

ICCBEI 2023

BANGKOK THAILAND



PROCEEDINGS
of the 5th International Conference
on Civil and Building Engineering Informatics
July 19-21, 2023

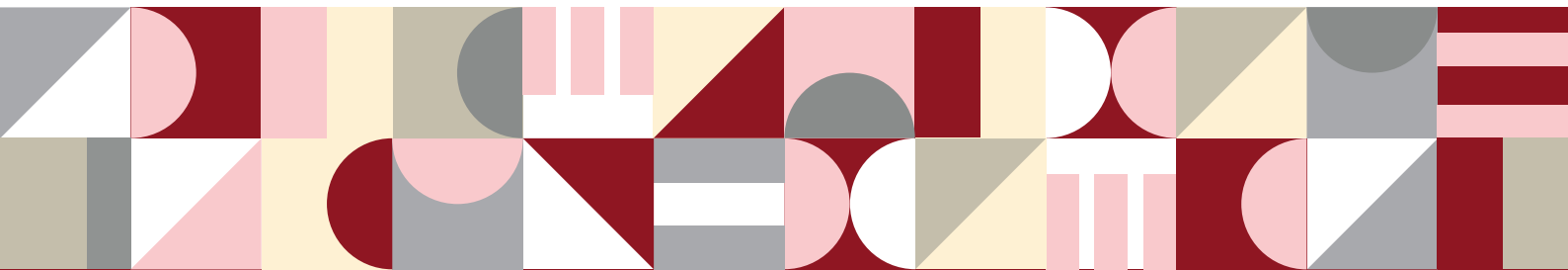
Edited by
Veerasak Likhitrungsilp, Charinee Limsawasd, and Nobuyoshi Yabuki
ICCBEI 2023 Organizing Committee

ICCBEI 2023

BANGKOK THAILAND

**Proceedings of the 5th International Conference
on Civil and Building Engineering Informatics**

Edited by
Veerasak Likhitrungsilp, Charinee Limsawasd, and Nobuyoshi Yabuki
ICCBEI 2023 Organizing Committee





**Funding for Academic and Research Cooperation with
the University Network and International Institutes
under the Second Century Fund, C2F B.E. 2562 (2019)
Chulalongkorn University**



PRE-BUILT

Pre-Built Public Company Limited

PROPERTY PERFECT

Perfect Prefab Company Limited

ISBN (e-book): 978-616-407-863-5

Edited by Veerasak Likhitrungsilp, Charinee Limsawasd, and Nobuyoshi Yabuki

Published by Chulalongkorn University, Bangkok 10330, Thailand

COPYRIGHT NOTICE: Copyright©2023 by the authors of individual papers

The full papers of this proceedings can be downloaded from

<https://civil.eng.chula.ac.th/iccbei2023/>

GREETINGS FROM THE CHAIR OF ICCBEI 2023

Sawasdee Krub. Welcome to the 5th International Conference on Civil and Building Engineering Informatics (ICCBEI 2023), Bangkok, Thailand. Chulalongkorn University is grateful and honored to host this prestigious conference. ICCBEI was organized from the previous series of Asian Construction Information Technology Roundtable Meeting, which had been sponsored by Japan Society of Civil Engineers (JSCE) and Japan Construction Information Center (JACIC). At that time, Asia did not have any international conferences on computing in civil and building engineering. The Board of Directors (BOD) of Asian Group for Civil Engineering Informatics (AGCEI) was established and organized the 1st ICCBEI in 2013. The following three conferences were held in Tokyo (2015), Taipei (2017), and Sendai (2019). Due to the COVID-19 pandemic, ICCBEI has not been organized since then.

In recent years, especially during the COVID-19 era, digital disruption has accelerated the digital transformation of every industry, especially construction. To be productive and competitive with their opponents, architecture, engineering, construction, and operations (AECO) organizations are obliged to smartly adopt and implement a variety of digital technologies to serve their various purposes. In addition to fundamental digital technologies such as building/construction information modeling (BIM/CIM), several modern information technologies have been emerging and widely used in construction business such as XR (VR, AR, MR); laser and image scanning; AI; big data; and ChatGPT.

ICCBEI 2023 covers a wide range of research fields in the application of Information and Communication Technology (ICT) to civil, building, and environmental engineering. The conference called for abstracts (optional) in January 2023, and the full papers were submitted in April 2023. With rigorous reviews by the scientific committee, the conference finally accepted 74 full papers, which are grouped into nine categories, namely, (1) Building and Construction Information Modeling, (2) Visualization and XR, (3) Laser and Image Scanning, (4) AI & Data Analysis, (5) Information Process and Management, (6) Construction Engineering and Asset Management, (7) Green Construction and Sustainability, (8) Digital Twin, and (9) Smart Cities and Infrastructure Management.

Finally, ICCBEI 2023 would like to express our gratitude for tremendous support from Professor Nobuyoshi Yabuki (the President of Board of Directors, AGCEI); Professor Supot Teachavorasinskun, Dean of Engineering, Chulalongkorn University; Professor Boonchai Stitmannathum, Head of Civil Engineering Department, Chulalongkorn University; the Organizing Committee members; the Scientific Committee members; all organizing staff; and many others. Without your devotion, this conference will never happen. We hope you enjoy the conference and Bangkok.



Veerasak Likhitrungsilp

Chair of the Organizing Committee ICCBEI 2023
Associate Professor, Chulalongkorn University, Thailand

Organization of ICCBEI 2023



Board of Directors

Asian Group of Civil Engineering Informatics (AGCEI)

President:

Nobuyoshi Yabuki, Osaka University, Japan

Members:

Jack Chin Pang Cheng, Hong Kong University of Science and Technology, Hong Kong

Patrick Shang-Hsien Hsieh, National Taiwan University, Taiwan

Sang-Ho Lee, Yonsei University, Korea

Veerasak Likhitrungsilp, Chulalongkorn University, Thailand

Zhiliang Ma, Tsinghua University, China

Koji Makanae, Miyagi University, Japan

Weng Tat Chan, National University of Singapore, Singapore

Xiangyu Wang, Curtin University, Australia

Committees of ICCBEI 2023

Organizing Committee

Advisors:

Supot Teachavorasinskun, Dean of Engineering, Chulalongkorn University

Boonchai Stitmannathum, Head of Civil Engineering Department, Chulalongkorn University

Chair:

Veerasak Likhitrungsilp, Dept. of Civil Engineering, Chulalongkorn University

Vice Chair:

Tirawat Boonyatee, Dept. of Civil Engineering, Chulalongkorn University

Members:

Nakhon Kokkaew, Dept. of Civil Engineering, Chulalongkorn University

Tidarut Wisuthseriwong, Dept. of Civil Engineering, Chulalongkorn University

Veerayut Komolvilas, Dept. of Civil Engineering, Chulalongkorn University

Chayut Ngamkhanong, Dept. of Civil Engineering, Chulalongkorn University

Sanphet Chunitipaisan, Dept. of Survey Engineering, Chulalongkorn University.

Aksara Puttividhya, Dept. of Water Resources Engineering, Chulalongkorn University

Kaweekrai Srihiran, Dept. of Architecture, Chulalongkorn University

Sutee Anantsuksomsri, Dept. of Urban and Regional Planning, Chulalongkorn University

Terdsak Tachakitkachorn, Dept. of Architecture, Chulalongkorn University

Chavanont Khosakitchalert, Dept. of Architecture, Chulalongkorn University

Manop Kaewmoracharoen, Dept. of Civil Engineering, Chulalongkorn University

Charinee Limsawasd, Dept. of Civil Engineering, Chulalongkorn University

Committees of ICCBEI 2023

Scientific Committee

Chair:

Nobuyoshi Yabuki (Osaka University, Japan)

Vice Chair:

Veerasak Likhitruangsilp (Chulalongkorn University, Thailand)

Members:

Jack Chin Pang Cheng (Hong Kong University of Science and Technology, Hong Kong)

Patrick Shang-Hsien Hsieh (National Taiwan University, Taiwan)

Sang-Ho Lee (Yonsei University, Korea)

Zhiliang Ma (Tsinghua University, China)

Koji Makanae (Miyagi University, Japan)

Weng Tat Chan (National University of Singapore, Singapore)

Xiangyu Wang (Curtin University, Australia)

Sutee Anantsuksomsri (Chulalongkorn University, Thailand)

Nilobol Aranyabhaga (Office of National Water Resources, Thailand)

Farrukh Arif (NED University of Engineering and Technology Karachi, Pakistan)

Nathee Athigakunagorn (Kasetsart University, Thailand)

Nida Azhar (NED University of Engineering and Technology Karachi, Pakistan)

Vacharapoom Benjaoran (Suranaree University of Technology, Thailand)

Tirawat Boonyatee (Chulalongkorn University, Thailand)

Apichat Buakla (University of Phayao, Thailand)

Krisada Chaiyasarn (Thammasat University, Thailand)

Saksith Chalermpong (Chulalongkorn University, Thailand)

Thongthit Chayakula (Chulalongkorn University, Thailand)

Albert Y. Chen (National Taiwan University, Taiwan)

Sanphet Chunithipaisan (Chulalongkorn University, Thailand)

Hiroaki Date (Hokkaido University, Japan)

Sy Tien Do (Ho Chi Minh City University of Technology (HCMUT), Vietnam)

Tomohiro Fukuda (Osaka University, Japan)

Vincent J.L. Gan (National University of Singapore, Singapore)

Brian Guo (University of Canterbury, New Zealand)

Tantri Handayani (Universitas Gadjah Mada, Indonesia)

Abdulrahman Haruna (Abubakar Tafawa Balewa University, Nigeria)

Wen-Yi Hung (National Central University, Taiwan)

Ryuichi Imai (Hosei University, Japan)

Manop Kaewmoracharoen (Chulalongkorn University, Thailand)

Satoshi Kanai (Hokkaido University, Japan)

Chavanont Khosakitchalert (Chulalongkorn University, Thailand)

Hongjo Kim (Yonsei University, South Korea)

Committees of ICCBEI 2023

Namgyun Kim (University of Dayton, USA)
Tuantan Kitpaisalsakul (Chulalongkorn University, Thailand)
Karun Klaycham (Kasetsart University, Thailand)
Nakhon Kokkaew (Chulalongkorn University, Thailand)
Veerayut Komolvilas (Chulalongkorn University, Thailand)
Nipawan Kunsuwan (Kasetsart University, Thailand)
Chollada Laofor (Mahanakorn University of Technology, Thailand)
Panon Latcharote (Mahidol University, Thailand)
Hang Thi Thu Le (University of Architecture Ho Chi Minh City, Vietnam)
Sutat Leelataviwat (King Mongkut's University of Technology Thonburi, Thailand)
Narong Leungbootnak (Future Engineering Consultants Co., Ltd, Thailand)
Ting Li (Shijiazhuang Tiedao University, China)
Charinee Limsawasd (Chulalongkorn University, Thailand)
Petcharat Limsupreeyarat (Burapha University, Thailand)
Ping Liu (Jiangsu University of Science & Technology, China)
Masaya Nakahara (Osaka Electro-Communication University, Japan)
Kenji Nakamura (Osaka University of Economics, Japan)
Sorawit Narupiti (Chulalongkorn University, Thailand)
Chayut Ngamkhanong (Chulalongkorn University, Thailand)
Vachara Peansupap (Chulalongkorn University, Thailand)
Patraphorn Phornthepkasemsant (Burapha University, Thailand)
Sarin Pinich (Chulalongkorn University, Thailand)
Lapyote Prasittisopin (Chulalongkorn University, Thailand)
Aksara Putthividhya (Chulalongkorn University, Thailand)
Pher Errol B. Quinay (University of the Philippines Diliman)
Damrongsak Rinchumphu (Chiang Mai University, Thailand)
Jittichai Rudjanakanoknad (Chulalongkorn University, Thailand)
Natthapol Saovana (King Mongkut's University of Technology North Bangkok, Thailand)
Kaweeakrai Srihiran (Chulalongkorn University, Thailand)
Natee Suriyanon (Chiang Mai University, Thailand)
Terdasak Tachakitkachorn (Chulalongkorn University, Thailand)
Wisuwat Taesombat (Kasetsart University, Thailand)
Takahiro Tanaka (Hiroshima University, Japan)
Wasaporn Techapeeraparnich (Mahidol University, Thailand)
Kongkoon Tochaiwat (Thammasat University, Thailand)
Tuan Van Tran (Can Tho University, Vietnam)
Kanok Weerawong (Chulalongkorn University, Thailand)
Tidarut Wisuthseriwong (Chulalongkorn University, Thailand)
I-Tung Yang (National Taiwan University of Science and Technology, Taiwan)
Xianzhong Zhao (Tongji University, China)
Jin Zhu (University of Connecticut, USA)
Yang Zou (University of Auckland, New Zealand)

TABLE OF CONTENTS

Keynote Lecture 1

Transforming Urban Living in Bangkok: The Role of Infrastructure Asset Management in Creating a Smart City

Assoc. Prof. Wisanu Subsompon (Vice Governor of Bangkok Metropolitan Authority)

18

Keynote Lecture 2

Engineering Brain: Metaverse for the Future Engineering

Prof. Xiangyu Wang (Curtin University, Australia)

20

Keynote Lecture 3

Decision Support Systems for Civil Engineering Construction

Prof. Photios G. Ioannou (University of Michigan (Ann Arbor), USA)

22

AI & Data Analysis

[AI1] Adaptive Kriging-Assisted Metaheuristic Method for Efficient Reliability-Based Design Optimization

Handy Prayogo (National Taiwan University of Science and Technology),
I-Tung Yang (National Taiwan University of Science and Technology)

24

[AI2] ChatGPT in the Construction Domain: Opportunities, Risks, and Recommendations

Taegeon Kim (Yonsei University), Seokhwan Kim (Yonsei University), Namgyun Kim (University of Dayton), Hongjo Kim (Yonsei University)

33

[AI3] Training Data Generation with 3D CAD Models for Point Cloud Deep Learning for Underwater Objects

Hiroshi Okawa (Eight-Japan Engineering Consultants Inc.), Shota Yagi (Eight-Japan Engineering Consultants Inc.), Seiji Itano (Eight-Japan Engineering Consultants Inc.), Kazuo Kashiwama (Chuo University)

38

[AI4] Evaluation of AI's Generalization Performance for Detecting Construction Machinery from Video Images

Kentaro Hayakawa (Miyagi University), Koji Makanae (Miyagi University)

45

[AI5] Intelligent Design of Simply-Supported Planar Truss based on Reinforcement Learning

Xianzhong Zhao (Tongji University), Zhiyuan Liu (Tongji University), Weifang Xiao (Tongji University), Ruifeng Luo (East China Architectural Design & Research Institute Co., Ltd.)

52

[AI6] Model Building for Lane Line Extraction Using High-Definition Map

Ryuichi Imai (Hosei University), Kenji Nakamura (Osaka University of Economics),
Yoshinori Tsukada (Setsunan University), Noriko Aso (Dynamic Map Platform Co., Ltd.),
Jin Yamamoto (Hosei University)

59

[AI7] Fundamental Study on Extraction Method of License Plate Classification Number Using Video Images

Ryuichi Imai (Hosei University), Daisuke Kamiya (University of the Ryukyus), Yuhei Yamamoto (Kansai University), Masaya Nakahara (Osaka Electro-Communication University), Wenyuan Jiang (Osaka Sangyo University), Koki Nakahata (Kansai University), Ryo Sumiyoshi (Hosei University)

66

[AI8] A Quantitative Evaluation of Rough Ground Truth Labeling on Construction Scaffolding Image Segmentation

Natthapol Saovana (King Mongkut's University of Technology North Bangkok)

73

[AI9] Analyzing the Impact of COVID-19 Pandemic on Traffic Volume through Textual Data: A Bert-Based Approach

Mu-Chieh Chung (National Taiwan University), Albert Y. Chen (National Taiwan University)

81

[AI10] Electric Vehicle Emission Analysis through Thermal Image-Based Vehicle Classification

Chun-Ping Liao (National Taiwan University), Ta-Chih Hsiao (National Taiwan University), Albert Y. Chen (National Taiwan University)

87

[AI11] CSS-Onto: Construction Safety Situation Ontology

Zhe Zhang (University of Canterbury), Brian H.W. Guo (University of Canterbury), Yonger Zuo (University of Canterbury), Bowen Ma (University of Canterbury), Alice Chang-Richards (University of Auckland), Zhenan Feng (Massey University), Yang Zou (University of Auckland)

92

[AI12] Risk Assessment of Railway Tracks in Floodplain Area Using Digital Surface Model and Computer Vision

Watcharapong Wongkaew (Chulalongkorn University), Wachira Muenyoksakul (Chulalongkorn University), Krittiphong Manachamni (Chulalongkorn University), Tanawat Tangjarusritaratorn (Chulalongkorn University), Chayut Ngamkhanong (Chulalongkorn University)

100

[AI13] Graph Neural Network Integrating with Metaheuristic Search for Automated Multi-Layer Rebar Design Optimization

Mingkai Li (The Hong Kong University of Science and Technology), Vincent J. L. Gan (National University of Singapore), Jack C. P. Cheng (The Hong Kong University of Science and Technology)

108

[AI14] Data Analysis for Prediction and Visualization of Sensor Data in Railroad Proximity Construction

Atsushi Takao (Okumura Corporation), Nobuyoshi Yabuki (Osaka University), Yoshikazu Otsuka (Okumura Corporation)

116

[AI15] An Approach for Generating Hybrid Datasets of Construction Material

Bo Cheng (Tongji University), Yujie Lu (Tongji University), and Xianzhong Zhao (Tongji University)

123

Building and Construction Information Modeling

[BIM1] Multi-Modal Deep Learning (MMDL)-Based Automatic Classification of BIM Elements for Construction Cost Estimation

Hao Liu (The Hong Kong University of Science and Technology), Shanjing Zhou (Imperial College London), Vincent J.L. Gan (National University of Singapore),
Jack C.P. Cheng (The Hong Kong University of Science and Technology)

131

[BIM2] An Automatic Translation Framework based on Ontology to Building Energy Models

Zhaoji Wu (The Hong Kong University of Science and Technology),
Jack C.P. Cheng (The Hong Kong University of Science and Technology),
Zhe Wang (The Hong Kong University of Science and Technology),
Helen H.L. Kwok (The Hong Kong University of Science and Technology)

139

[BIM3] GIS Based 3D Data Integration on Highway Tunnel through Lifecycle Management for Advanced Maintenance

Choiijilsuren Batbaatar (Kyushu University), Yasuhiro Mitani (Kyushu University),
Hisatoshi Taniguchi (Kyushu University), Hiroyuki Honda (Kyushu University)

147

[BIM4] A Building Information Model for Sensing and Simulation toward Net-Zero Energy Building Renovation

Kazuya Matsuba (Osaka University), Nobuyoshi Yabuki (Osaka University), Tomohiro Fukuda (Osaka University), Yoshiro Hada (Tokyu Construction Co., Ltd)

153

[BIM5] A Property Data Sharing Method of Building Information Models Using Remote Augmented Reality

Koji Yoshimura (Osaka University), Nobuyoshi Yabuki (Osaka University), Tomohiro Fukuda (Osaka University)

160

[BIM6] “To BIM or Not to BIM”: A Simulation Game for Teaching AEC Students the Key Mechanisms in Project Delivery

Yun-Tsui Chang (National Taiwan University), Aritra Pal (National Taiwan University),
Tzong-Hann Wu (National Taiwan University), Shang-Hsien Hsieh (National Taiwan University)

168

[BIM7] A BIM-Assisted Planning Tool for Facilitating the Application of an Aluminum Formwork System to Beam-Column Buildings

Kuan-Yi Chen (National Taiwan University), Tzong-Hann Wu (National Taiwan University),
Budy Setiawan (FBC Formworks Systems Co., Ltd.), Cecilia Clarita Tandri (FBC Formworks Systems Co., Ltd.), Shang-Hsien Hsieh (National Taiwan University), Wen-Tung Chang (FBC Formworks Systems Co., Ltd.)

176

[BIM8] Development of a BIM-Based System for Assessment and Optimization of GHG Emissions in the Early Design Stage

Thanasak Phittayakorn (Chulalongkorn University), Chavanont Khosakitchalert (Chulalongkorn University), Lapyote Prasittisopin (Chulalongkorn University)

184

[BIM9] BIM-COBie Based Bridge-Defect Integrated Model for Condition Assessment of Bridge Superstructure

Jung-Bin Lee (Yonsei University), Sangho Lee (Yonsei University), Inseop Yun (Yonsei University), Sang-Ho Lee (Yonsei University)

192

[BIM10] Situation of BIM Implementation in Comparison between the National University of Singapore and Chulalongkorn University

Gittigul Boonplien (Chulalongkorn University), Terdsak Tachakitkachorn (Chulalongkorn University), Kaweechai Srihiran (Chulalongkorn University)

200

[BIM11] Strategic Development of Building Information Modeling (BIM) Implementation for Thai Construction Contractors

Parit Martpaijit (Chulalongkorn University), Vachara Peansupap (Chulalongkorn University)

206

[BIM12] BIM-Based Precast Building Optimization by Optimality Criteria and NSGA-II-GD Considering Constructability for Precast Concrete Sizing and Rebar Detailing

Weng-Lam Lao (Hong Kong University of Science and Technology),
Ming kai Li (Hong Kong University of Science and Technology),
Billy C.L. Wong (Hong Kong University of Science and Technology),
Vincent J.L. Gan (National University of Singapore),
Jack C.P. Cheng (Hong Kong University of Science and Technology)

213

[BIM13] Improving the Efficiency of ICT Earthwork through Automated Planning Using BIM

Hitoshi Ishida (Penta-Ocean Construction Co., LTD), Nobuyoshi Yabuki (Osaka University)

223

[BIM14] New Era of Mapping Products From UAV-Based Oblique Camera System

Thirawat Bannakulpihat (Chulalongkorn University), Phisan Santitamnont (Chulalongkorn University)

231

[BIM15] Evaluation of Interoperability by Quantifying Data Integrity in the Integration of BIM and Structural Analysis for Multiple Levels of Development

Kayla Solis (University of the Philippines Diliman), Pher Errol Quinay (University of the Philippines Diliman), Karlo Daniel Colegio (University of the Philippines Diliman)

237

[BIM16] Quantitative Analysis for Applying Building Information Modeling(BIM) in Infrastructure Projects

Hwan Yong Kim (Hanyang University ERICA), Min Ho Shin (Woosong University),
Leen Seok Kang (Gyeongsang National University)

245

[BIM17] BIM: A Successful Alternative for the Construction Quantity Take-Off in the Large-Scale Construction Project

Hang Le Thi Thu (University of Architecture Ho Chi Minh City),
Huyen Nguyen Thi (University of Architecture Ho Chi Minh City),
Huong Pham Thu (University of Architecture Ho Chi Minh City),
Phong Thanh Nguyen (Ho Chi Minh City Open University)

252

[BIM18] Building Information Modeling Framework for Practical Implementation of a Mega-Project in Thailand

Pawaris Khammultri (Sino-Thai Engineering and Construction Public Company Limited),
Kritsada Lappanichayakul (Sino-Thai Engineering and Construction Public Company Limited),
Pithiwat Tiantong (Sino-Thai Engineering and Construction Public Company Limited),
Athasit Sirisonthi (Sino-Thai Engineering and Construction Public Company Limited)

258

[BIM19] State-of-the-Art of Historic Building Information Trends with Digitalization Integration on the Architecture Heritage Conservation in Vietnam

Thu Anh Nguyen (Ho Chi Minh City University of Technology (HCMUT)),
Nhu My Uy Le (Ho Chi Minh City University of Technology (HCMUT)),
Sy Tien Do (Ho Chi Minh City University of Technology (HCMUT)),
Son Hong Nguyen (Ho Chi Minh City University of Technology (HCMUT)),
Quang Trung Khuc (Ho Chi Minh City University of Technology (HCMUT))

266

[BIM20] On Practical Cases of Building Information Management in Construction Project Collaboration

Min Shih (Unique Engineering and Construction Public Company Limited),
Yen-Hung Chen (National Taiwan University of Science and Technology),
Shen-Guan Shih (National Taiwan University of Science and Technology)

275

[BIM21] Design and Implementation of BIM-Based Roadway Drainage Model

Jing-Ying Huang (Sinotech Engineering Consultants, Ltd.), Chi-Hsuan Lin (Sinotech Engineering Consultants, Ltd.), Jian-Bang Yang (Sinotech Engineering Consultants, Ltd.),
Yi-Chiang Tsao (Sinotech Engineering Consultants, Ltd.), Shih-Yao Lan (Taoyuan City Government)

283

[BIM22] Automatic Creation of 3D Textured Simplified Model for Supporting Piled Pier Maintenance

Tomohiro Mizoguchi (Nihon University), Kenichi Mizuno (Penta-Ocean Construction Co., Ltd.),
Osamu Taniguchi (Penta-Ocean Construction Co., Ltd.)

289

[BIM23] BIM Application for Resolving Construction Issues in Thailand: A Consultant's Case Study

Narong Leungbootnak (Khon Kaen University), Vuthea Min (Future Engineering Consultants Co., Ltd)

296

[BIM24] The Process of Applying AR/VR/MR in Design Implementation in Construction Projects

Nam Phuong Nguyen (Hanoi University of Civil Engineering),
Tuan Sy Ho (Ho Chi Minh City University of Technology (HCMUT)),
Sy Tien Do (Vietnam National University Ho Chi Minh City)

301

Construction Engineering and Asset Management

[CEA1] Modeling and Pricing of Multiple Renewal Options Embedded in Short-Term Lease Contracts

Nakhon Kokkaew (Chulalongkorn University), Wisanu Supsompon (Bangkok Metropolitan Administration), Chanon Atipanya (Chulalongkorn University)

312

[CEA2] A Bayesian Network Model for Quantifying the Cost Impacts of Claim Causes in Building Projects

Sang Van (Chulalongkorn University), Veerasak Likhitrungsilp (Chulalongkorn University), Photios G. Ioannou (University of Michigan)

321

[CEA3] Comparison of Immersive and Non-Immersive VR Games for Assessing Safety Knowledge

Sabnam Thapa (Chulalongkorn University), Vachara Peansupap (Chulalongkorn University)

328

[CEA4] Implementing the Circular Economy Concept in Construction Supply Chain Management of Modular Steel Projects

Thet Htar San (Chulalongkorn University), Veerasak Likhitrungsilp (Chulalongkorn University)

335

[CEA5] Markov Deterioration Hazard Model for Road Network Deterioration Forecast for National Road Networks in Lao PDR

Souvikhane Hanpasith (Osaka University), Kotaro Sasai (Osaka University), Kiyoyuki Kaito (Osaka University)

342

[CEA6] Promoting Flexible Use of Open Data through Service Link Platform for Infrastructure Management

Yinyongdong Ma (Yamaguchi University), Kei Kawamura (Yamaguchi University), Junha Hwang (Yamaguchi University), Shuji Sawamura (Yamaguchi Prefecture Government), Hisao Emoto (Tottori University)

352

Digital Twin

[DT1] Design of a Digital Twin for Real-Time Construction Pollution Management in Building Renovation Projects

Truong-An Pham (Chulalongkorn University), Veerasak Likhitrungsilp (Chulalongkorn University)

361

[DT2] Verification of Registration and Complementation of Point Cloud Data Obtained by Simplified Measurement

Ryuichi Imai (Hosei University), Kenji Nakamura (Osaka University of Economics), Yoshinori Tsukada (Setsunan University), Yasuhito Niina (Asia Air Survey Co., Ltd.), Ryo Komiya (Hosei University)

371

[DT3] Traffic Noise Simulation and Its Auralization Using VR Technology

Kazuo Kashiya (Chuo University)

379

[DT4] Smart Home Adoption: Challenge and Opportunity for Digital Twin Building

Chalumpon Thawanapong (Chulalongkorn University), Terdsak Tachakitkachorn (Chulalongkorn University), Kaweechai Srihiran (Chulalongkorn University)

386

[DT5] Consideration for Level of Digital Twin in Architecture

Terdsak Tachakitkachorn (Chulalongkorn University), Chalumon Thawanapong (Chulalongkorn University), Kaweechai Srihiran (Chulalongkorn University)

394

[DT6] From BIM to Digital Twin: A Case Study Experience

Prapaporn Rattanatamrong (Thammasat University), Jarunchai Srisawat (Thammasat University), Peemapat Podsoonthorn (Thammasat University), Thapana Boonchoo (Thammasat University), Wanida Putthividhya (Thammasat University), Veerasak Likhitrungsilp (Chulalongkorn University)

400

Green Construction and Sustainability

[GS1] Circular Economy Critical Success Factors for Sustainable Construction: An Exploratory Approach

Abdulrahman Haruna (Abubakar Tafawa Balewa University), Veerasak Likhitrungsilp (Chulalongkorn University)

406

[GS2] A Blockchain-Based Carbon Auditing Framework for Construction Material and Product Certification

Yuqing Xu (The Hong Kong University of Science and Technology), Xingyu Tao (The Hong Kong University of Science and Technology), Moumita Das (The Hong Kong University of Science and Technology), Helen H.L. Kwok (The Hong Kong University of Science and Technology), Hao Liu (The Hong Kong University of Science and Technology), Jack C.P. Cheng (The Hong Kong University of Science and Technology)

414

[GS3] Research on Visualization based on Climate Analysis of the Influence of Green Space on the Thermal Environment Using MSSG Model

Takumi Makio (Osaka Metropolitan University), Kaoru Matsuo (Osaka Metropolitan University), Shigeaki Takeda (Osaka Metropolitan University), Hiroyuki Kaga (Osaka Metropolitan University), Makoto Yokoyama (Fukuyama City University)

422

[GS4] Emissions Tracking Control Optimization to Support Sustainable Construction in Road Construction Projects

Phattadon Khathawatcharakun (Chulalongkorn University), Charinee Limsawasd (Chulalongkorn University), Nathee Athigakunagorn (Kasetsart University)

428

[GS5] Green Infrastructure Planning with Population Decreasing for Adapting to Climate Change by Using GIS and Numerical Models: Case of Kure City in Hiroshima Prefecture

Takahiro Tanaka (Hiroshima University), Shinji Hirai (Hiroshima University), Ryota Araki (Hiroshima University), Riki Yamaga (Hiroshima University), Shota Tamura (Hiroshima University), Makoto Yokoyama (Fukuyama City University), Kaoru Matsuo (Osaka Metropolitan University), Toru Sugiyama (Japan Agency for Marine-Earth Science and Technology)

433

[GS6] Comparative Analyses of Simulation and Measurement Data of Buildings Energy Consumption Using Typical Weather Data and Real Weather Data in Hot-Humid Climate

Sarin Pinich (Chulalongkorn University), Terdsak Tachakitkachorn (Chulalongkorn University), Atch Sreshtaputra (Chulalongkorn University)

438

Information Process and Management

[IPM1] The Integration of Design and Fabrication for Prefabricated UHPC Panels of Building Facades

Kevin Harsono (National Taiwan University of Science and Technology),
ShenGuan Shih (National Taiwan University of Science and Technology),
YenJui Chen (Taiwan Sobute New Materials Co. Ltd.)

444

[IPM2] Considering of BIM Data Scale Interfaces for Various Application: Case Studies of Smart Patrol Project in Chulapat 14 Building Chulalongkorn University

Kaweekrai Srihiran (Chulalongkorn University), Terdsak Tachakitkachorn (Chulalongkorn University), Chalumon Thawanapong (Chulalongkorn University)

452

[IPM3] Development of Roadway Geometric Design Process Model for Knowledge Management

Koji Makanae (Miyagi University)

457

Laser and Image Scanning

[LIS1] Footprint Detection of Ceiling Equipment from TLS Point Clouds

Riho Akiyama (Hokkaido University), Hiroaki Date (Hokkaido University), Satoshi Kanai (Hokkaido University), Kazushige Yasutake (Kyudenko Corporation)

465

[LIS2] An Alternative Method for Cable Tension Evaluation based on the Terrestrial Laser Scanning Data

Thaniyaphat Srimontriphakdi (King Mongkut's University of Technology Thonburi),
Peerasit Mahasuwanchai (King Mongkut's University of Technology Thonburi),
Phutawan Yawananont (King Mongkut's University of Technology Thonburi),
Chainarong Athisakul (King Mongkut's University of Technology Thonburi),
Ekkachai Yooprasertchai (King Mongkut's University of Technology Thonburi),
Sutat Leelataviwat (King Mongkut's University of Technology Thonburi),
Somchai Chucheeepsakul (King Mongkut's University of Technology Thonburi)

471

[LIS3] Integrating BIM into Web GIS to Enhance the Visualization of Port Infrastructure

Le Vin Tran (Ho Chi Minh City University of Technology (HCMUT)),
Minh Chung Bui (Ho Chi Minh City University of Technology (HCMUT)),
Van Tan Nguyen (Ho Chi Minh City University of Technology (HCMUT)),
Tuan Anh Le (Ho Chi Minh City University of Technology (HCMUT)),
Danh Thao Nguyen (Ho Chi Minh City University of Technology (HCMUT)),
Bao Binh Luong (Ho Chi Minh City University of Technology (HCMUT)),
Hiep Hoang (Portcoast Consultant Corporation)

477

Smart Cities and Infrastructure Management

[SCI1] On the Visual Aspect of the Information Scape in the Built Environment: Shilin Night as an Example

Ye Yint Aung (National Taiwan University of Science and Technology),
ShenGuan Shih (National Taiwan University of Science and Technology)

486

[SCI2] Accumulation and Classification of Smart Living Framework from Academic Studies and Real Sector

Suchanad Phuprasoet (Chulalongkorn University), Terdsak Tachakitkachorn (Chulalongkorn University), Kaweechai Srihiran (Chulalongkorn University)

494

[SCI3] Crack Detection of Bridges from Self-Weight Deformation Profiles

Suphanat Wang (Chulalongkorn University)

501

[SCI4] Dynamic Response Evaluation of Railway Track Transitions with Resilient Materials

Surapan Noppharat (Chulalongkorn University), Anand Raj (Chulalongkorn University), Chayut Ngamkhanong (Chulalongkorn University)

511

[SCI5] One-Dimensional Compression Model for Unsaturated Crushable Granular Materials

Pongsapak Kanjanatanalert (Chulalongkorn University), Veerayut Komolvilas (Chulalongkorn University)

519

[SCI6] A Combined Drought Index (CDI) System for Drought Early Warning, Monitoring, and Risk Assessment in EEC Thailand

Sasin Jirasirirak (Chulalongkorn University), Aksara Putthividhya (Chulalongkorn University), Somkiat Prajamwong (Eastern Economic Corridor Office), Wimonpat Bumbudsanpharoke Kamkanya (Office of the National Water Resources)

527

[SCI7] Disaster Education on Flood Prevention Using Card Game through Digital Platform

Mari Tanaka (Gunma University), Kenji Nakamura (Gunma University Center for Mathematics and Data Science)

536

Visualization and XR

[XR1] Construction of a Location-Based Mixed-Reality Visualization System Using Global Navigation Satellite System Data

Ryoudai Nakaso (Chuo University), Masahiro Suzuki (Chuo University), Hiroshi Okawa (Chuo University), Tsuyoshi Kotoura (Penta-Ocean Construction CO.), Kazuo Kashiya (Chuo University)

543

[XR2] Advanced Augmented Reality Object Placement in Construction Sites Using Geospatial API and Visual Positioning Systems

Haein Jeon (Seoul National University of Science and Technology), Youngsu Yu (Seoul National University of Science and Technology), Sihyun Kim (Seoul National University of Science and Technology), Bonsang Koo (Seoul National University of Science and Technology)

550

[XR3] Automated Dimensional Checking in Mixed Reality for Staircase Flight

Michelle Siu Zhi Lee (Osaka University), Nobuyoshi Yabuki (Osaka University), Tomohiro Fukuda (Osaka University)

557

[XR4] BIM-Based and Augmented Reality Combined with a Real-Time Fire Evacuation System for the Construction Industry

Somjintana Kanangkaew (Chulalongkorn University), Noppadon Jekkaw (Chulalongkorn University), Tanit Tongthong (Chulalongkorn University)

KEYNOTE LECTURE 1

TRANSFORMING URBAN LIVING IN BANGKOK: THE ROLE OF INFRASTRUCTURE ASSET MANAGEMENT IN CREATING A SMART CITY

Wisanu Subsompon

Ph.D., Associate Professor
Deputy Governor, Bangkok Metropolitan Administration

Abstract: The rapid urbanization and population growth in cities worldwide have presented numerous challenges, and Bangkok is no exception. In response to these challenges, the Bangkok Metropolitan Administration (BMA) has embarked on a transformative journey to establish a smart and sustainable metropolis. A crucial component of this transformation is Infrastructure Asset Management (IAM), which harnesses technology to enhance the efficiency, resilience, and quality of urban infrastructure. Two key areas of focus in this endeavor are Pavement Analysis for Maintenance and Lighting Control Systems. By integrating advanced technologies such as the Internet of Things (IoT), survey technology, artificial intelligence, and data analytics, the BMA effectively monitors, maintains, and optimizes the city's infrastructure assets.

The application of Pavement Analysis for Maintenance ensures that Bangkok's roads and sidewalks are in optimal condition. By utilizing survey technology, and data analytics, the BMA can proactively identify areas requiring maintenance, minimizing disruptions and enhancing overall transportation efficiency. This approach results in cost savings and improved safety for residents and commuters. The implementation of a sophisticated Lighting Control System is another significant aspect of Bangkok's smart city transformation. Through IAM, the BMA leverages advanced technologies to monitor and control street lighting. This enables efficient energy management, reduced light pollution, and enhanced safety in public spaces. By leveraging data analytics, the BMA can identify patterns and optimize lighting schedules, creating a more sustainable and citizen-centric urban environment. While Bangkok has made substantial progress in its smart city journey, several challenges remain. These include concerns related to privacy and security, the need for infrastructure upgrades, and ensuring equitable access to technology for all citizens. To address these challenges, Bangkok should continue to foster collaboration between the public and private sectors, invest in research and development, and place a strong emphasis on citizen engagement and inclusivity.

KEYNOTE LECTURE 1



Profile of Dr. Wisanu Subsompon

Dr. Wisanu Subsompon earned Ph.D. in Civil Engineering from Carnegie Mellon University, USA in 1996. He also received the Bachelor of Law degree from Sukhothai Thammathirat University, Thailand in 2001. After graduating Ph.D., he had been working at Department of Civil Engineering, Faculty of Engineering, Chulalongkorn University, Bangkok, Thailand. During his tenure at Chulalongkorn University, he served in many executive positions of the university, including the Vice President for Property and Physical Resources Management, the Vice President for Property and Innovation Management, the Assistant to the University President for Science and Technology Development, the Director General of Chulalongkorn University Intellectual Property Institute, and the Managing Director of Jamjuree Innovations Co., Ltd. (holding company). In addition, he was an advisor to the Minister of Transport (Dr. Chatchart Sittipunt), the Independent Director of Airports of Thailand Public Company Limited, the Independent Director of BFIT Securities Public Company Limited, and the Independent Director of Land and Houses Public Company Limited. He is currently the Vice Governor of Bangkok Metropolitan Authority.

KEYNOTE LECTURE 2

ENGINEERING BRAIN: METAVERSE FOR THE FUTURE ENGINEERING

Xiangyu Wang

Ph.D., Professor, School of Design and Built Environment, Faculty of Humanities,
Curtin University, Perth, Australia. Email: Xiangyu.Wang@curtin.edu.au

Abstract: Engineering Brain is a sophisticated system that uses AI algorithms to analyse data and provide valuable insights to engineers. It allows engineers to simulate various construction scenarios and predict their outcomes, enabling them to make informed decisions in real-time. By integrating BIM, engineers can create a digital twin of the project that captures every detail of the physical structure, from the design to the construction phase. This technology enhances collaboration between all parties involved, including architects, engineers, contractors, and owners. This keynote presentation will provide attendees with an in-depth understanding of the engineering brain concept and its application in construction and civil engineering. The presentation will begin by introducing the basic principles of the engineering brain and its components. Then, the presentation will delve into the benefits of using the engineering brain in construction and civil engineering, including improved accuracy, efficiency, and sustainability. The keynote presentation will also discuss various case studies and real-world examples of successful engineering brain implementations. Attendees will have the opportunity to learn about the challenges faced during implementation and the solutions that were employed to overcome them. Finally, the keynote presentation will conclude with a discussion of the future of the engineering brain in construction and civil engineering.

KEYNOTE LECTURE 2



Profile of Professor Xiangyu Wang

Professor Xiangyu Wang is a global “Highly Cited Researcher” recognized by Clarivate Analytics, and a Fellow of the EU Academy of Sciences. He is affiliated with Curtin University and also the Executive Director/Distinguished Professor at the Institute of Intelligent Construction and Maintenance of Civil Infrastructure at East China Jiaotong University. He served on the panel of the Australian Research Council College of Experts in 2016-2018. He was also the Woodside Chair for a five-year term, the Australia’s top ten ASX listed company and largest energy company. His research achievements have been applied in various sectors including energy, mining, infrastructure, and construction, resulting in billions of dollars in global economic benefits. He has published 400+ journal articles where over 30 articles were ranked as ESI top 1 % highly cited papers and nearly 10 articles were hot papers (top 0.1%). His Web of Science overall citation is over 10,000.

KEYNOTE LECTURE 3

DECISION SUPPORT SYSTEMS FOR CIVIL ENGINEERING CONSTRUCTION

Photios G. Ioannou

Ph.D., Professor, Civil & Environmental Engineering Department, University of Michigan, Ann Arbor, Michigan, USA 48109-2125. Email: photios@umich.edu

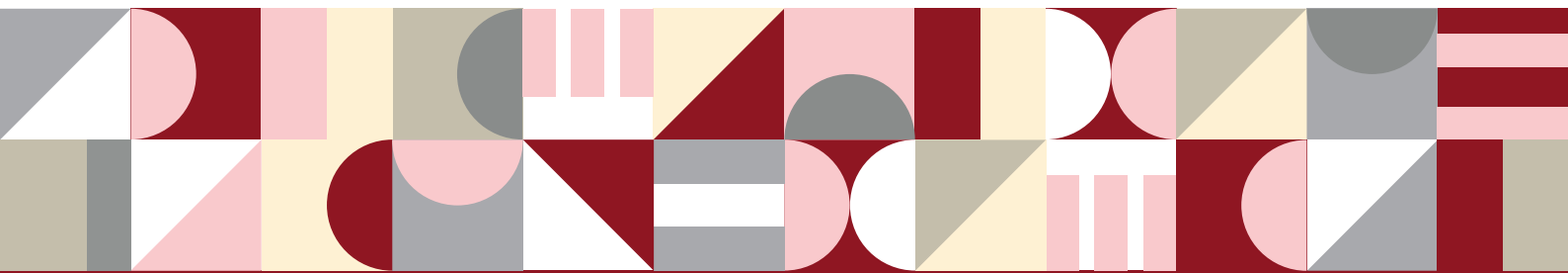
Abstract: Decision support systems have been developed and applied at all levels of civil engineering construction. This presentation will concentrate on two such applications. At the strategic level we will examine how competitive bidding models can help a contractor select the optimum price for a lump-sum construction contract. We will also examine the importance of cost uncertainty and the contractor's risk aversion on the optimum bid price. These are two factors that have traditionally been ignored even though they have a significant impact on how much the contractor should bid. At the operational level we will describe the discrete event simulation systems that have been developed at the University of Michigan, such as UM-CYCLONE, COOPS, STROBOSCOPE, and EZSTROBE, for modeling construction processes under uncertainty. The most modern of these, STROBOSCOPE and EZSTROBE, are used throughout the world for research, teaching, and practice, and are available from www.stroboscope.org. Applications of these systems to be presented include general earthmoving, dam construction, tunneling, and the scheduling of projects with repeating activities under uncertainty.



Profile of Professor Photios G. Ioannou

Photios G. Ioannou is Professor in the Department of Civil and Environmental Engineering at the University of Michigan, a Fellow of the ASCE, and a recipient of several awards including the Peurifoy Construction Research Award and the John O. Bickel Award from ASCE. Together with his former doctoral student J.C. Martinez are the designers and developers of the STROBOSCOPE Simulation System. He has also performed research in the development of other simulation systems, including UM-Cyclone, COOPS, EZStrobe, ProbSched, CPMAAddn, and Chastrobe. His research is in construction engineering and management in the areas of simulation, tunneling, competitive bidding models, project finance, innovative project delivery systems, and project scheduling. His email address is photios@umich.edu and his homepage is <https://www.ioannou.org>

AI and DATA Analysis



ADAPTIVE KRIGING-ASSISTED METAHEURISTIC METHOD FOR EFFICIENT RELIABILITY-BASED DESIGN OPTIMIZATION

Handy Prayogo¹, and I-Tung Yang²

1) Ph.D. Candidate, Department of Civil and Construction Engineering, College of Engineering, National Taiwan University of Science and Technology, Taipei, Taiwan. Email: d10905818@mail.ntust.edu.tw

2) Prof., Department of Civil and Construction Engineering, College of Engineering, National Taiwan University of Science and Technology, Taipei, Taiwan. Email: ityang@mail.ntust.edu.tw

Abstract: Reliability-based Design Optimization aims to find a design that minimizes the cost while adhering to the reliability constraints that consider the inherent uncertainties in the engineering process. Due to the ever-increasing complexity of today's engineering problems, an efficient way of solving RBDO problems is needed. Surrogate-based RBDO methods, particularly those that use Kriging or Gaussian Process Regression, have been studied intensively for their efficiency and accuracy. However, the existing methods still incur a high computation demand when paired with classical gradient-based optimization tools. This study proposed a new framework Meta-LAK that relies on the cooperation between metaheuristic optimization technique and Kriging model to tackle the RBDO problem. Using the information provided by the Kriging model, the method can avoid evaluating every sample, thus reducing the computation demand. The optimized design also limits the possible candidate samples used to enrich the Kriging model. The proposed algorithm is tested against a benchmark problem to evaluate its performance.

Keywords: Reliability-based design optimization, Adaptive Kriging, Metaheuristic

1. INTRODUCTION

Practical engineering problems typically involve a wide range of uncertainties such as: manufacturing tolerances, material properties, loading, and environmental condition. (Cheng et al., 2021; Meng et al., 2020). Traditional deterministic design optimization takes into account such uncertainties in the form of empirical safety factors. However, the use of empirical safety factors may result in a design that is too conservative and uneconomical. Reliability-Based Design Optimization (RBDO) is a method to find the best design that minimizes the cost while considering the various uncertainties that lie in the engineering system. The RBDO is generally formulated by:

$$\begin{aligned} & \min f(\mathbf{d}) \\ \text{s. t. } & \begin{cases} P(g_c(\mathbf{X}) \leq 0) \leq P_{fc}^t, & i = 1, 2, \dots, nc \\ \mathbf{d}^L \leq \mathbf{d} \leq \mathbf{d}^U \end{cases} \end{aligned} \quad (1)$$

where $f(\mathbf{d})$ is the cost function of design variable \mathbf{d} ; \mathbf{X} represent the vector of random variables; $g_c(\mathbf{X})$ denotes the c -th performance/limit-state function with $g_c(\mathbf{X}) \leq 0$ indicating structure failure; P_{fc}^t is the c -th target probability of failure; nc indicates the number of limit-state functions in the problem; the \mathbf{d}^L and \mathbf{d}^U are the lower and upper bounds respectively;

In real-world applications, the limit-state function is often a time-consuming model that involves complex calculations such as Finite Element Analysis (FEA). Due to the ever-growing complexities of engineering problems, the traditional RBDO methods such as double loop methods (Hao et al., 2019; Lee et al., 2015), decoupled methods (Jiang et al., 2020; Shi et al., 2020), and single-loop methods (Jiang et al., 2017; Meng & Keshtegar, 2019) may incur too high of a computational cost. Another alternative is to use a surrogate model to replace the expensive limit-state function. Out of the different surrogate models available, the Kriging model is the most widely used due to its capability in predicting the local variance (Jiang et al., 2021). This unique characteristic enables the active-learning/adaptive strategies, where the active-learning function is used to select the best point to enrich the model sequentially.

In adaptive Kriging-based RBDO methods, the model can be constructed using two of the following strategies: the global modeling strategy (Li et al., 2022b; Xiao et al., 2020) and the local modeling strategy (Li et al., 2022a; X. Zhang et al., 2021b). The global modeling strategy aims to approximate the limit-state function in the global design domain. Once the Kriging model reaches a certain level of accuracy, the optimization is then done using the constructed Kriging model. On the other hand, the local modeling strategy focuses only on the local region. In this strategy, the samples near the optimization result of each iteration are considered as candidate samples to enrich the Kriging model. This process of design optimization and model updating is done sequentially until the optimal solution converges.

While significant progress has been made in Kriging-based RBDO methods, several challenges still remain. For instance, the local modeling strategy is generally more efficient in terms of limit-state function evaluations, but it requires design optimization at every iteration. Although Kriging model evaluation is cheap, it is not completely free and when paired with classical gradient-based optimization, it may still incur a high

computational cost or yield an unsatisfactory result. For this reason, a new RBDO framework called Metaheuristic-optimized Local Adaptive Kriging (Meta-LAK) that combines metaheuristic optimization with adaptive Kriging is proposed. The framework relies on the cooperation between the two methods to reduce the computation demand of the local modelling strategy. By utilizing this framework, it is possible to accelerate the optimization process by making use of the information gained from the Kriging model to avoid the need for evaluating every design. The efficiency of the construction of Kriging model is also improved from this interaction, as it restricts the available candidate samples based on the optimum design.

2. METHOD

In the proposed Meta-LAK, there are two main components in the framework: the reliability estimation using Adaptive Kriging method and the optimization using metaheuristic method. The metaheuristic guides the search throughout the design space to find the optimal design based on the current Kriging model. Then, adaptive Kriging tries to improve the prediction accuracy by enriching the Kriging model centered around the optimum solution. The framework will stop once convergence of the optimum solution is achieved.

2.1 Probability of Failure Estimation

In this paper, all non-normal and correlated variables are mapped into the standard normal space for the calculation of reliability analysis. In order to improve the efficiency of the framework, an efficient and robust reliability analysis technique called Radial-Based Important Sampling (RBIS) is used (Xiong & Tan, 2018). It aims to reduce the number of samples needed for Monte-Carlo Sampling (MCS) by excluding the samples within the safe hypersphere. The probability of failure (P_f) can be estimated by:

$$P_f = P(g(\mathbf{X}) \leq 0 \mid \beta > 0) \times P(\beta > 0) \quad (2)$$

$$P_f = \frac{n_{fail}}{n_{rbis}} (1 - \chi_n^2(\beta^2)) \quad (3)$$

where β denotes the radius of the safe hypersphere determined by the most probable point (MPP), $\chi_n^2(\cdot)$ is the chi-square Cumulative Distribution Function (CDF) with n degree of freedom which is equal to the dimension of the problem, n_{fail} denote the number of failure samples, and n_{rbis} is the total samples outside the safe hypersphere. Since the safe hypersphere carries a large portion of the probability density, it can reduce the number of evaluations significantly. An example of the safe hypersphere is illustrated in Figure 1.

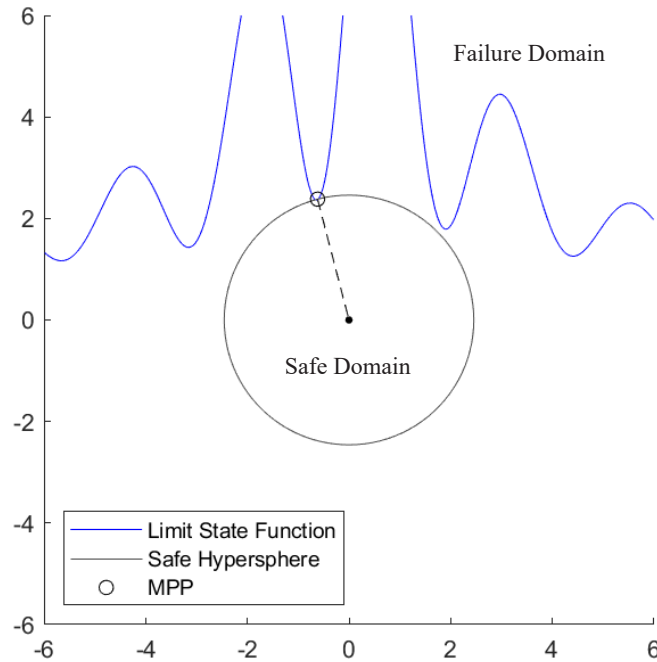


Figure 1. Illustration of the safe hypersphere in a standard normal space

Using Equation (3) and the target probability of failure, the maximum radius of the safe hypersphere that should be considered can be calculated by:

$$\beta_{max} = \sqrt{\chi_n^{2^{-1}}(1 - P_f^t)} \quad (4)$$

Any failure samples found outside β_{max} will result in a probability of failure less than the target probability of failure and thus can be ignored. To identify the safe hypersphere, the MPP needs to be determined,

which is defined as the closest point on the limit-state function to the origin. There are a few ways of obtaining the MPP, in this study, the radius is divided into multiple segments and the search is conducted from the outer radius (β_{max}) inward. Once no failure samples are found in a segment, the failure point closest to the origin point is accepted as the MPP. Once the MPP is found any MCS samples that are within the safe hyperball can be ignored, and the P_f can be calculated using Equation (3). On the other hand, if there are no failure samples in the first segment, then it can be concluded that the P_f must be lesser than the target.

2.2 Active-learning Function

The effectivity of an adaptive Kriging model depends on its ability to improve its predictive capability. learning function is an indicator that quantifies the amount of information that a candidate sample would bring if it is incorporated into the Kriging model. One of the most popular learning functions used in adaptive Kriging is the U -function (Echard et al., 2011):

$$U = |\mu_{\hat{G}}|/\sigma_{\hat{G}} \quad (5)$$

where $\mu_{\hat{G}}$ and $\sigma_{\hat{G}}$ is the mean and standard deviation of the Kriging predictor respectively. The U -function indicates the risk of misclassifying the state of failure of the prediction. The closer $\mu_{\hat{G}}$ to zero and the larger $\sigma_{\hat{G}}$ will make the U smaller implying more risk of mistakes. Thus, the best point to be added to the model is the sample with the minimum U value. Once the minimum U value is greater or equal to 2, the model is assumed to be good enough to represent the limit state function.

However, it is shown that value-based stopping conditions have been proven to be too conservative in most cases (Moustapha et al., 2022). Therefore, a new stopping condition based on the confidence interval of \hat{P}_f is proposed, which is formulated as:

$$\frac{\hat{P}_f - \hat{P}_{f_{lb}}}{\hat{P}_f} \leq \varepsilon_{bound} \quad (6)$$

$$\hat{P}_f = I(\mu_{\hat{G}} \leq 0)/n_{rbis} (1 - \chi_n^2(\beta^2)) \quad (7)$$

$$\hat{P}_{f_{lb}} = I(\mu_{\hat{G}} + 2\sigma_{\hat{G}} \leq 0)/n_{rbis} (1 - \chi_n^2(\beta^2)) \quad (8)$$

where $\hat{P}_{f_{lb}}$ is the probability of failure using the limit state $\mu_{\hat{G}} + 2\sigma_{\hat{G}}$, ε_{bound} is the convergence threshold for the confidence interval, and $I(\cdot)$ is an indicator function. In Equation (6), the $\hat{P}_{f_{ub}}$ is not used, because in RBIS the sample within the hyperball is not evaluated and therefore cannot be calculated.

2.3 Cooperation between Metaheuristic Algorithm and Adaptive Kriging

In a conventional Kriging-based RBDO method, a traditional gradient-based method, i.e. Sequential Quadratic Programming (SQP), is typically employed in conjunction with a Kriging model to determine the optimal design, disregarding the computational expense involved. Although Kriging is cheap to compute, it is not completely free, necessitating a more efficient optimization method. Therefore metaheuristic method which has been proven to be superior to the traditional gradient-based approaches is considered (Azizi et al., 2023). Metaheuristic can be defined as an iterative method that employs various strategies to efficiently explore and exploit the search space in order to attain a near-optimal solution. This study applies a robust and powerful metaheuristic algorithm called Symbiotic Organisms Search (SOS) (Cheng & Prayogo, 2014). The method employs a strategy that mimics the interaction between organisms in an ecosystem to achieve the optimal solution. One other benefit of SOS, in contrast to the majority of metaheuristic algorithms, is that it does not necessitate the use of tuning parameters.

In the present study, the SOS algorithm's efficiency is further enhanced by incorporating the information from the Kriging model. By determining the maximum considered radius (β_{max}) from the target probability of failure, the SOS avoids evaluating design points with β exceeding it, indicating P_f smaller than the target. Similarly, design points with origin residing in the failure domain are also excluded from the evaluation, as they would result in high P_f regardless. As a result, the reliability analysis is only performed when needed, reducing the amount of workload required for optimization.

2.4 Meta-LAK Framework

The flowchart of the proposed framework is shown in Figure 2. The detailed steps are as follows:

1. Generate the initial training samples: Latin Hypercube Sampling (LHS) is used to uniformly generate the N_0 training samples/design of experiment (DoE) over the design space $[d^L, d^U]$.
2. Construct the Kriging model for each constraint: Ordinary Kriging model with Gaussian correlation function from the DACE toolbox (Lophaven et al., 2002) is adopted in the framework.
3. Design optimization with SOS: The reliability assessment of the RBDO is done using the RBIS method with the constructed Kriging model as a substitute limit state function. When calculating the probability of failure, SOS uses information from the Kriging model to avoid unnecessary calculations, as explained in Section 2.3.

4. Find MPP for the current optimal design: Once the optimal solution for the current Kriging model is found, the reliability assessment is improved for each limit-state function/constraint in the problem. The MPP needs to be identified, to prepare the RBIS samples which are used in the learning process. The samples are generated by filtering out n_{mcs} MCS samples inside the safe hypersphere. The n_{mcs} can be determined by using the target probability of failure (P_f^t) and coefficient of variation (CoV) (Echard et al., 2011):

$$n_{mcs} = \frac{(1 - P_f^t)}{P_f^t CoV^2} \quad (9)$$

In this study, CoV of 0.05 is deemed to be acceptable.

5. Calculate the learning function for RBIS samples: Equation (5) is used to pick the best sample to enrich the Kriging model.
6. Check for learning stopping condition: The learning phase is stopped when the value or convergence threshold introduced in Section 2.2 is fulfilled. If none of the conditions is met, the chosen sample in Step 5 is incorporated into the Kriging model.
7. Check for convergence of β : Due to the improvement made to the Kriging model, the radius of the safe hyperball (β) may shift. As a result, the convergence of β needs to be checked before advancing to the next step. The convergence is calculated using the current and previous radius:

$$\frac{|\beta^j - \beta^{j-1}|}{\beta^j} \leq \varepsilon_{beta} \quad (10)$$

where ε_{beta} is the convergence threshold for β . If the convergence is not reached, the method will return to Step 4 to adjust the safe hyperball.

8. Check for convergence of optimal design: Similarly, the optimal design may change so the convergence needs to be checked. The convergence can be obtained by comparing the current and previous designs:

$$\frac{\|d_{opt}^k - d_{opt}^{k-1}\|}{\|d_{opt}^k\|} \leq \varepsilon_{design} \quad (11)$$

where ε_{design} denotes the convergence threshold for optimal design. If the current optimal design has converged, the method is terminated.

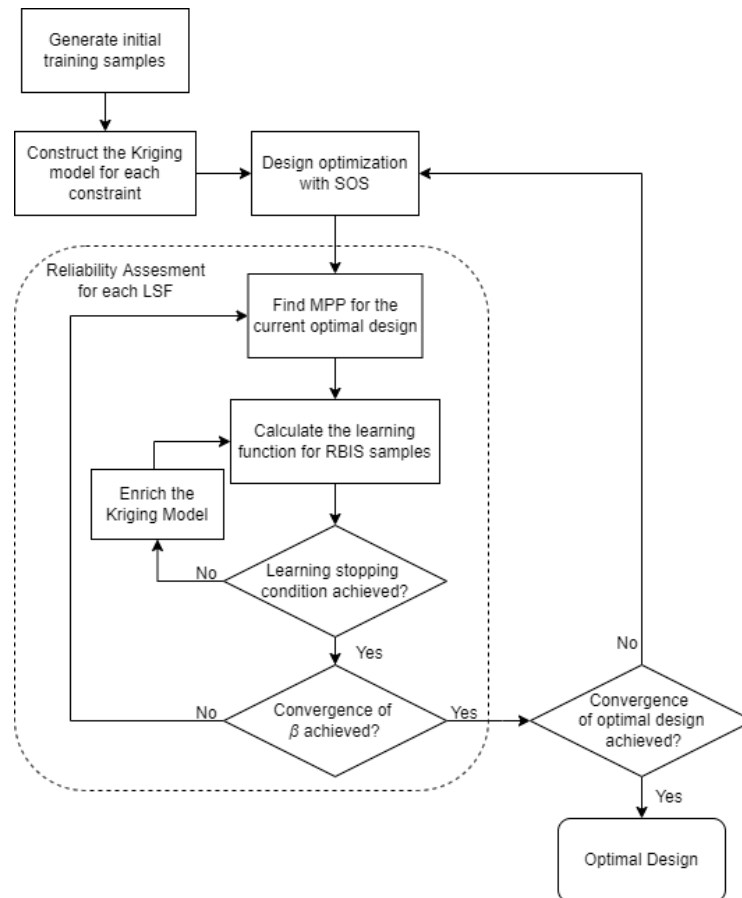


Figure 2. The Meta-LAK Framework

3. CASE STUDY

The parameter for Meta-LAK is set as follows. N_0 is set to $5 \times \dim$ which scale with the dimension of the problem (\dim). The convergence thresholds (ε_{bound} , ε_{beta} , and ε_{design}) are all set as 0.01. For the SOS algorithm, the population size and number of generations are set to 15 and 30, respectively. These parameter settings have been chosen according to preliminary results to optimize the performance of Meta-LAK. In order to verify the performance of the proposed Meta-LAK, the result is compared to other state-of-the-art Kriging-based RBDO methods such as: MCFPS (Li et al., 2022a), LAKAM-SLS (Yang et al., 2022), KSLA (Zhang et al., 2021a), RIFA-ADK (Zhang et al., 2021b). In order to showcase the robustness of Meta-LAK, the experiment is conducted 10 times of which the average value is shown in the result.

The first case study is a bi-variate mathematical example that combines a highly non-linear and a linear limit state function (Zhang et al., 2021b). Both variables follow a normal distribution $X_i \sim N(d_{X_i}, 0.1^2)$, $i = 1, 2$ with a target failure probability $P_{fc}^t = 2.275\%$, $c = 1, 2$. The problem is formulated as follows:

$$\begin{aligned}
 & \text{Find } \mathbf{d}_X = [d_{X_1}, d_{X_2}]^T \\
 & \text{Min } f(\mathbf{d}_X) = (d_{X_1} - 3.7)^2 + (d_{X_2} - 4)^2 \\
 & \text{s. t. } P(g_c(\mathbf{X}) \leq 0) \leq P_{fc}^t, c = 1, 2 \\
 & g_1(\mathbf{X}) = -X_1 \sin(4X_1) - 1.1X_2 \sin(2X_2) \\
 & g_2(\mathbf{X}) = X_1 + X_2 - 3 \\
 & 0 \leq d_{X_1} \leq 3.7, 0 \leq d_{X_2} \leq 4
 \end{aligned} \tag{12}$$

The RBDO solution obtained by the proposed Meta-LAK is illustrated in Figure 3. Comparative results are shown in Table 1. The Meta-LAK can obtain optimal solutions within the target probability of failure while achieving a superior average total number of samples ($N_{s_{total}}$) compared to the other methods. While LAKAM-SLS1 and LAKAM-SLS2 are more efficient, they produce inaccurate solutions that violate the reliability constraint. In addition to improving the efficiency of the number of samples, the proposed method can reduce the average computation time from 127.498 s to 26.997 s without any significant accuracy loss, thanks to the cooperation strategy between the two components: Adaptive Kriging method and Symbiotic Organisms Search.

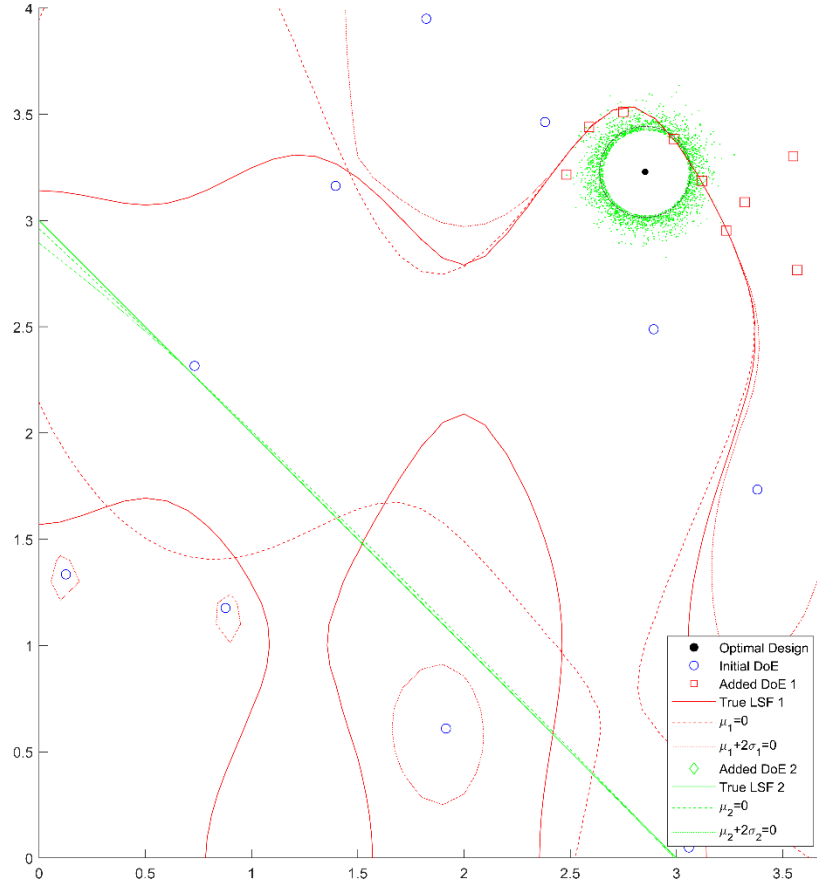


Figure 3. RBDO solution of the mathematical problem by Meta-LAK

Table 1. Comparative results of Kriging-based RBDO methods

Methods	Optimal Solution	N_{S1}	N_{S2}	$N_{S_{total}}$	P_{f1}	P_{f2}
Analytical	1.3258 (2.8421, 3.2320)	-	-	-	2.270E-02	0
MCFPS	1.3256 (2.8426, 3.2316)	28.2	10	38.2	2.272E-02	0
LAKAM-SLS1	1.3039 (2.8149, 3.2786)	17	7	24	3.208E-02	0
LAKAM-SLS2	1.3038 (2.8160, 3.2773)	14	7	21	3.181E-02	0
KSLA	1.3047 (2.8088, 3.2855)	18	18	36	3.363E-02	0
RIFA-ADK	1.3282 (2.8414, 3.2312)	50	12	62	2.223E-02	0
Meta-LAK	1.3258 (2.8367, 3.2382)	24.2	10.1	34.3	2.265E-02	0

The second case study is a short-column design problem (Jiang et al., 2017). The column is loaded with a compressive force (F), and bending moments (M_1 & M_2) with an allowed yielding stress (f_y). The objective is to find the optimal design of depth (h) and width (b) that fulfills the constraints formulated below:

$$\begin{aligned}
 &\text{Find } \mathbf{d}_X = [d_b, d_h]^T \\
 &\text{Min } f(\mathbf{d}_X) = d_b \times d_h \\
 &\text{s. t. } P(g_c(\mathbf{X}) \leq 0) \leq 0.135\% \\
 &g_1(\mathbf{X}) = 1 - \left(\frac{4M_1}{bh^2f_y} + \frac{4M_2}{b^2hf_y} + \frac{F^2}{(bhf_y)^2} \right) \\
 &g_2(\mathbf{X}) = \frac{b}{h} - 0.5 \\
 &g_3(\mathbf{X}) = 2 - \frac{b}{h} \\
 &d_b, d_h \geq 0
 \end{aligned} \tag{13}$$

where: $b \sim N(d_b, 0.05)$ m, $h \sim N(d_h, 0.05)$ m, $F = 2500$ kN, $M_1 = 250$ kNm, $M_2 = 125$ kNm, $f_y = 40$ MPa. The framework demonstrated remarkable efficiency in solving the RBDO problem by finding the optimal design (0.4270, 0.5174) using only 42, 29, and 16 samples for each limit-state function respectively, which is shown in Figure 4. In contrast, traditional methods would necessitate evaluating millions of samples at each potential candidate point to attain a similar result.

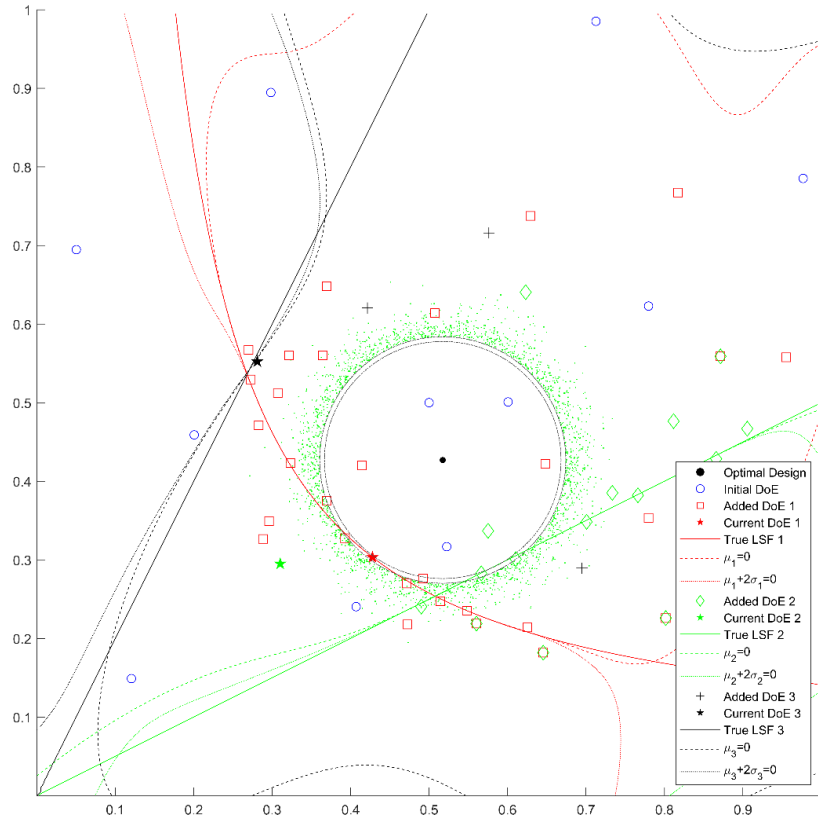


Figure 4. RBDO solution of short-column design by Meta-LAK

4. CONCLUSION

This paper presents a new RBDO framework called Meta-LAK. The framework combines Metaheuristic and an adaptive Kriging method to solve the RBDO problem effectively. The information from Kriging allows for efficient search from SOS, and Kriging enrichment can be limited to candidate samples within proximity of the optimal sample. Using an efficient sampling technique, the method can obtain the solution efficiently while maintaining a high level of accuracy. The effectiveness of the proposed method is demonstrated through the case studies. The first case study reveals that the proposed framework consistently generates reliable approximation with fewer samples than previous Kriging-based methods. The subsequent case study serves as a demonstration of the framework's applicability to real-world civil engineering problem. However, one of the drawbacks of the proposed framework is that by using RBIS, the framework may encounter challenges in dealing with high dimensional problems. In future studies, the framework can be improved further in this direction.

ACKNOWLEDGMENTS

The present study was supported by National Science and Technology Council, Taiwan under Grant No. 110-2221-E-011-032-MY3.

REFERENCES

- Azizi, M., Talatahari, S., and Gandomi, A. H. (2023). Fire Hawk Optimizer: a novel metaheuristic algorithm. *Artificial Intelligence Review*, 56(1), 287-363.
- Cheng, K., Lu, Z., Xiao, S., Zhang, X., Oladyshkin, S., and Nowak, W. (2021). Resampling method for reliability-based design optimization based on thermodynamic integration and parallel tempering. *Mechanical Systems and Signal Processing*, 156, 107630.
- Cheng, M.-Y., and Prayogo, D. (2014). Symbiotic Organisms Search: A new metaheuristic optimization algorithm. *Computers & Structures*, 139, 98-112.
- Echard, B., Gayton, N., and Lemaire, M. (2011). AK-MCS: An active learning reliability method combining Kriging and Monte Carlo Simulation. *Structural Safety*, 33(2), 145-154.
- Hao, P., Ma, R., Wang, Y., Feng, S., Wang, B., Li, G., Xing, H., and Yang, F. (2019). An augmented step size adjustment method for the performance measure approach: Toward general structural reliability-based design optimization. *Structural Safety*, 80, 32-45.
- Jiang, C., Qiu, H., Gao, L., Cai, X., and Li, P. (2017). An adaptive hybrid single-loop method for reliability-based design optimization using iterative control strategy. *Structural and Multidisciplinary Optimization*, 56(6), 1271-1286.
- Jiang, C., Qiu, H., Li, X., Chen, Z., Gao, L., and Li, P. (2020). Iterative reliable design space approach for efficient reliability-based design optimization. *Engineering with Computers*, 36(1), 151-169.
- Jiang, C., Yan, Y., Wang, D., Qiu, H., and Gao, L. (2021). Global and local Kriging limit state approximation for time-dependent reliability-based design optimization through wrong-classification probability. *Reliability Engineering & System Safety*, 208, 107431.
- Lee, I., Lee, B., and Lim, J. (2015). Sequential optimization and reliability assessment based on dimension reduction method for accurate and efficient reliability-based design optimization. *Journal of Mechanical Science and Technology*, 29, 1349-1354.
- Li, X., Han, X., Chen, Z., Ming, W., Cao, Y., and Ma, J. (2022a). A multi-constraint failure-pursuing sampling method for reliability-based design optimization using adaptive Kriging. *Engineering with Computers*, 38(1), 297-310.
- Li, X., Zhu, H., Chen, Z., Ming, W., Cao, Y., He, W., and Ma, J. (2022b). Limit state Kriging modeling for reliability-based design optimization through classification uncertainty quantification. *Reliability Engineering & System Safety*, 224, 108539.
- Lophaven, S. N., Nielsen, H. B., and Søndergaard, J. (2002). *DACE - A Matlab Kriging Toolbox, Version 2.0*. (IMM-TR-2002-12).
- Meng, Z., and Keshtegar, B. (2019). Adaptive conjugate single-loop method for efficient reliability-based design and topology optimization. *Computer Methods in Applied Mechanics and Engineering*, 344, 95-119.
- Meng, Z., Zhang, Z., and Zhou, H. (2020). A novel experimental data-driven exponential convex model for reliability assessment with uncertain-but-bounded parameters. *Applied Mathematical Modelling*, 77, 773-787.
- Moustapha, M., Marelli, S., and Sudret, B. (2022). Active learning for structural reliability: Survey, general framework and benchmark. *Structural Safety*, 96, 102174.
- Shi, Y., Lu, Z., Huang, Z., Xu, L., and He, R. (2020). Advanced solution strategies for time-dependent reliability based design optimization. *Computer Methods in Applied Mechanics and Engineering*, 364, 112916.

- Xiao, M., Zhang, J., and Gao, L. (2020). A system active learning Kriging method for system reliability-based design optimization with a multiple response model. *Reliability Engineering & System Safety*, 199, 106935.
- Xiong, B., and Tan, H. (2018). A robust and efficient structural reliability method combining radial-based importance sampling and Kriging. *Science China Technological Sciences*, 61(5), 724-734.
- Yang, M., Zhang, D., Wang, F., and Han, X. (2022). Efficient local adaptive Kriging approximation method with single-loop strategy for reliability-based design optimization. *Computer Methods in Applied Mechanics and Engineering*, 390, 114462.
- Zhang, H., Aoues, Y., Lemosse, D., and de Cursi, E. S. (2021a). A single-loop approach with adaptive sampling and surrogate Kriging for reliability-based design optimization. *Engineering Optimization*, 53(8), 1450-1466.
- Zhang, X., Lu, Z., and Cheng, K. (2021b). Reliability index function approximation based on adaptive double-loop Kriging for reliability-based design optimization. *Reliability Engineering & System Safety*, 216, 108020.

CHATGPT IN THE CONSTRUCTION DOMAIN: OPPORTUNITIES, RISKS, AND RECOMMENDATIONS

Taegeon Kim¹, Seokhwan Kim², Namgyun Kim³, Hongjo Kim⁴

1) Ph.D. Student, Department of Civil and Environmental Engineering, Yonsei University, Seoul, South Korea. Email: ktg9655@yonsei.ac.kr

2) Ph.D. Student, Department of Civil and Environmental Engineering, Yonsei University, Seoul, South Korea. Email: yyksh2019@yonsei.ac.kr

3) Ph.D., Assis. Prof., Department of Civil and Engineering and Engineering Mechanics, University of Dayton, OH, United States. Email: nkim01@udayton.edu

4) Ph.D., Assis. Prof., Department of Civil Engineering, Faculty of Engineering, Yonsei University, Seoul, South Korea. Email: hongjo@yonsei.ac.kr (corresponding author)

Abstract: Chatbot technology based on a large language model is expected to have a great impact on most industries including the construction industry. This paper examines the potential implications of the current state-of-the-art of large language models such as ChatGPT for the construction domain. Based on a literature review and the authors' experience using ChatGPT for different tasks, we provide our analysis and conjecture on the potential applications, opportunities, risks, and limitations of ChatGPT in the construction domain. We argue that ChatGPT can offer valuable information, insights and solutions for challenges and problems the construction industry is facing, as well as foster creativity, communication and collaboration among civil engineers. We also acknowledge some challenges and risks that ChatGPT entails, such as ethical, legal issues, and the problems of data quality. We conclude with recommendations on how to leverage ChatGPT for the construction domain.

Keywords: Chatbot, ChatGPT, Large Language Model, Natural Language Processing, Impact of Chatbot Technology in Construction.

1. INTRODUCTION

Natural language processing (NLP) is a branch of artificial intelligence that deals with natural language texts (Brown et al. 2020; Radford et al. 2019). NLP can help achieve smart construction by extracting useful information and insights from various text data sources. There has been a growing trend of research on applying NLP techniques in the construction domain. Recent studies (Salama and El-Gohary 2016; Wang et al. 2022; Yan et al. 2022) adopted four main types of NLP techniques for smart construction: text classification, text clustering, information extraction, and information retrieval.

Large language models (LLMs) are originated from NLP that can generate natural and coherent texts on various topics and domains (Radford et al. 2019). LLMs have been advancing rapidly in recent years, thanks to the availability of large-scale data and computational resources, as well as the development of novel architectures and algorithms. LLMs have shown remarkable performance in various natural language processing tasks, such as machine translation, text summarization, and question answering. LLMs can potentially assist engineers in the Architecture, Engineering, and Construction (AEC) industry in solving various problems by providing useful information, insights and solutions, as well as enhancing their productivity, and communication skills.

One of the most prominent examples of LLMs is ChatGPT. ChatGPT is a conversation chatbot that was released by OpenAI in 2022. ChatGPT is based on GPT-3.5, a deep neural network with 175 billion parameters that can generate texts on any given prompt or context (Hughes 2023). ChatGPT can produce natural and logical texts on various topics, ranging from casual conversations to technical reports. Despite the short time from its launch, ChatGPT has been widely used by more than 100 millions of active users for various purposes, such as entertainment, education, research and business. The recent study indicates that approximately 80% of the U.S. workforce answered that their work tasks will be affected by the introduction of ChatGPT (Eloundou et al. 2023). Therefore, the introduction of ChatGPT would also have a great impact on the construction industry where about 7.5 million people are employed (BLS 2022)

However, despite the popularity of ChatGPT, there is a lack of investigation on its impact on the construction domain. How can ChatGPT be used effectively and responsibly for construction engineering tasks? What are the opportunities and limitations of ChatGPT? What are the risks that ChatGPT poses for the construction domain? These are some of the questions that need to be answered to understand and leverage ChatGPT for researchers and practitioners in this domain.

Therefore, the main objective of this paper is to investigate the opportunities, limitations and risks of ChatGPT for academia and industry in the construction domain. To achieve this, we conducted a literature review and an empirical study based on our experience using ChatGPT for potential application areas related to construction engineering and management. The main contributions of this paper are: (1) We provide an overview of the current state-of-the-art of LLMs such as ChatGPT and their implications for the construction domain. (2) We present our analysis and conjecture on the potential applications, opportunities, risks and limitations of

ChatGPT in the construction domain based on a literature review and our experience using ChatGPT. (3) We offer some recommendations for both academia and industry on how to leverage ChatGPT effectively and responsibly for the construction domain.

2. EMERGENCE OF LARGE LANGUAGE MODEL

The development of LLMs can be traced back to the emergence of recurrent neural networks (RNNs) and long short-term memory (LSTM) units. These models were able to capture long-term dependencies and sequential patterns in natural language texts. However, they also suffered from some limitations, such as gradient vanishing or exploding problems, difficulty in parallelization, and high computational cost.

A breakthrough was achieved by Transformer models proposed by (Vaswani et al. 2017). Transformer models replaced RNNs with attention modules that allowed the model to focus on relevant parts of the input-output sequences. Transformer models also enabled parallelization by using self-attention layers that computed pairwise interactions between all tokens in a sequence, increasing scalability. Transformer models achieved state-of-the-art performances on various natural language processing tasks (Amer et al. 2021; Ko et al. 2021; Lee et al. 2023; Wu et al. 2021).

Another milestone was reached by BERT (Bidirectional Encoder Representations from Transformers) presented by Devlin et al. (2019). BERT is a pre-trained Transformer model that captures bidirectional contextual representations from a large corpus of unlabeled text data. BERT can be fine-tuned with a small amount of additional training data and achieved new records on several benchmarks. Since then, many variants of BERT have been proposed, such as RoBERTa (Liu et al. 2019), ALBERT (Lan et al. 2020), ELECTRA (Clark et al. 2020), demonstrating that better performance of BERT can be achieved by using larger datasets, longer training time, different pre-training objectives or architectures.

In 2019-2020, the trend shifted towards building larger and larger Transformer models with a huge number of parameters and text data. Well-known examples of such LLMs include GPT-2 (Radford et al., 2019), T5 (Raffel et al. 2020), GPT-3 (Brown et al. 2020). These models demonstrated impressive capabilities of generating fluent and diverse texts on various topics. They also showed remarkable generalization and transfer learning abilities on various tasks without fine-tuning or with few-shot learning.

ChatGPT is one of these LLMs based on GPT-3 architecture, which consists of a stack of decoder-only Transformer layers with self-attention. ChatGPT is trained on a large corpus of text data collected from various sources from social media, webpages, and electronic books. ChatGPT can generate responses for different types of dialogues, and also adapt to different styles and tones based on the context and user preferences.

3. NLP IN THE CONSTRUCTION DOMAIN

In the construction domain, NLP has gained significant attention in recent years due to its potential to improve efficiency, reduce costs, and enhance decision-making in many tasks, including automated document summarization, information extraction, and question-answering systems. For example, Padhy et al. (2021) developed an NLP-based system that can extract critical information from construction contracts, including project scope, schedule, and budget. Another NLP application in the construction domain is automated document summarization. Sun et al. (2020) developed a summarization algorithm that can extract the essential information from construction progress reports and summarize it into a few sentences. Kim et al. (2022) developed a question-answering system that can answer questions about infrastructure damage information based on data extracted from earthquake related textual data. NLP has also been used in construction safety management applications. Tixier et al. (2016) adopted NLP for classifying construction safety reports. The developed system was able to classify reported safety issues into different categories, such as near-misses, injuries, and accidents. Kim and Chi (2019) utilized NLP to identify safety hazards in the safety inspection reports. Another study analyzed construction workers' safety perception using NLP.

Although NLP has shown promising results in previous studies, the potential impact of chatbots, powered by Large Language Models (LLMs), in innovating a wide range of construction engineering and management tasks is yet to be explored. Exploring the potential of chatbots based on LLMs would benefit the reader in transforming various aspects of construction engineering and management tasks.

4. CAPABILITIES OF ChatGPT

ChatGPT can be used to search information related to a variety of construction tasks. This process is typically conducted by sequential prompting, illustrated in Table 1. We asked ChatGPT two sequential questions to obtain the information about OSHA standards for fall protection in construction sites. In the first question, ChatGPT gave some general information about OSHA standards for fall protection as well as a detailed part number (29 CFR 1926 Subpart M.). In the second question, ChatGPT provided specific standards about safety net systems. As shown in the answers, ChatGPT can provide domain-specific information and users can also ask more detailed information with additional questions.

To identify the quality and reliability of the ChatGPT's answer, we compared the ChatGPT's answer with the OSHA's actual standards. Although ChatGPT's answer included relevant information about Safety Net Systems, some details were omitted. For example, OSHA standards 1926.502(c)(7) (see Appendix) includes more detailed requirements about the maximum size of each mesh opening. However, ChatGPT selectively provided the information of that standard.

To examine the importance of sequential conversation with ChatGPT, we asked the second question without the first question (see Question 2 and Answer 2 in Table 1). ChatGPT's answer included more general information than the answer in the sequential conversation. Based on our experience, it's advantageous to ask ChatGPT with specific and detailed prompts sequentially to help it generate accurate and relevant responses. Providing context for the prompt can also help ChatGPT better understand what a user is looking for and generate more accurate results. For generating desirable responses, a user should write prompts multiple times to edit and revise the initial response of ChatGPT.

Table 1. Example use of ChatGPT in searching construction safety related contents

Question 1-1	What is the OSHA standard for fall protection in construction sites?
Answer 1-1	<p>The Occupational Safety and Health Administration (OSHA) has specific standards for fall protection in construction, which are outlined in 29 CFR 1926 Subpart M. The standard establishes requirements for fall protection systems, including:</p> <ol style="list-style-type: none"> 1. General Requirements: Employers must provide fall protection for employees working at heights of 6 feet or more above lower levels. 2. ... <p>The OSHA standard also outlines requirements for training, inspection, and maintenance of fall protection systems. Employers must ensure that ...</p>
Question 1-2	What are the OSHA's specific standards for the installation of safety net systems for fall protection?
Answer 1-2	<p>OSHA standards for the installation of safety net systems for fall protection are outlined in 29 CFR 1926.502(c). The specific standards include:</p> <ol style="list-style-type: none"> 1. Proper Installation: Safety net systems must be installed as close as practicable under the surface on which employees are working, but never more than 30 feet below the working surface. 2. ... <p>It's important to note that safety nets are not a substitute for other types of fall protection, ...</p>
Question 2	What are the OSHA's specific standards for the installation of safety net systems for fall protection?
Answer 2	<p>OSHA (Occupational Safety and Health Administration) has specific standards for the installation of safety net systems for fall protection under the Code of Federal Regulations, 29 CFR 1926.502(c)(6). Here are some of the key requirements:</p> <ol style="list-style-type: none"> 1. Safety nets must be installed as close as possible beneath the working surface but no more than 30 feet below. 2. ... <p>It's important to note that these are just some of the requirements for the installation of safety net systems for fall protection. ...</p>

5. OPPORTUNITIES OF USING NLP TECHNOLOGY

Utilizing chatbot technologies such as ChatGPT in the construction domain presents several opportunities for improving efficiency, particularly in the areas of information search, document proofreading, document summarization, and facilitating multilingual communication. Adopting chatbots based on LLMs would allow project stakeholders to expedite information retrieval from construction-related documents by processing large volumes of data and identifying relevant information quickly and accurately, thereby saving time and resources. Furthermore, chatbots can provide concise and informative summaries of lengthy or complex construction documents, enabling stakeholders to grasp essential information at a glance and make informed decisions more rapidly. Not only can project stakeholders retrieve information from large amounts of construction specifications without manual labeling of each specification (Kim et al. 2022a), but they can also check regulatory compliance using LLMs (Zhang and El-Gohary 2017). These advantages offered by NLP technologies have the potential to

streamline various construction processes, enhance communication, and ultimately contribute to greater overall project efficiency.

6. RISKS & LIMITATIONS OF ChatGPT

Several limitations of ChatGPT should be considered in the construction domain. First, while ChatGPT can process large volumes of data, it may not always deliver accurate or sufficiently detailed information, which could lead to misinformed decisions or safety hazards. Second, ChatGPT's language comprehension, although sophisticated, may not fully understand complex construction-specific terminology or idioms, resulting in unclear or incorrect interpretations. Third, it lacks domain-specific expertise, which is crucial in addressing intricate construction challenges that often require human intuition and experience. Fourth, ChatGPT might inadvertently perpetuate biases present in its training data, leading to ethical concerns or the reinforcement of stereotypes within the industry. Fifth, data privacy concerns are critical, as sensitive project information could be exposed to unauthorized parties without proper encryption and access controls. Lastly, ChatGPT can suffer from hallucination issues when providing correct references or original document sources, resulting in misleading or entirely fabricated information, which could compromise the reliability of its output.

7. RECOMMENDATIONS FOR USING CHATBOT TECHNOLOGY

ChatGPT's answers to the same questions could be different in each session. Thus, users are required to be equipped with prompting capabilities to effectively use ChatGPT. It would be beneficial for users to ensure the safety and legal compliance of information provided by ChatGPT. One could consider verifying the accuracy, reliability, and timeliness of responses to reflect changes in safety regulations, building codes, and zoning laws. It will be helpful to implement legal and safety compliance measures by adhering to relevant laws, regulations, and guidelines. Offering training to personnel on proper ChatGPT usage, including accessing information and validating chatbot responses, could be advantageous. Establishing authorities composed of construction experts would enable the training of LLMs with construction domain specific knowledge and providing feedback when an error or inaccurate information is reported. By adopting these suggestions, construction professionals might find it easier to utilize chatbot technology effectively while maintaining safety and legal compliance.

8. POTENTIAL APPLICATIONS IN THE CONSTRUCTION DOMAIN

Safety Training: ChatGPT can be a useful tool in safety training in the construction domain. It can be programmed to deliver safety protocols and guidelines in an interactive manner, making the learning process more engaging for workers. Its ability to understand and respond to natural language questions allows it to provide clarifications and additional information when required, ensuring that workers fully understand the safety measures in place. Moreover, ChatGPT can simulate various safety scenarios or situations, helping workers to better prepare for real-world situations.

Contract Risk Analysis: The vast amount of data and the complexity of legal language used in contracts often make contract risk analysis a challenging task. ChatGPT can be utilized to simplify this process by analyzing the text in contracts and identifying areas of potential risk. It can be trained to understand legal terms and clauses, enabling it to provide concise summaries and highlight critical points that require attention. This could help construction firms mitigate potential legal and financial risks associated with contractual agreements.

Project Report Generation: ChatGPT can automate the process of project report generation in the construction domain. By interpreting and organizing raw data from various sources like project management tools, site logs, and financial systems, it can generate comprehensive and accurate project reports. These reports can cover various aspects of a construction project including progress, budget, timelines, and issues encountered. By automating this process, construction firms can save time and resources, and ensure that stakeholders are kept well-informed about project status.

Searching Information for Specific Operations, Guidelines, and Stipulations: In the construction industry, there's a huge volume of information related to specific operations, guidelines, and stipulations that need to be adhered to. These may include regulatory guidelines, architectural standards, material specifications, and more. ChatGPT can be programmed to search and retrieve this information in real-time, saving workers from the time-consuming task of searching through multiple sources. By asking ChatGPT a question in natural language, workers can get the specific information they need, improving efficiency and compliance within the construction domain.

9. SWOT ANALYSIS

To summarize, this study conducted SWOT analysis to evaluate the application of LLM-based chatbot technology, as follows:

Strength:

- Knowledge representation and retrieval capabilities, enabling informative and accurate answers to user questions

- Potential to improve efficiency, reduce costs, and enhance decision-making in various applications, including automated document summarization, information extraction, and question-answering systems in the construction domain

Weakness:

- Dependency on large amounts of data for training, which can be difficult to obtain in certain specialized domains, such as construction engineering and management
- Risk of providing inaccurate information due to the hallucination problem, which can lead to safety issues or legal problems if not properly validated

Opportunity:

- Potential to innovate traditional challenges that the construction industry faces, such as training new workers in different languages
- Opportunity to enhance communication and collaboration between construction professionals, contractors, and clients

Threat:

- Ethical concerns, such as bias or discrimination in decision-making processes

While the emergence of ChatGPT and its use in the construction engineering and management domain presents numerous strengths and opportunities, there are also weaknesses and threats that must be carefully considered and addressed to ensure safe and effective implementation.

10. CONCLUSION

ChatGPT has the potential to significantly impact construction engineering and management by streamlining various processes, enhancing communication, and improving overall project efficiency. Its capabilities in information search, document proofreading, document summarization, and facilitating multilingual communication can save time and resources, foster collaboration, and support informed decision-making among stakeholders. Furthermore, AI-powered chatbots can provide critical assistance in navigating the increasingly complex construction landscape, addressing challenges in project management, customer support, and the dissemination of vital information.

However, caution must be exercised to avoid over-reliance on ChatGPT and to acknowledge its limitations, such as inaccuracies, miscommunication, lack of domain-specific expertise, and ethical concerns. To make the best use of this technology in the construction domain, potential applications and future studies could focus on enhancing the chatbot's understanding of complex industry-specific terminology, improving multilingual communication capabilities. Additionally, research could explore the development of hybrid systems that combine AI-driven insights with human expertise, ensuring that human intuition and critical thinking remain integral to the construction engineering and management process. By addressing these limitations and building on its strengths, the construction industry can fully realize the potential of chatbot-based technology to improve efficiency, reduce costs, and enhance decision-making.

ACKNOWLEDGMENTS

This research was conducted with the support of the “2022 Yonsei University Future-Leading Research Initiative (No. 2022-22-0102)” and the “National R&D Project for Smart Construction Technology (RS-2020-KA156488)” funded by the Korea Agency for Infrastructure Technology Advancement under the Ministry of Land, Infrastructure and Transport, and managed by the Korea Expressway Corporation. Any opinions, findings, and conclusions or recommendations expressed in this material are those of the author(s) and do not necessarily reflect the views of the funding agencies.

REFERENCES

- Amer, F., Y. Jung, and M. Golparvar-Fard. 2021. “Transformer machine learning language model for auto-alignment of long-term and short-term plans in construction.” *Autom. Constr.*, 132: 103929. Elsevier.
- Brown, T. B., B. Mann, N. Ryder, M. Subbiah, J. Kaplan, P. Dhariwal, A. Neelakantan, P. Shyam, G. Sastry, A. Askell, S. Agarwal, A. Herbert-Voss, G. Krueger, T. Henighan, R. Child, A. Ramesh, D. M. Ziegler, J. Wu, C. Winter, C. Hesse, M. Chen, E. Sigler, M. Litwin, S. Gray, B. Chess, J. Clark, C. Berner, S. McCandlish, A. Radford, I. Sutskever, and D. Amodei. 2020. “Language Models are Few-Shot Learners.” arXiv.
- Bureau of Labor Statistics. 2022. “Construction Laborers.” Accessed March 23, 2023. <https://www.bls.gov/oes/current/oes472061.htm>.
- Clark, K., M.-T. Luong, Q. V. Le, and C. D. Manning. 2020. “ELECTRA: Pre-training Text Encoders as Discriminators Rather Than Generators.” arXiv.
- Devlin, J., M.-W. Chang, K. Lee, and K. Toutanova. 2019. “BERT: Pre-training of Deep Bidirectional Transformers for Language Understanding.” arXiv.

- Eloundou, T., S. Manning, P. Mishkin, and D. Rock. 2023. "GPTs are GPTs: An Early Look at the Labor Market Impact Potential of Large Language Models." ArXiv Prepr. ArXiv230310130.
- Hughes, A. 2023. "ChatGPT: Everything you need to know about OpenAI's GPT-4 tool." BBC Sci. Focus Mag. Accessed March 23, 2023. <https://www.sciencefocus.com/future-technology/gpt-3/>.
- Kim, J., S. Chung, S. Moon, and S. Chi. 2022a. "Feasibility Study of a BERT-based Question Answering Chatbot for Information Retrieval from Construction Specifications." *2022 IEEE Int. Conf. Ind. Eng. Eng. Manag. IEEM*, 0970–0974.
- Kim, T., and S. Chi. 2019. "Accident case retrieval and analyses: Using natural language processing in the construction industry." *J. Constr. Eng. Manag.*, 145 (3): 04019004. *American Society of Civil Engineers*.
- Kim, Y., S. Bang, J. Sohn, and H. Kim. 2022b. "Question answering method for infrastructure damage information retrieval from textual data using bidirectional encoder representations from transformers." *Autom. Constr.*, 134: 104061. Elsevier.
- Ko, T., H. D. Jeong, and G. Lee. 2021. "Natural Language processing-driven model to extract contract change reasons and altered work items for advanced retrieval of change orders." *J. Constr. Eng. Manag.*, 147 (11): 04021147. *American Society of Civil Engineers*.
- Lan, Z., M. Chen, S. Goodman, K. Gimpel, P. Sharma, and R. Soricut. 2020. "ALBERT: A Lite BERT for Self-supervised Learning of Language Representations." arXiv.
- Lee, G., G. Lee, S. Chi, and S. Oh. 2023. "Automatic Classification of Construction Work Codes in Bill of Quantities of National Roadway Based on Text Analysis." *J. Constr. Eng. Manag.*, 149 (2): 04022163. *American Society of Civil Engineers*.
- Liu, Y., M. Ott, N. Goyal, J. Du, M. Joshi, D. Chen, O. Levy, M. Lewis, L. Zettlemoyer, and V. Stoyanov. 2019. "RoBERTa: A Robustly Optimized BERT Pretraining Approach." arXiv.
- Padhy, J., M. Jagannathan, and V. S. Kumar Delhi. 2021. "Application of natural language processing to automatically identify exculpatory clauses in construction contracts." *J. Leg. Aff. Dispute Resolut. Eng. Constr.*, 13 (4): 04521035. *American Society of Civil Engineers*.
- Radford, A., J. Wu, R. Child, D. Luan, D. Amodei, and I. Sutskever. 2019. "Language models are unsupervised multitask learners." OpenAI Blog, 1 (8): 9.
- Radford, A., J. Wu, R. Child, D. Luan, D. Amodei, and I. Sutskever. n.d. "Language Models are Unsupervised Multitask Learners."
- Raffel, C., N. Shazeer, A. Roberts, K. Lee, S. Narang, M. Matena, Y. Zhou, W. Li, and P. J. Liu. 2020. "Exploring the Limits of Transfer Learning with a Unified Text-to-Text Transformer." arXiv.
- Salama, D. M., and N. M. El-Gohary. 2016. "Semantic Text Classification for Supporting Automated Compliance Checking in Construction." *J. Comput. Civ. Eng.*, 30 (1): 04014106. *American Society of Civil Engineers*. [https://doi.org/10.1061/\(ASCE\)CP.1943-5487.0000301](https://doi.org/10.1061/(ASCE)CP.1943-5487.0000301).
- Sun, J., K. Lei, L. Cao, B. Zhong, Y. Wei, J. Li, and Z. Yang. 2020. "Text visualization for construction document information management." *Autom. Constr.*, 111: 103048. Elsevier.
- Tixier, A. J.-P., M. R. Hallowell, B. Rajagopalan, and D. Bowman. 2016. "Automated content analysis for construction safety: A natural language processing system to extract precursors and outcomes from unstructured injury reports." *Autom. Constr.*, 62: 45–56. Elsevier.
- Vaswani, A., N. Shazeer, N. Parmar, J. Uszkoreit, L. Jones, A. N. Gomez, L. Kaiser, and I. Polosukhin. 2017. "Attention Is All You Need." arXiv.
- Wang, N., R. R. A. Issa, and C. J. Anumba. 2022. "Transfer learning-based query classification for intelligent building information spoken dialogue." *Autom. Constr.*, 141: 104403. <https://doi.org/10.1016/j.autcon.2022.104403>.
- Wu, H., G. Q. Shen, X. Lin, M. Li, and C. Z. Li. 2021. "A transformer-based deep learning model for recognizing communication-oriented entities from patents of ICT in construction." *Autom. Constr.*, 125: 103608. Elsevier.
- Yan, H., M. Ma, Y. Wu, H. Fan, and C. Dong. 2022. "Overview and analysis of the text mining applications in the construction industry." *Heliyon*, 8 (12): e12088. <https://doi.org/10.1016/j.heliyon.2022.e12088>.
- Zhang, J., and N. M. El-Gohary. 2017. "Integrating semantic NLP and logic reasoning into a unified system for fully-automated code checking." *Autom. Constr.*, 73: 45–57. <https://doi.org/10.1016/j.autcon.2016.08.027>.

TRAINING DATA GENERATION WITH 3D CAD MODELS FOR POINT CLOUD DEEP LEARNING FOR UNDERWATER OBJECTS

Hiroshi Okawa¹, Shota Yagi², Seiji Itano³ and Kazuo Kashiya⁴

1) EJ Innovation Technology Center, Eight-Japan Engineering Consultants Inc., Tokyo, Japan. Email: ookawa-hi@ej-hds.co.jp

2) Disaster Mitigation and Facility Maintenance Department, Eight-Japan Engineering Consultants Inc., Okayama, Japan. Email: yagi-sho@ej-hds.co.jp

3) River and Port Division, Eight-Japan Engineering Consultants Inc., Tokyo, Japan. Email: itano-se@ej-hds.co.jp

4) Prof., Department of Civil and Environmental Engineering, Chuo University, Tokyo, JAPAN. Email: kaz.90d@civil.chuo-u.ac.jp

Abstract: This paper proposes developing a method to automatically classify underwater structures quickly and accurately using point cloud deep learning methods and point cloud data acquired using a narrow multi-beam bathymetric surveyor attached to an autonomous unmanned robot. We propose using a point cloud deep learning method to determine the current state of the underwater environment. Deep learning of point clouds requires a large amount of training data; however, training data can be quickly generated by replacing existing 3D CAD models of underwater structures with point clouds. Furthermore, discriminators trained by replacing point clouds created from 3D CAD models exhibit low discrimination with measured point clouds.

This presentation proposes a method that addresses these issues by collecting training data more efficiently and enhancing the accuracy of the correct answers. We applied the proposed method to measured underwater point cloud data to verify the effectiveness of the method.

Keywords: Point cloud, Deep learning, Underwater structure, Multi-beam echo-sounding, Classification

1. INTRODUCTION

Three-dimensional measurement devices have enabled the rapid development of point cloud measurement technology using acoustic equipment in underwater environments. This technology offers a new method of underwater inspection by acquiring wide-range, simple, safe, and high-resolution data using an autonomous surface vehicle (ASV) equipped with an acoustic depth sounder (Sugiyama et al., 2018). However, one of the challenges with underwater mapping data (Sawa & Oki, 2019) is that they are very large and have low readability owing to the lack of color information. Therefore, expert technicians are required to analyze them manually, which is time-consuming and error-prone. To address this challenge, this study aims to automatically and accurately classify underwater point cloud data by coloring them using a semantic segmentation model based on point cloud deep learning. We applied PointNet++ (Qi et al., 2017a), a state-of-the-art framework for land point cloud data, to underwater point cloud data.

The dataset for point-cloud deep learning is not only very limited but also confined to land-based datasets, with no datasets targeting underwater. Therefore, it is necessary to create these datasets, and most of them are manually annotated from actual measurement data and cannot be automatically collected. Therefore, we propose a new method to generate point clouds from 3D CAD models of prefabricated underwater structures and use them as learning data.

This paper presents the efficiency and accuracy of data collection. We evaluated the performance of our method by classifying underwater point cloud data using PointNet++ with the generated training data and comparing the accuracy results. Ultimately, we aimed to use the proposed method for debris surveys, but we adopted tetrapods as they are underwater and are common artificial objects. In addition, even with the limited use of tetrapods, rapid surveys, and disaster reports relying on human hands are required for scattered, moved, and damaged blocks in various disasters despite dangerous situations. In such situations, a breakthrough is expected by combining automatic navigation robots and AI during primary surveys. An accuracy of approximately 70% is considered sufficient in primary surveys.

2. UNDERWATER POINT CLOUD DATA AND DATA ACQUISITION METHOD

2.1 Equipment Used

Underwater mapping data combine images, terrain, water quality, time, and other information with location coordinates acquired underwater. The most common way of acquiring these data is to use acoustic exploration devices such as side-scan sonar and multi-beam echo sounders on a ship. In this study, we use an ASV (see Figure-1) as a platform to acquire point cloud data with a multi-beam acoustic depth sounder (iWBMSH; Norbit) mounted on it.

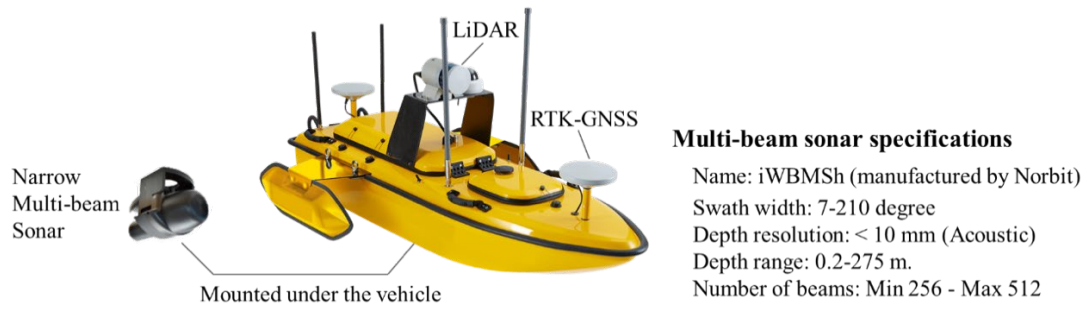


Figure 1. ASV and multi-beam sonar specification

2.2 Acquisition of Underwater Point Cloud Data

The bottom surface of the water can be measured using direct and indirect methods. We used one of the indirect methods, that is, multi-beam depth measurement, using the Mills Cross method. This method emits fan-shaped transmission beams from the sonar horizontally and receives them vertically with slits after they are reflected from the water bottom (Asada, 1999). Using this multi-beam depth sounder on an ASV, we can acquire point-cloud data without color information. Figure-2 illustrates an example of acquired point cloud data with only three-dimensional coordinate values.

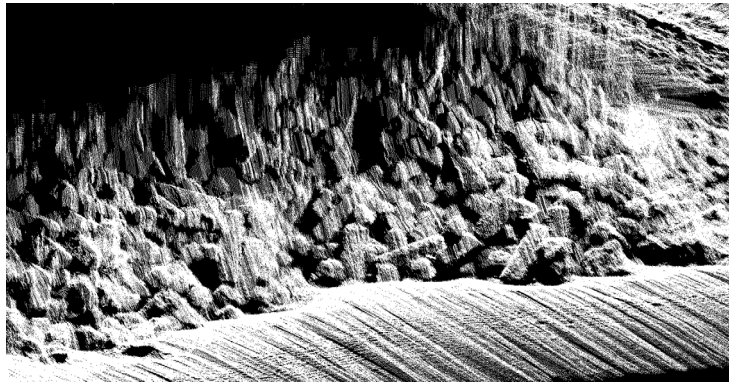


Figure 2. Example of data by multi-beam sonar

3. OBJECT RECOGNITION BY DEEP LEARNING ON 3D POINT CLOUDS

3.1 Deep Learning on 3d Point Clouds

As mentioned earlier, a 3D point cloud is a set of points having 3D coordinates and forming a 3D model. However, a 3D point cloud is also an unordered collection of points with varying densities and unclear adjacency relationships. Therefore, although each point does not have meaning by itself, a 3D shape can be expressed through multiple adjacent points. The positional relationship between adjacent points is imperative in deep learning. Previously, image-based methods that convert 3D point clouds into images using specific methods and learn them using convolutional neural networks (CNNs) were common. However, converting 3D data into 2D data may result in the loss or distortion of detailed geometric and spatial information. Therefore, in recent years, 3D point-cloud-based methods that directly input and learn 3D point clouds have become mainstream.

3.2 About the Learning Model

When performing 3D point cloud deep learning, it is necessary to consider the orderlessness of information, the relationship between points, and the invariance of movement. Therefore, conventionally, these properties were considered by voxelizing point clouds and treating each layer as an image using a 2D CNN approach. However, PointNet (Qi et al., 2017b) can directly take point cloud data as input without 2D conversion and consider these properties by applying an affine matrix to the input point cloud. PointNet has a problem that it cannot extract local features from 3D point clouds.

PointNet++ (see Figure 3) is an improved version of PointNet proposed by Qi et al., which has a hierarchical network structure where features are extracted for each local region. The local feature extraction part consists of three layers: sampling layer, grouping layer, and PointNet layer. The sampling layer samples points from the inputted 3D point clouds, the grouping layer groups neighboring points around the sampled points, and the PointNet layer computes feature values from the extracted neighboring points. Through these processes, it can learn the local features of inputted 3D point clouds. In addition, PointNet++ includes two abstract layers to obtain

multi-scale information according to point density to consider the local structure of inputted 3D point cloud data, which was an issue in PointNet. The first layer is a sampling layer, which performs sampling in distance space. We used the farthest point sampling (FPS) (Moenning et al., 2003) method to sample representative points at equal intervals from the inputted three-dimensional point clouds. Next, in the second grouping layer, we assigned the remaining three-dimensional point clouds that were not selected by FPS to the group with the closest representative point cloud among those selected by FPS. In PointNet++, there are two grouping methods: single-scale grouping (SSG), which groups at one distance, and multi-scale grouping (MSG) (Chen et al., 2021), which considers multiple distances. We adopted SSG because of its low computational cost. By recursively applying these two layers and PointNet, we aggregated multi-scale information and built a deep learning framework that considers the local structure of three-dimensional point clouds. As shown in Figure 3, the feature extraction part that aggregates information on the input data in PointNet++ is the same for both the class classification and semantic segmentation models.

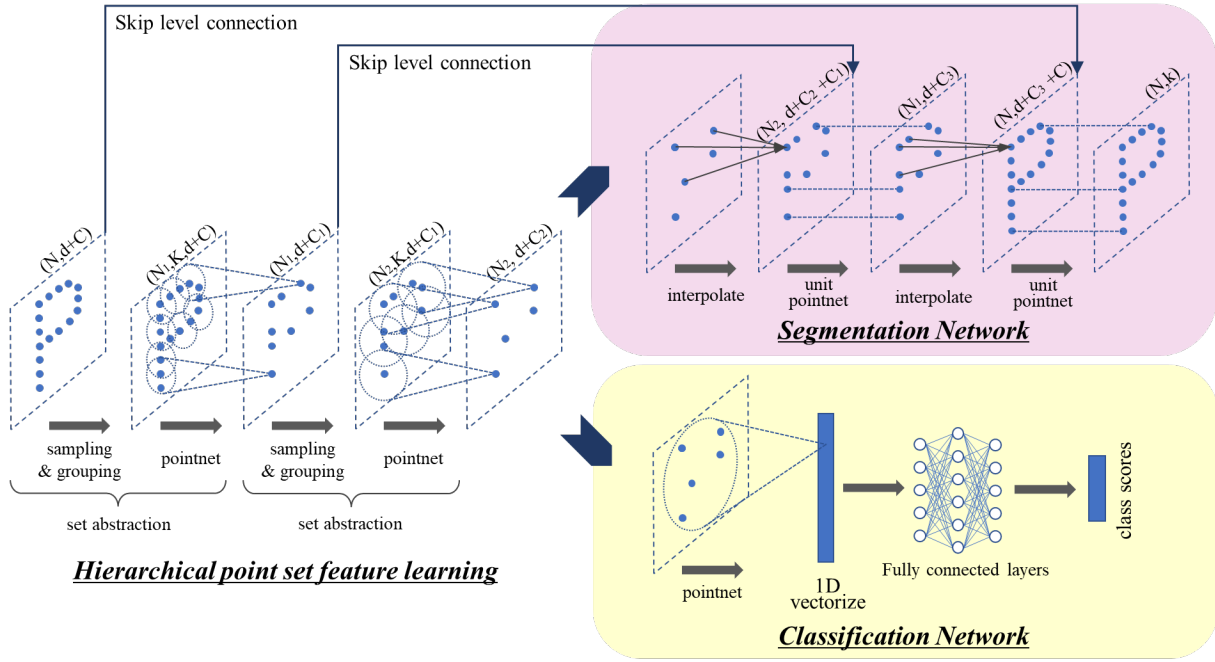


Figure 3. Network (PointNet++) (Qi et al., 2017a)

4. EFFICIENT AND HIGH-QUALITY CREATION OF TRAINING DATA

In this study, we used a supervised learning method to create datasets for point cloud deep learning models. We created training data and test data and used PointNet++ as a point cloud deep learning model to evaluate the learning results by classification and semantic segmentation. In the next section, we describe the method of creating training models, the method of acquiring test data, and the learning results.

4.1 CAD Models

Typical existing structures in water, such as rivers and coasts, include tetrapods and foot-protection blocks. These structures are prefabricated products; therefore, their shapes can be reproduced accurately. In this study, we created three-dimensional CAD models from two-dimensional drawings of foot protection blocks that are actually used on coasts. In addition, we created surface models because point cloud information only requires surface information and does not require internal information.

4.2 Method of Creating Point Cloud Data

We generated point clouds on the surface of the model created in the previous section and used them as training data. To generate point clouds, we used point cloud processing software (Cloud Compare), which allowed us to generate point clouds by specifying any number of points. The point cloud density was set separately by sampling and grouping in the feature extraction network described in the previous section. To use point cloud as training data, it is desirable to create training data similar to measured point cloud data. Therefore, we applied the following process to make the data as similar as possible:

(1) Processing of Point Cloud Data (Cutting Process)

For training data in classification models, we used individual point cloud models created as shown in Figure 4. Underwater point cloud data contain several data blocks with missing parts owing to shadows or blind spots from the water surface due to its acquisition method. Therefore, we devised a way to improve the classification accuracy by cutting off part of the original training data.

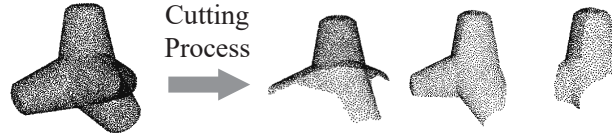


Figure 4. Cutting process

(2) Rotation Process

We applied rotation processing to the blocks processed in the previous section for data augmentation purposes. The rotation angle was set to rotate up to 360 °at 6° intervals for each of the X, Y, and Z axes with respect to each block so that it became 180 times per block. An example of the actual processed data is shown in Figure 5.

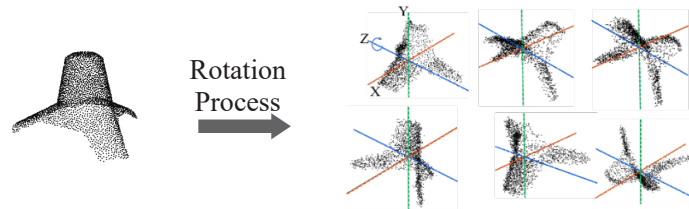


Figure 5. Cutting process

4.3 Creation of Training Dataset

In this study, we used the PointNet++ network to perform classification and semantic segmentation. However, it was necessary to prepare the training datasets for each task. Classification data can be reused to create training data for semantic segmentation. The details of each dataset are described in the following section.

(1) Dataset for Classification

The point cloud model created in the previous section was used as a training dataset for the classification task. Each model consisted of more than 5,000 points, which were controlled by a sampling-grouping layer within the feature extraction network.

(2) Dataset for Segmentation

The dataset for the semantic segmentation task was created by arbitrarily selecting and placing classification datasets based on rules. To create this dataset, we used three-dimensional CG software (Blender). Figure 6 illustrates an example of the created area dataset.

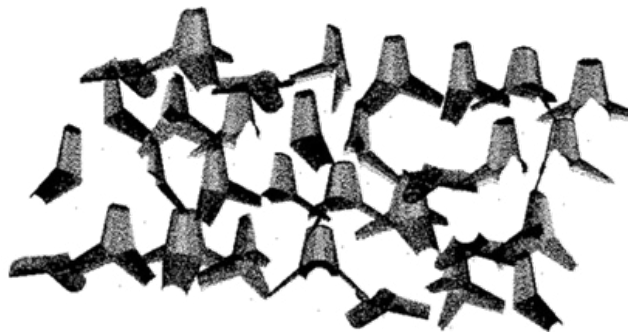



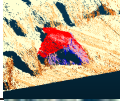




Figure 6. Dataset for semantic segmentation

4.4 Validation of Training Dataset

We validated our training dataset to apply the PointNet++ network to the underwater point-cloud dataset. Because the local region extraction network within the PointNet++ network was common between both tasks (classification and semantic segmentation tasks), we performed a validation process using only the classification dataset. As a test dataset, we extracted a real underwater measurement dataset and evaluated it against our trained model. We created training datasets and test datasets using the methods described above, as shown in Table 1.

Table 1. Dataset (Training data and Test data)

Block Type	Training datasets				Test datasets (ground truth)		
	Shape Example (by CAD)	Total Number of Models (Cut)	Total Number of Models (Rotation)	Total Number of Regions	Shape Example (ground truth)	Total Number of Models	Total Number of Regions
A		5	900	20		254	5
B		3	540	20		55	3
C		4	720	20		54	4

5. APPLICATION EXAMPLES

5.1 Analysis Target: Blocks A, B, AND C

As the analysis target for this study, we adopted point cloud data obtained by actual measurements in shallow water areas (around Hamada Port in Hamada City, Shimane Prefecture; around Kii Port in Oki District, Shimane Prefecture; around Saga Port in Kuroshio Town, Hata District, Kochi Prefecture) where tetrapods were scattered. Tetrapods are wave-dissipating concrete blocks used to prevent erosion caused by weather and longshore drift. We also selected tetrapods as targets for classification and semantic segmentation.

5.2 Training Data and Test Data

For the test data for the classification model, we used point cloud data extracted from the data acquisition area. However, for the test data for the semantic segmentation model, we directly used the acquired area data. Because tetrapods are prefabricated products, we created 3D CAD models based on design drawings and converted them into point cloud models to create training data. Figure 7 illustrates an example of the training data for each block. The total number of points composing each block model was approximately 5,000 points, and typical parameters were point number control 1,024 points and learning times were 500 times.

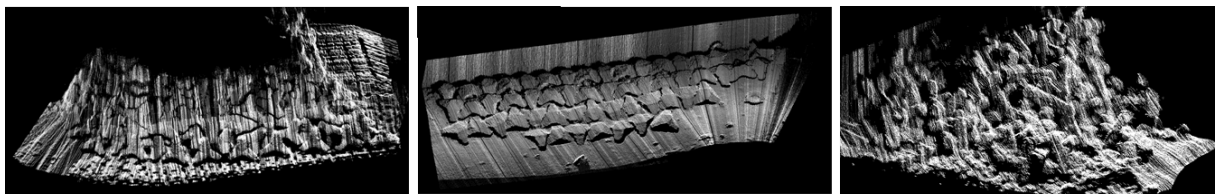


Figure 7. Test dataset for semantic segmentation (Left: for Block A, Center: Block B, Right: Block C)

5.3 Analysis Results

We classified the test data using the above training model and the results (confusion matrix) are shown in Table 2 and Table 3. We used the following classification metrics to evaluate and contrast the multiclass classification results derived from this architecture. These values range from 0 to 1, and the higher the value, the more optimal the model.

Precision (P), also known as positive predictive value, quantifies the ratio of predicted points that actually belong to a particular class to all predicted points for that class. For each class, precision is calculated as follows

$$P = \frac{TP}{TP+FP} \quad (1)$$

Recall (R), or true positive rate, measures the proportion of predicted points that are correctly classified out of all predicted points for a given class. The recall for each class is given by the following formula

$$R = \frac{TP}{TP+FN} \quad (2)$$

F1 score (F_1) combines precision and recall into one metric by calculating their harmonic mean. Generally, a model with an F1 score of 0.80 or higher is considered excellent.

$$F_1 = \frac{2 \cdot P \cdot R}{P+R} \quad (3)$$

Accuracy (A) is a metric that indicates how well the overall prediction results match the true values, and is derived by the following formula:

$$A = \frac{TP+TN}{TP+FP+TN+FN} \quad (4)$$

In the above formulas, TP is the number of true positives, FP is the number of false positives, TN is the number of true negatives, and FN is the number of false negatives for a given class. In general, the higher the values of P, R, F_1, A the better the performance of the deep-learning model. In the table below, we have also given the arithmetic mean of the F-values for each class division as the 'macro-average'. By calculating these values and seeing if they show similar trends, we can assess the classification accuracy of this architecture.

The macro-average F1 score was 0.85, which implies, a very high accuracy classification result. Figure 8 shows the results of semantic segmentation with different colors. Those identified as block A are colored red, block B is colored blue and block C is colored green. Mean IoU is a common metric for evaluating segmentation results. It measures the overlap rate between the predicted and the ground truth segments, as defined in equation (5).

$$IoU = \frac{TP}{TP+FP+FN} \quad (5)$$

It can also be interpreted as the pixel-wise accuracy of the classification. Mean IoU is computed by averaging the IoU values for each class in a single image, and then averaging over all classes. Although some parts were classified as different blocks, the mean IOU was also very high at 0.812.

Table 2. Classification report (Confusion Matrix)

		Predict Classification		
Class		A	B	C
Actual Classification	A	231	5	18
	B	3	50	1
	C	7	5	43

Table 3. Classification report (Precision, Recall, F1, Accuracy)

Class	Precision	Recall	F1	Accuracy
A	0.91	0.96	0.93	0.89
B	0.93	0.83	0.88	
C	0.78	0.69	0.74	
macro-average	0.87	0.83	0.85	—

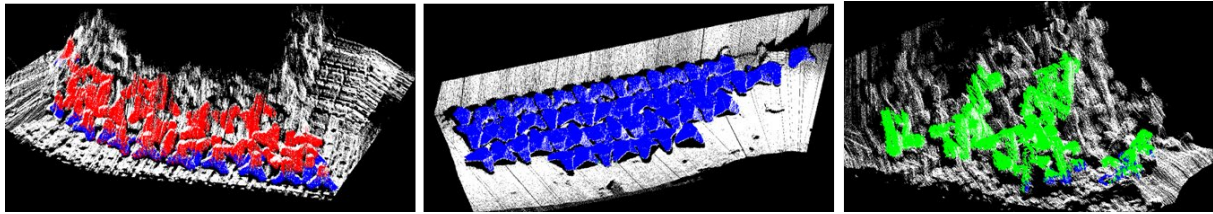


Figure 8. Results of semantic segmentation - Segmented point clouds are colored.
(Left: for Block A, Center: Block B, Right: Block C)

5.4 DISCUSSION

In the three-class classification, both accuracy and mean-IOU were over 80%, and we maintained high accuracy even in the multiclass classification. Thus, we achieved high-accuracy classification and semantic segmentation by adding point number control to PointNet++'s feature extraction layer and appropriately processing underwater point cloud features. However, the confusion matrix reveals that Block C has a lower accuracy than the other blocks. This is an issue because Block C has a complex installation pattern that is not well represented in the training data. In addition, we found many incorrect outcomes at the boundary parts with the bottom surface, that is, in blocks A and C in Figure 8, the areas that should have been colored red or green are blue, indicating that they were segmented as block B. This was owing to the similarity of the model shape; therefore, we need to consider this issue further.

6. CONCLUSION

In this study, we aimed to develop a method for automatically and quickly performing structure classification and current situation grasping using underwater point cloud data automatically acquired by an ASV, enabling automatic object classification of underwater point clouds using point cloud deep learning. In addition, considering the characteristics of underwater point clouds, we developed an efficient training data creation method by generating point clouds from three-dimensional CAD models of prefabricated underwater structures, obtaining the following conclusions.

- By applying PointNet++ to underwater point-cloud data, we achieved automatic and high-accuracy classification by coloring point-cloud data using semantic segmentation based on point-cloud deep learning.

- Using partially processed data generated from three-dimensional CAD models, we considerably improved the training data creation efficiency and discrimination performance and confirmed the applicability to actual measurement data.

REFERENCES

- Asada, A.(1999). Seabottom imaging by multi-beam sonar, *The Journal of the Acoustical Society of Japan*, 10 (55), 712-722.
- Chen, Y. Liu, G. Xu, Y. Pan, P. Xing, Y.(2021). PointNet++ Network Architecture with Individual Point Level and Global Features on Centroid for ALS Point Cloud Classification, *Remote Sensing*, 13 (3), 472.
- Moenning, C. and Dodgson, N. A.(2003). Fast Marching farthest point sampling for implicit surfaces and point clouds, *Computer Laboratory Technical Report University of Cambridge, UK*, 565.
- Qi, C. R., Su, H., Mo, K., and Guibas, L. J. (2017b). PointNet: Deep learning on point sets for 3D classification and segmentation, *Proceedings of the IEEE Conference on Computer Vision and Pattern Recognition*, CVPR 2017, 652–660.
- Qi, C.R., Yi, L., Su, H. and Guibas, L.J. (2017a). PointNet++: Deep Hierarchical Feature Learning on Point Sets in a Metric Space, *Proceedings of the 31st International Conference on Neural Information Processing Systems*, 5099–5108.
- Sawa, T. and Oki, T.(2019). Technique of underwater acoustic for seafloor mapping, *The Journal of the Acoustical Society of Japan*, 75 (1), 29-34.
- Sugiyama, F. Kiyonari, K. Iida, T. Komiyama, S. Suzuki, T. and Yamamoto, K.(2018). The Development of the Float Robot for the Efficiency of the River Facility Inspection, *Journal of the Robotics Society of Japan*, 36 (2), 168-174.

EVALUATION OF AI'S GENERALIZATION PERFORMANCE FOR DETECTING CONSTRUCTION MACHINERY FROM VIDEO IMAGES

Kentaro Hayakawa¹, Koji Makanae²

1) Ph.D. Candidate, Graduate School of Project Design, Miyagi University, Japan. Email: p2155002@myu.ac.jp

2) Ph.D., Prof., School of Project Design, Miyagi University, Japan. Email: makanae@myu.ac.jp

Abstract: We developed an object detection system that automatically detects construction machines in video images by performing machine learning. However, the detection accuracy was decreased when the object detection system was applied to a construction site different from where the training data was collected. Therefore, we improved the detection accuracy when the object detection system was applied to different sites by devising the structure of the training data used for machine learning.

As a result, the generalization performance was high by making the detection system include well-balanced training data on the orientation of construction machinery and its distance from the camera. By learning the appearance of various construction machines, we were able to construct a detection system that can be applied to different job sites without being influenced by specific situations.

Keywords: AI, Object detection, Generalization performance, Video image, Construction machinery

1. INTRODUCTION

Recently, it is common practice to monitor the construction status of a construction site with a fixed-point camera and check the site status through images from a remote location such as an office. As a more developed technology, efforts are being made to combine captured video with Artificial Intelligence (AI) to detect specific objects from the video. Pan and Zhang (2021) reviewed the current state of AI utilization in construction sites and cited computer vision as one of the research topics that can fully utilize the advantages of AI. The purpose of research on computer vision is to monitor construction sites, and it is evaluated that it can track and recognize workers, materials, equipment, etc., and can be responsible for prediction and evaluation. Specific use cases are reviewed by Mostafa and Hegazy (2021), citing construction safety, progress monitoring, and damage assessment as the main ones. Regarding safety, Mneymneh et al. (2019) use it for safety management at construction sites by judging workers on their wearing of helmets. In terms of progress, Xiao and Kang (2021) state that tracking construction machinery in a video can be useful for automatic monitoring of construction site productivity and progress.

In this way, techniques for managing construction sites using AI are attracting attention, but AI is vulnerable to situations outside its learning range and cannot respond flexibly (Chun, 2020). One possible way to create AI that can respond to diverse on-site situations is to collect training data for each site where it is applied. However, the problem is that it takes time and money to collect a large amount of training data each time. In order to save the time and effort of creating training data from scratch when applying AI to different sites, an AI with high generalization performance is needed. We believe that devising a training dataset for machine learning is critical to achieving it. Xiao and Kang (2021) propose a training dataset specific to construction machinery, focusing on the number of objects per image, the number of categories, and the size distribution of bounding boxes. However, they do not mention their balanced composition or generalization performance. We focused on the direction of the construction machinery and the distance from the camera. We created two types of detection engines, one with well-balanced training data related to them and the other without it, and applied them to two sites to compare which engine has higher generalization performance.

2. OUTLINE OF THE SYSTEM FOR AUTOMATIC DETECTION OF CONSTRUCTION MACHINERY

To evaluate the accuracy of the detection of construction machinery, we used the construction machine detection system we developed in the previous study (Hayakawa et al., 2020) to automatically detect construction machinery in a video. The construction machine detection system targets four types of construction machines commonly used in embankment construction (dump truck, excavator, bulldozer, vibration roller), and can detect these construction machines from unknown input images. Figure 1 shows the flow of operating the construction machine detection system.

1) A fixed-point camera installed at the construction site captures the state of embankment construction. Dump trucks, excavators, bulldozers, and vibrating rollers are recorded at 4K resolution (3,840×2,160), and image data is cut out from the obtained video and used as image data for learning.

2) As shown in Figure 2, the construction machine in the image data for learning is enclosed in a rectangle and registers the type of construction machine. By assigning such labels, we create a training dataset that associates the appearance and type of construction machinery. Normally, this work is done visually and manually, and it takes much time. Figure 2 is an example of labeled image data. When multiple

construction machines are shown in one image, all the objects are labeled.

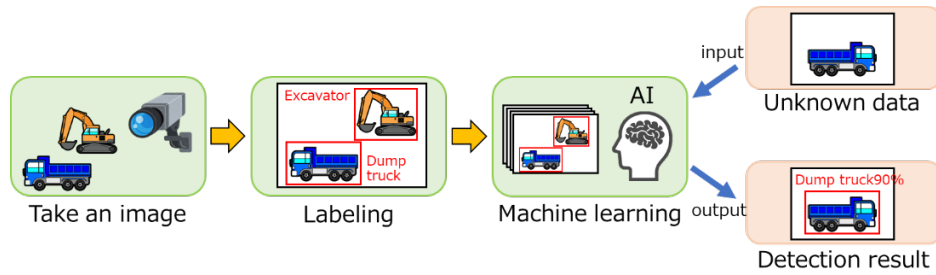


Figure 1. The operation flow of the construction machine detection system

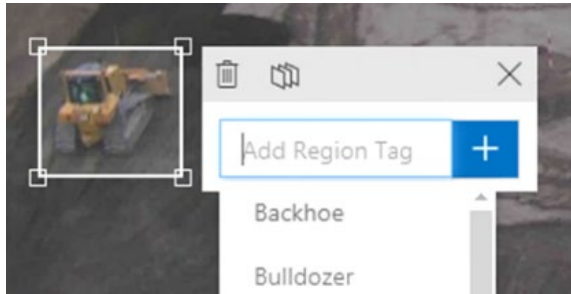


Figure 2. Appending a label to an object

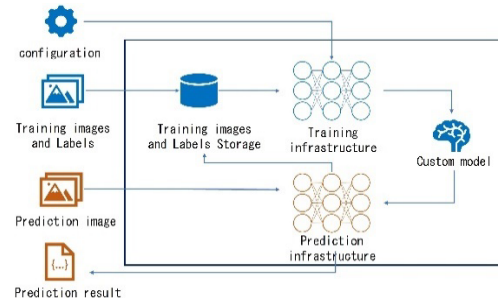


Figure 3. Process flow by Custom Vision



Figure 4. Detection result by machine learning

3) The training data set is input to Microsoft's Azure Cognitive Services Custom Vision, and machine learning is performed to create a construction machine detection system (Figure 3). This platform uses a deep learning algorithm that is strong in visual characteristics, and it is possible to create a learning model from images input as training data and create a model that detects learned objects.

4) When unknown image data is input to the construction machine detection system, inference is executed and objects similar to learned features are detected. Figure 4 shows the detection results. The detection result is represented by a bounding box (BB) with a different color for each type of construction machine, and the probability of inference is displayed above the BB. As shown on the left side of Figure 4, the object surrounded by a red BB indicates that it is a bulldozer with a probability of 90.5%.

3. EXPLANATION OF THE TWO TRAINING DATASETS AND DEMONSTRATION AT A CONSTRUCTION SITE

We created two types of detection engines, one is the engine that learned data on the orientation of construction equipment and its distance from the camera in a balanced manner, and another is the engine that learned data by randomly selecting data. We checked the detection accuracy of the construction machine detection engines for sites under different conditions. The flow for checking the detection accuracy is shown in Figure 5.

Table 1 shows the characteristics of the two types of detection engines. A total of 1,800 images were randomly extracted from the video of site A during the time period when the construction machinery was in operation, and 9,679 labels were assigned to them. One type of engine "Random AI" was obtained by machine learning this data set. In the other training data set, images were extracted from the video of site A, focusing on the direction of the construction machine (Figure 6) and the distance from the camera (Figure 7). When labeling the image data for learning, in addition to the name of the construction machine, information on the direction and

distance is also given. For example, the label might be [dump, leftward, short distance]. In order to prevent the appearance of the construction machines included in the training data set from biasing toward specific situations, we intentionally balance the number of 8 types of orientation labels and 3 types of distance labels so that they were uniform. We adopted 5,880 labels. Another type of engine “Balance AI” was generated by performing machine learning on this training dataset. Figures 8 and 9 show the number of labels for each direction of dump trucks in the training data sets used in Random AI and Balance AI. Random AI has different numbers of labels in each direction, but Balance AI is uniform.

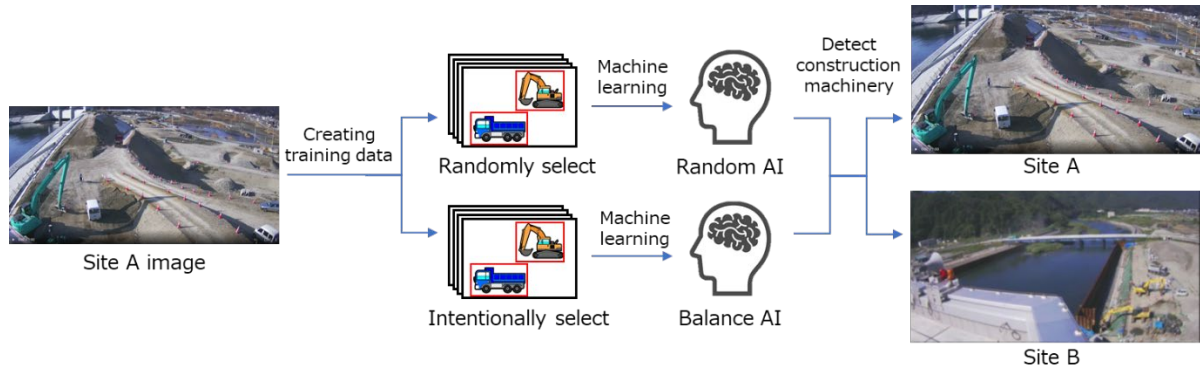


Figure 5. Flow for checking the detection accuracy of two types of detection engine at two sites

Table 1. Characteristics of Random AI and Balance AI

	collect Training data	Number of labels	Number of images	uniformize
Random AI	Site A	9,679	1,800	No
Balance AI	Site A	5,880	2,623	direction distance



Figure 6. Direction of construction machines



Figure 7. Distance from camera

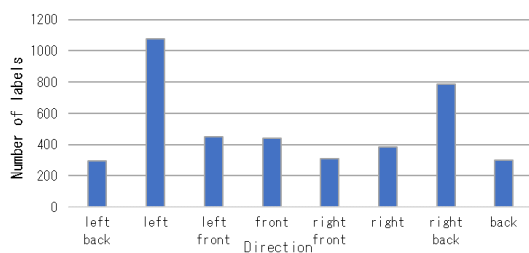


Figure 8. Number of Random AI labels (dump truck direction)

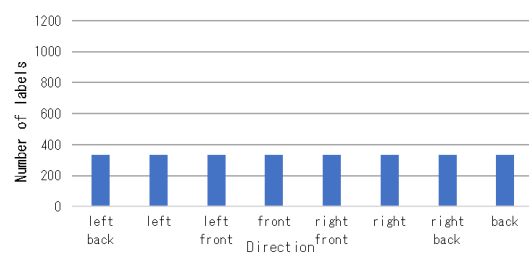


Figure 9. Number of Balance AI labels (dump truck direction)

The unknown data for the evaluation of the two types of engines were extracted from the images of site A (Figure 10) and site B (Figure 11). The unknown data for Site A was obtained from the fixed-point camera same as the training data, and it is characterized by many construction machines performing embankment work on seawalls within a short to medium range of about 100 m from the camera. In the case of site B, the camera type is the same as site A, but there are many construction machines that build river embankments at a distance of 100 to 150 m from the camera, and the angle of the camera and background conditions differ from site A. We used Intersection over Union (IoU) and accuracy as evaluation indicators of detection accuracy when the detection

engines infers unknown data. IoU judges that detection is correct if the overlap between the correct BB area given by visual observation and the BB area detected by detection engines exceeds the threshold (Figure 12). In this paper, when IoU is 30% or more, we regard the detection engine's judgment as correct. Accuracy is one of the indicators that expresses the accuracy rate of detection results and is calculated by $\text{Accuracy} = \text{number of correct answers} / (\text{number of correct answers} + \text{number of false positives} + \text{number of undetected cases})$.



Figure 10. Video of site A



Figure 11. Video of site B

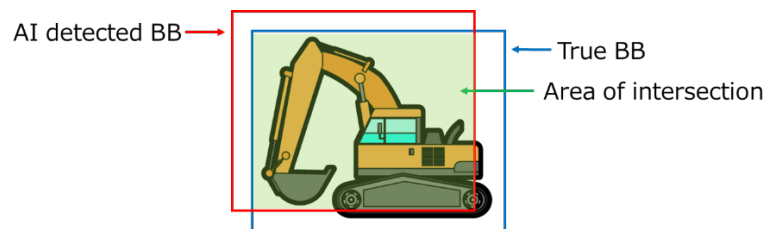


Figure 12. Judgment method using IoU

Table 2. Accuracy rate for two types of detection engines

	Accuracy (%)	
	Site A	Site B
Random AI	63.23	49.43
Balance AI	57.97	61.17

4. COMPARISON RESULTS OF BALANCE AI AND RANDOM AI

Table 2 shows the results of obtaining the accuracy rate by inputting the unknown data of site A and site B into Random AI and Balance AI. The accuracy rate was 63.23% when unknown data of site A was input to Random AI, and 57.97% for Balance AI. On the other hand, when the unknown data of site B was input, the accuracy rate of Random AI decreased to 49.43%, but the accuracy rate of Balance AI improved to 61.17% even when applied to different sites.

The result shows that the difference in the composition of the training dataset strongly affected the detection. The construction machines in the video of site A are often working at a short to medium distance from the camera, and due to the convenience of the carry-in route, the construction machines frequently face in a specific direction. Random AI that machine-learned a training data set with biased features has a high accuracy rate at site A, which has a similar bias, but the accuracy rate at site B, which has a different situation, decreases. On the other hand, Balance AI, which performs machine learning on a training data set that has a well-balanced number of labels for the direction and distance of construction machines is less susceptible to specific situations and has high generalization performance that can be applied to different sites.

5. CHANGE IN ACCURACY RATE DUE TO ADDITION OF TRAINING DATA

In the previous chapter, it was found that the balance AI has generalization performance. However, the detection rate is around 60% and not high. There is a need to further improve the detection accuracy in order to introduce a versatile balance AI engine when applying it to many sites in the future. However, this is contingent on minimizing the effort to create training data sets as much as possible. Therefore, improve the accuracy rate when Random AI and Balance AI are applied to site B, we added image data newly acquired at site B to the training data set and verified the change in the accuracy rate. Table 3 shows the breakdown of the training data set. Based on the training data set used for machine learning of Random AI and Balance AI described in Chapter 3, images are cut out from the video of site B and added to the training data set. For the additional training data, images were randomly cut out from the time period when the construction machinery was in operation at site B,

and 2,914 labels were assigned. For comparison, machine learning was performed using only the training data newly acquired at site B to create a new AI model.

Table 3. Breakdown of additional training data for Site B

	collect Training data	Number of labels	Number of images	uniformize
Random AI	Site A	9,679	1,800	No
	Site B (additional data)	2,914	1,020	No
Balance AI	Site A	5,880	2,623	direction distance
	Site B (additional data)	2,914	1,020	No

Table 4. Accuracy rate of AI with additional training data

	Accuracy (%)	
	Before adding training data	After adding training data
Random AI	49.43	63.11
Balance AI	61.17	71.00
Additional data only AI	–	54.17

The same unknown data from Site B as in Chapter 3 was input to Random AI and Balance AI with added training data, and the accuracy rate was calculated. Table 4 shows the results. The addition of training data to the Random AI resulted in an accuracy rate of 63.11%, while the addition of training data to the Balance AI resulted in an accuracy rate of 71.00%, with both improving the correct answer rate. The new AI model created with only the addition of training data resulted in a 54.17% accuracy rate. These results confirm that when detecting construction machinery from unknown data at site B, it is effective to train the Random AI and the Balance AI, which trained only the image data of site A, with the additional image data of site B. In particular, when training data was added to the Balance AI, the accuracy rate was high at over 70%, even though the number of labels for site B was relatively small at 2,914. Random AI also improved its accuracy rate by adding training data, but we think that it did not reach the accuracy rate like Balance AI because it adopted a data set with biased features. In addition, the new AI model created with only the additional training data was expected to have a high accuracy rate because it was specialized for the situation of site B. However, due to insufficiency of the absolute number of labels, the accuracy rate was about 54%.

6. PROPOSAL OF OPERATION METHOD OF CONSTRUCTION MACHINE DETECTION AI

Figure 13 shows the flow for more effective operation of construction machine detection system. Conventionally, when operating a construction machine detection system, the time and cost involved in collecting large amounts of image data for learning at each site was an issue. However, it will be possible to maintain the accuracy rate even in different sites by devising the composition of the training data set and creating a Balance AI with high generalization performance. It takes more time than usual to create a training data set that equalizes the number of labels for the direction of the construction machine and the distance from the camera. However, if you create a training data set in advance with image data from another site and create a Balance AI, you can quickly apply it to the target site. After applying Balance AI, if a higher accuracy rate is required, additional image data is collected from the on-site video and added to the training dataset to improve the accuracy rate of Balance AI. As additional image data does not need to consider the direction of the construction machine and the distance from the camera, the advantage is that training data can be collected in a short time. As described above, by operating Balance AI with high generalization performance, we believe that the time and cost required to collect training data each time it is introduced into the site can be greatly reduced.

7. CONCLUSION

In this paper, we evaluated the generalization performance of a detection system that automatically detects construction machinery in a video when the data set structure is devised. As a result of comparing two types of detection engine, Random AI and Balance AI, it was found that Balance AI has higher generalization performance, indicating the possibility of reducing the collection of training data for each site. The findings of this research are summarized below.

- When training data collected at Site A and infer unknown data from Site A, the Random AI's accuracy rate was about 5% higher than the Balance AI.
- When training data collected at Site A and infer unknown data from Site B, the Balance AI's accuracy rate was about 12% higher than the Random AI.

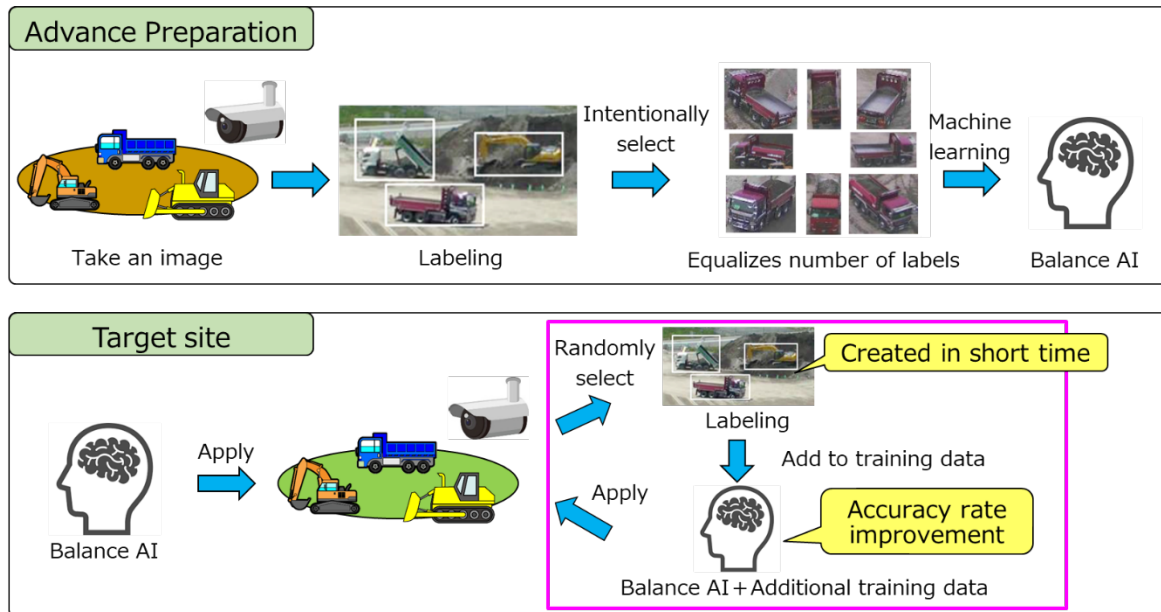


Figure 13. Flow of effective operation of construction machine detection AI

the Balance AI's accuracy rate was about 12% higher than the Random AI.

- When the training data from Site B was added to the Random AI and the Balance AI created from the training data collected at Site A to infer the unknown data from Site B, the Balance AI's accuracy rate was about 7% higher than the Random AI.
- By using Balance AI, it can be applied to other sites while maintaining a high accuracy rate.

On the other hand, the following issues also arose.

- Additional experiments on different sites will make the effectiveness of the proposed approach clearer.
- The performance of balance AI itself is insufficient. In practice, it may be desirable to be able to use enough training data for a site in different sites.

There are many efforts to utilize AI for construction management at construction sites, but we should also pay attention to the importance of preparing basic training data. In the development of the construction machinery detection system, considerable time is spent collecting high-quality training data. Balance AI can demonstrate stable performance at any site and is expected to make a significant contribution to labor savings and the advancement of construction management.

A Balance AI with high generalization performance facilitates deployment to a large number of sites, but the preliminary label selection and uniformity process are labor-intensive and more time-consuming than a random label assignment process. In the future, we will consider methods to improve the efficiency of label assignment and sorting.

REFERENCES

- Chun, P. J. (2020). A.I. in civil engineering: a roadmap for research and development, *Artificial Intelligence and Data Science*, (J1), pp. 9-15.
- Hayakawa, K., Kurodai, M., Masuda, H. and Makanae, K. (2020). Development of AI-based construction machine detecting system and examination on accuracy improvement, *Artificial Intelligence and Data Science*, (J1), pp. 313-319.
- Mneymneh, B. E., Abbas, M. and Khoury, H. (2019). Vision-based framework for intelligent monitoring of hardhat wearing on construction sites, *Journal of Computing in Civil Engineering*, 33 (2).
- Mostafa, K. and Hegazy, T. (2021). Review of image-based analysis and applications in construction, *Automation in Construction*, 122, 103516.

- Pan, Y. and Zhang, L. (2021). Roles of artificial intelligence in construction engineering and management, *Automation in Construction*, 122, 103517.
- Xiao, B. and Kang, S. (2021). Vision-based method integrating deep learning detection for tracking multiple construction machines, *Journal of Computing in Civil Engineering*, 35 (2).
- Xiao, B. and Kang, S. (2021). Development of an Image Data Set of Construction Machines for Deep Learning Object Detection, *Journal of Computing in Civil Engineering*, 35 (2).

INTELLIGENT DESIGN OF SIMPLY-SUPPORTED PLANAR TRUSS BASED ON REINFORCEMENT LEARNING

Xianzhong Zhao¹, Zhiyuan Liu², Weifang Xiao³, and Ruifeng Luo⁴

1) Ph.D., Prof., Department of Structural Engineering, Tongji University, and Shanghai Qi Zhi Institute, Shanghai, China. Email: x.zhao@tongji.edu.cn

2) Ph.D. Candidate, Department of Structural Engineering, Tongji University, and Shanghai Qi Zhi Institute, Shanghai, China. Email: 2211128@tongji.edu.cn

3) Ph.D., Assoc. Prof., Department of Structural Engineering, Tongji University, Shanghai, China. Email: weifangxiao@tongji.edu.cn

4) Ph.D. East China Architectural Design & Research Institute Co., Ltd., Shanghai, China. Email: ruifeng_luo@ecadi.com

Abstract: Intelligent design is a multidisciplinary research field involving artificial intelligence (AI), mathematical optimization, and human experience. The aim is to realize the automatic design of structures. As an important research topic of intelligent design in civil engineering, the truss design is characterized by high complexity, strict constraints and diversity of decision-making, which are the obstacles to the application of AI in designing the trusses. How to realize "brain-inspired design" by combining human knowledge with intelligent thinking is still a major challenge in the intelligent design of structures. This study develops an intelligent design algorithm for simply-supported planar truss based on reinforcement learning. The layout design problem of simply-supported planar truss is modeled as a Markov Decision Process (MDP). In order to solve the model, Monte Carlo Tree Search (MCTS), which performs well in sequential decision problems, is applied. Furthermore, MDP can include the engineering logic and knowledge that are extracted from the remarkable characteristics of simply-supported planar truss. This significantly condenses the initial solution space and optimizes the decision-making process. A contrast experiment is conducted to demonstrate the validity and efficiency of the proposed algorithm.

Keywords: Truss layout design, Intelligent design, Reinforcement learning, Markov decision process, Monte Carlo tree search

1. INTRODUCTION

Structural design plays a key role in engineering projects. Solving design problems is one of the most challenging processes in engineering (Simon & Herbert, 2019). Traditional design methods rely on the trial-and-error processes and the thinking patterns of experienced engineers. Parametric design methods convert some structural elements into parameters, but essentially it is no more than a programmatic way of traditional mode. Intelligent design makes more demands than traditional and parametric methods. Simulating the way that human brain works in engineering design by computers is the kernel of intelligent design. "Brain-inspired design" requires computers to sense and feed changes in the design environment and to be capable of evaluating, analyzing, and making decisions. Finally, the design task is completed through human-computer collaboration.

Intelligent design is a multidisciplinary research field involving AI, mathematical optimization, and human experience (Zhao, 2022). Although advancement in machine learning and computational modeling has brought machine intelligence beyond human levels in several problem-solving milestones (Mnih et al., 2015; Sliver et al., 2016; Brown & Sandholm, 2018), one common feature among these problems is that they are well-defined with rules and actions which are universally followed. Sheer complexity, constraint stringency, and decision diversity characterize design problems that become barriers to the application of AI. The abovementioned features make addressing design tasks require skills such as strategic planning, abstract decision-making, creativity, and explainability (Raina et al, 2021). This motivates AI to combine with civil engineering for facilitating solving design problems.

This paper investigates the intelligent design of structures and focuses on the layout design of simply-supported planar truss. Layout design is at the conceptual and project design phase of the overall construction activity. Engineering design generally focuses on construction drawing design now, yet early design can have a significant impact on the complete project cost and structural performance. The later the design change occurs, the higher the additional cost of the engineering incurred (Griem & Peter, 2009).

The way to achieve intelligent design is to build an algorithm. The construction of the algorithm should be tailored to the nature of the design. Design is essentially an iterative process. The designer first perceives the current design state, then utilizes prior knowledge and experience to modify it and produce a new design (Raina et al, 2019). Through subjective or objective indicators, the designer evaluates the new design to guide the revision process. The entire course can be represented as a sequential decision process. Inspired by AlphaGo (Sliver et al., 2016), this paper models truss layout design as a Markov Decision Process (MDP) (Bellman & Richard, 1957) based on the comprehension of the design principle. And a reinforcement learning algorithm called Monte Carlo Tree Search (MCTS) (Kocsis & Szepesvári, 2006) is applied to solve the model. During building MDP, the remarkable characteristics of simply-supported planar truss are extracted to optimize decision actions. The

integration of engineering logic and knowledge significantly condenses the initial solution space and optimizes the decision-making process.

The paper is organized as follows: Sec. 1 introduces the concept of intelligent design and builds up a foundation for the algorithm proposed in this study. Sec. 2 contains the background of the involved techniques and relevant studies. Sec.3 explains the MDP construction process for simply-supported truss design and outlines the solving of the model by MCTS. To demonstrate the validity and efficiency of the algorithm, a comparative experiment is conducted in Sec.4. The final conclusions and future work are mentioned at the end in Sec. 5.

2. BACKGROUND

2.1 Truss Layout Design

Truss layout design includes three decision variables and they are node positions, interconnectivity between nodes, and bar sections respectively. The independent optimization of these three decision variables corresponds to shape, topology, and size optimization. There is a great deal of research (Kaveh & Khosravian, 2022; Liu & Xia, 2022) into the optimal design of layout by applying heuristics based on the ground structure method (Dorn, 1964). However, these methods do not automate the design from scratch, but rather optimize existing structures. Even considering shape, topology, and size optimization simultaneously, the solution space is limited by the initial structure, which in turn affects the global optimality of the final result. Optimal design is a late-stage design approach whose important aspects of the design are already established, leaving exploration within narrow bounds (Krish, 2011).

In this paper, intelligent design requires the algorithm to create designs automatically. Under the premise of meeting constraint conditions, the design process will constantly lead to the trajectory approximating the design objective. The design transforms from scratch to existence, and then from existence to optimization. This approach, which differs significantly from optimal design is known as generative design (GD) (Watson et al., 2022). GD methods for truss layouts involve four main categories. Physics-based methods, such as using physical scaling models to predict the optimum topology of a structure, are an important tool for conceptual design of structures in the early days. With the maturity of modern computer technology, this primitive method is gradually becoming obsolete. Simulation-based methods are devoted to the identification of excellent structural configurations using numerical calculations through finite element analysis techniques. This method reflects a function-follow-form engineering intellection. However, it may result in a lot of post-processing work and is prone to producing nonstandard components. (Fenton et al., 2015). The homogenization method (Bensoussan et al., 2011), solid isotropic material with penalization method (Ho et al., 2022), and evolutionary structural optimization method (Xia et al., 2018) are widely used simulation-based methods. Graph-based methods, typically such as shape grammar (Shea, 1997) and triangulation algorithms (Zeng, 2023), control layout generation by combining and splitting the geometric elements of a structure. This approach is often combined with heuristics, reflecting a form-follow-function diagrammatic mindset. But graph-based methods have limitations in statically indeterminate structures and multiple load conditions. Another category is image-based methods. This method takes the image as a vehicle to optimize the layout by configuring the pixels (Raina, 2022). It is challenging to effectively represent designs of spatial structures and has shortcomings in interpretability.

2.2 Reinforcement Learning

According to the learning patterns, machine learning can be classified as supervised learning, unsupervised learning, and reinforcement learning (Jordan and Mitchell, 2015). The research aim of reinforcement learning is to enable computers to think, judge, reason, and make rational decisions like humans (Sutton & Barto, 2018). This is highly compatible with the idea of "brain-inspired design". Reinforcement learning is suitable for decision problems where there is insufficient understanding of the environment, i.e. where it is not possible to model experience, knowledge, and rules accurately. Its scope of application perfectly matches the characteristics of design tasks. Reinforcement learning relies on the interaction of agent with environment to achieve decision optimization. Agent refers to the algorithm that learns and makes decisions about the problem, while environment represents the mathematical model with which the agent interacts. In a reinforcement learning system, environment generates rewards based on the decisions of agent. The learning strategy of agent aims to find an exploration-exploitation trade-off. The rewards will assist agent to improve the learning strategy. Exploration refers to agent gaining more unknown information by interacting with the environment, while exploitation denotes agent making the best decision based on the current knowledge (Sutton & Barto, 2018).

The above features of reinforcement learning offer the possibility of constructing an algorithm in which computers can self-learn structural design. For applying reinforcement learning, the problem needs to be modeled mathematically first. MDP is a basic theoretical framework and classical formal representation of reinforcement learning problems. It consists of four elements, namely state, action, transition model, and reward. After the problem is modeled, a suitable algorithm needs to be adopted to solve it. MCTS is a reinforcement learning method that seeks the optimal decision by sampling actions in a decision tree. MCTS has a revolutionary impact on combinatorial games and dynamic planning problems. It is particularly suited to MDP where there are reward delays. Sec. 3 of this paper will explain in detail the process of constructing an MDP for simply-supported truss

layout design and briefly describe the process of applying MCTS to solve the model.

Reinforcement learning has received widespread attention after the emergence of AlphaGo. It is now widely used in games (Rajeswaran, 2020), automation control (Polydoros & Nalpantidis, 2017), financial investment (Charpentier et al., 2021), and other fields. However, the application of reinforcement learning is rarely visible in the field of truss structure design. Zhu et al. utilize a structure self-generation method that combines reinforcement learning with graph embedding methods for the truss layout design (Zhu et al., 2021). The authors of this paper have previously proposed an automated design framework for truss layouts, named AlphaTruss (Luo et al., 2022a; Luo et al., 2022b). The framework combines numerical and graphical approaches based on reinforcement learning, but does not model the decision process for a particular structural form. The algorithm proposed in this study builds on AlphaTruss. And the engineering properties of simply-supported planar truss are combined with the algorithm to achieve a more efficient generation of this specific structural form.

3. METHODOLOGY

3.1 Problem Definition

The truss design problem can be formulated in four parts: design objective, constraint conditions, input information, and output. The design objective represents the optimization orientation of the layout generation and can be used as the main evaluation indicator of the design results. The most common design objective is weight minimum. Constraint conditions are the necessary requirements that need to be met during the design process. In practical engineering, there are certain design specifications and user demands. And constraint conditions play this role. The input information refers to the initial design conditions that generally include design domain, support conditions, load conditions, fixed nodes, fixed bars, material properties, and other indispensable design information. The output denotes the optimal truss layout generated after the algorithm has been executed.

3.2 Markov Decision Process

MDP is a sequential decision model based on the interaction between agent and environment. It can be expressed as: agent observes an environment state s_t at moment t , then selects and takes an action a_t . As a consequence of a_t , environment transfers to the next state s_{t+1} according to transition model p and feeds a numerical reward r_t back to agent. This process is repeated until environment reaches the terminal state s_T . Figure 1 shows the schematic diagram of MDP.

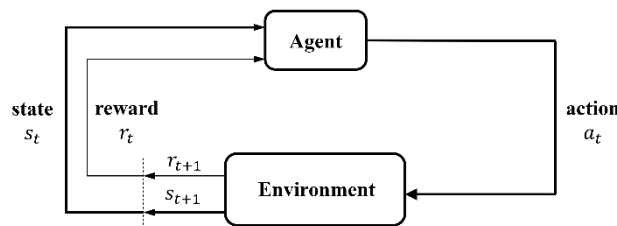


Figure 1. Schematic diagram of MDP

In truss design, state represents all information of the current layout. Action refers to the decision based on the characteristics of state. There are three kinds of state in the state space with different features and the corresponding three action categories are adding nodes, adding bars, and selecting bar sections. These three categories must be executed in strict order, which is logical by design. With an emphasis on versatility, the action can adopt the briefest rule, adding only one node, one bar, or selecting one section at each time. The briefest rule may be beneficial to maintain the original solution space. However, if the rule can be combined with the quality properties of the form-specific structure, restricting the actions enables the solution space to be optimized. Simply-supported truss has prominent symmetry. The most effective and efficient method of designing large structures is through the use of symmetry (Kicinger et al., 2005). Thus, the three action categories can be modified to symmetrically add nodes, bars, and select sections about the central axis of the truss. In symmetric designs, the medial axis node sometimes plays a more critical role, but the probability of having the added node fall on the symmetrical axis is small. A preprocessing state and its corresponding action are set to handle this downside. The preprocessing state analyzes whether the medial axis node needs to be added at the beginning of the entire generation process. The corresponding action is selecting the vertical position of the node. By introducing symmetry, the decision process and the solution space are drastically condensed.

In addition, simply-supported truss has a significant mechanical characteristic. Simply-supported truss can be considered as a hollow beam, with the upper and the lower chords taking the compression and tension, respectively. The shape of the truss can be designed into a shape similar to the moment curve. The arch shape makes the chords of the truss more evenly and reasonably stressed (Zhu & Yin, 2005). To control the shape of the truss, an arch mechanism is set up in the node generation process. The mechanism requires that the nodes can be added only when they can maintain the shape of the truss as an arch. This reduces the solution space of the search

and improves the efficiency of the decisions while giving the structure an excellent force transfer mechanism.

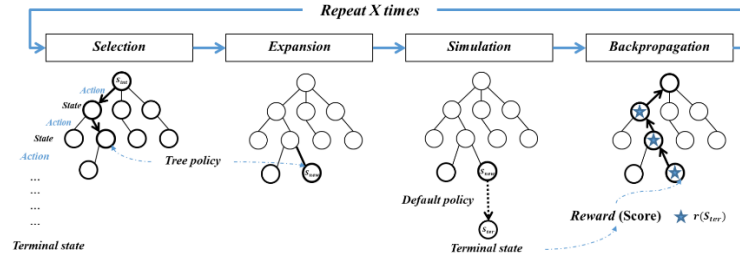
Transition model p describes the probability of transferring s_t to s_{t+1} after a_t is taken. In environment of design problem, p is defined as 1 which means, given s_t and a_t the resulting state s_{t+1} is determinate. The reward r_t is a numerical signal that characterizes the design objective. It drives the generation process towards a better trajectory. The setting of the reward mechanism is provided in the previous work (Luo et al., 2022a).

3.3 Monte Carlo Tree Search

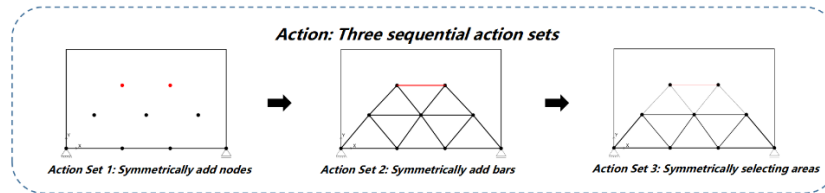
MCTS is applied to solve MDP. MCTS explores the decision space based on the exploration-exploitation heuristic mechanism by accumulating the action value estimates obtained from monte carlo simulation. It performs a large number of dynamic searches to estimate the reward value expectation of diverse actions. MCTS involves four steps: selection, expansion, simulation, and backpropagation. Selection: MCTS is given an initial state containing all the input information. It is called the root state s_r of the search tree. Starting at s_r , a tree policy is recursively applied to descend through the tree until the most urgent state is reached. The tree policy attempts to balance considerations of exploration (look in states that have not been well understood yet) and exploitation (look in states which appear to be potential). The formulation of tree policy is represented as Equation (1), where I_s is an indicator to measure whether a state is urgent or not. N_s and N_f respectively present the visited times of s and its previous state. Note that I_s is positive infinity if s has not been visited. The parameter c controls the exploration of tree policy and the effect of the parameter ϕ is balancing the average and maximum reward. r_s^{best} denotes the maximum reward obtained by s in all simulation processes. Expansion: A state is expandable if it represents a non-terminal state and has unvisited leaf states (leaf state refers to the possible next state). A leaf state will be added to the expandable state by taking an action. Simulation: A monte carlo simulation is run from the expandable state according to the default policy until reaching terminal state. The default policy is that all the actions are randomly selected. Backpropagation: The state value v_s is evaluated based on the simulation result. Equation (2) shows the calculation formula of v_s , where r_i denotes the i^{th} reward obtained by s in N_s simulations. The value will be backpropagated successively. Each sequential execution of the above four steps is called one time of search. These four steps are repeated until reaching the maximum search times. Figure 2 describes the flow of the algorithm and more details about MCTS are provided in previous work (Luo et al., 2022a).

$$I_s = \phi \frac{v_s}{N_s} + (1 - \phi)r_s^{best} + c \sqrt{\frac{2 \ln(N_f)}{N_s}} \quad (1)$$

$$v_s = \sum_{i=1}^{N_s} r_i \quad (2)$$



(a) Four steps in MCTS (Luo et al., 2022a)



(b) Three sequential action sets in MDP

Figure 2. The diagram describing the algorithm

4. EXPERIMENT

To prove that the action adjustment mentioned in Section 3.2 benefits the intelligent design of simply-supported truss, a comparative experiment is conducted in this section. The experiment demonstrates the effect of

considering symmetry and introducing the arch mechanism on the design results.

4.1 Experimental Setup

The experiment requires the design of a simply-supported truss in the rectangular design domain as in Figure 3. Six punctual loads are specified in the bottom part of the truss, a single loading scenario. All bars in this truss are selected from an AISC set of W sections that vary from W14×22 to W14×426 (Construction, A. I. O. S., 1989). Young's modulus E of steel is 201 Gpa, density ρ is 7.85103×10^3 kg/m³, and yield strength f_y is 248.8 Mpa. Constraint conditions are the following: the truss must be geometrically stable. The allowable tensile stress is $0.6f_y$. The highest compression stress σ_i^c of the bar i is obtained from in-plane buckling consideration, computed as Equation (3), where $\lambda_i = L_i/r_i$, $C = \pi\sqrt{2E/f_y}$, and L_i and r_i are the length and gyration radii of the cross section of the bar i , respectively. Permissible displacement of each node is limited to 70 mm. The minimum and maximum longitude of bars should be 5 m and 20 m, respectively.

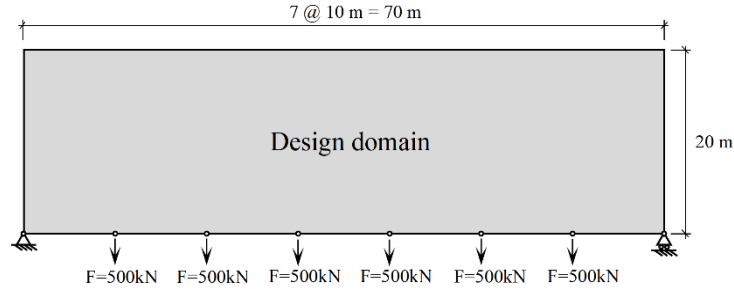


Figure 3. Design domain

$$\sigma_i^c = \begin{cases} \frac{12\pi^2 E}{23\lambda_i^2}, & \text{if } \lambda_i > C \\ \left(1 - \frac{\lambda_i^2}{2C^2}\right)f_y, & \\ \frac{5}{3} + \frac{3\lambda_i}{8C} - \frac{\lambda_i^3}{8C^3}, & \text{if } \lambda_i < C \end{cases} \quad (3)$$

Three tests are carried out in this experiment. The first test (test 1) does not take symmetry and arch mechanism into account. Only symmetry is considered in the second test (test 2). Another test (test 3) introduces both symmetry and arch mechanism. Each test runs five times independently. And all experimental parameters are set exactly the same to ensure fairness.

4.2 Results And Discussion

Table 1 shows the correlation data, where five independent runs are considered in each test. From the comparison results of test 2 and test 1, it can be seen that the former performs much better than the latter, both in terms of the lightest and the average weight. This indicates that the solution can be substantially improved by introducing symmetry. The best and average solutions for test 3 are 15.1% and 14.7% lighter, respectively, than those for test 2. And the best solution for test 3 also costs less search. It illustrates that the arch mechanism can effectively facilitate the design of truss layout.

Table 1. Correlation data of three tests

Test	Lightest weight (kg)	Search times	Average weight (kg)
Test 1	81008	1234439	93627
Test 2	45615	1379946	49273
Test 3	38744	1199925	42028

Figure 4 exhibits the best layouts for three tests. The term "weight" represents the total weight of the truss. Note that a bar in red/blue/yellow color indicates that it is in tension/compression/unstress, respectively. Orange nodes denote that they are newly generated. And the numbers of nodes and bars represent the order in which they are generated. The layout for test 1 is highly irregular. It is concluded that the algorithm can only generate feasible but poor solutions without considering symmetry. Even without introducing arch mechanism, the best layout for test 2 is still inclined to the arch shape. This indicates that the optimization process naturally prefers the arch shape. Due to the introduction of the arch mechanism, the layout for test 3 shows a more fluid and smooth arch profile. Its force transfer mechanism is more rational.

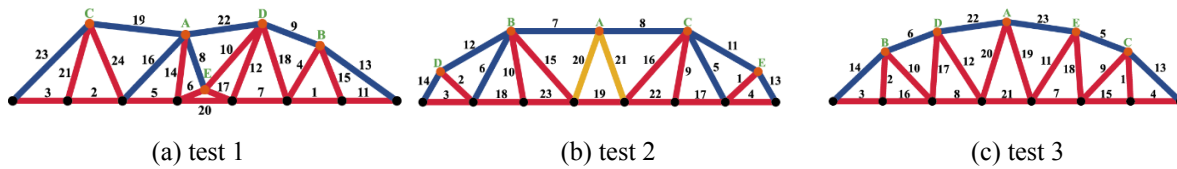


Figure 4. The best layouts for three tests

5. CONCLUSIONS

The paper introduces the concept and characteristics of intelligent design and distinguishes it from traditional design. The kernel of intelligent design lies in the computer simulation of the human brain to perform the design task. Constructing a valid and logical algorithm is the way to realize brain-inspired design. In this study, an intelligent design algorithm for simply-supported planar truss layout is developed. Based on reinforcement learning and understanding of design principles, the truss design process is abstracted as an MDP and solved by MCTS. To condense the solution space and decision process, some structural characteristics (viz. symmetry and arch mechanism) that exist in this particular truss form are abstracted and combined. Finally, through a comparative experiment, it is demonstrated that the introduction of symmetry and arch mechanism results in a more rational force transfer mechanism of the generated truss, which leads to more efficient utilization of materials.

In the experiment, although the algorithm can generate excellent truss layouts, it relies on a huge number of searches, since MCTS is inherently compute intensive. And each run of the algorithm solves an isolated design task offering no transfer of strategies or experience across analogous problems. Future works may aim at optimizing the design chain and introducing deep learning to reduce the reliance on computility and improve the generalization of the algorithm.

ACKNOWLEDGMENTS

This research is funded by Shanghai Qi Zhi Institute, grant number SYXF0120020110.

REFERENCES

- Bellman, R. (1957). A Markovian decision process, *Journal of mathematics and mechanics*, 679-684.
- Bensoussan, A., Lions, J. L., & Papanicolaou, G. (2011). *Asymptotic analysis for periodic structures* (Vol. 374), American Mathematical Soc..
- Brown, N., & Sandholm, T. (2018). Superhuman AI for heads-up no-limit poker: Libratus beats top professionals, *Science*, 359(6374), 418-424.
- Charpentier, A., Elie, R., & Remlinger, C. (2021). Reinforcement learning in economics and finance, *Computational Economics*, 1-38.
- Construction, A. I. O. S. (1989). Manual of steel construction: allowable stress design, *American Institute of Steel Construction: Chicago, IL, USA*.
- Dorn, W. S. (1964). Automatic design of optimal structures, *Journal de mecanique*, 3(6), 25-52.
- Fenton, M., McNally, C., Byrne, J., Hemberg, E., McDermott, J., & O'Neill, M. (2015). Discrete planar truss optimization by node position variation using grammatical evolution, *IEEE Transactions on Evolutionary Computation*, 20(4), 577-589.
- Ho, S. Y., Ko, P., & Lu, C. T. (2022). Scalar and fermion two-component SIMP dark matter with an accidental Z_4 symmetry, *Journal of High Energy Physics*, 2022(3), 1-32.
- Jordan, M. I., & Mitchell, T. M. (2015). Machine learning: Trends, perspectives, and prospects, *Science*, 349(6245), 255-260.
- Kaveh, A., & Khosravian, M. (2022). Size/layout optimization of truss structures using vibrating particles system meta-heuristic algorithm and its improved version, *Periodica Polytechnica Civil Engineering*, 66(1), 1-17.
- Kicinger, R., Arciszewski, T., & DeJong, K. (2005). Evolutionary design of steel structures in tall buildings, *Journal of Computing in Civil Engineering*, 19(3), 223-238.
- Kocsis, L., & Szepesvári, C. (2006). Bandit based monte-carlo planning, *Machine Learning: ECML 2006: 17th European Conference on Machine Learning Berlin, Germany, September 18-22, 2006 Proceedings 17* (pp. 282-293). Springer Berlin Heidelberg.
- Krish, S. (2011). A practical generative design method, *Computer-Aided Design*, 43(1), 88-100.
- Liu, J., & Xia, Y. (2022). A hybrid intelligent genetic algorithm for truss optimization based on deep neural network, *Swarm and Evolutionary Computation*, 73, 101120.
- Luo, R., Wang, Y., Xiao, W., & Zhao, X. (2022a). AlphaTruss: Monte Carlo tree search for optimal truss layout design, *Buildings*, 12(5), 641.
- Luo, R., Wang, Y., Liu, Z., Xiao, W., & Zhao, X. (2022b). A Reinforcement Learning Method for Layout

- Design of Planar and Spatial Trusses using Kernel Regression, *Applied Sciences*, 12(16), 8227.
- Mnih, V., Kavukcuoglu, K., Silver, D., Rusu, A. A., Veness, J., Bellemare, M. G., ... & Hassabis, D. (2015). Human-level control through deep reinforcement learning, *nature*, 518(7540), 529-533.
- Polydoros, A. S., & Nalpantidis, L. (2017). Survey of model-based reinforcement learning: Applications on robotics, *Journal of Intelligent & Robotic Systems*, 86(2), 153-173.
- Raina, A., Cagan, J., & McComb, C. (2022). Design strategy network: a deep hierarchical framework to represent generative design strategies in complex action spaces, *Journal of Mechanical Design*, 144(2).
- Raina, A., McComb, C., & Cagan, J. (2019). Learning to design from humans: Imitating human designers through deep learning, *Journal of Mechanical Design*, 141(11).
- Raina, A., Puentes, L., Cagan, J., & McComb, C. (2021). Goal-directed design agents: Integrating visual imitation with one-step lookahead optimization for generative design, *Journal of Mechanical Design*, 143(12).
- Rajeswaran, A., Mordatch, I., & Kumar, V. (2020, November). A game theoretic framework for model based reinforcement learning, *International conference on machine learning* (pp. 7953-7963). PMLR.
- Shea, K. (1997). *Essays of discrete structures: purposeful design of grammatical structures by directed stochastic search*. Carnegie Mellon University.
- Silver, D., Huang, A., Maddison, C. J., Guez, A., Sifre, L., Van Den Driessche, G., ... & Hassabis, D. (2016). Mastering the game of Go with deep neural networks and tree search, *nature*, 529(7587), 484-489.
- Simon, H. A. (2019). *The Sciences of the Artificial, reissue of the third edition with a new introduction by John Laird*. MIT press.
- Sutton, R. S., & Barto, A. G. (2018). *Reinforcement learning: An introduction*. MIT press.
- Watson, M., Leary, M., & Brandt, M. (2022). Generative design of truss systems by the integration of topology and shape optimization, *The International Journal of Advanced Manufacturing Technology*, 118(3-4), 1165-1182.
- Xia, L., Xia, Q., Huang, X., & Xie, Y. M. (2018). Bi-directional evolutionary structural optimization on advanced structures and materials: a comprehensive review, *Archives of Computational Methods in Engineering*, 25, 437-478.
- Zeng, Q., Zhu, S., Li, Z., & Guo, X. (2023). Self-adaptive triangular mesh generation framework for free-form single-layer reticulated shells based on virtual interaction forces, *Automation in Construction*, 148, 104750.
- Zhao, X. . (2022). AI in civil engineering, *AI Civ. Eng.* 1, 1.
- Zhu, C., & Yin, X. (2005). Analysis on significance of conceptdesign and its application, *Architecture Technology*, 36(8), 3.
- Zhu, S., Ohsaki, M., Hayashi, K., & Guo, X. (2021). Machine-specified ground structures for topology optimization of binary trusses using graph embedding policy network. *Advances in Engineering Software*, 159, 103032.

MODEL BUILDING FOR LANE LINE EXTRACTION USING HIGH-DEFINITION MAP

Ryuichi Imai¹, Kenji Nakamura², Yoshinori Tsukada³, Noriko Aso⁴, and Jin Yamamoto⁵

- 1) Ph.D., Prof., Faculty of Engineering and Design, Hosei University, Tokyo, Japan. Email: imai@hosei.ac.jp
- 2) Ph.D., Prof., Faculty of Information Technology and Social Sciences, Osaka University of Economics, Osaka, Japan. Email: k-nakamu@osaka-ue.ac.jp
- 3) Ph.D., Assoc. Prof., Faculty of Business Administration, Setsunan University, Osaka, Japan. Email: yoshinori.tsukada@kjo.setsunan.ac.jp
- 4) Managing Officer, Technology, Dynamic Map Platform Co., Ltd., Tokyo, Japan. Email: Aso.Noriko@dynamic-maps.co.jp
- 5) Ph.D. Candidate, Graduate School of Engineering and Design, Hosei University, Tokyo, Japan. Email: jin.yamamoto.2j@stu.hosei.ac.jp

Abstract: In public works projects in Japan, a large amount of point cloud data has been measured and accumulated at various locations through the introduction of mobile measurement system (MMS) and terrestrial laser scanners (TLS). Point cloud data, which is the outcome of laser surveying, is a huge collection of 3D points having position coordinates, reflection intensity, and RGB. Various uses of point cloud data are expected to be developed. One of the main uses of point cloud data is the preparation of HD maps, which serve as basic maps for autonomous driving. Currently, the HD maps in Japan cover about 30,000 km and will be expanded to about 130,000 km including expressways and ordinary roads. Since HD maps are prepared by manually joining and processing point cloud data, it is desirable to improve the efficiency of preparing HD maps. Therefore, it is required to establish an efficient and comprehensive method of developing lane lines for the development, maintenance, and updating of HD maps. In this study, we proposed a method for automatically generating AI training data for automatic extraction of lane lines using the area data of lane lines generated from HD maps. This allowed extraction of lane lines from point cloud data with an average F-measure of 0.9 or higher.

Keywords: HD map, Point cloud data, Lane line, Deep learning

1. INTRODUCTION

In public works projects in Japan, a large amount of point cloud data has been measured and accumulated at various locations through the introduction of mobile measurement system (MMS) and terrestrial laser scanners (TLS). Since point cloud data, which is the outcome of laser surveying, is a huge collection of 3D points having position coordinates, reflection intensity, and RGB, development of a variety of uses can be expected. Focusing on road space, examples include the maintenance and updating of High Definition Map (hereinafter referred to as "HD map") (Nikkei xTECH. Active, 2023), which is under research and development for autonomous driving. The performance of laser surveying instruments that obtain the basic data for HD maps is improving day by day. The sections that capture five or more satellites retain map information level 500, which satisfies the requirements of road management (Kitagawa et al., 2016). In addition, from the Cabinet Office's Strategic Innovation Promotion Program (SIP) "Automated Driving System," HD maps define road geographic features such as lane lines, road markings, road signs and traffic signals, which are essential for automated driving use cases (Koyama & Shibata, 2016). Currently, HD maps of Japan cover about 30,000 km. They are expected to be expanded to about 130,000 km including expressways and ordinary roads by Fiscal Year 2024 (Nikkei xTECH, 2021). Manual development of road features requires an enormous amount of labor for future maintenance of HD maps. In particular, lane lines, which are plane features painted on the roadway, require the highest cost among the roadway features as the HD maps are expanded. Consequently, an efficient and exhaustive method for developing lane lines using AI is required.

As one of its solutions provided in an existing study, Lingfei et al. (Lingfei et al., 2019) developed an algorithm to extract lane lines by setting a threshold for reflection intensity and a threshold for voxel grid by Otsu's method. Validated on approximately 20 million measured data points of roads and 22 million measured data points of intersections, the algorithm extracts lane lines with an accuracy of 0.97 for F-measure, which is the harmonic mean of the precision and recall. However, it is difficult to define a unique value for the threshold because the reflection intensity of a lane line varies depending on the weather conditions and laser survey equipment. Thus, Emori et al. (Emori et al., 2019) used machine learning to have it learn the position coordinates, reflection intensity, and RGB of the point cloud data and verified it for the data about 11 map borders. One of the map borders of verification data has a road distance of approximately 50 m and approximately 2 million points. As a result of calculating F-measure for each map border, the maximum and minimum F-measure were 0.94 and 0.18, respectively, and the average F-measure for the 11 map borders was 0.66. The cause for decrease in F-measure was that in some of the map borders the shadows of surrounding buildings overlapped with the white line paint and consequently the lane lines and crosswalks were not extracted. From the above, diversity of training data is

required to build a highly accurate lane line extraction model. Therefore, a large amount of training data is required. However, since the training data are created manually, there is a problem that generation of training data is time-consuming and labor-intensive.

In this study, we propose a method to automatically generate training data for AI to extract lane lines using area data that can specify 3D space generated from HD maps. Then, a model for automatic extraction of lane lines (hereinafter referred to as the "extraction model") is built by having AI learn the generated training data. This allows for reduction in the generation time of training data and building of an extraction model capable of handling the reflection intensity that varies depending on the laser measurement device and measurement environment. Furthermore, lane lines can be extracted efficiently and comprehensively by applying the extraction model to the measured point cloud data. Therefore, the model is expected to contribute to labor saving in preparing lane lines.

From the above, the purpose of this study is to build a model for extracting lane lines using area data generated from HD maps. In specific, first of all for data preprocessing, the reflection intensity of a lane line is normalized to 255, and the point cloud data is filtered by setting a threshold value based on the histogram of the reflection intensity. Then, the point cloud data of the lane line is extracted using the area data generated from the HD map, and an extraction model is built using the extracted point cloud data. Finally, the extraction model is applied to a section different from the training data to verify the usefulness of the extraction model.

2. METHOD

2.1 Process Flow

As shown in Figure 1, the proposed method consists of the learning part and the determination part. In the learning part, the point cloud data and HD map are used to generate training data for the extraction model. First, CSF filter of CloudCompare (Zhang et al., 2016) is applied to the point cloud data to separate the point cloud data into ground surface and non-ground surface. Since the lane line is a roadway feature located on the ground surface, the point cloud data of the ground surface is used in generating the training data. Next, a histogram of the reflection intensity is created for the point cloud data of the ground surface using the function of CloudCompare. Then, a threshold value is set based on the histogram and the point cloud data is filtered to extract candidate points for the lane line. The threshold value of the reflection intensity is defined as the mean of the reflection intensities plus the standard deviation, taking advantage of the characteristics that the reflection intensity of a lane line is higher than that of a roadway. In generating training data, the existing method (Imai et al., 2022) is used to generate area data from the HD map and extract lane lines from the filtered point cloud data. Figure 2 shows the relationship between the area data and point cloud data. The area data is created by making a closed polyline on an arbitrary plane and extruding its shape vertically at an arbitrary height. A three-dimensional space is specified with this area data to allow extraction of the lane line from the point cloud data. Finally, Training data is generated by assigning an attribute value indicating the lane line to the extracted point cloud data.

The determination part divides the point cloud data into the ground surface and the non-ground surface using the same procedure as the learning part. Then, it filters the point cloud data of the ground surface where the lane line is located with the threshold value. Finally, the extraction model built in the learning part is applied to the filtered point cloud data to determine the lane lines.

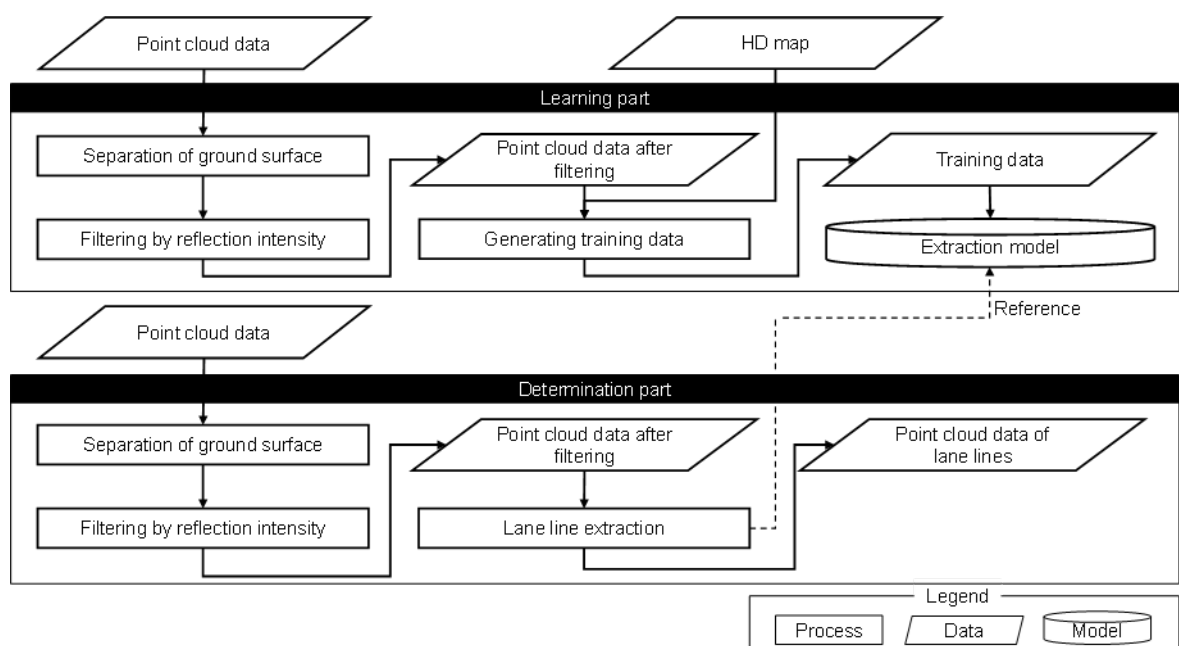


Figure 1. Process flow of the proposed method

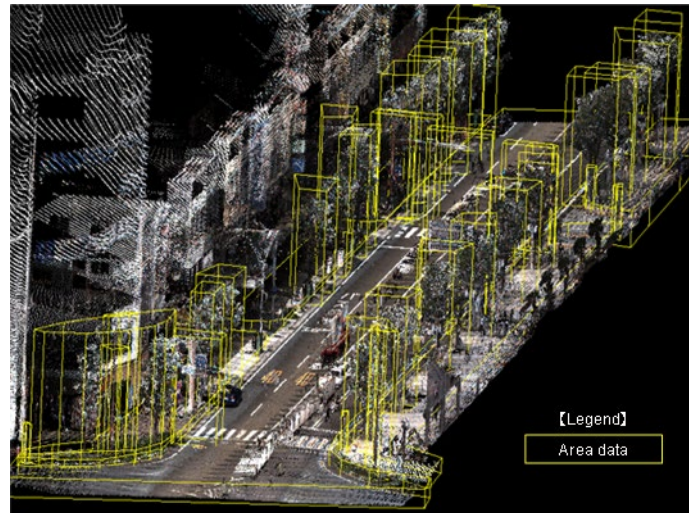


Figure 2. Relationship between area data and point cloud data

2.2 Specifications of Point Cloud Data

Point cloud data obtained by MMS or TLS retains the reflection intensity in addition to the position information based on an arbitrary coordinate system. On the other hand, RGB is not always given because superimposition processing of the point cloud data and a colored image is required. Therefore, although RGB is useful information for extracting lane lines, to ensure versatility of the extraction model in this study, the value of reflection intensity normalized to 255 was given to RGB using the function of CloudCompare to convert RGB of point cloud data. Figure 3 shows the point cloud data to which the reflection intensity values are given. In this study, we use the point cloud data with excellently measured lane lines shown on the left side of Figure 3. The histogram of reflection intensity is shown on the right side of Figure 3. In the histogram in Figure 3, the reflection intensity values are distributed between 0 and about 60,000, with the mean of about 30,648 and the standard deviation of about 9,522. Accordingly, the filtering threshold is approximately 40,170, which is the mean plus the standard deviation.

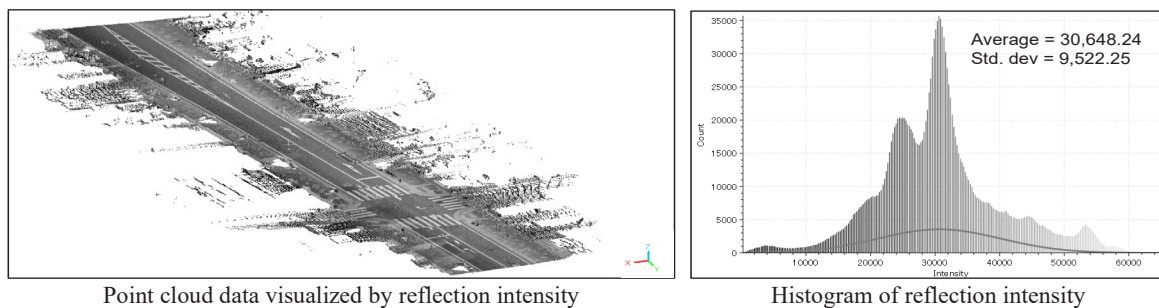


Figure 3. Point cloud data with reflection intensity given to RGB

2.3 Procedure for Generating Training Data

Figure 4 shows the details of generation of training data in the learning part of Figure 1. The details are described in STEP1 through STEP6 as shown in Figure 4. The processing steps are as follows.

STEP1: Apply CSF filter to the point cloud data and extract the point cloud data of the ground surface.

STEP2: Make a histogram of the reflection intensity, then filter the point cloud data above the threshold value calculated by adding the standard deviation to the mean value of the reflection intensity.

STEP3: Superimpose the area data generated from the HD map on the filtered point cloud data to extract the lane line.

STEP4: Give a label, which is the attribute value indicating the lane line, to the point cloud data extracted using the area data.

STEP5: Give other labels to point cloud data located in the vicinity other than the lane line.

STEP6: Combine the point cloud data from STEP4 and STEP5 to generate training data.

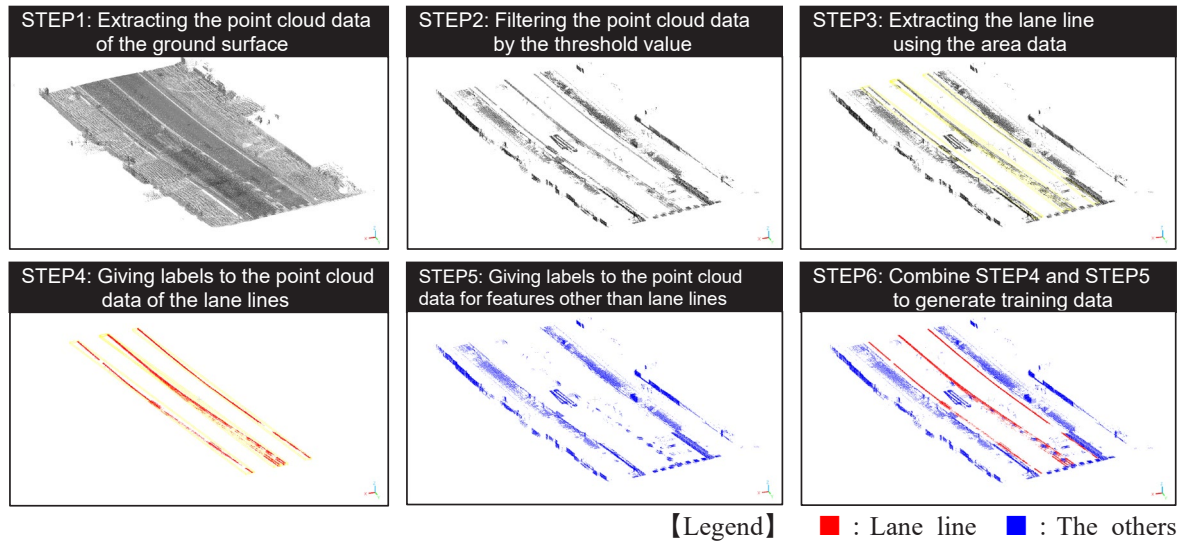


Figure 4. Procedure for generating training data

2.4 Conditions for Building the Extraction Model

In this study, we build a lane line extraction model using ConvPoint (Boulch, 2020), which is capable of acquiring excellent accuracy in determining road features from point cloud data. Since the object of extraction is limited to lane lines, the extraction model is build using binary classification of "lane lines" and "the others". For the parameters of the extraction model, that of Epoch was set to 100 and Iteration to 1,000 in reference to the default values. In addition, in consideration of over-learning, the model with the optimal Epoch is selected by applying early stopping, which stops learning when Loss cannot be minimized. In early stopping, a parameter can be set to stop learning when a specific Epoch is reached, at which the loss is not improved, and no further improvement is observed. In this study, this parameter was set to three patterns: 3, 5, and 7, to construct the model.

3. EXPERIMENT

3.1 Experiment Overview

In this experiment, the time required to generate training data manually is compared with the time using the proposed method. Then, the lane line extraction model is applied to the laser-measured point cloud data to verify the accuracy of the lane line determination. The target section of this experiment is an approximately 1.0-km stretch of an ordinary road in Shizuoka Prefecture, Japan. Table 1 shows a summary of the point cloud data used in this experiment. The number of points for the training data for the extraction model is 352,996 for lane lines, and 1,013,127 for the others. The range of reflection intensity for the verification data is the same as that of the training data. Therefore, the data was filtered by the reflection intensity threshold according to the procedure for generating the training data. For this validation data, we selected a different dataset than the training data. Additionally, correct answer data is generated for two map borders with a road section of approximately 50 meters. As Table 1 shows, the number of points for verification data 1 is 32,156 for lane lines and 40,221 for the others, while the number of points for verification data 2 is 33,655 for lane lines and 71,857 for the others.

The precision, recall, and F-measure are used as the evaluation indicators of the extraction model. In the accuracy evaluation, the point cloud data extracted using the area data is defined as the correct answer, and each evaluation indicator is calculated by aggregating the correct point cloud data and the point cloud data determined by the extraction model.

Table1. Point cloud data used for experiments

Label type	Number of points for the training data (points)	Number of points for verification data (points)	
		Verification data 1	Verification data 2
Lane line	352,996	32,156	33,655
Others	1,013,127	40,221	71,857

3.2 Results of Building an Extraction Model

Table 2 shows the time required to generate all of the training data for the target section manually and with the proposed method. Note that the time required to separate the ground surface and to create the histogram of reflection intensities are not included in the time required because these processes can be done automatically using the functions of CloudCompare. Table 2 shows that the time required for manual generation of training data was approximately 34 minutes for extracting lane lines and approximately 1 minute for assigning lane line attribute values to the point cloud data, for a total time of approximately 35 minutes. The proposed method required approximately 7 minutes for extracting lane lines and 8 seconds for giving lane line attribute values to the point cloud data, for a total time of approximately 7 minutes. As a result, the proposed method allowed reduction in the time required to generate training data by approximately 28 minutes.

Figure 5 shows the transition of the learning of the built extraction model. In the learning of the extraction model, Loss of the extraction model and the IoU, an indicator that expresses the degree of overlap of bounding boxes as a numerical value ranging from 0 to 1, are calculated. Also, since the early stopping parameter was set to 3, 5, and 7, the Epochs of the extraction model differ. As a result of building the extraction model, the model to which early-stopping was not applied continued to learn up to 100 Epochs, which is the default value. The model stopped training at 46 Epochs with parameter 3, and at 62 Epochs with parameter 5. On the other hand, with parameter 7, the model continued to learn up to the same 100 Epochs as without using early stopping. IoU at 100 Epochs was 0.975 and Loss was 1.96×10^{-7} . Similarly, IoU at 100 Epochs with parameter 7 was 0.975 and Loss was 1.85×10^{-7} . IoU at 62 Epochs was 0.969 and Loss was 2.41×10^{-7} . IoU at 46 Epochs was 0.964 and Loss was 2.85×10^{-7} . For this reason, both models learned well because Loss values for respective models are as close to 0 as possible.

Table 2. Time required for generating training data manually and with proposed method

Work item	Time required to generate training data	
	manually	Proposed method
Process to extract lane lines from point cloud data	34 minutes 26 seconds	6 minutes 59 seconds
Process for giving the lane line attribute values to point cloud data	53 sec.	8 sec.
Total processing time	35 minutes 19 seconds	7 minutes 7 seconds

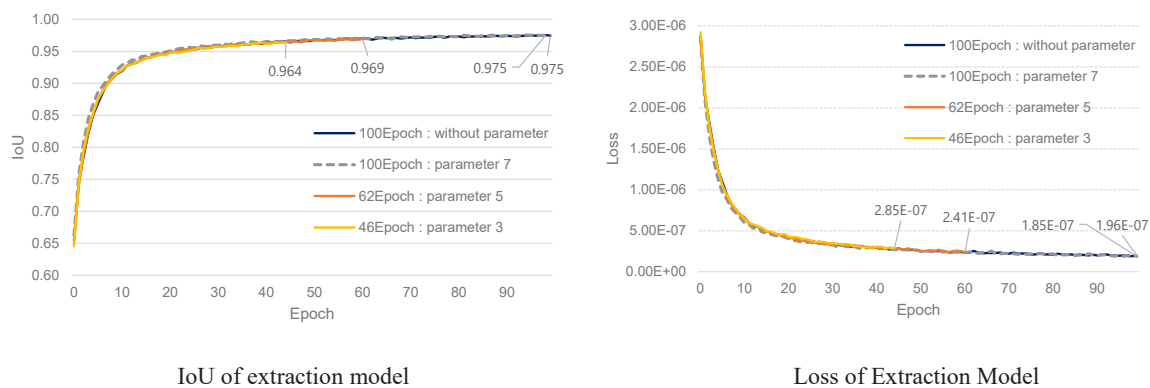


Figure 5. Transition of learning of the extraction model

3.3 Results of Applying the Extraction Model and Discussion

Table 3 shows the lane line determination accuracy. Parameters were set to 3, 5, and 7, and models with and without early stopping were applied to the validation data to calculate the lane line determination accuracy. It should be noted that both the model with a parameter of 7 and the model without early stopping continued learning up to 100 Epochs, resulting in identical accuracies for lane line determination. In validation data 1, the precision, recall, and F-measure of the model at 46 Epochs were all 0.96. At 62 Epochs, the precision was 0.95, the recall was 0.93, and the F-measure was 0.94. At 100 Epochs, the precision was 0.97, the recall was 0.94, and the F-measure was 0.95. For validation data 2, the model at 46 Epochs achieved a precision of 0.95, a recall of 0.89, and an F-measure of 0.92. At 62 Epochs, the precision was 0.97, the recall was 0.78, and the F-measure was 0.87. Additionally, at 100 Epochs, the precision was 0.95, the recall was 0.80, and the F-measure was 0.87. Consequently, the average F-measures for the models were 0.94 at 46 Epochs and 0.91 for both 62 Epochs and 100 Epochs.

Table 3. Accuracy of lane line determination

Model	Parameter	Evaluation indicator	Verification data		Average
			1	2	
Model of 46Epoch	3	precision	0.96	0.95	0.96
		recall	0.96	0.89	0.93
		F-measure	0.96	0.92	0.94
Model of 62Epoch	5	precision	0.95	0.97	0.96
		recall	0.93	0.78	0.86
		F-measure	0.94	0.87	0.91
Model of 100Epoch	7 and without parameter	precision	0.97	0.95	0.96
		recall	0.94	0.80	0.87
		F-measure	0.95	0.87	0.91

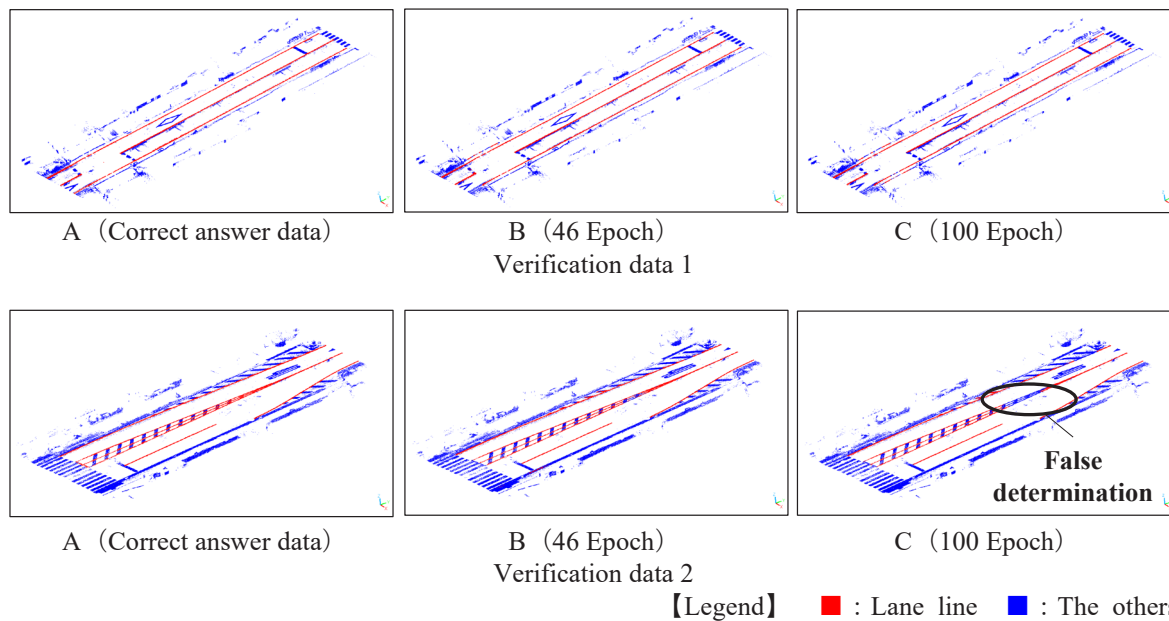


Figure 6. Determination results of lane lines

Comparing each model, the 46Epoch model was selected because the 46Epoch model estimated by early topping of parameter 3 has the highest decision accuracy. On the other hand, in validation data 2, the recall significantly decreased to 0.78 and 0.80 for 62 Epochs and 100 Epochs, respectively. The results in Table 3 show that the accuracy varies depending on the parameters adjusted at each Epoch. The AI used in this study does not return a constant value, and the numerical value of the result fluctuates from Epoch to Epoch. Therefore, it is difficult to determine the exact factor that caused the decrease in the value. Also, a lower F measure means that the model does not fit the validation data. However, comparing the mean of the F measure for Epoch 46 and Epoch 100, the difference is 0.03, which is considered to be within the margin of error. In addition, since the F measure is greater than 0.9 for both models, they are considered to be correctly trained.

Figure 6 shows the results of the lane line determination. In Figure 6, the results of 46 Epochs, which had the highest accuracy in Table 3, and the default 100 Epochs are shown as examples. A in Figure 6 is the correct answer data. B in Figure 6 shows the determination result using the 46 Epoch model with early stopping applied. C in Figure 6 shows the determination result using the 100 Epoch model without early topping. In the verification data 1-B and C, we confirmed that the correct lane lines were determined well in red. Furthermore, the fact that there was no part with false determination of lane lines suggests that the point cloud data for the lane lines were extracted without omission. Comparing the verification data 2-B and C, B showed better result of determining the point cloud data of the lane line. Focusing on the verification data 2-C, some part shows false determination of lane lines in blue, which were not properly determined. However, the part with false determination in 2-C was determined successfully as lane lines in the verification data 2-B. From these results, it can be considered that the application of early stopping allowed the selection of Epochs that are expected to improve the accuracy of the lane

line determination. In B and C of verification data 1 and 2, although there were crosswalks and road markings that had the same characteristics as the lane lines, they were properly determined as the points other than the lane lines. On the other hand, it is considered to be difficult to determine the lane lines in areas where the lane lines have completely disappeared due to deterioration over time.

4. CONCLUSIONS

In this study, point cloud data of the lane lines were extracted using the area data generated from the HD map, and the training data was automatically generated. Using the generated training data, an extraction model of lane lines was built. As a result of applying the extraction models to the validation data, the model with early stopping achieved a maximum F-measure of 0.94, while the model without early stopping reached a maximum F-measure of 0.91. Accordingly, it was made clear that either of these extraction models is capable of extracting the lane lines from the point cloud data with high accuracy. Compared to existing studies, the proposed method has a significant advantage in that it can automate the generation of training data for models that automatically extract lane lines. Furthermore, by utilizing the models developed in this study, the lane lines defined in the HD map can be automatically determined and extracted. Consequently, the models are expected to contribute to the continuous maintenance of lane lines and labor saving of updating work.

In the future, we will verify the accuracy of the lane line extraction model using point cloud data with different reflection intensities, as well as devise a method to enclose the outer shape of the lane lines with polygons in order to analyze the lane lines, which are the result of determination, in detail. In addition, there is a concern that filtering by reflection intensity may allow inclusion of the point cloud data of the lane lines of which the reflection intensity has deteriorated over time. Therefore, it is necessary to verify whether the point cloud data of the lane lines are not excessively filtered.

ACKNOWLEDGMENTS

Subsidy for this study by the Grant-in-Aid for Research and Development of Construction Technology from the Ministry of Land, Infrastructure, Transport and Tourism is gratefully acknowledged.

REFERENCES

- Boulch, A. (2020). ConvPoint: Continuous convolutions for point cloud processing, *Computers & Graphics*, 88, pp.24-34.
- Emori, H., Saito, M., Sada, T. and Okajima, M. (2019). A Study on Automatic Extraction of 3D Point Cloud by Machine Learning for Road Lines, *Ser. F3 (civil engineering informatics)*, Journal of Japan Society of Civil Engineers, 75 (2), pp. I_114-I_122.
- Imai, R., Nakamura, K., Tsukada, Y., Tsuchida, N. and Yamamoto, J. (2022). Generation on Semantic Point Cloud Data of Road Features Using Dynamic Maps, *Ser. F3 (civil engineering informatics)*, Journal of Japan Society of Civil Engineers, 78 (2), pp. I_93-I_102.
- Kitagawa, T., Tsuchida, N. and Yasui, Y. (2016). High-Precision Map Generation Technology, *Systems, Control and Information*, Control and Information Engineers, 60 (11), pp.475-480.
- Koyama, H. and Shibata, Y. (2016). Development of dynamic maps for autonomous driving, *Systems, Control and Information*, Control and Information Engineers, 60 (11), pp.463-468.
- Lingfei, M., Tianyu, W., Ying, L., Jonathan, L., Yiping, C. and Michael, C. (2019). Automated Extraction of Driving Lines from Mobile Laser Scanning Point Clouds, *29th International Cartographic Conference*, pp.1-6.
- Nikkei xTECH. Active (2023) High Definition 3D Map: website:
<https://active.nikkeibp.co.jp/atcl/act/19/00146/061000018/>
- Nikkei xTECH. (2023). HD map for autonomous driving on general roads website:
https://special.nikkeibp.co.jp/atclh/NXT/21/dynamic_maps1129/
- Zhang, W., Qi, J., Wan, P., Wang, H., Xie, D., Wang, X. and Yan, G. (2016) An Easy-to-Use Airborne LiDAR Data Filtering Method Based on Cloth Simulation, *Remote Sensing*, MDPI, 8 (6), pp.501-509.

FUNDAMENTAL STUDY ON EXTRACTION METHOD OF LICENSE PLATE CLASSIFICATION NUMBER USING VIDEO IMAGES

Ryuichi Imai¹, Daisuke Kamiya², Yuhei Yamamoto³, Masaya Nakahara⁴,
Wenyuan Jiang⁵, Koki Nakahata⁶, and Ryo Sumiyoshi⁷

- 1) Ph.D. Prof, Faculty of Engineering and Design, Hosei University, Tokyo, Japan. Email: imai@hosei.ac.jp
- 2) Ph.D. Assoc. Prof, Faculty of Engineering, University of the Ryukyus, Okinawa, Japan. Email: d-kamiya@tec.u-ryukyu.ac.jp
- 3) Ph.D. Asst. Prof, Faculty of Environmental and Urban Engineering, Kansai University, Osaka, Japan. Email: y_yamamo@kansai-u.ac.jp
- 4) Ph.D. Asst. Prof, Faculty of Information Science and Arts, Osaka Electro-Communication University, Osaka, Japan. Email: nakahara@oecu.jp
- 5) Ph.D. Assoc. Prof, Faculty of Engineering, Osaka Sangyo University, Osaka, Japan. Email: kyo@ce.osaka-sandai.ac.jp
- 6) Ph.D. Candidate, Graduate School of Informatics of Informatics, Kansai University, Osaka, Japan. Email: k964962@kansai-u.ac.jp
- 7) Graduate Student, Graduate School of Engineering and Design, Hosei University, Tokyo, Japan. Email: ryo.sumiyoshi.4t@stu.hosei.ac.jp

Abstract: Traffic surveys in Japan require a large number of people. However, it is becoming increasingly difficult to secure surveyors due to the population decline. In recent years, the Ministry of Land, Infrastructure, Transport and Tourism (MLIT) has been promoting survey methods using ICT and IoT; however, the cost of introducing machinery is huge. Against this background, survey methods that use AI for analyzing video images captured by CCTV cameras and video cameras installed to monitor roads are attracting attention. In existing studies, the number of passing vehicles is counted separately for light and heavy vehicles by using deep learning. We think that the survey method using AI can be advanced by adding an approach of subdividing vehicle types such as light passenger cars and heavy special-purpose vehicles based on the results of recognizing license plates to the function of this method for determining whether a vehicle is light or heavy. Vehicles in Japan can be distinguished between light and heavy vehicles by recognizing each classification number, which consists of three digits on the license plate. In this study, we devised a method for extracting classification numbers from the video images captured for traffic surveys, using an object detection technique based on deep learning. Experimental results show that the proposed method is capable of extracting classification numbers with high accuracy.

Keywords: License plate recognition, Vehicle type determination, Traffic volume investigation, Deep learning, Image processing

1. INTRODUCTION

1.1 Research Background and Objectives

In Japan, traffic surveys have been conducted in order to grasp the current status and problems of road traffic and to formulate future road development plans (MLIT, 2010). In these surveys, surveyors count the number of passing vehicles separately for light and heavy vehicles by visually checking the shape and license plates of the vehicles passing through the survey points. However, the survey costs expensive because it requires a large number of personnel. In addition, it has become hard to secure surveyors due to the population decline. Therefore, MLIT has been promoting a survey method that utilizes ICT and IoT (MLIT, 2017). However, the high cost of introducing machinery makes it difficult to introduce such a method, and more efficient and labor-saving surveys have not been realized yet.

Against this background, a method for counting the number of passing vehicles by analyzing the video images captured by CCTV cameras and video cameras installed for road surveillance with AI is attracting attention. An existing study (Nakahata et al., 2022) shows that it is possible to determine light and heavy vehicles and count their respective cross-sectional traffic volumes with high accuracy by using the methods of object detection, image area division, and image classification based on deep learning. However, There is a problem that the determination accuracy of light and heavy vehicles goes down in case of failure to identify the parts of vehicles. The determination results of the existing method can be corrected if this method can be supplemented by some other method that recognizes license plates, identifies the identical vehicle based on the recognition results, and classifies vehicles into smaller categories such as light passenger cars, standard freight vehicles, and heavy special-purpose vehicles. We considered that this would allow upgrading the existing AI-based survey method. A Japanese license plates (Figure 1) contains a serial designation number consisting of four digits as well as a classification number that allows determining whether a vehicle is light or heavy by recognizing its first digit. The methods of recognizing Japanese license plates include the automatic license plate reader (N system) installed on roads for criminal investigations (National Police Agency, 1985) and a method to recognize license plates from video images captured by the video cameras installed on the roadside (Ozaki et al., 2021). However, the former method has a problem

that it is not capable of counting the number of passing vehicles separately for light and heavy vehicles. The latter method has another problem that it is not capable of recognizing license plates of vehicles traveling on the adjacent lanes because the video cameras are installed at a low position. To solve these problems, we developed a method for extracting and recognizing serial designation numbers using video images captured from a high position with a wearable camera, which is easier to install than a video camera, having proved this allows recognition of serial designation numbers with high accuracy (Imai et al., 2023). Thus, we considered that it might be possible to extract and recognize the classification numbers of which the character size is smaller than that of the serial numbers. However, since the character size of a classification number is small, areas other than the classification number may be erroneously extracted. For this reason, we develop a highly robust method by using a deep learning method with high accuracy.

Therefore, the purpose of this study is to devise a method for extracting the classification numbers using video images captured from high positions as a first step toward recognizing the classification numbers.



Figure 1. Contents of a license plate

1.2 Japanese License Plate

The size of a Japanese license plate is 165 x 330 mm for light vehicles and 220 x 440 mm for heavy vehicles. A license plate consists of two-tiered character strings, with the Transport Branch Office and classification number in the upper row, and a hiragana letter and a serial designation number in the lower row. The size of each character is different for each type, with the size of the Transport Branch Office and hiragana letter being 40 x 40 mm for both light and heavy vehicles. The character size for the classification number is 40 x 23 mm for light vehicles and 40 x 33 mm for heavy vehicles. The size for serial designation number is 80 x 40 mm for light vehicles and 120 x 60 mm for heavy vehicles. The Transport Branch Office that has jurisdiction over the address where the vehicle owner lives is put as a name of its place on the left side of the upper row. These names of the places include "Sakai", "Osaka", "Naniwa", "Iseshima", and so forth, consisting of 2 names of places with 1 letter, 107 names with 2 letters, 20 names with 3 letters, and 2 names with 4 letters, 131 names in total. The classification number is put to the right of the Transport Branch Office, consisting of three digits. The vehicle type, such as light passenger cars, standard freight vehicles, and heavy special-purpose vehicles, can be determined by the first digit. License plates issued before 1998 may have a two-digit classification number, and as in the three-digit case, the vehicle type can also be determined by the first digit. Hiragana letter refers to the letter put on the left side of the lower row and can be used to determine the use of the vehicle, such as private, rental, or commercial use. The serial designation number refers to the characters to the left of the hiragana letter, consisting of 4-digit Arabic numerals, with combinations from "1" to "9999". License plates are available in four colors: yellow, white, black, and green, which can be used to identify light vehicles, standard vehicles, and commercial vehicles. The license plate comes in four colors: yellow, white, black, and green. In recent years, license plates have been diversified as those with some patterns have been issued to promote revitalization of a region or tourism.

In this study, we focused on classification numbers that can be used to distinguish between light and heavy vehicles in order to improve the accuracy of the determination between light and heavy vehicles. An existing study (Imai et al., 2023) has shown that serial designation numbers can be extracted with high accuracy using a process of detecting consecutive white pixels. However, since the character size of a classification number is smaller than that of a serial designation number, it is difficult to distinguish a noise from a classification number. Therefore, we considered that an object detection method based on highly accurate deep learning could be used to correctly extract the classification number.

1.3 Existing research on the extraction and recognition methods of license plates

Most research on license plates in Japan has focused on using the serial designation number to identify vehicles. For instance, one method concentrates on the luminance histogram of letter boundaries to extract the serial designation number (Nakao, 2011). This approach can accurately extract characters by focusing on minute changes in luminance in the gaps between characters. Another method utilizes the color difference between the license plate's background and its letters (Haneda, & Hanaizumi, 2013). This technique employs image binarization and labeling to separate the characters from the license plate's background. However, these methods can be challenging to apply when the vehicle cannot be captured from the front, or when the image is blurred.

Recently, methods based on deep learning have been garnering attention. An example of such is a method that uses a convolutional neural network (CNN) to recognize characters on license plates captured by security

cameras (Tsuji et al., 2018). This approach improved recognition accuracy in images containing degradation, such as insufficient resolution and noise, by using a multi-structured CNN. Another method detects vehicles in video images taken from the roadside and recognizes license plates (Ozaki et al., 2021). This technique can count vehicles separately for small and large vehicles using deep learning, and it can recognize license plates with high accuracy through template matching. However, these methods face challenges, including low recognition accuracy for moving vehicles and their applicability only to single-lane roads.

In existing research conducted outside of Japan, one method uses YOLO v2 to detect license plates and then employs Mask R-CNN to recognize characters (Cheng-Hung, & Ying, 2019). In this method, the use of deep learning has demonstrated that characters can be recognized with high accuracy if the shooting angle is within 45°. However, no existing studies have found a method for extracting license plate classification numbers from video images taken from high vantage points for traffic volume surveys. Therefore, in this study, we develop a method to extract license plate classification numbers by applying deep learning to video images of vehicles shot from oblique angles with a camera installed at a high location.

2. METHOD

2.1 Process Flow of the Proposed Method

Figure 2 shows the flow of the process proposed in this study. The method consists of the learning function, the cross-sectional line setting function, and the extraction function.

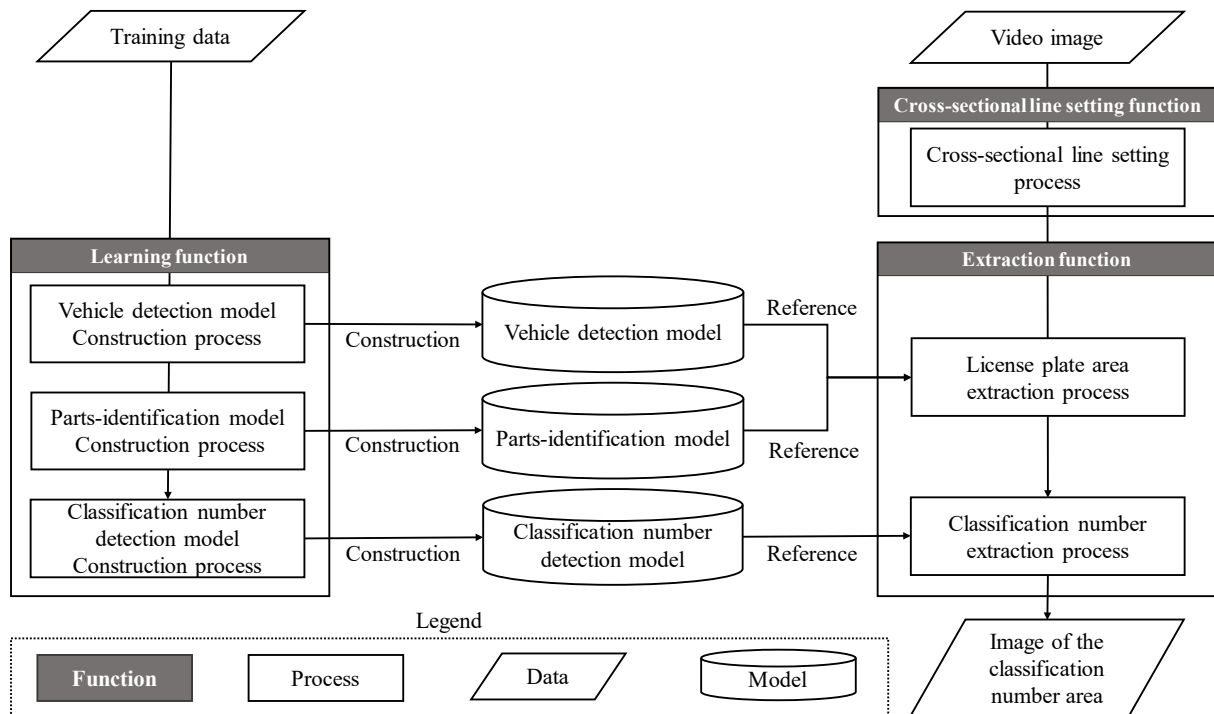


Figure 2. Process flow of the proposed method

2.2 Input/Output Data and Preprocessing

The learning function uses the images that labeled the area of the vehicle, the images that labeled parts of the vehicle such as the front and back, and the images that labeled the location of the classification number as the input, and the training model as the output. The extraction function, similar to an existing study (Imai et al., 2019), uses the video images captured at 4K resolution using a video camera set at a height of about 4.0 m from the ground and a vertical angle of about 20 degrees as the input, and the extraction results of the classification numbers as the output. As a pre-processing step for the estimation function, two cross-sectional lines are set on the video image using the cross-sectional line setting function.

2.3 Learning Function

This function consists of a process of constructing vehicle detection models, a process of constructing parts-identification models, and a process of constructing classification number detection models.

(1) Process of constructing vehicle detection models

The training data for this process is image labeling the area of the vehicle within the image shown in

Figure 3 a. The model is constructed using YOLOv4 (Bochkovskiy et al., 2020), which is a deep learning object detection method.

(2) Process of constructing parts-identification models

The training data for this process are gray-scaled vehicle area images shown in Figure 3 b and 9 kinds of manually labeled vehicle parts (front, back, left side, right side, top, front wheels, rear wheels, windshield, and license plate). The model is constructed using SegNet (Badrinarayanan et al., 2017), which is an image area division method based on deep learning.

(3) Process of constructing classification number detection models

The training data for this process is image labeling the classification number part of the license plate area image shown in Figure 3 c. The model is constructed using YOLOv4, as in the process of constructing vehicle detection models.

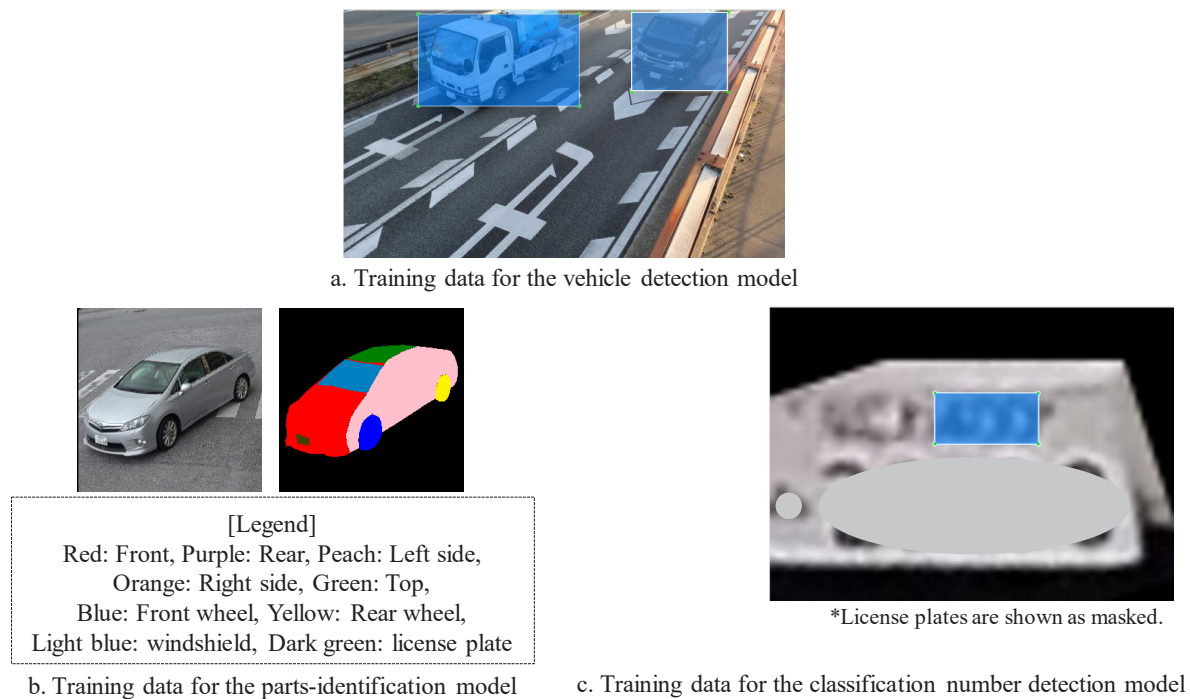
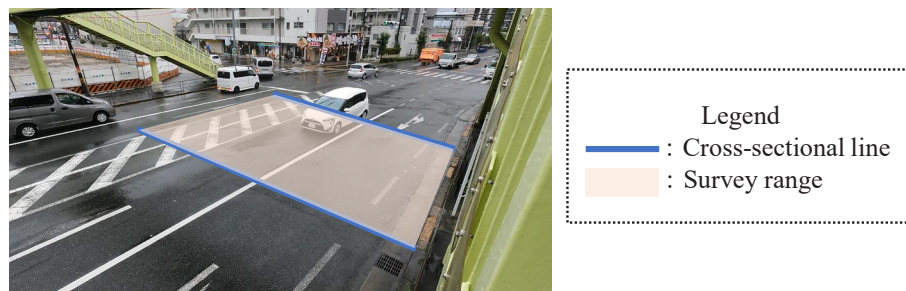


Figure 3. Training data for each model

2.4 Cross-sectional Line Setting Function

This function consists of the cross-sectional line setting process. The cross-sectional line setting process sets two cross sectional lines on the target road in the video (Figure 4). This allows limiting vehicles to those traveling in the front lane of the target road. In addition, by setting two cross-sectional lines, vehicles passing through the cross-sectional lines are detected and extracted over multiple frames. Moreover, to prevent excessive count of vehicles, a vehicle passing through two cross-sectional lines is counted as one vehicle.



2.5 Estimation Function

This function consists of the license plate extraction process and the classification number extraction process.

(1) License plate extraction process

This process detects a vehicle in the captured video image and extracts the area of the license plate from the vehicle (Figure 5). First, the captured video image is analyzed using the vehicle detection model to detect a vehicle passing through two sectional lines over multiple frames, and the detected vehicle is extracted as a vehicle area image. Next, the vehicle area image is analyzed using the parts-identification model to generate images that identify the parts of the vehicle (hereinafter referred to as parts-identification images). Then, among the areas identified as the license plate from the parts-identification images, the area with the largest area is extracted as the license plate area image.

(2) Classification number extraction process

This process extracts the classification number from the license plate area image (Figure 6). First, the license plate area image is analyzed using the classification number detection model to detect the place of the classification number. Then, using the coordinate values obtained at the time of detection, the place of the classification number is extracted as a classification number area image.

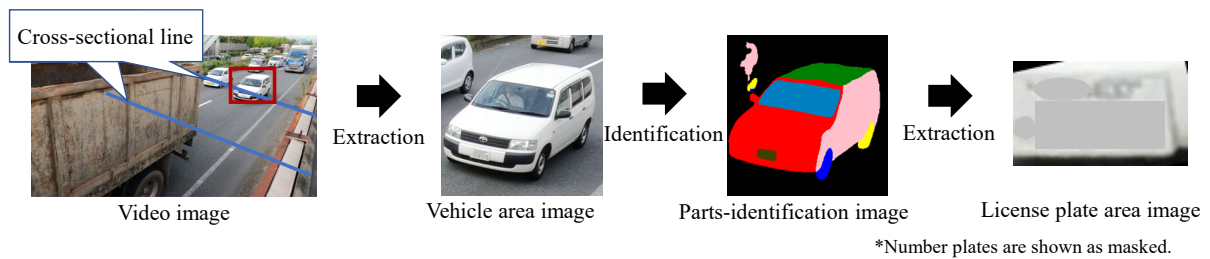


Figure 5. Flow of the license plate extraction process



Figure 6. Flow of the classification number extraction process

3. EXPERIMENT

3.1 Experiment Overview

In this experiment, the usefulness of the proposed method is verified by applying the proposed method to the video images captured by a video camera for the purpose of traffic surveys. The video images used for evaluation were taken with the video camera installed at a height of about 4.0 m from the ground and at a vertical angle of about 20 degrees, similar to the optimal shooting conditions clarified in the existing study (Imai et al., 2019). The video images were taken during the daytime with a resolution of 4K and a frame rate of 30 fps. The target road had two lanes on each side with a speed limit of 50 km/h. Evaluation was made using the Percentage of correct answers calculated by dividing the number of vehicles of which the classification numbers were correctly extracted by the total number of vehicles evaluated.

3.2 Experimental Conditions

This experiment employs an existing model of YOLOv4 as the vehicle detection model. It also uses the model from Tanaka et al.'s study (Tanaka et al., 2021) as the parts-identification model. Regarding the accuracy of the existing models, the F value of the license plate of the light vehicle is 0.907, and that of the heavy vehicle is 0.815. The classification number detection model was constructed using 1,893 images with labeling of the location of the license plate classification number that were cut from the video images taken at different spots from those for the evaluation data (Figure 3 c).

3.3 Experimental Results and Discussion

Table 1 shows the results of the experiment. Table 1 shows that extraction succeeded for 536 out of 539

vehicles, and the correct answer percentage was 99.4%, which means that it allowed to extract the location of the classification number with high accuracy. This result proved the usefulness of the classification number extraction method.

A detailed review of the results shows that, as Figure 7 shows, it was possible to extract the location of the classification number regardless of the color of the license plate. It is considered that this is because the training data contained enough license plate area images of all colors. In addition, as the right side of Figure 7 shows, it was found that even if a part of the license plate is missing from the image, the classification number can be extracted correctly if the classification number is clearly visible.

On the other hand, as Figure 8 indicates, the images with which extraction failed shows that when the Transportation Branch Office is put with three letters such as "Na-ni-wa" in the image, error of extraction tends to occur extracting the unnecessary parts other than the classification number. This is because most of the training data used to construct the classification number detection model consisted of 2-letter images such as "O-saka" and "Oki-nawa". Therefore, it can possibly be improved by reconstructing the learning model to include 3-letter images. In addition, as the right side of Figure 8 shows, the extraction of the classification number failed with the images in which the part of the classification number was not visible. This is because images with no visible characters cannot be prepared as training data, for a human visually confirms the location of the classification number and labels this part. In this regard, the use of a wearable camera capable of capturing images at 5.3K resolution may make it possible to capture images with the classification number visible. Furthermore, the purpose of extracting and recognizing the classification numbers is to determine whether the vehicle is a light or heavy. When the classification number is not visible, the shape of the vehicle can be applied to determine whether the vehicle is light or heavy. We think this result can be used to complement the determination. The authors' ultimate goal is to develop a method to identify the same vehicle using the license plate recognition results from video images captured by the cameras installed at multiple spots. An existing study (Imai et al., 2023) shows a potentiality to identify the same vehicle using the recognition results of serial designation numbers from the video images taken at multiple spots. Therefore, even for the vehicle of which extraction of the classification number failed at one spot, it may be possible to complement omissions of extraction of classification numbers by identifying the same vehicle from the recognition results of the characters other than the classification number.

Table 1. Extraction results of classification numbers

Number of vehicles evaluated	Extraction Succeeded (vehicles)	Extraction failed (vehicles)	Percentage of correct answers (%)
539	536	3	99.4

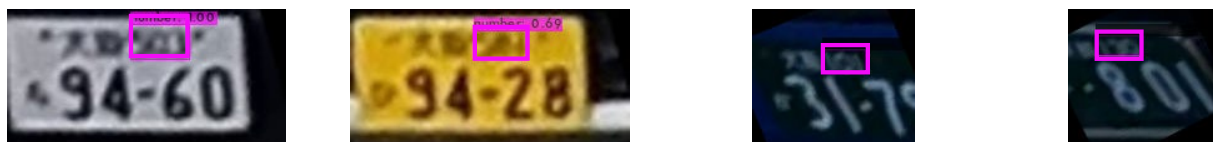


Figure 7. Images with success in extraction of the classification numbers



Figure 8. Images with failure in extraction of the classification numbers

4. CONCLUSIONS

In this study, we devised a method for extracting the classification numbers of license plates from the video images captured for the purpose of traffic surveys. As the classification numbers were extracted with high accuracy as a result of the demonstration experiment, the usefulness of the proposed method was verified.

In the future, we will devise a method for recognizing the classification numbers using deep learning. In addition, since we used video images taken in the daytime under sunny conditions in this experiment, we will verify whether the video images taken at different times of the day or under different weather conditions can

achieve the same level of accuracy. Furthermore, since some of the images captured at 4K resolution did not show visible classification numbers in the experiment, we will verify whether the extraction accuracy can be improved by using a higher resolution of 5.3K. Finally, since license plates with some patterns have been distributed in Japan in recent years, we will verify whether the proposed method is also useful for such license plates.

ACKNOWLEDGMENTS

We would like to express our gratitude to Survey Research Center Co., Ltd., CHUO KENSETSU CONSULTANT. Co., Ltd. and NIPPON INSIEK Co., Ltd. for providing us with video images and advice for practical application of this study.

REFERENCES

- Badrinarayanan, V., Kendall, A., and Cipolla, R. (2017). SegNet: A Deep Convolutional Encoder-Decoder Architecture for Image Segmentation, *Transactions on Pattern Analysis and Machine Intelligence*, 39 (12), 2481-2495.
- Bochkovskiy, A., Wang, C., and Liao, H. (2020). YOLOv4: Optimal Speed and Accuracy of Object Detection, website: <https://arxiv.org/pdf/2004.10934.pdf>
- Cheng-Hung, L. and Ying, L. (2019). A License Plate Recognition System for Severe Tilt Angles Using Mask R-CNN, *International Conference on Advanced Mechatronic Systems*.
- Haneda, K. and Hanaizumi, H. (2013). An Automated Method for Extracting and Recognizing Numbers on A License Plate, *Information Processing Society of Japan*, 2013 (1), 449-450.
- Imai, R., Kamiya, D., Yamamoto, Y., Tanaka, S., Nakahara, M., and Nakahata, K. (2019). A Basic Study on Traffic Census Using Generic Deep Learning, *Ser. F3 (Civil Engineering Informatics), Journal of Japan Society of Civil Engineers*, 75 (2), I_150-I_159.
- Imai, R., Yamamoto, Y., Nakahara, M., Kamiya, D., Nakahata, K., and Sumiyoshi, R. (2023). Research on a Method to Recognize Numbers on License Plates Toward Sophistication of Traffic Volume Investigation, *Ser. F3 (Civil Engineering Informatics), Journal of Japan Society of Civil Engineers*, 79 (22), 1-11.
- Ministry of Land, Infrastructure, Transport and Tourism. (2010). General traffic volume survey website: <https://www.mlit.go.jp/road/census/h22-1/data/kasyorep.pdf>
- Ministry of Land, Infrastructure, Transport and Tourism. (2017). Summary of the 2015 National Road and Street Traffic Conditions Survey General Traffic Volume Survey website: <https://www.mlit.go.jp/common/001187536.pdf>
- Nakahata, K., Imai, R., Kamiya, D., Yamamoto, Y., Tanaka, S., Nakahara, M., and Jiang, W. (2022). Research for Traffic Census Using Segmentation of Automobile Parts, *Ser. F3 (Civil Engineering Informatics), Journal of Japan Society of Civil Engineers*, 78 (2), I_82-I_92.
- National Police Agency. (1985). White Paper on Police website: <https://www.npa.go.jp/hakusyo/s60/s600101.html>
- Onoue, H., and Shiono, M. (1994). A License Number Plate Extraction in a Car Image and Recognition of All Characters Containing KANJI, *The Institute of Electronics, Information and Communication Engineers*, J77-D- II (3), 483-492.
- Ozaki, K., Sugawara, H., Hujii, J., Okubo, J., and Okano, M. (2021). Development of a system by roadside video that integrate traffic volume measurement by vehicle type and license plate recognition and verification of applicability to traffic flow analysis, *Japan Society of Traffic Engineers*, 41, 233-238.
- Tanaka, S., Yamamoto, Y., Imai R., Kamiya, D., Nakahara, M., and Nakahata, K. (2021). Research and Developed for Segmentation of Automobile Parts on Traffic Census, *Intelligence, Informatics, and Infrastructure*, 2 (J2), 821-832.

A QUANTITATIVE EVALUATION OF ROUGH GROUND TRUTH LABELING ON CONSTRUCTION SCAFFOLDING IMAGE SEGMENTATION

Natthapol Saovana¹

1) Ph.D., Lecturer, Department of Construction Design and Management, Faculty of Industrial Technology and Management, King Mongkut's University of Technology North Bangkok, Thailand. Email: Natthapol.s@itm.kmutnb.ac.th

Abstract: Scaffolding is a temporary structure supporting the construction and maintenance of buildings. Although it is a crucial component for construction progress, it does not receive much attention. Thus, there is a need for a tool assisting scaffolding supervision. Image segmentation from deep learning has proved its ability in various knowledge fields and may be applicable to this challenge. Nevertheless, accurate ground truth labeling is necessary for artificial intelligence training to get a satisfactory image segmentation result, but carefully labeling each image is very labor-intensive and time-consuming, especially with the scaffolding that usually got occluded by both natural and fabricated objects. Reducing the quality of the labeling can decrease the processing time but may significantly reduce the accuracy of the segmentation. Therefore, it is crucial to compromise between the time and quality of the labeling to raise the productivity of the entire process. The result shows that using rough labeling to train deep learning for scaffolding segmentation can reduce the data preparation time while sacrificing only a small amount of segmentation precision.

Keywords: Scaffolds, Deep learning, Image segmentation, Rough labeling

1. INTRODUCTION

The construction industry is one of the most important industries in numerous countries with millions of people involved in this supply chain. On the other hand, construction sites are dangerous because they have a high level of casualties (Kurien et al., 2018). One of the major causes of accidents on site comes from temporary structures, and scaffolding is responsible for one-fourth of this fatality rate in South Korea (J. Kim et al., 2022). In order to properly inspect scaffolding, the site practitioners have to do the site visit and climb up these structures to check by themselves although it can harm them in such process.



Figure 1. Scaffolding installation

Currently, some technologies can assist in the visualization of these temporary structures thus, the inspectors do not have to closely examine such as Xu et al. (2018) that utilized the Random Forest classifier and Random Sample Consensus (RANSAC) (Fischler & Bolles, 1981) to segment the point cloud of the scaffolding, which had only 40% accuracy for deck segmentation due to the occlusion and manual selection of reference. J. Kim et al. (2022) proposed the use of Simultaneous Localization and Mapping (SLAM) from a robotic dog to create point clouds and then utilized various techniques to clean and segment each bar that does not have occlusion. Their limitation is that the scaffoldings on sites are usually covered with safety sheets like the example in our manuscript, which will greatly reduce the number of point clouds of the bars. Moreover, segmenting the scaffolding as a whole is more realistic to the site practice and will reduce the computational time greatly. Khan et al. (2022) proposed the use of machine learning to detect the worker by combining the support from equipment with the Internet of Things (IoT) to know if the workers act along with the safety requirement. Then, they implemented computer vision to track if that worker is inside the scaffolding, which is already prespecified the boundary by the user. Their limitation is that there is no depth awareness in this study therefore, if the worker stands in front of the scaffolding, their system will treat this situation as if the worker is using the scaffolding.

The visualization from closed-circuit televisions (Cheng & Wang, 2018) and drones (Ham et al., 2016) may also be able to assist in the inspection of the scaffolding. Nevertheless, it is still challenging for safety issues because there is a need for expert individuals to judge whether the condition is safe. This limitation can be further supported by deep learning, which is one of the most trending technologies in artificial intelligence (AI). Deep learning, combined with computer vision approaches, provides computers with the skills to understand a specific pattern in an image or video by learning through preconstructed datasets (Kannan et al., 2019) and proves to be successful in various scopes, for example, medicine (Kannan et al., 2019), agriculture (Zabawa et al., 2020), and urban planning (Xia et al., 2021). This technique is widely called image segmentation.

However, the result of deep learning-based detection heavily relies on the quality of the training datasets (Karimi et al., 2020). Therefore, it is very difficult for some subjects to achieve satisfactory results due to the availability of data (Sun & Hardoon, 2010). This problem directly affects the utilization of deep learning with scaffolding because they are usually ignored by stakeholders (K. Kim et al., 2018) even though their cost can be up to 15 percent of the total construction cost (Hou et al., 2017). Another challenge of implementing deep learning-based image segmentation is the laborious and time-consuming preparation of image data, especially with scaffolding that is often occluded by prefabricated objects, existing buildings, and vegetation. Thus, the labelers have to spend more time and concentration highlighting the ground truth for the training of the deep learning model, which might not be favorable to the site practitioners who usually have diverse activities to be done daily (Yang et al., 2015).



Figure 2. Scaffolding occluded by vegetation

Reducing the quality of the ground truth by roughly labeling the scaffolding can decrease the workload of the labelers, but the wrongly trained pixels will be treated as noises and reduce the accuracy of the detection (Karimi et al., 2020). This tradeoff is tricky and needs to be evaluated because if it is feasible to sacrifice some detection accuracy for a better reduction of preparation time, it might encourage more stakeholders to support the use of deep learning to timely inspect the scaffolding without human intervention hence, decreasing the fatality rate from the construction site.

2. RESEARCH METHOD

To achieve the research objective of this study, which is to investigate the effect of rough labeling on scaffolding detection using deep learning, the research method is separated into four parts as follows:

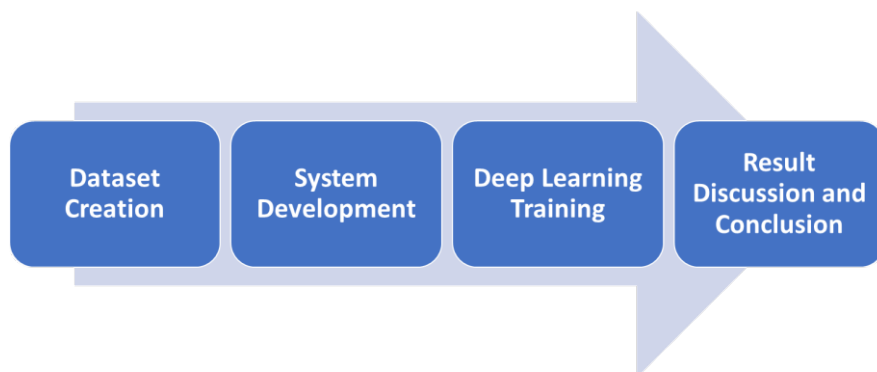


Figure 3. The research method of this study

2.1 Dataset Creation

The testing dataset in this study is separated into two datasets based on the quality of the labeling. The first dataset was created by labeling the scaffolding to be as realistic as possible. The existing buildings, objects, and vegetation were avoided when creating the boundary of each scaffold label. This dataset served as the ground truth of the current practice that the labelers must try their best not to create noise in the training. The second dataset was a roughly labeled dataset that did not remove the occluded components from the ground truth of the training. The difference between the two labelings is shown in Figure 4. It can be seen that the occluded objects such as fences and vegetation were omitted from the labeling in the detailed labeling dataset. In contrast, these occluded components were included in the labeling for the rough labeling dataset. The boundary in these two datasets was also a little different. In the detailed labeling dataset, the boundary tightly fits the scaffolding. On the other hand, the boundary in the rough labeling dataset does not exactly overlap with the real end of the scaffolding to reduce the preparation time of such dataset.

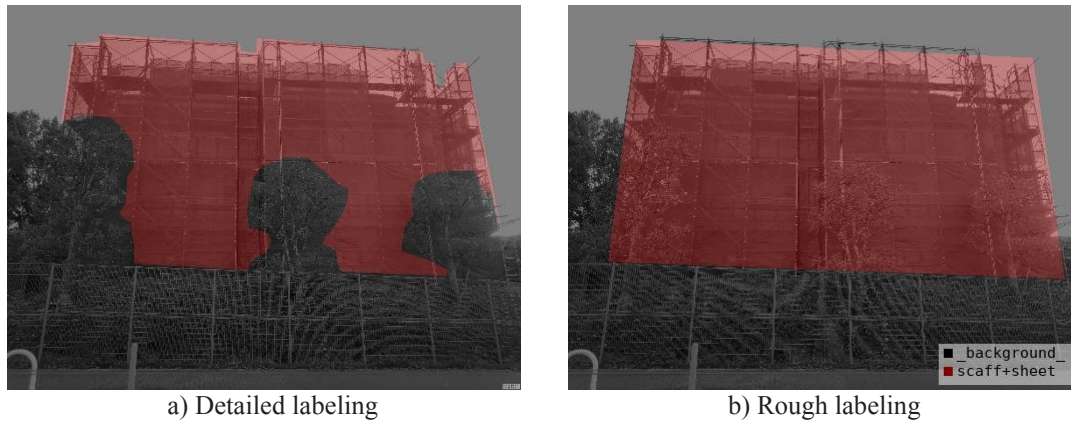


Figure 4. Example of apartment construction in the training set

The size of the training images was 512 x 384 pixels in PNG format. The original images in both datasets were the same to eliminate the bias of the result. They were digital images of the scaffolding from various construction sites in Japan captured using a commercial mobile phone. The mobile phone was selected as data acquisition equipment because site practitioners usually take images on their sites to do their field reports with mobile phones (Chen et al., 2015). The total images in each dataset were one hundred-forty images, one hundred-twenty images in the training set, and twenty images in the evaluation set. Please be noted that the images in each set did not appear in another set to raise the generalization of the testing.

2.2 System Development

The architecture of the system in this study was inspired by U-Net (Ronneberger et al., 2015) and YOLACT (Bolya et al., 2019). U-Net was able to achieve high-accuracy results from numerous scopes of studies that had a small amount of available training data (Izutsu et al., 2019). It consists of encoder and decoder parts that utilize copy-and-crop procedures to do the data augmentation from the available data. On the other hand, YOLACT separates tasks inside the network into two groups, which are prototype mask generation to roughly create possible masks and mask coefficient calculation that focus on the prepared prototype masks instead of the entire picture. The masks that have a higher set coefficient will be kept for the segmentation. The input of the system was the original images and the output was those images with highlights showing the possible scaffolding inside each image. U-Net and YOLACT were separated entirely from the training, testing, and evaluation.

2.3 Deep Learning Training

For U-Net, the training implemented a decay rate of 0.995 and the learning rate of 10^{-5} . Meanwhile, the training of YOLACT utilized the original setting of the network from Bolya et al. (2019). The batch size of both evaluations is eight. The training had continued for three hundred epochs. Finally, the minimization of the loss function was utilized for the training.

2.4 Result Discussion and Conclusion

The evaluation of the results relied on the F1 score, which can be calculated from the precision and recall of the system (Saovana et al., 2020) for the testing using U-Net. In contrast, the evaluation of the results from YOLACT testing implemented mean average precision (mAP) as the criteria for judging the impact of rough labeling. The average preparation time per image of each dataset was also recorded to justify the time difference between the two datasets.

3. RESULTS

The performances of the systems training on both datasets over learning time are shown in Figure 5 for U-Net and Figure 6 for YOLACT. Moreover, all of the final variable values for evaluation are shown in Table 1.

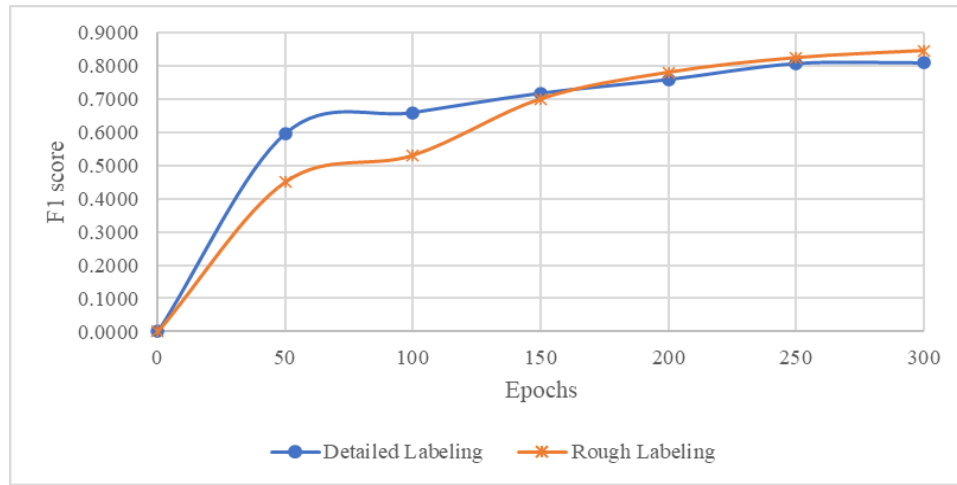


Figure 5. The F1 score of the segmentation from U-Net over the learning time of each dataset

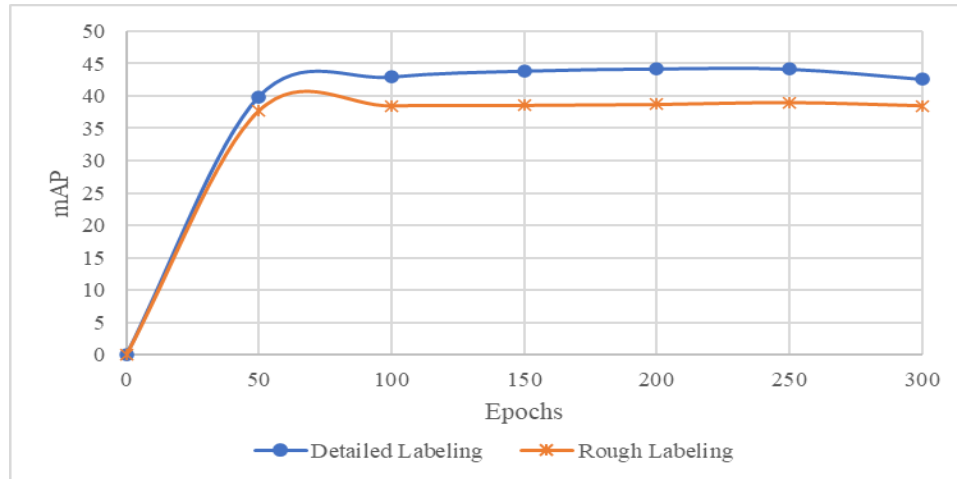


Figure 6. The mAP of the segmentation from YOLACT over the learning time of each dataset

Table 1. The performance of the system after training for 300 epochs

Datasets	The F1 score of the segmentation from U-Net	The mAP of the segmentation from YOLACT	The labeling time (minutes/image)
Detailed labeling	0.8073	42.57	1.32
Rough labeling	0.8445	38.50	0.45

Surprisingly, the F1 score of the detailed labeling dataset testing with U-Net was lower than the rough labeling dataset although, in theory, the quality of the labeling should be higher. The F1 score of the detailed labeling dataset was 0.8073 meanwhile, the F1 score of the rough labeling dataset was 0.8445. The difference is about 0.04. From the graph, it can be seen that although the detailed labeling dataset started with a better F1 score in the first one hundred fifty epochs, the F1 score of the rough labeling dataset kept gradually higher than the former one after that.

For YOLACT, the training using the detailed labeling dataset was able to achieve higher performance than its opponent for the entire training process. The final mAP of the training using the detailed labeling dataset was 42.57 and 38.50 for utilizing the rough labeling dataset as a training dataset, about 9.50% lower.

Furthermore, the time used for the labeler to finish preparing the ground truth for an image inside the rough labeling dataset was about three times shorter than when they had to finish an image for the detailed labeling dataset. The samples of the original images and their corresponding ground truths and results from using both datasets are shown in Figures 7 and 8.

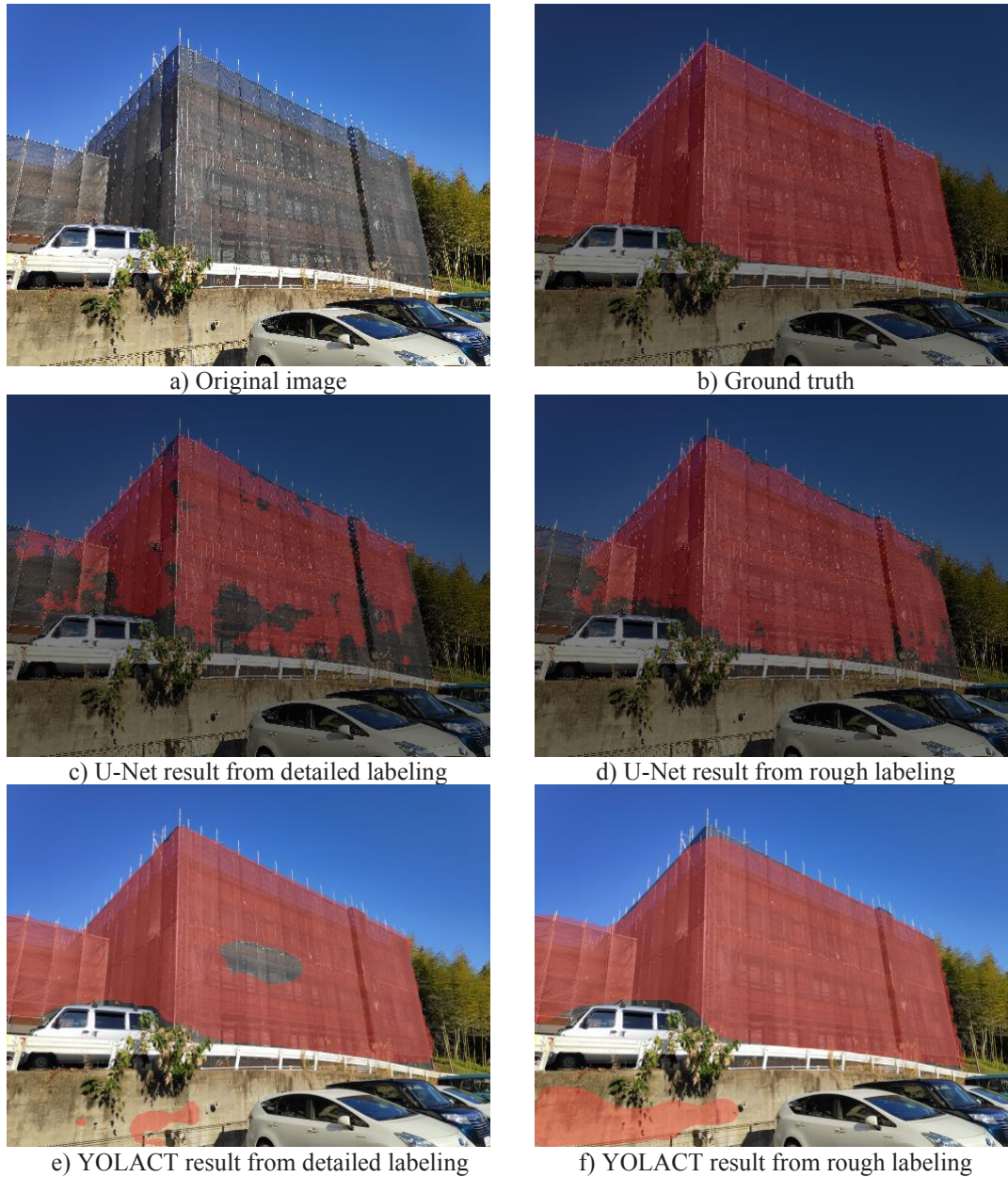


Figure 7. The first sample of an evaluating image and its corresponding images

4. DISCUSSION

From the result of the U-Net evaluation, the lack of performance from implementing the detailed dataset came from the reduction of generalization due to overfitting. It can be seen from Figures 7c and 8c that the system struggled to segment a vast area inside the scaffolding such as the center, the seams of the safety sheets, and the steel bars of the scaffolding. Introducing noise to the AI can decrease the performance of such AI however, a small amount of noise for a small set of data can raise the generalization of the detection hence better performance (Cires et al., 2010; Zur et al., 2009). As can be seen from utilizing the rough dataset for training, it affected the segmentation to be better, by about 5%. From Figures 7d and 8d, the segmentation was done smoothly in numerous parts of the image. However, because of the noise, some unrelated buildings were also segmented as a false positive, and parts of the scaffolding especially the boundary were left out of the highlighting.

For the evaluation of YOLACT, most of the scaffolding was properly segmented when implementing the detailed labeling dataset except for the central part of the scaffolding (Figures 7e and 8e). Nevertheless, although the segmentation from training using the rough dataset was able to segment the scaffolding fully, there were errors from detecting unrelated components such as a light pole and an adjacent structure resulting in a lower mAP of the segmentation (Figures 7f and 8f). Moreover, the boundary of the scaffolding also did not tightly fit the ground truth for training. This occurrence will make further processes complicated if the boundary of the scaffold is needed such as the projection of a three-dimensional mask to the point cloud (Saovana et al., 2021) or progress calculation.

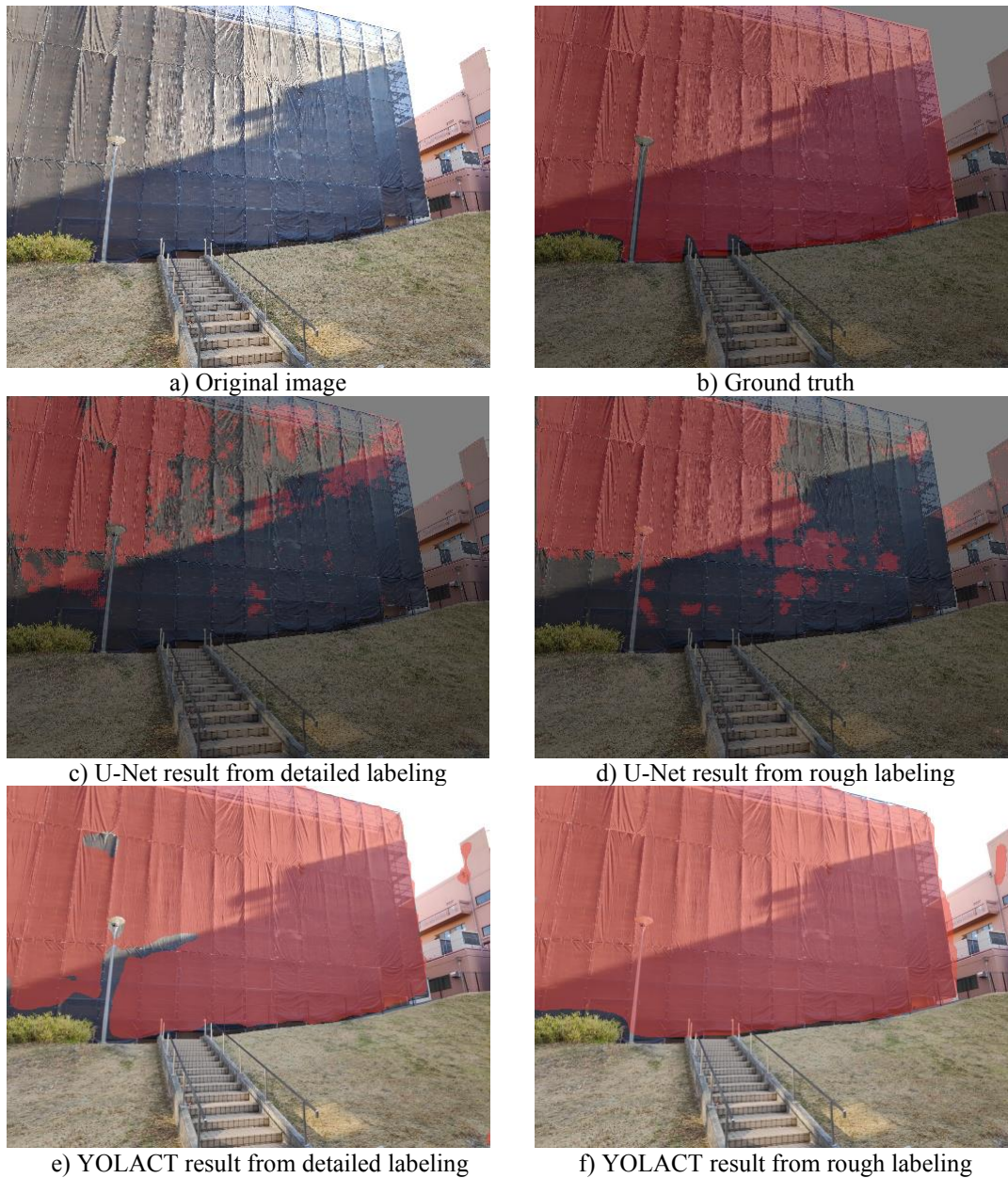


Figure 8. The second sample of an evaluating image and its corresponding images

The major advantage of implementing rough labeling for scaffolding image segmentation is the reduction of time and labor for dataset preparation. There was a 65.90% decrease in labeling time for making the ground truth of the training.

5. CONCLUSIONS

Scaffolding is the major cause of fatality in the construction industry. Therefore, there is a need for an assistance tool to visualize and monitor these temporary structures instead of a site visit by the staff that can expose them to dangers. One of the promising technologies is deep learning combined with computer vision, which can enable a computer to visualize such structures with pre-trained knowledge from a dataset. Nevertheless, scaffolding required a vast amount of time to prepare a dataset because it is usually obstructed by other components resulting in discouraging the busy site practitioners to implement this proposed process.

In conclusion, although the results from the detailed labeling dataset were inferior to the training with the rough labeling dataset for U-Net, the benefit of using the detailed labeling dataset is the clear boundaries between the scaffolding and other objects. However, there might be numerous voids hindering the performance that needed to be filled or modified before further utilization. The usage of a rough labeling dataset is possible because although the precision of the segmentation was sacrificed by 9.50% of mAP for YOLACT, the duration of time for data preparation was drastically decreased by 65.90%.

The limitation of this study is the small number of images in each dataset which may provide a disadvantage to the detailed labeling dataset because there are fewer patterns to learn. Furthermore, this situation can also raise the performance of the training using the rough labeling dataset due to better generalization (Cires et al., 2010; Zur et al., 2009). The suggestion for further research is to raise the number of images inside both datasets. If the data acquisition is difficult due to the availability of scaffolding images, the researcher may consider a data augmentation technique that can synthesize training data by adding flipping, brightness adjusting, and rotating to the existing data to create more trainable input images.

ACKNOWLEDGMENTS

This research is funded by the Faculty of Industrial Technology and Management, King Mongkut's University of Technology North Bangkok, Thailand.

REFERENCES

- Bolya, D., Zhou, C., Xiao, F., and Lee, Y. J. (2019). YOLACT: Real-time instance segmentation, *Proceedings of the IEEE International Conference on Computer Vision, 2019-Octob*, 9156–9165. <https://doi.org/10.1109/ICCV.2019.00925>
- Chen, Z., Chen, J., Shen, F., and Lee, Y. (2015). Collaborative Mobile-Cloud Computing for Civil Infrastructure Condition Inspection, *Journal of Computing in Civil Engineering*, 29(5), 04014066. [https://doi.org/10.1061/\(ASCE\)CP.1943-5487.0000377](https://doi.org/10.1061/(ASCE)CP.1943-5487.0000377)
- Cheng, J. C. P., and Wang, M. (2018). Automated detection of sewer pipe defects in closed-circuit television images using deep learning techniques, *Automation in Construction*, 95(June), 155–171. <https://doi.org/10.1016/j.autcon.2018.08.006>
- Cires, D. C., Meier, U., and Gambardella, L. M. (2010). *Deep Big Simple Neural Nets Excel on Hand- written Digit Recognition*. 1–14.
- Fischler, M. A., and Bolles, R. C. (1981). Random Sample Consensus: A Paradigm for Model Fitting with Applications to Image Analysis and Automated Cartography, *Communications of the ACM*, 24(6), 381–395. <https://doi.org/10.1145/358669.358692>
- Ham, Y., Han, K. K., Lin, J. J., and Golparvar-Fard, M. (2016). Visual monitoring of civil infrastructure systems via camera-equipped Unmanned Aerial Vehicles (UAVs): a review of related works, *Visualization in Engineering*, 4(1), 1–8. <https://doi.org/10.1186/s40327-015-0029-z>
- Hou, L., Zhao, C., Wu, C., Moon, S., and Wang, X. (2017). Discrete Firefly Algorithm for Scaffolding Construction Scheduling, *Journal of Computing in Civil Engineering*, 31(3), 1–15. [https://doi.org/10.1061/\(ASCE\)CP.1943-5487.0000639](https://doi.org/10.1061/(ASCE)CP.1943-5487.0000639)
- Izutsu, R., Yabuki, N., and Fukuda, T. (2019). As-built detection of steel frame structure using deep learning, *The 4th International Conference on Civil and Building Engineering Informatics (ICCBEI)*, 25–32.
- Kannan, S., Morgan, L. A., Liang, B., Cheung, M. G., Lin, C. Q., Mun, D., Nader, R. G., Belghasem, M. E., Henderson, J. M., Francis, J. M., Chitalia, V. C., and Kolachalama, V. B. (2019). Segmentation of Glomeruli Within Trichrome Images Using Deep Learning, *Kidney International Reports*, 4(7), 955–962. <https://doi.org/10.1016/j.ekir.2019.04.008>
- Karimi, D., Dou, H., Warfield, S. K., and Gholipour, A. (2020). Deep learning with noisy labels: Exploring techniques and remedies in medical image analysis, In *Medical Image Analysis* (Vol. 65). Elsevier B.V. <https://doi.org/10.1016/j.media.2020.101759>
- Khan, M., Khalid, R., Anjum, S., Tran, S. V.-T., and Park, C. (2022). Fall Prevention from Scaffolding Using Computer Vision and IoT-Based Monitoring, *Journal of Construction Engineering and Management*, 148(7). [https://doi.org/10.1061/\(asce\)co.1943-7862.0002278](https://doi.org/10.1061/(asce)co.1943-7862.0002278)
- Kim, J., Chung, D., Kim, Y., and Kim, H. (2022). Deep learning-based 3D reconstruction of scaffolds using a robot dog, *Automation in Construction*, 134(November 2021), 104092. <https://doi.org/10.1016/j.autcon.2021.104092>
- Kim, K., Cho, Y. K., and Kim, K. (2018). BIM-Based Decision-Making Framework for Scaffolding Planning, *Journal of Management in Engineering*, 34(6). [https://doi.org/10.1061/\(ASCE\)ME.1943-5479.0000656](https://doi.org/10.1061/(ASCE)ME.1943-5479.0000656)
- Kurien, M., Kim, M. K., Kopsida, M., and Brilakis, I. (2018). Real-time simulation of construction workers using combined human body and hand tracking for robotic construction worker system, *Automation in Construction*, 86(November 2017), 125–137. <https://doi.org/10.1016/j.autcon.2017.11.005>
- Ronneberger, O., Fischer, P., and Brox, T. (2015). U-net: Convolutional networks for biomedical image segmentation. In N. Navab, J. Hornegger, W. Wells, & A. Frangi (Eds.), *Medical Image Computing and Computer-Assisted Intervention – MICCAI 2015. MICCAI 2015. Lecture Notes in Computer Science* (Vol. 9351). Springer, Cham. https://doi.org/10.1007/978-3-319-24574-4_28
- Saovana, N., Yabuki, N., and Fukuda, T. (2020). Development of an unwanted-feature removal system for Structure from Motion of repetitive infrastructure piers using deep learning, *Advanced Engineering*

- Informatics*, 46(July), 101169. <https://doi.org/10.1016/j.aei.2020.101169>
- Saovana, N., Yabuki, N., and Fukuda, T. (2021). Automated point cloud classification using an image-based instance segmentation for structure from motion, *Automation in Construction*, 129(June), 103804. <https://doi.org/10.1016/j.autcon.2021.103804>
- Sun, S. and Hardoon, D. R. (2010). Active learning with extremely sparse labeled examples, *Neurocomputing*, 73(16–18), 2980–2988. <https://doi.org/10.1016/j.neucom.2010.07.007>
- Xia, Y., Yabuki, N., and Fukuda, T. (2021). Development of a system for assessing the quality of urban street-level greenery using street view images and deep learning, *Urban Forestry and Urban Greening*, 59(August 2020), 126995. <https://doi.org/10.1016/j.ufug.2021.126995>
- Xu, Y., Tuttas, S., Hoegner, L., and Stilla, U. (2018). Reconstruction of scaffolds from a photogrammetric point cloud of construction sites using a novel 3D local feature descriptor, *Automation in Construction*, 85(June 2017), 76–95. <https://doi.org/10.1016/j.autcon.2017.09.014>
- Yang, J., Park, M. W., Vela, P. A., and Golparvar-Fard, M. (2015). Construction performance monitoring via still images, time-lapse photos, and video streams: Now, tomorrow, and the future, *Advanced Engineering Informatics*, 29(2), 211–224. <https://doi.org/10.1016/j.aei.2015.01.011>
- Zabawa, L., Kicherer, A., Klingbeil, L., Töpfer, R., Kuhlmann, H., and Roscher, R. (2020). Counting of grapevine berries in images via semantic segmentation using convolutional neural networks, *ISPRS Journal of Photogrammetry and Remote Sensing*, 164(October 2019), 73–83. <https://doi.org/10.1016/j.isprsjprs.2020.04.002>
- Zur, R. M., Jiang, Y., Pesce, L. L., and Drukker, K. (2009). Noise injection for training artificial neural networks : A comparison with weight decay and early stopping, *Medical Physics*, 36(10), 4810–4818. <https://doi.org/10.1118/1.3213517>

ANALYZING THE IMPACT OF COVID-19 PANDEMIC ON TRAFFIC VOLUME THROUGH TEXTUAL DATA: A BERT-BASED APPROACH

Mu-Chieh Chung¹, and Albert Y.Chen²

1) Master Candidate, Department of Civil Engineering, Transportation Engineering Program, National Taiwan University, Taipei Taiwan. Email: r10521517@ntu.edu.tw

2) Ph.D., Prof., Department of Civil Engineering, National Taiwan University, Taipei, Taiwan. Email: AlbertChen@ntu.edu.tw

Abstract: The COVID-19 pandemic has caused a significant impact on various aspects of our lives, including transportation. This study aims to analyze transportation volume during the pandemic from a textual perspective using a BERT-based model. We collected textual data from the daily press release issued by Taiwan Centers for Disease Control (CDC) to capture people's reaction in terms of transportation under these pandemic-related information and policies. We explore people's behavior under the government's policy related to the pandemic by predicting the Taipei Metro's traffic volume based on the textual data. Our study demonstrates ways of using the Bidirectional Encoder Representations from Transformers (BERT) based models to predict the traffic volume during the pandemic through textual data. Policymakers could take our findings as reference to provide effective transportation services to meet people's changing needs during and after the pandemic.

Keywords: COVID-19, Transportation, Natural Language Processing (NLP), BERT

1. INTRODUCTION

The COVID-19 pandemic has had a significant impact on transportation systems across the globe. The spread of the virus has resulted in governments implementing various measures to contain it, such as lockdowns, travel restrictions and social distancing guidelines. These measures have led to a reduction in demand for transportation services, affecting various modes of transport, including aviation, rail, road, and marine transportation.

The Taipei Metro, also known as the Taipei Mass Rapid Transit (Taipei MRT), is a rapid transit system servicing the cities of Taipei and New Taipei in Taiwan, with an average daily ridership of approximately 2 million people. In response to the pandemic, the Taiwanese government implemented various measures, including universal mask wearing and launching extensive public education campaigns to raise awareness about the virus and how to prevent its spread. As a result, the Taipei Metro's ridership has been significantly impacted, with an average daily ridership of approximately 0.5 million during the peak of the pandemic in 2021, representing a 75% decrease compared to the normal situation. Figure 1. shows the daily confirmed cases of COVID-19 in Taiwan and Daily volume of the Taipei Metro.

The reduction in ridership has also led to a significant revenue loss for the Taipei Metro. To address this issue, the Taipei Metro has implemented various measures to reduce its operating costs, such as reducing train frequency during off-peak hours and limiting the use of air conditioning systems in stations and trains.

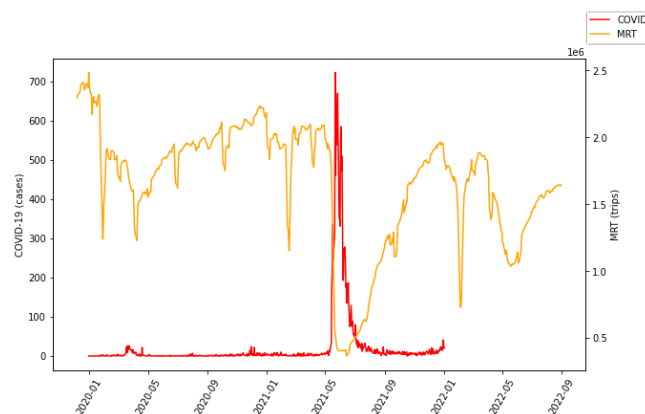


Figure 1. Daily confirmed cases of COVID-19 in Taiwan and Daily volume of Taipei Metro

To adjust to the change in traffic volume during the pandemic, transportation operators have implemented a range of strategies to optimize resources, reduce costs, and maintain safety for passengers. These strategies include flexible scheduling, promotion of alternative modes of transportation, implementation of contactless payment systems, regular cleaning and disinfection, and clear communication with passengers. Real-world examples of such strategies can be seen in cities like London, Sydney, and New York City. Transport for London (TFL) introduced a new timetable to reduce the number of buses and trains running during peak hours, reflecting

the reduced demand for services. In Sydney, Transport for NSW implemented new measures to promote social distancing on public transportation and increased cleaning and disinfection. In New York City, the Metropolitan Transportation Authority (MTA) reduced the frequency of subway services and introduced measures to increase cleaning and disinfection of vehicles and stations. A case study based on the COVID-19 pandemic revealed that a well-planned subway system in New York City can sustain 88% of transit flow while reducing the risk of disease transmission by 50% relative to fully-loaded public transit systems (Luo et al., 2022).

To implement the above strategies, it is crucial for operators to monitor and analyze the traffic data to understand the impact of the pandemic on traffic volume and patterns. This data can be helpful in decision-making and adjustments to operational strategies, accordingly. Previous studies have analyzed the link between COVID-19 and traffic volume. A big-data-driven analytical framework was proposed to assess the human mobility trend during COVID-19 pandemic (Hu et al., 2021). The effects of the COVID-19 pandemic on road traffic collisions are reviewed (Yasin et al., 2021). The changes in urban traffic volume and air pollutant concentrations before and after the outbreak of the pandemic was also investigated (Tian et al., 2021).

However, the situation is different in Taiwan. Taiwan was quick to recognize the potential danger of the COVID-19 pandemic and implemented a range of measures to prevent its spread. This means that the traffic volume in Taiwan has been reduced due to government policies and regulations even before the outbreak of the pandemic. As a result, an analysis based solely on the number of confirmed cases would not be able to accurately predict the actual increase or decrease in traffic volume. In order to capture the difference in travelers' behavior impacted by the government policies, an analysis through textual data containing the specific information is needed.

In this study, we utilize the daily press releases issued by the Taiwan Centers for Disease Control and Prevention (CDC), a government agency responsible for disease prevention and control, health promotion and emergency response, as our data source to predict the volume of Taipei Metro. The CDC issues daily press releases to provide the public with updates on the latest information related to infectious disease and other public health issues. During the pandemic, these press releases typically include information on the number of confirmed cases, suspected cases, and deaths of COVID-19, as well as updates any new measures being implemented to control the spread of the disease.

We propose to build a Bidirectional Encoder Representations from Transformers (BERT) based model to extract hidden information from the daily press releases issued by the CDC. BERT is a state-of-the-art Natural Language Processing (NLP) model that has shown great success in extracting information from unstructured text data. Our model will be trained using a large corpus of press releases during the pandemic and the daily volume of Taipei Metro from the same time periods. By analyzing the text data and traffic volume together, we aim to identify any patterns or correlations that may exist between the two. This approach could help to uncover hidden factors that contribute to changes in traffic volume during the pandemic, providing valuable insights for policymakers and transportation planners.

2. METHOD

2.1 Data Preprocessing

(1) Daily Press Releases Data

First, the date is included in the daily press releases issued by the CDC. Since this study could be seen as a time-series analysis, meaning the volume of public transportation and the severity of the pandemic are both highly dependent on the time, we analyzed the data with and without date information separately. This way, we can compare the results and explore the importance of date and time sequences in predicting traffic volumes.

Data preprocessing is a critical step in building any NLP model. In this study, we use the "bert" preprocess mode in the ktrain package in Python to preprocess the textual press releases issued by the CDC. This approach involves tokenizing the text into individual words and converting them into numeric representations that can be processed by the model. We use the pre-trained BERT model to embed the words into a 200-dimensional vector space, where words with similar meanings are grouped together. This helps to capture the semantic meaning of the text and provides a better representation of the data for the downstream model. Additionally, the standard text preprocessing techniques, such as removing stop words, is applied to improve the quality of the input data. Overall, our data preprocessing approach ensures that the text data is appropriately transformed and ready for use in training our BERT-based model.

(2) Daily Volume of Taipei Metro

To deal with the volume data of the Taipei Metro, we followed several steps. First, we added up the number of inbound passengers at all stations to get the total trips of the metro system for each day. We then computed a seven-day rolling average of the daily volumes to capture the trend and smooth out the noise in the data. In addition, we applied a one-day lag to the volume data to account for the temporal impact of the CDC press release. Finally, since the target value, which is the volume of Taipei Metro, has a large range of values, the model may struggle to make accurate predictions as the errors can be amplified by the large scale of the target value. To improve the stability of the model during training and also make it easier to interpret the predictions, the volume

data is scaled between 0 and 1 using the normalization technique. This preprocessing approach allowed us to capture more accurately the underlying trend in the volume of the Taipei Metro.

2.2 Model Construction

BERT is a state-of-the-art NLP model developed by Google AI (Devlin et al., n.d.). It revolutionized the field of NLP by introducing a pre-trained, context-aware language representation system. BERT is based on the Transformer architecture, which utilizes self-attention mechanisms to capture the relationships between words in a sentence.

Unlike previous models that predominantly relied on left-to-right or right-to-left contexts, BERT is designed to understand bidirectional language context. It is trained on a massive amount of text data to learn deep contextual representations of words. This pre-training involves masked language modeling, where random words in a sentence are masked, and BERT learns to predict them based on the surrounding context.

BERT's pre-training allows it to be fine-tuned for a wide range of downstream NLP tasks, such as sentiment analysis, named entity recognition, and question answering. By incorporating contextual information, BERT captures intricate nuances and semantic relationships in text, resulting in impressive performance on various benchmarks and outperforming previous NLP models. Its versatility, accuracy, and ability to handle various language tasks have made BERT a popular tool for many NLP applications, including applications in the transportation field (Rath & Chow, 2022).

In this study, the news releases published by the CDC are relatively complex in terms of vocabulary and article structure. Moreover, the text length of a single news release is approximately between 500 and 700 Chinese characters, requiring the model to possess strong language comprehension abilities. BERT's contextual understanding gained from the pretraining on a large corpus of text data is crucial in analyzing and predicting the factors affecting public transportation volume during the pandemic, such as government regulations and social distancing measures.

We created a BERT-based regression model that was trained on the preprocessed data. The model consisted of multiple layers of transformers, with each layer consisting of one or several multi-head self-attention layers, dropout layers, and fully connected layers.

Each transformer in the model performed a series of operations, including self-attention, feedforward neural networks and layer normalization. The self-attention mechanism enabled the model to identify the most important words and phrases in the input text by giving attention to different parts of the text at different levels of granularity. The feedforward neural network then processed the attended output to generate a set of feature representations, which were passed through the fully connected layer to produce the final prediction. Also, to prevent overfitting, we included dropout layers in the model. These layers randomly dropped out a certain percentage of the neurons during training, forcing the model to learn more generalizable features. Finally, we used layer normalization to normalize the output of each transformer, which helped to stabilize the training process and improve the model's performance.

The model was trained with a batch size of 6, learning rate of $2e-5$, and for 5 epochs. The batch size was chosen for computational efficiency, the learning rate for stable convergence, and the number of epochs to balance underfitting and overfitting. In addition, to evaluate the performance of the model, we used the Mean Absolute Error (MAE) as our evaluation metrics.

2.3 Random Split and Chronological Split

We split the data into training and validation sets using an 80-20 split, with the validation set used for early stopping during training.

As a time series regression problem, we observed that the order of the data points is important in the training and validation process. To address this, we experimented with splitting the data randomly and chronologically, where the first 80% of the data was used for training and the remaining 20% was used for validation. Comparing the results of the two splitting methods can provide valuable insights into the underlying characteristics of the data and inform the selection of an appropriate training strategy.

3. RESULTS

In this section, we present the results of our experiments using the BERT-based model to predict the volume of Taipei Metro based on daily press release issued by the CDC. We split the data into training set and validation set, and we experimented with two different approaches for splitting the data: randomly and chronologically (as mentioned in 2.3). Additionally, we experimented with two different types of input data: one including the date and one without (as mentioned in 2.1).

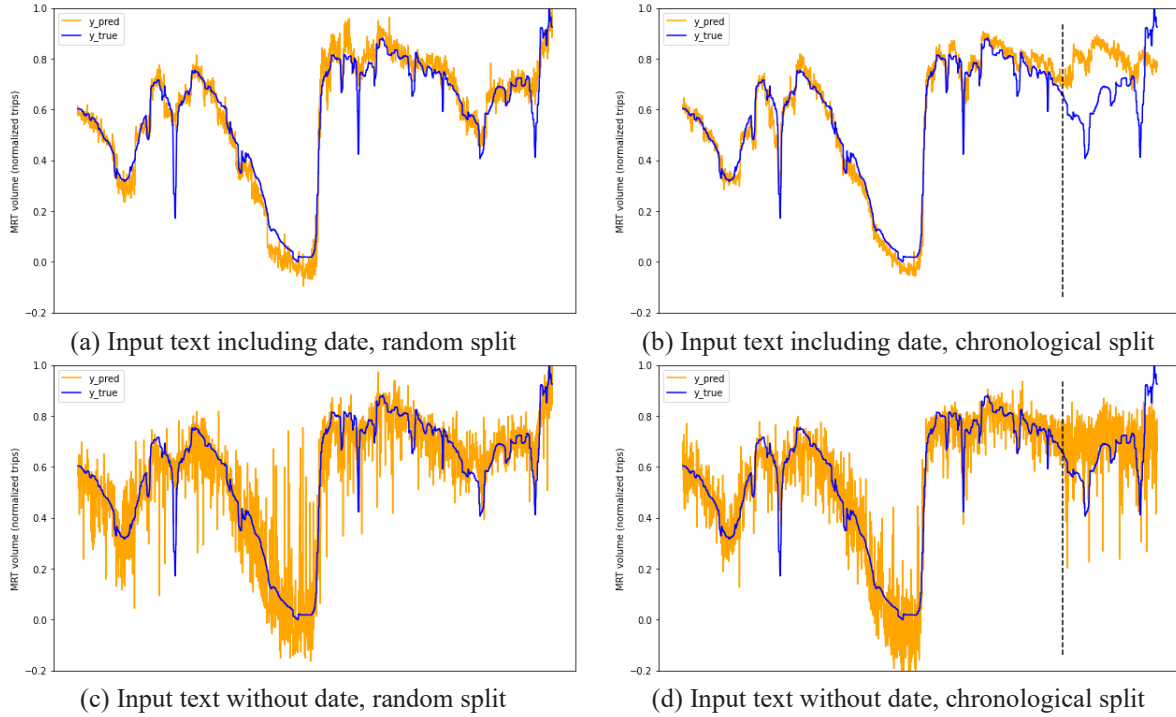


Figure 2. Training and validation curves for: (a) input text including date and using random split, (b) input text including date and using chronological split, (c) input text without date and using random split, (d) input text without date and using chronological split.

Table 1. Validation MAE of different experiments

	Random split	Chronological split
Input text including date	0.0534	0.1716
Input text without date	0.1086	0.1307

The results for the four different experiments are shown in Figure 2, and Table 1 shows the validation MAE in terms of normalized value of each experiment. To avoid verbosity, we will use Experiment (a), (b), (c), (d) to represent the four practices in the following content (corresponding to the numbering in Figure 2).

Figure 2 (a) shows the training and validation curves for using input texts including date and splitting training and validation set randomly. As we can see from the figure, the predicted volume of Taipei Metro closely follows the actual volume, with a validation MAE of 0.0534. Figure 2 (b) shows the training and validation curves for using input texts also including date but splitting training and validation set chronologically. The vertical dashed line in the figure indicates the boundary between training set and validation set. From the curves to the right of the dashed line in the figure, we can see that although the model is capable of roughly capturing the trend of the volume, the error is relatively higher with a validation MAE of 0.1716 comparing to the Experiment (a).

Figure 2 (c) shows the training and validation curves for using input texts without date and splitting training and validation set randomly. The validation MAE in this case, with a value of 0.1086, is slightly higher than the result of Experiment (a), but lower than the one of Experiment (b). Finally, Figure 2 (d) shows the training and validation curves for using input texts without date and splitting training and validation set chronologically, also with a vertical dashed line indicating the boundary between training set and validation set. In this case, the validation MAE is at 0.1307, which is between the results of Experiment (b) and (c).

4. DISCUSSION

The results of the experiments suggest that the choice of input text and training/validation split strategy has a significant impact on the performance of the BERT-based model for time series regression. Experiment (a), which used input texts including date and randomly split training and validation set, achieved the best validation MAE of 0.0534. In contrast, Experiment (b), which split the data chronologically, resulted in a higher validation MAE of 0.1716. Comparing these two results, we can conclude that randomly splitting the data leads to better performance in terms of validation MAE. However, it is important to note that in cases like this, splitting the data chronologically may still be preferable. This is because it better reflects the real-world scenario where the model is trained on historical data and used to make predictions on future data.

In Experiment (b), the model was still able to capture the trend of the volume but had relatively higher

error. This could be due to the fact that the model was not exposed to the data patterns that occurred after the training set, leading to poor generalization on the validation set. Another speculation is that since the text data contains date information, the model may predict the target value by interpolation-like methods based on the date of the data.

In order to test the validity of this speculation, Experiment (c) and (d) are proposed. First, comparing the results of Experiment (a) and (c), when we removed the date information from the input texts, the performance of the model decreased in terms of validation MAE, which is as expected. Although the difference between Experiment (a) and (c) may seem relatively small, we can observe from Figure 2 that the prediction curve tends to oscillate more when the date information is removed from the input texts. This indicated that including date information can help the model better capture the temporal patterns in the data.

Moreover, in Experiment (d) where the data was split chronologically but without date information, the model still achieved a validation MAE of 0.1307, making the difference between Experiment (c) and (d) much smaller than the difference between Experiment (a) and (b). This finding supports the above speculation. Without date information, the model may not be able to perform accurate interpolation for the predicted values.

To construct a more robust and generalizable model, it is crucial to avoid the interpolation effect. Interpolation-based predictions rely heavily on the input data's date information, which can lead to inaccuracies in the model's performance when predicting future data. Based on these findings above, we suggest adopting the approach utilized in Experiment (d), which is using input texts without date and splitting training and validation set chronologically, to avoid being misled by overfitting curves similar to that in Figure 2 (a) when dealing with this type of problem.

Furthermore, since the date information was obscured in both Experiment (c) and (d), we speculate that the difference in model performance between the two experiments may be attributed to the variations in the tone and writing format of the press releases across different periods during the pandemic. To improve the accuracy of the model in Experiment (d), we suggest adopting an adaptive approach to predict the target value on a daily basis and update the model accordingly in the future, which can lead to more effective predictions.

5. CONCLUSIONS

In this study, we conducted four experiments, each with a different format of input texts or a different way of splitting training and validation sets.

In conclusion, the results of these experiments highlight the importance of selecting appropriate input texts and training/validation split strategies when building BERT-based models for time series regression. The results indicate that including date information in the input texts can help the model better capture temporal patterns in the data, but also lead to potential overfitting when the data is split randomly. On the other hand, although chronological splitting of the data may lead to less favorable performance since the model is not exposed to the data patterns occurring after the training set, it can better reflect real-world scenarios and improve the model's generalization.

Our findings also suggest that the interpolation effect should be avoided to construct a more robust and generalizable model. Interpolation-based predictions rely heavily on the input data's date information, which can lead to inaccuracies in the model's performance when predicting future data. Therefore, we recommend adopting the analysis approach utilized in Experiment (d), which is using input texts without date and splitting training and validation sets chronologically, to avoid overfitting and achieve a more authentic and applicable performance.

Future work can focus on investigating the impact of variations in the tone of text data across different periods. Additionally, an adaptive approach is suggested to be adopted to predict the target value and update the model on a daily basis. Overall, these findings can provide insights for researchers and practitioners in the field of time series regression using BERT-based models.

REFERENCES

- Devlin, J., Chang, M.-W., Lee, K., Google, K. T., and Language, A. I. (n.d.). *BERT: Pre-training of Deep Bidirectional Transformers for Language Understanding*. Retrieved from website: <https://github.com/tensorflow/tensor2tensor>
- Hu, S., Xiong, C., Yang, M., Younes, H., Luo, W., and Zhang, L. (2021). A big-data driven approach to analyzing and modeling human mobility trend under non-pharmaceutical interventions during COVID-19 pandemic, *Transportation Research Part C: Emerging Technologies*, 124. <https://doi.org/10.1016/J.TRC.2020.102955>
- Luo, Q., Gee, M., Piccoli, B., Work, D., and Samaranayake, S. (2022). Managing public transit during a pandemic: The trade-off between safety and mobility, *Transportation Research Part C: Emerging Technologies*, 138. <https://doi.org/10.1016/J.TRC.2022.103592>
- Rath, S., & Chow, J. Y. J. (2022). Worldwide city transport typology prediction with sentence-BERT based supervised learning via Wikipedia, *Transportation Research Part C: Emerging Technologies*, 139.

- <https://doi.org/10.1016/J.TRC.2022.103661>
- Tian, X., An, C., Chen, Z., and Tian, Z. (2021). Assessing the impact of COVID-19 pandemic on urban transportation and air quality in Canada, *Science of the Total Environment*, 765. <https://doi.org/10.1016/J.SCITOTENV.2020.144270>
- Yasin, Y. J., Grivna, M., and Abu-Zidan, F. M. (2021). Global impact of COVID-19 pandemic on road traffic collisions, *World Journal of Emergency Surgery*, 16(1), 1–14. <https://doi.org/10.1186/S13017-021-00395-8/TABLES/2>

ELECTRIC VEHICLE EMISSION ANALYSIS THROUGH THERMAL IMAGE-BASED VEHICLE CLASSIFICATION

Chun-Ping Liao¹, Ta-Chih Hsiao², and Albert Y. Chen³

1) Master student, Department of Civil Engineering at National Taiwan University, Taipei, Taiwan. Email: r10521516@ntu.edu.tw

2) Ph.D., Prof., Graduate Institute of Environmental Engineering at National Taiwan University, Taipei, Taiwan. Email: tchsiao@ntu.edu.tw

3) Ph.D., Prof., Department of Civil Engineering at National Taiwan University, Taipei, Taiwan. Email: AlbertChen@ntu.edu.tw

Abstract: The increasing level of air pollution in urban areas has become a focus of many studies due to its detrimental impact on the health of the population. Vehicular emissions on roads have been identified as one of the primary sources of pollution. Numerous countries have proposed the complete electrification of vehicles as a measure to reduce pollution on roads; however, the actual impact of Electric Vehicles (EVs) versus conventional vehicles on pollution remains uncertain. Therefore, developing an accurate model to distinguish EVs on roads can enable us to better understand the impact of EVs on road pollution.

Since EVs and conventional vehicles have no significant visual differences, visible light-based object detection is highly unreliable. However, thermal imaging can accurately distinguish the differences among these two types of cars.

This study presents a transfer learning approach from a deep learning model and an open-source dataset with the thermal data we collected. Particularly, we count the portion of different type of cars with the car detection model and applied vehicle emission analysis.

This study could be applied for assessment of personal exposure to emissions and related health impacts. This work also provides a reliable method for distinguishing between EVs and conventional vehicles on roads using thermal imaging, which can be extended to the identification of other types of EVs such as electric motorcycles, electric buses, and electric trucks. The extracted data is expected to also facilitate in different domains such as environmental analysis, traffic control, smart cities, and other related research.

Keywords: Transfer learning, Deep learning, Object detection, Thermal imaging, Electric vehicle, Air pollution, Pollutant

1. INTRODUCTION

Air pollution has been considered a severe environmental problem recently. Besides climate change (Manisalidis et al., 2020), air pollution exposure is also harmful to the human health (Giugliano et al., 2005). In the field of transportation, we focus on the air pollution generated by vehicles, especially the pollution generated by vehicles on roads, which directly impacts people in proximity to the transportation network. For example, long-term health of drivers, pedestrians, and even residents and business owners and customers near the roads could be effected.

The electrification of transportation is a global trend, with many leading organizations and countries proposing similar policies to address pollution and carbon emissions. Examples include the United Nations Framework Convention on Climate Change (UNFCCC, 2022), the Zero Emissions Transportation Association (ZETA, 2023), the government of Norway which has set a target to sell only zero-emission cars by 2025 (Norsk elbilforening, 2023), and the United Kingdom which plans to phase out the sale of new gasoline and diesel cars by 2030 (GOV.UK, 2020).

Although EVs can reduce pollution caused by burning gasoline, other sources of pollution caused by their heavier weight (Galvin, 2022), such as tire wear and road dust, are also worth investigating. In recent studies on the pollution of EVs, both laboratory tests (Woo et al., 2022) and analysis using pollution models (Skipper et al., 2023) have been conducted.

We found that there is a lack of research that analyzes on the pollution caused by mixed traffic flow, composed of EVs and traditional vehicles, on actual roads. There are many methods for object detection, with Mask R-CNN (He et al., 2017) and YOLO (Redmon & Farhadi, 2018) being the most commonly used. However, the training data used by these models does not include EVs. We need to collect data on EVs ourselves to enable our model to distinguish between EVs and non-EVs on the road.

In their works, Takagi et al. (2014) and Li et al. (2017) distinguished EVs based on different acoustic features. In outdoor environments, there exist complex acoustic noise characteristics, which can worsen the model performance when the signal is captured by non-professional microphones.

Wüstenberg et al. (2014) distinguished EVs from fossil-fueled vehicles using a mobile phone to measure the frequency of engine vibrations when a vehicle is idling, which can be limited to individual vehicles and cannot represent the traffic conditions of an entire road section.

Automatic license plate recognition (ALPR) is also considered an approach to distinguish EVs because some countries have some policies that EVs have their own unique style of license plate. Such as in Taiwan, the word "Electric Car" on license plates, using the letter "E" as a prefix, or implementing distinctive color markings are all possible ways to indicate the presence of an EV. However, this policy is not mandatory and is not for every country in the world. The reliability of this approach appears to be questionable.

Švorc et al. (2020) suggested to detect EVs using thermal characteristics. The reason is because under adverse weather conditions, such as fog, snow, or heavy rain, the detection accuracy may be reduced considering visible spectrum image characteristics. It is necessary to replace or supplement the traditional camera-based methods with thermal imaging cameras. Also, some car manufacturers have introduced pure electric versions of popular models, which poses significant challenges in terms of visual recognition.

Our objective is to use thermal imaging camera to record traffic flow and utilize YOLOv7 (Wang et al., 2022) and transfer learning to develop a model that can distinguish EVs from non-EVs. IN addition, vehicles' respective numbers should be calculated, and the contribution of EVs to air pollution should be analyzed by comparing them with simultaneously field collected air pollution data.

2. METHOD

We are going to introduce our methodology in this chapter. As shown in Figure 1. it is the total workflow of our work. We first use the transfer learning method to transfer the open-source dataset, then train the object detection model with our collected thermal images. After that, we count the number of vehicles of different categories with the trained object detection model. Then, the methodology for emission analysis is described.

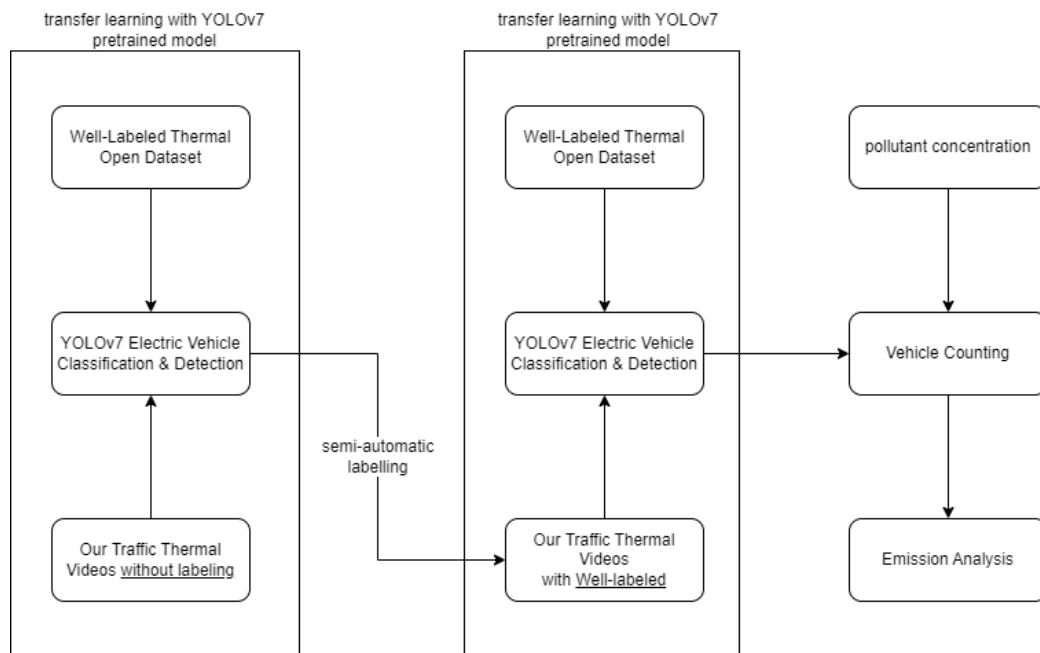


Figure 1. Total workflow

2.1 Transfer Learning with the YOLOv7 Model

Many prior studies require a dataset with accurate labels in order to extract image features, but creating such a dataset can be a time-consuming task. Transfer learning involves leveraging knowledge gained while solving one problem as source domain to address a different but related problem as target domain by capturing crucial information from the learning process.

We use YOLOv7 (Wang et al., 2022) pretrained model trained with MS-COCO (Lin et al., 2014) dataset as our source domain, an open-source and reliable FLIR thermal image dataset (FLIR Systems Inc., 2022) as our target domain. We hope the deep learning model could be trained and can collect data in thermal image.

2.2 Traffic Data Extraction

(1) Semi-Automatic Labeling

In this study, we utilized our model to recognize the collected traffic data. Specifically, the model was able to accurately classify different types of vehicles in the traffic flow, including motorcycles, cars, trucks, and buses. To modify the labels, we utilized the widely used labeling tool, labelImg, and changed the tag of certain targets from "car" to "EV".

(2) Vehicle & EV Classifier Model Construction

In order not to do too many transfer learning which may lead to a catastrophic forgetting (Kirkpatrick et al., 2017). We redo the training process we conduct at section 2.1. But this time our target domain is the FLIR thermal image dataset (FLIR Systems Inc., 2022) and our thermal EV dataset. Details of samples are shown in Table 1. Figure 2. And Figure 3. show examples of EV samples and Non-EV samples under thermal image.

Table 1. Quantity of EV and Non-EV samples.

Type	EV	Non-EV
Images#	1511	4127



Figure 2. Examples of EV samples.



Figure 3. Examples of Non-EV samples.

(3) Vehicle Counting by Categories

Whenever vehicles are detected by the deep learning model, detected vehicles are connected to the vehicles in the previous image frame. Specifically, the same vehicle in frame t and in frame $t+1$ would be associated. The Kalman Filter (Welch et al., 1995) and the Hungarian Algorithm (Kuhn, 1955) are applied for the association of detections into trajectories. we employed the Kalman Filter to estimate the position of a vehicle in the next frame by utilizing its current kinematic information. Then, we utilized the Hungarian Algorithm to match the predicted positions with the detected positions based on the minimum total distance with a constraint on the maximum distance between them. With the aid of the Kalman Filter, we could substitute the position of an undetected vehicle with its predicted position. Moreover, we combined the predicted position and the detected position to adjust the trajectory of a vehicle. StrongSORT (Du et al., 2022) is applied for the job Multi-Object Tracking (MOT), Kalman Filter and Hungarian Algorithm. The primary objective of developing this model is to count vehicles. To accomplish this objective, a counting line is defined in the image, which is used to count the number of vehicles that pass over it. The counts for EVs, Non-EVs, motorcycles, buses, and trucks are respectively counted.

2.3 Emission Analysis

(1) Data Collection

The monitoring site was set on the roadside of Keelung Road, one of the main arterials in Taipei City. Keelung Road is a two-way road with three lanes in each way.

(2) EV Contribution Analysis

In order to assess the potential emission reduction resulting from car electrification. This involves identifying the contribution of EVs to different pollutant emissions. To accomplish this, a multilinear regression analysis is applied to identify the impact of EVs on ambient pollutant concentrations. Once the contribution has been determined, an analysis is conducted to assess the emission reduction from replacing traditional cars with EVs. To estimate traffic-related CO₂ emissions, the background CO₂ concentration, which has a high background value, needs to be removed from the measured concentration. Additionally, analyses are conducted for black carbon (BC) and nitrogen oxides (NO_x) emissions.

3. RESULTS & DISCUSSION

In thermal imaging, the most significant difference between EVs and internal combustion engine vehicles lies in the engine that burns gasoline. The rear-engine design is now outdated and almost invisible on the road. The temperature difference in the front engine area will be the focus of our deep learning model. Initially, we believed that this was the case, but after experimentation, we found that this would lead to false positives, where internal combustion engine vehicles are classified as EVs. We explored the reasons for this and found several factors: the materials used in new generation vehicles are better at insulation and more efficient at dissipating heat, or the engine is just starting up, also known as a cold car. This situation causes the temperature in the engine area to be less noticeable, leading to our model misclassification.

However, we also found that even in a just-started vehicle, the tailpipe exhaust is very noticeable in the thermal image, while EVs do not produce exhaust emissions. Therefore, we hope to place the recognition judgment part in the rear view of the vehicle, hoping that the model can capture the difference and reduce the occurrence of misclassification.

4. CONCLUSIONS

This is an ongoing study, and the above results represent our current progress. Our goal is to develop a reliable deep learning model that can accurately identify EVs in traffic flow. Using this traffic flow data and measured pollution data, we aim to calculate the actual emissions from EVs in mixed traffic flow. We hope that this data will be useful for future research and serve as a reference for government policy-making. Furthermore, we hope that future researchers can develop models that can identify a wider range of vehicle types, and apply them to smart city and traffic control issues.

REFERENCES

- Du, Y., Song, Y., Yang, B., and Zhao, Y. (2022). StrongSORT: Make DeepSORT Great Again, *ArXiv*, *abs/2202.13514*.
- FLIR Systems Inc. (2022, January 19). *The Teledyne FLIR Free ADAS Thermal Dataset v2*. Retrieved from website: <https://www.flir.com/oem/adas/adas-dataset-agree/>.
- Galvin, R. (2022). Are electric vehicles getting too big and heavy, Modelling future vehicle journeying demand on a decarbonized US electricity grid, *Energy Policy*, 161, 112746. <https://doi.org/10.1016/j.enpol.2021.112746>
- Giugliano, M., Lonati, G., Butelli, P., Romele, L., Tardivo, R., and Grosso, M. (2005). Fine particulate (PM_{2.5}–PM₁) at urban sites with different traffic exposure, *Atmospheric Environment*, 39(13), 2421–2431. <https://doi.org/10.1016/j.atmosenv.2004.06.050>
- GOV.UK. (2020, November 18). *Government takes historic step towards net-zero with end of sale of new petrol and diesel cars by 2030*. Retrieved from website: <https://www.gov.uk/government/news/government-takes-historic-step-towards-net-zero-with-end-of-sale-of-new-petrol-and-diesel-cars-by-2030>
- He, K., Gkioxari, G., Dollár, P., and Girshick, R. B. (2017). Mask R-CNN. *CoRR*, *abs/1703.06870*. Retrieved from website: <http://arxiv.org/abs/1703.06870>
- Kirkpatrick, J., Pascanu, R., Rabinowitz, N., Veness, J., Desjardins, G., Rusu, A. A., Milan, K., Quan, J., Ramalho, T., Grabska-Barwinska, A., Hassabis, D., Clopath, C., Kumaran, D., and Hadsell, R. (2017). Overcoming catastrophic forgetting in neural networks, *Proceedings of the National Academy of Sciences*, 114(13), 3521–3526. <https://doi.org/10.1073/pnas.1611835114>
- Kuhn, H. W. (1955). The Hungarian Method for the Assignment Problem, *Naval Research Logistics Quarterly*, 2(1–2), 83–97. <https://doi.org/10.1002/nav.3800020109>
- Li, S., Fan, X., Zhang, Y., Trappe, W., Lindqvist, J., and Howard, R. E. (2017). Auto++: Detecting Cars Using Embedded Microphones in Real-Time, *Proc. ACM Interact. Mob. Wearable Ubiquitous Technol.*, 1(3). <https://doi.org/10.1145/3130938>
- Lin, T.-Y., Maire, M., Belongie, S. J., Bourdev, L. D., Girshick, R. B., Hays, J., Perona, P., Ramanan, D., Dollár, P., and Zitnick, C. L. (2014). Microsoft COCO: Common Objects in Context. *CoRR*, *abs/1405.0312*. Retrieved from website: <http://arxiv.org/abs/1405.0312>
- Manisalidis, I., Stavropoulou, E., Stavropoulos, A., and Bezirtzoglou, E. (2020). Environmental and Health Impacts of Air Pollution: A Review, *Frontiers in Public Health*, 8. <https://doi.org/10.3389/fpubh.2020.00014>
- Norsk elbilforening. (2023, January 3). *Norwegian EV policy*. Norwegian EV Policy. Retrieved from website: <https://elbil.no/english/norwegian-ev-policy/>
- Redmon, J. and Farhadi, A. (2018). YOLOv3: An Incremental Improvement. *ArXiv*.
- Skipper, T. N., Lawal, A. S., Hu, Y., and Russell, A. G. (2023). Air quality impacts of electric vehicle adoption in California, *Atmospheric Environment*, 294, 119492.

- <https://doi.org/https://doi.org/10.1016/j.atmosenv.2022.119492>
- Švorc, D., Tichý, T., and Růžička, M. (2020). Detection of the electric vehicle using thermal characteristics, *2020 Smart City Symposium Prague (SCSP)*, 1–5. <https://doi.org/10.1109/SCSP49987.2020.9133981>
- Takagi, M., Fujimoto, K., Kawahara, Y., and Asami, T. (2014). Detecting Hybrid and Electric Vehicles Using a Smartphone, *Proceedings of the 2014 ACM International Joint Conference on Pervasive and Ubiquitous Computing*, 267–275. <https://doi.org/10.1145/2632048.2632088>
- UNFCCC. (2022, May 23). *Electric Future*. Electric Future. Retrieved from website: <https://unfccc.int/blog/electric-future>
- Wang, C.-Y., Bochkovskiy, A., and Liao, H.-Y. M. (2022). *YOLOv7: Trainable bag-of-freebies sets new state-of-the-art for real-time object detectors*.
- Welch, G., Bishop, G., and others. (1995), *An introduction to the Kalman filter*.
- Woo, S.-H., Jang, H., Lee, S.-B., and Lee, S. (2022). Comparison of total PM emissions emitted from electric and internal combustion engine vehicles: An experimental analysis, *Science of The Total Environment*, 842, 156961. <https://doi.org/https://doi.org/10.1016/j.scitotenv.2022.156961>
- Wüstenberg, M., Blunck, H., Grønbæk, K., and Kjærgaard, M. B. (2014). Distinguishing Electric Vehicles from Fossil-Fueled Vehicles with Mobile Sensing, *2014 IEEE 15th International Conference on Mobile Data Management*, 1, 211–220. <https://doi.org/10.1109/MDM.2014.32>
- ZETA. (2023). Retrieved from website: <https://www.zeta2030.org/>. <https://www.zeta2030.org/>

CSS-ONTO: CONSTRUCTION SAFETY SITUATION ONTOLOGY

Zhe Zhang¹, Brian H.W. Guo², Yonger Zuo³, Bowen Ma⁴, Alice Chang-Richards⁵, Zhenan Feng⁶, and Yang Zou⁷

1) Ph.D. Candidate, Department of Civil & Natural Resources Engineering, University of Canterbury, New Zealand. Email: zhe.zhang@pg.canterbury.ac.nz

2) Senior. Lecturer., Department of Civil & Natural Resources Engineering, University of Canterbury, New Zealand. Email: brian.guo@canterbury.ac.nz

3) Ph.D. Candidate, Department of Civil & Natural Resources Engineering, University of Canterbury, New Zealand. Email: yonger.zuo@pg.canterbury.ac.nz

4) Ph.D. Candidate, Department of Civil & Natural Resources Engineering, University of Canterbury, New Zealand. Email: bowen.ma@pg.canterbury.ac.nz

5) Senior. Lecturer., Department of Civil and Environmental Engineering, University of Auckland, New Zealand. Email: yan.chang@auckland.ac.nz

6) Senior. Lecturer., School of Built Environment, Massey University, New Zealand. Email: Z.Feng1@massey.ac.nz

7) Senior. Lecturer., Department of Civil and Environmental Engineering, University of Auckland, New Zealand. Email: yang.zou@auckland.ac.nz

Abstract: Despite research efforts in the digital technology-driven third wave of construction occupational health and safety (OHS) management since the early 2000s, the construction industry is still plagued by numerous accidents. This underscores the persistent need for a comprehensive approach to improving safety. The objective of this research is to develop a Construction Safety Situation Ontology (CSS-Onto) that enables a formal definition of “safety situation” and facilitates the development of intelligent systems that improve situation awareness on construction sites. The NeOn methodology was adopted to reuse ontological and non-ontological resources to develop the CSS-Onto. The ontology consists of 11 core classes: actor, physiological state, psychological state, group, social dynamics and norms, climatic conditions, equipment, material, building element, digital technology, and task. The CSS-Onto was evaluated through a showcase to demonstrate its competency in accurately representing the safety situation. The paper concludes with a discussion on defining safety situations in construction sites, underpinned by a two-part examination. Firstly, a set of principles was outlined to serve as a foundation for identifying safety situations. Secondly, philosophical perspectives (both monism and dualists) on matter and mind were explored aiming to provide a deeper understanding of the ontological assumptions on safety situation. The discussion endeavors to contribute to ongoing conversations around situation awareness in construction safety. The framework bridges the knowledge gap by providing formal language to facilitate future information fusion, retrieval, mapping, and reasoning. Future research should be conducted to evaluate the coverage and usefulness of the CSS-Onto.

Keywords: Situation awareness, Situational awareness, Construction safety, Ontology, Safety situation

1. INTRODUCTION

The construction sector has been criticized for its elevated frequency of incidents worldwide. According to a report from Safe Work Australia (SWA), the employers’ 5-year average fatality rate in the Australian construction industry is 2.9, much higher than the national average of 1.1, thereby positioning it fifth among all industries (Safe-Work-Australia-(SWA), 2018).

One of the primary obstacles faced by site workers is effectively managing site dynamics. In a bustling construction site, numerous actors, materials, and equipment operate concurrently. Maintaining an adequate level of attention during hazardous situations can be an arduous task for laborers. For instance, a heavy equipment operator may cause accidents by failing to notice other workers in their blind spot. Often, accidents occur because workers are unaware of their surroundings, such as a rigger working beneath a crane's load. Therefore, achieving and maintaining a sufficient level of situation awareness holds the potential to enable individuals to identify potential hazards, make informed decisions, and take proactive measures against accidents. Situation awareness (SA) has been defined as “the perception of the elements in the environment within a volume of time and space, the comprehension of their meaning, and the projection of their status in the near future” (Endsley, 1995).

The information related to SA can be referred as SA requirements. SA requirements refer to the information that an operator ideally needs to know to make decisions and achieve goals. In the domain of construction safety, Goal-Directed Task Analysis (GDTA) is one of the most widely accepted methods for investigating SA requirements (Choi et al., 2020; Gheisari et al., 2010; Irizarry & Gheisari, 2013). However, GDTA has been criticized for several disadvantages. Firstly, it oversimplifies activities into an isolated hierarchy of goals, decisions, and information requirements that poorly model the contextual relationship between SA requirements. Secondly, it heavily relies on the subjective judgments of small groups of participants (10 to 20). Thirdly, it is time-consuming. Finally, it gives poor consideration to non-routine or unexpected tasks. The GDTA could have

been more compelling if it had included an evaluation of the effectiveness of SA requirements. Defining what constitutes a safety situation is another fundamental issue in measuring the effectiveness of SA requirements. Kärkkäinen et al. (2019) have proposed a conceptual model known as the "situation picture" to improve digital and social information communication. However, the definition and modeling of a "safety situation" have been largely overlooked in the domain of construction safety research.

Providing adequate and timely information is a highly effective strategy to achieve and maintain a safety situation. However, simply having an abundance of data does not guarantee meaningful insights. To convert data into useful information, a generic framework is needed to efficiently fuse, retrieve, map, and reason relevant data. This is particularly important when considering the intelligent-oriented third wave of construction occupational health and safety (OHS) management that emerged in the early 2000s (Gondia et al., 2023; Jin et al., 2019; Niu et al., 2019). Previous research has often focused on a single scenario. For example, Cheng and Teizer (2014) programmed an algorithm to create a visual representation of blind spots around tower crane. Elelu et al. (2023) developed an audio-based algorithm to detect potential collisions between equipment and labors. To facilitate effective construction OHS management, a systematic approach is required to gather and integrate contextual, heterogeneous construction safety data into meaningful information and useful knowledge. One theoretical framework that underpins the concept of a safety situation is situation theory, developed by Barwise and Perry (1983). The theory abstracts situations into three fundamental building blocks: individuals, properties and relations, and locations. Allowing mathematical precision in analyzing and describing complex situations is the main advantage of situation theory. Previous research efforts has conducted to provide safety insights. For example, Huang et al. (2018) developed a big data-driven safety decision-making framework to extract hidden safety insight from safety-related big data by data mining. To push the envelope further, effective construction OHS management requires a generic safety situation to define safety information, establish relationships between information, and measure SA.

Ontology originates from metaphysics and refers to the nature of existence. In computer science, ontology is used to model and represent domain knowledge in a machine-readable format. In the data fusion community, Llinas et al. (2004) argued that ontology has the significant capacity to partition "situation" into hierarchical frameworks to support future algorithm development. In information science, ontology serves as a structured domain knowledge representation that includes classes, properties, and relationships aimed at facilitating the fusion, retrieval, mapping, and reasoning of information. An ontology has the capacity to automatically organize diverse data and transform it into contextual safety information.

The objective of this paper is to develop a construction safety situation ontology (CSS-Onto). The goals of CSS-Onto are to establish an ontological framework for situational awareness requirements that enable computers to describe construction sites using formal language, and to facilitate the definition of "safety situation" in the context of construction sites.

2. METHODOLOGY

The research methodology employed for developing the CSS-Onto is the NeOn Methodology. Suárez-Figueroa et al. (2015) developed this methodology, which consists of four fundamental phases: initiation, reuse, reengineering, and design (refer to Figure 1). Utilizing the NeOn Methodology provides numerous advantages, primarily focused on the capacity to reuse both ontological and non-ontological resources to ensure efficiency and strong consistency with other ontologies.

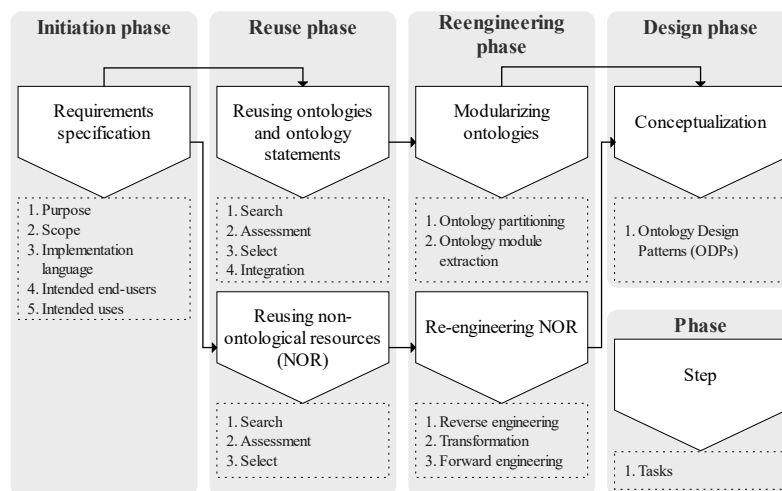


Figure 1. Ontology development framework

The objective of specifying ontology requirements is to elicit the criteria that the CSS-Onto must satisfy. The purpose of the CSS-Onto is to model the dynamic construction sites in formal language to facilitate computer-based SA improvement. The CSS-Onto centers on the domain of ensuring safety at construction sites. Physiological and psychological state of individual, social state of group, and state of other physical environmental elements represent three main levels of granularity in CSS-Onto. The CSS-Onto utilizes the Web Ontology Language 2 (OWL 2) (Group, 2012) as the formal language. The CSS-Onto is intended to be used by a diverse group of end-users, including frontline workers, safety managers, and inspectors. Furthermore, the CSS-Onto is expected to be used for various purposes in the future, such as information fusion, retrieval, mapping, and reasoning.

The reuse phase involves two sources of information: ontologies and non-ontological resources (NOR). Ontologies are categorized into two fundamental types: general ontology and domain ontology. The reuse of general ontologies aims to ensure maximum reusability across various domains by defining concepts such as space and time. After searching, assessing, and selecting a general ontology, OWL 2 was used to conceptualize the basic categories and relationships of the ontology. Nevertheless, the objectives of reusing domain ontology were to save time, reduce costs, and increase overall quality. In this specific research, the Active Fall Protection System Ontology (AFPS-Onto) (Guo & Goh, 2017) was reused. Subsequently, ontology statements selected from both general and domain ontologies were integrated to generate an extended ontology network. The NOR adopted in the research were 148 accident reports from the City-of-New-York (2023) and the Industry Foundation Class (IFC) from BuildingSMART-International-Limited (2020).

In the reengineering phase, the AFPS-Onto underwent a modularization process that was facilitated by a combination of ontology partitioning and ontology module extraction techniques. This approach was employed to decompose the AFPS-Onto into interrelated modules, and to create more specialized sub-ontologies that could be reused in CSS-Onto. On the other hand, NOR were re-engineered through three steps. First, NOR were reverse engineered to information granules such as task, occupation, equipment, material, building element, environmental element, immediate factor, accident type, industry, spatial relationship, and temporal relationship. Second, the transformation was conducted to identify patterns, schemas, data models, and relationships that exist among information granules. Finally, the forward engineering generated an ontological model based on the information granules, patterns, relationships, etc. In the design phase, the process of integrating sub-ontologies from modularization and the ontological model from NOR re-engineering was undertaken by utilizing ontology design patterns (ODPs), resulting in the conceptualization of CSS-Onto.

3. CONSTRUCTION SAFETY SITUATION ONTOLOGY

3.1. The Purpose of CSS-ONTO

Figure 2 depicts two blocks that are vertically stacked, each representing a cognitive process involved in achieving human SA. Conventional workers on construction sites typically rely on traditional cognitive processes to perceive and maintain SA. This involves complex cognitive processes such as attention, working memory, long-term memory, and decision-making, which are driven by sensory inputs. However, this traditional approach may have its limitations. For example, when presented with ample data, information overload may occur, hindering accurate perception, comprehension, and projection. Moreover, biases inherent in individuals may impact their SA. Furthermore, cognitive processes like working memory and attention may not always be sufficient in volatile environments.

Although research leveraging DT has been conducted to enhance workers' SA in construction sites (Cheng & Teizer, 2014; Elelu et al., 2023), the fragmented nature of the provided information (such as blind spots of equipment operators and collision warnings through auditory signals emitted by equipment) has led to significant gaps in knowledge, resulting in significant deficiencies in constructing the safety situation. The proposed ontology-based DT-driven cognitive process aims to address these challenges by introducing a CSS-Onto that models the dynamic construction sites in a formal language to facilitate computer-based SA. Additionally, the development of a knowledge-based system to support computer-based perception, comprehension, and projection can be facilitated by integrating a reasoning engine such as case-based reasoning and rule-based reasoning (Goh & Guo, 2018). In summary, it is expected that the combination of ontology-based DT-driven SA information requirements and a reasoning engine will assist computers in achieving perception, comprehension, and projection. Thereafter, human SA can be improved or maintained through SA information from computer systems.

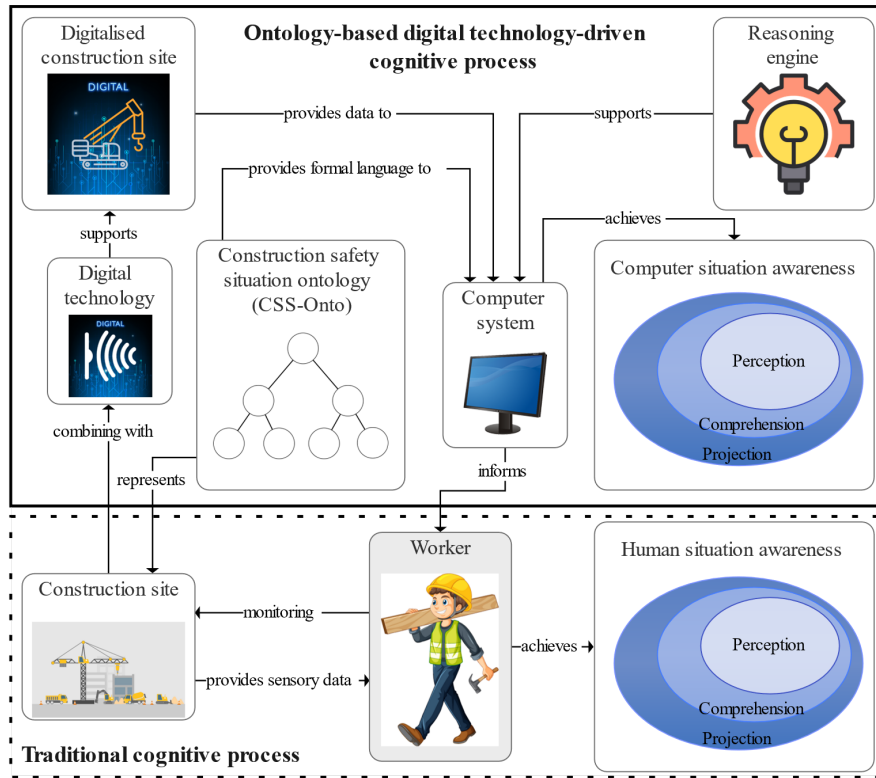


Figure 2. The purpose of construction safety situation ontology

3.2. An Ontological Model of Safety Situation

Figure 3 is a graphical representation of CSS-Onto. The ontological framework is composed of four fundamental components: individual (i.e. psychological state), group (i.e. social dynamics and norms), physical environmental element (i.e. equipment), and task. The individual component encompasses three concepts: actor, physiological state, and psychological state, which are employed to model a human in construction sites. The group component comprises two concepts: group and social dynamics and norms, aimed at creating an abstract concept of a team as a unified whole, which can be applied to future contexts where groups are viewed as the fundamental unit of analysis. The physical environmental element includes five concepts: climatic conditions, equipment, material, building element, and digital technology, which are employed in combination to provide environmental information about construction sites. The concept of task is central, as it represents the primary activity around which all other elements revolve. In considering the big picture, the four components are interdependent, as a group of individuals work together within an environment to accomplish tasks.

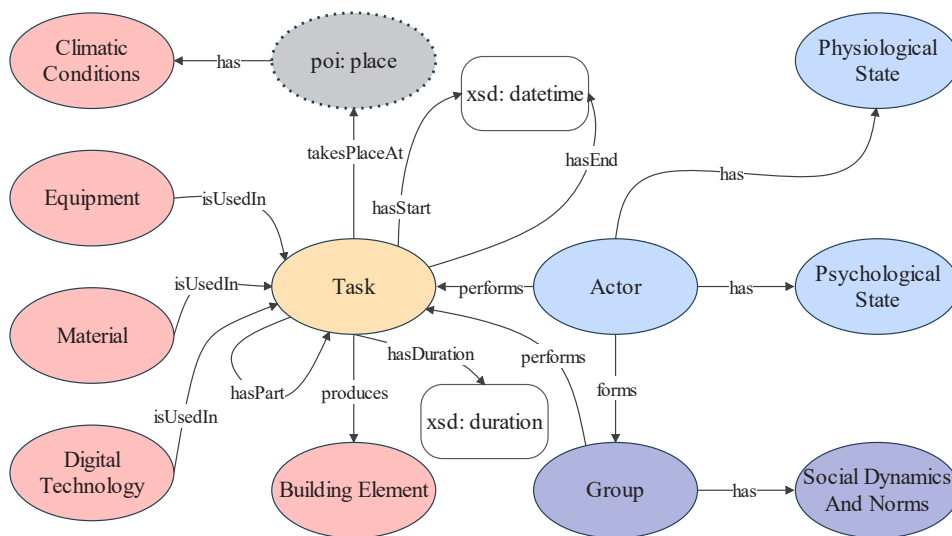


Figure 3. An ontological model of safety situation

3.3. Class

The notion of an actor encompasses all stakeholders involved in construction sites. The CSS-Onto defines actor roles based on the Australian and New Zealand Standard Classification of Occupations (ANZSCO) (Stats-NZ & Australian-Bureau-of-Statistics-(ABS), 2022). For instance, the actor role comprises five major groups, namely managers, professionals, technicians and trades workers, machinery operators and drivers, and laborers.

Physiological status refers to the overall condition of an individual's bodily functions at a particular moment. It can encompass various aspects of an individual's health and well-being, such as physical fatigue, heart rate, reaction time, and more.

Psychological status can be defined as the state of an individual's mental and emotional well-being at a specific time. It encompasses a range of interconnected aspects of psychological functioning, including safety knowledge, safety attitude, safety consciousness, mental load, situational awareness, and so forth.

A group is a collective of two or more stakeholders who collaborate to accomplish a shared task. Social dynamics and norms refer to the interaction approaches and unwritten rules between and among and within groups. The purpose of defining the group is to facilitate the modeling of attributes such as peer pressure, production pressure, and safety culture.

Equipment refers to the machinery and tools utilized to execute various tasks, such as loaders, cranes, dumpers, and excavators. Materials are defined as a variety of substances utilized in constructing structures, such as concrete, steel, wood, and water. In the context of construction sites, building elements are characterized as distinct and separable components that combine to form a building or structure, including but not limited to flooring, columns, walls, beams, stairs, and roofs. Climatic conditions in construction sites encompass a range of meteorological and environmental factors, including wind, soil, air, and dust. Digital technology in construction sites refers to the use of digital tools and systems to improve safety, such as building information modeling (BIM), internet of things (IoT), and virtual reality (VR).

The task in CSS-Onto is built upon the task definitions offered by IFC. Tasks in construction sites refer to the specific activities that need to be performed to complete a construction project. The IFC provides 12 types of tasks: attendance, construction, demolition, dismantle, disposal, installation, logistic, maintenance, move, operation, removal, and renovation (BuildingSMART-International-Limited, 2020).

3.4. Relations

Khoo and Na (2007) define semantic relations as “meaningful associations between two or more concepts, entities or sets of entities”. By providing a framework for establishing relationships between different entities, semantic relations facilitating the representation of contextual information in a structured and organized manner. The semantic relations adopted in the CSS-Onto can be grouped into the following types:

- Hyperonym-hyponym relations: these refer to the hierarchical relationship between a general class (hypernym) and a more specific class (hyponym), also known as a supertype-subtype relation. Variations include “is_equivalent_to”, “is_similar_to”, “is_disjoint”, “is_opposite”, and “is_subclass_of” (El-Diraby & Osman, 2011). A representative instance in the CSS-Onto is: “Laborers <has_subclass> Concreters”.
- Meronym-holonym: these pertain to the interdependence between a whole entity (holonym) and its constituent parts (meronyms), also called a part-whole relation. An example in the CSS-Onto is: “Actor <has_subpart> Leg”.
- Concept-object (instance-of) relations: these refer to the relationship between a concept (class) and an object (instance) that is an instance of that concept. For example, in the CSS-Onto, “A specific inspector <is_instance_of> Safety inspector”.
- Cause-effect relations: these are elucidated by lexical causatives (also known as causative verbs). These lexical causatives include: “performs”, “produces”, and “is_used_in”. An example in CSS-Onto is: “Actor <performs> Task”
- Spatial relations: these refer to spatial relationships between instances, such as “adjacent”, “inside”, “outside”, “intersect”, “has_distance”, “up”, “down”, “left”, “right”, “forward”, and “backward”. For example, Worker <under> Crane.
- Temporal relations: these pertain to the relationships between instances in time. Variations including “before”, “after”, “concurrent_with”, “partially_overlapping_with”, “during”. To illustrate, “Crane flip over injury Worker <in the process>”

3.5. Data Property

El-Gohary and El-Diraby (2010) have provided a definition of property as “a characteristic that describes a thing”. Figure 4 shown the representative properties of main classes in CSS-Onto. The majority of these properties were obtained through reengineering processes of accident reports. However, it is important to note that certain properties were extracted through knowledge engineering processes, such as safety attitude, safety motivation, and trust in co-workers.

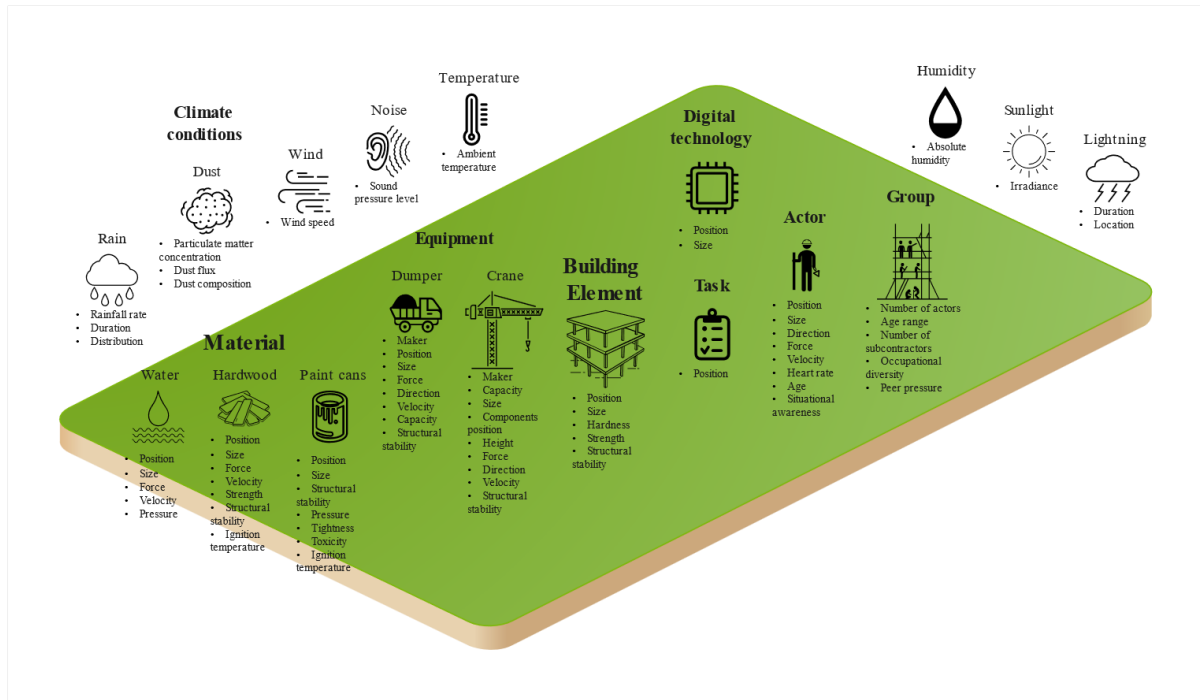


Figure 4. Key properties of main classes

4. EVALUATION

The competency of CSS-Onto was evaluated by describing a safety situation in an actual accident report from the City-of-New-York (2023). The classes, relations, and properties were highlighted in Figure 5 to showcase its competency in accurately representing the safety situation.

A department of buildings (DOB) inspector reported that a tower crane was <engaged with> loading a four foot piece of scaffolding material on <top> of a trailer within the job site. <After> the load was <lowered> into place, a worker began unhooking the rigging gear so that the crane could <proceed> with the <next> lift. The gear was <detached> from the load and the crane hoisted <up> to clear the trailer and the loaded scaffolding <when>, unbeknownst to the worker, the rigging gear <snagged> the corner of the load that had just landed, which <caused> the load to <flip over> the <side> of the trailer and <bring> the worker <down>, injuring him <in the process>. The worker was found bleeding, but conscious, and was <taken to> a hospital by ambulance.

Class

<Relations>

Property

Figure 5 Safety situation description

5. DISCUSSION

The term “safety situation” refers to the current state of safety in construction sites, encompassing several key aspects such as safety conditions, the presence of potential hazards and risks, the severity of risk, and the measures to mitigate risk. The CSS-Onto can be utilized to define and describe the safety situation. The following principles can aid in defining the safety situation:

- The status of individual elements, including both classes and properties.
- The spatial-temporal and cause-effect relationship amount individual elements.
- A situation entails certain hazards, risks, and corresponding measures.

The CSS-Onto can be utilized in conjunction with techniques such as data fusion, retrieval, mapping, and reasoning to facilitate comprehension of vast and intricate data, with the aim of supporting hazard identification, risk assessment, and risk mitigation in the context of construction safety.

Firstly, for hazard identification, CSS-Onto can be used to model the safety situation in terms of individuals, groups, physical environmental elements, and tasks. This modeling approach, combined with data fusion techniques that integrate data from various sources, such as sensor data, guidelines, and accident reports, can be utilized to identify potential hazards. Retrieval techniques can also be utilized to extract safety information from safety databases that can assist in hazard identification. Additionally, mapping techniques can be used to visualize the location of hazards. Reasoning techniques can be utilized to identify potential hazards by analyzing

the relationships between instances as modeled in the ontology.

Secondly, in terms of risk assessment, CSS-Onto can be employed to model the safety situation regarding the likelihood and severity of potential hazards. Data fusion techniques can be used to integrate various hazard data to assess the likelihood and severity of risks. Retrieval techniques can be utilized to extract relevant information on the severity and likelihood of similar hazards from safety databases. Furthermore, mapping techniques can be employed to visualize the risks associated with each hazard on the construction site, while reasoning techniques can be used as an analysis method to evaluate the risks.

Finally, CSS-Onto can be utilized to model the safety situation in terms of risk mitigation measures. Data fusion techniques can be used to integrate safety standards, best practices, and safety guidelines to identify potential risk mitigation measures. Retrieval techniques can be employed to extract effective risk mitigation measures from safety databases. Mapping techniques can also be utilized to visually identify potential risk mitigation measures on the construction site. Reasoning techniques can be employed to evaluate the effectiveness of different risk mitigation measures in reducing risks.

A future ontology-based DT-driven construction safety situation aware site is likely to be an intelligent system that can provide the appropriate safety information to the correct stakeholders at the right time. Firstly, real-time safety data is likely to be gathered from a wide range of sensors. Secondly, artificial intelligence (AI) might power the safety data analysis. Thirdly, VR could be used to support remote safety inspection. Fourthly, augmented reality (AR) has the capacity to visualize real-time safety information. Finally, the system may be developed based on a cloud-based infrastructure, allowing ubiquitous access.

The definition of a safety situation requires grappling with a fundamental inquiry surrounding its ontological nature, particularly whether it pertains to matter and/or mind. One notable perspective, namely monism, posits that matter and mind are the same. Material monism, as a form of monism, suggests that physical matter and natural laws can explain all things in the universe, including but not limited to mind, mental process, and consciousness. In defining the safety situation, the CSS-Onto aligns with the material monist perspective. This perspective is adopted due to the belief that the mind emerges from physical brain activity, and scientific investigation and experimentation of the brain can facilitate comprehension and elucidation of the mind. In other words, the mind is generally considered knowable within material monism. Conversely, mentalistic monism proposes that there is only one fundamental substance in the universe, and that substance is of a mental or spiritual nature. However, natural monism points out that matter and mind are one common substance. Specifically, mind and matter are considered as two sides of the same coin. On the other hand, dualism believes that matter and mind are two fundamentally different kinds of entities in the universe. Dualists maintain that the mind is a non-physical entity that exists independently of the body and brain, and the mind cannot be explained by physical processes in the brain alone. In conclusion, the philosophical perspectives on matter and mind have significant implications for defining and comprehending safety situations in construction sites. Specifically, the way we conceptualize the relationship between matter and mind impact how we perceive, comprehend, and project safety situation on construction sites.

6. CONCLUSION

The research employed NeOn to create a CSS-Onto that enables structured and standardized formal language representation on construction sites, with the primary goal of facilitating computer-based perception, comprehension, and projection of safety situations. Moreover, the study proposes several principles to define safety situations and elucidate the philosophical thinking behind them. The utilization of ontology-based systems in construction safety management can also aid in data fusion, retrieval, mapping, and reasoning to support hazard identification, risk assessment, and risk mitigation.

Although the CSS-Onto provides a promising approach to enhance safety in the construction industry. The CSS-Onto has several limitations: (1) the ontology reuse is limited to AFPS-Onto due to time constraints; (2) the NOR is restricted to accident reports and IFC; (3) due to limited sample size (148) from accident reports, the CSS-Onto cannot representing all domain knowledge in construction site safety practice; (4) accident reports as secondary data negatively impact the analysis results; (5) accident report data sources is only from City-of-New-York (2023); and (6) ontology evaluation was oversimplified.

The CSS-Onto can be extended and updated over time to encompass more comprehensive safety knowledge and practices, and to adapt to changing circumstances and requirements. Future research is recommended as follows: (1) more construction safety ontology should be considered in reuse phase; (2) more NOR should be included. For example, safety standards, safety regulations, best practices, and safety guidelines; (3) cross-culture multi-disciplines GDTA should be conducted to gather comprehensive domain knowledge; (4) an objective historical hazards information collection method should be developed; and (5) task-based ontology evaluation should be conducted to evaluate coverage and usefulness of the CSS-Onto.

REFERENCES

- Barwise, J. and Perry, J. (1983). *Situations and attitudes*. MIT Press
- BuildingSMART-International-Limited. (2020). Industry Foundation Classes 4.0.2.1 - Version 4.0 - Addendum 2 - Technical Corrigendum 1. Retrieved from BuildingSMART-International-Limited website: https://standards.buildingsmart.org/IFC/RELEASE/IFC4/ADD2_TC1/HTML/
- Cheng, T. and Teizer, J. (2014). Modeling tower crane operator visibility to minimize the risk of limited situational awareness, *Journal of Computing in Civil Engineering*, 28 (3),
- Choi, M., Ahn, S. and Seo, J. (2020). VR-Based investigation of forklift operator situation awareness for preventing collision accidents, *Accident analysis and prevention*, 136 105404
- City-of-New-York. (2023). Construction Related Accident Reports. Retrieved from City-of-New-York website: <https://www.nyc.gov/site/buildings/dob/construction-related-accident-reports.page>
- El-Diraby, T. E. and Osman, H. (2011). A domain ontology for construction concepts in urban infrastructure products, *Automation in construction*, 20 (8), 1120-1132
- El-Gohary, N. M. and El-Diraby, T. E. (2010). Domain Ontology for Processes in Infrastructure and Construction, *Journal of construction engineering and management*, 136 (7), 730-744
- Elelu, K., Le, T. and Le, C. (2023). Collision Hazard Detection for Construction Worker Safety Using Audio Surveillance, *Journal of Construction Engineering and Management*, 149 (1),
- Endsley, M. R. (1995). Toward a Theory of Situation Awareness in Dynamic Systems, *Human factors*, 37 (1), 32-64
- Gheisari, M., Irizarry, J. and Horn, D. B. (2010). Situation awareness approach to construction safety management improvement, *26th Annual Conference of the Association of Researchers in Construction Management, ARCOM 2010*, Leeds, pp.311-318.
- Goh, Y. M. and Guo, B. H. W. (2018). FPSWizard: A web-based CBR-RBR system for supporting the design of active fall protection systems, *Automation in construction*, 85 40-50
- Gondia, A., Moussa, A., Ezzeldin, M. and El-Dakhakhni, W. (2023). Machine learning-based construction site dynamic risk models, *Technological Forecasting and Social Change*, 189 122347
- Group, W. C. O. W. (2012). OWL 2 Web Ontology Language Document Overview (Second Edition). Retrieved from Group, W. C. O. W. website: <https://www.w3.org/TR/owl2-overview/>
- Guo, B. H. W. and Goh, Y. M. (2017). Ontology for design of active fall protection systems, *Automation in construction*, 82 138-153
- Huang, L., Wu, C., Wang, B. and Ouyang, Q. (2018). Big-data-driven safety decision-making: A conceptual framework and its influencing factors, *Safety Science*, 109 46-56
- Irizarry, J. and Gheisari, M. (2013). Situation Awareness (SA), a qualitative user-centered information needs assessment approach, *International Journal of Construction Management*, 13 (3), 35-53
- Jin, R., Zou, P. X. W., Piroozfar, P., Wood, H., Yang, Y., Yan, L. and Han, Y. (2019). A science mapping approach based review of construction safety research, *Safety science*, 113 285-297
- Kärkkäinen, R., Lavikka, R., Seppänen, O. and Peltokorpi, A. (2019). Situation picture through construction information management, *10th Nordic Conference on Construction Economics and Organization*, Tallinn, Estonia, pp.155-161.
- Khoo, C. S. G. and Na, J.-C. (2007). Semantic relations in information science, *Annual Review of Information Science and Technology*, 40 (1), 157-228
- Llinas, J., Bowman, C., Rogova, G., Steinberg, A., Waltz, E. and White, F. (2004). Revisiting the JDL data fusion model II, *SPACE AND NAVAL WARFARE SYSTEMS COMMAND SAN DIEGO CA*
- Niu, Y., Lu, W., Xue, F., Liu, D., Chen, K., Fang, D. and Anumba, C. (2019). Towards the “third wave”: An SCO-enabled occupational health and safety management system for construction, *Safety science*, 111 213-223
- Safe-Work-Australia-(SWA). (2018). Work-related traumatic injury fatalities Australia 2018. Retrieved from Safe-Work-Australia-(SWA) website: <https://www.safeworkaustralia.gov.au/doc/work-related-traumatic-injury-fatalities-australia-2018>
- Stats-NZ and Australian-Bureau-of-Statistics-(ABS). (2022). Australian and New Zealand Standard Classification of Occupations (ANZSCO). Retrieved from Stats-NZ and Australian-Bureau-of-Statistics-(ABS) website: <https://www.abs.gov.au/statistics/classifications/anzsco-australian-and-new-zealand-standard-classification-occupations/latest-release>
- Suárez-Figueroa, M. C., Gómez-Pérez, A. and Fernández-López, M. (2015). The NeOn Methodology framework: A scenario-based methodology for ontology development, *Applied ontology*, 10 (2), 107-145

RISK ASSESSMENT OF RAILWAY TRACKS IN FLOODPLAIN AREA USING DIGITAL SURFACE MODEL AND COMPUTER VISION

Watcharapong Wongkaew¹, Wachira Muenyoksakul¹, Krittiphong Manachamni², Tanawat Tangjarusritatorn³ and Chayut Ngamkhanong⁴

1) Department of Civil Engineering, Faculty of Engineering, Chulalongkorn University, Bangkok, Thailand. Email: 6230481521@student.chula.ac.th, 6230464921@student.chula.ac.th

2) Department of Environmental Engineering, Faculty of Engineering, Chulalongkorn University, Bangkok, Thailand. Email: 6330011321@student.chula.ac.th

3) Ph.D., Department of Water Resources Engineering, Faculty of Engineering, Chulalongkorn University, Bangkok, Thailand. Email: tanawat.ta@chula.ac.th

4) Ph.D., Department of Civil Engineering, Faculty of Engineering, Chulalongkorn University, Bangkok, Thailand. Email: chayut.ng@chula.ac.th

Abstract: Monsoon region, which Thailand is situated in, experiences frequent heavy rainfall, leading to recurring flooding problems. This is one of the serious natural disasters that cause significant damage to Thailand's Infrastructure. Furthermore, human activities, such as the construction of railway tracks that obstruct the flow of water, and the inadequate natural drainage system also contribute to the problem. In order to analyze the area-based risk factors that cause railway track flooding, 5 major factors, including average total rainfall in rainy season, waterway density, land use, slope, and elevation must be considered. The study utilizes computer vision techniques such as Digital Surface Model (DSM) and flooding simulation to illustrate the topography of the flood-prone area and the right of way of railway tracks. A Digital Surface Model (DSM) is used to illustrate the topography of the flood-prone area and right of way of railway tracks. A comprehensive map showing the likelihood of railway track flooding in the area can be generated via the digital surface model and flooding simulation. Moreover, the results from these techniques can help identify the railway tracks damage, track structure, and surrounding areas due to the influences of different flooding conditions. The outcome of this study will provide a robust flood risk management process that can effectively prevent railway track's damages from natural disasters by utilizing computer vision technology to improve flood modeling accuracy.

Keywords: Digital Surface Model, Disaster risk, Flood, Railway tracks, Computer vision

1. INTRODUCTION

Railway track flooding is a common occurrence in Thailand, especially during the monsoon season when heavy rainfalls lead to flash floods and river overflows which cause extensive damage to railway infrastructure up to 1.3 billion THB (SRT Annual Report, 2017). Flooding of railway tracks disrupts transportation and poses a significant risk to the safety of railway rolling stocks along with passengers and personnel. With the increasing frequency and intensity of extreme weather events due to climate change, railway infrastructure in monsoon regions is facing greater challenges to maintain operational efficiency and safety in long term.

The issue of railway track flooding in Thailand is closely related to the country's floodplains. Western and Southern Thailand's geography are characterized by a network of rivers, which overflow their banks during the monsoon season, leading to extensive flooding (W. Jomwinya, 2017). The railway tracks, which run closely to the rivers, are often located in low-lying areas that are prone to flooding. When floodwaters rise, the tracks and fields become submerged, making the area unpassable.

Moreover, flooded tracks can cause the soil beneath them to erode, wash the ballast away, leading to mud pumping and destabilization of the track bed and compromising the safety of the trains passing over them. This has led to a growing need for effective flood mitigation strategies and better disaster and extreme event management plans to minimize the impact of flooding on railway transportation. In this context, understanding the risk and prediction of railway track flooding in the regions, as well as exploring potential modelling solutions, are crucial for ensuring the predictability, reliability, and resilience of railway infrastructure.

The area that we selected is the floodplain area in the Amphoe Meung Phetchaburi, Phetchaburi Province. The area between the Nong Pla Lai Station and Phetchaburi Station since area of interest had repeated flood over the course of 11 years from GISTDA data. (GISTDA Thailand Flood Monitoring System, 2023) The area, shown below in satellite imagery in Figure 1, is floodplain with some discharge network, land use of paddy fields, elevation between 0 – 10 meters.

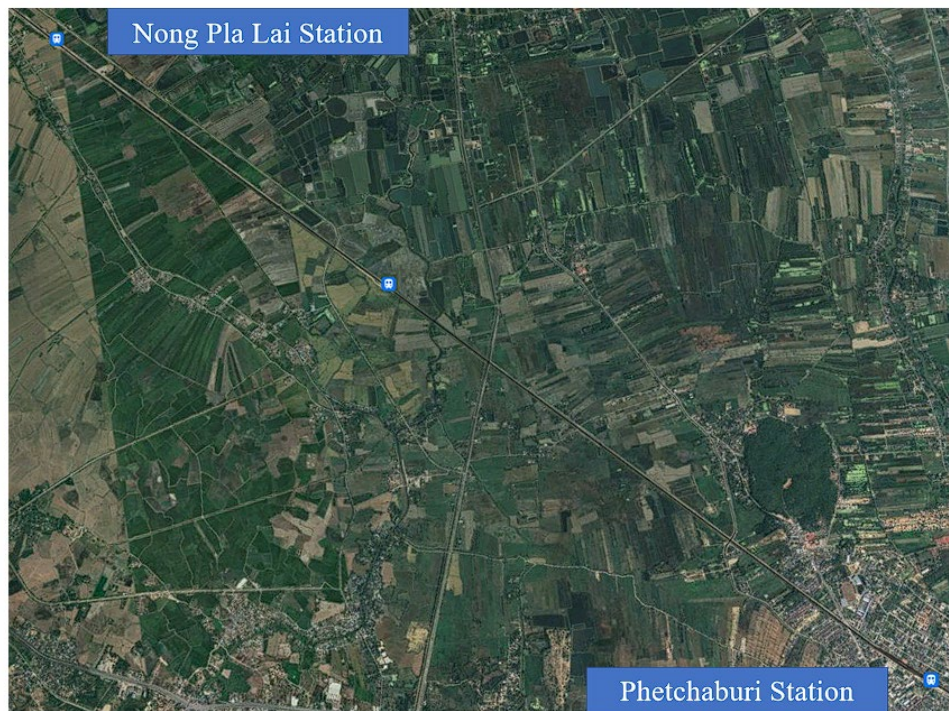


Figure 1. Satellite image of area of interest

2. METHOD

2.1 Data Collection

We associated some factors with a part of secondary data as in land use and slope since the primary data is incomplete or unavailable. By far, the secondary data that we use is the land use data that determine and label by photogrammetry method and usage of satellite imagery, and slope that determined by the 1-meter interval contour of the area which slope can be calculated by differences of elevation. The collection of data involved 5 major area-based risk factors including average total rainfall in rainy season, waterway density, land use, slope, and elevation, in railway tracks flooding, from various sources in Table 1.

Table 1. Data sources

Data	Sources	Type of data	Boundary of data
Digital Surface Model	GTOPO30/ NASA SRTM DEM30	numeric	-15 – 1506 m.
Land Use	Google Earth Imagery	nominal	field, residential
Average Total Rainfall in rainy season	Thai Meteorological Department	numeric	0 – 13.6 cm.
Elevation/ Slope	Contour maps from Department of Geology, Chulalongkorn University	numeric	-15 – 1506 m.
Railway Tracks	NASA SRTM DEM30	Line	-
Flood history	Department of Geography, Chulalongkorn University	area and ordinal	0 – 9
Waterway density	Geo-Informatics and Space Technology Development Agency	line	-
Catchment Area	Department of Geology, Chulalongkorn University	area	0 – 2,210 km ²
Administrative District	Department of Geology, Chulalongkorn University	nominal	-
Extreme Weather Condition	Department of Geography, Chulalongkorn University	numeric	0 – 20
	Thai Meteorological Department		

2.2 Flood Risk Index Calculation

To estimate the risk of the railway tracks in floodplain area, we use the Flood Risk Index (MarshMcLennan, 2021), which describe the flood risk in 3 components which we modified to better suited for local area in Thailand and railway industry which will be described in the table 2 below.

Table 2. Index Components, indicators and data sources

Index components	Indicators	Data Sources
Hazard	Riverine Flood	Digital Surface Model Average Total Rainfall and thunderstorm in rainy season Elevation/ Slope Waterway density
Exposure	Railway Track Exposure	Flood Area Maps: GISTDA Railway Tracks Elevation: SRT
Vulnerability	Railway vulnerability	Flood History: GISTDA

To calculate the Flood Risk Index or FRI, the methodology that we used is to combine 3 components of risk as hazard in form of Flood Hazard Score (FHS), exposure as Flood Exposure Score (FES) and vulnerability as in Flood Vulnerability Score (FVS) into index in the form of Equation (1) which gives us the index to interpret and into risk map

$$FRI = 0.5(FHS) + 0.3(FES) + 0.2(FVS) \quad (1)$$

All of the data in Table 2 is interpreted into one score as in FHS, FES and FVS which can be obtained by Equation (2), (3), (4).

$$FHS = f(Elevation, Slope, Precipitation, Thunderstorm) \quad (2)$$

$$FES = f(ArialExtent, RailTrackElevation) \quad (3)$$

$$FVS = f(FloodHistory) \quad (4)$$

Which $f(x)$ is functions of variable that model automatically tunes

FRI will be classified into 4 categories ranging from 0 – 1 which expressed in Table 3

Table 3. Flood Risk Index

Flood Index Range	Risk Class	Interpretation	Potential Damages
0 – 0.25	Low Risk Area	The area potentially have some flood over the years that can be prevented or mitigated (Low FHS, FES, FVS)	- Embankment seepage - Mud pumping
0.25 – 0.5	Medium Risk Area	The area potentially have some flood over the years that poses risk to railway embankment and needed to be repaired (Medium FHS, FES, FVS)	- Embankment seepage - Mud pumping and track settlement
0.5 – 0.75	High Risk Area	The area mostly flooded over the years and poses threats to railway embankment which damages may extend through ballast and rail track, which needed to be close for operation and repair (High FHS, FES, FVS)	- Embankment seepage - Ballast washaway - Mud pumping and track settlement - Track settlement due to ballast
0.75 – 1	Repeated Flood Area	The area potentially have repeated flood every other year. It poses significant threats to the railway tracks and embankment, which needed to be repaired and closed for unspecified period of time (Highest FVS)	- Ballast washaway - Embankment scour - Mud pumping and track settlement - Track settlement due to ballast

2.3 Risk Index Interpretation

(1) Idealize Track Condition.

To reference the ideal condition of track. We use State Railway of Thailand's standard for double track construction project. Which include engineering parameters, material properties and geometry of the track. Those data are presented in Table 4.

Table 4. Engineering parameters, material properties and geometry of the track.

Engineering Parameters	Data
Track Gauge	1 Meter
Rail Section	Bs100a
Sleeper Type	Prestress Concrete
Sleeper Dimension	200 X 50 X 25 cm
Ballast Material	Andesite, Rhyolite
Ballast Depth	70 cm
Embankment Height	2-6 m

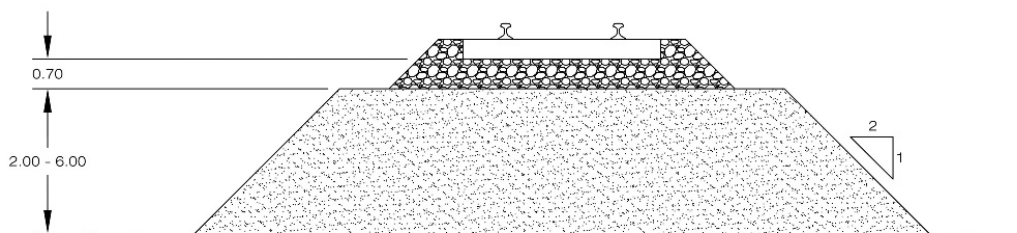


Figure 2. Railway Embankment

(2) Track Damage Interpretation from Flood Risk Index.

Track damage can be interpreted from flood risk index by categorizing character of flood area. Which can be categorized into 2 characters. One-sided flood and Two-sided flood. Those 2 categories are different in behavior of failure.

1.) One-sided flood

One-sided flood can be determined as a section of track which has high flood risk index area on one side but low or insignificant flood risk index on the other side. Or both of them are very different in value. This type of flood tends to have high movement and force, which causes damage to the track structure via 3 different processes.

Categorized by height and speed of the flood, 3 processes are described as in and in Figure 3 denoting by the letter (a), (b), and (c)

(a.) Embankment seepage

Embankment seepage caused by one-sided flood with water level is lower than ballast level. Or described as water level are within the area of embankment. According to State Railway of Thailand's standard for double track construction project. Track embankment is constructed by compacting earth materials. This type of material can have a phenomenon that existing water on one side of the material tends to move to the other side. Called water seepage. This phenomenon creates seepage force which can damage the track embankment. Causing embankment material to wash away on the other side of the flood.

(b.) Ballast washaway

Ballast washaway caused by one-sided flood with water level is higher than ballast level. Creating overtopping flow of flood. Which can wash away ballast with it. Track with missing ballast can affect strength and stiffness of the track.

(c.) Embankment scour

Embankment scour caused by one-sided flood with water level is higher than ballast level and have extreme velocity. A great amount of force created by water streams can damage whole structure, making the whole embankment fail and collapse.

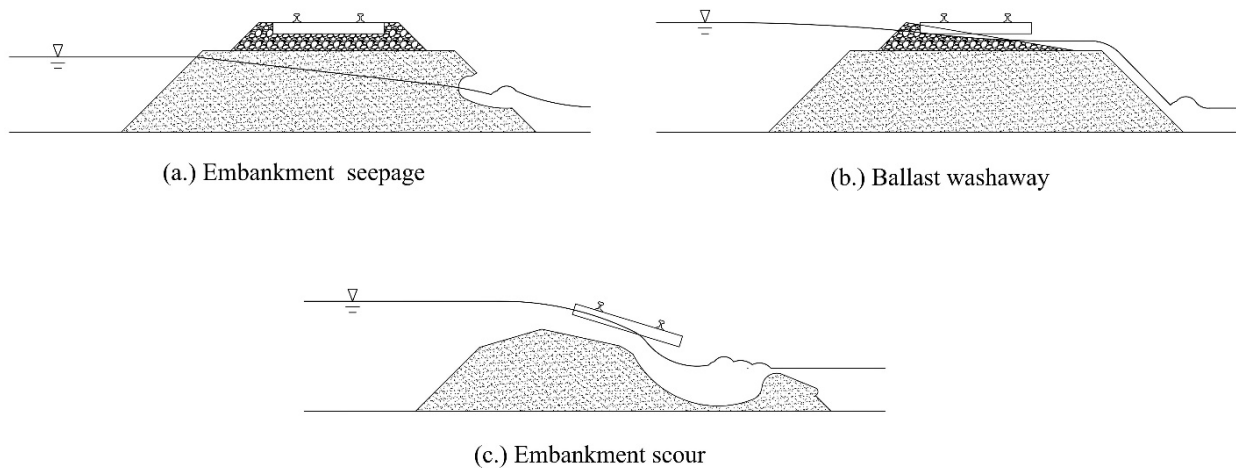


Figure 3. Type of Railway tracks failure in one-sided flood condition

2.) Two-sided flood

Two-sided flood can be determined as a section of track which area in both sides have high flood risk index, and no significant differences in term of value. This type of flood tends to remain stationary with no or negligible stream flow. With that, this type of flood causes damage to the track structure via 2 different processes,

Categorized by level of the flood. 2 processes are described as in and in Figure 4 denoting by the letter (a), and (b)

(a.) Mud pumping and track settlement due to embankment material movement

This type of damage is caused by flood on both sides of the track with water level lying within the area of embankment. When embankment material is soaked. Material swells and loses its compactness and becomes slurry substances. This mud-like substance is poor in performance of withstanding train load due to its high fluidity. This substance can seep through ballast layer and eject out caused by high pressure from train load when train is passing by. This phenomenon is mud pumping. Which can reduce stiffness of the track and increase track settlement.

(b.) Track settlement due to reduction of ballast interlocking

This type of damage is caused by flood on both sides of the track with water levels higher than the ballast level. The presence of water in the ballast layer acts like a lubricant causing the ballast aggregate to lose its skin friction and interlocking. Which can reduce stiffness of the track and increase track settlement.

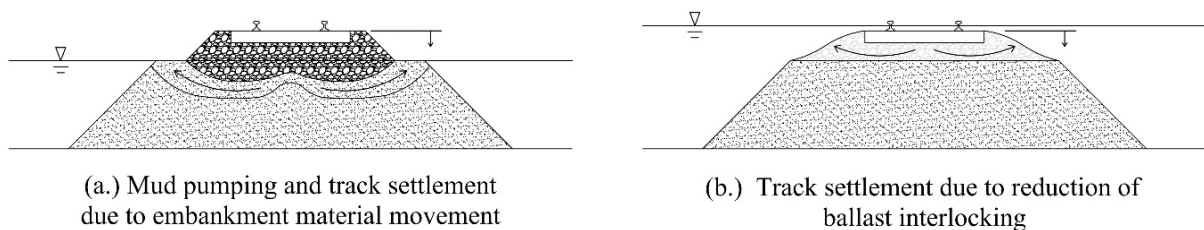


Figure 4. Type of Railway tracks failure in two-sided flood condition

2.4 Risk of Hazard in Floodplain Area Around Railway Tracks

To estimate the risk of floodplain area around railway tracks, making computers understand the physical parameters surrounding railway tracks from geological data is needed. This involves collecting data such as the elevation of the tracks, the distance from the nearest water source, and the surrounding rail track characteristics such as embankment, ballast. Also, we need flood history to be able to correctly predict and calculate the flood risk index (FRI).

Once we have this data, we can select candidate estimators that might be able to accurately estimate the area of the floodplain. The model which we select will be called estimators which calculate and predict the flood risk index that will be able to represent the flood history. These estimators include machine learning algorithms, statistical models, and other computational methods via transferring data from numerical data into raster and then transform into dataframe which can be used in the model.

Table 5. Floodplain estimators

Model	Type of processing
Multinomial Logistic Regressor*	Classifier
Multinomial Naïve Bayes*	Classifier
Multi-Layer Perceptron (MLP)*	Fully connected ANN
Convolutional Neural Network based	Backpropagation
Transformers based model	Attention-based

*Model use for classified flood on rail

(1) Model Inputs

The input of the model is digitalised into raster data and put into the python which then integrated with DEM data, all of the input can be found in Table 2. Then, transformation of independent variables and integrated into the dataframe and put into the model as explained in Figure 5.

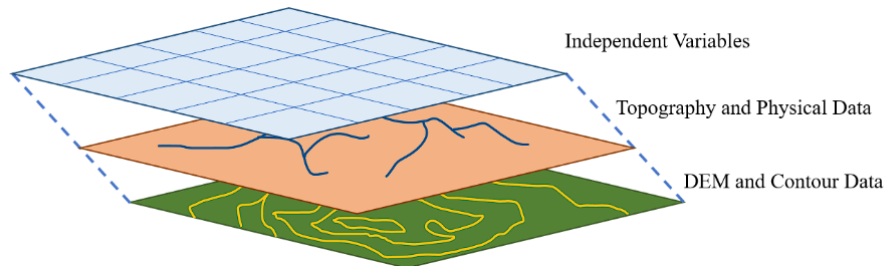


Figure 5. Process of creating model inputs

After the data overlayed, integrated and expressed in the form of raster data, the data can be converted into dataframe as explained in Figure 6.

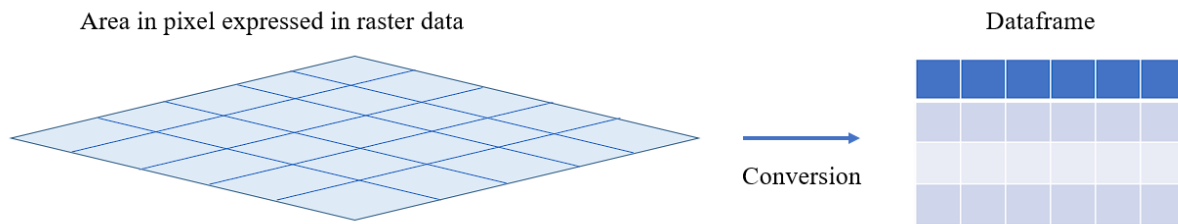


Figure 6. Process of conversion into model inputs

(2) Train-Validation-Test Split

After the data in the form of dataframe, the process of splitting data and validation take place, which is crucial in training the machine learning model, the process is done by splitting the raster data between 16 years into test set, validation set, and training set using KFold cross-validation method, 6 folds.

Prediction of the model is done by parameters of splitting in Table 6.

Table 6. Floodplain estimators

Splitting Type	Number of years
Training	10
Validation	2
Tests	4

(3) Metrics

After selecting the candidate estimators, we evaluate the results based on the accuracy of measuring the basic criteria of the floodplain. This can include measuring the amount of correctly estimated area and other metrics such as precision and recall. To quantify the area, we use Intersect over Union (IoU) (Hamid Rezatofighi, Nathan Tsoi, JunYoung Gwak, Amir Sadeghian, Ian Reid, Silvio Savarese, 2019), which provides the intersect segment area of the real floodplain compared to the estimated floodplain. This allows us to compare the estimated floodplain to the actual floodplain and determine how accurate our estimator is.

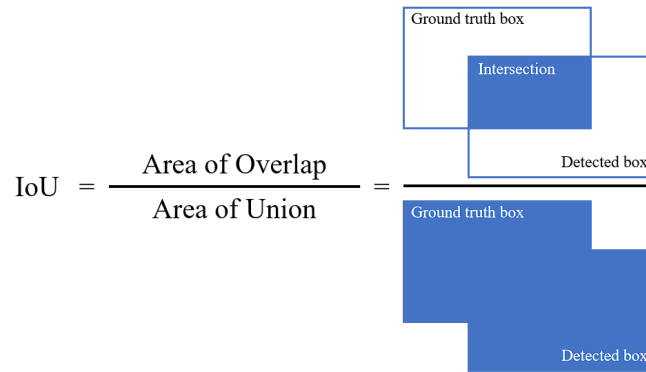


Figure 7 Explain how Intersect over Union (IoU) metrics works.

Overall, accurately estimating the floodplain area around railway tracks is crucial for assessing the risk of flooding and ensuring the safety of the railway system. By using computational methods and statistical models, we can make these estimations with a high degree of accuracy, allowing us to take the necessary steps to prevent flooding and minimize the risk to both the railway system and the surrounding area.

The performance metrics interpretation is described in Table 7.

Table 7. Metrics interpretation

Metrics	Range	Interpretation
IoU	0 - 1	IoU > 0.8 as excellent score, IoU > 0.5 as good, and any other score as poor
Dice Index	0 - 1	0, indicating no spatial overlap to 1, indicating complete overlap, meaning if the score is closer to 1, the better
F1 Score	0 - 1	The closer it is to 1, the better the model.
Precision	0 - 1	A measure of quality if the score is closer to 1 more ground truth to all data (True Positive)
Recall	0 - 1	A measure of quantity if the score is closer to 1 the more ground truth to the relevant data.

3. RESULTS

Using Computer vision technology to explore the impact of flooding on railway tracks and surrounding areas, examining track damage and structure. We divided flood risk into 4 categorical types as shown in Table 8 with the result of specific metrics.

Table 8. Performance results on the snapshot image dataset.

	Validation set					Testing set				
	Precision	Recall	F1 score	IoU	Dice Index	Precision	Recall	F1 score	IoU	Dice Index
Logistic Regression (Macro-average)	0.68	0.69	0.68	-	-	0.50	0.50	0.50	-	-
Naïve Bayes (Macro-average)	0.54	0.53	0.52	-	-	0.27	0.35	0.40	-	-
MLP (Macro-average)	0.95	0.93	0.94	-	-	0.83	0.75	0.73	-	-
CNN (Macro-average)	0.54	0.51	0.52	0.62	0.66	0.42	0.43	0.47	0.55	0.61
Transformer (Macro-average)	0.62	0.63	0.66	0.68	0.73	0.59	0.57	0.61	0.67	0.72

Table 9. Prediction results on FRI

FRI Range	Arial Extent
Low Risk area	0.12
Medium Risk area	0.35
High Risk area	0.25
Repeated Flood area	0.28

4. DISCUSSION

According to Tables 8 and 9, the results show the performance on the snapshot image dataset for each condition. Table 8 displays the precision, recall, and F1 score for each model, including categorical and area digitized in macro-averages due to limited samples. Due to the small testing set, the performance of the model can be explored further if we expand the study area to include more samples.

The results show that the Multi-Layer Perceptron (MLP) area has the highest precision, recall, and F1 score, indicating that the model is most effective when applied with this category of area. For others, overall results are not good because the small area and number of years, but the results would suggest that this model can be used as a tool for identifying flood risk areas more efficiently if provided more data.

5. CONCLUSIONS

The study considers five main major factors, including average total rainfall in the rainy season, waterway density, land use, slope, and elevation, to analyze the area-based risk factors that cause railway track flooding. Using computer vision technology, we had generated a comprehensive map showing the flood risk index of railway track flooding in the area. The digital surface model used in this study help in identifying the damages to railway tracks, track structures, and surrounding areas due to the influences of different flooding conditions.

This study is expected to provide us with an understanding of the relationship between flooding conditions and railway embankment and track damages, which can be used to develop more effective flood risk management strategies. With a remarkable potential, the findings of this study will contribute to the development of a more resilient railway infrastructure that can withstand the impacts of natural disasters.

Utilizing this process, railway operators will be able to mitigate the risks of flooding and prevent future damages to the railway embankment efficiently. The study is expected to provide a more comprehensive understanding of the relationship between flooding conditions and railway track damages and provides a useful framework for analyzing and preventing railway track flooding using computer vision technology and risk factor analysis. The findings can be applied to other regions with similar flooding problems to develop a more resilient railway infrastructure that can withstand natural disasters.

ACKNOWLEDGMENTS

The authors would like to thank all of the data sources including Thai Meteorological Department, GISTDA, Department of Geology, Chulalongkorn University, and Department of Geography, Chulalongkorn University. Also, the authors would like to thank Associate Professor Dr. Pannee Cheewinsiriwat, and Dr. Phathinan Thaihatkul for the advice, methodology and the data on Geographic Information System (GIS) which we used QGIS and Python 3 in visualizing.

REFERENCES

- Fu, H., Yang, Y. and Kaewunruen, S. (2023). Multi-Hazard Effects of Crosswinds on Cascading Failures of Conventional and Interspersed Railway Tracks Exposed to Ballast Washaway and Moving Train Loads, *Sensors* 2023, 23(4), 1786. Retrieved from <https://www.mdpi.com/1424-8220/23/4/1786>
- Jomwinya, W. (2017). *Geography of Thailand*. Faculty of Social Science, Udon Thani Rajabhat University.
- MarshMcLennan. (2021). *Marsh McLennan Flood Risk Index: Methodology*. Retrieved from MarshMcLennan website: <https://www.marshmcclennan.com/insights/publications/2021/september/marsh-mclennan-flood-risk-index.html>.
- Rezatofighi, H., Tsoi, N., JunYoung, G., Sadeghian, A., Reid, I., Savarese, S. (2019). Generalized Intersection over Union: A Metric and A Loss for Bounding Box, 1-9 doi:<https://doi.org/10.48550/arXiv.1902.09630>
- State Railway of Thailand. (2017). *State Railway of Thailand Annual Report*. Retrieved from SRT website: <https://www.railway.co.th/AboutUs/AnnualReport>
- Tsubaki, R., Bricker, J. D., Ichii, K., Kawahara, Y. (2016). Development of fragility curves for railway embankment and ballast scour due to overtopping flood flow, *Natural Hazards and Earth System Sciences*.
- Wongthadam, T. (2016). *Assessment of flood hazard areas using Analytical Hierarchy Process*. 1-83. Retrieved April 11, 2023

GRAPH NEURAL NETWORK INTEGRATING WITH METAHEURISTIC SEARCH FOR AUTOMATED MULTI-LAYER REBAR DESIGN OPTIMIZATION

Mingkai Li¹, Vincent J. L. Gan², and Jack C. P. Cheng³

1) Ph.D. Candidate, Department of Civil and Environmental Engineering, School of Engineering, The Hong Kong University of Science and Technology, Hong Kong, China. Email: mlicj@connect.ust.hk

2) Ph.D., Assistant Prof., Department of the Built Environment, College of Design and Engineering, National University of Singapore, Singapore. Email: vincent.gan@nus.edu.sg

3) Ph.D., Prof., Department of Civil and Environmental Engineering, School of Engineering, The Hong Kong University of Science and Technology, Hong Kong, China. Email: cejcheng@ust.hk

Abstract: Rebar design is a crucial aspect of reinforced concrete structures, and existing optimization methods based on metaheuristic algorithms (MAs) are time-consuming. Emerging machine learning techniques like graph neural networks (GNNs) have the potential to solve the problem. This paper presents an automated design optimization approach for multi-layer rebar layouts integrating GNN and MA (GNN-MA). The graph representation of multi-layer rebar layouts is developed, integrating design information of rebars and interrelationship between them. The rebar design problem is formulated as a node prediction task, and a GNN with three outputs is trained to provide an initial design, including the number of rebar layers, the diameter and bar number of the outmost layer. MA is then employed to check and optimize the design from GNN. GNN-MA could learn from previous design and generate the same optimal design with that generated by MA alone for more than 97.92% of design cases, while saving about 60-80% of computational time. GNNExplainer is adopted to explain the behaviour of the GNN network and important features and edges leading to the prediction could be identified.

Keywords: Reinforced concrete structure, Steel reinforcement design, Graph Neural Network, Metaheuristic algorithm

1. INTRODUCTION

Reinforced concrete (RC) structures are a commonly used format in building structures, and optimizing the design of rebar is a crucial aspect of the RC design process. Rebar design optimization plays a significant role in meeting strength and ductility requirements, reducing material consumption, and minimizing labour costs. However, the design process is often carried out manually or semi-automatically, relying heavily on the expertise of engineers (Mohit, 2021). Although previous studies have proposed metaheuristic algorithms (MAs) to automate the rebar design process (Eleftheriadis et al., 2018; Li et al., 2021), most of these algorithms generate populations randomly and rely on iterative searching techniques. As a result, these methods are time-consuming and could not progressively learn from previous design processes, hindering their practical application.

The development of machine learning (ML) in recent years has brought hope to solve the above problems. Graph neural networks (GNNs) are good at handling unstructured data like networks and graphs, by aggregating information through graph structures that define the relationship between different elements. GNNs have just been adopted in the field of building engineering in recent years. Nauata et al. (2020) encoded the constraints of the house layout problem into the graph structure of its relational networks, and applied GNN to aggregate the information of adjacent nodes in the rational networks and construct the feature vector to generate various of floorplans with high quality. Chang and Cheng (2020) formulated the building structures as graphs by simplifying the components as joints and their connectivity as edges, based on which GNNs were trained to understand the structural layout, predict structural simulation results, and propose the optimal cross-sections of elements. Results found that the GNN-based method could dramatically reduce the optimization time required by GA. Gan (2022) applied GNN to process the graph data model for volumetric modules with spatial attributes, topological relationship, geometrics and semantics. The application of GNN in rebar design had not been reported before Li et al. (2023) proposed to integrate GNN and MA to improve computational efficiency. The use of GNNs is advantageous because of their ability to incorporate complex structural information and interactions between different rebar groups. However, the proposed method only focused on single-layer rebar layout.

Though GNNs are promising to solve the rebar design problem, they are often criticized due to their non-transparent calculation processes. This is a common problem of ML-based techniques, and the complexity of GNNs makes it more challenging to understand the reasoning behind their predictions, compared to traditional neural networks. The lack of transparency can be a significant barrier to their adoption, particularly in civil engineering, where the consequences of incorrect or poorly justified decisions can be significant. In this regard, studying explainability of GNN model is of great significant for building trust and confidence in the model's predictions, ensuring compliance with regulations and standards, and facilitating integration with existing processes. Besides, understanding how GNNs arrive at their results could also help developers improve model performance. Yuan et al. (2022) categorized existing GNN explanation techniques into two categories: model-level methods and instance-level methods. Model-level methods provide input-independent and high-level

explanations, aiming at explaining general behaviours (Yuan et al., 2020). However, the explanation from model-level methods may not be human-interpretable since the obtained graph patterns may not exist in the real world. Instance-level methods identify important input features and edges for each GNN's prediction, which are easier to understand (Pope et al., 2019; Luo et al., 2020). GNNExplainer is an instance-level method that could quantitatively indicate the importance of node features and edges in the graph by introducing perturbations and monitoring the change of prediction. Without any need for architectural modification or re-training, GNNExplainer has the capability to offer valuable insights into any GNN that adheres to the neural message-passing scheme, regardless of the type of prediction task being performed on graphs (Ying et al., 2019). In this regard, GNNExplainer is suitable for the explanation of GNN-based rebar design.

To address these limitations, this paper presents an automated rebar design optimization approach for multi-layer rebar layouts by integrating explainable GNN and MA. The representation of multi-layer rebar layout is presented, following with the tailor-made GNN model and post-processing algorithm. Six famous MAs are evaluated for post-processing. The experiment found that the hybrid mechanism integrating GNN and MA (GNN-MA) could achieve the optimal design for more than 97.92% of design cases, while saving about 60-80% of computational time required by MA alone. The explainability of GNN model is also investigated using GNNExplainer.

2. METHODOLOGY

The workflow of the proposed method is shown in Figure 1. Firstly, structural analysis is conducted based on structural model derived from BIM model or established by engineers. The structural analysis results, geometrical information, supporting conditions, etc., are then extracted to construct graph representations for beams. The graph representation of rebar is proposed to define the parametric relationship between different rebar groups in a single RC component. Based on the graph representation, GNN can aggregate the design information among related rebar groups and provide an initial design. However, GNN alone cannot guarantee that the proposed design can satisfy all the code-stipulated requirements, since it is basically a data-driven method and those requirements are not included in the model as constraints. Therefore, a MA is then applied to further optimize the rebar design from the GNN and check all the requirements. Since the prediction from GNN is close to the optimal solution, the MA can only search the neighbor of the GNN's prediction, which dramatically narrows down the searching space, significantly improving the optimality of design and efficiency of optimization.

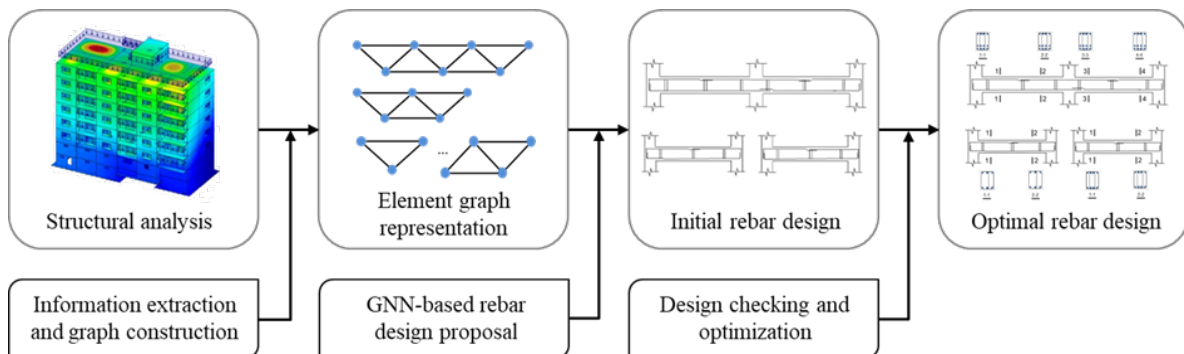


Figure 1. Proposed GNN-based rebar design optimization method

2.1 GNN-based Rebar Design

(1) Multi-layer Rebar Layout

To conduct the multi-layer rebar design, the first step is to clarify the format and variables of the multi-layer rebar layout. Compared with single-layer rebar layouts, multi-layer rebar layouts need to consider the quantitative relationship between different layers of reinforcement. According to industrial practices and the convenience of onsite installation, as shown in Figure 2, four assumptions are made for multi-layer rebar layouts.

a) In the same layer of steel bars, only one steel bar diameter is used. b) The number of steel bars in the outer layer must be greater than or equal to the number of steel bars in the inner layer. c) The diameter of the outer layer of steel bars must be greater than or equal to the diameter of the inner layer. d) When the number of steel bars in the outer layer is even, the number of steel bars in the adjacent inner layer also needs to be even. Assumption a) provides convenience for the installation of steel bars and can reduce the probability of errors in construction. Assumption b) and c) are straightforward because placing more rebars on the outside provides higher load carrying capacity while using the same steel area. Assumption d) is specified in order to avoid asymmetric reinforcement distribution. These assumptions are applied to the selection of multi-layer rebar layouts, during the dataset preparation and further design checking and optimization of the results from GNN.

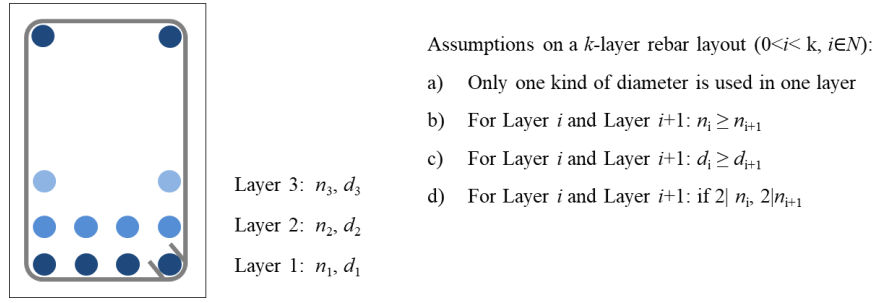


Figure 2. Definition and assumptions of multi-layer rebar layouts

(2) Graph Representation of Rebar Design

Since GNNs perform inference on data with graph structure, the adoption of GNNs in rebar design requires formulation of rebar design problem in graph format. As shown in Figure 3, given a RC beam with structural analysis results, the typical rebar layout is identified and the rebars are divided into groups according to the design codes and preference of industrial practices. Then the graph representation is constructed according to the interrelationship between different rebar groups. Each node in the graph represents a rebar group, while each edge represents the interrelationship between two rebar groups. The design-related information of each rebar group like geometrical, positional information, etc., is integrated into the graph and works as node attributes. Each node has 6 attributes including width, depth, length, required steel area, “top or bottom” and “end or mid”. For middle nodes in continuous beam (such as Node 2 in Figure 3), the length is taken as the average value of the two adjacent two spans. The last two attributes are categorical variable and would be processed using one-hot encoding when training GNN. “Top or bottom” indicates the position from the vertical perspective, denoting whether this rebar group belong to top or bottom rebars. “End or mid” indicates the position of rebars from the horizontal perspective, showing whether the rebar group is located at the end span, which determines whether the rebar group should be anchored into the end supports (such as Group 1 and 4).

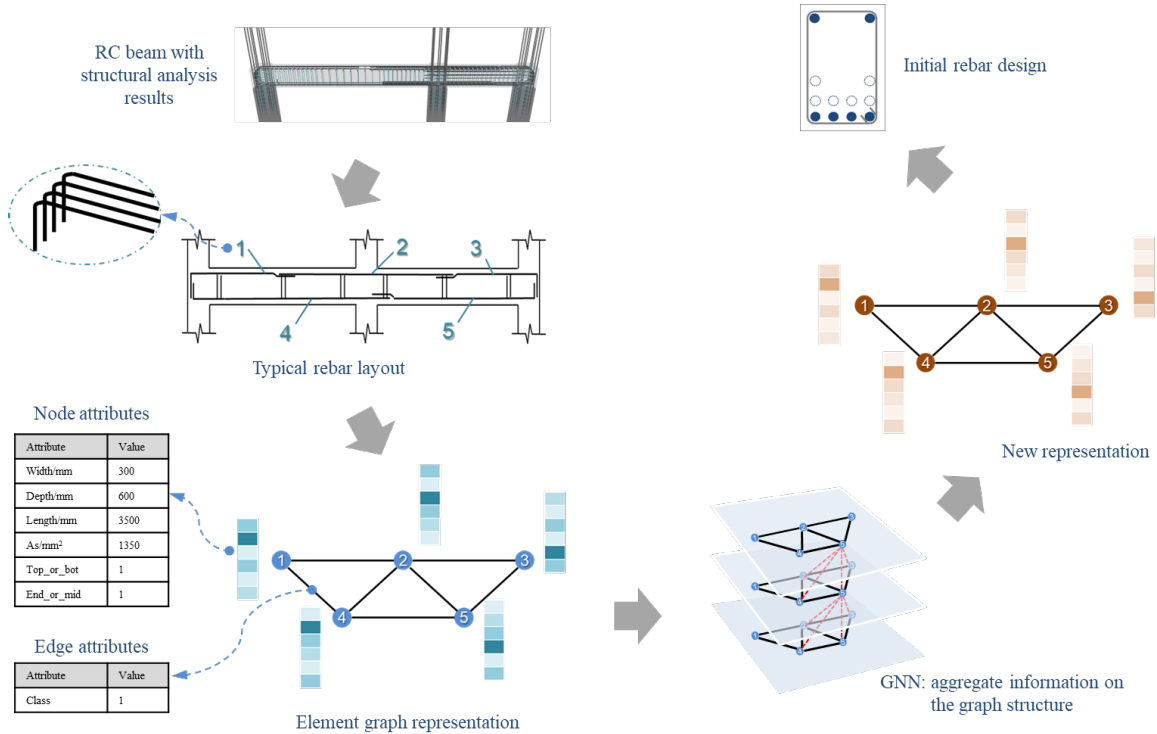


Figure 3. Graph representation of rebar layout and GNN-based rebar design

Edge denotes the interrelationship between rebar groups, and edge attribute could provide additional information to describe the interrelationship. We classify the edge into two categories: the edges among top/bottom rebars, and the edges between top and bottom rebars. For the rebars in the same half, the number of rebars should be compatible since the rebars will be lapped together if their diameters are different, as shown in Figure 4(a). Hence, the edges among top/bottom rebars represent this constraint on bar numbers of two rebar groups. The edges

between top and bottom rebars represents another kind of constraint on bar numbers. As shown in Figure 4(b), when multi-layer layouts are adopted, the bar numbers of top and bottom rebars should be compatible. Besides, building codes also restrict the ratio between the top and bottom steel areas. Therefore, the edge attribute of the proposed graph presentation is a categorical variable to distinguish between two types of interrelationships between rebar groups, which will be utilized by the GNN for information aggregation and learning.

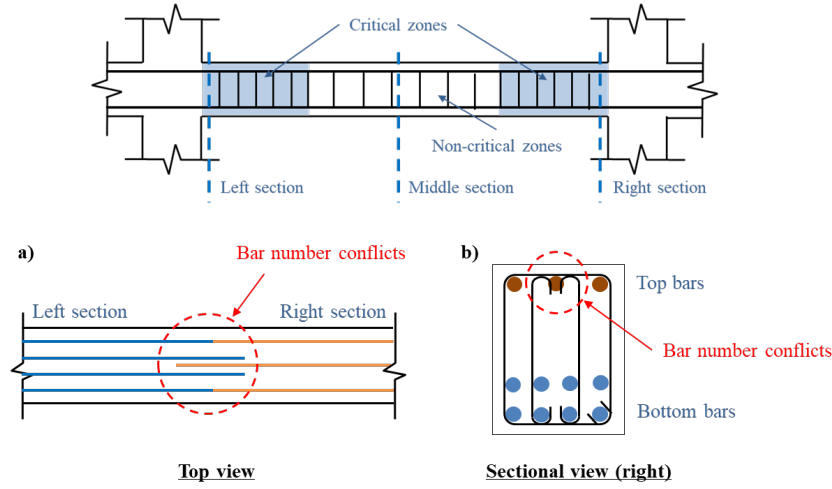


Figure 4. Interrelationships between rebar groups

Compared to single-layer rebar layout, the difficulty in multi-layer rebar design is that the number of rebar layers is unknown. This is also must-solve problem for neural networks, since they are more commonly used for coping with tasks with fixed number of outputs. Besides, when the number of outputs becomes larger, it becomes more difficult to accurately predict the number and diameter of multi-layer reinforcement at the same time. Therefore, we use the number of layers of bars, the number of outermost bars, and the diameter of outermost bars as the outputs of the neural network to roughly determine the layout of multi-layer layout, and then apply MA for further checking and optimization. The rebar design problem is formulated as a node-level prediction task. For a given graph with nodes having 6 features and edges with 1 feature, the GNN will learn to predict the number of rebar layers, bar number and bar diameter for the outmost layer for each node in the graph. From manual design experience, engineers will first determine the number of layers and then select feasible bar number and diameter. Therefore, the GNN starts with the network for layer number prediction, and then the predicted values are integrated as one of the features to improve the prediction accuracy of next output, as shown in Figure 5.

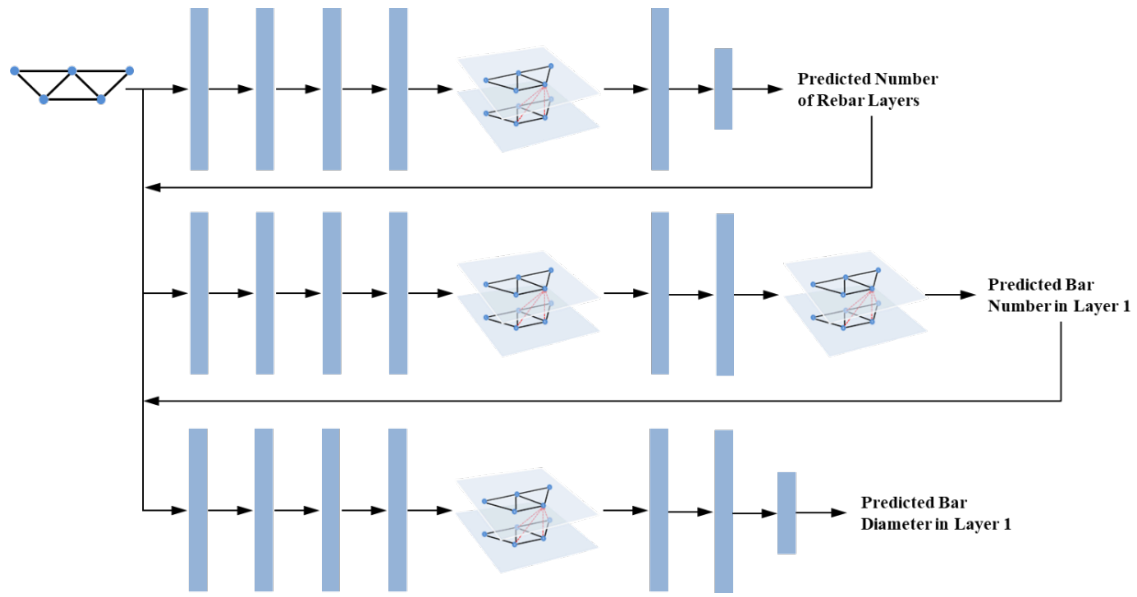
(3) Dataset Preparation

The collection of training dataset is a crucial step of GNN model training. Hundreds of RC beam design cases are first collected from real-life projects. Some perturbations are then introduced to the geometric dimensions and required steel areas of these RC beams to generate more cases, expanding the training dataset. Since the optimal designs of these design cases are unknown, we adopted the optimization formulation proposed by Li et al. (2021), considering both material cost and installation cost. 4 well-known metaheuristic algorithms are then applied for search the optimal design, including genetic algorithm (GA) (Mirjalili, 2019; Katoch et al., 2021), firefly algorithm (FA) (Ying and He, 2013), cuckoo search (CS) (Yang and Deb, 2010), and exploratory genetic algorithm (Li et al., 2023). To ensure the optimality of the final design, the best design among the outcomes from these four algorithms is selected as the optimal design. During the optimization, the four assumptions in 2.1 (1) are applied for the selection of multi-layer rebar layouts, and the interrelationship described in 2.1 (2) are also followed. For each design case with its optimal design, a graph is constructed as described in Section 2.1 (2), which serves as an instance in the training dataset. Finally, a dataset with 3,000 design cases was prepared, containing 1,000 simply-supported beams, 1,000 2-span continuous beams, and 1,000 3-span continuous beams. 75% of the dataset is used for training and the remaining 25% is used for testing.

(4) Post-processing

Since GNN is essentially a data-driven technique, there is no guarantee that the predicted reinforcement layout is optimal and complies with the code-stipulated requirements. Therefore, design checking and further optimization are necessary for the initial design proposed by GNN. Given the predicted values V_p from GNN, MAs only need to search the rebar layout in the solution space $[V_p - 1, V_p + 1]$, which is much smaller than the original one and could reach the optimum much faster. Besides, code-stipulated requirements are checked during the

optimization process of MA, making sure the final design is practical and code-compliant.



Note. The bars denote the fully connected layers. Long bar refers to layer with 64 nodes, while short bar refers to layer with 18 nodes. Each layer in this model has a LeakyRelu activation function with negative slope equals to 0.05. Huber loss is adopted for loss functions, with δ equals to 0.235, 0.210 and 0.230 for the three predicted values, respectively. Adam optimizer is adopted for training with learning rate equals to 0.005.

Figure 5. GNN model architecture

2.2 Explainability Techniques

GNNExplainer (Ying et al., 2019) can be used for any GNN task including node prediction and graph classification, and it can provide local interpretation that identifies the most important nodes and edges in the graph for a given prediction. It is adopted in this paper to explain the behavior of the GNN for rebar design because of its versatility and robustness. GNNExplainer could highlight the important subgraph structure by identifying the edges that are most relevant to the prediction. The explanation process starts by selecting a node of interest and performing a forward pass through the GNN model to obtain the predicted label. Then the relevance score for each feature and edge in the subgraph around the node of interest is computed using a gradient-based method. Finally, the explanation is generated by selecting the features and edges whose scores exceed a certain threshold.

To evaluate the contribution of different features, GNNExplainer utilizes attention mechanisms. It uses graph convolutional networks to capture structural information from graphs and generate embeddings for nodes that can be used as input to attention mechanisms. Then the weights for different subset of features are computed by multiple attention mechanisms. The process allows GNNExplainer to capture both local and global structural information from graphs while also considering rich node features.

3. EXPERIMENTAL RESULTS

3.1 GNN Model Training

The model accuracies during training processes are presented in Figure 6 and Table 1. Accuracy is defined as the percentage of nodes that GNN provides the same predictions as the optimal design generated by MAs. Expect for accuracy of prediction, another indicator called “closeness” is defined in this paper, which counts those predictions that are close to the ground truth within a certain value. This value is set as 1 in this paper. ‘GT’ in Figure 6 refers to ‘ground truth’. The accuracies of predictions on testing set are about 60%, which may be caused by the limited size of dataset, unbalanced feature distribution in the dataset and non-optimal GNN architecture for graph learning, and further investigation is required to improve the accuracies. However, the closeness of these three outputs is close to 100%, which means the prediction falls into the neighbor of ground truth, laying down the foundation of applying MAs for further optimization. The last two columns in Table 1 show the accuracy and closeness when three outputs from GNN are correct, and the closeness reaches 99.40% and 97.92% on training and testing dataset, respectively. As the post-processing algorithms will take the neighbor of the initial design from GNN as the solution space for optimization, ensuring the predictions from GNN are closed to the optimal design is more important than predicting the optimal design in one step. Therefore, closeness of the predictions can serve as an indicator to performance of the hybrid mechanism of GNN and MA. Our experiments found that when the

GNN's predictions are close to the optimal design, the mechanism integrating GNN and MA can always generate the same optimal design generated by MA alone, which means for these 99.40% (or 97.92%) design cases, GNN with MA for post-processing can always arrive at the optimum.

Table 1. Accuracies of the GNN model on training and testing datasets

Output	Number of layers		Bar number in Layer 1		Bar diameter in Layer 1		All three outputs	
	Accuracy	Closeness	Accuracy	Closeness	Accuracy	Closeness	Accuracy	Closeness
Training	61.69	99.20	69.96	100.00	71.61	99.39	36.94	99.40
Testing	59.89	98.93	64.93	100.00	65.57	98.61	35.76	97.92

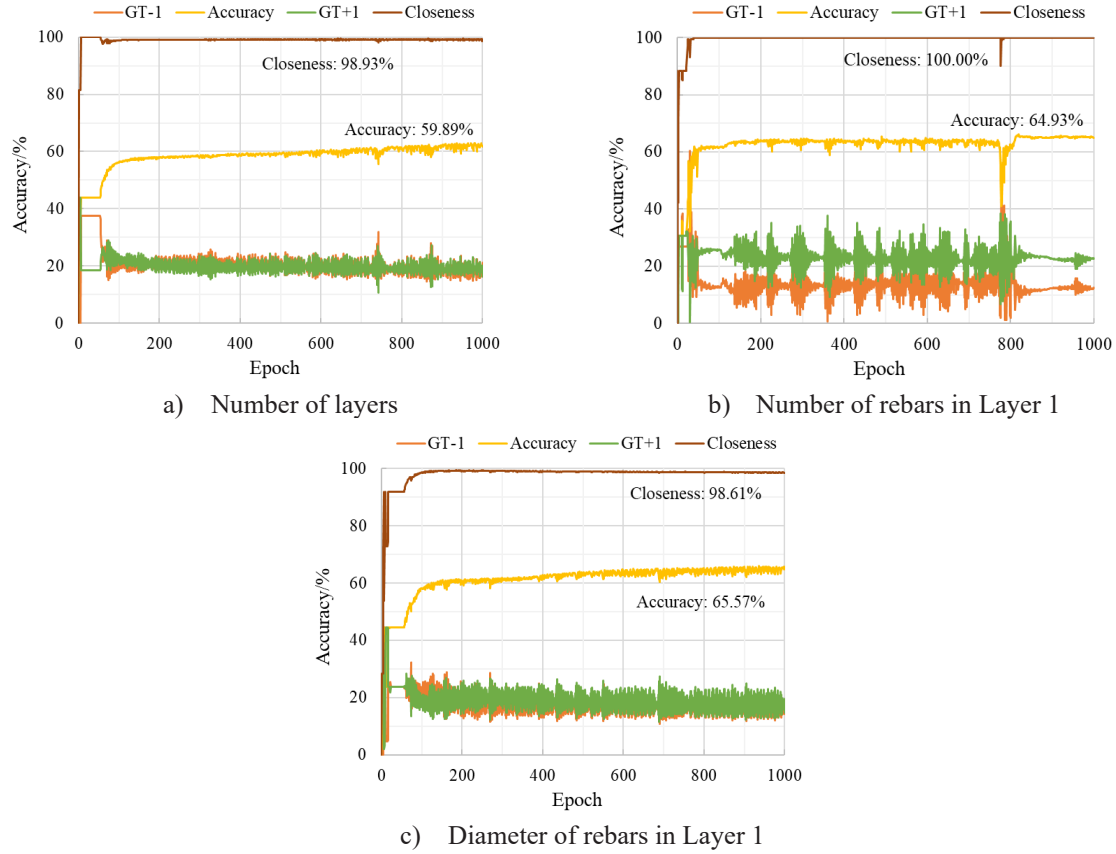


Figure 6. Accuracies on testing dataset during the training process

3.2 Performance Evaluation

Six famous MAs are applied for post-processing of the initial designs generated by GNN, including GA, particle swarm optimization (PSO) (Kennedy and Eberhart, 1995), ant colony optimization (ACO) (Dorigo et al., 2006), FA, artificial bee colony (ABC) (Karaboga and Basturk, 2008), and CS. To have a fair evaluation, the algorithmic parameters of these algorithms are finetuned (Ezugwu et al., 2020), and the parameter settings are shown in Table 2. Same population size and iteration number are adopted.

Table 2. Parameter settings of the metaheuristic algorithms.

GA	PSO	ACO	FA	ABC	CS
$p_c = 0.75$	$w = 1.6$	$n_s = 50$	$\gamma = 1.4$	$p_0 = 1$	$d = 0.45$
$p_m = 0.95$	$w_d = 0.99$	$q = 0.7$	$\beta_0 = 2.7$	$b = 1$	$\beta = 1$
$m = 0.45$	$c_1 = 1.6$	$\zeta = 1$	$\alpha = 0.15$	$a = 1.9$	
	$c_2 = 1.7$		$\alpha_d = 1$		

Note. p_c – crossover percentage; p_m – mutation percentage; m – mutation rate; w – inertia coefficient; w_d – damping ratio of inertia coefficient; c_1 – personal acceleration coefficient; c_2 – social acceleration coefficient; n_s – sample size; q – intensification factor; ζ – deviation-distance ratio; γ – light absorption coefficient; β_0 – base value of attraction coefficient; α – mutation coefficient; α_d – damping ratio of mutation coefficient; p_0 – percentage of

onlooker bees; b – abandonment limit parameter; a – acceleration coefficient; d – discover rate; β – Levy flights parameter.

Figure 7 show the mean computational time required by 6 considered MAs on RC beams with different number of spans. It shows that the saving of computational time becomes more significant as the number of spans goes up. When the number of spans reaches 3, GNN-MA could save about 60~80% of the computational time.

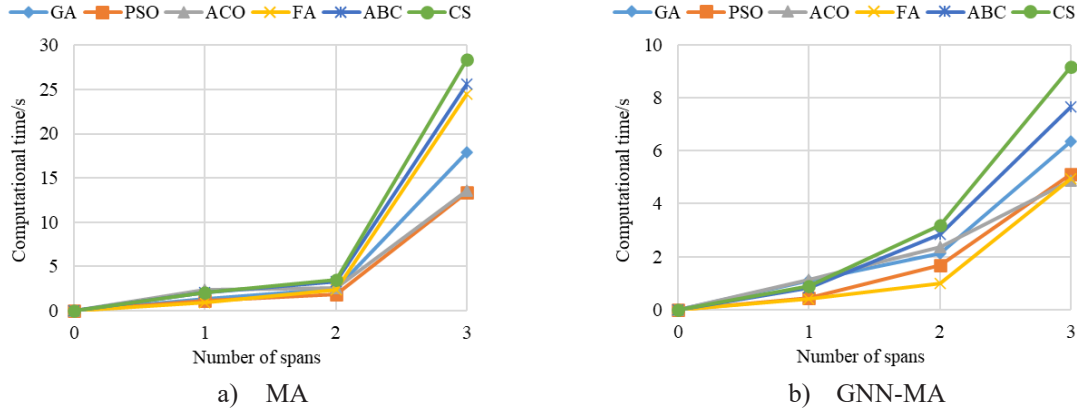


Figure 7. Computational time comparison between MA and GNN-MA

3.3 Explainability Results

An example of employing GNNExplainer to interpret the prediction is shown in Figure 8. For the RC beam, its typical rebar layout is to divide the rebars into three groups, namely group 1, 2 and 3 in Figure 8. The histograms beside the nodes represent the top four features contributing to the prediction of rebar layer numbers. The subgraphs show the importance level of pathways. The darkness of the edge represents its importance, and darker edge has higher importance. For Node 1, the importance score of “As” is much larger than that of other features, which coincides with the fact that Group 1 has larger required steel area. From design experience from practices, a large steel area usually leads to a larger number of rebar layers. For Node 3 with relatively larger steel area, “As” is also the feature with highest importance. For Node 2 that requires minimal steel area, “As” only ranks third in the top four features. Except “As”, geometric features like depth and width are also of great importance to the prediction of layer number.

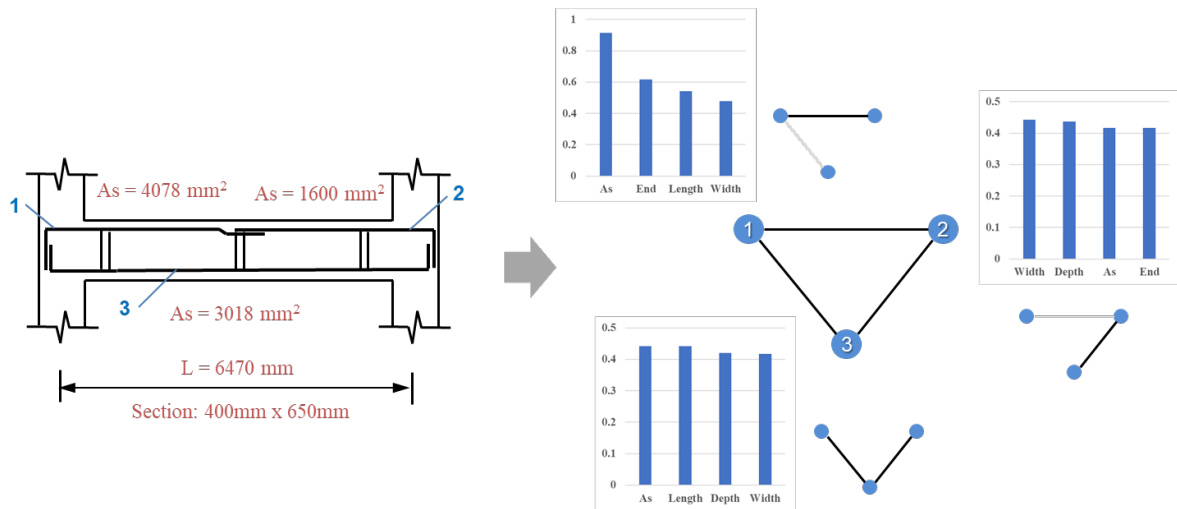


Figure 8. Important edges and node features when predicting the number of rebar layers

4. CONCLUSIONS AND DISCUSSION

In this paper, we present an automated approach for multi-layer rebar design optimization integrating GNN and MA. Graph representation of rebar design is proposed, and the rebar design problem is formulated as a node prediction task. GNN is then adopted to learn from collected design cases, aiming to provide an initial design that is close to the optimal design to accelerate the design process. To ensure the code-compliance and optimality

of final design, MAs are employed to further optimize the initial design from GNN, code-stipulated requirements are checked during the process. Since the closeness of GNN's prediction is about 100%, MAs could only search the neighbor of the initial design from GNN. Experiments show that GNN-MA can obtain the optimal design for more than 97.92% of design cases, and save about 60~80% of the computational time required by using MA alone. The computational time saving is more remarkable as the number of spans goes up. GNNExplainer is adopted to provide human-interpretable explanation for the predicted initial layout, and the important features identified are consistent with our design experience.

Though the proposed method is promising, there are some limitations requiring future efforts. Firstly, this study focuses on continuous beams with 1-3 spans, the proposed method has not been validated on RC beams with more spans and other types of RC beams. Secondly, the post-processing algorithms relies on the prediction accuracies of GNN, and the scenario that GNN's prediction is far away from ground truth has not been discussed. Thirdly, the generated explanations of GNN only indicate the importance of features and edges, more aspects of the model should be investigated to provide a more comprehensive understanding of the GNN-based rebar design.

REFERENCES

- Chang, K. H., & Cheng, C. Y. (2020). Learning to simulate and design for structural engineering. In *International Conference on Machine Learning*. pp. 1426-1436. PMLR.
- Dorigo, M., Birattari, M., & Stutzle, T. (2006). Ant colony optimization. *IEEE computational intelligence magazine*, 1(4), 28-39.
- Eleftheriadis, S., Duffour, P., Stephenson, B., & Mumovic, D. (2018). Automated specification of steel reinforcement to support the optimisation of RC floors. *Automation in construction*, 96, 366-377.
- Ezugwu, A. E., Adeleke, O. J., Akinyelu, A. A., & Viriri, S. (2020). A conceptual comparison of several metaheuristic algorithms on continuous optimisation problems. *Neural Computing and Applications*, 32, 6207-6251.
- Gan, V. J. (2022). BIM-based graph data model for automatic generative design of modular buildings. *Automation in Construction*, 134, 104062.
- Karaboga, D., & Basturk, B. (2008). On the performance of artificial bee colony (ABC) algorithm. *Applied soft computing*, 8(1), 687-697.
- Katoch, S., Chauhan, S. S., & Kumar, V. (2021). A review on genetic algorithm: past, present, and future. *Multimedia Tools and Applications*, 80, 8091-8126.
- Kennedy, J., & Eberhart, R. (1995). Particle swarm optimization. In *Proceedings of ICNN'95-international conference on neural networks*. Vol. 4, pp. 1942-1948. IEEE.
- Li, M., Wong, B. C., Liu, Y., Chan, C. M., Gan, V. J., & Cheng, J. C. (2021). Dfma-oriented design optimization for steel reinforcement using bim and hybrid metaheuristic algorithms. *Journal of Building Engineering*, 44, 103310.
- Li, M., Liu, Y., Wong, B. C., Gan, V. J., & Cheng, J. C. (2023). Automated structural design optimization of steel reinforcement using graph neural network and exploratory genetic algorithms. *Automation in Construction*, 146, 104677.
- Luo, D., Cheng, W., Xu, D., Yu, W., Zong, B., Chen, H., & Zhang, X. (2020). Parameterized explainer for graph neural network. *Advances in neural information processing systems*, 33, 19620-19631.
- Mirjalili, S., & Mirjalili, S. (2019). Genetic algorithm. *Evolutionary Algorithms and Neural Networks: Theory and Applications*, 43-55.
- N. Nauata, K. Chang, C. Cheng, G. Mori, Y. Furukawa, House-gan: Relational generative adversarial networks for graph-constrained house layout generation, *European Conference on Computer Vision*, Springer, 2020, 162-177.
- Pope, P. E., Kolouri, S., Rostami, M., Martin, C. E., & Hoffmann, H. (2019). Explainability methods for graph convolutional neural networks. In *Proceedings of the IEEE/CVF conference on computer vision and pattern recognition*. pp. 10772-10781.
- Yang, X. S., & Deb, S. (2010). Engineering optimisation by cuckoo search. *International Journal of Mathematical Modelling and Numerical Optimisation*, 1(4), 330-343.
- Yang, X. S., & He, X. (2013). Firefly algorithm: recent advances and applications. *International journal of swarm intelligence*, 1(1), 36-50.
- Ying, Z., Bourgeois, D., You, J., Zitnik, M., & Leskovec, J. (2019). GNNExplainer: Generating explanations for graph neural networks. *Advances in neural information processing systems*, 32.
- Yuan, H., Tang, J., Hu, X., & Ji, S. (2020). XGNN: Towards model-level explanations of graph neural networks. In *Proceedings of the 26th ACM SIGKDD International Conference on Knowledge Discovery & Data Mining*. pp. 430-438.
- Yuan, H., Yu, H., Gui, S., & Ji, S. (2022). Explainability in graph neural networks: A taxonomic survey. *IEEE Transactions on Pattern Analysis and Machine Intelligence*.

DATA ANALYSIS FOR PREDICTION AND VISUALIZATION OF SENSOR DATA IN RAILROAD PROXIMITY CONSTRUCTION

Atsushi Takao¹, Nobuyoshi Yabuki², and Yoshikazu Otsuka³

1) Deputy manager, ICT Management Center, Okumura Corporation, Tokyo, Japan. Email: atsushi.takao@okumuragumi.jp

2) Ph.D., Prof., Division of Sustainable Energy and Environmental Engineering, Graduate School of Engineering, Osaka University, Suita, Japan. Email: yabuki@see.eng.osaka-u.ac.jp

3) Ph.D., General Manager, Environmental Technology, Engineering Headquarters, Okumura Corporation, Tokyo, Japan. Email: yoshikazu.otsuka@okumuragumi.jp

Abstract: It is essential to lessen the effect of construction on railroads at sites where construction is taking place close to them. Therefore, various types of sensors are installed at various locations throughout the construction site to monitor its condition. In order to better utilize sensor data for monitoring, we developed a system that links live sensor data with the BIM 4D model of the construction site. The data is then consolidated into a centralized monitoring system to facilitate the management of the construction site. Using this data, the current state of the site can be easily grasped, and more accurate predictions can be made about the effects of construction on the nearby railroads. After that, we used the monitoring system to investigate the relationship between various types of construction works and the site conditions as measured by the sensors. We demonstrated that the construction work content and sensor observations are indeed correlated. Future work includes further clarification of the correlations of the observed data, and prediction of the effects of the various construction works on nearby railroads.

Keywords: Sensor, Visualization, Site condition prediction, 4D models, Data analysis

1. INTRODUCTION

Construction done close to railroad tracks is referred to as "railroad proximity construction". For instance, when excavation work is done close to railroad tracks, significant accidents like train derailments could occur if subsidence or swelling of the railroad occurs as a result of the construction activity. To prevent such accidents, regular measurement of the settlement of both the railroad foundation and the tracks is conducted. Early understanding of problematic site conditions is for quickly addressing any issues before serious damage is caused. However, this requires frequent or real-time measurements, which require time and effort to collect, manage, and interpret the data.

Accordingly, this research focuses on the visual presentation and interpretation of sensor data using building information modeling (BIM). We constructed a sensor management system that can associate 4D sensor data with a 4D model (McKinney et al., 1996) and visualize changes in sensor measurements as construction progresses. This system enables the visualization of sensor installation locations, orientations, and measurements with time directly on a 4D representation of the construction site. The developed system can be used to simulate future structures, existing structures, and various installed sensors while carrying out construction work in railroad proximity. This paper demonstrates how information regarding the installed sensors can be managed centrally and visualized alongside the progress of the project.

However, the installation and monitoring cost increases with the number of sensors, so it is desirable to use minimize their number. In this work, we statistically analyze the data of multiple types and multiple locations of sensors accumulated in the system to evaluate potential correlations. If suitable strong correlations exist, it will be possible to optimize the sensor system and decrease its cost by minimizing the number of installed sensors.

2. LITERATURE REVIEW

Several works have been published on the visualization of sensor data on BIM models. Ghen et al. (2018) conducted fire simulations on existing structures, and used the API of Autodesk Revit to visualize the results on a BIM model. Further, they associated fire detection sensor data stored in the database with the BIM model. However, since the research dealt with fire simulation and monitoring for existing structures, use cases in which the BIM model changes over time, such as during construction were not shown.

Wang, J. et al. (2022) conducted research on data visualization using BIM for the health monitoring of heritage structures. The 3D model of the sensor was displayed on the BIM model, and the sensing data was visualized. Furthermore, they displayed the 3D model of the sensor on the BIM model and visualized the sensing data. However, there was no example of simultaneously displaying structural changes occurring in a structure under construction and sensor information.

Research was conducted on a method to reflect building data in facility management to the digital twin platform in real time (Xie et al., 2023). The efficiency of facility management was improved by reflecting the information obtained from the sensors in the building on the digital twin platform in real time. However, the visualization of sensor data on the BIM model that associates sensor data and BIM has not been done.

A study was conducted to visualize information from environmental sensors inside a building on a BIM model (Wang, T. et al., 2022). Visualization of sensor data was performed by coloring the BIM model with gradation based on sensor information. However, since the target was the environmental sensor of the existing structure, there was a problem in applying it to the construction site where both the structure and the sensor change over time.

At the construction site, research was conducted on the progress of the construction site and the application to the quality control of the completed form using the point cloud data generated from the image (Vincke & Vergauwen, 2022). Although the temporal change of the construction site was expressed on the BIM model based on the image data, the measurement data of the sensors installed on the construction site could not be expressed on the BIM model.

Therefore, the key issue is that during the construction stage, the condition of the structure where the sensors are installed changes daily, and in some cases the installed sensors themselves are moved or replaced. Therefore, when linking the 3D model with the sensor data, it is necessary to coordinate and manage the BIM model and sensor data in response to changes over time. However, in the existing system, there was a problem in visualizing the temporal change of the sensor data in the construction stage on the BIM model.

3. METHODOLOGY

3.1 Visualization of Sensor Data

The goal of this work is to develop a comprehensive system that can visualize sensor data onto a 4D BIM model, and that can address time changes in the 3D model and sensor placement. This developed system combines BIM 4D models of construction objects, surrounding structures and sensors; a sensor database that stores sensor data from multiple types of sensors; a sensor database management system that stores sensor management values; and a construction process management system.

The BIM 4D model is constructed to represent the temporal change of the construction site by associating construction process data with 3D models of construction objects, surrounding structures, and sensors. Surrounding structures included in the model are existing roads and buildings in the vicinity of the construction site, and are included as construction objects when they are modified due to construction.

First, 3D models are created by dividing each member according to the construction procedures. Second, process data is created by setting start/end dates and a unique ID for each work. By associating the IDs of each type of work in the process data with the IDs of corresponding objects in the 3D model, the 3D model and the process data are linked. By switching display/hide based on the process data associated with the object, changes over time are displayed on the BIM 4D model.

In the comprehensive system, we will build a sensor database management system that stores data from the sensors installed at the construction site and associates it with the BIM 4D model. The sensor database management system has the role of storing sensor data in the sensor database and managing sensor quality control values. The BIM 4D model and the sensor data are linked by importing the sensor data into the sensor database and associating the 3D objects of each sensor with its corresponding sensor data. This makes it possible to change the placement of the 3D object of the sensor associated with the sensor data in response to the time change of the BIM 4D model. An example of collected subsidence data and its corresponding control values is shown in Figure 1.

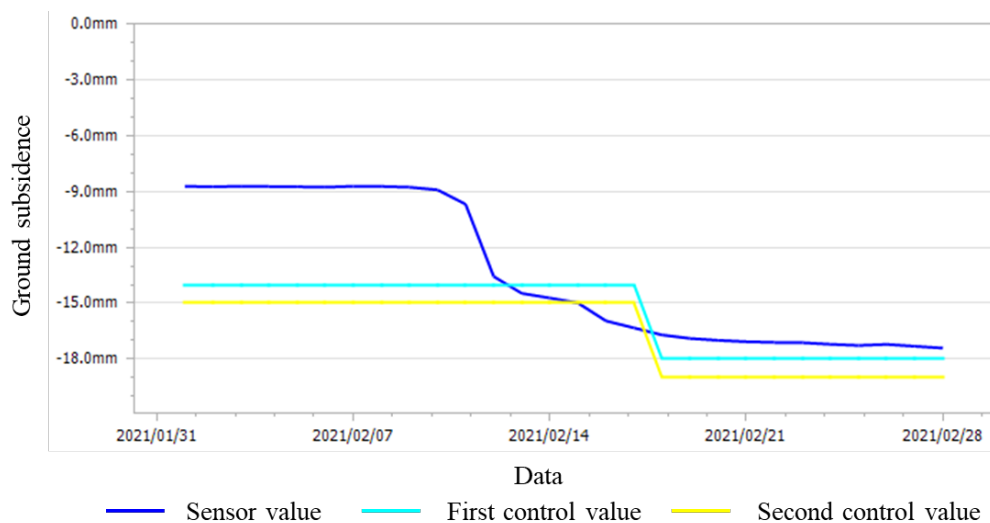


Figure 1. An example of collected sensor data and its corresponding quality control values

3.2 Data Analysis

The method of statistical analysis of the sensor data is described below. First, we classified the sensor data by sensor type and installation position. The classification of sensor type is called sensor group, and the classification of installation position is called distance group. In addition, we also classified the work content that affects the sensor data. The classification of work content is called a task group.

Second, we performed an exploratory analysis of the dataset and identified task, sensor, and distance groups that have sufficient valid observations for use in the statistical analysis. Next, we codified the analysis variables based on their sensor and distance groups. Within each distance group, several sensors of the same type were installed at different locations. The data for all sensors of the same type within the same distance group were aggregated by calculating their median. This median was taken to represent the distance group (Shrivastava et al., 2004).

Next, we used the data of groups with sufficient observations to calculate the correlation coefficients between all sensor and distance groups. Correlation analysis is a statistical method used to determine the relationship between two variables, and it can help identify which sensor groups and/or distance groups are redundant, if any. Pearson's correlation coefficient, which measures the linear correlation between two variables, was primarily used for the analysis. Pearson's correlation coefficient between two datasets is given by equation (1) as follows:

$$\gamma = \frac{S_{xy}}{S_x S_y} = \frac{\frac{1}{n} \sum_{i=1}^n (x_i - \bar{x})(y_i - \bar{y})}{\sqrt{\frac{1}{n} \sum_{i=1}^n (x_i - \bar{x})^2} \sqrt{\frac{1}{n} \sum_{i=1}^n (y_i - \bar{y})^2}} \quad (1)$$

Where the subscripts x and y denote each dataset, S_x and S_y denote the standard deviations of each dataset, S_{xy} denotes the covariance, x_i and y_i denote the measurements of each dataset, \bar{x} and \bar{y} denote the means of each dataset, and n denotes the number of measurements. The correlation coefficients were calculated between all sensor groups to create the correlation matrix, where each row and column represents one sensor group and one distance group, and the value in each cell represents the correlation coefficient between the corresponding sensor groups. To better visualize the matrix, we created a heat map where the color of each cell represents the strength of the correlation coefficient. Sensors that have high correlation coefficients with other sensors can be judged as redundant because they are measuring the same action. Therefore, it will be possible to remove such redundant sensors with little impact on the effectiveness of the monitoring system.

In geo-monitoring systems, sensors inherently provide redundant information due to the inter-related measurements that are required. Although such redundancy allows for better robustness against environmental impact, and potential outlier measurement, it can increase the cost of installation and computation, creating complexity in the model (Holst & Lohweg., 2021). Accordingly, we could identify ways to eliminate redundant sensors and/or redundant measurements depending on the primary objectives for the installation of sensors.

3.3 Case Study

The developed system was applied to the construction project called "A" in Japan, scheduled from 2016 to 2024. Construction project A was carried out as part of an underground railroad project, and involved work to build retaining walls and box culverts for a subway section at the transition section between the over ground and underground tracks. The excavation was carried out in the vicinity of a preexisting in-service track to construct the structure of the underground railroad. The construction length is adjacent to the pre-existing track along its whole length distance of 646m. Accordingly, the monitoring of the construction impact on the pre-existing track is required along the entire construction line. The construction length is divided into 35 construction blocks to facilitate the construction management and the simultaneous construction of multiple blocks. After the construction of the retaining walls, soil near the preexisting track is excavated, and struts are installed. Then, the skeleton of the railroad section is constructed, after which the shoring is removed and the excavated area is backfilled. When constructing the frame, the lining board is removed from the construction site and the work is carried out underground.

In order to constantly monitor the impact of construction work on the preexisting track, several site conditions were measured at regular intervals along the construction length. Subsidence gauges, which measure the subsidence of the construction base, were installed at the preexisting track side between the earth retaining wall and the track at intervals of 10m along the construction length. Small inclinometers were installed on the overhead contact poles of the existing track at intervals of 40m to measure the inclination of the poles. Strain gauges and thermometers were installed on the struts of the shoring to measure the axial force of the struts. Since the shoring to be installed differed depending on the excavation depth, strain gauges were installed not at regular intervals, but each time a shoring was installed. Multistage inclinometer and laser distance sensors were used to measure the horizontal displacement of the retaining wall and change in the inner space. Both the multi-stage inclinometer and the laser distance sensor measure the displacement of the retaining wall, but from the viewpoint

of installation cost, they were used according to the depth of excavation to be measured. Laser distance sensors were used for the construction blocks where the excavation depth is shallow, and multi-stage inclinometers were used for deeper blocks. The total number of sensors installed was 61 subsidence gauges, 17 small inclinometers, 33 strain gauges, 68 multistage inclinometers, 3 laser distance sensors. The distance group and sensor groups, and their associated labels are summarized in Tables 1, 2, and 3. The number of installed sensors and collected measurements from distance group 1 were insufficient to perform the statistical analysis, so their data were excluded from the analysis. Furthermore, aggregating the strain and temperature data of the struts by their distance groups does not yield meaningful information, as the sensors were not installed at regular intervals, and the shoring design changes along the construction length. Therefore, the strain and temperature data of the struts were excluded from the current statistical analysis.

3.4 Visualization Using 4D Models

A 3D model of the construction target, surrounding structures, and sensors was created as a component of the BIM 4D model. The 3D model of the construction object was divided into task groups according to the work content in order to associate it with the process data. The task groups included in the analysis are summarized in Table 4. The 3D objects representing the sensors were enlarged to facilitate visualizing changes in their measurements. Additionally, multiple process data could be associated with the same object if the processes were conducted simultaneously.

For each sensor installed at the construction site, information on the measuring device ID, measurement type, installation position, measurement date and time, and measured value was stored in the database. Since the measurement frequency of sensor data differs depending on the sensor, it is necessary to determine the representative value when outputting the measurement data to the system. Since the process data is daily data, we output the data at 17:00 when construction work concludes for the day. This allows monitoring of the site condition on a daily basis. The quality control value of sensors was set based on the design value of the displacement of the earth retaining and shoring predicted from the results of structural analysis of the shoring. Since this design value changes according to the excavation progress, it is updated daily in the database system as the construction progresses.

The 3D model object was associated with the sensor ID stored in the sensor database, and the sensor data was linked to the BIM 4D model as attribute information. Based on the date and time specified in the BIM 4D model, the database is referenced based on the sensor ID associated with the model, and the measurement and management values are displayed in the model. The 3D object of the sensor in the BIM 4D model was associated with the database through their corresponding sensor IDs. By setting the process data in the BIM model, the daily construction status was reflected on the BIM 4D model according to each type of work, and the daily measurement values of the sensor and the construction status was visualized simultaneously. In addition, we were able to visualize the trend of the sensor data with time by using a time-lapse chart.

Table 1. Distance groups for which sensor data was aggregated

Group no.	Construction Blocks	Start location (m)	End location (m)	Length (m)
1	BL1 →BL6 (Excluded due to insufficient data)	0	110	110
2	BL7 →BL13	110	240	130
3	BL14→BL23	240	410	170
4	BL24→BL28	410	510	100
5	BL29→BL35	510	650	140

Table 2. Sensor groups installed at each distance group

Notation.	Measurement	Sensor Type
dis	Displacement of retaining wall	Multistage inclinometer and Laser distance sensors
sub	Subsidence of construction base	Subsidence gauges
inc	Inclination of overhead poles	Small inclinometers

Table 3. Labels uses for various measurements at distance group

		Distance groups				
		1	2	3	4	5
Sensor groups	dis	dis-1	dis-2	dis-3	dis-4	dis-5
	sub	sub-1	sub-2	sub-3	sub-4	sub-5
	inc	inc-1	inc-2	inc-3	inc-4	inc-5

Table 4. Task group

Task no.	Type of work
task1	Soil excavation
task2	Soil backfill
task3	Sheet pile installation
task4	Strut assembly
task5	Strut disassembly
task6	Overburden increase
task7	Overburden decrease
task8	Unrelated
task9	Water level lowering
task10	Rebar assembly and formwork

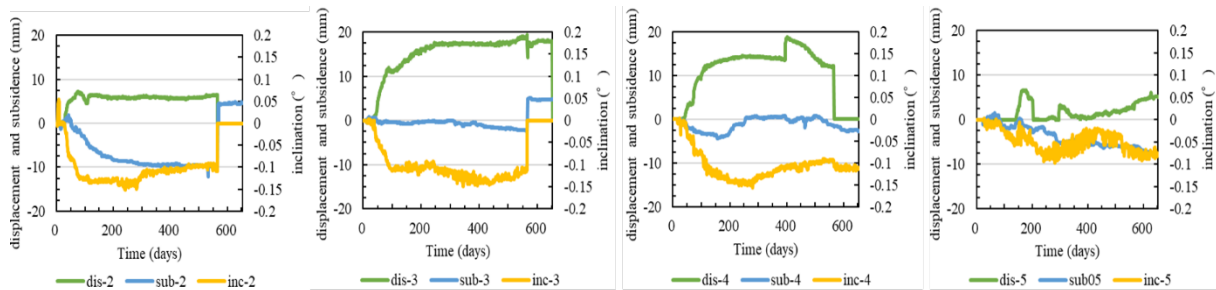


Figure 2. Time series plots of displacement, subsidence, and inclination sensors of distance groups 2 to 5

4. RESULTS

We analyzed the sensor data acquired from May 2020 to February 2022. The 35 construction blocks were divided into 5 distance groups as shown in Table 1. As shown in Table 2, there were multiple time series data for 4 sensor types, (1) displacement, (2) subsidence, (3) inclination. Each time series was aggregated for the 5 distance groups shown in Table 1 (distance group 1 was excluded due to insufficient data). Table 3 shows the codification used for the sensor and the distance groups. Five distance groups were associated with each of the three sensor groups. The task groups conducted throughout this data collection period are summarized in Table 4.

4.1 Sensor Measurements and Statistical Analysis

The time series plots were created for sensor data at all distance groups to visually investigate potential correlations (Figure 2). This graph shows the daily sensor values for the multistage inclinometer, subsidence gauge and small inclinometers for each distance group. Some correlations were clearly visible, such as the inverse correlation between retaining wall displacement and base subsidence data at distance group 5. Boxplots of sensor data versus construction tasks for each distance group are shown in Figure. 3. Distance groups 2 and 4 were chosen as representative groups for the data.

4.2 Correlation Matrix

Pearson Correlation between all sensor groups and distance groups 2, 3, 4 and 5 was calculated, and the heat map shown in Figure. 4 was generated. In Figure. 4, positive correlations are shown in red, and negative correlations in blue. The darker the color, the higher the correlation. Using 0.75 as the cut-off for significant correlation, the following observations were made from the heat map.

- For distance within the same distance group, displacement and inclination groups at distance groups 3 and 4 showed high correlations (dis-3 & inc-3: -0.89, dis-4 & inc-4: -0.79).
- Across adjacent distance groups, 3 and 4, displacement and inclination sensors showed significant correlation (dis-3 & inc-4: -0.78, dis-4 & inc-3: -0.9).
- Displacement sensor groups at these distance groups 3 & 4 were highly correlated (0.9).

A few other correlations were also observed across the non-adjacent distance groups such as sub-2 with dis-3 (-0.97), sub-2 with dis-4 (-0.9), sub-2 with inc-4 (0.75), inc-2 with inc-4 (0.79), dis-3 with sub-5 (-0.77), and sub-2 with sub-5 (0.83). Subsidence groups were correlated with inclination groups, and sensor group 4 and sensor group 1 within each of 5 different distance groups.

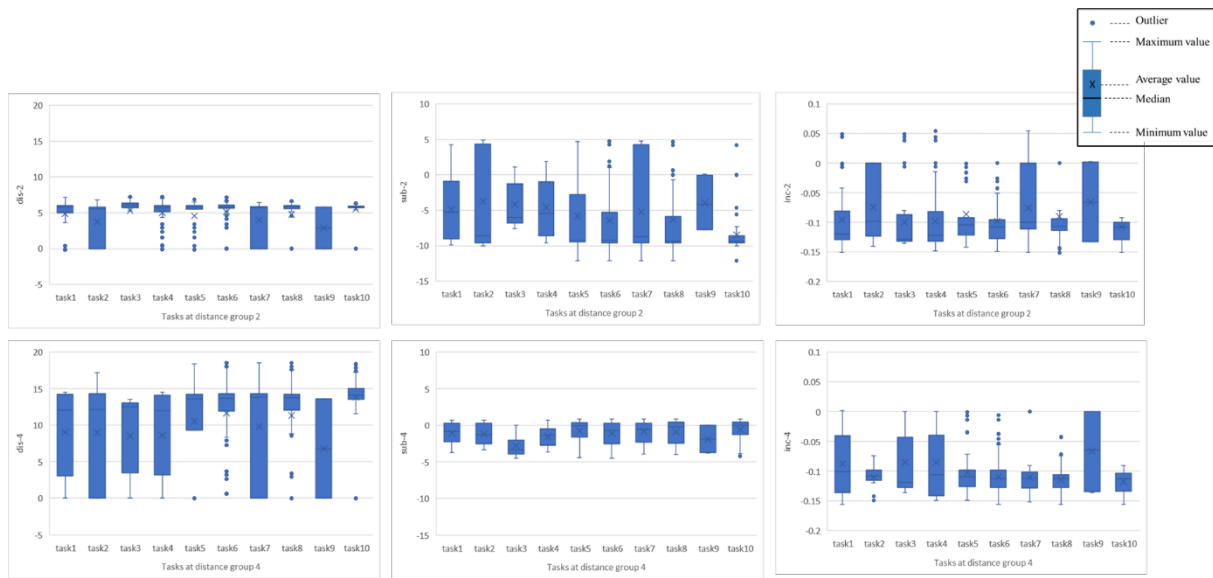


Figure 3. Task group plots of sensor data

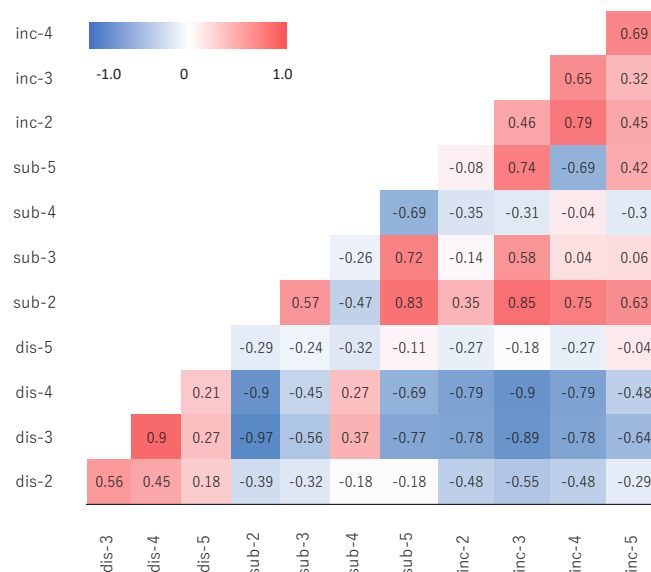


Figure 4. Pearson's correlation coefficient matrix of the sensor groups

5. DISCUSSION

By associating the sensor data with the BIM model and reproducing the construction progress, we could visualize the time variation of the sensor data. Since the situation can be checked visually on the system, the effort required to prepare materials such as process charts to investigate the cause was reduced. In this study, since the construction data is updated daily, the construction progress was reproduced in the model using the progress of the previous day when the process data was updated. However, more frequent measurements will be needed if the cause of sudden changes during construction is to be evaluated using the current system. Therefore, the method of capturing various sensor data needs to be considered in order to determine the optimal frequency of updating the construction progress and visualizing the sensor data in the system.

By associating the sensor data with the construction status on the BIM model and visualizing it, site engineers no longer need to manually compare and evaluate site conditions in relation to sensor data. In future work, we plan to incorporate sensors and construction management information other than those tested in the current work, as well as improve the model so that it can be managed centrally. Currently, sensor information in this system is updated on a daily basis, so we will increase updating the frequency to reflect real-time site conditions and enable fast responses to sudden site condition changes.

Some observations could be made from the descriptive analysis. For example, at distance group 5, displacement and subsidence data were correlated. Regarding the land subsidence, there is a correlation between the cut beam axis force and the sediment meter. To validate the findings, future work could perform a principal component analysis (PCA) on the sensor data. PCA is a technique that reduces the dimensionality of the data by identifying the most important components. The first principal component will capture the largest amount of variance in the data, and it can help identify which sensors are most important. Using the information about what tasks are happening at each distance, we can determine which sensors are necessary for monitoring those tasks. For example, if a particular task only affects one sensor type, there is no need to monitor the other sensor types at that distance.

6. CONCLUSIONS

In order to improve the efficiency of measurement at the construction stage, we constructed a system that associates sensor information with BIM 4D models. We applied the developed system at an actual construction site and confirmed that the sensor data linked to the construction status could be visualized. Regarding ground subsidence, which is an important metric for construction work near railroads, correlation between the inclinometers and the horizontal displacement of the retaining wall was observed from the data analysis.

Statistical analysis was conducted to investigate potential correlations between multiple sensor types along different construction distances across 2 years. Pearson's correlation coefficient heat map pointed to the existence of correlation across sensor groups, however, there was also some correlation across the distance groups and not just within the specific distance groups. For further research, task information, especially the key task which impacts all sensors in the given distance group, should be populated across the entire observed data set.

This would allow for the inclusion of task groups in the analysis and testing for potential correlations. Further data cleaning and data population would help improve the quality of the analysis.

REFERENCES

- Ghen, X.S., Liu, C.C., and Wu, I.G. (2018). A BIM-based visualization and warning system for fire rescue, *Advanced Engineering Informatics*, 37, 42-53.
- Holst, C. A., and Lohweg, V. (2021). A redundancy metric set within possibility theory for multi-sensor systems, *Sensors*, 21(7), 2508.
- McKinney, K., Kim, J., Fischer, M., and Howard, C. (1996). Interactive 4D-CAD, *3rd Congress on Computing in Civil Engineering, ASCE*, 383-389.
- Shrivastava, N., Buragohain, C., Agrawal, D., and Suri, S. (2004). Medians and beyond: new aggregation techniques for sensor networks, *Proceedings of the 2nd international conference on Embedded networked sensor systems*, 239-249.
- Vincke, S., and Vergauwen, M. (2022). Vision based metric for quality control by comparing built reality to BIM, *Automation in Construction*, 144, 104581
- Wang, T., Gan, V.J.L., Hu, D., and Liu, H. (2022). Digital twin-enabled built environment sensing and monitoring through semantic enrichment of BIM with SensorML, *Automation in Construction*, 144, 104625
- Wang, J., You, H., Qi, X., and Yang, N. (2022). BIM-based structural health monitoring and early warning for heritage timber structures, *Automation in Construction*, 144, 104618
- Xie, X., Merino, J., Moretti, N., Pauwels, P., Chang, J.Y., and Parlikad, A. (2023). Digital twin enabled fault detection and diagnosis process for building HVAC systems, *Automation in Construction*, 146, 104695

AN APPROACH FOR GENERATING HYBRID DATASETS OF CONSTRUCTION MATERIAL

Bo Cheng¹, Yujie Lu², and Xianzhong Zhao³

1) Ph.D. Candidate, Department of Structural Engineering, College of Civil Engineering, Tongji University, Shanghai, China. Email: 1810775@tongji.edu.cn

2) Ph.D., Prof., Department of Structural Engineering, College of Civil Engineering, and Key Laboratory of Performance Evolution and Control for Engineering Structures of Ministry of Education, and Shanghai Institute of Intelligent Science and Technology, Tongji University, Shanghai, China. Email: Lu6@tongji.edu.cn

3) Ph.D., Prof., Department of Structural Engineering, College of Civil Engineering, Tongji University, and Shanghai Qi Zhi Institute, Shanghai, China. Email: x.zhao@tongji.edu.cn

Abstract: The emergence of computer vision technology makes automatic quantity counting of construction materials possible. However, the industry and academia still face the problem of a lack of training data, resulting in weak performance of trained models. To solve the problem, this study utilizes Unreal Engine and data augmentation techniques to create digital construction material assets, generating ultra-realistic 2D and 3D renders of construction material for model training. Our experiments show that a hybrid of the real and generated data improves model performance. To demonstrate the effectiveness of the proposed method, a hybrid scaffold dataset containing several 3D digital models, and 907 2D images with 165,901 scaffold pipe instances is constructed. The results show that models trained with hybrid scaffold data gain about 4.6% promotion in average precision (AP) and 4.1% in average recall (AR), revealing that our method can generate high-quality hybrid data and improve the performance of the trained models.

Keywords: Hybrid dataset generating, Construction material, Unreal Engine, Data augmentation, Digital model.

1. INTRODUCTION

Construction materials are key factors on construction sites. During the construction period, materials are kept in the on-site warehouse, and warehouse keepers must check the quantity and quality of materials for management purposes. Traditionally, such management of construction materials relies on manpower. Keepers need to manually check the amount of materials during storage and use, which is time-consuming, laborious, and error-prone.

With the rapid development of deep learning and computer vision technology, such as image classification, detection, and segmentation in recent years, industry and academia have begun to utilize these technologies to achieve automatic recognition and management of construction materials. For instance, to monitor changes on jobsite, material appearance was recognized by the filter bank and principal Hue-Saturation color value with an accuracy of 97% (Dimitrov & Golparvar-Fard, 2014). In another research, a deep convolutional neural network (DCNN) was applied to identify different construction materials and achieved 94% classification accuracy (Davis et al., 2021). To reduce the cost of labor and time, researchers proposed a YOLOv3-based method to automatically detect and count steel bars, and their method achieved a high average precision of 99.7% (Yang Li et al., 2021). Researchers also build construction material datasets and used state-of-the-art computer vision technology to recognize construction material. This study revealed that high-quality datasets are important for training deep-learning models (Sun & Gu, 2022).

Despite the emergence of plentiful research work, academia and industry still face the problem of lacking high-quality data for model training (Paneru & Jeelani, 2021), causing limited generalization ability of the trained models. For example, although the study achieves high precision, false detections occur in complicated real-world scenarios such as insufficient illumination and occlusion (Yang Li et al., 2021). Early study also implicates that training models with small-scale datasets can lead to overfitting and weak generalization (Karystinos, G. N., & Pados, D. A., 2000). To solve the problem of lacking data, this study proposes an approach for generating high-quality hybrid data using data augmentation and Unreal Engine, a powerful 3D modeling and game developing software. The generated data have the characteristics of diversity and verisimilitude, and experiments show that with hybrid data, models get over 4% improvement in both precision and recall, revealing the effectiveness of the proposed approach.

This study selects scaffold, the commonly used construction material, as the research object. As shown in Figure 1(a), a scaffold pipe has the appearance characteristics of a circular steel tube, with an adapter plug on both sides. Typically, these scaffolds are stored in stacks when not in service, thus the stacked scaffolds get spatial characteristics, including occlusion, dense placement, and irregular placement on depth, as shown in Figure 1(c). Such spatial characteristics of stacked materials raise significant challenges for computer vision-related research, including material recognition and detection. Thus this study will contribute to solving the challenge from the data level.

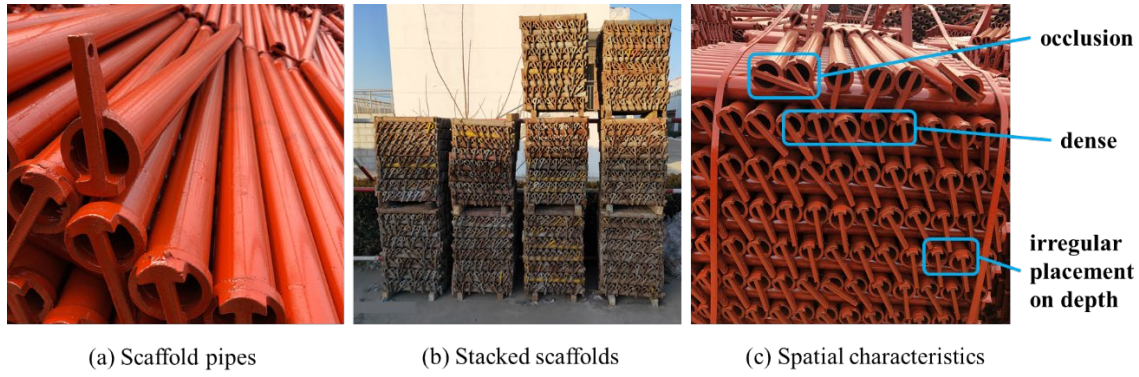


Figure 1. Appearance and spatial characteristics of the scaffold

2. METHOD

There are two problems that hinder the development of vision-based research on material. One is that industry and academia lack high-quality data for model training, and the other is that stacked materials bring challenges for recognition and detection. To address the mentioned problems, this study proposes an approach for generating high-quality hybrid data with Unreal Engine and data augmentation. The approach consists of three parts, 3D digital model generating, 2D image generating, and data augmentation.

There have been various vision tasks in construction material-related research, including classification, detection, tracking, etc. Different tasks focus on different features, such as shape, material, texture, angle of view, and so on. To obtain data that can serve more vision tasks, this study takes the mentioned factors into account when generating data.

The overall framework of the approach is shown in Figure 2.

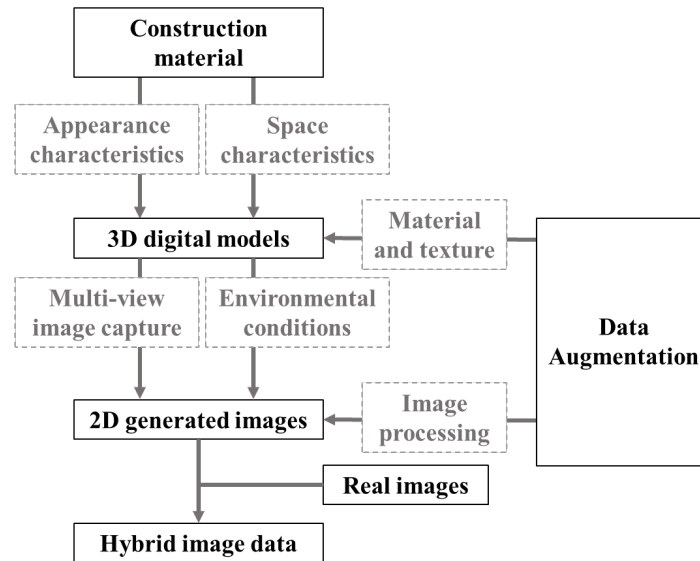


Figure 2. Framework of approach

2.1 3D Digital Model Generating

Generating 3D digital models with appearance and spatial characteristics is the key to the approach. Firstly, a three-dimensional model of the scaffold is constructed in Unreal Engine 4 (UE4). The obtained model must be consistent with the real scaffold in appearance characteristics, as shown in Figure 3(a). Secondly, a stacked scaffold model is generated by stacking massive scaffolds together, like how they are stored on real construction sites. The spatial characteristics of the real scaffold stack, including occlusion, dense placement, and irregular placement on depth are reproduced in digital models, making the generated models more realistic, as shown in Figure 3(b). Lastly, material texture, illumination, and rendering effect are applied to generated models in UE4. With an appropriate combination of factors mentioned above, an ultra-realistic three-dimensional scaffold model can be established, as shown in Figure 3(c).

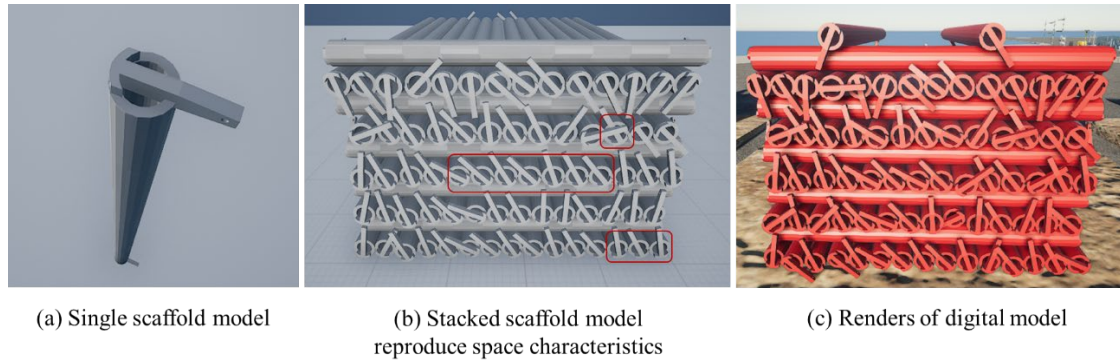


Figure 3. Process of 3D model generating

2.2 2D Images Generating

Capturing images from 3D scaffold models under multi-view and various environmental conditions is a vital way to obtain diverse and high-quality image data. With the generated 3D models, high-quality images can be acquired through two main ways: multi-views and distances, and various environmental conditions.

For 3D models look different under different views and distances, this study captures images from 3D scaffold models under multi-views and distances, aiming to better depict the features of scaffolds. Figure 4 shows how to capture images from multi-views and distances. The view of the camera changes from front view, top view to side view, and the distances vary from close to middle range.

Changing environmental conditions is another way to obtain diverse image data. In the real world, collecting image data from various environments is a tough task. However, in UE4, it's just the click of a button to change environmental conditions such as illumination and weather, making it easy to obtain a large amount of image data. In this study, a series of environmental conditions, including strong light, dim light, shadow, fog, and so on, are applied to simulate the real world, and then diverse image data are captured.

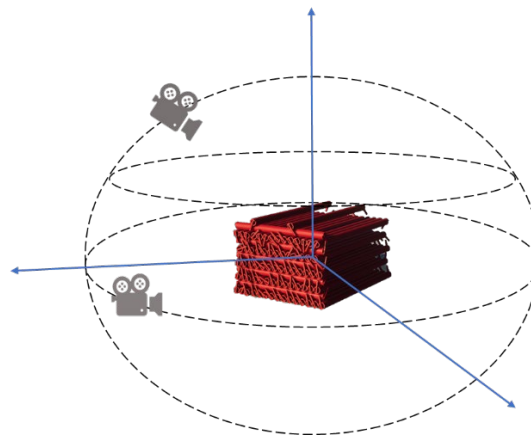


Figure 4. Capture images from multi-views and distances

2.3 Data Augmentation

Two types of data augmentation methods are applied in this study to add diversity to data. At the 3D model level, data augmentation is achieved by changing the material textures of the 3D model. Textures such as steel, copper, wood, rock, and concrete are utilized so as to make the 3D model diverse and realistic, as shown in Figure 5. At the 2D image level, HSV augmentation is applied. HSV augmentation is an image processing method that performs color space conversion on an image and randomly enhances or weakens the HSV(hue, saturation, and value) components in the color space to generate a new image. With the two types of data augmentation methods, the generated 3D models and 2D images get more diversity, which is important for constructing high-quality datasets.



Figure 5. different materials and textures

To measure the effectiveness of the data generated by this method, this study utilizes the generated scaffold dataset to train Faster R-CNN (Ren et al., 2017), a classic detection algorithm, and applies average precision (AP) and average recall (AR) as evaluation metrics. $AP@ \alpha$ is the average precision at a fixed intersection over union (IoU) threshold of α . In this study, $AP@50$ (coarse metric) and $AP@75$ (strict metric) are used. In a nutshell, trained models with high AP are more accurate, and models with high AR are not prone to missed detection.

3. RESULTS

Figure 6 shows the results of 2D image generating. Figure 6(a)(b)(c) give a glance of images captured from the front view, side view and overhead view, and the features of the scaffold are well presented through multi-view images. Figure 6(d)(e)(f) show the images captured under three environmental conditions, bright light, dim light, and foggy. It can be found that such image data have the characteristic of diversity and reality.

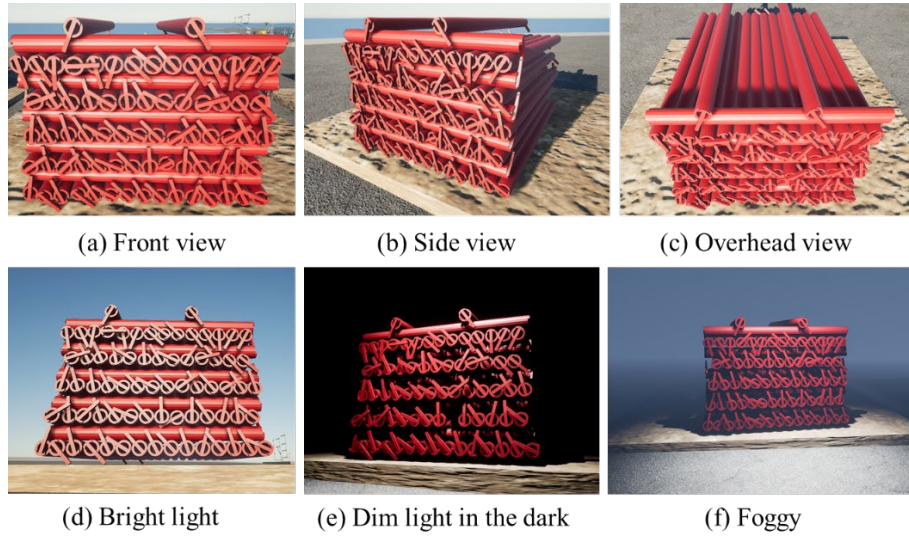


Figure 6. Results of 2D images generating

The results of data augmentation are shown in Figure 7. It can be found that, with the HSV augmentation, the original images generate two new images with different color features. In this way, more features of the scaffold are available, and the diversity of data is improved. Thus models are possible to learn better from features and avoid overfitting with diverse training data.

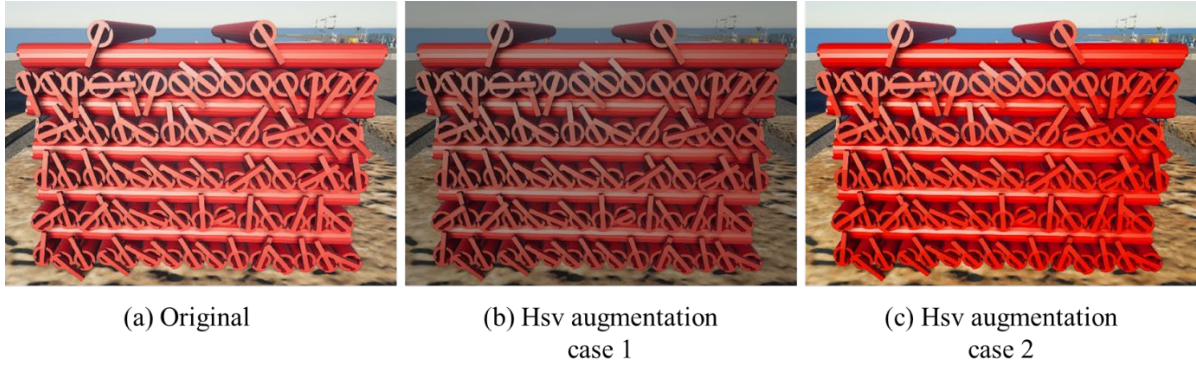


Figure 7. Results of data augmentation

With the method proposed in this study, 10 three-dimensional digital models of the scaffold, as well as 126 high-quality 2D images, were generated. Based on these data, a hybrid scaffold dataset was established. The dataset consists of 3D digital models and 2D hybrid images, and the hybrid images contain 126 generated images and 781 real images. For model training, all images were labeled with bounding box information (shown in Figure 8) in two formats, COCO format (Lin et al., 2014) and VOC format (Everingham et al., 2015). In short, the hybrid scaffold dataset contains 10 digital models, and 907 images, with a total amount of 165, 901 scaffolds.

Table 1. Dataset details

Data type	Data information	Number	Annotation
3D model	Digital models in UE4	10	Semantic label, integrated in models
Generated image	Captured from UE4, JPG format	126	Bounding box, COCO&VOC format
Real image	Collected from 6 construction sites, JPG format	781	Bounding box, COCO&VOC format



Figure 8. Bounding box annotation

A comparison of the images from the hybrid dataset is shown in Figure 9. The generated images are listed in the first row, and the second row consists of real images collected from construction sites. It can be found that the two kinds of images get high similarity in appearance. However, the generated images have more diversity in the angle of views and environments, and this characteristic can contribute to related research at the feature level and data level.



Figure 9. Images of the hybrid dataset

4. DISCUSSION

4.1 Effectiveness of Generated Data

To reveal the effectiveness of the method and the quality of the generated data, comparative experiments were carried out. A classic detection algorithm, Faster R-CNN, was selected as the baseline model. Four models A, B, C, and D are trained with datasets a, b, c, and d respectively, with the same training strategies and configurations. After training, the outcoming models were evaluated on the same validation dataset, and the evaluation metrics measure the performance of the trained models, as well as measuring the quality of different data. The experiment results are shown in Table 2.

Table 2. Experiment results

Model	Training data	AP	AP@50	AP@75	AR
A	Dataset a: 100 real images	0.507	0.950	0.830	0.540
B	Dataset b: 100 generated images	0.497	0.930	0.830	0.535
C	Dataset c: 100 real images and 100 generated images	0.553	0.950	0.914	0.581
D	Dataset d: 50 real images and 50 generated images	0.540	0.949	0.910	0.570

The results from Table 2 show that, compared to model A which only utilizes real images, model C, which is trained with a hybrid dataset, achieved approximately 4.6% improvement in AP and 4.1% in AR. These findings reveal that using a mixture of real and generated image data can enhance the algorithm's performance, and the hybrid dataset proposed in this study has characteristics of high quality and effectiveness. Another finding is that model B, which is trained with only generated images, has an inferior performance to model A. This result demonstrates that generated image data cannot completely replace real data, and it is better to combine real and generated images to form hybrid data.

Model D is set to show the impact of the number of data. The performance of model D is slightly inferior to that of model C but much better than that of model A and model B, showing that more data do benefit the performance of models, but the main contribution of improvement is the hybrid data.

4.2 Application

The hybrid data-generating approach proposed in this study is applicable to materials that are densely stacked, such as steel bars, scaffolds, and timber. The steel bar, for instance, is another common material and has some similar characteristics such as irregular placement and occlusion. Following the framework in Figure 2, one can generate 3D steel bar models and 2D images without much effort, and these generated data can contribute to research such as steel bar management and construction progress monitoring. The high-quality data can also be used for computer vision tasks such as image classification, object detection, and semantic segmentation. Furthermore, the proposed method can also be effective in cases when the target objects have unique appearance characteristics or when there is a lack of data.

5. CONCLUSIONS

The academia and industry have faced the problem of a lack of data for a long time. In this study, the main idea is to combine Unreal Engine and data augmentation to generate ultra-realistic 3D digital models and 2D diverse images of construction material. With the proposed method, a hybrid scaffold dataset containing 10 3D

digital models, and 907 2D images with 165,901 scaffold pipe instances is constructed. Further experiments show that the generated hybrid data can improve the performance of the trained models.

Nevertheless, the proposed method is not fully automatic, and manual effort is required during 3D digital model generating and 2D image generating. It is possible to run the whole process automatically in the future study.

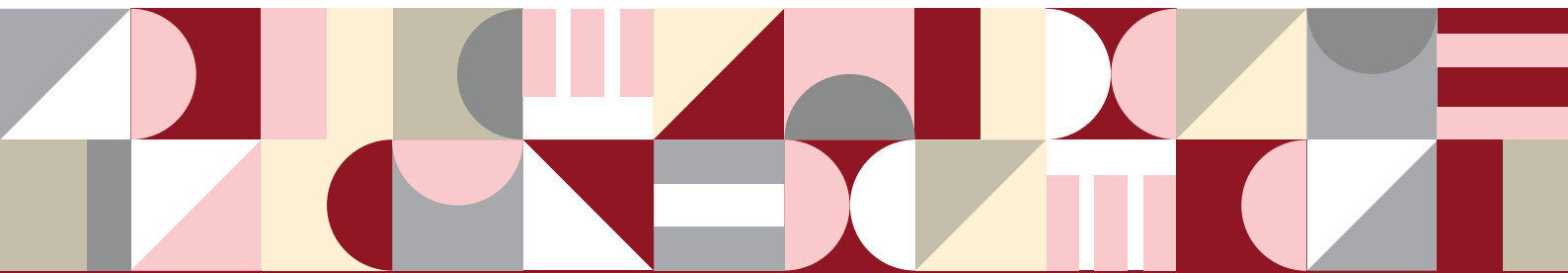
ACKNOWLEDGMENTS

The authors would like to acknowledge the financial support by Shanghai Qi Zhi Institute, grant number SYXF0120020110, and Glodon Company Limited.

REFERENCES

- Davis, P., Aziz, F. B., Newaz, T., Sher, W., & Simon, L. . (2021). The classification of construction waste material using a deep convolutional neural network. *Automation in Construction*, 122.
- Dimitrov, A. , & Golparvar-Fard, M. . (2014). Vision-based material recognition for automated monitoring of construction progress and generating building information modeling from unordered site image collections. *Advanced Engineering Informatics*, 28(1), 37-49.
- Everingham, M. R., Eslami, S., Gool, L. J., Williams, C., Winn, J. M., & Zisserman, A. . (2015) The PASCAL Visual Object Classes Challenge: A Retrospective[J]. *International Journal of Computer Vision*, 2015,111(1):98-136.
- Karystinos, G. N., & Pados, D. A. . (2000). On overfitting, generalization, and randomly expanded training sets. *IEEE Transactions on Neural Networks*.
- Lin, T. Y., Maire, M., Belongie, S., Hays, J., & Zitnick, C. L. . (2014). Microsoft COCO: Common Objects in Context. *European Conference on Computer Vision*. Springer International Publishing.
- Paneru, S. , & Jeelani, I. . (2021). Computer vision applications in construction: current state, opportunities & challenges. *Automation in construction*, (132-Dec.),
- Ren, S., He, K., Girshick, R., & Sun, J. . (2017). Faster r-cnn: towards real-time object detection with region proposal networks. *IEEE Transactions on Pattern Analysis & Machine Intelligence*, 39(6), 1137-1149.
- Sun, Y. , & Gu, Z. . (2022). Using computer vision to recognize construction material: a trustworthy dataset perspective. *Resources, Conservation and Recycling*, (183-), 183.
- Yang, Li. , Yujie, Lu. , & Jun, C. .(2021). A deep learning approach for real-time rebar counting on the construction site based on yolov3 detector. *Automation in Construction*, 124.

Building and Construction Information Modeling



MULTI-MODAL DEEP LEARNING (MMDL)-BASED AUTOMATIC CLASSIFICATION OF BIM ELEMENTS FOR CONSTRUCTION COST ESTIMATION

Hao Liu¹, Shanjing Zhou², Vincent J.L. Gan³, and Jack C.P. Cheng⁴

1) Ph.D. Candidate, Department of Civil and Environmental Engineering, The Hong Kong University of Science and Technology, Hong Kong. Email: hliuci@connect.ust.hk

2) Ph.D., Centre for Systems Engineering and Innovation, Department of Civil and Environmental Engineering, Imperial College London, London, UK. Email: shanjing.zhou18@imperial.ac.uk

3) Ph.D., Asst. Prof., Department of the Built Environment, National University of Singapore, Singapore. Email: vincent.gan@nus.edu.sg

4) Ph.D., Prof., Department of Civil and Environmental Engineering, The Hong Kong University of Science and Technology, Hong Kong. Email: cejcheng@ust.hk

Abstract: In Building Information Modeling (BIM)-based cost estimation, elements shall be classified in a way that aligns with measurement standards and estimating practice. Traditional rule-based and machine learning methods are either time-consuming or cannot meet fine-grained classification requirements in cost estimation. To overcome this challenge, this paper presents a novel framework based on BIM and Multi-Modal Deep Learning (MMDL) for automatic fine-grained BIM element classification. It begins with the transformation of multi-modal (i.e., graphical and non-graphical) element features from BIM models. Subsequently, an MMDL model is developed and deployed to fuse the multi-modal BIM element features for end-to-end fine-grained classification. The framework is validated with a BIM element classification dataset. The results show that fine-grained elements can be classified with high accuracy (over 99%) in an end-to-end manner.

Keywords: Building information modeling, Multi-modal deep learning, BIM data fusion, Classification, Interoperability, Cost estimation

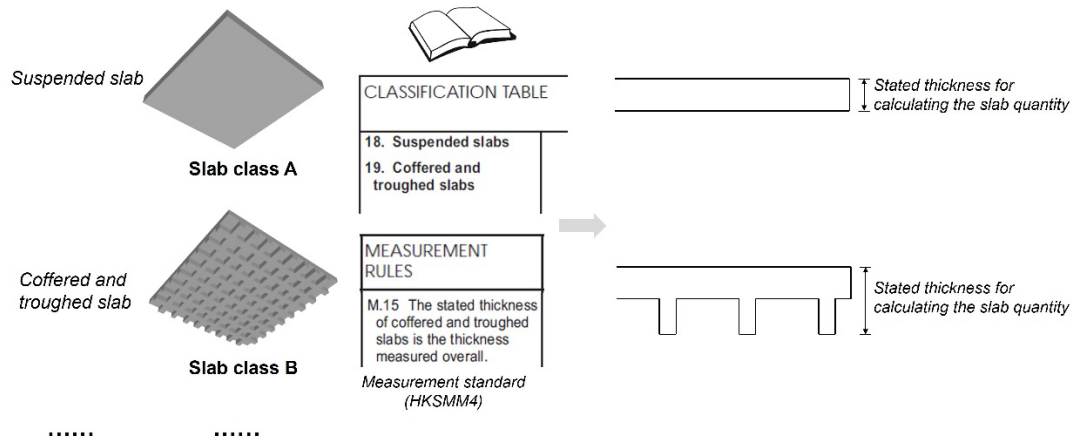
1. INTRODUCTION

Construction cost estimation is a process of classifying construction items that constitute a building project, measuring their quantities, and computing the project cost (Ma et al., 2013). Traditionally, it is time-consuming and error-prone as it requires quantity surveyors and cost estimators to interpret 2D designs (e.g., drawings, specifications) to determine appropriate cost parameters manually (Liu et al., 2022a). In recent years, the development of Building Information Modeling (BIM) creates a paradigm shift in this process. Design information can be automatically extracted from BIM models and associated with cost parameters to produce accurate cost estimations while significantly reducing human effort (Elghaish et al., 2020).

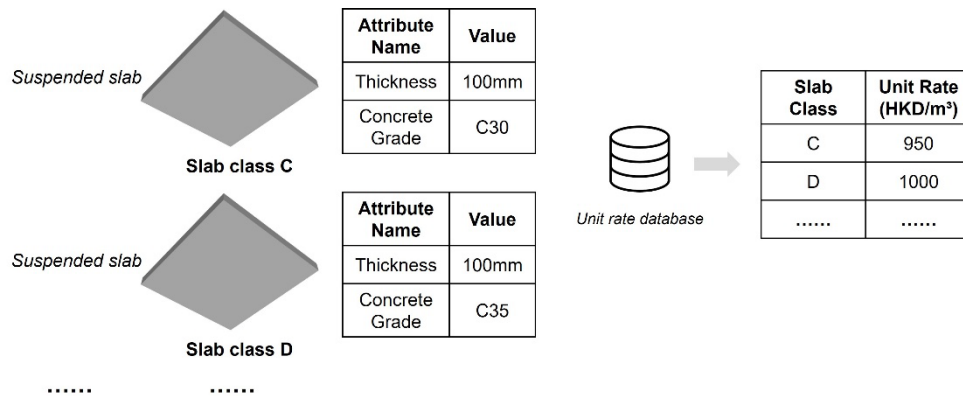
To automatically extract accurate design information from BIM models, how to classify BIM elements in compliance with cost estimation requirements is a major challenge (Fazeli et al., 2020). In BIM-based cost estimation, elements are supposed to be classified in a way that allows interoperability with measurement standards and estimating practice (Wu et al., 2014). Figure 1 illustrates the fine-grained element classification method under such cost estimation requirements. Fine-grained classification means that a general category of element, such as slab, shall have multiple domain-specific sub-categories. This is different from normal BIM classification where elements only have general categories (e.g., slab, beam, wall). For example, according to the Standard Method of Measurement (SMM) for building works (e.g., (Hong Kong Institute of Surveyors, 2018)) commonly used in commonwealth countries (the UK, Singapore, etc.), suspended slabs and coffered slabs should be measured separately with reference to different measurement rules. Thus, slab elements in BIM should be classified as two fine-grained categories to be associated with different measurement rules, as shown in Figure 1 (a). In addition, slabs with different geometry and/or semantics need to have fine-grained classifications linked with different unit rates for accurate cost estimation, as shown in Figure 1 (b). Nevertheless, native BIM models usually do not have such cost-related fine-grained element classifications since they are structured by the built-in classification system in the original BIM authoring software, and it is not uncommon to see that designers do not incorporate fine-grained classifications in BIM models (Lee et al., 2014). Thus, quantity surveyors need to map BIM elements to fine-grained classes for accurate cost estimation.

However, the classification criteria are implicitly buried in various measurement rules and estimating practice (Wu et al., 2014). Heavy human intervention is required to align BIM elements with the cost-specific classifications. Thus, an automatic method to classify BIM elements into fine-grained categories is needed to alleviate the considerable human effort in this process. As a data-driven end-to-end approach where rules are learned from the data itself and mappings between inputs and outputs are achieved directly without intermediate intervention (Akinoshio et al., 2020), deep learning provides new possibilities for human-free BIM element

classifications. In particular, Multi-Modal Deep Learning (MMDL) (Ngiam et al., 2011), a subset of deep learning that jointly utilizes various data modalities (i.e., data representation forms, such as image, text, and audio, to store information) for learning and reasoning, brings new insights to integrate graphical and non-graphical BIM data for fine-grained classification that needs to distinguish elements at both the graphical and non-graphical levels (as shown in Figure 1). Previous studies have demonstrated the potential of deep learning in BIM semantic reasoning and enrichment (Zabin et al., 2022), however, the application of MMDL for BIM element classification is still in its infancy. Therefore, this study aims to develop a novel data-driven end-to-end framework based on BIM and MMDL to automatically classify fine-grained BIM elements for construction cost estimation.



(a) Different fine-grained slab classifications with graphical differences considering measurement standards – A and B shall be associated with different measurement rules



(b) Different fine-grained slab classifications with non-graphical differences considering estimating practice – C and D shall be associated with different unit rates

Figure 1. Element classification under cost estimation requirements – A slab example

2. PROPOSED METHOD

Figure 2 presents the overall proposed method. BIM element graphical (i.e., visual element images) and non-graphical (i.e., textural geometric and semantic attributes) features are extracted from BIM models, where the elements are graphically represented as specific objects in terms of quantity, size, shape, location, orientation, etc. (Construction Industry Council, 2021) and contain the necessary cost estimation-related information including the material type (Liu et al., 2022b). Following this, a fine-grained BIM element classification dataset integrating the graphical and non-graphical BIM data is established based on specific classification criteria for cost estimation (e.g., Figure 1). An MMDL model is then developed to fuse the BIM graphical and non-graphical features. In this study, the term Multi-Modal (MM) refers to the consideration of both BIM graphical and non-graphical information. Afterwards, the trained MMDL model is utilized to automatically classify elements from new BIM models into fine-grained categories for subsequent cost estimation. Details of the method are provided in the following subsections.

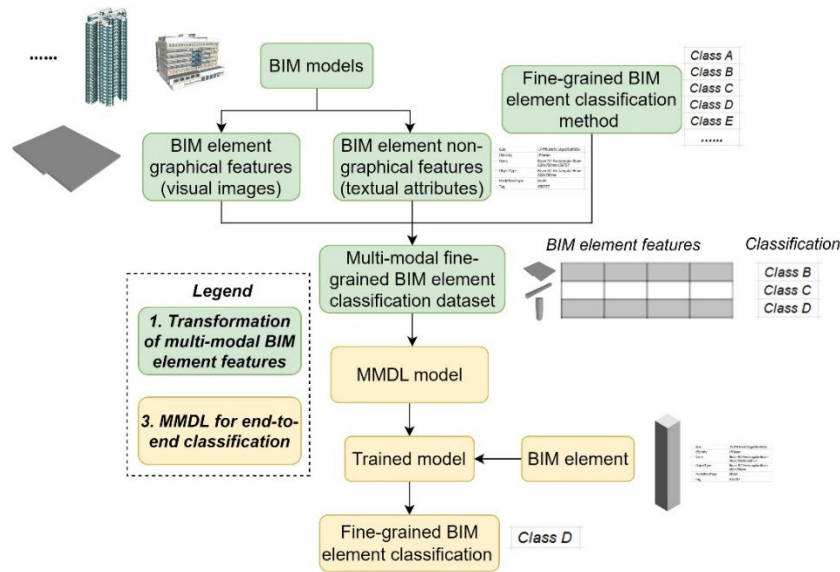


Figure 2. Proposed method based on BIM and MMDL

2.1 Transformation of Multi-modal BIM Element Features

Based on BIM models with specific graphical representations and necessary cost estimation-related non-graphical information, a transformation method is developed to extract the multi-modal BIM element features, as shown in Figure 3. The graphical features, which are represented by elemental images, are normalized by calibrating pixel intensities into a normal distribution to allow faster convergence in the subsequent model training (Shin et al., 2020). The non-graphical features containing the elemental geometric and semantic attributes are represented as numerical and string values, respectively. The numerical values (e.g., element size) are kept in their original forms, whereas the string values including family name become computable through natural language processing. Text preprocessing steps such as tokenization, and stop word removal are first conducted for string values. Then, word embedding (Jurafsky and Martin, 2008) is introduced to represent the preprocessed string values in a computable form. It converts words into real-valued vectors that encode the word meanings, in which case the vectors of similar words are closer in the vector space. Subsequently, the word embeddings are summed and averaged to maintain the same dimension as the numerical values. Finally, the transformed graphical and non-graphical BIM features are integrated to form the base of the multi-modal inputs for the element classification.

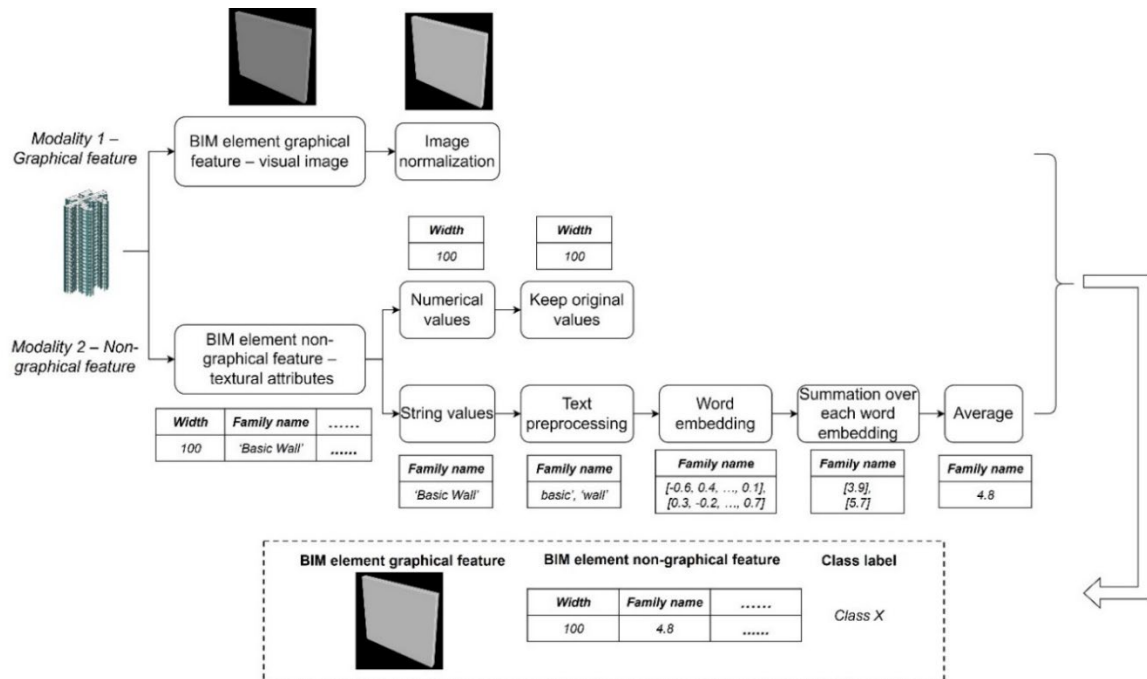


Figure 3. Transformation of multi-modal BIM element features (take one wall as an example)

2.2 MMDL for End-to-end Classification

As seen in Figure 1 and Introduction, the BIM element fine-grained classification for cost estimation requires both graphical and non-graphical information for distinguishment. Traditional unimodal deep learning methods that consider a single data modality cannot classify the elements at the fine-grained level due to the lack of discriminative information. Therefore, an MMDL model is developed to fuse the BIM graphical and non-graphical modalities for fine-grained end-to-end element classification.

Figure 4 illustrates the architecture of the proposed MMDL model, which comprises a graphical and a non-graphical branch to handle the BIM visual element image and textural element attribute modalities, respectively. The graphical branch utilizes the Convolutional Neural Network (CNN), a deep learning model that excels in visual imagery analysis (Valueva et al., 2020). Specifically, the input element image undergoes a convolutional layer that multiplies the color values of the convolved image patch (i.e., a pixel and its neighborhood) by a filter kernel matrix. The Rectified Linear Unit (ReLU) activation function is applied after the convolutional layer to introduce nonlinearity to the model, followed by max-pooling to extract a down-sampled feature map. This stack of layers is repeated in the graphical branch. The final max-pooling layer's output is flattened for fusion with the non-graphical branch.

Motivated by the superiority of the self-attention mechanism in capturing a wide range of global contextual information into local features (Vaswani et al., 2017), an attention-based module is developed in the non-graphical branch to encode the rich BIM element attributes. This module first decomposes each input element attribute into three items, namely query, key, and value, through three trainable transformation weight matrices in the linear transformation. Based on this, a scaled dot product attention mechanism is applied. For each query, the model learns the information from the global input features through an attentive process. More details about the attention mechanism can be found in (Vaswani et al., 2017). Finally, the attention readout is fused with the graphical branch to integrate the visual image and textural attribute modalities of BIM elements.

The flattened output from the graphical branch and the attention readout from the non-graphical branch are transformed through fully-connected layers into values with the same dimension. Then, a weighted addition strategy is employed to fuse the encoded graphical and non-graphical features, as shown in Eq. (1), where O_{fused} is the fusion output after the weighted addition layer, $O_{graphical}$ and $O_{non-graphical}$ denote the outputs from the graphical and non-graphical branches with the same dimension, respectively, and λ and γ are trainable influential factors of graphical and non-graphical information, respectively, to reveal the impact of each modality. This modality-aware design enables the model to selectively absorb and synthesize information from various BIM data modalities that may differ in importance. The fusion output is then sent to two fully-connected layers with the ReLU activation function to produce fine-grained BIM element classification.

$$O_{fused} = \lambda \cdot O_{graphical} + \gamma \cdot O_{non-graphical} \quad (1)$$

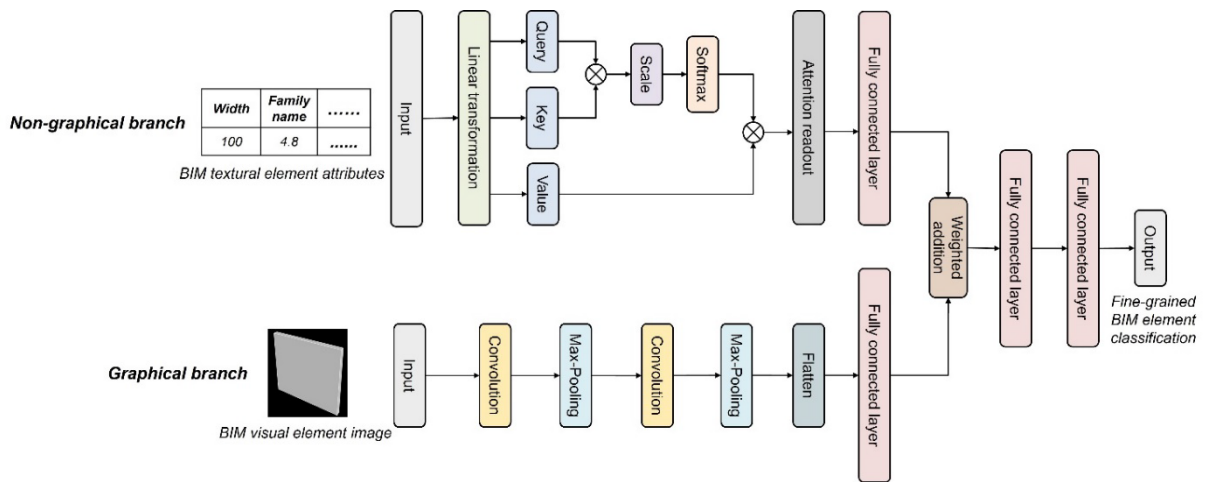


Figure 4. The proposed MMDL model fusing BIM graphical (i.e., visual element image) and non-graphical (i.e., textural element attributes) information

A classification model is obtained after training the proposed MMDL model with the BIM element multi-modal features as the inputs. For elements in new BIM models that also have specific graphical representations and necessary cost estimation-related information, the trained model can automatically deduce the corresponding fine-grained classifications, which greatly reduces the required human workload. The BIM models enriched with fine-grained classification information can then be smoothly utilized in subsequent cost estimation activities.

3. EXPERIMENTS AND RESULTS

3.1 Experimental Design

The proposed method was implemented in a desktop computer with the Windows 10 system, one Intel(R) Core(TM) i7-11700KF @ 3.60GHz processor, one NVIDIA GTX 3060Ti graphical processing unit (GPU), and 32GB random-access memory (RAM). The BIM models used in this study are vendor-neutral IFC models. IfcOpenShell 0.7.0 (IfcOpenShell, 2022) and BlenderBIM 0.0.220619 (BlenderBIM, 2022) are used to perform the transformation of multi-modal BIM element features. PyTorch 1.11.0 (Linux Foundation and Meta AI, 2022) is adopted as the deep learning platform to develop the MMDL model.

For illustration, a multi-modal fine-grained BIM element classification dataset is created based on the BIM models shown in Figure 5. They are from two real BIM-based cost estimation projects in Hong Kong. Elements are obtained from the collected BIM models. Figure 6 and Figure 7 show the classes of the elements in the dataset and the number of elements in each class, respectively. The dataset covers typical concrete building element types including slab, beam, column, and wall, each of which has fine-grained sub-categories regarding their graphical and/or non-graphical differences. The multi-modal BIM element features are obtained according to the data transformation method (Figure 3). The elements in the dataset are classified and labeled according to standard methods of measurement (Hong Kong Institute of Surveyors, 2018) and cost estimation practice from cost experts.

The model training is based on the recommendations and practices in previous studies (Emunds et al., 2022). The dataset is randomly split into training and testing sets with a ratio of 8:2, resulting in 2345 and 587 elements in the training and testing sets, respectively. 30% of the training set is further separated as a validation set. Then, the model is trained over the remaining 70% of the training set and evaluated using the validation set according to the classification metrics shown in Figure 8 and Eqs. (2) – (5) to determine optimal hyperparameters, where i stands for a class, N_{total} is the total number of samples, and n means the total number of classes. After the hyperparameter tuning, the model is trained over the whole training set for 200 epochs with a batch size of 64, and the Adam optimizer (Kingma and Ba, 2017) is adopted with a learning rate of 0.001. Finally, the trained model is evaluated using the testing set to reveal the classification performance.

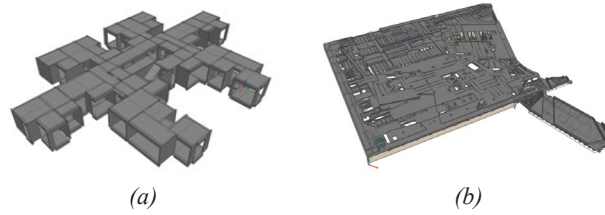


Figure 5. Collected BIM models (typical floors) where elements are obtained for the fine-grained classification: (a) A residential building; (b) A commercial building

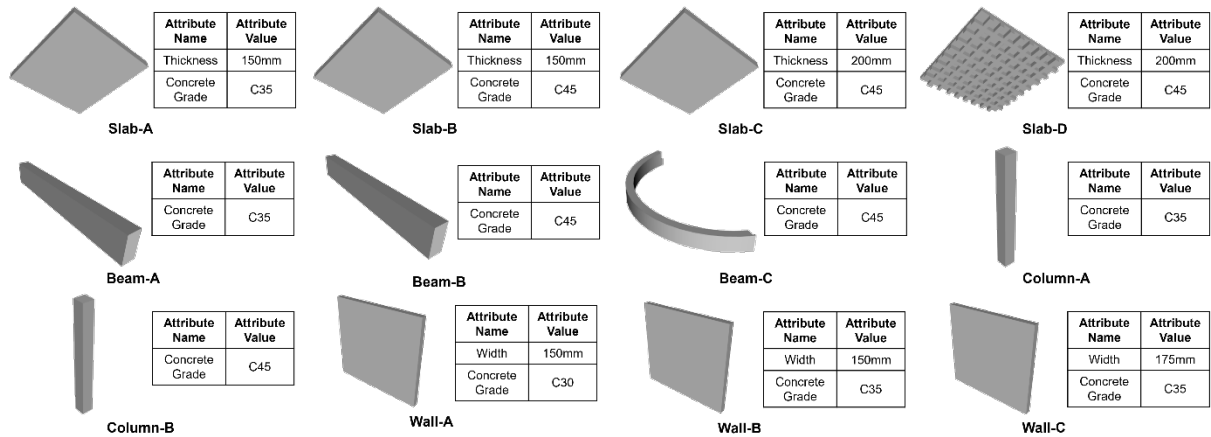


Figure 6. 12 Typical BIM element classes for cost estimation in the dataset (For simplicity, different letters are used to represent different classes)

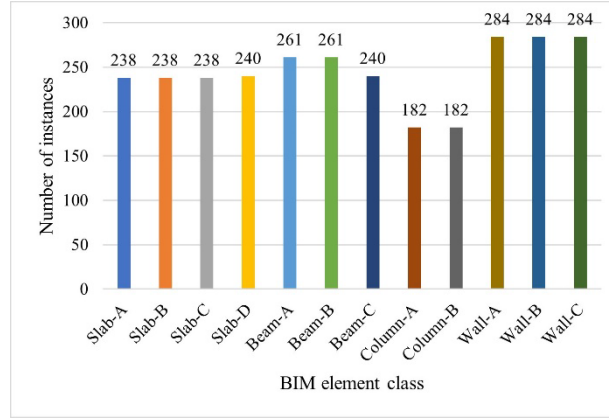


Figure 7. The number of elements per class

		True Class	
		Positive	Negative
Predicted Class	Positive	True Positive (TP)	False Positive (FP)
	Negative	False Negative (FN)	True Negative (TN)

Figure 8. Confusion matrix (TP: the number of positive samples being classified as positive; FN: the number of positive samples being classified as negative; FP: the number of negative samples being classified as positive; TN: the number of negative samples being classified as negative)

$$Accuracy = \frac{\sum_i TP_i}{N_{total}} \quad (2)$$

$$Precision = \frac{TP_i}{TP_i + FP_i} \quad (3)$$

$$Recall = \frac{TP_i}{TP_i + FN_i} \quad (4)$$

$$F1 - score = \frac{\sum_{i=1}^n \frac{2 \times TP_i}{2 \times TP_i + FP_i + FN_i}}{n} \quad (5)$$

3.2 Classification Results

The MMDL model (Figure 4) was developed and trained to automatically classify BIM elements into fine-grained categories. As shown in Figure 9, it achieves high classification performance in most categories.

The influential factors of graphical and non-graphical branches in the modality-aware fusion strategy shown in Eq. (1) are 0.1963 and 0.8037, respectively, indicating that the rich non-graphical information plays a more important role in the fine-grained BIM element classification for cost estimation. This makes sense because of two reasons. First, the non-graphical features provide classification patterns (e.g., material property information via *concrete grade* attributes) that only originate from them. In addition, they also contain part of the information explicitly (e.g., general type information through *family name* attributes) that is encoded in the graphical features. Nevertheless, the graphical features still have certain impacts since they are indispensable to the distinguishment of fine-grained classes that are non-graphically the same but graphically different (e.g., the suspended slab *Slab-C* and coffered slab *Slab-D*).

Effectiveness of multi-modality. Table 1 shows the performance differences between the multi-modal and unimodal deep learning models. The multi-modality design enhances the performance by about 30% and 6%, respectively, compared with the graphical and non-graphical modalities alone, indicating the significant effectiveness of the multi-modality in facilitating the BIM element classification.

Effectiveness of deep learning. The performance of the deep learning model and a typical machine learning model (i.e., random forest (RF)) with the fixed modality is studied to investigate the effectiveness of the deep learning module. As shown in Table 2, the deep learning model provides remarkably higher performance than the machine learning model in both graphical and non-graphical modalities. This implies that the deep learning module can significantly improve the BIM element classification results.

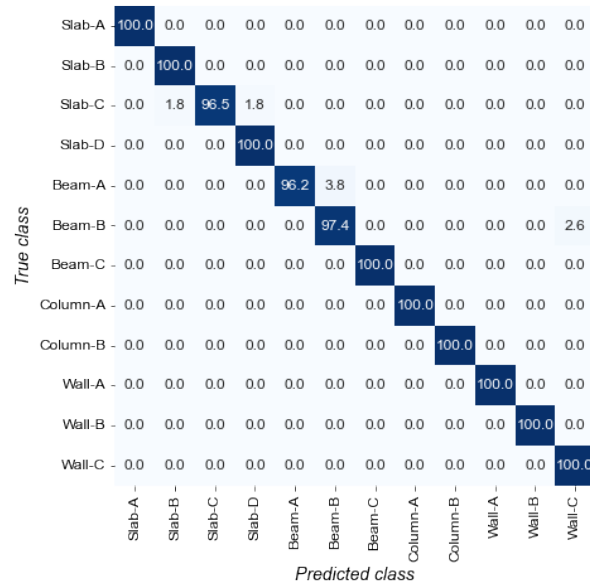


Figure 9. Confusion matrix of the proposed method (Each cell represents the percentage of elements in a class in the vertical axis being classified as a class in the horizontal axis. For example, the 100.0 in the first row and first column means that 100% of the elements in Slab-A class are classified as Slab-A class. The 0.0 in the first row and second column denotes that 0% of the elements in Slab-A class are classified as Slab-B class.)

Table 1. Classification metrics of multi-modal and unimodal deep learning model

	Accuracy	Precision	Recall	F1-score
MMDL	0.9915	0.9911	0.9917	0.9913
MMDL graphical branch	0.6848	0.6950	0.6924	0.6902
MMDL non-graphical branch	0.9267	0.9489	0.9313	0.9256

Table 2. Classification metrics of deep learning model and typical machine learning model with fixed modality

	Accuracy	Precision	Recall	F1-score
MMDL graphical branch	0.6848	0.6950	0.6924	0.6902
RF with graphical input	0.5451	0.5338	0.5831	0.5327
MMDL non-graphical branch	0.9267	0.9489	0.9313	0.9256
RF with non-graphical input	0.9097	0.8531	0.9041	0.8664

4. CONCLUSIONS

Fine-grained BIM element classification is vital to ensure interoperability for BIM-based domain applications. This paper presents a novel fusion approach to classifying BIM elements into fine-grained categories for cost estimation. The contributions are mainly twofold. (1) A BIM data fusion framework that synthesizes graphical and non-graphical modalities in BIM models as training sources for data-driven element classification. To the authors' best knowledge, this study pioneers the integration of various BIM data modalities for BIM element classification, which can eliminate the required human effort in developing classification rules and break through the bottleneck of unimodal learning. (2) A MMDL model to classify the fine-grained BIM elements. The modality-aware MMDL architecture integrates CNN and attention modules with a weighted addition strategy to reveal the impacts of BIM graphical and non-graphical modalities, respectively, which allows selective recognition of various BIM data modalities and end-to-end classification of the fine-grained element categories.

However, there are several limitations as follows. First, preparing the fine-grained BIM element classification dataset for model training requires time-consuming manual annotating effort. In the future, semi- or unsupervised deep learning techniques that require less labeled data will be explored to alleviate this aspect. In addition, this study mainly covers typical building elements (i.e., slab, beam, column, wall) of concrete structures

in cost estimation for illustration. More types of building elements and structures, as well as domain classification applications, will be investigated in future work to make the proposed framework more comprehensive.

ACKNOWLEDGMENTS

This research is partially supported by NUS Start-up Grant (No. R-296-000-233-133). Any opinions and findings are those of the authors and do not necessarily reflect the views of the grantor.

REFERENCES

- Akinosho, T.D., Oyedele, L.O., Bilal, M., Ajayi, A.O., Delgado, M.D., Akinade, O.O., and Ahmed, A.A. (2020). Deep learning in the construction industry: A review of present status and future innovations, *Journal of Building Engineering*, 32, 101827.
- BlenderBIM. (2022). *An add-on for beautiful, detailed, and data-rich OpenBIM with Blender*. Retrieved from: <https://blenderbim.org/>
- Construction Industry Council (CIC). (2021). *CIC BIM Standards - General (Version 2.1 - 2021)*. Retrieved from: https://www.bim.cic.hk/zh-hant/resources/publications_detail/100
- Elghaish, F., Abrishami, S., Hosseini, M.R., and Abu-Samra, S. (2020). Revolutionising cost structure for integrated project delivery: a BIM-based solution, *Engineering, Construction and Architectural Management*, 28(4), 1214-1240.
- Emunds, C., Pauen, N., Richter, V., Frisch, J., and van Treeck, C. (2022). SpaRSE-BIM: Classification of IFC-based geometry via sparse convolutional neural networks, *Advanced Engineering Informatics*, 53, 101641.
- Fazeli, A., Dashti, M.S., Jalaei, F., and Khanzadi, M. (2020). An integrated BIM-based approach for cost estimation in construction projects, *Engineering, Construction and Architectural Management*, 28(9), 2828-2854.
- Hong Kong Institute of Surveyors. (2018). *Hong Kong Standard Method of Measurement of Building Works, Fourth Edition Revised 2018*, Retrieved from: https://www.hkis.org.hk/en/publication_sales.html
- IfcOpenShell. (2022). *IfcOpenShell: Open source IFC library and geometry engine*. Retrieved from: <https://github.com/IfcOpenShell/IfcOpenShell>
- Jurafsky, D. and Martin, J. (2008). *Speech and Language Processing, 2nd edition*. Prentice Hall.
- Kingma, D.P. and Ba, J. (2014). Adam: A method for stochastic optimization, *arXiv preprint*, <http://arxiv.org/abs/1412.6980>.
- Lee, S.K., Kim, K.R., and Yu, J.H. (2014). BIM and ontology-based approach for building cost estimation, *Automation in construction*, 41, 96-105.
- Linux Foundation and Meta AI (2022). *PyTorch*. Retrieved from: <https://pytorch.org/>
- Liu, H., Cheng, J.C., Gan, V.J., and Zhou, S. (2022a). A knowledge model-based BIM framework for automatic code-compliant quantity take-off, *Automation in Construction*, 133, 104024.
- Liu, H., Cheng, J.C., Gan, V.J., and Zhou, S. (2022b). A novel Data-Driven framework based on BIM and knowledge graph for automatic model auditing and Quantity Take-off. *Advanced Engineering Informatics*, 54, 101757.
- Ma, Z., Wei, Z., and Zhang, X. (2013). Semi-automatic and specification-compliant cost estimation for tendering of building projects based on IFC data of design model, *Automation in Construction*, 30, 126-135.
- Ngiam, J., Khosla, A., Kim, M., Nam, J., Lee, H., and Ng, A.Y. (2011). Multimodal deep learning, *Proceedings of the 28th International Conference on International Conference on Machine Learning*, Bellevue, Washington, USA, pp. 689–696.
- Shin, Y., Kim, M., Pak, K.W., and Kim, D. (2020). Practical methods of image data preprocessing for enhancing the performance of deep learning based road crack detection, *ICIC Express Letters, Part B: Applications*, 11(4), 373-379.
- Valueva, M.V., Nagornov, N.N., Lyakhov, P.A., Valuev, G.V., and Chervyakov, N.I. (2020). Application of the residue number system to reduce hardware costs of the convolutional neural network implementation, *Mathematics and Computers in Simulation*, 177, 232-243.
- Vaswani, A., Shazeer, N., Parmar, N., Uszkoreit, J., Jones, L., Gomez, A.N., Kaiser, Ł., and Polosukhin, I. (2017). Attention is all you need, *Proceedings of the 31st International Conference on Neural Information Processing Systems*, Long Beach, California, USA, pp. 6000–6010.
- Wu, S., Wood, G., Ginige, K., and Jong, S.W. (2014). A technical review of BIM based cost estimating in UK quantity surveying practice, standards and tools, *Journal of Information Technology in Construction*, 19, 534-562.
- Zabin, A., González, V.A., Zou, Y., and Amor, R. (2022). Applications of machine learning to BIM: A systematic literature review, *Advanced Engineering Informatics*, 51, 101474.

AN AUTOMATIC TRANSLATION FRAMEWORK BASED ON ONTOLOGY TO BUILDING ENERGY MODELS

Zhaoji Wu¹, Jack C.P. Cheng², Zhe Wang³, and Helen H.L. Kwok⁴

1) Ph.D. Student, Department of Civil and Environmental Engineering, The Hong Kong University of Science and Technology, Hong Kong SAR. Email: zwubz@connect.ust.hk

2) Ph.D., Prof., Department of Civil and Environmental Engineering, The Hong Kong University of Science and Technology, Hong Kong SAR. Email: cejcheng@ust.hk

3) Ph.D., Asst. Prof., Department of Civil and Environmental Engineering, The Hong Kong University of Science and Technology, Hong Kong SAR. Email: cezhewang@ust.hk

4) Ph.D., Postdoc, Institute for the Environment, The Hong Kong University of Science and Technology, Hong Kong SAR. Email: hlkwokab@connect.ust.hk

Abstract: Under the trend of carbon neutrality, building energy is being paid more attention to in recent years. Building Energy Modeling (BEM) is a powerful and essential tool that assists building designers and managers to predict and manage building energy performance. Manually collecting data related to BEM from various sources is time- and expertise-demanding. Building Information Modeling (BIM) facilitates automatic BEM by the integration of multiple data, but recent studies showed that the seamless transfer of BIM to BEM has not been fully achieved. Ontology-based approaches provide another feasible solution to automatic BEM. Previously, we proposed an ontology model for BEM which can integrate data for BEM from key data domains, i.e., weather, building, internal heat gain and Heating, Ventilation, and Air-conditioning (HVAC) system. Automatic thermal zoning can be conducted via cross-domain reasoning based on the ontology model. However, to fully achieve automatic BEM, translation from the ontology model to the building energy model is needed. In this study, we propose an automatic ontology-to-BEM translation framework using instance-based mapping, dynamic data conversion and template-based configuration file generation. By the instance-based method, fields between the two different models can be identified and mapped at the entity level and the property level. By the dynamic data conversion algorithm, temporally-changing data can be retrieved from original databases based on the information provided by the ontology model, and the data can be automatically written to BEM configuration files. By the template-based configuration file generation workflow, the completeness of the BEM model is ensured. One floor of a campus building was selected as an illustrative example of the framework. The results showed that the proposed framework could automatically generate the building energy model while reducing the modeling time by over 99% with consistency of the manually dedicated modeling.

Keywords: Building energy modeling, Ontology, Model translation, Data mapping

1. INTRODUCTION

More attention is being paid to building energy efficiency, especially under the regulatory trend for carbon neutrality. To reduce building energy consumption and achieve energy efficiency, building energy management is essential throughout the entire building lifecycle. Building energy modeling (BEM) is a prerequisite of building energy management, and can help building designers and managers predict the energy demand and adopt optimal design or control strategies. However, data required for BEM, including location, weather, building geometry, construction typologies, internal loads, Heating, Ventilation, and Air-conditioning (HVAC) systems, operating strategies, schedules, etc. (Gao et al., 2019), are in different types and come from various information sources. For example, building geometries may be provided by Building Information Modeling (BIM) while the operation strategies and schedules of HVAC may be provided by Building Management Systems (BMS). The lack of precise input data results in low accuracy of prediction (Zhao & Magoulès, 2012). Manual collection of different data from various sources can be an error-prone and time-consuming job. In addition, inputting the data into the energy simulation engine usually requires expertise in BEM. Manual preparation of the input data and modeling process of BEM can scarcely achieve timely prediction and decision-making. Consequently, both efficient data model for data integration from multiple information sources and automatic BEM model generation are urgently needed for building energy management.

BIM can serve as a building information hub which provides uniform data models and enhances data integration and interoperability. Therefore, BIM can be a solution to the issue of BEM data preparation and model generation. Previous studies focused on the adoption of BIM-based schemas (e.g., Industry Foundation Classes (IFC) and Green Building XML (gbXML)) for BEM, and have reported overcoming the hindrances to BIM-BEM process, including incorrect geometry translation, lack of material libraries, lack of space load, and lack of HVAC transformation (Gao et al., 2019). However, recent studies (Bastos Porsani et al., 2021; Bracht et al., 2021) still show that full interoperability between BIM and BEM had not yet been achieved. Some functions, e.g., thermal zoning and dynamic data conversion, need to be developed in a smooth and seamless BIM-BEM process.

Ontology-based approaches have the potential to overcome the shortages of BIM-BEM. Recent studies

(Corry et al., 2015; Degha et al., 2019; Han et al., 2015; Hu et al., 2021; Lork et al., 2019; Schachinger & Kastner, 2017; Zhang et al., 2021) have shown that ontology-based approaches are practical and efficient in building energy management with advantages including structured data schema for knowledge management, convenient bridging for cross-domain linking, and efficient logic inference for implicit knowledge discovery. However, ontology-based BEM is less studied. Only the ontology-based SimModel (Pauwels et al., 2014) was proposed for building energy simulation purposes but limitations still exist in that important elements for energy simulation, e.g., materials, space types, thermal zones and space loads, are not considered (Farzaneh et al., 2019; Gao et al., 2019). Consequently, further studies of ontology-based approaches should be conducted.

Data integration and automatic modeling are two important issues of BEM. For data integration, we have proposed an ontology model (Figure 1) which covers four key information domains for BEM including weather, building, internal heat gain and HVAC system (Wu et al., 2022). Based on the model, we proposed inference rules and automatic thermal zoning that can be conducted in accordance with the criteria of internal heat gain, external heat gain and HVAC control. However, to achieve timely prediction and decision-making for building energy management, fully automatic modeling is essential. In this study, we propose an automatic ontology-to-BEM translation framework using instance-based mapping and dynamic data conversion. Fields between the two models can be identified and mapped at the entity and property level using the instance-based method. The temporally-changing data (e.g., weather data and equipment operation schedules) can be retrieved from the original databases based on the information from the ontology model, and written to the BEM configuration files using the dynamic data conversion algorithm. One floor of a campus building was selected as an illustrative example of the framework.

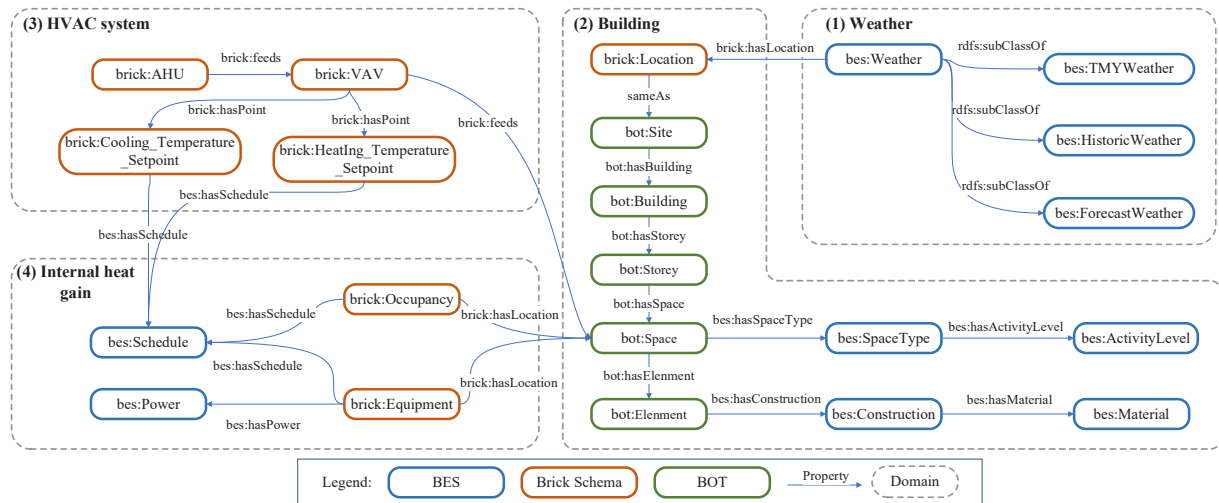


Figure 1. Ontology model for BEM

2. METHOD

2.1 Instance-Based Mapping

Representations of entities and properties are different between the ontology model and the building energy simulation model. The first issue is to achieve the accurate mapping of the same entities and properties in different models. It is a common issue in BIM-BEM studies, but it is less studied in ontology-to-BEM. The Instance-based method maps corresponding fields individually between two models in different schemas and it is by far the most effective way for schema mapping between complex schemas with the guarantee of mapping accuracy (Deng et al., 2016). Objects are written separately as individual items (Figure 2) in both ontology models (e.g., Web Ontology Language ontologies (OWL) file in Turtle syntax) and BEM models (e.g., EnergyPlus Input File (IDF)), which facilitates the implementation of the instance-based method for field mapping.

Two levels of field mapping are studied. The first level is entity mapping, in which the corresponding entities are identified between the two models (e.g., CYT4001Occupancy in Figure 2). The second level is property mapping, in which the corresponding properties are identified under the same entity between the two models (e.g., occupancy name, space where the occupancy is located, etc. in Figure 2). Figure 3 takes the occupancy as an example to clearly show how the properties are translated from the proposed ontology model (Figure 3 (b)) to the building energy simulation model (Figure 3 (a)). There are three types of property mapping. Some properties (the red arrows) can be mapped directly. Some properties (the green arrows) should be calculated based on the ontology model and the database. Some properties (e.g., number of people) are set as default values. After field mapping, an automatic translation framework from OWL files and IDF files is established based on the Python scripts as shown in Figure 2. The Python library rdflib (RDFLib Team, 2022) is adopted to parse the ontology model and extract the information of the targeted fields via SPARQL Protocol and RDF Query Language

(SPARQL) query. The Python library eppy (Santosh Philip, 2022) is implemented to write the IDF file based on the extracted information.

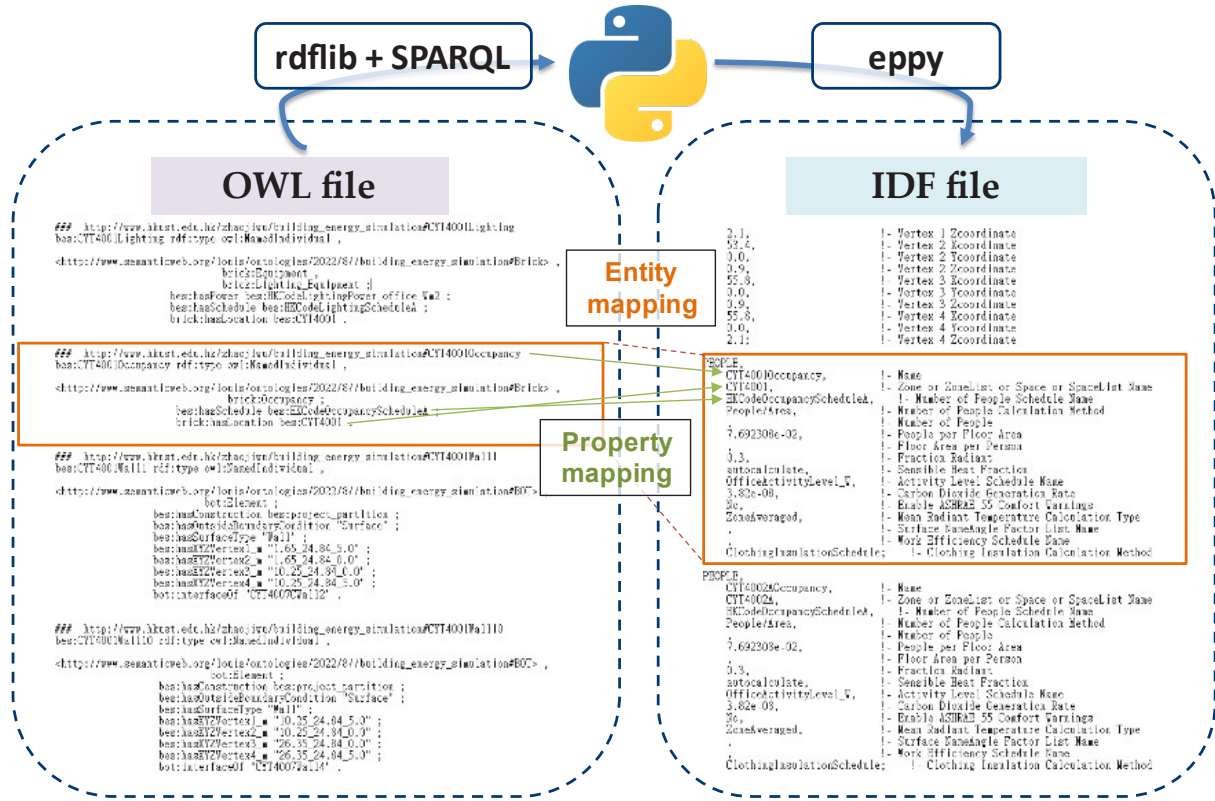


Figure 2. Instance-based mapping between the ontology model and BEM model.

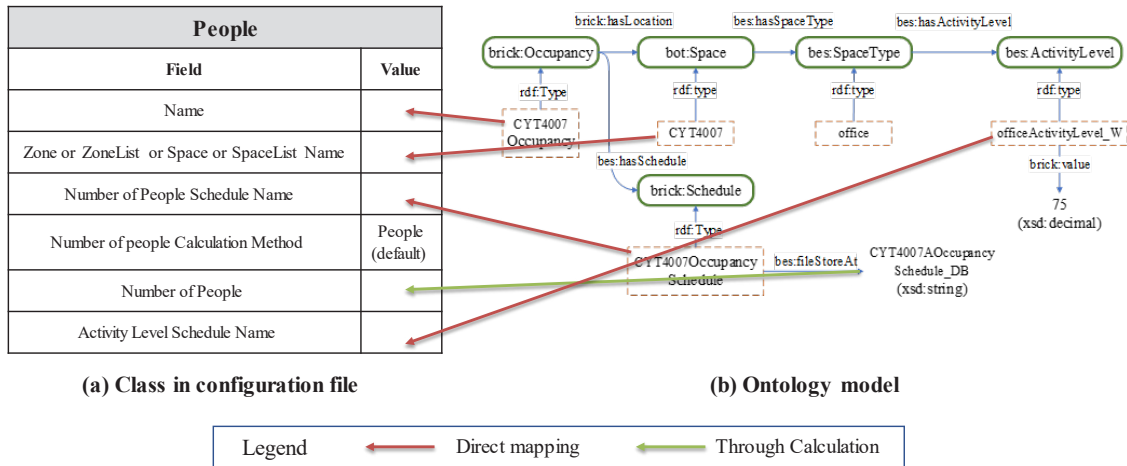


Figure 3. Property mapping between the ontology model and the BEM model

2.2 Dynamic Data Conversion

In the operation phase, temporally-changing data from multiple sources. Weather data and schedules of equipment and occupancy are two main dynamic data which should be translated into the BEM model. To simulate building energy consumption in one past or future period, corresponding weather data should be selected according to the period and input into the energy simulation engine. For schedules of equipment and occupancy, the selection also depends on the simulation period. For the simulation in past periods, the historical records of the people counting or equipment status should be selected. For the simulation in future periods, since there are no records, the common practice is to use the historic data to represent the future conditions (e.g., to use the average number in one past period). Consequently, dynamic data conversion is a process of data selection from which they are stored in and data written in BEM configuration files.

Figure 4 shows the overall workflow of dynamic data conversion from the database to the BEM model. Dynamic data are stored in the original addresses instead of the ontology model and storage address information is provided by the proposed ontology model. Firstly, the data address information is retrieved from the ontology model via SPARQL query. Secondly, with address information and the simulation period, the query in Structured Query Language (SQL) can be constructed and sent to the databases which store the dynamic data. Finally, data can be retrieved according to the query and translated to EnergyPlus Weather Format (EPW) file or IDF file via Python scripts and the library eppy.

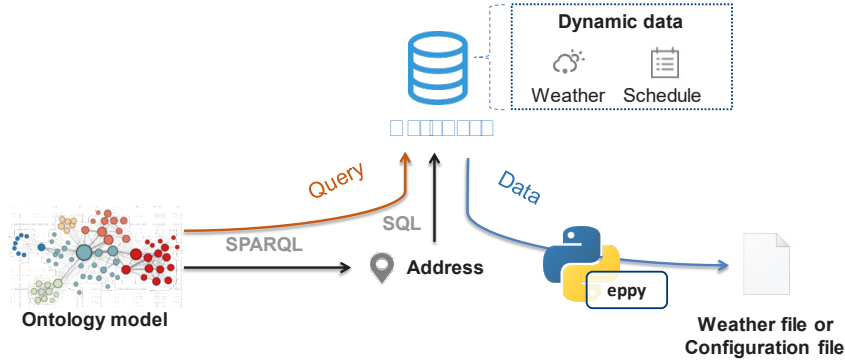


Figure 4. Dynamic data conversion workflow

Table 1 shows the algorithm to translate weather data to the BEM model. The inputs include the simulation period, weather file template and ontology model. The weather file template is the local weather file in EPW format. Recorded historic or forecast weather data, which contain relevant parameters, e.g., temperature and relative humidity, in time series, are retrieved from the database. The columns (parameter values) and the rows (timestamps) in the weather file template are located according to the simulation period. The template data in these columns and rows are covered by the actual data. Finally, the EPW file with the actual data is generated and inputted into the energy simulation engine.

Table 1. Algorithm to translate weather data to the BEM model

Algorithm 1: Weather file generation	
Input: start timestamp T_s , end timestamp T_e , ontology model O , weather database D , weather file template F	
1	query and retrieve $weather_address \leftarrow O$
2	query and retrieve $weather_data[] \leftarrow D$ according to $weather_address$
3	open F do
4	for each $weather_parameter$ in $weather_data[]$ do
5	$parameter_data_list[] \leftarrow$ hourly data from $weather_data[]$ between T_s and T_e
6	locate $column$ of $weather_parameter$ in F
7	locate row between T_s and T_e in F
8	write $parameter_data_list[]$ in $column$ and row
9	end for
10	close F
Output: EPW file F	

Table 2 shows the algorithm to translate the equipment schedule to the BEM model. There are two types of equipment schedules for two scenarios. If spaces are equipped with equipment status recorders, the running status (e.g., the percentage of full operation) can be recorded and serves as the historic data for schedule construction. If spaces are not equipped with equipment status recorders, the common practice is to use schedules provided by guidelines or standards according to the space types. Consequently, in the equipment schedule translation, schedules should be identified as guideline-based or record-based. In the building energy simulation engine, e.g., EnergyPlus (U.S. Department of Energy's (DOE) Building Technologies Office (BTO) & National Renewable Energy Laboratory (NREL), 2022), schedules usually consist of hourly data. For guideline-based scenarios, hourly data are provided by guidelines directly. For record-based scenarios, data may be collected in different intervals and hence they should be translated into hourly data, e.g., by calculating the hourly average in the same hour every weekday or weekend. Table 3 shows the algorithm to translate the occupancy schedule to the BEM model. The occupancy schedule translation is similar to the equipment schedule translation, whereas the occupancy is usually recorded by the number of people and should be translated into the percentages of the maximum occupancy. In the record-based scenario, the fields Number of People and People per Area should be

calculated automatically according to the people counting records.

Table 2. Algorithm to translate equipment schedule to the BEM model

Algorithm 2: Lighting / Electrical equipment schedule translation	
Input: start timestamp T_s , end timestamp T_e , ontology model O , schedule file or database S , IDF file F	
1	query and retrieve $space_list[] \leftarrow O$
2	open F do
3	for each $space$ in $space_list[]$ do
4	query and retrieve $schedule_address, area, power \leftarrow O$
5	query and retrieve $schedule[] \leftarrow S$ according to $schedule_address$
6	if the schedule is guideline-based then
7	$equipment_hourly_status_list[] \leftarrow$ hourly data from $schedule[]$
8	write $equipment_hourly_status_list[]$ to $Schedule:Day:Hourly$ in F
9	$level_per_area \leftarrow power$
10	write $level_per_area$ to $Watts\ per\ Zone\ Floor\ Area$ in F
11	if the schedule is record-based then
12	$equipment_status_list[] \leftarrow schedule[]$ between T_s and T_e
13	for each $hour$ every weekday or weekend do
14	$equipment_hourly_status_list[] \leftarrow$ average($equipment_status_list[]$ in $hour$)
15	$level_per_area \leftarrow power / area$
16	write $level_per_area$ to $Watts\ per\ Zone\ Floor\ Area$ in IDF file
17	write $equipment_hourly_status_list[]$ to $Schedule:Day:Hourly$ in F
18	end for
19	write $Schedule:Week:Daily$ in F
20	write $Schedule:Year$ in F
21	end for
22	close F
Output: IDF file F	

Table 3. Algorithm to translate occupancy schedule to the BEM model

Algorithm 3: Occupancy schedule translation	
Input: start timestamp T_s , end timestamp T_e , ontology model O , schedule file or people counting database S , IDF file F	
1	query and retrieve $space_list[] \leftarrow O$
2	open F do
3	for each $space$ in $space_list[]$ do
4	query and retrieve $schedule_address, area \leftarrow O$
5	query and retrieve $schedule[] \leftarrow S$ according to $schedule_address$
6	if the schedule is guideline-based then
7	$occupancy_hourly_ratio_list[] \leftarrow$ hourly data from $schedule[]$
8	write $occupancy_hourly_ratio_list[]$ to $Schedule:Day:Hourly$ in F
9	$people_per_area \leftarrow$ people per area given by the guideline
10	write $people_per_area$ to $People\ per\ Floor\ Floor\ Area$ in F
11	if the schedule is record-based then
12	$occupancy_count_list[] \leftarrow schedule[]$ between T_s and T_e
13	$number_of_people \leftarrow \max(occupancy_count_list[])$
14	$people_per_area \leftarrow number_of_people / area$
15	write $people_per_area$ to $People\ per\ Floor\ Floor\ Area$ in F
16	for each $hour$ every weekday or weekend do
17	$occupancy_hourly_ratio \leftarrow$ average($occupancy_count_list[]$ in $hour$) / $number_of_people$
18	write $occupancy_hourly_ratio$ to $Schedule:Day:Hourly$ in F
19	end for
20	write $Schedule:Week:Daily$ in F
21	write $Schedule:Year$ in F
22	end for
23	close F
Output: IDF file F	

2.3 Template-Based Configuration File Generation

Through instance-based mapping and dynamic data conversion, the information from the proposed ontology model and the databases can be translated into the BEM model automatically. However, to complete the simulation configuration file and run the simulation successfully, some indispensable fields still need to be supplemented. These fields usually are related to the settings of the simulation, e.g., simulation control, calculation methods and output parameters (Figure 5). For the same simulated object, these settings seldom change in different simulation scenarios, and hence they can be set as the default in a template configuration file. Figure 6 shows the workflow of the template-based configuration file generation. The fields related to the simulation settings are written in the template configuration file. Other fields are written to the template through instance-based mapping and dynamic data conversion by the Python scripts for model translation. The full configuration file is generated after writing and can be imported into the energy simulation engine.

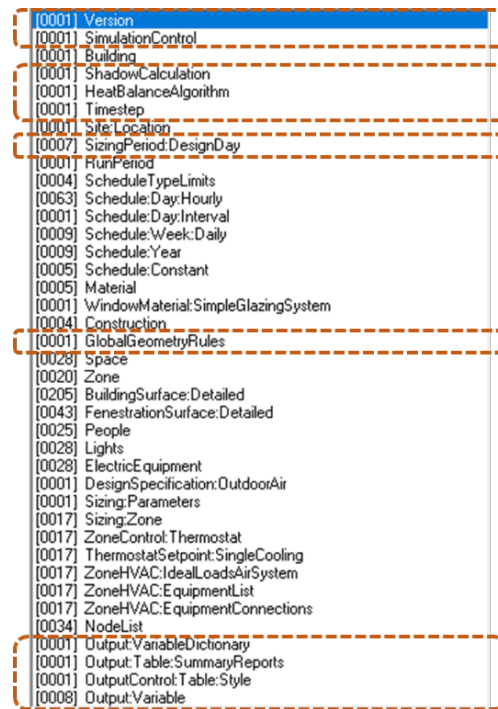


Figure 5. Fields of simulation settings, etc. (framed), which should be set in the template configuration file

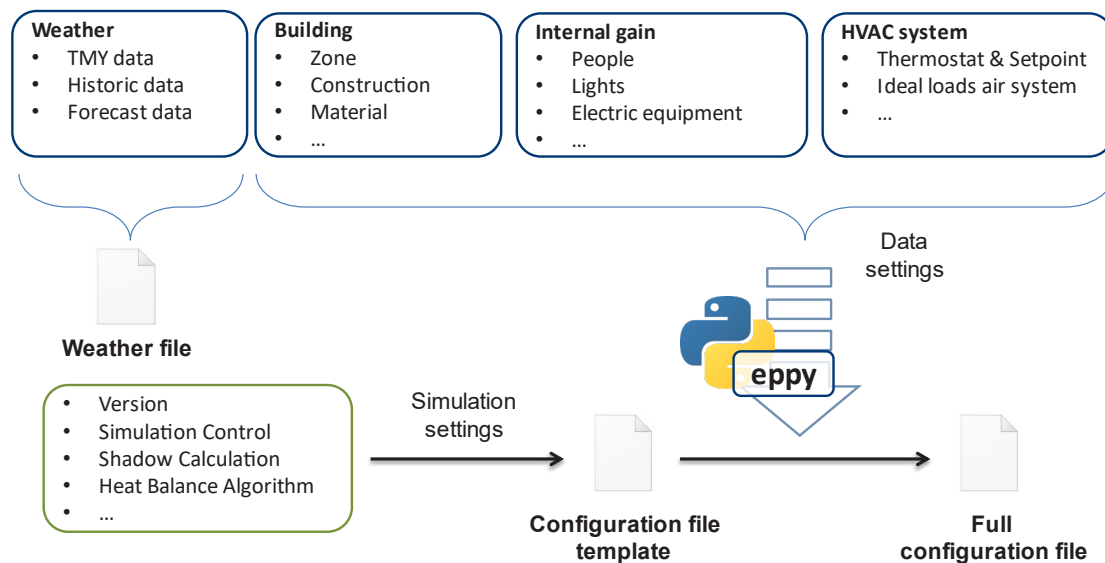


Figure 6. Workflow of Template-based configuration file generation

3. ILLUSTRATIVE EXAMPLE

3.1 Introduction of the Example

One floor of a campus building of a university was selected as the case object (Figure 7). The floor is used for academic purposes with an area of around 2200 m² and contains approximately 30 rooms. The building managers planned to verify the building energy simulation results by EnergyPlus on this floor to support predictive control studies in the future. The building energy model was developed by the proposed framework. In addition, to compare with the performance of the proposed framework, five PhD students, who had 5-to-9-year experience in thermal load simulation by EnergyPlus, were invited to manually develop the energy simulation model with the same information as the proposed framework, using IDF Editor provided by EP-Lauch, the official EnergyPlus tool. To ensure the accuracy of the manual modeling, the students checked each other's models after each step and finally submitted one BEM model on which they reached a consensus. The overall working time was recorded. A desktop served as the platform for the implementation of the framework, whose specifications are listed as follows: Intel Core CPU i7-6700 at 3.40 GHz 8 cores, 32 GB RAM memory, and Windows 64 operating system. The versions of tools or software used are listed as follows: Python 3.9.13 and EnergyPlus 9.6.

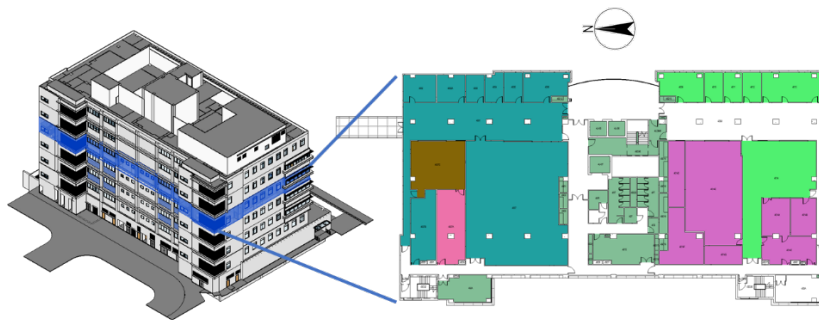


Figure 7. Location and layout of the example

3.2 Results

Precision and speed are two main aspects of the framework's performance. For precision, the EPW file and IDF file generated by the proposed framework were compared with the files by manual modeling. The two IDF files were imported into the software EP-Lauch and checked the consistency field by field. Simulations were conducted based on the files generated by the proposed framework and manually modeling respectively. Their simulation results of the cooling load during the same period were identical. The results showed the consistency between the automatically generated model and the manual dedicated model.

For speed, the time consumption consisted of two parts, i.e., EPW file generation, and IDF file generation. The EPW file generation was finished in 0.545 s and the IDF file generation was done in 2.702 s using Python scripts. In total, 3.247 s was consumed for the BEM process. The manual modeling process took approximately 8.5 h for information retrieval from different sources, and EPW and IDF file editing. The modeling time can be reduced by over 99% ($(4.772 \text{ s} - 8.5 \text{ h}) / 8.5 \text{ h} \times 100\%$) by the proposed framework compared with the manual modeling. Consequently, the proposed framework can keep the same precision as the manual modeling while substantially reducing the BEM time consumption.

4. CONCLUSIONS

In this study, we propose an automatic ontology-to-BEM translation framework using instance-based mapping, dynamic data conversion and template-based configuration file generation. Three goals which ensure seamless model translation are achieved. Firstly, entities, properties and relationships between ontology models and BEM models are identified and mapped. Secondly, temporally-changing data can be retrieved from original databases, and automatically written to BEM configuration files, which is seldom achieved in BIM-BEM methods. Thirdly, simulation settings are considered and the completeness of the BEM model is ensured. We selected one floor of a campus building as an illustrative example to implement the proposed framework and evaluate its performance. The results showed that the proposed framework could automatically generate the building energy model while reducing the modeling time by over 99% with consistency of the manually dedicated modeling. Although the main parts of BEM were considered in this study, other minor but important components, e.g., shading and infiltration, were excluded. Further extensions need to be included in the future.

REFERENCES

- Bastos Porsani, G., Del Valle de Lersundi, K., Sánchez-Ostiz Gutiérrez, A., & Fernández Bandera, C. (2021). Interoperability between Building Information Modelling (BIM) and Building Energy Model (BEM). *Applied Sciences*, 11(5), 2167. <https://doi.org/10.3390/app11052167>
- Bracht, M. K., Melo, A. P., & Lamberts, R. (2021). A metamodel for building information modeling-building energy modeling integration in early design stage. *Automation in Construction*, 121, 103422. <https://doi.org/10.1016/j.autcon.2020.103422>
- Corry, E., Pauwels, P., Hu, S., Keane, M., & O'Donnell, J. (2015). A performance assessment ontology for the environmental and energy management of buildings. *Automation in Construction*, 57, 249–259. <https://doi.org/10.1016/j.autcon.2015.05.002>
- Degha, H. E., Laallam, F. Z., & Said, B. (2019). Intelligent context-awareness system for energy efficiency in smart building based on ontology. *Sustainable Computing: Informatics and Systems*, 21, 212–233. <https://doi.org/10.1016/j.suscom.2019.01.013>
- Deng, Y., Cheng, J. C. P., & Anumba, C. (2016). Mapping between BIM and 3D GIS in different levels of detail using schema mediation and instance comparison. *Automation in Construction*, 67, 1–21. <https://doi.org/10.1016/j.autcon.2016.03.006>
- Farzaneh, A., Monfet, D., & Forgues, D. (2019). Review of using Building Information Modeling for building energy modeling during the design process. *Journal of Building Engineering*, 23, 127–135. <https://doi.org/10.1016/j.jobbe.2019.01.029>
- Gao, H., Koch, C., & Wu, Y. (2019). Building information modelling based building energy modelling: A review. *Applied Energy*, 238, 320–343. <https://doi.org/10.1016/j.apenergy.2019.01.032>
- Han, J., Jeong, Y.-K., & Lee, I. (2015). A Rule-Based Ontology Reasoning System for Context-Aware Building Energy Management. *2015 IEEE International Conference on Computer and Information Technology; Ubiquitous Computing and Communications; Dependable, Autonomic and Secure Computing; Pervasive Intelligence and Computing*, 2134–2142. <https://doi.org/10.1109/CIT/IUCC/DASC/PICOM.2015.317>
- Hu, S., Wang, J., Hoare, C., Li, Y., Pauwels, P., & O'Donnell, J. (2021). Building energy performance assessment using linked data and cross-domain semantic reasoning. *Automation in Construction*, 124, 103580. <https://doi.org/10.1016/j.autcon.2021.103580>
- Lork, C., Choudhary, V., Hassan, N. U., Tushar, W., Yuen, C., Ng, B. K. K., Wang, X., & Liu, X. (2019). An Ontology-Based Framework for Building Energy Management with IoT. *Electronics*, 8(5), 485. <https://doi.org/10.3390/electronics8050485>
- Pauwels, P., Corry, E., & O'Donnell, J. (2014). Representing SimModel in the Web Ontology Language. *Computing in Civil and Building Engineering (2014)*, 2271–2278. <https://doi.org/10.1061/9780784413616.282>
- RDFLib Team. (2022). *Rdflib 6.2.0*. Retrieved from website: <https://rdflib.readthedocs.io/>
- Santosh Philip. (2022). *Welcome to eppy's documentation!*. Retrieved from website: <https://eppy.readthedocs.io/>
- Schachinger, D., & Kastner, W. (2017). Ontology-based generation of optimization problems for building energy management. *2017 22nd IEEE International Conference on Emerging Technologies and Factory Automation (ETFA)*, 1–8. <https://doi.org/10.1109/ETFA.2017.8247565>
- U.S. Department of Energy's (DOE) Building Technologies Office (BTO), & National Renewable Energy Laboratory (NREL). (2022). *EnergyPlus*. Retrieved from website: <https://energyplus.net/>
- Wu, Z., Cheng, J. C. P., & Wang, Z. (2022). An ontology-based framework for building energy simulation in the operation phase. *The 19th International Conference on Computing in Civil and Building Engineering (ICCCBE 2022)*, Cape Town, South Africa.
- Zhang, Y.-Y., Hu, Z.-Z., Lin, J.-R., & Zhang, J.-P. (2021). Linking data model and formula to automate KPI calculation for building performance benchmarking. *Energy Reports*, 7, 1326–1337. <https://doi.org/10.1016/j.egyr.2021.02.044>
- Zhao, H., & Magoulès, F. (2012). A review on the prediction of building energy consumption. *Renewable and Sustainable Energy Reviews*, 16(6), 3586–3592. <https://doi.org/10.1016/j.rser.2012.02.049>

GIS BASED 3D DATA INTEGRATION ON HIGHWAY TUNNEL THROUGH LIFECYCLE MANAGEMENT FOR ADVANCED MAINTENANCE

Choijsilsuren Batbaatar¹, Yasuhiro Mitani², Hisatoshi Taniguchi³, and Hiroyuki Honda⁴

1) Department of Civil Engineering, Graduate School of Engineering, Kyushu University, Fukuoka, Japan. Email: batbaatar.choijsilsuren.546@s.kyushu-u.ac.jp

2) Ph.D., Prof., Disaster Risk Reduction Research center, Graduate School of Engineering, Kyushu University, Fukuoka, Japan. Email: mitani@doc.kyushu-u.ac.jp

3) Ph.D., Assoc. Prof., Disaster Risk Reduction Research center, Graduate School of Engineering, Kyushu University, Fukuoka, Japan. Email: taniguchi@doc.kyushu-u.ac.jp

4) Ph.D., Assist. Prof., Disaster Risk Reduction Research center, Graduate School of Engineering, Kyushu University, Fukuoka, Japan. Email: h.honda@doc.kyushu-u.ac.jp

Abstract: Building Lifecycle Management (BLM) is becoming more important for the building and construction production process since that improves efficiency and productivity of the building and construction production process by considering each process from investigation, design, and construction to maintenance process in lifecycle. However, in the Lifecycle Management of tunnel, information on each process of the construction production process is managed in various formats and databases. Consequently, if it was able to be lifecycle management information on each process of the tunnel construction production process, advanced maintenance that considers the causes of deformation in tunnel from multiple aspects would be possible.

In this research, a candidate is an existing tunnel (Phase I) and a newly constructing tunnel (Phase II). Firstly, the Building and Construction Information Modeling (BIM/CIM) model for tunnel construction is created from the information of the construction production process for investigation, design, construction, and maintenance (inspection and repair) of the existing Phase I tunnel by integrating all information into 3D space by using ArcGIS Pro and other software. Then, the tunnel BIM/CIM model from Phase I tunnel information is updated to become a comprehensive BIM/CIM model that can be effectively used for the maintenance process of each tunnel by the construction information of the new tunnel Phase II is added in real time. Finally, a 3D geological model around each tunnel based on BIM/CIM model with integrated information is developed.

As a result, we have been able to centrally manage the information of each tunnel through the tunnel BIM/CIM model on ArcGIS Pro. The effectiveness of the tunnel BIM/CIM model for maintenance has been clarified through more advanced analysis of cracks and road surface deformations on the Phase I tunnel considering the real condition of the around tunnels.

Keywords: Building Lifecycle Management, Maintenance, Building and Construction Information Modeling, tunnel

1. INTRODUCTION

Building Information Modeling (BIM) is used for the building production process to improve efficiency and quality by adding attribute data such as cost and management information to 3D digital model of building, which is then utilized consistently from design through construction to maintenance and management (Yoshikai et al., 2018). Currently, BIM is receiving much attention in industry and research (Hegemann et al., 2020). This system has been rapidly developed in the building production process since around the 1990s as shown in Figure 1. Furthermore, BIM has been developed not only for building processes but also for infrastructure projects such as roads, bridges, tunnels, etc. Meanwhile, in Japan, the Ministry of Land, Infrastructure, Transport, and Tourism (MLIT) has been implementing Construction Information Modeling (CIM) model project since 2012s, which aims to improve quality and safety management of construction production process by using 3D models in design and construction sites (Yamaoka et al., 2016). For structures such as roads and bridges, it is sufficient to use BIM for the infrastructure, because these structures include concretes and management systems, like common buildings. However, for tunnel construction, in addition to these structures, the surrounding ground becomes a part of the structure, therefore, it is necessary to consider both BIM and CIM. In addition, BIM/CIM model is developed for each process of the building and construction production process: BIM/CIM for the investigation, BIM/CIM for the design, and BIM/CIM for the construction and maintenance. Therefore, National Building Information Modeling Standards (NBIMS) vision for BIM/CIM is an improved planning, design, construction, operation, and maintenance processes using a standardized information model throughout the lifecycle management for all information in the building and construction production process (Sacks et al., 2018).

Tunnel structures present a challenge for maintenance management due to the various databases and formats used to manage each stage of the construction production process, with most of the information being in two-dimensional format. Therefore, it is difficult to identify spatial relationship of such information, and the fact that the stored data is not effectively used for maintenance management has become a problem for tunnel maintenance. In addition, tunnel structures can only be seen from inside once construction is finished, and it is

difficult to understand what cracks have occurred in what kind of geological conditions. Therefore, the original purpose of this research is to integrate all information on each process of the tunnel's whole construction production process into BIM/CIM model for building lifecycle management and to clarify effectiveness of BIM/CIM model for advanced maintenance.

This research focuses on an existing tunnel (Phase I) and a newly constructing tunnel (Phase II) adjacent to Phase I. Firstly, the information on the investigation to maintenance process of the Phase I tunnel is spatially integrated. Subsequently, the new tunnel Phase II's construction information is added in real time to BIM/CIM model with ArcGIS Pro. Then, BIM/CIM model is used to predict geological condition around tunnel, some deformation analysis, and for maintenance.

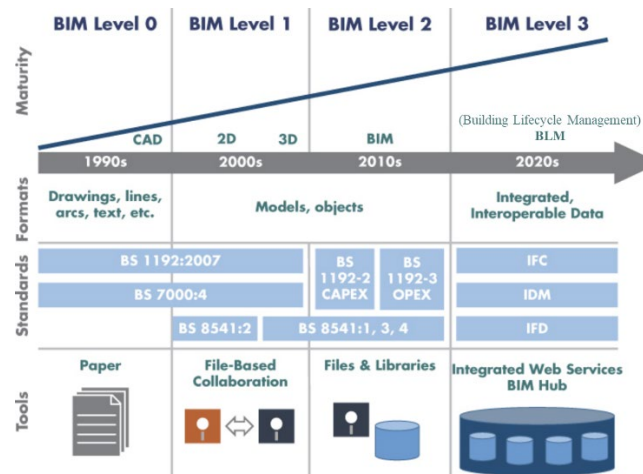


Figure 1. The BIM maturity model Levels: from 0 to stage 3 (Sacks et al., 2018)

2. METHOD

2.1 Development of The New BIM/CIM Model For Tunnel Construction

In this study, GIS software was selected as the method for constructing the BIM/CIM model of the tunnel. The reason for this approach is that GIS can automatically integrate multiple different types of information using a common global coordinate as a key. In addition to this, GIS also offers several spatial analysis tools, which enhances the utility of the integrated information for various kinds of analysis. Therefore, for constructing the GIS-based BIM/CIM model, the following five processes are conducted in ArgGIS Pro.

Firstly, on investigation process of Phase I tunnel, to effectively plan the design and construction methods for a tunnel project based on the results of investigation process, it is most important to clarify geological conditions of target area using various geotechnical investigation methods before start of tunnel design and construction. Information on geological investigation process includes many types of information such as borehole investigation (rock types, crack condition, RQD, etc.) and standard penetration tests (N values), physical properties from uniaxial compressive strength and coefficient of permeability, etc. by laboratory test, tunnel geological longitudinal profile. Therefore, in this research, borehole models are created and visualized using these physical properties for integration and digitalization. This is done by placing a cylindrical model vertically downward from the initial excavation position of the borehole investigation based on the coordinates where borehole investigation is conducted. Some physical property values are stored in the boring model as attribute information according to depth. To model the geologic longitudinal profile, first, a 3D central line model of the tunnel's route is created based on the road location coordinates from the tunnel planning process. Then, the geological longitudinal profiles are placed along the central line model of tunnel's route.

Secondly, on design process of Phase I tunnel, tunnel design process includes tunnel cross-section design drawings and detailed information such as lining concretes and rock bolts, which are determined based on the various geological conditions from investigation process. A 3D model of the tunnel is produced by creating a lining cross-section from the design drawings and stretching it along the central line model of the tunnel's route. Then, the tunnel 3D model stores the detailed information on the thickness of lining concrete, shotcrete, and tunnel invert at the design process as attribute information. In addition to the tunnel model, a rock bolt model is also created by tracing the rock bolt extension spacing along the central line model.

Thirdly, on construction process of Phase I tunnel, tunnel construction relies on the tunnel design information, but modifications are sometimes made based on deformation measurements and geological conditions encountered during the excavation process. As a result, the actual tunnel construction information, measurement data, and engineering sketches of the tunnel cutting face are all included in the tunnel construction process.

Information on the actual construction process and measurement data is integrated as attribute information into the 3D model of the tunnel created by the tunnel design process. Furthermore, an engineering sketch of the tunnel cutting face is placed on the central line model of the tunnel's route based on the distance from tunnel entrance.

Fourthly, on maintenance process of Phase I tunnel, tunnel maintenance procedures encompass traditional manual inspection reports, point cloud data from laser inspection, tunnel wall surface images from image inspection, and monitoring data such as road surface deformation. Initially, the 3D tunnel model, as created by the information on design process, is modified based on actual coordinates and position from tunnel point cloud data from laser inspection, and tunnel wall surface image layer is superimposed on that modified 3D tunnel model (Yasuda et al.,2020). Then, a line model is created to represent the degradation information, such as cracks, water leakage, and repair data using the inspection images. Crack width and history of crack occurrence and repair are integrated into this line model as attribute information. Traditional manual tunnel inspection reports and monitoring data are stored as attribute information in the 3D tunnel model.

Finally, on investigation to construction process of Phase II tunnel, the ongoing construction of Phase II tunnel adjacent to Phase I tunnel aims to alleviate highway traffic congestion. The CyberNATM system is employed in the construction process of Phase II tunnel to manage tunnel construction information (CyberNATM, 2023). Therefore, in this research, a comprehensive BIM/CIM model that can be used for the maintenance process of both Phase I and Phase II tunnels is created by adding the construction process information from the CyberNATM system, such as tunnel progress, measurement results, and tunnel cutting face images in real time based on location coordinates of each piece of information in the same way as the modeling of Phase I tunnel information. Each information model design and integrated model of each tunnel's construction production process is shown in Figure 2.

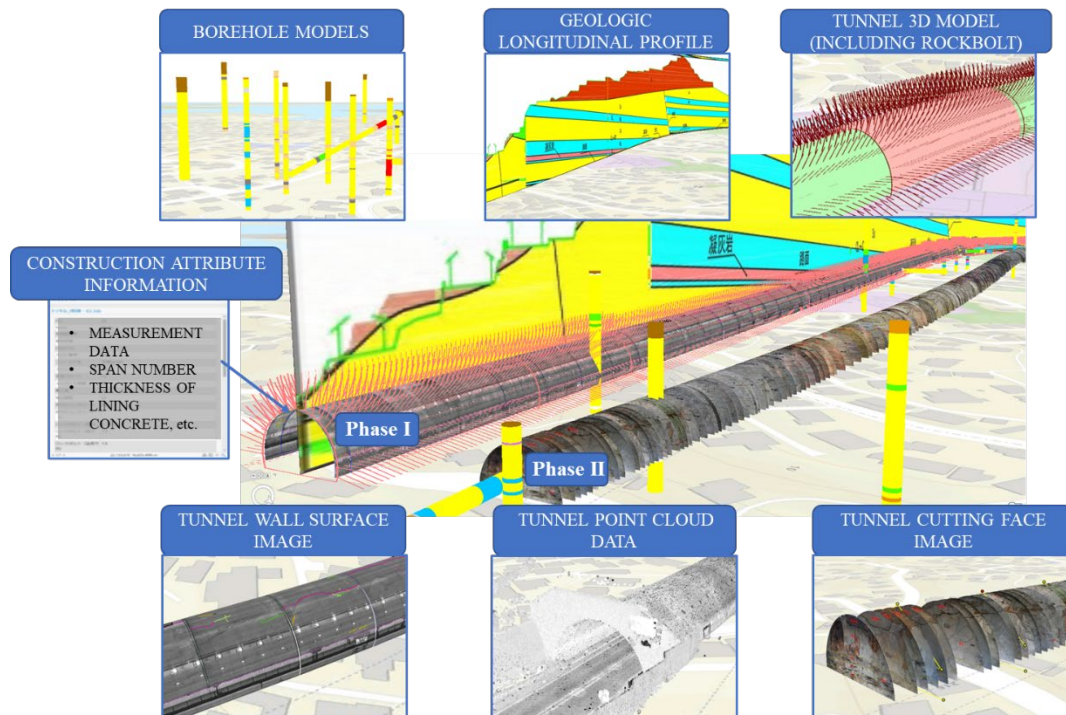


Figure 2. BIM/CIM design of tunnel construction production process on the ArcGIS Pro

2.2 3D Geological Modeling

3D geological model is created using borehole models from the investigation process, engineering sketch of tunnel cutting face from construction process, additional borehole models from the maintenance process of Phase I, and tunnel cutting face images information from construction process of Phase II integrated into the BIM/CIM model of the tunnel. To create a 3D geological model, point features are initially created at the geological boundary for the tunnel cutting face image. This construction process information pertains to Phase I and Phase II tunnels. Then, geological boundary layer model around tunnels is created in raster format by using kriging as a spatial interpolation method for these point features and borehole models of investigation information as shown in Figure 3. Finally, geological boundary layers in raster format are converted to TIN (triangulated irregular network), and each geologic boundary layer is combined three-dimensionally to create a 3D geological model by the extrude between tool of ArcGIS Pro as shown in Figure 4. Geological 3D model includes information on rock formations, geological structure, the attitude of rocks, and other information. In addition, tunnel geological

surface model is created by considering positional relationship between 3D geological model and tunnel 3D model from the design process information of Phase I tunnel.

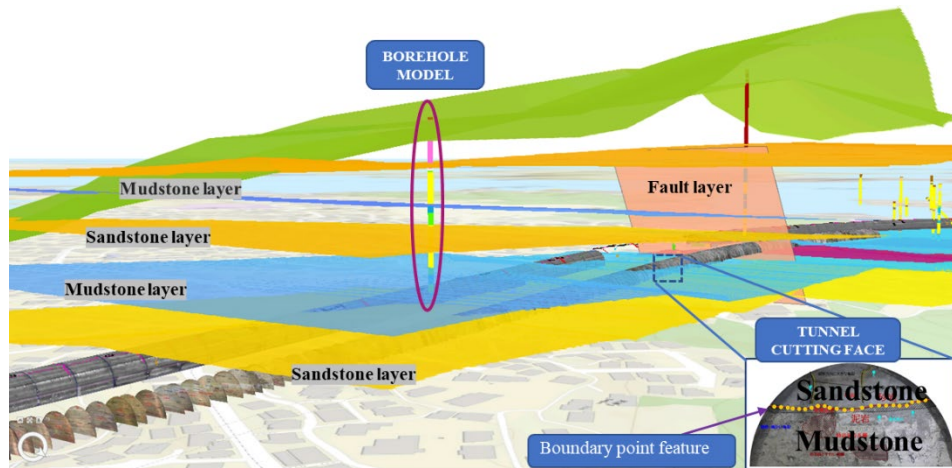


Figure 3. Geological boundary layer model from borehole models and tunnel cutting faces

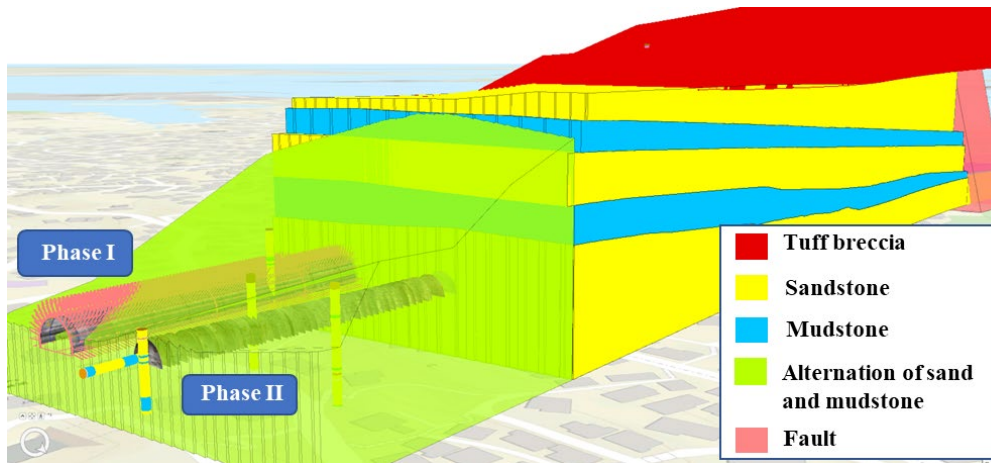


Figure 4. 3D geological model based geological boundary layer model

3. RESULTS

This research has enabled the lifecycle management of each stage of the tunnel construction production process through the creation of a comprehensive BIM/CIM model. It integrates and visualizes different types of information from each tunnel's construction production process in 3D space, using ArcGIS Pro. Then, that comprehensive BIM/CIM model has been used to create new information models which could be effectively used for maintenance process of Phase I tunnel.

Currently, deformations such as cracks and deformation of road surface have often been observed in the Phase I tunnel. Therefore, by using a BIM/CIM model of the tunnel construction, it is possible to determine the causes of cracks in the tunnel by considering many aspects such as location and history of cracks, progression, their actual length, direction, and surrounding geological conditions as shown in Figure 5. By way of illustration, the outcome of an analysis of a crack in a tunnel that extends throughout its length can be seen in Figure 6. This evaluation takes into account both the geological conditions of the surrounding area, as determined in the investigation process, and the crack line model recorded during the maintenance process. The result revealed that cracking near the sandstone-mudstone boundary is prone to occur.

In addition, by adding construction information of Phase II tunnel to the BIM/CIM model that was initially created for Phase I tunnel, a 3D geological model of tunnel's surroundings has been created, which enabled a spatial relationship between deformation area of road surface and surrounding geological conditions. In the past, the deformation of road surface was analyzed for deformation mechanism using only the results of monitoring from the maintenance process and a general 2D geological longitudinal profile of the tunnel. Therefore, in this research, it has been able to identify in 3D that the deformation area of road surface exists in a fault and there are surrounding mudstones and tuff stone that can be swelled by water and affect road surfaces as shown in Figure 7.

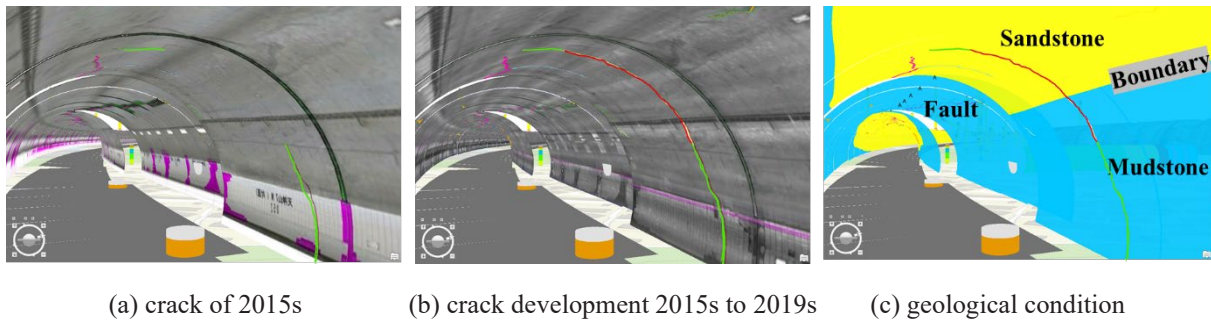


Figure 5. Digitalization of crack and inspection data

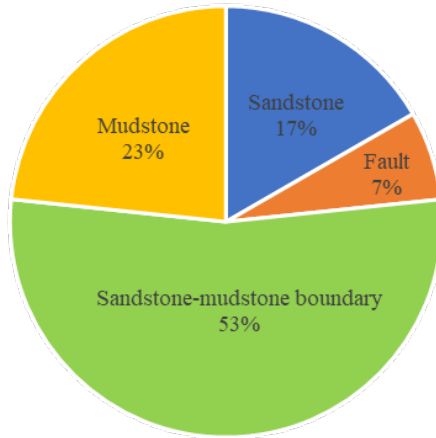


Figure 6. Percentage of crack progression relative to geological type

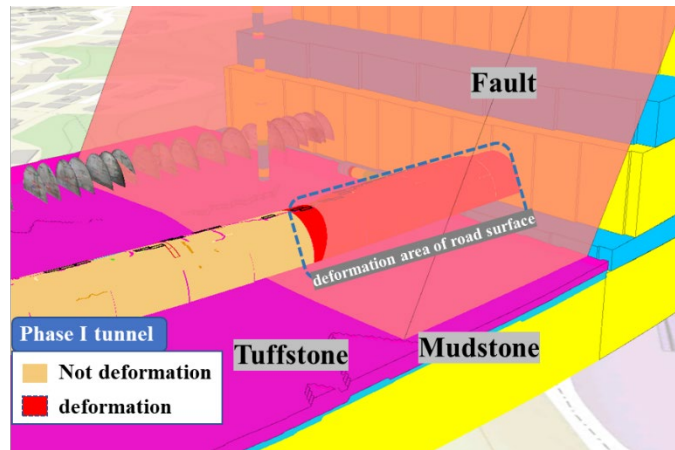


Figure 7. Surrounding geological condition of road surface's deformation area

4. DISCUSSIONS

This study presents two primary findings regarding the infrastructure construction production process: (1) Integration of different types information on each process of the infrastructure construction production process into centralized management in 3D space based on their location coordinates (focus on the method of creating BIM/CIM model); (2) By considering the spatial relationship of multiple pieces of information integrated into a BIM/CIM model, a new information model is created that can be effectively used in the construction production process of the target object. For example, for tunnel construction, a deformation model based on construction and inspection information, and a geological 3D model based on survey and construction information could be developed (focus on the effective use of integrated information).

Our research confirmed utility of GIS software approach for the tunnel's BIM/CIM model with visualization and other analysis tools. It indicates that the various information of tunnels which are managed in different forms and databases based on their location coordinates can be integrated and centralized by utilizing GIS. Furthermore, based on information integrated with this BIM/CIM model, geological prediction models, deformation models, etc. can be created using spatial analysis, modeling, and other tools in GIS software. Then, it has been possible to deformation analysis with spatial consideration of information on each process of the tunnel's whole construction production process. Acquiring analytical geological models and tunnel attribute information, physical property of geology, and monitoring information from BIM/CIM model in GIS can be used for other analysis software. The results of deformation and excavation construction processes arising from the analysis can be integrated into the BIM/CIM model, which enables BIM/CIM model to be linked with other analysis software for the tunnel construction production process as shown in Figure 8.

The study results reveal that by using the geological 3D model created in the tunnel BIM/CIM model, it is possible to understand the details of previously unknown geological conditions, which is useful for the construction process of the Phase II tunnel, including the selection of the construction method and the support design modifications during construction process. Furthermore, by adopting this BIM/CIM model, other construction processes: investigation, design, construction, and tunnel information (Phase II tunnel) have been also effectively utilized for tunnel maintenance (Phase I tunnel). In other words, in the maintenance process of Phase I tunnel, by simultaneously considering the progress of cracks and the surrounding geological condition, it becomes possible to provide a more specific indication of the causes of cracks and other deformation. Moreover, based on

the results of our deformation analysis, future inspection and repair methods for tunnel maintenance can be informed.

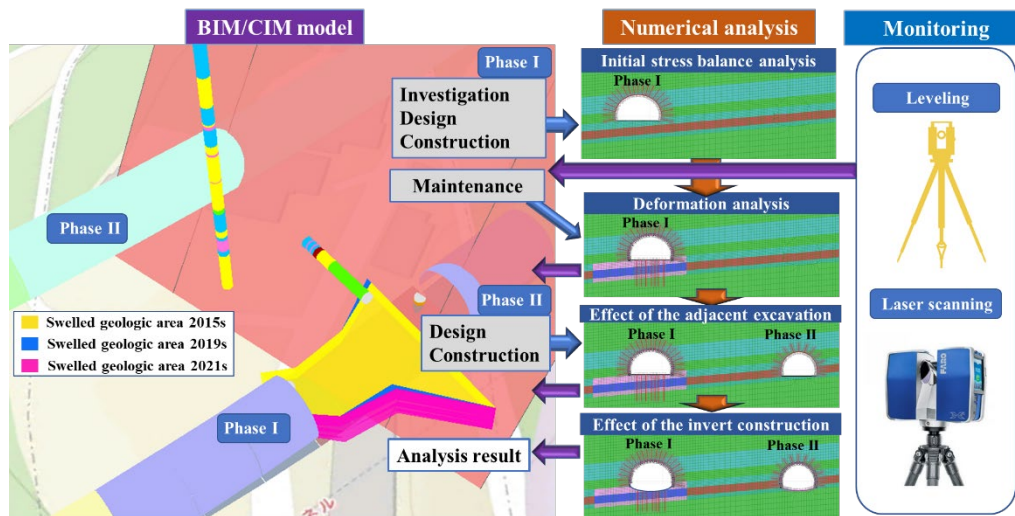


Figure 8. Utilization of BIM/CIM model in numerical analysis

5. CONCLUSIONS

This paper introduces a novel approach to tunnel construction using Building Information Modeling (BIM/CIM). This approach integrates information from each process of tunnel construction into a single platform for lifecycle management and advanced maintenance. The developed BIM/CIM model enables evaluation of cracks and deformations in tunnels not only from aspect of inspections in maintenance process, but also from multiple aspects using information from other processes of tunnel investigation, design, and construction. In other words, more effective maintenance is enabled by considering more accurate information on tunnel deformation, such as tunnel construction records and geological conditions surrounding tunnels.

In a case study of an existing tunnel (Phase I) and a newly constructing tunnel (Phase II) adjacent to Phase I, a comprehensive BIM/CIM model was developed using ArcGIS Pro. This model integrates various information from both Phase I and Phase II tunnels and can be used for the maintenance process of each tunnel. The results indicate that this BIM/CIM model enables effective use of construction process information from adjacent Phase II tunnel in addition to the information from other processes of Phase I tunnel for maintenance process. Such an approach enables effective planning of repairs for tunnel deformations and has advantages in terms of time and cost.

ACKNOWLEDGMENTS

We would like to express my deepest appreciation to the West Nippon Expressway Company for providing valuable data and cooperation in this research.

REFERENCES

- CyberNATM. (2023). ENZAN KOUBOU| ICT Solutions & automation for construction and civil engineering industry website : <https://www.enzan-k.com/eng/service/cybernatm.html>
- Hegemann, F., Stascheit, J., Maidl, U. (2020). As-Built documentation of segmental lining rings in the BIM representation of tunnels, *Tunneling and Underground Space Technology*, Vol. 106, pp.1-10.
- Sacks, R., Eastman, C., Lee, G., and Teicholz, P. (2018). BIM Handbook: A Guide to Building Information Modeling for Owners, Designer, Engineers, and Contractors (3rd ed.)
- Yamaoka, D., Aoyama, N., Kawano, K., Shigetaka, K., and Sekiya, H. (2016). Verification of how to create the CIM model of the bridge which assumed the use by the maintenance, *Journal of JSCE*, Vol. 72, pp.I_21-I_28
- Yasuda, T., Yamamoto, H., Enomoto, M., and Nitta, Y. (2020). Smart Tunnel Inspection and Assessment using Mobile Inspection Vehicle, Non-Contact Radar and AI, *37th International Symposium on Automation and Robotics in Construction*, pp.1373-1379.
- Yoshikai, K., Tsutsui, T., Takaguchi, H. (2018). Evaluation of design efficiency improvement by utilizing BIM by proceeding analysis, *J. Archit. Plan., AIJ*, Vol.83, pp.1297-1303.

A BUILDING INFORMATION MODEL FOR SENSING AND SIMULATION TOWARD NET-ZERO ENERGY BUILDING RENOVATION

Kazuya Matsuba¹, Nobuyoshi Yabuki², Tomohiro Fukuda³, and Yoshiro Hada⁴

1) Master Course Student, Division of Sustainable Energy and Environmental Engineering, Graduate School of Engineering, Osaka University, Suita, Japan. Email: matsuba@it.see.eng.osaka-u.ac.jp

2) Ph.D., Prof., Division of Sustainable Energy and Environmental Engineering, Graduate School of Engineering, Osaka University, Suita, Japan. Email: yabuki@see.eng.osaka-u.ac.jp

3) Ph.D., Assoc. Prof., Division of Sustainable Energy and Environmental Engineering, Graduate School of Engineering, Osaka University, Suita, Japan. Email: fukuda.tomohiro.see.eng@osaka-u.ac.jp

4) Dr. Eng., Principal Researcher, Heat and Wind Group, Institute of Technology, Tokyu Construction Co., Ltd. Email: hada.yoshiro@tokyu-cnst.co.jp

Abstract: Net-zero energy buildings (ZEBs) are expected to become more widespread as efforts proceed to promote carbon neutrality and energy conservation in the building sector. Means to transform buildings into ZEBs include optimizing energy operations by detecting energy waste through in-building sensing, and optimizing heating, ventilation, and air conditioning (HVAC) design by simulating the indoor environment at the design stage. In addition, building information modeling (BIM) is increasingly being used in the construction industry. Linking data measured by sensors with BIM is expected to visualize equipment usage and the indoor environment. Furthermore, using BIM data for simulation is expected to facilitate the simulation process. However, BIM data operations often depend on the type and capabilities of the BIM software, making them less versatile. Therefore, the Industry Foundation Classes (IFC) are deployed for interoperable data management. However, there are two challenges with sensors and simulations for IFC: First, the definition of compound sensors is not provided; second, IFC data for HVAC equipment cannot be used for indoor environment simulation. This research attempts to overcome both challenges by developing a new integrated IFC data model for BIM and sensors. The integrated IFC data model clearly shows the relationship between the BIM model and sensors. Furthermore, a generic representation of sensors is demonstrated by developing an IFC data model of a compound sensor. In addition, a new IFC data model for HVAC equipment is developed to enable the use of IFC data for HVAC equipment as input data for indoor environment simulation. Future work will use the IFC data model developed in this research to operate data measured by sensors and to perform simulations.

Keywords: Net-zero energy building, Building information modeling, Sensing, Indoor environment simulation, Industry Foundation Classes

1. INTRODUCTION

As efforts to introduce carbon neutrality and to reduce energy consumption in the building sector proceed, net-zero energy buildings (ZEBs), which aim to reduce the balance of energy consumed within the building to zero while achieving comfortable indoor environments, are expected to become widespread. Means to transform buildings into ZEBs include optimizing energy operations by detecting energy waste through in-building sensing (Zhong et al., 2023), and optimizing heating, ventilation, and air conditioning (HVAC) design by simulating the indoor environment at the design stage. In construction, the use of Building Information Modeling (BIM), in which data is shared and used centrally and efficiently by all stakeholders using a 3D building model with attribute information, is also advancing. Linking data measured by sensors with BIM is expected to visualize equipment usage and the indoor environment (Eftekhari et al., 2018). In addition, computational fluid dynamics (CFD), an analysis that automates mathematical principles to simulate aerodynamics, heat transfer, and turbulence on 3D models, is used to simulate indoor environments in buildings. The use of BIM data as input data for CFD analysis is expected to facilitate the analysis process (Lee et al., 2021). Although many studies have explored linking BIM and sensors (Zhang et al., 2022) and investigated BIM for indoor environment simulations (Kwok et al., 2020), the results have been largely dependent on the types and capabilities of BIM software, so limited versatility of BIM is a concern.

The organization buildingSMART International (bSI) has established Industry Foundation Classes (IFCs) as an international standard for BIM. IFC allows data conversions to and from various BIM software formats, thus enabling data operations that do not rely on specific BIM software. In addition, IFC data are represented by an object-oriented data model comprising associations between “entities,” and its open schema approach allows users to develop their own data models and add their own property sets within the scope of the specification (Yabuki et al., 2016; Zhang et al., 2021).

With these backgrounds in mind, this study had two objectives. The first was to demonstrate a generic representation of sensors in IFC by developing a new integrated IFC data model for BIM and sensors and creating a property set for sensors. The second was to develop a new IFC data model and create property sets for HVAC systems and use these IFC data for indoor environment simulation.

2. LITERATURE REVIEW

2.1 Research on IFC Sensors

Under IFC 4.3, the most recent IFC data specifications, an “IfcSensor” is an entity that represents a sensor, but it assumes a single-function sensor and does not indicate how to define compound sensors. Research has been conducted to determine how to extend IFC sensors in order to accommodate their use with IFC data. Rio et al. (2013) created new IFC property sets to represent and operationalize structural system sensors in the IFC. Eftekharirad et al. (2018) developed a new IFC data model to represent relations between sensors, occupants, and rooms in the IFC. Xu et al. (2022) managed sensor data by creating new IFC property sets representing sensor product information, positioning data, and so on. These studies created their own property sets to represent the sensors intended for use in the IFC, but they have not demonstrated a generic IFC representation applicable to the numerous existing sensor types. This study will solve the problem by developing an integrated IFC data model of BIM and sensors, which shows the relationship between the BIM model and sensors, creating the necessary property sets for the sensors, and also developing an IFC data model for compound sensors.

2.2 Research on the Relation between the IFC and Indoor Environment Simulations

Using geometry and attribute data in BIM models is expected to save significant time and effort in CFD model design and reduce data inconsistencies and human error (Lee et al., 2022). Studies on CFD analysis using IFC data have also been conducted. D’Amico et al. (2020) proposed new IFC property sets to represent the data needed for indoor air quality analysis. However, they did not indicate how to use the created IFC data for such analyses. O’Grady and Keane (2006) developed an application based on the IFC format to make CFD analysis more accessible to building designers. However, users must define and grant their own properties. Lee et al. (2022) presented a method for generating highly accurate CFD models using geometry and attribute data from IFC models. However, the attribute data only considered the insulation performance of walls and apertures, not the HVAC equipment. The present study demonstrates how to use IFC data for CFD analyses applicable to HVAC equipment by creating IFC property sets for air-conditioning vents and developing a data model to facilitate the use of air-conditioning vent data for CFD analysis.

3. DEVELOPMENT OF AN INTEGRATED IFC DATA MODEL FOR BIM AND SENSORS

3.1 Overview of the Model

We created an IFC data model integrating a BIM model and a sensor data model (Figure 1). The integrated data model can show relations between sensors and the BIM model, including which rooms the sensors are installed in, which components the sensors are installed on, and the correspondences between sensors and building equipment. In addition, we created a new property set that includes basic sensor information, detailed positioning data, installation information, and other attribute information necessary for representing the sensor in the BIM model. Table 1 shows the developed property set.

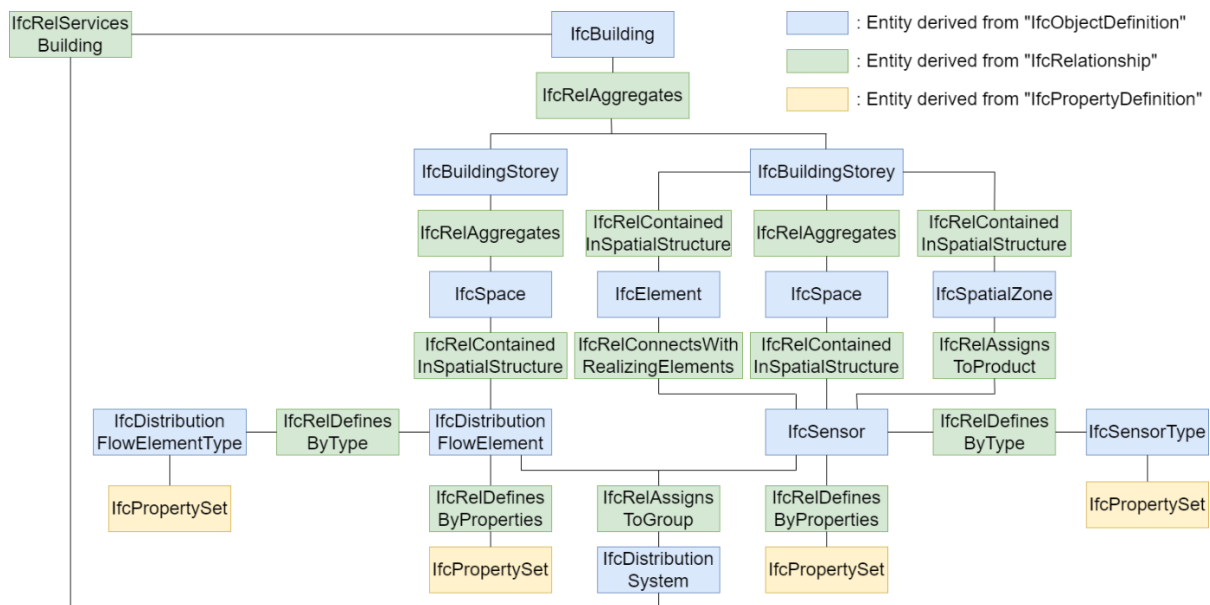


Figure 1. Integrated IFC data model for BIM and sensors

Table 1. Developed IFC property set for application to sensors

Property set name	Description
mPset_SensorInformation	Defines properties related to basic sensor information (ProductName, ModelNumber, etc.)
mPset_SensorPosition	Defines properties related to sensor location information (SensorID, InstallationMemberID, LengthFromSmallBaseLineX, etc.)
mPset_SensorInstallation	Defines properties related to sensor installation information (FasteningMethod, Information of measuring direction, etc.)
mPset_SensorOperation	Defines properties related to sensors' activity state (IsOperating, IsOutOfOrder)

However, we have found that the model may not work for some cases, such as compound sensors and some air-conditioning control vents. Therefore, we developed a new data model for compound sensors and air-conditioning control vents, as described in the following sections.

3.2 Development of a New IFC Data model for Compound Sensors

3.2.1 Property set for compound sensors

A compound sensor is a single sensing device that has multiple functions; for example, a temperature and humidity sensor would measure both temperature and humidity. The properties applicable to compound sensors can therefore be divided into two types. The first is properties like those in the property set shown in Table 1, which have only one value per sensor device, such as the product name, model number, or position coordinates. The second is properties with a number of values equal to the number of functions the sensor device has, such as accuracy or measurement range. A property set containing such properties is applied to compound sensors according to their number of functions. The property set name indicates the function. For example, in addition to the four property sets shown in Table 1, property sets named “mPset_SensorTypeTemperatureSensor” and “mPset_SensorTypeHumiditySensor” can be applied to temperature and humidity sensors. The property set specific to each sensor function includes four common properties: “MeasurementMethod,” “MeasurementRange,” “Accuracy,” and “Resolution,” and additional properties can be added as needed.

3.2.2 Data Model for Compound Sensors

Figure 2 shows the compound sensor data model developed for this study, using a temperature and humidity sensor as an example. In the data model for compound sensors, the “PredefinedType” value in the “IfcSensor” attribute is “USERDEFINED,” the “ObjectType” value is “COMPOUND SENSOR,” and the “Description” value is the function name (“Temperature, Humidity” for a temperature and humidity sensor). Here, we apply the property set described in Section 3.2.1.

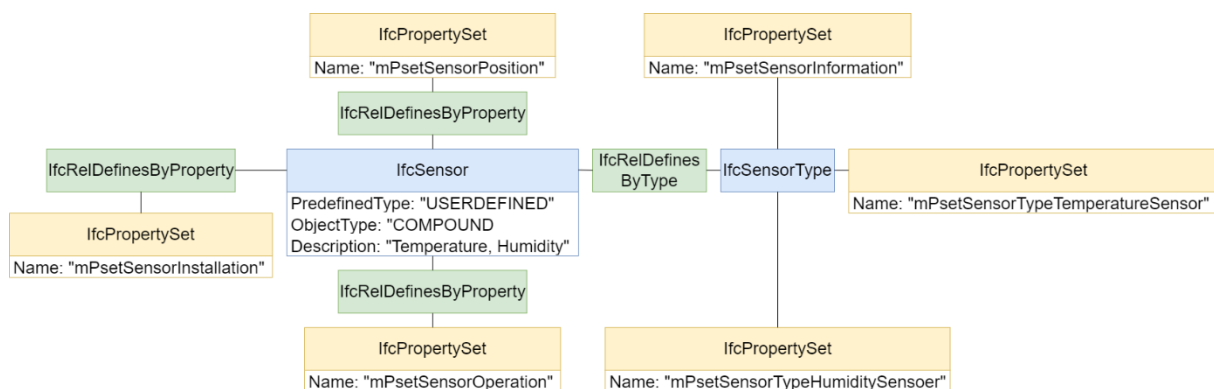


Figure 2. Data model for compound sensors (temperature and humidity sensor)

3.3 Development of a new IFC data model for air-conditioning control vents

3.3.1 Creation of property sets for air-conditioning control vents

IFC data for air-conditioning equipment are expected to be applied to boundary condition parameters for air outlets and inlets in CFD analysis. Therefore, in addition to the original role of BIM data as properties required as a building database, we created new IFC property sets for air-conditioning vents as properties for use in CFD analysis (Table 2).

Table 2. New IFC property set for air-conditioning vents

Property set name	Description
mPset_AirTerminalPosition	Defines properties related to air terminal location information (AirTerminalID, ConnectedAirConditionerID, LengthFromSmallBaseLineX, etc.)
mPset_AirOutletPerformance	Defines properties related to air outlet performance (AirVelocityVector, SupplyAirFlowRate, PerpendicularDistanceInCooling, etc.)
mPset_AirInletPerformance	Defines properties related to air inlet performance (FlowArea, OpeningRatio, ExhaustAirFlowRate, etc.)

3.3.2 Data Model for Air-conditioning Vents

Air-conditioning vents can be categorized into two types: those in which air is sent to or from an air-conditioning unit in the building via ducts, such as Anemo or nozzle types (the “duct-connected” type, below), and those integrated with the structure of the air-conditioning unit, such as the outlet of a four-way cassette-type indoor unit (the “air-conditioner-integrated” type, below). The IFC data specifications represent the former as “IfcAirTerminal,” and the latter, along with its air-conditioning unit, as “IfcUnitaryEquipment.” Because the entity applied in IFC differs depending on the category of the air-conditioning unit, it is impossible to collectively extract data related to air-conditioning units in IFC during CFD analysis. To illustrate this issue using IFC data models, Figure 3 shows conventionally operated IFC data models for air vents of the duct-connected and air-conditioner-integrated type.

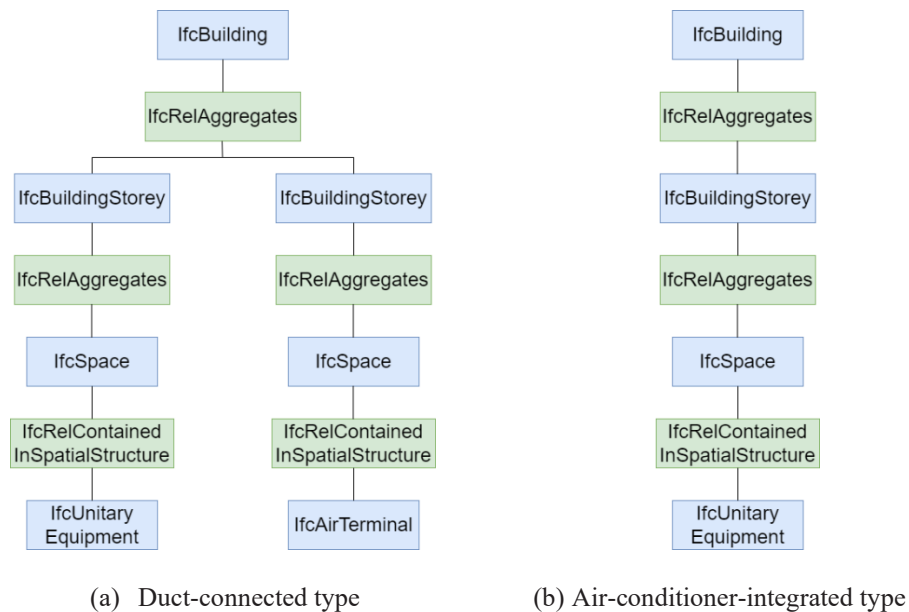


Figure 3. Conventional IFC data model for air-conditioning vents in operation

As shown in Figure 3a, “IfcAirTerminal” and “IfcUnitaryEquipment” are unconnected in the conventional data model for duct-connected vents, so the relation between each air-conditioning vent and the air-conditioning unit connected to it is not explicit. Therefore, in the data model created for this study (Figure 4a), we used “IfcDistributionSystem” to connect “IfcAirTerminal” and “IfcUnitaryEquipment” in order to show the relations between these systems. As shown in Figure 3b, the conventional data model for an air-conditioner-integrated vent cannot extract the air-control vent portion because it represents the entire indoor unit as a single entity. Therefore, in the data model created for this study (Figure 4b), air-conditioning vents are represented as “IfcAirTerminal” to allow batch extraction of air-conditioning vents regardless of their classification. In addition, we used “IfcGroup” to link “IfcAirTerminal” and “IfcUnitaryEquipment” in order to show that the indoor unit and the air vent are integrated. Furthermore, as with duct-connected air vents, “IfcDistributionSystem” represents relations in the equipment system. The bold font and bold line in Figure 4 indicate parts of the data model that have been modified from the conventional data model.

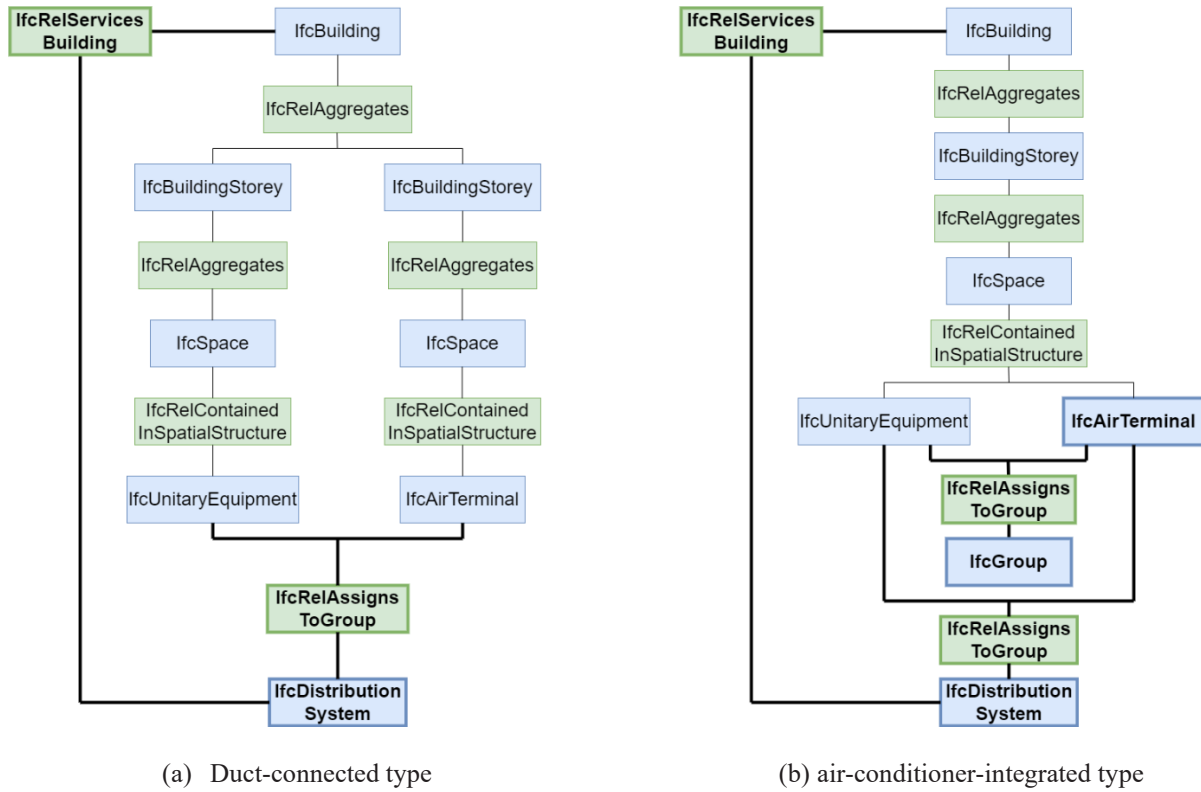


Figure 4. New IFC data model for air-conditioning vents

4. APPLICATION TO INPUT DATA CREATION FOR CFD ANALYSIS

Figure 5 shows the flow of CFD analysis using IFC data, as performed in this study. For BIM software, the BIM model is designed based on the data model presented in Section 3 and output to IFC data. Next is the process for generating a mesh for CFD analysis, using geometry data from IFC data and using the properties to generate boundary condition data for CFD analysis. The data model developed in this study allows data related to air-conditioning vents to be extracted from the BIM model in a single step, thereby facilitating the process shown in Figure 5.

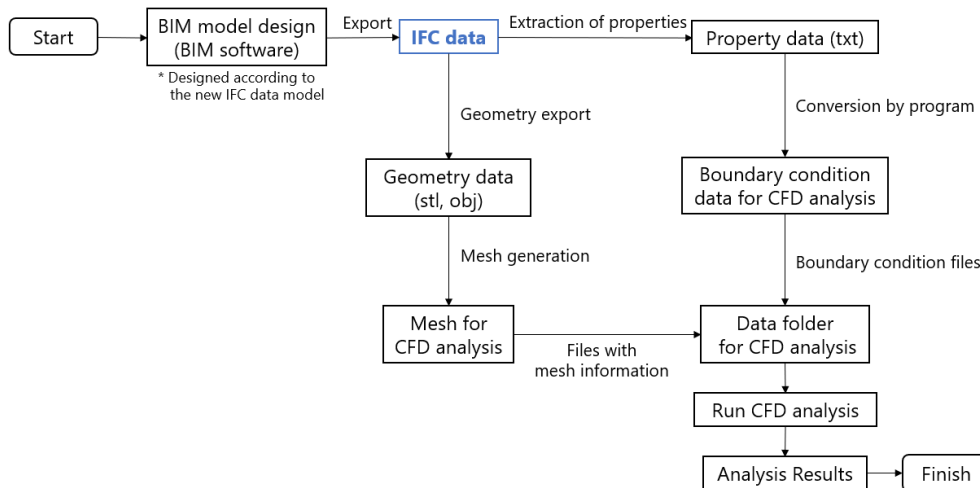


Figure 5. CFD analysis process using IFC data

4.1 Mesh Generation Using IFC Geometry Data

BIM models are not designed for CFD analysis, and their geometries are too complex and computationally expensive to perform CFD analysis. Therefore, research has been conducted with the aim of reducing analysis costs by simplifying BIM model geometries after converting them to CAD format (Porter et al., 2018; Utkucu et al., 2020). In the present study, we used the geometry of “IfcSpace,” an entity representing a specific building

space. Using the IfcSpace geometry simplifies geometries for walls and other complex shapes, and even if unwanted gaps exist in the BIM model due to design errors and the like, they will not interfere with the analysis.

For IFC geometry data, we used IfcConvert from the IfcOpenshell (IfcOpenshell, 2023), an open-source library for analyzing and editing IFC, to extract only the geometries of entities used in the analysis (e.g., the analysis space, air-conditioning vents, heat sources) and output them in the OBJ file format. Next, we use mesh-generation software to generate a mesh. The mesh used for CFD analysis must have boundary surfaces. By specifying the IFC entity and “Tag” of the member attribute as the boundary surface name in the “IfcSpace” geometry, we can link each boundary surface to IFC data, and the insulation performance of walls, floors, ceilings, and so on can be extracted from the IFC. Figure 6 shows the process for generating the mesh for CFD analysis.

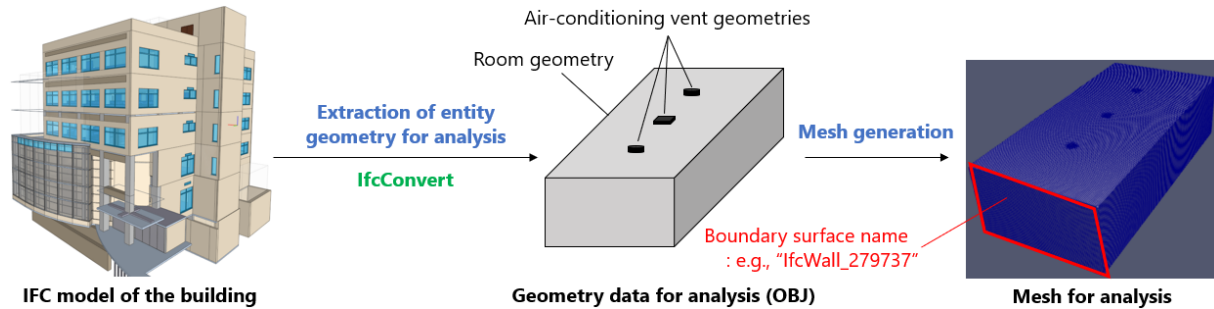


Figure 6. Mesh-generation process for CFD analysis of IFC geometry data

4.2 Use of IFC Properties for Boundary Condition Data

This study presents a method for obtaining from IFC properties parameters that can be defined as BIM attribute information in the boundary condition parameters of CFD analysis, including inflow/outflow conditions for air-conditioning vents and conditions related to the insulation performance of walls and windows. Table 3 lists the boundary condition parameters for which BIM attribute information values can be used and their corresponding IFC properties. The IFC properties shown in Table 3 include both properties defined in the existing IFC and those newly developed for this study.

Table 3. Correspondences between boundary condition parameters and IFC properties

Object	Parameter	Unit	IFC entity	IFC property (property set)
Air-conditioning vents	Inflow/outflow velocity vector	m/s	IfcAirTerminal	AirVelocityVector (mPset_AirOutletPerformance)
	Velocity normal to the surface	m/s	IfcAirTerminal	AirVelocityVector (mPset_AirOutletPerformance)
	Volumetric flow rate	m ³ /s	IfcAirTerminal	SupplyAirFlowRate (mPset_AirOutletPerformance)
Wall, window	Heat transfer coefficient	W/m ² *K	IfcWall, IfcWindow	ThermalTransmittance (Pset_WallCommon, Pset_WindowCommon)
Lighting equipment	Heat flux, Energy consumption	W/m ²	IfcLightFixture	HeatFlux (mPset_LightFixturePerformance)
System equipment	Heating value	W	IfcDistributionElement	NominalPowerConsumption (Pset_ElectricalDeviceCommon)

We used IfcOpenshell to extract IFC properties. IfcOpenshell is capable of extracting entity attributes. We used IfcOpenshell to extract “NominalValue,” which is an attribute of “IfcPropertySingleValue,” an entity representing an IFC property. The boundary condition file was generated as an arrangement using the extracted properties. As an example, the process of generating a boundary condition file by extracting property values related to the airflow rate applied to an air-conditioning vent is shown in Figure 7, along with the data structure of the IFC properties.

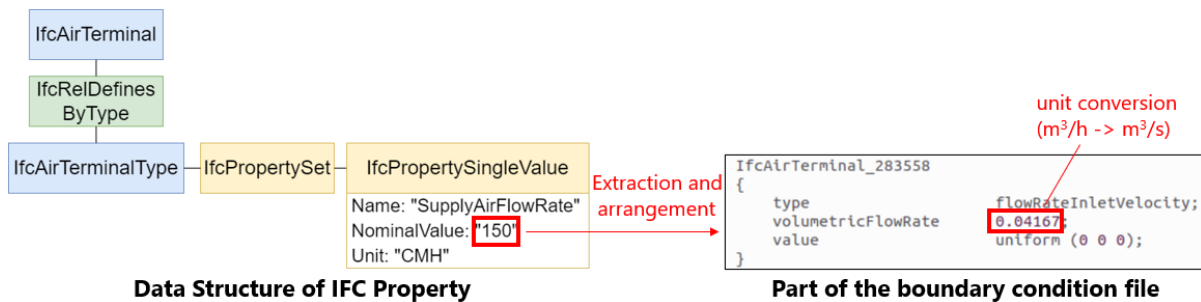


Figure 7. Process for using IFC properties to generate a boundary condition file

5. CONCLUSIONS

Given that strengthening the connections between BIM, sensing, and simulations will be essential for ZEB building conversions, in this study, we developed a new integrated IFC data model for BIM and sensors, and developed a new IFC data model for compound sensors, thereby demonstrating a generic method for representing sensors in IFC. In addition, we developed a new IFC data model for air-conditioning vents to enable centralized data extraction in the IFC, and we presented a method for CFD analysis using IFC data that includes data for HVAC equipment.

Future research will investigate the management of sensor-measured data in BIM by linking sensor-measured data with sensors in IFC data, generating a prototype system for CFD analysis using the IFC data presented in this study, and evaluating that analysis method.

REFERENCES

- D'Amico, A., Bergonzoni, G, Pini, A., and Currà, E. (2020). BIM for Healthy Buildings: An Integrated Approach of Architectural Design Based on IAQ Prediction, *Sustainability*, 12 (24), 1-31.
- Eftekharirad, R., Bakht, N.M., and Hammad, A. (2018). Extending IFC for Fire Emergency Real-Time Management Using Sensors and Occupant Information, *35th International Symposium on Automation and Robotics in Construction*, 985-992.
- IfcOpenShell. (2023). *IfcOpenShell - The open source IFC toolkit and geometry engine*. Retrieved from IfcOpenShell website: <https://ifcopenshell.org/index.html>
- Kwok, H.H.L., Cheng, J.C.P., Li, A.T.Y., Tong, J.C.K., and Lau, A.K.H. (2020). Multi-zone indoor CFD under limited information: An approach coupling solar analysis and BIM for improved accuracy, *Journal of Cleaner Production*, 244.
- Lee, M., Park, G., Jang, H., and Kim, C. (2021). Development of Building CFD Model Design Process Based on BIM, *Journal of Asian Architecture and Building Engineering*, 11 (2), 313-320.
- O'Grady, W., and Keane, M. (2006). Specification of an IFC based software, *Joint International Conference on Computing and Decision Making in Civil and Building Engineering*, 3627-3636.
- Porter, S., Tan, T., Wang, X., and Paree, V. (2018). LODOS - Going from BIM to CFD via CAD and model abstraction, *Automation in Construction*, 94, 85-92.
- Rio, J., Ferreira, B., and Martins, P.J. (2013). Expansion of IFC model with structural sensors, *Informes de la Construcción*, 65 (530), 219-228.
- Utkucu, D., and Sözer, H. (2020). Interoperability and data exchange within BIM platform to evaluate building energy performance and indoor comfort, *Automation in Construction*, 116.
- Xu, Z., Ran, Y., and Rao, Z. (2022). Design and integration of air pollutants monitoring system for emergency management in construction site based on BIM and edge computing, *Building and Environment*, 211.
- Yabuki, N., Lebegue, E., Gual, J., Shintani, T., and Zhantao, L. (2016). International Collaboration for Developing the Bridge Product Model "IFC-Bridge", *Joint International Conference on Computing and Decision Making in Civil and Building Engineering*, 1927-1936.
- Zhong, H., Guo, M., Wang, Y., and Wang, Z. (2023). Quantify the magnitude and energy impact of overcooling in a sub-tropical campus building, *Building and Environment*, 231.
- Zhang, S., and Wan, Y. (2022). Software for Mapping and Extraction of Building Land Remote Sensing Data Based on BIM and Sensor Technology, *Journal of Sensors*, 2022, 1-7.
- Zhang, Y., Xing, X., and Afari, A.F.M. (2021). Semantic IFC Data Model for Automatic Safety Risk Identification in Deep Excavation Projects, *Applied Sciences*, 11 (21).

A PROPERTY DATA SHARING METHOD OF BUILDING INFORMATION MODELS USING REMOTE AUGMENTED REALITY

Koji Yoshimura¹, Nobuyoshi Yabuki², and Tomohiro Fukuda³

1) Master Course Student, Division of Sustainable Energy and Environmental Engineering, Graduate School of Engineering, Osaka University, Suita, Japan. Email: yoshimura@it.see.eng.osaka-u.ac.jp

2) Ph.D., Prof., Division of Sustainable Energy and Environmental Engineering, Graduate School of Engineering, Osaka University, Suita, Japan. Email: yabuki@see.eng.osaka-u.ac.jp

3) Ph.D., Assoc. Prof., Division of Sustainable Energy and Environmental Engineering, Graduate School of Engineering, Osaka University, Suita, Japan. Email: fukuda.tomohiro.see.eng@osaka-u.ac.jp

Abstract: Building Information Modeling (BIM) is being promoted to increase efficiency in Architecture, Engineering, and Construction (AEC). Augmented Reality (AR) is also being used to display BIM models at sites. However, when property data is modified on AR devices, the modifications are not reflected in the BIM models so it takes time to transfer them to other phases. Furthermore, the technology for multiple geographically remote users to share information in an AR environment is limited. Therefore, the purpose of this research is to develop a property data sharing system that allows users to synchronously modify property data of BIM models in the AR environment, and automatically reflect the modifications into data files that are effective for collaboration with other phases. As a proposed method, first, property data and 3D models are extracted from BIM models and uploaded to the server. Next, users retrieve the specified models and property data from the server and display them correspondingly by a given ID using a developed application on AR devices. The property data modifications entered by users are reflected in the BIM models via the server. Finally, Industry Foundation Classes (IFC) files reflecting the modifications are exported. Construction Operations Building information exchange (COBie) data can also be modified on AR devices. These processes can be implemented simultaneously by multiple users using each AR device. The result of the verification shows it is possible to modify the property data of various BIM models in the AR environment and reflect them to BIM and IFC models. This research can improve the efficiency of data collaboration because property data modifications can be shared with other users among multiple phases in the AR environment. Future challenges include enabling users to modify the geometry of BIM models with other users in the AR environment to further accelerate information sharing.

Keywords: Building Information Modeling, Property data, Augmented Reality, Industry Foundation Classes, Construction Operations Building information exchange

1. INTRODUCTION

In the construction industry, the chronic shortage of labor has become a major problem, and there are concerns about the decline in the number of workers as well as the retirement of personnel with a wealth of knowledge and experience, known as veterans. In addition, many of Japan's civil engineering structures, such as bridges and tunnels, have been in continuous use since their completion during Japan's period of rapid economic growth, and their deterioration is becoming increasingly serious (Ministry of Land, Infrastructure, Transport and Tourism, 2020). To protect the safety of users, it is necessary to carry out urgent renewal work on these civil engineering structures in a planned way. However, revenue and labor shortages will make it difficult to accomplish renewal works completely in a timely manner.

To address these issues, the government has begun to introduce Building Information Modeling (BIM) into the construction industry. This is expected to speed up discussions by visualizing parts and materials, automate quantity calculations and clash detections, and improve the efficiency of process control and progress monitoring compared to the use of paper-based design plans and models in the past (Ministry of Land, Infrastructure, Transport and Tourism, 2023). In addition, to increase the efficiency of visualizing parts and materials in 3D models, there are increasing opportunities to display BIM models using Augmented Reality (AR). By displaying BIM models at specific locations on a construction site using AR, it is possible to confirm the completed image of the structure to be built at the actual scale and visualize invisible parts such as underground buried structures. Besides, by displaying the BIM model in AR and allowing users to view the model's property data, it is possible to easily obtain the necessary structural information. This will make it easier to understand the structure overview and construction flow, and further promote smooth information sharing and opinion exchange (Ren et al., 2016; Wang et al., 2013).

However, the problem is that the property data of BIM models displayed in AR can only be used within the AR device. Typically, when BIM models are displayed in AR, the 3D models and property data are extracted from the BIM software that created the model and imported into the 3D engine to create the AR environment. In other words, the property data exists only in a one-way data flow from the BIM software to the AR environment. Therefore, even if changes are made to property data in the AR device, these changes are not reflected in the BIM models (Alizadehsalehi et al., 2020; Ratajczak et al., 2019; Schiavi et al., 2022).

Another issue is the limited technology for multiple users in different geographic environments to share information through the AR environment. Most of the research on AR and BIM collaboration is mainly concerned with improving model visibility and operability, and these studies focus on the convenience of individual users, while not so much has been seen on data collaboration among multiple users and multiple devices in an AR environment. Therefore, when workers are geographically distributed, information cannot be transferred in the AR environment and means through other communication systems are used (Garbett et al., 2022; Tavares et al., 2019; Thabet et al., 2022).

It is true that more opportunities to visualize BIM models and property data with AR, in order to promote information sharing and opinion exchange, will make it easier to grasp the overview of the structure and construction flow. On the other hand, due to the problems mentioned above, even if users make changes to the property data in the AR environment, these changes cannot be reflected in the BIM models, nor can they be shared with other users in real time. In addition, it may take time and effort to communicate the changes not only between users within each phase of design, construction, and maintenance but also between each phase. These influences can reduce the efficiency of information sharing and opinion exchange and the productivity of the whole project, leading to delays in the construction schedule.

This research proposes a system that enables multiple users to synchronously modify property data while displaying BIM models in AR at each phase of design and construction, without being limited by geography. At the same time, the changes are automatically reflected in the BIM models and data files, which can be effectively linked to other phases, such as Industry Foundation Classes (IFC). With this system, when property data is modified in AR, the changes can be shared among users in real-time. In addition, because the changes are automatically reflected in various data files such as IFC, they can be quickly shared between the design, construction, and maintenance phases of the project (Wong et al., 2022). This is expected to improve the productivity and efficiency of the entire project, reduce construction time, and eliminate long hours of labor.

2. PROPOSED METHOD

An overview of the proposed method is shown in Figure 1. In this research, the device used by users to visualize the 3D models and property data by AR is called the AR device, the PC that extracts the 3D models and property data from the BIM models and reflects the changes is called the local PC, and the server that connects the local PC and the AR devices and has a database is called the remote server.

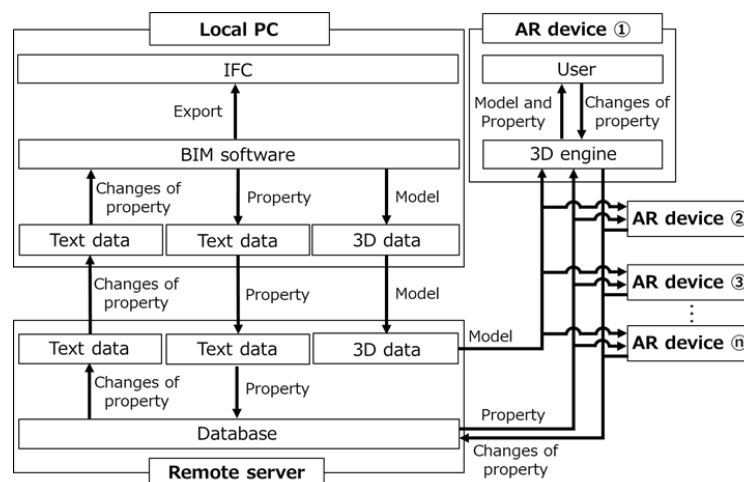


Figure 1. Overview of the proposed method

Users use the 3D engine on the AR device to obtain the 3D model and property data of the specified BIM model from the remote server. When the model is displayed in AR and the user selects a component on the AR device, the property data corresponding to that component is displayed on the screen by its ID set in the BIM software. Then, the changes in the property data entered by the user on the AR device are sent to the remote server.

The remote server acquires the text data containing the property data sent from the local PC and the property data modifications sent from the AR device and reflects them in the database. The modified property data in the database is immediately exported as text data and sent to the local PC.

Once the local PC receives the text data, it is imported into the BIM software. The BIM software uses the file name and the text to determine which property data of which components of which models have been modified, and the data is reflected in the BIM model as property data accordingly. Finally, when the changes are reflected in the BIM model, the type of each property data, such as instance parameter or type parameter, is determined, and the IFC model is exported with the appropriate property set.

3. PROTOTYPE SYSTEM IMPLEMENTATION

The processing of this system takes place at the AR device, the remote server, and the local PC. The process of acquiring the 3D models and property data from the remote server and sending the changes to the remote server on the AR device was developed in C# using Unity as the platform. The process of displaying the models in AR was developed using ARCore, an augmented reality application developed by Google.

A free rental server, StarServerFree, was used for the remote server. And MySQL, an open-source relational database, was used as the database for storing property data. In addition, MySQL, which is a standard feature of StarServerFree, was used in this system, and the process of reflecting property data in MySQL and extracting property data of a specific model from MySQL was developed using the PHP language. These PHP processes are executed in response to requests from Unity on the AR device.

The BIM software on the local PC was Revit provided by Autodesk. The process of extracting the 3D models and property data of the BIM models from Revit and the process of reflecting the modified property data were developed using Dynamo, a visual programming system. The programming language used in Dynamo is Python. The program of sending the extracted 3D models and property data to the remote server and the program of retrieving the property data modifications from the remote server were developed in C# using Unity on the local PC as the platform.

The libraries, software, and services used in the development and implementation of this system are listed in Table 1. The flowchart of the implemented prototype system is shown in Figure 2. In addition, Internet connections are established between the AR device and the remote server and between the remote server and the local PC using UnityWebRequest programmed in Unity.

Table 1. The libraries, software, and services used in the prototype system

Name, Version	Outline	Purpose
Unity 2020.3.7f1	3D engine	Transmission and acquisition of 3D models and property data
ARCore	AR application	Displaying AR of 3D models
StarServerFree	Remote server	Keeping 3D model and property data files and PHP scripts
MySQL	Database	Keeping property data
Revit2022	BIM software	Opening BIM model
Dynamo	Visual programming	Extracting 3D models and property data from BIM models in Revit, and reflecting changes in property data

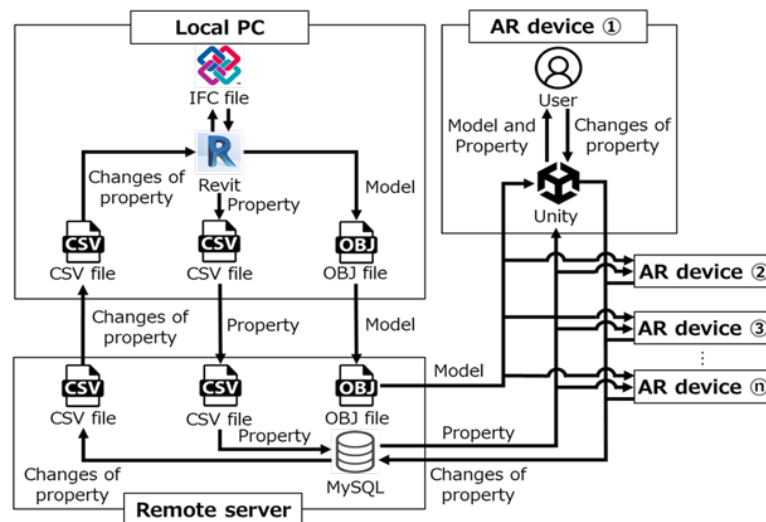


Figure 2. Overall flow chart of the prototype system

Finally, details of the devices used for the prototype system are shown in Table 2. The desktop PC in Table 2 was used as the local PC, and the smartphone was used as the AR device. The AR device and the remote server, and the local PC and the remote server were connected via the wireless LAN shown in Table 2.

Table 2. Details of the devices used for verification

Type	Product name	Item	Name
Desktop PC	Z270-S01	OS	Windows 10 Education
		CPU	Intel Core i5-7400CPU@ 3.00GHz
		RAM	16GB
		GPU	NVIDIA GeForce GTX 1060
Smartphone	Google Pixel 2	OS	Android 11
		CPU	Qualcomm Adreno 540, 710MHz
		RAM	4GB
		Camera	Built-In
Network equipment (Wireless LAN access point)	BUFFALO AirStation Pro WAPM-1166D	Transfer speed	IEEE802.11ac: Max 866Mbps IEEE802.11n: Max 300Mbps IEEE802.11a: Max 54Mbps IEEE802.11g: Max 54Mbps IEEE802.11b: Max 11Mbps
		Interfaces	2.4GHz and 5GHz

4. VALIDATION OF THE PROPOSED METHOD

In this chapter, the implemented prototype system is used with a model to validate the proposed method. Specifically, the property data and the Construction Operations Building Information Exchange (COBie) data of a pier model are shown along with images. In addition, examples of strings that did not reflect the changes in the BIM models are shown.

4.1 Verification of Pier Model Property Data

In this verification, a pier model of an elevated bridge was used. This model was used in an expressway construction project in Japan. The Revit model of the pier is shown in Figure 3. Note that the property data changed in the validation were not used in the actual project but are all hypothetical contents.

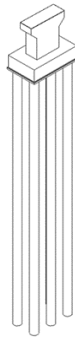


Figure 3. The Revit model of the pier

When any component of the 3D model displayed in AR on the device is selected, the corresponding property data is displayed on the screen according to the given ID. In this way, the 3D model and property data can be compared and viewed. After viewing the 3D model and the property data, and finding the property data that needs to be changed, the user enters the changes on the AR device. The changes are reflected in the database on the remote server. Therefore, they can be viewed not only on the device where the changes were entered but also on other users' AR devices at the same time.

The 3D model and property data displayed on the AR device when a component called “footing” of the pier model is selected is shown in Figure 4. From this, users can recognize that the “elementID” of this component is “148243” and the “Design_strength_of_concrete” is “25N/mm²”. In this verification, the “Design_strength_of_concrete” has been changed from “25N/mm²” to “30N/mm²” to increase the strength of the component whose “elementID” is “148243”. In addition, a property data item named “contractor” has been added and the item of the component whose “elementID” is “148243” has been set to “A_construction_company”. The data changes on the AR device are shown in Figure 5.



Figure 4. AR device screen when selecting the footing of the model

elementID	Design_strength_of_concrete	Object_classification	elementID	Design_strength_of_concrete	Object_classification	contractor
147198		foundation_crushed_stone	147198		foundation_crushed_stone	
148033	25N/mm2	cast-in-place_pile	148033	25N/mm2	cast-in-place_pile	
148114	18N/mm2	levelling_concrete	148114	18N/mm2	levelling_concrete	
148243	25N/mm2	footing	148243	30N/mm2	footing	A construction company

Figure 5. AR device screen before and after changing property data (left: before, right: after)

The modified or added property data is reflected in the Revit model on the local PC via the remote server. The property data items added to the Revit model are automatically appended to the appropriate location in the text file for proper mapping to the IFC objects. When the text file is read, the IFC model is exported with the property data changes and newly added items. The property data of the Revit model before and after changing is shown in Figure 6 and the IFC model is shown in Figure 7.

Text		Text	
IFCExportAs	IfcBridgePart	IFCExportAs	IfcBridgePart
id	Bri001-AC01-006	id	Bri001-AC01-006
Object_classification	footing	Object_classification	footing
Discriminant_information	Kusozu_elevated_bridge_P2_pier_f...	Discriminant_information	Kusozu_elevated_bridge_P2_pier_f...
Standard_of_reinforcing_bar	SD345	Standard_of_reinforcing_bar	SD345
Design_strength_of_concrete	25N/mm2	Design_strength_of_concrete	30N/mm2
		contractor	A_construction_company

Figure 6. The property data of the Revit model before and after changing (Left: before, Right: after)

Y_Pset		Y_Pset	
Design_strength_of_concrete	25N/mm2	contractor	A_construction_company
ID	Bri001-AC01-006	Design_strength_of_concrete	30N/mm2
IFCExportAs	IfcBridgePart	ID	Bri001-AC01-006
Object_classification	footing	IFCExportAs	IfcBridgePart
Standard_of_reinforcing_bar	SD345	Object_classification	footing
		Standard_of_reinforcing_bar	SD345

Figure 7. The property data of the IFC model before and after changing (Left: before, Right: after)

From Figure 6 and 7, it can be seen that “Design_strength_of_concrete” has been changed from “25N/mm2” to “30N/mm2” and “contractor” has been added and its property data has been changed to “A_construction_company” in both the Revit model and the IFC model.

4.2 Verification of Pier Model COBie Data

This section shows the verification of the modification of the COBie data in the property data of the pier model used in 3.1, together with the images. In order to handle COBie data in Revit, a function called Autodesk Cobie Extension for Revit was installed in Revit (Autodesk, 2023) in advance. This extension allows COBie data to be handled as property data in the Revit model. In addition, the COBie data can be exported as a spreadsheet.

The “COBie.CreatedOn” of the component identified in 3.1 whose “elementID” is “148243” has been changed from “2022/11/27” to “2023/01/11” on the AR device to change the completion date of this component. The data change on the AR device is shown in Figure 8. The changed COBie data is reflected in the Revit model on the local PC via the remote server. In addition, the COBie data changed on the AR device is automatically overwritten in the spreadsheet containing the COBie data on the local PC. The property data of the Revit model before and after changing is shown in Figure 9, and the spreadsheet is shown in Figure 10.

elementID	COBie_CreatedOn	COBie Component Description	COBie_CreatedBy	elementID	COBie_CreatedOn	COBie Component Description	COBie_CreatedBy
147198	2022/11/27	Bri001-AC01-003	chocolatecocoa6492@gmail.com	147198	2022/11/27	Bri001-AC01-003	chocolatecocoa6492@gmail.com
148033	2022/11/27	Bri001-AC01-005	chocolatecocoa6492@gmail.com	148033	2022/11/27	Bri001-AC01-005	chocolatecocoa6492@gmail.com
148114	2022/11/27	Bri001-AC01-004	chocolatecocoa6492@gmail.com	148114	2022/11/27	Bri001-AC01-004	chocolatecocoa6492@gmail.com
148243	2022/11/28	Bri001-AC01-006	chocolatecocoa6492@gmail.com	148243	2023/01/11	Bri001-AC01-006	chocolatecocoa6492@gmail.com

Figure 8. AR device screen before and after changing COBie data (left: before, right: after)

Data		Data	
COBie	<input checked="" type="checkbox"/>	COBie	<input checked="" type="checkbox"/>
COBie.ExternalIdentifier	なし	COBie.ExternalIdentifier	なし
COBie.CreatedBy	chocolatecocoa6492@gmail.com	COBie.CreatedBy	chocolatecocoa6492@gmail.com
COBie.CreatedOn	2022/11/28	COBie.CreatedOn	2023/01/11
COBie.Component.Name	Kusozu_elevated_bridge_P2_pier	COBie.Component.Name	Kusozu_elevated_bridge_P2_pier
COBie.Component.Space	n/a	COBie.Component.Space	n/a
COBie.Component.Description	Bri001-AC01-006	COBie.Component.Description	Bri001-AC01-006

Figure 9. The COBie data of the Revit model before and after changing (left: before, right: after)

CreatedOn	Type Name	Description	CreatedOn	Type Name	Description
2022/11/27	foundation_crushed_stone	Bri001-AC01-003	2022/11/27	foundation_crushed_stone	Bri001-AC01-003
2022/11/27	cast-in-place_pile	Bri001-AC01-005	2022/11/27	cast-in-place_pile	Bri001-AC01-005
2022/11/27	levelling_concrete	Bri001-AC01-004	2022/11/27	levelling_concrete	Bri001-AC01-004
2023/1/11	footing	Bri001-AC01-006	2023/11/28	footing	Bri001-AC01-006
2022/11/27	column_part	Bri001-AC01-002	2022/11/27	column_part	Bri001-AC01-002
2022/11/27	beam_part	Bri001-AC01-001	2022/11/27	beam_part	Bri001-AC01-001

Figure 10. The COBie data of the spreadsheet before and after changing (left: before, right: after)

4.3 Property Data That Cannot be Reflected in the Model

In this prototype system, it was found that property data changes entered at the AR device may not be reflected correctly in the BIM model due to the following factors.

The first is the use of CSV files. CSV files are text files in which each data item is separated by commas. Therefore, if there is a comma in a single property data string, the property data will be split, and the BIM model will not be able to properly reflect the property data.

The second issue is the data type of the property data in the BIM model. The property data of the BIM model can contain a variety of strings, but the BIM software must be preconfigured with a data type that matches the string. This prototype system does not have a feature that allows the user to freely change this data type, and was designed with the data type of all property data set to “Text”. Therefore, if a string of only integers is entered, that property data will not be reflected in the BIM model.

Third, there is an issue with the output from MySQL to text data. When property data changes are extracted from MySQL to a CSV file, if there are spaces in the property data, the string is enclosed in double quotes.

Table 3 shows examples of property data that are not correctly reflected in the BIM model, reasons for the problems, and examples of modifications that can be made to correctly reflect the property data in the BIM model.

Table 3. Examples of property data whose changes are not properly reflected and examples of modifications to those property data

Examples of incorrect reflection	Reasons not reflected	Examples of modifications
Koji,Yoshimura	Containing a comma	KojiYoshimura
30	Only numbers	30N/mm ²
2022,10,03	Containing commas	2022/10/03
the elevated bridge	Containing spaces	the_elevated_bridge
Maintenance day, 10/03	Containing commas and spaces	Maintenance_day_10/03

5. DISCUSSION

First, verification using the prototype system confirmed that property data modified in the AR environment can be automatically reflected in BIM models and IFC models. By using this system, the modified property data can be immediately shared with other site workers, office workers, and users from other businesses or phases when the model is displayed in the field for landscape and shape verification in the design phase, or for correcting schedule delays and errors in the construction phase. This is expected to reduce construction time.

However, in this prototype system, the IFC entity to which property data is assigned is unified to “IfcProduct”. Therefore, property data changes could be reflected in all IFC objects, but detailed settings, such as the user's intention not to reflect them in certain objects, are not possible. In order to output more flexible IFC models in the future, it is necessary to allow users to select IFC entities.

Second, from 3.3, it was found that when property data is reflected in the BIM model, it may not be reflected correctly due to commas, spaces, or strings that do not match the data type. However, the prototype system is designed to log property data before and after changing and send emails with the same contents to all concerned. This is expected to allow the original property data to be restored by referring to the log, even if unintended changes are reflected in the BIM model. In addition, this logging system records not only the contents before and after the change but also the name of the modifier and the date and time of the modification. This will play a significant role in ensuring data consistency and clarifying where responsibility lies if there are collaborators.

The email sent when property data changed, which is not reflected in the BIM model is shown in Figure 11. This email indicates that the user named Yoshimura wanted to change “Design_strength_of_Concrete” from “25N/mm²” to “30N/mm²”.

Modifier: yoshimura
 Date: 03/01/2023, 12:13:57
 Device Name: DT-16
 Target: Kusoze_elevated_bridge_P2_pier_instance
 Contents: Changed [Design_strength_of_concrete] of [148243] from [25N/mm2] to [30]

Figure 11. Emails sent to concerned persons informing them of the changes

Third, in this study, the pier model created in Revit was used to verify the proposed method. Although only the pier model is mentioned in the text, it has been confirmed that property data of piping models, one of the building elements, is also able to be shared between the AR environment and the BIM models in this system. However, there are various types of BIM models, including terrain models, geology and soil models, linear models, earthwork shape models, structure models, and integrated models that combine these models. To make data exchange more efficient in an AR environment, the system needs to be compatible with those BIM models as well.

On the other hand, Revit can import IFC models and their property data. This allows various BIM models created in other software to be imported into Revit via IFC files and their property data to be modified in the proposed method. For example, a linear model created in Civil 3D and exported to an IFC model could be supported in this system.

6. CONCLUSIONS

In this research, a method was proposed to enable property data modifications of BIM models on an AR system using a mobile device and to speed up the sharing of such modifications among users. The proposed method connects AR devices and local PCs to remote servers via the Internet and automatically reflects property data modifications in BIM models and IFC models. In addition, a prototype system was implemented to verify the proposed method. The following points were clarified through the verification.

- Property data modifications of each model are appropriately reflected in the BIM models and the IFC models.
- Not only property data, but also COBie data can be modified in the AR environment.
- Some strings cannot be properly reflected as property data in the BIM and IFC models.
- Because the IFC object to which the property data is assigned is unified into a single entity, it is not possible for users to intentionally not reflect the changes in a particular object.

Therefore, when the model is displayed in the field using AR, it is possible to modify the property data of the BIM model in the AR environment if there is an Internet environment, and these modifications can be automatically shared with other site workers and office staff, as well as users in other phases or businesses. This is expected to increase the efficiency and speed of data linkage.

Several prospects are mentioned. First, to build a more versatile system, various data formats and IFC entities should be able to be specified by users. Second, to make the system easily accessible to a wider range of users, the proposed method can be developed as a web system that does not require the installation of an application on the device and can be easily updated. Finally, the proposed method and the prototype system in this research do not allow users to change the shape of the 3D model while displaying the model in AR. If a method can be found that allows users to change the shape of a model synchronously with other users in an AR environment, information sharing will be accelerated.

REFERENCES

- Alizadehsalehi, S., Hadavi, A., and Huang, J.C. (2020). From BIM to extended reality in AEC industry, *Automation in Construction*, 116, 103254.
- Autodesk. (2023). *Autodesk COBie extension for Revit*. Retrieved from Autodesk website: <https://interoperability.autodesk.com/cobieextensionrevit.php>
- Garbett, J., Hartley, T., and Heesom, D. (2022). A multi-user collaborative BIM-AR system to support design and construction, *Automation in Construction*, 122, 103487.
- Ministry of Land, Infrastructure, Transport and Tourism. (2020). *Summary of the white paper on land, infrastructure, transport and tourism in Japan, 2020*. Retrieved from Ministry of Land, Infrastructure, Transport and Tourism website: <https://www.mlit.go.jp/hakusyo/mlit/r01/hakusho/r02/pdf/English%20Summary.pdf>
- Ministry of Land, Infrastructure, Transport and Tourism. (2023). *BIM/CIM Portal Site*. Retrieved from Ministry of Land, Infrastructure, Transport and Tourism website: <http://www.nilim.go.jp/lab/qbg/bimcim/bimcimindex.html>
- Ratajczak, J., Riedl, M., and Matt, D.T. (2019). BIM-based and AR Application Combined with Location-Based Management System for the Improvement of the Construction Performance, *Buildings*, 9 (5), 118.
- Ren, J., Liu, Y., and Ruan, Z. (2016). Architecture in an Age of Augmented Reality: Applications and Practices for Mobile Intelligence BIM-based AR in the Entire Lifecycle, *International Conference on Electronic Information Technology and Intellectualization*, 978-1-60595-364-9, 664-674.
- Schiavi, B., Havard, V., Beddiar, K., and Baudry, D. (2022). BIM data flow architecture with AR/VR technologies: Use cases in architecture, engineering and construction, *Automation in Construction*, 134, 104054.
- Tavares, P., Costa, C.M., Rocha, L., Malaca, P., Costa, P., Moreira, A.P., Sousa, A., and Veiga, G. (2019). Collaborative Welding System using BIM for Robotic Reprogramming and Spatial Augmented Reality, *Automation in Construction*, 106, 102825.
- Thabet, W., Lucas, J., and Srinivasan, S. (2022). Linking life cycle BIM data to facility management system using Revit Dynamo, *Organization, Technology and Management in Construction*, 14 (1), 2539-2558.
- Wang, X., Love, P.E.D., Kim, M., Park, C., Sing, C., and Hou, L. (2013). A conceptual framework for integrating building information modeling with augmented reality, *Automation in Construction*, 34, 37-44.
- Wong, M.O. and Lee, S. (2022). IFC-based information exchange for multi-agency response to indoor fire emergencies, *Automation in Construction*, 144, 104623.

"TO BIM OR NOT TO BIM": A SIMULATION GAME FOR TEACHING AEC STUDENTS THE KEY MECHANISMS IN PROJECT DELIVERY

Yun-Tsui Chang¹, Aritra Pal², Tzong-Hann Wu³ and Shang-Hsien Hsieh⁴

1) Ph.D. Candidate, Department of Civil Engineering, Faculty of Engineering, National Taiwan University, Taipei, Taiwan. Email: ytchang@caece.net

2) Ph.D. Candidate, Department of Civil Engineering, Faculty of Engineering, National Taiwan University, Taipei, Taiwan. Email: apal@caece.net

3) Ph.D., Post-Doc Researcher, Department of Civil Engineering, Faculty of Engineering, National Taiwan University, Taipei, Taiwan. Email: tzonghannwu@ntu.edu.tw

4) D. Eng., Prof., Department of Civil Engineering, Faculty of Engineering, National Taiwan University, Taipei, Taiwan. Email: shhsieh@ntu.edu.tw

Abstract: Architecture, Engineering, and Construction (AEC) projects face various opportunities, challenges, and risks when adopting different information management technologies and collaboration strategies among stakeholders. Considerations for adopting new information management technologies go beyond the technical requirements. They are also related to the business value and culture of different stakeholders, the trust between them, the project delivery models, and so on. University students often face difficulties understanding the multifold considerations held by various project stakeholders in adopting different information management technologies, the complex relationships between stakeholders, and the diverse AEC project delivery models through didactic lecture-based teaching. A simulation game was designed and embedded in the course "BIM Technology & Application" offered by the Department of Civil Engineering at National Taiwan University to help students understand the actual AEC project delivery process.

Keywords: AEC education, Classroom teaching, Simulation game, Project delivery model

1. INTRODUCTION

Delivering Architectural, Engineering, and Construction (AEC) projects can be challenging since they involve collaboration between various stakeholders and intense information management between them (Zhang & Wang, 2009). Unfortunately, traditional paradigms and information management technologies for AEC project delivery often result in poor performance since they frequently lead to limited collaboration and inadequate interoperability (Franz et al., 2017). Thus, Alternative Project Delivery Methods (APDMs) such as Integrated Project Delivery (IPD) and information management technologies such as Building Information Modeling (BIM) have drawn much attention from the AEC industry and academia recently because of their potential to improve AEC project delivery (Aldossari et al., 2021; Gu & London, 2010). As a result, universities worldwide have also started integrating these new concepts and skills into their curriculum for AEC students (Chegu Badrinath et al., 2016; Solnosky et al., 2014). However, one of the main barriers to this integration identified by the educationalists is that they are primarily taught in traditional ways, failing to provide students with opportunities to experience and explore the relationships between project stakeholders, the differences between project delivery methods, and the roles of information management technologies (Hedayati et al., 2015; Mills & MacDonald, 2013).

Simulation games have been used for AEC education since the 1990s (Rounds et al., 1986, Veshosky, & Egbers, 1991). These games are mostly designed for the students to understand the roles of construction managers. The roles of other parties in the AEC projects are little addressed. Later, more simulation games are developed to address specific challenges in the AEC projects, e.g., bidding, procurement and negotiation (Dzeng & Wang, 2016; Perng et al., 2006). A more general simulation game is needed for AEC students to learn and understand the basic mechanisms of AEC projects, the relationship between different stakeholders, and the role of emerging technologies. And how different tools and media (e.g., LEGO, a board game) can be used for these simulation games are to be explored further (Dancz et al., 2017).

Our research team at the Department of Civil Engineering at National Taiwan University (NTUCE) has developed a simulation game named "To BIM or Not to BIM." This game aims to help our students (both undergraduate and graduate) experience and understand the process and mechanisms of AEC projects and the meaning behind the adoption of different information management technologies. In this game, participants play the role of different stakeholders: clients, designers, and contractors. The game is divided into two phases: design and construction. Clients set the project delivery requirements at the beginning of the game, and designers and contractors are chosen through competitive bidding. The designers and contractors are responsible for allocating appropriate resources for execution and determining the right technologies for information management. Finally, project delivery success is measured by profit and loss, and the quality of delivery is ensured in each phase of the game. Since 2019, the game has been embedded in the "BIM Technology & Application" course offered by NTUCE. So far, approximately 90 university students (undergraduate and graduate) have played the game and shared their feedback.

2. METHOD

2.1 The Design of the Simulation Game

The simulation game aims to allow university students to experience the process and mechanisms of real-world AEC projects, allowing them to explore the relationship between project stakeholders and the role of information management technologies in project delivery. The critical elements of this simulation game are as follows.

(1) Role Playing

The players (course students) can play one of the three essential roles in AEC projects: the client representative, the principal architect, and the main contractor (as shown in Figure 1). The client party owns capital to invest in a new asset and aims to profit from it. The architectural firm manages and delivers the design of the new asset, and the main contractor manages and delivers its construction.

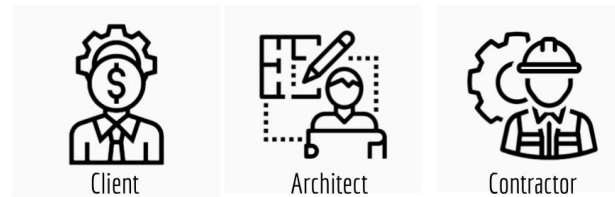


Figure 1. The three main roles in our simulation game

(2) Project Delivery Process

The players go through several steps, representing critical phases in a typical AEC project: the planning, design, and construction (as shown in Figure 2). We use one of the project delivery models called Design-Bid-Build (DBB) in the simulation game. Firstly, the client party issues a proposal for their new asset in the planning phase. In this phase, they set the project's expected cost, quality, and duration and collect information about related building regulations and limitations. Secondly, they find a suitable architectural firm to deliver the design of the new asset, usually via a bidding process (but not limited to it). In this step, the client conveys the proposal of their new asset to the architectural firm(s), who in turn make their proposal(s). Finally, the final design proposal (including the final design fee and expected quality and duration to be delivered in the design phase) is decided via negotiation between the client representative and the principal architect or the winning firm that provided the most appealing offer in the bidding process.

Thirdly, the principal architect decides which architect in the firm will be responsible for the design delivery and which information management technology will be used for their work. Three types of architects can be chosen, super, senior, and junior, and two information management technologies are available: computer-aided Design (CAD) and Building Information Modeling (BIM). After the selection of the desired workforce and tools, the design of a new asset is conducted. The player who plays the role of the principal architect will roll dice to determine the outcome of their design delivery. More information about the dice and risk incorporated into this game is explained in the next section. In the final step of the design phase, the client representative and principal architect need to check whether the design delivery is acceptable. If not, more design work must be conducted, and the architectural firm is responsible for the extra cost and associated overdue penalties.

Similar to the design phase, at the beginning of the construction phase, the client finds a suitable main contractor to deliver the construction of their new asset, usually but not limited to being decided via a bidding process. In this step, they also convey the proposal of their new asset to the contractor(s), who in turn make their proposal(s). Finally, the final construction proposal (including the final construction fee and expected quality and duration to be delivered in this phase) is decided via negotiation between the client representative and the main contractor or the winning firm that provided the most appealing offer in the bidding process.

Like the design phase, the main contractor will decide which engineer in the firm will be responsible for construction delivery and which information management technology will be used for their work. Three types of engineers can be chosen, super, senior, and junior, and two information management technologies are available: CAD and BIM. After the selection of the desired workforce and tools, the construction of the new asset is conducted. The player who plays the role of the main contractor will roll dice to determine the outcome of their construction delivery. More information about the design of the dice and risk in this game is explained in the next section. In the final step of the construction phase, the client representative and the main contractor need to check whether the construction delivery is acceptable. If not, more work must be conducted, and as for the architectural firm, the main contractor is responsible for the extra cost and associated overdue penalties.

The client then reviews the final project delivery outcomes- total cost, quality, and duration. The potential profit generated by the new asset and losses caused by project setbacks is also evaluated.

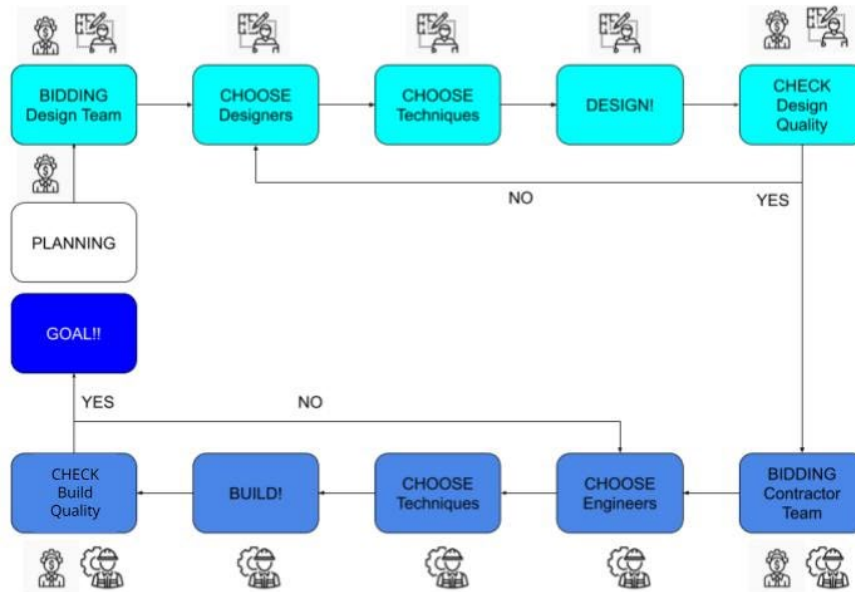


Figure 2. The twelve main steps in our simulation game

(3) Risk

The risk factors in AEC project delivery are also considered and incorporated into our simulation game. As mentioned in the previous section and shown in Figure 3, the workforces of the architectural firms and contractors are categorized into three levels based on their level of work experience: super (most experienced), senior (less experienced), and junior (least experienced). Two information management technologies, CAD and BIM, are available for project delivery (as shown in Figure 4), with the latter considered the more advanced technology. In theory, the cost of hiring super architects and engineers is higher, but they deliver better project outcomes (higher quality and shorter duration). The cost of senior personnel is lower, but they perform less well, and the cost of junior architects and engineers is the least, but they perform the worst (lowest quality and longest duration). BIM is theoretically more costly but ensures better project delivery and vice-versa for CAD. In reality, however, there is the chance that these workforces and technologies might perform differently than expected, and dice are used to reflect this risk factor.

Our simulation game uses three dice colors (as shown in Figure 5). The green dice have the highest probability of a better project outcome, the yellow dice have a lower probability, and the red dice have the lowest. As mentioned in the previous section, once the players (i.e., the principal architect and the main contractor) have chosen their desired workforce and technology for that round, they must roll the corresponding dice to determine the project delivery outcome. Green dice are used for super architects and engineers and BIM, yellow for senior personnel and CAD, and red for junior personnel.

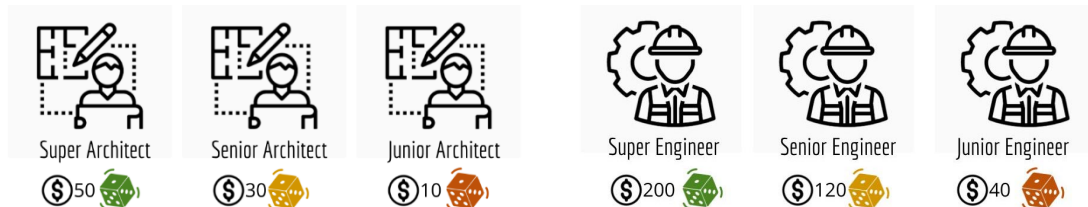


Figure 3. Three levels of architects and engineers

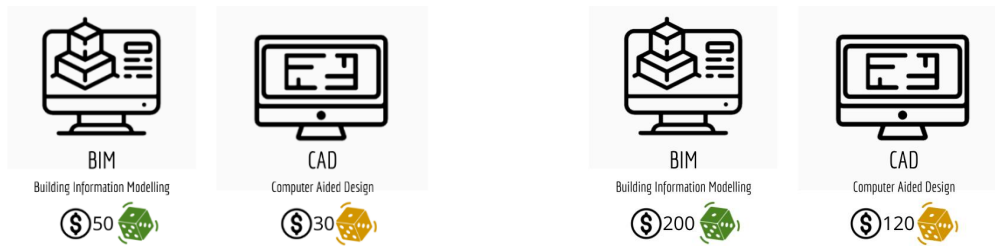


Figure 4. Two types of information management technology

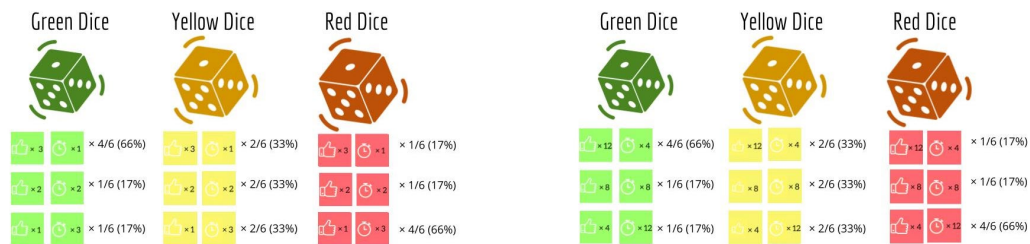


Figure 5. Three types of dice were used in the design and construction phase

(4) Cost, Quality, and Duration

The representative numbers and relationships between project cost, quality, and duration across project phases have been carefully designed in our simulation game to reflect real situations encountered in actual AEC projects. For example, the design fee in Taiwan is usually 10 ~ 20% of the estimated construction fee. Thus, in our simulation game, the project cost, quality, and duration in the construction phase are four times more than in the design phase (as shown in Figures 3, 4, and 5), and 50 units of cost are equivalent to one unit of quality. This math is relevant to the design of the dice and the costs of the different workforces and information technologies.

(5) Winning Criteria

Since the amount of capital and the profit method vary greatly between the client, architectural firms, and main contractors, the winner of our simulation game is not the one who profits the most. Students are divided into various groups when this game is played and can play their roles with their strategies; therefore, the relationships between the client, architectural firms, and main contractors will differ from one group to another. The ideal outcome for an AEC project is a win-win situation for all project stakeholders. The group that achieves such a balance is to be considered the winner.

(6) Bonus

We have designed another mechanism to reflect the benefits of adopting BIM for different stakeholders. For example, if the architectural team delivers their design using BIM, the cost of adopting BIM for the main contractor will be lower (25% discount). Whether earlier delivery of the new asset will benefit the project stakeholders is considered but not yet designed into this version of the simulation game.

(7) Penalty

We also design a penalty mechanism for the simulation game. If the architect or contractor exceeds their expected duration, one unit of duration delay will get 50 units of penalty. They must take this penalty as their cost in the final balance process. This penalty will pay to the client.

2.2 The Way to Play

We play two rounds in a typical class. First, students are formed into groups of five to six people. The first round is relatively simple, aiming to enable students to understand the process and mechanisms of the game. In this round, the project scale is also smaller (with an estimated construction cost of 1000 units). One or two students play the role of the client representatives of the same company, another act as the principal architect of the same firm, and another act as a representative of the same main contractor. The second round becomes more challenging and complex, and the project scale is bigger (with an estimated cost of 5000 units). Students still play the same roles as in the last round, but this time the two principal architects work for different firms, and there are two contractors. These architectural firms and contractors must compete to win the project, representing the traditional AEC project delivery model- "Design-Bid-Build."

More details about how we play the simulation game in class are shown in Table 1. During an in-class activity, group-to-group results were compared, and insights were given on how certain choices led to specific outcomes. Also, an ideal group was chosen, and their choices, outcomes, and strategies were discussed in detail in class. Later in the reflection session, participating groups were given time to analyze their performance and were encouraged to share their thoughts and "takeaways" from the game. At the end of the session, player suggestions were taken through an online feedback form.

Table 1. A breakdown of the gameplay

Session	Description	Duration
Introduction	The purpose, rules, and process of the game are introduced.	10 mins
Grouping and Role Assignments	First, students are grouped as 5 - 6 people. Second, the roles are assigned by teachers or decided by students. Third, students playing different roles are gathered separately. Then, key information and tips for each role are given to them separately by teaching assistants.	10 mins
1 st round	The estimated construction cost of a new asset is set at 1000 units. Usually, the design and construction requirements are met after one selection of the workforce and tools. There is only one client, an architectural firm, and the main contractor. Therefore, no bidding process is required.	30 mins
Discussion	The results (profit) of different project stakeholders in different groups are collected and compared. The reasons for the winning and losing are discussed, as is how the students understand the relationships between different project stakeholders and the role of BIM.	10 mins
Break	A short break is arranged for students to reflect on the game.	10 mins
2 nd round	The estimated construction cost of a new asset is set at 5000 units. Usually, the design and construction requirements are met after five selections of the workforce and tools. There is one client, two architectural firms, and two contractors. Therefore, a bidding process is required.	40 mins
Discussion	The results (profit) of different project stakeholders in different groups are collected and compared. The reasons for the winning and losing are discussed, as is how the students understand the relationships between different project stakeholders and the role of BIM.	10 mins

3. RESULTS & VALIDATION

3.1 History and Evolution

This game was first introduced to students in a summer course in 2019. Later, this became part of the "BIM Technology and Application" course. Table 2 shows the details of the game played at different times. So far, it has been played around 50 times by more than 90 participants. The players have included undergraduate university students in 2nd year and above up to doctorate students.

Table 2. Game details of recorded games

Course Title	Year	Format	No. of Students	Player's profile
NTU Summer School	Summer 2019	Physical	9	B
BIM Technology & Application	Fall 2019	Physical	30	B, M, D
BIM Technology & Application	Fall 2020	Physical	22	B, M, D
BIM Technology & Application	Fall 2021	Digital	24	B, M, D
NTU CAE Summer Internship	Summer 2022	Digital	8	B

B: Bachelor, M: Masters, D: Ph.D.

The initial version of the game was developed as a paper-based board game, where students could play with paper cards and dice, as shown in Figure 6. Although playing the game in that fashion was fun, maintaining the manual calculations was challenging. Sometimes faulty records led to unexpected game results and discussions. Similar feedback was also received from students. Over the years, the game evolved from paper-based to digital due to continuous development efforts. During the COVID-19 pandemic, the digital version of the game was used when physical classes were discouraged. The digital version retained all the attributes of the paper-based version,

utilizing a simple single-window User Interface (UI). Only the processes after the competitive bidding step were digitized. Figure 7 shows a screenshot of the game's UI. Spreadsheet extraction of each round's results was one of this version's key features. The digital version reduces the chance of human errors during calculations and the time required for playing each round. The results are exported in a spreadsheet so that group results can be easily compared and presented in the class.

As part of future development efforts, it is planned to convert the game into a web version. The current version supports the design-build-build project delivery scenario. However, other delivery methods, such as IPD, that promote ultimate stakeholder collaboration by integrating the latest information management technologies, such as BIM, are planned for future versions.



Figure 6. A paper version of the simulation game

Project Details		NTUCE BIM Board Game®		Estimate	
Budget(\$)	Group	Time(W)	Revenue(\$)	Expense(\$)	Savings/Loss(\$)
Design Stage		Construction Stage			
Architect's Levels Super Architect, Senior Architect, Junior Architect Please select the architect: [Dropdown] Please select the architect's tool: [Dropdown] BIM usage [Dropdown]		Engineer's Levels Super Engineers, Senior Engineers, Junior Engineers Please select the engineer: [Dropdown] Please select the engineer's tool: [Dropdown] BIM usage [Dropdown]			
Green Dice 1-2, 3-4, 5-6 1-2, 3-4, 5-6 1-2, 3-4, 5-6		Yellow Dice 1-2, 3-4, 5-6 1-2, 3-4, 5-6 1-2, 3-4, 5-6			
Red Dice 1-2, 3-4, 5-6 1-2, 3-4, 5-6 1-2, 3-4, 5-6		Green Dice 1-2, 3-4, 5-6 1-2, 3-4, 5-6 1-2, 3-4, 5-6			
Final outcome of the design stage Agreed Price(\$), Actual Cost(\$), Savings/Loss(\$) Quality Achieved, Time Spent(W), Time Penalty(\$) Lets Design!!		Final outcome of the construction stage Agreed Price(\$), Actual Cost(\$), Savings/Loss(\$) Quality Achieved, Time Spent(W), Time Penalty(\$) Lets Construct!!			

Figure 7. UI of the digital version

3.2 Close Observations

Eight bachelor's students played the latest version of the simulation game during their 2022 NTU CAE Summer Internship (see Figure 8). Close observations of their gameplay in the first round are presented in the following sections as examples of how students perform from our simulation game.

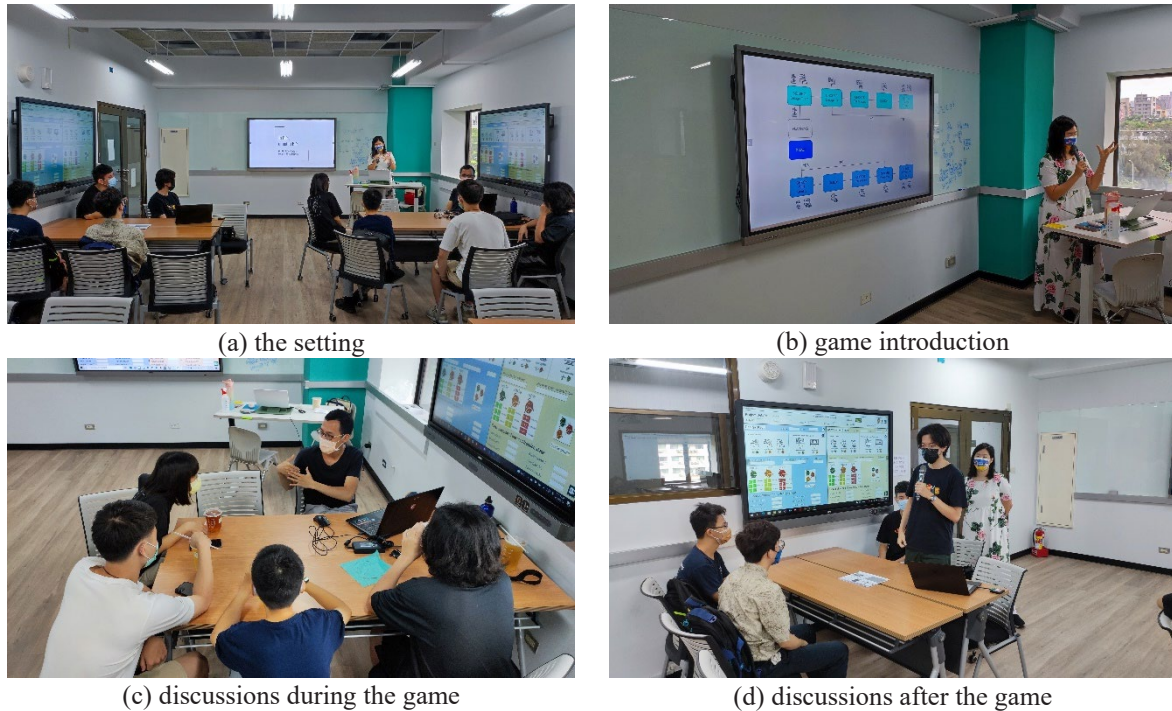


Figure 8. Photos of gameplay during the 2022 NTU Summer Internship

A comparison of the two groups' results is shown in Table 3. The project budget, minimum quality and maximum duration in the first round of game are set by the game designers, which represent the clients' estimation of project budget (including construction cost, contractor's and designer's service fee) and building authority's requirements. Whether the clients aim for higher quality or shorter duration is decided by the game players themselves. The clients should make reasonable planning for design and construction phase and agreements with designer and contractor based on the information provided (e.g. minimum/ maximum amount of quality and duration to gain in one round of design and construction work, the set ratio difference between design and construction phase). From the agreed prices for the two projects, it is clear that negotiation plays a vital role in project bidding. Risk is an integral part of the construction, and this is also evident from the outcome. Both groups chose a senior architect and a CAD tool during the first design round; however, the first group did not perform as well, so they had to play another design round, which incurred more cost and time. This scenario highlights the philosophy of doing things right at the very first attempt. In the case of Group 2, all stakeholders were satisfied because of the balanced savings in each phase of the project; however, stakeholder satisfaction was not equally achieved. The classroom discussions helped students to find resemblances with actual construction scenarios.

Table 3. Comparison of results of two student groups in the first round of the game

Project Budget (\$) = 1000			Group-1			Group-2		
Stakeholders	Client	Designer	Contractor	Client	Designer	Contractor		
Minimum Quality (Tokens)	20	-	-	20	-	-		
Maximum Duration (Weeks)	20	-	-	20	-	-		
Agreed Quality (Tokens)	20	6	14	20	4	16		
Agreed Duration (Weeks)	16	4	12	19	4	15		
Agreed Amount (\$)	1050	330	720	665	180	485		
Quality Achieved (Tokens)	30	6	24	25	5	20		
Time Spent (Weeks)	18	10	8	15	3	12		
Revenue (\$) ^(a)	1800	330	720	1250	180	485		
Expense (\$) ^(b)	1050	140	350 ^(c)	665	60	320		
Time penalty (\$) [50/unit time]	-	300	-	-	-	-		
Savings/loss (\$)	750	-110	370	585	120	165		
Choices (Person, Tool)		1 Senior Architect +1 CAD, 1 Senior	1 Super Engineer +1 BIM		1 Senior Architect +1 CAD	1 Super Engineer +1 CAD		

Architect
+1 BIM

Note:

- a) Revenue: Client = $50 * \text{Quality Achieved} + \text{Time penalty from designer \& contractor}$; Designer and Contractor = *Agreed amount*
- b) Expense: Client = *Agreed amount by designer and contractor*; Designer and Contractor = *Actual cost*
- c) If the designer uses BIM, the contractor can enjoy 25% savings on the BIM expense.

4. CONCLUSIONS AND FUTURE WORKS

This research addressed the issue that traditional teaching methods cannot help students experience and explore the relationships between project stakeholders, the differences between project delivery methods, and the roles of information management technologies. Therefore, we proposed a simulation game, "To BIM or not to BIM," that allows students to experience resource trade-offs with appropriate risk management to maximize their profit. We have introduced the game into the class since 2019, and from class observation, we found that although the project budget and quality requirements were the same, team performance was very different. This phenomenon reflects AEC project uniqueness.

In the future, we will design pre- and post-game questionnaires for the participating students to investigate whether they gain the knowledge about the AEC project delivery we aim for when designing this simulation game. We will also conduct simulation analysis via computer to validate that the mechanisms are well designed according to our expectations. Furthermore, we plan to simplify the game environment setup process and enrich the game with more scenarios so that students can have more experience by rapidly playing the game several times with different strategies within a specific time. In addition, the current simulation game follows the Design-Bid-Build (DBB) project delivery method as its game process, but this can be extended with other project delivery methods, such as Integrated Project Delivery (IPD). This would allow students to gain wider experience.

REFERENCES

- Aldossari, K. M., Lines, B. C., Smithwick, J. B., Hurtado, K. C., and Sullivan, K. T. (2021). Alternative project delivery method adoption in the AEC industry: An organizational change perspective, *International Journal of Construction Education and Research*, 1-16.
- Chegu Badrinath, A., Chang, Y. T., and Hsieh, S. H. (2016). A review of tertiary BIM education for advanced engineering communication with visualization, *Visualization in Engineering*, 4(1), 1-17.
- Dancz, C. L., Parrish, K., Bilec, M. M., & Landis, A. E. (2017). Assessment of students' mastery of construction management and engineering concepts through board game design, *Journal of Professional Issues in Engineering Education and Practice*, 143(4), 04017009.
- Dzeng, R. J., and Wang, P. R. (2016). Educational games on procurement and negotiation: Perspectives of learning effectiveness and game strategies, *Journal of Professional Issues in Engineering Education and Practice*, 142(3), 04016004.
- Franz, B., Leicht, R., Molenaar, K., and Messner, J. (2017). Impact of team integration and group cohesion on project delivery performance, *Journal of Construction Engineering and Management*, 143(1), 04016088.
- Gu, N. and London, K. (2010). Understanding and facilitating BIM adoption in the AEC industry, *Automation in Construction*, 19(8), 988-999.
- Hedayati, A., Mohandes, S.R., and Preece, C. (2015). Studying the obstacles to implementing BIM in educational system and making some recommendations, *Journal of Basic Applied Science Research*, 5(3), 29-35.
- Mills, J., and MacDonald, J. (2013). An IPD approach to construction education, *Australasian Journal of Construction Economics and Building*, 13(2), 93-103.
- Perng, Y. H., Juan, Y. K., and Chien, S. F. (2006). Exploring the bidding situation for economically most advantageous tender projects using a bidding game, *Journal of Construction Engineering and Management*, 132(10), 1037-1042.
- Rounds, J. L., Hendrick, D., and Higgins, S. (1986). Project management simulation training game, *Journal of Management in Engineering*, 2(4), 272-279.
- Solnosky, R., Parfitt, M. K., and Holland, R. J. (2014). IPD and BIM-focused capstone course based on AEC industry needs and involvement, *Journal of Professional Issues in Engineering Education and Practice*, 140(4), A4013001.
- Veshosky, D. and Egbers, J. H. (1991). Civil Engineering project management game: teaching with simulation, *Journal of Professional Issues in Engineering Education and Practice*, 117(3), 203-213.
- Zhang, Y. and Wang, G. (2009, September). Cooperation between building information modeling and integrated project delivery method leads to change in thinking of AEC industry, *In 2009 International Conference on Management and Service Science*. IEEE. pp. 1-4.

A BIM-ASSISTED PLANNING TOOL FOR FACILITATING THE APPLICATION OF AN ALUMINUM FORMWORK SYSTEM TO BEAM-COLUMN BUILDINGS

Kuan-Yi Chen¹, Tzong-Hann Wu², Budy Setiawan³, Cecilia Clarita Tandri⁴, Shang-Hsien Hsieh⁵, and Wen-Tung Chang⁶

1) MS. Student, Department of Civil Engineering, National Taiwan University, Taipei, Taiwan. Email: r11521609@ntu.edu.tw

2) Postdoctoral Research Fellow, Department of Civil Engineering, National Taiwan University, Taipei, Taiwan. Email: tzonghannwu@ntu.edu.tw

3) Chief Eng., FBC Formworks Systems Co., Ltd., Taipei, Taiwan. Email: huangwenren88@gmail.com

4) Eng., FBC Formworks Systems Co., Ltd., Taipei, Taiwan. Email: cecilctandri@gmail.com

5) Prof., Department of Civil Engineering, National Taiwan University, Taipei, Taiwan. Email: shhsieh@ntu.edu.tw

6) CEO., FBC Formworks Systems Co., Ltd., Taipei, Taiwan. Email: tonylook@ms52.hinet.net

Abstract: Aluminum formwork systems are an onsite labor-saving and sustainable construction method. However, it requires detailed planning before construction, which is more challenging for beam-column buildings, commonly seen in regions facing seismic hazards, than slab-wall buildings. Also, the existing CAD-based planning tool for beam-column buildings is labor-intensive and time-consuming. Therefore, this research develops a BIM-assisted tool for formwork engineers to efficiently and effectively conduct layout planning. The tool is implemented by Revit API and consists of six modules: (1) Preparation of Layout Planning, (2) Corner Panel Initial Placement, (3) Flat Panel Generation, (4) Flat Panel Refinement, (5) Corner Panel Generation, and (6) Formwork Accessory Planning. The tool also considers the inventory of panels and assists in deciding the production of new panels during layout planning. Finally, a real case evaluation shows that the developed tool can save at least 50% of layout planning time, compared to the existing CAD-based layout planning tool.

Keywords: Aluminum formwork, Layout planning, BIM, Design automation, Beam-Column buildings

1. INTRODUCTION

Aluminum formwork systems are now increasingly applied in Taiwan's Architecture, Engineering & Construction (AEC) industry. Compared with conventional timber formwork systems, aluminum formwork systems have a lower cost in onsite labor because it does not need many handcraft tasks on-site. Gaddam and Aravindan (2020) conducted a case study that shows that the aluminum formwork system took the least construction time and the second least cost by comparing 4 types of formwork systems. However, aluminum formwork systems require detailed planning before construction. Any on-site machining tasks (cutting, welding, and drilling) should be conducted in the factory because it is safer and less costly than onsite. Moreover, the formwork planning for the connections of beam-column buildings is more complex than that of slab-wall buildings, making formwork planning more challenging. Biruk and Jaskowski (2017) proposed a mixed integer linear programming modeling approach to support the formwork planning process. They focus on wall panel planning but do not consider the columns and beams in their examples. Lee et al. (2018) proposed an advanced planning model to conduct slab panel planning considering structural obstacles, such as columns. Lee et al. (2021) developed a prototype of an automatic tool that focuses on wall and slab planning. However, the examples or cases in the previous studies are often using slab-wall buildings. It cannot directly be used for beam-column buildings. In addition to labor-saving, the aluminum formwork system is also a sustainable construction method because each panel can be reused 200 to 300 times before it is recycled. Thus, the formwork planning should consider the inventory of formwork panels to reduce the need for creating new panels because of the long-term lifecycle of each panel. Lee and Ham (2018) developed an automatic slab form layout system, which maximizes the standard formwork panels on the slab and automatically determines the layout of standard and nonstandard formwork panels, but they only focus on slab panels. Mei et al. (2021) proposed a BIM-based framework for formwork planning considering potential reuse, but we only see the preliminary layout planning result presented in their paper. It seems that their planning layout is only preliminary. The above-mentioned studies can help engineers conduct wall and slab planning in slab-wall buildings and consider potential reuse, but they cannot be directly used for Taiwan's beam-column buildings. Therefore, this research aims to propose and develop an automatic planning tool to help aluminum formwork engineers conduct detailed planning. The detailed planning considers panel alignment, panel assembly, and panel management for Taiwan's beam-column buildings.

2. THE BIM-ASSISTED ALUMINUM FORMWORK PLANNING TOOL

This research proposes a BIM-assisted formwork planning tool and uses the API (Application Programming Interface) of Autodesk Revit, a BIM (Building Information Modeling) software, to implement the

tool. The aluminum formwork system adopted is from FBC Formworks Systems Co., Ltd. (<https://www.fbcformworks.com/>). Their formwork system is a transformation from that of Aluforms Co., Ltd. (<https://www.aluforms.net/>) to fit the demands of Taiwan's beam-column buildings.

The development of the proposed planning tool uses the layout planning principle of walls, columns, and beams from FBC Formworks Systems Co., Ltd. as a reference. There are five main principles to be considered in layout planning: (1) The number of panels should not be too many to cause poor construction efficiency; (2) Layout corner panels on the connection between the flat panels with different orientations; (3) Make sure flat panels are aligned with their opposite flat panels for screwing pull ties; (4) Make sure part of holes between adjacent panels are aligned for assembly; (5) Make sure all panels are fastened and supported by accessories. Figure 1 shows an example of layout planning based on the rules (Chen et al., 2022). Besides, before using the tool, the BIM model should satisfy three constraints: elements should be rectangular cuboids; elements should be unjointed; and contact areas between elements should be rectangular.

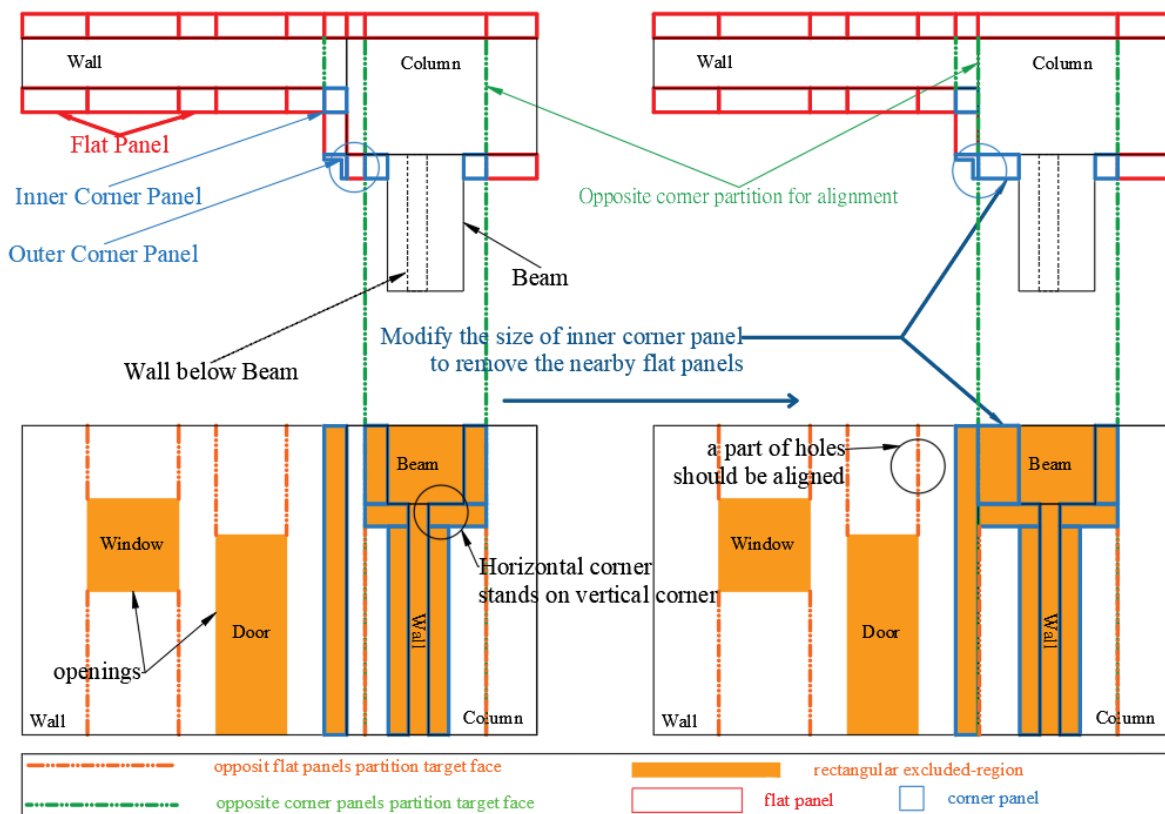


Figure 1. An example of layout planning (Chen et al., 2022)

Finally, the developed tool consists of six modules: (1) Preparation of Layout Planning, (2) Corner Panel Initial Placement, (3) Flat Panel Generation, (4) Flat Panel Refinement, (5) Corner Panel Generation, and (6) Formwork Accessory Planning. Modules 2 to 4 are based on the previous approach proposed (Chen et al., 2022). This research makes Modules 2 to 4 more automatic and then develops Modules 1, 5, and 6 to complete the planning process. The comprehensive planning process is shown in Figure 2. The functions in the modules are categorized into 3 types: automatic, semi-automatic, and manual function. Semi-automatic functions mean that the tool can accelerate this operation. In addition, any function that may create, modify, or delete panels or accessories would connect with a formwork management module. The following sections show the implementation of each module.

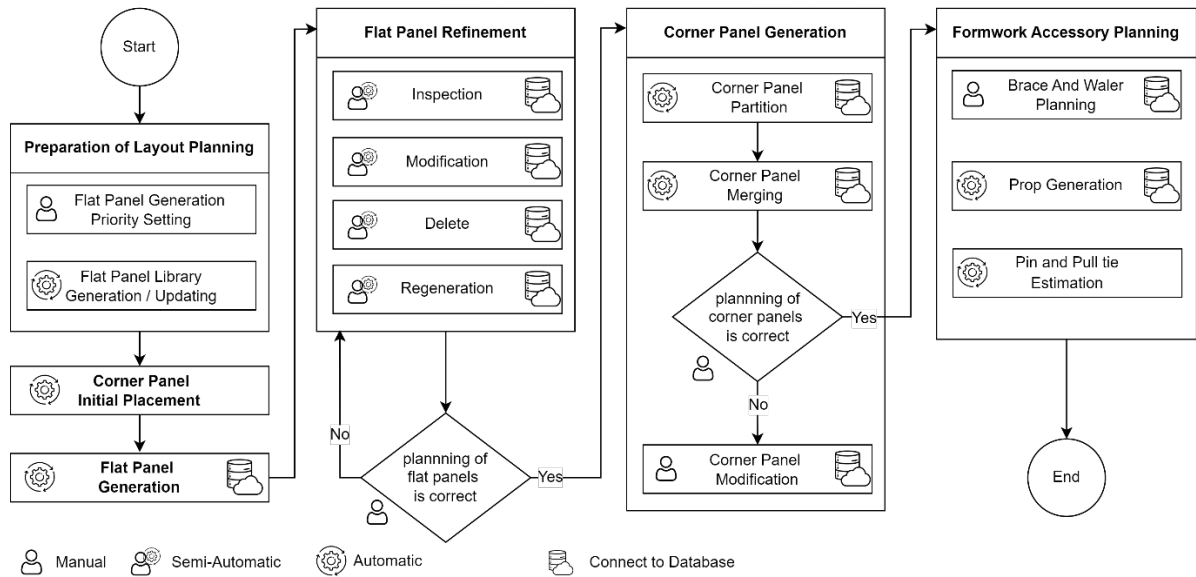


Figure 2. The comprehensive planning process of the proposed tool

2.1 Preparation of Layout Planning

Engineers can decide what kinds of flat panels should be used and set their generation priority by editing a CSV (comma-separated values) file. The file has all the panel types that may be used in a project. The generation priority is the same as the appearing sequence in the CSV file. Figure 3 shows an example of the generation results from two different CSV files.

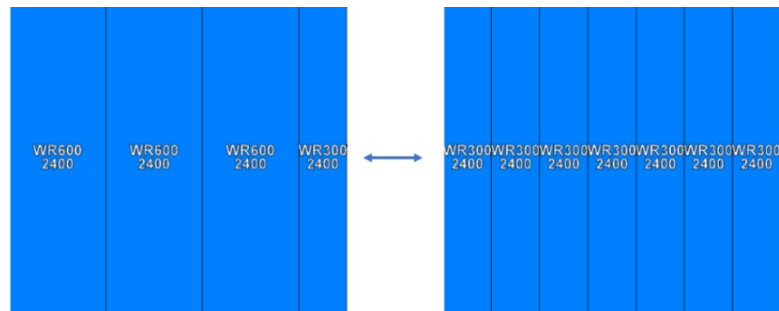


Figure 3. An example of the generation results from two different CSV files

The panel library is automatically generated or updated according to the CSV file. Engineers can edit a flat panel's property parameter to adjust the positions of the holes on the panel. Figure 4 shows an operation example of the parametric flat panel library.

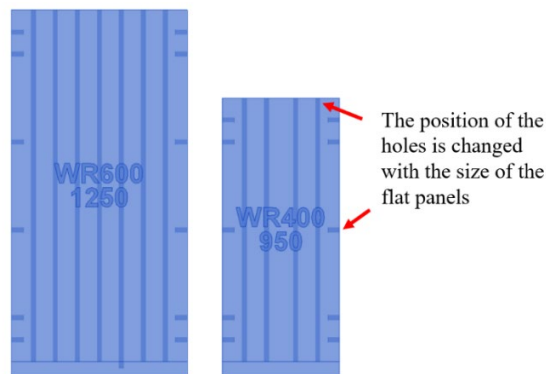


Figure 4. An operation example of the parametric flat panel library

2.2 Corner Panel Initial Placement

The planning tool analyzes all corner types of all elements in the same story and then follows the principles decided by engineers to define the respective types and locations of corner panels. The inner corner of an opening does not need corner panels. The connections between all corner panels follow the rules defined by engineers. For example, the horizontal corner panels should stand on the vertical corner panels. Figure 5 shows an example result after the corner panel initial placement. The initial placement can be modified by engineers and influence the result of following flat panel generation.

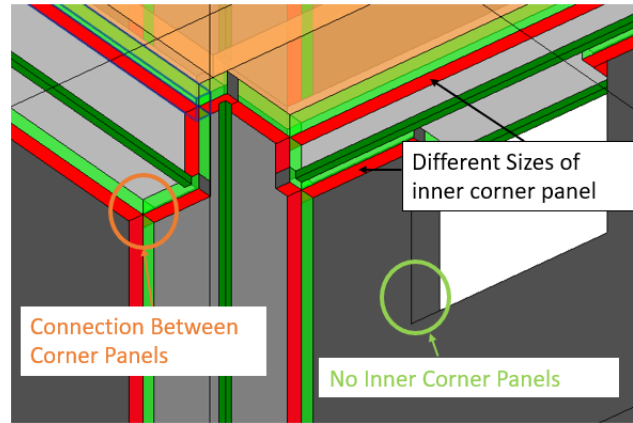


Figure 5. An example of the result after corner panel initial placement

2.3 Flat Panel Generation

The planning tool automatically generates flat panels on each element with six steps: (1) Category Identification, (2) Beam Partition, (3) Face Partition, (4) Story Interface Checking, (5) Flat Panel Generation, and (6) Hole Position Modification. Steps 1 and 3 are the same as the previous approach (Chen et al., 2022). Step 2 is to confirm that the part of the panels' holes on the beam can align with the part of the panels' holes on the wall below the beam. This step partitions beams according to the panel layout of the walls, as shown in Figure 6. Step 4 is to check whether a special type of panel (the base for next-story panels) should be placed on the partitioned face (as shown in Figure 7). Step 5 is to generate panels on partitioned faces by the planning sequence from the preparation of formwork planning. This step connects with the formwork management module to make an appointment, Step 6 is to modify the arrangement of holes according to the elevation of the flat panels as shown in Figure 8.

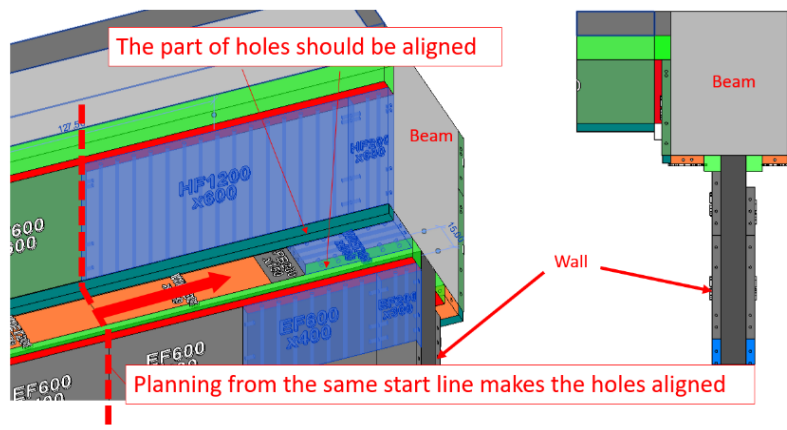


Figure 6. Partitioning beam for the alignment of the holes

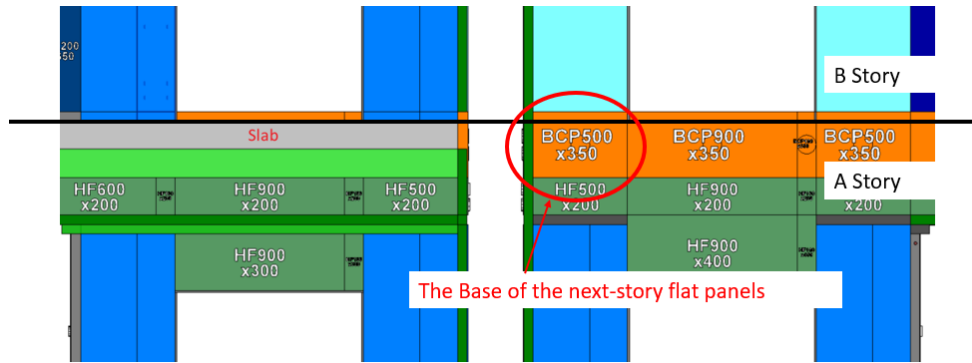


Figure 7. Story interface checking

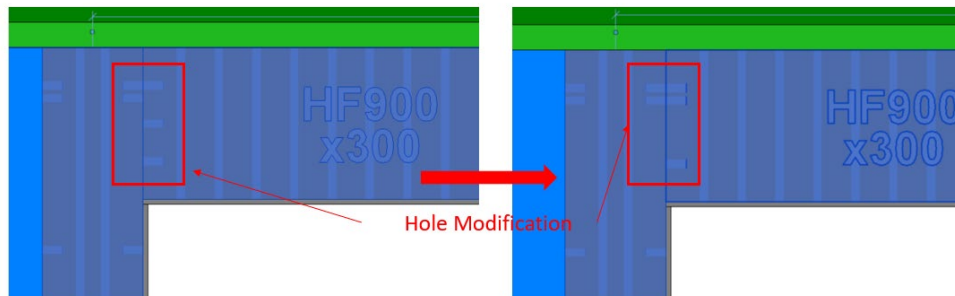


Figure 8. The alignment of the hole position in the same elevation

2.4 Flat Panel Refinement

This module consists of four functions including Inspection, Modification, Delete, and Regeneration for engineers to refine the flat panel generation result. The Inspection function can analyze the components selected by engineers and then produce a list that indicates all unfinished faces, as shown in Figure 9(a). The Modification function provides tools for engineers to resize, merge, and split panels. Figure 9(b) shows the example of merging panels. The operation can be done more quickly and can be connected to the database to check whether the panel needs to be produced. The Delete function is to help engineers delete all panels on a single face or a single component, as shown in Figure 9(c). The Regeneration function allows engineers to draw reference lines on a face and then regenerate the panels on it, as shown in Figure 9(d). These functions assist engineers to inspect and adjust panel configurations more quickly and retain some flexibility to deal with potentially more complex cases.

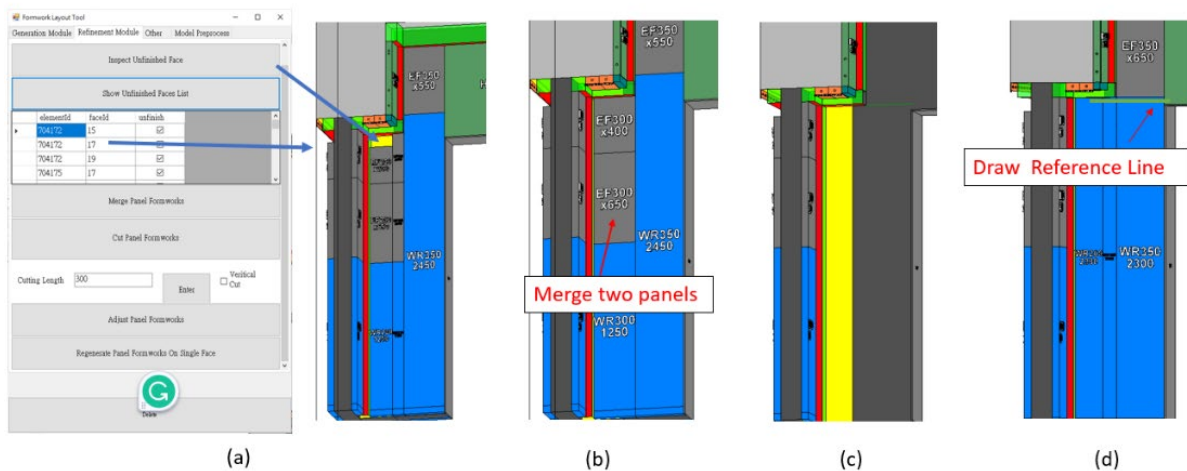


Figure 9. Flat panel refinement: (a) Inspect unfinished faces and show original planning of (b), (c), and (d); (b) Merge flat panels; (c) Delete flat panels on faces; and (d) Regenerate flat panels based on the reference line.

2.5 Corner Panel Generation

The developed tool automatically cuts corner panels by near flat panels and then combines two corner panels into an L shape corner panel, if needed, by the engineer's defined rules. Figure 10 shows an example of cutting and merging corner panels. Engineers can also quickly merge, cut, and adjust the corner panel manually if they want to address any issue they find.

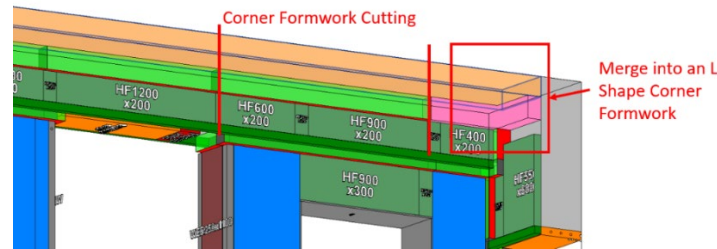


Figure 10. An example of corner panel cutting and merging

2.6 Formwork Accessory Planning

Formwork accessory planning is one of the subtasks in aluminum formwork planning. It plays an important role in fastening and supporting aluminum formwork panels. Formwork accessories have five types (brace, waler, prop, pin, and pull tie). The developed tool can support manual planning of braces and walers, automatic planning of props, and estimation of the number of pins and pull ties. The planning result of the formwork accessory is shown in Figure 11. To obtain the estimation of pins and pull ties, this tool adds all the number of pins and pull ties and subtracts overlapping numbers of them between flat panels.

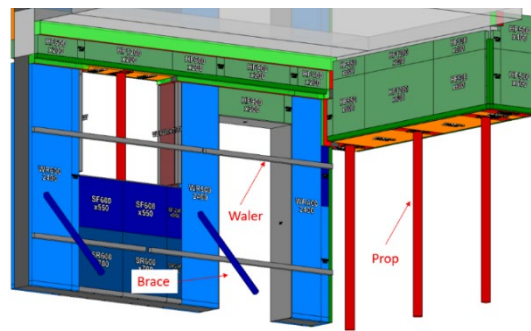


Figure 11. An example of Formwork Accessory Planning

3. CASE STUDY

This research took one-twelfth of the single-story building model as our evaluation model, which has 27 walls, 4 columns, 6 beams, 4 slabs, and 7 openings, as shown in Figure 12(a). The original single-story model has 340 walls, 20 columns, 63 floors, 71 beams, and 70 openings, resulting in a total panel area of 3,353 square meters, excluding the panel area on the slab. Figure 12(b) shows the relationship between the evaluation and original models.

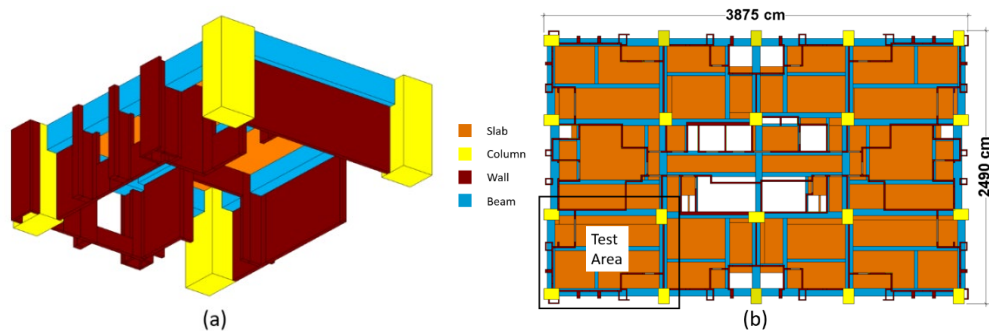


Figure 12. The evaluation model: (a) The 3D view; (b) The relationship with the original model

Table 1 shows that the proposed BIM-assisted tool saves 77.2% of the operation time of panel planning (flat panel planning and corner panel planning) in the evaluation model. In total planning (panel and accessory planning), the saving time is reduced from 77.2% to 59.2%. This is because accessory planning still requires many manual operations. The final panel planning result is shown in Figure 13. However, the operation time of the CAD-based tool in the table was assumed as one-twelfth of the operation time in the original model, so this result was a preliminary comparison and might vary with the different complexity of test cases.

Table 1: The operation time of the steps for planning in BIM-assisted and CAD-based tool

Operation	Operation Time (minutes)		Saving Time Percentage
	BIM-assisted	CAD-based	
Panel Planning	255	1120	77.2%
Total Planning	620	1520	59.2%

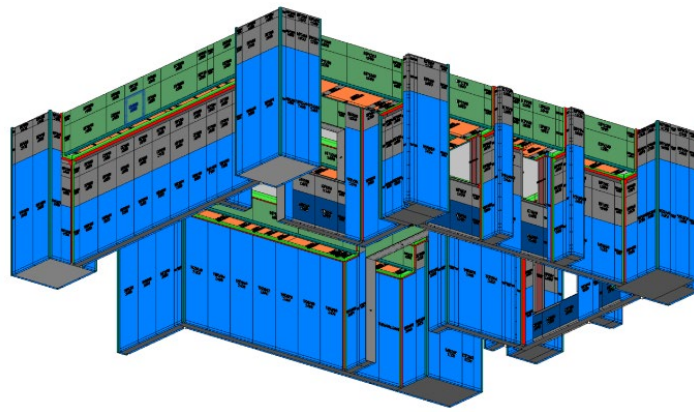


Figure 13. The final layout planning results

Engineers spent a lot of time on the flat panel refinement and corner panel modification, especially in conducting the planning on the bottom face of the beams. Many generation issues occurred on the face because of its complex contacting relationship and the consideration of support flat panel, as shown in Figure 14. In addition, hole alignment between a flat panel on the bottom face and a flat panel on the side face should be reviewed by engineers, as shown in Figure 15.

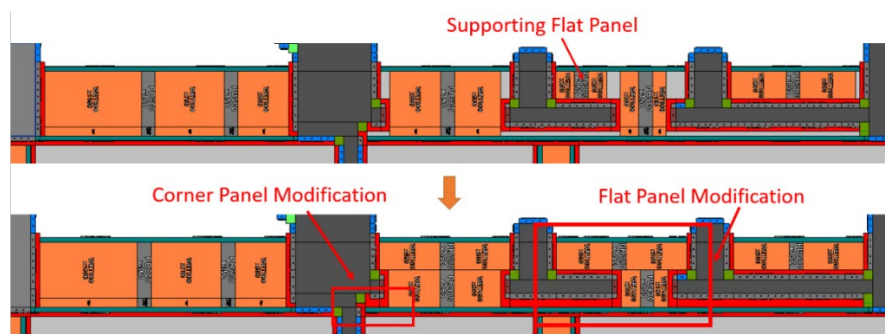


Figure 14. The condition of formwork layout planning on the bottom face of a beam

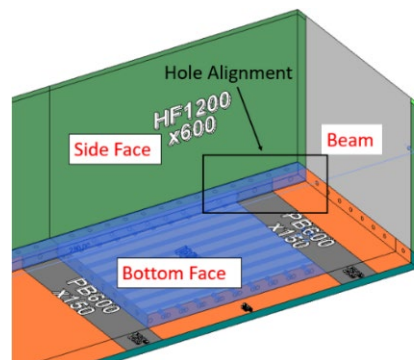


Figure 15. Hole alignment between flat panels on different faces

4. CONCLUSIONS

This research develops a planning tool to support efficient formwork layout planning for beam-column buildings, which are commonly seen in regions with seismic hazards. The tool is implemented by Revit API. This tool has six modules including (1) Preparation of Layout Planning, (2) Corner Panel Initial Placement, (3) Flat Panel Generation, (4) Flat Panel Refinement, (5) Corner Panel Generation, and (6) Formwork Accessory Planning. A real case evaluation of a beam-column building shows the tool can save at least 50% of layout planning time than the existing CAD-based layout planning tool. In the future, the BIM-assisted tool can be further improved in reducing constraints of models, supporting complex connection situations in panel generation, providing more advanced refinement functions, considering the slab and the stair category in layout planning, and providing more automatic planning for the formwork accessory.

REFERENCES

- Biruk, S. and Jaskowski, P. (2017) Optimization of Vertical Formwork Layout Plans Using Mixed Integer Linear Programming, *International Journal of Civil Engineering*, 15, 125–133. <https://doi.org/10.1007/s40999-016-0090-6>
- Chen, K. Y., Wu, T. H., Hsieh, S. H., Setiawan, B., Tandri, C. C., and Chang, W. T. (2022, November). A BIM-Based Layout Planning Approach for the Aluminum Formwork System, In *Proceedings of the International Conference on Construction Applications of Virtual Reality* (p. 1280-1284)
- Gaddam, S. M. and Aravindan, A. (2020). A Comparative Study on Newly Emerging Type of Formwork Systems with Conventional Type of Form Work Systems, *Materials Today: Proceedings*, 33(1), 736–740. <https://doi.org/https://doi.org/10.1016/j.matpr.2020.06.090>.
- Lee, B., Choi, H., Min, B., Ryu, J., and Lee, D. E. (2021). Development of Formwork Automation Design Software for Improving Construction Productivity, *Automation in Construction*, 126(103680). <https://doi.org/10.1016/j.autcon.2021.103680>
- Lee, C. and Ham, S. (2018). Automated System for Form Layout to Increase the Proportion of Standard Forms and Improve Work Efficiency. *Automation in Construction*, 87, 273-286. <https://doi.org/10.1016/j.autcon.2017.12.028>
- Lee, D., Lim, H., Kim, T., Cho, H., and Kang, K. I. (2018). Advanced Planning Model of Formwork Layout for Productivity Improvement in High-rise Building Construction, *Automation in Construction*, 85, 232-2. <https://doi.org/10.1016/j.autcon.2017.09.019>.
- Mei, Z., Xu, M., Wu, P., Luo, S., Wang, J., and Tan, Y. (2021). BIM-Based Framework for Formwork Planning Considering Potential Reuse, *Journal of Management in Engineering*, 38(2), 04021090. [https://doi.org/10.1061/\(ASCE\)ME.1943-5479.0001004](https://doi.org/10.1061/(ASCE)ME.1943-5479.0001004)

DEVELOPMENT OF A BIM-BASED SYSTEM FOR ASSESSMENT AND OPTIMIZATION OF GHG EMISSIONS IN THE EARLY DESIGN STAGE

Thanasak Phittayakorn ¹, Chavanont Khosakitchalert ^{2*}, and Lapyote Prasittisopin ³

1) Ph.D. Candidate, Department of Architecture, Faculty of Architecture, Chulalongkorn University, Bangkok, Thailand. Email: 6471004925@student.chula.ac.th

2) Ph.D., Assistant Professor, Department of Architecture, Faculty of Architecture, Chulalongkorn University, Bangkok, Thailand. Email: Chavanont.k@chula.ac.th

3) Ph.D., Assistant Professor, Department of Architecture, Faculty of Architecture, Chulalongkorn University, Bangkok, Thailand. Email: Lapyote.p@chula.ac.th

* Corresponding author

Abstract: Greenhouse gas (GHG) emissions from the building sector are a significant contributor to global warming due to embodied and operational carbon produced during the entire building design and construction process. While the design process has the potential to effectively reduce GHG emissions, it is crucial for architects to integrate methods for minimizing environmental impact at each stage. Building Information Modeling (BIM) and Life Cycle Assessment (LCA) are widely used tools and methods for evaluating GHG emissions in the building sector. However, in the early design stage, there are numerous uncertainties and a lack of information on materials and processes that make it difficult to evaluate and minimize environmental impact. This research aims to develop a BIM-based system for evaluating and minimizing GHG emissions during the early design stage of a building when it is still in the conceptual mass stage. The focus of the research is on office buildings. The parameters that can be adjusted include the shape of the building, the windows-to-wall ratio (WWR), and the number of floors. The system calculates the GHG emissions and adjusts the parameters until the desired total floor area is reached with the lowest GHG emissions possible. The proposed system was developed using Visual programming in Rhinoceros with Grasshopper plug-in and the Environment Product Declarations (EPDs) database. The results demonstrate that the BIM-based system for conceptual design can effectively assist architects in assessing GHG emissions during the early design stage.

Keywords: Life cycle assessment, Building Information Modeling, Greenhouse gas emission, Design process, Design optimization, Parametric design.

1. INTRODUCTION

Climate change is one of the most serious issues we are facing today, with a negative impact on the environment and living creatures worldwide. The building sector is one of the main contributors to carbon emissions due to extensive energy and natural resource consumption during construction projects. According to the Intergovernmental Panel on Climate Change (IPCC) and Architecture 2030 (Grubert & Stokes-Draut, 2020; Lewis et al., 2018), the building sector is responsible for up to 40% of total greenhouse gas emissions worldwide.

Life Cycle Assessment (LCA) is a valuable tool for evaluating the environmental impact of products and systems, including buildings. It considers the entire life cycle of a product or system, from raw material extraction to disposal, to identify potential environmental impacts at each stage (Finkbeiner, 2014; ISO, 2006; Sereewatthanawut et al., 2021). However, conducting an LCA for buildings can be challenging due to the significant amount of information and time required. The process involves collecting data on the quantity and quality of building materials, which can be difficult and time-consuming (Hollberg et al., 2021; Lasvaux et al., 2013). The Life Cycle Inventory (LCI) and Life Cycle Impact Assessment (LCIA) phases involve analyzing the collected data and assessing the potential environmental impacts of building materials and the entire building system.

Inaccurate material quantities can result in unreliable results, emphasizing the need for accurate data when performing an LCA. Thus, it may not always be practical to conduct an LCA for a building if material quantities are unknown (Díaz et al., 2014; Eastman et al., 2011). However, simplifying the LCA process for buildings is possible, such as using existing data from similar projects or relying on industry-wide averages for material quantities. New technologies such as Building Information Modeling (BIM) can aid in automating data collection and analysis, making LCA more feasible for building projects (Bernstein et al., 2020; Khosakitchalert et al., 2020).

During the early stages of design, many unknowns related to materials, processes, and other factors can impact the environmental impact of a product or system. This can make it challenging to accurately assess and minimize the environmental impact (Budig et al., 2021; Nembrini et al., 2014; Victoria & Perera, 2018).

To address this challenge, designers can incorporate environmental considerations into the design process from the outset, using a proposed system to improve a building mass for minimizing greenhouse gas (GHG) emissions and identifying potential environmental hotspots from designing the building mass, such as the shape of the building mass, the windows-to-wall ratio (WWR), and the number of floors.

The main objective of this paper is to develop a BIM-based system for evaluating and optimizing building

GHG emission reductions during the early stages of the design and evaluation process. The system aims to improve the optimum value by using a genetic algorithm to evaluate the fitness score and achieve the specified results, namely maximizing gross floor area (GFA) and minimizing GHG emissions.

2. PROPOSED METHODOLOGY

The study focuses on office building types. The proposed methodology consists of four steps: 1) generating a building mass, 2) inputting a materials database, 3) calculating the GHG emissions from the LCA database, and 4) optimizing the building mass.

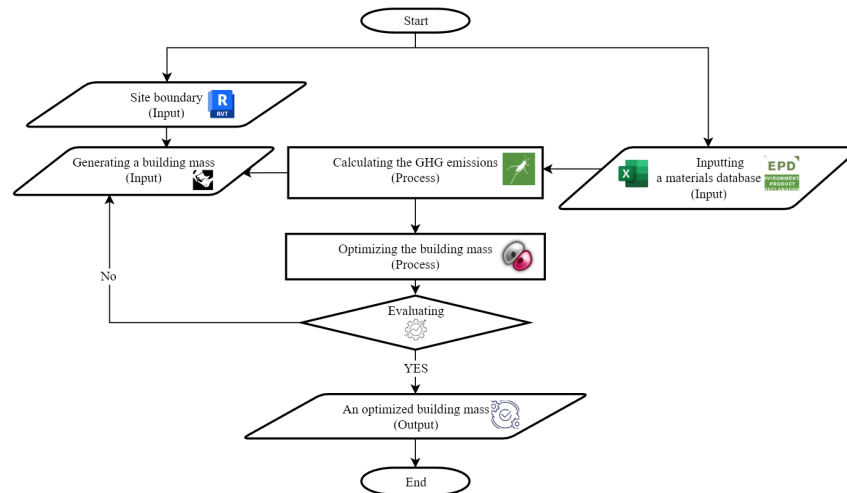


Figure 1. The proposed methodology.

2.1 Generating a Building Mass

First, a site model of the project was created in BIM software to accurately locate the building at the correct geolocation, taking into account factors such as climate conditions and geography. This can help avoid mistakes later in the project and facilitate collaboration between architects, engineers, and contractors. Line boundaries, including the site boundary and setback site boundary, were created to limit the building shape and determine the area for optimizing the GFA, as shown in Figure 2.

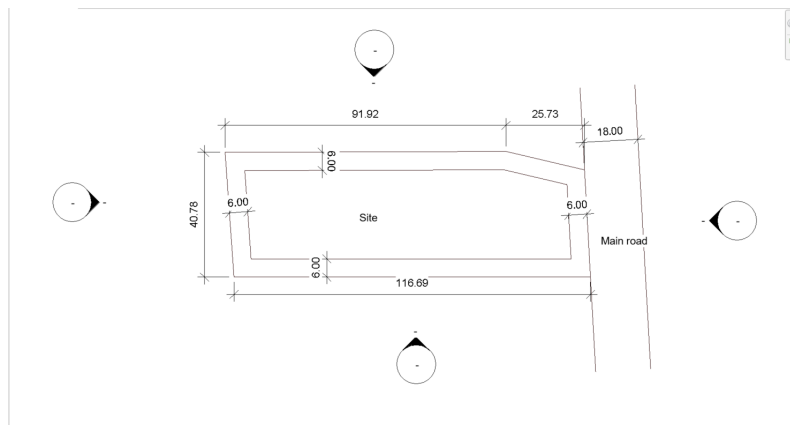


Figure 2. Site boundary and setback site boundary.

After importing the site model to Rhinoceros, the building mass was generated using Grasshopper, a visual programming (VP) plug-in. The setback site boundary was used as the base geometry for generating the building floor plates, which could be scaled in both X and Y directions. Another rectangle geometry was used to trim the floor plates, and its width, length, and rotation could be adjusted. Additionally, the floor plates were trimmed by the slope setback on the Z axis. Finally, the windows and exterior walls were created from the floor plates by extruding them, as illustrated in Figure 3. The proportion of windows and exterior walls, or the window-to-wall ratio (WWR), could be adjusted by the user, ranging from 0.3 or 30% to 0.5 or 50.

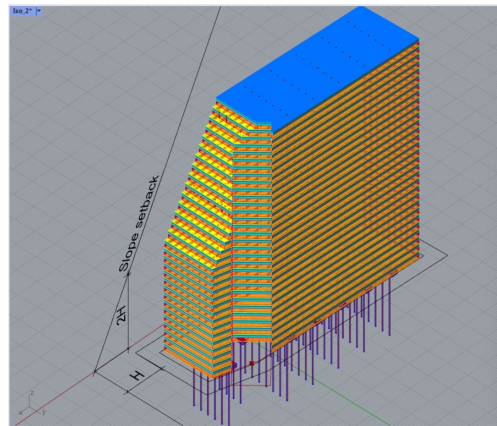


Figure 3. 3D model of the building mass in the conceptual mass stage.

2.2 Inputting a Material Database

In order to calculate the embodied carbon of the building during the early design phase when it is still a mass study, it was considered that the building includes foundations, piles, floors, columns, ceilings, exterior walls, interior walls, windows, doors, and roof slabs. Data on the GHG emissions of each material were gathered from the Environment Product Declarations (EPDs) database, and the information was compiled in an Excel file. Table 1 presents the building elements, materials, material density, and GHG embodied in each material.

Table 1. Building elements, materials, material density, and GHG embodied in each material.

Building elements	Materials	Density (kg/m ³)	Green House Gases Embodied (kg CO ₂ -eq/kg)
Foundations	Concrete	2,500	400
Piles	Concrete	2,500	400
Floors	Concrete	2,500	400
Columns	Concrete	2,500	400
Ceilings	Gypsum	1,200	636
Exterior walls	Brick	900	225
Interior walls	Brick	900	225
Windows	Glass and PVC Frame	50	11,400
Doors	Medium density fiberbord	6	57.4
Roof slabs	Concrete	2,500	400

2.3 Calculating the GHG Emissions from the LCA Database

The embodied carbon impact of a building can be calculated by multiplying the mass of each material (M) with its specific impact factor (IF) (Hollberg & Ruth, 2016). The mass of each material is calculated by multiplying its volume (V) with its density (D). The embodied carbon impact of all components is then added together to obtain the embodied carbon impact of the entire building, as shown in Equation (1).

$$I_E = \sum M(V \times D \times IF) \quad (1)$$

where I_E is the embodied carbon impact; M is the amount of specific material; and IF is the impact factor.

The building elements used for calculating the embodied carbon include foundations, piles, floors, columns, ceilings, exterior walls, interior walls, windows, doors, and roof slabs. The volume of floors, ceilings, and roofs can be calculated from the floor plates of the building mass, while the volume of exterior walls and windows can be calculated from the sides of the building mass. To calculate the volume of columns, piles, and foundations, the surface of the floor plates is divided into points of 8 x 8 meters, and then the piles and foundations are placed on the first floor plates, and columns are placed on all floor plates. The volume of these elements can be extracted accordingly. The volume of the interior walls is calculated by using the typical layout of small group office (Neufert & Neufert, 2012) divided by the floor plate area after deducting the building core areas. The number of possible office rooms per floor and the area of the building's core are then used to calculate the possible interior wall and door numbers according to the dimensions for Net Internal Area (NIA) floor areas defined for office (open plan) multiple occupation (RICS, 2018), as shown in Figure 4.

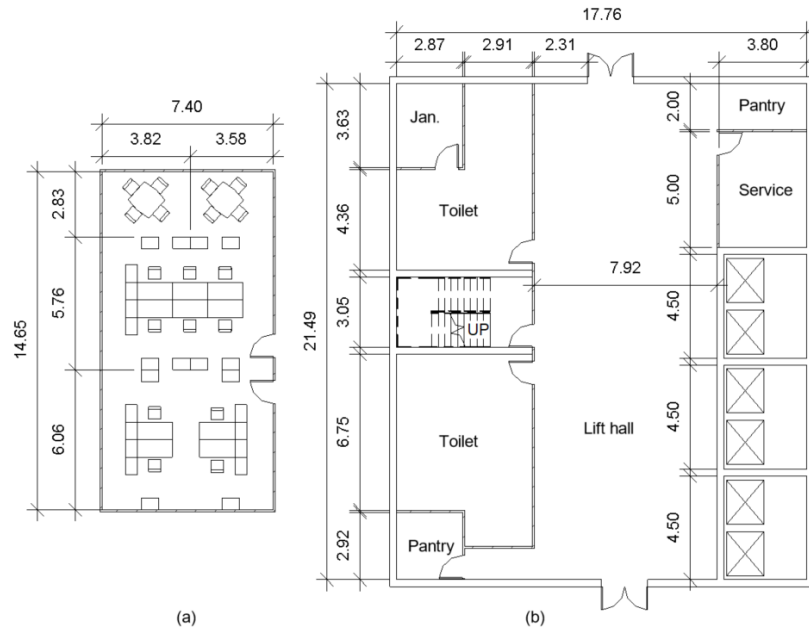


Figure 4. (a) Example layout of a small group office and (b) dimensions for NIA of an office building.

2.4 Optimizing the Building Mass

In this study, Galapagos, a Grasshopper plugin, was used to apply genetic algorithms (GA) for optimizing the building mass. GA is an optimization algorithm that simulates natural selection and the survival of the fittest to solve optimization problems. They have been shown to be effective in finding near-optimal solutions for complex problems with multiple objectives (González & Fiorito, 2015). However, implementing GA requires knowledge of computer programming and mathematics, which can be a barrier for many professionals. Galapagos is a tool developed by David Rutten that integrates GA into the Grasshopper software, providing an intuitive and accessible way for users to explore different optimization problems without needing advanced skills. With Galapagos, users can set up an optimization problem by defining the design variables, objectives, and constraints, and then let the algorithm run to find the best solution. This tool has the potential to make optimization more accessible to a wider range of professionals, allowing them to solve complex problems efficiently and effectively.

(1) Genomes

Genomes in genetic algorithms are the collection of parameters that define a potential solution to an optimization problem. In this study, genomes were used to define the parameters that influence the generating building mass in the optimization process. The building mass was generated in Rhinoceros, and a limited number of selected variables were managed through Grasshopper using genetic algorithms. The genomes used in this study included the base geometry of the building floor plates, which can be scaled and varied linearly from 0.00 to 1.00 in both the x and y directions, the height of the floor, which varied linearly from 3.5 to 4.00 meters, and the number of floor plates, which varied as a positive integer from 0 to 30 floors. Another genome was used to define a rectangle that trimmed the floor plates, which varied in width, length, and rotation on the XY plane. The final genome defined the proportion of the windows to walls, or WWR, which varied linearly from 30% to 50%. All of these genomes were used to generate the building mass that minimized greenhouse gas emissions and gross floor area, which were the objectives of the optimization process.

(2) Fitness Function

The fitness function in this study combines three objectives. The first objective is to maximize the GFA, the second objective is to minimize GHG emissions, and the third objective is to maximize the WWR within a range of 30% to 50%. When optimizing for multiple objectives, the challenge is to develop a fitness function that balances these objectives into a single value. They cannot be directly compared, as they have different units and scales. Therefore, it is by developing a custom script that normalizes all objectives, multiplies them by weighting factors, and then sums them together.

To maximize the GFA, the maximum floor area ratio (FAR) is used as the desired GFA to calculate the score. If the GFA equals the maximum FAR, the score is 1. The score decreases when the GFA is less than the desired GFA, and if it exceeds the desired GFA, the score is 0.

To minimize GHG emissions, the maximum possible GHG emissions are set to calculate the score. If the calculated GHG emissions equal 0, the score is 1. The score decreases when the GHG emissions increase, and if

they equal the maximum possible GHG emissions, the score is 0. If the GHG emissions are negative, the score is 0.

To maximize the WWR, a WWR of 50% is scored 1, and a WWR of 30% is scored 0.

The weights are multiplied by the three objectives. The GFA is weighted 3.5, the GHG emissions are weighted 5.5, and the WWR is weighted 1. The nodes used to calculate the scores are shown in Figure 5.

The scores with the weights of all objectives are added together to form a score out of 10. Then, we use 2 to the power of the score to form the exponential function, as shown in Equation (2). The top score is 2^{10} or 1024. The exponential function is a good way to separate lower scores from higher scores. If the GFA equals 0, the fitness function equals 0 as punishment in the case where 0 GFA produces the best GHG emissions.

$$\text{Total of fitness score} = 2^{(\text{GFA score} + \text{WWR score} + \text{GHG score})} \quad (2)$$

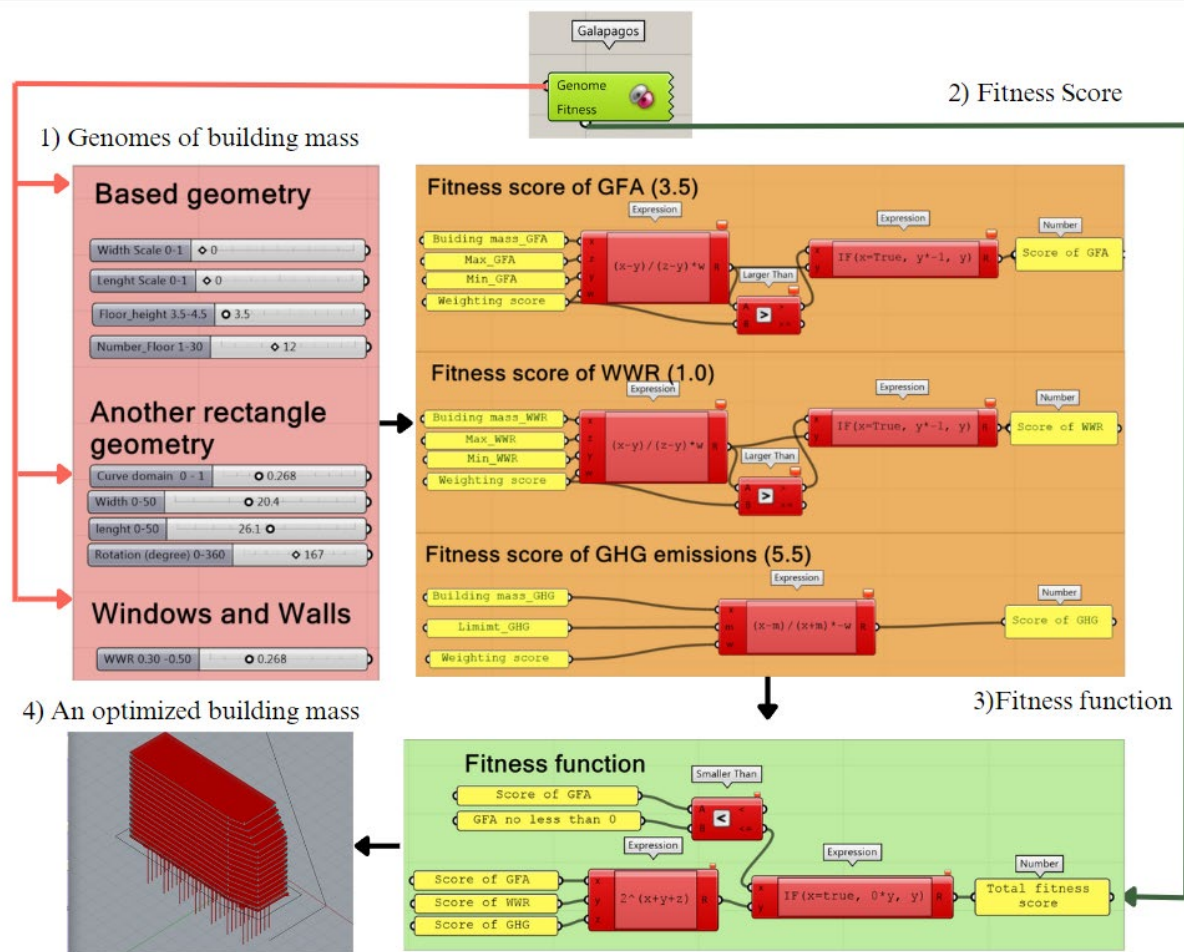


Figure 5. Genomes and fitness function of the prototype system.

(3) Galapagos Settings

In this study, the population was set at 50 individuals per generation with an initial boost of 2 individuals. Fifty percent of individuals were allowed to pass to the next generation, and a maximum inbreeding factor of 25% was ensured to maintain reasonable variability among generations. The maximum stagnation was set to stop the solver if there was no improvement in the fitness function after 50 generations. These settings were defined to balance simulation time and the accuracy of the optimization process.

3. CASE STUDIES

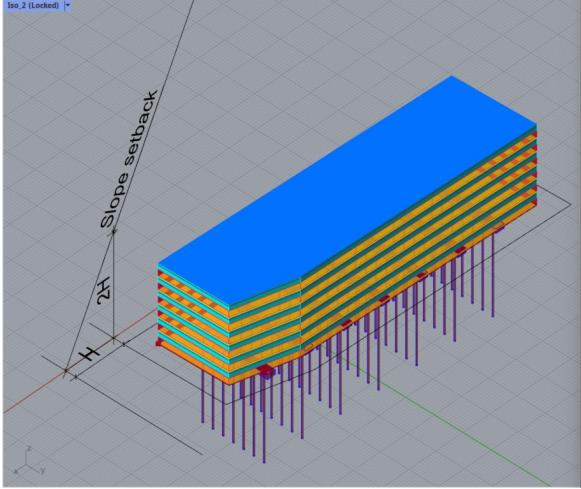
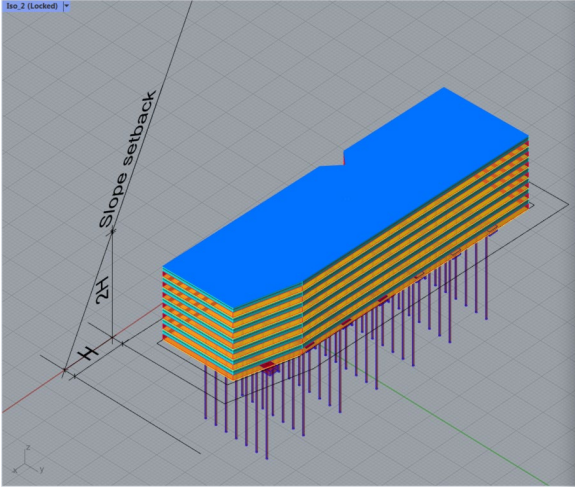
To test the proposed method, two case studies were conducted. Both studies used the same site boundary, but the first study aimed to optimize the GHG emissions of the GFA closest to 20,000 m², while the second study aimed to optimize the GHG emissions of the GFA closest to the maximum FAR. Before optimization, the building mass in each case was set by hand to the closest desired GFA (20,000 m² and maximum FAR). The results of the optimization are presented in Tables 2 and 3, which show the building mass before and after optimization. Additionally, the tables present important information such as the number of floors, floor height, building footprint

area, GFA, WWR, GHG emissions, fitness score, weighting total score, GFA score, WWR score, and GHG emission score.

3.1 Optimize the GHG Emissions of the GFA Closest to 20,000 m²

The first case study focused on optimizing GHG emissions for a building with a GFA closest to 20,000 m². The optimization process involved decreasing the floor height by 22.22% from 4.5 to 3.5 m, increasing the number of floors by 16.67% from 6 to 7, and reducing the building footprint by 6.66% from 2,610.98 m² to 2,437.08 m². As a result, the GFA increased from 17,955.89 to 19,983.20 m², while the (WWR remained unchanged at 0.5 or 50%. Moreover, the GHG emissions decreased from 8.15 x 10⁶ kg CO₂-eq to 7.85 x 10⁶ kg CO₂-eq, which represents an 3.68% reduction. The fitness score, weighting total score, GFA score, WWR score, and GHG emissions score were also improved, representing a difference of 52.65%, 13.41%, 17.06%, 0.00%, and 16.67%, respectively.

Table 2. Optimizing the GHG emissions of the GFA closest to 20,000 m².

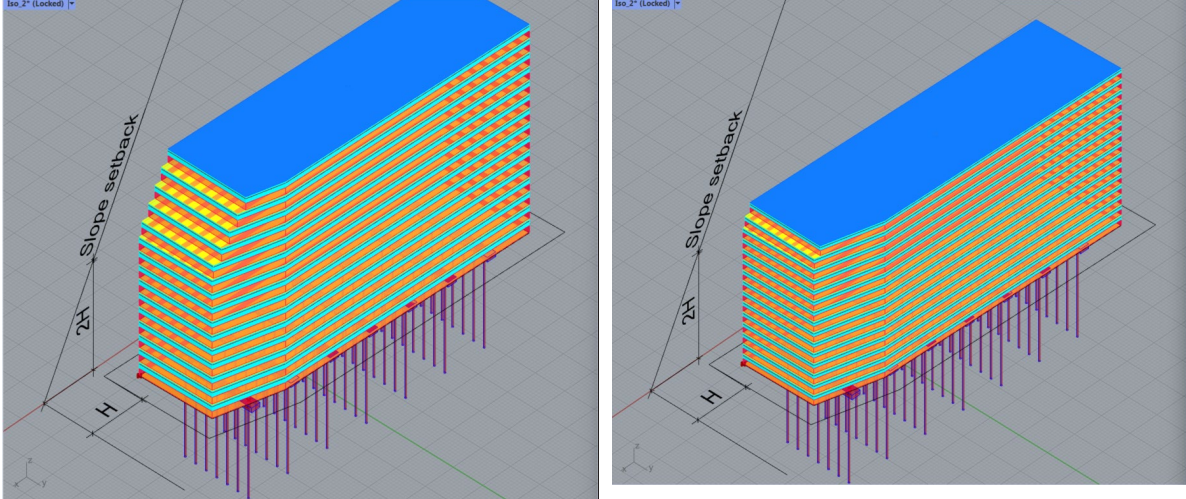
Site area: 4,717.54 m ²				
Maximum FAR: 47,175.40 m ²				
Maximum possible GHG emissions: 12 x 10 ⁶ kg CO ₂ -eq				
Desired GFA = 20,000 m ²				
				
Optimization	Before	After	Unit	Percentage difference
Number of floors	6	7	Storey	16.67%
Floor height	4.5	3.5	m	-22.22%
Building footprint	2,610.98	2,437.08	m ²	-6.66%
GFA	17,955.89	19,983.20	m ²	11.29%
WWR	0.50	0.50	-	0.00%
GHG emissions	8.15	7.85	x 10 ⁶ kg CO ₂ -eq	-3.68%
Fitness score = 2 ^(GFA+WWR+GHG score)	23.42	35.75	-	52.65%
Weighting total score = 10	4.55	5.16	-	13.41%
GFA score (3.5)	2.99	3.50	-	17.06%
WWR score (1)	1.00	1.00	-	0.00%
GHG emissions score (5.5)	0.50	0.66	-	16.67%
Solver runtime	90 minutes			

3.2 Optimize the GHG Emissions of the GFA Closest to the Maximum FAR

The second case study aimed to optimize GHG emissions for a building with a GFA closest to the maximum (FAR of 47,175.40 m²). The optimization process involved decreasing the floor height by 22.22% from 4.5 to 3.5 m, while the number of floors remained the same at 15 stories. The building footprint remained unchanged. The optimization resulted in an increase in GFA from 44,490.84 to 44,880.35 m², while the WWR remained unchanged at 0.5 or 50%. The GHG emissions were reduced from 18.19 x 10⁶ kg CO₂-eq to 15.73 x 10⁶ kg CO₂-eq, representing a 13.52% reduction. The fitness score, weighting total score, GFA score, WWR score, and GHG emissions score were also improved, representing a difference of 52.65%, 13.41%, 17.06%, 0.00%, and 16.67%, respectively.

and GHG emissions score were also improved, representing a difference of 35.68%, 9.82%, 1.24%, 0.00%, and 153.85%, respectively.

Table 3. Optimizing the GHG emissions of the GFA closest to the maximum FAR.

Site area: 4,717.54 m ²				
Maximum FAR: 47,175.40 m ²				
Maximum possible GHG emissions: 20 x 10 ⁶ kg CO ₂ -eq				
Desired GFA = 47,175 m ²				
				
Optimization	Before	After	Unit	Percentage difference
Number of floors	15	15	Storey	0.00%
Floor height	4.5	3.5	m	-22.22%
Building footprint	2,610.98	2,610.98	m ²	0.00%
GFA	44,490.84	44,880.35	m ²	0.88%
WWR	0.50	0.50	-	0.00%
GHG emissions	18.19	15.73	x 10 ⁶ kg CO ₂ -eq	-13.52%
Fitness score = 2 ^(GFA+WWR+GHG score)	22.31	30.27	-	35.68%
Weighting total score = 10	4.48	4.92	-	9.82%
GFA score (3.5)	3.22	3.26	-	1.24%
WWR score (1)	1.00	1.00	-	0.00%
GHG emissions score (5.5)	0.26	0.66	-	153.85%
Solver runtime	50 minutes			

5. CONCLUSION

The study developed a BIM-based system for assessing and optimizing GHG emissions in the early design stages of an office building. The prototype system used Grasshopper to generate a conceptual mass and calculate the GHG emission. The GA was used to optimize the building mass to minimize GHG emissions and maximize the GFA and WWR.

The results of the two case studies demonstrate that the proposed BIM-based system, which uses a genetic algorithm to optimize building mass, can effectively reduce GHG emissions in buildings. In the first case study, the building mass was optimized for a GFA closest to 20,000 m². The optimization resulted in a decrease in floor height and building footprint and an increase in the number of floors, which increased the GFA. The WWR remained constant. The optimization reduced GHG emissions by 3.68%. In the second case study, the building mass was optimized for a GFA closest to the maximum FAR of 47,175.40 m². The optimization resulted in a decrease in floor height, but the number of floors and building footprint remained constant. The GFA increased and the WWR remained constant. The optimization reduced GHG emissions by 13.52%. In both cases, the optimization resulted in significant improvements in the fitness score, weighting total score, and GHG emissions score, indicating that the optimization method was effective in reducing GHG emissions while increasing building size.

Overall, this study provides a valuable tool for architects to assess and optimize GHG emissions in the early design stages of their building projects. This study makes a significant contribution to the field of sustainable building design and underscores the importance of considering GHG emissions in the early design stages.

ACKNOWLEDGMENTS

The authors would like to thank the Thailand Science Research and Innovation Fund, Chulalongkorn University (SOC66250010), and the Faculty of Architecture at Chulalongkorn University.

REFERENCES

- Bernstein, W. Z., Tensa, M., Praniewicz, M., Kwon, S., and Ramanujan, D. (2020). An automated workflow for integrating environmental sustainability assessment into parametric part design through standard reference models, *Procedia CIRP*, 90, 102–108. <https://doi.org/10.1016/j.procir.2020.02.058>
- Budig, M., Heckmann, O., Hudert, M., Ng, A. Q. B., Xuereb Conti, Z., and Lork, C. J. H. (2021). Computational screening-LCA tools for early design stages, *International Journal of Architectural Computing*, 19(1), 6–22. <https://doi.org/10.1177/1478077120947996>
- Díaz, J., engineering, L. A.-C. in civil and building, & 2014, undefined. (2014). Sustainable construction approach through integration of LCA and BIM tools, *Ascelibrary.Org*, 283–290. <https://doi.org/10.1061/9780784413616.036>
- Eastman, C. M. C., Eastman, C. M. C., Teicholz, P., Sacks, R., and Liston, K. (2011). *BIM Handbook: A guide to building information modeling for owners, managers, designers, engineers and contractors*. John Wiley & Sons.
- Finkbeiner, M. (2014). *The International Standards as the Constitution of Life Cycle Assessment: The ISO 14040 Series and its Offspring* (pp. 85–106). Springer, Dordrecht. https://doi.org/10.1007/978-94-017-8697-3_3
- González, J. and Fiorito, F. (2015). Daylight design of office buildings: Optimisation of external solar shadings by using combined simulation methods, *Buildings*, 5(2), 560–580. <https://doi.org/10.3390/buildings5020560>
- Grubert, E. and Stokes-Draut, J. (2020). Mitigation life cycle assessment: Best practices from LCA of energy and water infrastructure that incurs impacts to mitigate harm, *Energies*, 13(4), 992.
- Hollberg, A., Kiss, B., Röck, M., Soust-Verdaguer, B., Wiberg, A. H., Lasvaux, S., Galimshina, A., and Habert, G. (2021). Review of visualising LCA results in the design process of buildings, *Building and Environment*, 190(December 2020). <https://doi.org/10.1016/j.buildenv.2020.107530>
- Hollberg, A. and Ruth, J. (2016). LCA in architectural design—a parametric approach, *International Journal of Life Cycle Assessment*, 21(7), 943–960. <https://doi.org/10.1007/s11367-016-1065-1>
- ISO. (2006). *Environmental Management - Life Cycle Assessment - Principles and Framework (ISO 14040:2006)*. Retrieved from website: <https://www.iso.org/standard/37456.html>
- Khosakitchalert, C., Yabuki, N., and Fukuda, T. (2020). Automated modification of compound elements for accurate BIM-based quantity takeoff, *Automation in Construction*, 113, 103142. <https://doi.org/10.1016/j.autcon.2020.103142>
- Lasvaux, S., Gantner, J., Schiopu, N., Nibel, S., Bazzana, M., Bosdevigie, B., and Sibiude, G. (2013). Towards a new generation of building LCA tools adapted to the building design process and to the user needs, *Sustainable Building*, September, 406–417.
- Lewis, E., Chamel, O., Mohsenin, M., Ots, E., and White, E. T. (2018). Architecture 2030, In *Sustainspeak* (pp. 24–26). <https://doi.org/10.4324/9781315270326-12>
- Nembrini, J., Samberger, S., and Labelle, G. (2014). Parametric scripting for early design performance simulation, *Energy and Buildings*, 68(PART C), 786–798. <https://doi.org/10.1016/J.ENBUILD.2013.09.044>
- Neufert, E. and Neufert, P. (2012). Neufert Architects’ Data Fourth Edition, In *Journal of Chemical Information and Modeling* (Vol. 53, Issue 9).
- RICS. (2018). *Code of Measuring Practice: A Guide for Property Professionals*. (Issue May). Retrieved from website: <https://www.rics.org/uk/upholding-professional-standards/sector-standards/real-estate/code-of-measuring-practice/>
- Sereewatthanawut, I., Pansuk, W., Pheinsusom, P., and Prasittisopin, L. (2021). Chloride-induced corrosion of a galvanized steel-embedded calcium sulfoaluminate stucco system, *Journal of Building Engineering*, 44, 103376. <https://doi.org/10.1016/j.job.2021.103376>
- Victoria, M. F., and Perera, S. (2018). Parametric embodied carbon prediction model for early stage estimating, *Energy and Buildings*, 168, 106–119. <https://doi.org/10.1016/j.enbuild.2018.02.044>

BIM-COBIE BASED BRIDGE-DEFECT INTEGRATED MODEL FOR CONDITION ASSESSMENT OF BRIDGE SUPERSTRUCTURE

Jung-Bin Lee¹, Sangho Lee², Inseop Yun³ and Sang-Ho Lee⁴

1) Research Assistant, Department of Civil and Environmental Engineering, Yonsei University, Seoul, South Korea. Email: j.b.lee@yonsei.ac.kr

2) Research Assistant, Department of Civil and Environmental Engineering, Yonsei University, Seoul, South Korea. Email: csemlsh@yonsei.ac.kr

3) Graduate Student, Department of Civil and Environmental Engineering, Yonsei University, Seoul, South Korea. Email: dbstdlstjq921@yonsei.ac.kr

4) Ph.D., Prof., Department of Civil and Environmental Engineering, Yonsei University, Seoul, South Korea. Email: lee@yonsei.ac.kr

Abstract: In this study, various types of defects occurring on bridges were expressed as object elements to create a Building Information Modeling (BIM)-based bridge-defect model, and a methodology was proposed to digitally assess the condition grade of the bridge affected by defects by generating Construction Operations Building information exchange (COBie) files to a database. The presented method determined the level of development of the bridge superstructure member, classified the 10 representative types of defect, and defined its properties that mainly occur in bridge superstructure to create the bridge-defect model. Then, bridge members and defect information were parameterized based on bridge alignment, and a method for modeling based on parameters using Revit Dynamo was suggested. COBie data was derived and extracted from the bridge-defect model through the Add-in program of the BIM authoring tool and managed through the Structured Query Language (SQL) program to evaluate the condition rating of the bridge. Most of the condition assessment process was automated by making it easy to reference and use the information required at each stage of the condition assessment. The developed methodology was validated through testing based on inspection data of actual bridges, and its practicality and efficiency were verified. This study can be expanded to the entire bridge and has yielded much more accurate results than existing methods. Information on each type of defect can be individually managed and flexibly utilized in other maintenance activities.

Keywords: BIM, COBie, Defect element, Bridge-defect model, Bridge superstructure, Condition assessment

1. INTRODUCTION

As the number of aging bridges is rapidly increasing worldwide, more efficient and advanced management technologies are required in the future compared to the existing management methods. In Korea, most bridge inspections are based on visual inspections, recording defects on 2D drawings and reports to manage the defects and determine bridge condition grades. While a considerable amount of inspection data is accumulated for each bridge, and various survey information from different sources is provided in database format, most management systems are highly inefficient because each piece of information is discrete, and difficult to reuse data for purposes beyond their predetermined objectives. Therefore, the defect information must be managed digitally to support systematic and efficient decision-making and perform in-depth analysis.

Utilizing Building Information Modeling (BIM), a representative technology in the construction industry for digitizing and managing project or structure information, can further advance and enhance the technology for maintaining aging bridges more efficiently. Damage management using BIM models facilitates cost savings and automates maintenance planning through clear visualization, data management, and evaluation. However, there are some challenges to overcome to utilize BIM technology in bridge maintenance due to problems with standardization in BIM-based management, workers' proficiency, and difficulties in the digital transformation of document-oriented data (Honghong et al., 2023).

Therefore, this study proposed a method to digitalize defects occurring in bridges as defect object elements, integrate them with the bridge model, and interconnect and utilize the information necessary for maintenance work. An integrated model was created, which was converted to Construction Operations Building information exchange (COBie) data, allowing for hierarchically structured transmission to manage maintenance information contained in the BIM model in a standardized manner. Finally, the study verified the practicality and usefulness of the approach by conducting a condition assessment based on damages on actual bridges.

2. LITERATURE REVIEW

Various attempts have been made to visually express, standardize, and manage the expression of damage occurring in structures using BIM technology for bridge maintenance. (Anil et al., 2016; Artus & Koch, 2020; Hamdan & Scherer, 2019; Hühwohl et al., 2018; Isailović et al., 2020). Ways to express damage, including location, amount, and severity, as a cube-type object using BIM software are presented (McGuire et al., 2016). A bridge management framework that integrates BIM technology and advanced computing and imaging technology

is proposed (Chan et al., 2016). The development of a next-generation integrated bridge inspection system, Seebridge, with bridge defect identification, classification, modeling, and visualization functions, was also carried out (Sacks et al., 2018). A bridge information modeling implementation framework that can allocate damage information to individual model elements and enable life-cycle bridge data management is proposed (Xu & Turkan, 2019).

The main focus of these existing studies is to propose new frameworks using BIM technology for bridge maintenance or to manage bridge damage by applying advanced technologies such as cutting-edge computing. On the other hand, there has been a lack of research on efficiently converting accumulated raw data from regular field inspections into standardized digital data, integrating it into a bridge model based on BIM, linking them with COBie, and using this information to support condition assessment. From a bridge maintenance perspective, damage data recorded in regular inspection reports should be reusable for engineering judgment in mid- to long-term bridge management and various maintenance tasks. Therefore, research on technologies that efficiently convert related data into BIM-based information and standardize information utilization methods for operational management is vital.

The most significant advantages and strengths of using COBie data derived from the proposed bridge damage model in this study for managing damage information are as follows:

1. It is easy to digitally model various defects expressed on the exterior damage map.
2. It efficiently utilizes raw data; such as defect quantity tables in spreadsheet format linked with COBie files.
3. Any modified, supplemented, deleted, or updated information in the bridge damage model or COBie files can be synchronized in real-time on the model and file.
4. It allows for easy database conversion of data supporting maintenance tasks and easy selection and utilization of only the necessary information for decision-making activities such as calculation, judgment, and evaluation through queries.

3. METHODOLOGY

The flowchart for managing bridge defects using BIM in this study is shown in Figure 1. The colors are expressed differently in each stage in the figure, and the corresponding color will be used to distinguish each step in the upcoming explanation. Each stage is described step by step in Chapter 4. In Step 1, to minimize memory usage when managing a bridge and defect models, which is necessary for maintenance tasks that require managing a significant number of facilities simultaneously, the scope of the representation that should be expressed to create an optimized maintenance model was defined, and family files were created for each object. Step 2 involves extracting basic information and parameters from the drawings required for model construction. Parameters were extracted from inspection data consisting of images and tables, and the properties of bridge components and defects were organized by objects in a spreadsheet. In Step 3, a model integrating the bridge and defects was created by conducting necessary modeling based on parameters using Revit Dynamo according to the defined model of bridge members and damage. Step 4 is the phase of damage information management and condition assessment using COBie data. COBie data was exported using the Add-in program of the BIM authoring tool, and structured query language (SQL) programs were used to manage COBie data. The procedure for the bridge condition assessment was programmed, and necessary information was extracted to automate most of the computational and judgment processes. The results of the condition grading evaluations for each type of damage and bridge member are managed in a spreadsheet composed of COBie data. Information is shared and obtained through an information linkage system based on identification codes within the bridge damage model. Furthermore, whenever information is added or updated in the integrated model or COBie file, it is simultaneously reflected on both sides.

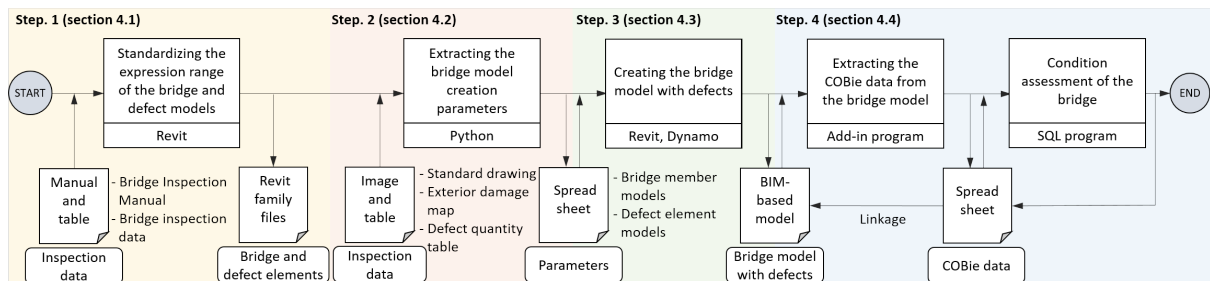


Figure 1. Flowchart of BIM-COBie defect information management










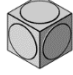
4. DIGITAL INFORMATION MODEL FOR CONDITION ASSESSMENT

4.1 Element Models of Defects and Bridge

For digital informatization of various defects, this study analyzed domestic and international bridge inspection manuals (AASHTO, 2003; Austroads, 2018; Caltrans, 2017; FHWA, 2012; IOWADOT, 2014; KISTEC,

2019; MnDOT, 2019; MTO, 2008; QGOV, 2016) and inspection reports to classify the types of defects and determine the significant attributes. It is necessary to classify and manage major defects that significantly impact the bridge's condition rather than deal with all types of defects to digitalize defect objects based on BIM and efficiently manage their information. The individual properties and the properties to be dealt with in general to quantitatively evaluate the bridge's condition by the type of damage that occurs in each part of the bridge are defined (Lee, 2022). In this study, nine defects frequently occurring in the bridge's superstructure were derived as representative defect items (crack, crazing, spalling, delamination, segregation, efflorescence, rebar exposure, failure, and a water leak). Lastly, 'other defect' was added to contain other damage. A total of 10 types of defects were classified and digitalized, as shown in Table 1. The defect element is in the form of a small cube, and on each face, the defect is symbolized and objectified to be easily distinguished. Damage has representative attributes that can express its characteristics, status, and level, and those attributes are used as properties for object models for each defect element. Defect elements were generated as family files in the form of individual objects to be used as primary data for bridge condition assessment by reflecting the characteristics and numerical values of defects collected during a bridge inspection.

Table 1. Shape and properties of damage models by type

Type and Shape	Required properties	General properties
 Crack (CR)  Crazing (CZ)  Scaling & Spalling (SC)  Delamination (DL)  Segregation (SG)  Efflorescence (EF)  Rebar Exposure (RE)  Failure (FA)  Water Leakage (WL)  ETC (ET)	Crack width Crack length Cracking ratio Damage length Damage width Damage area Damage rate Exposure length Exposure width Exposure rate Failure length Rate of failure(%) - Damage rate (%)	Defect type, Detailed damage type, Bridge defect ID, Grade of the damage, Latest inspection date, Repair status, Specifications

All defects to the bridge were investigated and analyzed to determine the scope of expression for each bridge member model that can be used in maintenance work. The elements each bridge member should represent were determined based on the importance of the defects considered in the condition assessment (Lee, 2022). The Level of Development (LOD) for each component was then set. Considering the condition assessment procedure, which involves determining the grade of individual members by dividing them into minimum units by span or point, the elements that should be represented according to the minimum unit for each component were included in the bridge component family files. Bridge member models ranging from LOD 200 to LOD 300 were created for the actual bridges to be applied in this study.

An identification code based on a standard classification code was used to manage information by linking the bridge and the defect model. The defined bridge object identification code is a code that can identify the location of damage by unit member based on the structural hierarchical division system of the bridge system (Kim, 2010). The sequence numbers are assigned in sequential order, from the starting point to the endpoint, left to right, to distinguish elements of the same type with multiple units. The identification code of the defect object consists of abbreviations that express information about the damage number and the type of defect (Lee et al., 2023). A unique identification code was input as property for each bridge and defect element model, enabling object-oriented information management by linking digital damage-related information to bridge members. The process

of creating the bridge member and defect element models and the framework for assigning identification codes to each object of the damage and bridge member models is shown in Figure 2.

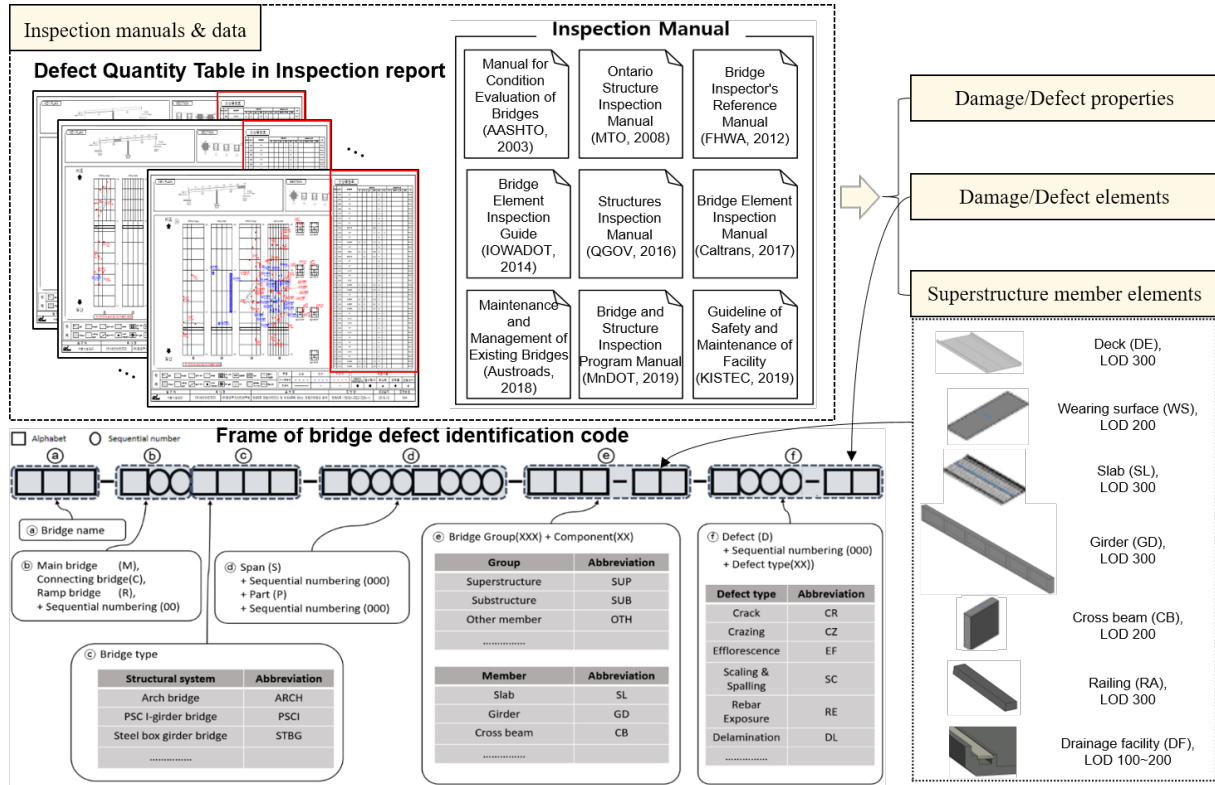


Figure 2. Process of standardizing the expression range of the bridge and defect element models

4.2 Parameter Extraction for the Bridge-Defect Model Creation

Properties and arrangement information of bridge members and defects must be organized in a specific format for each object to build a bridge-defect model using parameters. Standard drawing, defect quality table, and exterior damage map were used to obtain the information necessary to build the model. Since the location of various defects is integrally expressed in the drawing in symbol forms in the exterior damage map, obtaining individual damage locations is required. Therefore, to derive three-dimensional coordinates from the two-dimensional image, coordinates of the reference point of the bridge member's corners and the defect points indicated in the damage symbols were derived from the exterior damage map. The previously developed Python code (Kim, 2020) with the function of sequentially recording coordinates of selected points in the image was improved and utilized. These coordinates can be easily converted into three-dimensional linear coordinates on the BIM bridge model through the following equation (1) - (3) (Lee et al., 2023).

$$Y_{3D_d.p} = \frac{Y_{3D_e.p} - Y_{3D_s.p}}{Y_{2D_e.p} - Y_{2D_s.p}} \times (Y_{2D_d.p} - Y_{2D_s.p}) + Y_{3D_s.p} \quad (1)$$

$$Z_{3D_d.p} = \frac{Z_{3D_e.p} - Z_{3D_s.p}}{Y_{2D_e.p} - Y_{2D_s.p}} \times (Y_{2D_d.p} - Y_{2D_s.p}) + Z_{3D_s.p} \quad (2)$$

$$X_{param3D_d.p} = \frac{1}{X_{2D_e.p} - X_{2D_s.p}} \times (X_{2D_d.p} - X_{2D_s.p}) \quad (3)$$

Here, d.p represents the coordinates of each defect, s.p represents the starting point among the reference coordinates, and e.p represents the end point among the reference coordinates. Using the 2D coordinates (X_{2D} , Y_{2D}) of the extracted defect objects from the image, we can obtain the damage's 3D linear coordinates ($X_{param3D_d.p}$, $Y_{3D_d.p}$, $Z_{3D_d.p}$). When the linear coordinate-based arrangement concept is schematized, the Z-axis faces downward according to the direction of the X-axis centerline type of Revit used in this study. The three-dimensional linear location and attribute information for each defect object can be used to create the defect model collectively. Finally, the information extracted from the three data types was organized in a spreadsheet.

4.3 Bridge and Defect Integrated Information Model

The bridge-defect model was created by collectively placing defect objects with properties necessary for the damage assessment in the bridge superstructure model generated through the BIM authoring tools. The bridge model was created by placing bridge member objects based on the central alignment using data extracted from

standard drawings as parameters. For the placement of damage elements on the bridge model, the center of the occurrence location on the corresponding member of the bridge model was calculated, the placement reference point was matched using Revit Dynamo, and the properties were input. Figure 3 shows some key content of the Dynamo code developed to create a bridge-defect model automatically.

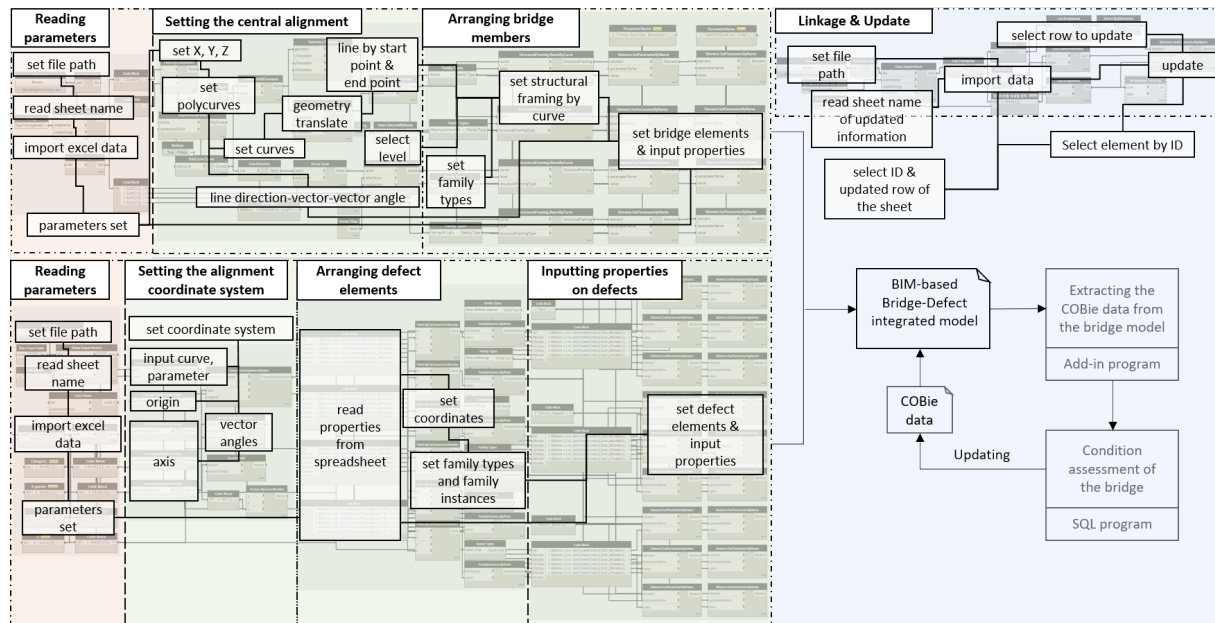


Figure 3. Key contents of developed Dynamo codes

4.4 Assessing Condition of a Bridge Using COBie

Identification codes and naming principles of COBie parameters based on the standard classification system must be established to hierarchically manage the components of each member of the bridge-defect model and condition assessment information for each bridge part. Through the BIM Interoperability Tool function, a property that allows for the input of COBie parameters for each model object was added, identification information for the bridge components and defect object elements was input into the added property, and COBie data was extracted. Among the output COBie data, the information stored in the Component sheet and Attribute sheet represents standardized digital data of bridge damage generated from the BIM model, which can be used to support engineering judgments, evaluations, and decision-making. The information in each COBie file sheet can be interdependent and managed object-oriented. Based on the individually sorted property data, a condition assessment of the bridge was performed according to the bridge maintenance guidelines. The guidelines provide rating criteria for each bridge member and defect type to determine each component's defect grade at each span or point. The minimum grade of defect grade at each span or point is determined as the final grade, and the final grade for each member is determined by the minimum grade at all spans or points. The member grades for all structural types are converted into defect indices, and the average for each member is calculated, taking into account the weight of each component, to obtain a weighted average. The resulting value is then used to calculate the final grade according to the corresponding defect degree score range. Table 2 shows the criteria for the grade based on the defect score range and the defect index.

Table 2. Defect index by grade and grade based on defect degree score range

Grade	Defect index	Defect degree score range
A	0.10	$0 \leq X < 0.13$
B	0.20	$0.13 \leq X < 0.26$
C	0.40	$0.26 \leq X < 0.49$
D	0.70	$0.49 \leq X < 0.79$
E	1.00	$0.79 \leq X$

The assessment results were linked to the model via external identifiers in the COBie data. In order to reconstruct the necessary data from the COBie file to support maintenance tasks such as condition assessment, the necessary damage element information and bridge element in the COBie file should be collected using a database management program that uses SQL as a standard. Information such as the maximum width of damage or the area ratio by type of defect required for condition grading can be automatically calculated and stored through SQL

queries using data from the defect element table, and the condition assessment of the bridge by part can be automated through appropriate programming techniques. Finally, Revit Dynamo was used to add the functionality of immediately reflecting changes in some data in the table to the BIM model. The key contents can be seen in Figure 3. These functions facilitate user-side decision-making of maintenance tasks and enable history management of damage and reflection of the latest model updates after maintenance.

5. CASE STUDY AND VALIDATION

BIM modeling and assessing conditions of defects were performed based on the safety inspection reports, exterior damage maps, and defect quantity tables to verify the effectiveness of the research results presented in Chapter 4. Two actual bridges were selected for verification: one was a concrete deck with a high incidence of damage to show the results by type of defect, and the other was the superstructure of a PSC I-girder bridge to show the results by bridge component.

5.1 Condition Assessment of the Concrete Deck

The bridge covered in the verification was a seven-span steel box girder bridge with a total length of 330m constructed in 1999. The condition assessment of the bridge was conducted on the concrete deck plate, focusing on four of the seven spans that had significant damage. The 384 damage records that occurred on the targeted floor panels were digitalized using defect elements. The research methodology was tested to determine if the condition assessment of the concrete deck could be performed using the built bridge maintenance BIM model. The accuracy of evaluation for each defect type was confirmed to be automated. The necessary values in the database could be calculated in conjunction with the developed programming code and the condition assessment process. The accuracy of the judgment process that determined the component condition grade based on the lowest rating among the evaluation results for each type of defect was also verified. Figure 4 shows the deck of the bridge-defect BIM model containing defects created through the research methodology and the condition assessment results. Defect elements were accurately placed in the model of each deck plate component by the coordinate transformation equations (1) - (3) and the developed Dynamo code by type of damage. Additionally, information necessary for the bridge's condition assessment and COBie parameters were well managed as properties for each defect element. By confirming that the condition assessment results are consistent with the safety inspection report results, the practicality and usefulness of the proposed method of creating a bridge maintenance model containing defects and linking it to COBie data to assess condition were validated through practical application.

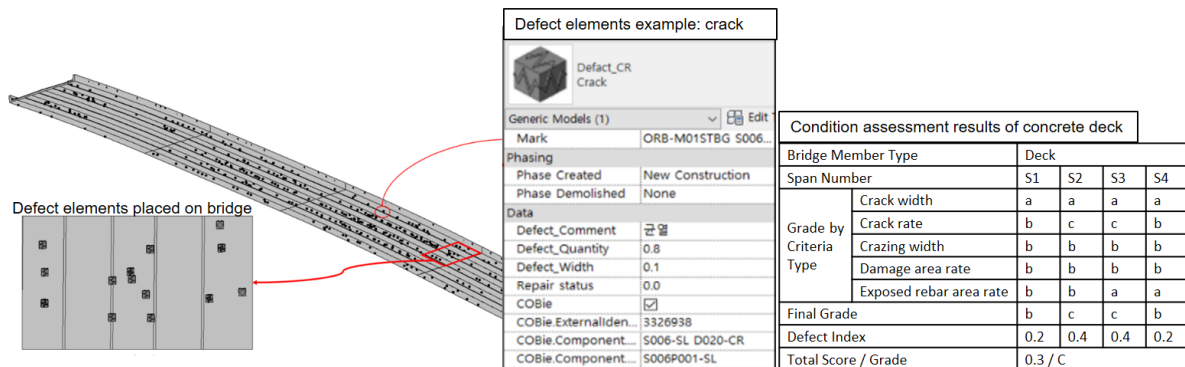


Figure 4. Results of the condition assessment of the concrete bridge deck model containing defect elements

5.2 Condition Assessment of the Superstructure of PSC I-girder Bridge

The second bridge selected to verify the effectiveness of the presented methodology is a four-span PSC I-girder bridge with a total length of 120 m built in 1994. 229 damage recorded in the inspection data and 128 bridge members constituting the bridge superstructure were implemented as BIM-based models by applying the method presented in Chapter 4. Based on the COBie data generated for each bridge member from the bridge-defect BIM model, the condition assessment results of the bridge were derived by automatically calculating the condition grade of the bridge through Dynamo and SQL programs. It was confirmed that all aspects were consistent by comparing the results with the safety inspection report of the verification bridge. The validity and effectiveness of the proposed methodology could be verified by reflecting the results directly in the BIM model and implementing the visualization of ratings according to the judgment grades of bridge members. Figure 5 shows the appearance of the bridge-defect model implemented as an integrated model, examples of the defect objects and properties managed in the model, and the condition assessment results.

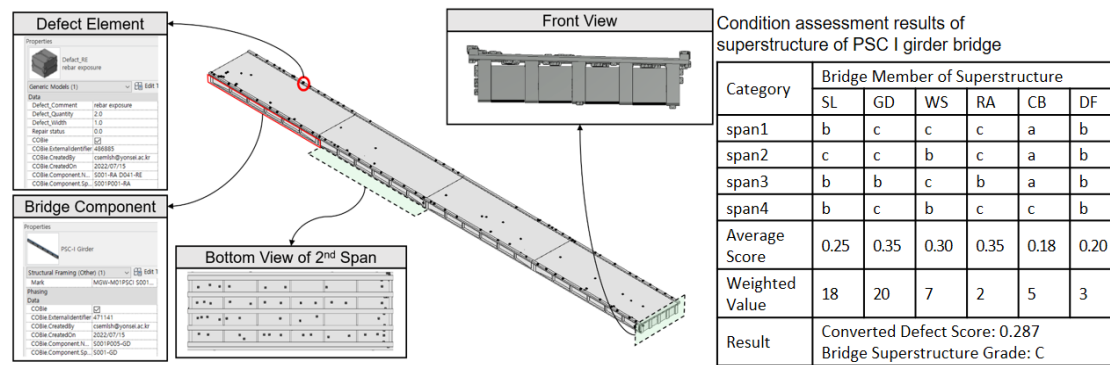


Figure 5. Overview of BIM-based bridge damage condition assessment model and the results

6. DISCUSSION AND CONCLUSIONS

This study proposed a method to generate a bridge-defect model using a developed Dynamo code by creating family models for each bridge component at the minimum level of detail that can contain maintenance information, classifying and objectifying defects into ten representative types according to the frequency of damage occurrence, defining and digitalizing defect properties in a standardized way. This study suggested parameterizing defect and bridge object information needed for the model formation and presenting a method to interlink the information of defect elements existing in the bridge components using identification codes. Additionally, this study developed a methodology to automatically perform condition assessment grading based on damage using COBie data and SQL program utilizing the constructed bridge-defect model.

To verify the core technology proposed in this study, the detailed process according to the condition assessment procedure was programmed for a concrete deck and the superstructure of a PSC I-girder bridge. The condition assessment results were compared with those recorded in the inspection report, thus verifying the effectiveness and efficiency of the proposed methodology, technology, and the accuracy of the developed tools. The digital transformation technologies presented in this study could be applied to various maintenance tasks for bridges when combined with history management, decision-making, and other interface technologies tailored to specific purposes.

ACKNOWLEDGMENTS

This work was supported by the National Research Foundation of Korea (NRF) grant funded by the Korea government (MSIT) (No. 2022R1A2C1092514).

REFERENCES

- American Association of State Highway and Transportation Officials (AASHTO) (2003). *Manual for Condition Evaluation of Bridges 2nd Edition*. Washington D.C.
- Anil, E.B., Akinci, B., Kurc, O., and Garrett, J.H. (2016). Building information modeling based earthquake damage assessment for reinforced concrete walls. *Journal of Computing in Civil Engineering*, 30 (4), 04015076.
- Artus, M. and Koch, C. (2020). Modeling geometry and semantics of physical damages using IFC. *Intelligent Computing in Engineering, Proceedings*, 144–153.
- Association of Australian and New Zealand Road Transport and Traffic Authorities (Austroads) (2018). *Maintenance and Management of Existing Bridges*. Australia.
- California Department of Transportation (Caltrans) (2017). *Bridge Element Inspection Manual*. California
- Chan, B., Guan, H., Hou, L., Jo, J., Blumenstein, M. and Wang, J. (2016). Defining a conceptual framework for the integration of modelling and advanced imaging for improving the reliability and efficiency of bridge assessments. *Journal of Civil Structural Health Monitoring*, 6 (4), 703-714.
- Federal Highway Administration (FHWA) (2012). *Bridge Inspector's Reference Manual*. FHWA NHI 12-049.
- Hamdan, A. and Scherer, R.J. (2019). A generic model for the digitalization of structural damage. *Life-Cycle Civil Engineering*, 2549–2556.
- Honghong, S., Gang, Y., Haijiang, L., Tian, Z., & Annan, J. (2023). Digital twin enhanced BIM to shape full life cycle digital transformation for bridge engineering. *Automation in Construction*, 147, 104736.
- Hüthwohl, P., Brilakis, I., Borrmann, A., and Sacks, R. (2018). Integrating RC bridge defect information into BIM models. *Journal of Computing in Civil Engineering*, 32 (3), 04018013.
- Iowa Department of Transportation (IOWADOT) (2014). *Bridge Element Inspection Guide*. Iowa.
- Isailović, D., Stojanovic, V., Trapp, M., Richter, R., Hajdin, R., and Döllner, J. (2020). Bridge damage: Detection, IFC-based semantic enrichment and visualization. *Automation in Construction*, 112, 103088.

- Kim, B. G. (2010). *Integration of a 3-D Bridge Model and Structured Information of Engineering Documents*. Doctoral Dissertation, Yonsei University, Seoul, Korea.
- Kim, J. S. (2020). *Extract mouse click coordinate values from an image*, Available at: https://gaussian37.github.io/vision-opencvcoordinate_extraction/ (Accessed: Feb. 10, 2020) (in Korean).
- Korea Infrastructure Safety and Technology Corporation (KISTEC) (2019). *Guideline of Safety and Maintenance of Facility (Safety Inspection and Diagnosis)* (in Korean).
- Lee, J. B. (2022). *IFC BIM-based Optimized Information Model Construction for Damage Condition Assessment of Cable Bridges*, M.S. Thesis, University of Yonsei, Seoul, Korea.
- Lee, S. Lee, J.B., Kim, J.H.J, and Lee, S.H. (2023). Digitalization of damage in concrete bridge deck using information modeling technique, *Journal of the Korea Concrete Institute*, 35 (2). (in press)
- McGuire, B., Atadero, R., Clevenger, C. and Ozbek, M. (2016). Bridge information modelling for inspection and evaluation. *Journal of Bridge Engineering*, 21 (4), 04015076.
- Ministry of Transportation (MTO) (2008). *Ontario Structure Inspection Manual*. Ontario, Canada.
- Minnesota Department of Transportation (MnDOT) (2019). *Bridge and Structure Inspection Program Manual*. State of Minnesota.
- Queensland Government (QGOV) (2016). *Structures Inspection Manual*. Queensland, Australia.
- Sacks, R., Kedar, A., Borrmann, A., Ma, L., Brilakis, I., Hühwohl, P., Simon, D., Uri, K., Raz, Y., Thomas, L., Burcu, E. B. and Sergej, M. (2018). SeeBridge as next generation bridge inspection: overview, information delivery manual and model view definition. *Automation in Construction*, 90, 134-145.
- Xu, Y. and Turkan, Y. (2019). BrIM and UAS for bridge inspections and management. *Engineering, Construction and Architectural Management*, 27 (3), 785-807.

SITUATION OF BIM IMPLEMENTATION IN COMPARISON BETWEEN THE NATIONAL UNIVERSITY OF SINGAPORE AND CHULALONGKORN UNIVERSITY

Gittigul Boonplien¹, Terdsak Tachakitkachorn², and Kaweekrai Srihiran³

1) Ph.D. Student, Department of Architecture, Faculty of Architecture, Chulalongkorn University, Bangkok, Thailand. Email: yoggbp@gmail.com

2) Ph.D., Asst. Prof., Architecture for Creative Community Research Unit, Department of Architecture, Faculty of Architecture, Chulalongkorn University, Bangkok, Thailand. Email: Terdsak.t@chula.ac.th

3) Assoc. Prof., Regional, Urban, and Built Environmental Analytics: RUBEA, Department of Architecture, Faculty of Architecture, Chulalongkorn University, Bangkok, Thailand. Email: Kaweekrai.s@chula.ac.th

Abstract: Building Information Modelling (BIM) is a part of the development of systems in the architecture, engineering, and construction (AEC) industry. It is acknowledged that the National University of Singapore (NUS) and Chulalongkorn University (CU) are the first educational institutions in the region to have led BIM since the 2010s. Nonetheless, Singapore is more substantially progressive than Thailand. Consequently, differences in level of implementation, standardization, and integration arise. For this reason, this research aims to study the BIM implementation on both Singapore and Thailand campuses. The objectives are to collect and compare the current BIM implementation and campus physical development plan by analyzing documents and interviewing those involved in this area.

As a result, this study found that Singapore possesses the BIM Roadmap, set up by the government, which has a standard and also integrates both professional and academic stakeholders. Hence, NUS built its own BIM standards. There is a prototype building for BIM operations, providing benefits for both learning and research. Whereas in Thailand, CU implements BIM into the campus physical development plan by gathering building data and utilizing it to manage some buildings on campus. In the case of a more complete level of implementation, it is still an incomplete process, unstandardized, and lacking the responsible organization for BIM implementation. However, the process of making the full system for BIM implementation part of the campus physical development plan will require modifications and developments in terms of academics, research and development, and responsible organization for the more complete implementation of BIM.

Keywords: BIM, BIM implementation, Campus physical development plan

1. INTRODUCTION

BIM also includes many of the capabilities needed to model the life cycle of a building, providing the basis for new design possibilities, changing roles, and relationships among project teams. Proper implementation of BIM facilitates a more integrated design and construction process, resulting in higher-quality buildings at lower costs and shorter project durations. (Eastman et al., 2011) That is a set of technologies and solutions that enable the 3D representation of geometric and functional attributes of building elements. Its objective is to improve the collaboration of different stakeholders and enhance productivity in the architecture, engineering, and construction (AEC) industry. (Jiang et al., 2022) Despite significant technical advancements in BIM, industry stakeholders have not completely embraced it or taken advantage of its undeniable advantages. AEC companies must make substantial investments in software, hardware, training, and other necessities for BIM adoption to be successful. (Ghaffarianhoseini et al., 2017) That depends on ongoing support from the many academic sectors, particularly the government, the main stakeholder. (Mustaffa et al., 2017) The awareness and experience of those involved in construction are expected to make BIM deployment easier. To aid in the decision-making process, more trustworthy information and statistics must be provided. (Rahim et al., 2021) Decision-makers can use the identified cluster of factors to perform various analyses of the BIM adoption process and to develop adoption strategies by providing information and observations within organizations. (Faisal Shehzad et al., 2022)

Since international governmental institutions have required and/or recommended that all public works be certified in the BIM methodology, public and private institutions and universities have developed ways to integrate BIM into their production and educational processes. (Besné et al., 2021) The physical campus is a space of special significance. It has affected the quality of students' lives, and it can reflect the academic atmosphere and scientific research level of universities and directly or indirectly affect the quality of education and teaching. (Zhao, 2022) The traits of a smart campus or digital campus include a personalized, collaborative, network-based, and intelligent Internet of Things. Early campus modelling using BIM and VR, followed by later building model display using VR and AR, is the ideal fusion of education, scientific research, management, and campus life. (Wu et al., 2021) The competitive advantage can be achieved with collaborative project delivery and productive information modelling. BIM is the use of a shared digital indicator of built environment data. (Grilo and Jardim-Goncalves 2010)

Universities are attempting to implement BIM into their curricula, whether for architecture, civil engineering, or building degrees, but they are doing so without the backing of a common strategy or standards. (Adamu et al., 2016) Such standards would help institutions make the leap to BIM by giving them guidelines to follow, which would accelerate the process, and by providing good practices. (Besné et al., 2021) Like the National University of Singapore (NUS), one of the BIM R&D Steering Committee members sets the Singapore BIM roadmap, concentrating on strategies, practices, and technologies operating towards overall construction productivity improvement and supporting local industry's BIM adoption attempts. (BCA, 2013a) NUS builds its own BIM standards. There is a prototype building for BIM operations, providing benefits for both learning and research. Whereas in Thailand, Chulalongkorn University (CU) implements BIM into the campus physical development plan by gathering building data and utilizing it to manage some buildings on campus.

This study is based on a review of NUS and CU as well as policy initiatives towards BIM adoption, while at the same time highlighting the level of implementation and adoption in the Singapore BIM Roadmap. This paper also highlights the relevant initiatives required to ensure the success of BIM implementation in the campus physical development plan.

2. BACKGROUND OF BIM IMPLEMENTATION

2.1.1 BIM Implementation in Singapore

Singapore is Asia's most notable pioneer in BIM implementation and has strict governmental BIM mandates (Zaia et al., 2023). That implemented and led a multiagency effort in 2008 to allow the world's first Building Information Modelling (BIM) electronic submission (e-submission) by the Building and Construction Authority (BCA) via the Construction Real Estate Network (CORENET). (Das et al., 2011) In 2009, Singapore's government created a BIM Roadmap Industry to aid in the adoption and implementation of BIM. (Fatt, 2011) BCA implemented the BIM Roadmap in 2010 with the aim that 80% of the construction industry will use BIM in 2015 and to improve the construction industry's productivity by up to 25% by 2025. (Das et al., 2011) aim to green 80% of our buildings' gross floor area by 2030 and provide platforms for the research and development of innovative green building solutions. (BCA, 2023) National BIM e-submission guidelines regulate and standardize the overall BIM adoption in the industry in Singapore. (Cheng and Lu, 2015) The BIM Guide aims to outline the various possible deliverables, processes, personnel, and professionals involved when BIM is being used in a construction project. to clarify the roles and responsibilities of project members, which are then captured in a BIM execution plan to be agreed upon between the employer and project members. (BCA, 2013b) Integrated Digital Delivery (IDD) is a whole-lifecycle project delivery approach introduced by BCA in 2017 that aims to digitally integrate the stakeholders and work activities involved in the value chain using digital technology. (Hwang et al., 2020).

Table.1 BIM implementation journey in Singapore

BIM goals/roadmap	BIM mandates	Regulator Standards/guidelines release and updates	Educator Training/courses	Funding agency BIM funds	Researcher R&D programs
<p>(2010–2015) 1st BIM roadmap: 1) Public sector taking the lead; 2) Regulatory approvals; 3) Removing impediments; 4) Building BIM capabilities and capacity; 5) Incentivizing BIM adopters</p> <p>(2016–2020) 2nd BIM roadmap: 1) Drive BIM collaboration throughout virtual design and construction (VDC); 2) BIM for design for manufacturing and assembly; 3) New training programs; 4) BIM for facility management and smart city; 5) R&D</p>	<p>(2012) BIM was mandatory as part of public sector building project procurement, (2013) Mandatory architecture BIM e-submission for all new building projects > 20,000 m², (2014) Mandatory engineering BIM e-submission for all new building projects > 20,000 m², (2015) Mandatory architecture and engineering BIM e-submission for all new building projects > 5000 m²</p>	<p>(2010-2011) E-submission guidelines, templates (2012-2013) Singapore BIM guide (2013-2015) BIM Particular Conditions, Standard for 3D Topographic Surveying, BIM Essential Guides (2016) Code of Practice for Building Information Modeling (BIM) e-Submission, BIM for DfMA (Design for Manufacturing and Assembly) Essential Guide (2017) Singapore VDC Guide (2018) BIM Guide for Asset Information Delivery</p>	<p>(Since 2011) Hosted by BCA Academy: 1) Training; 2) Handholding; 3) Outreach programs; 4) Certificate course; 5) Specialist diploma</p> <p>(Since 2016) new training programs at all levels</p>	<p>(2010-2018) BIM Fund: Construction Productivity and Capability Fund (CPCF)</p>	<p>The BIM Centre (Center of Excellence): 1) National University of Singapore (NUS) focus on the Life Cycle Approach; 2) Nanyang Technological University (NTU) focus on the pre-casting</p> <p>(Since 2016) R&D as one of the five strategies</p>

2.1.2 BIM Implementation in Thailand

In 2015, the Association of Siamese Architects under Royal Patronage (ASA) and the Institute of Siamese Architects created the Thailand BIM Guideline. (ASA, 2015) The Architect Council of Thailand (ACT), Council of Engineers (COE), and Engineering Institute of Thailand under H.M. the King's Patronage (EIT) created the BIM Guide in 2017. (ACT et al., 2017) According to the cooperation policy between the Federation of Thai Industries (FTI), the Thai BIM Association (TBIM), and the Siam Cement Public Company Limited (SCG), the Thailand BIM Object for Construction Material Guideline was created in 2022. (FTI et al., 2022)

Table.2 BIM implementation journey in Thailand

BIM goals/roadmap	BIM mandates	Regulator Standards/guidelines release and updates	Educator Training/courses	Funding agency BIM funds	Researcher R&D programs
Not yet	Some projects will appear in the Terms of Reference (TOR).	(2015) Thailand BIM Guideline (2017) BIM guide (2022) Thailand BIM Object for Construction Material Guideline	Academy: 1) Training; 2) Short Course 3) Certificate course; 4) Course levels in university	From Independent entity and Education agency	From Independent entity and Education agency

2.2.1 Campus Physical Development Plan in National University of Singapore (NUS)

To build up Singapore's BIM R&D capability, Center of Excellence (COEs) have been set up, one at the National University of Singapore (NUS). At the NUS BIM Centre, a BIM Integration Roadmap has been developed to augment the BIM capability of the Singapore Construction Industry for the up-and-coming areas related to BIM. A series of BIM research projects to develop and implement best practices focused on the Life Cycle Approach aims to transform BIM value, enhance BIM technology, and differentiate BIM education, research, and practice locally and globally. (Teo Ai Lin, 2014) The NUS Centre for 5G Digital Building Technology (5GDBT), hosted by the Department of the Built Environment, aims to increase productivity by using digital building technology innovation and practice to transform the way people design, deliver, and manage the built environment. (NUS, 2023a) Sustainability and climate action have gained impetus nationally with the launch of the inter-ministerial Singapore Green Plan 2030 and the NUS-developed Campus with three main goals: carbon neutrality at NUS 2030, a cool NUS Living Lab, and zero waste at NUS 2030. They do at University Campus Infrastructure (UCI) and will continue to integrate various goals and develop infrastructure to shape sustainable behaviors. (NUS, 2023b) The structure of the organization has been adjusted according to Table 3.

Table.3 Campus physical development organization of NUS, Singapore

NUS - University Campus Infrastructure (UCI)	Organizational Structure of UCI and Related offices				
	2015	2016	2019	2020	2023
Senior Vice-President (Campus Infrastructure)			✓	✓	
Vice-President (Campus Infrastructure)	✓	✓		✓	✓
Senior Director (Campus Operation & Maintenance)	✓	✓			
Assoc Vice-President (Campus Operation & Maintenance)			✓		
Assoc Vice-President (Campus Life)			✓		
Office of University Campus Infrastructure (Shared Services)	✓	✓	✓	✓	
U1 - Administrative Services Unit (ASU)					✓
U2 - Campus Planning & Management Unit (CPMU)					✓
U3 - Digital Transformation Unit (DTU)					✓
U4 - Sustainability Strategy Unit (SSU)					✓
D1 - Division of Campus Asset Management (DCAM)					✓
D2 - Division of Campus Emergency and Security (DCES)					✓
D3 - Division of Campus Life (DCL)					✓
Office of Environmental Sustainability (OES)	✓	✓	✓	✓	U4
Office of Estate Development (OED)	✓	✓	✓	✓	D1
Special Projects e.g., Utown, Yale-NUS, Transport System	✓	✓			
Office of Facilities Management (OFM)	✓	✓	✓	✓	D1
Office of Campus Amenities (OCA)	✓	✓	✓	✓	D3
Office of Safety, Health & Environment (OSHE)	✓	✓	✓	✓	
Office of Campus Security (OCS)	✓	✓	✓	✓	D2
Office of Housing Services (OHS)	✓	✓	✓	✓	D3
Conference & Events Management Unit (CEU)			✓	✓	D3
Sports & UTown Management Unit (SUU)			✓	✓	D3

Head Office Division Related offices

2.2.2 Campus Physical Development Plan in Chulalongkorn University (CU)

Chulalongkorn University (CU) was the first institution of higher learning established in Thailand. Founded by King Vajiravudh (King Rama VI) in March 1917 to take the lead in creating knowledge and innovations that will build and support a sustainable society in 2024. (CU, 2021) The Office of Physical Resources Management (PRM) has responsibility for building facilities that provide energy assistance to the environment. The remaining resources and transportation will provide an efficient and conducive atmosphere for learning, research, and operation to achieve the goals of the university. (CU, 2023) The campus area consists of 70% of the academic area, 10% of the government-occupied area, and 30% of the commercial area. CU developed its campus with five main goals: city within the city, architectural identity, university life, social distribution, and income. (CU, 2017) The structure of the organization has been adjusted according to Table 4.

Table.4 Campus physical development organization of CU, Thailand

CU - Office of Physical Resources Management (PRM)	Organizational Structure of PRM		
	2013	2016	2018 - Present
Vice President (Property and Physical Resources Management)	✓	✓	✓
Assistant Vice President (Property and Physical Resources Management)	✓	✓	✓
Administration	✓	✓	✓
Architecture and Infrastructure	✓	✓	D1
Facilities Management and Physical Information Systems	✓	✓	D2
Energy and Environment	✓	✓	D4
D1 - Building and Premises	✓	✓	✓
D2 - Planning, Design and Physical Information Systems			✓
D3 - Maintenance			✓
D4 - Infrastructure Energy Management and Environment			✓
D5 - Physical Contracts Management and Vehicles Management			✓

■ Head ■ Office ■ Division

3. CONCLUSION

This section clarifies Singapore's government started with BIM implementation for BIM mandates, led the way to BIM e-submission, and created a BIM Roadmap Industry in 2010 with the aim of enhancing BIM for the construction industry's productivity by up to 25% by 2025. They have had a national BIM guide and various guides for BIM users since 2012, as shown in Table 1. While Thailand has had a National BIM Guide and handbooks for BIM users since 2015, it does not yet have a BIM Roadmap or BIM e-submission agency, as shown in Table 2.

Accordingly, setting up a roadmap for a country obviously requires research, and the transformation of digital building permits (Beach et al., 2020) can provide input for policy formulation, BIM organization, information exchange capability, research area identification, promotion, presentation, and coordination of BIM for an effective BIM implementation in a country. (Wong et al., 2010) That relates to a successful BIM implementation, which depends on continuous support from the different rules and preferably the primary participant, which is the government. (Mustaffa et al., 2017) But the BIM implementation process differs across regions; this is due to the government's force, cultural diversity, building and construction practices, and inhabitants. (Faisal Shehzad et al., 2022) In generally developed nations, the mission of the government in supporting and transforming technology is significant to BIM's successful implementation in the AEC industry, and most of the main obstacles to BIM implementation involve the project stakeholders and people of technology. (Chan et al., 2019)

This section clarifies The NUS BIM Centre integrated BIM Roadmap of Singapore was developed from a series of BIM education, research, and practice initiatives focused on the life cycle approach aimed at digitization, such as the 5GDBT in the Department of the Built Environment. NUS is advancing campus sustainability and climate action for smart campuses in 2030, handled by University Campus Infrastructure (UCI). From data accumulation and review, this study found that:

- There was a change in the structure of the organization of NUS in 2023 by emphasizing the Digital Transformation Unit to support the management and the Sustainability Strategy, as shown in the red frame in Table 3. While CU aims to be a leader in creating knowledge and innovation that will create and support a sustainable society in 2024, this is handled by the Office of Physical Resources Management (PRM).
- There was a change in the structure of the organization of NUS in 2018 to present with a merger of Planning, Design, and Physical Information Systems, which is taking care of many aspects, not just digitalization, as shown in the red frame in Table 4.

The quality of the campus environment reflects the level of academic and research activity on campus. which directly or indirectly affects the quality of education and teaching. (Zhao, 2022) The smart campus will feature the Internet of Things, intelligent personal, collaborative, networked, and intelligent systems, and an advanced digital campus for the perfect combination of education, research, management, and campus life. (Wu et al., 2021) BIM training and conferences should be facilitated within the framework of university and industry

links. (Belay et al., 2021) Successful implementation of BIM requires substantial investment from AEC industries, including investments in software, hardware, training, and other requirements. (Ghaffarianhoseini et al., 2017) The competitive advantage can be achieved with collaborative project delivery with BIM through the use of a shared digital representation of built environment data. The main challenges to the construction industry are automation, digitization, economics, and return on investment. (Grilo and Jardim-Goncalves 2010)

Compared to existing BIM implementations, governments are important for adoption since they play a key role in the adoption of BIM as initiators and drivers, regulators, educators, funders, demonstrators, and researchers due to the rapid development of BIM technology through pilot and R&D initiatives. To help the industry and further develop knowledge of BIM. (Cheng and Lu, 2015) Anywise, the various agencies required and/or recommended buildings be certified in the BIM methodology, and the industries and universities have support to integrate BIM into their production and educational processes. To be competitive with BIM users, universities must be able to train their students, and it is necessary to apply BIM in education and research. (Vimonsatit and Htut, 2016)

This paper concludes that BIM is being used at just two universities. It does not include other universities that may have different levels of BIM implementation. Therefore, BIM implementation at the university level should focus on initiators and drivers, regulators, educators, funders, demonstrators, and researchers with universities and industry partners. To provide guidance at the national level to create a BIM roadmap and standards or guidelines. In addition, relevant agencies both at the university and national level should focus on enhancing digital transformation.

REFERENCES

- ACT, COE, EIT. (2017). *Building Information Modelling Guide*. Engineering Institute of Thailand under H.M. the King's Patronage (EIT).
- Adamu, Z., & Thorpe, T. (2016). How universities are teaching BIM: A review and case study from the UK. *Journal of Information Technology in Construction*, 21, 119-139.
- ASA. (2015). *Thailand BIM Guideline*. Association of Siamese architects under royal patronage (ASA) by Institute of Siamese architects.
- BCA (2013a). *BIM technology paves the way for greater industry collaboration*. Retrieved from The Building and Construction Authority (BCA) website: <https://www1.bca.gov.sg/about-us/news-and-publications/media-releases/2013/07/30/bim-technology-paves-the-way-for-greater-industry-collaboration/>
- BCA (2013b). *BIM technology paves the way for greater industry collaboration*. Retrieved from The Building and Construction Authority (BCA) website: https://www.corenet.gov.sg/media/586132/Singapore-BIM-Guide_V2.pdf/
- BCA (2023). *About BCA*. Retrieved from The Building and Construction Authority (BCA) website: <https://www1.bca.gov.sg/about-us/about-bca/> (Accessed 01.04.23).
- Beach, T. H., Hippolyte, J. L., & Rezgui, Y. (2020). Towards the adoption of automated regulatory compliance checking in the built environment. *Automation in construction*, 118, 103285.
- Belay, S., Goedert, J., Woldesenbet, A., & Rokooei, S. (2021). Comparison of BIM adoption models between public and private sectors through empirical investigation. *Advances in Civil Engineering*, 2021, 1-13.
- Besné, A., Pérez, M. Á., Necchi, S., Peña, E., Fonseca, D., Navarro, I., & Redondo, E. (2021). A systematic review of current strategies and methods for BIM implementation in the academic field. *Applied Sciences*, 11(12), 5530.
- Chan, D. W., Olawumi, T. O., & Ho, A. M. (2019). Perceived benefits of and barriers to Building Information Modelling (BIM) implementation in construction: The case of Hong Kong. *Journal of Building Engineering*, 25, 100764.
- Cheng, J. C., & Lu, Q. (2015). A review of the efforts and roles of the public sector for BIM adoption worldwide. *Journal of Information Technology in Construction (ITcon)*, 20(27), 442-478.
- CU. (2017). *100 years Land and Property Management Chulalongkorn University*. Office of Property Management, Chulalongkorn University (CU).
- CU. (2021). *Chulalongkorn University Sustainability Report 2020-2021*. Chulalongkorn University For Sustainable Development, Chulalongkorn University (CU).
- CU. (2023). *About Office of Physical Resources Management*. Retrieved from Office of Physical Resources Management (PRM), Chulalongkorn University (CU) website: <http://www.prm.chula.ac.th/about/history/>
- Das, J., Leng, L. E., Lee, P., Kiat, T. C., Palanisamy, L., Leong, N. K., & Jun, Z. H. (2011). All set for 2015: the BIM roadmap. *Build Smart-The BIM Issue*, (09).
- Eastman, C. M., Teicholz, P., Sacks, R., & Liston, K. (2011). *BIM handbook: A guide to building information modeling for owners, managers, designers, engineers and contractors*. John Wiley & Sons.

- Faisal Shehzad, H. M., Binti Ibrahim, R., Yusof, A. F., Mohamed khaidzir, K. A., Shawkat, S., & Ahmad, S. (2022). Recent developments of BIM adoption based on categorization, identification and factors: a systematic literature review. *International Journal of Construction Management*, 22(15), 3001-3013.
- Fatt, C. T. (2011). BIM Road Map For Singapore Construction Industry. *BIM Journal*.
- FTI, TBIM, SCG. (2022). *Thailand BIM Object for Construction Material Guideline*. Federation of Thai Industries (FTI).
- Ghaffarianhoseini, A., Tookey, J., Ghaffarianhoseini, A., Naismith, N., Azhar, S., Efimova, O., & Raahemifar, K. (2017). Building Information Modelling (BIM) uptake: Clear benefits, understanding its implementation, risks and challenges. *Renewable and sustainable energy reviews*, 75, 1046-1053.
- Grilo, A., & Jardim-Goncalves, R. (2010). Value proposition on interoperability of BIM and collaborative working environments. *Automation in construction*, 19(5), 522-530.
- Hwang, B. G., Ngo, J., & Her, P. W. Y. (2020). Integrated Digital Delivery: Implementation status and project performance in the Singapore construction industry. *Journal of Cleaner Production*, 262, 121396.
- Jiang, R., Wu, C., Lei, X., Shemery, A., Hampson, K. D., & Wu, P. (2022). Government efforts and roadmaps for building information modeling implementation: Lessons from Singapore, the UK and the US. *Engineering, Construction and Architectural Management*, 29(2), 782-818.
- Mustaffa, N. E., Salleh, R. M., & Ariffin, H. L. B. T. (2017). Experiences of Building Information Modelling (BIM) adoption in various countries. In *2017 International Conference on Research and Innovation in Information Systems (ICRIIS)*, pp. 1-7).
- NUS (2023a). *About Centre of 5G Digital Building Technology*. Retrieved from Department of the Built Environment (DBE), National University of Singapore (NUS) website: <https://cde.nus.edu.sg/dbe/5gdbt/about-us/overview/> (Accessed 01.04.23).
- NUS (2023b). *About University Campus Infrastructure*. Retrieved from University Campus Infrastructure (UCI), National University of Singapore (NUS) website: <https://uci.nus.edu.sg/about-us/>
- Rahim, N. S. A., Zakaria, S. A. S., Romeli, N., Ishak, N., & Losavanh, S. (2021, November). Application of Building Information Modeling toward Social Sustainability. In IOP Conference Series: *Earth and Environmental Science*, 920 (1), 012007.
- Teo Ai Lin, E. (2014). Singapore BIM Roadmap: An Update. *BIM forum & academic conference 2014*, 11, 42-44.
- Vimonsatit, V., & Htut, T. (2016). Civil Engineering students' response to visualisation learning experience with building information model. *Australasian Journal of Engineering Education*, 21(1), 27-38.
- Wong, A. K., Wong, F. K., & Nadeem, A. (2010). Attributes of building information modelling implementations in various countries. *Architectural engineering and design management*, 6(4), 288-302.
- Wu, B., Hao, R., Li, H., Chai, Q., & Wang, Y. (2021). Research on intelligent campus system design based on BIM & VR/AR technology. In *Journal of Physics: Conference Series*, 1885 (5), 052050.
- Zaia, Y. Y., Adam, S. M., & Abdulrahman, F. H. (2023). Investigating BIM level in Iraqi construction industry. *Ain Shams Engineering Journal*, 14(3), 101881.
- Zhao, L. (2022). *Security Design of University Campus Landscape Based on BIM*. Wireless Communications and Mobile Computing, 2022.

STRATEGIC DEVELOPMENT OF BUILDING INFORMATION MODELING (BIM) IMPLEMENTATION FOR THAI CONSTRUCTION CONTRACTORS

Parit Martpaijit¹, and Vachara Peansupap²

1) Department of Civil Engineering, Faculty of Engineering, Chulalongkorn University, Bangkok, Thailand. Email: 6372088621@student.chula.ac.th

2) Ph.D., Assoc. Prof., Department of Civil Engineering, Faculty of Engineering, Chulalongkorn University, Bangkok, Thailand. Email: vachara.p@chula.ac.th

Abstract: Currently, BIM implementation is found in complex procedures involving people, processes, technology, and strategy. These characteristics may cause unsuccessful BIM implementation, adversely affecting several construction processes. Since the implementation of BIM is still new to the Thai construction industry; it requires a study of the factors affecting the construction organization. This research aims to study internal and external factors by applying SWOT analysis tools to analyze strengths, weaknesses, opportunities, and threats in BIM implementation for Thai construction contractors. The data analysis revealed that certain opportunities for BIM implementation in Thai contractor organizations differed when compared to contractor organizations in foreign countries. For instance, one notable difference is the absence of BIM regulations in the Thai construction industry. Moreover, they share similar weaknesses with contractor organizations in foreign countries, including the high cost of implementation and the time required to learn the program. Lastly, by utilizing all four factors, strategies will be developed through the TOWS matrix to promote and recommend suitable strategies for BIM implementation in Thai construction contractors. For example, an experimental BIM strategy could be employed for a pilot study, which would assess its advantages and disadvantages to inform future projects.

Keywords: Building Information Modeling, SWOT factors, BIM Implementation, Strategy

1. INTRODUCTION

Nowadays, construction projects are increasingly large and complex, resulting in conflicts during the construction process. These conflicts can arise from conflicting construction designs, unadjusted construction drawings, an excessive amount of material, inaccurate price estimates, and more. These issues result in delivery delays and higher construction costs. To address these challenges, the concept of Building Information Modeling (BIM) has been developed, which is a process that uses computer technology and software for building modeling (Williams, 2017).

According to a study of the construction of office buildings in Warsaw, it was found that BIM can be up to 10% faster than traditional design methods and up to 80% more accurate during the design phase. This results in reduced design corrections and changes. Furthermore, BIM can be applied to every process in a construction project, from the start of the project until maintenance after construction is completed (Czmoch & Pękala, 2014).

The application of BIM depends on the nature of the work and the liability of each organization in the construction industry. For instance, architects can apply BIM to provide a better view and overview of the project using 3D models, while contractors can use BIM to reduce errors in the construction site, save work time, and lower construction costs. Owners can also use BIM to reduce work time and increase work productivity (McGraw-Hill, 2009).

Implementation of building technology, including BIM, requires effective study and management. This approach has been successful in both enterprise and industrial applications. The use of information technology in architecture necessitates the joint development of strategies and tactics (Betts, 1995), such as establishing the CORENET project. Singapore's construction and real estate network plans to restructure the business processes of the construction industry to achieve a leap in productivity, quality, and timeliness through the application of building technology.

Especially since the implementation of BIM is still new to the Thai construction industry, it requires a study of the factors affecting the construction organization. This research aims to study internal and external factors by applying SWOT analysis tools to analyze strengths, weaknesses, opportunities, and threats in BIM implementation for Thai construction contractors. The factors obtained will be used to develop strategies for the implementation of BIM for Thai construction contractors by applying TOWS matrix.

2. LITERATURE STUDIES

2.1 Identify Factors That Affect BIM Implementation in Organizations.

This research uses SWOT analysis as a tool to evaluate the situation and determine strategic factors by analyzing internal and external factors. According to past research, there are many factors that affect BIM implementation for construction contractors.

(1) Internal Factors

Strength (S) is a positive ability and internal environment that can be used for organizational development as shown in Table 1.

Table 1. Strength factors affecting BIM implementation in contractor organizations.

List	Factors	Reference
Strength Factors (S)		
S1	Intelligent modeling process reduce errors that may occur from personnel.	(1), (2), (4)
S2	BIM technology can create 3D building models quickly and easily.	(1), (2), (4)
S3	Operations with BIM technology helps to organize the construction process.	(1), (3), (5)
S4	BIM reduces errors and avoids risks that may occur during construction.	(1), (3)
S5	BIM technology analyzes usage or contributes to reductions in energy consumption over the entire lifecycle.	(1), (4)
S6	BIM technology improves the quality and management of information and documents.	(1), (3)
S7	BIM reduces operational errors before the actual construction.	(1), (2)
S8	BIM technology promotes good synergies between architecture, structure, and system work.	(1), (5)

Weakness (W) is the ability and situation within the organization in a negative way that cannot be used for the purpose of working to achieve the objectives and needs to be corrected as shown in Table 2.

Table 2. Weakness factors affecting BIM implementation in contractor organizations.

List	Factors	Reference Number
Weakness Factors (W)		
W1	BIM technology requires high operating costs of software and supporting hardware.	(1), (6), (7), (8)
W2	BIM is necessary to apply BIM from beginning to end.	(11), (12)
W3	BIM tools require a long period of learning and understanding.	(2), (7)
W4	BIM technology is designed to focus on modeling rather than building information.	(6), (8)
W5	BIM implementation in different sectors has resulted in reduced workflow flexibility compared to traditional workflows.	(2), (6), (9), (10)
W6	BIM software can lead to issues with data transmission between software.	(2)
W7	BIM technology often encounters processing errors in building virtual reality models based on software errors. and system work.	(2)
W8	BIM requires high-quality labor to develop the correct BIM model.	(2), (6), (7), (12)

(2) External Factors

Opportunity (O) are external situations that is conducive to the development and driving the work of the organization to success as shown in Table 3.

Table 3. Opportunity factors affecting BIM implementation in contractor organizations.

List	Factors	REF
Opportunity Factors (O)		
O1	BIM technology is applicable in government procurement in many countries. It gives Thai companies the opportunity to expand their markets and work with companies in those countries.	(1), (6), (8), (9)
O2	BIM adoption is an opportunity to connect with international BIM leaders in education and the construction industry	(2), (6)
O3	BIM may be a key process for future implementation of architectural design and construction, therefore requiring knowledgeable workforce.	(2), (6), (7)
O4	Implementation of BIM develops new skills and knowledge of organizational personnel.	(2), (6), (11)
O5	Construction market leaders are increasingly interested in BIM, leading to an increase in BIM investment in the construction industry.	(6), (10), (13)
O6	BIM education and knowledge promotion will make the use of BIM more widespread in the future.	(14), (15)

Threat (T) are external situations that impede development and drive success of the organization as shown in Table 4

Table 4. Threat factors affecting BIM implementation in contractor organizations.

List	Factors	REF
Threat Factors (T)		
T1	Lack of knowledge gathering on BIM technology from academics and experts. As a result, it is difficult to study and apply BIM.	(1), (6), (9), (11)
T2	The construction industry in Thailand lacks personnel with BIM knowledge and capabilities.	(2), (6)
T3	Stakeholders in the construction industry lack confidence and knowledge in using BIM technology in construction projects.	(1), (7), (12)
T4	BIM implementation may lead to changes in the traditional working methods of the construction industry.	(1), (6), (8)
T5	The limited number of companies using BIM technology in the Thai construction industry has led to a decrease in the demand for BIM personnel in the industry.	(1), (6), (9), (10)
T6	Lack of support from the government.	(1), (6)
T7	There are no legal regulations and binding standards regarding BIM in Thailand.	(6), (12)

Note: (1) = (Utomo & Rohman, 2019), (2) = (Azhar, 2011), (3) = (Pickup, 2013), (4) = (Chimhundu, 2016), (5) = (Smith, 2014), (6) = (Ben Mahmoud et al., 2022), (7) = (Siebelink et al., 2020), (8) = (Leśniak et al., 2021), (9) = (Majrouhi Sardroud et al., 2018), (10) = (Ahmed, 2018), (11) = (Enshassi et al., 2019), (12) = (Zima et al., 2020), (13) = (McGraw-Hill, 2009), (14) = (Odubiyi et al., 2019), (15) = (Manzoor et al., 2021)

3. RESEARCH METHODOLOGY

This research is survey research in which the researcher uses a questionnaire as a tool to collect data and analyze the study results by statistical mean factor analysis and analysis of possible strategies for BIM implementation for Thai construction contractors.

3.1 Data Collection

This research uses a questionnaire as a data collection tool for the sample. The sample group of the questionnaire is personnel of Thai construction contractor. Determine the appropriate and sufficient minimum sample size by using the following methods: The central limit theorem should have not less than 30 samples (Kwak & Kim, 2017). This research has collected data from 32 samples with steps The process of constructing the questionnaire for data collection is as follows:

(1) Study the concepts and literature related to factors and strategies in applying BIM in the organization.

(2) Develop questions from the literature review. It is divided into 3 parts as follows:

Part 1: Question about general information of the respondents. This is general information, including the name of the organization, and work experience.

Part 2: Question about BIM application status, including BIM work experience, the meaning of BIM from work experience, and characteristics of the use of BIM concepts in organizations.

Part 3: Survey to assess the strengths, weaknesses, opportunities, and threats of BIM implementation for Thai construction contractors. It consists of 8 strength factors, 8 weakness factors, 6 opportunities factors, and 7 threat factors.

3.2 Analyzing Data

The data obtained from the survey will be used for statistical calculations and make a comparative analysis to find the application strategy of BIM implementation for Thai construction contractors according from data collecting as follows:

Part 1: General information of respondents. Researchers use the data to allocate frequency and calculate percentages.

Part 2: BIM application status. Researchers use data to allocate frequencies and calculate percentages.

Part 3: Analyzes strengths, weaknesses, opportunities, and threats of BIM implementation for Thai contractor organizations. Using statistics and presenting the analysis results as a table for accompanying the lecture.

4. RESULTS

4.1 Identification of Factors

According to data of respondents, 32 sample companies responded.

In a question about work experience, it was found that the proportion of the first respondents was “more than 5 years” or 59% as shown in Table 5

Table 5. Data of respondents about work experience

Range	Frequency	Percentages
More than 5 years	19	59%
3-5 years	7	22%
1-3 years	5	16%
Less than 1 year	1	3%
Total	32	100%

In a question about BIM work experience, it was found that the proportion of the first respondents was “1-3 years” or 41% as shown in Table 6

Table 6. Data of respondents about BIM work experience

Range	Frequency	Percentages
More than 5 years	3	9%
3-5 years	8	25%
1-3 years	13	41%
Less than 1 year	5	16%
No Experience	3	9%
Total	32	100%

In a question about the meaning of BIM from work experience, it was found that the proportion of the first respondents was “BIM is Collaboration Process” and “BIM is Creation of 3D Model) or 75% of respondents as shown in Table 7

Table 7. Data of respondents about the meaning of BIM from work experience

Meaning of BIM	Frequency	Percentages
Collaboration Process	24	75%
Creation of 3D Model	24	75%
3D Visualization	22	69%
3D Software	20	63%
Construction Documentation	18	56%
Data and Information	17	53%

In a question about characteristics of the use of BIM concepts in organizations, it was found that the proportion of the first respondents was “Construction Method and Process” or 75% as shown in Table 8

Table 8. Data of respondents about characteristics of the use of BIM concepts in organizations

Characteristics of the use of BIM	Frequency	Percentages
Construction Method and Process	24	75%
Construction Documentation	22	69%
Cost Estimation	20	63%
Design Analysis	19	59%
Bidding and Procurement	16	50%
Time Planning and Scheduling	15	47%

The result from calculating the weighted arithmetic mean score of the strength factors found that the first rank was “BIM technology promotes good synergies between architecture, structure, and system work”, Average score 4.66 points. For weakness factors the first rank was “BIM technology requires high operating costs of software, supporting hardware, and high costs of training.”, Average score 4.25 points as shown in Table 9.

Table 9. Top 4 mean score of strength factors and weakness factors

Strength factors	Score	Weakness factors	Score
BIM technology promotes good synergies between architecture, structure, and system work.	4.65	BIM requires high-quality labor to develop the correct BIM model.	4.31
BIM reduces errors and avoids risks that may occur during construction.	4.48	BIM is necessary to apply BIM from beginning to end.	4.26
BIM reduces operational errors before the actual construction.	4.44	BIM technology requires high operating costs for software and supporting hardware.	4.24
Operations with BIM technology helps to organize the construction process.	4.29	BIM tools require a long period of learning and understanding.	4.13

For opportunity factors the first rank was “BIM may be a key process for future implementation of architectural design and construction, therefore requiring knowledgeable workforce.”, Average score 4.59 points. For Threat factors the first rank was “Lack of support from the government.”, Average score 4.28 points as shown in Table 10.

Table 10. Top 4 mean score of opportunity factors and Threat factors

Opportunity factors	Score	Threat factors	Score
BIM education and knowledge promotion will make the use of BIM more widespread in the future.	4.58	Lack of support from the government.	4.37
BIM may be a key process for future implementation of architectural design and construction, therefore requiring a knowledgeable workforce.	4.52	There are no legal regulations and binding standards regarding BIM in Thailand.	4.34
Construction market leaders are increasingly interested in BIM, leading to an increase in BIM investment in the construction industry.	4.39	Lack of knowledge gathering on BIM technology from academics and experts. As a result, it is difficult to study and apply for BIM.	4.13
Implementation of BIM develops new skills and knowledge of organizational personnel.	4.35	The construction industry in Thailand lacks personnel with BIM knowledge and capabilities.	4.08

4.2 BIM Strategy Development

After analyzing the internal and external factors of BIM implementation to identify strengths, weaknesses, opportunities, and threats, the next step is to utilize the TOWS matrix tool for strategy development. The TOWS matrix is a strategic tool that generates new strategies based on the organization's current environment by aligning internal and external factors identified in the SWOT analysis, as depicted in Figure 1. Based on the matching between internal and external factors, four strategies can be created as follows.

- Strength-Opportunity (SO) are strategies that use strengths to maximize opportunities.
- Weakness-Opportunity (WO) are strategies that minimize weaknesses by taking advantage of opportunities.
- Strength-Threat (ST) are strategies that use strengths to minimize threats.
- Weakness-Threat (WT) are strategies that minimize weaknesses and avoid threats.

Contractor Firm

	Strength Factors S1. BIM technology promotes good synergies between architecture, structure, and system work. S2. BIM reduces errors and avoids risks that may occur during construction. S3. BIM reduces operational errors before the actual construction. S4. Operations with BIM technology helps to organize the construction process.	Weakness Factors W1. BIM requires high-quality labor to develop the correct BIM model. W2. BIM is necessary to apply BIM from beginning to end. W3. BIM technology requires high operating costs for software and supporting hardware. W4. BIM tools require a long period of learning and understanding.
Opportunity Factors O1. BIM education and knowledge promotion will make the use of BIM more widespread in the future. O2. BIM may be a key process for future implementation of architectural design and construction, therefore requiring a knowledgeable workforce. O3. Construction market leaders are increasingly interested in BIM, leading to an increase in BIM investment in the construction industry. O4. Implementation of BIM develops new skills and knowledge of organizational personnel.	(S1O1) Utilize the concept of BIM to introduce BIM based work, accelerate the development of organizational potential, and increase opportunities for working abroad. (S3O4) Establish a training center to develop personnel for the organization, reduce outsourcing costs, and improve the company's image.	(W2O4) Create an experimental strategy for BIM in the pilot study and be prepared to examine the advantages and limitations of other development projects. (W4O3) Develop a strategy to identify companies with specific abilities to form partnerships and help train employees in areas where the company still has weaknesses.
Threat Factors T1. Lack of support from the government. T2. There are no legal regulations and binding standards regarding BIM in Thailand. T3. Lack of knowledge gathering on BIM technology from academics and experts. As a result, it is difficult to study and apply for BIM. T4. The construction industry in Thailand lacks personnel with BIM knowledge and capabilities.	(S1S2S3S4T2) Develop corporate standards or refer to international standards and adapt them accordingly. (S1S2S3T4) Develop the potential of suppliers by organizing training sessions for those involved in BIM use, to enhance the work of main contractors and promote collaboration among them.	(W2T4) Begin by learning how to apply and experiment in specific construction stages, and then make necessary adjustments in subsequent stages.

Figure 1. TOWS matrix of factors for BIM implementation among Thai construction contractors.

5. DISCUSSIONS

The first purpose of this study is to analyze the strengths, weaknesses, opportunities, and threats of BIM implementation for Thai construction contractors. Thirty-two samples of construction contractors using BIM in Thailand were examined through SWOT analysis. The findings indicate that the strength factor of BIM implementation for Thai construction contractors had the highest average level of agreement, which is "BIM technology promotes good synergies between architecture, structure, and system work". This finding aligns with the research conducted by Utomo and Rohman (2019). Regarding weakness factors of BIM implementation for Thai construction contractors, the highest average level of agreement is "BIM requires high-quality labor to develop the correct BIM model." This is consistent with research by Zima et al. (2020). For the opportunity factors of BIM implementation for Thai construction contractors, the highest average level of agreement is "BIM education and knowledge promotion will make the use of BIM more widespread in the future". This findings is consistent with research by Manzoor et al. (2021). In term of threat factors of BIM implementation for Thai construction contractors, the highest average level of agreement is "Lack of support from the government". This is different from the research of Zima et al. (2020), which focuses on regulatory, standard, and legal factors of applying BIM at the organizational level, rather than the promotion in the public sector. Unlike some countries, BIM in Thailand is not a mandatory procedure for some public organizations.

Another purpose of this study is to provide strategies for BIM implementation for Thai construction contractors. The strategies analyzed using the TOWS Matrix have different objectives. For example, the SO strategy is suitable for organizations that have already adopted BIM and want to increase future opportunities. Considering this, the researcher proposes a strategy of "Establish a training center to develop personnel for the organization, reduce outsourcing costs, and improve the company's image". This strategy is based on the observation that organizations with strengths in BIM implementation can effectively disseminate knowledge to other organizations. The idea for this strategy is derived from Smith (2014).

On the other hand, the ST strategy is ideal for organizations that need to adopt BIM to address emerging threats. Therefore, this research findings proposes the strategy of "Development of corporate standards or referring to standards outside the country to apply". His strategy is based on the notion that adopting BIM application standards from other countries not only encourages broader BIM adoption but also exerts pressure on the government to enforce legal requirements and establish its own standards. The idea for this strategy is supported by Manzoor et al. (2021).

6. CONCLUSIONS

Based on the research results of Strategic Development of Building Information Modeling (BIM) Implementation for Thai Construction Contractors, it is a guide for considering various factors. However, it is important that organizational personnel should have a better understanding of BIM, in terms of SWOT analysis, analyzing the strengths, weaknesses, opportunities, and threats of the organization, as well as engaging in brainstorming and strategy development. The integration of these factors through the TOWS matrix is key to enhancing strategic efficiency. The transformation of an organization into a BIM-enabled entity is a time-consuming process; organizations must continually research and store evolving data to enable effective BIM implementation, considering that factors and circumstances can change at any time. Therefore, observing the surrounding environment and situational changes is also beneficial for organizational strategic planning.

REFERENCES

- Ahmed, S. (2018). Barriers to Implementation of Building Information Modeling (BIM) to the Construction Industry: A Review. *Journal of Civil Engineering and Construction*, 7, 107-113. <https://doi.org/10.32732/jceec.2018.7.2.107>
- Azhar, S. (2011). Building Information Modeling (BIM): Trends, Benefits, Risks, and Challenges for the AEC Industry. *Leadership and Management in Engineering*, 11(3), 241-252. [https://doi.org/doi:10.1061/\(ASCE\)LM.1943-5630.0000127](https://doi.org/doi:10.1061/(ASCE)LM.1943-5630.0000127)
- Ben Mahmoud, B., Lehoux, N., Blanchet, P., & Cloutier, C. (2022). Barriers, Strategies, and Best Practices for BIM Adoption in Quebec Prefabrication Small and Medium-Sized Enterprises (SMEs). *Buildings*, 12(4). <https://doi.org/10.3390/buildings12040390>
- Betts, M. (1995). Technology planning frameworks to guide national IT policy in construction. *Automation in Construction*, 3(4), 251-266. [https://doi.org/https://doi.org/10.1016/0926-5805\(94\)00013-D](https://doi.org/https://doi.org/10.1016/0926-5805(94)00013-D)
- Chimhundu, S. (2016). A study on the BIM adoption readiness and possible mandatory initiatives for successful implementation in South Africa.
- Czmoch, I., & Pękala, A. (2014). Traditional Design versus BIM Based Design. *Procedia Engineering*, 91. <https://doi.org/10.1016/j.proeng.2014.12.048>
- Enshassi, M. A., Al Hallaq, K. A., & Tayeh, B. A. (2019). Limitation Factors of Building Information Modeling (BIM) Implementation. *The Open Construction & Building Technology Journal*, 13(1), 189-196. <https://doi.org/10.2174/1874836801913010189>
- Kwak, S. G., & Kim, J. H. (2017). Central limit theorem: the cornerstone of modern statistics. *Korean J Anesthesiol*, 70(2), 144-156. <https://doi.org/10.4097/kjae.2017.70.2.144>
- Leśniak, A., Górka, M., & Skrzypczak, I. (2021). Barriers to BIM Implementation in Architecture, Construction, and Engineering Projects—The Polish Study. *Energies*, 14(8). <https://doi.org/10.3390/en14082090>
- Majrouhi Sardroud, J., Khorramabadi, A., Ranjbar, A., & Mehdizadeh Tavasani, M. (2018). *Barriers Analysis to Effective Implementation of BIM in the Construction Industry*. <https://doi.org/10.22260/ISARC2018/0009>
- Manzoor, B., Othman, I., Gardezi, S. S. S., & Harirchian, E. (2021). Strategies for Adopting Building Information Modeling (BIM) in Sustainable Building Projects—A Case of Malaysia. *Buildings*, 11(6). <https://doi.org/10.3390/buildings11060249>
- McGraw-Hill. (2009). *THE BUSINESS VALUE OF BIM Getting Building Information Modeling to the Bottom Line*.
- Odubiyi, T., Aigbavboa, C., Thwala, W., & Netshidane, N. (2019). Strategies for Building Information Modelling Adoption in the South African Construction Industry. *Modular and Offsite Construction (MOC) Summit Proceedings*, 514-519. <https://doi.org/10.29173/mocs133>
- Pickup, J. (2013). *A Strategic Guide to Adoption and Implementation*.
- Siebelink, S., Voordijk, H., Endedijk, M., & Adriaanse, A. (2020). Understanding barriers to BIM implementation: Their impact across organizational levels in relation to BIM maturity. *Frontiers of Engineering Management*, 8(2), 236-257. <https://doi.org/10.1007/s42524-019-0088-2>
- Smith, P. (2014). BIM Implementation – Global Strategies. *Procedia Engineering*, 85, 482-492. <https://doi.org/10.1016/j.proeng.2014.10.575>
- Utomo, F. R., & Rohman, M. A. (2019). The Barrier and Driver Factors of Building Information Modelling (BIM) Adoption in Indonesia: A Preliminary Survey.
- Williams, T. (2017). The Nature of Risk in Complex Projects. *Project Management Journal*, 48, 55-66. <https://doi.org/10.1177/875697281704800405>
- Zima, K., Plebankiewicz, E., & Wiczorek, D. (2020). A SWOT Analysis of the Use of BIM Technology in the Polish Construction Industry. *Buildings*, 10(1). <https://doi.org/10.3390/buildings10010016>

BIM-BASED PRECAST BUILDING OPTIMIZATION BY OPTIMALITY CRITERIA AND NSGA-II-GD CONSIDERING CONSTRUCTABILITY FOR PRECAST CONCRETE SIZING AND REBAR DETAILING

Weng-Lam Lao¹, Mingkai Li², Billy C.L. Wong³, Vincent J.L. Gan⁴, and Jack C.P. Cheng⁵

- 1) MPhil Candidate, Department of Civil and Environmental Engineering, Hong Kong University of Science and Technology, Hong Kong. Email: wllao@connect.ust.hk
- 2) Ph.D. Candidate, Department of Civil and Environmental Engineering, Hong Kong University of Science and Technology, Hong Kong. Email: mlicj@connect.ust.hk
- 3) Ph.D. Candidate, Department of Civil and Environmental Engineering, Hong Kong University of Science and Technology, Hong Kong. Email: clwongah@connect.ust.hk
- 4) Ph.D., Assistant Professor, Department of Building, National University of Singapore, Singapore. Email: vincent.gan@nus.edu.sg
- 5) Ph.D., Associate Head and Professor, Department of Civil and Environmental Engineering, Hong Kong University of Science and Technology, Hong Kong. Email: cejcheng@ust.hk

Abstract: Constructability is adopted as a concept to improve construction performance, including precast construction. Despite many attempts to enhance constructability factors such as logistics, sequencing, and transportation, standardization remains an area in need of development. The framework initiates by using Building Information Modeling techniques to extract semantic information from architectural plans, then uses gradient-based Optimality Criteria method to optimize the sizing variables of precast components. Finally, a hybrid approach called NSGA-II-GD, which combines Non-dominated Sorting Genetic Algorithm II and Great Deluge Algorithm, is used to optimize the rebar layout design of each precast component. Results from an illustrative example demonstrate an optimal point between construction cost and standardization, particularly for components subjected to similar stresses. The proposed NSGA-II-GD algorithm improves the searching efficiency in terms of convergence, computational time, and searching space.

Keywords: Precast optimization, Building information modeling, Constructability, NSGA-II, Optimality criteria

1. INTRODUCTION

Constructability is a widely adopted concept in the construction industry, including in the precast sector. Several factors, such as standardization, installation, resource availability, and economic impacts, have been identified as key factors affecting constructability (Hijazi et al., 2009; Zhang et al., 2016). Previous research has focused on improving installation by identifying the best component assembling sequence (Chen et al., 2010; Liu et al., 2023), and ensuring resource availability by considering the supply chain between production factories and on-site assembly (Pasandideh et al., 2015; Soleimani et al., 2017). Additionally, there have been studies to improve logistics (Chen et al., 2017) and reduce precast production's economic costs (de Albuquerque et al., 2012). Standardization, which involves using components with the same dimensions to reduce the number of mold changes and enhance productivity, is also an important factor. However, little research has been conducted on leveraging standardization in the precast design stage.

Optimizing structural element sizing and rebar detailing has been the subject of much research. Gan et al. (Gan et al. 2019) utilized a gradient-based optimality criteria-genetic algorithm (OC-GA) approach to optimize component topology and dimension sizing, but ignored downstream design such as rebar detailing. Li et al. (Li et al., 2023, Li et al., 2021) adopted a Hooke and Jeeves enhanced GA (GA-HJ) method to provide a clash-free rebar layout, but upstream processes such as structural dimensioning were not considered. Although Leyva et al. (Leyva et al., 2018) attempted to use NSGA-II with a coding system based on the combination of dimensions and rebar detailing, the available detailing was oversimplified, allowing only one layer of rebar. All three studies only focused on cost-related attributes of reinforced concrete structures and did not take into account constructability factors such as standardization.

The paper presents a framework for promoting standardization in precast reinforced concrete design. The framework adopts Building Information Modelling (BIM) techniques to extract information from a pre-defined structural layout plan and optimize precast structural elements such as columns, beams, and walls. The optimization is done using a multi-objective formulation that considers both construction costs and constructability scores. Optimality Criteria (OC) method is used in component sizing, while a new method called NSGA-II-GD is proposed to optimize the rebar detailing design for each precast element. The NSGA-II-GD method is a hybrid of the Non-dominated Sorting Genetic Algorithm II (NSGA-II) and the Great Deluge Algorithm (GDA), which improves the efficiency of the solution search.

The novelties of this research includes:

- (1) Development of a novel BIM-based framework for optimizing the structural design of precast elements.
- (2) Formulation of an optimization strategy that takes into account construction costs and constructability for precast elements to achieve standardization.
- (3) Integration of OC with NSGA-II-GD for element sizing and rebar detailing optimization.
- (4) Hybridization of NSGA-II with GD to improve computational efficiency for rebar detailing optimization.

2. METHOD

2.1 Proposed BIM-Based Framework for Precast Component Sizing And Rebar Layout Design Optimization

The framework, illustrated in Figure 1, is divided into two primary components: (1) the extraction of building model information automatically, including semantic information such as loading and topology, and (2) the optimization of precast element design by integrating the OC method for element dimensions and a proposed NSGA-II-GD method for rebar layout design. Designers can choose from alternatives design from the Pareto Front which can be used for downstream processes, such as the automatic generation of shop drawings and visualization.

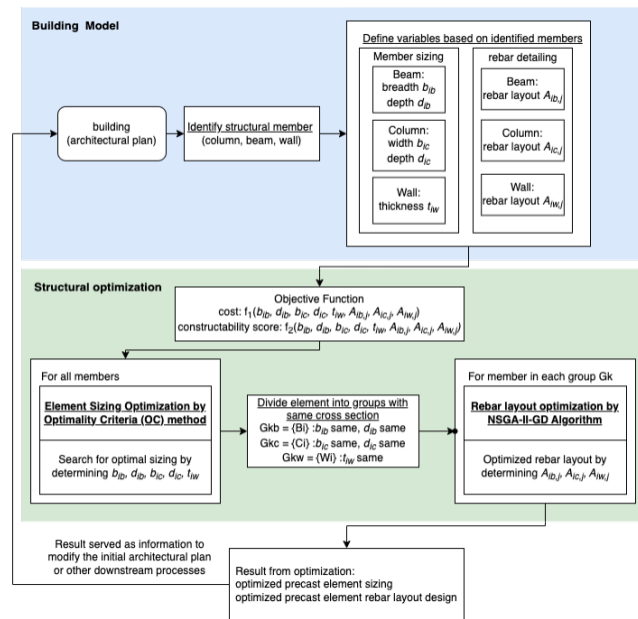


Figure 1. Framework of structural optimization for precast components

2.2 Formulation of Optimal Design

(1) Constructability consideration in precast component design

The present study aims to enhance the constructability of precast components by promoting standardization. According to the 3S principle, which is the basis of the Buildable Design Appraisal System (BDAS) (Building and Construction Authority, 2019) in Singapore and the Buildability Evaluation System (BSE(E)) (Development Bureau, 2022) in Hong Kong, standardization in precast construction involves three key elements:

1. Repeated grid layout, structural plan, and floor height to expedite on-site assembly of precast components.
2. Repeated sizing of structural elements or external cladding to minimize the number of mold changes required in the factory.
3. Standard reinforcement detailing of similar size, span, and loading components to increase the speed of production and installation.

While the first element is typically governed by the architectural plan, the other two can be controlled during the component design stage. To evaluate the relationship between standardization and construction cost, the present study extends the constructability scoring method developed by BSE(E).

(2) Variables for Precast Component

In order to consider the distinct structural behaviors of beams, columns, and walls, the study employs separate variables to describe their dimensions and rebar layout designs. Figure 2 presents all the variables used in the calculations, with the independent variables highlighted. The layout design variables were initially a vector to represent the number (n), diameter (d), and spacing (s) of bars in different sub-sections. Designers can extend these vectors to include more layout formulation rules. These variables will be transformed into discrete integers during the optimization procedure.

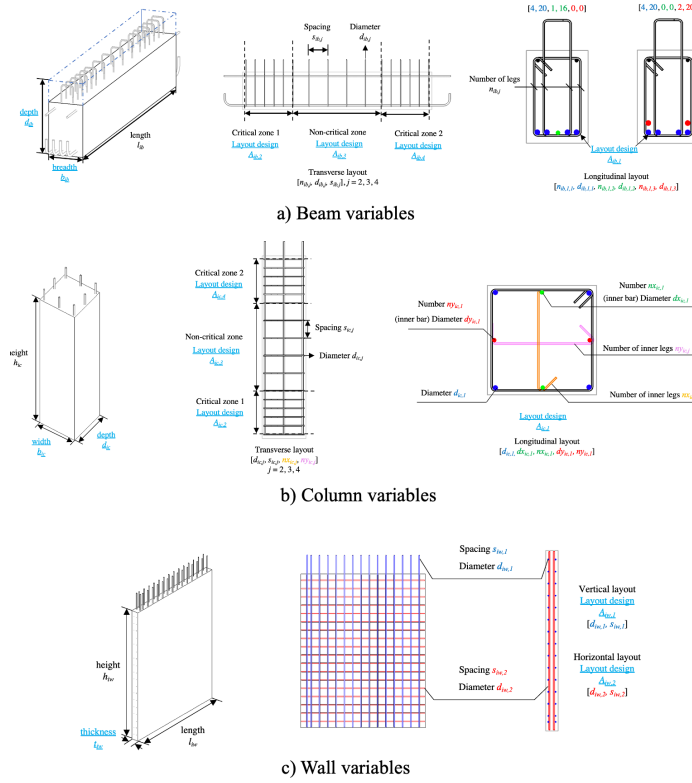


Figure 2. Definition of variables for (a) beams, (b) columns, and (c) walls

In rebar layout design, several bar diameters and multiple bar layers are also practical. To represent the wide range of rebar layout designs in precast reinforced concrete components, databases are created to map all existing layouts to an index. These databases filtered infeasible solutions according to the following criteria:

1. The provided steel area from the layout must be within the minimum required and maximum allowable steel area.
2. The cross-sectional sizing in each direction of the component must be within the dimension constraint.

(3) Objective Function

A) First objective: maximizing constructability score

In BSE(E), the standardization level is based on the ratio between the types of dimensions and the total number of components. The score contains a continuous linear value when the ratio is between 15% to 70%. In this study, the method established by BSE(E) for component dimension standardization is extended to evaluate not only the type of cross-section but also the rebar layout. The constructability score is assessed by combining the standardization of component dimension and rebar layout design and is formulated as follows:

$$G_{ratio} = N_{groups}/N_{components} \quad (1)$$

$$score = 1, G_{ratio} < 0.15 \quad (2)$$

$$score = \frac{0.7 - G_{ratio}}{0.55}, 0.15 < G_{ratio} < 0.7 \quad (3)$$

$$score = 0, G_{ratio} > 0.7 \quad (4)$$

where G_{ratio} is the group ratio; N_{groups} is the number of groups of components that are identical, which have the same cross-sectional dimension and rebar layout design; $N_{components}$ is the total number of components having the same cross-sectional dimension, score is the constructability score.

B) Second objective: minimizing construction cost

The construction cost of precast concrete components is composed of material costs, including the cost of concrete and steel reinforcement, and labor costs, which mainly include rebar placement and tying.

$$Cost = C_c + C_s + C_l \quad (5)$$

$$C_c = \sum_{iw}^{lw} \sum_{ic}^{lc} \sum_{ib}^{lb} \sum_j^J \left(V_{ci,w}(t_{iw}, A_{iw,j}) + V_{ci,c}(b_{ic}, d_{ic}, A_{ic,j}) + V_{ci,b}(b_{ib}, d_{ib}, A_{ib,j}) \right) \times c_c \quad (6)$$

$$C_s = \sum_{iw}^{lw} \sum_{ic}^{lc} \sum_{ib}^{lb} \sum_j^J \left(V_{si,w}(A_{iw,j}) + V_{si,c}(A_{ic,j}) + V_{si,b}(A_{ib,j}) \right) \times \gamma \times c_s \quad (7)$$

$$C_l = \sum_{iw}^{lw} \sum_{ic}^{lc} \sum_{ib}^{lb} \sum_j^J \left(T_{i,w}(A_{iw,j}) + T_{i,c}(A_{ic,j}) + T_{i,b}(A_{ib,j}) \right) \times c_l \quad (8)$$

$$T_i = \sum_l^I \sum_j^J \frac{N_{bar}(A_{i,j})}{p_p} + \frac{N_{tie}(A_{i,j})}{p_t} \quad (9)$$

where C_c , C_s , and C_l are the cost of concrete, steel and labor (in HKD); $V_{ci,w}$, $V_{ci,c}$, and $V_{ci,b}$ are the volume of concrete excluding the volume of steel reinforcement (in m³); $V_{si,w}$, $V_{si,c}$, and $V_{si,b}$ are the volume of steel reinforcement (in m³); $T_{i,w}$, $T_{i,c}$, $T_{i,b}$ are the time for rebar installation (in min); c_c is the concrete cost per unit volume (in HKD/m³), c_s is the steel cost per unit weight (in HKD/kg), c_l is the labor cost per unit time (HKD/min); γ is the density of steel (in kg/m³), N_{bar} is the number of bars installed inside a component, N_{tie} is the number of ties used to fix the bars, p_p is the rebar placing time (in bar/min), p_t is the rebar tying time (in tie/min); b, c and w denotes the beam, column and wall components, i and j refers to the component index and rebar design subsection index respectively, I and J refers to the total number of component and total number of subsection inside the component respectively.

(5) Design Constraints

Constraints include those specified by the designers (dimension limits) and those provided by design codes. Equation (10) describes the maximum allowable serviceability total lateral drift ratio \bar{d}_H of the whole building; Equation (11) defines the upper limit of lateral inter-story drift \bar{d}_f ; Equation (12) sets the component strength constraints. Other constraints related to rebar design include those specified in the code of practice (Building Department, 2020), and the main one is illustrated in the database filtering procedures in Section 2.2.2

$$\frac{\delta_T}{H} \leq \bar{d}_H \quad (10)$$

$$\frac{(\delta_f - \delta_{f-1})}{h_f} \leq \bar{d}_f, f = 1, 2, \dots, F \quad (11)$$

$$\sigma_i \leq \bar{\sigma}_i \quad (12)$$

where δ_T is the total lateral drift at the top floor, and H is the building height; δ_f and δ_{f-1} are the lateral displacements of two adjacent floors, and h_f is the corresponding floor height; σ_i and $\bar{\sigma}_i$ represents the individual element stress and its allowable limit; l and u denote the lower and upper limits of each dimension variable, respectively.

2.3 Integrate OC and NSGA-II-GD for Precast Building Optimization

(1) Two-stage optimization

In this study, we have developed a two-stage optimization strategy that aims to optimize component sizing and rebar layout design simultaneously while considering constructability and construction costs. In the first stage, the gradient-based OC algorithm is applied to iteratively adjust the component dimensions and minimize structural costs while satisfying strength and lateral drift serviceability constraints. In the second stage, we employ a hybrid algorithm called NSGA-II-GD, which combines the NSGA-II algorithm and the GDA. This approach is used to optimize the rebar layout design for each sub-group of components that share the same type and dimensions. By limiting the search space to feasible regions only, the GDA improves the search efficiency.

(2) Gradient-based OC

To obtain the gradient required for iterative variable updates, explicit formulations of lateral drift constraints are necessary. The lateral drift constraints can be explicitly represented using the virtual work principle, which is shown in Equation (13)

$$d_l = \sum_{iw}^{lw} \left(\frac{e_{0iw,l}}{t_{iw}} + \frac{e_{1iw,l}}{t_{iw}^3} \right) + \sum_{ic}^{lc} \left(\frac{e_{0ic,l}}{b_{ic}d_{ic}} + \frac{e_{1ic,l}}{b_{ic}d_{ic}^3} + \frac{e_{2ic,l}}{b_{ic}^3d_{ic}} \right) + \sum_{ib}^{lb} \left(\frac{e_{0ib,l}}{b_{ib}d_{ib}} + \frac{e_{1ib,l}}{b_{ib}d_{ib}^3} + \frac{e_{2ib,l}}{b_{ib}^3d_{ib}} \right) \leq \bar{d}_l \quad (13)$$

where $e_{0iw,l}$, $e_{1iw,l}$, $e_{0ic,l}$, $e_{1ic,l}$, $e_{2ic,l}$, $e_{0ib,l}$, $e_{1ib,l}$, and $e_{2ib,l}$ are the virtual strain energy coefficient calculated from internal moments and forces of the precast components under actual loading and virtual loading; l is the lateral constraints index.

The design formulation can be converted to unconstrained functions using Lagrangian multipliers to form a recursive formula, as shown in Equations (14-16). The recursive formula is derived from the gradient obtained from the partial derivatives of the unconstrained function with respect to each dimension variable. Derivation of the recursive relationship is demonstrated in this reference (Chan, 2001).

$$(b_i)_{v+1} = (b_i)_v \times \left\{ 1 + \frac{1}{\eta} \left(\sum_l^L \frac{\lambda_l}{c_i} \left(\frac{e_{0i,l}}{b_i^2 d_i^2} + \frac{e_{1i,l}}{b_i^2 d_i^4} + \frac{3e_{2i,l}}{b_i^4 d_i^2} \right) - 1 \right) \right\}_v \quad (14)$$

$$(d_i)_{v+1} = (d_i)_v \times \left\{ 1 + \frac{1}{\eta} \left(\sum_k^L \frac{\lambda_l}{c_i} \left(\frac{e_{0i,l}}{b_i^2 d_i^2} + \frac{3e_{1i,l}}{b_i^2 d_i^4} + \frac{e_{2i,l}}{b_i^4 d_i^2} \right) - 1 \right) \right\}_v \quad (15)$$

$$(t_i)_{v+1} = (t_i)_v \times \left\{ 1 + \frac{1}{\eta} \left(\sum_l^L \frac{\lambda_l}{c_i} \left(\frac{e_{0i,l}}{t_i^2} + \frac{3e_{1i,l}}{t_i^4} \right) - 1 \right) \right\}_v \quad (16)$$

where v and $v + 1$ signify the iteration number; η is a parameter to controls the pace of convergence of the recursive relationship; l is the index of lateral drift constraints and L represents the total number of lateral drift constraints; c_i is the cost coefficient of each component i respectively; λ_l denotes the Lagrangian multipliers of the l th constraint.

(3) NSGA-II-GD

Figure 3 illustrates the optimization procedure using the NSGA-II-GD algorithm. The optimization procedure adopts a tournament binary selection, a two-point crossover operator, and a random mutation operator to produce offspring based on parents from the previous generation. Then, a feasibility check is conducted to verify whether the children produced fall within the feasible region and adjust the child's genes if it falls within the infeasible region. After that, all feasible offspring are merged with their parents and undergo non-dominated sorting and crowding distance sorting. Individuals with larger front ranks or smaller crowding distances are filtered until the number of individuals in the new population equals the initial population. This process is repeated until the maximum number of iterations, which serves as the stopping criterion, is reached.

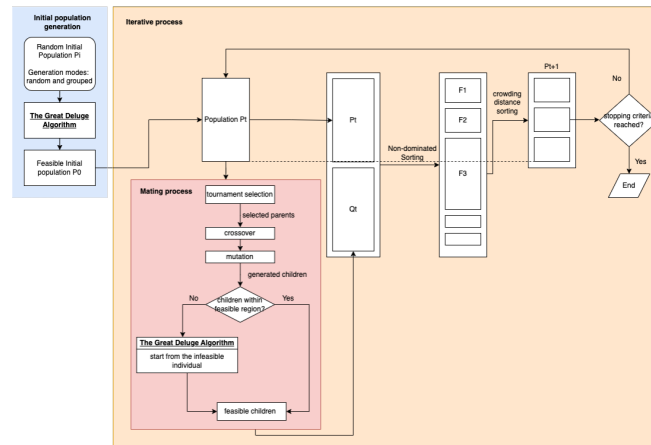


Figure 3. NSGA-II-GD optimization procedure

GDA is integrated to find feasible solutions. The constraints are formulated such that it returns zero if there is no violation, and the more a solution violates the constraints, the higher the return value. This integration allows NSGA-II to only search inside the feasible region, which eliminates the computational efforts in exploring the infeasible region.

3. ILLUSTRATIVE EXAMPLE

To demonstrate the optimization framework and the correlation between standardization level and construction cost, a 5-story building is used as an example. The building's structural layout and 3D architectural model are shown in Figure 4. Design attributes are listed in Table 1. Table 2 includes the parameter tuning in the NSGA-II-GD algorithm.

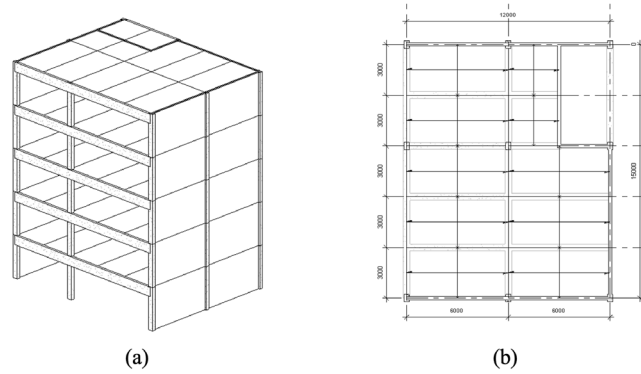


Figure 4. (a) 5-story 3D architectural model and (b) structural layout plan in the illustrative example

Table 1. Design attributes of the illustrative example

Design attribute	value
Typical Beam Dimension	750 mm x 600 mm
Typical Column Dimension	600 mm x 600 mm
Typical Wall Thickness	300 mm
Beam Breadth Range	300 mm to 800 mm
Beam Depth Range	400 mm to 1000 mm
Column Width and Depth Range	300 mm to 1000 mm
Wall Thickness Range	150 mm to 500 mm
Concrete Strength	45 MPa
High-yield Rebar Grade	500 MPa
Mild Steel Rebar Grade	250 MPa
Longitudinal Rebar Diameter	12, 16, 20, 25, 32, 40 mm
Transverse Rebar Diameter	8, 10, 12, 16, 20 mm
Concrete Costs	771.9 HKD/m ³
High-Yield Rebar Cost	5075 HKD/ton
Mild Steel Rebar Cost	5961 HKD/ton
Labor cost	4420 HKD/day (assume two workers)

Table 2. Parameter Tuning of NSGA-II-GD

Parameter	Value
NSGA-II	
Crossover rate	0.75
Mutation rate	0.25
Population/variable number ratio	~10
generation	200-300 (depends on variable number)
GDA	
population	20
Step value	0.001

4. RESULT AND DISCUSSION

4.1 Optimized Dimension of Precast Component

Figure 5 displays the optimized dimensions of each precast component, while Table 3 summarizes the grouping of these components. Notably, all beams share the same cross-sectional dimension of 300 mm x 400 mm. The optimized dimensions of the components mostly fall within the smallest dimension defined by the designer. The sub-groups with the smallest dimension contain the highest number of components, while other sub-groups only contain a few components as they are subjected to distinct stresses.

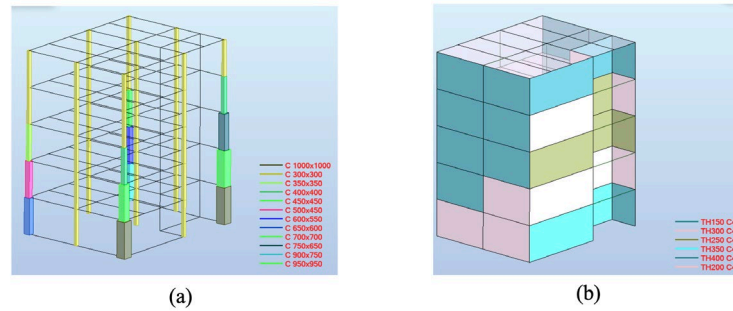


Figure 5. (a) Columns sizing and (b) wall sizing after sizing optimization

Table 3. Grouping of components with identical dimensions in beams, columns and walls

Type	Beam	Column	Wall		Total
Number of Components	66	45	35		146
Number of Sub-Groups	3	14	13		30

4.2 Relationship Between Construction Cost and Constructability Score

Figure 6 depicts the correlation between construction cost and constructability score for all three types of components in a typical sub-group. Each graph is obtained by merging five solutions from the random and group modes. For beams and columns, it is observed that the construction cost stop decreasing at an optimal point. This occurs because the optimal point already provides the best layout for each component subjected to similar stresses. Any further attempt to include another layout will result in sub-optimal solutions, having an increasing cost instead of a decreasing one. Wall components only show an increasing trend due to their simpler design.

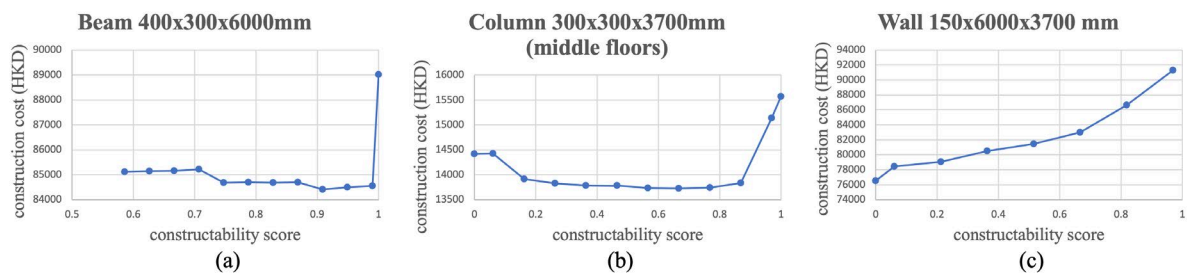


Figure 6. Aggregated Pareto front from rebar detailing optimization by NSGA-II-GD for (a) beam group 400 x 300 x 6000 mm, (b) column group 300 x 300 x 3700mm and (c) wall group 150 x 6000 x 3700 mm

Figure 7 demonstrates how the rebar layout transforms inside the beam precast component as the constructability score changes. Beyond the optimal point, alterations mainly occur inside the longitudinal reinforcement. In contrast, for constructability scores below the optimal point, modifications are primarily observed in the transverse reinforcement.

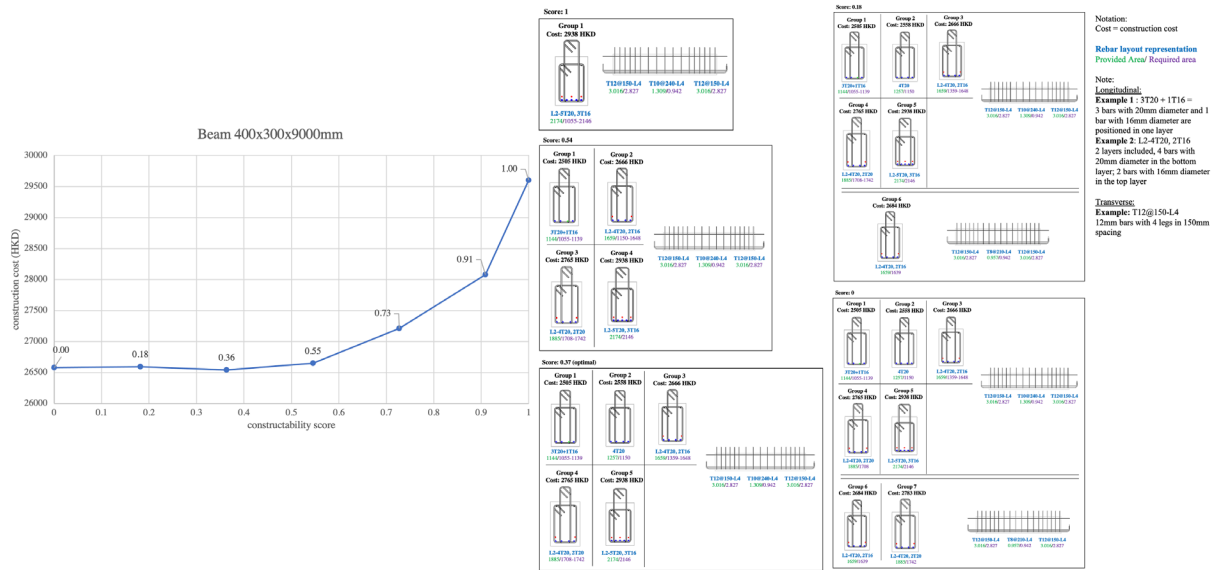


Figure 7. Rebar detailing of beam group 400 x 300 x 9000 mm according to different constructability scores

4.3 Cost Distribution in Precast Components

Figure 8 presents a cost portion analysis of construction costs. The concrete costs are approximately half of the reinforcement costs across all three components while the labor cost varies from 6% to 31%. This difference may be attributed to the highly congested rebar detailing arrangement observed in beams and columns.

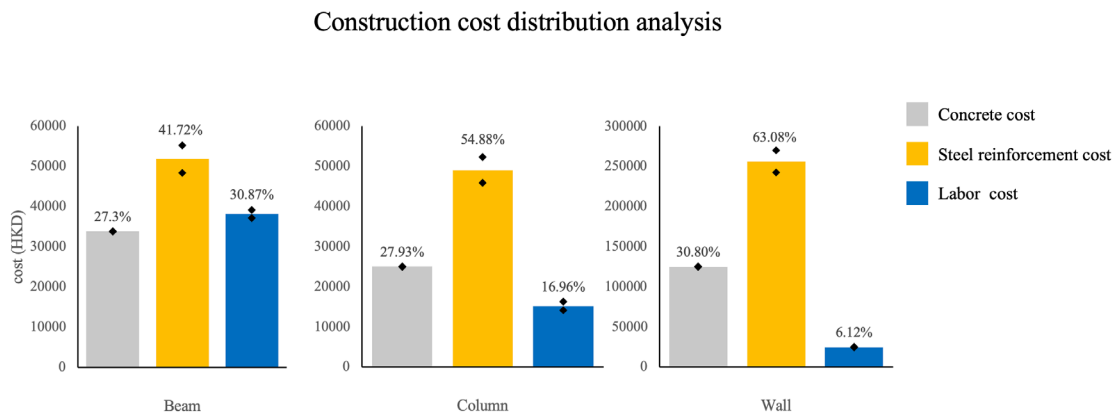


Figure 8. Construction cost distribution analysis for (a) beam, (b) column, and (c) wall

(4) Comparative Study of NSGA-II-GD to Standard NSGA-II and Weighted GA

Figure 9 depicts the aggregated Pareto front for each of the algorithms for beams, columns, and walls. For all three component categories, NSGA-II-GD provides solutions with lower construction costs at the same constructability score. Moreover, the aggregated results of the two modes of NSGA-II-GD not only include solutions with low constructability scores but also those in the high score region. In contrast, the solutions provided by both the standard NSGA-II and the weighted GA are mainly concentrated in the low constructability score region, but the solution range they provide falls into the sub-optimal region, which is not within the region of interest in finding the relationship between standardization level and construction cost.

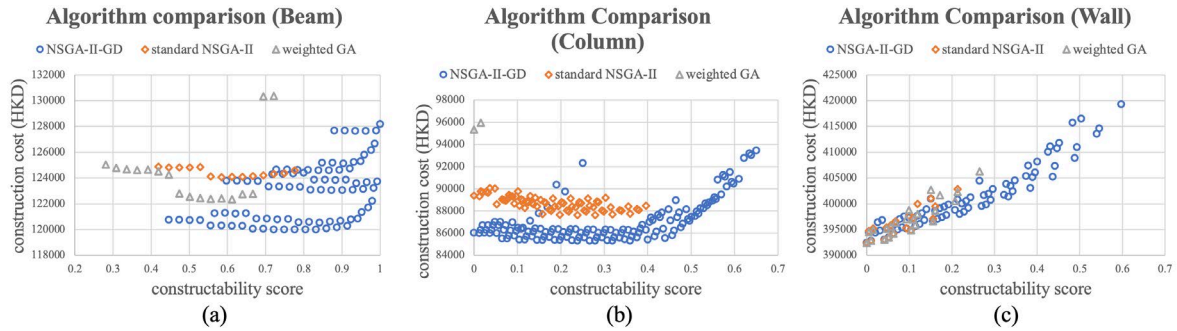


Figure 9. Comparison of aggregated permutating Pareto front between NSGA-II-GD, standard NSGA-II and GDA for (a) beam, (b) column and (c) wall

Table 4 provides information on the computational time required by the three algorithms in different scenarios. Each scenario was executed ten times, and the average computational time was recorded. Both NSGA-II and weighted GA require a higher population and generation setting to provide a converged solution. Therefore, the actual time required for a converged solution provided by the random mode of NSGA-II-GD is half that required by the other two algorithms. Furthermore, when the number of variables is very large, standard NSGA-II and weighted GA are unable to provide a converged solution, and the total computational time is not recorded in the table.

Table 4. Computation time comparison of NSGA-II-GD, standard NSGA-II and weighted GA under different scenarios

	NSGA-II-GD (random mode)	NSGA-II-GD (grouped mode)	Standard NSGA-II	Weighted GA
Beam: 400x300x3000mm, number of variables = 24, number of components = 11 (6 with different required areas)				
Converged population	100	100	300	300
Converged generation	100	100	200	200
Time (s)	26.081	61.623	58.907	45.949
Beam: 400x300x9000mm, number of variables = 40, number of components = 10 (10 with different required areas)				
Converged population	300	300	1200	1500
Converged generation	200	200	200	500
Time (s)	100.321	593.603	184.420	394.2
Beam: 400x300x6000mm, number of variables = 152, number of components = 45 (38 with different areas)				
Converged population	1500	1500	-	-
Converged generation	400	400	-	-
Time (s)	1469.679	1748.090	-	-

5. CONCLUSION

In summary, this study makes a significant contribution to the field of structural design optimization for precast building components by proposing a BIM-enabled framework that optimizes their dimensions and rebar detailing designs. The framework incorporates a gradient-based OC optimization technique for component sizing and a proposed NSGA-II-GD algorithm for rebar detailing designs. The study demonstrates that a balance between standardization and construction cost is necessary for optimal results for components with similar stress levels. The proposed NSGA-II-GD algorithm significantly improves searching efficiency in terms of computational time, searching space, and convergence.

However, the study has some limitations. Firstly, the formulation does not consider logistics costs associated with precast components, such as transportation and assembly, which can be difficult to quantify and highly project-specific. This limitation may lead to atomistic results since the precast fabrication process is more complex than the fabrication of structural components on-site. Secondly, only simple geometries, such as rectangular beams and columns, were studied. However, the approach could be extended to various shapes by incorporating more variables and applying a relationship to transform non-rectangular shapes into rectangular ones during the gradient-based OC optimization. Lastly, labor costs may change in the future as the precast industry adopts more automation for prefabrication, and machine-related costs should be introduced to account for this.

ACKNOWLEDGMENTS

The authors would like to acknowledge the support by the Hong Kong Construction Industry Council, Grant No. CIC19EG03. Any opinions and findings are those of the authors, and do not necessarily reflect the views of the Hong Kong Construction Industry Council.

REFERENCES

- Building and Construction Authority. (2019). *Code of Practice of Buildability*. Retrieved from Building and Construction Authority. website https://www1.bca.gov.sg/docs/default-source/docs-corp-news-and-publications/publications/for-industry/buildability-series/cop-on-buildability-2019.pdf?sfvrsn=d8526675_0
- Building Department. (2020). *Code of Practice for Structural Use of Concrete 2013 (2020 Edition)*. Retrieved from Building Department. website https://www.bd.gov.hk/doc/en/resources/codes-and-references/code-and-design-manuals/CoP_SUC2013e.pdf
- Development Bureau. (2022). *Buildability Evaluation System for Public Engineering Work Projects (BSE(E))*. Retrieved from Development Bureau. website https://www.devb.gov.hk/en/publications_and_press_releases/publications/BESE/index.html
- Chan, C. M. (2001). Optimal lateral stiffness design of tall buildings of mixed steel and concrete construction. *The Structural Design of Tall Buildings*, 10(3), 155-177.
- Chen, J. H., Yan, S., Tai, H. W. and Chang, C. Y. (2017). Optimizing profit and logistics for precast concrete production. *Canadian Journal of Civil Engineering*, 44(6), 393-406.
- Chen, Y., Okudan, G. E. and Riley, D. R. (2010). Decision support for construction method selection in concrete buildings: Prefabrication adoption and optimization. *Automation in Construction*, 19(6), 665-675.
- De Albuquerque, A. T., El Debs, M. K. and Melo, A. M. C. (2012). A cost optimization-based design of precast concrete floors using genetic algorithms. *Automation in Construction*, 22, 348-356.
- Gan, V. J. L., Wong, C. L., Tse, K. T., Cheng, J. C. P., Lo, I. M. C. and Chan, C. M. (2019). Parametric modelling and evolutionary optimization for cost-optimal and low-carbon design of high-rise reinforced concrete buildings. *Advanced Engineering Informatics*, 42, 100962.
- Hijazi, W., Alkass, S. and Zayed, T. (2009). Constructability Assessment Using BIM/4D CAD Simulation Model.
- Leyva, H. A., Bojórquez, E., Bojórquez, J., Reyes-Salazar, A., Castorena, J. H., Fernández, E. and Barraza, M. A. (2018). Earthquake Design of Reinforced Concrete Buildings Using NSGA-II. *Advances in Civil Engineering*, 2018, 5906279.
- Li, M., Liu, Y., Wong, B. C. L., Gan, V. J. L. and Cheng, J. C. P. (2023). Automated structural design optimization of steel reinforcement using graph neural network and exploratory genetic algorithms. *Automation in Construction*, 146, 104677.
- Li, M., Wong, B. C. L., Liu, Y., Chan, C. M., Gan, V. J. L. and Cheng, J. C. P. (2021). DfMA-oriented design optimization for steel reinforcement using BIM and hybrid metaheuristic algorithms. *Journal of Building Engineering*, 44, 103310.
- Liu, C., Zhang, F., Zhang, H., Shi, Z. and Zhu, H. (2023). Optimization of assembly sequence of building components based on simulated annealing genetic algorithm. *Alexandria Engineering Journal*, 62, 257-268.
- Pasandideh, S. H. R., Niaki, S. T. A. and Asadi, K. (2015). Bi-objective optimization of a multi-product multi-period three-echelon supply chain problem under uncertain environments: NSGA-II and NPGA. *Information Sciences*, 292, 57-74.
- Soleimani, H., Govindan, K., Saghafi, H. and Jafari, H. (2017). Fuzzy multi-objective sustainable and green closed-loop supply chain network design. *Computers & Industrial Engineering*, 109, 191-203.
- Zhang, C., Zayed, T. and Hijazi, W. (2016). Quantitative Assessment of Building Constructability Using BIM and 4D Simulation. *Open Journal of Civil Engineering*, 6(3).

IMPROVING THE EFFICIENCY OF ICT EARTHWORK THROUGH AUTOMATED PLANNING USING BIM

Hitoshi Ishida¹ and Nobuyoshi Yabuki²

1) Senior Manager, ICT Promotion Office, Penta-Ocean Construction Co., LTD., Japan. Email: hitoshi.ishida@mail.penta-ocean.co.jp

2) Ph.D., Prof., Division of Sustainable Energy and Environmental Engineering, Graduate School of Engineering, Osaka University, Suita, Japan. Email: yabuki@see.eng.osaka-u.ac.jp

Abstract: In Japan, Information and Communication Technology (ICT) earthwork has been deployed under the "i-Construction" policy proposed by the Ministry of Land, Infrastructure, Transport and Tourism (MLIT) in 2015, which aims to improve the productivity in construction through the consistent use of 3D data, Global Navigation Satellite System (GNSS), Total Station (TS), and sensors. In the creation of plans for ICT earthwork, efficiency is being improved through the use of Building Information Modeling (BIM) models. Specifically, a BIM model is created for each construction stage based on the BIM model of the final shape, and the way of proceeding with construction up to the final shape is visualized and studied. However, there are many small- and medium-scale earthworks in Japan, and there is a lack of personnel in charge of BIM modeling at such sites. In this study, we developed a method to automate daily earthwork planning by applying BIM to earthwork projects in which ICT earthwork was introduced and compared it with the construction flow in actual construction sites.

Keywords: ICT earthwork, BIM, 3D Model, Automated planning

1. INTRODUCTION

The construction industry is facing a serious shortage of workers as society's birthrate declines and the population ages, making it an urgent issue to improve productivity and supplement the know-how that is lost due to the retirement of skilled workers. In response, the Ministry of Land, Infrastructure, Transport and Tourism (MLIT) has been promoting an initiative called "BIM/CIM" (Building/Construction Information Modeling, Management) since 2012 to streamline the entire construction production process from survey to design, construction, and maintenance management, mainly through the use of 3D models. Furthermore, the use of 3D data at construction sites is rapidly expanding due to "i-Construction" announced by the MLIT in November 2015. In "i-Construction," the MLIT has created a series of standards corresponding to new surveying instruments and new construction machinery while expanding the types of work such as "ICT earthwork", "ICT pavement", "ICT dredging" and so on. ICT Earthworks aims to improve productivity by consistently using 3D data throughout the entire process of surveying, design, construction, and inspection. In the creation of plans for ICT earthwork, efficiency is being improved through the use of BIM models. Specifically, a BIM model is created for each construction stage based on the BIM model of the final shape, and the way of proceeding with construction up to the final shape is visualized and studied. However, there are many small- and medium-scale earthworks in Japan, and there is a lack of personnel in charge of BIM modeling at such sites. On the other hand, the ICT earthwork plan is used as data to instruct the ICT construction equipment on the shape of the target fill or cut. This earthwork plan can be created with a construction step model, but for complex construction projects, it is necessary to create a number of these construction steps. In addition, the staff on site and the operator of the ICT construction equipment must change the system as needed to cope with daily changes in the situation. Daily changes in the situation are mainly delays in work due to weather conditions and delays in the supply of materials due to changes in soil quality. These factors include the fact that the construction site is too small to provide sufficient temporary storage space for the fill and that there are not always enough runways to transport the soil and gravel. Thus, it is often difficult to operate ICT earthwork efficiently in small- and medium-scale earthwork projects in Japan due to the small number of manpower and the narrowness of construction sites.

2. AUTOMATED PLANNING METHOD FOR ROAD EARTHWORKS

2.1 Use of Construction History Data

Although many efforts have been made to utilize BIM models at construction sites, updating BIM models during construction is still a heavy workload. On the other hand, it is known that ICT construction machinery has improved the productivity and quality of road construction projects, and that applying BIM modeling to ICT construction machinery planning can reduce planning rework and improve productivity. (Kim et al., 2017)

ICT construction machinery (Figure 1) is becoming popular in road earthwork projects, and studies are in progress to utilize the construction records (such as Global Navigation Satellite System (GNSS) log files) of the construction process for construction management. Imai et al. (2017) evaluate the application of ICT construction records data from ICT construction machinery to shape management for road pavement construction, suggesting

the practicability and usefulness of using 3D data generated from construction history data. The MLIT has established guidelines for the use of construction history data for workmanship management, considering the fact that workmanship can be grasped at an early stage and that it can be obtained in areal forms to be an advantage, and it is expected to be used in the future to improve productivity (MLIT, 2021).

Kim et al. (2017) pointed out that it is inefficient to manually transfer planning information for ICT construction machinery, which is created from BIM models of road earthworks, to ICT construction machinery, as it requires manual information transfer, and to automate these linkages, they proposed an earthwork calculation module using BIM models and an ICT construction machinery module to generate TIN surfaces is proposed. This study further attempts to automatically generate design information for ICT construction machinery by using both BIM models and construction history records data. Specifically, 3D shape data generated from construction history data of ICT construction machinery is automatically reflected in the BIM model to plan the next layer, thereby facilitating the use of ICT construction machinery on site.

The ICT construction machinery used is shown in Figure 1. All of them are equipped with a machine guidance system and can send and receive data to and from a cloud server using communication equipment. The ICT vibration rollers generate reports as shown in Figure 2 as evidence of the construction. The flow of data files and plan files is shown in Figure 3, where the tracking data from the ICT vibration roller is sent to the cloud server, which converts it into 3D shapes for the next layer plan, which is then sent to the ICT bulldozer. By establishing a system that automatically generates planning information for each layer and automatically transmits it directly from the cloud to ICT construction machinery, construction can be performed efficiently in response to changing conditions.



Figure 1. ICT construction machinery

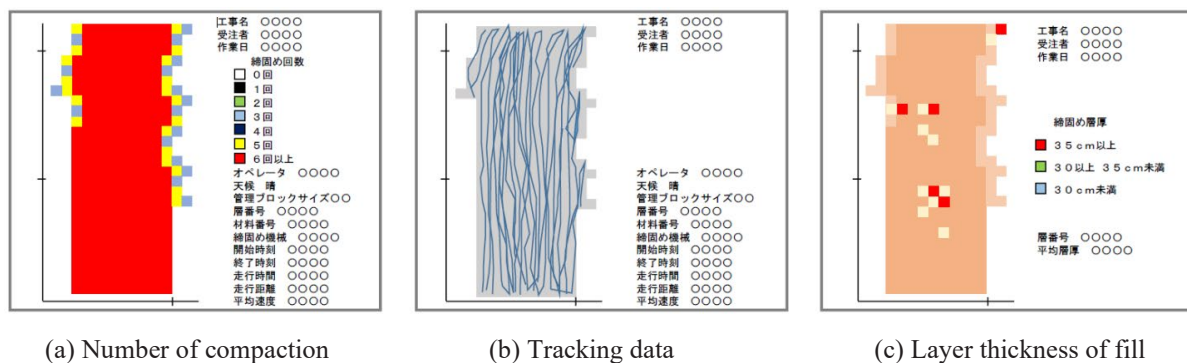


Figure 2. Construction history data map

The situations we envision using this method include re-planning when the height of the fill layers changes (even within the allowable limits of each layer) due to construction errors or differences in soil compaction rates, and re-planning after filling the site differently from the plan. Examples of changes in embankment plans include the following.

- 1) Temporary drainage measures are taken in response to rainfall during fill operations.
- 2) Insufficient inventory of fill material to fill the planned area.
- 3) Modifications have been made to provide temporary roads for construction.
- 4) Changes due to adjustments to the life of neighboring residents.

The automatic planning of the next layer, using construction history data, reduced the amount of work and management by the field staff.

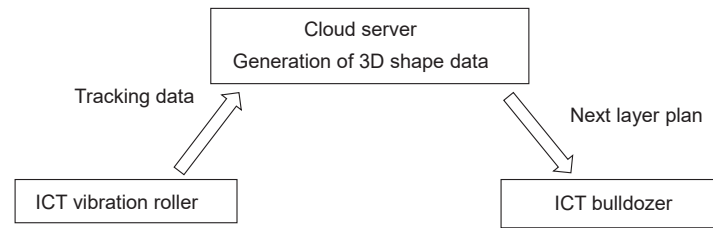


Figure 3. Flow of data files and plan files

2.2 Automated Planning for ICT Construction Machinery

Generally, we create a BIM model for each construction phase based on the BIM model of the final shape to visualize and study how to proceed with construction up to the final shape. However, in Japan, there are many small- and medium-scale earthworks, and there is a lack of personnel in charge of BIM modeling at such sites.

Raza et al. propose a method that handles 3D models parametrically and provides flexibility for modification in order to make the 3D model of roadway earthworks more complete during design. The method allows the program to automatically calculate and modify the geometric shape of the model (2017b). The National Institute for Land and Infrastructure Management (NILIM) of the MLIT has published a "Draft Concept of Parametric Models for Data Exchange" (2019) as a method to reduce modeling work and improve the efficiency of BIM operations.

In this study, to establish a mechanism for automatic updating of the BIM model, we created a parametric model for road earthworks. The parametric model developed in this study consists of road center alignment and cross sections, which are used with terrain geometry. The parametric BIM model of road earthwork constructed in this study is shown in Figure 4 and 5. Figure 4 is the actual system screen, showing a bird's-eye view of the road earthwork model in 3D. The semi-transparent orange areas extending to the left and right are the design model of the road. The two arrows in the figure indicate the longitudinal direction of the road, which is toward the right at the upper right side of the figure, and the transverse direction, which is toward the right front from the center area. The red area in the center of the figure represents the progression of the embankment from the bottom to the top, one layer at a time. The lower layer of fill in this parcel is striking the terrain in both the longitudinal and transverse directions. Figure 5 is a schematic of the cross-section viewed from the back of Figure 4. The planning model for the next layer is automatically generated at the height of one layer above the layer compacted by the ICT vibration roller. If there is a terrain in the cross-sectional direction (left side of the figure), the model is generated up to the intersection with the terrain; if there is no terrain (right side of the figure), the model is generated using the parameters of the cross-section. If a layer becomes thinner due to construction errors or different soil compaction rates, the height of the next layer is automatically adjusted lower by that amount.

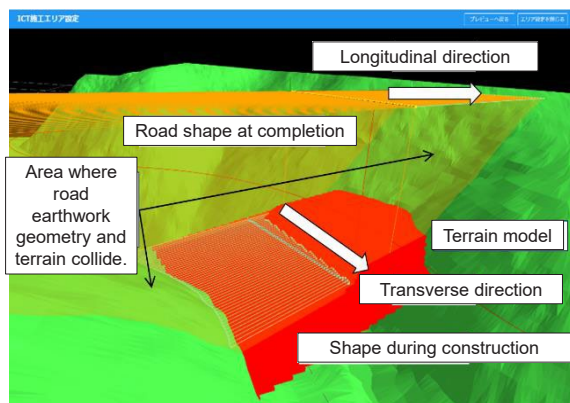


Figure 4. Composition of the parametric model (3D view)

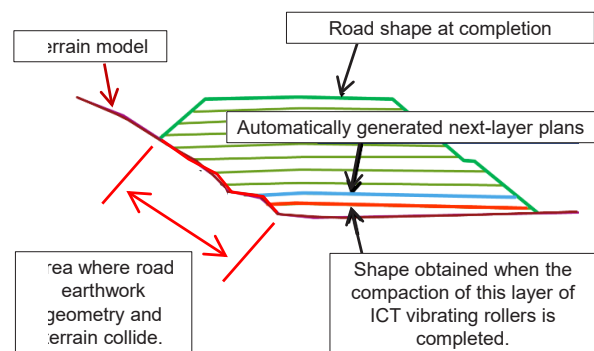


Figure 5. How to generate the plan for the next-layer

2.3 Comparison with conventional ICT construction machinery operation methods

Raza et al.(2017a) applied BIM modeling to a road construction project and verified its effectiveness. The BIM model facilitated alignment changes of the route by parametrically handling the road centerline. Furthermore, the BIM model visualizes the relationship between the road centerline, the TIN model of the ground surface

obtained by the laser scanner, and the cross-sectional subassemblies, which facilitates adjustments. The necessary parameters are extracted from the 2D drawings. It has been demonstrated by Raza et al. that BIM can be used to efficiently create a 3D model of the final geometry. Autodesk Civil3D was used to create the BIM model.

In this study, we applied BIM to the day-to-day management of performing construction and automatically modeled the daily plans for operating ICT construction machinery. Conventionally, earthwork planning using BIM is based on a BIM model of the final shape, and BIM models are created for each construction phase to visualize and study how to proceed with construction up to the final shape. As a detailed procedure, the construction plan is developed based on the BIM model of the final shape and 2D drawings taken over from the design process. The BIM model inherited from the design process includes a rough terrain. This rough terrain may be a digital elevation model (DEM) (5m or 10m mesh) provided by the Geospatial Information Authority of Japan, Shuttle Radar Terrain Mission (SRTM) data (30m or 90m mesh), or various other types of data. In this study, BIM was applied to the day-to-day management of construction activities and automatic modeling of daily plans for operating ICT construction machinery. Prior to creating the construction plan, the current terrain is surveyed using a laser scanner or drone in necessary areas, and replaced with the terrain of the BIM model of the finished form, which is then updated.

Based on the updated BIM model of the finished configuration, an earthwork plan is created using modeling software such as Autodesk Civil3D. The model to be created is a layered TIN model separated by approximately 30 cm in height from the existing terrain until it is filled in to the finished shape. Using this model, planning files for ICT bulldozers and vibration rollers are created.

Based on this, the bulldozer will perform the spreading and the vibration roller will perform the compaction. Based on the construction record of each layer finished by the vibration roller, a two-dimensional map-like management form is created and submitted to the client.

A comparison of the flow of the conventional and proposed methods is shown in Figure 6. This method does not require a BIM modeler for day-to-day management. As can be seen from the resources and inputs shown in Figure 7, the conventional method requires more effort to change the plan and to ensure the consistency of the management forms when the plan is changed.

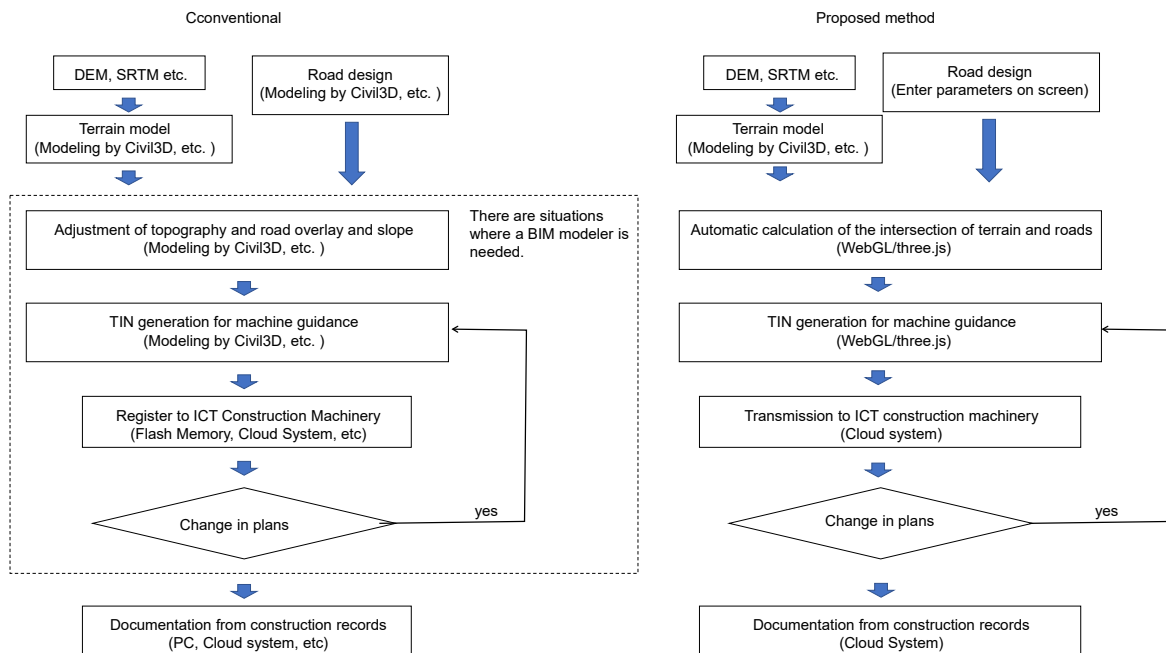


Figure 6. Comparison of the flow of the conventional and proposed methods

2.4 System Operation Flow

This system is a web program using WebGL (Ishida et al., 2015). A particularly important function in generating the planned TIN model in automatic planning is the collision determination for the terrain model. For this, we used Raycaster from three.js, a JavaScript 3D Library. The points where the parametrically expressed longitudinal and cross-sectional shapes collide with the terrain model are determined, and the construction area is obtained by connecting them.

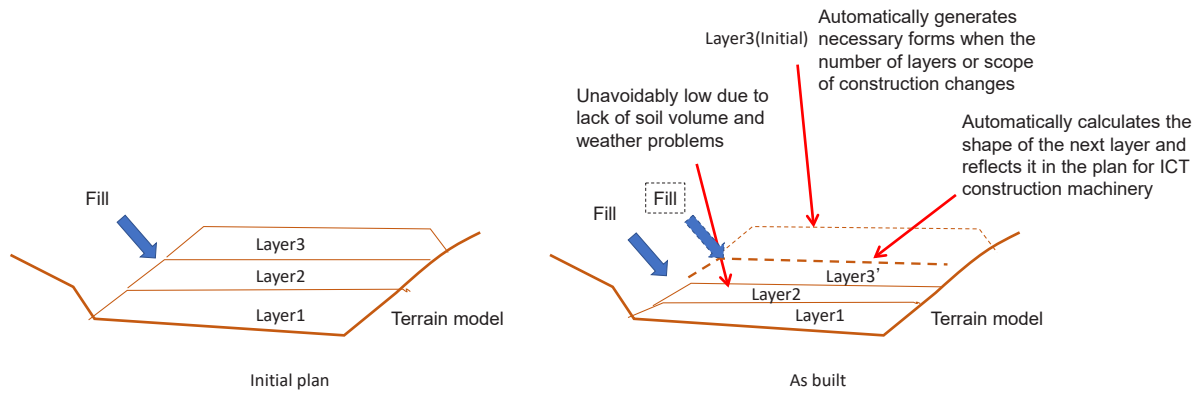


Figure 7. Automatic adjustment for construction that differs from the plan

The operational flow of the system is shown in Figure 8. The terrain models are registered, and the parameters for road center alignments and cross-sections are registered. The terrain model registered this time is a TIN model created from 5m mesh DEM. The parameters registered this time were 30 sections of road center alignments and 50 types of cross-sections. Figure 9 shows a screen shot of the road centerline registration screen and a plan view of the registered results. Figure 10 is a registration screen showing the cross-section profile and the registered results in a cross section view. On the upper left side of the registration screen, select cut or fill and specify the width of the road, pavement thickness, and slope of the road surface. On the lower left side of the registration screen, you register the slope shape. Specify the slope height and slope gradient, and multiple slopes can be registered repeatedly. On the right side of the registration screen, berm shapes can be registered. Width, height, and slope can be specified. The cross-sectional shape registers the shape of one side. When placing the transect shape on the road center alignment, you can select symmetry, left, or right as the placement target. Figure 10 shows the screen for placing a cross section on the road center alignment. In this screen, the beginning and end points of the cross section are specified on the road center alignment. Symmetry, left, and right can be specified. The result of the placement is given in the list on the right side of the screen.

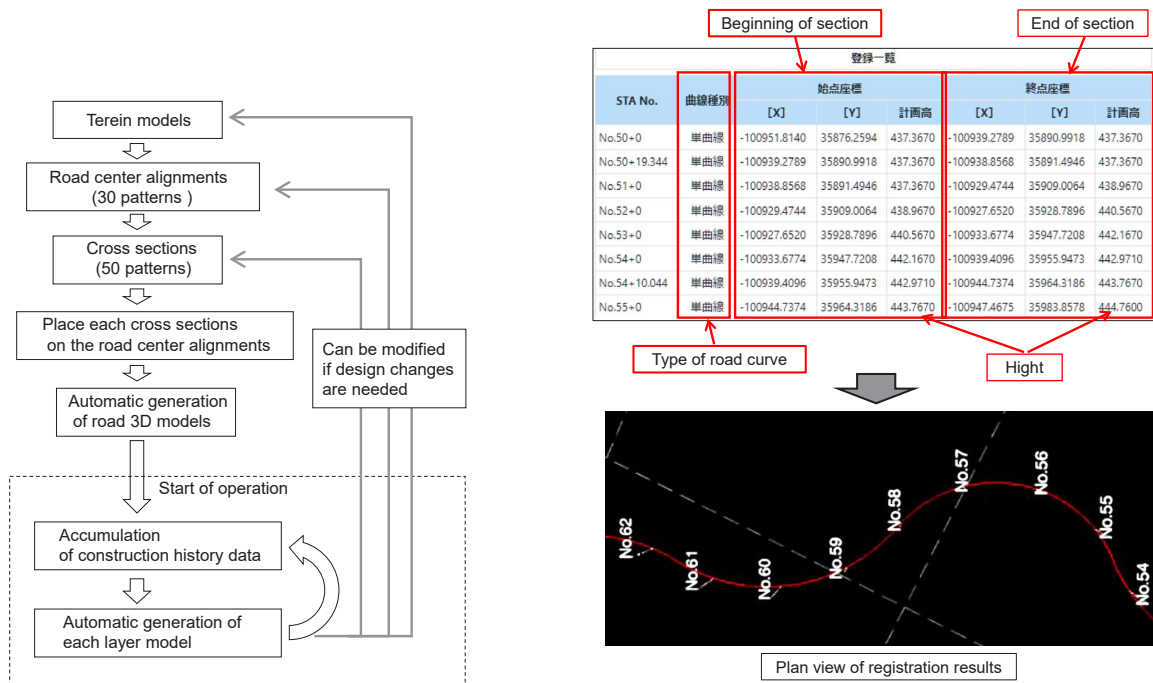


Figure 8. Operation flow

Figure 9. Registration of road center alignments

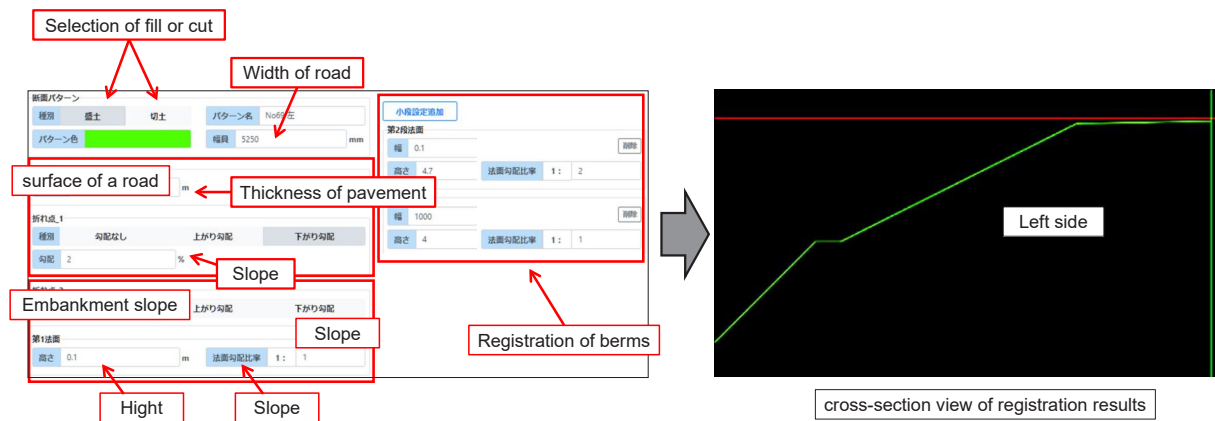


Figure 10. Registration of cross-sectional profiles

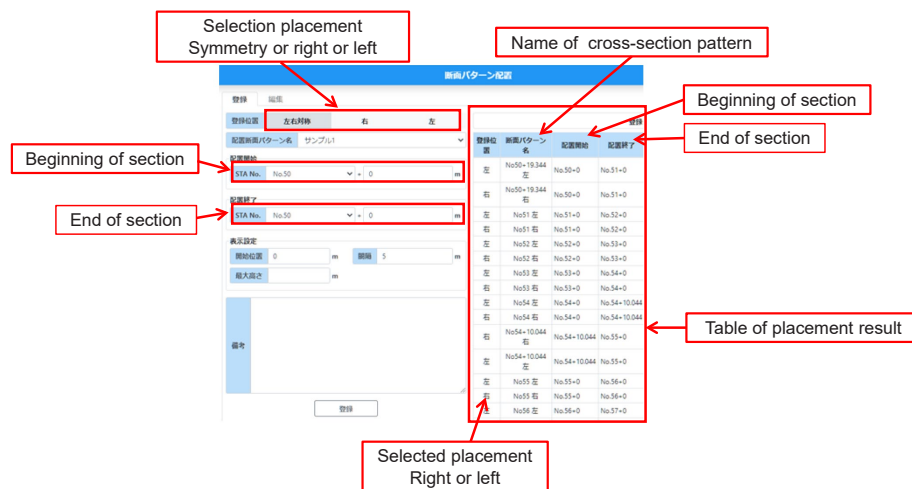


Figure 11. Placement of cross sections on road center alignments

3. RESULTS AND DISCUSSION

The work to which this system was applied was the construction of a carrying road for the Shitara Dam planned for Shitara-cho, Kitashitara-gun, Aichi Prefecture, ordered by the Chubu Regional Development Bureau of the MLIT. Table 1 shows the construction information. The work did not include the dam embankment, but involved the construction of a conveyance road, and the main work type was road earthwork.

Table 1. Construction site information

Name	FY 1991: Construction of a road for transporting waste rock aggregate from Shitara Dam
Orderer	Chubu Regional Development Bureau, Ministry of Land, Infrastructure, Transport and Tourism (MLIT)
Construction Period	July 6, 2019 – March 31, 2021
Construction Site	Shitara-cho, Kitashitara-gun, Aichi Prefecture,
Construction Outline	Siuki Section Embankment Excavation V = 187,970m ³ , Forensic A = 13,460m ² , Drainage structures 1 type Egasawa Section Soil V = 154,920m ³ , Forensic A = 1,987m ² , Reinforced Soil 30,300m ³ , Wall holder 1 type Tajiri Section Steel bridge L = 568m, Wall holder A = 319m ²

The results of the application of automatic planning are shown in Figure 12. When this system was applied, the next layer of embankment plan was automatically generated from the results of the vibration roller construction

and used for the bulldozer construction. When this system was applied, the next layer of embankment plan was automatically generated from the results of the ICT vibration roller construction and used for the construction of the ICT bulldozer. The construction history used for the automatic planning is stored in a BIM model, and when the BIM model was checked using VR (Figure 13), it was found to be more efficient than the conventional management method, as it was easier to grasp the consistency. When plans are changed, the BIM model is automatically updated and the planning files for ICT construction machinery are automatically output, eliminating the need for on-site staff to edit the BIM model. As a use case, the plan was modified when it became necessary to construct with dump trucks passing halfway across the embankment against the cross section of the embankment (Figure 14). The width of the embankment must be divided in half, and the sliding must be site matched so that the difference in elevation between the left and right sides is not too large.

The work efficiency when changes occur in the plan is shown in Table 2. While the conventional method required modeling work for new plans, this method does not, and the instructions to the operators of the ICT construction machinery are easier to follow, thus reducing staff labor by 0.8 man-days. Thus, changes in plans can be made easily. In addition, construction records and plan changes on the BIM model could be accurately confirmed even from remote locations such as the office, since the details are integrated into the VR space at any time. Daily planning can be facilitated in this way. In addition, in confirming the construction records and plan changes on the BIM model, the details were integrated into the VR space at any time so that they could be accurately identified from remote locations such as the office. By managing construction records in BIM, it is possible to visualize the status of workmanship and compaction in an easy-to-understand manner, eliminating the need to create conventional forms. In addition, since the details of the BIM model, including construction records, can be checked via a web system, construction sites with many hazardous areas can be managed safely from a remote location.

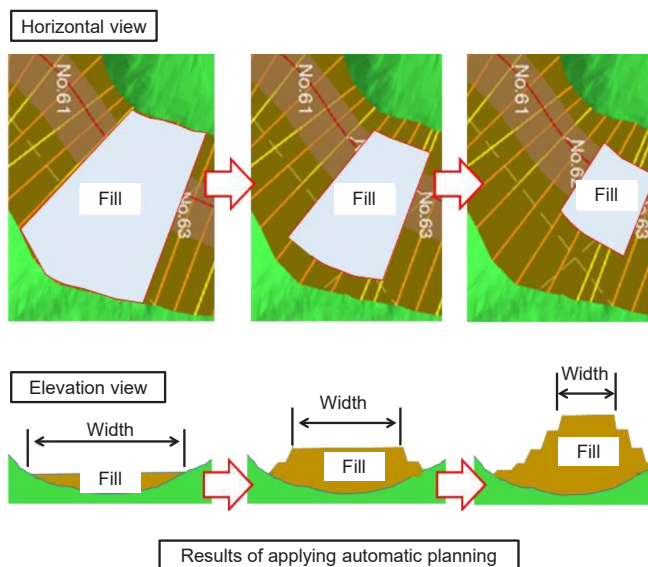


Figure 12. Results of applying automatic planning

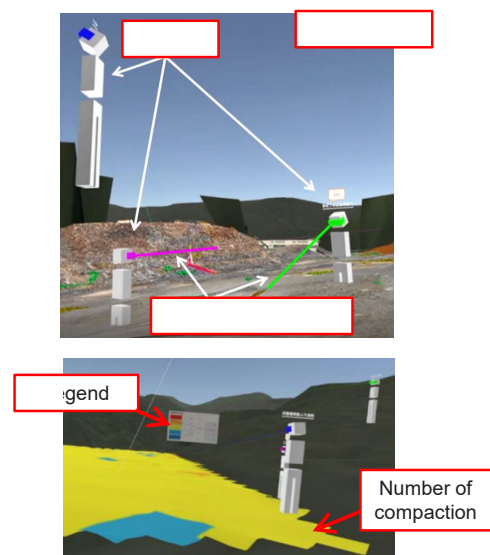


Figure 13. VR confirmation of construction data registered in BIM (VR-space)

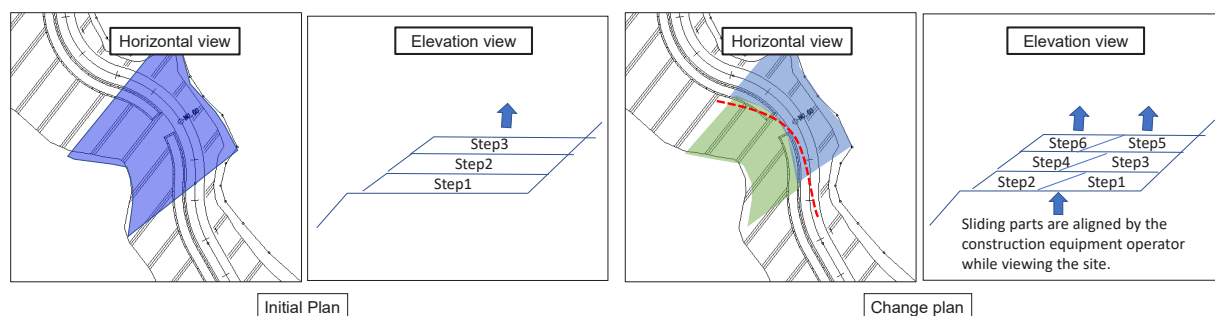


Figure 14. Use Case

Table 2. The work effort

	Conventional(min)	Proposed method(min)
Re-planning	180	0
on-the-spot check/Instructions to ICT construction machinery operators	180	120
Report	60	20
Total	420	140
(420-140)/360=0.8 man-days (Calculate a day as 8 hours)		

In addition, although it was only a part of the construction project, it was possible to automatically generate plans for ICT construction machinery from the construction history data, and to perform the embankment according to those plans. During the process of earthwork, daily minor plan changes occur frequently, but it is difficult to quickly make changes to plans in BIM and to maintain consistency in the management of quality records. This method is likely to eliminate this gap.

Automatic planning will be an important component of automated construction in the future (Otsuki et al., 2020). It is also very important to ensure safety by making the sites where automated construction is performed unmanned. We believe that the automatic planning method and VR-based site confirmation technology demonstrated here are important for the future of the construction industry, and we intend to make improvements and expand the functionality of the system.

ACKNOWLEDGMENTS

The field trial of this method was subsidized by the "Project on the Introduction and Use of Innovative Technology for Dramatic Improvement of Construction Site Productivity," a project implemented by the MLIT. In conducting this research, we also received a great deal of cooperation from the Technical Management Division of the Chubu Regional Development Bureau, Shitara Dam Construction Office, and other related parties.

REFERENCES

- Ishida, H. and Yabuki, N. (2015). Application of WebGL to Maintenance and Management of Civil Engineering Structures, *Journal of Japan Society of Civil Engineers*, Series F3 (Civil Engineering Informatics), 71 (2), 58-65
- Imai, R., Taniguchi, H., and Matsuura, G. (2017). As-Built Management Using the Execution History of Construction Machines in Pavement Construction. *Journal of Japan Society of Civil Engineers*, Series F3 (Civil Engineering Informatics), 73 (2), 416-423
- Kim, J., Kim H., Tanoli, W. A., and Seo, J. W. (2009). 3D Earthwork BIM Design and its Application in an Advanced Construction Equipment Operation, *Architecture and Engineering*, 4 (2), 22-26
- Ministry of Land, Infrastructure, Transport and Tourism (MLIT). (2021). *Guidelines for Supervision and Inspection of Formwork Management Using Construction History Data* (Earthworks) (Draft), p.1.
- National Institute for Land and Infrastructure Management (NILIM). (2020). *Concept of parametric model for data exchange* (draft), pp.1-2.
- Otsuki, T., Morikawa, H., Shiiba, Y., Ogata, S., and Moteki, M. (2020). Research on standardization of construction site time-series change information as learning data for automatic generation of work plan of construction machinery in earthworks, *Proceeding of the 37th International Symposium on Automation and Robotics in Construction (ISARC)*, Kitakyushu, Japan, pp.1053-1060.
- Raza, H., Park, S., Lee, S. S., Tanoli, W. A., and Seo, J. W. (2017a). 3D Earthwork BIM Design Process for a Road Project, *Journal of KIBIM*, Vol.7, No.2, Korean Institute of Building Information Modeling, pp.8-15.
- Raza, H., Tanoli, W. A., Lee, S. S., and Seo, J. W. (2017b). Flexible Earthwork BIM Module Framework for Road Project, *Proceeding of the 34th International Symposium on Automation and Robotics in Construction (ISARC)*, Taipei, Taiwan, pp.410-415.

NEW ERA OF MAPPING PRODUCTS FROM UAV-BASED OBLIQUE CAMERA SYSTEM

Thirawat Bannakulpiphat¹ and Phisan Santitamnon²

1) Researcher, Department of Survey Engineering, Faculty of Engineering, Chulalongkorn University, Bangkok, Thailand. Email: thirawat.bannakulpiphat@gmail.com

2) Dr.-Ing., Associate Professor, Department of Survey Engineering, Faculty of Engineering, Chulalongkorn University, Bangkok, Thailand. Email: phisan.chula@gmail.com

Abstract: Unmanned aerial vehicles (UAVs), equipped with small and compact oblique camera systems, are revolutionizing the field of mapping and surveying by providing highly detailed and accurate 3D maps of terrain that were previously difficult to generate. By processing oblique images captured by these systems, a range of products can be generated, including true orthophotos, 3D city models by colorized point cloud, 3D textured city models, oblique viewer with easy 3D measuring capability, and precise multi-view 3D object measurement. These products offer unparalleled flexibility and all-purpose applications with accuracy, making UAV-based oblique camera systems well suited for a wide range of applications supporting city administration, such as Building and Construction Information Modeling (BIM/CIM), urban planning, infrastructure development, building control regulation/legislation, and finally the digital twin. This paper explores the potential of these modern mapping products and highlights their benefits and limitations in the case of megacities, e.g., Bangkok. The paper discusses the impact of small and compact UAV-based oblique camera systems on the mapping and surveying industry and emphasizes the need for ongoing research and development in this rapidly evolving field.

Keywords: UAVs, Oblique camera system, 3D city model, 3D geoinformation, Multi-view object measurement

1. INTRODUCTION

The use of multi-head camera systems mounted on unmanned aerial vehicles (UAVs) has emerged as a game changer in the field of mapping and surveying by capturing nadir and oblique photographs simultaneously; these camera systems provide a rich source of geometric information, which significantly enhances the interpretation and classification of terrain features (Remondino & Gerke, 2015; Gerke et al., 2016). The technology not only improves mapping efficiency, but it also facilitates the acquisition of multi-view images, resulting in a higher number of images for further multi-view geometry and point cloud processing (Bannakulpiphat et al., 2022). With the advent of UAVs equipped with oblique camera systems, the generation of highly accurate and detailed 3D terrain maps, especially in urban areas, has become feasible for applications such as urban planning, infrastructure development, building control regulation/legislation, and building and Construction Information Modeling (BIM/CIM). These systems have dramatically improved the interpretation and classification of terrain characteristics, such as structures and vegetation cover, that were previously difficult to identify using traditional mapping methods.

This article aims to explore the potential of oblique camera systems mounted on unmanned aerial vehicles (UAVs) in mapping and surveying, highlighting their benefits and limitations in the context of megacities. The paper focuses on the products that can be generated by processing oblique images, such as true orthophotos, 3D city models with colorized point clouds, 3D textured city models, oblique viewers with easy 3D measuring capability, and precise multi-view 3D object measurements. These products provide unparalleled flexibility and accuracy, making UAV-based oblique camera systems suitable for a wide range of applications.

2. UAV-BASED OBLIQUE CAMERA SYSTEMS FOR MAPPING AND SURVEYING

To successfully utilize UAV-based oblique camera systems for mapping and surveying, several essential steps are required. First, planning and preparing flights, including obtaining the necessary permits. The ground control point (GCP) coordinates are then established and measured to ensure accurate positioning and project control. During the mission flight, on-site image quality checks are performed and aerial triangulation is computed and adjusted for nadir images for quality control purposes (Bannakulpiphat et al., 2023). A key difference of the oblique camera compared to the nadir camera mission is the introduction of the rig parameter. A photogrammetry camera rig is a system of multiple cameras that are arranged in a specific configuration and synchronized to capture a series of overlapping images of an object or scene from multiple angles. The design and selection of optimal rig parameters are critical to determining the best model for an oblique camera system. Bundle Block Adjustment (BBA) with constraint rig parameters is used to compute and adjust aerial triangulation. Finally, precise geotagged images with their orientations are generated, providing a foundation for producing those potential products, such as true orthophotos, 3D city models by colorized point cloud, 3D textured city models, oblique viewer with easy 3D measuring capability, and precise multi-view 3D object measurement. Figure 1 illustrates the workflow to process images from an oblique camera system.

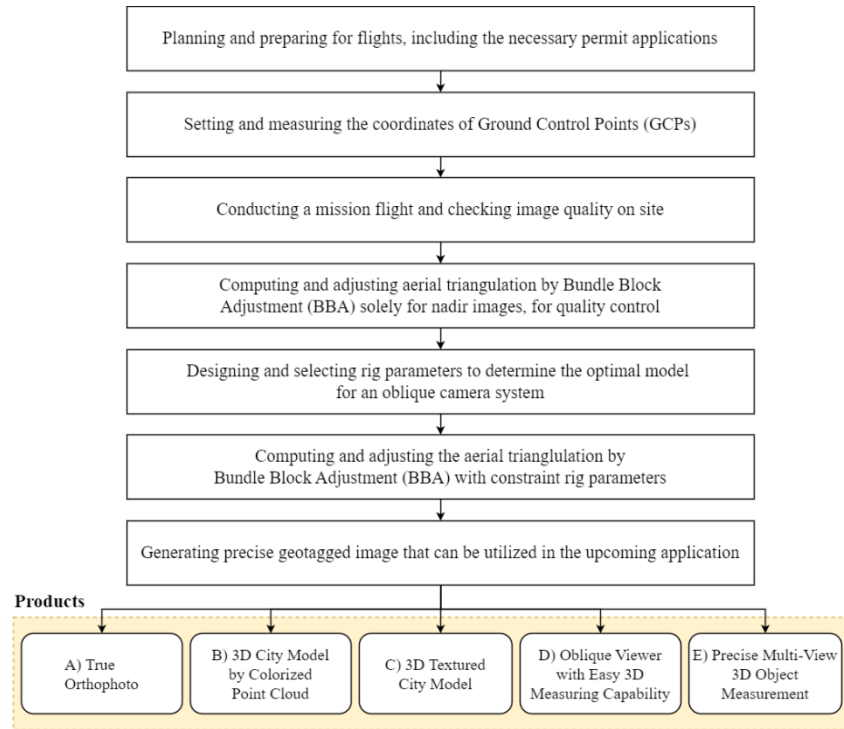


Figure 1. The workflow for processing images from an oblique camera system

3. APPLICATIONS OF PRODUCTS FROM THE UAV OBLIQUE CAMERA MISSION

There are five major mapping products from a UAV oblique camera mission, each of which can be applied to a variety of applications:

3.1 True Orthophoto

The “true orthophoto” accurately represents the Earth's surface by removing distortion and displacement caused by terrain relief in aerial photographs. The generation of true ortho needs to correct not only terrain distortion and relief displacement but also building and tree heights. True orthophotos are preferred for applications such as urban planning, engineering, and city administration, where accurate measurement of ground features is critical and there is no occlusion from high-rise buildings. Figure 2 compares two types of orthophoto generated by processing nadir and oblique images with the Google satellite image, called “ground ortho” captured at the same location, revealing significant differences. While the ground ortho offers a broad overview of the area with occlusion, the true orthophoto offers a more detailed, building standing-up, and accurate representation of the terrain due to its higher resolution and corrected distortion. True orthophoto facilitates the identification of individual features such as buildings, roads, and vegetation, unlike the satellite image, which suffers from distortion in areas with high-rise buildings and high vegetation that hide important details for most city applications.

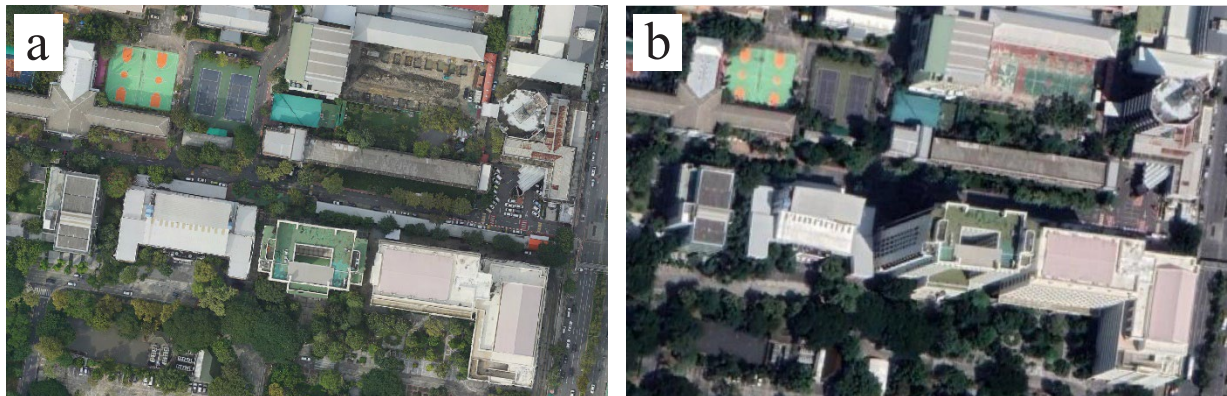


Figure 2. A comparison between the orthophotos (a) true ortho from UAV and (b) ground ortho from the very high-resolution satellite image from Google Map

3.2 3D City Model by Colorized Point Cloud

The 3D colorized point cloud city model is a mapping product based on dense point clouds generated from photogrammetry and computer vision techniques. The model generates a highly detailed representation of urban areas. It uses colored point cloud data to allow precise measurements and visualizations of buildings and structures (see Figure 3a). The colorization of point cloud data also facilitates the identification of different materials, such as buildings, roads, and trees, making it a useful tool for visualization and communication purposes. From the Chulalongkorn University block, we found that the 3D colorized point cloud model can be successfully reconstructed for most parts of the area, even in the corner of the city jungle. Overall, the 3D colorized point cloud city model is a powerful and versatile tool for analyzing and understanding urban environments. The 3D measurement directly on the point cloud data is also possible.

3.3 3D Textured City Model

A 3D textured city model refers to a digital 3D representation of a city or urban area that includes realistic surface textures applied to the geometry (see Figure 3b). This model is created using photogrammetry techniques that involve processing multiple overlapping images taken from different angles to create dense point clouds that represent the 3D geometry of the area. The textures are then applied to the point cloud to create a realistic representation of the city. This model has numerous applications in urban planning, architecture, and cultural heritage.



Figure 3. Examples of (a) the 3D city model by colorized point cloud data and (b) the 3D textured city model generated from processing nadir and oblique images. The yellow rectangle in the image shows the area of the Engineering Centennial Memorial Building, located in the Faculty of Engineering at Chulalongkorn University.

3.4 Oblique Viewer with Easy 3D Measuring Capability

The oblique viewer with easy 3D measuring capability is a product that offers a comprehensive and accurate representation of objects or surfaces in three dimensions from nadir and oblique images captured by UAVs. This mode of application is probably suited for urban planning and building control regulation/legislation by allowing users to view images taken from different angles, providing a more detailed understanding of the object's shape, texture, and other characteristics (see Figure 4).

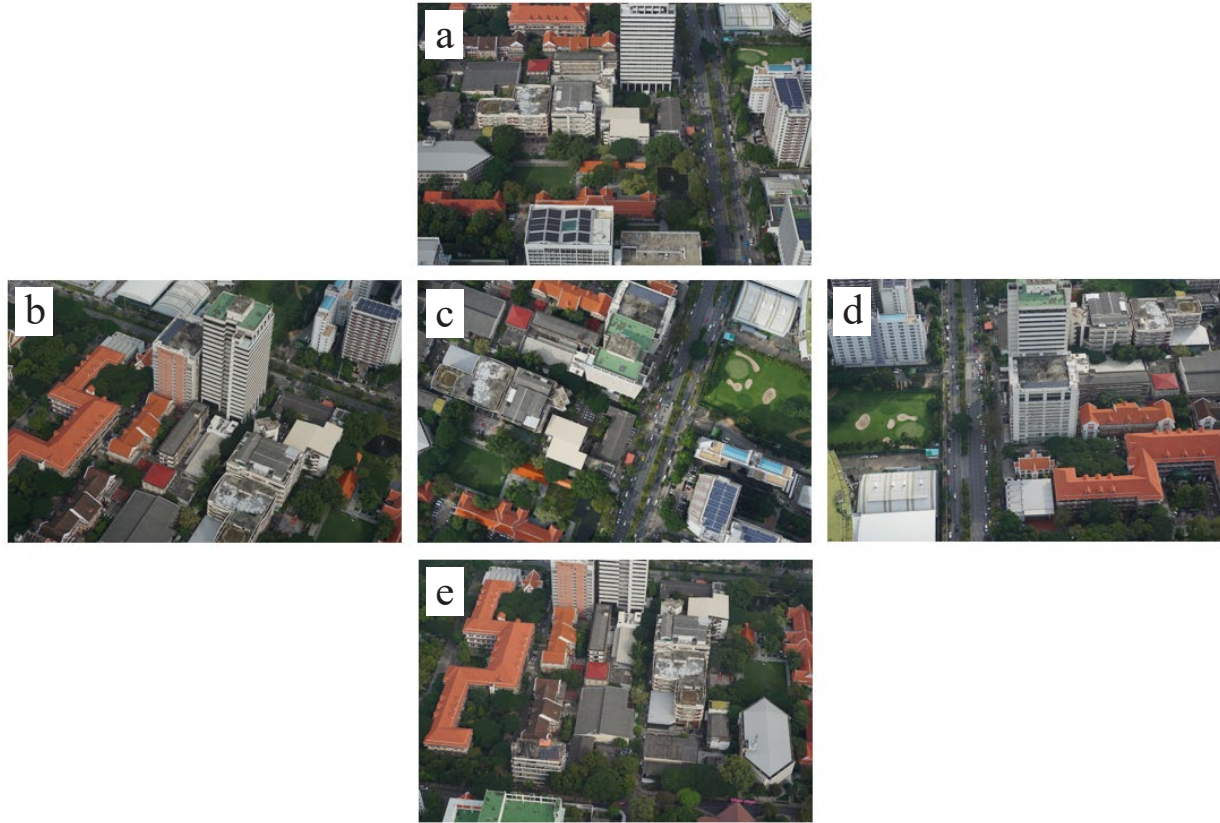


Figure 4. Example of images from an oblique viewer (a) front image, (b) left image, (c) nadir image, (d) right image, and (e) rear image

3.5 Precise Multi-View 3D Object Measurement

Precise multi-view 3D object measurement is a state-of-the-art photogrammetry technique that generates a highly accurate geometry of a UAV image block by retaining precise Interior Orientation Parameter (IOP) and Exterior Orientation Parameter (EOP) supporting 3D pointwise calculation from multiple images captured from different viewpoints (see Figure 5a). Unlike conventional 3D measurement photogrammetry, which relies on only two images and a two “stereo” projection ray. This multi-view approach uses the intersection of multiple projection rays to achieve greater precision and detail in modeling complex objects (see Figure 5b). This product is designed to provide a high level of precision when measuring 3D objects from multiple viewpoints. The system works by creating a bundle of 3D rays from the key point on the objects appearing from both nadir and oblique images. The resulting model can be viewed from various angles, allowing for precise measurements of the object's dimensions with an accuracy level up to the ‘centimeter’. In summary, the precise multi-view 3D object measurement technique is a powerful tool that provides high-precision measurements of 3D objects from multiple viewpoints, with numerous applications across building and construction information management.

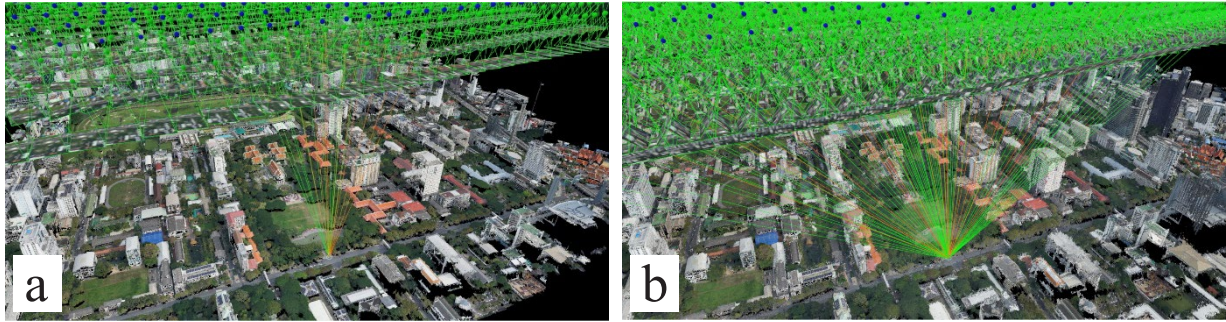


Figure 5. Comparison of the intersection of the number of projection rays between processing (a) only nadir images and (b) nadir and oblique images

The precise multi-view 3D object measurement enables highly accurate 3D measurements to be taken from nadir and oblique images captured by UAVs. By allowing users to view and measure objects from multiple angles, it provides a more comprehensive and accurate analysis of the data. The viewer's measurement capability is highly precise, enabling measurements of distance, height, and area with exceptional accuracy. In a city with dense high-rise buildings, measuring over the façade is important, as oblique images can capture the top of the object more accurately than vertical images. The product can be used to measure various objects, such as buildings, billboards, flags, and building signs (as shown in Figure 6), and provides coordinates and errors of the measured objects (as shown in Table 1). This kind of measurement can help to assess land, housing, and billboard taxation.

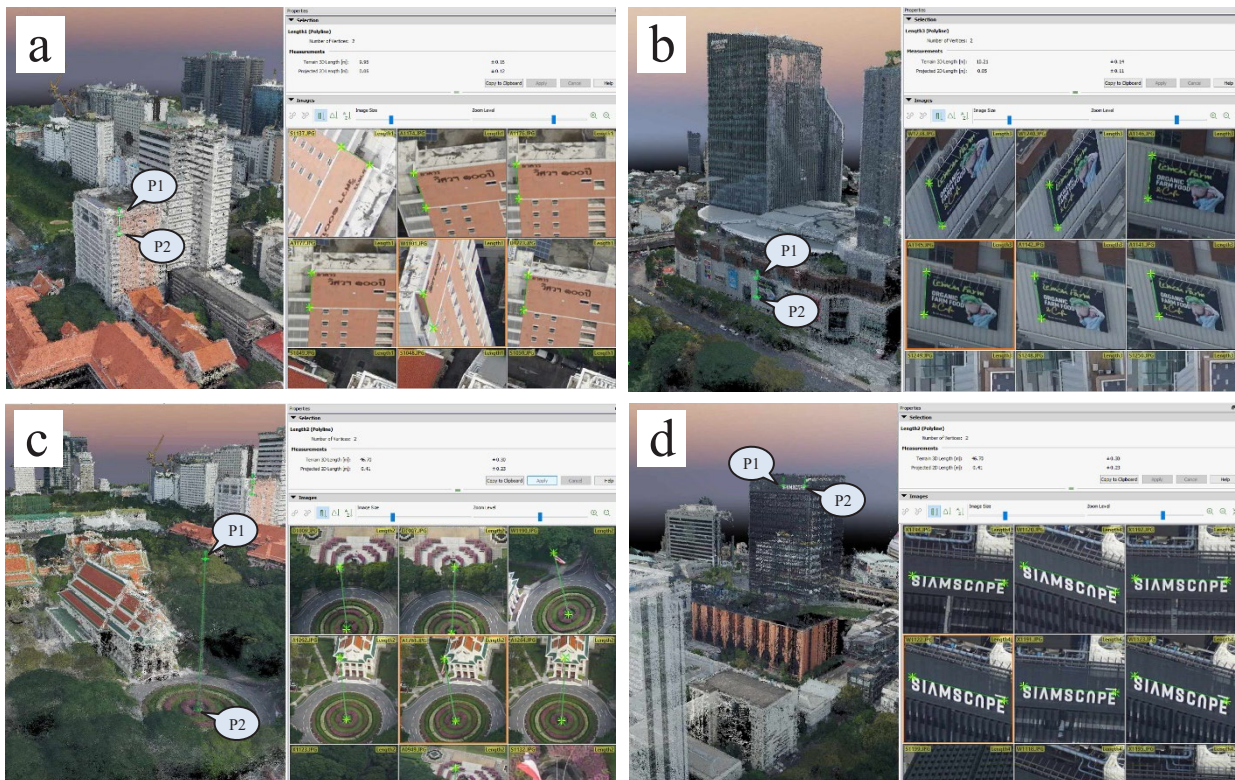


Figure 6. Precise 3D measurement by oblique images of: (a) building, (b) billboard, (c) flag, and (d) building sign

Table 1. Result of the measurement of 3D precise points (Easting, Northing, Height Above Ellipsoid; HAE) with their error statistics.

Name	Point	Coordinate (m)			Error Statistics (m)		
		Easting	Northing	HAE	Easting	Northing	HAE
Line 1 (a) building	P1	665833.42	1519109.99	28.46	0.05	0.03	0.07
	P2	665833.44	1519109.94	18.51	0.07	0.04	0.09
Line 2 (b) billboard	P1	665289.89	1518862.05	-6.63	0.04	0.03	0.05
	P2	665289.94	1518862.06	-16.85	0.06	0.04	0.08
Line 3 (c) flag	P1	665654.77	1519316.82	17.43	0.14	0.13	0.18
	P2	665655.15	1519316.67	-29.27	0.08	0.08	0.12
Line 4 (d) building sign	P1	665584.37	1519972.94	95.73	0.04	0.20	0.20
	P2	665600.05	1519970.24	95.75	0.04	0.18	0.18

4. CONCLUSIONS

In conclusion, the processing of nadir and oblique image data captured by small and compact UAV-based oblique camera systems has resulted in the creation of valuable products for BIM/CIM applications. The true orthophoto accurately represented and completely revealed the ground surface, while the 3D city model and the 3D textured city model provide detailed visual representations of urban areas with 3D measurement capability. Moreover, the oblique viewer and precise multi-view 3D object measurement products enable precise measurements and analysis of structures and objects in the captured images. These products have significantly impacted the mapping and surveying industry by enabling more efficient and accurate data collection and analysis for Building and Construction Information Modeling (BIM/CIM), urban planning, infrastructure development, building control regulation/legislation, and finally the digital twin. In addition, the mission of the UAV-based oblique camera has made mapping and surveying operations safer and more cost-effective by decreasing the need for manned aircraft and perhaps a small amount of ground survey work. However, ongoing research and development in this field is necessary to address challenges such as a huge amount of image capture with five-time data growing, successive data processing, and future design of the service platform. Further advances in this rapidly evolving field have the potential to revolutionize the mapping and surveying industry and contribute to various applications, including urban planning, infrastructure development, and disaster management.

ACKNOWLEDGMENTS

The authors express their gratitude to the Metropolitan Electricity Authority (MEA) for providing support for the data, software, and hardware used in this research.

REFERENCES

- Bannakulpiphat, T., Santitamnont, P., and Maneenart, T. (2022). A Case Study of Multi-Head Camera Systems on UAV for the Generation of High-Quality 3D Mapping. *Engineering Journal of Research and Development*, ISSN: 2730-2733, 33 (4).
- Bannakulpiphat, T., Santitamnont, P., Maneenart, T., and Wongweeranimit, W. (2023). Best Practice for Mapping Production from UAV Imagery. *Engineering Journal of Research and Development*, ISSN: 2730-2733, 34 (1).
- Gerke, M., Nex, F., Remondino, F., Jacobsen, K., Kremer, J., Karel, W., Huf, H., and Ostrowski, W. (2016). Orientation of oblique airborne image sets-experiences from the ISPRS/EUROSDR benchmark on multiplatform photogrammetry. *The International Archives of Photogrammetry, Remote Sensing, and Spatial Information Sciences 41-B1*, 41, 185-191.
- Remondino, F., and Gerke, M. (2015, September). Oblique aerial imagery—a review. In *Photogrammetric Week 15* (2), 75-81.

EVALUATION OF INTEROPERABILITY BY QUANTIFYING DATA INTEGRITY IN THE INTEGRATION OF BIM AND STRUCTURAL ANALYSIS FOR MULTIPLE LEVELS OF DEVELOPMENT

Kayla Solis¹, Pher Errol Quinay², and Karlo Daniel Colegio³

1) BSCE, Institute of Civil Engineering, College of Engineering, University of the Philippines Diliman, Quezon City, Philippines. Email: kgsolis1@up.edu.ph

2) D.Eng, Associate Professor, Institute of Civil Engineering, College of Engineering, University of the Philippines Diliman, Quezon City, Philippines. Email: pbquinay2@up.edu.ph

3) MSCE Candidate, Instructor, Institute of Civil Engineering, College of Engineering, University of the Philippines Diliman, Quezon City, Philippines. Email: kqcolegio@up.edu.ph

Abstract: In the Architecture, Engineering, and Construction (AEC) Industry, the model generation of structures and structural analysis are generally done in separate phases of a project. In order to achieve a more streamlined and efficient process for these phases, the interoperability of Building Information Modeling (BIM) and structural analysis was examined in this study. Since the integration of BIM and structural analysis involves data transfer between different platforms, there are interoperability challenges related to the accuracy and consistency of transferred data. This research study aimed to evaluate interoperability considering data integrity in the integration of BIM and structural analysis for multiple Levels of Development (LOD). Firstly, five LODs were considered to target a specific detail of structural analysis and digital modeling for a load-bearing system of a structure. Digital models employing BIM were created using the information gathered and identified LODs. Secondly, models suitable for structural analysis were generated and analyzed. Next, the data integrity was quantified based on a criterion involving different properties of the model, such as orientation, element type, connection, cross-section, length, compressive strength, and modulus of elasticity. In application to a study model and a model for an actual church wall structure, it is found that aside from data formats significantly affecting the data integrity, the mentioned properties influence the data integrity to varying degrees, thus, highlight the need for improvement in data transfer process for higher LODs. This study provides an evaluation of interoperability that may guide designers on how to proceed when conducting integration procedures during the modeling-analysis process by providing the data integrity values to be expected after the data transfer processes.

Keywords: Interoperability, Data Integrity, Structural Analysis, BIM, LOD

1. INTRODUCTION

The Building Information Modeling (BIM) is predominantly utilized in the design and construction phase, and is widely used in the Architecture, Engineering, and Construction industry to help architects, engineers, and managers achieve the best practice of the different phases in the life cycle of a structure. There are other processes involved under each phase, such as modeling, design, structural analysis, construction, facility management, demolition, etc. However, there is no single software that can be used to perform all these processes. Hence, data transfer processes are done between different platforms to account for the inability of these platforms to perform all procedures. Moreover, since there are multiple processes involved, there are also multiple stakeholders and professionals that need to collaborate in order to complete a project (Sampaio & Gomes, 2021).

With the goal to integrate different processes and ensure that throughout the different phases, the data gathered and obtained from each collaborator is kept as accurate and consistent as possible, this study focuses on the integration of modeling and analysis, specifically, the BIM process that involves different extents of model detailing and the structural analysis of a structure. It evaluates interoperability by quantifying the data integrity throughout the integration process that could describe the accuracy and consistency of the data being transferred which is essential in achieving a collaborative and efficient process in construction and design projects.

Interoperability is the ability of ICT systems and of the business processes they support to exchange data and to enable the sharing of information and knowledge mainly through different data formats (EIF, 2004). It improves communication while increasing the quality of information management during data transfer processes. However, given the limitations of data transfer processes, interoperability may be a problem when different platforms are used. To address this, file formats that enable interoperability were developed. BuildingSMART, formerly known as International Alliance for Interoperability (IAI), developed the Industry Foundation Classes (IFC) format. IFC is a platform neutral, open file format that is developed to enable interoperability between different platforms to improve collaborations between different stakeholders. Aside from IFC, another file format that enables interoperability is the Drawing Interchange Format or Drawing Exchange Format (DXF). However, unlike IFC which is used in BIM platforms, DXF is used mostly for CAD and similar programs. IFC and DXF are two of the few file formats that are available as export and import formats in different platforms.

With the increasing adoption of BIM in engineering practice in the Philippines, it is important to address

the limited references focusing on interoperability in the integration of BIM and structural analysis. Interoperability can be evaluated through the quantification of data integrity which is the overall accuracy, completeness, and consistency of data over its lifecycle (Brook, 2020). A related study by Sampaio & Gomes (2021) analyzes BIM interoperability in structure design where several BIM and structural analysis software were used and compared. However, interoperability is not only affected by the software used. There are also other factors to look into such as the data transfer format and the BIM LOD which takes into consideration the variation in the elements included in the BIM model. These factors are considered in this study to further evaluate the BIM interoperability. Such studies may guide designers on how to proceed when conducting integration procedures during the modeling-analysis process by providing the data integrity values to be expected after the data transfer processes.

2. METHOD

2.1 Objectives and Scope of the Study

The objective of the study is to evaluate interoperability considering data integrity in the integration of BIM and structural analysis for multiple LODs. The study proposes a quantification of the data integrity for multiple cases of data transfer involving different LODs and data formats. For this objective, the following activities were undertaken: (1) created the digital study models of a structure based on the selected LODs, and performed structural analysis; (2) proposed a scoring based on a criterion that involves different parameters in the model and evaluated the interoperability through the quantification of the data integrity after the data transfer processes; (3) applied the quantification on a model of an actual church wall structure.

The created study models include structural features such as walls, reinforcements, supports, beams, columns, material properties, and foundations. Architectural features such as the windows and doors were not considered. The quantification of data integrity is limited to these elements following the evaluation criteria applied to such structural configurations in the study by Muller et al. (2017).

Five LODs were used in the study, namely, LOD 100, LOD 200, LOD 300, LOD 400, and LOD 500. To describe each LOD: LOD 100 includes the main volume of the load bearing system; LOD 200 includes the main volume of the load bearing system and its material properties; LOD 300 includes the correct dimensions of the load bearing system (beams and columns) and the supports of the structure; LOD 400 includes the correct dimensions of the load bearing system (beams and columns), supports of the structure, reinforcements, and structural walls; LOD 500 includes the correct dimensions of the load bearing system (beams and columns), supports of the structure, reinforcements, structural walls, and foundations of the structure (Bertin et al., 2020).

Two data formats were used to transfer the BIM models to the structural analysis platforms: Drawing Interchange Format (DXF) and Industry Foundation Classes (IFC).

In this paper, the following softwares were used: BIM software (BS): Autodesk Revit 2021; structural analysis softwares: Autodesk Robot 2021 (SS1), CSI ETABS 2016 (SS2). SS1 and SS2 are two software tools that are widely-used for structural analysis and design of buildings in the Philippines. SS1 is from the same developer as BS, while SS2 is from a different developer.

2.2 Methodology

Figure 1 shows the methodology used in the study. It consists of the data gathering, use of BIM design software, use of structural analysis software, and evaluation of interoperability considering the parameters shown on the lower right side of the figure.

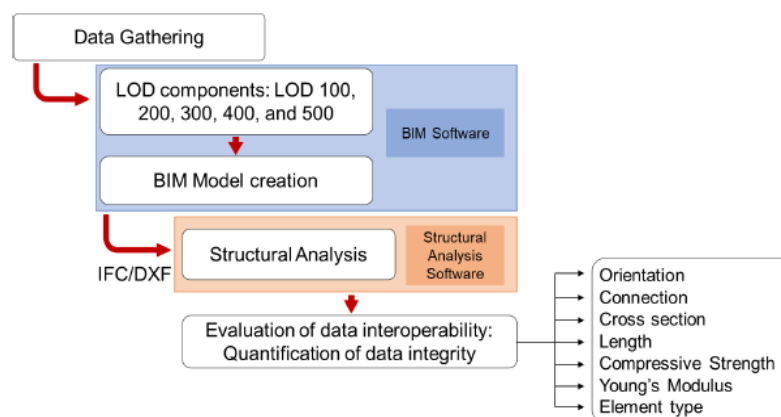


Figure 1. The methodology used in the study.

(1) BIM model creation

A study model was created for the developed procedure. Shown in Figure 2 are the dimensions of the

study model. The columns are 450 mm×600 mm cast-in-place concrete while the beams are 400 mm×800 mm cast-in-place concrete. The smaller column connecting the footing and the bigger column are 300 mm×450 mm cast-in-place concrete. The footings at the bottom are 1200 mm×1200 mm cast-in-place concrete that are 450 mm thick. The walls are 300 mm thick cast-in-place concrete. The material properties of cast-in-place concrete defined in BS is 23.250 GPa for the Young's Modulus and 24.1 MPa for the concrete compressive strength. Reinforcements are 22 mm diameter steel bars, arbitrarily placed 300 mm away from the sides and 300 mm apart from each other.

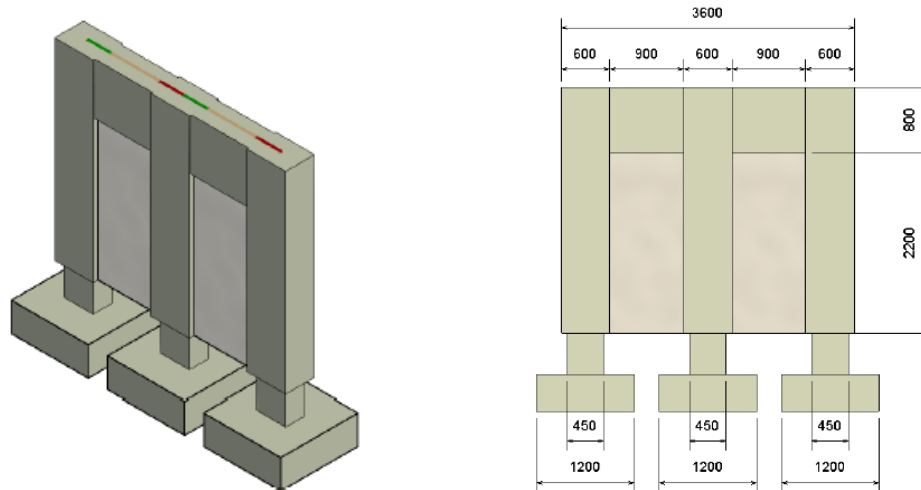


Figure 2. Description of the Study Model

(2) Structural Analysis

The structural models were generated using the DXF and IFC data formats of the BIM models as inputs in SS1 and SS2. The structural details specified in the BIM (enumerated in the previous section) are carried over to the structural analysis model through the exported data formats and spreadsheets. Structural analysis was then performed using a superimposed uniformly distributed in-plane vertical load of 10 kN/m applied at the beams and the self-weight. It should be noted that prior to the structural analysis, corrections on member connectivity and boundary conditions may be introduced to the structural model to satisfy the stability requirement.

(3) Evaluation of Interoperability by Quantification of Data Integrity

After the structural analysis, the interoperability was evaluated by quantification of data integrity. During the model transfer process and data correction in the structural analysis part, the properties and data that were changed or lost after transferring were identified. Some of these are the changes in orientation (or proper position of the member axes), length, or material properties, some member connections are lost, and some elements are not transferred such as supports.

The quantification of data integrity was based on an evaluation criteria adopted from a study by Muller et al. (2017). Muller et al. (2017) computes the data integrity by simply averaging the scores obtained without considering the weight of each property. In the current study each property is given a corresponding weight since each one has varying degree of accuracy required in structural analysis. To assign the weights of these properties, a decision matrix procedure was conducted which was adapted from The Quality Toolbox (Tague, 2005). The computation of the weights is shown in Table 1 where the decision matrix procedure was conducted.

The decision matrix procedure starts with the assignments of rating. The rating scale was decided for member connectivity, length, orientation, cross section, mechanical property, and support condition, as described by related studies (Kim, 2021; Mugahed Amran et al., 2019; Porter, 2007). The rating scale values are values from 1.0 to 3.0 that describe the required degree of accuracy of the property in structural analysis, with 1.0 being the lowest and 3.0 being the highest. The sum total of each rating scale was computed and the rating scales were all divided by this total amount. The results obtained are the weights for each property which was used for computing the weighted average of the quantification values of the data integrity.

Table 2 shows the scoring system used for the quantification of data integrity. For unquantifiable parameters such as orientation and element type, a scoring similar to the Likert scale was used. In Muller et al.'s study, the scoring was limited to 0 (incomplete), 0.5 (partial), and 1 (complete). This does not take into consideration the value transferred, hence, for quantifiable parameters, the percentage amount of transferred data relative to the quantity of the original data in BS was computed instead.

Table 1. Assignments of weights for the weighted average

Property	Rating Scale	Weight
Modulus of Elasticity (E)	1.0	1.0/13.5 = 0.074
Compressive Strength (f'_c)	1.0	1.0/13.5 = 0.074
Element type	1.5	1.5/13.5 = 0.111
Length	2.0	2.0/13.5 = 0.148
Cross Section	2.5	2.5/13.5 = 0.185
Orientation	2.5	2.5/13.5 = 0.185
Connection	3.0	3.0/13.5 = 0.223
Total	13.5	1.000

Table 2. Scoring system used in the evaluation

Property	Score
Modulus of Elasticity (E)	$E1 / E2$, where $E1 \leq E2$
Compressive Strength (f'_c)	f'_{c1} / f'_{c2} , where $f'_{c1} \leq f'_{c2}$
Element type	1 – correct; 0.5 – incorrect; 0 – no element
Length	Transferred length / Total initial length
Cross Section	Transferred area / Total initial area
Orientation	1 – correct; 0.5 – incorrect; 0 – no element
Connection	No. of correct connections / No. of total connections

2.3 Application to a Model of a Church Wall Structure

This study applied the evaluation procedure to a model of an actual church wall structure. The dimensions and material properties were obtained from site-inspection and material survey: the columns are 450 mm×850 mm cast-in-place concrete while the beams are 350 mm×800 mm cast-in-place concrete. The walls are 300 mm thick cast-in-place concrete. The modulus of elasticity of concrete is 23.25 GPa and the concrete compressive strength is 25.3 MPa. Reinforcements with 22 mm diameter were used. The rebar cover used was 100 mm and the reinforcements were placed 600 mm apart alternately. The LODs modeled were LOD 100, LOD 200, LOD 300, and LOD 400. LOD 500 was not considered due to insufficient information available for the foundation structure.

Similar to the study model, BIM model was created and structural analysis was performed. Gravity loads were applied based on the actual structural settings. Lateral loads were applied in-plane and out-of-plane to the model following the earthquake loading specified in National Structural Code of the Philippines 2015 (NSCP 2015).

3. RESULTS

3.1 Study Model

Shown in Figure 3 below is the graph comparing the properties and elements for each LOD. As shown, LOD 200 has 9.6% more elements and properties than LOD 100; LOD 300 has 16.9% more elements and properties than LOD 200; LOD 400 has 33.3% more elements and properties than LOD 300; and LOD 500 has 16.7% more elements and properties than LOD 400.

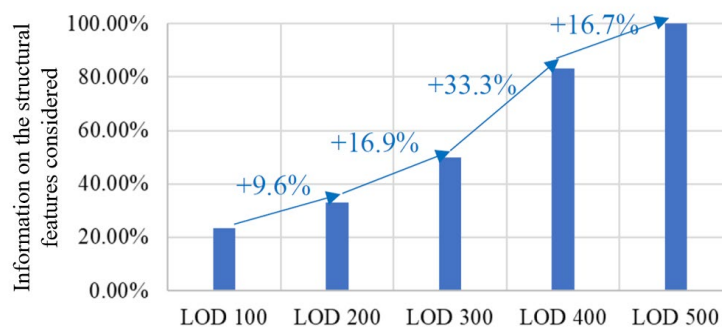


Figure 3. Comparison of elements and properties present on each LOD for the study model

Shown in Table 3 is a sample of the quantification values of the data integrity for a case of a study model (the nomenclature, case 500-I-SS1 of the table pertains to: “500” for LOD 500, “I” for IFC data format, and “SS1” for structural analysis software 1). Firstly, for the supports and reinforcements, since they are not transferred at all, a score of zero for all parameters was given. For the orientation, since the beams are incorrectly oriented, a score of 0.5 was given. For the foundations, the columns are incorrectly oriented, hence scored as 0.5. Since all the

elements are disconnected from each other, a score of zero was given for the connections. For the lengths, the length of the beams and the walls are originally both 1.5 m but the transferred lengths are only 0.9 m. Computing the percentage by dividing 0.9 m by 1.5 m, a value of 0.6 was obtained. For the material properties, the value of the compressive strength of concrete in BS (BIM software) is 24.1 MPa while the compressive strength value interpreted in SS1 is 25 MPa. The percentage was then determined to be 0.964. Moreover, the value of Modulus of Elasticity (Young's Modulus) in BS is 23.25 GPa while in SS1, it is 25 GPa. Computing for the percentage, a value of 0.93 was obtained. Lastly, for the rest of the elements with correct parameters transferred, a score of 1 was given. The same scoring procedure was done for all other cases. Figure 4 gives a summary of the quantification for all the cases considered.

Table 3. Quantification of data integrity for study model case 500-I-SS1

	Placement		Geometry		Materials			Weighted Sum
	Orientalion	Connec-tion	Cross Section	Length	f _c	E	Element type	
Columns	1	0	1	1	0.964	0.93	1	0.769
Beams	0.5	0	1	0.6	0.964	0.93	1	0.617
Support	0	0					0	0.000
Walls	1	0	1	0.6	0.964	0.93	1	0.710
Reinforce-ments	0	0	0	0	0	0	0	0.000
Foundations	0.5	0	1	1	0.964	0.93	0	0.566
								0.444

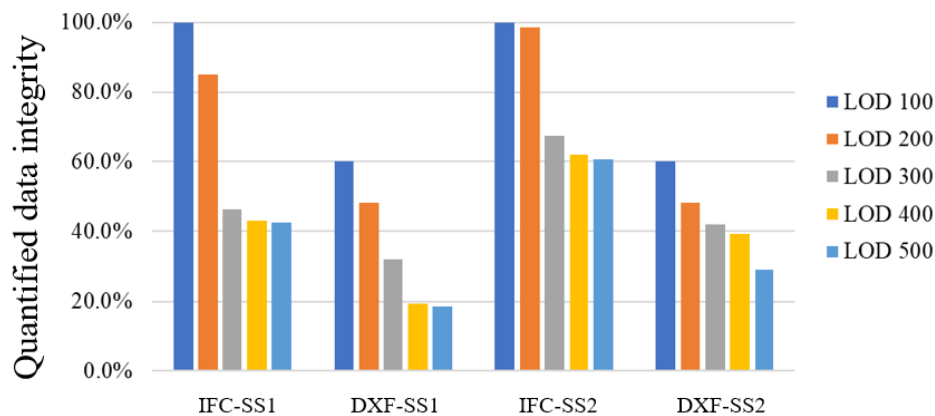


Figure 4. Quantification of data integrity for all cases of the study model

3.2 Model of a Church Wall Structure

Figure 5 shows the BIM model of the church wall structure created using BS. Following the methodology, multiple LOD models was created for this structure.

Figure 6 shows the graph comparing the properties and elements for each LOD. LOD 200 has 5.71% more elements and properties than LOD 100, LOD 300 has 43.81% more elements and properties than LOD 200, and LOD 400 has 40.00% more elements and properties than LOD 300.

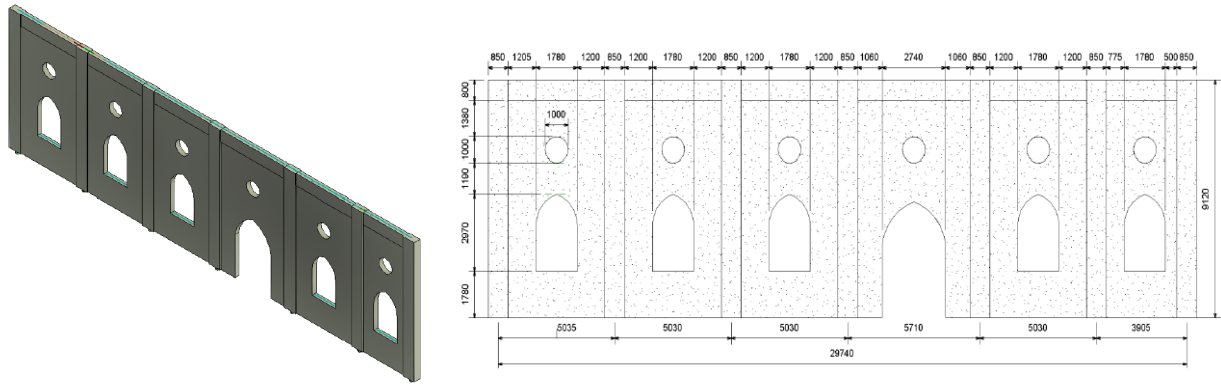


Figure 5. Model for the church wall structure created in BS and its dimensions

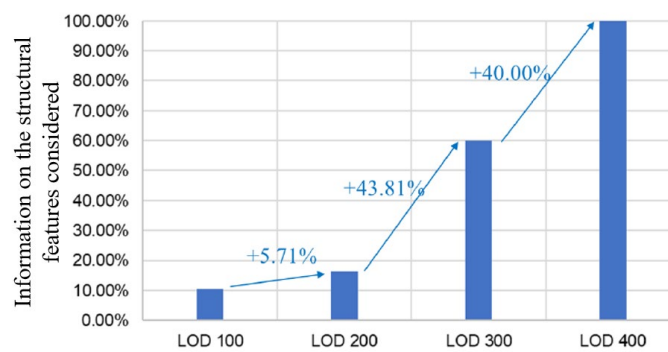


Figure 6. Comparison of elements and properties present on each LOD for the church wall model

Figure 7 shows a sample of the deformed shape after performing structural analysis (the nomenclature, case 400-I-SS1 pertains to: “400” for LOD 400, “I” for IFC data format, and “SS1” for structural analysis software 1).

Shown in Figure 8 is a graph of the quantification values of the data integrity for all cases checked in the church wall model. Similar observations in the study model can be seen. Lower LODs have higher data integrity than higher LODs, and that as the LOD increases, the data integrity decreases. Higher LODs consist of more elements which makes it more challenging to transfer all the data correctly. Therefore, there is a need to improve the interoperability, especially for higher LODs.

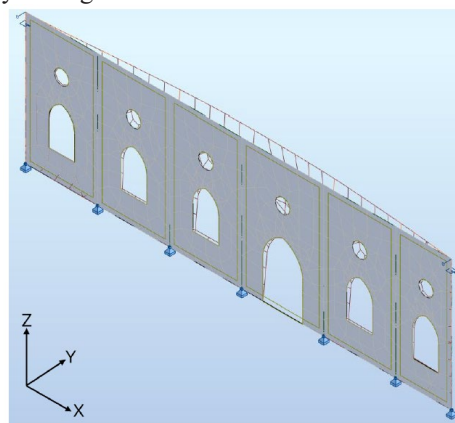


Figure 7. Deformed shape for the case 400-I-SS1 of church wall (displacement magnified 25×).

Shown in Table 4 is a sample of the quantification values of the data integrity for a case of the church wall model (the nomenclature, case 400-I-SS1 of the table pertains to: “400” for LOD 400, “I” for IFC data format, and “SS1” for structural analysis software 1). Similar to the study model, since the supports and reinforcements are not transferred at all, a score of zero for all parameters was given. For the orientation, since the beams are incorrectly oriented, a score of 0.5 was given. Since all the elements are disconnected from each other, a score of zero was given for the connections. For the lengths, the length of the beams transferred was only 85.8% of the

original model, hence, the value assigned was 0.858. For the material properties, the value of the compressive strength of concrete in BS (BIM software) is 25.3 MPa while the compressive strength value interpreted in SS1 is 25 MPa. The percentage was then determined to be 0.988. Moreover, the value of Modulus of Elasticity (Young's Modulus) in BS is 23.25 GPa while in SS1, it is 25 GPa. Computing for the percentage, a value of 0.93 was obtained. Lastly, for the rest of the elements with correct parameters transferred, a score of 1 was given.

Table 4. Quantification of data integrity for the church wall model case 400-I-SS1

	Placement		Geometry		Materials			Weighted Sum
	Orienta-tion	Connec-tion	Cross Section	Length	f _c	E	Element type	
Columns	1	0	1	1	0.988	0.93	1	0.771
Beams	0.5	0	1	0.858	0.988	0.93	1	0.657
Support	0	0					0	0.000
Walls	1	0	0.692	1	0.988	0.93	1	0.714
Reinforce-ments	0	0	0	0	0	0	0	0.000
								0.428

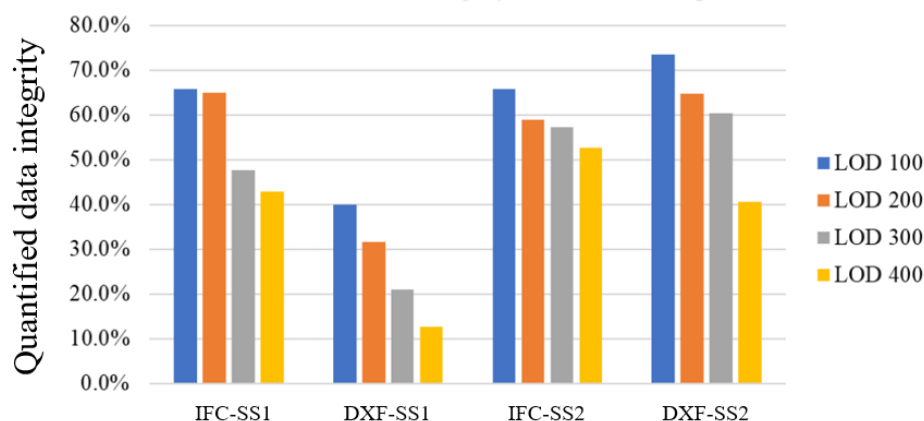


Figure 8. Quantification of data integrity for all cases of the model of a church wall structure

4. DISCUSSION

The following are obtained after post processing the results for the cases: LOD 100 resulted to the highest average data integrity with a value of 80% for the study model, while LOD 500 was the lowest with 37.7% average data integrity. For the church wall model, LOD 100 also resulted to the highest average data integrity of 61.3% and LOD 400 had the lowest value, 37.2%. Based on the data formats used, IFC resulted to 70.6% average data integrity, while DXF resulted to 39.7% average data integrity for the study model. For the church wall model, IFC also resulted to a higher average data integrity than DXF (57.0% for IFC and 43.1% for DXF).

Based on the elements of the study model, the columns obtained the highest average data integrity which is 63.41%, while reinforcements obtained the lowest with a value of 0.00% since no reinforcements were transferred. For the elements of the church wall model, columns also obtained the highest average data integrity of 56.82%, while reinforcements also obtained 0.00% data integrity. Lastly, for the properties, the length obtained the highest average data integrity of 81.70%, while the compressive strength obtained the lowest value of 33.18% for the study model. For the church wall model, the length also obtained the highest value which is 87.52% and the compressive strength also obtained the lowest value which is 26.88%.

Based on the results above, it is observed that aside from data formats significantly affecting the data integrity, the mentioned properties influence the data integrity to varying degrees. Through the computation of percentage in the scoring of quantifiable parameters, a clearer description of the transferred data was obtained rather than simply assigning scale values of 0, 0.5, and 1. Additionally, computing the average considering the weight of each parameter affected the overall results since the required degree of accuracy of the parameters on structural analysis was taken into account. This highlights the need for further studies on quantification of the data integrity to improve the data transfer process, especially for the case of higher LODs.

5. CONCLUSION

This study evaluated interoperability considering data integrity in the integration of BIM and structural analysis for multiple LODs. The study proposed an approach to quantify the data integrity for multiple cases of data transfer involving different LODs, data formats, and structure analysis tools used. The evaluation procedure involves quantifying the data based on different parameters – orientation, element type, connection, cross-section, length, compressive strength, and modulus of elasticity.

The study demonstrates a procedure that may help in maximizing the efficiency of a design and minimizing errors in the entire design and management processes through the integration of BIM and structural analysis. The study presents a procedure on the quantification of data integrity through visual inspection and scoring based on a criterion that involves different parameters in the model. This procedure can be performed using different data formats and structural analysis tools, aside from those used in this study.

Data correction consumes a lot of human and computer effort, hence, higher time and financial costs. However, this study provides an evaluation of interoperability that may guide designers on how to proceed when conducting integration procedures during the modeling-analysis process by providing the data integrity values to be expected after the data transfer processes.

ACKNOWLEDGMENTS

The authors would like to thank the members of the Structural Engineering Group of the Institute of Civil Engineering, University of the Philippines Diliman for the helpful comments provided in this study. The authors would also like to thank the engineers of AMH Philippines, Inc. for the assistance in the model settings for the church wall structure.

REFERENCES

- Bertin, I., Mesnil, R., Jaeger, J.-M., Feraille, A., and Le Roy, R. (2020). A BIM-based framework and databank for reusing load-bearing structural elements. *Sustainability*, 12(8), 3147.
- Brook, C. (2020). *What is Data Integrity? Definition, best practices & more*. Retrieved from Digital Guardian website: <https://digitalguardian.com/blog/what-data-integrity-data-protection-101>
- EIF (2004) *European Interoperability Framework for pan-European eGovernment services*. Luxembourg: European Communities.
- Kim, M.T. (2021). *Geometric Properties of Sections Part II - Moment of Inertia*. Retrieved from Midas Bridge website: <https://www.midasbridge.com/en/blog/bridgeinsight/geometric-properties-of-sections-part-2>
- Mugahed Amran, Y.H., Alyousef, R., Alabduljabbar, H., Alrshoudi, F., and Rashid, R. (2019). Influence of slenderness ratio on the structural performance of lightweight foam concrete composite panel. *Case Studies in Construction Materials*, 10.
- Muller, M., Garbers, A., Esmanioto, F., Huber, N., Loures, E., and Canciglieri Jr., O. (2017). Data Interoperability Assessment through IFC for BIM in structural design – a five-year gap analysis. *Journal of Civil Engineering and Management*, 23(7), 943–954.
- National Structural Code of the Philippines. (2015) (7th ed.). Quezon City, Philippines: Association of Structural Engineers of the Philippines, Inc.
- Porter, D. (2007). Multiscale modelling of Structural Materials. *Multiscale Materials Modelling*, 261–287.
- Sampaio, A., and Gomes, A. (2021). BIM Interoperability Analyses in Structure Design. *CivilEng*, 2(1), 174–192.
- Tague, N. (2005). *The quality toolbox* (2nd ed.). ASQ Quality Press.

QUANTITATIVE ANALYSIS FOR APPLYING BUILDING INFORMATION MODELING(BIM) IN INFRASTRUCTURE PROJECTS

Hwan Yong, Kim¹, Min Ho, Shin², and Leen Seok, Kang³

1) Ph.D., Associate Professor, School of Architecture and Architectural Engineering, Hanyang University ERICA, Ansan, S. Korea. Email: hwankim@hanyang.ac.kr

2) Ph.D., Professor, School of Railroad Civil System Engineering, Woosong University, Daejeon, S. Korea, Email: mhshin57@gmail.com

3) Ph.D., Professor, Department of Civil Engineering, Gyeongsang National University, Jinju, S. Korea. Email: lskang@gnu.ac.kr

Abstract: Building Information Modeling(BIM) opened up many possibilities for construction industry. However, most studies focus mainly on its overall uses and management areas. By investigating real projects that could utilize BIM in design phases for a railway construction, the authors try to examine possible advantages and disadvantages in BIM implementation. To do so, the authors have selected three projects with BIM implementation during design process and three other projects with non-BIM, traditional design working environment. Similar scale projects were carefully chosen and their differences in costs, man-hours, and labor forces were analyzed quantitatively. In addition, an in-depth interview was conducted with four BIM designing firms to provide a more comprehensive perspective on advantages and issues in BIM implementation. The average results show that BIM implemented projects spent \$65,800 less than their counterparts and can increase about 2.9% of productivity. More importantly, the difference between BIM and non-BIM projects are in their man-hours. BIM adopted projects spend 103.5 days less than non-BIM projects on average and required 3 less professional labor forces during the entire design process.

Keywords: Building Information Modeling(BIM); Cost Analysis; BIM Environments; Rail BIM

1. INTRODUCTION

Building Information Modeling(BIM) provides nD Computer-Aided Drawing (CAD) services that are traditionally not available in many cases (Mesároš, Smetanková et al. 2019, Jo 2020, Raja Mohd Noor, Che Ibrahim et al. 2021). BIM is an effective tool to manage construction process in a number of different circumstances, and its information-oriented interface is a powerful tool for every step in construction (Enshassi, Hamra et al. 2018, Kim, Hadadi et al. 2018, Hong, Hammad et al. 2019, Ahuja, Sawhney et al. 2020, Malik, Nasir et al. 2021). With its capability of representing physical and functional characteristics of a facility in a digital representation, BIM is regarded as a key ingredient for future construction industry.

One of the significant features of BIM is in its transparent information sharing and facility abilities. In addition, interactive operations for the clients or users through the entire project life cycle is considered another important dimension (Liu, Wang et al. 2017, Sepasgozar, Costin et al. 2022). For example, BIM-enabled facility management includes visualization, interoperability, and real-time data accessibility as the top most cited benefits realized (Pishdad-Bozorgi 2017). BIM capabilities save the costs associated with inadequate interoperability and the time often wasted in searching of information, manually inputting data, and analyzing data (Sepasgozar, Costin et al. 2022). Using new information systems and models such as 5D BIM, all the design options, including the associated costs of each design scenario, can be evaluated concurrently (Sacks, Bloch et al. 2019).

However, although its numerous possibility for construction innovation, the utility and effectiveness have not been tested properly. Some studies have articulated the use of BIM and its advantages in construction, but most of them are theoretical, not practical (Chang and Hsieh 2020, Teng, Xu et al. 2022, Xia, Liu et al. 2022). Many of the studies emphasize the theoretical perspectives of using BIM and thus, do not suggest a more specific argument in economic terms (Enshassi, Hamra et al. 2018, Gupta, Jha et al. 2020, Manzoor, Othman et al. 2021).

If BIM is an effective tool to support construction industry and change the way we design a facility, then its advantages in terms of costs should be studied in a more detailed manner. This study is to provide an insight to such obstacles in BIM research. By investigating real projects that have utilized BIM in design phases for a railway construction, the authors try to examine possible advantages and disadvantages in BIM implementation. To do so, the authors have selected three projects with BIM implementation during design process and three other projects with non-BIM, traditional design working environment. Similar scale projects were carefully chosen and their

differences in costs, man-hours, and labor forces were analyzed quantitatively. In addition, an in-depth interview was conducted with four BIM designing firms to provide a more comprehensive perspective on advantages and issues in BIM implementation.

2. METHOD

2.1 Research Framework

To properly understand the working environment of BIM in a railway construction, the authors conducted a comprehensive survey on BIM designing process. The first part of the survey involves quantitative measures, such as man-hour changes, labor charge, and others. The other part of the survey is designed to capture qualitative measures, such as difficulties in BIM working environment or benefits of using BIM. For survey collection, two professionals from each firm were selected from firm A, B, and C: BIM manager and BIM coordinator. A total of 6 experts had spent approximately 2.5 hours to answer the quantitative measures, and the authors have reorganized survey answers to properly put into equations. Some firms had very specific records to answer each of the quantitative measure, but some had to decide based on managers' memory, requiring more scrutiny in interpreting answers. In addition to those 6 professionals, a BIM manager from firm D had participated in an in-depth interview for qualitative measures. In-depth interviews took about 5 hours (in a 2-day visiting) to complete the survey.

Table 1. Basic information about the selected 6 firms and projects

BIM Use	Firms	Project Type	Total Project Length	Total Project Duration	Total No. of Professional Engineers	No. of Professional BIM Engineers	Project Location
BIM	A	Subway Extension	1.96km	60months	51	15	Seoul Vicinity
	B		5.21km	95months	78	18	In Seoul
	C		1.73km	60months	48	12	Seoul Vicinity
Non-BIM	D		2.15km	60months	60	N/A	Daejeon Vicinity
	E		4.97km	95months	85		In Seoul
	F		1.81km	60months	50		Seoul Vicinity

To properly conduct a comparative research, the authors have selected similar scale projects from both BIM and non-BIM sides. All of the projects are coming out from subway line extensions. Three of them are located inside of Seoul Metropolitan area, whereas two exist in the vicinity of Seoul and one is part of Daejeon Metropolitan area, the 6th largest city in Korea. As can be seen, firm A and D indicate similar project length, duration, number of engineers, and the location. Firm B and E, and firm C and F can be matched with their similar characteristics. Because all of the projects are still under construction, other information, such as total budget, exact location, specific participants, is considered confidential and cannot be disclosed at this moment. Table 1 summarize this result.

2.2 Quantitative Measurements

Quantitative measures are divided into four categories asking 14 different questions, whereas qualitative measures are divided into 5 categories with 16 questions. Four categories for quantitative questions are: 1) planning stage; 2) BIM modeling; 3) education and support; and 4) relevant meetings, and qualitative questions are divided into: 1) the Level-Of-Detail(LOD) for the products; 2) design errors and difficulties; 3) budget change in BIM application; 4) satisfaction rate; and 5) the use of guidelines for BIM. Table 2 indicates quantitative survey questions.

Table 2 Survey questions for quantitative and qualitative measures

Quantitative Measures	
Categories	Areas of Questions
Planning Stage	Planned budget for design and planning stage
BIM Modeling	Man-hour for creating BIM modeling based on different LODs
	Error processing time and amount of labor force for BIM modeling
	Man-hour and the number of labors for designing phase
	Labor charge for BIM coordination

	Man-hour for model check and quality management
	Total working hours for creating BIM models
Education & Support	Hours of education for BIM utilization
	Initial investment for adopting BIM
	Types of software and the cost of maintaining it
Relevant Meetings	Additional meetings required for using BIM
	Meetings for error and interference check for BIM model

* Same questions were delivered to non-BIM firms but without using BIM

The authors were dispatched to each firm and met BIM managers and coordinators to properly collect the required survey questionnaires. In addition, in-depth interviews were conducted with BIM managers for qualitative questions. All of the projects are for subway extensions, started the design process between 2019 and 2020, and thus price inflation was not a consideration for the cost estimates. Table 4 shows the measurements results for BIM applied projects. Total costs, man-hour and the estimated labor fees for each survey question are estimated.

Table 3. Man-hour and the number of labor for BIM projects

Item	Code	Descriptions	Firm A			Firm B			Firm C		
			Man-hour (days)	No. of labor	Cost estimates (\$)	Man-hour (days)	No. of labor	Cost estimates (\$)	Man-hour (days)	No. of labor	Cost estimates (\$)
Planning	(a)	Plan management	3.3	1	8,000	5	2	17,000	3.3	1	15,000
BIM Modeling	(b)	Drawing & scheduling	70	4	14,000	60	2	40,000	70	4	26,500
	(c)	Design stage	30	2*	94,000	60	1*	168,000	30	1*	70,000
			30	3**		90	2**		30	2**	
			30	2***		60	2***		30	2***	
	(d)	Model coordination	30	10	50,000	90	4	72,000	30	7	70,000
	(e)	Model check & quality control	7	2	10,000	30	2	12,000	1.6	2	5,000
Education & Support	(f)	BIM education	0.2	5	3,000	0.3	2	900	1.6	6	2,500
	(g)	BIM initial investment	N/A		10,000	N/A		68,000	N/A		10,000
	(h)	Maintenance costs			20,000/yr			20,000/yr			30,000/yr
Relevant Meetings	(i)	Emergency meetings	0.4	2	600	0.1	2	600	0.1	2	1,200
	(j)	Model check meetings	0.5	2	1,200	0.1	2	1,200	0.3	2	4,800
Total			201.4	33	210,800	395.5	21	410,500	196.9	29	235,000
Average for three firms			263.6days / 27.7men / \$283,285								

*: BIM manager **: BIM coordinator ***: BIM modeler

1. Labor charge for BIM manager differs but the average among three firms was \$10,000/month.
2. Labor charge for BIM coordinator differs but the average among three firms was \$14,000/month.
3. Labor charge for BIM modeler differs but the average among three firms was \$16,000/month.

As can be seen in table 3, each project requires about 200~300 days for design stage. The longest duration for designing stage was BIM modeling. Firm A and C spent about 160 days for model design and another 30 days for its coordination, whereas firm B spent 270 days for modeling and another 90 days for coordination. According to the BIM manager, the project for firm B was a larger scale project and had a hard time for its difficult geographical location, requiring for more in-depth modeling and checking time for a BIM model. As a result, even

though the total number of input labor was the smallest, the total amount for BIM costs and man-hour came out as the highest. Due to the different size, and geographic situation, firm B generally shows higher costs in project planning and BIM modeling.

As for the BIM modeler, coordinator, and manager, each firm provides different labor charge based on the level of experiences and contract details. Therefore, the average among three firms was implemented to calculate BIM modeling costs. BIM education and urgent meetings were not the major parts of the total estimates (16.5% for firm A, 22.1% for firm B, 21% for firm C). However, a big difference comes from BIM investments. Firm A and C mainly use AutoDesk Revit for its BIM modeling, but firm B uses a number different packages combined paying for higher fees for its license charge.

Table 4. Man-hour and the number of labor for non-BIM projects

Item	Code	Descriptions	Firm D			Firm E			Firm F		
			Man-hour (days)	No. of labor	Cost estimates (\$)	Man-hour (days)	No. of labor	Cost estimates (\$)	Man-hour (days)	No. of labor	Cost estimates (\$)
Planning	(a)	Plan management	1.0	1*	11,000	2	2*	11,000	4.5	2*	12,000
Design Drawings	(b)	Drawing & scheduling	90	2*	24,000	80	2* 1**	28,000	60	2**	16,000
	(c)	Design stage	100	10*	159,000	300	6* 2**	270,000	210	7* 1**	175,000
	(d)	Detail drawing	40	12*	63,600	100	2** 1**	35,000	60	4* 1**	32,000
	(e)	Drawing check & quality control	10	10*	13,300	20	5*	10,000	10	3*	3,000
	(f)	Emergency meetings	3	1** 1***	1,250	2	2**	600	3	1* 2**	1,100
Relevant Meetings	(j)	Drawing check meetings	3	2* 1** 1***	2,050	3.3	1* 2**	1,330	2.3	2**	1,230
Total			247	41	274,200	507.3	26	355,930	349.8	25	240,330
Average for three firms			368.1days / 30.7men / \$290,153								

*: Entry level professional engineers

**: Intermediate level professional engineers

***: Experienced level professional engineers

Engineers' fee was calculated based on national labor standard for Korean construction industry.

Table 4 is the man-hour and labor charge for non-BIM projects. According to the results, firm E shows higher costs than the other two firms. The chief designer indicated that firm E's project was relatively large in its size and more complicated compared to general projects, requiring for more time and labor during design and detail drawing stage. Firm F consumed more man-hour than firm D (349.8 days vs. 247 days), but their project difficulty was relatively low and for that reason, the number of labor and the level of expertise for the engineers were lower than firm D.

According to the results, the average man-hours for three firms to complete design task took about 368.1 days with 30.7men, costing \$290,153. Non-BIM projects took longer than a year to complete the design process. We can see that the average man-hours for BIM projects was 263.6 days, whereas non-BIM projects took about 368.1 days. It means non-BIM projects needed about 105 more days to complete the project. In addition, BIM projects required 27.7 labors to end up the projects and non-BIM needed 30.7 men to finish the projects, making it about 3 labor differences. Lastly, the average costs for BIM adopted projects was \$283,285/year and the same item for non-BIM projects was \$290,153/year, creating the difference about \$6,868. This may not be a significant difference but considering that man-hour and labor inputs also vary based on BIM utilization, the effectiveness of using BIM can be understood in a greater magnitude.

3. RESULTS

Table 5 explains cost difference between BIM and non-BIM projects. As can be seen, firms with BIM implementation required an average of \$13,333 and non-BIM spent \$11,333, making it about \$2,000 difference in planning stage. For designing, firms with BIM spent an average of \$210,500 for its design and modeling, whereas non-BIM firms spent an average of \$276,300, making the difference about \$65,800. This is a notable difference as BIM utilized firms spent an additional cost for its software purchase and support. The average cost for BIM education and support came out as an average of \$54,800 annually. But the total costs for BIM projects were not too significantly different.

According to the average costs, although BIM firms spent more investments on education and support, planning stage, and relevant meetings, the entire design work took \$65,800 less than non-BIM firms, making all other spending compensated. This is an interesting result because once BIM model is set up, then there are not too much associated costs for other related works, such as detail design, 3D modeling, and so forth. Therefore, BIM may require more investments upfront, but durability and utility of the products are more versatile and the costs can be compensated with subsequent works.

Table 5. Costs comparison between BIM and non-BIM projects

		Planning stage	BIM modeling	Design drawings	Education & support	Relevant meetings	Total
BIM Projects	Firm A	8,000	168,000	N/A	33,000	1,800	210,800
	Firm B	17,000	292,000	N/A	88,900	1,800	399,700
	Firm C	15,000	171,500	N/A	42,500	6,000	235,000
	Average	13,333	210,500	N/A	54,800	3,200	281,833
Non-BIM Projects	Firm D	11,000	N/A	259,900	N/A	3,300	274,200
	Firm E	11,000	N/A	343,000	N/A	1,930	355,930
	Firm F	12,000	N/A	226,000	N/A	2,330	240,330
	Average	11,333	N/A	276,300	N/A	2,520	290,153

* All costs are calculated in yearly basis.

Table 6 indicates labor and man-hour difference between BIM and non-BIM implementations. According to the results, firm B spent the highest number of man-hours in BIM projects but the number of labor was the smallest. The difference between firm A and B in terms of man-hour is about 194 hours and firm C showed the least amount of man-hours for designing. Firm A shows the highest number of labor for its project, about 12 more than firm B and about for more than firm C. The average revealed that BIM projects require about 264.6 man-hours and 27.7 labor forces.

Table 6. Man-hour and labor comparison between BIM and non-BIM projects

			Planning stage	BIM modeling	Design drawings	Education & support	Relevant meetings	Total
BIM Projects	Firm A	Man-hour	3.3	197	N/A	0.2	0.9	201.4
		Labor	1	23	N/A	5	4	33
	Firm B	Man-hour	5	390	N/A	0.3	0.2	395.5
		Labor	2	13	N/A	2	4	21
	Firm C	Man-hour	3.3	191.6	N/A	1.6	0.4	196.9
		Labor	1	18	N/A	6	4	29
	Average	Man-hour	3.9	259.5	N/A	0.7	0.5	264.6
		Labor	1.3	18	N/A	4.3	3	27.7
Non-BIM Projects	Firm D	Man-hour	1	N/A	240	N/A	6	247
		Labor	1	N/A	34	N/A	6	41
	Firm E	Man-hour	2	N/A	500	N/A	5.3	507.3
		Labor	2	N/A	19	N/A	5	26
	Firm F	Man-hour	4.5	N/A	340	N/A	5.3	349.8
		Labor	2	N/A	18	N/A	5	25
	Average	Man-hour	2.5	N/A	360	N/A	5.5	368.1
		Labor	1.7	N/A	23.7	N/A	5.3	30.7

Firm E spent about 500 hours for design drawing with 19 labors, making it the longest number of man-hours among non-BIM projects. Firm D spent the highest number of labor for design stage and firm F shows the least amount of labor for its design process. The average results show that non-BIM projects require about 368.1 man-hours to complete the projects with 30.7 professionals. Comparing to BIM projects, non-BIM projects spent about 103.5 more man-hours with 3 more labor forces. This could be a significant result because the average cost difference between BIM and non-BIM projects was about \$65,800 but the number of man-hours differ to a greater degree. Observing the average, non-BIM projects took about 103.5 days longer than BIM projects to complete its design process. Although \$65,800 could not be a significant difference in terms of investments per year, the time difference seems a noteworthy result.

According to the cost comparison, firm A spent \$210,800 for its project design, whereas firm D spent \$274,200 for the same process. It could be understood that BIM utilization may increase the productivity by 23.1% roughly. On the other hands, based on the result between firm B and E, BIM implementation did not increase productivity of the design process, rather the productivity has gone down by about 11%. This cannot be a complete measure to judge about BIM efficiency in a larger scale projects, but we could understand that education and support costs created a slight difference. Lastly, the productivity difference between firm C and F was about 2.2%, meaning that BIM has created about 2.2% efficient results in terms of the total costs. On average, BIM utilization for a similar scale project could induce cost differences, making it about 2.9% increase in productivity. Figure 1 illustrates the results.

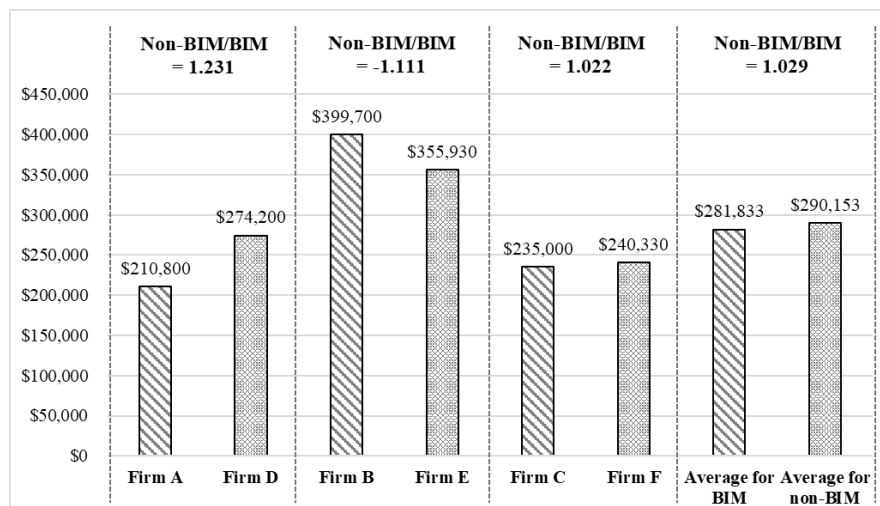


Figure 1. Productivity difference between BIM and non-BIM projects

4. DISCUSSION

It is certain that only with 6 firms' analysis results cannot be generalized for BIM effectiveness. However, this study provided a holistic view on the differences between BIM and non-BIM projects for a railway design process. Based on the survey and in-depth interviews, the authors tried to identify possible benefits and hurdles in BIM utilization, and possibly suggest a future direction for a smarter and sustainable construction environment.

5. CONCLUSIONS

This study is designed to understand the advantages and issues of using BIM in design process. In specific, similar scale and budget projects were selected for BIM and non-BIM utilization. As the analysis results indicated, BIM can provide a certain types of benefits in design process. The average results show that BIM implemented projects spent about \$65,800 less than their counterparts, and could increase about 2.9% of productivity. More importantly, the difference between BIM and non-BIM projects are in their man-hours. BIM adopted projects spend 103.5 days less than non-BIM projects on average, and required 3 less professional labor forces during the entire design process.

This could be an interesting point because BIM utilizing firms spent more investments on hardware and software costs. In addition, BIM education resources were a mandatory for a more effective working environment. Due to these reasons, the upfront costs for BIM projects showed higher expenses, but the final analysis came out

as lower costs, less labor forces, and less man-hours than the traditional working environment. If BIM can be a continuous effort for these selected firms, then the initial investments could minimize and eventually pay off the additional charges.

ACKNOWLEDGMENTS

This study was funded by the Ministry of Land, Infrastructure, and Transport in South Korea (Grant number: 22RBIM-C158185-03), and the authors would like to thank for their generous support.

REFERENCES

- Ahuja, R., A. Sawhney, M. Jain, M. Arif and S. Rakshit (2020). "Factors influencing BIM adoption in emerging markets—the case of India." *International Journal of Construction Management* 20(1): 65-76.
- Chang, Y.-T. and S.-H. Hsieh (2020). "A review of Building Information Modeling research for green building design through building performance analysis." *J. Inf. Technol. Constr.* 25: 1-40.
- Enshassi, A. A., L. A. A. Hamra and S. Alkilani (2018). "Studying the Benefits of Building Information Modeling (BIM) in Architecture, Engineering and Construction (AEC) Industry in the Gaza Strip." *Jordan Journal of Civil Engineering* 12(1): 87-98.
- Gupta, S., K. N. Jha and G. Vyas (2020). "Proposing building information modeling-based theoretical framework for construction and demolition waste management: strategies and tools." *International Journal of Construction Management*: 1-11.
- Hong, Y., A. W. Hammad and A. Akbarnezhad (2019). "Impact of organization size and project type on BIM adoption in the Chinese construction market." *Construction Management and Economics* 37(11): 675-691.
- Kim, J.-U., O. Hadadi, H. Kim and J. Kim (2018). "Development of A BIM-Based Maintenance Decision-Making Framework for the Optimization between Energy Efficiency and Investment Costs." *Sustainability* 10(7): 2480.
- Liu, X., X. Wang, G. Wright, J. C. Cheng, X. Li and R. Liu (2017). "A state-of-the-art review on the integration of Building Information Modeling (BIM) and Geographic Information System (GIS)." *ISPRS International Journal of Geo-Information* 6(2): 53.
- Malik, Q., A. R. Nasir, R. Muhammad, M. J. Thaheem, F. Ullah, K. I. A. Khan and M. U. Hassan (2021). "BIMp-Chart—A Global Decision Support System for Measuring BIM Implementation Level in Construction Organizations." *Sustainability* 13(16): 9270.
- Manzoor, B., I. Othman, S. S. S. Gardezi and E. Harirchian (2021). "Strategies for adopting building information modeling (Bim) in sustainable building projects—A case of Malaysia." *Buildings* 11(6): 249.
- Mesároš, P., J. Smetanková and T. Mandičák (2019). *The fifth dimension of BIM—implementation survey*. IOP Conference Series: Earth and Environmental Science, IOP Publishing.
- Pishdad-Bozorgi, P. (2017). "Future smart facilities: State-of-the-art BIM-enabled facility management." *Journal of Construction Engineering and Management* 143(9): 02517006.
- Raja Mohd Noor, R. N. H., C. K. I. Che Ibrahim and S. Belayutham (2021). "The nexus of key attributes influencing the social collaboration among BIM actors: a review of construction literature." *International Journal of Construction Management*: 1-11.
- Sacks, R., T. Bloch, M. Katz and R. Yosef (2019). "Automating design review with artificial intelligence and BIM: State of the art and research framework." *Computing in Civil Engineering 2019: Visualization, Information Modeling, and Simulation*: 353-360.
- Sepasgozar, S. M., A. M. Costin, R. Karimi, S. Shirowzhan, E. Abbasian and J. Li (2022). "BIM and Digital Tools for State-of-the-Art Construction Cost Management." *Buildings* 12(4): 396.
- Teng, Y., J. Xu, W. Pan and Y. Zhang (2022). "A systematic review of the integration of building information modeling into life cycle assessment." *Building and Environment*: 109260.
- Xia, H., Z. Liu, E. Maria, X. Liu and C. Lin (2022). "Study on City Digital Twin Technologies for Sustainable Smart City Design: A Review and Bibliometric Analysis of Geographic Information System and Building Information Modeling Integration." *Sustainable Cities and Society*: 104009.

BIM: A SUCCESSFUL ALTERNATIVE FOR THE CONSTRUCTION QUANTITY TAKE-OFF IN THE LARGE-SCALE CONSTRUCTION PROJECT

Hang Le Thi Thu¹, Huyen Nguyen Thi², Huong Pham Thu³, and Phong Thanh Nguyen⁴

1) Dr., Lecturer, Faculty of Civil Engineering, University of Architecture Ho Chi Minh City, Ho Chi Minh City, Vietnam. Email: hang.lethithu@uah.edu.vn

2) Student, Department of Civil Engineering, University of Architecture Ho Chi Minh City, Ho Chi Minh City, Vietnam. Email: huyen.nguyenthi2420@gmail.com

3) Student, Department of Civil Engineering, University of Architecture Ho Chi Minh City, Ho Chi Minh City, Vietnam. Email: huong.pt2201@gmail.com

4) Dr., Lecturer, Professional Knowledge and Project Management Research Team, Ho Chi Minh City Open University, Ho Chi Minh City, Vietnam. Email: phong.nt@ou.edu.vn

Abstract: Building Information Modeling (BIM) is the effective process of creating and managing information in construction projects through a 3D virtual model that has been applied to a number of construction projects all over the world. From 2023, the BIM application will be compulsory for work class I or higher in public investment projects, projects funded by nonpublic investment state capital, and PPP projects in Vietnam. However, the accuracy of BIM in volume take-off is a big barrier to its application in practice. Therefore, in this paper, the authors present a successful alternative for using a BIM quantity take-off in a large-scale construction project (class I) in Vietnam. Revit is selected as a potential BIM authoring program for developing the 3D model and conducting semi-automatic quantity take-off in this study. Microsoft Excel is selected as an implicit spreadsheet tool for reporting the results. The authors compared the results from two methods: the BIM method and the traditional method, to evaluate the advantages and disadvantages of BIM technology for construction quantity take-off in large-scale construction projects.

Keywords: Building Information Modeling (BIM), Successful alternative, Construction quantity take-off, Large-scale construction project.

1. INTRODUCTION

Nowadays, digital transformation is the trend in almost all industries including the construction industry. Building information modeling (BIM) is a potential technology that can help architects, engineers, and contractors with their digital transformation progress. BIM is not only understood as the software like Revit, Tekla, Navisworks, etc. but also as a closed process of creating and using information models in all stages of the project life-cycle including design, construction, operation, and decommissioning. In construction investment projects, BIM had shown outstanding advantages in managing information more effectively; it was described as a tool to improve the consistency of data in construction management (Kocakaya, 2019; Likhitrungsilp et al., 2019). BIM helped to save time for estimating construction costs and improving construction planning (Le et al., 2021). BIM supported the faster evaluation of building life-cycle costs progress through a visualized approach, the consistency of information, and the time savings for huge repetitive calculations (Le et al., 2020). BIM was applied in many construction fields such as energy simulation, asset management, risk management, cost measurement, and estimation (Azhar, 2011; Si et al, 2016; Stenstrand, 2010; Taghaddos et al., 2016; Toan et al, 2020).

Although BIM technology provided many advantages for construction management, the number of BIM research for construction quantity take-off in large-scale projects is limited in Vietnam. Olsen and Taylor research pointed out several limiting factors of BIM application for quantity take-off (Olsen & Taylor, 2017). Some research presented the benefits and challenges of BIM application in quantity surveying practice (Harrison & Thurnell, 2015; Muhannad, 2015; Raphael & Priyanka, 2014). Other studies proposed solutions to make BIM application in quantity take-off more efficient, such as using BIM quality standards for quantity take-off (Kwon et al., 2011) and proposing an open BIM-based quantity take-off system for schematic estimation of building frames to improve the reliability of estimating results in the preliminary design phase (Choi et al., 2015). Wijayakumar and Jayasena proposed a method to measure quantity through model-based mass extraction techniques. BIM not only helps increase the accuracy of the estimation process but also helps reduce unexpected volumes from the estimation errors. Therefore, BIM research for construction quantity take-off is very necessary.

In Vietnam, BIM is a mandatory standard in many legal documents. BIM is officially included in the Government's Decree No. 15/2021/ND-CP about regulations on the management of construction projects in Vietnam (Vietnamese Government, 2021). A roadmap for BIM application in the construction sector is issued in 2023 (The Prime Minister of Vietnam, 2023) and mentions that from 2023, the application of BIM is compulsory for works in class I and higher in public investment projects; from 2025, the application of BIM is compulsory for works in class II and higher in public investment projects, projects funded by non-public investment state capital, and PPP projects. In addition, for new investment projects funded by other capital sources, main investors are required to provide BIM files to serve the appraisal of feasibility study reports, construction designs carried out

after fundamental designs, applications for construction permits, and acceptance testing tasks according to the following roadmap: class I and special class works from 2024; all class I, class II, and special class works from 2026. However, the Vietnamese contractors still face a lot of difficulties in applying BIM to their projects. Therefore, this paper presented a successful alternative for the construction quantity take-off in a large-scale construction project with BIM technology in Vietnam.

2. METHOD

In this paper, the authors propose a method to take-off the quantity of all building components in a large-scale building project using BIM technology. The proposed method consists of four steps, as shown in Figure 1. There are many BIM authoring programs that can be used to create 3D BIM models. However, the authors selected Revit as a potential BIM authoring platform because it is the most popular BIM platform in Vietnam. It is also a powerful tool that Vietnamese BIM users usually use to create and release drawings for construction projects.

The first step is to determine the list of construction work for the building project using the spreadsheet platform. All design drawings, specifications, and calculation regulations are used to analyze and calculate. This step is done manually by the estimating engineer, who will create a calculation form. The outcome of this step is the list of works according to the construction orders, the volume of each work, the unit price, and the cost of each work to implement the projects. In order to compare the accuracy of the list of works with the actual construction order, the quantity surveyor (QS) needs to have practical experience to know how to divide the volume of work components correctly for each activity. In addition, the QS also needs to understand the construction method for performing the project, for example, the kind of concrete, formwork, or steel used for each building component.

The second step is to create BIM models. The BIM models of building projects are usually divided into three types: architectural models, structural models, mechanical, electrical, and plumbing models. The designer will start with the project library, which consists of all families of columns, beams, floors, doors, windows, and other building components. Each family included the geometry information (length, width, and height dimensions) and the non-geometry information (material type, unit cost) following their specification. It is very important to unify the coordinate points and axis grid of the project in the model. Because the project works are assigned to many project participants; therefore, the errors, duplication, and mistakes may occur in subsequent phases (Vietnam Ministry of Construction, 2021a; Vietnam Ministry of Construction, 2021b).

In this paper, the 3D BIM models are not only used to calculate the mass but also to test the collisions between disciplines. The QS and designers can visualize the problems encountered and handle them before the project is implemented in practice. In this step, the QS must come up with rules for calculating the volumes of the intersecting positions of the 3D objects. Each QS will have its own calculation rules; for example, the intersection mass between beam and floor will be prioritized in the calculation for beam or floor from the edge of the beam as shown in Figures 2 and 3.

The third step is to create the relevant statistical table for each task component. At the beginning, the QS needs to develop a statistical table template to store the required information. In Revit, the QS can organize project information into fields. For example, the QS needs to get the volume of the concrete column, so the statistics table only needs to set up data such as floor, column name, type of material, and volume of concrete (Thao et al., 2020). Each project will need different information, so statistical tables also need to be created differently depending on the project type, as shown in Figure 4. The quantity of each 3D element model will be computed automatically.

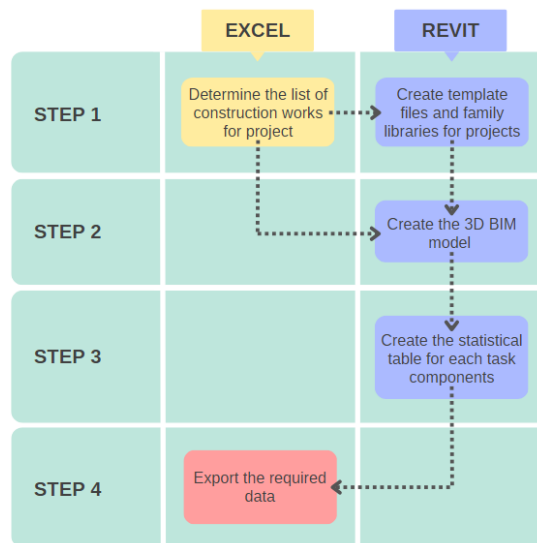


Figure 1. A construction quantity take-off method for the large-scale project with BIM

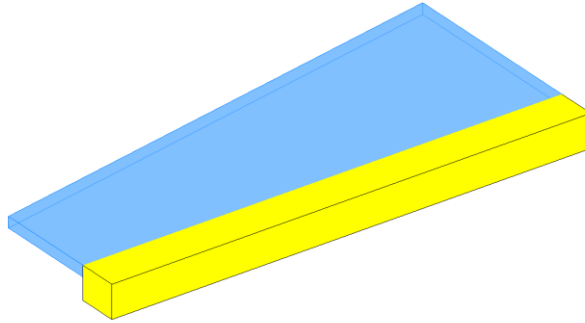


Figure 2. The prior calculation of the intersection between beam and floor is beam mass.

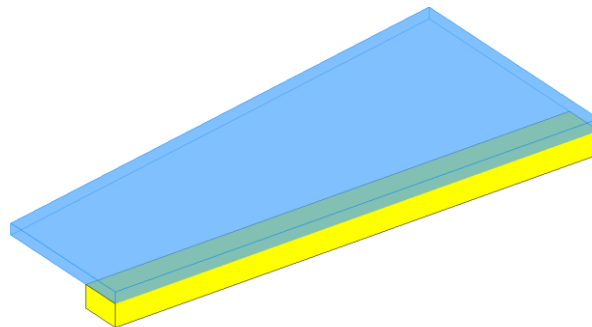


Figure 3. The prior calculation of the intersection between beam and floor is floor volume.

However, Revit still has some shortcomings. For example, when the QS wants to calculate the formwork areas of the beam, Revit only calculates the area of the entire beam. However, the actual formwork area of the beam is the total area of two sides and the bottom area of the beam. In addition, Revit does not exclude intersections among components. Therefore, the results from Revit must take time to solve the above problems.

The fourth step is to export the required data. In this study, Microsoft Excel is selected as a useful calculation tool. After receiving the quantity take-off from Revit, the QS created the necessary spreadsheet table for the construction cost estimation in Microsoft Excel. Currently, Revit still cannot export the quantity take-off files to the available spreadsheet template (Vasen, 2021). BIM users must use more add-ins to export their necessary data.

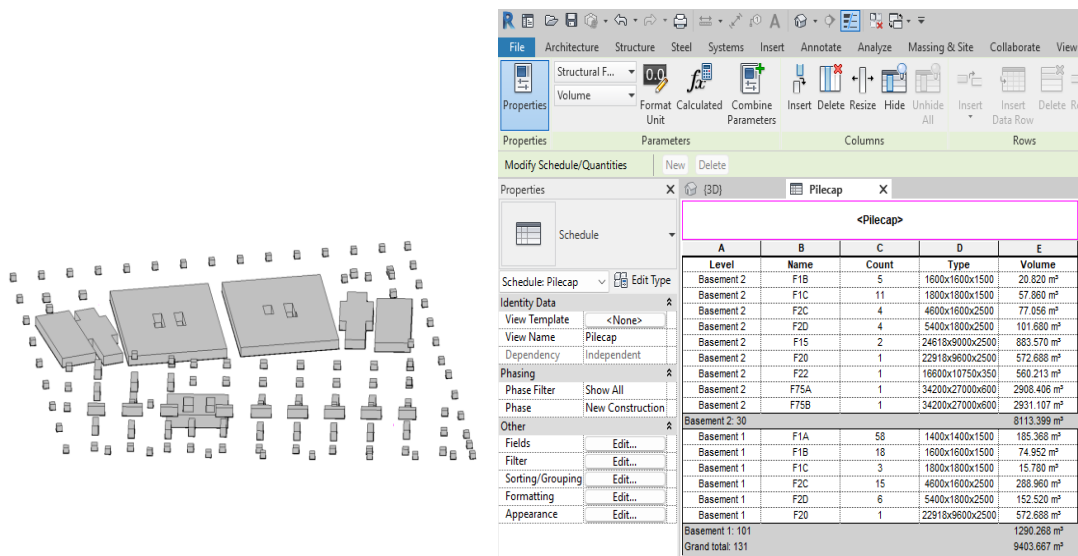


Figure 4. The statistical table of foundation components in Revit

3. RESULTS

In order to evaluate the efficacy of BIM for construction quantity take-off. The authors applied it to a real project in Ho Chi Minh City. This is a large-scale building project with a total floor area of more than 100,000 m². This building included two basements, eight podium floors, and 35 floors. The authors used Revit software to create the 3D models and calculate the quantities for all building components using the proposed method as presented in Section 2. After comparing the quantity from the proposed method and the quantity from the actual construction contract, the authors found near-similar results from both approaches, as shown in Figure 5. It indicates that the reliability of the proposed system is acceptable.

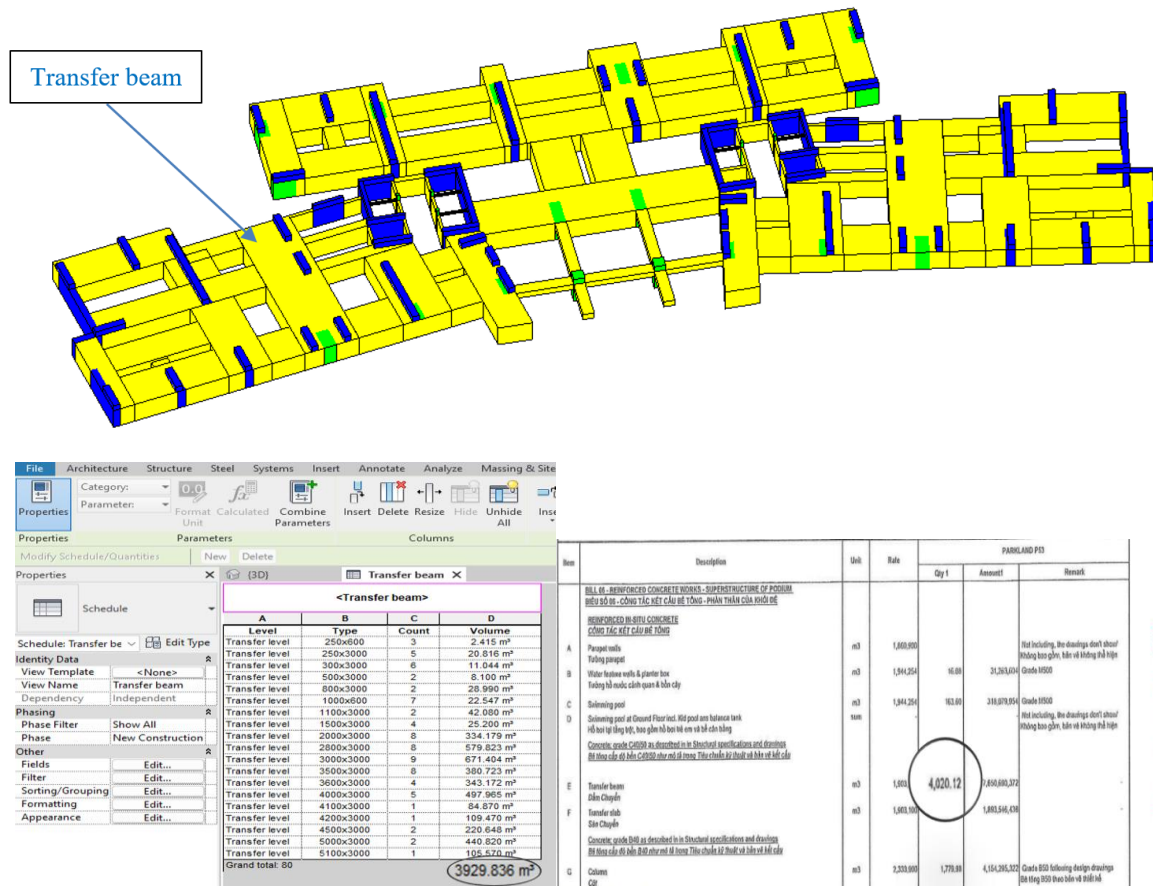


Figure 5. The quantity of transfer beam was calculated from the 3D BIM model and the quantity of transfer beam in the actual construction contract.

4. DISCUSSION

In order to take-off quantity effectively with BIM, the QS needs to prepare the standards or guidelines at the beginning of the project to ensure consistency of information. For the traditional method, the QS normally makes mistakes in the estimating process because they do not understand the project designs. In addition, the QS often takes more time to read many 2D drawings and conduct a huge equation for areas, volumes, etc. of each project component. BIM provided a better visual for the QS, who did not have experience in quantity take-off.

The BIM provided automatically taken-off information about quantity, material type, and unit cost of all building components, which helped save time compared with the traditional method. The authors conducted a comparison of the time to execute a part of the 5th floor using the manual calculation and the Revit calculation. The results showed that Revit helped save more than 70% of the time for quantity take-off compared to the manual method with 2D CAD.

Currently, there is much research showing the benefits of Revit in the construction industry. According to the in-depth interviews, the Vietnamese QS does not want to apply BIM to their projects because of the accuracy of measuring results. The authors conducted a comparison of the cost to execute a part of the 5th floor using the hand calculation and the Revit calculation. The results showed that the cost difference of mold use is very high, around 15%, between the hand calculation and the Revit calculation. In addition, the cost difference in concrete volume is also high around 10% compared to the two methods. The QS often ignores the intersection for faster

calculation. Therefore, in this study, the authors proposed an intersectional rule among the component models in Revit to improve the accuracy of measuring results.

The BIM helped to update the design changes from the designers, the work task changes from the owner, or the practical volume changes from the contractor faster compared with the traditional method, especially in cases where the changes happen continuously.

With BIM, the QS can save time and money on the documents because the BIM model is uniform throughout the tender, construction, and as-built phases. The project participants can make faster decisions with adequate information.

The BIM was an innovative approach to data organization. For future projects, the BIM library will help the designer save a lot of time when creating the 3D BIM model. It also helps to increase the synchronism of projects.

5. CONCLUSIONS

This paper presented a successful alternative for construction quantity take-off in large-scale construction projects with BIM technology. The authors indicated the advantages and disadvantages of BIM for quantity take-off in the actual project in Vietnam. In order to evaluate the effectiveness of the proposed method, the authors compared the results of the proposed method with those of the traditional 2D method.

Currently, BIM is an obligatory part of large-scale public projects in Vietnam. The Vietnamese government issued many legal documents, such as proposals, guidelines, and decisions, about approving a roadmap for the application of BIM in the construction industry. Therefore, it is only natural that BIM will gradually replace the traditional process. Although BIM technology is still inadequate and cannot be optimized, the benefits of BIM are very obvious. In this study, BIM helped to improve the information exchange among project stakeholders, including the owner, designer, consultant, and contractor. BIM helped save time and money on updating the changes throughout the life cycle of the project. BIM helped to increase the accuracy of quantity take-off and also save time and money for this process. This is something that the traditional method cannot do.

ACKNOWLEDGMENTS

The authors would like to thank the Faculty of Civil Engineering, University of Architecture Ho Chi Minh City, for funding this research project.

REFERENCES

- Azhar, S. (2011). Building information modeling (BIM): Trends, benefits, risks, and challenges for the AEC industry, *Leadership and management in engineering*, 11(3), 241-252.
- Choi, J., Kim, H., and Kim, I. (2015). Open BIM-based quantity take-off system for schematic estimation of building frame in early design stage, *Journal of Computational Design and Engineering*, 2(1), 16-25.
- Harrison, C. and Thurnell, D. (2015). BIM implementation in a New Zealand consulting quantity surveying practice, *International journal of construction supply chain management*, 5(1), 1-15.
- Kocakaya, M.N. (2019). Building information management (BIM), a new approach to project management, *Journal of sustainable construction materials and technologies*, 4(1), 323-332.
- Kwon, O., Jo, C.W., and Cho, J.W. (2011). Introduction of BIM quality standard for quantity take-off, *Journal of the Korea Institute of Building construction*, 11(2), 171-180.
- Le, H.T.T., Likhitrungsilp, V. and Yabuki, N. (2021). A BIM-database-integrated system for construction cost estimation, *ASEAN Engineering Journal*, 11(1): p. 45-59.
- Le, H.T.T., Likhitrungsilp, V. and Yabuki, N. (2020). A BIM-integrated relational database management system for evaluating building life-cycle costs, *Engineering Journal*, 24(2): p. 75-86.
- Likhitrungsilp, V., Le, H.T., Yabuki, N., and Ioannou, P.G. (2019). Integrating building information modeling and visual programming for building life-cycle cost analysis, In Proc., *Interdependence between Structural Engineering and Construction Management 10th Conf*, pp. 1-6.
- Muhammad, M.R.R. (2015). The significance of building information modelling to the quantity surveying practices in the UAE construction industry, In *6th international conference on structural engineering and construction management* (pp. 22-32).
- Mustafa, N. K., Ersin, N., and Umit, I. (2019). Building Information Management (BIM), A New Approach to Project Management, *Journal of Sustainable Construction Materials and Technologies*, 4(1), 323-332.
- Olsen, D. and Taylor, J.M. (2017). Quantity take-off using building information modeling (BIM), and its limiting factors, *Procedia engineering*, 196, 1098-1105.
- Raphael, V. and Priyanka, J. (2014). Role of building information modelling (BIM) in quantity surveying practice, *International Journal of Civil Engineering and Technology*, 5(12), 194-200.
- Stenstrand, J. (2010). The use of building information models in quantity takeoff for cost estimation and construction site management, *Aalto University School of Science and Technology*

- Si, H.V.V., Duc, H.N., Thang, V.D., Nguyen Thi Bich Thuy, N.T.B. (2016). Application of BIM on construction works quantities taking-off, *Journal of Science and Technology*, 4(17), pp.68-74.
- Taghaddos, H., Mashayekhi, A., and Sherafat, B. (2016). Automation of Construction Quantity Take-Off: Using Building Information Modeling (BIM), *Construction Research Congress 2016*, 2218-2227.
- Thao, T.N.H. and Dung, L.A. (2020). Automatic Workflow for Quantity Take Off in Cost Estimation, *Journal of Science and Technology*.
- The Prime Minister of Vietnam. (2023). Decision No. 258/QĐ-TTg approving roadmap for application of building information modeling (BIM) in construction sector.
- Toan, N.Q., Hang, N.T.T., Nam, L.H., Duyen, D.H., and Nam, T.P. (2020). Application of Building Information Modeling (BIM) for automatic integration of construction costs management information into 3D models in consideration of Vietnamese regulations, *Faculty of Construction Economics and Management*.
- Vassen, S.A. (2021). Impact of BIM-based Quantity Take off for Accuracy of Cost Estimation, *International Journal of Construction Engineering and Management*, 10(3), 55-69.
- Vietnam Ministry of Construction. (2021a). Research and propose the process of measuring the volume of BIM application in accordance with Vietnamese conditions, *Journal of Construction Economics*.
- Vietnam Ministry of Construction. (2021b). General guidance document on the application of BIM building information modeling, *Journal of Construction Economics*.
- Vietnamese Government. (2021) . Decree No. 15/2021/ND-CP detailing on management of construction investment project.

BUILDING INFORMATION MODELING FRAMEWORK FOR PRACTICAL IMPLEMENTATION OF A MEGA-PROJECT IN THAILAND

Pawaris Khammultri¹, Kritsada Lappanichayakul², Pithiwat Tiantong³, and Athasit Sirisonthi⁴

1) M. Sc., Engineering Department, Sino-Thai Engineering and Construction Public Company Limited, Bangkok, Thailand. Email: Pawaris_kh@stecon.co.th

2) B. Eng., Engineering Department, Sino-Thai Engineering and Construction Public Company Limited, Bangkok, Thailand. Email: Kritsada_la@stecon.co.th

3) Ph.D., Engineering Department, Sino-Thai Engineering and Construction Public Company Limited, Bangkok, Thailand. Email: Pithiwat_ti@stecon.co.th

4) Ph.D. Candidate, Engineering Department, Sino-Thai Engineering and Construction Public Company Limited, Bangkok, Thailand. Email: Athasit@stecon.co.th

Abstract: Building Information Modeling (BIM) is used to create, collaborate and manage data throughout the engineering, procurement, and construction (EPC) as well as operations phases of the building. U-Tapao international airport (UTP airport) are a public-private partnership project and one of the mega-projects in Thailand (≈6500 rai) which utilized as a case study in the paper. However, UTP airport projects are divided into six categories including passenger terminal building, airside, landside, airport facilities, cargo terminal, and utilities. The 2nd runway, high speed railway, motorway M7, power supply, water supply, and aircraft fuel supply are other projects that require close coordination and collaboration. Therefore, the purpose of this paper is to provide a BIM framework for real-world mega-projects that focuses on issues of practicability. The complexity of the project and the number of parties involved cause the implementation of BIM to be planned from the design phase to the construction phase. The data transfer strategy was implemented for the future of operation and maintenance phase. Single data source, data migration to the cloud, design collaboration, and combining all disciplines with a BIM are essential to the successful implementation of BIM in this project. This paper demonstrated that BIM could overcome project constraints and resulted in a framework for realistic BIM execution which is able to be utilized in EPC projects to alleviate the problem of a lack of information and eliminate conflicts between another parties.

Keywords: Building Information Modeling (BIM), Engineering Procurement Construction (EPC), Airport.

1. INTRODUCTION

U-Tapao Airport (UTP) is a joint civil-military public airport located in Ban Chang District of Rayong Province, approximately 170 km southeast of Bangkok (Thailand). The location of the airport is in a special economic zone, the Eastern Economic Corridor (EEC), which covers three provinces in Eastern Thailand, namely, Chonburi, Rayong, and Chachoengsao. The EEC development is a key driver of “Thailand 4.0” economic policy in Thailand. With the EEC policy, the government plans to develop these 3 provinces as a prime area for technology-based manufacturing and services, including first S-Curve and new S-Curve industries, and to strengthen Thailand’s strategic location as a hub of regional multimodal connectivity.

The development of UTP is one of the primary infrastructure mega-projects to increase tourism and industrial development within the EEC. Bangkok Airways Public Company Limited (BA), BTS Group Holding Public Company Limited (BTS), and Sino-Thai Engineering & Construction Public Company Limited (STECON) under the name of “BBS Joint Venture” was the bidder who proposed the best offer for the U-Tapao International Airport and Eastern Aviation City Development Project. U-Tapao International Aviation Co., Ltd. (UTA), a joint venture company incorporated under the BBS Joint Venture Agreement to operate the U-Tapao International Airport Expansion Project, has entered into the Public Private Partnership (PPP) or Concession Agreement for the U-Tapao International Airport Expansion Project with the Eastern Economic Corridor Office of Thailand (the EECO). PPP is a long-term agreement between the government and the private sector. Multiple nations have implemented public-private partnerships, which are primarily utilized for infrastructure initiatives. The design-build procurement strategy alters the conventional order of work. It satisfies the client's desire for a single point of accountability in an effort to lower hazards and overall costs. It is now widespread in many nations, and contract templates are broadly accessible. UTP will provide accessibility to suppliers, workers, and visitors to the EEC. The high-speed railway (HSR) project which will be linked the three airports in the Bangkok metropolitan area, including Don Mueang Airport (DMK), Suvarnabhumi Airport (BKK) and UTP, aims to create faster and more comprehensive connections between airports, ports, and industrial clusters. The HSR will allow passengers to commute from Bangkok and its suburbs to UTP in less than one hour. Investment in the transport sector will allow trade and tourism to achieve full potential in EEC.

STECON has been awarded as Engineering, Procurement, and Construction Contractor (EPC) to implement the Project, that is to carry out designs, procurements, and construction of U-Tapao International Airport Expansion Project. EPC is a form of construction contract wherein the contractor is responsible for all engineering, procurement, and construction activities necessary to deliver the completed project to the owner

within a predetermined time and budget. However, UTP airport projects are separated into six categories, which include passenger terminal building, airside, landside, airport facilities, cargo terminal, and utilities. Other initiatives that require close coordination and collaboration include the second runway, high-speed railway, M7 motorway, power supply, water supply, and aircraft fuel supply. It is evident that the airport's construction and infrastructure work will be extremely complex. So, BIM has become central topic to the improvement of the AECOO stands for Architecture, Engineering, Construction, Owner Operator (AECOO) industry around the world (Bradley et al, 2016)

Building information is managed using a three-dimensional software method to be capable of correcting flaws in architectural and engineering construction designs prior to real implementation. Modeling data was used to support the design by employing three-dimensional geometry parameters as a guide for operations and by providing relevant data to support cost estimation or different construction steps (Jung & Joo, 2011). The global growth of the BIM business and strategies for adopting BIM were also studied in order to create the framework (Smith, 2014). The paper discusses how changes in technology and project delivery processes are generating positive outcomes and efficiencies in the construction industry. A framework is a methodical arrangement of relationships or a conceptual scheme, structure, or system. Establishing a framework aims to direct work procedure, improve communication through shared comprehension, and integrate pertinent concepts into a descriptive or predictive model. In the previous project of STECON, numerous difficulties were encountered. The experience from previous work was used as a lesson to improve the BIM framework in various aspects. Therefore, the objective of this study is to develop BIM framework LOD100 to LOD300 of design phase to practical implementation of UTP airport project. The collaboration plan of building work, infrastructure work and interfacing work was developed. The data for facility management was prepared for delivery to the construction phase in the future.

2. PROCEDURE OF WORK

2.1 Experience And Fundamental of BIM

Since the 2013s, BIM for construction projects were implemented by STECON. Initially, construction projects used BIM to facilitate work. However, design and construction projects have been executed recently to promote greater BIM usage. as shown in Table 1.

Table 1. Previous mega-project work of STECON

Year	Project Name	Construction Type	Scope of Works	Level of Detail
2013	CAT Telecom	Building	Build Only	400 - 500
2016	BOB	Building	Build Only	400
2016	Sewage Tunnel	Infrastructure	Build Only	400 - 500
2018	PK-YL	Infrastructure	Design & Build	100 - 500
2020	MCC	Building	Build Only	400 - 500
2021	GCC	Building	Build Only	400 - 500

In Thailand, there is currently no apparent BIM standard. In this study, BIM Forum, American Institute of Architects (AIA), Engineering Institute of Thailand (EIT), and The Association of Siamese Architects under Royal Patronage (ASA) standards were referenced to determine the appropriate framework for application in the project. The level of detail (LOD) defines the quantity and quality of building data that must be included in a BIM model (LOD 100: conceptual mass, LOD 200: approximate size and shape in model, LOD300: accuracy size and shape in model, LOD 400: represented in LOD 300 with installation information, LOD 500: Elements are modeled as constructed assemblies for maintenance and operations). LOD100-500 (Grytting et al., 2017) were used in STECON previous work. BIM has been used in a variety of projects of STECON. Especially, during 2014 to 2018, the passenger terminal of Phuket airport, Thailand was constructed by STECON. This experience would be encouraged to develop the BIM framework in this study.

The majority of STECON's projects are built only with BIM implementation that is both defined and undefined in the TOR. The initial issue encountered was that the requirements were not specified. Model resolution including may not contain a reference to the applicable standards. Therefore, STECON presents the BIM process and BIM objective in order to identify working instances and achieve a predefined BIM workflow through collaboration. A workshop is required at the outset of the work. Develop communication with all related disciplines, whether they are employed by the prime contractor or a subcontractor. The majority of STECON's activity involves large-scale projects. The task must be divided into several sections. Consequently, process collaboration absence of communication and coordination would result in a lack of data when dividing the scope of a project. There would be a problem with the conventional method of sending and receiving work at the beginning of the project. It results in a lack of data and out-of-date information in AEC (Architecture, Engineering and Construction) area (Arayici et al., 2018).

2.2 Project Information Analysis

To initiate each new construction undertaking project data acquisition and project analysis should be the initial steps such as project information pertaining to contracts, budgets, conditions, project forms, and associated agencies. The project data is then analyzed to begin outlining the framework that would be used for the project's execution. Additionally, it is essential to examine research on the evolution of frameworks, such as BIM in airport construction projects (Keskin et al., 2018).

The phase analysis of a project begins with an examination of the project's baseline, project type, and contract form. Many details are included in airport-related projects, which must be developed in accordance with the project plan. The BIM system for the project has been designed with models and tools that are appropriate for the nature of the project and the work involved. The BIM application of the project were detailed in the BEP, which consist of BIM Goals, workflows, software, clash detection, and model development. All this information was submitted to BIM consultant and owner to be implemented with the Subcontractor who operates within the framework of the EPC.

2.3 Framework Development

The establishment of a project framework begins with the incorporation of project analysis data, BIM standards and methodologies. STECON has undertaken different initiatives and studied the growth of the framework of various research being created around the world (Bradley et al, 2016). Leading to the establishment of the structure from the big picture, as well as the creation of work processes were studied. It can be divided into three major sections, as follows:

- 1) Overall framework: designation of an overarching framework that takes into consideration the project's form, scope of work, and the relationship between each department and the organization's external stakeholders were studied. It will be divided into two parts.
 - Role and responsibilities: a significant number of individuals are involved in the U-Tapao Airport initiative. Therefore, it is necessary to define the duties and responsibilities of everyone involved in the project, as well as the person who is primarily accountable or liable secondarily.
 - BIM workflow: It describes the overall operations of each department and task. BIM workflow is divided into two major phases of the project consist of the design phase and the construction phase.
- 2) Data and information exchange: to guarantee the project's achievement, it is crucial to define data forwarding, storage to prevent errors, and duplicate operations. It can be divided into the following two sections:
 - Tool: Autodesk Construction Cloud (ACC) was primarily utilized for design data exchange on projects alongside using ProjectWise. The majority of the design work utilized Autodesk applications, such as Revit, Civil 3D, Navisworks, and AutoCAD, which will determine the version of each application and the format for transmitting data via IFC.
 - Folder structure management: it is essential that the information exchanged between project participants is accurate including with data storage, formatting, and file access.
- 3) Collaboration clash detection: visual inspection and Navisworks were used to determine the detection of defects in each component.

2.4 Planning The Utilization of The Framework During Construction

The BIM framework for the project is intended primarily for use during the construction phase. In the context of a PPP project, concessionaires as investors need to always validate of the correct quantity and budget during the construction phase. BIM framework with the continuity of information transmission from design phase to the pre-construction, and construction phase were prepared. In order to reduce construction duration, BIM expertise is also applied to prefabrication planning. Moreover, BIM framework has been implemented to better facility management in the future.

3. RESULTS

Several reasons can be used to analyze specific BIM implementation concerns in Thailand. The majority of BIM implementation issues in Thailand are the result of inadequate attention from the relevant departments. The project owner's absence of detailed BIM requirements has resulted in insufficient data for the implementation of BIM. The lack of coordination in the BIM work at the beginning of the project included the absence of a BIM Execution Plan (BEP). Therefore, the risk management plan and establishing of BIM framework are the significant importance of BIM implementation in the mega-project. The project area of UTP is approximately 6,500 rai. The design works in the EPC contract were divided into 6 packages including passenger terminal building, airside, landside, airport facilities, cargo terminal, and utilities. It can be seen that UTP airport consists of both building work and infrastructure work. The collaboration and combined information of the 6 packages were controlled by BIM consult to verification the conflict in the model of each package. The discipline of each package was verified before combined the model. To create a conceptual framework for the whole project, the BIM framework focused on practical implementation was divided into 3 parts consisting of goals, collaboration, and data and model

management. The overall BIM framework was summarized in Figure 1 to understand all processes in the project. BIM Execution Plan (BEP) was produced for utilizing on U-Tapao international airport phase 1 project (UTP) to define as a BIM standard identifying the BIM implementation, defining role and responsibility of each party in the project as well as describing the information exchanges between parties. A project's BEP was defined the appropriate uses of BIM on the project, along with a detailed design and documentation of the process for executing BIM throughout a project's lifecycle in order to achieve goals and objectives of the project throughout the project.



Figure 1. Overall BIM framework

3.1 Goals

3.1.1 Project Goals & BIM Goals

The BIM Strategy Plan should be suited to the project's human and physical resources, operating time, and quality standards. A project's Traditional goals (i.e., time, cost, and quantity) and productivity are impacted by a lack of information and conflict. Nevertheless, BIM-based approaches reduce complexity and difficulty, increase productivity and efficiency, and evaluate time. Consequently, construction practices have shifted towards BIM-based practices (Al-Ashmori, et.al, 2020). The development of national and international BIM standards was identified as one of the most essential factors and strategies for the successful implementation of BIM (Smith, 2014). It can be seen that the owner, who may be government or corporate leaders, plays a significant role in determining the project's direction. Include setting objectives for the project's implementation as well.

A BIM strategy seeks to optimize the use of advanced BIM technology and processes in order to improve the quality of the built environment and project outcomes while reducing costs and optimizing performance. The BIM goals for UTP emphasize 4 main criterions including design, visualization, and estimation as shown in Table 2.

Table 2. BIM goals for building work

BIM goals	Priority	Description	Potential BIM Uses
Design	High	The utilization of BIM technology from the conceptual design stage through the construction stage in accord with the standard and regulation.	- 3D model LOD300 for detailed design (DD) - Construction Reference Drawing (CRD)
Visualization	Medium	The simulation from the BIM model for presentation and walkthrough.	- Virtual Reality (VR) - Walkthrough
Coordination	High	The process of clash detection to identify the conflicts in design and construction's limitation.	- 3D coordination - Clash detection
Estimation	High	The quantity of materials and equipment in each stage of design	- Quantity take-off (QTO)

Design, Coordination, and Estimation are among the BIM Goals in the high priority section, as shown in Table 2. Beginning with the architectural design, followed by all engineering aspects, and concluding with clash detection, which identifies design flaws so they can be resolved, or the design improved to meet the specifications, each of the three components utilizes a continuous process. The quantity is subsequently extracted from the model data to be used as information for constructing BOQ and presenting to decision holders.

3.1.2 Model Development Workflow

The development of the BIM model in accordance with the BIM goals established for each phase initiated the development of the LOD for the design and construction phases. The document from preliminary design throughout as-built drawing were showed in Figure 2 consists of drawing, BOQ, and model with various accuracy

depending on each stage. BIM element is able to mae cost and schedule data automatically (Charef et al., 2018). This is possible due to the close interconnection between costs and schedules. Each stage was evaluated by stakeholders in terms of its investment potential and appropriate for engineering.

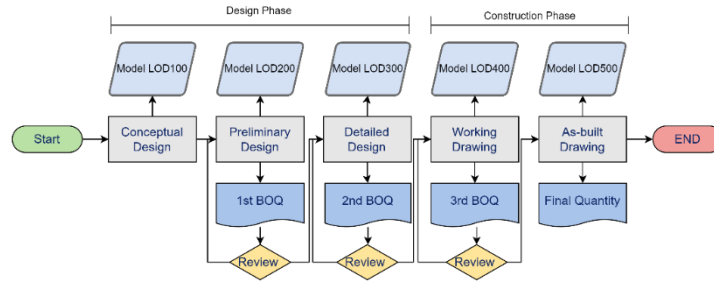


Figure 2. Model development workflow

3.1.3 Role and Responsibility

It is essential to comprehend each party's BIM responsibilities and duties. There are 5 main BIM roles in this project include BIM Manager including with BIM expert, BIM coordinator, BIM specialist and modeler/BIM operator. BIM Roles and responsibilities for a user in Building Information Modeling shown as Table 3.

Table 3. BIM Roles and responsibilities

Roles	Responsibilities
BIM Manager	Plan and manage the workflow with BIM, communicate and reach agreements, and establish work policies and objectives.
BIM Expert	Technical program specialist, an adviser of technique and process of the programs in order to make BIM work continuously, planning in creating a model.
BIM Coordinator	Inspecting and controlling BIM process. Coordinating within a team and others to meet BIM Protocol, BIM Standard, and BEP
BIM Specialist	Giving advice of technique and process of the programs and controlling in creating/editing a model to meet BIM Protocol, BIM Standard, and BEP. Be able to teach and develop working skills for a member of the team.
Modeler/BIM Operator	Creating, editing and controlling a model of their own discipline to meet the project's requirements

The BEP of a project defines the appropriate uses of BIM on a project, as well as a detailed design and documentation of the process for executing BIM throughout a project's lifecycle, in order to achieve the project's aims. The BIM Manager is responsible for all BIM-related project coordination. The primary responsibilities of a BIM manager are to delegate authority to each professional involved in a project to develop, modify, or transfer their respective project component (Sampio, 2022).

3.2 Collaboration

3.2.1 BIM Workflow

For the BIM coordination workflow in the pre-construction phase were prepared by focusing on the BIM model's quality that must have sufficient detail and information as well as the reduction of the amount of clash detection occurred in throughout the phase as shown in Figure 3. The result showed the BIM workflow from collaboration of conceptual model throughout the preparing documentation including a detailed design drawing with a construction reference drawing (CRD) and Bill of Quantities (BOQ).

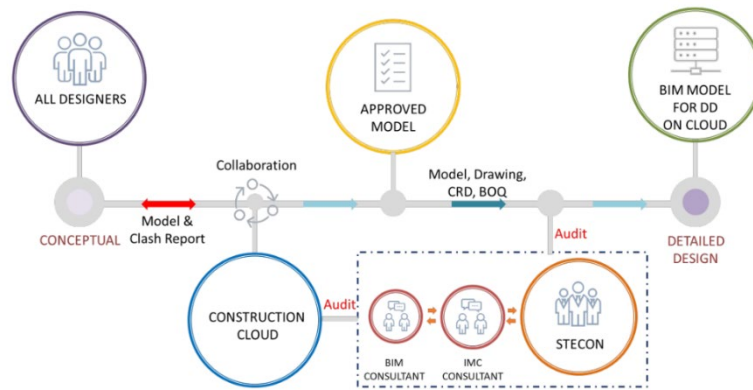


Figure 3. BIM Coordination Workflow for Pre-Construction Phase

3.2.2 Clash Detection Workflow: Design Phase

Figure 4 illustrates the workflow for clash detection during the design phase of the project. BIM manager investigated and reported conflict detection by zone with project file configuration in addition to grouping on typical clash result. All clash results from the clash detection procedure were categorized according to the significance of the conflict, and these results were used as the primary topic of discussion at the BIM meeting. In PDF, XML, HTML, or another format, a clash report is a document shared with all involved parties that details problems or conflicts that have arisen in the project based on the clash detection criteria or rules. The HTML (Tabular) report format was utilized in the project, which can be viewed in a web browser.

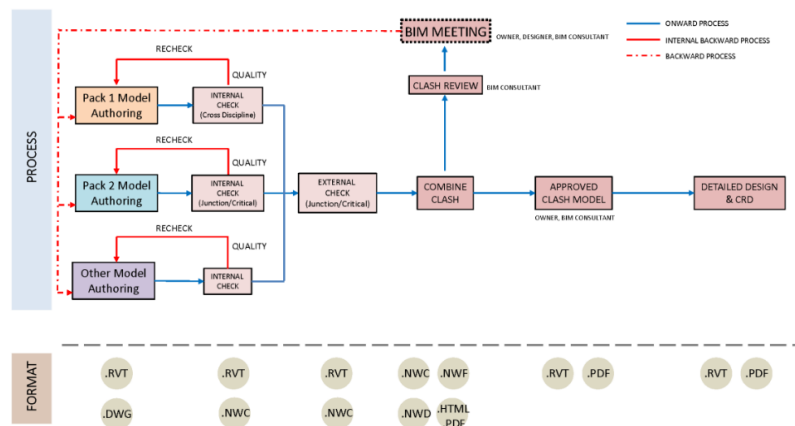


Figure 4. Clash detection workflow

3.2.3 Interface meeting

Throughout the stages of preliminary design and detail design, each party's BIM model was updated weekly. Bi-weekly meeting for BIM-related discussion with other coordination topics was organized in order to check the clash in the model. An additional BIM-related agenda can be added to the meeting. The BIM Manager will lead BIM meetings, as well as internal coordination and a review of the project's standards and procedures.

3.3 Data and Model Management

The Autodesk Construction Cloud (ACC) and ProjectWise were used in the project throughout all design phases for the project data management in different type of documents (Alvarez et al, 2021). The account and configure project access and permissions were conducted by BIM manager. The agreed-upon files to the consultant at each design milestone were provided by each package design team. The file storage for collaboration with all designer team was summarized in Table 4. Table 4 displayed the file type from each project-related software used to manage the file format system.

Table 4. Model file storage for collaboration

File location	Description
Hub	Sino-Thai Engineering and Construction
Project	U-Tapao International Airport Phase 1 (UTP)
File type	RVT - Type of file for all disciplines model on Revit DWG - Type of file for Civil & Site Utilization NWC – Type of file for Navisworks Cache NWF - Type of file for Navisworks File Set NWD - Type of file for Navisworks Document DWG - Type of file for Detailed Design Drawing submit as package PDF - Type of file for Detailed Design Drawing submit as package XLSX - Type of file for Bill of Quantities (BOQ)
Passwords protect	Sign in by Autodesk account ID after receiving invitation from admin
File maintainer	STECON

The folder structure management for BIM data were used based on the standard, which is classified the structure into 3 main parts as work in progress (WIP), shared, and published with the archive folder used as backup within each folder as shown in Figure 5.

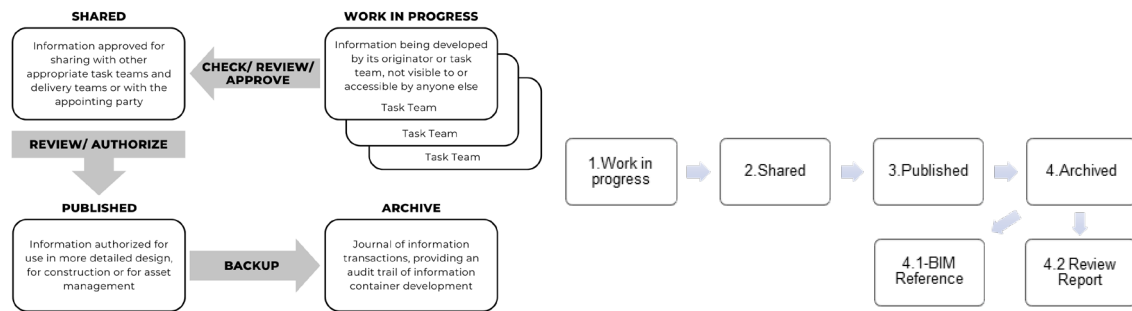


Figure 5. Folder structure management

The folder structure was used to categorize any input information uploading into platform, Autodesk Construction Cloud (ACC), and ProjectWise. The folder was classified into 4 main parts including work in progress (working), shared (input), published (output), and archived (process & information) as shown in figure 5. In addition, BIM reference is another folder used to gather other information necessary for the project. Each main folder will be subdivided into subfolders for each milestone in order to collect milestone-related data.

3.4 Project Implementation for UTP

3.4.1 Base Reference File

BIM was utilized on the project to facilitate the division of work between parties, more distinctly, reduce the likelihood of blunders and conflicts occurring in project due to the project's complexity. Base Reference File is a central file to divide data and distinct division of the scope of task for each section as shown in Figure 6. LOD100 resolution is utilized to generate a base reference file, each of which is accountable for designing within its own scope without affecting the work scope of other departments.

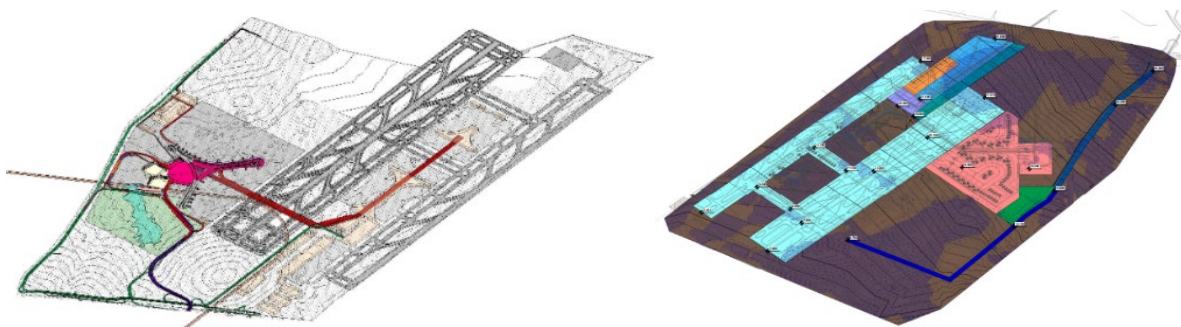


Figure 6. Base reference file and project terrain of UTP

3.4.2 Project Terrain

In the UTP Project, the implemented BIM also facilitated the management of earthwork volumes. The survey team's information was transferred to a CSV file and then plot in AutoCAD Civil 3D to calculate the excavation volume and fill volume. In case the elevation was changed during design phase, it can be real-time calculated the excavation volume and fill volume by using BIM.

4. CONCLUSIONS

This paper presents comprehensive the BIM framework of U-Tapao international airport which is the mega-projects in Thailand with area approximately 6,500 rai. STECON has been awarded as Engineering, Procurement, and Construction Contractor (EPC) to implement the UTP project. BIM framework for practical implementation was proposed by STECON. Findings revealed the following:

- The BIM application for cloud-based data transmission is categorized as a standard storage structure. and preserved in a systematic manner. This section contains central information for use by all departments as a resource or to develop a model. This system reduced the problem of a lack of information and eliminated conflicts between other parties.
- A BIM workflow is established for model coordination and validation. The BIM goals at each stage must be appropriate in terms of resources, time, and quality for the UTP project. BIM 3D and BIM 5D, respectively, were responsible for conflict resolution and quantification for updating real-time information.
- As an outcome of this paper, a BIM framework with a method for transmitting information to the pre-construction and building-operation stages has already been developed. In the future, when it will be utilized, it will require further development.
- The BIM framework for practical implementation was developed including three categories such as goals, collaboration, and data management. The BEP contains the BIM framework's specifications. To ensure the project's success, all participants must work together and rigorously adhere to the plan.

The BIM framework for this project must be consistently developed until the construction phase so that its usability can be confirmed. This work is expected to benefit the BIM industry in Thailand to ensure that it can be utilized in the future.

ACKNOWLEDGMENTS

The authors thankful to the Sino-Thai Engineering & Construction Public Company Limited (STECON) for providing necessary supports.

REFERENCES

- Arayici, Y., Fernando, T., Munoz, V., & Bassanina, M. (2018). Interoperability specification development for integrated BIM use in performance based design, *Automation in Construction*, 85, 167-181.
- Alvarez, A. P., Ordieres-Mere, J., Loreiro, A. P., & Marcos, L. (2021). Opportunities in airport pavement management: Integration of BIM, the IoT and DLT, *Journal of Air Transport Management*, 90, 101941.
- Al-Ashmori, Y. Y., Othman, I., Rahmawati, Y., Amran, Y. H. M., Sabah, S. H. A., Rafindadi, A. D., & Mikic, M. (2020). BIM benefits and its influence on the BIM implementation in Malaysia, *Ain Shams Engineering Journal*, 11, 1013-1019.
- Bradley, A., Li, H., Lark, R., & Dunn, S. (2016). BIM for infrastructure: An overall review and constructor perspective, *Automation in Construction*, 71, 139-152.
- Charef, R., Alaka, H., & Emmitt, S. (2018). Beyond the third dimension of BIM: A systematic review of literature and assessment of professional views, *Journal of Building Engineering*, 19, 242-257.
- Jung, Y., & Joo, M. (2011). Building information modelling (BIM) framework for practical implementation, *Automation in Construction*, 20, 126-133.
- Keskin, B., Ozorhom, B., & Koseoglu, O. (2018). BIM Implementation in Mega Projects: Challenges and Enablers in the Istanbul Grand Airport (IGA) Project, *Advances in Informatics and Computing in Civil and Construction Engineering*, pp.881-888.
- Grytting, I., Svalestuen, F., Lohne, J., Sommersteth, H., Augdal, S., & Laedre, O. (2017). Use of LoD decision plan in BIM-projects, *Procedia Engineering*, 196, 407-414.
- Sampaio, A. Z. (2022). Project management in office: BIM implementation, *Procedia Computer Science*, 196, 840-847.
- Smith, P. (2014). BIM implementation – global strategies, *Procedia Engineering*, 85, 482-492.

STATE-OF-THE-ART OF HISTORIC BUILDING INFORMATION TRENDS WITH DIGITALIZATION INTEGRATION ON THE ARCHITECTURE HERITAGE CONSERVATION IN VIETNAM

Thu Anh Nguyen¹, Nhu My Uy Le², Sy Tien Do³, Son Hong Nguyen⁴, Quang Trung Khuc⁵

1) Ph.D., Department of Construction Engineering and Management, Faculty of Civil Engineering, Ho Chi Minh City University of Technology (HCMUT), 268 Ly Thuong Kiet Street, District 10, Ho Chi Minh City, Vietnam National University Ho Chi Minh City, Linh Trung Ward, Thu Duc District, Ho Chi Minh City, Vietnam. Email: nathu@hcmut.edu.vn

2) M.Eng., Department of Construction Engineering and Management, Faculty of Civil Engineering, Ho Chi Minh City University of Technology (HCMUT), 268 Ly Thuong Kiet Street, District 10, Ho Chi Minh City, Vietnam National University Ho Chi Minh City, Linh Trung Ward, Thu Duc District, Ho Chi Minh City, Vietnam. Email: uynhule@hcmut.edu.vn

3) Ph.D., Assoc. Prof., Department of Construction Engineering and Management, Faculty of Civil Engineering, Ho Chi Minh City University of Technology (HCMUT), 268 Ly Thuong Kiet Street, District 10, Ho Chi Minh City, Vietnam National University Ho Chi Minh City, Linh Trung Ward, Thu Duc District, Ho Chi Minh City, Vietnam. Email: sy.dotien@hcmut.edu.vn

4) Master Student, Department of Construction Engineering and Management, Faculty of Civil Engineering, Ho Chi Minh City University of Technology (HCMUT), 268 Ly Thuong Kiet Street, District 10, Ho Chi Minh City, Vietnam National University Ho Chi Minh City, Linh Trung Ward, Thu Duc District, Ho Chi Minh City, Vietnam. Email: 1612968@hcmut.edu.vn

5) M.Eng., Department of Construction Engineering and Management, Faculty of Civil Engineering, Ho Chi Minh City University of Technology (HCMUT), 268 Ly Thuong Kiet Street, District 10, Ho Chi Minh City, Vietnam National University Ho Chi Minh City, Linh Trung Ward, Thu Duc District, Ho Chi Minh City, Vietnam. Email: khucquangtrung@hcmut.edu.vn

Abstract: The protection of constructed heritage is increasingly intertwined with the routine upkeep of structures, making conservation a practical requirement daily. Despite the recent considerable development in the usage of BIM in the field of Cultural Heritage (CH), the application of Heritage Building Information Modeling (HBIM) of cultural property intended for preservation is still limited. One of them is the unique diversity of Vietnamese traditional architecture that needs to be considered to assess the status of restoration and conservation. The improvement of data capturing technologies like 3D Laser Scanning and enhanced photogrammetry, along with the ongoing capability of HBIM authoring tools, not only enables the storage of spatial information and metadata but also offers the means for recording structural changes. This research aims to overview the state of art implementation for digital historical building, specifically in the Scan-to-HBIM application, and propose a database of historical structures using HBIM that focuses on the measurement information contained in the model, particularly related to conservation from the Scan-to-HBIM process to apply in a specific case study, namely Hung Kings Temple. The research methodology is using a questionnaire survey to collect data from the sampling to evaluate the frequency of using the component information in the Heritage Building. It sought to demonstrate the efficacy of HBIM there in the information recording of small-scale historical monuments. The utilization of digital tools and data recording formats in the creation of object models presents opportunities for future modifications and the integration of HBIM technology for Vietnam in particular and works in the world in general.

Keywords: Cultural Heritage; Heritage Building Information Modeling (HBIM); 3D Laser Scanning; Conservation; Level of Development (LOD).

1. INTRODUCTION

Named monuments, buildings, and landscapes are all examples of physical heritage, as are collections of art and scientific knowledge. Intangible heritage includes cultural practices and beliefs that have been passed down through generations (Machete, Falcão, Gonçalves, Godinho, & Bento, 2020). Fundamental to the study of architectural heritage is surveying and archival research. To evaluate a building's present condition, diseases, architectural style, and various phases of construction, it is necessary to gather, store, and analyze all types of information about it (López, Lerones, Llamas, Gómez-García-Bermejo, & Zalama, 2017). The most noteworthy aspect of the World Heritage Convention of 1972 is that it combines in a single treaty the themes of natural protection and cultural property preservation. At the beginning of this year, the municipality commissioned research to support the preliminary design of the preservation plan for the earthquake-damaged church of St. Francesco in the hamlet of Arquata del Tronto (Italy) that was struck in 2016 by static and dynamic terrestrial laser scanning (TLS) to acquire massively geometric and material information supporting the three-dimensional (3D) and the creation of the Heritage Building Information Modeling (HBIM) (Banfi et al., 2022).

Many of the issues that cultural collections, sites, and assets are dealing with are the consequence of long-term neglect or a lack of management and maintenance (Fund, September 2017). This involves having the appropriate skills and processes in place to guarantee that they are properly maintained. Poor management and upkeep put legacy in danger, and it may result in greater expenses in the long run (Heritage Victoria, August 2020). Therefore, it is imperative to identify and evaluate the existing models of heritage promotion and conservation in

Ho Chi Minh City in particular and Vietnam in general to develop an appropriate product evaluation framework for each heritage conservation purpose.

2. LITERATURE REVIEW

2.1. The Heritage Building Information Modeling Applying to Culture Heritage

Heritage building information models (HBIM) must grow into a widely used system (Boboc et al., 2019; Khaja, Seo, & McArthur, 2016). The advancement of technology over the last several decades has enabled the deployment of new methods of digital information distribution, which has also had a significant impact on the evolution of Cultural Heritage (CH) dissemination (Borri & Corradi, 2019). Despite these attempts to preserve the urban legacy of Saudi Arabia, several heritage buildings in the country have been plagued by major difficulties for years due to improper maintenance and operation. The construction of a geometric model to serve as an inventory of cultural assets is a necessary step in the restoration of architectural structures. Architecture is culture, an important part of national culture. The national identity and advanced nature of the culture must be permeated not only in cultural and artistic work but also in all material construction and creation activities (Minister, July 19, 2021). Nonetheless, one of the most difficult tasks today is to resolve the problem of information management, which is scattered by the many parties participating in the restoration process. In terms of minimizing incoherence and duplication of effort, it is necessary to digitize and link the information processing process.

The majority of notable heritage structures are legally protected, with many of them being owned and/or managed by trusts, public or religious institutions, and museums, among others. The standardization system comprises organizations responsible for standardization activities conducted on national, European as well as international levels in general and Vietnamese in specific. European and worldwide standards are produced following the idea of the national delegation, with each country sending a delegation of specialists to represent its point of view throughout the development process. The notion of national delegation provides stakeholders with a clear channel to European and worldwide standards while also encouraging industry self-regulatory efforts (Anne-Kathrin Schäfer, 2020).

Table 1 is a list of existing standards according to CEN and BSI standards for the management and operation of historical monuments.

Table 1. Legal Document Related to Facility Management in Culture Heritage

Standard Code	Standard Name
CEN EN 16893:2018	Conservation of Cultural Heritage - Specifications for location, construction, and modification of buildings or rooms intended for the storage or use of heritage collections
CEN/TC 442	Building information modeling
CEN/TC 346	Conservation of cultural property
CSN EN 16096	Conservation of cultural property - Condition survey and report of built cultural heritage
BS EN 16141:2012	Conservation of cultural heritage — Guidelines for management of environmental conditions — Open storage facilities: definitions and characteristics of collection centers dedicated to the preservation and management of cultural heritage.

The architecture of Vietnam is stunning and diverse, and it may be divided into five separate sections: vernacular, Chinese, ethnic, colonial, and Indochina architecture (Cadière, 1987). The old monuments in traditional forms that can be seen all around the nation are a source of great pride for the Vietnamese people (Nhr, 2020). Wooden houses and layer roofs are common features of traditional Vietnamese architecture. Preservation of architectural heritage may not be a hindrance to economic progress, but rather a significant asset to it (Linh, 2018). Up to now, in Vietnam, there have been no sets of standards for architectural heritage management practices issued. Legal congress provisions are still implemented according to the **Law on Cultural Heritage No. 28/2001/QH10** dated June 29, 2001, of the National Assembly, as amended and supplemented by Law No. 32/2009/QH12 dated June 18, 2009 (Assembly, 2001), promulgated on July 23, 2013, to strengthen the effectiveness of state management and enhance the responsibility of the people in participating in protection and development to promote cultural heritage. On December 25, 2018, **Decree No. 166/2018/ND-CP** (Government, 2018), issued by the Government, stipulated the competence, order, and procedures for formulating, appraising, and approving planning, preservation, and restoration projects. restore and restore historical-cultural relics and scenic spots. **Circular No. 15/2019/TT-BVHTTDL** (Culture, 2019) dated December 31, 2019, of the Ministry of Culture, Sports and Tourism detailing several regulations on preservation, renovation, and restoration of monuments, the repair dossiers urgent, periodical preservation of relics or objects of relic inventory.

According to (Khalil, Stravoravdis, & Backes, 2021), as HBIM reviews the many data types that could be included in the documentation and investigation process of the built heritage, it is poised to play a pivotal role in the digital documentation of heritage buildings by combining quantitative and qualitative data and facilitating the integration of different stakeholders and specialized data into the digital management of the various phases of dealing with heritage buildings. However, this research merely discusses the correlations between these aspects as consideration factors to be utilized for the document, without proposing a particular procedure to apply to the works.

In 2023, the HBIM research (Hou, Lai, Wu, & Wang, 2023) investigated the theoretical and practical connections between Digital Twin (DT) applications in Heritage Facility Management (HFM) from a lifecycle management perspective and guide development directions. This modern review was carried out using a systematic literature review method. The overall implication of this study is that it shows the potential of heritage sites in facilitating HFM in the context of urban development. From there, this study aims to conduct an overview of Vietnamese applications for heritage management with digital support tools.

2.2. The General Status of Vietnam Heritage Architecture Conservation

Digital transformation in the field of culture and tourism is taking place continuously, new technologies are applied regularly. According to cultural experts, the application of technology and digital transformation in the field of culture and tourism has brought about positive effects, helping viewers to approach cultural heritage in many different ways. This is completely in line with the development trend, meeting the needs of the public and visitors to enjoy and learn. Table 2 below showed the list of digital heritage activities in Vietnam for five years from several Hi-tech companies and Laboration in Ho Chi Minh City and Hanoi City such as Star Global 3D company, Portcoast, Sen Heritage Group, Seagate and CyArk, etc.

Table 2. The List of Digital Heritage Activities in Vietnam

No.	Heritage Architecture	Technology Application					
		Photogrammetry	360 View	Ontology	3D Laser scanning	Hologram	3D Mapping
1	The Temple of Literature	x		x			x
2	Hoa Lu Ancient Capital	x		x			
3	Vietnam National Museum of History	x	x	x			
4	Tien Le communal	x					
5	Bo Da pagoda		x				
6	The Hung Kings Temple		x				
7	Na Tu historical sites		x				
8	ATK Dinh Hoa historical sites		x				
9	27/7 historical sites		x				
10	Tu Duc tomb				x		
11	An Dinh palace				x		
12	Khai Dinh tomb	x			x		
13	Hue Imperial City		x		x		
14	Da Nang Fine Arts Museum	x					
15	My Son Sanctuary	x			x		
16	Hue Ancient Capital Heritage Site						
17	South Women's Museum	x				x	
18	Vietnam Museum of History		x				
19	Tan Dinh church		x		x		
20	Saigon Notre-Dame Cathedral		x		x		
21	Nha Rong Wharf		x		x		
22	Saigon Opera House	x	x	x	x		
23	L'Opera de Hanoi	x	x	x	x		
24	Oc Eo Cultures			x			
25	Ho Chi Minh Museum		x	x			

No.	Heritage Architecture	Technology Application					
		Photogrammetry	360 View	Ontology	3D Laser scanning	Hologram	3D Mapping
26	Hoang Thanh Thang Long Museum		x	x			

As a result, heritage digitization is a trend that is no longer strange in the world, Vietnamese heritage sites have also approached this trend for many years, but to a relatively limited extent. The 360 views and 3D Laser Scanning dominate the technology application at heritage works. When using HBIM, each component of the total construction plan is represented by component objects, while the required granularity of information of HBIM objects is expressed through the parameter LOD. Along with the geometric information, the non-geometric information of the HBIM object is necessary for the management of heritage information in record keeping, so each of these objects should contain specific information related to the target. of conservation and maintenance stages, i.e., have different LODs. LOD includes many different levels, according to the American Institute of Architects (AIA), LOD is divided into 6 levels:

- LOD 100 – Conceptual
- LOD 200 - Approximate Geometry
- LOD 300 - Precise Geometry
- LOD 350 - Precise Geometry with Connections
- LOD 400- Fabrication-ready Geometry
- LOD 500 - Operational/As-built Models


In previous studies, the model was also evaluated through the Level of Knowledge (LOK) (Barontini et al., 2021). The LOD concept cannot be transferred to the HBIM property in terms of the development of the project because the project already exists; instead, the transfer must relate to the project's LOK and property administration, both of which this LOK can provide appropriate information.

3. METHOD

3.1. The Case Study in Vietnam

The Temple of Hung Kings (Table 3) at the Zoo and Botanical Garden built by the French in 1926 is called the Temple of Memory (Temple de Souvenir) and was chosen as the typical case study for collection data. In June 2015, Hung Kings Temple was ranked as a historical-cultural relic, a city-level scenic spot (Son, 2015).

Table 3. Hung Kings Temple information

<p>Location The Hung Kings Temple in the Botanical Garden (District 1) was built in 1926 and is one of the typical ancient architectures of Saigon.</p>	
<p>Architect Style The temple has a square plan, bearing the architectural style of the Nguyen Dynasty with overlapping roofs, forming three curved roofs. In general, the long-standing counterattack work of Minh Mang Tomb in Hue.</p>	

Besides that, the whole temple is decorated with decorative motifs in the shape of cranes, unicorns, turtles, and phoenixes representing the noble descendants of Vietnamese dragons and fairies, most notably the pair of blue dragons carved on both sides (Dien, 2016). The Hung Kings are revered as the common ancestor of the whole Vietnamese nation. Therefore, the worship of Hung Vuong has become a unique type of religious and cultural belief in the spiritual/cultural life of generations of Vietnamese people; is the spiritual fulcrum that creates the strength of the Vietnamese nation (Van, Long, Thanh, Dong, & Van Luong, 2020).

3.2. Scan-to-HBIM application

Figure 1 presented the Scan-to-HBIM with the obtained data processed. The process included 5 stages from collecting data through the 3D Laser Scanning method to the visualization through the emulator software. In 2nd step, before the HBIM model was built, the 3D component model identified the Level of Development (LOD) through the questionnaire survey and the LOD standard based on the BIM Forum LOD Specification 2021. When the HBIM model is established by Autodesk Revit software, which is going to upload to the BIM Platform such as Autodesk 360, Bentley, Trimble Website, etc.

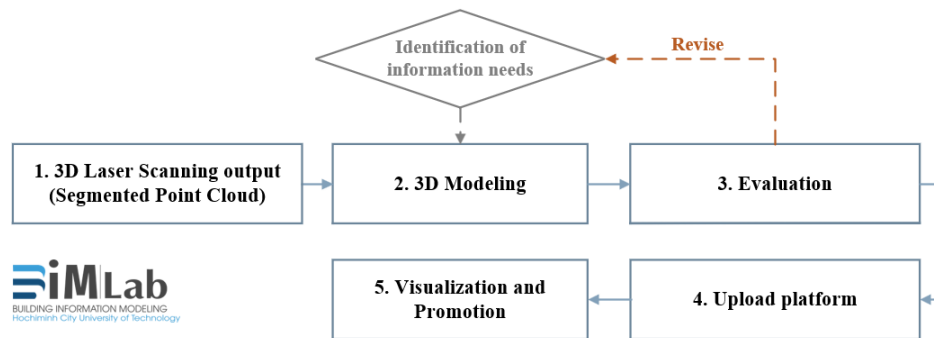


Figure 1. Scan-to-HBIM activities process

3.3. Database Framework Establishment

After proposing the survey tables from the reviews of related documents and studies, the author surveys the frequency of using the information on the components in a historical monument. The survey consists of two main phases:

- Phase 1: Survey the frequency of information use of building components.
- Phase 2: Primary survey with the first participants with the required amount of information for each element in the heritage model setting.

After establishing a database, the authors apply the proposal to a real project to evaluate the performance of the database. The application implementation will be applied to specific software and types of components included in the proposed HBIM-FM model to evaluate the ability to provide information in the project. These recommendations represent a minimum information requirement during the operational phase. Therefore, when other projects adopt this information set, it is possible to customize more or less the development level of the information model in the project rather than the fixed LOD level. Figure 2 below presents the process of carrying out a 2-stage surveyor from which to propose an appropriate LOD level for the pilot heritage project, specifically here at the Hung King temple.

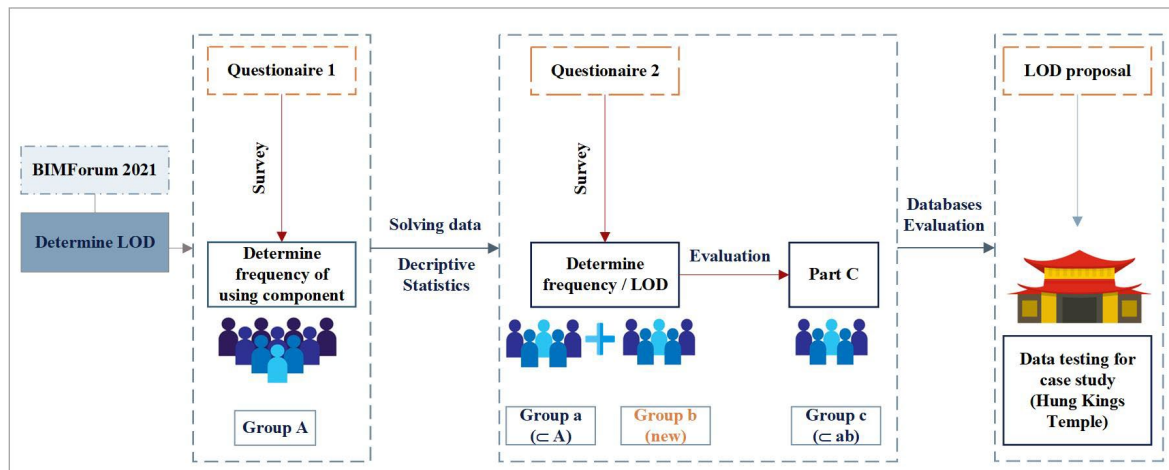


Figure 2. Data collection process

4. RESULTS

The characteristics of this study are that the survey subjects are all individuals involved in the archeology and construction field, meanwhile, a very large number of surveys, distributed on a large scale and requiring resources such as time, cost as well as human resources, is extremely large. The time to carry out this study is limited, and the application of the sample population survey seems impossible. Therefore, the author chooses the sample survey method in the research. A descriptive statistical data analysis method was used in this study. The phase 1 survey was completed in April 2021 and the survey was sent to more than 200 subjects who are architects, engineers, and managers in the field of architecture - construction. Then, the author received 74 responses from individuals, of which 69 responses were valid. Survey subjects give feedback through Microsoft Office Form Online and paper copies are sent directly to individuals participating in heritage conservation projects and projects as well as individuals involved in management. operating management. In the statistics for the questionnaire

survey, in Figure 3, the majority of survey participants are consulting units (including engineers and architects) accounting for 39.1%, followed by investors and first-time operating management units. are 29% and 18.8% respectively. Since the units directly involved in the management and operation of the heritage and the conservation and restoration of the monuments are usually consulting and management units of the facility, the number of differences is biased towards the industry groups listed.

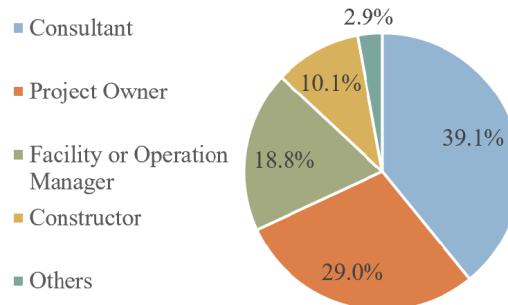


Figure 3. Roles in the Construction Project

The survey panels on the methods used in the conservation, archiving, and preservation of monuments and the problems encountered were shown in Figure 4. One of the outstanding problems in the process of managing and operating historic sites today is the loss of detailed information about historical structures (44) and the change, expansion, and adjustment of the functions of the heritage (39). The accuracy of hand-drawn drawings is not high as well as the lack of drawings, information, and documents related to heritage works are equally important, due to the application of new technologies such as AutoCAD or Revit over the past two decades while the historical works have existed for a long time.

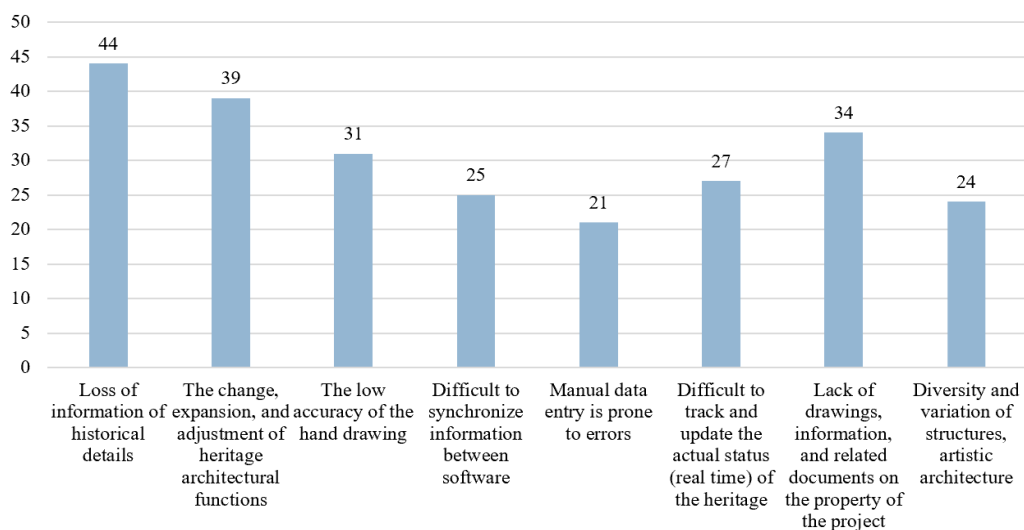


Figure 4. The common problems in the management and operation of historical monuments nowadays

The author uses the Likert scale method and SPSS tool to process the obtained data. In Table 4 in which questions 1 and 2, the integration of HBIM is necessary to build a unified information model for the management and operation of the monument plays an important role in the concept, which in higher mean, 4.64 and 4.7, the conservation of historical buildings, made through energy refurbishment or retrofit and restoration works on existing buildings.

Table 4. The integration of HBIM is necessary to build a unified information model for management and operation

	N	Minimum	Maximum	Mean	Std. Deviation
1. The integration of building information modeling (BIM) for the heritage, namely Heritage building information modeling (HBIM)	69	2	5	4.64	.766
2. It is necessary to build a unified information model for the management and operation of the monument	69	2	5	4.70	.692

One of the first important steps in building an HBIM-FM model is to establish a LOD system following the standards and requirements of the building operation management unit. To do this work in the real project, the authors use the proposed LOD system. Figure 5 displays a model of bronze burners in the style of the Nguyen Dynasty, which is more than 50 years old in Hung Kings Temple. The geometric and informational complexity that architectural models can achieve requires the determination of the complexity of the model and the degree of precision achieved in the geometrical definition and quantity and reliability of information related to an element or project through LOD. Because of LOD500 in which the model element is a field-verified representation accurate in terms of size, shape, and location with orientation, the Hung Kings temple also includes the axis which meant the LOD400 is adaptiveness to the detailing, fabrication, assembly, and installation information.






Ký hiệu/ Code	Cấu kiện/ Element	Mức độ phát triển của cấu kiện/ Component Level of Development (LOD)				
		LOD 100	LOD 200	LOD 300	LOD 350	LOD 400
E2050.39**	Đỉnh Brass burners					
		Khối chung chung, sơ đồ hoặc các cấu kiện được mô hình sơ bộ.	Sơ bộ các kích thước, hình dáng, và vị trí của cấu kiện	Mô hình có các kích thước và vị trí, khoảng cách như chỉ định của thiết kế.	Mô hình với thực tế tại công trường, bao gồm kích thước, hình dáng, khoảng cách, vị trí và liên kết của cấu kiện.	Các phụ kiện của phụ kiện được thêm vào để nhằm phục vụ việc chế tạo và lắp đặt.
		General model information and position are not shown accurately	Schematic layout with approximate size, shape, and location of equipment	Modeled as design-specified size, shape, spacing, and location of equipment and associated components.	Modeled as actual size, shape, and location of service connections and support structure/pads.	Supplementary components added to the model required for fabrication and field installation.

Figure 5. HBIM LOD sample identification

5. DISCUSSION

The construction of a shared digital data warehouse also needs to be done methodically, consistently, and scientifically. Units that have digitized data and have their database need to soon integrate and share data with stakeholders. Through the preliminary survey, the 3D Laser Scanning technology group is dominant in the conservation, maintenance, and restoration of historical monuments in Vietnam. Combined with current research trends in the world, the research team has chosen the 3D Laser Scanning method because of its effectiveness, popularity, and optimal support for the HBIM modeling process in the future.

The process adopted for HBIM creation of structural covering systems, beginning with 3D Laser Scanning surveys and orthoimage synthesis, may be summed up as follows:

- 1) Definition of the structural element macrofamily component.
- 2) The BIMForum LOD proposal-based definition of the hierarchical aggregation of the many object elements within the object family.
- 3) Material specification for each object element. The establishment of such hierarchies of objects is the beginning point for the definition of a database of structural elements finished for the building of HBIMs, which account for the condition of the surveyed structures and the integrated information on the geometry and construction methods.

HBIM involves the integration of geometric 3D information with heritage property survey and analysis. As the Legacy Information Model progresses toward a higher level of precision, the expansion of parameter groups, subgroups, and individual parameters becomes possible. By building a database with a suitable LOD, the study builds a suitable HBIM model for each use purpose such as renovating, restoring, and replacing components when

necessary. In the following research step, the research team conducts a demand survey using model information to accurately identify components with specific LOD requirements. In this research, the author proposes the LOD application in 5 levels (from LOD 100 to LOD 400) because lacking software and the information stored, identification of the information needs plays an important role in the mockup project in Heritage Architecture in Ho Chi Minh City, Vietnam.

6. CONCLUSIONS

A Hung Kings model created in a BIM environment enabled the management of data about the properties of the materials and the geometry of the surfaces. This is particularly beneficial for the storing and exchanging of geometric and semantic data to manage architectural features of historical significance. In addition, Revit software allowed for the management of information inherent to the features of the materials, as well as the acquisition of semantic information. Consequently, it is feasible to correlate historical and architectural information with each object. This can be accomplished by the creation of a basic local database or a centralized one, i.e., one with standard requirements that catalog all the artifacts on the national territory that are recognized as belonging to the cultural heritage. The HBIM model of the temple after determining the appropriate LOD level and after processing the data in the next phase, the author proceeds to build a suitable HBIM model.

In addition, to promote the value of the intangible cultural heritage data warehouse, it is necessary to apply virtual reality (VR), and augmented reality (AR), which to help improve education and preserve heritage, including intangible cultural heritage. Through the proposal to build a scale of model development from the above Scan-to-HBIM process, the creation of digital data on cultural heritage based on new construction and integration openly access digital data will serve to store, manage, research, conserve, exploit, promote heritage, and promote sustainable tourism development.

ACKNOWLEDGMENTS

This research is funded by Vietnam National University Ho Chi Minh City (VNU-HCM) under grant number DS2022-20-03. We acknowledge Ho Chi Minh City University of Technology (HCMUT), VNU-HCM for supporting this study. The authors also would like to thank BIMLab for helping with this research.

REFERENCES

- Anne-Kathrin Schäfer, S. M. D. (2020). *State of Art Report*. Retrieved from EU: Assembly, N. (2001). *Law on Cultural Heritage No. 28/2001/QH10 as amended and supplemented by Law No. 32/2009/QH12*.
- Banfi, F., Brumana, R., Landi, A. G., Previtali, M., Roncoroni, F., & Stanga, C. (2022). Building archaeology informative modeling turned into 3D volume stratigraphy and extended reality time-lapse communication. *Virtual Archaeology Review*, 13(26), 1-21. doi:10.4995/var.2022.15313
- Boboc, R., Duguleană, M., Voinea, G.-D., Postelnicu, C.-C., Popovici, D.-M., & Carrozzino, M. (2019). Mobile Augmented Reality for Cultural Heritage: Following the Footsteps of Ovid among Different Locations in Europe. *Sustainability*, 11(4). doi:10.3390/su11041167
- Borri, A., & Corradi, M. (2019). Architectural Heritage: A Discussion on Conservation and Safety. *Heritage*, 2(1), 631-647. doi:10.3390/heritage2010041
- Cadière, L. M. (1987). *L'Art à Hué: Imp. de l'Extrême-Orient*.
- Culture, M. o. (2019). *Circular 15/2019/TT-BVHTTDL, Sports and Tourism detailing several regulations on preservation, renovation, and restoration of monuments, the repair dossiers urgent, and periodical preservation of relics or objects of relic inventory*.
- Dien, L. (2016). Đền Hùng trong Thảo cầm viên Sài Gòn bị “bao vây”. Retrieved from <https://tuoitre.vn/den-hung-trong-thao-cam-vien-sai-gon-bi-bao-vay-1170957.htm>
- Fund, H. L. (September 2017). *Management and maintenance plan guidance*.
- Government, V. (2018). *Decree No. 166/2018/ND-CP stipulated the competence, order, and procedures for formulating, appraising, and approving planning, preservation, and restoration projects. restore and restore historical-cultural relics and scenic spots*.
- Heritage Victoria, N. S., East Melbourne 3008. (August 2020). Heritage Victoria Minimum standards for maintenance and repair of heritage places. *Heritage Act 2017* 19.
- Hou, H., Lai, J. H. K., Wu, H., & Wang, T. (2023). Digital twin application in heritage facilities management: systematic literature review and future development directions. *Engineering, Construction and Architectural Management, ahead-of-print(ahead-of-print)*. doi:10.1108/ECAM-06-2022-0596
- Khaja, M., Seo, J. D., & McArthur, J. J. (2016). Optimizing BIM Metadata Manipulation Using Parametric Tools. *Procedia Engineering*, 145, 259-266. doi:10.1016/j.proeng.2016.04.072
- Khalil, A., Stravaravdis, S., & Backes, D. (2021). Categorisation of building data in the digital documentation of heritage buildings. *Applied Geomatics*, 13(1), 29-54. doi:10.1007/s12518-020-00322-7

- Linh, Đ. (2018). Phát triển du lịch bền vững gắn với bảo tồn, phát huy giá trị di sản. *Báo Nhân Dân*. Retrieved from <https://nhandan.vn/du-lich/phet-trien-du-lich-ben-vung-gan-voi-bao-ton-phet-huy-gia-tri-di-san-322835>
- López, F. J., Leronés, P. M., Llamas, J., Gómez-García-Bermejo, J., & Zalama, E. (2017). A Framework for Using Point Cloud Data of Heritage Buildings Toward Geometry Modeling in A BIM Context: A Case Study on Santa Maria La Real De Mave Church. *International Journal of Architectural Heritage*, 1-22. doi:10.1080/15583058.2017.1325541
- Machete, R., Falcão, A. P., Gonçalves, A. B., Godinho, M., & Bento, R. (2020). Development of a Manueline Style Object Library for Heritage BIM. *International Journal of Architectural Heritage*, 15(12), 1930-1941. doi:10.1080/15583058.2020.1740825
- Minister, P. (July 19, 2021). *Decision No. 1246/QĐ-TTg approving Vietnam's architecture development orientations through 2030, with a vision toward 2050*.
- Như, B. (2020). Số hóa di sản: Không chỉ cần nhà công nghệ. Retrieved from <https://tiasang.com.vn/-van-hoa/So-hoa-di-san-Khong-chi-can-nha-cong-nghe-26726>
- Son, T. (2015). Đền Hùng Vương ở Thảo Cầm Viên được xếp hạng di tích. Retrieved from <https://vnexpress.net/den-hung-vuong-o-thao-cam-vien-duoc-xep-hang-di-tich-3241090.html>
- Van, V. H., Long, N. T., Thanh, T. T., Dong, T. K., & Van Luong, P. (2020). The Worship of Ancestors Belief of Vietnamese People. *B P International*. doi:10.9734/bpi/mono/978-93-89816-92-1

ON PRACTICAL CASES OF BUILDING INFORMATION MANAGEMENT IN CONSTRUCTION PROJECT COLLABORATION

Min Shih¹, Yen-Hung Chen², and Shen-Guan Shih³

1) BIM Consultant, Unique Engineering and Construction Public Company Limited, Bangkok, Thailand, Former BIM Director of AECOM International Company. Email: minshih99@gmail.com

2) Assist. Prof., Department of Architecture, National Taiwan University of Science and Technology, Taipei, Taiwan. Email: jerome@anyday.com.tw

3) Prof., Department of Architecture, National Taiwan University of Science and Technology, Taipei, Taiwan. Email: sgshih@mail.ntust.edu.tw

Abstract: While traditional project management contracts tend to focus on delineating the work responsibilities of different teams, construction projects often require close collaboration between stakeholders to integrate various interfaces. Building Information Modeling (BIM) is not only a virtual modeling tool for detecting interface clashes but also an audit tool for streamlining information flow among all stakeholders. The exchange of information and mutual support between stakeholders is critical to successful teamwork in construction projects. This report draws on the practice in construction projects as cases to highlight the often-overlooked role of building information management in the project lifecycle. We demonstrate how BIM facilitates collaboration and enhances communication between stakeholders, ultimately leading to more successful project outcomes.

Keywords: Building information management, Multi-stakeholder team collaboration, Information transparency.

1. INTRODUCTION

Construction project management often involves hierarchical contracts between the client, architect, contractor, consultants, sub-contractors, and suppliers, with a focus on clearly defining the responsibilities of each stakeholder team. However, traditional contracts that allocate responsibilities may not align with the proactive collaboration needed in construction projects. Building Information Modeling (BIM) can facilitate information exchange and efficient communication between different stakeholder teams. Rather than simply using 3D drafting tools for modeling, BIM is a database that captures a wide range of information about building elements and their attributes and relationships (McArthur 2015). Despite its potential benefits, some contractors are hesitant to share information or use BIM with owners, hindering its adoption. Research suggests that improving information transparency in construction management could greatly enhance collaboration among stakeholder teams (Brady et al. 2018).

The objective of this paper is to demonstrate effective BIM management strategies for promoting its integration benefits within traditional contract structures. To successfully apply BIM at the management level, four key elements must be in place: “the Policy, Process, People, and Technology”, also known as the “3P & 1T” framework (Hamed 2011) (Lee & Borrmann 2020). The “Policy” involves the inclusion of BIM implementation in traditional contracts. The “Process” pertains to the integration of BIM workflows within the traditional interface responsibility division system. The “People” focus on the cognitive readiness of project managers (non-modelers) to implement and apply BIM, while the “Technology” refers to the technical ability of project participants to use modeling software. With these elements in place, the stakeholder team can provide accurate models (Technology), project execution or management can address interface problems (People), BIM managers can control the workflow execution (Process), and the Owner or project manager can use BIM models as a contract review tool (Policy). This allows the project's execution and management levels to apply model information to the information management level. The practical BIM management cases presented in this paper are based on these principles.

2. INTERGRADATION OF BIM TO TRADITIONAL PROJECT CONTRACTS

Integrating BIM into traditional project contracts requires clear communication of the reasons and expectations for its use in the contract documents. The following keynotes are considered:

1. Define BIM integration based on the project's nature, objectives, and goals.
2. Integrate BIM requirements into contract documents, including scope of work, specifications, drawings, and output items.
3. Clearly define the roles and responsibilities of all stakeholders in relation to BIM in the contract.
4. Define the BIM deliverables in the contract documents, including the required models and associated data.
5. Incorporate BIM into project management processes, including design review, coordination meetings, and construction management.

Integrating BIM into traditional project contracts can lead to increased transparency and improved collaboration among project stakeholders, ultimately resulting in better project outcomes with reduced risks. When BIM is used as a collaborative tool throughout the project lifecycle, it can increase efficiency, reduce errors, and improve project outcomes. However, traditional design or construction contracts have not typically included BIM as a key component, with BIM often only required as a tool for generating deliverables or design integration in the appendixes. Therefore, successfully implementing BIM requires a comprehensive approach that incorporates concepts such as Policy, Process, People, and Technology (3P & 1T), as well as adjusting the workflow under the guidance of ISO 19650 CDE. This approach can include providing a visual platform for multi-discipline interface integration, upgrading it to a design audit core, and utilizing it as a decision-making judgment tool.

Case1: The underground station of the Bangkok MRT

As an example, consider the design and build project for the Bangkok MRT underground station. The contract is divided into three stages: Definitive Design, Detailed Design, and Construction Reference Design. BIM review milestones are set, including 25% Definitive Design LOD 200, 50% Detailed Design LOD 250, 75% Detailed Design LOD 300, and 100% Construction Reference Drawings LOD350. The process is illustrated with the BIM standard of another project for confidentiality (Figure 1). By setting these milestones, the project team can ensure that BIM is used as a collaborative tool throughout the project lifecycle, increasing efficiency, reducing errors, and improving project outcomes. Effective design integration of all construction items, linking CSD (combined service drawings) and SEM (structure, electrical and mechanical), is crucial for project success. One key challenge is integrating BIM into traditional design workflows.

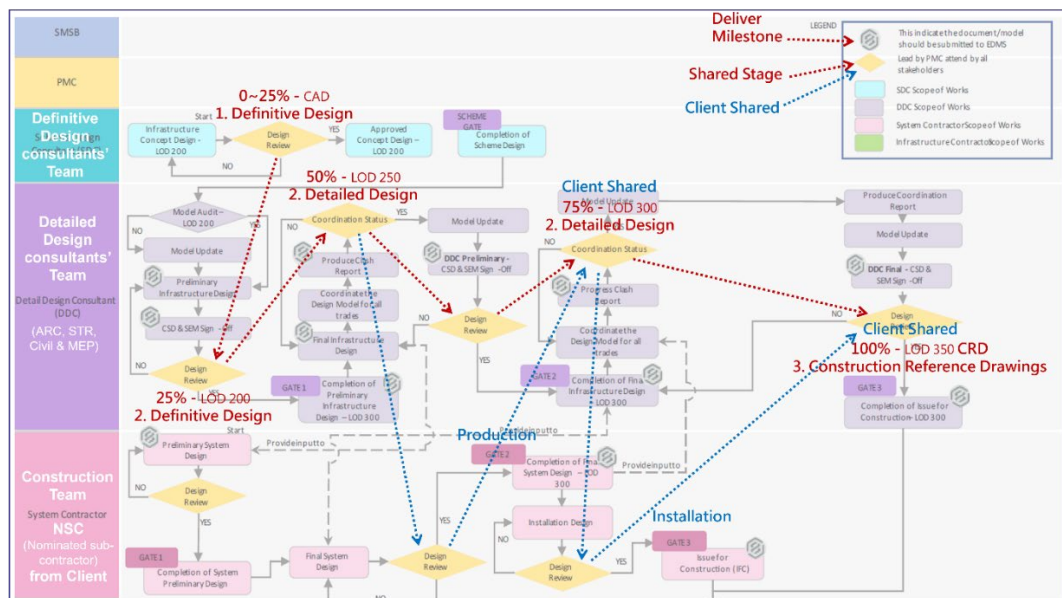


Figure 1. An integrated process of building information management (KUTS 2011)

Detailed Design consultants create a Preliminary Model using the Definitive Design CAD drawings and then further integrated into the federated model. It is illustrated with false models and drawings in Figure 2 and Figure 3 for confidentiality. The model is LOD 200 and includes discipline models for architecture, structure, civil engineering, and MEP (Mechanical Electrical Plumbing). It is important to check the overall CAD drawings of each discipline model to identify conflicts in design content and coordination priority, as shown in Figure 5.

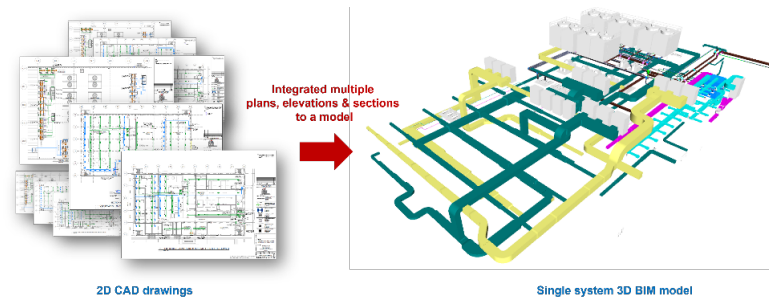


Figure 2. From 2D CAD drawings to single system building information modeling (from the authors)

The second segment (25~50%) and the third segment (50~75%) of the project are developed in the Design Details stage, which are corresponding to LOD 250 and 300 respectively. The focus of this stage is on detailed integration between systems, as shown in Figure 3. Coordination priorities are referred to in Figure 5. BIM is used as an audit tool to coordinate and integrate the three stages into LOD 350, which matches the Design Program.

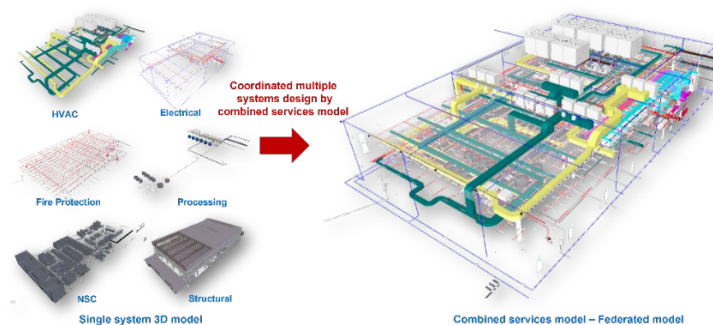


Figure 3. From 2D CAD drawings to the federated model (from the authors)

The fourth segment involves reaching 100% completion of the 3rd stage, which is the Construction Reference Drawings (CRD). This stage involves the integration of design and construction, resulting in a LOD 350 modeling. The LOD 350 segment is a shared component that combines the construction team and the subcontractor chosen by the owner (NSC), who is the client shared at ISO 19650 CDE. The integration process is illustrated in Figure 4.

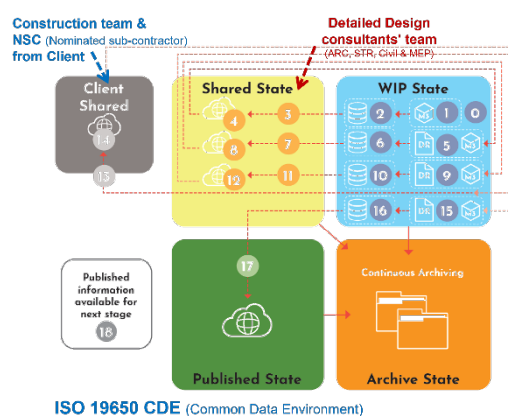


Figure 4. ISO 19650 Common Data Environment workflow (from ISO 19650-3-2020, with annotations by the authors)

Element Importance Order			
Priority	Priority Definition	Selection Groups	
1	Major elements requiring coordination to avoid major issues during construction	Architecture	Vertical / Horizontal Circulation (Staircases, Escalators, Lifts, Shafts, Corridors, Exit/Entrance Gate...)
		Structure	Diaphragm wall, Skeleton Structure, Internal major structure (Columns, Framing Beams, Slabs, Foundation, Pit)
		M&E	Large HVAC duct runs, Major Gravity fed MEP services pipes, Major pressure Pipes > 300 mm Diameter, Major power cable track, Vertical MEP shafts
2	Elements can be moved / adjusted, but will require a certain degree of coordination	Architecture	Doors & Windows, Non-load bearing walls, Major Indicator / Signage, Space layout
		Structure	Internal Structural walls, shear walls, girders, Ramp, Floor level change, Recessed floor
		M&E	Gravity & non-gravity fed pipes >100mm ; <300mm diameter, Equipment room layout
3	Elements can be moved / adjusted, with no difficulty if found clashing (not necessary in the clash list)	M&E	Cables & Pipes less than 100mm diameter

Figure 5. MRT project coordination priority (from the authors)

At each stage, VDR (Virtual Design Review) is used for integration, and then CAD drawings are sent out from the integrated model to complete the published process. Refer to the BIM workflow in Figure 6.

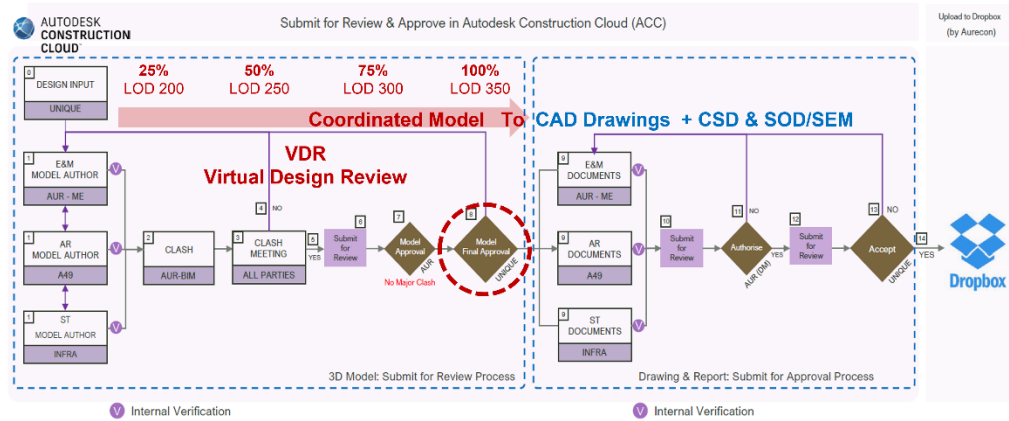


Figure 6. The MRT project BIM execution plan (with annotations by the authors)

3. AN INTEGRATED WORKFLOW OF BUILDING INFORMATION MANAGEMENT

Case 2: Western Digital high-tech plant project

The second case study involves integrating BIM into the traditional Request for Information (RFI) workflow during the construction phase of the Western Digital high-tech plant project. In the traditional RFI process (represented by the yellow route in the figure below), the main contractor sends an RFI to the owner's project management team, which is then reviewed by the design team. The design team must then review and respond, discuss with the owner's group, seek solutions to the problem, and then reply to the main contractor to close the RFI process. During the construction phase, RFIs typically relate to interface problems or incomplete design information and may involve the owner's Nominated Sub-Contractor (NSC) or inconsistencies between different design contracts. With BIM integration (represented by the blue route in the figure below), the model connects different stakeholders' teams for integration on RFI issues, seeking solutions, and responding to the design team for design revisions. This enhances collaboration and efficiency and helps to resolve issues more quickly. Refer to Figure 7 for a visual representation of the process.

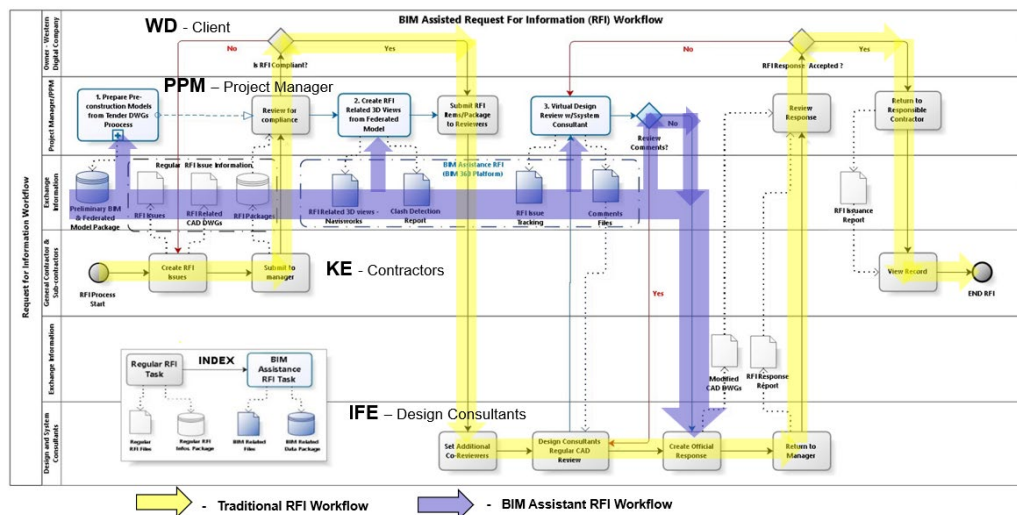


Figure 7. The BIM-augmented RFI process of the Western Digital expansion project (from the authors)

To ensure adherence to ISO 19650 CDE guidelines, BIM integration follows a structured approach. First, a preliminary model is developed from tender drawings to establish a baseline. During the Work in Progress (WIP) stage, the main contractor submits an RFI application form with supporting drawings and material clarification needs. The project management team reviews the RFI and uses the preliminary model to integrate the relevant regional model. This integration stage is referred to as shared coordination, and all project stakeholders are invited to participate. After thorough discussions, negotiations, and integrations, a proposed solution is submitted to the Owner for approval and publishing. The Owner then instructs the construction team to execute the decision and

complete the Archive stage. Refer to Figure 8 for a visual representation of this process. The subsequent cases (3 and 4) highlight the positive impact of BIM integration in this RFI process.

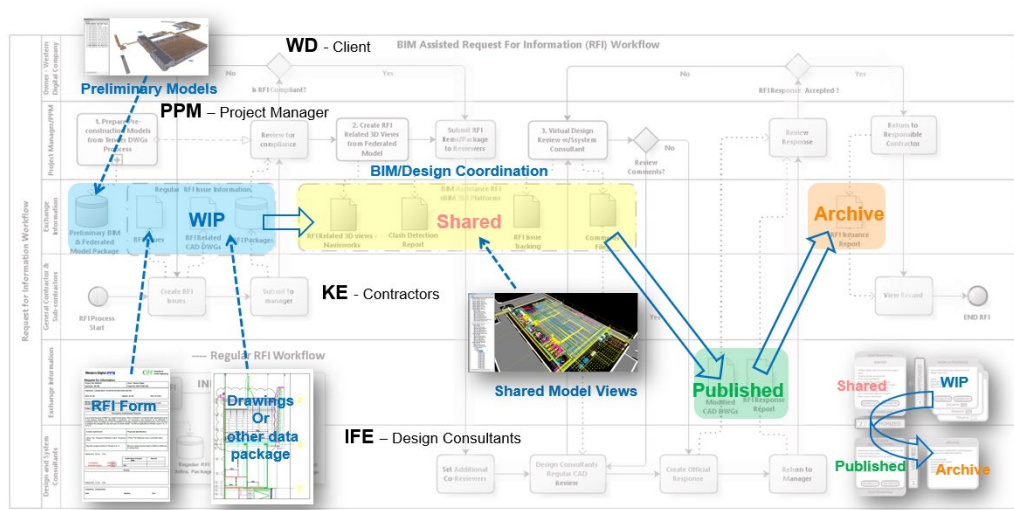


Figure 8. The ISO-19650 process of the Western Digital expansion project (from the authors)

Case 3: Western Digital high-tech factory

The Western Digital high-tech factory expansion project had a construction cost of approximately 1.1 billion US dollars. During the pre-construction phase, the initial design model was created. However, as the production equipment data and factory engineering data were provided by different stakeholders' teams, inconsistencies arose due to asynchronous information. To address this issue, BIM was implemented into the project during the initial construction period, resulting in better integration. During the initial design model stage, the pipeline data provided by production equipment manufacturers (NSC - Nominated Subcontractor) was vague, particularly in the series connection of equipment and machine pipelines, which are known as the Single Line System. As shown in Figure 9, the left side represents the Integrated BIM 3D Coordination Model, while the right side shows the Single Line System.

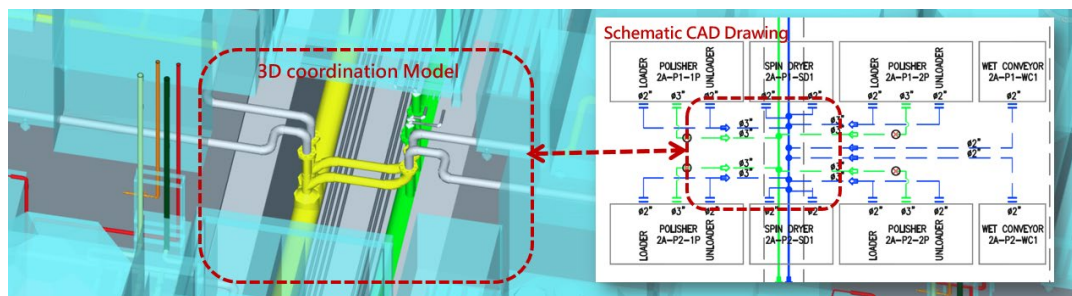


Figure 9. The 3D BIM coordination model and Schematic CAD drawing (from the authors)

The equipment plan in the design phase only provided preliminary information on the location, quantity, and interface of the pipeline, without details on the pipeline itself as shown on the right side of Figure 10. The lack of detailed information on the equipment resulted in the imprecise location of the interface, and only a rough arrangement of the interface was possible. BIM integration allowed for a more detailed diagram of the equipment machine, as shown on the left side of the figure.

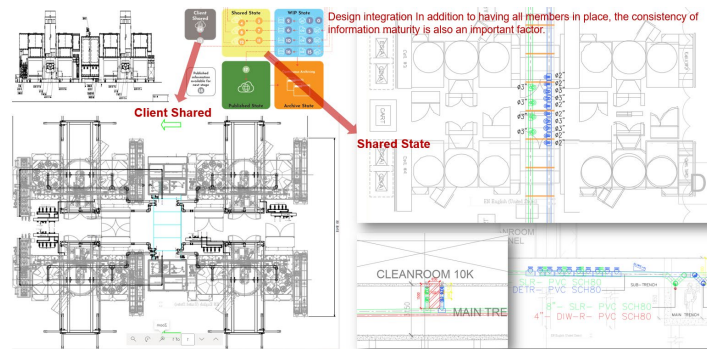


Figure 10. The Detailed Drawing after Integration of BIM (Left, from the authors), and the pipeline drawing in the Design stage (Right, from the authors)

During the construction phase, it was assumed that all the production equipment planning was completed. However, significant discrepancies were revealed in the federated model, which highlighted an obvious gap in the equipment space and a lack of serial connection design and definition of construction responsibility in the interface. This is depicted in Figure 11, where the left-hand side shows displacements found when the detail drawings were laid on top of the system drawing. On the other hand, after BIM integration, the right-hand side shows that the conflicting arrangement of the pipes was corrected by BIM.

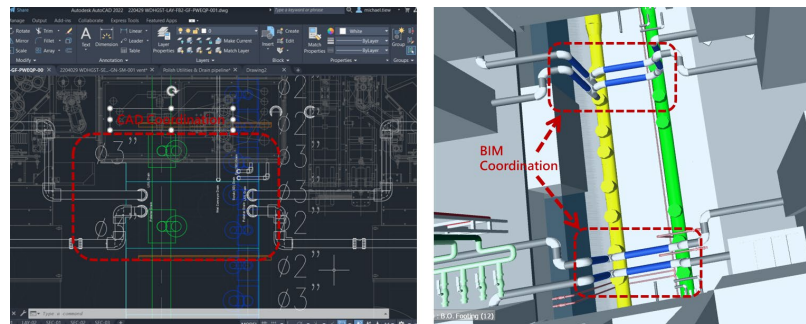


Figure 11. Detail pipeline drawings are overlaid on the system diagram (left, from the authors). BIM showed the conflict situation of pipelines (right, from the authors).

The final solution to the discrepancies and problems encountered in the construction stage was to revise the contract and add an additional 'Hook up' subcontractor, as well as provide detailed information about the production equipment. BIM integration played a crucial role in resolving these issues, as shown in Figure 12.

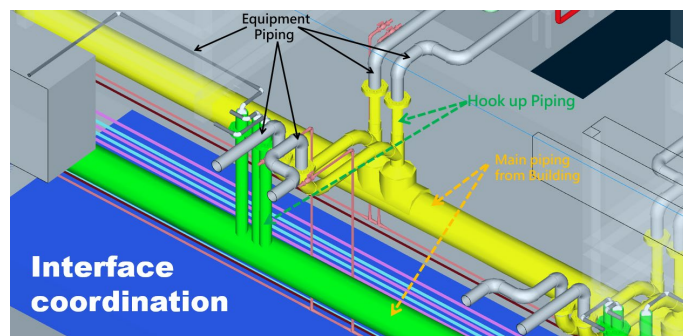


Figure 12. Resolving the piping conflict (from the authors).

Interface issues can often be overlooked during the bidding process due to the lack of vertical height information in 2D CAD drawings. This issue is unavoidable when the contract maker relies solely on CAD drawings as the “Policy”. To address this issue, a comparison should be made between the 2D CAD drawings and 3D models based on BIM “Technology”, and “People” involved in the integration process should adopt a new mindset. This can be achieved by changing their perspective toward the integration “Process”.

Case 4: Western Digital high-tech factory

BIM integration promotes information transparency and can facilitate collaboration among stakeholders, transforming their previously independent attitudes into active problem-solving. In the Western Digital high-tech factory project, the bundle pipeline (red pipeline) belonged to the owner's subcontractor, while the platform water tanks and discharge pipeline belonged to the contract of the plant engineering contractor. In the original design, the bundle pipeline passed through the lower platform of the water tank and extended to the upper platform to connect to the production equipment series. However, BIM integration revealed a conflict between the two systems in the area marked with a blue circle in Figure 13. This conflict had to be resolved through collaboration and coordination among the stakeholders.

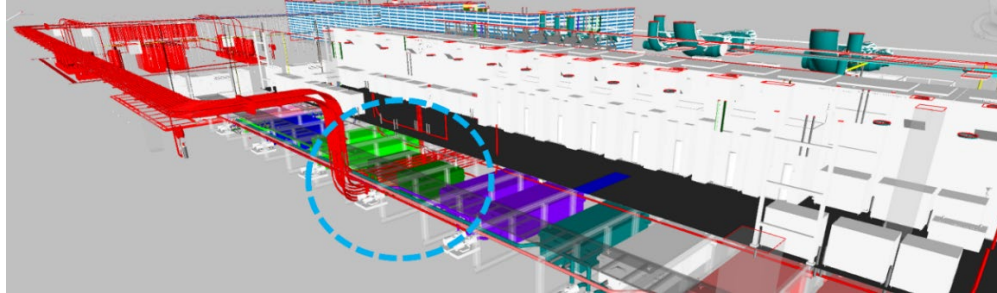


Figure 13. The pipeline conflict in case 4 (from the authors).

In this case, BIM was utilized as a transparent platform for integrating information provided by the model to facilitate communication, planning, and resolving discrepancies and missing interfaces in contracts prior to construction. To effectively integrate BIM into design project information management, it should be included at the preliminary construction stage, right from the beginning. 2D CAD drawings often do not provide enough information to determine equipment space, leading to synchronization and simultaneity issues in management information and design models. BIM provides a solution to these issues by improving transparency and enabling active collaboration among stakeholders' teams. Thus, BIM should be considered as a communication tool for resolving issues and improving the overall project outcomes. The project manager, production equipment manager, equipment subcontractor, pipeline subcontractor, plant contractor, water tank subcontractor, design unit, and project management unit held joint negotiations to resolve the issue with the help of BIM integration. The stakeholders worked together to find a solution and decided to change the pipeline route, connecting it from the left equipment room to the top of the platform, as illustrated in Figure 14. This decision was reached through collaborative discussions and effective use of BIM, which allowed all parties to visualize the problem and agree on a viable solution.

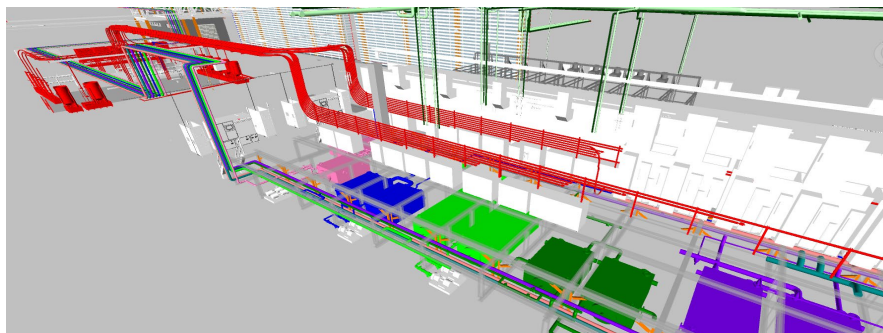


Figure 14. The resolution of pipeline conflict in the case 4 (from the authors).

BIM integration in this case provided visibility into design deficiencies and conflicts, allowing decision-makers at the owner's level to make informed decisions. To establish a successful BIM integration process, it is crucial to involve all project stakeholders and change the mindset of executive and management personnel. This can be achieved by timely addressing major design deficiencies prior to construction. BIM models provide detailed and transparent information, enabling better cooperation and coordination among stakeholders and achieving better design outcomes. Moreover, the BIM model allows for easier comprehension of construction difficulties and future maintenance needs, emphasizing the importance of collaboration among all stakeholders.

5. CONCLUSION

BIM highlights the importance of exchanging information and making project information visible to all stakeholders involved in the project. This approach brings several benefits, such as improved design quality, increased collaboration, reduced errors and duplication of work, and significant risk reduction. By promoting information transparency, BIM facilitates effective information management, thereby enhancing project coordination and management. The adoption of BIM enables project teams to shift from traditional contracts with passive cooperation to more proactive integrated work, leading to better project outcomes.

The combination of 3P plus and 1T is a crucial aspect that helps overcome the limitations of traditional contracts. By utilizing a transparent platform, it promotes cooperation among all stakeholders' teams, allowing them to make decisions through discussions and integrate them into the model process, which ultimately fosters the integration of BIM. Breaking down the barriers between contracts, this approach encourages collaboration and helps to achieve better outcomes in terms of design, construction, and risk management.

The promotion of BIM currently faces a limitation in the industry due to the lack of implementation of 3P and 1T cooperation. It is important to emphasize the participation of owners and the transparent application of BIM to improve collaboration among teams and effectively utilize its functions. Practical BIM management experience cases are used to demonstrate workflow, model integration, and decision-making results to uncover the key to BIM's success.

REFERENCES

- Brady, D.A., Tzortzopoulos, P., Rooke, J., Formoso, C.T., and Tezel, A. (2017) Improving transparency in construction management: a visual planning and control model, *Engineering, Construction and Architectural Management*, 25 (10), 1277-1297.
- Guo, H., Yu, R., and Fang, Y. (2019), Analysis of negative impacts of BIM-enabled information transparency on contractors' interests, *Automation in Construction*, 103, 67-79
- Hamed, W. (2011), BIM Transformation, Retrieved from BIMCITY website:
<https://bimcity.wordpress.com/2011/10/04/bim-transformation/>
- ISO 19650-3-2020: Organization and digitization of information about buildings and civil engineering works, including building information modelling (BIM) - Information management using building information.
- KUTS, (2011), Sarawak Metro Kuching Urban Transportation System (KUTS) project BIM Standards.
- Lee, G., & Borrmann, A., (2020) BIM policy and management, *Construction Management and Economics*, 38:5, 413-419, DOI: 10.1080/01446193.2020.1726979
- McArthur, J. J. (2015). A building information management (BIM) framework and supporting case study for existing building operations, maintenance and sustainability, *Proceeding of International Conference on Sustainable Design, Engineering, and Construction*, Procedia Engineering 118 (2015) 1104-1111
- PAS 1192-2:2013 Incorporating Corrigendum No. 1 Specification for information management for the capital/delivery phase of construction projects using building information modelling.

DESIGN AND IMPLEMENTATION OF BIM-BASED ROADWAY DRAINAGE MODEL

Jing-Ying Huang ¹, Chi-Hsuan Lin ², Jian-Bang Yang ³, Yi-Chiang Tsao ⁴, and Shih-Yao Lan ⁵

1) Engineer, Department of Land Development, Highway & Aviation Engineering, Sinotech Engineering Consultants, Ltd., Taipei, Taiwan. Email: jingying@mail.sinotech.com.tw

2) Planner, Department of Land Development, Highway & Aviation Engineering, Sinotech Engineering Consultants, Ltd., Taipei, Taiwan. Email: chihhsuanlin@mail.sinotech.com.tw

3) Project Manager, Department of Land Development, Highway & Aviation Engineering, Sinotech Engineering Consultants, Ltd., Taipei, Taiwan. Email: bon@mail.sinotech.com.tw

4) Associate Vice President, Department of Land Development, Highway & Aviation Engineering, Sinotech Engineering Consultants, Ltd., Taipei, Taiwan. Email: tyc@sinotech.com.tw

5) Chief Engineer, Office of Aerotropolis Public Construction, Taoyuan City Government, Taoyuan, Taiwan. Email: 10017459@mail.tycg.gov.tw

Abstract: Despite the vigorous development of Building Information Modeling (BIM), research on the application of BIM for drainage systems mainly focuses on building drainage systems, while BIM applications for roadway drainage systems are less discussed. The most significant difference between the two systems is that roadway drainage systems are designed based on the geographic environment and hydraulic analysis, resulting in different object types, object usage, and object properties. For example, the design of a roadside ditch must conform to roadway alignment, and the upstream/downstream connection between roadway drainage objects may be one-to-many instead of one-to-one. Therefore, the existing frameworks for building drainage systems are not applicable to roadway drainage systems.

Drawing upon experience in major civil engineering projects in Taiwan dating back to 1994, Sinotech Engineering Consultants, Ltd. proposes a BIM-based roadway drainage model. Based on the framework of the model, a computer-aided design system for roadway drainage, SinoDrain, is developed to refine the design process. The model and SinoDrain provide a data structure to store massive data about the roadway drainage system, simplifying the design process and significantly reducing the likelihood of human error. Furthermore, SinoDrain has been verified in multiple projects, enhancing accuracy, and realizing significant cost and time savings, and bringing theoretical and practical benefits to the field of roadway drainage design. This research cites the Taoyuan Aerotropolis - Zone B2 project as an example. Sinotech Engineering Consultants, Ltd. first performed the detailed design of the roadway drainage system using traditional design methods, and then re-performed the detailed design using the proposed model and SinoDrain to establish the BIM model.

Keywords: BIM, Computer-Aided Design System, Roadway Drainage Model, Taoyuan Aerotropolis

1. INTRODUCTION

Extreme weather events are occurring with increasing frequency, and impermeable surfaces are increasingly used in urban areas. The roadway drainage system, therefore, plays a crucial role in rainwater drainage, which relates to traffic safety, road maintenance, soil and water conservation, and disaster prevention. Without proper roadway drainage system design, runoff can cause traffic accidents, road damage, or environmental disasters such as flooding, landslides, and water pollution (Aranda et al., 2021). Owing to its strong relationship with rainwater and the roadway, the design of a roadway drainage system is subject to terrain, hydraulic characteristics, and roadway alignment (Mukherjee, 2014), setting it apart from other drainage systems. Even though BIM-based design tools for building drainage systems are numerous, and can provide engineers with an efficient way to build an integrated 3D model (Rabia & Kumar, 2022; Wei et al., 2017), these existing tools are not applicable to roadway drainage systems because of the differences between the two systems.

With the vigorous development of BIM, several open standards for data exchange have been defined, such as LandXML, InfraGML, and IFC4 Add 2 (buildingSMART, 2023; LandXML.org, 2023; OGS, 2023). Many extended models for use in roadway infrastructure design have also sprung up; nevertheless, the roadway drainage system is simply defined within those models, and these open standards and open models cannot clearly express the object types, properties, and relationships for the roadway drainage system (Amann et al., 2013; Amann et al., 2014; Amann et al., 2015; Gao et al., 2016; Kim et al., 2016). Moreover, commonly used BIM software for civil engineering in Taiwan, e.g., Civil 3D and OpenRoads, also lack such data structures. For example, a roadside ditch is classified as a roadway object in Civil 3D, whereas its drainage functionality is ignored, meaning engineers cannot use Civil 3D for drainage design. Furthermore, research on the application of models for roadway drainage systems is severely lacking, with only a few cases in which researchers developed automation systems (Atencio et al., 2022) or achieved early-stage drainage system planning with existing software (Kuok et al., 2022). Hence, many processes, such as modeling and tabulation, are still being conducted manually in conventional drainage design, leading to insufficient documentation, visualization, and coordination, and resulting in duplication of

efforts, time consumption for iterative revisions, and human error. In addition, the Construction and Planning Agency, Ministry of the Interior, R.O.C., began promoting the adoption of BIM in civil engineering projects in 2014, and began mandating the use of BIM in some public civil engineering projects (Yang, 2017). As of May 2023, however, the Construction and Planning Agency has not yet announced specific criteria for when BIM must be used in a project.

In order to address these deficiencies of BIM, namely how engineers lack adequate data structures and tools for use in roadway drainage system design, and so that engineering firms in Taiwan can comply with any requirements to use BIM, this research (1) proposes a BIM-based roadway drainage model, which encompasses comprehensive and interdisciplinary data structure, and (2) develops a computer-aided design system, SinoDrain, for roadway drainage to verify the model's validity and practicality. The workflow is as follows: (1) define object types, properties, and relationships for the roadway drainage model by interviewing engineers, (2) using the model, develop SinoDrain on Civil 3D, (3) validate SinoDrain using several real-world projects, (4) modify the model according to the validation results from step (3), and (5) repeat steps (3) and (4) until the roadway drainage model and SinoDrain can meet the design requirements for the Taoyuan Aerotropolis - Zone B2 project.

2. ROADWAY DRAINAGE MODEL

Roadway drainage system design usually takes place after large-scale land development. In addition to the terrain, hydraulic characteristics, and roadway alignment, underground pipelines also need to be considered as pipeline conflicts tend to occur when designing the roadway drainage system. Due to the interdisciplinarity of roadway drainage system design, iterative revision is inevitable during the design process. Also, the upstream/downstream connection between objects in a BIM model may be one-to-many instead of one-to-one. Roadway drainage objects are unique in their types, usage, and properties, and simply dividing them into pipe and structure (i.e., Civil 3D) is insufficient for practical use. Given the above-mentioned problems, this research proposes a proper and applicable BIM-based roadway drainage model. As shown in Figure 1, the proposed model clarifies the classification and the relationships of roadway drainage objects by referring to the concept of object-oriented programming. In the model, each object type has a specific property set that can store geometric and non-geometric properties of the roadway drainage object, while the relationships specify a given object's upstream object(s), downstream object, and its association with roadway alignment and terrain, thereby establishing a comprehensive roadway drainage system data structure.

The scope of the proposed model is limited to roadway drainage objects in the Taiwan context, but for closely related roadway objects, i.e., alignment and terrain, the model provides a data structure to achieve data exchange for relevant properties, such as surface elevation and alignment station. Additionally, the model is mainly designed for the implementation of land development projects on flat terrain.

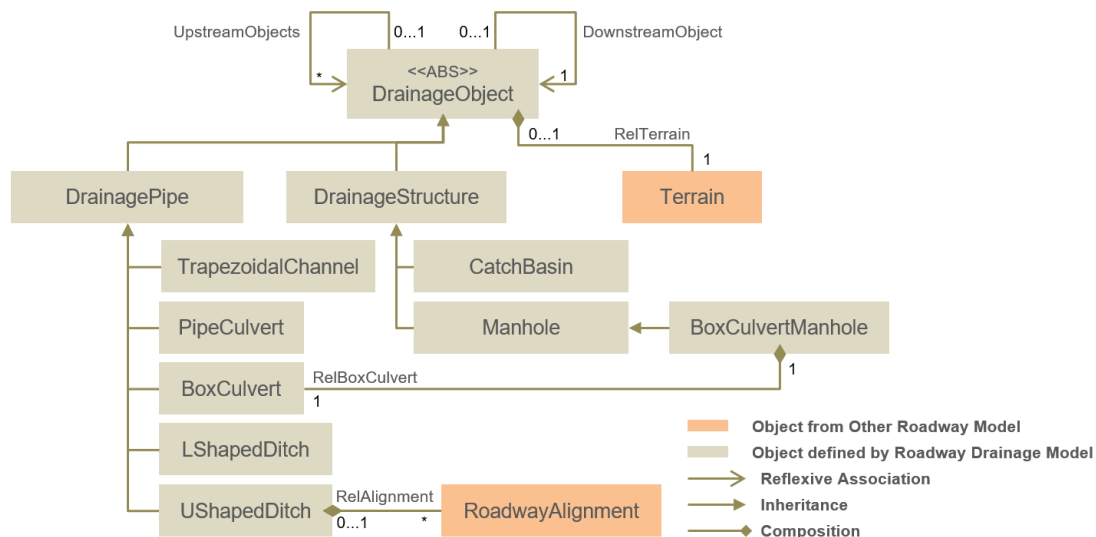
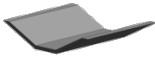

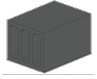






Figure 1. BIM-based roadway drainage model

(1) Object Classification

Firstly, according to their geometric characteristics, roadway drainage objects are divided into 2 types, namely drainage pipe and drainage structure, and are then subdivided according to their usage. In total, 7 object types are defined. With different usages and section shape types, each object type has its specific geometric and non-geometric property set. The definition and diagram of each object type are illustrated in Table 1.

Table 1. Classification of roadway drainage objects

Type	Shape	Definition
- Drainage Pipe		The geometric characteristic of drainage pipe is composed of an alignment and one or many section(s).
- Trapezoidal Channel		Trapezoidal channels collect rainwater or standing water into an existing drainage system.
- Pipe Culvert		A pipe culvert connects a catch basin to a box culvert.
- Box Culvert		Box culverts act as arteries for roadway drainage; for example, they have sufficient space for large flows and electrical conduits.
- L-shaped Ditch		L-shaped ditches are designed for interception, and are usually larger than U-shaped ditches.
- U-shaped Ditch		U-shaped ditches are usually located at the edge of roadways or sidewalks to collect rainwater, standing water, and surface runoff.
- Drainage Structure		The geometric characteristic of drainage structure is a single component.
- Catch Basin		Catch basins are designed to collect and store rainwater or surface runoff.
- Manhole		Manholes are vertical tunnels that provide personnel access to sewers for inspection and maintenance.
- Box Culvert Manhole		Box culvert manholes are located on box culverts.

(2) Object Relationships

As shown in Table 2, a roadway drainage object generally has one/many upstream object(s), a downstream object, and associated terrain. However, trapezoidal channel, L-shaped ditch, and box culvert manhole do not have the relationships defined in the scope of the model. This is because trapezoidal channel and L-shaped ditch are usually the starting point where there is no object upstream, and downstream there is usually an external drainage system; and because a box culvert manhole is not a water channel. The remaining object types have certain upstream/downstream connections depending on their usage. Taking box culvert as an example, its upstream object(s) can be another box culvert and/or one/many pipe culvert(s), while its downstream object can only be another box culvert (it may also be a detention basin or an external drainage system, both of which are not in the scope of the model). On the other hand, U-shaped ditch has one/many associated roadway alignment(s), and the U-shaped ditch follows roadway alignment(s). Moreover, box culvert manhole has an associated box culvert on which the box culvert manhole is located. In summary, the relationships defined in the model conform to the design principle of the roadway drainage system and the engineers' design logic.

Table 2. Roadway drainage object relationships

Type	Upstream Object(s)	Downstream Object	Terrain	Roadway Alignment	Box Culvert
Trapezoidal Channel	-	-	V	-	-
Pipe Culvert	Catch Basin	Box Culvert	V	-	-
Box Culvert	Box Culvert, Pipe Culvert	Box Culvert	V	-	-
L-shaped Ditch	-	-	V	-	-
U-shaped Ditch	Catch Basin, U-shaped Ditch	Catch Basin, U-shaped Ditch	V	V	-
Box Culvert Manhole	-	-	V	-	V
Catch Basin	Pipe Culvert, U-shaped Ditch	Pipe Culvert, U-shaped Ditch	V	-	-

* V: The referred object relationship exists.

3. SYSTEM DEMONSTRATION

Based on the model, a computer-aided design system for roadway drainage, SinoDrain, is developed. SinoDrain is a Civil 3D application programming interface (API). As shown in Figure 2, the whole design process consists of three major steps, using Civil 3D for design and Revit for BIM model management and visualization. First, engineers utilize the object design and management tools provided in the aided design module to conduct roadway drainage system design. Second, based on the design results, the engineers use the data exchange module to create two tables, namely an object properties table and an object geometric data table. Last, the engineers use the data exchange module developed in Revit to automatically remodel the roadway drainage system as a BIM model with the two tables and family components, which are built based on the object types and properties defined in the roadway drainage model. The object properties table can be used for drawing and modeling, and it provides sufficient data for conducting hydraulic analysis in EPA SWMM or similar software. Moreover, the hydraulic analysis results can be entered into SinoDrain to automatically adjust the design. Figure 3 shows a roadway drainage object properties table format that is commonly used in Taiwan.

To verify the model and the system's validity and practicality, SinoDrain was used to perform detailed design work for the roadway drainage system in Taoyuan Aerotropolis - Zone B2. The detailed design work had originally been performed using traditional design methods, and was then re-performed using the proposed model and SinoDrain to establish the BIM model. Taoyuan Aerotropolis is a land development project that aims to accelerate industrial and economic prosperity around Taoyuan International Airport. Zone B2 is located in the southwest of Taoyuan Aerotropolis, with an area of 184.85 hectares that is mainly planned for residential development.

With the implementation of SinoDrain, the roadway drainage system of zone B2, which comprises 630 drainage pipes and 326 drainage structures, is successfully built. This successful implementation demonstrates that the standardized and parameterized objects, which are developed based on the roadway drainage model, can store the properties, and it demonstrates that the BIM model can be built effectively and efficiently. In addition, the model structure is capable of managing interdisciplinary data while coordinating with other fields, significantly reducing time consumption for iterative revision and human error. The detailed design results of the roadway drainage system for Taoyuan Aerotropolis - Zone B2 are displayed in Figure 2.

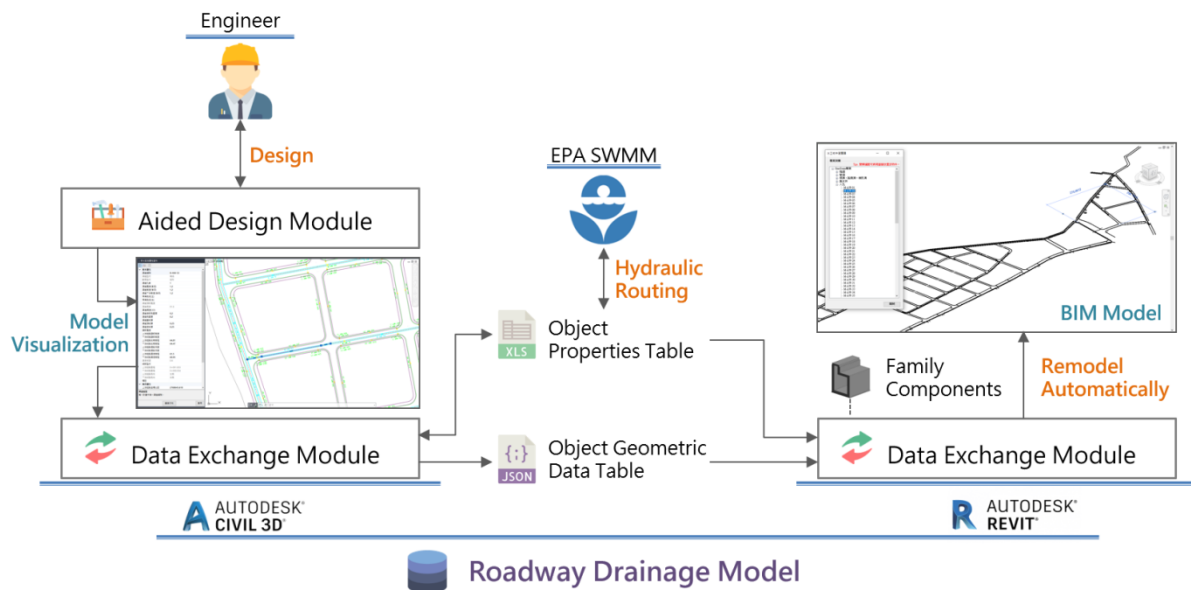


Figure 2. SinoDrain workflow

TAOYUAN AEROTROPOLIS - ZONE B2 (DRAINAGE PIPE)												
No	Type	Section Shape	Number of Cell(s)	Width(Diameter)	Upstream Height(Diameter)	Downstream Height(Diameter)	Length	Upstream Surface Elevation	Downstream Surface Elevation	Roadway Alignment	Upstream Alignment Station	Downstream Alignment Station
3	B-AW-01	Box Culvert	Rectangle	1	4.5	3	54.5	57.46	0	6-90-15M-2	0+306.379	0+296.769
4	B-AW-02	Box Culvert	Rectangle	1	4.5	3	94.39	57.8	57.46	6-90-15M-2	0+400.754	0+306.379
5	B-AW-03	Box Culvert	Rectangle	1	4.5	3	128.57	58.43	57.8	6-90-15M-2	0+529.305	0+400.754
6	B-AW-04-1	Box Culvert	Rectangle	1	4.5	2.5	22.65	58.67	58.43	6-90-15M-2	0+551.951	0+529.305
7	B-AW-04-2	Box Culvert	Rectangle	1	4.5	2.5	159.69	59.6	58.68	6-90-15M-3,6-90-15M-2	0+005.864	0+552.955
8	B-AW-05-1	Box Culvert	Rectangle	1	4	2	57.8	59.78	59.6	6-90-15M-3	0+063.660	0+005.864
9	B-AW-05-2	Box Culvert	Rectangle	1	4	2	44.64	59.83	59.78	6-90-15M-3	0+110.382	0+065.660
10	B-AW-06	Box Culvert	Rectangle	1	4	2	89.22	60.73	59.83	6-90-15M-3	0+200.237	0+110.382
11	B-AW-07-1	Box Culvert	Rectangle	1	4	2	65.09	60.79	60.73	6-90-15M-3	0+265.330	0+200.237
12	B-AW-07-2	Box Culvert	Rectangle	1	4	2	121.43	60.83	60.79	6-90-15M-3	0+387.762	0+266.330
13	B-AW-08	Box Culvert	Rectangle	1	4	2	125.1	61.23	60.83	6-90-15M-3	0+512.866	0+387.762
14	B-AW-09	Box Culvert	Rectangle	1	3	2	122.74	61.58	61.23	6-5-15M-1,6-90-15M-3	0+041.122	0+512.866
15	B-AW-10	Box Culvert	Rectangle	1	3	2	93.76	62.12	61.58	6-90-15M-3,6-5-15M-1	0+729.156	0+041.122
16	B-AW-11-1	Box Culvert	Rectangle	1	3	2	44.78	62.54	62.12	6-90-15M-3	0+773.938	0+729.156
17	B-AW-11-2	Box Culvert	Rectangle	1	3	2	51.19	62.66	62.54	8-26-10M,6-90-15M-3	0+003.821	0+774.938
18	B-AW-12	Box Culvert	Rectangle	1	3	2	64.32	62.98	62.66	6-90-15M-3,8-26-10M	0+889.982	0+003.821
19	B-AW-13	Box Culvert	Rectangle	1	2.5	2	71.74	63.67	62.98	8-9-10M,6-90-15M-3	0+221.564	0+889.982
20	B-AW-14-1	Box Culvert	Rectangle	1	2.5	2	42.82	64.07	63.67	6-90-15M-3,8-9-10M	1+004.289	0+221.564
21	B-AW-14-2	Box Culvert	Rectangle	1	2.5	2	40.52	64.47	64.08	6-90-15M-3	1+046.312	1+005.789
22	B-AW-15-1	Box Culvert	Rectangle	1	2.5	2	39.71	64.92	64.47	6-90-15M-3	1+086.023	1+046.312
23	B-AW-15-2	Box Culvert	Rectangle	1	2.5	2	43.64	65.47	64.94	6-90-15M-3	1+131.160	1+087.523
24	B-AW-16-1	Box Culvert	Rectangle	1	2	2	40.74	65.97	65.47	6-90-15M-3	1+171.999	1+131.160
25	B-AW-16-2	Box Culvert	Rectangle	1	2	2	41.52	66.51	65.99	6-90-15M-3	1+215.071	1+173.499
26	B-AW-17-1	Box Culvert	Rectangle	1	2	2	28.67	66.85	66.51	6-90-15M-3	1+243.724	1+215.071
27	B-AW-17-2	Box Culvert	Rectangle	1	2	2	50.03	67.4	66.87	6-90-15M-3	1+295.113	1+245.224
28	B-AW-18-1	Box Culvert	Rectangle	1	2	2	33.74	67.54	67.4	6-90-15M-3	1+325.711	1+295.113
29	B-AW-18-2	Box Culvert	Rectangle	1	2	2	55.53	67.74	67.54	6-90-15M-3	1+385.243	1+325.711
30	B-AW-19	Box Culvert	Rectangle	1	1.2	1.2	129.7	59.63	57.55	8-6-10M,6-90-15M-2	0+137.829	0+306.379
31	B-AW-20	Box Culvert	Rectangle	1	1.2	1.2	106.61	59.63	59.63	8-6-10M	0+244.443	0+137.829
32	B-AW-21	Box Culvert	Rectangle	1	1.2	1.2	198.87	59.78	59.63	8-6-10M	0+443.317	0+244.443

Figure 3. Object properties table

Thanks to the proposed model and SinoDrain, overall working time in the detailed design was reduced by 33% compared to traditional design methods, with significant reductions in time spent on system design (46%), drawings and modeling (71%), and tabulation (83%), thereby boosting efficiency and saving labor costs. Moreover, SinoDrain and the roadway drainage model are proven to fulfill the practical requirements of roadway drainage system design.

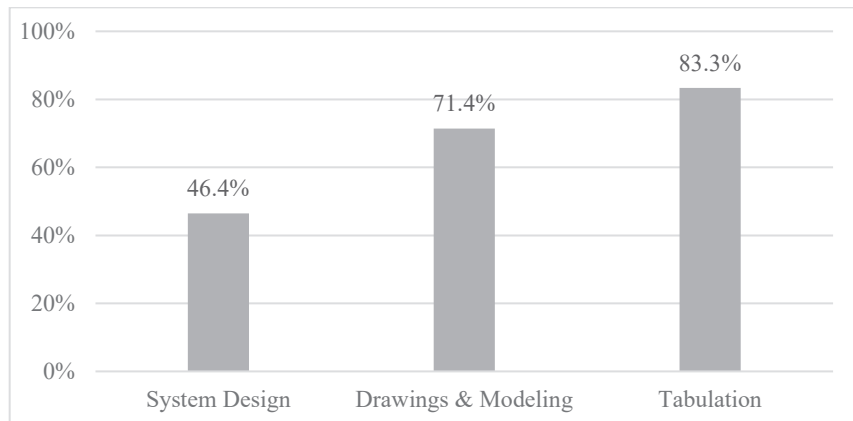


Figure 4. Time savings

4. CONCLUSIONS

This research proposes a BIM-based roadway drainage model which clarifies the types, properties, and relationships of the roadway drainage model, and further develops a computer-aided design system, SinoDrain, which is an API of Autodesk BIM software Civil 3D. The model provides a data structure for roadway drainage objects, and SinoDrain assists engineers throughout the whole design process. In conclusion, the implementation of SinoDrain in the Taoyuan Aerotropolis - Zone B2 project verifies SinoDrain's applicability and the model's validity. Furthermore, by simplifying the process and reducing manual operation, the proposed model and SinoDrain effectively improve design accuracy and efficiency. These research results can be used to promote the development of BIM in the field of roadway drainage system design, and further boost the quality of public civil engineering projects in Taiwan.

Three suggestions are given for future studies. First, aside from the roadway drainage objects included in this research, more roadway drainage objects can be added to meet the various requirements of different projects. Second, as elevation design is an important issue in roadway drainage design, a function that generates vertical profiles can be developed to enhance design efficiency. Third, further integration of the proposed model with other BIM-based models, in particular roadway models or software, can be studied in order to improve data exchange across platforms.

REFERENCES

- Amann, J., Borrmann, A., Hegemann, F., Jubierre, J., Flurl, M., Koch, C., & König, M. (2013). A Refined Product Model for Shield Tunnels based on a Generalized Approach for Alignment Representation. *Paper presented at the 1st International Conference on Civil and Building Engineering Informatics (ICCBEI)*, Tokyo, Japan.
- Amann, J., Flurl, M., Jubierre, J. R., & Borrmann, A. (2014). An alignment meta-model for the comparison of alignment product models. *Proceedings of the 10th European Conference on Product and Process Modelling in the Building Industry (ECPM)*, Vienna, Austria, 351.
- Amann, J., Singer, D., & Borrmann, A. (2015). Extension of the upcoming IFC Alignment standard with cross sections for road design. *Paper presented at the 2nd International Conference on Civil and Building Engineering Informatics*, Tokyo, Japan.
- Aranda, J. A., Beneyto, C., Sánchez-Juny, M., & Bladé, E. (2021). Efficient Design of Road Drainage Systems. *Water*, 13(12), 1661.
- Atencio, E., Araya, P., Oyarce, F., Herrera, R. F., Muñoz-La Rivera, F., & Lozano-Galant, F. (2022). Towards the Integration and Automation of the Design Process for Domestic Drinking-Water and Sewerage Systems with BIM. *Applied Sciences*, 12(18), 9063.
- Bradley, A., Li, H., Lark, R., & Dunn, S. (2016). BIM for infrastructure: An overall review and constructor perspective. *Automation in Construction*, 71, 139-152.
- buildingSMART. (2023). *IFC4 Add2*. Retrieved from buildingSMART website: <https://standards.buildingsmart.org/IFC/RELEASE/IFC4/ADD2/HTML/>
- Gao, G., Liu, Y. S., Wu, J. X., Gu, M., Yang, X. K., & Li, H. L. (2016). IFC railway: A semantic and geometric modeling approach for railways based on IFC. *Proceedings of the 16th International Conference on Computing in Civil and Building Engineering*, Osaka, Japan, 6-8.
- Kim, H., Shen, Z., Moon, H., Ju, K., & Choi, W. (2016). Developing a 3D intelligent object model for the application of construction planning/simulation in a highway project. *KSCE Journal of Civil Engineering*, 20(2), 538-548.
- Kuok, K. K., Kingston Tan, K. W., Chiu, P. C., Chin, M. Y., Rahman, M. R., & Bin Bakri, M. K. (2022). Application of Building Information Modelling (BIM) Technology in Drainage System Using Autodesk InfraWorks 360 Software. *Proceedings of the 5th International Conference on Water Resources (ICWR) – Volume 1*, 209-224.
- LandXML.org. (2023). *LandXML 2.0*. Retrieved from LandXML.org website: <http://www.landxml.org/Spec.aspx>
- Mukherjee, D. (2014). Highway surface drainage system & problems of water logging in road section. *The International Journal of Engineering Science*, 3(11), 44-51.
- OGS. (2023). *OGC InfraGML 1.0*. Retrieved from OGS website: <https://www.ogc.org/standard/infra/gml/>
- Rabia, M. P. R., & Kumar, D. S. (2022). Applications of Building Information Modelling for Water Infrastructure Development. In R. Jha, V. P. Singh, V. Singh, L. B. Roy, & R. Thendiyath (Eds.), *Hydrological Modeling: Hydraulics, Water Resources and Coastal Engineering* (pp. 221-230): Springer Cham.
- Rebolj, D., Tibaut, A., Čuš-Babič, N., Magdič, A., & Podbreznik, P. (2008). Development and application of a road product model. *Automation in Construction*, 17(6), 719-728.
- Saad, A., Ajayi, S. O., & Alaka, H. A. (2022). Trends in BIM-based plugins development for construction activities: a systematic review. *International Journal of Construction Management*, 1-13.
- Wei, T., Chen, G., & Wang, J. (2017). Application of BIM Technology in Building Water Supply and Drainage Design. *IOP Conference Series: Earth and Environmental Science*, 100.
- Yang, J. B. (2017). 機關辦理公共工程導入建築資訊建模 BIM 技術 [BIM Implementation in Public Construction Works]. Taiwan: Public Construction Commission, Executive Yuan, R.O.C.

AUTOMATIC CREATION OF 3D TEXTURED SIMPLIFIED MODEL FOR SUPPORTING PILED PIER MAINTENANCE

Tomohiro Mizoguchi¹, Kenichi Mizuno² and Osamu Taniguchi³

1) Ph.D., Assoc. Prof., Department of Computer Science, College of Engineering, Nihon University, Japan. Email: mizoguchi.tomohiro@nihon-u.ac.jp

2) Penta-Ocean Construction Co., Ltd., Japan. Email: kenichi.mizuno@mail.penta-ocean.co.jp

3) Penta-Ocean Construction Co., Ltd., Japan. Email: osamu.taniguchi@mail.penta-ocean.co.jp

Abstract: For efficient and effective maintenance of aging piled piers, the camera-mounted radio-controlled boat was developed. This enabled the acquisition of 3D dense polygonal model with rich texture of undersurface of superstructure of piled pier by SfM/MVS process to multiple images. In this paper, for the effective use of 3D model in maintenance stage, we propose the method for automatically converting it to a simplified textured model. From a viewpoint of design and functionality of piled pier, multiple beam and pile head are arranged so that they configure orthogonal grid. By utilizing such a domain specific knowledge of piled piers, our method automatically segments a dense polygonal model into major parts, such as slab, beam, and pile head, and converts it to a simplified polygonal model where each constituent region is represented by a planar surface. We also create ortho image of each planar region and reconstruct a 3D simplified textured model. We demonstrate the effectiveness of our proposed method through various experiments.

Keywords: Piled pier maintenance, SfM/MVS, Semantic segmentation, 3D modeling

1. INTRODUCTION

Many port structures in Japan are aging, and the importance of efficient and effective maintenance and renewal has been pointed out. Among them, for inspection of piled pier, the current situation is that professional engineers take a small boat and visually inspect it in a confined environment. However, in addition to the limited number of engineers, the work on the boat is a heavy burden. And there is another problem such as a limited time for inspection considering the tide level. Against this background, a radio-controlled boat equipped with a camera was developed to improve efficiency and manpower-saving (Mizuno, 2018). As a result, it became possible to acquire image data of the undersurface of the pier superstructure without the presence of professional engineers, and inspection based on these images has become established as an effective means.

In the process of diagnosing the degree of deterioration of a pier, it is necessary to evaluate the degree of each member. Therefore, in image-based diagnosis, it is effective to first construct a high-density 3D model with rich textures from the obtained images by structure from motion and multi-view stereo (SfM/MVS). In addition, it is expected to convert point cloud to simplified model by automatically extracting end points and intersection points of each member from the model, performing semantic segmentation to divide the model into each member to be diagnosed, such as floor slabs, beams, and pile heads, and approximating each region with a primitive shape. In addition, it is valid to create an orthoimage for each planar region that constitutes each member, extract deterioration such as cracks and spalling on this orthoimage and manage the results by associating them with the 3D model. This makes it possible not only to diagnose the degree of deterioration for each member, but also to draw the results on a 3D model. In addition, since the built model is lightweight, it is possible to manage the model on the cloud and view it on a PC or mobile terminal via the Internet. In addition, the use of 3D models has the advantage of making it easier to visually understand the positional relationship of deterioration and damage compared to the inspection results summarized in the current 2D developed view, and to share them among related parties.

However, at present, there is no software that can automatically perform processing such as semantic segmentation and 3D simplified model construction on the 3D scanned polygon model of piled pier. Therefore, all these processes must rely on interactive work by the operator, and it takes a huge amount of time to select one by one while visually checking the region boundaries of the high-density model. Therefore, the development of a method to automate this 3D processing is required.

2. RELATED WORKS

In recent years, in addition to the conventional terrestrial laser scanning (TLS), mobile 3D scanning technology has spread rapidly and has become widely used for 3D scanning of civil engineering structures. It is also widely used for scanning by mounting it on a mobile platform such as an Unmanned Aerial Vehicle (UAV) (Mohammadi et al., 2021). Along with this, semantic segmentation which decomposes the measured point cloud into each member and 3D modeling have been actively studied in recent years, especially for road bridges.

For example, in the study (Lu et al., 2019), they deal with a laser scanned point cloud of RC bridge as a target and proposed a method for decomposing it into main members, such as slab, pier, pier cap, girder, by slicing

the point cloud at regular intervals and evaluating local shape characteristics of the partial point cloud obtained. In the study (Yan et al., 2022), 3D scanned point cloud of steel girder bridge by TLS or UAV-based laser scanner is targeted and a method is presented to divide the point cloud into main members such as bridge deck, steel girder, and cross frame based on clustering and segmentation method. In (Truong-Hong and Lindenbergh, 2022), the method targets the measurement point cloud of RC bridge and proposes a method to divide it into main members based on surface clustering. The common idea of these methods is that they all target a specific class of structures, use common design rules and domain-specific knowledge, and propose geometric methods specialized for that class. Since piled pier we deal with in this research has different shape characteristics from these structures, they cannot be used directly, and the development of a method specialized for piled pier is necessary.

On the other hand, in the research (Li et al., 2016), 3D point clouds constructed by SfM/MVS processing from building images taken by UAV are targeted, and 3D models consisting of plane sets are constructed. In this method, the building point cloud is converted into a height image based on the ground for processing. In the height image, the boundary line of the building is extracted using the outline of the roof as a clue, and it is approximated by a set of line segments using Douglas-Peucker method. Finally, 3D model can be constructed by extruding the region bounded by the line segments to the corresponding height. In this method, by introducing 2.5D processing based on height images, 3D models can be constructed stably even from low-quality point clouds. However, the model construction process is performed in pixel units, and the extraction accuracy of the building contour line depends on the pixel size, so the model construction accuracy remains a problem. However, such 2.5D processing should be effective for piled piers with relatively flat structures, thus we use this strategy with special customization.

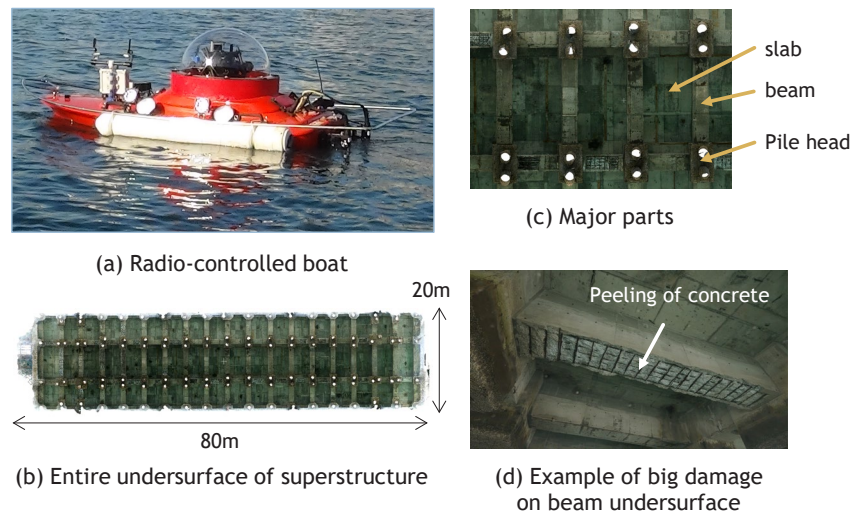


Figure 1. Example of undersurface of superstructure of piled pier

3. AN EXAMPLE OF OUR DATA SET

Here we explain the outline of the 3D measurement of the piled pier treated in this research. The boat shown in Figure 1(a) was used for the measurement. This boat is equipped with a high-resolution camera through a gimbal which is a shaking-suppression device. This gimbal is a three-axis control-type and automatically regulates roll, pitch, and yaw motion. And it suppresses camera shake caused by waves and captures high-quality movie with little blurring. This camera can capture movie of 8.4 million pixels (3,840×2,180). Since the area under the pier is a dark environment where sunlight does not reach, LED lighting is installed to ensure brightness. Figure 1(b) shows an example of a pier. 45 years have passed since its construction, and it is about 80m long and 20m wide. Figure 1(b) shows an example of a 3D model of the undersurface of the superstructure of this pier. To build this model, we made several round trips under the piled pier at a speed of about 0.5m/sec and it took about two hours in total for camera capture. The imaging resolution was set to 1 mm/pixel or less even for slabs far from the boat. A 3D model was constructed by SfM/MVS from about 2,000 images extracted at an every second from the acquired movie. As a field condition for investigation, the boat can enter under the pier if about 0.8m can be secured between the bottom surface of the pier superstructure and the water surface. In the example of Figure 1, it was about 0.8m to 4.0m. For more details, refer to the work of (Mizuno, 2018). Data for other piers used in this study were obtained in the same way.

Here, we analyze the shape characteristics of the piled pier. As shown in Figure 1(c), the underside of the pier superstructure consists mainly of slabs, beams, and pile heads. The following four points can be mentioned as the shape characteristics of the pier.

1. From the viewpoint of their functionality, beams and pile heads have a structure in which they are arranged regularly to form an orthogonal grid.
2. The surface shape of slabs, beams, and pile heads, which are the main members, is composed only of planar surfaces.
3. The structure has a large horizontal spread and a small vertical depth.
4. As shown in Figure 1(d), in the vertically downward region, there are many places where the concrete has largely peeled off, and the unevenness of the surface of the scanned data is large. On the other hand, in the horizontally oriented region, the degree of deterioration is slight, and the surface unevenness is small.

4. RESEARCH PURPOSE AND METHOD OVERVIEW

In this research, we propose a method for constructing a 3D simplified models with textures from the 3D high-density textured polygon model obtained by SfM/MVS which can be effectively used for pier deterioration diagnosis. Utilizing the general knowledge of piled pier design mentioned in chapter 3, we aim to develop a method that reflects the unique shape characteristics of piled pier such as regularity.

The proposed method mainly consists of five steps. First, the barycenter of the polygon corresponding to the sides of beams and pile heads are projected onto the xy plane after aligning the 3D model along the vertical direction (step 1). Next, initial semantic segmentation is performed by RANSAC-based linear fitting on this projection plane, and an initial 3D model is constructed based on member class classification and region height calculation (step 2). After that, a 3D simplified model is constructed by fitting a template to the pile head area (step3). Also, if the structure includes haunch, local 3D models of these haunch is optionally constructed, and the simplified model is updated (step4). Finally, an orthoimage of each planar region in the simplified model is created and output as a textured model (step5).

The features of the proposed method are as follows.

1. **Use of domain-specific knowledge:** By utilizing general design knowledge about piled piers and using information such as the regular arrangement of piled pier specific members, semantic segmentation and 3D simplified model construction can be performed stably.
2. **Robust 3D reconstruction by 2.5D processing:** The 3D model is aligned vertically and converted to a height map representation to introduce 2.5D processing. In the model construction process, we effectively use the triangles in the structure where the surface deterioration is relatively light. As a result, compared to the conventional method of directly processing the 3D scanned polygon model, not only is it less susceptible to degradation, but the model construction process can be made more efficient, and a high-quality simplified model that closely approximates the input polygons can be stably constructed.

5. OUR PROPOSED METHOD

The developed 3D simplified model construction method consists of the following five steps. The input is a high-density 3D polygonal model generated by SfM/MVS. The output is a simplified model with 3D textures consisting of a set of planes that make up each region and an orthoimage for each region. In this method, the RANSAC method (Fischler et al., 1981) is applied in various stages. RANSAC is a probabilistic approach that extracts plausible data from data containing noise, and its effectiveness has been demonstrated in detecting planes and curved surfaces in measured point clouds. Details of each step are described below.

5.1 Alignment (step1)

Three dominant axes in the structure are detected by Gaussian mapping of triangle unit normal vectors and RANSAC method, and coordinate transformation is performed to align the model vertically. First, we map the unit normal vector of each triangle in the model onto the Gaussian sphere. Due to the structural characteristics of the piled pier, the normal vector of the floor slabs and beams, which occupy most of the surface area, points vertically downward. Therefore, these unit normal vectors should be concentrated at one point on the Gaussian sphere, and the point density should be higher than other regions. Therefore, the point where the point density is maximum on this spherical surface is found by the RANSAC-based method, and the model is rotated so that the averaged normal vector coincides with the -z direction and aligned in the vertical direction.

Next, the triangles whose normal vector after rotation points to the horizontal direction are extracted by threshold processing. Here, we calculated the angle between normal vector and the vertical direction at each triangle, and extracted the triangles whose angle is greater than the threshold. The threshold was set to 85.0deg, and good results were obtained for all models. These triangles mainly correspond to the sides of the beam where the degree of deterioration is relatively small. After that, we project the barycenter of the extracted horizontally oriented triangles onto the xy plane. The straight line is found with the largest number of points distributed by

RANSAC on the projection plane, and model is rotated around the z-axis to align so that it coincides with the x-axis. This aligns beams and pile heads with respect to x- and y-axis, making it easier to extract members and perform modeling later. Figure 2 shows the polygon model after alignment.

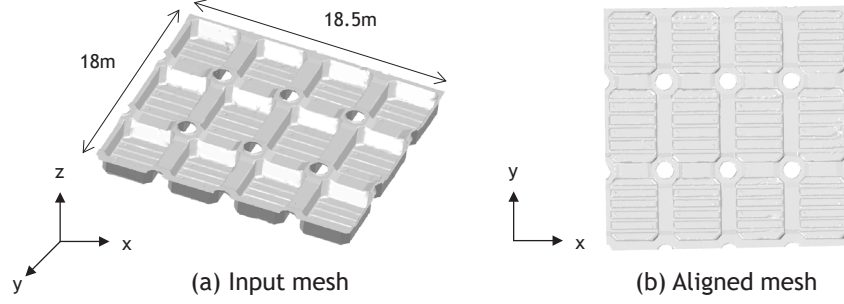


Figure 2. Model alignment

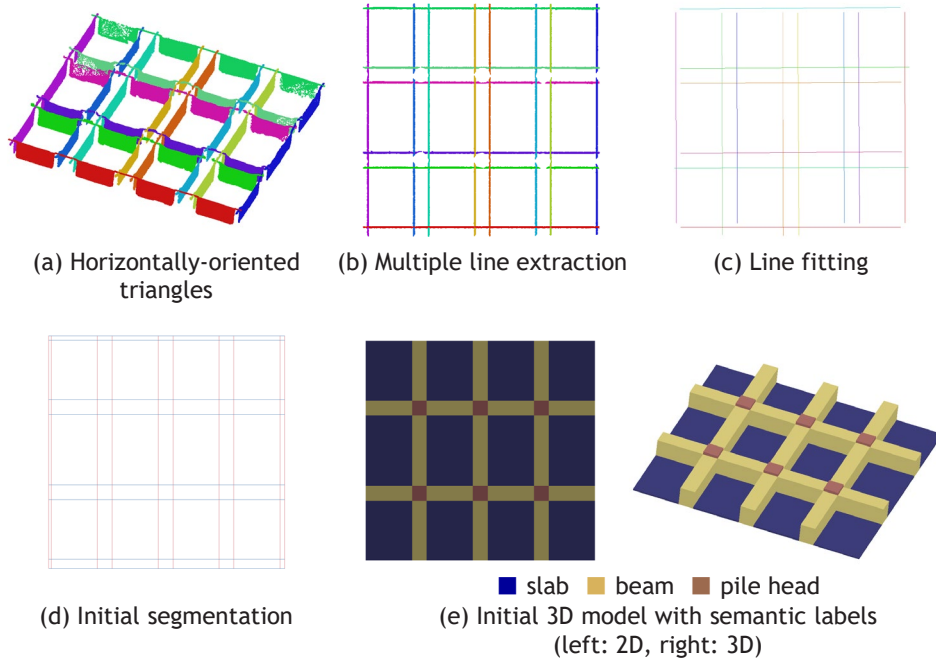


Figure 3. Initial semantic segmentation and 3D modeling

5.2 Initial Semantic Segmentation (step 2)

Next, the horizontally oriented point cloud projected onto the xy plane are effectively used in the same way as in the previous step to perform initial segmentation as shown in Figure 3(a). Since beams are generally arranged in two orthogonal directions, the barycenter of the horizontally oriented triangular are distributed on straight lines parallel to the x and y directions on the projection plane. Therefore, we exhaustively extract multiple barycenter by RANSAC-based line fitting and fit a least-squares line to each as shown in Figure 3 (b) and (c). Let $\{l_i^x\}$, $\{l_j^y\}$ be the sets of straight lines perpendicular to the x- and y-axes respectively. Furthermore, these straight lines are extended, and an initial segmentation is performed with the area surrounded by the four line segments as one as shown in Figure 3 (d). Here the region $R_{i,j}$ is the one surrounded by two pairs of adjacent straight lines $\langle l_i^x, l_{i+1}^x \rangle$, $\langle l_j^y, l_{j+1}^y \rangle$. For each region $R_{i,j}$, the region length along the x and y directions are calculated as $d_{i,j}^x$ and $d_{i,j}^y$ respectively.

Next, each area is classified into three classes, slab, beam, and pile head, by thresholding for each area size using Eq. (1).

$$label(i, j) = \begin{cases} 0 & \text{(pile head) if } (d_{i,j}^x < th_{class} \text{ and } d_{i,j}^y < th_{class}) \\ 1 & \text{(beam) else if } (d_{i,j}^x < th_{class} \text{ or } d_{i,j}^y < th_{class}) \\ 2 & \text{(slab) else} \end{cases} \quad (1)$$

Good results are obtained by setting the threshold to $th_{class} = 3.0m$ from the experiment.

Finally, the triangles included in each region are extracted, and the planes parallel to the z direction are detected by RANSAC for the vertically downward point cloud, and the height $h_{i,j}$ of each region is calculated. An initial 3D model is constructed by sweeping the obtained boundary to this height. As for the height reference, the slab is set to 0 in common, and the beam and pile head are calculated by plane fitting by the RANSAC method. Figure 3 (d) shows an example of the semantic segmentation.

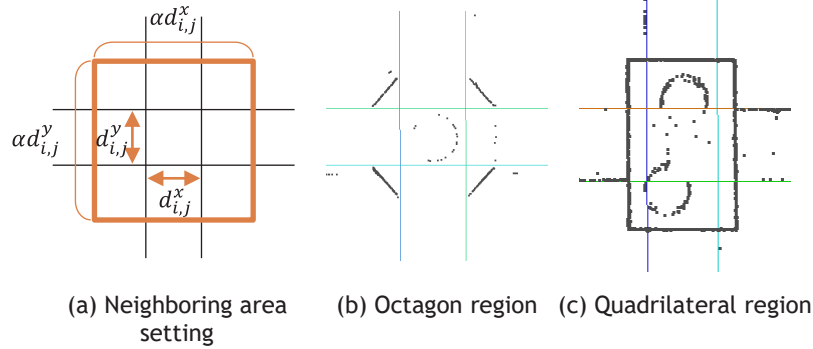


Figure 4. Examples of pile head points in neighboring area

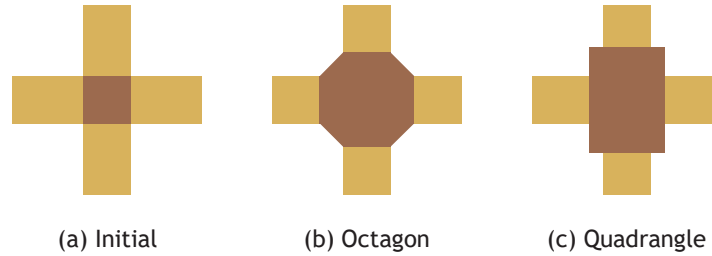


Figure 5. Examples of 3D modeling of pile head

5.3 Classification of Pile Head Region and Template Fitting (step 3)

Modeling is performed by fitting a template model to the region classified as the pile head in the previous step. In this study, we focused on two types of widely used squares and octagons. First, we extract the horizontally oriented point cloud within a certain range from the center of the region. Here, as shown in Figure 4(a), the range is defined as α times of the pile head region sizes $d_{i,j}^x$, $d_{i,j}^y$ in both the x and y directions. We set $\alpha=3.0$ based on the several experiments.

Next, a template model is fitted locally to the extracted projected point cloud using straight-line fitting by RANSAC. First, in the case of an octagon, as shown in Figure 4(b), points are generated only from four areas inclined at an angle of 45 degrees to the x and y directions in most pile head shapes. Four line segments are generated. In addition, in some cases, points on the side of the round pile often remain. The octagonal pile head is designed to be reflectively symmetrical in the vertical and horizontal directions on the 2D surface. Therefore, the four line segments on the projection plane should also have reflection symmetry with respect to the x and y axes. Therefore, to reflect such symmetry in the constructed model, our method first extracts point clouds distributed on four line segments by the RANSAC method separately, and then four lines are fitted simultaneously under the constraints that they are symmetrical each other and the inclination is 45 degrees. After that, the points of intersection with the four straight lines of the beam side that have already been applied to the point cloud are extracted, and the pile head 3D model is updated as shown in Figure 5(b). An example of modeling is shown in Figure 7(b).

On the other hand, in the case of quadrangle, a point cloud distributed on a straight line parallel to the x-axis and y-axis can be confirmed, as shown in Figure 4(c). Since most of them also have a relationship of reflection symmetry with each other. Therefore our method extracts each partial point group by the RANSAC method in the same way as above, and four lines are fitted simultaneously by imposing a constraint to be symmetric each other and parallel to one of the axes. The 3D model is updated as shown in Figure 5(c).

5.4 3D Modeling of Haunch Region (step 4)

A haunch is an area created at the joint between the pile head and the beam to increase the strength of the

joint. If a haunch is included, the cross-sectional shape of the beam is evaluated, and the haunch region is created as shown in Figure 6(a). As shown in this figure, there are obliquely distributed point clouds corresponding to haunches at the boundary with the pile head at both ends of the beam. Therefore, as shown in Figure 6(b), only the points where the angle between the triangle normal vector and the vertical downward direction is within a certain range are extracted. Then a straight line is fitted as shown in Figure 6(c) and a cross-sectional shape as shown in Figure 6(d) can be created. After that, we can calculate the depth according to the width of the beam and create a haunch 3D model. An example of modeling is shown in Figure 7(c).

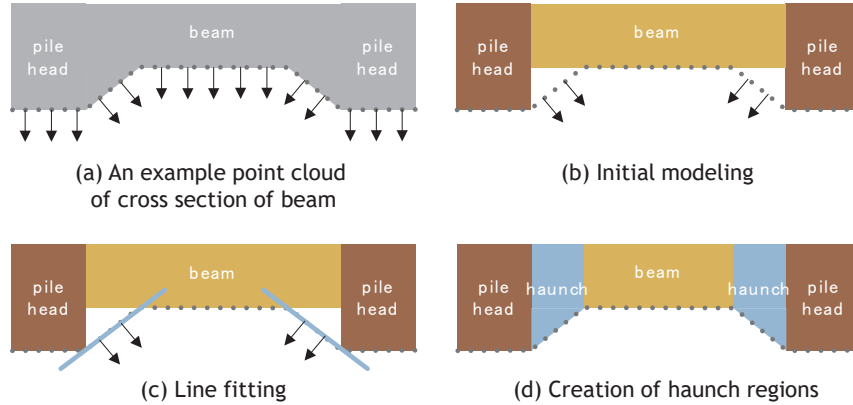


Figure 6. 2D cross-sectional view of haunch region creation

5.5 Ortho Image Creation (step 5)

For the input high-density textured model, each plane area that constitutes the floor slab, beam, pile head, and haunch of the simplified model is extracted. An orthoimage is created by using off-screen rendering mapping at each planar region. By applying ortho image to the simplified model, a simplified model with 3D textures can be constructed. For details, see the literature (Kessenich, 2016).

6. RESULTS AND DISCUSSION

In this section, we describe the experimental results of the proposed method. For the experiment, we used the polygonal model that was cut out from the 3D polygon model of the entire pier by SfM.

Figure 7 shows an example of the simplified model that was constructed. The number of triangles in the input polygon model is about 1.8 million which are evenly sampled in space. It can be confirmed that the models for each member are constructed appropriately including the octagonal pile heads and haunches. It is also possible to confirm that labels are appropriately assigned to each member. Figure 8 shows the result of comparison of the reconstructed model and input polygon model. It can be confirmed that the model can be constructed with high accuracy because the two are roughly aligned visually. The simplified model consists of 189 regions, most of which are rectangular except for the slab. Therefore, the number of triangles in the final simplified model is about 400, which is about 1/4,500 of the input model. Figure 9 shows an example of constructing a textured model. We were able to build a visually high-quality model with no conspicuous seams between the generated textures.

The current problem is that the outer circumference cannot be modeled. In the 3D reconstruction processing from the images by SfM/MVS, the quality of the SfM model reconstructed in the outer part is significantly lower than the inner part due to the influence of sunlight, so it is excluded from the processing. Another issue is that the pile head shape cannot be automatically classified. At present, users visually specify squares or octagons. In fact, even one pier may have multiple types including other shapes, so it is necessary to develop an automatic classification method using machine learning.

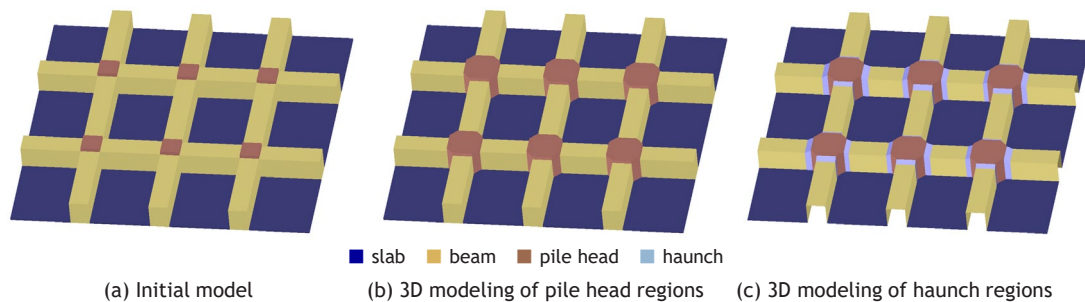


Figure 7. Process for a 3D simplified model reconstruction

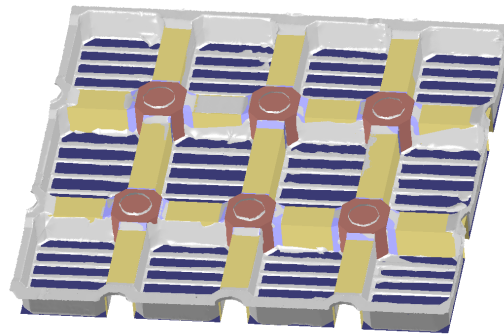


Figure 8. Comparison of input polygon model and reconstructed simplified model

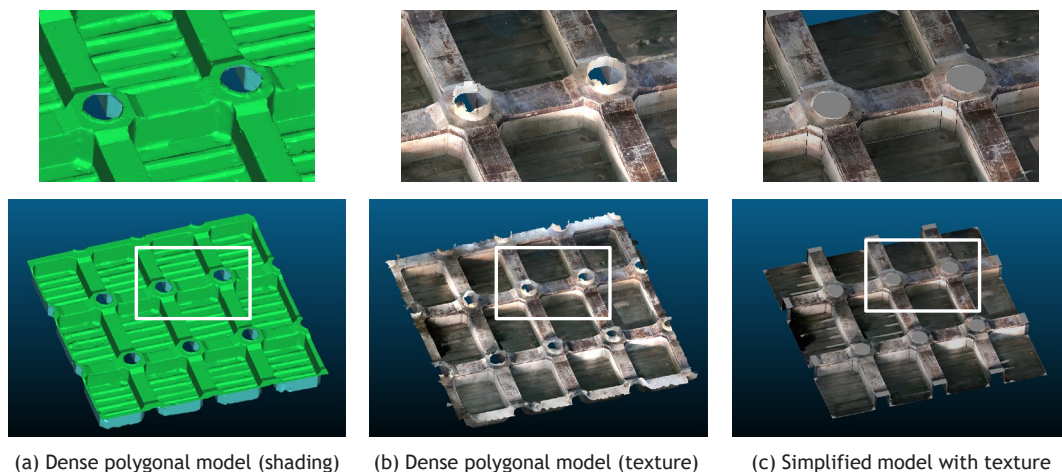


Figure 9. Reconstructed 3D simplified model with texture

5. CONCLUSIONS

In this paper, we proposed a new method that can automatically construct simplified models with textures based on member recognition from high-density polygon models, 3D model construction, and automatic orthoimage creation to support the maintenance and management of piled piers. We also verified the effectiveness through various experiments. In the future work, we will conduct experiments on various piers and proceed with quantitative performance verification of the proposed method.

REFERENCES

- Fischler, M. A. and Bolles, R. C., (1981). Random Sample Consensus: A Paradigm for Model Fitting with Applications to Image Analysis and Automated Cartography, *Communications of the ACM*, 24(6), 381–395.
- Kessenich, J., Sellers, G., and Shreiner, D. (2016). OpenGL Programming Guide: The Official Guide to Learning OpenGL, Addison-Wesley Professional.
- Li, M., Nan, L., Smith, N., and Wonka, P. (2016). Reconstructing building mass models from UAV images. *Computers & Graphics*, 54, 84-93.
- Lu, R., Brilakis, I., and Middleton, C. R. (2019). Detection of structural component in point clouds of existing RC bridges, *Computer-Aided Civil and Infrastructure Engineering*, 34, 191-212.
- Mizuno, K. (2018). System of Inspection and Diagnosis for Port Structures Using Unmanned Boat, *PIANC Yearbook*.
- Mohammadi, M., Rashidi, M., Mousavi, V., Karami, Al, Yu, Y., and Samali, B., (2021). Quality evaluation of digital twins generated based on UAV photogrammetry and TLS: Bridge case study, *Remote Sensing*, 13, 3499.
- Truong-Hong, L. and Lindenbergh, R. (2022). Automatically extracting surfaces of reinforced concrete bridges from terrestrial laser scanning point clouds, *Automation in Construction*, 135, 104127.
- Yan, Y., and F. Hajar, J. (2021). Automated Extraction of structural elements in steel girder bridges from laser point clouds, *Automation in Construction*, 125, 103582.

BIM APPLICATION FOR RESOLVING CONSTRUCTION ISSUES IN THAILAND: A CONSULTANT'S CASE STUDY

Narong Leungbootnak^{1,2}, Vuthea MIN³

1) Emeritus professor, Construction Engineering and Management Division, Department of Civil Engineering, Khon Kaen University, Thailand. Email: NarongL.FEC@gmail.com

2) Chairman, Future Engineering Consultants Co., Ltd, Bangkok, Thailand

3) Former project manager, Future Engineering Consultants Co., Ltd, Bangkok, Thailand

Abstract: This technical paper reports on the benefits of implementing Building Information Modeling (BIM) in construction projects, drawing on two case studies. The first case study discusses the application of BIM to resolve an unanticipated issue that arose during the bore pile drilling work in the construction of a hospital in Bangkok. The second case study details the use of BIM to detect a significant design flaw in a hospital building in northeastern Thailand. The employment of BIM facilitated the optimization of the design and construction process, improved communication among project teams, and prevented the occurrence of safety hazards, variation orders, rework, project delays, and additional costs. Consequently, the adoption of BIM in these construction projects can enhance the efficiency and accuracy of the construction process.

Keywords: Construction Management, BIM, Building project, Construction issue, Thailand

1. INTRODUCTION

The construction industry has been continuously evolving and adopting new technologies to improve efficiency, reduce costs, and ensure successful project delivery (Oraee *et al.*, 2019). One such technology that has gained popularity in recent years is Building Information Modelling (BIM) (Autodesk, 2023; Flamini *et al.*, 2023). BIM has been increasingly adopted as a tool for construction project management, enabling better visualization, coordination, and communication among stakeholders involved in the project. This paper presents two case studies showcasing the use of BIM in hospital construction projects in Thailand. The first case study highlights the benefits of BIM in the construction supervision phase, especially in overcoming unexpected challenges during the bore piling work. The second case study demonstrates the significance of BIM in identifying and resolving a significant design flaw, thereby preventing potential project delays and additional costs. This article also provides recommendations for future construction projects, emphasizing the importance of requesting information from concerned authorities before commencing work on any underground project and storing BIM data in big data for efficient utilization. These case studies illustrate the potential of BIM in improving construction project management and ensuring successful project delivery.

2. LITERATURE REVIEW

Building Information Modeling (BIM) is an emerging technology that challenges traditional work procedures and practices in the construction industry. BIM enables the integration of structured, multi-disciplinary data to create a digital representation of a building throughout its lifecycle (Autodesk, 2023). The adoption of BIM in developing countries is limited, with its implementation remaining low in the construction industry (Olanrewaju *et al.*, 2022). Theoretical developments in BIM suggest that it can be useful for not only geometric modeling but also for the management of construction projects. The most frequently reported benefits of BIM include cost reduction and control, significant time savings, and improved project practices (Bryde *et al.*, 2013).

Furthermore, BIM characteristics have a direct influence on awareness, and in turn, has a direct influence on BIM adoption among Thai engineers (Ngowtanawan, 2017). The quality of BIM software, relative advantage of BIM over previous software, trialability of BIM, ease of use, and compatibility with other software are the most critical factors that reflect BIM adoption. While Thai private developers request the use of BIM for over 60% of large projects, most use BIM below its potential and receive only limited benefits. The primary barriers to BIM adoption are the negative effect on schedule/productivity at the beginning of projects, high initial investment, lack of knowledge and information about BIM, lack of government leadership to promote change, resistance to change of practice, and long adoption periods (Sierra *et al.*, 2020).

Despite the limitations and challenges of BIM adoption, the digital model resulting from BIM design represents a valuable tool to support building construction management. However, at present, its potential is limited to the project phase (Flamini *et al.*, 2023). As BIM implementation continues to spread from design activity to other phases of construction projects, its potential to improve project practices is becoming more apparent.

3. METHOD

This article is taking directly from our projects experience of two building projects that implemented BIM during two hospital buildings construction, as undertaken by our construction management consultancy in

Thailand. It is imperative to highlight that this technical paper is primarily intended to serve as a platform for experience sharing, rather than being a formally structured academic research paper with specific methodology.

4. CASE STUDIES

In our capacity as a consulting firm, we have leveraged BIM as a tool for managing the construction of several projects, commencing from 2013. Over the course of our engagement, we have been involved in roughly 20 such undertakings, of which two have been selected as case studies for inclusion within this paper.

4.1 Case Study Number 1: Construction Management of a Hospital Project in Bangkok

The construction of this hospital project started in 2021 till present (2023). This case study is about the use of BIM in this construction project. Prior to the start of this construction, BIM was employed to integrate various design drawings, including architectural, structural, MEP, medical gas, and interior drawings. Clash detection was performed for the entire building, allowing us to identify conflicts and avoid issues. By building the project virtually on a computer before actual construction, we were able to save time, reduce costs, and enhance the quality of work by minimizing variation orders, design revisions, and reworks during the construction process. Notably, BIM encountered unexpected challenges during the bore piling work in this project. This case study highlights the advantages of BIM in construction management and explains how it was implemented to resolve the issues that arose during the construction phase, especially providing recommendations for future underground construction projects in order to prevent similar challenges.

Issue: During the construction of this hospital, a bore piling drilling machine encountered an unknown concrete structure at a depth of -17m underground. Our construction team could not identify what kind of structure it was, so we consulted the project owner and residents, but no information was available. Our team decided to hire a concrete drilling specialist company to drill the underground concrete in order to check the quality of the concrete and determine the structure type. However, during the drilling process, the concrete drilling machine caused water leakage, revealing a water-stop and a concrete structure with steel lining. It turned out to be a tunnel for water supply that had been built over 43 years ago and in active. The tunnel had a diameter of 2m. This unexpected issue delayed the construction and incurred additional costs. It is noted that a survey was conducted at the beginning of the project to determine the presence of substructures underground, by asking the project owners and residents in the area. The responses were that they did not recognize any underground activity before.

Solution: To solve the issue, BIM was used to integrate all construction drawings, including structural, water tunneling, retaining wall, and platform, to generate an accurate 3-dimensional view for ease of repair. The retaining wall, platform, and pile wall were analyzed, and the designers incorporated H-Beams to reinforce the retaining wall during the repairing process. The use of BIM in this project enabled the construction team to obtain an overview and details of structures and helped to solve the issue more efficiently.

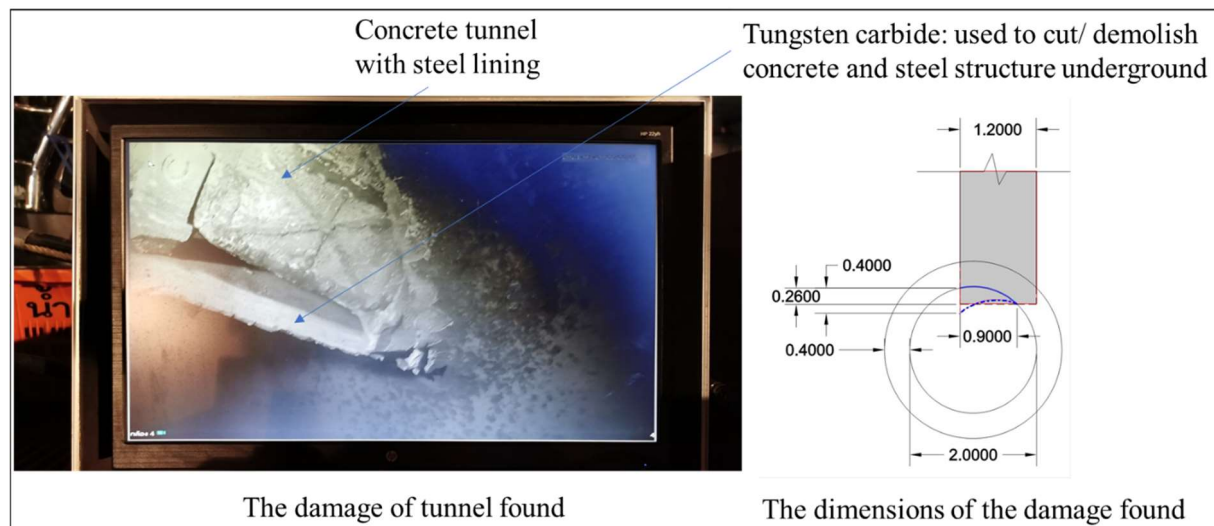


Figure 1. Concrete tunnel damage and dimensions of tunnel with a steel lining 17m underground

Conclusion and recommendation: The implementation of BIM in this project proved to be an effective solution to overcome the challenges faced during the construction phase. BIM provided an accurate 3-dimensional view of the structures, which enabled our design team to analyze and reinforce the retaining wall and adjustment of piles length and their locations in order to avoid the damaging of tunneling. However, the issue could have been prevented if the construction team had identified the type of underground structure before commencing work. It is recommended that before commencing work on any underground project, construction teams should request

information from concerned authorities to prevent delays and additional costs. Furthermore, it is essential to transform BIM to be more efficiently utilized in Thailand and stored in big data to enable all stakeholders to access the information easily and work on each project without disrupting public services. Figure 1 depicts the concrete tunnel damage and dimensions of tunnel with a steel lining 17m underground. Figure 2 depicts a typical output of BIM utilization to solve the problem in this case study.

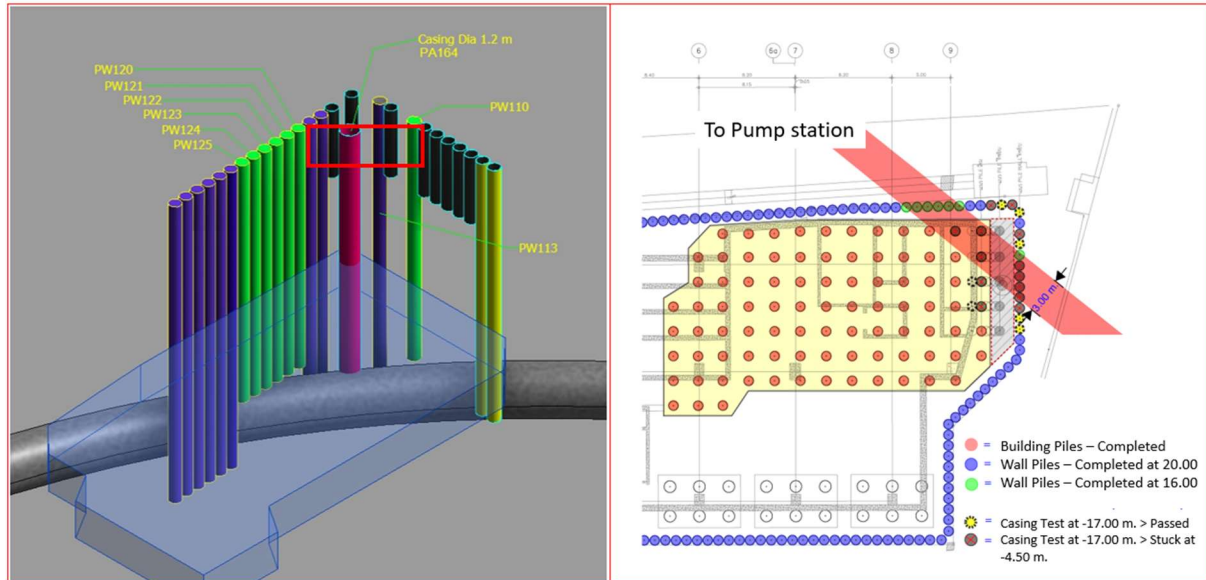


Figure 2. Typical output of BIM utilization to solve problem of case study number 1

4.2. Case Study Number 2: Construction Management of a Hospital Project in Northeast Thailand

This case study examines the use BIM in a hospital building project located in the northeast region of Thailand. The project was initiated in 2021 and completed in the earlier of 2023. It highlighted the benefits of utilizing BIM technology in construction projects, and presents a specific challenge faced during the project and how it was resolved. The hospital building project utilized BIM technology to construct the building virtually, allowing for better visualization and identification of potential design and construction issues. This technology enabled the team to integrate the architectural, structural drawings and MEP drawing, allowing for a more efficient and coordinated design process.

Issue: After the integration of all drawings by using BIM, the team discovered a significant issue with the design drawing of the canopy with no supporting structure. This was due to a lack of synchronization between the architectural and structural drawings, resulting in a significant design flaw that could have had serious problem of project which could result in variation order, rework, project delay, and extra cost.

Solution: The team quickly realized the severity of the problem and conducted a meeting with the contractor to find a solution. After thorough consideration, it was determined that extending the concrete slab and adding a stainless-steel gutter could provide the necessary support for the canopy. By utilizing BIM technology to identify the issue, the team was able to resolve the problem efficiently and effectively, preventing potential variation order, rework, project delay, and extra cost.

Conclusion and recommendation: This case study highlights the benefits of using BIM in construction projects, specifically in identifying design issues that could have significant safety implications. It is recommended that BIM is implemented in all construction projects to prevent similar design issues and to streamline the design and construction process. The use of BIM can enhance communication between project teams, improve efficiency and accuracy, and prevent potential safety hazards, variation order, rework, project delay, and extra cost. Figure 3 is depicted typical example of synchronization between architectural and structural drawings by using BIM and detection of canopy with no supporting structure. Figure 4. is depicted the actual construction of canopy after application of BIM in case study number 2.

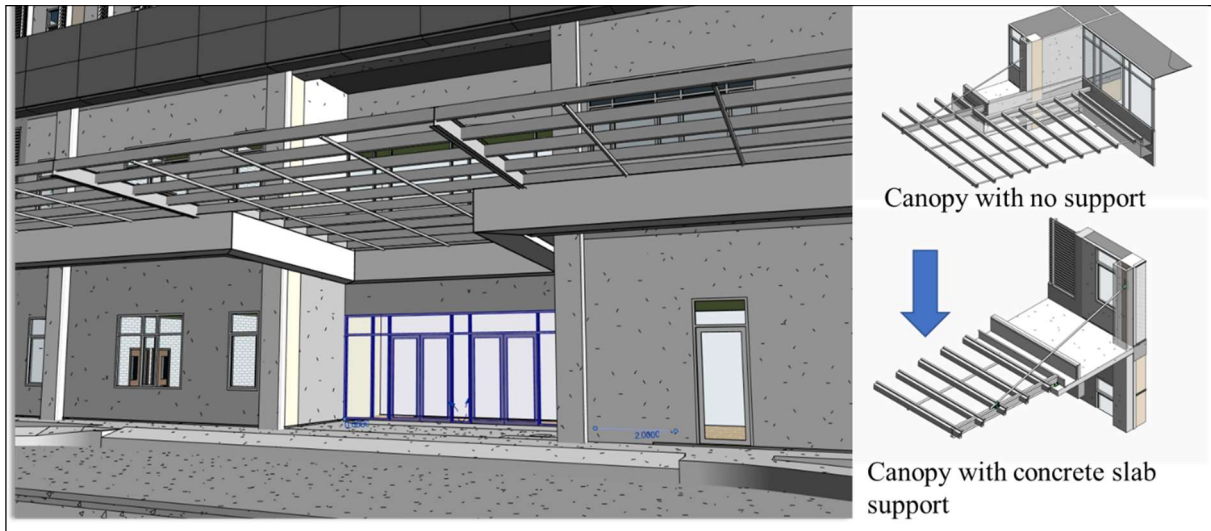


Figure 3. Typical example of synchronization between architectural and structural drawings by using BIM and detection of canopy with no supporting structure

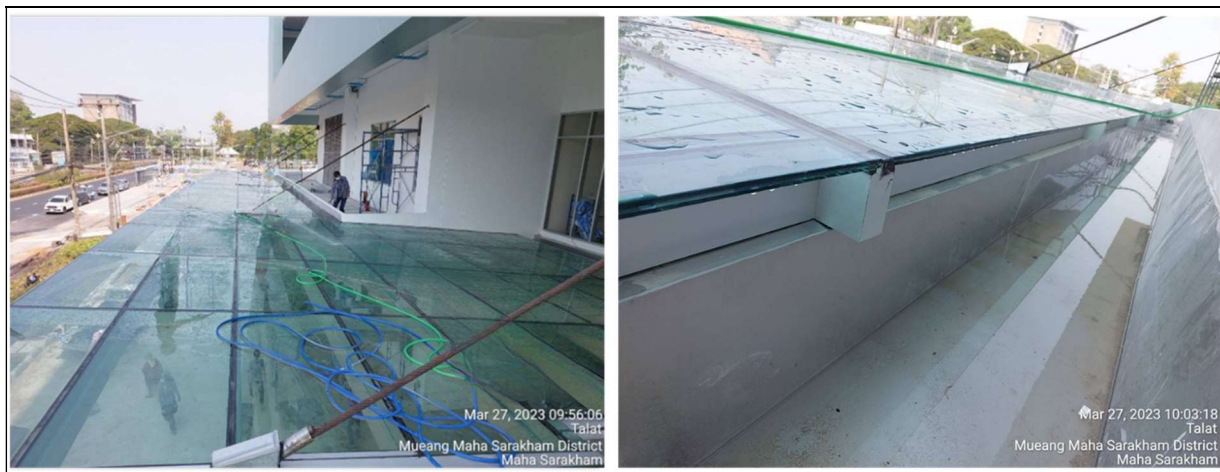


Figure 4. Actual construction of canopy after application of BIM in case study number 2

5. BENEFIT OF USING BIM FOR OUR PROJECTS

As a consultant with experience in utilizing BIM for construction management, we would like to share our insights on the advantages of BIM implementation in two hospital projects.

One of the most significant benefits of BIM implementation is the ability to identify and address issues within each discipline and element of the building during the computerized construction. This allows for adjustments to be made to synchronize the entire building and reduce the need for rework during the physical construction phase. BIM implementation requires the hiring of BIM modelers and coordinators to manage the process, which can be seen as an investment in project success. However, the long-term benefits of BIM implementation justify the cost. Another advantage of BIM implementation is the ability to solve problems before construction begins, resulting in cost savings of approximately 2% of the overall project cost. Additionally, BIM implementation can save up to 10% of the overall project time compared to traditional construction methods and reduce approximately 50% of rework. Utilizing BIM also results in improved work quality, with an improvement of almost 7% compared to work done without BIM. Incorporating BIM into the construction process can also reduce variation orders by approximately 2%, resulting from design errors that can be identified when combining all disciplines such as architectural drawings, structural, mechanical, electrical, and plumbing systems design, etc. Finally, the implementation of BIM also facilitates the proper linking of buildings, particularly in our cases where covered walkways are required to connect new and existing structures.

Therefore, our consultancy experience in utilizing BIM for the construction management of two hospital projects demonstrates that the benefits of BIM implementation are significant, resulting in improved work quality, cost savings, and reduced project duration and rework.

6. DISCUSSION

The two case studies presented highlight the benefits of utilizing BIM in construction projects. The first case study involves the construction of a hospital in Bangkok, where BIM was used to solve an unexpected issue during the bore piling work, which caused water tunneling to break. The use of BIM helped to generate an accurate 3-dimensional view of the structures, which enabled our designers to analyze and reinforce the retaining wall and adjusting piles length and coordination thereby solving the problem more efficiently.

In the second case study, BIM was used in a hospital building project in the northeast region of Thailand. During the BIM integration process, the team discovered a significant issue with the design drawing of the canopy, which with no supporting structure. By utilizing BIM to identify the issue, the team was able to resolve the problem efficiently and effectively, preventing potential safety hazards, quality issue, variation order, rework, project delay, and extra cost.

The use of BIM in both case studies helped to streamline the design and construction process, improve communication between project teams, and prevent potential safety hazards, variation order, rework, project delay, and extra cost. It is recommended that BIM is implemented in all construction projects to prevent similar design issues and to enhance the overall efficiency and accuracy of the construction process. The implementation of BIM in construction projects has proven to be an effective solution in managing construction projects and minimizing issues that may arise during construction.

7. CONCLUSION AND RECOMMENDATION

In conclusion, these two case studies demonstrate the benefits of utilizing BIM in construction projects. BIM enables construction teams to better visualize and coordinate their work, identify potential design flaws and issues, and efficiently resolve them, resulting in improved efficiency, accuracy, and cost savings. In the first case study, BIM was used to overcome unexpected challenges during the bore pile drilling of construction of a hospital, resulting in a more efficient and effective resolution of the issue. In the second case study, BIM was used to identify a significant design flaw in the canopy of a hospital building project, which was resolved efficiently and effectively, preventing potential safety hazards and additional costs. These case studies emphasize the importance of implementing BIM in construction projects to streamline the design and construction process, enhance communication between project teams, and prevent potential safety and additional costs. It is recommended for all construction projects in Thailand and beyond for the implementation of BIM.

8. LIMITATION

This technical paper provided a practical account of our experience as consultants in construction project management. It is not an academic research paper, and is based solely on our own experience, which may not be representative of all construction projects in Thailand and elsewhere. Our goal is to share our knowledge and experience of using BIM in project management and encourage all key construction stakeholders in Thailand and beyond to implement BIM in their construction projects. However, we must acknowledge that we have only presented two projects, which limit the generalizability of our findings to all BIM applications in building construction management.

REFERENCES

- Autodesk. (2023). *Design and build with BIM*. Retrieved from website: <https://www.autodesk.com/industry/aec/bim>
- Bryde, D., Broquetas, M., & Volm, J. M. (2013). The project benefits of Building Information Modelling (BIM). *International Journal of Project Management*, 31(7), 971-980.
- Flamini, A., Loggia, R., Massaccesi, A., Moscatiello, C., & Martirano, L. (2023). Building Information Modeling and Supervisory Control and Data Acquisition Integration: The Lambda Lab Digital Twin. *IEEE Industry Applications Magazine*, 29(1), 57-66. <https://doi.org/10.1109/MIAS.2022.3214015>
- Ngowtanasawan, G. (2017). A Causal Model of BIM Adoption in the Thai Architectural and Engineering Design Industry. *Procedia Engineering*, 180, 793-803.
- Olanrewaju, O. I., Kineber, A. F., Chileshe, N., & Edwards, D. J. (2022). Modelling the relationship between Building Information Modelling (BIM) implementation barriers, usage and awareness on building project lifecycle. *Building and Environment*, 207, 108556.
- Orace, M., Hosseini, M. R., Edwards, D. J., Li, H., Papadonikolaki, E., & Cao, D. (2019). Collaboration barriers in BIM-based construction networks: A conceptual model. *International Journal of Project Management*, 37(6), 839-854.
- Sierra, F., & Rodboonpha, C. (2020). BIM Implementation models in Thailand: drivers, benefits, barriers, and lessons learned. *Journal of Construction in Developing Countries*. Retrieved from website: <https://uwe-repository.worktribe.com/preview/10262587/2022%20BIM%20implementation%20in%20Thailand.pdf>

THE PROCESS OF APPLYING AR/VR/MR IN DESIGN IMPLEMENTATION IN CONSTRUCTION PROJECTS

Nam Phuong Nguyen¹, Tuan Sy Ho¹, Sy Tien Do^{2,3}

1) Engineer, Portcoast Consultant Corporation, Ho Chi Minh City, Vietnam. Master's Student in Hanoi University of Civil Engineering. Email: nam.np@portcoast.com.vn; tuan.hs@portcoast.com.vn

2) PhD, Assoc. Prof., Department of Construction Engineering and Management, Faculty of Civil Engineering, Ho Chi Minh City University of Technology (HCMUT), Ho Chi Minh City, Vietnam. Email: sy.dotien@hcmut.edu.vn

3) Vietnam National University Ho Chi Minh City, Ho Chi Minh City, Vietnam

Abstract: Despite the prospective advantages of using virtual reality (VR), augmented reality (AR), and mixed reality (MR) in the construction industry, there are still obstacles that must be overcome, including high initial investment costs, equipment and application synchronization, and staff training. The purpose of this research was to establish a method for utilizing VR/AR/MR in the implementation of design in construction projects. This study employs design software and VR/AR/MR applications to generate 3D models, identify and resolve errors and problems, generate a virtual tour, and optimize 3D models. The primary outcome is a procedure for applying VR/AR/MR to design implementation that specifies personnel requirements and construction project implementation processes. This research will contribute to the development of best practices for implementing VR/AR/MR in the construction industry, thereby enhancing construction processes and project management.

Keywords: AR (Augmented Reality), VR (Virtual Reality), MR (Mixed Reality), Design phase, Interaction, Feasibility evaluation.

1. INTRODUCTION

The accelerated development of Virtual Reality, Augmented Reality, and Mixed Reality (VR/AR/MR) technologies is transforming the construction industry. They are revolutionizing the conceptualization, presentation, and execution of designs, thereby augmenting the efficiency and effectiveness of project management and construction processes.

One of the key advantages of VR/AR/MR is that it allows architects, engineers, and builders to visualize and test their designs in a virtual environment. This enables them to identify and correct design defects and construction issues early on, reducing the need for costly and time-consuming modifications later on. It also enables stakeholders to experience the design in a more immersive and interactive manner, thereby enhancing communication and collaboration.

Despite the prospective benefits, utilizing VR/AR/MR in the construction industry still presents obstacles. The cost of apparatus and software which can be substantial, is one of the primary obstacles (Gu et al. 2021). In addition, high-quality 3D models are required, and synchronization between devices and applications can be difficult (Wang et al., 2020). Furthermore, training and skill development are required for effective use of this technology (Cao et al., 2020).

To surmount these obstacles, construction companies must invest in research and development, as well as their employees' training and education. By doing so, they can realize the full potential of VR/AR/MR and obtain an industry advantage.



Figure 1. Applying technology in construction (Portcoast Consultant Corporation)

In conclusion, VR/AR/MR technologies are revolutionizing the construction industry, offering significant benefits. By utilizing these technologies to enhance design, communication, safety, and training, construction companies can boost efficiency, cut costs, and deliver improved client service (Figure 1). To stay competitive, it is crucial for the industry to stay informed about new advancements and embrace them. This article aims to investigate and assess the potential and effectiveness of AR/VR/MR technologies in construction project design and implementation. The study will specifically examine the applications of AR/VR/MR in streamlining the design process, minimizing errors, improving efficiency, and reducing costs in project management and construction operations.

2. LITERATURE REVIEW

BIM and AR/VR/MR technologies are promising trends in the construction industry, offering significant benefits in design improvement and collaboration among stakeholders. BIM enables the creation of detailed virtual models, enhancing design quality, reducing errors, and improving communication (Huang et al., 2019). AR/VR/MR applications in construction enhance collaboration, communication, safety, and training, though challenges like cost and skill shortages exist (Shen et al., 2021; Gu et al., 2021).

Despite the challenges, the benefits of using BIM and AR/VR/MR technologies in the construction industry are significant, and they have the potential to transform the industry's processes and outcomes. As such, it is crucial for industry stakeholders to continue exploring and adopting these technologies to improve the construction industry's overall performance.

Table 1. Research around the world using Bim in the design and application AR/ VR /MR technology

No.	Title	References	Problem Statement	Objectives	Research Methodology	Results
1	Augmented Reality for Maintenance and Inspection in Civil Engineering: A Systematic Review ^[1]	Liu et al., 2022	The limited understanding of the potential applications and benefits of AR in maintenance and inspection tasks in civil engineering	To identify the potential applications of AR in maintenance and inspection tasks in civil engineering and to evaluate the benefits of AR in improving these tasks	Systematic literature review	AR can improve the accuracy and efficiency of maintenance and inspection tasks, reduce downtime and maintenance costs, and provide a more intuitive and interactive user interface for inspection software
2	Mixed Reality for Building Information Modeling: A Review ^[2]	Park et al., 2021	The lack of research on the application of MR in building information modeling (BIM)	To identify the potential applications of MR in BIM and to evaluate the benefits of MR in improving BIM processes	Systematic literature review	MR can improve the visualization and interaction of BIM models, increase collaboration and coordination among stakeholders, and provide a more intuitive user interface for BIM software
3	Virtual Reality Training for Construction Safety: A Review of the Literature ^[3]	Huang et al., 2021	The need for more effective and engaging training methods for construction safety	To evaluate the effectiveness of VR training for construction safety and to identify the factors that contribute to the success of VR training programs	Systematic literature review	VR training can improve the engagement and retention of safety training, increase worker awareness and preparedness for hazardous situations, and reduce the risk of on-site accidents and injuries
4	Augmented reality, virtual reality, and mixed reality in construction: A systematic review ^[4]	Shen et al., 2021	To assess the use of AR, VR, and MR in construction	To identify the benefits, challenges, and future directions of AR, VR, and MR in construction	Systematic literature review	Identified the benefits, challenges, and future directions of AR, VR, and MR in construction

No.	Title	References	Problem Statement	Objectives	Research Methodology	Results
5	The Application of Virtual Reality in the Construction Industry [5]	Gu et al., 2021	To assess the use of VR in the construction industry	To identify the applications, benefits, and challenges of VR in the construction industry	Literature review	Identified the applications, benefits, and challenges of VR in the construction industry
6	BIM-based sustainability analysis in building design: A systematic literature review [6]	Wang et al., 2020	The lack of systematic literature review of BIM-based sustainability analysis in building design	To conduct a systematic literature review of BIM-based sustainability analysis in building design	Systematic literature review	Identified the current state of BIM-based sustainability analysis in building design and highlighted the gaps in the existing research
7	Design and Implementation of VR/AR/MR-Based Education System [7]	Cao et al., 2020	To design and implement a VR/AR/MR-based education system	- To design a VR/AR/MR-based education system - To implement the education system using Unity 3D and Vuforia SDK - To evaluate the usability and effectiveness of the education system	Design and implementation study	- The VR/AR/MR-based education system was successfully designed and implemented - The education system can provide immersive and interactive learning experiences - The education system can improve students' learning motivation and performance
8	Application of augmented reality for simulating 3D model from point cloud and photogrammetry – A study case of construction site inspection [8]	Thu et al., 2020	The limitations of traditional methods in construction site inspection	To evaluate the effectiveness of AR in simulating 3D models for construction site inspection	Case study	AR was found to be an effective tool for simulating 3D models and improving efficiency in construction site inspection
9	Integrating point cloud from 3D Laser scanning and Unmanned Aerial Vehicle (UAV) equipment in order to collect construction [9]	Sy et al., 2019	The need for improved efficiency and accuracy in data collection in construction	To integrate point cloud from 3D Laser scanning and UAV equipment for improved data collection in construction	Case study	The integration of point cloud from 3D Laser scanning and UAV equipment was found to improve efficiency and accuracy in data collection in construction
10	A systematic review of building information modeling (BIM) in the construction industry: Current status, challenges, and future directions [10]	Huang et al., 2019	To assess the current status, challenges, and future directions of BIM in the construction industry	To identify the current status, challenges, and future directions of BIM in the construction industry	Systematic literature review	Identified the current status, challenges, and future directions of BIM in the construction industry

In conclusion, using BIM in the design and VR/AR/MR applications in construction design provides significant benefits in enhancing collaboration, reducing errors, improving safety, and minimizing environmental impact. While there may be initial investment costs and technical requirements, the long-term benefits make it a valuable tool for construction companies looking to improve their processes and stay competitive in the industry.

3. RESEARCH METHODOLOGY

The application of 3D modeling and AR/VR/MR technology in construction projects has revolutionized the industry by providing enhanced visualization and interactivity, streamlining communication and decision-making processes, and minimizing errors and costs. With 3D models, stakeholders can better understand the

project design and identify potential issues before construction begins. Moreover, AR/VR/MR technology allows for immersive experiences that enhance user engagement and understanding. This technology has the potential to greatly improve the efficiency and effectiveness of construction projects, ultimately leading to better outcomes for all parties involved.

Application implementation process

The process to deploy this application, stakeholders will follow several steps (Figure 2) such as:

Step 1: Collecting information about the project, including architectural, structural, and MEP (Mechanical, Electrical, and Plumbing)

Step 2: Using design software and AR/VR/MR technologies to create a 3D model of the project

Step 3: Checking and evaluating the 3D model to detect and address errors and issues

Step 4: Enhancing user interaction with the 3D model by creating diverse interactive experiences, such as creating a virtual tour of the construction space.

Step 5: Optimization and tuning the 3D model on various AR/VR/MR devices

Step 6: Using the 3D model to make decisions and solve problems during the construction process

4. RESULTS AND DISCUSSION

4.1 Results

In recent years, the adoption of AR/VR/MR technologies in the design phase of construction projects has brought significant benefits to the industry. By leveraging the power of virtual environments, architects, engineers, and builders are able to visualize and test their designs in a more intuitive and immersive manner, leading to improved work efficiency. As a result, potential design defects and construction issues can be identified and addressed early on, saving both time and costs that would have otherwise been spent on modifications during the construction phase.

Furthermore, the collaborative nature of these technologies enables project stakeholders to communicate and make decisions more effectively, leading to faster project progress. For example, by using virtual reality (VR) technology, stakeholders can experience a 3D model of a building before it's constructed and make informed decisions based on their virtual experience. The use of augmented reality (AR) can also help workers on construction sites visualize where to place components or identify potential hazards, improving safety and reducing the risk of errors.

These benefits are exemplified in Figure 2 and Figure 8, which shows a virtual model of a construction project being viewed and modified by architects, engineers, and builders. Through the use of AR/VR/MR technologies, the team is able to collaborate more effectively, address design issues early on, and ultimately deliver a higher quality project.

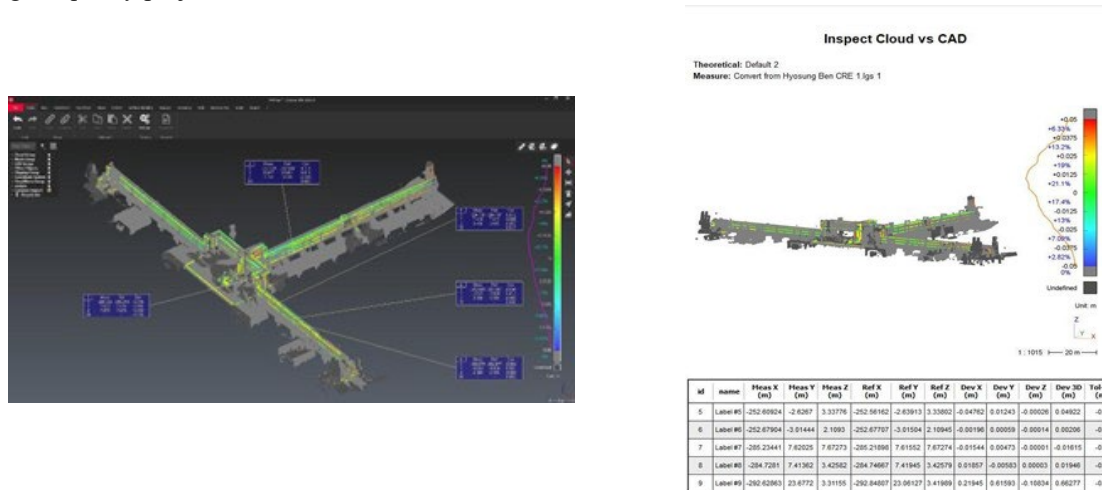


Figure 2. Checking and evaluating the 3D model

The adoption of AR/VR/MR technologies in the construction industry has enabled the creation of virtual tours that offer a more immersive and interactive experience than traditional 2D renderings or physical models. As a result, stakeholders are able to better visualize and understand the project design, leading to more informed decision-making.

One notable example of the benefits of virtual tours can be seen in Figure 3, where a virtual tour of a building design is being conducted. Through the use of AR/VR/MR technologies, the tour provides a realistic and engaging experience for users, allowing them to explore the building design in detail and gain a deeper understanding of its layout and features.

In addition to being engaging, user feedback from virtual tours has been overwhelmingly positive. Many individuals have reported that the immersive experience provided by AR/VR/MR technologies is not only enjoyable but also informative. This feedback highlights the potential of virtual tours to improve communication and collaboration among project stakeholders, ultimately leading to higher quality construction projects that better meet the needs of users.



Figure 3. The owner's experience when visiting their construction site through VR.

The adoption of AR/VR/MR technologies in the construction industry requires an investment in both equipment and skills, but the long-term benefits are significant. Figure 4 illustrates the use of laser scanning equipment, which can create 3D models of a construction site. This technology can help to identify potential issues in the early stages of the project, allowing for prompt and cost-effective resolution.

In addition to cost savings, the use of AR/VR/MR technologies can also lead to faster decision-making and project progress, thanks to improved communication and collaboration between stakeholders. By leveraging these technologies, project teams can work together more effectively, regardless of their physical location.

While the initial investment in AR/VR/MR technologies may be substantial, the decreasing cost of equipment and software is expected to make it more accessible and cost-effective for construction companies in the future. In fact, training employees to use laser scanning equipment and other AR/VR/MR tools is becoming increasingly common, reflecting the growing recognition of the benefits of these technologies.



Figure 4. Training employees to use laser scanning equipment

4.2 Discussion

The application of 3D and AR/VR/MR technology in construction design and project management brings many benefits to contractors, investors, and other stakeholders. By using interactive 3D models, users can experience a more realistic and comprehensive understanding of the project design and details, which helps to minimize errors during the construction process. Moreover, AR/VR/MR applications allow users to interact with 3D models and view details that are difficult to discern in reality. In addition, the use of this technology improves work efficiency and reduces costs for all parties involved in the design and construction processes. The application of 3D and AR/VR/MR technology in construction projects is an unstoppable trend and will continue to be developed in the future.

This application also has the potential to reduce costs and time in the design and construction process, while minimizing errors and risks during implementation.

To effectively employ this technology, however, designers and project managers will require investments in equipment and skills. Additionally, the accuracy and reliability of the 3D model must be ensured in order to make the correct design and construction decisions.

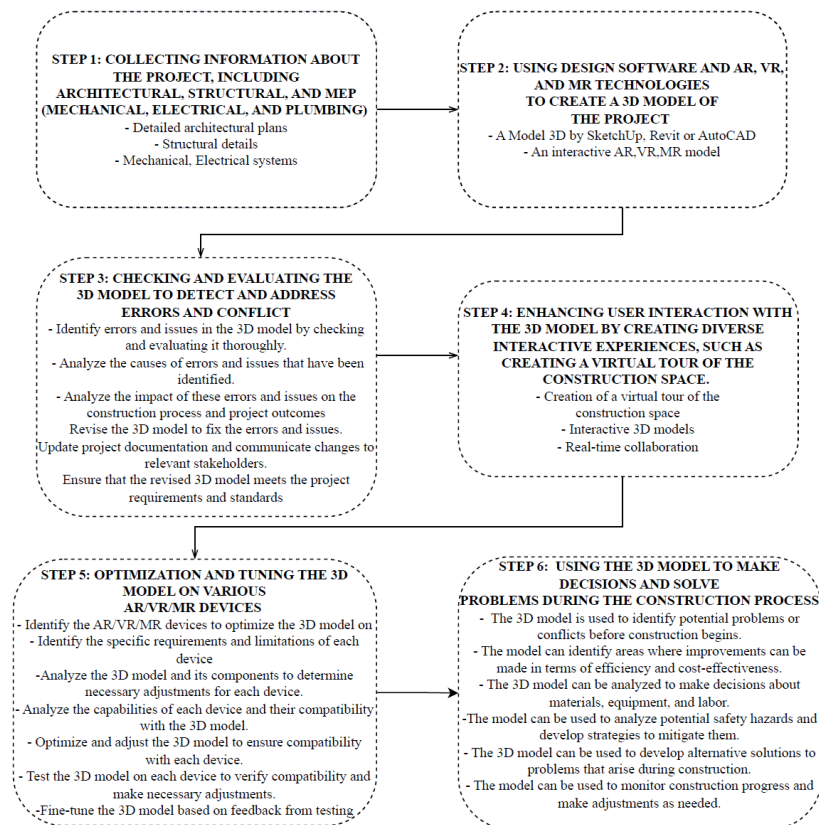


Figure 5. Research process for applying AR/VR/MR in design implementation

The following is a detailed step-by-step implementation to apply in the design phase.

Step 1: Collecting information about the project, including architecture, structural, and MEP (Mechanical, Electrical, and Plumbing) (Figure 6)

In the first step of the process, the researchers gathered information about the construction project, including its purpose, area, architecture, and structure. This involved collecting data and documents related to the project, such as drawings, blueprints, specifications, and site plans. The goal was to obtain a comprehensive understanding of the project's requirements, constraints, and objectives, and to identify any potential issues or challenges that might arise during the construction process.

To collect this information, the researchers employed various research methods, such as surveys, interviews, or site visits. They may have also used computer-aided design (CAD) software to analyze and visualize the project's architectural and structural features. This step was crucial in laying the foundation for the subsequent stages of the process, as it provided the necessary input data for creating the 3D model and evaluating its performance.



Unmanned Aerial Vehicle (UAV)



3D Laser Scanning equipments

Figure 6. Collecting the basis information for construction design

Step 2: Using design software and AR/VR/MR technologies to create a 3D model of the project (Figure 7)

After gathering sufficient project information, the next crucial step in implementing AR/VR/MR in the construction industry is creating a 3D model of the construction project. This comprehensive model incorporates various elements such as architecture, structure, electrical and water systems, and landscape. However, creating a detailed 3D model can be challenging, considering factors like precision, time, cost, and designer expertise. Fortunately, AR/VR/MR technology has simplified this process. Modern design tools like SketchUp, Revit, and AutoCAD enable engineers and designers to rapidly create accurate and comprehensive 3D models.

Once the 3D model is ready, it serves multiple purposes in construction. Virtual walk-throughs provide immersive and interactive experiences for stakeholders. It also facilitates problem identification and modifications before construction commences, minimizing errors and delays. Additionally, the 3D model enhances communication and collaboration by providing a clear, shareable depiction of the project.

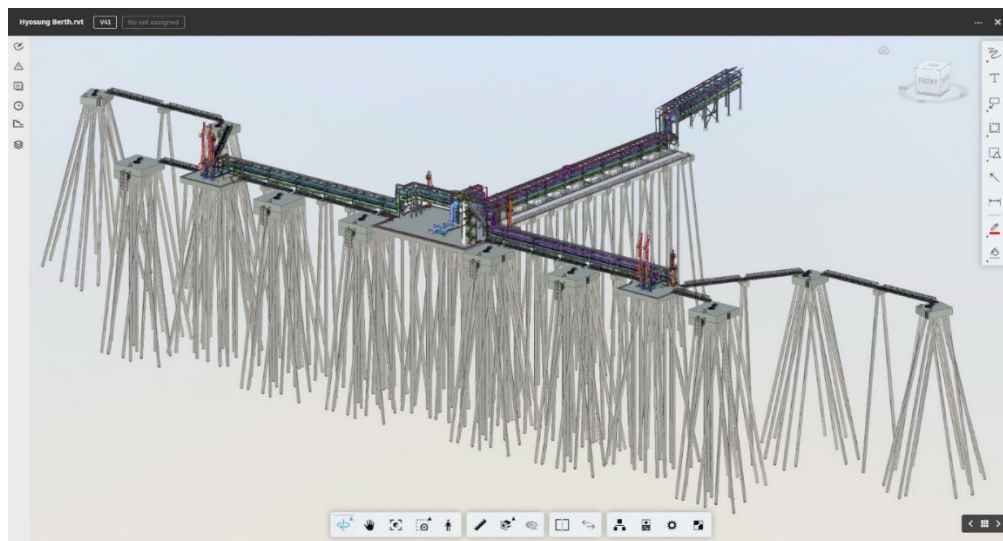


Figure 7. Creating 3D Model

Step 3: Checking and evaluating the 3D model to detect and address errors and conflict (Figure 2)

Once the 3D model has been created and visualized using AR/VR/MR technology, the next critical step is to conduct a thorough inspection and evaluation to identify any errors or issues. This stage is vital in ensuring the accuracy and compliance of the final product.

Various tools and methods are available for examining and evaluating the 3D model. Commonly, software is used to analyze the model, identifying errors related to size, shape, structural integrity, and other factors that may impact functionality or safety.

During the review and evaluation process, it is crucial to ensure that the 3D model can be effectively utilized as intended. For instance, if it is designed for architectural purposes, it must accurately depict the building's construction and be compatible with the software commonly used by architects and engineers. Similarly, if it is intended for virtual or augmented reality applications, optimization for the appropriate hardware and software platforms is essential.

Overall, the review and evaluation of the 3D model are critical stages in the AR/VR/MR construction design process. By ensuring accuracy, error-free representation, and compatibility with its intended use, high-quality designs can be created that meet project requirements and serve as valuable resources for architects, engineers, and other construction professionals.

Step 4: Enhancing user interaction with the 3D model by creating diverse interactive experiences, such as creating a virtual tour of the construction space (Figure 8)

After creating and refining the 3D model, the next step is to incorporate interactive features to enhance the user's experience. One way to achieve this is by creating a virtual tour of the construction site, using virtual reality (VR) technology to enable users to explore the virtual space and interact with various aspects of the construction design.

For example, in a commercial building project, users can take a virtual tour of the foyer and examine the various design elements such as layout, furniture, and decor. They can also interact with virtual elements like doors, elevators, and lighting to see how they function in the space.

Another method to improve the user experience is by creating interactive simulations. In a residential construction project, for instance, users can interact with a kitchen simulation to visualize how various appliances and materials will appear and function in the space. They can experiment with different layouts and designs to find the optimal solution for their needs.

By providing these interactive experiences, users can better understand and interact with the building's design, enabling them to make better decisions and achieve a better outcome.



Figure 8. Interacting with the model in real space

Step 5: Optimizing and Fine-tuning the 3D Model for Different AR/VR/MR Devices (Figure 9)

After creating and enhancing the 3D model with interactive features, it is crucial to optimize and fine-tune it for various AR/VR/MR devices. This involves adjusting the resolution, frame rate, and other settings to ensure the model runs smoothly and looks good on different devices.

As different AR/VR/MR devices have varying technical specifications and capabilities, it is important to optimize the 3D model for each device to ensure the best user experience. A 3D model that looks fantastic on a high-end VR headset may not perform well on a lower-end AR app for a smartphone.

Optimizing the 3D model may also involve modifying the user interface and interactions to ensure they are intuitive and easy to use on each device.

Overall, optimizing and fine-tuning the 3D model for various AR/VR/MR devices is a crucial stage in ensuring the success of the project as it can significantly impact the user experience and engagement.

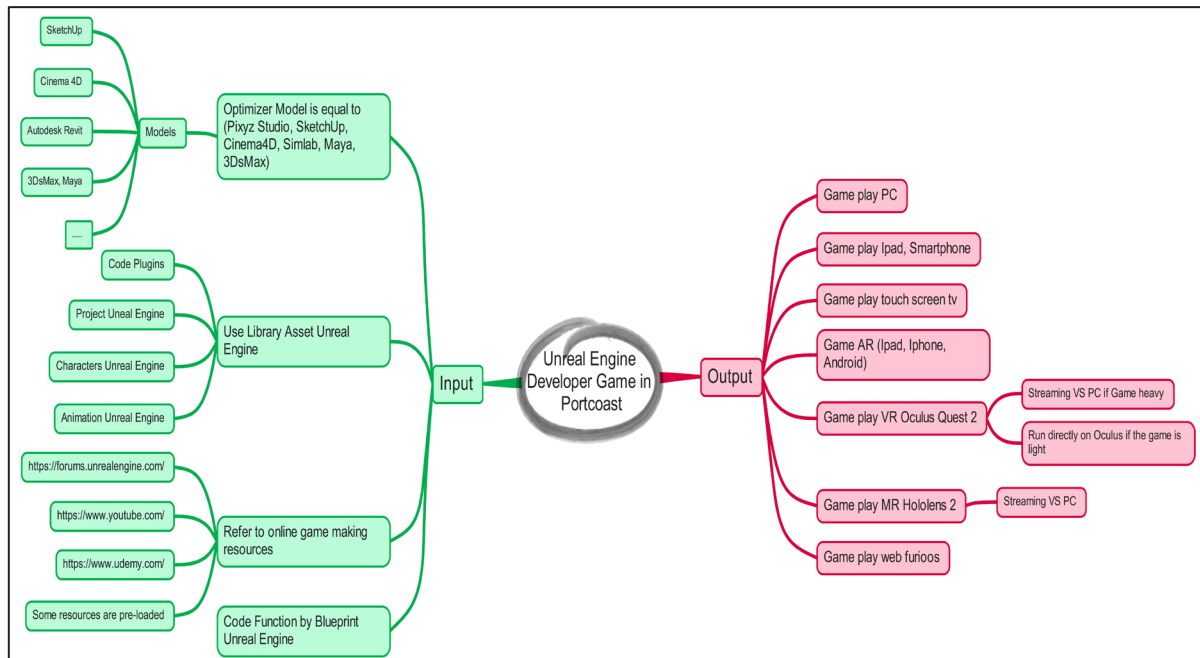


Figure 9. Optimizing process on AR, VR,MR devices projects

Step 6: Using the 3D model to make decisions and solve problems during the construction process (Figure 10)

The 3D model created through AR/VR/MR technology serves as a valuable asset throughout the construction process, aiding decision-making and problem-solving.

Before construction begins, the 3D model enables early detection and resolution of potential issues. By visualizing the project in 3D, conflicts or discrepancies between different building components can be easily identified, thus preventing costly construction errors.

During construction, the 3D model facilitates coordination among teams and subcontractors. For instance, the electrical team can visualize the installation of electrical components and ensure accurate placement. Similarly, the plumbing team can examine the interconnections of plumbing components and ensure proper installation.

Furthermore, the 3D model allows for real-time monitoring of construction progress. By overlaying the model onto the construction site, areas falling behind schedule can be pinpointed, and the overall progress can be assessed.



Figure 10. Illustration of applying virtual reality technology in desgín

Using the 3D model during construction can ultimately speed up the process and reduce the likelihood of errors. It can help ensure that the project is completed on time, within budget, and to everyone's satisfaction.

5. CONCLUSIONS

The use of 3D technology and AR/VR/MR in the design and management of construction projects offers numerous benefits to contractors, developers, and other stakeholders. By utilizing an interactive 3D model, users can gain a more authentic and comprehensive understanding of the project's design and details, which can help to minimize errors during the construction process. Moreover, the use of AR/VR/MR technology allows users to interact with the 3D model and view difficult-to-see details in the real-world environment. In addition, this technology can increase work efficiency and save costs for all parties involved in the design and construction process. In summary, the application of 3D and AR/VR/MR technology in construction projects is an unstoppable trend that will continue to be developed in the future.

The popularity of using AR/VR/MR technology in the construction industry is increasing rapidly, enhancing the interactivity and visuality of the 3D model while improving the ability to evaluate and manage construction projects. This application also has the potential to reduce costs and time in the design and construction process while minimizing errors and risks during implementation.

However, to effectively apply this technology, it is necessary to invest in equipment and training for designers and project managers. Additionally, ensuring the accuracy and reliability of the 3D model is essential to make the right decisions during the design and construction process.

ACKNOWLEDGEMENTS

We would like to acknowledge Portcoast Consultant Corporation for their support and for providing the data used in this study.

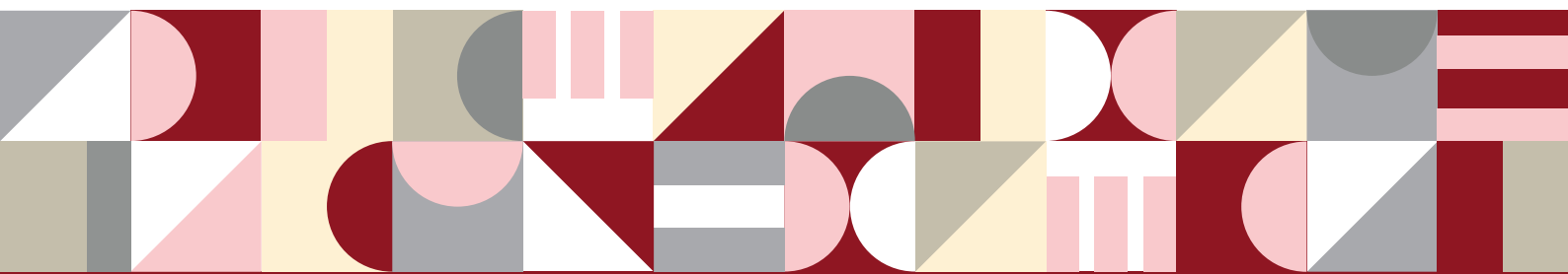
We acknowledge Hanoi University of Civil Engineering (HUCE) for supporting this study.

We acknowledge Ho Chi Minh City University of Technology (HCMUT), VNU-HCM for supporting this study.

REFERENCES

- Cao, D., Yang, J., Zhang, Y., & Ding, Y. (2020). Design and Implementation of VR/AR/MR-Based Education System. *In Advances in Computer Science and Education Applications*.
- Gu, H., Guo, Y., & Zhou, Y. (2021). The Application of Virtual Reality in the Construction Industry. *In 3rd International Conference on Communication and Information Processing*.
- Huang, Y., Gu, N., & Wu, D. (2021). *Virtual Reality Training for Construction Safety: A Review of the Literature. Automation in Construction*.
- Huang, T., Ren, Z., Shi, Y., Liu, S., & Wang, X. (2019). *A systematic review of building information modeling (BIM) in the construction industry: Current status, challenges, and future directions. Sustainability*.
- Liu, Y., Huang, Y., Zhang, H., & Qiu, Z. (2022). Augmented Reality for Maintenance and Inspection in Civil Engineering: A Systematic Review. *Automation in Construction*.
- Park, K., & Lee, G. (2021). Mixed Reality for Building Information Modeling: A Review. *Automation in Construction*.
- Shen, W., Liu, Y., Zheng, X., & Qiu, H. (2021). Augmented reality, virtual reality, and mixed reality in construction: A systematic review. *Automation in Construction*.
- Sy, T. D., Thu, A. N., Hiep, H., Loan, T. V., Phuoc, N. T. L., Truong, V. V., Vi, N. T. N., Quang, M. D., An, T. T. P. (2019). Integrating point cloud from 3D Laser scanning and Unmanned Aerial Vehicle (UAV) equipments in order to collect construction project information modeling. *Vietnam Journal of Construction*.
- Thu, A. N., Sy, T. D., Hiep, H., Khanh, D. T. N., Dai, H. N., Dat, H. Q. C., Hai, P. H. (2020). Application of augmented reality for simulating 3D model from point cloud and photogrammetry – A study case of construction site inspection. *Vietnam Journal of Construction*.
- Wang, C., Li, Y., Li, Y., & Li, Y. (2020). The application of virtual reality technology in architecture and construction industry. *In International Conference on Civil, Architecture and Sustainable Development*.

Construction Engineering and Asset Management



MODELING AND PRICING OF MULTIPLE RENEWAL OPTIONS EMBEDDED IN SHORT-TERM LEASE CONTRACTS

Nakhon Kokkaew¹, Wisanu Supsompon², and Chanon Atipanya³

1) Assoc. Prof., Department of Civil Engineering, Faculty of Engineering, Chulalongkorn University, Bangkok, Thailand.
Email: nakhon.k@chula.ac.th

2) Vice Governor of Bangkok, Bangkok Metropolitan Administration, Bangkok, Thailand

3) Master student, Department of Civil Engineering, Faculty of Engineering, Chulalongkorn University, Bangkok, Thailand

Abstract: Leaseholds have been increasingly used in real estate projects because of their flexibility advantages, such as flexible-use and contract renewal options. This paper presents a financial model for real estate development by which developers may employ short-term lease contracts (STLCs) with multiple renewal options (MROs) instead of a single long-term lease. To price flexibility value of renewal option embedded in short-term lease contracts under an equilibrium model, this paper proposes a computational framework based on market lease present value (*MLPV*) and a Monte Carlo option pricing method. The multiple renewal options are modeled as a series of European call options. The future *MLPV* of STLCs, an important underlying variable of renewal options, is then assumed to follow a stochastic process called geometric Brownian motion. The proposed method is then applied to a real estate project under construction in Bangkok. The results of our analysis revealed that using multiple short-term lease contracts with multiple renewal options may provide benefits for both developers and leaseholders.

Keywords: Building economics, Lease, Real estate, Renewal options, Monte Carlo Simulation

1. INTRODUCTION

The growth of the construction industry is believed to be positively correlated with the wellbeing of the real estate market. For example, the Thai construction industry was valued in 2019 at about \$US43,000 million or about 7.7% of the country's GDP, while the Thai real estate market was valued at about 45% of the total construction value. The real estate market is certainly large, and it includes a wide range of projects. For instance, it can be divided into the four basic groups of *residential, commercial, industrial, and infrastructure* (Folch, 2008).

For residential projects, they can be developed using either *freehold* or *leasehold* methods. However, as the prices of land in the center areas of big cities like Bangkok become more and more expensive, freehold property also become unaffordable to general people, especially young workers. For young workers, they usually have low incomes and may be reluctant to buy freehold residential properties because they are not certain about their work in the future. For example, they may find a better job elsewhere and decide to move so as to live close to their new workplaces. Therefore, young workers may find it more sensible to rent instead of buying.

As for leasehold, it can be viewed as purchasing the use of property over a fixed period of time (Bellalah, 2002). One of the several benefits of a leasehold property is that it can provide leaseholders (tenants or lessees) flexibility throughout the holding period. Examples of flexibility in a typical lease contract include flexible-use options and contract renewal options. Elements of strategic flexibility in leasehold contracts (leases), such as renewal and flexible-use options, have been studied since the works of Miller and Upton (1976), McConnell and Shallheim (1983), and Grenadier (1995). Myers (1987) believed that flexibility in real assets should be viewed as real options. Real options may be defined as the right, but not the obligation, to take certain actions on real assets. The main purpose of the use of real options is to supplement the discounted cash flow (DCF) method in valuing a project under uncertainty, where the DCF may simply ignore the values of strategic actions, such as renewal, delay, postponement, and abandonment (Hayes & Abernathy, 1980; and Hayes & Garvin, 1982).

In Thailand, leasehold properties typically have 30-year term. Due to the limited time of use, with all things being equal, leasehold properties are usually sold at about 70% of the prices of freehold ones, which may still be expensive in case the projects are in prime areas. Therefore, to help address the issue of housing affordability crisis, especially in a city center, we consider a residential property development model using a short-term leasehold contract (STLC) with multiple renewal options (MROs). This approach to real estate development may essentially help lower the initial lease prices of the developed property, thereby making it more affordable. This is because STLCs require smaller down payments and less borrowing from banks to finance the transaction. Moreover, since the property developed using the proposed method becomes more affordable, developers can tap a greater pool of *real and local demand* accordingly. Thus, the benefits can be potentially mutual.

The remainder of this paper is organized as follows. The next section provides a brief background of Thailand's real estate market, and it summarizes the previous studies about real estate valuation and real options analysis. In Section 3, a proposed computation framework is presented. Then, in Section 4, we provide the details of the case study project. Section 5 presents the risk modelling and analysis of the case study project, followed by the results of the analysis. Finally, the paper closes with the conclusion in Section 6.

2. BACKGROUND

2.1 Thailand's Residential Property Market

As observed by Folch (2008), infrastructure developments, such as transportation improvements, can help increase the demand for residential properties in the improving area. For example, the development of mass rail transit in the center of Bangkok city essentially helped spur the development of high-rise condominiums along the rail lines because of the high demand for residential properties in the area. As a result, the price index of Bangkok's condominiums, which are mostly located along the developed rail lines, grew on average about 6% per year over the past decade (2012–2020), while single-detached houses grew about 3.5% per year (see Fig. 1).

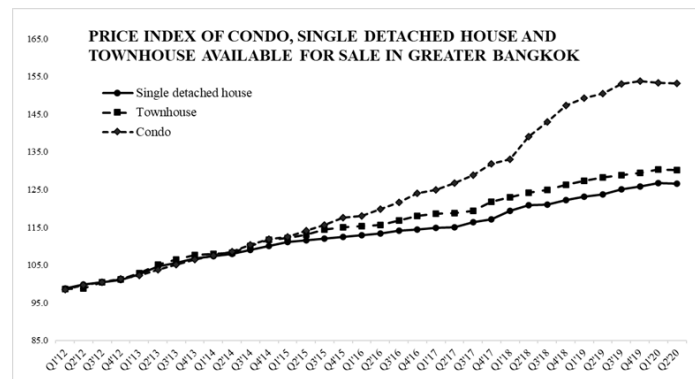


Figure 1. Housing price index in Bangkok (Source: Bangkok Post, 2020)

2.2 Leasehold Property

Leasing has grown increasingly popular in market-oriented economies because of its special ability to boost economic activity by putting the financing party's (lessor's) own assets to work (Katner, 2011). The use of leasing is not confined to real estate but includes other types of assets, such as satellites, trucks, and power plants (Bellalah, 2002).

Recently, it has been successfully adopted in the infrastructure market (e.g., build-lease-operate-transfer, asset recycling, or leasing of government-owned assets). For real estate projects, each market is perceived as unique, and its development process is so much a creation of the political process that society may negotiate, debate, and reconsider how that market relates to the basic issues of an enterprise economy: who pays, who benefits, who risks, and who has standing to participate in the decision process (Grasskamp, 1981).

2.3 Flexibility as Real Options

Flexibility as real options is an emerging concept in contemporary decision analysis. Basically, an option gives the holder the right, but not the obligation, to buy (call option) or to sell (put option) a designated asset at a predetermined price (the strike or exercise price). The designated asset that can be bought or sold is called the underlying asset.

Real options were proposed as an alternative method to conventional project evaluation, such as DCF. Conventional approaches work well when the future cash flow and decisions are predictable. However, when projects contain a high degree of uncertainty and strategic interactions, they tend to underestimate the project value or lead to a wrong decision regarding the project's financial feasibility. As Schwartz and Trigeorgis (2001) highlighted, flexibility of decision and strategic interactions should be considered to have financial value even though DCF methods fail to fully take account of that value. Real options have been widely studied and successfully applied to various fields, such as R&D (e.g., Lee & Paxson, 2001; Herath & Park, 2002), natural resources (e.g., Brennan & Schwartz, 1985; Kelly, 1998), strategy (e.g., Bernardo & Chowdhry, 2000; Kogut & Kulatilaka, 1994), technology (e.g., McGrath, 1997), and infrastructure (e.g., Nuefville, 2011; Chiara et al., 2007).

Real options research in lease contracts include, for example, a study on the use of ROA to endogenously derive the entire term structure of lease rates (Grenadier, 1995), the use of a ROA to the valuation of lease contracts under incomplete information (Bellalah, 2002), and the application of real options to lease contracts in the maritime transport industry (Al Sharif and Qin, 2014).

2.4 MC-Based Option Pricing Method (OPM)

The valuing or pricing of options can be done using (1) analytical, (2) numerical, and (3) simulation methods. We provide a summary of each method as follows.

Analytical methods, also named closed form methods, are widely used for valuing financial options whose underlying risk variables are assumed to follow a geometric Brownian motion (GBM). The first and most popular analytical method is the Black-Scholes (B/S) formula (Black and Scholes, 1973). The B/S can be used to price

European options, a type of option that can be exercised only at the maturity date. However, this analytical method strictly requires that the underlying risk variable follows a GBM.

The numerical or approximation analytical methods were mainly developed to deal with options that have early exercise features, such as American options, a type of option that can be exercised any time prior to the maturity date. Binomial lattices and finite difference methods are examples of often-used numerical methods (Hull, 2006).

The third group of methods are based on simulations, such as MC simulations, and involve two main processes. The first is the “forward projection” of the underlying risk variables, which is performed by MC simulation. The second involves determining the optimality of decision at each time step in a backward fashion, where dynamic programming and least squares regression are two of the methods used to find the optimal exercise decision (Longstaff & Schwartz, 2004). The main purpose of the backward algorithm is to compare and select, at each time step, the maximum value between an immediate payoff (if exercised now) and an expected continuing payoff (if exercised later). The underlying risk assumption of simulation methods need not follow a GBM, making the method extremely useful for pricing real options.

In this study we adopted this approach to option pricing for our analysis of the renewal option embedded in lease contracts.

2.5 Renewal Options In Real Estate

Real options in real estate development have been explored by several researchers. For example, Shilling et al. (1985) was among the first to apply option pricing theory (OPT) to value the right to property development as a call option (Hui & Fung, 2009). In another study (Throupe et al., 2012) proposed using a ROA valuation to mitigate the risk and to find the optimal strategy for developing a mixed-use property. In a recent article by Yeh and Lien (2020), they evaluated a real estate development project using a binomial MC-OPM. As for valuing renewal options embedded in leases, Hendershott and Ward (2002) applied OPT to value retail leases with renewal and average options using the B/S formula. Geltner et al. (2013) also applied decision tree analysis (DTA) to valuing a lease renewal option.

In this paper, we propose using the MC for valuing leases with MROs embedded in residential real estate whose underlying risk variable is the *market lease present value (MLPV)* backed by rent incomes. We also add into the valuation model the assumption of *aging property* that may affect the income growth over the holding period of leases, thereby making the valuation more realistic and conservative.

3. COMPUTATIONAL FRAMEWORK

In this section, we first present the conceptual framework of using multiple STLCs (Alternative “B” in Fig. 2) with renewal options as a substitute for a single LTLC (Alternative “A” in Fig. 2).

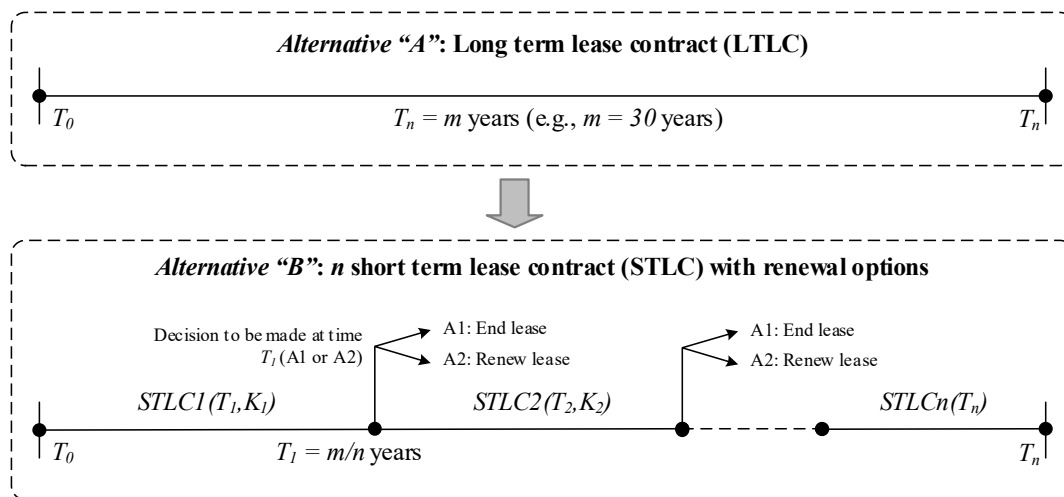


Figure 2. Conceptual framework of n short term leases with multiple renewal options

As shown in Fig. 2, a m -year lease contract may be replaced by using n of STLCs with $n-1$ renewal options. In order to make such a decision rationally, a tenant would have to calculate the *expected* net benefits (the PV of the stream of expected rent incomes) to be received from holding the subsequent lease and the financing costs of lease renewal. Therefore, if the PV of the stream of expected rent incomes falls below the cost of lease renewal (i.e., exercise price of contract renewal, K), a rational leaseholder should not exercise a renewal option and end the lease (i.e., decision A1: End lease). However, if the opposite is assumed to occur, the leaseholder should exercise

the right to renew the lease (i.e., decision A2: Renew lease).

Based on the conceptual framework presented in Fig. 2, the computational framework for pricing MROs in STLCs and the equilibrium option lease value can be developed as described in the following steps.

The first step is to determine the *MLPV* of LTLC (T_n -year with no option), denoted by $LPV_{t=0}(A)$, using the *income or investment method*.

The income or investment approach uses the DCF method, which is based on the implicit assumptions concerning all income streams produced by an investment (Johnson & Thomson, 2014). It employs the concept of time value for money, and the discount rate (r) for the calculation is adjusted based on the level of risk exposure: the greater the risk exposure, the higher the discount rate to be used. Risk-free cash flow, such as coupons from the investment in government bonds, is denoted by r_f . Therefore, for risky investments, such as real estate investment, the discount rate should be the sum of the risk-free rate (r_f) and the risk premium. This theory is known as a capital asset pricing model (CAPM). Accordingly, the present value (PV) of a stream of cash flow CF_t can be computed as shown in Eq. (1):

$$PV = \sum_{t=0}^{t=N} \frac{CF_t}{(1+r)^t}, \quad (1)$$

where CF_t is the net cash flow generated in year t , and r is a risk-adjusted discount rate. For a 30-year leasehold property unit, the expected market *lease present value* at year $t=0$ can be computed as:

$$MLPV_{t=0} = \sum_{t=0}^{t=30} \frac{(S_t \times 12)}{(1+r)^t}, \quad (2)$$

where S_t is monthly rent income in year t .

Based on Eq. (2), the expected market LPV (i.e., *MLPV*) can be modified as;

$$MLPV_{t=0}(A) = \sum_{t=0}^{t=T_n} \frac{(\hat{S}_t \times 12)}{(1+r)^t}, \quad (3)$$

where r is a risk-adjusted discount rate; and, \hat{S}_t is an *expected* monthly market rent income for year t .

For alternative “B”, the expected *MLPV* of the succeeding lease can be computed by Eq. (4);

$$MLPV_{t=T_j}(B) = \sum_{t=1+T_j}^{t=T_{j+1}} \frac{(\hat{S}_t \times 12)}{(1+r)^{t-T_j}}, \quad (4)$$

where T_j is the end year of the lease j . For example, if a lease with one renewal option were employed, the tenant would like to know the *MLPV* of the second lease, which is computed at the end year of the first lease ($T_{j=1}$).

A renewal option embedded in STLCs can be modeled as a *European* call option with an exercise price of K at maturity date. Grenadier (1995), for example, a pioneer in this study, provided technical details on the valuation of options to renew or cancel a lease using an *equilibrium model*. Under the equilibrium model, the value of two leases, lease “A” for T_2 years with no options and lease “B” for T_1 years with an option to renew for additional $(T_2 - T_1)$ years, must be equal since each provides the same service flow from the underlying asset (Grenadier, 1995). Therefore, the equilibrium option rent can be determined by equating the PVs of the first and second leases, and the *option premium* is the difference between the equilibrium rent on a lease of term T_2 with no renewal option and the equilibrium option rent on a lease of term T_1 with a renewal option.

3.1 Determining Exercise Prices (K)

Once the expected *MLPV* for each lease contract is determined, a *fair renewal price* (hereafter exercise or strike price) corresponding to the short-term lease contract j , denoted by K_j , can be determined as,

$$K_{j \in \{1, 2, \dots, n-1\}} = MLPV_{T_j}(B). \quad (5)$$

For example, the strike price of the first 10-year STLC with two renewal options ($n = 3, m = 30$) can be computed as $K_{j=1} = MLPV_{T_{j=1}}(B) = MLPV_{t=10}(B)$.

3.2 Modeling of The Underlying Risk Variable (X_t)

The underlying risk variable of renewal options embedded in STLCs is the future rent income in year t , denoted as S_t , and can be modeled using the stochastic GBM process. Therefore, the uncertain future monthly rent income in year t may be presented mathematically as shown in Eq. (6);

$$dS_{t+1} = \mu S_t dt + \sigma S_t dz, \quad (6)$$

where μ and σ is the drift rate, and the volatility of the stochastic process S_t , respectively; and, dz is a stochastic process called a Wiener process, defined as $dz = \varepsilon_t \sqrt{dt}$, and is a standard normal random variable (i.e., $\varepsilon_t \sim N(0,1)$). However, in this study, we incorporated the assumption about aging property into the model. The aging property assumption leads to different drift rate (μ) for each lease. Therefore, the $MLPV$ in year T_j (X_{T_j}) can be modeled as shown in Eq. (7);

$$X_{t=T_j} = MLPV_{t=T_j}(S_t) = \sum_{t=T_j}^{t=T_{j+1}} \frac{(S_t \times 12)}{(1+r)^{t-T_j}}, \quad (7)$$

where $MLPV_{t=T_j}$ is a function of a random variable S_t , which has a parameter μ_j for the j lease contract. The MC simulation can be used to generate the future $MLPV$ of X_{T_j} . For example, the $MLPV$ of the second lease, measured in year $T_{j=1}$ for simulated path i , denoted as $\omega(i)$ for $i=1,2,\dots,N$, can be mathematically presented as $X_{T_{j=1},\omega(i)}$.

3.3 Modeling of A Payoff Function of MROs

The MROs in lease contracts can be modeled as a *series of European call options* whose payoff (Π) can be computed by

$$\Pi(t, X_{T_j,\omega(i)}; K_j) = \max(X_{T_j,\omega(i)} - K_{j \in \{1,2,\dots,n-1\}}, 0) \quad (8)$$

where $\Pi(t, X_{T_j,\omega(i)}; K_j)$ is the payoff function of the renewal option at time t ; $X_{T_j,\omega(i)}$ is the market lease value at time T_j for the simulated path $\omega(i)$; n is the number of STLCs; and, $K_{j \in \{1,2,\dots,n-1\}}$ is a vector of strike prices corresponding to the j lease contract. From Eq. (4), the payoff function is non-negative, and its value is the maximum between $X_{T_j,\omega(i)} - K_j$ and zero.

3.4 Revision of Future Payoff

Since MROs (i.e., two or more renewal options) are path dependent, then *dynamic programming* must be employed to determine the optional decision of the leaseholder. For example, the exercise of the first renewal option will provide the tenant the right to renew for another lease. Therefore, if the tenant decides to end the lease, there will be no right to renew the lease for another term, and the future payoff from the following renewal options must be set to zero.

3.5 The MC-OPM/Valuation

Once the $MLPV$ matrix represented by X_t and the payoff function have been determined, the expected present value ($C_{t=0}$) of renewal options modeled as a European call option at time t can be computed as;

$$C_{t=0}(X_{T_j}; K_j) = E^* \left[e^{-r_f T_j} \Pi(t, X_{T_j,\omega(i)}; K_j) \right] = e^{-r_f T_j} \sum_{i=1}^{i=N} \frac{\max(X_{T_j,\omega(i)} - K_{j \in \{1,2,\dots,n-1\}}, 0)}{N} \quad (9)$$

where $E^*[\cdot]$ is the expected value under a risk-neutral world and requires a risk-free discount rate (r_f). The reason for using a risk-free rate as the discount rate for valuing options is that options must be priced under a risk-neutral world to avoid arbitrage opportunity (Marshall, 2000; Hull, 2006).

4. CASE STUDY PROJECT: A MIXED-USE LEASEHOLD PROJECT

In this study, a mixed-use project under construction in the center of Bangkok (see Fig. 3) is employed as a case study for this paper. The project was scheduled to be opened in 2024, but it was postponed to 2025 due to the effect of the COVID-19 pandemic. A major part of this project is a residential property, which can be sold on a leasehold contract with a period of no more than 30 years. However, the developer also wants to know if shorter STLCs (e.g., 10 years with 2 renewal options) could make the development more attractive to buyers who may prefer short-term lease over rent.



Figure 3. A mixed-use project under construction in the center of Bangkok

5. ANALYSIS AND RESULTS

5.1 Base Case Analysis: 35-M2 Property Unit for A LTLC

The case project is a residential property, which can be sold on a leasehold contract with a period of no more than 30 years. However, the developer also wants to know if shorter STLCs (e.g., 10 years with renewal options) could make the development more attractive to buyers who prefer to lease rather than rent. The main assumption used in this analysis is that the expected growth (drift) rate of rent income for each lease contract is constant over the term of the lease contract. However, the drift rate for the next lease contract is assumed to be decreased to account for the *aging property*. For example, in Fig. 4, the expected drift rate for the first, second, and third lease contract is assumed to be $\mu_1 = a$, $\mu_2 = b$, and $\mu_3 = c$, respectively, where $a > b > c$.

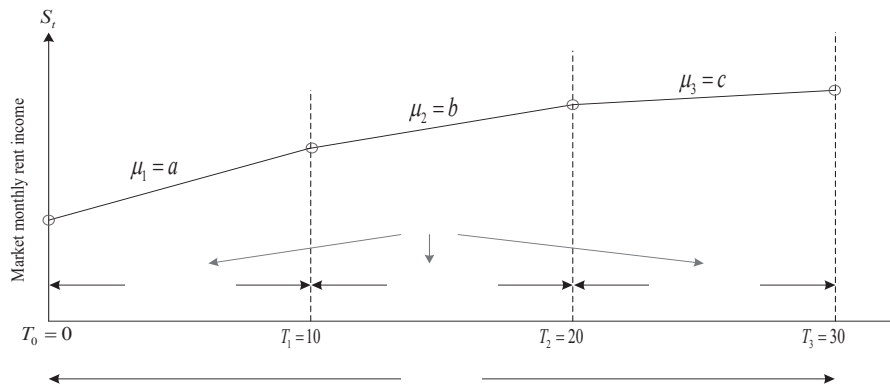


Figure 4. Drift rate (μ_j) of average market monthly rent income over the lease period

Market research to determine the competitive monthly rent in the area that the project is being developed is presented in Table 1. It was assumed that the expected drift rate for the first, second, and third lease contract was $\mu_1 = 4\%$, $\mu_2 = 3\%$, and $\mu_3 = 2\%$, respectively. Accordingly, the expected *MLPV* of LTLC was calculated, and the results are shown in Table 1.

Table 1. The DCF analysis of the case project using LTLC

Year	Average monthly rent (THB/month)	Estimated yearly value (THB/year)	Effective rent (THB/ m ² /month)
1	18,843	226,112	795.46
2	19,596	235,157	795.46
3	20,380	244,563	795.46
⋮	⋮	⋮	⋮
28	42,230	506,754	795.46
29	43,074	516,890	795.46
30	43,936	527,227	795.46

Based on the data shown in Table 1, the expected *MPVL(A)* is about 4,598,742 THB. As for a 10-year term lease contract with two renewal options, we can compute the expected *MLPV* of the first (*STLC1*), second (*STLC2*), and third (*STLC3*) lease using Eq. (4), which can be mathematically presented as;

$$MLPV(STLC1) = \sum_{i=1}^{i=T_1} \frac{(\hat{S}_i \times 12_i)}{(1+r)^i}, MLPV(STLC2) = \sum_{i=11}^{i=T_2} \frac{(\hat{S}_i \times 12_i)}{(1+r)^{i-10}}, MLPV(STLC3) = \sum_{i=21}^{i=T_3} \frac{(\hat{S}_i \times 12_i)}{(1+r)^{i-20}}. \quad (10)$$

Accordingly, the expected $MLPV$ of the three STLCs can be calculated as shown in Table 2.

Table 2. The DCF analysis of the case project using three STLCs

Lease	$MLPV$	Effective rent (Baht/m ² /month)	Present value
<i>STLC1</i>	1,960,837	634.32	1,960,837
<i>STLC2</i>	2,757,541	892.05	1,539,797
<i>STLC3</i>	3,521,781	1,139.28	1,098,108
Total $MLPV$ (B)			4,598,742

As can be seen in Table 2, by using the discount rate of 6%, the total $MLPV(B)$ comprising of three STLCs was indeed equal to that of the 30-year lease (i.e., $MLPV(A) =$ THB 4.59 million). When the three STLCs were employed, the $MLPV$ at the *beginning* of the first, second, and third lease was 1.96, 2.75, and 3.52 million THB, respectively, as shown in Fig. 5.

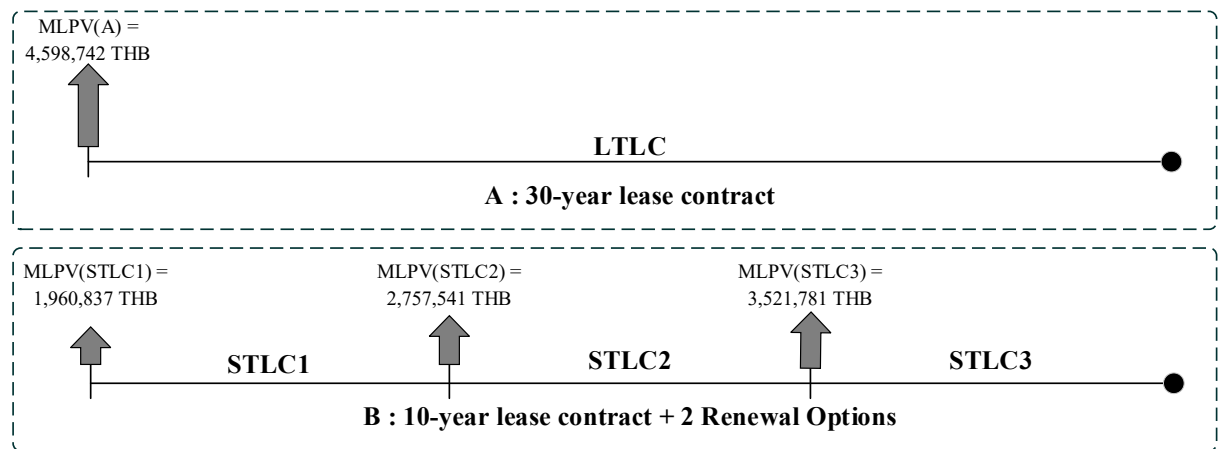


Figure 5. Market lease present value ($MLPV$) for each alternative

As mentioned earlier, there is a hidden value in the two renewal options, which must be priced. To price the options to renew the lease contract, the strike price to be specified in the lease contract must be determined. Based on the results shown in Table 3, the strike prices of renewal options for the first and second lease contracts can be specified, using the $MLPV$ at the beginning of each lease, as 2.75 and 3.52 million baht, respectively, (i.e., $K_1 = 2.75$ and $K_2 = 3.52$). Accordingly, under the equilibrium model, *equilibrium option rents* of lease “B” should be lower than those specified in the lease contract since the tenant may choose to end the lease if the market rent rate turned out to be cheaper than the rate specified in the contract to be renewed.

5.2 Modeling of Underlying Risk Variable

The underlying risk variable of this study is market lease present value ($MLPV$) backed by rent incomes. From Eq. (10), the $MLPV$ of a property unit in year $T_{j \in \{1,2\}}$ can be computed by

$$MLPV_{t=T_j} = X_{t=T_j} = \sum_{i=1+T_j}^{i=T_{j+1}} \frac{(S_i \times 12)}{(1+r)^{i-T_j}}, \quad (11)$$

where S_t is the market *monthly rent rate* in year t , which is assumed to behave as a random variable following a GBM with an expected drift rate of μ_j and a variance of σ^2 over the period of lease j ; and r is the risk-adjusted discount rate. The market monthly rent used in this study is different from the *monthly rent rate* specified in the lease contract, which is assumed to be constant over the lease period. This is because the actual monthly rent rate will vary or fluctuate for each unit in the same property. The GBM is defined by the stochastic differential equation (SDE) as given in Eq. (6).

5.3 Pricing of MROs Embedded in Lease Contracts

Future payoff was computed using Eq. (8). To increase the accuracy of the estimated option premium of

the three STLCs, we can increase the number of simulations. In this study, we used *MATLAB 2021a* for the simulation with $N = 10,000$. Based on the results of the simulation, the present values of the first and second renewal options were estimated to be **0.1598** and **0.1869**, respectively. Accordingly, the total value of the two renewal options for a 10-year lease (modelled as a series of European call options) is estimated to be about THB **0.3467** million in present value (i.e., $C_{t=0} = 0.3467$ million).

5.4 Results of Multiple Renewal Options (MROs) Analysis and Valuation

The results of the analysis presented in the previous section indicated that the *MLPV* of lease “A” for a 35-m² property unit is about THB 4.59 million or an *effective rent* (R_{T_0, T_3}) of about THB 795/m²/month. For lease “B”, the *contract effective rent* for each lease is $R_{T_0, T_1} = 634$, $R_{T_1, T_2} = 892$, and $R_{T_2, T_3} = 1,139$ baht/m²/month (Table 2). Therefore, the *effective rents* to be specified in the lease contract (contract effective rents) for 30-year term lease and 3 short-term leases are indeed equal, which satisfies the equilibrium model requirement.

However, for leaseholders, two renewal options in the lease contract provide the leaseholders an “exit option,” which is estimated to have a value of THB 0.3468 million in present value. Because the total value of effective rent must also meet the equilibrium model requirement in which the value of two leases, one for T_2 years with no options and another for T_1 years with an option to renew for additional $(T_2 - T_1)$ years, must be equal, the *equilibrium option rent* (denoted by $R_{T_j, T_{j+1}}^o$ for the equilibrium option rent for lease j) of the three short leases, therefore, can be calculated as $R_{T_0, T_1}^o = 582.62$, $R_{T_1, T_2}^o = 810.42$, and $R_{T_2, T_3}^o = 1,139.28$ baht/m²/month for the first, second, and third lease, respectively. For the calculation of the equilibrium option rent of the first lease contract (R_{T_0, T_1}^o) with the renewal option value of 0.1598 million in present value, the equilibrium option rent is therefore estimated to be the difference between the *MLPV*(SLTC1) (i.e., THB 1,960,837) and the first renewal option value, thereby reducing the cost to leaseholder to about THB 1,801,016 in present value for 10 years which is equivalent to the effective rent of 582.26 baht/m²/month. As for the equilibrium option rent (R_{T_1, T_2}^o) of the second lease contract, it can be estimated in the same way.

6. CONCLUSIONS

In this paper, we explored the option values embedded in a STLC (e.g., a 10-year term) with MROs, instead of a single LTLC. Valuing the fair price of MROs in leases can be a challenge for both developers and buyers who want to know the hidden option values in those leases. This paper has illustrated step-by-step how MROs embedded in leases can be priced using an equilibrium model and MC-OPM. With the increasing computing power of today’s personal computer, our proposed method is considered a simple and straightforward method for pricing a series of European call options.

The results of the analysis using a 35-m² property unit with a 30-year lease (Alternative A: a single LTLC) as a case study showed that the effective rent rate is about 795 baht/m²/month, with the *MPVL*(A) of about THB **4.59** million. When three STLCs, each with a 10-year term, are employed, the effective rent rate is about 634, 892, and 1,139 baht/m²/month for the first, second, and third lease, with the *MPVL*(SLC1), *MPVL*(SLC2), *MPVL*(SLC3) of about **1.96**, **2.75**, and **3.52** million, respectively. The present value (PV) of the three SLCs is **4.59** million. Two renewal options embedded in the lease contracts had been estimated to be about THB **0.3468** million. Therefore, the equilibrium optimal rent rate for leaseholders was reduced to 582.62 and 810.42 baht/m²/month for the first and second lease, respectively. This, therefore, makes the development more affordable and flexible to local people who may be reluctant to commit to the long-term financial obligation of a LTLC. Developers, on the other hand, can attract a greater pool of demand. The benefits can be mutual. However, as mentioned earlier, project development conditions worth considering in the adoption of the proposed method are those in the area with high workforce rotation and improving infrastructure, a key factor that could help drive the price appreciation of property units, accordingly.

The model presented in this paper, we hope, may help developers and leaseholders to appreciate the implicit benefits of shorter-term leases with flexible options, such as renewal options.

REFERENCES

- Al Sharif, A. A., & Qin, R. (2014). Valuation of Lease Contracts with a Price Adjustment Option: An Application to the Maritime Transport Industry, *The Engineering Economist*, 59:1, 30-54, DOI: 10.1080/0013791X.2013.869646
- Bangkok Post (2020). Back down to earth. Available: <https://www.bangkokpost.com/property/2011047/back-down-to-earth> [2021, February 1].

- Bellalah, M. (2002). Valuing lease contracts under incomplete information: a real options approach. *The Engineering Economist*, 47(2), 194–212.
- Bernardo, A., & Chowdhry, B. (2000). Resources, Real Options, and Corporate Strategy, Working Paper, The Anderson School at UCLA.
- Black, F., & Scholes, M. (1973). The Pricing of Options and Corporate Liabilities, *Journal of Political Economy*, 81, 637-659.
- Brennan, M., & Schwartz, E. (1985). Evaluating Natural Resource Investments, *Journal of Business*, 58(2) 135-157.
- Chiara, N., Garvin, M. J., & Vecer, J. (2007). "Valuing Simple Multiple-Exercise Real Options in Infrastructure Projects." *Journal of Infrastructure Systems*, 13(2), 97-104.
- Folch, M. (2008). Note on real estate investments, *Ivy Management Services*, Richard Ivey School of Business, The University of Western Ontario
- Geltner, D. M., Miller, M. G., Clayton, J., & Eichholtz, P. (2013). *Commercial Real Estate Analysis and Investments*. Oncourse Learning, 3rd Edition.
- Grasskamp, J. (1981). *Fundamentals of real estate development*, Washington, D.C.: ULI-the Urban Land Institute.
- Grenadier, S. R. (1995). Valuing lease contracts: A real-options approach, *Journal of Financial Economics*, 38(3), 297-331.
- Hayes, R. H., & Abernathy, W. J. (1980). Managing our Way to Economic Decline, *Harvard Business Review*, July-August, 67-77.
- Hayes, R. H., & Garvin, D. (1982). Managing as if tomorrow mattered, *Harvard Business Review*, May-June, 70-79.
- Hendershott, P. H., & Ward, C. W. (2002). Valuing and Pricing Retail Leases with Renewal and Overage Options, *NBER Working Paper No. 9214*.
- Herath, H. S. B., & Park, C. S. (2002). Multi-Stage Capital Investment Opportunities as Compound Real Options, *The Engineering Economist*, 47(1) 1-27.
- Hui, E. C., & Fung, H. (2009). Real estate development as real options, *Construction Management and Economics*, 27:3, 221-227, DOI:10.1080/01446190902759017
- Hull, J.C. (2006). *Options, Futures, and Other Derivatives*. Prentice Hall.
- Johnson, L., & Thomson, B. (2014). The discounted cash flow approach to valuing property investments (18.7). In E. Jowsey (Ed.), *Real estate concepts: a handbook*. London, UK: Routledge.
- Katner, W. (2011) Leasing in the Polish Civil Code, *Uniform Law Review*, 16(1-2), 401–414.
- Kelly, S. (1998). A Binomial Lattice Approach for Valuing a Mining Property IPO, *The Quarterly Review of Economics and Finance*, 38 (Special Issue), 693-709.
- Kogut, B., & Kulatilaka, N. (1994). Options Thinking and Platform Investments: Investing in Opportunity, *California Management Review*, 36(2), 52-67.
- Lee, J., & Paxson, D. (2001). Valuation of R&D Real American Sequential Exchange Options, *R&D Management*, 31(2) 191-201.
- Longstaff, F. A., & Schwartz, E. S. (2004). Valuing American Options by Simulation: A Simple Least-Squares Approach, *Review of Financial Studies*, 14(1), 113-147.
- Marshall, J.F. (2000). *Dictionary of financial engineering*. Hoboken, NJ: Wiley.
- McConnell, J. J. and Schallheim, J. S. (1983) Valuation of asset leasing contracts, *Journal of Financial Economics*, 12(2), 237-261.
- McGrath, R. (1997). A Real Options Logic for Initiating Technology Positioning Investment, *Academy of Management Review*, 22(4), 974-996.
- Miller, M. H. & Upton, C. W. (1976). Leasing, buying, and the cost of capital services, *The Journal of Finance*, Vol. 31, No. 3, pp.761-786.
- Myers, S. C. (1987). Financial Theory and Financial Strategy, *Midland Corporation Financial Journal*, Spring, 6-13.
- Nuefville, R. (2011). *Flexibility in Engineering Design*, MIT Press, Cambridge MA
- Schwartz, E.S., & Trigeorgis, L. (2001). *Real Options and Investment under Uncertainty*, MIT Press, Cambridge, MA.
- Shilling, J. D., Benjamin, J. D., & Sirmans, C. F. (1985). Contracts as options: some evidence from condominium developments. *AREUEA Journal*, 13(2): 143–52.
- Throupe, R., Sewalk S., Juncheng Z., & Huo C. (2012). Real Option Analysis: A Switching Application for Mixed-Use Real Estate Development, *Pacific Rim Property Research Journal*, 18:3, 277-291, DOI: 10.1080/14445921.2012.11104363
- Yeh, I-C, & Lien, C-H (2020). Evaluating real estate development project with Monte Carlo based binomial options pricing model, *Applied Economics Letters*, 27:4, 307-324, DOI: 10.1080/13504851.2019.1616049

A BAYESIAN NETWORK MODEL FOR QUANTIFYING THE COST IMPACTS OF CLAIM CAUSES IN BUILDING PROJECTS

Sang Van¹, Veerasak Likhitrungsilp², and Photios G. Ioannou³

1) Ph.D. Candidate, Department of Civil Engineering, Faculty of Engineering, Chulalongkorn University, Bangkok, Thailand. Email: quangsangek@gmail.com

2) Ph.D., Assoc. Prof., Department of Civil Engineering, Faculty of Engineering, Chulalongkorn University, Bangkok, Thailand. Email: Veerasak.L@chula.ac.th

3) Ph.D., Professor, Department of Civil and Environmental Engineering, University of Michigan, Ann Arbor, Michigan, USA. Email: photios@umich.edu

Abstract: Claims are a troublesome issue and often result in adverse consequences in construction projects. Claims stem from various causes. Even though these causes may or may not finally lead to claims, they still affect certain project objectives such as project cost, time, and quality. Thus, it is necessary to develop a tool that can assess the impacts of claim causes during project execution. In this paper, we quantify the cost impacts of claim causes in building projects using a Bayesian network (BN) model. Claim causes were first compiled by a comprehensive literature review and were then verified by a group of nine experts. Face-to-face interviews with the experts were conducted to define the cause-and-effect relationships among 13 claim causes, which were in turn used for developing a BN model. An ordinal scale was established for rating the cost impact of each claim cause, which is expressed by a cost overrun level of building projects. Through a structured questionnaire survey, the historical data of claim causes in 112 building projects were gathered to demonstrate the proposed model. The results show that the proposed BN model can be used to predict the cost impact levels of claim causes along with their associated probabilities. The proposed model can characterize critical claim causes in building projects, which can subsequently be used to choose appropriate response measures.

Keywords: Bayesian network model, Building projects, Construction claims, Claim causes, Claim responses.

1. INTRODUCTION

The construction industry has been witnessing a sharp rise of claims in terms of both frequency and severity (Apte & Pathak, 2016). Zaneldin (2006) reported that 35% of the construction projects in the United Arab Emirates (UAE) encountered claims. Although claims are sometimes necessary and can be settled in a non-confrontational manner (Kumaraswamy, 1997), for other times claims can lead to negative effects such as cost overruns and schedule delays (Apte & Pathak, 2016; Khahro & Ali, 2014). Noticeably, if claims are not settled amicably, they may lead to disputes, which often contribute to project failure, loss of time and money, and jeopardize the relationships among project participants (Cheung et al., 2001; Cheung & Pang, 2013). Construction disputes cost the United States \$43.4 million and last 14.8 months on average (Arcadis, 2018).

Several research works have focused on the quantification of claim severity, including the cost impacts of claims. For example, Semple et al. (1994) performed a content analysis on 24 construction claims submitted by the Canadian contractors and concluded that half of them were above 30% of respective contract sums. It is worth noting that most of the previous studies have approached claims from a reactive perspective, rather than a proactive perspective. Specifically, a limited amount of studies investigated the interdependences among claim causes to predict the cost impacts of claim causes during project execution (Likhitrungsilp et al., 2022).

In this paper, we quantify the cost impacts of claim causes in building projects using a Bayesian network model. This study focuses on building projects (e.g., residential or housing, office, hospital, and hotel) recently completed in Vietnam. The results can be used to predict the severity levels of claim causes in terms of cost, thereby we can prepare appropriate strategies to prevent or mitigate their likelihood of occurrences and consequences.

2. BACKGROUND

2.1 Cost Impacts of Claims

Costs associated with claims are often substantial (Olanrewaju & Anavhe, 2014). The average cost growth caused by claims was about seven percent of the original contract value in the US and Thailand (Sakate & Dhawale, 2017). The 18 percent of the contract sum was paid to contractors as claim fees in Portugal (Moura & Teixeira, 2007). The 50 percent of claims constituted 30% of the original contract price, and 33 percent of claims amounted to at least 60% of the original contract price (El-Adaway & Kandil, 2009). In some cases, the claim costs were as high as the original contract prices (Cheeks, 2003).

2.2 Cost Impacts of Claim Causes

Even though claim causes may or may not finally lead to claims, they still affect certain project objectives such as project cost, time, and quality. This depends on the claim causes' impact levels in each circumstance and

the relationships between contractors and owners. Predicting and recognizing the cost impacts of claim causes may help contractors plan their work related to claim causes better. For example, they can adequately allocate or reserve their budgets resulting from the project owners' delay in payment. If contractors submit a claim, they may sufficiently prepare an evidence (e.g., documents) to show their losses and damages of events causing claims.

2.3 Bayesian Networks

Bayesian networks (BNs) are directed acyclic graphs (DAG) used for descriptive and predictive purposes (Jensen, 2001). BNs can visually represent probabilistic cause-and-effect relationships among a set of random variables (Heckerman, 1997), including dependencies and independencies, which are closely aligned with real-world conditions (McCabe et al., 1998). For causal modeling, a BN is the best-fit methodology (Sharma et al., 2019).

Figure 1 shows an example of a BN. Nodes in the BN represent probabilistic variables. Root nodes (RN) are the nodes without any parent node, whereas leaf nodes (LN) are the nodes without any child node. Directed edges from a parent node to a child node depict the interdependences or causal relationships among variables (Guan et al., 2020).

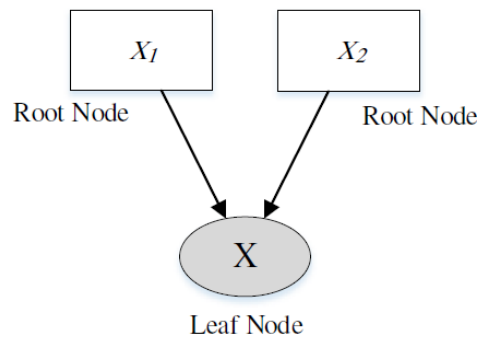


Figure 1. A Bayesian network with a directed acyclic graph (DAG) and causal relationships among nodes (Mohamad & Tran, 2021)

Bayes' theorem is the basis of the Bayesian approach. Assuming X and Y are two random events, then Bayes' theorem presenting the conditional probability dependencies among variables (Cárdenas et al., 2014) can be expressed by Equation (1):

$$P(X|Y) = P(Y|X) \times P(X) / P(Y) \quad (1)$$

where $P(X)$ and $P(Y)$ are the probabilities of X and Y , respectively. $P(Y|X)$ is the probability of Y given X . $P(X|Y)$ is the probability of X given Y .

3. RESEARCH METHODOLOGY AND RESULTS

Figure 2 depicts the five steps of this study. The details and results of each step are as follows.

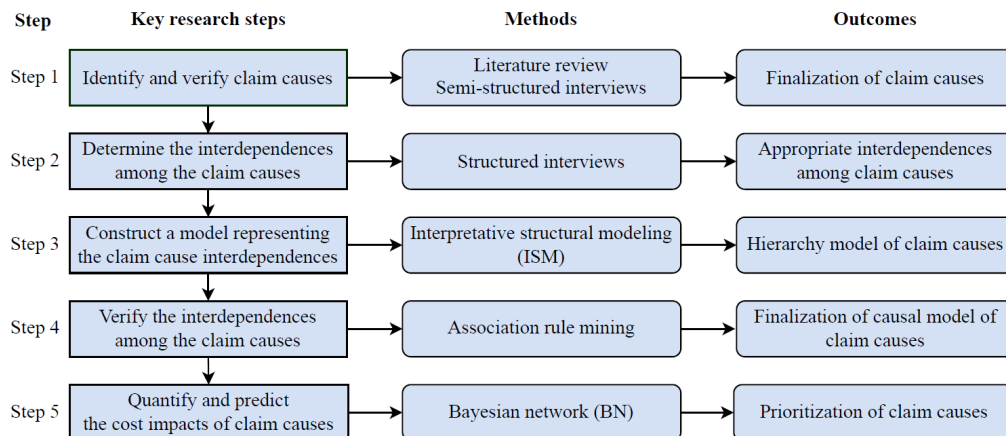


Figure 2. Research methodology

3.1 Identify and Verify Claim Causes

A comprehensive literature review was carried out to identify the preliminary list of claim causes by focusing on the claims made by contractors against owners during the construction phase in building projects. Semi-structured interviews were then conducted with nine claim experts with at least 10 years of experience in claim management to verify the list. Some claim causes were removed from the list due to their low frequency and lack of basis to claim, whereas some were combined because they share the common meanings. Table 1 shows 13 claim causes in this study.

Table 1. Potential claim causes

Code	Claim cause	Sources
CC01	Issues related to site possession	[1], [2], [3], [4], [5], [6], [9]
CC02	Issues related to inadequate documents	[1], [3], [4], [6], [7], [8], [11]
CC03	Change orders by owners	[1], [2], [3], [4], [5], [6], [7], [8], [10], [11]
CC04	Third-party interferences	[1], [3], [6]
CC05	Owner's delay	[1], [2], [3], [5], [6], [7], [8], [9], [10], [11]
CC06	Owner's procurement of material or equipment	[1]
CC07	Owner's failure to obtain licenses/permits	[1], [9], [10], [11]
CC08	Issues related to payment	[1], [2], [3], [5], [6], [7], [8], [10]
CC09	Termination/suspension of works	[1], [2], [3], [4], [6], [7], [8], [9], [10]
CC10	Differing site conditions	[1], [2], [3], [5], [8], [10], [11]
CC11	Unexpected increase in or escalation of material, labor, and equipment prices	[1], [3], [4], [6], [7], [8], [9], [10], [11]
CC12	Acts of God	[2], [3], [4], [9], [11]
CC13	Issues related to delivery/completion of work	[1], [9]

Sources: [1] Jalal et al. (2019), [2] Stamatiou et al. (2019), [3] Mishmish & El-Sayegh (2018), [4] Bu-Bshait & Manzanera (1990), [5] Cheung & Yiu (2006), [6] Enshassi et al. (2009), [7] Assaf et al. (2019), [8] Zanelidin (2018), [9] Yousefi et al. (2016), [10] Olanrewaju & Anavhe (2014), [11] Levin (2016)

3.2 Determine the Interdependences among the Claim Causes

The structured interviews with the previous nine experts were performed to identify the interdependences among the claim causes by construction contractors against project owners. A structured questionnaire, which is partially presented in Table 2, was used to support the experts in selecting an appropriate relationship between any two claim causes i and j (by ticking in the check box (☐)). The final relationship between any two claim causes was the one agreed by most of the experts. The guideline was provided in the questionnaire as follows.

- O means that claim cause i and claim cause j are not related.
- V means that claim cause i may lead to or influence claim cause j .
- A means that claim cause j may lead to or influence claim cause i .
- X means that claim cause i and claim cause j may lead to or influence each other.

Table 2. A structured questionnaire to determine the interdependences among the claim causes

Claim cause ' i '	O	V	A	X	Claim cause ' j '
Site possession	<input type="checkbox"/>	<input type="checkbox"/>	<input type="checkbox"/>	<input type="checkbox"/>	Inadequate documents
Site possession	<input type="checkbox"/>	<input type="checkbox"/>	<input type="checkbox"/>	<input type="checkbox"/>	Change orders by owners
Site possession	<input type="checkbox"/>	<input type="checkbox"/>	<input type="checkbox"/>	<input type="checkbox"/>	Third-party interferences
Site possession	<input type="checkbox"/>	<input type="checkbox"/>	<input type="checkbox"/>	<input type="checkbox"/>	Owner's delay
Site possession	<input type="checkbox"/>	<input type="checkbox"/>	<input type="checkbox"/>	<input type="checkbox"/>	...
Site possession	<input type="checkbox"/>	<input type="checkbox"/>	<input type="checkbox"/>	<input type="checkbox"/>	Delivery/completion of work

3.3 Construct A Model Representing the Claim Cause Interdependences

Based on the relationships among the claim causes determined in the previous step, interpretative structural modeling (ISM) was employed to construct a model which represents the interdependences among claim causes. ISM is a technique that can be used to establish the causal relationships among variables based on experts' opinions (Rezaee et al., 2019; Ruiz-Benitez et al., 2018). ISM processes can be found in Etemadinia & Tavakolan (2021) and Viswanathan et al. (2020). The ISM model in this study consists of 60 causal relationships among the claim causes.

3.4 Verify the Interdependences among the Claim Causes

Since the number of causal relationships in the ISM model is relatively large, the lift indexes of association rule mining (ARM) were calculated to check the reliability of interdependences among the claim causes. To achieve this, a questionnaire survey was conducted to collect the data related to claim causes from past building projects. There is a question in the questionnaire to determine the ‘occurrence’ or ‘no occurrence’ of each claim cause in the building projects in which the respondents were involved. The survey data was then encoded into values of “1” and “0” to support calculating lift indexes. The median value of lift indexes was considered a threshold to eliminate the weak-association relationships. Finally, 13 claim causes and 30 corresponding causal relationships were concluded, as displayed in Figure 3.

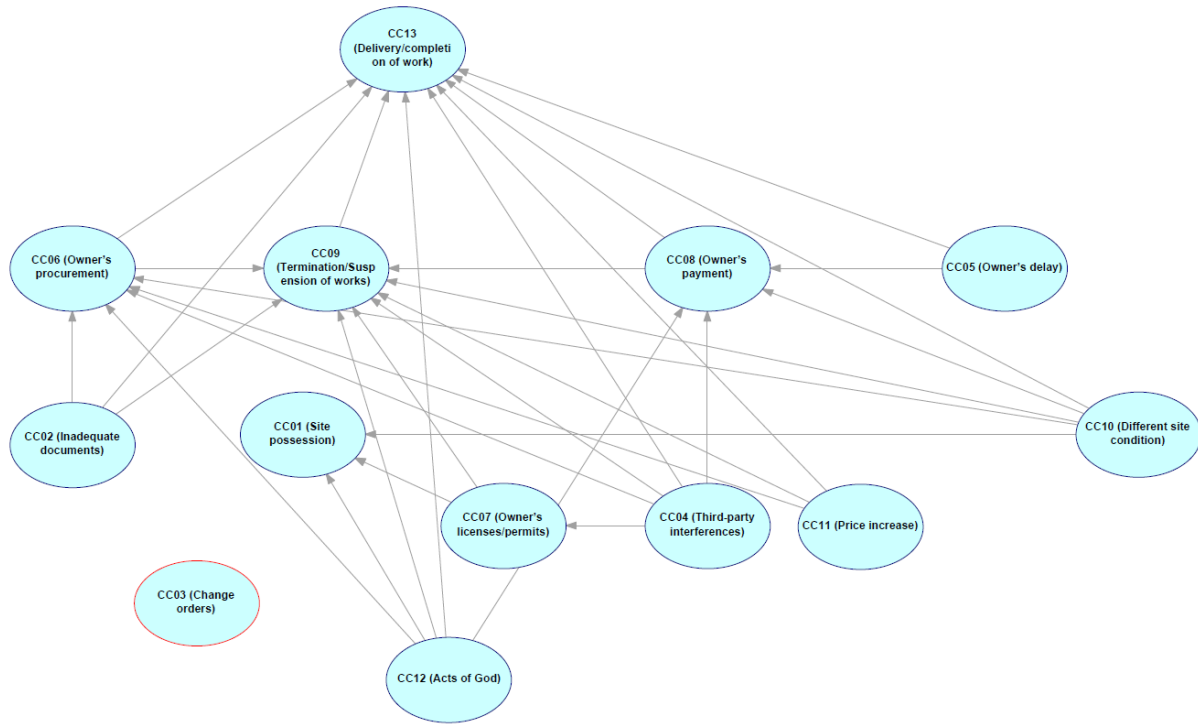


Figure 3. Refined ISM model

3.5 Quantify and Predict the Cost Impacts of Claim Causes Considering the Interdependences

In this step, we created a BN model of the claim causes considering their interdependences from the refined ISM model. Transforming an ISM model into a BN model is based on two main assumptions. First, a BN is a directed acyclic graph (DAG); that is, there is no cycle (Cinar & Kayakutlu, 2010). Thus, the cycles which exist in the ISM model must be eliminated while transforming it into a BN model. Another critical assumption is conditional independence. BN is an independence map, which guarantees that separated variables are conditionally independent given other variables. In the ISM model, $A \rightarrow B \rightarrow C$ refers to the effect of A on B and the effect of B on C, so there is an indirect effect of A on C. In the BN model, A is relevant to C, but if we know the true state of B, knowledge of A is irrelevant to C. So, C and A are conditionally independent given B (Cinar & Kayakutlu, 2010). Thus, the procedure needs to eliminate indirect relationships between claim causes. For this purpose, the direct and indirect relationships between claim causes are first identified. Then, the indirect effects should be eliminated (Cinar & Kayakutlu, 2010). In this paper, a total of 13 indirect relationships were eliminated, and the remaining 17 relationships were taken into the BN model.

In the questionnaire, a five-point ordinal scale was used to assess the impact level of each claim cause in terms of cost (cost overrun percentage). The scale ranged from 1 to 5, where 1 means very low (cost overrun $\leq 0.05\%$), 2 means low ($0.05\% < \text{cost overrun} \leq 0.1\%$), 3 means moderate ($0.1\% < \text{cost overrun} \leq 0.25\%$), 4 means high ($0.25\% < \text{cost overrun} \leq 0.5\%$), and 5 means very high (cost overrun $> 0.5\%$).

To construct a BN model, we used software GeNIe Academic Version 4.0.2304.0 by “BayesFusion, LLC” (<http://www.bayesfusion.com/>). Data of claim causes’ cost impact levels were encoded and input into the BN model. The five-point ordinal scale of cost impact is encoded by using the following rules: “1” (very low) and “2” (low) are changed into “1” (low), “3” (moderate) is changed into “2” (changes value but still remains moderate level), whereas “4” (high) and “5” (very high) are changed into “3” (high). Finally, each claim cause consists of three cost impact states (i.e., low, moderate, and high). Each state provides its corresponding probability. Figure 4 shows the BN model.

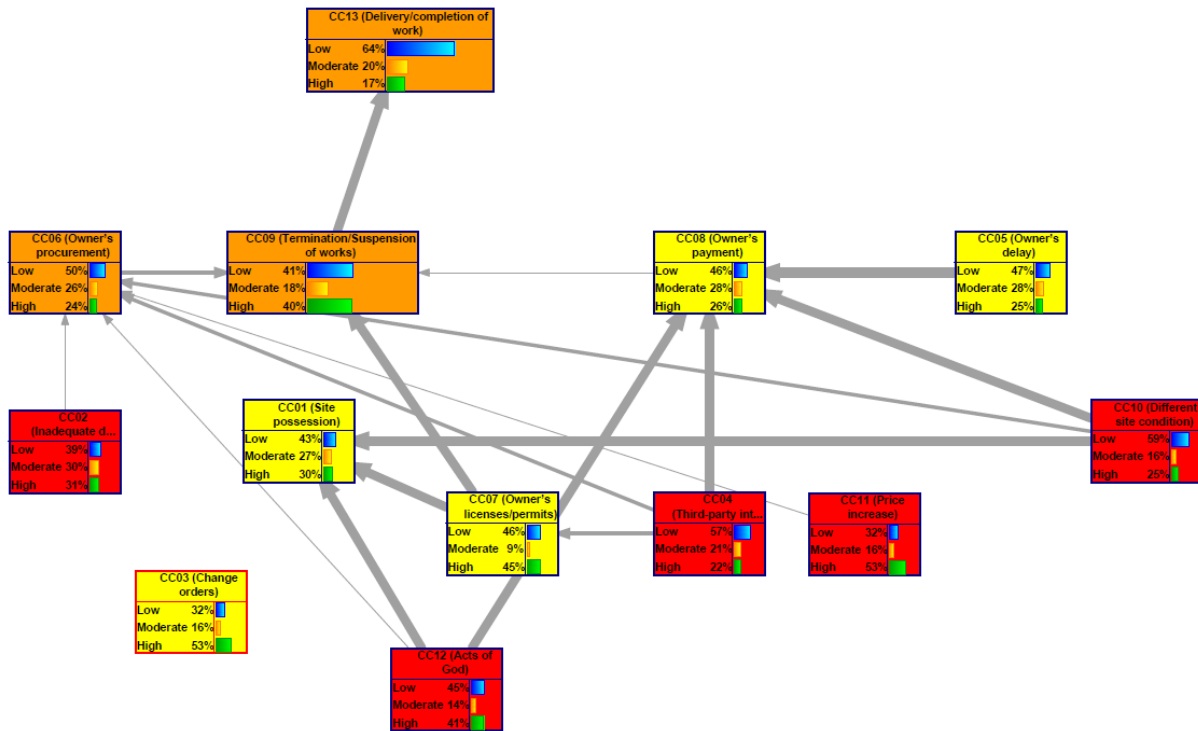


Figure 4. Bayesian network model and claim causes' states developed in GeNIe

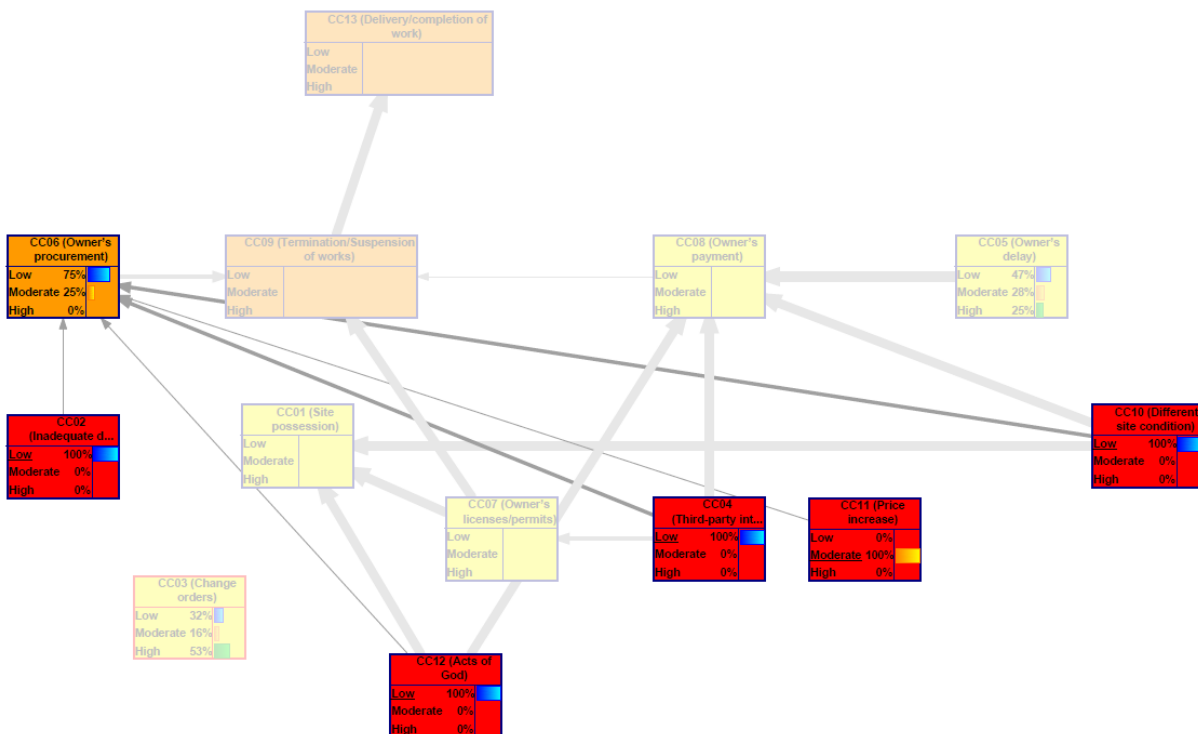


Figure 5. Bayesian network model presenting states of claim cause CC06, given states of claim causes CC02, CC04, CC10, CC11, and CC12

In this paper, we used claim cause *Owner's procurement of material or equipment* (CC06) in a project that was not included in the training data to demonstrate the predictive capability of the BN model. This claim cause is children node of 5 parent nodes, including *Issues related to inadequate document* (CC02), *Third-party interferences* (CC04), *Differing site condition* (CC10), *Unexpected increase in or escalation of material, labor,*

and equipment prices (CC11), and Acts of God (CC12). The states of CC02, CC04, CC10, CC11, and CC12 are low, low, low, moderate, and low, respectively. The BN model predicted that the probability of claim cause CC6 for the state “low” is 75%, 25% for the state “moderate,” and 0% for the state “high.” Accordingly, claim cause CC6 tends to create a “low” cost impact on the project. Figure 5 depicts the predictive results of the cost impact levels of claim cause CC6, along with associated probabilities, given the states of claim causes CC02, CC04, CC10, CC11, and CC12.

4. CONCLUSION AND RECOMMENDATION

This paper employs a Bayesian network (BN) approach to quantify and predict the cost impacts of claim causes on building projects. The BN model was developed based on 13 claim causes and their interdependences. Past building projects were used to demonstrate the applicability of proposed model. The model provides the probabilities associated with the three states of cost impact levels of claim causes. Critical claim causes, which lead to high impacts, must be focused while we prepare and implement appropriate response strategies and methods.

There are some limitations of the proposed model that need to be addressed in future research works. First, the proposed model focuses on the claims made by construction contractors against project owners only. Second, our model is primarily designed to use for the construction phase. Third, the model is structured to quantify the cost impacts of claim causes of building projects. As a result, further studies may investigate other types of claim causes, different phases of building projects, or other types of projects (e.g., industrial projects and infrastructure projects).

ACKNOWLEDGMENTS

The authors gratefully appreciate financial supports for this research project from the ASEAN University Network/Southeast Asia Engineering Education Development Network (AUN/SEED-Net) and the Department of Civil Engineering, Faculty of Engineering, Chulalongkorn University.

REFERENCES

- Apte, B. and Pathak, S. (2016). Review of types and causes of construction claims, *International Journal of Research in Civil Engineering, Architecture and Design*, 4 (2), 43-50.
- Arcadis. (2018). Global construction disputes report 2018: Does the construction industry learn from its mistakes. Arcadis Amsterdam, Netherlands.
- Assaf, S., Hassanain, M. A., Abdallah, A., Sayed, A. M., and Alshahrani, A. (2019). Significant causes of claims and disputes in construction projects in Saudi Arabia, *Built Environment Project and Asset Management*.
- Bu-Bshait, K. and Manzanera, I. (1990). Claim management, *International Journal of Project Management*, 8 (4), 222-228.
- Cárdenas, I. C., Al - Jibouri, S. S., Halman, J. I., and Van Tol, F. A. (2014). Modeling risk - related knowledge in tunneling projects, *Risk analysis*, 34 (2), 323-339.
- Cheeks, J. R. (2003). Multistep dispute resolution in design and construction industry, *Journal of Professional Issues in Engineering Education and Practice*, 129 (2), 84-91.
- Cheung, S. O., Ng, S. T., Lam, K. C., and Sin, W. S. (2001). A fuzzy sets model for construction dispute evaluation, *Construction Innovation*.
- Cheung, S. O. and Pang, K. H. Y. (2013). Anatomy of construction disputes, *Journal of construction engineering and management*, 139 (1), 15-23.
- Cheung, S. O. and Yiu, T. W. (2006). Are construction disputes inevitable?, *IEEE Transactions on Engineering Management*, 53 (3), 456-470.
- Cinar, D. and Kayakutlu, G. (2010). Scenario analysis using Bayesian networks: A case study in energy sector, *Knowledge-Based Systems*, 23 (3), 267-276.
- El-Adaway, I. H. and Kandil, A. A. (2009). Contractors' claims insurance: A risk retention approach, *Journal of construction engineering and management*, 135 (9), 819-825.
- Enshassi, A., Choudhry, R. M., and El-Ghandour, S. (2009). Contractors' perception towards causes of claims in construction projects, *International Journal of Construction Management*, 9 (1), 79-92.
- Etemadinia, H. and Tavakolan, M. (2021). Using a hybrid system dynamics and interpretive structural modeling for risk analysis of design phase of the construction projects, *International Journal of Construction Management*, 21 (1), 93-112.
- Guan, L., Liu, Q., Abbasi, A., and Ryan, M. J. (2020). Developing a comprehensive risk assessment model based on fuzzy Bayesian belief network (FBBN), *Journal of Civil Engineering and Management*, 26 (7), 614-634.
- Heckerman, D. (1997). Bayesian networks for data mining, *Data mining and knowledge discovery*, 1 (1), 79-119.

- Jalal, M. P., Noorzai, E., and Yavari Roushan, T. (2019). Root cause analysis of the most frequent claims in the building industry through the SCoP3E Ishikawa diagram, *Journal of Legal Affairs and Dispute Resolution in Engineering and Construction*, 11 (2), 04519004.
- Jensen, F. V. (2001). *Bayesian networks and decision graphs*. Springer.
- Khahro, S. H. and Ali, T. H. (2014). Causes leading to conflicts in construction projects: A viewpoint of pakistani construction industry, *International Conference on challenges in IT, Engineering and Technology (ICCIET'2014) July*, 17-18.
- Kumaraswamy, M. M. (1997). Conflicts, claims and disputes in construction, *Engineering Construction and Architectural Management*, 4 (2), 95-111.
- Levin, P. (2016). *Construction contract claims, changes & dispute resolution*. American Society of Civil Engineers.
- Likhitrungsilp, V., Ioannou, P. G., and Van, S. Q. (2022). Analyzing the interdependences of claim causes in construction projects, *Proceedings of International Structural Engineering and Construction*, 9 (1).
- Mccabe, B., Abourizk, S. M., and Goebel, R. (1998). Belief networks for construction performance diagnostics, *Journal of Computing in Civil Engineering*, 12 (2), 93-100.
- Mishmish, M. and El-Sayegh, S. M. (2018). Causes of claims in road construction projects in the UAE, *International Journal of Construction Management*, 18 (1), 26-33.
- Mohamad, M. and Tran, D. Q. (2021). Risk-Based Prioritization Approach to Construction Inspections for Transportation Projects, *Journal of Construction Engineering and Management*, 147 (1), 04020150.
- Moura, H. M. P. and Teixeira, J. M. C. (2007). Types of construction claims: a Portuguese survey.
- Olanrewaju, A. A. and Anavhe, P. J. (2014). Perceived claim sources in the Nigerian construction industry, *Built Environment Project and Asset Management*.
- Rezaee, M. J., Yousefi, S., and Chakraborty, R. K. (2019). Analysing causal relationships between delay factors in construction projects: A case study of Iran, *International Journal of Managing Projects in Business*.
- Ruiz-Benítez, R., López, C., and Real, J. C. (2018). The lean and resilient management of the supply chain and its impact on performance, *International Journal of Production Economics*, 203, 190-202.
- Sakate, P. and Dhawale, A. (2017). Analysis of claims and dispute in construction industry, *Int. J. Eng. Sci. Res. Technol*, 6 (5), 523-535.
- Semple, C., Hartman, F. T., and Jergeas, G. (1994). Construction claims and disputes: causes and cost/time overruns, *Journal of construction engineering and management*, 120 (4), 785-795.
- Sharma, V. K., Sharma, S. K., and Singh, A. P. (2019). Risk enablers modelling for infrastructure projects using Bayesian belief network, *International Journal of Construction Management*, 1-18.
- Stamatiou, D. R. I., Kirytopoulos, K. A., Ponis, S. T., Gayialis, S., and Tatsiopoulos, I. (2019). A process reference model for claims management in construction supply chains: the contractors' perspective, *International Journal of Construction Management*, 19 (5), 382-400.
- Viswanathan, S. K., Panwar, A., Kar, S., Lavingiya, R., and Jha, N. K. (2020). Causal Modeling of Disputes in Construction Projects, *Journal of Legal Affairs and Dispute Resolution in Engineering and Construction*, 12 (4), 04520035.
- Yousefi, V., Yakhchali, S. H., Khanzadi, M., Mehrabanfar, E., and Šaparauskas, J. (2016). Proposing a neural network model to predict time and cost claims in construction projects, *Journal of Civil Engineering and Management*, 22 (7), 967-978.
- Zaneldin, E. K. (2006). Construction claims in United Arab Emirates: Types, causes, and frequency, *International Journal of Project Management*, 24 (5), 453-459.
- Zaneldin, E. K. (2018). Investigating the types, causes and severity of claims in construction projects in the UAE, *International Journal of Construction Management*, 20 (5), 385-401.

COMPARISON OF IMMERSIVE AND NON-IMMERSIVE VR GAMES FOR ASSESSING SAFETY KNOWLEDGE.

Sabnam Thapa¹ and Vachara Peansupap².

1) Master's candidate, Department of Civil Engineering, Faculty of Engineering, Chulalongkorn University, Bangkok, Thailand. Email: 63721244021@student.chula.ac.th

2) Ph.D., Assoc. Prof., Department of Civil Engineering, Faculty of Engineering, Chulalongkorn University, Bangkok, Thailand. Email: vachara.p@chula.ac.th

Abstract: One of the major causes of accidents on construction sites is the unsafe behavior of construction personnel. Studies have shown that due to a lack of safety knowledge and experience, workers engage in unsafe behavior. By evaluating the existing safety knowledge, we can develop more specific safety programs, identify individuals prone to accidents, and improve safety knowledge. Recently, Virtual Reality (VR) has been extensively applied in hazard identification, training, and in classroom programs due to its immersive and interactive properties. Furthermore, VR games are effective for safety training, supporting dynamic learning in the classroom, and assessing knowledge, performance, and behavior. Past studies using VR games as assessment tools have employed either fully immersive or non-immersive setups. Both mediums offer equally convincing reasons for being effective in assessing safety knowledge, considering their advantages and disadvantages. However, determining which one, immersive VR or non-immersive, offers better options or preference effects in knowledge assessment could be beneficial for game developers. Thus, the objective of this research is to compare the experience of assessing safety knowledge with immersive and non-immersive VR to determine user preference and fundamental differences in their application. For this purpose, a pilot study was conducted, developing two VR games—an immersive VR game and a non-immersive VR game—and analyzing user preferences. The pilot study determined that most of the participants 63.33% of desktop games and, by extension, expressed a preference for the VR game instead for assessment of their safety knowledge.

Keywords: Safety knowledge, Safety assessment tools, Immersive VR games, Non-immersive VR games, Construction safety management.

1. INTRODUCTION

Despite increased investment in construction safety over the years (as reported by the BLS in 2021), unsafe behavior that leads to fatal and nonfatal accidents remains common on construction sites. A study on why workers engage in unsafe behavior identified eleven factors, and lack of education was one of them. The study found that workers with lower safety knowledge and experience had more accidents. Additionally, it was also stated that if safety knowledge was not improved, the workers continued to practice unsafe behavior. (Choudhry & Fang, 2008). Another research study in aviation, which examined the effect of education on knowledge, behavior, and attitude, concluded that an increase in knowledge positively affected behavior (Chang & Liao, 2009). Moreover, educational field trips and site visits are conducted with the primary objective of imparting site experience to students while enhancing their knowledge and hazard-detection skills (Pham et al., 2018). Thus, safety knowledge is necessary to bring about behavioral change in construction personnel, thereby mitigating accidents.

Virtual reality (VR) games, due to their properties of immersion, interaction, and motivation, have been extensively used in safety management (Wang et al., 2018). In safety training, VR games have been used to train the workforce in safety measures, hazard recognition, and procedural training due to their ability to simulate hazardous conditions while engaging players and giving them a sense of control (Kiral & Comu, 2017; Li et al., 2018; Wang et al., 2018). In education, the immersive simulation, multiplayer interaction, and dynamic learning offered by VR games have been used to impart practical knowledge and skills to students (Wang et al., 2018). Furthermore, VR games are effective in enhancing safety knowledge and skill gain through their ability to facilitate role-playing, dialogic learning, and interaction (Le et al., 2015). Even in children, the use of immersive VR for fire hazard training has been found to increase motivation to learn and interact (Smith & Ericson, 2009). Thus, VR games are reliable tools for enhancing safety education and training.

Most of the previous studies comparing immersive and non-immersive VR have focused on assessing their effectiveness in knowledge gain, knowledge retention, and the type of learning suitable for each. In a study that assessed the knowledge retention of passengers after training them on aviation safety, it was concluded that the use of immersive VR resulted in longer knowledge retention due to higher participant engagement compared to traditional cards (Chittaro & Buttussi, 2015). Another study demonstrated that VR immersion improved memorization powers and provided participants with in-depth experiences through realistic simulations, leading to enhanced practical safety knowledge gain (Froehlich & Azhar, 2016; Xu & Zheng, 2020). Recent studies have compared the impact of immersive and non-immersive VR on procedural and conceptual learning in fire safety and have concluded that immersion improves procedural learning but has no effect on conceptual knowledge.

These studies also found that the feeling of presence did not affect both procedural and conceptual knowledge (Morélot et al., 2021). Another study compared the efficiency of immersive and non-immersive VR as a learning approach and concluded that immersive VR using head-mounted displays (HMDs) is a better option for improving both knowledge and skills. Further research has compared the effects of different types of displays on long-term knowledge gain, sense of presence, and engagement in aviation procedure training, revealing that immersive VR games had the highest sense of presence and engagement, but knowledge gain was achieved with all three types of displays (Buttussi & Chittaro, 2018). Overall, the impact of immersive and non-immersive VR games on knowledge gain is still subject to mixed conclusions (Buttussi & Chittaro, 2017; Morélot et al., 2021).

While much research has been conducted to understand the impact of immersion on safety knowledge attainment, it is also important to determine effective assessment tools to accurately evaluate safety knowledge. There is a need to compare immersive and non-immersive VR in assessing safety knowledge, as different assessment methods evaluate different skills (Assessment methods). Furthermore, the evaluation of safety knowledge has primarily been done through interviews and questionnaires (Checa & Bustillo, 2020; Wu et al., 2020). However, there are other tools, such as VR games, that have proven to be reliable safety assessment tools (Li et al., 2012). Therefore, the objective of this research is to determine user preferences for immersive or non-immersive VR when assessing safety knowledge.

2. METHOD

The main objective of this research is to compare immersive and non-immersive VR games in their role as assessment tools for safety knowledge. To achieve this, two games were developed: one using immersive VR and the other using non-immersive VR, both using the same scenarios and contents. To determine user preferences, participants in the pilot study were required to play both immersive and non-immersive VR games, and their opinions were collected through a Google survey. This study employed an experimental qualitative research approach. The following section provides detailed information about the system design, development, and pilot phase.

2.1 System Framework

A scenario serves as the setting where the game unfolds, and the player engages with the environment. To enhance realism and promote immersion, the developed scenarios were designed with objects, lighting and audio arrangements, and animations. To create the virtual environments, characters, and 3D models were required, which were imported from Maximo, Sketchup, Turbosquid, Free3D, and BIM models, among others. Some models were reconfigured using Blender to ensure they were suitable for the scene. All the models were then imported into Unity software, where the virtual environment was developed. Coding was done using Visual Studio to make the game functional and interactive.

After developing the virtual environment, the input system varied based on the type of module. For the immersive VR game, Unity's paid asset, VRIF framework, was utilized, enabling interactions between the XR Advanced Rig and the environment. In the case of the non-immersive VR game, Unity's First-person starter pack was used, and the interaction occurred between the capsule player and its environment. These choices aligned with the conceptual framework outlined.

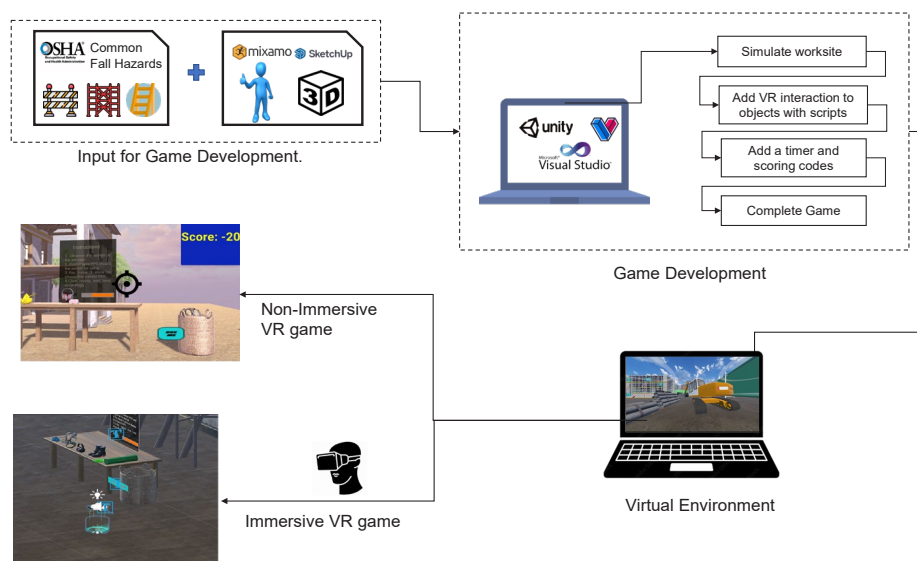


Figure 1 Conceptual framework for Game development.

2.2 Theme of the Game

The game's theme was to evaluate a player's safety knowledge, focusing on their understanding of personal protective equipment (PPE), knowledge of different parts of safety equipment, and comprehension of equipment functions and inspection procedures.

Level I was designed as the easiest level, assessing the player's ability to recognize the appropriate PPE for specific tasks. Level II required players to answer multiple-choice questions, evaluating their capability to identify the parts of safety equipment and understand their functions. Level III aimed to assess the player's knowledge of equipment specifications and inspection procedures. Each category of hazard such as scaffolding had at least three scenes to evaluate the player's knowledge. For non-immersive VR, the scenery and themes were the same. However, they were different in how input was perceived by the game system. In level I of the desktop game, the player had to drag and drop the correct object in the basket. In level II, the player had to use the quiz UI to go to a higher level of say scaffolding. In level II too, the player had to interact with the UI to go to higher levels.

2.2 Comparison of The Immersive and Non-Immersive

The main differences between immersive and non-immersive VR games were in the way players interacted with the virtual environment. In Level I, where players had to drag and drop objects, the immersive VR game utilized controllers for players to perform the dragging and dropping actions, while in the non-immersive VR game, players used the mouse key for this interaction. The controls for player movement also varied, as in the immersive VR game, players used controllers to move anywhere within the virtual environment, whereas, in the non-immersive VR game, movements were achieved using keyboard inputs or mouse clicks.

These distinctions in input and interaction were implemented during the game development process through coding. Specifically, coding was done to enable the controllers' functionality for dragging and dropping objects in the immersive VR game. In the non-immersive VR game, coding was implemented to respond to mouse clicks for object manipulation. Additionally, coding was done to enable controller-based movement in the immersive VR game, while the non-immersive VR game utilized keyboard or mouse click inputs for player movement.

2.3 Pilot Study

A pilot study was conducted with thirty students to assess their preferences for the assessment of safety knowledge. Among the participants, thirty percent had prior safety training, while the remaining seventy percent of construction management students had no prior safety training. However, they had some awareness of safety practices and knowledge related to construction site safety.

In the immersive VR game, the players used an HTC Vive Head-Mounted Display (HMD) and controllers. Of the total of thirty participants, forty percent of them had some experience using this equipment, while the rest sixty percent of the students had no prior experience with VR. To ensure familiarity with the HMD and controllers, a practice session was conducted before the actual gameplay. During this session, each participant practiced grabbing movements and controller-based movements.

The students were made to play the VR game first followed by the desktop game after taking breaks. Immediately following their experience with the non-immersive VR game, the players were required to complete a questionnaire.

3. RESULTS

In this section, we present a set of questions designed to gather valuable insights into the preferences of participants regarding VR games, specifically the use of immersive and non-immersive VR games for assessing safety knowledge. These questions aim to explore various aspects, including participants' prior experience with safety training, their perception of the developed game, their preference for desktop games versus VR games, the influence of immersion on knowledge evaluation, and the effectiveness of immersion for hazard detection. Collecting their responses was aimed at gaining a deeper understanding of the potential of VR technology in safety training and assessment. The following are the Likert scale-based questions that were asked of the players:

- Did you attend any safety training before this study?
- The VR game offered realistic scenarios that required me to apply safety knowledge.
- I prefer desktop games over VR immersive games to check my safety knowledge.
- Level of immersion does not impact my performance in knowledge evaluation.

The following Likert scale evaluation range was referenced from the study (Nyutu et al., 2021) to interpret the results from the questionnaire:

Table 1. Five-point Likert scale evaluation range.

Likert Scale description	Likert- scale	Interval
Strongly disagree	1	1.00 - 1.80
Disagree	2	1.81 - 2.60
Neutral	3	2.61 - 3.40
Agree	4	3.41 - 4.20
Strongly agree	5	4.21 - 5.00

The first question was aimed at assessing if the developed VR game was a good simulation of real-life work conditions and to find if the players find the VR game to be an effective way to learn safety knowledge. The average range was 4.43 meaning that on average the players strongly agree that developed scenarios were realistic and that safety knowledge was necessary to be applied in the scenarios portrayed. About 93.33% of the players agreed or strongly agreed with this statement.

The players' preference between non-immersive VR games and immersive VR games was assessed using the question, "I would prefer a desktop game over a VR game to evaluate my safety awareness," which yielded an average score of 2.23. This indicates that, on average, participants did not prefer desktop games over VR games for knowledge assessment. Approximately 63.33% of the participants favored VR games over desktop games. When asked why some participants chose desktop games, they cited their familiarity and comfort with desktop games as the main reasons. Some also mentioned being new to VR games and experiencing discomfort such as dizziness or having eye problems (wearing glasses), which influenced their preference for desktop games. On the other hand, those who preferred immersive games highlighted the sense of immersion, realism, and overall enjoyable assessment experience. They found the immersive nature of VR games to be engaging and less stressful during the evaluation. Participants who expressed a neutral stance mentioned that immersive VR was like their experience with first-person player games on a desktop, thus they remained neutral. Overall, these findings suggest a positive inclination towards VR games for evaluating safety knowledge, with factors such as immersion, interest, familiarity, and comfort influencing participants' preferences. The discomfort associated with VR experiences and the presence of eye problems were cited as reasons for some participants' preference for desktop games. These factors align with the findings of the study (Pardini et al., 2022). Figure 2 illustrates the results.

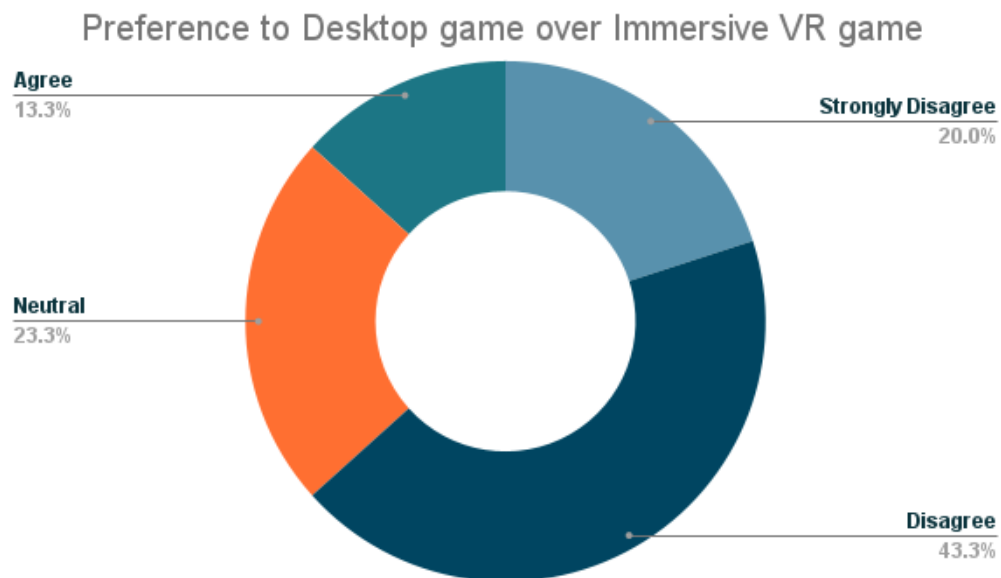


Figure 2. Result of player's preference of Desktop game over VR game for knowledge assessment.

To assess the impact of immersion on knowledge evaluation, we investigated whether the level of immersion affected players' performance. The average Likert scale score indicates that participants had a neutral stance regarding the impact of immersion on their knowledge assessment. Approximately 30% of the participants expressed a neutral response, stating that immersion neither positively nor negatively affected their knowledge assessment. A similar number of participants either agreed (23.3%) or disagreed that the level of immersion influenced their performance. However, most participants did not provide strong reasoning to support either claim

or stated that immersion had minimal influence on their ability to accurately evaluate safety knowledge. These findings align somewhat with the conclusions of a study that suggests immersion does not necessarily enhance conceptual learning (Morélot et al., 2021). The results obtained from our study are demonstrated as follows:

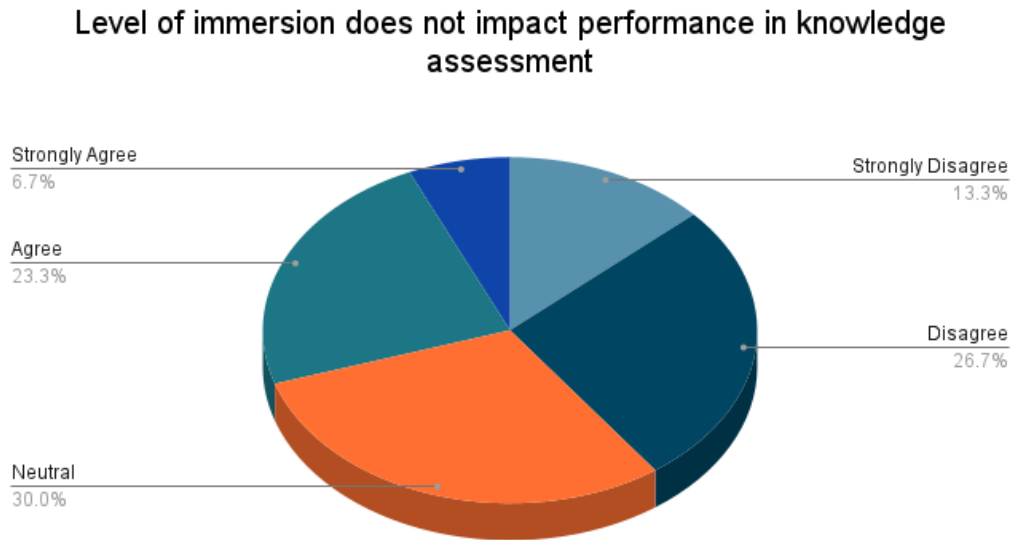


Figure 3. Results about the impact of immersion on performance in Knowledge assessment.

4. DISCUSSION

With the participation of thirty players, the study has reached the following conclusions about the comparison of immersive and non-immersive VR:

1. Participants found immersive VR (IVR) to be more realistic and engaging compared to non-immersive VR (NIVR).
2. Most players preferred IVR over NIVR for their knowledge evaluation due to its realism, higher engagement, and interest, resulting in a more enjoyable assessment experience. This indicates that IVR provides a superior assessment method. The study also highlights the influence of factors such as immersion, interest, familiarity, and comfort on participants' VR preferences.
3. The impact of immersion level on players' performance in knowledge evaluation is moderate. Participants did not perceive a significant influence of immersion on their ability to assess safety knowledge.
4. The study aimed to determine the correlation between training and performance in knowledge assessment, but no significant relationship could be identified.
5. The developed VR game was perceived as an effective simulation of real-life work conditions, scoring an average of 4.43 on the Likert scale. Consequently, the developed VR games serve as reliable assessment tools.

The results align with previous research findings that higher immersion leads to a greater sense of presence, engagement, motivation, and the ability to relate to real-world conditions, which in turn enhances motivation to learn (Checa & Bustillo, 2020). Additionally, the findings resemble another study's conclusion that immersive VR is preferable for procedural knowledge but not for conceptual knowledge (Morélot et al., 2021). The impact of immersion on the performance of participants in knowledge assessment was moderate. The impact of immersion on performance varied amongst the participants. Some participants in the study agreed that immersion had a positive impact on their performance, while others disagreed. This suggests that the impact of immersion may vary depending on the individual's learning style and preferences. However, further research is required to explore this topic and investigate potential factors that may affect the effectiveness of immersion in assessing safety knowledge. Future studies could aim to identify the factors influencing the relationship between immersion and safety knowledge assessment, utilizing larger study groups. Moreover, additional studies could assess the influence of immersion on performance in safety knowledge evaluations.

5. CONCLUSIONS

This study aimed to compare the effectiveness of immersive and non-immersive VR in assessing safety knowledge. It involved thirty participants who played both types of VR games. The results indicate that the developed VR game was perceived as an accurate simulation of real-life work conditions. Most participants preferred immersive VR for their knowledge evaluation due to its realism, higher engagement, and overall enjoyment of the assessment experience. However, factors such as immersion, interest, familiarity, and comfort influenced participants' inclination toward non-immersive VR games. The study also found that the impact of immersion level on participants' performance in knowledge evaluation was moderate, aligning with previous research on the impact of immersion on conceptual learning (Morélot et al., 2021). This information can be valuable for trainers in designing safety training programs tailored to their objectives. In conclusion, the study supports the acceptance of immersive VR over non-immersive VR for assessing safety knowledge, primarily due to participants' higher interest in immersive VR games.

The drawback of this research is that the study participants were limited, and the questionnaire was limited. Further studies could investigate the effects of immersion on performance in safety knowledge evaluations. More studies could aim to identify the factors that influence the connection between immersion and safety knowledge assessment, employing larger study groups.

REFERENCES

- Buttussi, F., & Chittaro, L. (2017). Effects of different types of virtual reality display on the presence and learning in a safety training scenario. *IEEE Transactions on Visualization and Computer Graphics*, 24(2), 1063-1076.
- Buttussi, F., & Chittaro, L. (2018). Effects of Different Types of Virtual Reality Display on Presence and Learning in a Safety Training Scenario. *IEEE Transactions on Visualization and Computer Graphics*, 24(2), 1063-1076. <https://doi.org/10.1109/TVCG.2017.2653117>
- Chang, Y.-H., & Liao, M.-Y. (2009). The effect of aviation safety education on passenger cabin safety awareness. *Safety science*, 1337-1345. <https://doi.org/10.1016/j.ssci.2009.02.001>
- Checa, D., & Bustillo, A. (2020). A review of immersive virtual reality serious games to enhance learning and training. *Multimedia Tools and Applications*, 79(9), 5501-5527. <https://doi.org/10.1007/s11042-019-08348-9>
- Chittaro, L., & Buttussi, F. (2015). Assessing Knowledge Retention of an Immersive Serious Game vs. a Traditional Education Method in Aviation Safety. *IEEE Transactions on Visualization and Computer Graphics*, 21(4), 529-538. <https://doi.org/10.1109/TVCG.2015.2391853>
- Choudhry, R. M., & Fang, D. (2008). Why operatives engage in unsafe work behavior: Investigating factors on construction sites. *Safety science*, 46(4), 566-584. <https://doi.org/10.1016/j.ssci.2007.06.027>
- Froehlich, M. A., & Azhar, S. (2016). Investigating virtual reality headset applications in construction. Proceedings of the 52nd Associated Schools of Construction Annual International Conference,
- Kıral, I., & Comu, S. (2017). *Safety Training for Scaffolding and Formwork Construction by Using Virtual Environment*. <https://doi.org/10.24928/JC3-2017/0281>
- Le, Q. T., Pedro, A., & Park, C. S. (2015). A social virtual reality based construction safety education system for experiential learning. *Journal of Intelligent & Robotic Systems*, 487-506.
- Li, H., Chan, G., & Skitmore, M. (2012). Visualizing safety assessment by integrating the use of game technology. *Automation in Construction*, 22, 498-505. <https://doi.org/10.1016/j.autcon.2011.11.009>
- Li, X., Yi, W., Chi, H.-L., Wang, X., & Chan, A. P. (2018). A critical review of virtual and augmented reality (VR/AR) applications in construction safety. *Automation in Construction*, 150-162.
- Morélot, S., Garrigou, A., Dedieu, J., & N'Kaoua, B. (2021). Virtual reality for fire safety training: Influence of immersion and sense of presence on conceptual and procedural acquisition. *Computers & Education*, 166, 104145. <https://doi.org/10.1016/j.compedu.2021.104145>
- Nyutu, E. N., Cobern, W. W., & Pleasants, B. A. (2021). Correlational Study of Student Perceptions of Their Undergraduate Laboratory Environment with Respect to Gender and Major. *International Journal of Education in Mathematics, Science and Technology*, 9(1), 83-102.
- Pardini, S., Gabrielli, S., Dianti, M., Novara, C., Zucco, G. M., Mich, O., & Forti, S. (2022). The Role of Personalization in the User Experience, Preferences and Engagement with Virtual Reality Environments for Relaxation. *International Journal of Environmental Research and Public Health*, 19(12), 7237.
- Pham, H. C., Dao, N., Pedro, A., Le, Q. T., Hussain, R., Cho, S., & Park, C. (2018). Virtual field trip for mobile construction safety education using 360-degree panoramic virtual reality. *International Journal of Engineering Education*, 34(4), 1174-1191.
- Smith, S., & Ericson, E. (2009). Using immersive game-based virtual reality to teach fire-safety skills to

- children. *Virtual Reality*, 13(2), 87-99. <https://doi.org/10.1007/s10055-009-0113-6>
- Wang, P., Wu, P., Wang, J., Chi, H.-L., & Wang, X. (2018). A Critical Review of the Use of Virtual Reality in Construction Engineering Education and Training. *International Journal of Environmental Research and Public Health*, 15, 1204. <https://doi.org/10.3390/ijerph15061204>
- Wu, B., Yu, X., & Gu, X. (2020). Effectiveness of immersive virtual reality using head-mounted displays on learning performance: A meta-analysis. *British Journal of Educational Technology*, 51(6), 1991-2005.
- Xu, Z., & Zheng, N. (2020). Incorporating Virtual Reality Technology in Safety Training Solution for Construction Site of Urban Cities. *Sustainability*, 13, 243. <https://doi.org/10.3390/su13010243>

IMPLEMENTING THE CIRCULAR ECONOMY CONCEPT IN CONSTRUCTION SUPPLY CHAIN MANAGEMENT OF MODULAR STEEL PROJECTS

Thet Htar San¹ and Veerasak Likhitrungsilp²

1) Master's student, Department of Civil Engineering, Faculty of Engineering, Chulalongkorn University, Bangkok, Thailand.
Email: 6272042621@student.chula.ac.th

2) Ph.D., Assoc. Prof., Department of Civil Engineering, Faculty of Engineering, Chulalongkorn University, Bangkok, Thailand.
Email: veerasak.l@chula.ac.th

Abstract: The circular economy (CE) is a modern economic model where the value of products, materials, and resources is maintained in the economy as long as possible, whereas the generation of waste is minimized. The CE primarily encompasses adding value to technological and biological cycles through design, material manufacturing, construction, and material recycling. Yet, it is a relatively new construction practice, which has been limitedly investigated. This paper examines how to implement the CE concept in construction supply chain management by focusing on modular steel projects. The supply chain, value chain, and life cycle of modular steel projects are thoroughly analyzed to define a modular steel supply chain, which consists of essential activities such as design, manufacturing, fabrication, and construction in a chronological order. We then identify all supply chain actors associated with these activities, their collaboration and interaction, as well as their responsibilities. The paper then examines the actions each actor must carry out in the pre-construction, construction, and post-construction stages. The main actors include architects, contractor, engineer, manufacturer, fabricator, supplier, and dismantler. Implementing circular economy principles in modular steel projects requires effective strategies for the stakeholders' engagement, collaboration, and knowledge sharing. Our results highlight new roles and responsibilities associated with the CE practice each supply chain actor must perform. These findings are a preliminary step toward the implementation of the CE concept in the supply chain of modular steel construction. They can subsequently lead to comprehensive circular supply chain management in the construction industry and can provide valuable insights and recommendations to advance sustainability, resource-efficient, environmentally-friendly built environments, and the circularity in the modular steel construction sector.

Keywords: Circular economy, Construction supply chain management, Circular supply chain, Sustainable construction, Modular steel project

1. INTRODUCTION

The circular economy (CE) is a new economic model that aims to improve the efficiency of resource consumption by reducing waste and increasing the long-term value retention of materials, which reduces the demand for primary resources (Morseletto, 2020). The CE concept focuses on the creation of circular loops of materials, products, energy, and waste flows (Masi et al., 2018). By reducing the depletion of resources and protecting the environment, it significantly contributes to sustainable economic development. Since materials are recycled and reused, the CE also allows the sustainability of resources once a product reaches its end-of-life (EoL) (Di et al., 2017). The rapid rise of CO₂ emissions poses a crucial threat to the environment and a challenge for modern society, which cause people more concern about global climate change (Lou et al., 2017). The use of resources and the economic growth are correlated because both lead to releasing CO₂ (Wang et al., 2011). The connections between energy use, pollution, and economic growth have received a great deal of attention from researchers and politicians in the last decade. This is because obtaining the sustainable economic growth has emerged as the world's leading goal (Antonakakis et al., 2011). The CE is an approach to operating business that supports the economic growth while promoting environmental protection and social advantages (Pisitsankhakarn & Vassanadumrongdee, 2020). A rapidly growing economy of developing countries is the steel industry. Yet, this industry consumes an extensive number of resources and energy. It also generates a great deal of pollutions and emissions (Masi, 2018). Greenhouse gases (GHGs) in the atmosphere are primarily produced by CO₂ emissions, which contribute to climate change and global warming. Unfortunately, a majority of steel manufacturers in emerging countries ignore the value of the environment. According to the CE concept and practices, companies have opportunities and business models to address this issue (Pomponi & Moncaster 2016). By enabling the use of secondary raw materials to build new value networks, the CE expands business opportunities for the steel construction sector (Mura et al., 2020). Organizations can become more competitive by implementing a circular economy since it can enhance both economic and environmental performances. However, there are still many fundamental questions that need to be addressed such as what drives the CE, what challenges it faces, and what opportunities it offers. This paper examines how the circular economy can be implemented by focusing on the steel construction industry in Thailand as a case study. The research gap in implementing circular economy in modular steel projects is determined from the existing knowledge in this specific area. It indicates the need for further research to address the gaps and advance the concept of circular economy principles in the context of

modular steel construction.

1.1 Circular Economy for Steel Construction

In the context of circular economy initiation, design, and construction for steel, several key principles and practices can be implemented to promote sustainability and circularity. Figure 1 displays the framework for measuring CE performance adapting from Wibowo et al. (2018).

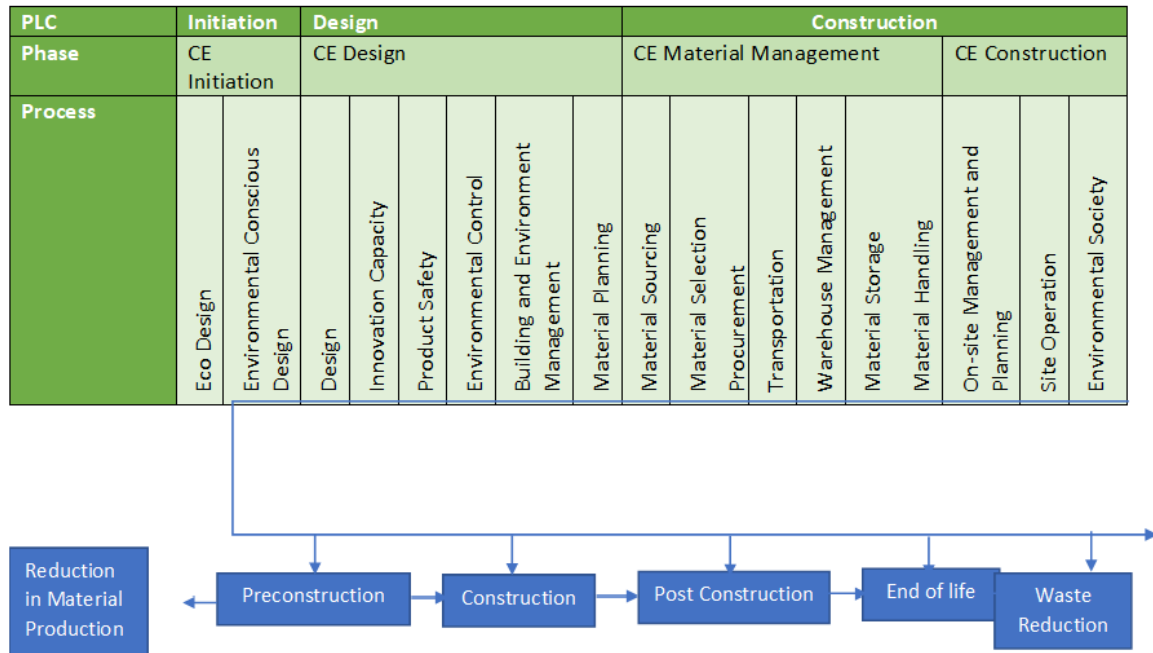


Figure 1. Framework for measuring CE performance (adapted from Wibowo et al., 2018)

Steel materials can be produced from high recycled contents through environmentally friendly manufacturing processes. Suppliers can perform sustainable sourcing practices such as using recycled scrap steel or renewable energy for steel production. Utilizing the modular and prefabricated construction techniques allows efficient assembly and disassembly of steel components. This approach facilitates easy replacement or reconfiguration of building elements, reducing waste, and enabling future adaptability. In this paper, we propose a comprehensive methodology to identify various barriers that hinder the sustainable development of the construction sector. We begin with summarizing the current state of the CE knowledge for modular steel buildings. Then, we investigate actors, actions, and factors that influence the circular economy concept in construction and foster collaboration and communication among stakeholders involved in modular steel construction. Engaging architects, engineers, contractors, and steel manufacturers contributes to a holistic approach to circular economy principles. We should encourage knowledge sharing of CE, innovation, and the adoption of best practices throughout modular steel projects.

2. METHODOLOGY

Implementing circular economy principles in construction requires a systematic approach that integrates sustainable practices throughout the project life cycle. First, we need to compile and analyze the existing knowledge and practice about the circular economy (CE) adoption in the Thai construction sector. Since the existing knowledge and practice about the CE in practice was quite limited, a qualitative research approach was adopted. Saunders et al. (2009) defined those interviews be a purposeful discussion among two or more parties, which can facilitate deriving valuable and in-depth insights regarding a particular area of study. Capturing the opinions of the subject matter experts provides an opportunity to gather in-depth insights through their experience and knowledge (Dawson, 2007). Thus, pursuant to the qualitative research approach and the nature of this research problem, semi-structured interviews were adopted for the main data collection technique for this research. Semi-structured interviews can be used to gather specific information for comparisons and simultaneously collect additional information expressed by interviewees during the data collection process. This may involve various methods such as surveys, interviews, site visits, and document analysis. The data collected should be sufficient to address the research questions and provide insights into circular economy practices in construction. Before interviewing them, we need to create the workflow activities of steel project, which is integrated with the main

actors of each activity of modular steel projects first. This will assist in developing a clear roadmap for implementing circular economy principles throughout the project life cycle, setting specific targets, and identifying key actions for every activity. Herein, we interviewed seven parties, namely, architects, contractors, engineers, manufacturers, fabricators, suppliers, and dismantler, who are aware of the CE concepts and have diverse backgrounds, experiences, or perspectives related to the CE. They are construction professionals with a minimum of 5 years of experience in roles such as construction project managers, architects, engineers, contractors, or subcontractors.

3. RESULTS

Table 1 displays the profile of the participants in this research. This paper is based on the implementation of 6R principles of the circular economy: reduce, reuse, recycle, redesign, reclassification, and renewability. The 6R principles provide a set of guidelines that promote sustainability and resource efficiency. Table 2 summarizes the CE practices in the pre-construction, construction, and post-construction stage of modular steel projects. It also displays the responsibilities of each actor in each stage of the project. The details of these findings associated with the 6R principles are as follows.

3.1. Awareness on the CE Concept in The Thai Construction Industry

The interviewees opined that knowledge and awareness on the concepts of CE was at a very primitive stage in the Thai construction industry. Furthermore, although the CE concept is not popular, certain CE principles is currently being implemented in construction projects.

Table 1. Profile of the research participants

Interview code	Designation	Experience in the construction sector (years)
A	Architects	12
C	Contractor	10
E	Engineer	14
M	Manufacturer	20
F	Fabricator	15
S	Supplier	6
D	Dismantler	5

3.2. Reduction Principle (R1)

The reduction principle (R1) can be implemented during the pre-construction phase by adopting construction standard practices. For example, the architects who participated in this research emphasized the importance of designing building elements which conform with the globally used standard sizes. Meanwhile, the other research participants highlighted the importance of reviewing the designs to reduce resource consumption and minimize wasteful resource allocation.

3.3. Reuse Principle (R2)

The reuse principle (R2) is identified by a majority of respondents. It encompasses the reuse of material recovered from disposal waste. Among all the actors, the supplier is most experienced in identifying which construction materials can be reused. Per the interviews, the contractors, engineers, and architects agreed that proper scheduling and record-keeping to determine the number of times (years) of usage of material (e.g., formwork) and equipment (e.g., site furniture and computers) can promote reuse in the construction sector. Furthermore, the contractor should double-check quantities before ordering materials to ensure that they are entirely used or reused (if possible). The contractor should also render the detailed specifications of materials in implementing the reuse principle. Ultimately, all the interviewees agreed that the public agencies must initiate, promote, and support construction waste recycling.

3.4. Recycle Principle (R3)

All the research participants were familiar recycling. However, they opined that the full benefits of recycling were not reaped for the Thai construction industry. A majority of the experts suggested that it be necessary to develop a schedule of recyclable resources. Since construction materials usually have long life cycles, specifying recycling methods at the design stage might not be feasible due to changes of construction and recycling technologies over time. However, this is viable for temporary structures and structures designed for a short-term use. Contractors have a significant role in steel construction material reuse. Some participants, including the contractor, fabricator, and engineer pointed out that many simple acts of recycling waste could be implemented during the pre-construction stage. For example, tendering and procurement activities, which rely heavily on paper-based approaches, should be digitally transformed.

3.5. Redesign Principle (R4)

According to a designer who participated in this research, during the design process, architects tend to focus more on aesthetics over effective resource utilization. If a CE model is to be adopted, architects should be encouraged to focus on effective use of resources without solely focusing on aesthetic aspects. The use of modular building designs, which facilitates prefabrication and factory-based production was also advocated by architects because it improves resource optimization and minimizes the generation of construction waste. Engineers emphasized the necessity to consider the potential for disassembly at the end-of-life during project design, particularly for the structures erected for a shorter use phase. In addition, the industry must promote using standardized connections that facilitate dismantling and reuse, minimizing the use of composite materials, and developing accurate as-built drawings. A majority of the research participants believed that although the CE concept is not well established in Thailand, it is worthwhile to note that certain aspects of the CE have already been implemented in practice.

Table 2. Circular economy practices and the responsibilities of each actor in the three project stages

Pre-construction	Construction	Post-construction
Practices The circular economy approach focuses on designing buildings or infrastructures with the goal of minimizing the amount of steel required. This can be achieved by using alternative materials or designing structures, which are more efficient, durable, and lightweight. By reducing the amount of steel needed, we can minimize the environmental impact of steel production and save resources.	Practices During construction, the circular economy approach involves using sustainable practices to reduce waste and maximize the use of resources. For example, construction waste can be minimized by recycling and repurposing materials such as steel scrap. Steel structures can also be designed to be disassembled and reused in future construction projects, which can further minimize waste and conserve resources.	Practices After construction, the circular economy approach involves designing steel products for long-term use and recycling at the end of their useful life. Steel products should be designed for easy disassembly and recycling, which make it possible to recover and reuse valuable resources such as steel, iron, and other metals. Recycling steel also reduces the need for virgin materials and minimizes the environmental impact of steel production.
Responsibilities Clients: Initiate the project and determine the requirements of the steel product Designer: Create the designs and engineering specifications for steel products Manufacturer: Produce the steel products according to the specifications provided by the designer Supplier: Supply the steel products to the construction site Contractor: Work with customers, designers, and manufacturers to plan and design the installation or construction of the steel product. Subcontractor: Provide accurate cost estimates, collaborating with the project team, offering technical expertise, ensuring regulatory compliance, and negotiating subcontract agreements Consultants: Collaborate with the project owner to define project objectives, scope, budget, and schedule	Responsibilities Clients: Maintain effective communication and collaboration with project stakeholders, including the project team, regulatory authorities, and local communities Contractors: Install and construct the steel products Supplier: Supply materials and equipment required for the installation or construction of the steel products Subcontractor: Hired by the contractor to perform specialized tasks such as welding Consultants: Evaluate and respond to requests for design changes, assessing impacts on cost, schedule, and quality	Responsibilities Clients: End users of the steel products and are responsible for their maintenance and repair Contractor: Provide maintenance and repair services for the steel products Supplier: Provide replacements parts or materials as needed Subcontractor: Effectively communicate, collaborate, and promptly resolve any outstanding issues, which is key to ensuring client satisfaction and maintaining positive working relationships Consultants: Assess the performance and functionality of the completed project based on user feedback, operational data, and sustainability goals. Recycler: Involved in the end-of-life stage of the steel products, recycling it to reduce waste and conserve resources

3.6. Reclassification Principle (R5)

This concept was new to our interview participants because its implementation is quite limited in the Thai construction industry. Only a few participants could opine about this issue. Based on the definition of reclassification, they stated that the pre-construction stage is the ideal stage for the implementation of this principle because most material-related decisions are made in this stage. The lack of understanding on this principle was considered by the interviewees as a crucial barrier towards its implementation and highlighted the necessity of improving awareness among all actors of the construction sector in Thailand.

3.7. Renewability Principle (R6)

Renewability or renewable energy strategies are currently implemented by all interview participants with the aim of reducing the environmental impact created by non-renewable energy sources. The CE concept places renewable energy as their main energy source in order to improve the flexibility of the economic system. It highlights the dominant role of clients in implementing this principle. This is because the high initial cost of renewable energy repels clients for adopting the CE. It is the responsibility of construction actors to make clients aware of the potential life-cycle cost savings that can be achieved through renewable energy despite the high initial capital. Moreover, convincing stakeholders to use renewables was identified as means of implementing this principle.

4. DISCUSSION

In this paper, we compiled the consensus of a group of experts' opinion on the adoption of the CE concept (6R principles) during the pre-construction stage of modular steel projects in Thailand. It was found that the 6R-related decisions should be enforced since the design process. This is endorsed by the findings of Bragança et al. (2014) and Tennakoon et al. (2019a) on the importance of making crucial decisions during the preconstruction stage. For the reuse principle (R2), it was suggested that we must increase the reuse of construction waste materials. This result conforms with the findings by Barker (2008), which discouraged sending waste materials for landfilling. For the recycle principle (R3), the strategies that can be implemented during the pre-construction stage include obtaining materials from green-certified suppliers and creating a schedule of recyclable resources. These results are consistent with the findings by Adi and Wibowo (2020) on the application of the CE concept to construction practices. To ensure the circularity of resources, construction materials should ideally be procured from green certified suppliers. The redesign approaches (R4) have been adopted by the construction industry through initiatives such as design for deconstruction (Chileshe et al., 2016b), which focuses on disassembly during building design. According to the design concept, it is also acceptable to adopt modular designs, which have been mentioned in the reuse principle (R2) (Patwa et al., 2020). Regarding the renewability principle (R6), it was recommended that the construction industry adopts new technologies for power generation. These recommendations are in accordance with the findings by Hargroves et al. (2014), which discovered how to design buildings such that renewable energy sources may be implemented more easily. Adoption of CE principles extent to which the interviewed stakeholders in the steel construction industry have embraced the 6R principles of circular economy. The results also include the benefits and challenges associated with implementing circular economy principles in modular steel construction and the positive environmental impacts such as reduced resource consumption, minimized waste generation, and lower carbon footprint. We also observe potential challenges faced by stakeholders, such as technological limitations, cost considerations, and regulatory constraints. This could include advancements in material recycling, energy recovery, or design methodologies that promote reuse and remanufacturing. The importance of collaboration among stakeholders in the steel construction industry for effective implementation of circular economy principles where interviewees mentioned collaborations with suppliers, contractors, or other industry partners to optimize resource utilization and promote circular practices. Finally, the research participants emphasized the significance of knowledge sharing and the role of industry networks and associations in disseminating best practices. Table 3 summaries the activities of each circular supply chain actor according to the 6R principles in the pre-construction stage.

5. CONCLUSIONS

The circular economic model (resources-production-waste-renewable resources) is replacing the conventional linear economic model (take-make-dispose), which ensures that maximum use is realized from available resources. Due to the greater flexibility offered for adopting change and the lower cost of change, the pre-construction stage was chosen in this paper as the ideal stage for implementing the principles of CE. This paper focuses on how the 6R principles of CE (i.e., reduce, reuse, recycle, redesign, reclassification, and renewability) can be implemented during the pre-construction stage of a construction project. We identified various activities related to each of the 6R principles that should be taken during the pre-construction phase. Understanding the current and potential applications of the 6R principles is an initial step towards realizing the practical implementation of CE. Implementing CE principles in the pre-construction stage of modular steel construction presents a valuable opportunity to create more sustainable and resource-efficient circularity buildings. By

considering design optimization, sustainable material sourcing, waste reduction, and resource optimization, stakeholders can contribute to a more circular and resilient construction industry, reducing environmental impacts while unlocking economic and social benefits. Per our findings, the current expertise regarding the concept of CE is quite limited in the Thai construction industry. This is a major barrier for the successful implementation of CE. Thus, it is necessary to disseminate knowledge about CE to every actor in the construction industry. Meanwhile, important issues concerning the implementation of CE need to be addressed via research works.

Table 3. Activities of each actor for the 6R principles in the pre-construction stage

Circular Economy Principle	Activities	Architect	Contractor	Engineer	Manufacturer	Fabricator	Supplier	Dismantler
Reduce	Adopt standard dimensions in designs	/						
	Review completed designs to identify opportunities for waste minimization		/	/	/	/	/	/
	Obtain experts' input for the design process	/		/				
Reuse	Reuse construction waste materials	/			/	/	/	/
	Double-check material quantities before ordering		/	/				
	Maintain detailed specifications of materials		/	/				
	Properly schedule to keep track of material usage	/	/	/				
	Adopt new technologies for services		/					
Recycle	Develop a schedule of recyclable resources		/	/	/	/	/	/
	Procure materials from green certified suppliers		/					
	Create channels for selling or transferring waste materials, which cannot be treated at site level to third parties			/				
Redesign	Follow design optimization techniques	/	/	/	/	/	/	/
	Balance aesthetics with effective material utilization	/						
	Adapt modular construction techniques	/						
	Focus on disassembly during building design			/				
	Follow environmental standards and sustainable construction guidelines	/		/				
	Review completed project designs to ensure circularity principles envisaged are achieved		/	/	/	/	/	/
Re-classification	Introduce new product specifications focusing re-classification	/	/	/				
Renewable	Convince clients on the potential for life cycle cost savings through the use of renewables	/	/	/	/	/	/	/
	Adopt new technologies for power generation (e.g., recovery of waste energy)		/	/	/	/	/	/

ACKNOWLEDGMENTS

The authors gratefully appreciate financial supports for this research from the Chulalongkorn University's Graduate Scholarship Programme for ASEAN or Non-ASEAN Countries and Department of Civil Engineering, Faculty of Engineering, Chulalongkorn University.

REFERENCES

- Adi, W.T.J. and Wibowo, P. (2020), “Application of circular economy in construction industry”, *IOP Conference Series: Materials Science and Engineering*, 849, 012049.
- Antonakakis, N., Chatziantoniou, I. and Filis, G. (2017) ‘Energy consumption, CO2 emissions, and economic growth: *An ethical dilemma*’, *Renewable and Sustainable Energy Reviews*. Elsevier, 68(October 2015), pp. 808–824. doi: 10.1016/j.rser.2016.09.105.
- Barker, M. (2008), “Time to bin industry’s lavish habits”, available at: <https://www.constructionnews.co.uk/archive/time-to-bin-industrys-lavish-habits-18-03-2008/>.
- Bragança, L., Vieira, S.M. and Andrade, J.B. (2014), “Early-stage design decisions: the way to achieve sustainable buildings at lower costs”, *Science World Journal*, Vol. 2014, 365364.
- Chileshe, N., Rameezdeen, R. and Hosseini, M.R. (2016a), “Drivers for adopting reverse logistics in the construction industry: a qualitative study”, *Engineering Construction and Architectural Management*, 23(2), 134–157.
- Carrascosa, D.H.; van Hove, E.P.; Bolea, J.; Toran, J.I.T.; Muñoz, L.R. Grupo de trabajo GT-6 Congreso Nacional del Medio Ambiente 2018 Fundación Conama,. Available online: http://www.conama.org/conama/download/files/conama2018/GTs%202018/6_final.pdf (accessed on 16 November 2021).
- Dawson, C. (2007), *A Practical Guide to Research Methods: A User-Friendly Manual for Mastering Research Techniques and Projects*, 3rd ed., Oxford: How to Books, Oxford.
- Di, F., Carlo, P., Baldé, K. and Polder, M. (2017) ‘Resources, Conservation and Recycling Measuring resource efficiency and circular economy: *A market value approach*’, *Resources, Conservation & Recycling*. Elsevier B.V., 122, 163–171. doi: 10.1016/j.resconrec.2017.02.009.
- Hargroves, K., Gockowiak, K., Wilson, K., Lawry, N. and Desha, C. (2014), *An Overview of Energy Efficiency Opportunities in Structural Engineering*, The University of Adelaide and Queensland University of Technology (The Natural Edge Project), commissioned by the Australian Government Department of Industry, Canberra.
- Lou, E. C. W., Lee, A. and Welfle, A. (2017) ‘Greenhouse gases (GHG) performance of refurbishment projects – Lessons from UK higher education student accommodation case studies’, *Journal of Cleaner Production*, 154, 309–317. doi: 10.1016/j.jclepro.2017.03.226.
- Masi, D., Kumar, V., Garza-Reyes, J. A. and Godsell, J. (2018) ‘Towards a more circular economy: exploring the awareness, practices, and barriers from a focal firm perspective’, *Production Planning and Control*, 29(6), 539–550. doi: 10.1080/09537287.2018.1449246.
- Morseletto, P. (2020) ‘Targets for a circular economy’, *Resources, Conservation and Recycling*. Elsevier, 153 (October 2019), p. 104553. doi: 10.1016/j.resconrec.2019.104553.
- Makanae, K. and Dawood, N. (2009). *Development and evaluation of a tangible terrain representation system for highway route planning*, *Computer-Aided Civil and Infrastructure Engineering*, 24 (3), 225–235.
- Mura, M., Longo, M. and Zanni, S. (2020) ‘Circular economy in Italian SMEs: *A multi-method study*’, *Journal of Cleaner Production*. Elsevier Ltd, 245, 118821. doi: 10.1016/j.jclepro.2019.118821.
- Patwa, N., Sivarajah, U., Seetharaman, A., Sarkar, S., Maiti, K. and Hingorani, K. (2020), “Towards a circular economy: an emerging economies context”, *Journal of Business Research*, 122, 725–735.
- Pisitsankhakarn, R. and Vassanadumrongdee, S. (2020) ‘Enhancing purchase intention in circular economy: Empirical evidence of remanufactured automotive product in Thailand’, *Resources, Conservation and Recycling*. Elsevier, 156(November 2018), p. 104702. doi: 10.1016/j.resconrec.2020.104702.
- Pomponi, F. and Moncaster, A. (2016) ‘Circular economy for the built environment: *A research framework*’, *Journal of Cleaner Production*. Elsevier Ltd, 143, pp. 710–718. doi: 10.1016/j.jclepro.2016.12.055.
- Saunders, M.N., Lewis, P. and Thornhill, A. (2009), *Research Methods for Business Students*, 5th ed., Pearson Education, Harlow.
- Tennakoon, G.A., Waidyasekara, A. and Ekanayake, B.J. (2019a), “A conceptual framework to optimize the impact of embodied energy and operational energy in buildings during the design stage”, *International Conference on Industrial Engineering and Operations Management*.
- Wang, S. S., Zhou, D. Q., Zhou, P. and Wang, Q. W. (2011) ‘CO2 emissions, energy consumption and economic growth in China: A panel data analysis’, *Energy Policy*. Elsevier, 39(9), 4870–4875. doi: 10.1016/j.enpol.2011.06.032.
- Wibowo, M.A.; Handayani, N.U.; Mustikasari, A. Factors for implementing green supply chain management in the construction industry. *J. Ind. Eng. Manag.* 2018, 11, 651–679.

MARKOV DETERIORATION HAZARD MODEL FOR ROAD NETWORK DETERIORATION FORECAST FOR NATIONAL ROAD NETWORKS IN LAO PDR

Souvikhane Hanpasith¹, Kotaro Sasai², and Kiyoyuki Kaito³

1) Ph.D. Candidate, Department of Civil Engineering, Division of Global Architecture, Graduate School of Engineering, Osaka University, Osaka, Japan. E-mail: souvikhane@civil.eng.osaka-u.ac.jp; Department of Planning and Finance, Ministry of Public Works and Transport, Vientiane Capital, Lao PDR, E-mail: souvikhane@gmail.com

2) Specially Appointed Researcher, Department of Civil Engineering, Division of Global Architecture, Graduate School of Engineering, Osaka University, Osaka, Japan. E-mail: k.sasai@civil.eng.osaka-u.ac.jp

3) Ph.D., Assoc. Prof.; Department of Civil Engineering, Division of Global Architecture, Graduate School of Engineering, Osaka University, Osaka, Japan. E-mail: kaito@ga.eng.osaka-u.ac.jp

Abstract: The primary objectives of road management systems are to estimate short- and long-term budget demands and establish a priority list of projects under fiscal constraints. Understanding road network deterioration is critical for predicting future conditions and developing appropriate maintenance and rehabilitation strategies. Various factors affect the deterioration speeds of road surfaces including traffic volume and environmental conditions, which are also the main uncertainties in developing the deterioration model, particularly for the Lao road management system. This paper aims to develop a road deterioration forecasting model using a Markov deterioration hazard model for prediction of the deterioration process for the national road network in Lao PDR using the international roughness index. The Markov deterioration hazard model estimates the hazard rates which are used to determine the Markov transition probabilities between the pavement's condition states defined on a discrete scale during inspection time. Then, the estimated transition probabilities can be used to forecast and predict life expectancy. The Markov deterioration hazard model is also capable of handling roughness condition data containing irregular inspection intervals. The empirical study used historical roughness index records to develop the model, incorporating traffic volume and pavement type data from the Lao national road maintenance system. The data set from the Lao road management system was composed of 22 road sections totaling 2,769 km in length. The results reveal the service life expectancy of two core networks, core network 1 and core network 2, to be 9.28 and 7.51 years, respectively. The analyses on deterioration process and life expectancy help the Lao road management system improve its road maintenance strategy, determine the maintenance period, and prioritize road network sections for maintenance. Furthermore, this study's results could support decision-making in terms of performance-based road contracts for maintenance.

Keywords: Road management; Deterioration prediction; Markov hazard model; Bayesian estimation method; Laos RMS.

1. INTRODUCTION

The Highway Development Management Application (HDM-4) (Kerali, 2001) is used by the Lao PDR's road maintenance management system to set priorities and allocate maintenance funds. The Laos national road network used the concept of core network level to classify the road hierarchy by different pavement structures, traffic, and environmental conditions. Three levels of the core network were introduced in order to classify the hierarchy of the national roads. The level of the core network is the key to determining inspection and maintenance frequencies. The total length of the road network in 2021 is 58,875 km and was categorized into six types: 1) National Roads, 2) Provincial Roads, 3) District Roads, 4) Urban Roads, 5) Rural Roads, and 6) Special Roads (MPWT, 2022). The lengths of the road network by category are shown in Figure 1.

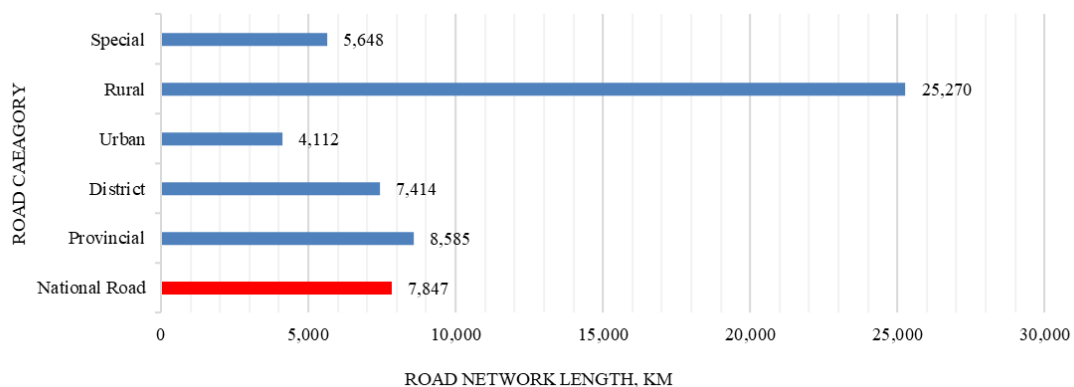


Figure 1. Lao PDR road network length by category in Year 2021

HDM-4, which is a mechanistic model, is a tool to predict road network maintenance needs (Li et al., 1997). Besides, the Pavement Management System (PMS) is the Road Management System's module for optimal road maintenance in Lao PDR. However, the main objections to implementing road management system are budget constraints and limited technical resources. Furthermore, PMS is used to calculate road network deterioration and estimate maintenance needs by relating roughness to many explanatory variables such as pavement aging, surface distress, and the environment where the road is located for precise estimation, evaluate road damages based on current condition inspection data, and then allocate funding (Robinson et al., 1998). However, the number of data records is small and inspection intervals are uneven because data collection is time-consuming, resource-intensive, and costly, which are the major challenges for the Department of Roads (DoR) and the Ministry of Public Works and Transport (MPWT) in implementing the PMS.

The international roughness index (IRI) was introduced by researchers from the United States, Brazil, Belgium, France, and England (Sayers et al., 1986). IRI has been used globally as one significant indicator for evaluating the pavement quality of the road network. This research intends to construct a road deterioration forecasting model to estimate the life expectancy based on the IRI by using Markov transition probability (Madanat et al., 1995). The empirical analysis was conducted using historical inspection data from the Lao road database and covered two core networks (core networks 1, which are the ASEAN Highways, and core network 2, which represents the National Roads) composed of 22 road sections totaling 2,769 km in length. The findings of this study will enable the road authorities (DoR, MPWT) to understand the service life expectancy of each different level of the core network and determine the best maintenance management plan, particularly for the approval of performance-based contracts for road maintenance projects.

2. METHOD

The Markov models have been adapted to meet the needs of various study fields and are now extensively used as a probabilistic estimation model for infrastructure performance. To estimate the Markov deterioration hazard model (Han et al., 2014; Tsuda et al., 2006), the explanatory variables that are anticipated to be related to the rate of deterioration together with the pair of two conditions from a single point and their interval time of inspection have been acquired and collected. Therefore, past inspection data of the road network have been gathered and analyzed, and the road database has been acquired from the DoR and MPWT of Lao PDR in order to develop a road deterioration prediction model utilizing the Markov deterioration hazard model. According to a time series, the condition state of each road section is designated in a rank order. In order to compare the lifespan of each type of pavement, the 2,769 km of road sections' conditions have been collected and categorized.

2.1. Markov Deterioration Hazard Model Estimation

The following presumptions are required in order to apply the Markov deterioration hazard model (Kobayashi et al., 2010):

1. No maintenance or restoration projects were required throughout the inspection period.
2. The deterioration of the road surface begins as soon as it is made available to the public at time τ_0 .

The deterioration of road sections is accumulated in time series. It is expressed in terms of calendar time by $\tau_1, \tau_2, \tau_3, \dots, \tau_i$ and the condition state is increased in unitary unit, the condition state at each point in the time axis is restricted by the time at the inspection was carried out as shown in Figure 2, τ represent a calendar time and condition state is expressed by a rank represents a state variable $i (i = 1, 2, \dots, j)$ where $i = 1$ represents for a section that has not deteriorate at all (in good condition), and the state variable value j is assumed to increase as deterioration progresses. Where $i = j$ indicates that a section has reached its service life (absorbing state of

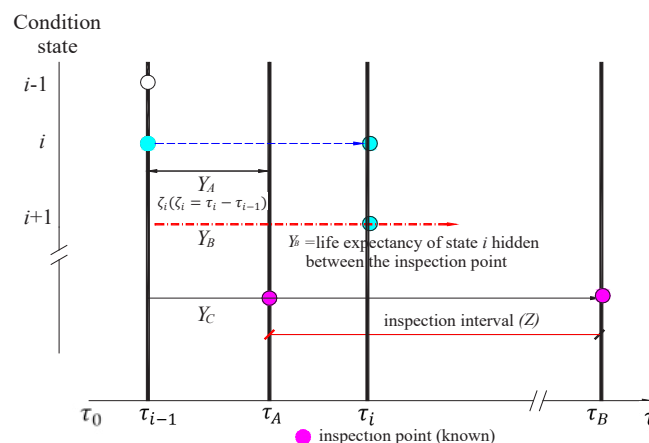


Figure 2. Deterioration process and inspection times.

the Markov chain which requires maintenance activities)

The information on the periodic deterioration process of the road section is derived at the time of inspections. However, data on condition state based on continuous inspection is difficult to obtain due to the high cost, time, and resources required. Therefore, the Markov chain concept, it is assumed that the pavement conditions are discrete condition states. This model considers two periodical inspections at time τ_A and τ_B on the time axis which its interval is denoted by $Z(Z = \tau_B - \tau_A)$ and the duration from $i = 1$ to $i = j$ is called the life expectancy of the road sections. Based on these definitions, we can determine the Markov transition probability matrix (MTP) (Norris, 1998) or Π which composed of probability π_{ij} with the preconditions that $\pi_{ij} \geq 0$ and $\sum_{j=1}^J \pi_{ij} = 1$ are required to satisfy the axioms of probability, since the model does not consider repairs, $\pi_{ij} = 0(i > j)$ and $\pi_{ij} = 1$ become additional preconditions.

$$\text{Prob}[h(\tau_B) = j | h(\tau_A) = i] = \pi_{ij} \quad (1)$$

$$\Pi = \begin{bmatrix} \pi_{11} & \cdots & \pi_{1J} \\ \vdots & \ddots & \vdots \\ 0 & \cdots & \pi_{JJ} \end{bmatrix} \quad (2)$$

In Figure 2, it is supposed that at time τ_A , the condition state observed by inspection is i ($i=1, 2, \dots, J-1$). The deterioration process in future times is uncertain. Among the infinite set of possible scenarios describing the deterioration path, only one path is finally realized. For simplicity there are four possible sample paths described in Figure 3, as follows (Tsuda et al., 2006) :

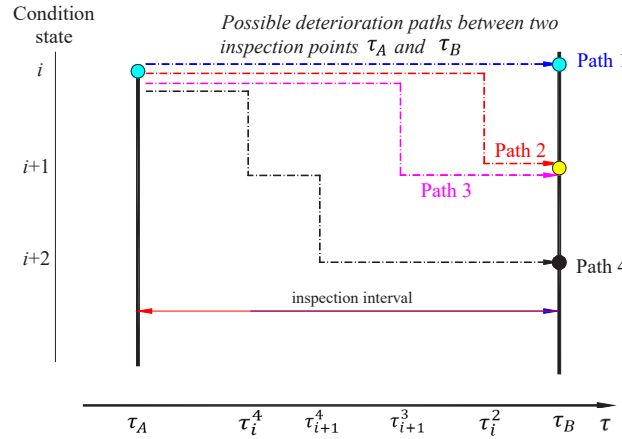


Figure 3. Condition states and possible paths (Kobayashi et al., 2010) (Tsuda et al., 2006)

- Path 1 indicates no transition in the condition state i during the periodic inspection interval.
- Path 2 indicates the transition of the pavement from condition state i to $i + 1$ at time τ_i^2 .
- Path 3 indicates the transition of the pavement from condition state i to $i + 1$ at time τ_i^3 .
- Path 4 indicates the transition of the pavement from condition state i to $i + 1$ and $i + 2$ at time τ_i^4 and τ_{i+1}^4 respectively. The condition state observed at τ_B is $i + 2$

Referring to Figure 2, the deterioration paths of the road pavement condition by the Markov chain concept are expressed, when deterioration status changes from i to $i + 1$ at τ_i , the duration remains at status i can be expressed by $\zeta_i(\zeta_i = \tau_i - \tau_{i-1})$. The life expectancy of a condition state i is assumed to be a stochastic variable with a probability density function $f_i(\zeta_i)$ and distribution function $F_i(\zeta_i)$. The distribution function $F_i(\zeta_i)$ represents the cumulative probability of the transition in the condition state for i to $i + 1$ when i is set at the initial point $y_i = 0$ (time τ_{i-1}). The cumulative probability $F_i(y_i)$ of a transition in the condition state i during the time points interval $y_i = 0$ to $y_i \in [0, \infty]$ is defined as:

$$F_i(y_i) = \int_0^{y_i} f_i(\zeta_i) d\zeta_i \quad (3)$$

Accordingly, the survival function $R_i(y_i)$ becomes $R_i(y_i) = \text{prob}\{(\zeta_i \geq y_i) = 1 - F_i(y_i)$. The deteriorating process that satisfies the Markov property can be represented by the exponential hazard function. The probability density $\lambda_i(y_i)$, which is referred to as the hazard function, is defined in the domain $[0, \infty]$ as:

$$\lambda_i(y_i) = \frac{f_i(y_i)}{R_i(y_i)} = \frac{\frac{dR_i(y_i)}{dy_i}}{R_i(y_i)} = \frac{e}{dy_i} (-\log R_i(y_i)) \quad (4)$$

By hazard function $\lambda_i(y_i) = \theta_i$, the probability $R_i(y_i)$ that the life expectancy of the condition state i

remains longer than y_i and its probability density function $f_i(\zeta_i)$ are expressed by the following:

$$R_i(y_i) = \exp\left[-\int_0^{y_i} \lambda_i(u) du\right] = \exp(-\theta_i y_i) \quad (5)$$

$$f_i(\zeta_i) = \theta_i \exp(-\theta_i \zeta_i) \quad (6)$$

2.2. Determination of Markov Transition Probability

Again, in Figure 3 the various deterioration paths are classified into $\pi_{ii}, \pi_{i,i+1}, \pi_{i,i+2}$, and π_{ij} . The Markov transition probabilities for these possible paths are based on the exponential hazard model can be explained for the three cases considering the condition state observed at periodic inspection time point as shown in Figure 4.

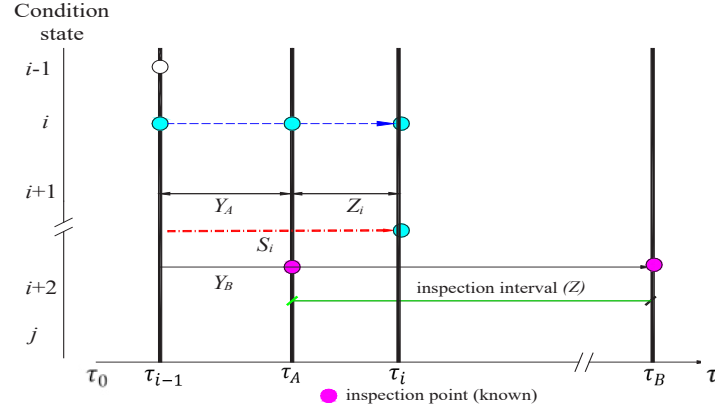


Figure 4. Periodic inspection practice of the condition state.

- **Case 1:** The condition state i keeping the current condition until the next inspection time

The condition state i obtain by inspection at time point y_A , the probability that the same state condition will be observe at the time point $y_B = (y_A + Z)$ is expressed by the following:

$$\pi_{ii} = \text{Prob}[h(y_B) = i | h(y_A) = 1] = \exp(-\theta_i Z) \quad (7a)$$

Eq (7a), π_{ii} is dependent only on the hazard rate (θ_i) and inspection interval (Z). Moreover, without using deterministic information at the time point y_A and y_B , it is still possible to estimate the transition probabilities.

- **Case 2:** The condition state changes from i to $i + 1$ during the inspection interval Z .

For the condition state i observed at inspection time point y_A changes to condition state $i + 1$ at time point y_B , the transition is assumed by exponential hazard function as: 1) the condition state i remain constant between a time point y_A to a time point $s_i = y_A + z_i$, ($z_i \in [0, Z]$), 2) the condition state changes to $i + 1$ at time point $y_A + z_i$, and 3) the condition remain constant from $y_A + z_i$ and y_B . However, the exact time in which transition from i to $i + 1$ cannot be trace by periodical inspection, and it can be temporally assumed that the transition occurs at the time point $(y_A + \bar{z}_i) \in [y_A, y_B]$. The Markovian transition probability that the condition state change from i to $i + 1$ during the time points y_A and y_B is expressed by:

$$\begin{aligned} \pi_{i,i+1} &= \text{Prob}[h(y_B) = i + 1 | h(y_A) = i] \\ \pi_{i,i+1} &= \frac{\theta_i}{\theta_i - \theta_{i+1}} \{-\exp(-\theta_i Z) + \exp(-\theta_{i+1} Z)\} \end{aligned} \quad (7b)$$

Where, $\pi_{i,i+1} < 1$.

- **Case 3:** The condition state changes from i to j ($j \geq i + 2$) during the inspection interval time Z .

The transition from the condition state from i to j during the inspection time interval Z , the transition is assumed to occur as 1) the condition state i remains constant between a time point y_A , $\bar{s}_i = y_A + \bar{z}_i \in [y_A, y_B]$, 2) the condition state changes to $i + 1$ at the time point $\bar{s}_i = y_A + \bar{z}_i$, 3) the condition state $i + 1$ remains constant during the time interval $\bar{s}_i = y_A + \bar{z}_i$, $\bar{s}_{i+1} = \bar{s}_i + \bar{z}_{i+1} (\leq y_B)$, and at this time point changes to $i + 2$. After repeating the same process 4) the condition state changes to j at some time point $\bar{s}_{j-1} (\leq y_B)$ remains constant until the time point y_B .

Therefore, the Markov transition probability changes from i to j ($j \geq i + 2$) during the inspection time y_A and y_B is expressed by:

$$\pi_{ij} = \text{Prob}[h(y_B) = j | h(y_A) = i]$$

$$\pi_{ij} = \sum_{k=i}^j \prod_{m=i}^{k-1} \frac{\theta_m}{\theta_m - \theta_k} \prod_{m=k}^{j-1} \frac{\theta_m}{\theta_{m+1} - \theta_k} \exp(-\theta_k Z) \quad (7c)$$

where:

$$\prod_{m=i}^{k-1} \frac{\theta_m}{\theta_m - \theta_k} = 1, \text{ at } (k \leq i + 1) \text{ and } \prod_{m=k}^{j-1} \frac{\theta_m}{\theta_{m+1} - \theta_k} = 1 \text{ at } (k \geq j)$$

In equation (7c), $\pi_{ij} [0 < \pi_{ij} < 1]$, and π_{ij} is arranged using the Markov transition probabilities conditions as follows:

$$\pi_{ij} = 1 - \sum_{j=1}^{j-1} \pi_{ij} \quad (7d)$$

From equation (7a) - (7d), the Markov transition probability depend on the inspection interval Z . The Markov transition probability is expressed as $\pi_{ij}(Z)$, Therefore, the transition probability matrix related to the inspection interval Z is expressed as follows

$$\Pi(Z) = \begin{bmatrix} \pi_{11}(Z) & \cdots & \pi_{1J}(Z) \\ \vdots & \ddots & \vdots \\ 0 & \cdots & \pi_{JJ}(Z) \end{bmatrix} \quad (8)$$

The MTP matrices $\Pi(Z)$ and $\Pi(nZ)$ describe the same deterioration process for two different intervals for an integer value n two inspection intervals (Z) and (nZ) . Therefore, the MPT $\Pi(nZ)$ is expressed as $\{\Pi(Z)\}^n$ as the time adjustment condition of the MTP.

In equation (7), the multistage exponential hazard model has been defined. However, considering the explanatory variable to estimate hazard rate θ_i which is defined as the function of explanatory variables x^k and unknown parameters β_i . where $\beta_i = (\beta_{i,1}, \dots, \beta_{i,M})$, M ($m=1, \dots, M$) is the number of explanatory variable and k ($k=1, \dots, K$) is an individual sample of inspection data.

$$\theta_i^k = f(x^k; \beta_i) \quad (9)$$

In summary, the elements of the MTP matrix π_{ij} are estimated using $\pi_{ij}(Z^k, x^k; \beta_i)$. The unknown parameter β_i ($i=1, \dots, J-1$) is determined with Bayesian estimation method to obtain the hazard function θ_i^k ($i=1, \dots, J-1$), the life expectancy of each condition state i can be defined by means of the survival function $R_i(y_i^k)$ (Lancaster, 1990).

$$LE_i^k \int_0^\infty \exp(-\exp(\theta_i^k y_i^k dy_i^k)) = \frac{1}{\theta_i^k} \quad (10)$$

$$\text{Life expectancy from } i \text{ to } J \text{ can be estimated using } \sum_{i=1}^{J-1} LE_i^k. \quad (11)$$

For detailed description, it is recommended to refer to the reference (Tsuda et al., 2006).

2.3. Application of Bayesian Estimation for the Markov Hazard Model.

Because the classic Markov chain using the maximum likelihood estimation frequently fails to converge for a variety of reasons (Han et al., 2014), the initial values of the parameters are frequently crucial (Train, 2009). Therefore, the Bayesian estimator is used to get around those issues, the Bayesian estimation is an iterative approach to statistical inference that uses data and prior knowledge to estimate the model's parameters. Bayesian estimation can be very helpful in the setting of a Markov deterioration hazard model to estimate the unknown parameter β_i ($i=1, \dots, J-1$). Bayesian estimation can be defined by 3 processes:

- 1) define the prior probability distribution $\pi(\beta)$,
- 2) define the likelihood function $L(\beta|\xi)$ by applying newly obtained data $\bar{\xi}$, and
- 3) modify the prior distribution $\pi(\beta)$ using Bayes' theorem and then update the posterior distribution $\pi(\beta|\xi)$ for parameter (β) .

However, the normalizing constant $L(\bar{\xi}) = \int L(\beta|\bar{\xi}) \prod_{i=1}^{J-1} g(\beta_i|\mu_i, \Sigma_i) d\beta$ is difficult to calculate. Therefore, we directly extract the statistical value for the posterior distribution of parameters using the Metropolis-Hastings algorithm, also known as the M-H algorithm (Hastings, 1970; Metropolis et al., 2004), in the Markov chain Monte Carlo (MCMC) simulation. The M-H algorithm procedure is explained below:

1. Define initial value of parameter vector $\beta(0)$.
2. Calculate current probability density $\pi(\beta(n))$ by using current $\beta(n)$.
3. Find a candidate value as $\tilde{\beta}(n) = \beta(n) + \varepsilon(n) \sim N(0, \sigma^2)$ where ε is the step width of the random walks.

4. Calculate the proposal density by using $\tilde{\beta}(n)$ as a candidate parameter $\pi(\tilde{\beta}(n))$.
5. Apply the updating rule by comparing $\pi(\tilde{\beta}(n))$ and $\pi(\beta(n))$ with the following conditions

$$\beta(n+1) = \begin{cases} \pi(\tilde{\beta}(n)) > \pi(\beta(n)), & \beta(n+1) = \tilde{\beta}(n) \\ \pi(\tilde{\beta}(n)) \leq \pi(\beta(n)), & \begin{cases} R \leq r, & \beta(n+1) = \tilde{\beta}(n) \\ \text{Otherwise,} & \beta(n+1) = \beta(n) \end{cases} \end{cases} \quad (12)$$

Where, $r = \pi(\tilde{\beta}(n)) / \pi(\beta(n))$, and R is a standard uniform for $R \sim U(0,1)$

6. Do sufficiently large numbers of iterations from step 2 to step 5, until sequence β^n becomes a stationary condition (that is close to convergence).
7. Cut burn-in samples and take the average of sample parameters.

The MCMC does not include any method to confirm that the initial value $\beta(0)$ reaches stationary distribution. Therefore, the Geweke's test is utilized to determine whether the Markov chain reaches the convergence to a maximum (Geweke, 1991). Refer to the following reference for a full explanation of the M-H method and the Geweke's test to verify the Markov chain's convergence (Han et al., 2014).

3. EMPIRICAL STUDY

3.1.1. Data Processing

The historical inspection data from the Lao RMS was inquired and examined following the model's estimation. Data inspection from the Lao RMS database for the years 2014–2016 and 2020 has been obtained. However, it was difficult to attain the maintenance history from 2016–2020 and the conditions in 2020 being almost as good as those in 2016. Therefore, only the dataset from 2014–2016 has been used. Pavement materials, the IRI, and average annual daily traffic (AADT) are the only available data that have been gathered and analyzed because environmental uncertainty parameters like weather, rainfall, etc. have not been sufficiently covered by data collection. Without taking any maintenance action, the aberrant condition examined under improved conditions has been evaluated and checked (Madanat et al., 1995). According to the DoR, MPWT Lao PDR classification, two core road networks (core networks 1 and 2) are evaluated. The model's basic tenet is to anticipate the target core networks' life expectancy, IRI degradation process, and hazard rate in relation to the Lao road network's deterioration process.

The collected data set of the IRI is applied to the model. The IRI data has been derived from periodic inspections since 2014–2016. In order to measure the IRI, the Dynamic Response Vehicle Intelligent Monitoring System equipment, which was supported by the Japan International Cooperation Agency (JICA) in 2012, has been used. The IRI was measured at a speed of around 80 km/h for each segment of 100 meters (Gharieb and Nishikawa, 2021; JICA, 2018). The IRI circumstances are then classified into five groups based on preset criteria for roughness sufficiency (MPWT, 2021) in order to estimate the Markov transition probability based on the exponential hazard model, according to Table 1. The IRI roughness scale, which ranks the conditions from excellent to failed (absorption state), indicates the need for maintenance or rehabilitation activities.

Table 1. The IRI Roughness Scale (condition state)

Pavement condition (State)	Excel/Good (1)	Fair (2)	Poor (3)	Bad (4)	Failed (5)
IRI (m/km)	$IRI \leq 3$	$3 < IRI \leq 5$	$5 < IRI \leq 7$	$7 < IRI \leq 9$	$9 < IRI$

After rejecting the incorrect information, the atypical condition, the data of road sections was divided into two core networks based on the definition and classification from DoR and MPWT. The total length was 2,769 km, or 35.29% of the total 7,847 km (national road network length), as presented in Table 2.

Table 2. Summary of data observation and variables

Core network	Total No. of road sections	Total length of observations (km)	Number of sample (pairs)	Explanatory Variables	Length of AC/ST (km)
Core 1	8	1,900	18998	AADT, Road surface (AC/ST) *	778/1,122
Core 2	14	869	8690	AADT, Road surface (AC/ST)	50/819

*AC=Asphalt concrete; ST=Surface treatment

Asphalt concrete pavement and surface treatment (single and double bituminous) are the two main types of pavements. The traffic volume is gathered from the number of vehicles passing the counting location in each road section. The methodology for counting is either automatic or manual (by the traffic count form), and the

vehicles are classified into 14 classes in order to generate the adjustment factors (MPWT, 2009). A number of adjustment factors are related to classified traffic counts to derive the average annual daily traffic. To normalize the traffic volume, the AADT has been classified into 3 bands: low, medium (mean), and high, as shown in Table 3.

Table 3. Traffic band classification

Band	From (AADT)	To (AADT)
Low	0	500
Mean	501	2000
High	2001	99999

3.1.2. Results

The transition probability matrix of Core Networks 1, 2 were determined using the Markov Deterioration Hazard Model. The MTP for Core Networks 1 and 2 are shown in Tables 4, and 5 respectively.

Table 4. MTP of the Core Network 1

State	1	2	3	4	5
1	0.487	0.442	0.063	0.006	0.002
2	0	0.761	0.203	0.026	0.010
3	0	0	0.732	0.167	0.101
4	0	0	0	0.378	0.622
5	0	0	0	0	1.000

Table 5. MTP of the Core Network 2

State	1	2	3	4	5
1	0.342	0.529	0.110	0.016	0.003
2	0	0.683	0.254	0.051	0.012
3	0	0	0.652	0.254	0.094
4	0	0	0	0.539	0.461
5	0	0	0	0	1.000

As a result of Tables 4 and 5, the transition probability in states 1-1, 2-2, and 3-3 shows that the core network 1 has a higher transition probability compared to the core network 2, meaning that the core network 1 will deteriorate more slowly than the core network 2, which in turn leads to a longer life expectancy.

The road network's hazard rate (deterioration rate) and interval life expectancy of each condition state of core networks 1 and 2 are computed using equations (10) and (11), the results are shown in Tables 6 and 7:

Table 6. IRI mean hazard rate (θ_i) and life expectancy (LE_i) of Core Network 1

State	Mean hazard rate (θ_i)	Hazard rate (θ_i) (ST)	Hazard rate (θ_i) (AC)	LE_i (Year) (AV)	LE_i (Year) (ST)	LE_i (Year) (AC)
1-2	0.720	0.944	0.487	1.39	1.06	2.05
2-3	0.273	0.303	0.234	5.06	4.36	6.32
3-4	0.313	0.278	0.372	8.25	7.96	9.01
4-5	0.974	0.738	1.452	9.28	9.32	9.70

Table 7. IRI mean hazard rate (θ_i) and life expectancy (LE_i) of Core Network 2

State	Mean hazard rate (θ_i)	Hazard rate (θ_i) (ST)	Hazard rate (θ_i) (AC)	LE_i (Year) (AV)	LE_i (Year) (ST)	LE_i (Year) (AC)
1-2	1.074	1.133	0.445	0.93	0.88	2.25
2-3	0.380	0.382	0.362	3.56	3.50	5.00
3-4	0.428	0.427	0.446	5.90	5.85	7.25
4-5	0.619	0.586	1.526	7.51	7.56	7.90

The estimation results for the unknown parameters, which indicates the statistic properties (coefficient) of the explanatory variables of each parameters (traffic and surface pavement), and Geweke's z score, which verifies the convergence (stationary distribution) of the parameter (Geweke, 1991), are shown in Tables 8 and 9 as follow:

Table 8. Unknown parameter and Geweke's test of Core Network 1

State	(β_0) Absolute	(β_{i1}) Traffic	(β_{i2}) Pavement	(β_0) Geweke's	(β_{i1}) Geweke's	(β_{i2}) Geweke's
1-2	-0.0005	-0.264	-0.661	0.203	0.276	-0.915
2-3	-1.256	0.284	-0.256	-0.275	0.382	-0.346
3-4	-0.824	-2.107	0.292	-0.369	0.248	1.352
4-5	0.497	-3.691	0.677	-0.342	0.021	0.567

Table 9. Unknown parameter and Geweke's test of Core Network 2

State	(β_0) Absolute	(β_{i1}) Traffic	(β_{i2}) Pavement	(β_0) Geweke's	(β_{i1}) Geweke's	(β_{i2}) Geweke's
1-2	0.632	-1.378	-0.934	0.719	-0.779	0.685
2-3	0.017	-2.663	-0.051	-1.455	1.595	0.097
3-4	-0.753	-0.269	0.045	-0.103	-0.217	-0.587
4-5	-0.630	0.257	0.958	1.337	-1.946	0.519

In Table 8, the β_{i1} indicate that the traffic volume had a significant impact on deterioration rate in condition 2-3. Higher traffic leads to faster deterioration rate. In order to verify the chain convergence, Geweke's test value for all β values should fall between the range $[-1.96, 1.96]$, where a value of 0 denotes perfect convergence.

The expected degradation path (deterioration processes) for 2 core networks is illustrated in Figures 5 and 6 as a graph, describing the typical deterioration process over the duration of the core networks' life expectancy condition states from the starting state (excellence condition) to the absorption stage by time order in years.

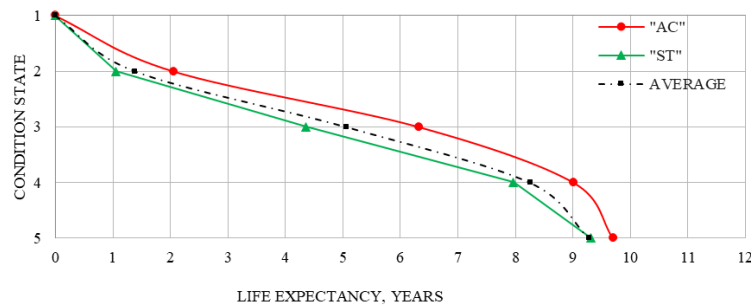


Figure 5. Core Network 1 deterioration process

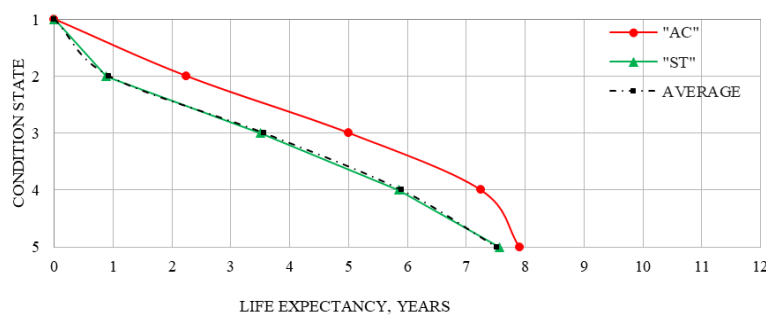


Figure 6. Core Network 2 deterioration process

4. DISCUSSION

While an extensive and high-quality Lao RMS database is necessary for validating the results, the life expectancies of the two networks were shorter than the expected design life, which is about 10-20 years from the design life (MPWT, 1996). This was probably due to the explanatory variables or the quality of the dataset. However, others researchers performed validation of the model (Han et al., 2014; Kobayashi et al., 2010; Kobayashi et al., 2012; Tsuda et al., 2006) which may point to the model being robust enough to generate acceptable estimates, Han et al., (2014) validated the model by comparing its predictions with an accumulated dataset spanning eight years and confirmed its reliability. The results of the empirical study were based on historical inspection data gathered by the Lao RMS from 2014 to 2016. In other words, this study examined the

three-years deterioration trend of the Lao road network using IRI data. Due to financial and technical limitations of the Department of Road, MPWT, part of the Lao Road Authority aims to collect data on the condition state of the road network in 2024, the final year of the current long-term maintenance financial plan 2016–2025. They were unable to conduct the inspection every year; hence, some years' data were omitted. Due to incomplete data, the traffic volume sample data led to a convergence issue due to the number of observations and the difficulty in identifying the precise location of the traffic on specific road sections. However, the outcomes indicated that the two significant core road networks had different life expectancies considering traffic volume and pavement parameter; the deterioration process of network 1 was estimated to take 9.28 years on average, while that of network 2 was estimated to last for 7.51 years. Furthermore, the life expectancy of the AC pavement road section in network 1 was 9.70 years, while that in network 2 was 7.90 years. Due to the ST pavement road section being the majority portion of the road network, both networks 1 and 2. Therefore, the predicted life expectancy of the ST pavement road section was nearly the same as the life expectancy of the whole networks 1 and 2 (average), which was 9.32 and 7.56 years, respectively. However, the life expectancies of two core road networks in this paper were evaluated using only the traffic and pavement type parameters, which may not be the only factors that affect the deterioration process of the two road networks in Lao PDR. The results, which indicate the transition year, can be used to evaluate the maintenance plans of each network in order to restore their condition. Moreover, it gives the road decision-maker time for intervention in terms of the maintenance plan.

5. CONCLUSIONS

Understanding the lifespan of infrastructure is important for asset management for planning and prioritizing maintenance activities. The Markov deterioration hazard model was used to forecast the deterioration of the road network in Lao PDR because this is an important step before carrying out infrastructure planning. The estimated life expectancy of the core network 1 and the core network 2 in the Lao road network shown in Tables 6 and 7, respectively, using the IRI data in the historical inspection dataset from RMS is an important prerequisite to maintenance planning for the two road groups. This information could be used for determining the maintenance frequency and prioritization at the network level. However, this study has only taken into account the traffic volume AADT and pavement type variables to predict the deteriorate process because of the incomplete Lao RMS data sets. Nonetheless, some important elements, such as the commercial vehicle weight, the Pavement's Structure Number (pavement strength), and other uncertainty environmental variables, such as rainfall, temperature, and terrain, should be taken into account for better prediction. Therefore, in future studies, these significant parameters should be collected and included in the model in order to generate more precise information that can be used for prioritization and allocation of the maintenance fund.

Furthermore, in the interest of developing the unpaved road network, other key performance measures, such as the Surface Integrity Index (SII), which is used to evaluate the condition of unpaved roads, should be considered in future. However, the authors believe that the results from this study will assist in improving the PMS, which will be utilized to determine the performance-based contract for upcoming road maintenance projects in Lao PDR.

REFERENCE AND DATA AVAILABILITY STATEMENT

All the data used in this study was provided by a third party. Direct requests for these materials may be made to the provider as indicated in the acknowledgements. The restricted data include road condition, traffic volume, and inventory data.

ACKNOWLEDGEMENTS

The authors would like to thank the Department of Road, The Ministry of Public Works and Transport of Lao PDR for kindly providing Lao national roads data including Road design manual, Road asset management plan, traffic survey manual, IRI condition, traffic volume, and pavement inventory data for this study.

REFERENCES

- Geweke, J. (1991). Evaluating the accuracy of sampling-based approaches to the calculation of posterior moments. In: St. Louis: Federal Reserve Bank of St Louis.
- Gharieb, M., & Nishikawa, T. (2021). Development of Roughness Prediction Models for Laos National Road Network. *CivilEng*, 2(1), 158. doi:<https://doi.org/10.3390/civileng2010009>
- Han, D., Kaito, K., & Kobayashi, K. (2014). Application of Bayesian estimation method with Markov hazard model to improve deterioration forecasts for infrastructure asset management. *KSCE Journal of Civil Engineering*, 18(7), 2107-2119. doi:<https://doi.org/10.1007/s12205-012-0070-6>
- Hastings, W. K. (1970). Monte Carlo sampling methods using Markov chains and their applications. *Biometrika*, 57(1), 97-109. doi:10.1093/biomet/57.1.97
- JICA. (2018). The Project for Improvement of Road Management Capability in Lao PDR; Japan International Cooperation Agency. doi:https://openjicareport.jica.go.jp/pdf/12309456_01.pdf

- Kerali, H. R. (2001). *The role of HDM-4 in road management*. Paper presented at the Proceedings, First Road Transportation Technology Transfer Conference in Africa, Ministry of Works, Tanzania.
- Kobayashi, K., Do, M., & Han, D. (2010). Estimation of Markovian transition probabilities for pavement deterioration forecasting. *KSCE Journal of Civil Engineering*, 14(3), 343-351.
doi:<https://doi.org/10.1007/s12205-010-0343-x>
- Kobayashi, K., Kaito, K., & Lethanh, N. (2012). A statistical deterioration forecasting method using hidden Markov model for infrastructure management. *Transportation Research Part B: Methodological*, 46(4), 544-561. doi:<https://doi.org/10.1016/j.trb.2011.11.008>
- Lancaster, T. (1990). *The econometric analysis of transition data*: Cambridge university press.
- Li, N., Haas, R., & Xie, W.-C. (1997). Investigation of Relationship Between Deterministic and Probabilistic Prediction Models in Pavement Management. *Transportation Research Record*, 1592(1), 70-79.
doi:10.3141/1592-09
- Madanat, Mishalani, & Hashim, I. W. (1995). Estimation of Infrastructure Transition Probabilities from Condition Rating Data. *Journal of Infrastructure Systems*, 1(2), 120-125. doi:10.1061/(ASCE)1076-0342(1995)1:2(120)
- Metropolis, N., Rosenbluth, A. W., Rosenbluth, M. N., Teller, A. H., & Teller, E. (2004). Equation of State Calculations by Fast Computing Machines. *The Journal of Chemical Physics*, 21(6), 1087-1092.
doi:10.1063/1.1699114
- MPWT. (1996). Road Design Manual.
- MPWT. (2009). Road Management System, Traffic Survey Manual.
- MPWT. (2021). Road Asset Management Plan.
- MPWT. (2022). MPWT yearly statistic 2021.
- Norris, J. R. (1998). *Markov chains*: Cambridge university press.
- Robinson, R., Danielson, U., & Snaith, M. S. (1998). *Road maintenance management: concepts and systems*: Macmillan International Higher Education.
- Sayers, M., Gillespie, T., & Queiroz, C. (1986). The international road roughness experiment: A basis for establishing a standard scale for road roughness measurements. *Transportation Research Record*, 1084, 76-85.
- Train, K. E. (2009). *Discrete choice methods with simulation*: Cambridge university press.
- Tsuda, Y., Kaito, K., Aoki, K., & Kobayashi, K. (2006). Estimating Markovian transition probabilities for bridge deterioration forecasting. *Structural Engineering Earthquake Engineering*, 23(2), 241s-256s.

PROMOTING FLEXIBLE USE OF OPEN DATA THROUGH SERVICE LINK PLATFORM FOR INFRASTRUCTURE MANAGEMENT

Yinyongdong Ma¹, Kei Kawamura², Junha Hwang³, Shuji Sawamura⁴, and Hisao Emoto⁵

1) Graduate School of Sciences and Technology for Innovation, Yamaguchi University, Yamaguchi, Japan. Email: c118vgw@yamaguchi-u.ac.jp

2) D. Eng., Prof., Graduate School of Sciences and Technology for Innovation, Yamaguchi University, Yamaguchi, Japan. Email: kay@yamaguchi-u.ac.jp

3) Graduate School of Sciences and Technology for Innovation, Yamaguchi University, Yamaguchi, Japan. Email: b088vgv@yamaguchi-u.ac.jp

4) Department of construction, Yamaguchi Prefecture Government, Yamaguchi, Japan. Email: sawamura.shiyuuji@pref.yamaguchi.lg.jp

5) Social Systems and Civil Engineering, Faculty of Engineering, Tottori University, Tottori, Japan. Email: emoto@tottori-u.ac.jp

Abstract: In 2014, periodical inspections of major infrastructure facilities in Japan became mandatory, and a large amount of periodical inspection data was generated. In addition, in 2012, the Electronic Government Open Data Strategy was enforced, and the Japanese government began promote utilizing open data for citizens. However, the data format and preservation method differ for each local government, and the level of Open Data is not sufficient. In this study, the authors focus on the utilization of periodical inspection data of infrastructure facilities, propose a method of distributing inspection data as machine-readable open data over the Internet, and put forward an efficient generation and distribution method of open data using a prototype system developed for this purpose. Moreover, as an example of open data utilization, a data visualization application was developed, which allows the user to instantly check the condition states of infrastructure facilities on a map.

Keywords: Infrastructure management, Open data, Web API, Data management, Data visualization.

1. INTRODUCTION

In Japan, road networks have developed rapidly during a period of rapid economic growth, and many bridges, tunnels, and other infrastructures have been constructed. These infrastructures have become an integral part of socioeconomic activities. However, the 2012 Sasago Tunnel roof fall accident brought to light the aging and deterioration of bridges over 50 years old, now a growing social problem, and proper and effective maintenance and management of infrastructure has become an urgent issue. Against this backdrop, the Japanese government enacted the "Regulation and Notification on Road Maintenance and Repair "(Ministry of Land, Infrastructure, Transport and Tourism, 2014) in 2014, making it mandatory to conduct periodic inspections every five years, which has resulted in infrastructure management organizations generating and accumulating a large amount of periodic inspection data. Since the Japanese government established an open data strategy for e-government in 2012, an environment in which citizens can easily use public data via the Internet is taking shape. However, most of the open data released by local governments, such as infrastructure information and map data, are provided in data formats such as PDF and JPEG, that are difficult to read by machines, and therefore must be manually re-entered and processed before they are used. In addition, it is difficult for local government officials to generate machine-readable open data on their own, making it necessary to develop new data conversion software. Further more, since each organization has its own record format and storage format, it takes a lot of time to collect and organize the data when utilizing it. Here, machine-readable means that the content described in a document, for example, can be easily processed by a computer program.

The study focus on the use of regular inspection data of infrastructures, propose a method to publish inspection data as open data in machine-readable format on the Internet, and propose a prototype system for efficient generation and publication of open data. Moreover, as an example of the use of open data, the authors developed a data visualization system that provides a bird's-eye-view of the infrastructure on a map.

Specifically, data extraction software and an open data system were developed based on the level of information literacy of municipal employees. Currently, most of the municipalities responsible for maintenance and management store data that are frequently used in maintenance and management work, such as information on infrastructure and the results of periodic inspections in Excel format. The study demonstrate a method for selecting data to be distributed from Excel and converting it into machine-readable open data web as data extraction software. Next, to increase the circulation of open data on the Internet, the authors developed a web application that utilizes Web API (Web Application Programming Interfaces) (Takaku, 2014), which has become common in web development, and implemented a data circulation function. In addition, as an example of the use of open data by Web API, the authors developed a system for visualizing and publishing bridge conditions which can be used to periodically check open data. Web API exchanges information between applications and systems over the network using HTTP and HTTPS communication. Web API is a mechanism that makes some functions managed

by the operating system or software available to external programs and applications. Using Web API, it is easy to incorporate the functions of other services into self-developed websites and applications and also to create new functions and services.

This study utilizes advances by previous researchers. Regarding research on the distribution of infrastructure data, Fujimoto et al. (2020) proposed a file management method to distribute data in JSON (JavaScript Object Notation) format using Web API as a data management method in order to make bridge inspection data openly available. Kameda et al. (2021) Proposed a method combining LoRa-based LPWA communication and MQTT protocol as a method to simplify the supply of monitoring data for infrastructure. Yuda et al. (2020) Organized data science processes in the field of infrastructure management and examples of data utilization. Yamamoto et al. (2021) Considered the preparation of information systems as part of pre-disaster reconstruction from the perspective of pre-disaster reconstruction, and studied the construction and use of information platforms. Abe et al. (2022) Organized the functions required for a data platform to utilize infrastructure data and proposed an infrastructure operating system. In our previous studies (Fujimoto et al. 2020), infrastructure data was distributed in the form of JSON files, but further openness was required to make it open data. In this study, the data could be simply extracted from an Excel format into a machine-readable JSON format for uploading to cloud storage services and an API was provided to the public for accessing the data. In addition, to make this basic open data more valuable, this study used data visualization tools to present the data in chart form and map form, making it easier for general public and government agent to understand the condition of the infrastructure. Moreover, this study proposes the concept of Service Link Platform (SLP). SLP is a system that allows for the combination of a wide variety of APIs, promoting the development of application software related to the maintenance and management of infrastructure. However, a large number of open data and tools need to be registered with SLP to make it practical. In this study, an application software was developed that enables civil engineers to efficiently create open data, contributing to the generation of open data. Although only the API of open data was implemented in this study, in the future, APIs of application software with processing functions will be developed and implemented.

2. MAINTAINING DATA DISTRIBUTION AND UTILIZATION

This section describes the flow of regular inspection data from acquisition to utilization, as shown in Figure 1. In this study, open data and utilization of maintenance and management data were modeled under the assumption of regular inspection of bridges in Yamaguchi Prefecture.

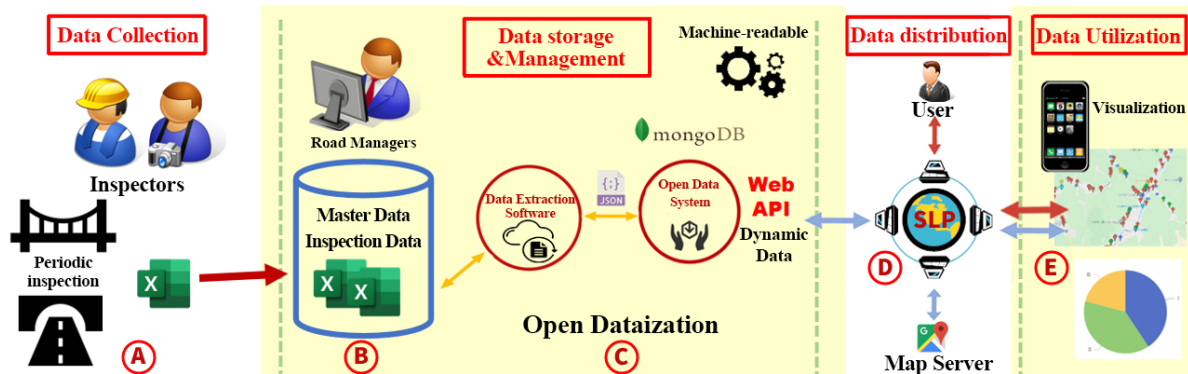


Figure 1. The Acquisition to Utilization of Periodic Inspection Data

2.1 Data Collection

As of October 2008, Yamaguchi Prefecture manages approximately 4,300 bridges, and regular inspections of 800 to 900 bridges are conducted annually. Regular inspections of these bridges are based on the Yamaguchi Prefectural Bridge Inspection Guidelines (Draft) (Yamaguchi Prefecture Civil Engineering Construction Department, 2017), and the inspection results are compiled into an inspection record sheet (Excel) as shown in A of Figure 1. Figure 2 shows a part of the inspection record sheet, in which the results of the periodic inspections are recorded. As shown in B of Figure 1, road managers in the Yamaguchi Prefecture store frequently used data in Excel as master data for maintenance and management purposes. These master data include bridge numbers, bridge specifications, addresses, regular inspection schedules, and judgment results of major components transcribed from the inspection record sheet. Figure 3 shows an example of master data stored in Excel. Practitioners use this master data to develop periodic inspection schedules.

2.2 Data Storage and Management

Although government agencies are currently working to publish the aforementioned data, the work of opening up data has become difficult due to the fact that each local government uses different data formats and storage methods. In addition, Open data should be available in a format that facilitates secondary use/processing and should be distributed in a machine-readable, easily searchable, and linked data format. This will lead to a reduced data processing burden and efficient data utilization. For example, the 5-star Open data (Omukai, 2013) has been proposed to codify the five conditions that must be met for open data.

Therefore, as shown in C of Figure 1, in this study a mechanism for converting master data (Excel) used by road managers into a machine-readable data format and improving data distribution on the Internet using Web API was developed and implemented as software. The details of the mechanism are described in section 3.

橋梁名 → Name	路線名 → Road	所在地 → Address	起点側	緯度 Latitude	経度 Longitude	橋梁ID → ID
(フリガナ)	一般国道	山口県				
管理者名 → Office	定期点検実施年月日	路下条件	代替路の有無	自専道or一般道	緊急輸送道路	占用物件 (名称)
山口県土木建築事務所	2020.11.1	水路	有	一般道	一次	上水
Inspect Date			定期点検者 → Inspectors			
部材単位の診断 (各部材毎に最も厳しい健全性の診断結果を記入)						
定期点検時に記録	判定区分 (I~IV)	変状の種類 (II以上の場合に記載)	備考 (写真番号、位置等が分かるように記載)	応急措置後に記録	判定区分	応急措置内容及び判定実施年月日
上部構造	主桁 I	→ Shugeta				
	横桁	→ Yokoketa				
	床版	→ Shouban				
下部構造	I	→ Kabukozo				
支保部	I	→ Shishobu				
その他		→ Other				
道路橋毎の健全性の診断 (判定区分 I~IV)						
定期点検時に記録	判定区分	所見				
I		早期に対応すべき損傷は認められない。				
Year Rank Length Width						
写真写真 (起点側、終点側を記載すること)						
架設年次	橋長	幅員				
1988年	6m	30.4m				
橋梁形式 → Type						
単径間PC床版橋						

Figure 2. Example of Inspection Record Sheet

国交省 点検データ 登録システム 作業用番号	橋梁ID (施設ID)	事務 所名	旧 事務 所名	橋梁名	フリガナ	橋区別	路線 種別	路線名	現道旧 道区分	一般 有料 区分	所在地
											① ②
		柳井	大島			B	一般道	437号	現道	一般	周防大島町 大字伊保田
		柳井	大島			橋	一般道	437号	現道	一般	周防大島町 大字伊保田
		柳井	大島			橋	一般道	437号	現道	一般	周防大島町 大字伊保田
		柳井	大島			B	一般道	437号	現道	一般	周防大島町 大字伊保田
		柳井	大島			B	一般道	437号	現道	一般	周防大島町 大字和田
		柳井	大島			B	一般道	437号	現道	一般	周防大島町 大字和田
		柳井	大島			橋	一般道	437号	現道	一般	周防大島町 大字和田
		柳井	大島			橋	一般道	437号	現道	一般	周防大島町 大字和田
		柳井	大島			B	一般道	437号	現道	一般	周防大島町 大字和田
		柳井	大島			橋	一般道	437号	現道	一般	周防大島町 大字神浦
		柳井	大島			橋	一般道	437号	現道	一般	周防大島町 大字森

→Sagayou →Id →Name →Road →Address1,Address2

Figure 3. Example of Bridge Master Data

2.3 Data Distribution

An open data system refers to systems that use web APIs to make infrastructure data publicly available, with the aim of providing developers with more opportunities for application development. This system allows developers to obtain data and develop various infrastructure management applications. These applications can help people better manage infrastructure, and improve urban management efficiency and quality of life.

Although the open data system opens up data, developers find it difficult to collect various APIs for development. To solve these problems, as shown in D of Figure 1, the authors propose to establish a Service Link Platform (SLP), which provides developers with a simple way to search for APIs, so that developers can develop new applications faster. In addition, SLP provides API documentation and code examples to help developers better understand how to use APIs.

SLP can also provide a wide variety of APIs. For example, a map API can allow users to search for specific infrastructure data on a map, and a data conversion API can help developers easily extract data from a certain format, thereby achieving more flexible data processing. Figure 4 shows the flow of the SLP used in development of applications.

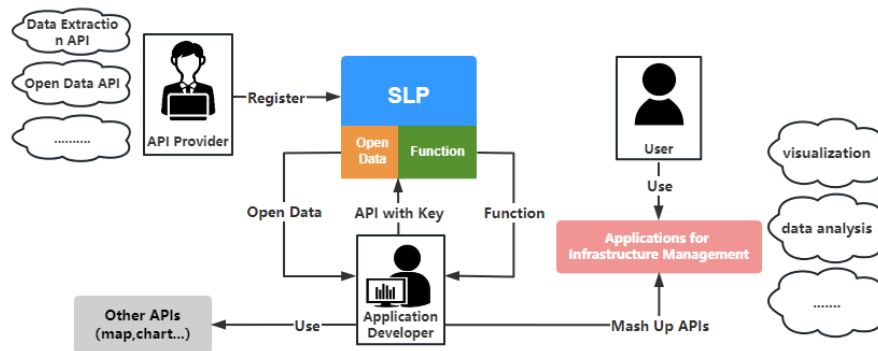


Figure 4. SLP system usage flow

2.4 Data Utilization

The ultimate goal of this study is to make data utilization more efficient. Establishing new data utilization models in the cloud is essential to advance infrastructure maintenance and management, such as collecting large amounts of data from different road management agencies, analyzing damage trends, and predicting damage with high accuracy. Efficiency and sophistication of open data and data distribution are important foundations to support data utilization, but managers and software developers of infrastructure do not yet understand how to utilize open data and how to leverage Web API. As shown in E of Figure 1, the authors developed a visualization system of bridge inspection data as an example of using open data in a machine-readable format and making it available through a Web API mechanism. The details of this system are described in section 4.

3. DATA EXTRACTION SOFTWARE AND OPEN DATA SYSTEMS

3.1 Overview of the Conversion to Open Data

Open data consists of data extraction, conversion, storage, and publication. The purpose of this study is to develop a system that can publish data held by road managers to the Internet in a machine-readable format and to develop data extraction and conversion software. The data extraction and conversion were developed as data extraction software, and the data storage and distribution were developed as an open data system.

Specifically, the data extraction software automatically extracts data from the master data in Excel format managed by the road manager and converts it to JSON format when the user decides on the range of data to be published. The system stores the JSON data output by the extraction software in a non-relational (NoSQL) database and publishes the data on the Internet.

NoSQL distinguishes itself from relational databases (RDB) by not guaranteeing the ACID (Atomicity, Consistency, Isolation, Durability) attributes of relational data. Also, the persistence of relational data is not guaranteed. Therefore, NoSQL has the advantage of fast processing and high system scalability and flexibility compared to traditional RDB because there is no strict relationship between data. NoSQL is not limited to table structures like RDB and can use various data models such as key/value pairs, column-oriented, document, and graph types. In other words, there is no predefined shape for the data.

API is a mechanism for exchanging functions of one program so that they can be used by another program. The advantages are that even if Web API uses HTTP/HTTPS communication with different programming languages, they still work on web browsers. Typical Web API include Google Maps API, YouTube API, and Twitter API, etc.

3.2 Process of Data Extraction Software

JSON is a data structure designed for use in JavaScript and is therefore highly compatible with JavaScript. This data structure is stored and transmitted as a combination of key/value pairs, which is easy for humans to understand, easy for machines to analyze and generate, and can effectively improve the distribution of data on the Web. In addition, JSON has gained widespread adoption in recent years due to the standard use of JavaScript in web development. Data extraction software converts data into JSON format, which is easier to disseminate on the Internet than Excel format data, through the following steps.

Step 1 Select the extracted data: In this step, first, the master data file shown in Figure 3 is parsed using JavaScript to detect the columns, the output is displayed on the user's web page, the user selects the data to be converted, as shown in A of Figure 5. For example, and the user selects the data to be converted to JSON format, as shown in the red box in Figure 3. Here, the user further enters the names of the keys for the selected Excel columns. This saves the data in the Excel rows as the value of the key.

Step 2 Convert from Excel format to JSON format: In this step, the data selected in step 1 above is converted to a JSON string text and saved. The data in JSON format shown in B of Figure 5 is an example of data conversion for the selected part of the master data (Excel) shown in Figure 3.

In this case, the authors have established standards for implementation within Yamaguchi Prefecture. These standards were developed to meet the needs of a specific area and therefore are not applicable to other areas. However, when other areas also want to make road data public, the local road manager needs to develop standards that are applicable to the local area to ensure the accuracy and reliability of data extraction. In the future, in order to publish and use the open data of each road management organization as big data, it is necessary to manage the IDs of structures and components, and to standardize the data structures published in JSON format.

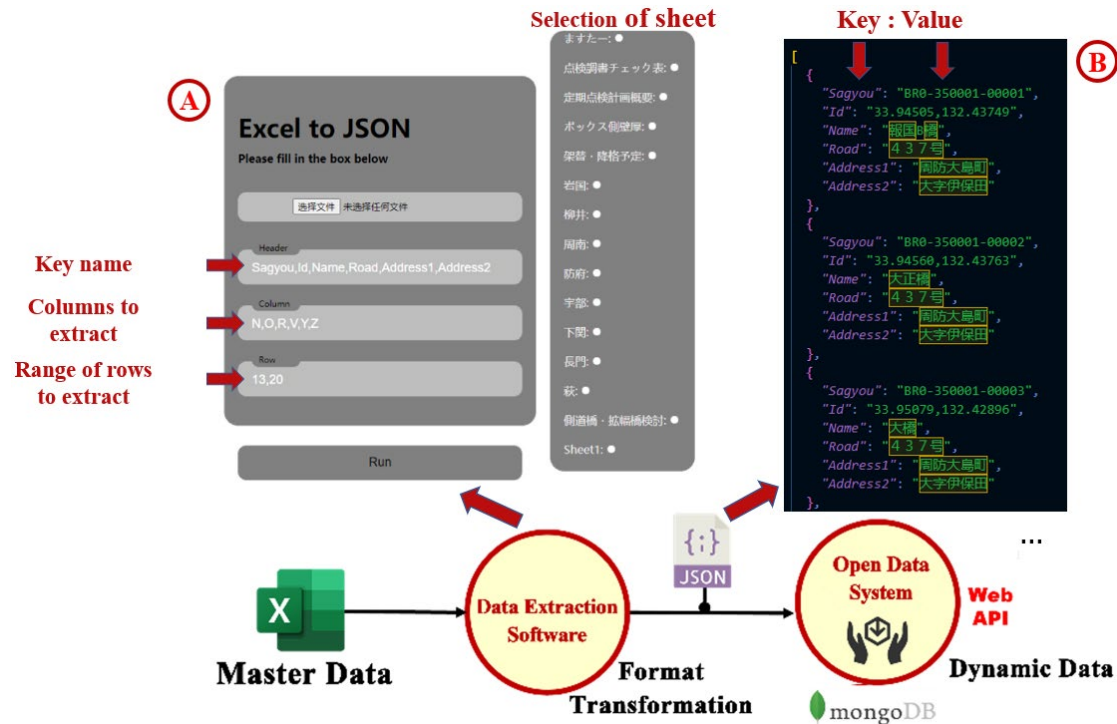


Figure 5. Converting Excel Data to JSON

3.3 Process of the Open Data System

The Open Data System stores the data extracted from the master data in JSON format in the following steps and makes the stored data available to system developers and other users.

Step 1 Save the data: In this step, the data provider transfers and stores the data in JSON format into the NoSQL database using an upload page, and this data is published as open data. In the implementation of this study, the NoSQL database MongoDB is used. MongoDB is a document-oriented database developed by MongoDB Inc. And is available as open-source code. The data storage format is BSON format, which is derived from JSON format.

Step 2 Issuing API keys: When a user accesses the application, this system issues a unique API key. In this system, the key is issued by clicking a button on the application screen. The number of the issued API key is stored in a database and used for user authentication. API key is an authentication message issued independently by the API service provider. This checks the user's usage status, prevents unauthorized connections, and is expected to improve security.

Step 3 Open data distribution through RESTful API: RESTful API is an API that can access unique URL on the web using HTTP methods (GET, POST, PUT, etc.) REST stands for Representational State Transfer and is a system design concept. In this study, GET and POST are provided in the open data system to conform to this RESTful API. GET is used to retrieve resources in the server, and POST is used to modify resources in the server. Therefore, in the open data system, GET is used to retrieve data from the open data system for use in the visualization system, while POST is used to upload data to the open data system.

Step 4 (Handling access from external systems) Open Data Collection: The external system (client) retrieving data from the open data system sends a GET request with a pre-issued API key in the URL. If the key is valid, the data is provided by the server.

4. DATA VISUALIZATION SYSTEM

4.1 Overview of System Requirements

This section describes how to use the open data provided by the open data system explained in section 3. In this study, the authors developed a system to provide the visualization results of open data published by Web

API as a service. Figure 6 shows an example of the output screen of the visualization system. Visualization is a theory, method, and technique that uses computer graphics and image processing techniques to interactively visualize and display data on a screen. The advantage of visualization is that information that is difficult to grasp using only numerical values can be illustrated with graphics, allowing people to understand and highlight important information more intuitively.

Currently, the users of the visualization system developed in this study are considered to be those responsible for providing maintenance and management of open data, as well as the general public. The main purpose of the system is to visualize bridge data with graphic and map information so that the health of bridges managed by Yamaguchi Prefecture can be easily understood from a bird's eye view. The system development requirements are shown in Table-1.

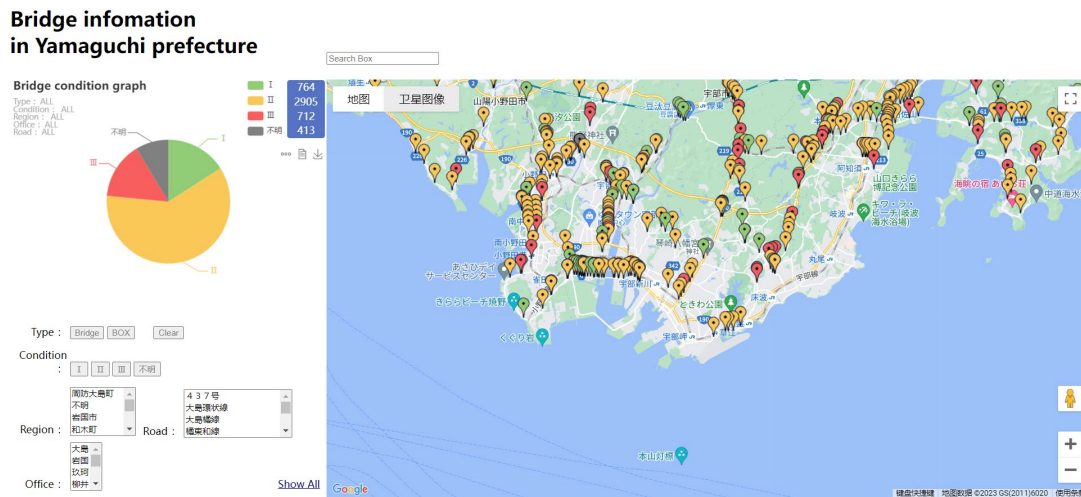


Figure 6. Visualization system (displaying data for system validation, not actual data)

4.2 System Construction

The system is a web-based system, hosted on a web server.

The visualization system publishes information about the health condition of bridges in the form of a web page. The visualization system acquires bridge data from the open data system developed by the authors and uses Google Maps API (map server) to obtain map information and map-related functions. Figure 7 shows the structure diagram of the visualization. This system was created by mixing the Web API developed by the authors and the Google map API provided by Google.

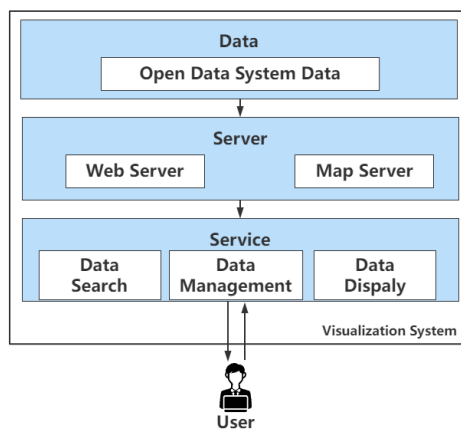


Figure 7. Visualization Structure

Figure 8 shows the communication between a web page and an open data system. The web page accesses MongoDB of the open data system through the Web API, requests to send open data, and the server returns the result (open data). A similar exchange as in Figure 8 is done with the Google Maps API. This visualization system uses the Express framework, JavaScript, and HTML technologies to create dynamic web pages. Node.js is a platform for running JavaScript to create web pages on the server side, and the Express framework is a development platform for efficiently developing web applications using Node.js.

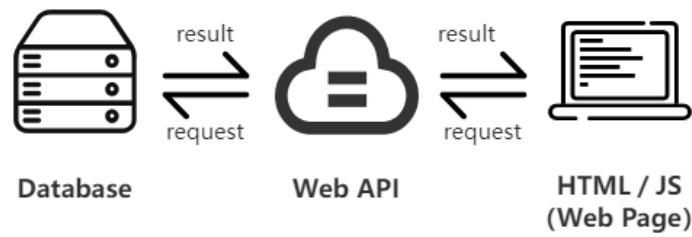


Figure 8. Visualization System (web page) and Open Data System Communication

4.3 System Functions

The visualization system developed in this study, shown in Figure 6, has the functions listed in Table 2. In the visualization system (bottom left corner of Figure 6), clicking or selecting the buttons for the functions listed in Table 2 displays the contents of the selected items on the map (right side of Figure 6) and displays statistical data in the form of graphs or values (top left side of Figure 6).

Table 1. Requirements for the visualization system

Head of Maintenance and Management	General users
<ul style="list-style-type: none"> The health condition of the bridge should be understandable to users who do not have expertise in bridges. The health condition of the bridge should be easily accessible in the form of maps or diagrams. The health condition of the bridge should be understandable to users who do not have expertise in bridges. The health condition of the bridge should be easily accessible in the form of maps or diagrams. 	<ul style="list-style-type: none"> The health condition of the bridge should be understandable to users who do not have expertise in bridges. The health condition of the bridge should be easily accessible in the form of maps or diagrams. The health condition of the bridge should be understandable to users who do not have expertise in bridges. The health condition of the bridge should be easily accessible in the form of maps or diagrams.

Table 2. Selection of visualization system

Selection Item	Options	Description
Type	Bridges	Bridges managed by Yamaguchi Prefecture (bridges 2m long or longer).
	Boxes	Ditch bridges (box culverts) with a soil layer of less than 1 meter are managed by Yamaguchi Prefecture.
Robustness	I	Healthy: A state of unimpaired function. Level I is indicated in green on maps and charts.
	II	Preventive maintenance stage: a state in which function is not impaired, but measures should be taken from a preventive maintenance point of view. Level II is indicated in yellow on maps and charts.
	III	Early Action Phase: A state in which the function of a road or bridge may be impaired and action should be taken at an early stage. Level III is indicated in red on maps and charts.
	IV	Urgent Action Phase: A state of impaired or likely impaired function that warrants urgent action. Level IV is indicated in black on maps and charts.
	Unknown	No data entry status. Unknown is shown in gray on maps and charts.
Region	Area names of Yamaguchi Prefecture	Location of the facility. By selecting the name of an area in the area list, you can display information about bridges in the specified area (multiple selections are possible).
Roads	Name of each road in Yamaguchi Prefecture.	The name of the route on which the facility is located. Bridge information for a given road can be displayed by selecting a road name from the road list (multiple selections are possible).
Office	Name of each office in Yamaguchi Prefecture	Management offices of the facility. By selecting the office name in the office list, you can display information about the bridges for which the specified office is responsible (multiple selections are possible).

5. CONCLUSIONS

In this paper, the authors have proposed a method for the effective conversion of data accumulated by municipalities for periodic inspections of infrastructure into open data and presented an example of its use. Taking into account the level of expertise of municipal employees and the circulation of open data on the Internet, applications were developed to convert data from Excel, which municipal employees usually use in their work, into machine-readable data, and to make the data available on the Internet using Web API. These developments will enable the regular inspection data accumulated annually to be released as public data at an earlier stage.

It is also expected to stimulate data utilization outside of road management agencies and the development of various software to improve maintenance and management. For example, visualization is used as an example of data utilization in this paper, but if a large amount of data is available from various road management agencies, it is expected to improve the accuracy of damage trend analysis and deterioration prediction. Furthermore, if these methods can be turned into software and made available on the Internet through Web API, it is possible to create new services. These methods can then be transformed into software and made available on the Internet through Web API.

Currently, in this study, only the open data of the open data system is provided via web API. As a future plan, this study proposes a concept of a SLP, which aims to provide developers with a simple way to search for APIs, thereby accelerating the development and promotion of applications. It can also better manage the web APIs that have already been made public, ensuring the quality and accuracy of the data. At the same time, SLP can also provide functional web APIs. In addition, in order to publish and use the open data of each road management organization as big data, it is necessary to manage the IDs of structures and components, and to standardize the data structures published in JSON format.

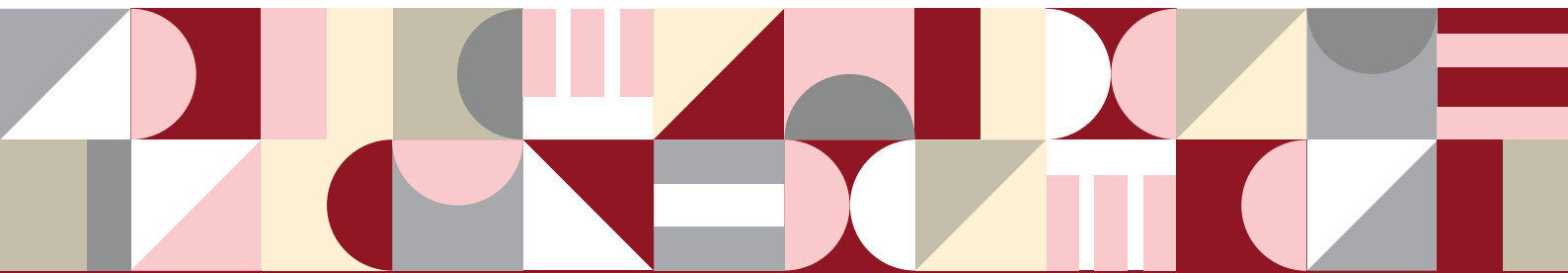
ACKNOWLEDGMENTS

Parts of this study were supported by a grant from the Japan Society of Civil Engineers for research activities related to promoting the local implementation of new technologies in 2021 and by the Yamaguchi Prefectural Construction Technology Center.

REFERENCES

- Abe, M., Sugisaki, K., and Zen, K. (2022). A study on basic functions required for infrastructure OS for infrastructure management, *Proceedings of AI and Data Science*, 3 (J2), 608-620.
- Fujimoto, K., Kawamura, K., and Sawamura, S. (2020). A study on data management methods for open data of periodic bridge inspection data, *Proceedings of Information Science and Technology*, pp.1-8.
- Kameda, T., Nakagawa, Y., Nakagawa, R., Omachi, M., and Umemoto, S. (2021). Fundamental Study on Efficiency of Data Supply to Data Platform, *Proceedings of AI and Data Science*, pp.1-6.
- Ministry of Land, Infrastructure, Transport and Tourism. (2014). *Enactment of Ministerial Ordinances and Notifications Concerning Maintenance and Repair of Roads (Partial Revision of Enforcement Regulations of Road Law, etc.)* website: <https://www.mlit.go.jp/common/001034659.pdf>
- Omukai, K. (2013). Open Data and Linked Open Data, *Proceedings of AI and Data Science*, 54 (12), 1204-1210.
- Takahisa, Y. (2014). Web API Past, Present, and Future (<Feature> Web API Utilization Techniques), *Journal of AI and Data Science*, pp.1-8.
- Yamaguchi Prefecture Civil Engineering Construction Department. (2017). *Yamaguchi Prefecture Bridge Inspection Procedure (Draft)* website: <https://www.pref.yamaguchi.lg.jp/uploaded/attachment/67403.pdf>
- Yamamoto, K., Shingu, K., Moriwaki, R., and Hato, E. (2021). Construction and Utilization of Information Platform as a Foundation for Advance Reconstruction, *Proceedings of AI and Data Science*, pp.1-9.
- Yuda, Y., Inomura, H., and Ishikawa, Y. (2020). Data Science in Infrastructure Management and Data Utilization Infrastructure to Support its Rapid Implementation, *Proceedings of AI and Data Science*, pp.1-10.

Digital Twin



DESIGN OF A DIGITAL TWIN FOR REAL-TIME CONSTRUCTION POLLUTION MANAGEMENT IN BUILDING RENOVATION PROJECTS

Truong-An Pham¹ and Veerasak Likhitrungsilp²

1) M. Eng. Candidate, Department of Civil Engineering, Faculty of Engineering, Chulalongkorn University, Bangkok, Thailand. Email: 6470308421@student.chula.ac.th or phamtruongansos@gmail.com

2) Ph.D., Associate Professor, Department of Civil Engineering, Faculty of Engineering, Chulalongkorn University, Bangkok, Thailand. Email: Veerasak.L@chula.ac.th

Abstract: Construction pollution (e.g., dust, noise, and vibration) is a critical issue that must be addressed by every party in building renovation projects. Real-time data on noise, dust, and vibration parameters need to be collected and analyzed to issue prompt warnings when certain thresholds are exceeded. Comprehensive data management can promote site conditions that are environmentally friendly for construction workers and building users. In this paper, we develop a digital twin that combines a building information modeling (BIM) model with a behavioral model for real-time construction pollution monitoring and control. The real-time noise, dust, and vibration data is collected via sensors, and transmitted and integrated with an as-is/as-planned BIM model by the Internet of Things (IoT) technology. The proposed platform allows project supervisors to detect construction pollution problems in building renovation projects instantaneously. This paper also designs the common data environment (CDE) of the digital twin. It delineates the structure and components of the database associated with construction pollution monitoring and control. An actual renovation project of the auditorium at the Faculty of Engineering, Chulalongkorn University is used to illustrate the proposed digital twin platform.

Keywords: As-is BIM models, As-designed BIM models, Building renovation project, Common Data Environment (CDE), Construction pollution, Digital twin, Internet of Things (IoT)

1. INTRODUCTION

When undertaking construction in urban areas, it is often unavoidable that site works will impact neighboring homes and businesses. High-end lodging establishments, museums, and apartment complexes often use information gathered by instruments to ensure that nearby construction is within acceptable limits and will not negatively impact their business or their guests (Zou et al., 2020). Even though most municipalities have rules to prevent these abuses, construction firms are ultimately responsible for monitoring their sites to ensure that no one is harmed. Construction superintendents, building owners, and neighbor dwellers need to address indoor air quality and vibration issues during new construction and renovation projects. Construction workers and other employees are also exposed to poor indoor air quality in these projects. Thus, on-site construction environmental monitoring can help control the behavior of project stakeholders in terms of pollutant emissions and environmental protection (Hong et al., 2019; Zhong et al., 2022). Noise, dust, and vibration are common pollutions in building renovation projects. They can have a crucial impact on the health, safety, and well-being of building occupants, as well as the surrounding community (Chennamsetty & Ravikumar, 2022). Construction activities emit various sizes of particulate matter, including total suspended particles (TSP), particulate matter 10 (PM10), and particulate matter 2.5 (PM2.5), in liquid or solid form during different construction phases. These particles can pose serious health risks to workers and nearby residents, particularly PM2.5, which can penetrate deeper into the lungs than larger particles (Rosman et al., 2019; Segersson et al., 2017).

Several Internet of Things (IoT)-related technologies have been developed to evaluate and monitor various parameters of air quality in an effort to mitigate air pollution problems. Saini et al. (2021) showed that 28 studies (70%) encompassed an indoor thermal comfort assessment, 26 studies (65%) involved CO₂ sensors, and 12 studies (30%) investigated CO sensors. In addition, they concluded that 77.5 percent of the analyzed literature lacks calibration specifications, and that 39.4 percent of sensors lack accuracy specifications. Using 5G wireless networks and blockchain, Han et al. (2019) proposed a platform for measuring an air pollution index in real-time. Chennamsetty and Ravikumar (2022) designed an IoT-based air pollution monitoring system that uses internet to monitor air quality and sounds alerts when the air quality falls below a predetermined threshold. Alam et al. (2018) developed an IoT-based application for real-time gas, sound, dust, and temperature detection. This system can be connected to a web via Wi-Fi, a customer's tablet, or a smart phone via an android application. Zhao et al. (2020) reviewed the fundamental characteristics of the IoT by comparing and analyzing radio frequency identification (RFID), machine-to-machine (M2M), and sensor networks. They then proposed an intelligent and multifunctional monitoring platform for reducing air pollution. Past research works monitored dust, noise, and vibration on construction sites using various instruments such as sound level meters (Mellert et al., 2008; Zou et al., 2020), vibration meters, dust monitors, and IoT-based monitoring systems (Trigona et al., 2022; Zou et al., 2020).

Integrating IoT and sensors with building information modeling (BIM) can create a real-time pollutant

monitoring system in the form of a digital twin. In the real world, dynamic non-geographic and geographic asset data usually does not correspond to documentation managed by building owners (Teicholz, 2013). BIM benefits are proved in the whole life cycle of a building (Kasim et al., 2016; Matejka et al., 2016). Applying BIM to FM includes documentation, quality control (Kim et al., 2014), construction monitoring (Likhitrungsilp et al., 2022), life cycle cost analysis (Likhitrungsilp et al., 2020), energy management (Hong et al., 2019; Kim et al., 2018), space management (Abrishami et al., 2020; Lucas, 2018), retrofit planning (Broderick et al., 2017; Hammond et al., 2014), as well as design and fabrication (Tuvayanond & Prasittisopin, 2023). Well-structured, up-to-date building information can reduce errors and financial risks through data management, cost calculation, and renovation progress tracking (Gökgür, 2015). Using BIM can increase the consistency of information and reduce data waste in construction information management (Likhitrungsilp et al., 2020). BIM databases are dynamic and integrated. We can combine a design model (geometrical and non-geometrical data) with a behavioral model (change management) to enable real-time model information coordination, resulting in better-coordinated design and construction changes (Menassa, 2021). Time-series sensing data such as energy and water consumption, temperature, CO₂ emissions, occupancy, electricity usage, and humidity can be collected to measure energy performances in the O&M phase (Ahankob et al., 2019; Hajian et al., 2009). Collected data can serve as a legal defense against challenges to service operations. Sensor data can also be used for real-time energy simulation and monitoring with statistical data handling methods. One of the most pressing questions in the field of building digital twin is how BIM can be used to assess the viability of different approaches to retrofitting existing buildings (Zhao et al., 2021). To achieve this, BIM models must be able to manage both static and dynamic data. The Common Data Environment (CDE) can be used by all parties involved to store, share, manage, and process information. The concept of CDE was originally proposed in BSI (2007) and BSI (2013). CDE-based management delineates information format, structure, classification, and attribute names for metadata (BSI, 2018). There are discrepancies between the CDE for as-is renovation projects and new construction projects or projects with BIM models from the design stage, including the Level of Development (LOD) of the BIM model, information exchange processes, and data types.

In this paper, we develop the CDE of a BIM-based digital twin for real-time construction pollution management in building renovation projects. The main objective of using BIM, sensors, and IoT for pollution monitoring in renovation projects is to create a comprehensive and integrated view of the construction site that allows real-time monitoring and control of pollution impacts such as noise, dust, and vibration. This can be achieved by collecting and analyzing data from various sensors and then integrating the dynamic data with the BIM model, which creates the digital representation of a construction site. This representation can then be used to optimize construction processes, minimize environmental impacts, and ensure that construction activities comply with environmental regulations. Additionally, the integration of BIM and digital twin for pollution monitoring can enhance the collaboration between stakeholders, leading to more efficient decision-making during the construction phase. The development of an IoT system for real-time construction pollution management in building renovation projects using a BIM-based digital twin is also a promising solution for sustainable construction practices. The system allows real-time monitoring and management of construction pollution, promotes sustainable construction practices, and provides valuable data for further analyses.

2. RESEARCH METHODOLOGY

Figure 1 displays the five steps of this research: (1) a comprehensive literature review, (2) data gathering through interviews, (3) identification of BIM requirements for the database in CDE, (4) design of a digital twin for real-time construction pollution management in building renovation projects, and (5) validation of the proposed system through a case study, as well as drawing conclusions and recommendations. The first step involves conducting a comprehensive literature review on online and printed articles related to construction pollution management, BIM, digital twins, and IoT technology. This literature review provides a theoretical foundation for the development of the proposed digital twin. Two rounds of in-person interviews were conducted to gather data concerning renovation projects and identify the components of construction pollution management system. In the first round of interviews, the emphasis was directed towards the present state of construction pollution management. The discussions encompassed the hurdles and constraints encountered in executing these practices, the existing CDE, as well as the life cycle of information within a construction renovation project. In the second round of interviews, an attention was directed towards the application of BIM technology, the digital twin concept, and its potential to enhance construction pollution management. Subsequently, all data gathered was synthesized and analyzed to establish the fundamental parameters that are incorporated into a noise, dust and vibration monitoring workflow within a CDE with the owner as the authorized party. The BIM requirements for the database of the proposed digital twin were identified based on these parameters. To validate the proposed system, a case study is investigated involving developing a digital twin for construction pollution management. The entire research process draws conclusions on the objectives achieved, and recommendations are made for future research in this area. To illustrate its efficacy and practicality, the proposed digital twin for real-time construction pollution management is applied to the renovation project of the Faculty of Engineering auditorium,

located at Building 3, Faculty of Engineering, Chulalongkorn University, Bangkok, Thailand. This system is called ACU-PM. Due to time constraints and the greater health impact of PM2.5 particles compared to that of PM10, this research focuses on PM2.5. This decision is based on the serious health consequences associated with prolonged exposure to PM2.5, including respiratory and cardiovascular diseases, lung inflammation, heart disease, lung cancer, and stroke. While PM10 is also a major concern in the construction industry, the PM2.5 impact is essential to ensure effective pollution management and protect human health (Rahman et al., 2019).

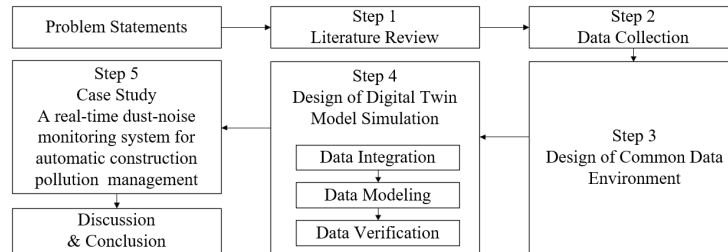


Figure 1. Research Methodology

In this research, an as-built BIM model is referred to as a BIM model that represents the final state of the building after construction, which may include additional information such as equipment specifications, maintenance records, and operating manuals. This model consists documentation, non-geometrical information and geometrical information defining the delivered project. However, since the project owner of the case study did not have the as-built drawings or as-built BIM models of the existing auditorium, we created a federated BIM model by combining the as-is BIM model generated from the scan-to-BIM technique using point cloud data and the as-designed BIM model generated from the CAD file of the designer for this renovation project. An as-designed BIM model is referred to a BIM model that represents the design intent of the building created by the design team during the pre-construction phase. Meanwhile, an as-is BIM model is referred to a BIM model that represents the current state of the building, including any modifications or changes made after construction. Creating an as-is BIM model is a process of 3D reconstruction, which requires data collection equipment to collect 3D spatial data, which is subsequently used to generate a 3D representation of the object's appearance.

To effectively manage construction pollution of this renovation project, a real-time, dust-noise-vibration monitoring system was developed by employing sensor devices installed at various locations on the site to detect the pollution. After testing the system, the hardware and software of the IoT system were set up. Six sensor devices were installed at different locations, as shown in Figure 2. As can be seen, each device consists of a cluster of sensors for detecting dust, noise, vibration, and air quality. The codes of these sensors consist of two parts. The first part is the name of the sensor cluster. The second part defines the location of the vibration sensor. For example, 2W is the sensor system number 2, which is attached to a wall to measure the wall (W) vibration during construction. 4G is the sensor system number 4, which is attached to a floor to measure the ground floor (G) vibration during construction. In this study, the sensors primarily collected data associated with the demolition activities. Each sensor was assigned with a specific number and to a location based on the criteria outlined in Table 1. The sensor placement strategy involved positioning sensors at both boundary and center of the construction site to provide comprehensive monitoring of the demolition activities and enable the detection of any potential issues.

The ACU-PM system developed in this study was built from Arduino IDE and various sensors for noise, dust, and vibration monitoring such as the grove loudness sensor, grove vibration sensor, grove air quality sensor v1.3, and sharp GP2Y10 dust sensor PM2.5, which can be connected using an ESP32 Node MCU USB – C CH340 and Breadboard Power Module MD-102. The collected sensor data can be transmitted over Wi-Fi to Hivemq, which is a message broker for the MQTT protocol and can then be forwarded to Node-RED for processing. Node-RED, which is a visual programming tool for IoT devices, can transform the sensor data into JSON format and send it to Firebase for real-time storage and analysis. Additionally, the data can be sent to a computer server in CSV format for further analysis. The JSON file can then be used in software like *Autodesk Forge* to develop the CDE of a BIM-based digital twin. When the sensor data is integrated with the BIM model, 6D BIM is used for energy analysis. This digital twin can enable real-time monitoring and management of construction pollution, promoting sustainable construction practices and reducing the negative impact on the environment. In this study, both static and dynamic data were managed via the BIM model in the digital twin platform, which was created based on interoperability and integrability considerations.

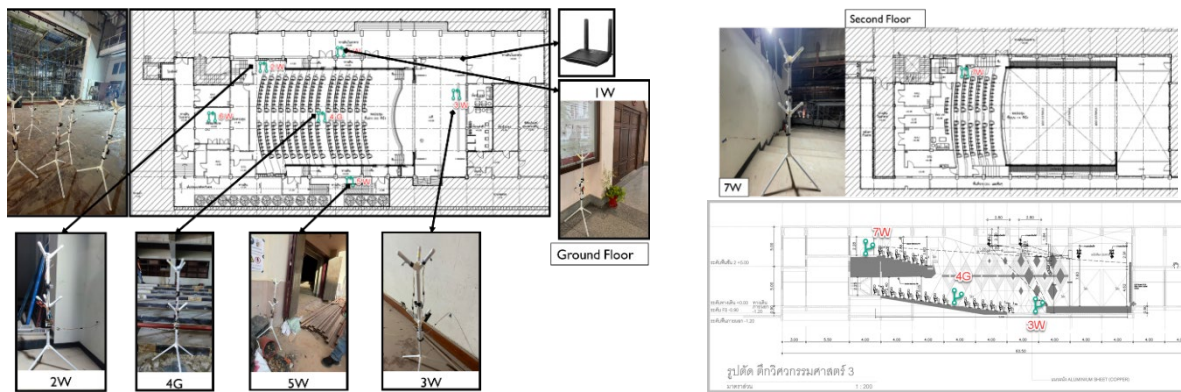


Figure 2. Six sensors devices installed on the ground floor and the second floor of the auditorium

Tables 2 and 3 show the examples of the design values for the data analysis and the trigger setting for the ACU-PM. In Thailand, the allowable levels of noise, dust, and vibration in a construction project are regulated by the Ministerial Regulation- Specification about the standard of administration and operation in respect of Occupational Safety and Health about heat, light and sound BE 2559 (2016). Noise level standards for construction activities vary depending on several factors such as the location and type of construction activity. In particular, the noise levels near residential areas must not exceed 70 dB(A) during the daytime and 60 dB(A) at night. Notification of the National Environment Board, No.15, B.E.2540 (1997) sets two additional criteria for steady and fluctuation noise, with the maximum levels of L_{max} less than 115 dB(A) and Leq 24 hr less than 70 dB(A), respectively. The employer must control the noise level to prevent the employees from being exposed to noise in the workspace where the peak sound pressure level of impact or impulse noise exceeds 140 dB or being exposed to continuous steady noise of more than 115 dB(A). The weighted equivalent continuous sound level (Leq) must be monitored and maintained below 75 dB(A) for an 8-hour period and below 70 dB(A) for a 24-hour period as stipulated by the Notification of the Ministry of Natural Resources and Environment, B.E.2548 (2005). These standards are crucial in protecting the health and well-being of workers and minimizing the impact of construction activities on surrounding communities. According to the Notification of National Environmental Board No. 10, B.E 2538 (1995) and the Notification of the National Environment Board, No.37, B.E.2553 (2010), the auditorium is classified as "Building Type 2."

3. RESULTS

Figure 3 depicts the CDE, which was developed for the ACU-PM system of this renovation project. In this CDE, we can see an integrated project information model, which every party in the project team can access at the same time and in real-time. Real-time pollution management involves monitoring and controlling the emission of particulate matter and other pollutants during construction activities to ensure the safety and well-being of workers and nearby residents. This CDE allows all stakeholders, including designers, contractors, and clients, to share project information and data using a centralized platform. By integrating real-time pollution data into the CDE, stakeholders can access and analyze the data in real-time, enabling them to make informed decisions and take appropriate measures to mitigate the risks associated with particulate matter emissions. This information can be shared across the project team and used to adjust construction activities, such as modifying construction schedules or altering work methods to reduce the emission of pollutants. As can be seen, this CDE structure is quite different from that of a new construction project in several aspects. In a new project, the CDE is usually established from the beginning and is a complete representation of the design, construction, and operation of the building. In a renovation project, however, the existing building conditions, infrastructures, and systems need to be taken into account, which can be more complex and challenging. The as-is BIM model for a renovation project typically requires more detailed information about the existing building conditions, including the location and condition of existing structures, systems, and equipment. This information is used to create a digital twin of the existing building, which can be compared to the design information for the renovation project to identify any potential conflicts and ensure that the renovation project is feasible. Another difference is that the CDE for a renovation project needs to be updated and maintained over the course of the project as changes to the existing building are made, and the design of the renovation project evolves. This requires the close collaboration between the design team and the construction team to ensure that the CDE remains accurate and up-to-date throughout the project.

From the project owner's perspective, 6D and 7D BIM can be valuable tools for pollution management during construction activities. By including pollution data in the 6D BIM model, the owner can monitor and manage pollution levels in real-time, allowing for an early intervention to reduce pollution and maintain a safe environment for workers and nearby residents. In 7D BIM, facility management data is integrated into the BIM

model, allowing the project owner to monitor and manage the building's performance over its life cycle. This includes data on energy consumption, water usage, waste management, and maintenance schedules. By incorporating pollution data into the 7D BIM model, the owner can maintain a comprehensive record of pollution levels during the construction phase, as well as the performance of the building's pollution control systems. This information can be used to identify areas for improvement and ensure compliance with environmental regulations.

Table 1. Sensors fitting locations

Sensor	Fitting criteria
Noise sensor	To ensure accurate measurements, the noise sensor must be placed in a free field at a minimum distance of one meter away from any reflective façade or barrier. Additionally, the sensor should be installed at a height of approximately 1.2 to 1.5 meters above the ground level.
Dust sensor	The dust sensors should be positioned in a clear and unobstructed location, several meters away from large structures that could disrupt the airflow, and open to the sky without any overhanging trees or structures. Ideally, the air inlet should be mounted between 1.5 to 4 meters above the ground level. To ensure the directivity of the pollution, it is typical to have at least one dust and noise monitor on each boundary of the construction site.
Vibration	The fitting of the vibration sensor should adhere to the relevant works, standards, and guidelines, which may necessitate the installation of multiple measurement points. The sensor itself must be securely attached to a rigid surface, such as a wall, floor, or heavy metal plate.
Cluster 1	This cluster is located on the ground floor outside, in front of the construction site. A vibration sensor has been attached to the wall to monitor the vibration of the outer wall. This wall is particularly vulnerable to vibration due to the construction works, dismantling of the site, and knocking down of wall panels at various locations in the corridor area where a significant amount of foot traffic passes. The sensor has been carefully positioned to ensure accurate readings and to comply with the required standards and guidelines. The door leading to this area is kept always closed to minimize the impact of external factors on the sensor readings.
Clusters 2,3,4	This cluster is situated on the construction site's ground floor, and measurement devices are placed in boundary and center positions. The selected areas are known to be significantly impacted by high levels of dust and noise, which can pose a severe risk to the health and safety of the workers on site. As such, these sensors are critical in monitoring and controlling pollution levels, providing valuable insights to aid in the management of construction site safety.
Cluster 5	In the steel processing area of the construction site, this cluster has been installed with a vibration sensor attached to the wall. This open area is particularly prone to generating noise and dust that can significantly impact the surrounding environment.
Cluster 7	A vibration sensor has been attached to the wall to monitor the vibration of the outer wall. This cluster is focused on areas where high dust and noise levels can significantly impact workers' health and safety on site. By monitoring these areas, the cluster aims to provide valuable data that can be used to inform better occupational health and safety practices.

Table 2. Design of pollutants trigger for vibration

Area	Frequency (Hertz)	Velocity (mm/s)
Building type 2		Vibration Case 1
2.1 Foundation or ground floor of building	$f \leq 10$ $10 < f \leq 50$ $50 < f \leq 100$ $f > 100$	5 $0.25f + 2.5$ $0.1f + 10$ 20
2.2 Top floor of building	Every	15*
2.3 Each building floor	Every	20**

Remark:

f = Frequency of vibration at the time of peak particle velocity is expressed as hertz

* = Standards specified for peak particle velocity on the horizontal axis

** = Standards specified for peak particle velocity on the vertical axis

Table 3. Design of pollutants trigger for ambient air standard on construction site

Pollutants	Average	Standard
Carbon monoxide (CO)	1h	Not exceed 30 ppm. (34.2 mg/m ³)
	8h	Not exceed 9 ppm. (10.26 mg/m ³)
Nitrogen Dioxide (NO ₂)	1h	Not exceed 0.17 ppm. (0.32 mg/m ³)
	1 year	Not exceed 0.03 ppm. (0.057 mg/m ³)
PM-2.5 (Particulate Matter Ø < 2.5 µm)	24h	Not exceed 0.05 mg/m ³ (50 µg/m ³)
	1 year	Not exceed 0.025 mg/m ³ (25 µg/m ³)

To develop the ACU-PM system, it is necessary to have a database that contains all necessary information about the construction site. This includes the location of the site; the sensors used to monitor dust, noise, and vibration levels; and the data collected by these sensors. To create a digital twin from an as-is BIM model, we first gathered and input the relevant data into the BIM model. This data includes the existing physical structure and systems such as architectural plans, engineering drawings, and asset management data. This data can then be used to create a virtual replica of the physical building, including its geometry, spatial relationships, and systems. This virtual replica can be updated and modified as needed throughout the project to reflect changes and updates to the physical building. The creation of the as-built BIM can be achieved by updating the digital twin with information collected during construction. This can include data from field inspections, construction progress photos, and as-built drawings. This information can be used to update the virtual model to reflect the actual physical conditions of the building after construction is completed. The goal is to create a comprehensive and accurate representation of the building, which can be used for maintenance, operation, and future renovation. The BIM database is designed to meet the level of development (LOD) requirements necessary for effectively monitoring and managing construction pollution. In this study, we designed the federated BIM model with LOD 300 and 350. The BIM model mainly focuses on architectural and structural elements, as shown in Figure 4.

The key parameters included in the noise, dust and vibration monitoring workflow of this CDE include sensor data, location data, time and dates when data was collected, analysis data, and visualization data. Data analysis and visualization are critical for effective pollution management. Data analysis involves examining sensor data such as trend analysis, threshold alerts, and predictive modeling. Data visualization encompasses processes to create visualizations of the collected data such as graphs, charts, and maps, as shown in Figure 5. These tools are essential for interpreting the data and making informed decisions about pollution management strategies. The sensor data is sent to the MTTQ broker, with node-red, real-time monitoring and control enabled by feeding sensor data into the digital twin, as shown in Figure 6. The concept of digital twin (DT) in *Autodesk Forge* refers to the creation of a virtual model of a physical building or asset that can be used to simulate and monitor its performance in real-time. By integrating data from various sources such as sensors, BIM models, and other systems, the DT provides a comprehensive view of the building's behavior and enables real-time monitoring and management of various aspects, including pollution levels. In the context of real-time pollution management, the DT can be used to monitor and analyze the behavior of the building's pollution control systems, as well as the environmental conditions inside and outside the building. By integrating sensor data into the ACU-PM, the system can provide real-time information on pollution levels, enabling early intervention to reduce pollution and maintain a safe environment for workers and nearby residents.

Federated BIM models can also be integrated into the ACU-PM system, providing a comprehensive view of the building's design and construction. This enables real-time monitoring and management of construction activities, allowing for early identification of potential sources of pollution and proactive measures to mitigate pollution levels. The preliminary results show that the data collected by the sensors on the renovation site consistently exceeds the regulations. The real-time monitoring of the pollution levels on the site is crucial for effective pollution management. *Autodesk Forge*, web API, and Firebase allow real-time monitoring of data collected from sensors, providing both the project owner and the contractor with up-to-date information on the pollution levels on the site.

4. DISCUSSION

While traditional dashboards can be useful for monitoring dust, noise, and vibration levels in a renovation project, they do not provide the same level of detail and insight as a BIM-enabled digital twin platform. This platform enables stakeholders to create a highly detailed 3D model of the building and its systems, including the location of sensors and other monitoring devices. This model can also be used to simulate different scenarios and assess the potential impact of construction activities on dust, noise, and vibration levels in real-time. In addition, the digital twin platform can be integrated with other building systems and sensors, providing stakeholders with real-time data on building performances and environmental conditions. This data can be used to optimize building performances, reduce energy consumption, and identify potential issues before they become major problems. Furthermore, the BIM-enabled digital twin platform can be used to manage the

entire life cycle of a building from the design, construction, operation and maintenance (O&M) stages. This allows stakeholders to make more informed decisions about building design and construction and to optimize building O&M plans to reduce life-cycle costs and improve performance over time.

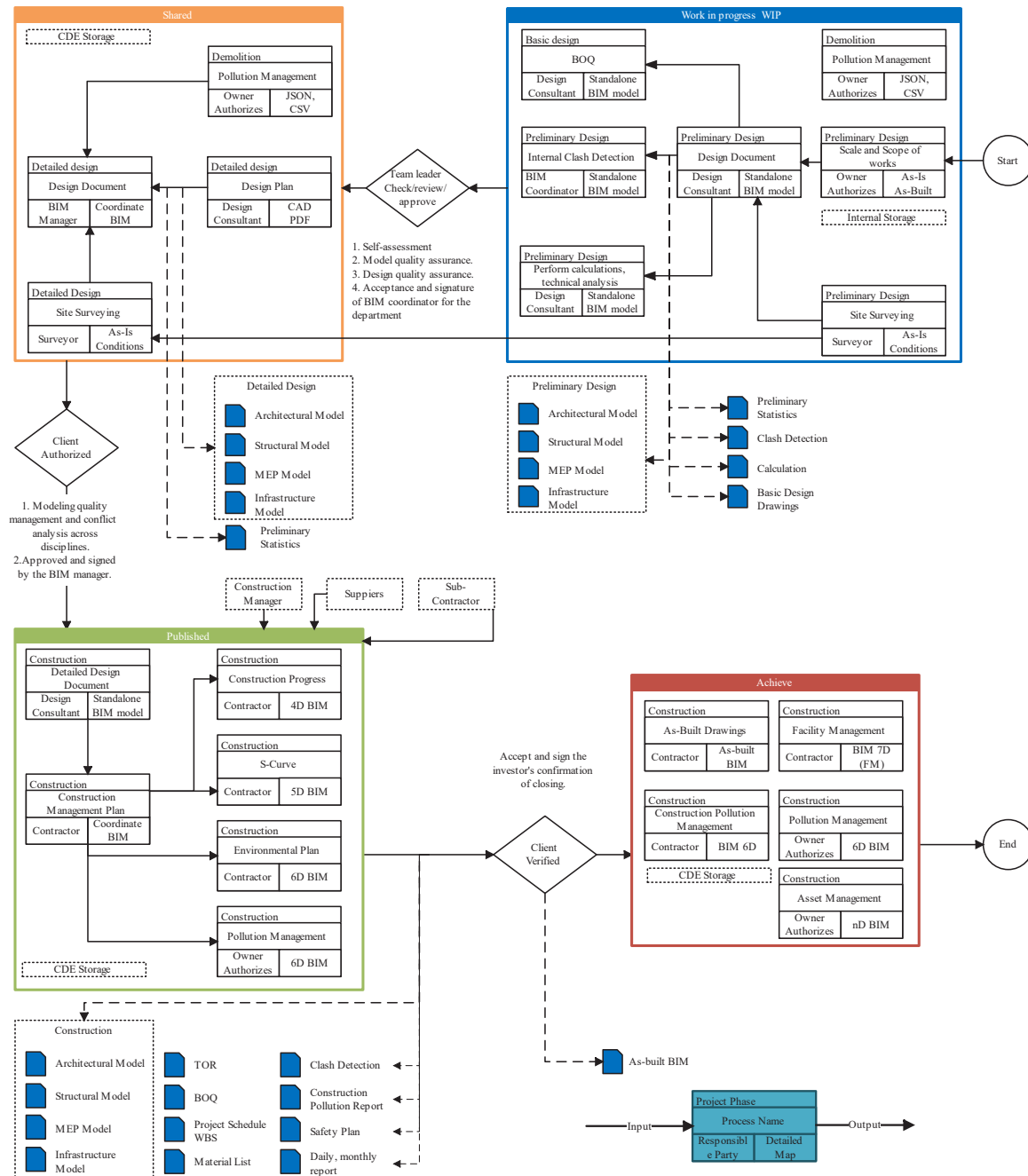


Figure 3. CDE of the digital twin of the case study



Figure 4. Federated BIM model used for the ACU-PM system: (a) Point-cloud model, (b) As-is BIM model, (c) As-designed BIM model of the Faculty of Engineering Auditorium, Chulalongkorn University

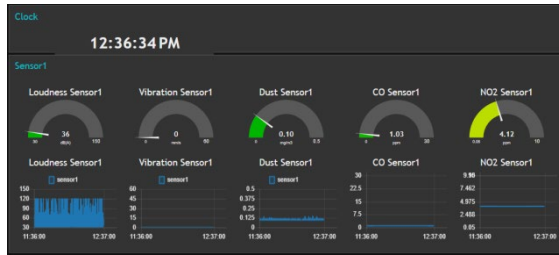


Figure 5. Dashboard on node-red – Cluster 1

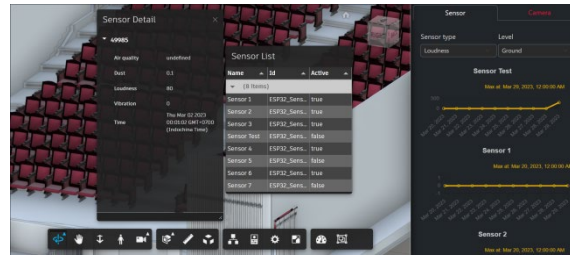


Figure 6. Real-time construction pollution management by ACU-PM on Autodesk Forge

The main difference between the conventional CDE and the CDE of the proposed ACU-PM system is that our system is designed to support digital creation and management. In the proposed CDE framework, stakeholders can store and manage data related to the building's physical characteristics, sensor data, and simulation results. With the BIM-based digital twin, the ACU-PM system serves as a tool for visualizing and analyzing necessary data to support decision-making. Regarding dust, noise, and vibration management specifically, the proposed system can store data related to the building's existing conditions and the proposed renovation scenarios. It can also simulate the impacts of these scenarios on dust, noise, and vibration levels and provide insights into potential mitigation strategies. In addition, the system enables the collaboration between different stakeholders involved in dust, noise, and vibration management such as the project owner, the contractor, the design team, and the building management team. In order to manage the emission of particulate matter on a construction site, it is important to implement effective time management practices and establish a schedule for construction activities. Additionally, baseline data should be collected to measure PM2.5 levels and map the distribution of PM2.5 emissions from the construction site. By using this baseline data, it is possible to create models to predict PM2.5 emissions during construction activities.

It should also be noted that the CDE for a digital twin can also support the ongoing maintenance and performance optimization of renovated buildings. By storing data related to the building's ongoing performances such as energy consumption, indoor air quality, and occupant comfort, the CDE can be used to identify areas where improvements should be made and optimize the building's performance over time. Furthermore, the proposed system can also support the use of emerging technologies such as artificial intelligence (AI) and machine learning (ML) to analyze data and make predictions about the building's performances.

Adopting an as-is BIM model and an as-designed (i.e., new design after renovation) BIM model can enhance the efficacy of construction pollution management of building renovation projects. As-is BIM models provide stakeholders with detailed and accurate views of existing buildings and their systems. This can be used to identify potential issues and constraints during the planning and design phase of the renovation project. By analyzing as-is BIM models, they can determine the potential impacts of construction activities on the surrounding environment and develop appropriate responsive strategies. As-designed BIM models can be used to simulate the construction process and assess the potential impacts of dust, noise, and vibration on the surrounding environment. This can help stakeholders identify potential issues before they actually occur and develop strategies to mitigate them. We can also use as-designed BIM models to optimize construction methods and materials as well as reduce the potential impacts of construction activities on the environment. Even though adopting as-is and as-designed BIM models cannot provide as complete information as as-built BIM models can, they can still provide valuable information for stakeholders to make informed decisions and optimize the construction process to minimize their impacts on the surrounding environment.

5. CONCLUSION

Both as-is and as-built BIM models in the digital twin can provide stakeholders with a comprehensive view of renovation projects and allow them to monitor the potential impacts of construction activities on the environment in real-time. This can ensure that construction projects be completed successfully and with minimal impacts on the surrounding environment. Designing a digital twin for real-time construction pollution management in building renovation projects can mitigate the impacts of pollution in various aspects. By providing a real-time monitoring function, the digital twin can be used to monitor construction activities in real-time, which can identify potential sources of pollution such as dust, noise, and vibration. Stakeholders can take an immediate action to mitigate the impact of pollution on the environment. Besides, the proposed digital twin can be used to simulate the construction process and predict the potential impact of pollution on the environment. However, several challenges must be addressed to realize the full benefit of the proposed digital twin, including the accuracy and reliability of data collection and management, the integration with other systems and stakeholders, and effective communication and collaboration. Thus, possible improvements on

designing and implementing a digital twin for real-time construction pollution management in building renovation projects include developing reliable and efficient data collection and management systems, introducing the integration of the digital twin with other systems and stakeholders, and improving communication and collaboration among stakeholders. Additionally, it is necessary to investigate how to assess the effectiveness of digital twins in reducing the environmental impacts of construction activities, including their impacts on cost and schedule performances, as well as how to identify best practices for their implementation.

ACKNOWLEDGMENTS

The authors gratefully appreciate financial supports for this research from the Chulalongkorn University's Graduate Scholarship Programme for ASEAN or Non-ASEAN Countries and Department of Civil Engineering, Faculty of Engineering, Chulalongkorn University.

REFERENCES

- Abrishami, S., Goulding, J., & Rahimian, F. (2020). Generative BIM workspace for AEC conceptual design automation: prototype development. *Engineering, Construction and Architectural Management*.
- Ahankoob, A., Manley, K., & Abbasnejad, B. (2019). The role of contractors' building information modelling (BIM) experience in realising the potential values of BIM. *International Journal of Construction Management*, 1-12. <https://doi.org/10.1080/15623599.2019.1639126>
- Alam, S. S., Islam, A. J., Hasan, M. M., Rafid, M. N. M., Chakma, N., & Imtiaz, M. N. (2018). Design and development of a low-cost IoT based environmental pollution monitoring system. 2018 4th international conference on electrical engineering and information & communication technology (iCEEICT),
- Broderick, A., Byrne, M., Armstrong, S., Sheahan, J., & Coggins, A. M. (2017). A pre and post evaluation of indoor air quality, ventilation, and thermal comfort in retrofitted co-operative social housing. *Building and Environment*, 122, 126-133.
- British Standards Institution. (2007). BS 1192:2007+A2:2016, *Collaborative production of architectural, engineering and construction information - code of practice*.
- British Standards Institution. (2013). PAS 1192-2:2013, *Specification for information management for the capital/delivery phase of construction projects using building information modelling*.
- British Standards Institution. (2018). BS EN ISO 19650-1:2018, *Organization and digitization of information about buildings and civil engineering works, including building information modelling (BIM) - Information management using building information modelling. Part 1: Concepts and principles*.
- Chennamsetty, S., & Ravikumar, C. (2022). Efficient and enhanced air pollution monitoring and controlling using IoT.
- Gökgür, A. (2015). Current and future use of BIM in renovation projects.
- Hajian, Hamid, & Becerik-Gerber, B. (2009). A research outlook for real-time project information management by integrating advanced field data acquisition systems and building information modeling. *Computing in Civil Engineering*, 83-94.
- Hammond, R., Nawari, N., & Walters, B. (2014). BIM in sustainable design: strategies for retrofitting/renovation. In *Computing in Civil and Building Engineering (2014)* (pp. 1969-1977).
- Han, Y., Park, B., & Jeong, J. (2019). A novel architecture of air pollution measurement platform using 5G and blockchain for industrial IoT applications. *Procedia Computer Science*, 155, 728-733.
- Hong, J., Hong, T., Kang, H., & Lee, M. (2019). A framework for reducing dust emissions and energy consumption on construction sites. *Energy Procedia*, 158, 5092-5096.
- Kasim, A., John, G., & Michael J., O. (2016). Role of BIM and 3D Laser Scanning on Job Sites from the Perspective of Construction Project Management Personnel. In *Construction Research Congress*, 2532-2541.
- Kim, J., Hadadi, O. A., Kim, H., & Kim, J. (2018). Development of A BIM-based maintenance decision-making framework for the optimization between energy efficiency and investment costs. *Sustainability*, 10(7), 2480.
- Kim, M.-K., Jack C.P., C., Hoon, S., & Chih-Chen, C. (2014). A framework for dimensional and surface quality assessment of precast concrete elements using BIM and 3D laser scanning. *Automation in Construction*, 14.
- Likhitrungsilp, V., Ioannou, P. G., & Nantapanuwat, P. (2022). A BIM-Enabled Dashboard System for Construction Project Monitoring and Control. Construction Research Congress 2022,
- Likhitrungsilp, V., Le, H., Yabuki, N., & Ioannou, P. (2020). A Relational Database Management System for Life-Cycle Cost Analysis of BIM Projects. *Proceedings of International Structural Engineering and Construction*, 7. [https://doi.org/10.14455/ISEC.res.2020.7\(1\).CON-05](https://doi.org/10.14455/ISEC.res.2020.7(1).CON-05)
- Lucas, J. (2018). Immersive Vr In The Construction Classroom To Increase Student Understanding of Sequence, Assembly, and Space of Wood Frame Construction *J. Inf. Technol. Constr.*, 23, 179-194.

- <http://www.itcon.org/2018/9>
- Matejka, P., Kosina, V., Tomek, A., Tomek, R., Berka, V., & Šulc, D. (2016). The integration of BIM in later project life cycle phases in unprepared environment from FM perspective. *Procedia Engineering*, 164, 550-557.
- Mellert, V., Baumann, I., Freese, N., & Weber, R. (2008). Impact of sound and vibration on health, travel comfort and performance of flight attendants and pilots. *Aerospace Science and Technology*, 12(1), 18-25.
- Menassa, C. C. (2021). From BIM to digital twins: A systematic review of the evolution of intelligent building representations in the AEC-FM industry. *Journal of Information Technology in Construction (ITcon)*, 26(5), 58-83.
- National Environment Board (2016). *Ministerial Regulation- Specification about the standard of administration and operation in respect of Occupational Safety and Health about heat, light and sound BE 2559 (2016)*.
- National Environment Board (1995). *Notification of National Environmental Board No. 10, B.E 2538 (1995)*.
- Royal Government Gazette (2005). *Notification of the Ministry of Natural Resources and Environment, B.E.2548 (2005)*.
- National Environment Board (1997). *Notification of the National Environment Board, No.15, B.E.2540 (1997)*.
- National Environment Board (2010). *Notification of the National Environment Board, No.37, B.E.2553 (2010)*.
- Rahman, S. A. A., Yatim, S. R. M., Abdullah, A. H., Zainuddin, N. A., & Samah, M. A. A. (2019). Exposure of particulate matter 2.5 (PM_{2.5}) on lung function performance of construction workers. AIP Conference Proceedings,
- Rosman, P. S., Samah, M. A. A., Yunus, K., & Hussain, M. (2019). Particulate Matter (PM_{2.5}) at construction site: a review. *Int J Recent Technol Eng*, 8(IC2), 255-259.
- Saini, J., Dutta, M., & Marques, G. (2021). Sensors for indoor air quality monitoring and assessment through Internet of Things: a systematic review. *Environmental Monitoring and Assessment*, 193(2), 66.
- Segersson, D., Eneroth, K., Gidhagen, L., Johansson, C., Omstedt, G., Engström Nylén, A., & Forsberg, B. (2017). Health impact of PM₁₀, PM_{2.5} and black carbon exposure due to different source sectors in Stockholm, Gothenburg and Umea, Sweden. *International journal of environmental research and public health*, 14(7), 742.
- Teicholz, P. (2013). *BIM for facility managers*. John Wiley & Sons.
- Trigona, C., Costa, E., Politi, G., & Gueli, A. M. (2022). IoT-Based Microclimate and Vibration Monitoring of a Painted Canvas on a Wooden Support in the Monastery of Santa Caterina (Palermo, Italy). *Sensors*, 22(14), 5097.
- Tuvayanond, W., & Prasittisopin, L. (2023). Design for Manufacture and Assembly (DfMA) of Digital Fabrication (Dfab) and Additive Manufacturing (AM) in Construction: A Review.
- Zhao, L., Zhang, H., Wang, Q., & Wang, H. (2021). Digital-Twin-based evaluation of nearly zero-energy building for existing buildings based on scan-to-BIM. *Advances in Civil Engineering*, 2021.
- Zhao, Y.-L., Tang, J., Huang, H.-P., Wang, Z., Chen, T.-L., Chiang, C.-W., & Chiang, P.-C. (2020). Development of IoT technologies for air pollution prevention and improvement. *Aerosol and Air Quality Research*, 20(12), 2874-2888.
- Zhong, B., Guo, J., Zhang, L., Wu, H., Li, H., & Wang, Y. (2022). A blockchain-based framework for on-site construction environmental monitoring: Proof of concept. *Building and Environment*, 217, 109064.
- Zou, C., Zhu, R., Tao, Z., Ouyang, D., & Chen, Y. (2020). Evaluation of building construction-induced noise and vibration impact on residents. *Sustainability*, 12(4), 1579.

VERIFICATION OF REGISTRATION AND COMPLEMENTATION OF POINT CLOUD DATA OBTAINED BY SIMPLIFIED MEASUREMENT

Ryuichi Imai¹, Kenji Nakamura², Yoshinori Tsukada³, Yasuhito Niina⁴, and Ryo Komiya⁵

1) Ph.D., Prof., Faculty of Engineering and Design, Hosei University, Tokyo, Japan. Email: imai@hosei.ac.jp

2) Ph.D., Prof., Faculty of Information Technology and Social Sciences, Osaka University of Economics, Osaka, Japan. Email: k-nakamu@osaka-ue.ac.jp

3) Ph.D., Assoc. Prof., Faculty of Business Administration, Setsunan University, Osaka, Japan. Email: yoshinori.tsukada@kjo.setsunan.ac.jp

4) Advanced Technologies Research Laboratory, Asia Air Survey Co.,Ltd., Kanagawa, Japan. Email: ysh.niina@ajiko.co.jp

5) Graduate Student., Graduate School of Engineering and Design, Hosei University, Tokyo, Japan. Email: ryo.komiya.5p@stu.hosei.ac.jp

Abstract: In recent years, digital twin has been attracting attention toward the realization of smart cities. In Japan, the Ministry of Land, Infrastructure, Transport and Tourism is promoting Project PLATEAU to construct a 3D urban model from photographs and point cloud data collected by aerial survey. The current 3D urban model faces the problems of collecting data on indoor spaces and areas shaded by street trees, which aerial survey is unable to obtain, and of collecting data on local deformations. These problems may be solved by utilizing point cloud data measured simply with inexpensive equipment. In this study, we improved the registration method and verified whether or not different point cloud data obtained by simplified measurement can complement each other. In the experiment, we registered point cloud data measured with a mobile terminal, which is one of the simplified measurement methods, using a transformation matrix calculated by an existing method, to complement the missing parts. As a result, it was proved that different sets of point cloud data obtained by two different applications of the mobile terminal allow complementing the missing parts of the respective cloud data with each other. The experimental results suggest the applicability of point cloud data obtained by mobile terminals to complement 3D urban models.

Keywords: 3D urban model, Point cloud data, Voxel, GICP, Point cloud registration

1. INTRODUCTION

In recent years, digital twins have been attracting attention towards building smart cities that utilize ICT and IoT. Digital twin is a mechanism for measuring in real time information on urban activities such as the movement of people and vehicles in the physical space and environmental information such as changes in weather and vegetation to utilize for simulation and analysis in the cyberspace. In Japan, various local governments are building digital twins of cities in order to utilize them for efficient urban development and provision of new services (Tokyo Metropolitan Government, 2021a).

In Japan, the Ministry of Land, Infrastructure, Transport and Tourism (MLIT) has been promoting the development and utilization of digital twins, working on the development of a 3D urban model in an open format, "Project PLATEAU" (MLIT, 2020). The 3D urban model of PLATEAU is created from 2D maps such as the basic urban planning map, aerial survey data obtained by public surveys and so on, and the basic urban planning survey data on building digital twins (MLIT, 2022). In specific, photos and point cloud data measured by aerial laser profilers and oblique cameras are used. While aerial survey is able to efficiently measure a wide area, it is unable to measure the point cloud data on the indoor space or the areas shaded by buildings and street trees. Consequently, a detailed 3D urban model that covers all over Japan has not yet been built. Another problem for 3D urban models is how to collect 3D information on the parts of deformation caused by construction works or natural disasters. For example, in the Virtual Singapore, a project led by the National Research Foundation, Singapore (Government of Singapore, 2021), the 3D urban model built from aerial survey data has not been updated since 2017 due to the technical problems mentioned above in addition to administrative problems. (Tokyo Metropolitan Government, 2021b).

Acquisition of point cloud data requires expensive equipment such as laser scanners, and specialized knowledge is also needed for measurement and data processing. In recent years, however, the cost reduction of measurement equipment and technological innovations such as AI have made it possible to acquire point cloud in a simplified way with mobile terminals and other devices (Imai et al., 2023; Ben et al., 2020). Given this background, the preparation to collect a large amount of 3D information in urban spaces is in order, and the next challenge is to establish a method for integrating and managing the large amount of 3D information to be collected. To integrate separately measured point cloud data, it is necessary to register the unique coordinate systems of the respective point cloud data into a single coordinate system. If point cloud data can be registered to the coordinate system in real space, it can be applied to visualization on the digital twin or complementing the existing 3D urban

model. Generally, point cloud registration can be achieved by using algorithms to minimize the distance between point cloud data such as Iterative Closest Point (ICP) (Szymon and Marc., 2001) and Generalized Iterative Closest Point (GICP) (Aleksandr et al., 2009). The registration of point cloud data using the ICP algorithm is also a standard feature in the point cloud data processing software CloudCompare. However, depending on the initial position and shape of the point cloud data, a problem of falling into a local solution may occur, which obstructs accurate registration. As a solution to this problem, we devised in this study a method to perform GICP on the point cloud data by applying the extracting process of the overlapped parts based on manually set initial position as well as the downsampling process using voxels. From the above, the purpose of this study is to verify whether or not it is possible to mutually complement point cloud data obtained by simplified measurement using the improved registration method.

2. METHOD

In the proposed method, two preprocessing processes of "extraction of overlapped parts" and "downsampling" are applied to the point cloud data to be registered in order to improve the accuracy of registration and the efficiency of calculation of the transformation matrix (Figure 1). In this paper, the point cloud data with coordinates that are the basis for registration is referred to as "target point cloud data" and the point cloud data to be registered as "source point cloud data".

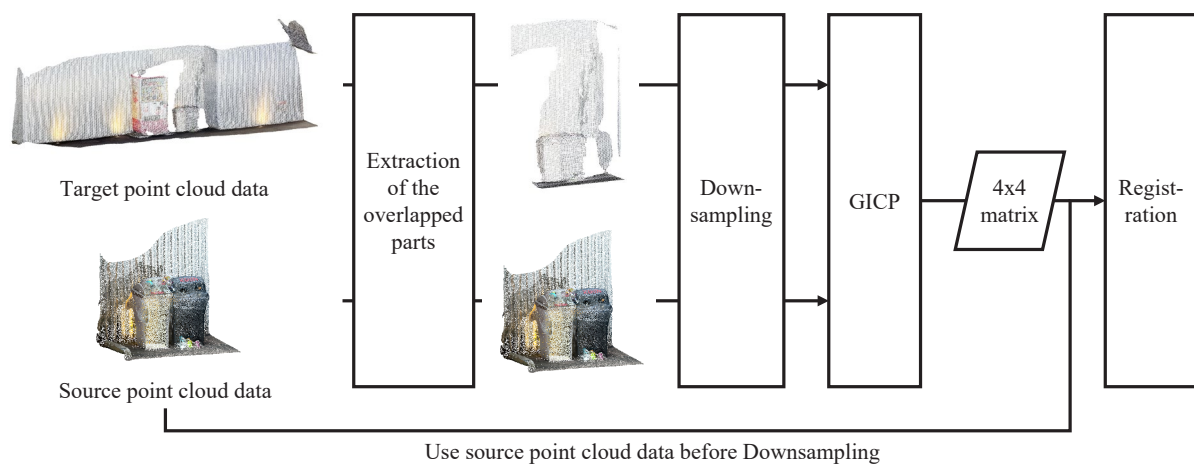


Figure 1. Flow of calculating the transformation matrix

2.1 Extraction Process of Overlapped Parts

In this method, in order to treat local solutions, the position and rotation of the source point cloud data are manually adjusted on the target point cloud data using CloudCompare, a software program for processing point cloud data. Then, the vertex coordinates of bounding boxes of both data are obtained, and a new cuboid is generated at the point where the two bounding boxes overlap in 3D. The overlapped parts are extracted from both target- and source- point cloud data by obtaining only the points that are contained within the cuboid.

2.2 Downsampling Process

When processing a large number of points, neighboring point search is a bottleneck. In this method, the Voxel grid is utilized for downsampling of the point cloud data to improve the efficiency of neighboring point search. A voxel grid is created in the bounding box of point cloud data with arbitrary length on one side. For downsampling, data is processed so that the number of points in each voxel grid becomes at most one by replacing the points in each voxel grid with the centroid of all points contained inside. The downsampling process is applied to both target and source point cloud data.

2.3 Calculating the Transformation Matrix

GICP is adopted for the transformation matrix. GICP is an algorithm that extends ICP and is a registration method that, in addition to the point location information used in ICP, uses a covariance matrix to consider the local geometric structure of the two-point groups. By obtaining the normal information for each point, GICP improves the matching accuracy. The transformation matrix calculated by GICP is a 4-by-4 matrix that provides translations and rotations of the 3D coordinates of each point. This method uses point cloud data to which the overlap extraction and downsampling processes have been applied to calculate the transformation matrix and register the source point cloud data to the target point cloud data.

3. EXPERIMENT

The source point cloud data, with the initial position given by CloudCompare, is registered by applying the proposed method and conventional GICP. In 3.1, we describe the measurements and details of the point cloud data used in this process. In 3.2, we describe the details of the application method and the indicators used to evaluate the results. In 3.3, we describe the registration results for the respective methods of calculating the transformation matrix. In 3.4, we describe the complementing results from the complementary point cloud data to which the preprocessing method with the voxel grid of 0.05 m was applied.

3.1 Measurement of Point Cloud Data

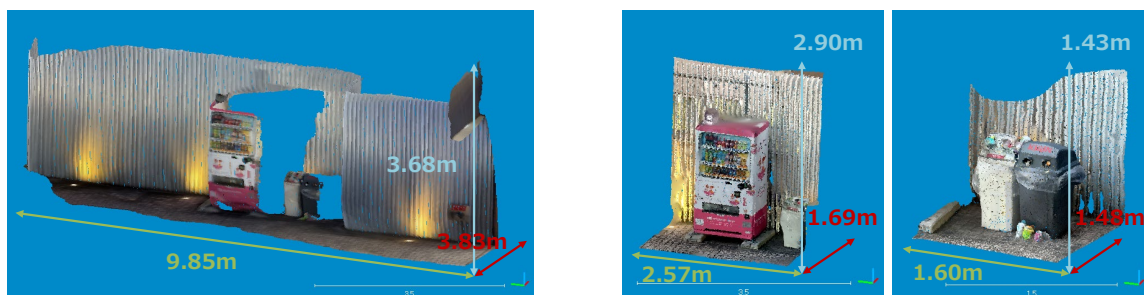
iOS applications were used to obtain the point cloud data. The measurement device used is iPhone 13 Pro Max sold by Apple Inc. Two applications, Scaniverse and Polycam, were used (Table 1). Figure 2, Figure 3, and Table 2 show the target environment, obtained point cloud data, and the details respectively. The target point cloud data was obtained roughly using Scaniverse, covering a relatively large area. The source point cloud data was measured in detail by measuring the missing parts of the target point cloud data twice separately using Polycam. Figure 3 and Table 2 show that the point cloud data used for the target point cloud measures a wider area than the source point cloud data, but there is only a difference of 20,000 to 30,000 points between the two. Therefore, as shown in Fig. 4, there are differences in the shape of the point cloud data acquired by different measurement applications, even if the point cloud data measured the same points. Figure 4 also shows that the point cloud data measured with the iPhone is distorted even on flat surfaces, such as the ground surface and the side of a vending machine.

Table 1. Applications used

Application	Provider	Version at the time of measurement
Scaniverse	Toolbox AI	1.6.1
Polycam	Polycam Inc.	3.0.8



Figure 2. Photos of the surrounding area



A. Target point cloud data

B. Source point cloud data (left: vending machine, right: trash can)

Figure 3. Measured point cloud data

Table 2. Details of point cloud data

Point cloud data	Applications used	Number of Points (points)
Target point cloud data	Scaniverse	183,132
source point cloud data (Vending machine)	Polycam	164,180
source point cloud data (Trash can)	Polycam	147,940

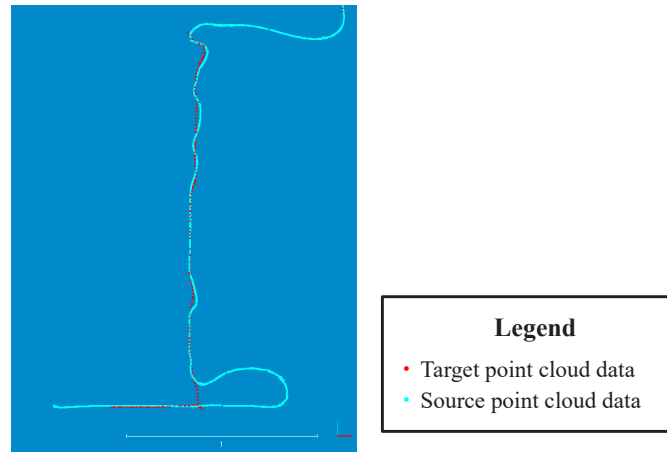


Figure 4. Comparison of cross sections of target and source point cloud data

3.2 Application of Methods and Evaluation Methods

In this experiment, the source point cloud data was registered with the voxel grid used for downsampling set to 0.05 m, 0.10 m, 0.15 m and 0.20 m. The accuracy is evaluated by comparing the results with the registration results using from CloudCompare's ICP and GICP. The evaluation items include quantitative distance of the point cloud data after registration, cross-sectional shape confirmed by visual inspection, and processing time. For evaluating the distance of the point cloud data, the average value of the M3C2 distance, which indicates the distance between each point and its neighboring point. The M3C2 distance is computed for every point within the source point cloud data subsequent to registration, serving as an assessment of the registration outcome. Put differently, the target and source point cloud data, utilized in the evaluation of the M3C2 distance, do not undergo down-sampling; instead, they encompass the identical quantity of points as those obtained during the measurement process. As indicated in Section 3.1, the point cloud data measured with the iPhone exhibited distortions. Therefore, we consider that not only quantitative indicators but also visual evaluation was necessary. Consequently, in the evaluation of the cross-section, we used the registration results of a vending machine as an example and visually checked the cross-section of the point cloud data in the two orientations of the X-axis and Y-axis directions. The processing time is the time required to calculate the transformation matrix, which is an evaluation indicator aimed at verifying the improvement in efficiency of the neighbor search by downsampling.

3.3 Registration Results for Each Calculation Method of Transformation Matrix

The number of points in the target and source point clouds after the application of downsampling is shown in Table 3. Table 3 demonstrates that the number of points in the point cloud data after the application of downsampling is significantly reduced compared to the point cloud data before the application of downsampling, as shown in Table 2.

The M3C2 distances for each method of calculating the transformation matrix are shown in Table 4. From Table 4, the M3C2 distances for the non-ICP methods were smaller than those for the initial position. Comparing the results of the devised method with those of the GICP, the registration of both vending machine and trash can point cloud data was more accurate than that of the GICP when the voxel grid used for downsampling was 0.10 m. The vending machine point cloud data was more accurate than that of the GICP when the voxel grid used for downsampling was 0.10 m. The registration results for the vending machine point cloud data did not outperform the GICP registration accuracy when a voxel grid other than 0.10 m was used. In the registration of the trash can point cloud data, the registration results slightly exceeded the GICP accuracy when a voxel grid of 0.20 m was used in addition to 0.10 m. The registration results using CloudCompare's ICP function were slightly better than the GICP accuracy when a voxel grid of 0.20 m was used. The results of the registration using the ICP function of CloudCompare show that the distances between the point clouds are larger than those of the original point cloud data, confirming that the registration is less accurate.

In the evaluation of the M3C2 distance, the registration results from the method that successfully reduced the M3C2 distance and the cross-section of each point cloud data after registration are shown in Figure 5. Figure

5.A shows that in all cases, the source point cloud data can be registered in the correct position. As shown in Figures 5.B and 5.D, in the cross-section of the ground surface, in both cross-sections along the X- and Y-axes, the voxel grid with a 0.10 m distance as evaluated by the M3C2 method has the closest points to the target point cloud. On the other hand, as shown in Figs. 5.C and 5.E, there are cases where the voxel grid is closer to the target point cloud than the voxel grid of 0.10 m, such as in the cross-section of the vending machine.

Table 5 shows the calculation time of the transformation matrix. From Table 5, it is confirmed that the processing time of the proposed method is about 1 to 2 second shorter than that of the conventional GICP for both of the two source point cloud data. This indicates that the downsampling process using a voxel grid has a certain effect in improving the efficiency of the nearest neighbor search

Table 3. Number of points after downsampling

Source point cloud data	Applied method	Target point cloud (points)	Source point cloud (points)
Vending machine	Proposed method (0.05m)	4,826	7,651
	Proposed method (0.10m)	1,304	2,077
	Proposed method (0.15m)	607	861
	Proposed method (0.20m)	420	477
Trash can	Proposed method (0.05m)	2,512	3,390
	Proposed method (0.10m)	671	872
	Proposed method (0.15m)	335	395
	Proposed method (0.20m)	197	208

Table 4. M3C2 Distance

Source point cloud data	Applied method	Average of M3C2 distance (cm)
Vending machine	Before Registration	2.14
	ICP (Cloud Compare)	5.58
	GICP	1.05
	Proposed method (0.05m)	1.34
	Proposed method (0.10m)	1.01
	Proposed method (0.15m)	1.36
	Proposed method (0.20m)	1.48
Trash can	Before Registration	3.44
	ICP (Cloud Compare)	12.23
	GICP	1.49
	Proposed method (0.05m)	1.56
	Proposed method (0.10m)	1.18
	Proposed method (0.15m)	1.74
	Proposed method (0.20m)	1.43

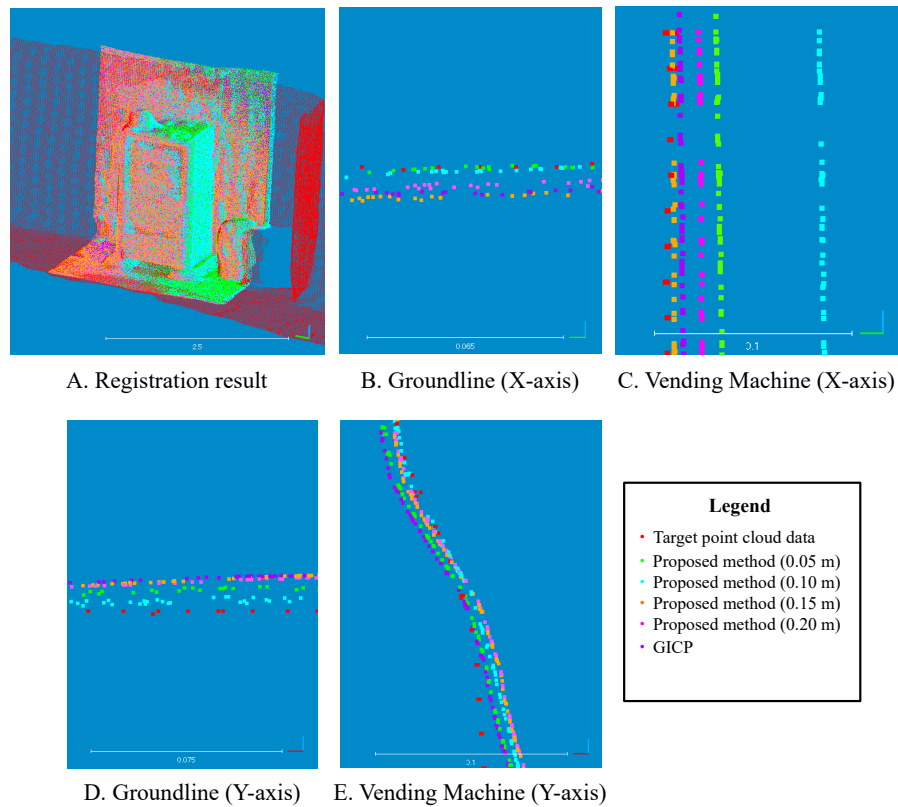


Figure 5. Registration Results of Vending Machine

Table 5. Comparison of calculation time for transformation matrix

Source point cloud data	Applied method	Processing time (seconds)
Vending machine	GICP	3.48
	Proposed method (0.05m)	2.55
	Proposed method (0.10m)	2.63
	Proposed method (0.15m)	1.92
	Proposed method (0.20m)	1.96
Trash can	GICP	3.64
	Proposed method (0.05m)	2.23
	Proposed method (0.10m)	2.32
	Proposed method (0.15m)	1.75
	Proposed method (0.20m)	1.76

3.4 Results of Complementing the Missing Parts

From the previous section, the use of a voxel grid of 0.10 m allows registration with an accuracy higher than that of the GICP. The results of complementing the target point cloud data with two source point cloud data sets registered using a 0.10 m voxel grid are shown in Figure 6. Figure 6 indicates that the side and top surfaces of the vending machine, which were missing in the target point cloud data, as well as the detailed shape of the trash can were successfully complemented.

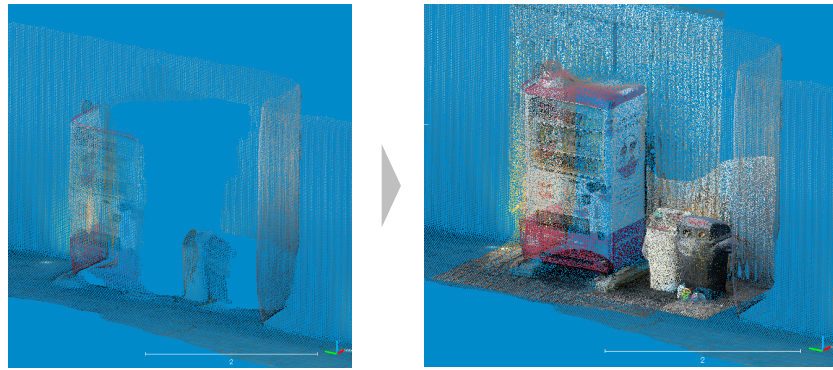


Figure 6. Result of complementation of target point cloud data

4. DISCUSSION

Comparison of the registration results of the devised method with existing methods shows that the quantitative evaluation of the registration of the entire point cloud data by the M3C2 distance indicates that the registration is more accurate than the GICP when using a voxel grid of 0.10 m. There are two possible reasons for the improved accuracy despite the reduction in the number of points used to calculate the transformation matrix due to downsampling. The first is that the two-point cloud data sets were measured by different applications: as indicated in Section 3.1, point cloud data acquired by different measurement applications have different point densities and shapes for each application, even when measuring the same location. In the proposed method, by downsampling the point cloud data, the point density and shape characteristics between the target and source point cloud data are brought closer, which may have resulted in successful registration. The second point relates to the distortion in the point cloud data measured with the iPhone: from Section 3.1, the point cloud data measured with the iPhone tends to be slightly distorted, even on a flat surface, unlike point cloud data measured with high-precision equipment. Therefore, the downsampling method of obtaining the centroid may have reduced the effect of irregular distortions in the point cloud data and improved the registration accuracy. In addition, the fact that the evaluation of the cross-section by visual inspection is partially inconsistent with the evaluation using the M3C2 distance is thought to be due to the distortions occurring in the point cloud data. On the other hand, the downsampling of this method uses the center of gravity of the point cloud data in the voxel grid as a new point, which may change the geometrical characteristics of the point cloud data due to downsampling. Therefore, it is considered that the smaller voxel grids accurately reflect the distribution characteristics of the original point cloud data, and the larger the voxel grid, the less accurate the registration. Tables 2 and 3 show that downsampling significantly reduces the number of points in the target and source point cloud data. Therefore, it is considered that the larger the voxel grid used for downsampling, the more difficult it becomes to preserve the geometrical characteristics of the original point cloud data. Indeed, when the voxel grid exceeds 0.15 m, the accuracy is inferior to that of the Generalized Iterative Closest Point (GICP) method. The registration accuracy also diminishes when employing a voxel grid of 0.05 m, compared to a grid of 0.10 m. As illustrated in Table 3, the point cloud data downsampled using the 0.05m voxel grid has approximately quadruple the number of points as the 0.10m voxel grid. This implies that each voxel grid contains fewer points when subjected to downsampling. It further suggests that a voxel grid must contain an ample number of points to mitigate the effects of distortion in the point cloud data. Therefore, a voxel grid of 0.10m proves optimal for preserving the geometrical characteristics of the original point cloud data while minimizing distortion effects, which is a notable characteristic of point cloud data measured with the iPhone. The devised method took approximately 1 to 2 seconds less processing time than the GICP in registering approximately 150,000 point cloud data acquired over an area of approximately 3 m. The processing time of the devised method was approximately 1 to 2 seconds shorter than that of the GICP. This means that voxel-grid downsampling outperforms existing methods in terms of accuracy and processing time. Moreover, since this experiment evaluated the registration of different sets of point cloud data with each other within a narrow area, such as installations in an urban space, it is necessary to make verification using point cloud data with a large number of points, such as promenades and indoor spaces in an urban space.

In the experiment, quantitative evaluation of the accuracy of registration suggested the possibility that point cloud data obtained by simplified measurement using a mobile terminal may help to collect 3D information on the missing parts. The importance of this partial complementation by point cloud data does not lie in the accuracy of the measurement data, but in the capability of reflecting information about what is where in real time on the 3D urban model. Unlike buildings and civil engineering structures that are already in place on PLATEAU, installations such as vending machines and trash cans are moved, removed, or newly built with high frequency. Therefore, in order to improve the accuracy of real-time analysis on the digital twin, it is necessary to establish a method to efficiently collect and complement the missing parts of 3D information from aerial surveys with simple measurements.

5. CONCLUSIONS

In this study, in order to efficiently calculate the transformation matrix made by GICP, we applied overlap extraction and voxel grid downsampling as preprocessing to the point cloud data used for registration. As a result, we succeeded in improving the processing efficiency while maintaining the accuracy of the existing GICP, proving that it is possible to complement the missing parts between point cloud data obtained by simplified measurement with a mobile terminal. From the above, it is made clear that point cloud data obtained in a simple way with a mobile terminal can be utilized as a means of collecting 3D information about the missing parts of indoor space and aerial survey data, which has been a challenging issue in building 3D urban models.

Since aerial survey data is originally used in PLATEAU, we would like to use the point cloud data obtained by the aerial laser profiler or aerial photogrammetry as the target point cloud data to verify whether or not the point cloud data obtained in a simplified way can be used to complement the data. Furthermore, it is necessary to utilize point cloud data over a wider area to clarify the conditions under which this method can be applied. Based on these verifications, we will build up a mechanism to efficiently collect a large amount of point cloud data and establish a method to reflect the results of complementation on the actual 3D urban model.

ACKNOWLEDGMENTS

We would like to thank Yutaka Matsubayashi and Ichijiro Yamamoto of Asia Air Survey Co., Ltd.. This work was supported by JSPS KAKENHI Grant Number JP20K14854.

REFERENCES

- Aleksandr, S., Dirk, H., and Sebastian, T. (2009). Generalized-icp, *Robotics: Science and Systems (RSS)*, 25, pp.26-27.
- Ben, M., Pratul, S., Matthew, T., Jonathan, B., Ravi, R., and Ren, N. (2020). NeRF: Representing Scenes as Neural Radiance Fields for View Synthesis, *Proceedings of the European Conference on Computer Vision (ECCV)*.
- Government of Singapore. (2021). *Virtual Singapore*. Retrieved from National Research Foundation Prime Minister's Office Singapore website: <https://www.nrf.gov.sg/programmes/virtual-singapore>
- Imai, R., Nakamura, K., Tsukada, Y., and Komiya, R. (2023). Basic Research on Creation of Indoor 3D Models By Voxel Representation Using LiDAR of Portable Terminal, *Ser. F3 (Civil Engineering Informatics)*, *Journal of Japan Society of Civil Engineers*, 79 (22), 1-9.
- Ministry of Land, Infrastructure, Transport and Tourism. (2020). *About*. Retrieved from PLATEAU by MLIT website: mlit.go.jp/plateau/about/
- Ministry of Land, Infrastructure, Transport and Tourism. (2022). *ucg01 Use Case Development Guide - Municipalities / 01. What is PLATEAU?*. Retrieved from PLATEAU by MLIT website: <https://www.mlit.go.jp/plateau/learning/ucg01/>
- Szymon, R., and Marc, L. (2001). Efficient Variants of the ICP Algorithm, *Proceedings Third International Conference on 3-D Digital Imaging and Modeling*, pp.145-152.
- Tokyo Metropolitan Government. (2021a). *Digital Twin Realization Project*. Retrieved from Tokyo Metropolitan Government website: <https://info.tokyo-digitaltwin.metro.tokyo.lg.jp/>
- Tokyo Metropolitan Government. (2021b). *Latest Trends in Virtual Singapore*. Retrieved from Tokyo Metropolitan Government website: https://www.toshiseibi.metro.tokyo.lg.jp/bunyabetsu/machizukuri/pdf/digital04_san02.pdf

TRAFFIC NOISE SIMULATION AND ITS AURALIZATION USING VR TECHNOLOGY

Kazuo Kashiya¹

1) Prof., Department of Civil and Environmental Engineering, Chuo University, Tokyo, JAPAN. Email:kaz.90d@civil.chuo-u.ac.jp

Abstract: This paper presents a traffic noise evaluation system based on geometrical acoustic theory. The computation of noise level is performed by the geometric acoustic theory. In order to investigate the validity and efficiency of the method, the present method is applied to several traffic noise problems. The computed results are compared with the measurement results. The present system is useful for planning and designing tool for various transportation facilities in an urban area, and also for consensus building for designers and the local residents.

Keywords: Traffic noise, Auralization, VR

1. INTRODUCTION

The evaluation of traffic noise is very important for planning and designing of various transportation facilities in an urban area. There have been presented a number of evaluation methods for noise simulation. Based on the frame of reference used, those methods can be classified into two categories: 1) Methods based on the geometrical acoustic theory and 2) Methods based on acoustic wave theory. Both methods have advantages and disadvantages. For the methods based on the geometrical acoustic theory, the CPU time is very short but the numerical accuracy is low comparing with the methods based on the acoustic wave theory. On the other hand, the method based on the acoustic wave theory gives accurate solution but the simulation becomes a large scale simulation. In the conventional studies, the computed noise level is described by the visualization using computer graphic such as iso-surface. Although the visualization is a powerful tool to understand the distribution of noise, it is difficult to recognize the noise level intuitively.

The authors have developed a noise evaluation system based on the geometric acoustic theory using virtual reality (VR) technology (Tajika et al., 2009, Shibata et al., 2010, Tanigawa et al., 2014, kashiya et al. 2015, Ishida et al., 2016, Kinoshita et al., 2017). The system exposes to the users the computed noise level with both the auditory information using sound source signal and the visual information using CG image. In order to investigate the validity and efficiency of the method, the present method is applied to several traffic noise problems. The computed results are compared with the measurement results in VR space. The present system is useful for planning and designing tool for various transportation facilities in an urban area, and also for consensus building for designers and the local residents.

This paper presents a traffic noise evaluation system using VR technology, and introduces examples of verification of the validity and effectiveness of this system through its application to actual noise problems on roads, railways, and aircraft. .

2. VR ENVIRONMENMENTS

The large scale visualization system based on virtual reality can be classified into two types; head mount display (HMD) and cave automatic virtual environment (CAVE). Each system has merit and demerit. In this study, we employed a CAVE system since it is easy to share the common VR space with multiple people.

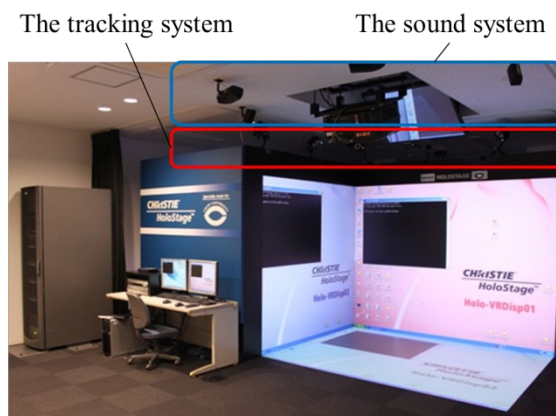


Figure 1. CAVE system

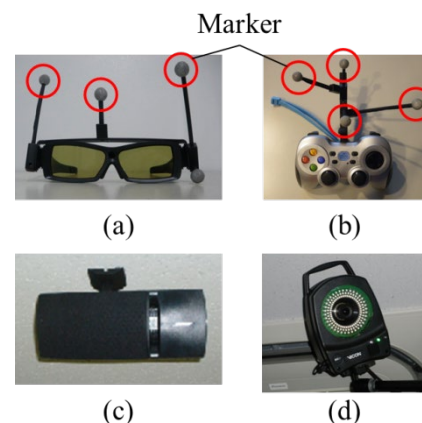


Figure 2. Device of VR system

Figure 1 shows a CAVE system “HoloStage” of Chuo University. This system is composed of three large and flat screens and high-performance projectors corresponding to the screen. The front and side screens are transmissive ones and the bottom screen is reflective one. The user wears the liquid crystal shutter glasses as shown in Figure 2 (a), which are synchronized to the computer display through infrared emitters alternating the left and right eye viewpoint at 120 Hz. The user can change the magnification of the VR system and move to the arbitrary position using the controller as shown in Figure 2 (b). This system has 7.1ch sound system in order to create the stereoscopic sound field as shown in Figure 2 (c). The user’s motion is captured by a motion tracking system “VICON” as shown in Figure 2 (d), which is the optics type motion tracking system. The positions of markers fitted to shutter glasses and controller are tracked by the tracking system.

3. NOISE EVALUATION SYSTEM

3.1 System Overview

Figure 3 shows the flow chart of this system. As input data, we set the driving conditions of automobiles, railway vehicles, aircraft, etc., the acoustic power level of sound sources, and the geometric shapes of structures and sound barriers. Also, in each time loop, the position of the sound source and the user (sound receiving point) in the VR space are obtained from the tracking device. Then, using those information, the noise level at the user's position in the VR space is calculated by a model based on geometric acoustic theory; ASJ RTN-Model 2018 (Research Committee of Road Traffic Noise in the Acoustical Society of Japan, 2019).

In the visualization part, 3D cars, railway vehicles, aircraft and target areas are drawn on each screen by the stereoscopic image. On the other hand, in the auralization section, the calculation of sound pressure is performed and the stereophonic sound are presented by speaker using the acoustic programming software MAX. Sharing of visualization and auralization information is performed by UDP/IP communication.

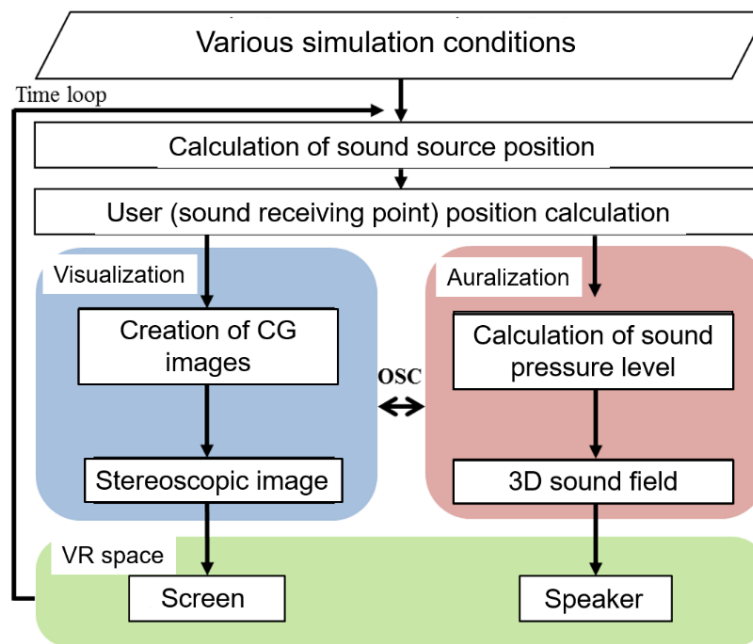


Figure 3. Flowchart of the present system

3.2 Noise Source

In this system, in order to calculate the temporal change of the noise level, the calculation formula of the point sound source is used by the ASJ model. The sound sources of automobiles and aircraft are set at the engine position, and the sound sources of railway vehicles are set on the bogie. In the case of railroad noise, the impact sound generated from the joints of railroad tracks is also taken into consideration.

3.3 Acquisition of Sound Source Data and Conversion to Stationary Sound

In order to implement the sound source data for auralization in the VR system, we collected the sound source data from the actual running and flying.

The stationary sound is created by extracting the minute time interval data passing through the front of the installed sound level meter and connecting them. At that time, in order to remove the discontinuity of the sound generated at the joint, the phase is shifted and synthesized. Also, since the sound source data acquired by the sound

level meter includes distance attenuation, processing is performed to remove the effect. (Tanigawa et al. 2014).

3.4 Acoustic Calculation by Geometric Acoustic Theory

In this system, the ASJ model is employed for the calculation of sound pressure level. The A-weighted sound pressure level at the observation point (at the user's position) is given by the following equation.

$$L_{A,i} = L_{WA,i} - 8 - 20 \log_{10} r_i + \Delta L_{dir} + \Delta L_{cor} \quad (1)$$

Where L_{WA} is the sound power level of the sound source, the second and third terms denote the geometric diffusion, r_i is the distance in a straight line between observer and sound source positions, ΔL_{dir} is the correction concerning with the directivity of sound source, ΔL_{cor} is the correction concerning with attenuation factors (attenuation caused by diffraction, ground effect, atmospheric absorption and so on).

In case that it is necessary to consider plural sound propagations such as direct sound, reflection and diffraction sounds (see Figure 4), the A-weighted sound pressure level at observer's position is computed as:

$$L_A = 10 \log \left(\sum_{i=0}^{i_{max}} 10^{\frac{L_{A,i}}{10}} \right) \quad (2)$$

where i_{max} is the number of the sound propagations, $L_{A,i}$ is the sound pressure level corresponding the sound propagation. In case of the railway noise, it is necessary to handle multiple sound sources for one trainset as shown in Figure 5. Figure 6 shows the directivity for noise source of railway, which is given by the following formula.

$$\Delta_{dir} = 10 \log_{10} (\cos^n \theta \cdot (0.1 + 0.9\phi)) \quad (3)$$

Here, n is a parameter related to directivity, and θ is the horizontal angle and ϕ is the vertical angle from the point closest to the running line seen from the observation point (see Figure 6).

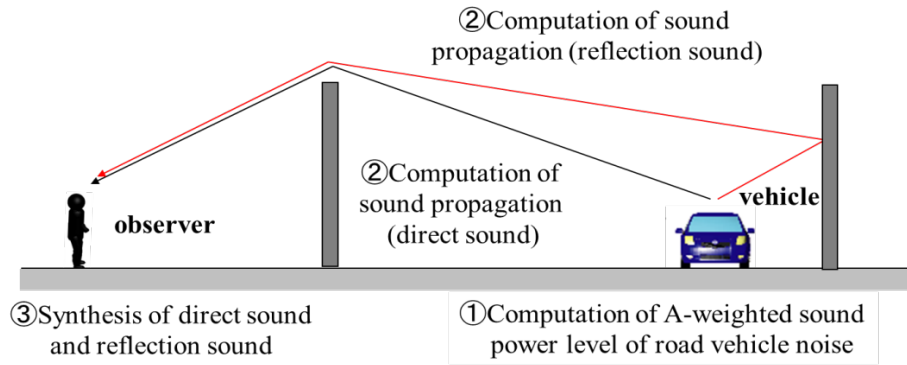


Figure 4 Computation using ASJ RTN-Model 2008

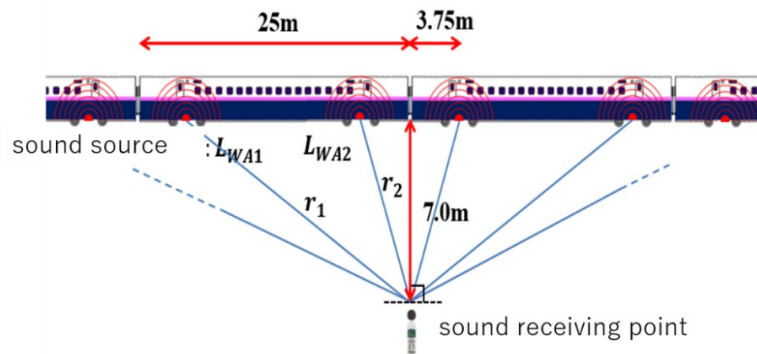


Figure 5. Source location of railway noise

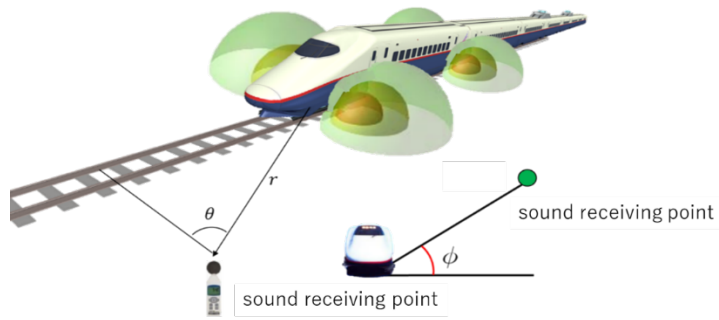


Figure 6. Directivity of railway noise

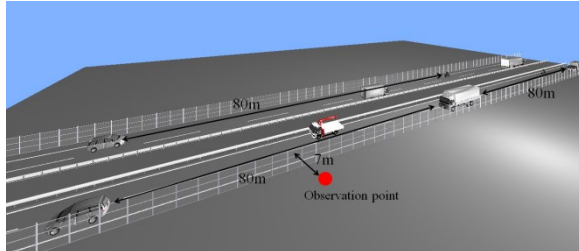
3.5 Acoustic Control of VR Equipment Using MAX

In this system, Max is used to construct a stereophonic field in VR space. Auralization of traffic noise is performed by loudspeaker control by Max using the computed sound pressure level. For the volume to be reproduced, the computed sound pressure level at the observation point is sent to Max using OSC (Open Sound Control), and based on that value, the speaker volume and stereophonic sound are controlled. The ambisonics method (Ward et al., 2001), which is based on the spherical harmonic expansion method, is used to construct the stereophonic field.

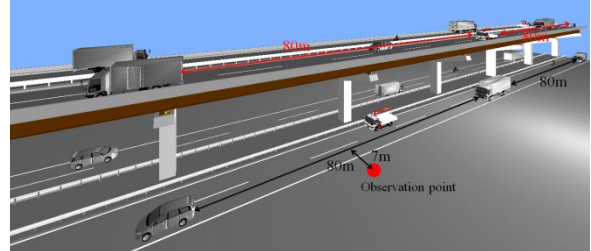
4. APPLICATION EXAMPLE

4.1 Application to Road Traffic Noise

The present system is applied to the mixed traffic simulations with various type of vehicle as shown in Figure 7: case A is a plain road, case B is a plain road with a viaduct road. The following simulation conditions are employed, vehicle speed: 100 km/h, type of pavement: drainage pavement, passage years of pavement: 0 year (new pavement). Figure 8 shows the scene that the observer uses the system. The computed results are compared with the measured results by the noise level meter as shown in Figure 9.



(a) Case A: plane road



(b) Case B (plain road with a viaduct road)

Figure 7. Mixed traffic simulation

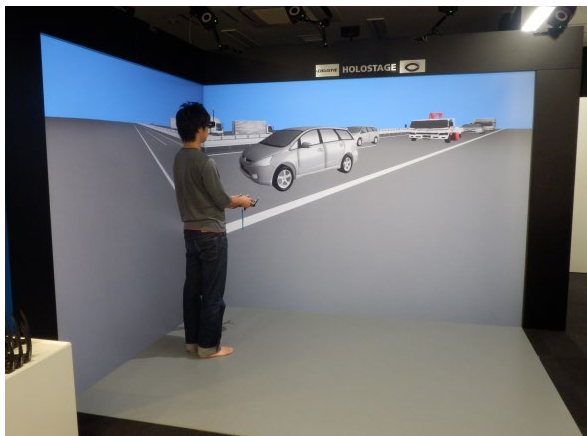


Figure 8. Observer uses the system

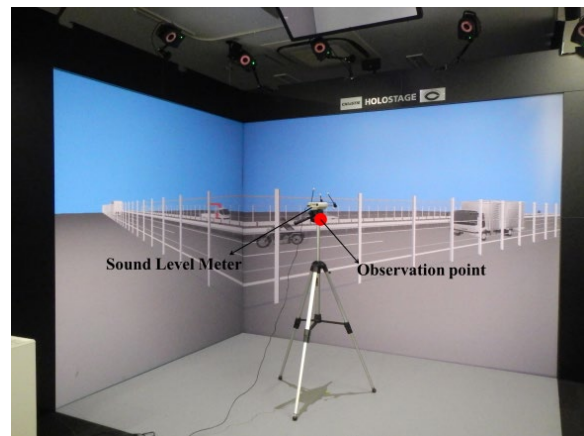


Figure 9. Observation of sound pressure

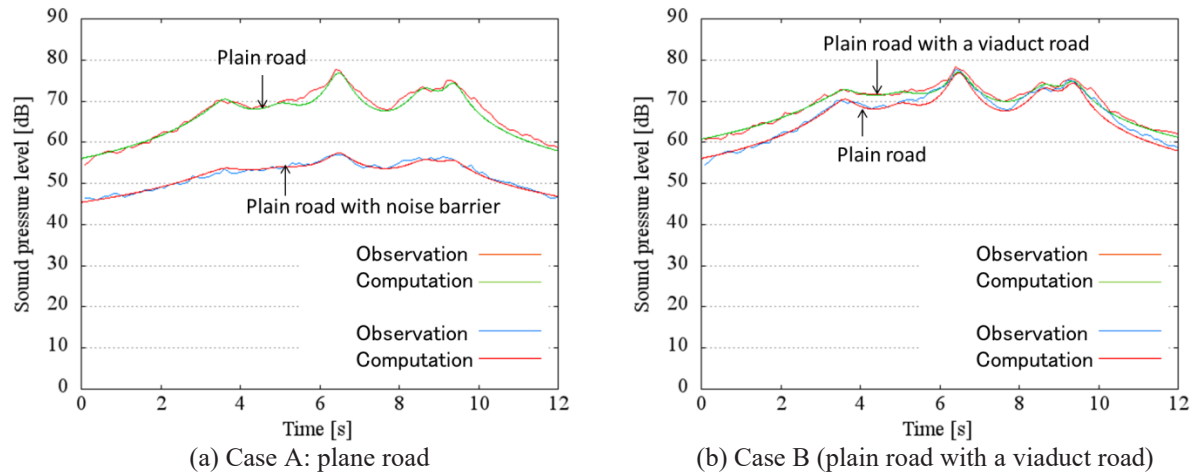


Figure 10. Comparison of computational and measured results

Figure 10 (a) shows the comparison of computed and observed results for case A. From this figure, it can be seen that the computational results are good agreement with the measurement, and the traffic noise level is reduced by the effect of noise barrier. Figure 10 (b) shows the comparison of computed and observed results for case B. In this figure, the computed results without a viaduct road are added in order to investigate the effect of viaduct road. From this figure, it can be seen that the computational results are good agreement with the measurement, and the traffic noise level is increased by the effect of viaduct road.

4.2 Application to Aircraft Noise

In order to verify the validity of the aircraft noise system, the present method is applied to two aircraft noise problem taking off from Tokyo International Airport (Haneda Airport) as shown in Figure 11.

In case 1, an aircraft (Boeing 737-8) taking off from runway C of Haneda Airport is targeted, and the actual measurement results and calculation results are compared at Jonanjima Seaside Park on the opposite shore of the takeoff direction (see Figure 11). Figure 12 shows the seen an observer uses the system. For the flight path, we used the average of the flight paths for 28 aircraft, and used the 90-degree dipole model for the directional model (Ishida et al. 2016). Figure 13 shows a comparison of the sound pressure level of the measured results and the calculated results. The slant distance is the distance from the aircraft to the observation point. From the figure, it can be seen that the occurrence time of the noise peak shows a good agreement with the actual measurement result by considering the directivity. However, it can be seen that a large difference in the sound pressure level after the peak. For this reason, examination of directivity models is essential in our future work.

In case 2, an observer is assumed to be indoors in order to evaluate the soundproofing measures. The building model used for the indoor simulation is a rectangular parallelepiped with a depth of 3.6m, a width of 3.6m, and a height of 3m. Figure 14 shows a user experiencing noise in a VR space. Figure 15 shows a comparison with the measurement results in the VR space. From this figure, it can be seen that the computational results are good agreement with the measurement in the VR space above the background noise (approximately 48 dB).

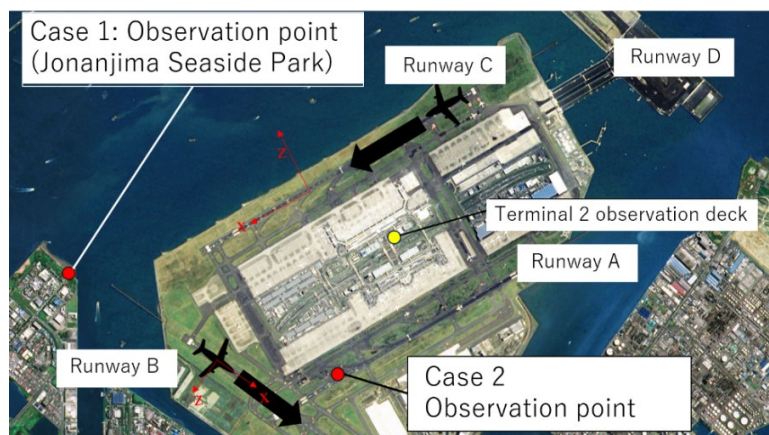


Figure 11. Comparison of computational and measured results



Figure 12. Observer uses the system (case 1)

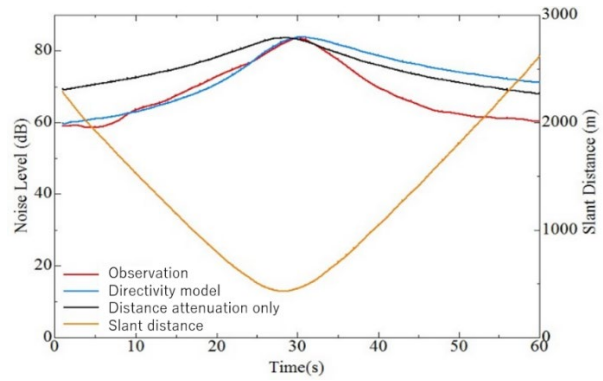


Figure 13. Comparison of results

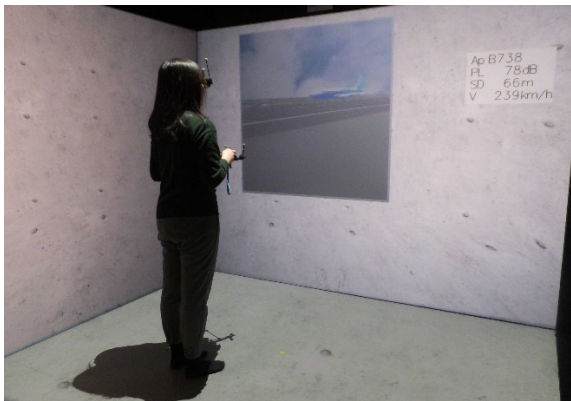


Figure 14. Observer uses the system (case 2)

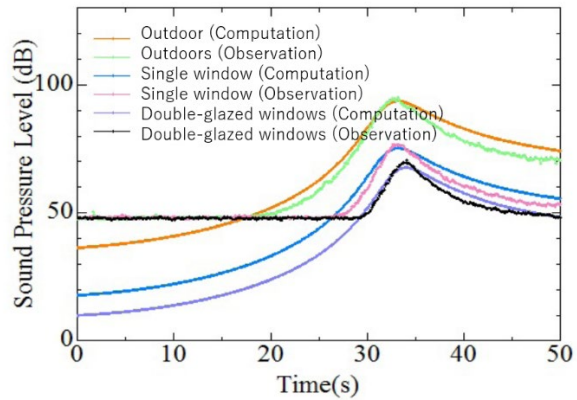


Figure 15. Comparison of results

4.3 Application to railway noise

As an application example of this railway noise system, we targeted the noise of the Tohoku Shinkansen around Oyama Station in Tochigi Prefecture. Figure 16 shows the seen an observer uses the system. The CAD model is created using topographical data, building data, track data, etc. issued by the Geospatial Information Authority of Japan.

Figure 17 shows a comparison between the measured values of the running sound of the E2 system and the computed results. The running speed of the train at this time was 274 km/h, and the observation point was 7 m from the track center (see Figure 5). In Figure 17, n is a coefficient related to directivity in equation (3), and it can be seen from the figure that the computed results and the measured values for a directivity coefficient of $n=1.0$ show good agreement when a train is approaching. However, the measured sound pressure level after passing the Shinkansen is higher than that when approaching, and it can be seen that the directivity is different between the front part and the rear part.

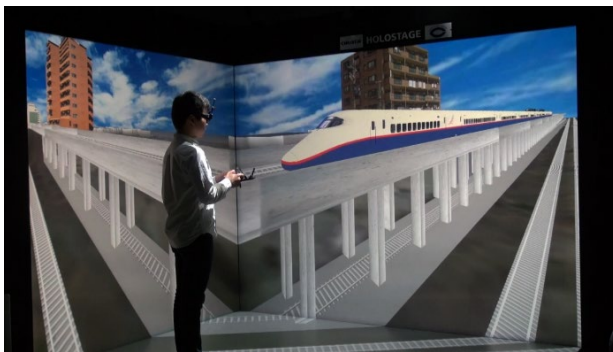


Figure 16. Application to high-speed train

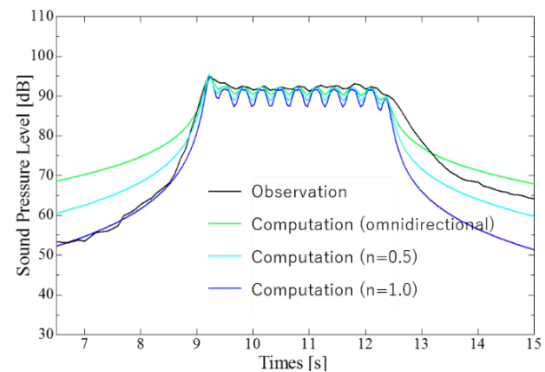


Figure 17. Comparison of results

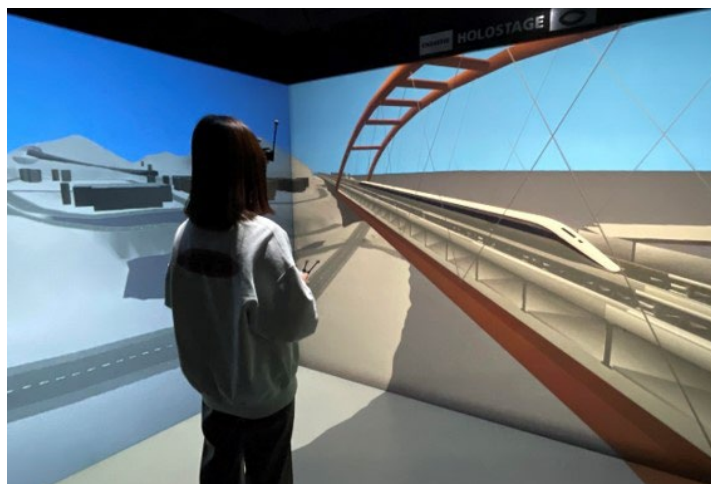


Figure 18. Application to magnetic levitation high-speed railways

We are currently studying the application of this system to magnetic levitation high-speed railways as shown in Figure 13. The results will be shown at the presentation.

5. CONCLUSION

This paper has been presented a traffic noise evaluation system and investigated its applicability to road, railway and aircraft noise.

This system can calculate various traffic noises in real time based on geometric acoustic theory, and present the calculation results as sounds in the VR space using actual sound source data. Since this system can be applied to various traffic noises with different sound source data, it can be effectively used in the planning and design stages of new traffic facilities and soundproofing works. In addition, it can be expected to be an effective tool for obtaining consensus with residents.

We plan to investigate the directivity of the sound source and various correction terms in order to improve the accuracy of the system in our future work.

ACKNOWLEDGMENTS

I would like to thank Dr. Masayuki Shimura of Construction Environment Research Institute and Dr. Masanori Tanigawa of Shimizu Corporation for their great support and cooperation in developing this system.

REFERENCES

- Ishida, A., Yamamoto, K., Yoshimachi T., Kashiyaama K. and Shimura, M. (2016), Development of an experience-based aircraft noise evaluation system using virtual reality technology, *Journal of JSCE, Division F3 (Civil Engineering Informatics)*, 72 (2), 140-147 (in Japanese)
- Kashiyaama, K., Ejima K., Yoshimachi T., Ishida A., Tanigawa M. and Shimura M. (2015), A road traffic noise evaluation system using virtual reality, *Proceedings of the 15th International Conference on Construction Applications of Virtual Reality*, Paper ID-81
- Kinoshita, K., Yoshimachi T., Kashiyaama K. and Shimura, M. (2017), Development of a railway noise evaluation system using virtual reality technology, *Journal of JSCE, Division F3 (Civil Engineering Informatics)*, 73(2), 372-379 (in Japanese)
- Research Committee of Road Traffic Noise in the Acoustical Society of Japan. (2019), Road traffic noise prediction model ASJ RTN-Model 2018, *Journal of Japan Acoustical Society of Japan*, 75, 188-250.
- Shibata, K. Tajika S. Kashiyaama K. and Shimura M. (2010), Development of an experienced-based road traffic noise evaluation system using VR technology, *Proc.of the 10th Int. Conf. on Construction Applications of Virtual Reality*, Sendai, Japan, 513-522.
- Tajika S. Kashiyaama K. and Shimura M. (2009), Development of a road traffic noise estimation system using virtual reality technology, *Proc.of the 9th Int. Conf. on Construction Applications of Virtual Reality*, Sydney, Australia, 305-314.
- Tanigawa M. Moriya Y. Ejima K. Kashiyaama K. Shimura M. (2014), Development of mixed traffic noise evaluation system using VR and acoustic spatialization technology, *Journal of JSCE, Division A2 (Applied Mechanics)*, 70(2), 195-202 (in Japanese)
- Ward, D.B. and Abhayapala, T.D. (2001), Reproduction of a plane wave sound field using an array of loudspeakers, *IEEE Transactions on speech and audio processing*, 9, 697-707.

SMART HOME ADOPTION: CHALLENGE AND OPPORTUNITY FOR DIGITAL TWIN BUILDING

Chalumporn Thawanapong¹, Terdsak Tachakitkachorn², and Kaweekrai Srihiran³

1) Ph.D. Student, Department of Architecture, Faculty of Architecture, Chulalongkorn University, Bangkok, Thailand. Email: Jchalumporn@gmail.com

2) Ph.D., Asst. Prof., Architecture for Creative Community Research Unit, Department of Architecture, Faculty of Architecture, Chulalongkorn University, Bangkok, Thailand. Email: Terdsak.t@chula.ac.th

3) Assoc. Prof., Regional, Urban, and Built Environmental Analytics: RUBEA, Department of Architecture, Faculty of Architecture, Chulalongkorn University, Bangkok, Thailand. Email: Kaweekrai.s@chula.ac.th

Abstract: Wireless Sensing Network (WSN) development in a household level has emerged smart home device with benefit of affordable cost, user friendly interface, easy entry in initial stage, has accelerated the widespread of smart building. Digital Twin (DT), a digital counterpart of physical object for monitoring, analysis, simulation, etc., has been use in manufacture, healthcare, building. DT building studies, integration of BIM and IoT data from WSN in virtual building platform, has create new possibility in operation and maintenance phase of smart building, with a real world demonstrator in Aalto university and Cambridge university, which emerge a DT system architecture, a framework for constructing DT building from the technical perspective. However, the existing framework is not compatible with smart home devices adoption in smart building since the lack of physical details of device installation on-site and various building data management. An inclusive DT framework with smart building involvement would increase the practicality of DT building development. According to the literature review on the existing DT framework and OSI reference model, the international standards of computer networks, this study proposes 6 layers of DT framework which clarify the whole details of DT development from the physical smart building to its digital counterpart. Based on the framework, a real world demonstrator, Pine and Grass building, DT was implemented in smart building development to improve the building aspect of well-being, performance, safety with smart home devices. The result provides the clarification in each layer, benefit and limitation of smart home device adoption in DT development, to improve understanding of DT building for building owner and building admin, an initiator and end users of DT building, which accelerate widespread of DT technology in the field of smart building.

Keywords: WSN, DT, Smart home device, Smart building

1. INTRODUCTION

Digital Twin (DT) is a concept of creating digital companions of the physical object in digital format to serve as the virtual representation for monitoring, analysis, simulation, etc. (Grieves & Vicker, 2017; Stanford-Clark & Frank-Schultz, 2022) The development of Internet of Things (IoT) recently, DT has been applied in many industries such as smart cities, health care, manufacturing. (Fuller et al., 2020) Building Information Modeling (BIM), a digital representation of the building process to facilitate the exchange and interoperability of information in digital format (Lee, 2022) has play a role as an IoT data management middleware in the field of smart building and smart cities. (Deng et al., 2021) The accomplished DT buildings with real world demonstrator has been done in a campus building, by developing DT platform with the integration of BIM and IoT data from Wireless Sensing Network (WSN), and real time application for building monitoring to enhance Building Management System (BMS) in Aalto university and Cambridge university. (Dave et al., 2018; Lu et al., 2020)

Smart home device, a life related IoT enabling device to utilize in a household level. (Li et al., 2021; Ricquebourg et al., 2006) With the benefit from affordable cost and user friendly interface, smart home devices have accelerated the widespread of smart building, both new building and existing building without BMS.

However, compare with the accomplished case in Aalto university and Cambridge university, the aspect of smart home device adoption for smart building development might be difference, since the existing building might not deploy BMS, and the adoption could transform the whole building into smart building with DT technology.

This study aims to create an inclusive framework for DT building development, by comparing the existing DT framework with Open Systems Interconnection (OSI) reference model, the common ICT framework, to identify a problem of the existing framework in case of smart home device adoption in the building without BMS in section 2.2, and propose DT building framework in section 3, with a real-world DT demonstrator to proof of concept in section 4.

The clear framework with a real-world demonstrator in this study, reveal the benefit and limitation of smart home device adoption in DT development, to improve understanding of DT building for building owner and building admin, initiator and end user of DT building, which accelerate widespread of DT technology in the field of smart building.

2. LITERATURE REVIEW

2.1 Smart Home Device for Smart Building Development

The concept of smart homes is to utilize residence as a platform, integrating life-related facilities and devices via taking advantage of a range of techniques including wiring, computers, network service, automated control, security systems, and multimedia to build a smart and efficient residential facility. (Riquebourg et al., 2006) With the IoT development, smart home provider has integrated hardware, software systems and cloud computing platforms to eradicate the barriers and risks of smart home adoption such as financial consideration, technology anxiety, etc. (Li et al., 2021) e.g., Ikea home smart (Ikea, 2023), Philips hue smart lights (Philips-hue, 2023). However, there is a complication in deploying smart home devices from multiple providers since each provider usually offers their own platform, 613 IoT platforms were available on the market in 2021. (IoTAnalytics, 2021) The previous study in 2021 reveal that BIM has a capability to connect with the real time sensing data for building environment monitoring and management in any phases of the building life cycle (Deng et al., 2021), and also an open platform to interoperability of information (Lee, 2022), indicated that DT building from BIM and IoT integration has a potential to established smart building with smart home devices.

2.2 Analysis on DT System Architecture

According to the review of related studies, 2 papers of a real world DT experimental study in the whole building scale were found. The selected papers were the DT platform development with BIM and IoT integration with the physical sensing data from WSN to enhance BMS in the existing building in (Case1) Aalto university and (Case2) Cambridge university, with a difference in a context of development e.g., objective, enabling technology, which affect to the result of studies, a system architecture. While (Case 1) Aalto university was aim to develop open communication standard for BIM and IoT integration called O-MI and O-DF with custom WSN devices, has define 3 components of development consist of IoT device, back end, front end (Dave et al., 2018), (Case 2) Cambridge university was aim to develop system architecture to integrate heterogenous data from Commercial Off-the-Shelf (COTS) WSN, has define 5 layers of development consist of data acquisition, transmission, digital modeling, data integration, service. (Lu et al., 2020) The existing framework might be fit with DT development in a similar context, but not compatible with smart home devices adoption in building without BMS, since IoT and DT technology could transform the whole building into a smart machine for living in, physical details of smart home device installation on-site and various IoT data management are required. The author has considered the OSI reference model for wider perspective, since the model is the highest level of abstraction in the OSI scheme by ISO in 1977, to create the international standards of computer networks to utilize its full potential (Day, 1989), According to the content analysis of the existing framework, the separation between physical details of device from the measured data from device could improve practicality in DT building development specified in Table 1, by categorizing smart home device in the building system with its physical condition and the measured data .

Table 1. DT building framework comparison in this study

OSI	Physical	Data	Network	Transport	Session	Presentation	Application
Case 1	IoT Device (lack of detail)			Back End (IoT)	Back End (BIM)	Front End	
Case 2		Data Acquisition	Transmission		Digital Modelling	Data Integration	Service
Proposed Framework	Physical	Data	Transmission		Digital Modelling	Data Integration	Application & Service

Note: ■ = consists of concrete detail

3. DT BUILDING FRAMEWORK

According to the analysis on the existing DT framework and OSI reference model, this study proposes 6 layers of DT framework in the context of smart home device adoption in the building without BMS.

- (Layer 1) Physical Layer, focuses on specification of device and how it was installed in the building.
- (Layer 2) Data Layer, clarifies data acquisition from smart home devices in the building system.
- (Layer 3) Transmission Layer, clarifies data path from the device to the provider.
- (Layer 4) Data Modelling Layer, focuses on BIM modeling technique for smart home device management.
- (Layer 5) Data Integration Layer, provides a whole picture of data integration in DT building, between BIM and IoT.
- (Layer 6) Application and Service Layer, clarifies the utilization of smart home devices, related to the IoT service in DT building.

4. DT BUILDING DEMONSTRATOR

Pine and Grass (PNG) building opened in 2018 for retail and office rent, with basic building equipment including lighting system, split type air conditioner, power outlets, magnetic door lock with RFID cards for building access. Since the aspect of smart building development in PNG building was focuses on well-being, performance, and safety, (p2) IoT Service was designed to achieve the development goal, specified in Table 2 and 3 via DT building application on BIM and IoT integration platform.

Table 2. Summary of the designed (p2) IoT service for PNG building

(p2) IoT Service	Smart building aspect		
	Well-being	Performance	Safety
a) Built environment monitoring	●		
b) Equipment control and monitoring	●	●	
c) Energy management		●	
d) Smart evacuation			●
e) On site notification			●
f) Customize space	●		
g) Smart access	●		

(Layer 1) Physical Layer

This section has clarified smart home devices installation in the building to achieve the requirement of (p2) IoT service, in the context of the building without BMS, except network device (device No. 14,20,21), the installed devices can be classified into 3 types according to the (p6) Related Device to achieve the objective of (p2) IoT Service with 3 kinds of (p7) Power Supply.

- Stand-alone device, a device that can work to achieve the objective of the service without other related device, with (p7) Power Supply from batteries consist of device No. 1,4,5, from DC power consist of device No. 2, from AC power consists of device No. 8 and 10.
- Existing system improvement device, the device that was deployed to operate with the existing device to achieve the objective of the service, with (p7) Power Supply from DC power consist of device No. 7,11,15,18, from AC power consist of device No. 6 and 9.
- New system installation, the group of installed devices that must be operated together to achieve the objective of the service, with (p7) Power Supply from batteries consist of device No. 3 and 12, from DC power consist of device No. 17, from AC power consist of device No. 13,16,19.

(Layer 2) Data Layer

This section has clarified device operation data in PNG building, which can be classified in term of (p3) Building System and (p4) Data Connection. While Physical to Virtual (P2V) is the real time measurement data from smart home sensors, Virtual to physical (V2P) connection is a command data for smart home actuator.

- Lighting data, P2V connection is an ambient light data in term of Lux from device No. 2, V2P connection are commands data for artificial light control with device No. 8 and 18, and natural light control with device No. 11.
- HVAC data, P2V connection are indoor air temperature data in term of Celsius and humidity data in term of percentage of Relative Humidity (RH) from device No. 1, and energy usage data of air conditioner in term of kWh from device No. 6, V2P connection is commands data for split type air conditioner control with device No. 7.
- Electrical Power data are P2V and V2P connection thru device No. 10, P2V connection is energy usage data of in term of kWh and V2P connection is commands data for the device.
- Sanitary data, P2V connection is a water leakage detection data from device No. 4.
- Fire alarm data, P2V connection is a smoke detection data from device No. 3 and outlet overheat detection data from device No. 15, V2P connection is commands data for device No. 9 and 12.
- Building envelopment data, focuses on door and window monitoring, P2V connection are physical access control data in term of user id from device No. 16 and QR code id from device No. 17, and window status data from device No. 5, V2P connection are command data for device No. 19 to automatically open the inner door and device No. 13 to unlock the front door.

(Layer 3) Transmission Layer

Since the (p2) IoT Service requirement of PNG building covers the whole building operations and more than 90 IoT devices were installed in PNG building, mesh Wi-Fi network has been deployed with device No. 21 for efficient Wi-Fi signal distribution (Saha et al., 2014), for COTS devices from Tuya Smart and custom devices from Digital Transformation, data transmission could be clarified by the (p9) Provider and (p8) Communication

Protocol of the devices.

- For Tuya Smart, device No. 2,6,7,8,11 require Wi-Fi signal for devices operation, device No. 1,3,4,5,9,10,12,13 has taken the advantage from IEEE 802.15.4 Zigbee 2.4 GHz on zigbee 2.0 protocol, since the protocol has been uses to reduce the network load on the router, as it has characteristics suitable for the operation of IoT devices with low data transfer rates (Dibley et al., 2015) which need device No. 14 to send data to Tuya IoT cloud platform via internet.
- Digital Transformation Co., Ltd. is the IoT solution company, take responsibility for the devices which have not been developed into COTS products, consist of device No. 15,16,17,19 with Wi-Fi connection, and device No. 18 with Radio Frequency (RF) 2.4 GHz network, which need device No. 20 to send data to Digital Transformation server via internet.

Table 3. Summary of smart home devices adoption in PNG building

No.	(p1) Friendly Name	(p2) IoT Service						(p3) Building System	(p4) Data Connection		(p5) Value	(p6) Related Device	(p7) Power Supply	(p8) Proto col	(p9) Provider
		a)	b)	c)	d)	e)	f)		g)	P2V					
1	T&H Sensor	•						HVAC	•		°C, RH%	No	Battery	Zigbee	Tuya Smart
2	Light Sensor	•						Light	•		Lux	No	DC	WiFi	
3	Smoke sensor		•		•			Fire	•		normal/ alarm	[12]	Battery	Zigbee	
4	Water sensor		•			•		Sanitary	•		normal/ alarm	No	Battery	Zigbee	
5	Door sensor		•					Envelope	•		open/ close	No	Battery	Zigbee	
6	Energy meter		•	•				HVAC	•		kWh	A/C	AC	WiFi	
7	IR Controller		•				•	HVAC		•	on/off, °C	A/C	DC	WiFi	
8	Smart Bulb		•		•	•		Light		•	on/off, 0-100, color	No	AC	WiFi	
9	Smart Switch				•			Fire		•	on/off	Emergency light	AC	Zigbee	
10	Smart Outlet		•	•				Electrical Power	•	•	on/off, kWh	No	AC	Zigbee	
11	Curtain Controller		•		•		•	Envelope		•	0-100	Curtain	DC	WiFi	
12	Siren				•			Fire		•	normal/ alarm	[3]	Battery	Zigbee	
13	Magnetic Lock Controller		•		•		•	Envelope		•	open/ close	[17], Magnetic lock	AC	Zigbee	
14	Zigbee Gateway							Network					DC	WiFi	
15	Temperature sensor		•			•		Fire	•		normal/ alarm	Power outlet	DC	WiFi	Digital Transformation
16	Face Scanner		•				•	Envelope	•		User id	[19]	AC	WiFi	
17	QR Scanner		•				•	Envelope	•		QR code id	[13]	DC	WiFi	
18	LED Controller		•		•	•	•	Light		•	on/off, 0-100, scene id	LED strip	DC	RF	
19	Automatic Door		•		•		•	Envelope		•	open/ close	[8]	AC	WiFi	
20	RF Gateway							Network					DC	WiFi	
21	Router							Network					DC		

Note: a) Built Environment Monitoring, b) Equipment Control and Monitoring, c) Energy Management, d) Smart Evacuation, e) On Site Notification, f) Customize Space, g) Smart Access

(Layer 4) Data Modeling Layer

According to the amount and complexity of smart home devices installed in PNG building. BIM play a role as a device management and coordination tool for contractor and building admin, for an accurate installed location on site, via Autodesk Revit (Autodesk, 2022a) BIM software.

Since the installed device has been classified with (p3) Building System, the device data classification has been transferred to model categorization in BIM software, together with unique element id, BIM parameter for geometry model identification (Kunkel, 2018), each device model capable to be developed to a virtual device (Dave et al., 2018; Lu et al., 2020) in DT building application as shown in Figure 1.

For user interface development of virtual devices, (p1) Friendly Name and (p5) Value has taken a role in design principle. For example, all device in DT application provides a logical naming with a (p1) Friendly Name and its location from BIM, devices with (p5) Value in term of Boolean data will be displayed in toggle switch style, consist of device No. 3,4,5,7,8,9,10,12,13,15,18,19.

(Layer 5) Data Integration Layer

This section clarifies BIM and IoT data integration. The real time IoT data of smart home devices operation will be connected from each (p9) Provider through an API to BIM server with Hypertext Transfer Protocol (HTTP), for data visualization and devices control in 2D and 3D graphical user interface in DT building application, via APIs in Autodesk Forge web service [36], which can be classified with (p4) Data Connection.

- P2V connection of measurement data will be called, using GET method from BIM server with 2 different calling period, defined by the propose of (p2) IoT Service. While the data for a) Built Environment Monitoring, b) Equipment Control and Monitoring, c) Energy Management, real time data from device No. 1,2,5,6,10 will be calling from BIM server every 1 minute for storing in database, waiting for the calling from BIM server for data display, the data for devices automation in d) Smart Evacuation, e) On Site Notification, f) Customize Space, g) Smart access from device No. 3,4,15,16,17 will be calling from BIM server every 1 second to reassure data recentness, and automatically operate the devices in response system even though there is no data calling from the application.
- V2P connection of smart home actuator command data for devices No. 7,8,9,11,12,13,18,19 will be sent from BIM server to the device provider thru API with POST method. BIM server will store only command data with successful response returned from device provider, for data display in b) Equipment Control and Monitoring as shown in Figure 1.

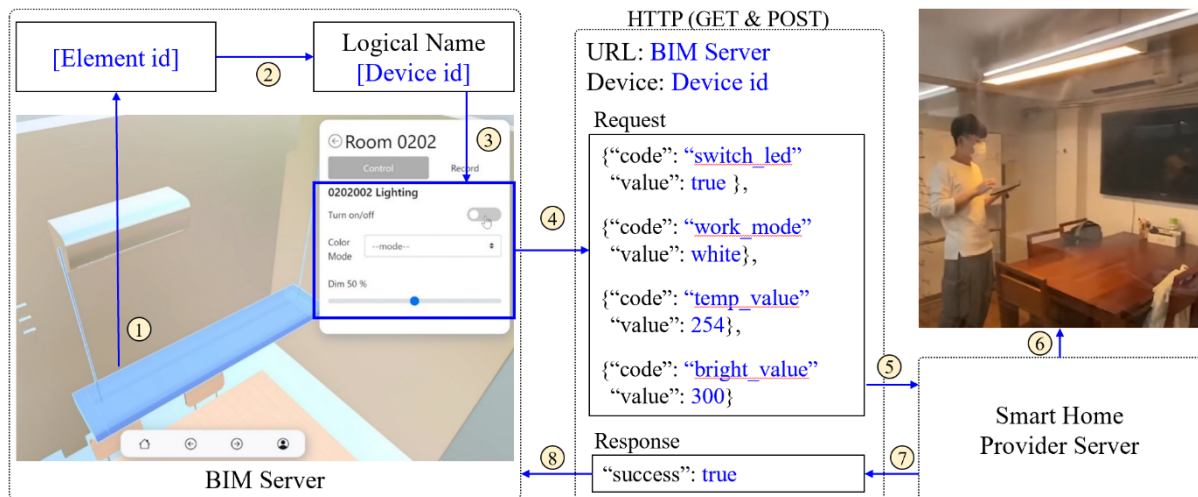


Figure 1. Demonstration of virtual device No. 18 in DT building application

(Layer 6) Application and Service Layer

DT building application is a BIM-based real time web application, in 2D and 3D graphical user interface, with cross platform IoT operation to accomplish PNG smart building development goal specified in Table 1. For example, in Smart evacuation system, when Smoke sensor detects an abnormality, a notification will be shown in the application to specifies location of the incident and smart home devices will automatically response for the evacuation assist e.g., green light flashing for evacuation guidance, automatic door opening, magnetic door lock disabling. DT application and service in PNG building can be clarified in term of smart home device utilization with (p2) IoT Service and (p4) Data Connection.

- a) Built Environment Monitoring is the indoor physical data display, with P2V connection from devices No. 1 and 2.

- b) Equipment Control and Monitoring is the virtual device for building equipment and smart home devices operation, with P2V and V2P connection from devices No. 3,4,5,6,7,8,10,11,13,15,16,17,18,19.
- c) Energy Management is the energy consumption data display in each area of the building with P2V connection from devices No. 6 and 10.
- d) Smart Evacuation is the automation of all smart home devices to support fire evacuation, with P2V connection from devices No. 3, and V2P connection from devices No. 8,9,11,12,13,18,19.
- e) On Site Notification is the lighting automation to notify the anomaly situation in unseen place, with P2V connection from devices No. 4 and 15, and V2P connection from devices No. 8 and 18.
- f) Customize Space is the device automation according to the preset scene of each user, when the user gets into the area physically, the devices will be adjusted follow the personal configuration, with P2V connection from devices No. 16, and V2P connection from devices No. 7,11,18,19.
- g) Smart Access is the building access control and monitoring system, with P2V connection from devices No. 17, and V2P connection from devices No. 13.



Figure 2. Demonstration of smart home devices automation in d) Smart Evacuation

4. DISCUSSION AND CONCLUSION

Comparing with the existing DT building framework, the separation between physical details of device from data acquisition, which originate the 6 layers of DT building framework in this study, could improve practicality in DT building development especially in the building without BMS, the details in each layer might be difference, according to the end user of the framework shown in Figure 3.

Well-considered requirement of IoT services for the smart building development should be appeared in (Layer 6) Application and Service Layer. The services lead to the proper smart home device deployment, by focusing on and the capability of API in (Layer 5) Data Integration Layer, and installed condition in (Layer 1) Physical Layer, which effect to the building network in (Layer 3) Transmission Layer. The DT demonstrator in this study has adopt smart home devices with minimum amount of IoT service provider to reduce the complication in each layer.

While the devices installation in the physical context has been clarify in (Layer 1) Physical Layer, smart home devices data classification which related to the building system in (Layer 2) Data Layer has improve the correlation between BIM and IoT in (Layer 4) Digital Modelling Layer, and emphasize the utilization of BIM as an IoT data management middleware.

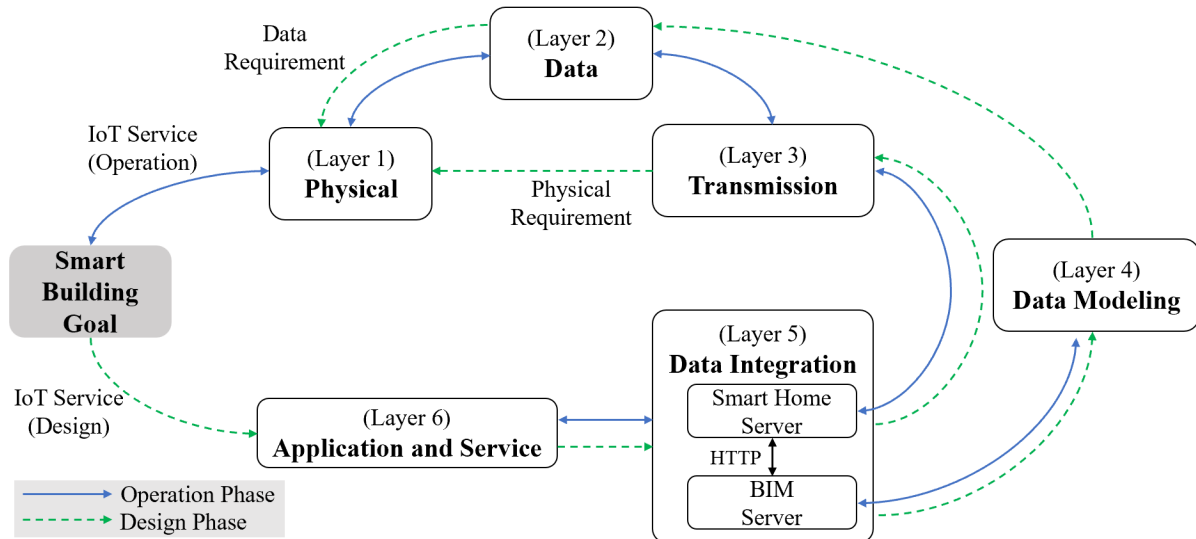


Figure 3. Workflow diagram of DT building framework in this study

ACKNOWLEDGMENTS

This study was supported by Digital Transformation Co., Ltd., Power Partners Co.,Ltd., and the National Research Council of Thailand (NRCT) under Grant No. 7369.

REFERENCES

- Autodesk. (2022a). *Revit Key Features 2022: Upcoming Advanced Features 2023*. Retrieved from Autodesk website: <https://www.autodesk.com/products/revit/features>
- Autodesk. (2022b). *Autodesk.Viewing. GuiViewer3D*. Retrieved from Autodesk website: <https://aps.autodesk.com/en/docs/viewer/v2/reference/javascript/guiviewer3d/>
- Dave, B., Buda, A., Nurminen, A. and Främling, K. (2018). A Framework for Integrating BIM and IoT Through Open Standards, *Automation in Construction*, 95, 35-45.
- Day, J. (1989). The Reference Model for Open Systems Interconnection in *Computer Network Architectures and Protocols* (2nd ed.). Springer.
- Deng, M., Menassa, C. and Kamat V. (2021). From BIM to digital twins: A systematic review of the evolution of intelligent building representations in the AEC-FM industry, *Journal of Information Technology in Construction*, 26, 58-83.
- Dibley, M., Li, H., Rezgui, Y. and Miles J. (2015). An integrated framework utilising software agent reasoning and ontology models for sensor based building monitoring, *Journal of Civil Engineering and Management*, 21 (3), 356-375.
- Fuller, A., Fan, Z., Day, C. and Barlow, C. (2020). Digital Twin: Enabling Technologies, Challenges and Open Research. *IEEE*, 8, 108952-108971.
- Grieves, M. and Vickers, J. (2017). *Transdisciplinary Perspectives on Complex Systems*. Springer.
- Ikea. (2023). *Home smart*. Retrieved from Ikea website: https://www.ikea.com/th/th/cat/home-smart-hs001/?gclid=Cj0KCQjwpPKiBhDvARIsACn-gzBNaBR_My3tQd8sd_mToP_VfiWW3FPpDeOyI_5pYAX5QwZu9haZBQMEaAjv4EALw_wcB&gclsrc=aw.ds
- IoTAnalytics. (2021). *IoT Platforms Competitive Landscape 2021*. Retrieved from Autodesk website: <https://iot-analytics.com/product/iot-platforms-competitive-landscape-2021/>
- Kunkel, J. (2018). *Revit Element ID - How to Get It and What to Do with It*. Retrieved from CADD microsystem website: <https://www.caddmicrosystems.com/blog/revit-element-id-how-to-get-it-and-what-to-do-with-it/>
- Lee, J. (2022). Advanced BIM Application in Construction and Buildings, *Buildings*, 12 (8).
- Li, W., Yigitcanlar, T., Erol, I., Liu A. (2021). Motivations, barriers and risks of smart home adoption: From systematic literature review to conceptual framework, *Energy Research & Social Science*, 80, 102211.
- Lu, Q., Parlikad, A.K., Woodall, P., Don Ranasinghe, G., Xie, X., Liang, Z., Konstantinou E., Heaton, J. and Schooling, J. (2020). Developing a digital twin at building and city levels: Case study of West Cambridge campus, *Journal of Management in Engineering*, 8 (3).
- Philips-hue. (2023). *Philips-hue personal wireless lighting*. Retrieved from Ikea website: <https://www.philips-hue.com/en-us>

- Ricquebourg, V., Menga, D., Durand, D., Marhic, B., Delahoche, L. and Loge, C. (2006). The Smart Home Concept : our immediate future, *1ST IEEE International Conference on E-Learning in Industrial Electronics*, Hammamet, Tunisia, pp. 23-28.
- Saha, S., Acharjee, U. and Tahzib-Ul-Islam M. (2014). A Survey on Wireless Mesh Network and its Challenges at the Transport Layer, *International Journal of Computer Engineering and Technology*, 5, 169-177.
- Stanford-Clark, A. and Frank-Schultz, E. (2022). *IBM Digital Twin Point of View December 2020*. Retrieved from IBM website: <https://www.ibm.com/blogs/academy-of-technology/wp-content/uploads/2022/04/AoT-DigitalTwin-PoV.docx.pdf> IBM Academy of Technology.

CONSIDERATION FOR LEVEL OF DIGITAL TWIN IN ARCHITECTURE

Terdsak Tachakitkachorn¹, Chalumporn Thawanapong², and Kaweechai Srihiran³

1) Ph.D., Asst. Prof., Architecture for Creative Community Research Unit, Department of Architecture, Faculty of Architecture, Chulalongkorn University, Bangkok, Thailand. Email: Terdsak.t@chula.ac.th

2) Ph.D. Student, Department of Architecture, Faculty of Architecture, Chulalongkorn University, Bangkok, Thailand. Email: Jchalumporn@gmail.com

3) Assoc. Prof., Regional, Urban, and Built Environmental Analytics: RUBEA, Department of Architecture, Faculty of Architecture, Chulalongkorn University, Bangkok, Thailand. Email: Kaweechai.s@chula.ac.th

Abstract: Digital Twin has been mentioned into the stage of application for many working fields both practical and theoretical, since a decade ago. However, lack of implementation with marketing approaches in architectural sector and enormous theoretical simulation without real on-site experiment, would mislead end-user or investor, and inevitably devalue its potential. Study from implemented case studies of Digital Twin utilization in architecture led to key points clarification, such as proportion of IoT device and networking for smart-living preparation, readiness of procedure framework, targeting function and its usage, that could be developed into a concept of Level of Digital Twin in architecture. This definition framing could regenerate perception from end-user perspective righteously, and reconvince for expansive utilization of DT in architectural sector.

Keywords: Level of Digital Twin, Demonstration, DT Building framework

1. INTRODUCTION

Development of IoT technology and Smart Home market growth (IoTAnalytics, 2021) have led to the rapid future expectation from Digital Twin building and Facility Management (FM) system, as it can provide and handle various types of physical data efficiently. Thus, Digital Twin has been mentioned as the significant tool dealing with exponentially arising enormous complex Data. (Dave et al., 2018; Lu et al., 2020) However, the most of current Digital Twin research often refer to the concept of operation and data integration through simulation without real implement, which would cost a lot of budgets with unpredictable result due to a lack of previous practical experiment. Therefore, some of marketing-approach sector, who bet mainly on Digital Twin investment opportunity, has tried to promote Digital Twin in real estate sector using only theoretical simulation without any prove from real on-site experiment. This would mislead end-user or investor, and inevitably devalue of Digital Twin real potential.

This paper aims to establish an initial concept of the Level of Digital Twin in Architectural sector through a common logical process to clarify an existing of different Digital Twin status by means of demonstration of 5 selective cases, with a concrete evidence, input into Digital Twin Building Framework (DT Building Framework). The framework has been developed from the Digital Twin experiment projects in Chulalongkorn university, consists of 6 layers specified in Table 1. This could clarify any questions, through representative cases, whether we should call it Digital Twin or not. Moreover, it could be clear on the level of each case, quantitative and qualitative, after identifying as Digital Twin. With this initial concept prove, it would be developed to an idea of standard and led to regenerate righteous perception about Digital Twin in architectural sector from user side, and would reconvince any investors for expansive utilization of Digital Twin into real estate sector furthermore.

Table 1. Clarification of 6 layers of DT building framework

Layer	Description
(Layer 1) Physical Layer	clarifies physical quality of IoT device in the project and how it was installed on site.
(Layer 2) Data Layer	clarifies data acquisition from IoT technology in the project.
(Layer 3) Transmission Layer	clarifies data path and IoT protocol from devices to servers.
(Layer 4) Data Modeling Layer	clarifies graphical and no - graphical data modeling technique of the physical entities for IoT data management.
(Layer 5) Data Integration Layer	clarifies a whole picture of data integration in DT environment.
(Layer 6) Application and Service Layer	clarify the utilization of IoT service in DT environment.

2. STUDY PROCESS

2.1 Case Study Selection

(1) Case1: Typical Digital Twin simulation: this case has the most enormous numbers among all cases, with main purpose firstly to convince engagement of Digital Twin in architectural sector. On the other hands, some individual marketing promotion approach, without appropriate understanding, would mislead potential stake holder and finally would devalue real essence, with skeptical perception to apply Digital Twin in architectural field. A study of Simulation on typical research and development project (Autodesk, 2016) as shown in Figure 1, was selected as case representative to reconfirm fulfillment in 6 framework layers, and emphasize its Digital Twin implement status.

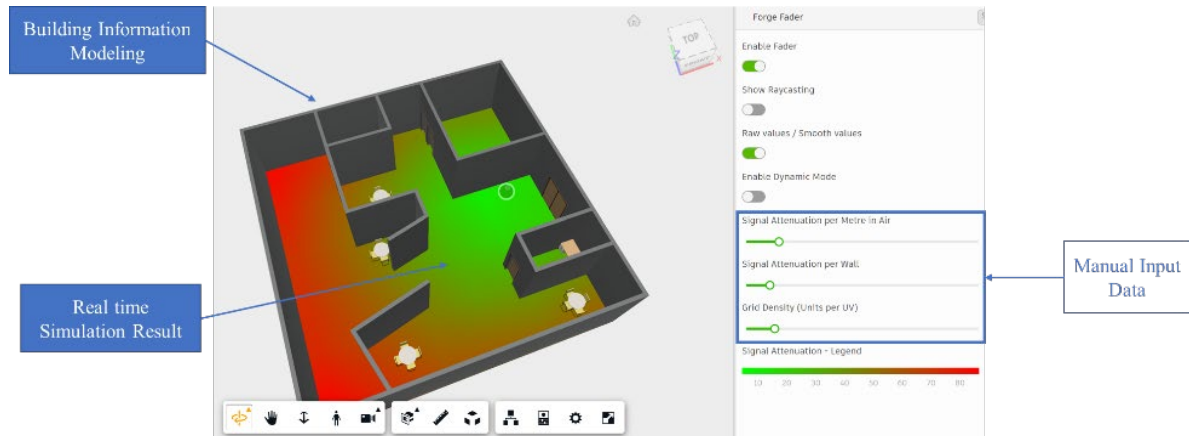


Figure 1. User interface of Case1

(2) Case2: Typical Home IoT solution: Numbers of Home IoT solution service and related products has risen abundantly these few years. Most of them have been adapted based on conventional ICT platforms. ZEN smart-living unit, based on its experimental objective focusing on developing Indoor Air Quality (IAQ) management system in a house-hold level thru IoT devices as shown in Figure 2 and 3, was selected as case representative to reconfirm fulfillment in 6 framework layers whether its implement status could be perceived as Digital Twin in architectural sector. On the other hand, analysis through 6 layers of framework could identify its potential upgrade component, which support Digital Twin fulfillment.

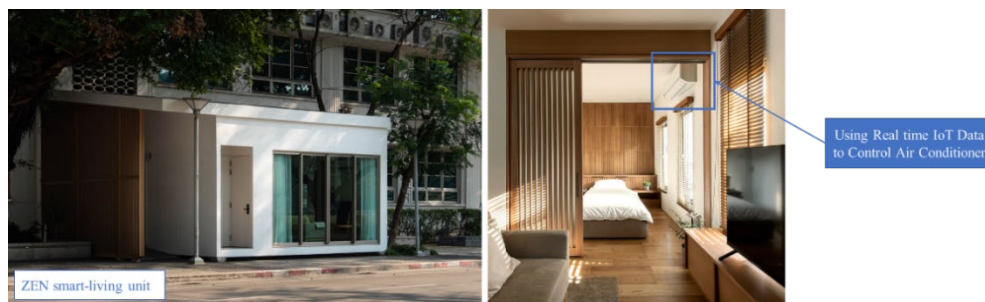


Figure 2. Real world experimental of Case2

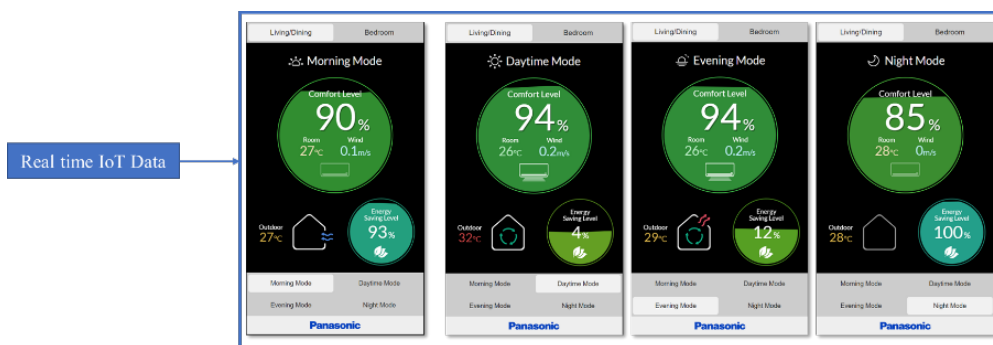


Figure 3. User interface of Case2

(3) Case3: Digital Twin experimental implement 01: In Thailand, while Building Management system (BMS) Building has been employed as the main conventional practice for more than decades, BIM platform DT Building could rarely be identified. Smart patrol project in Chulapat 14 building was selected as case representative Digital Twin Building, based on its experimental objective focusing on IoT data visualization in Digital Twin space as shown in Figure 4, with multi-sensing IAQ moveable gear as shown in Figure 5, to reconfirm its 3 basic functional interaction status in each of 6 framework layers.

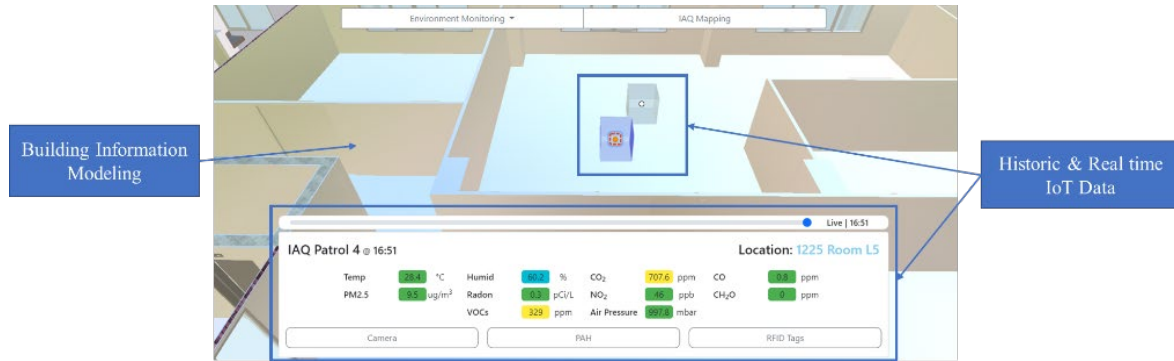


Figure 4. User interface of Case3

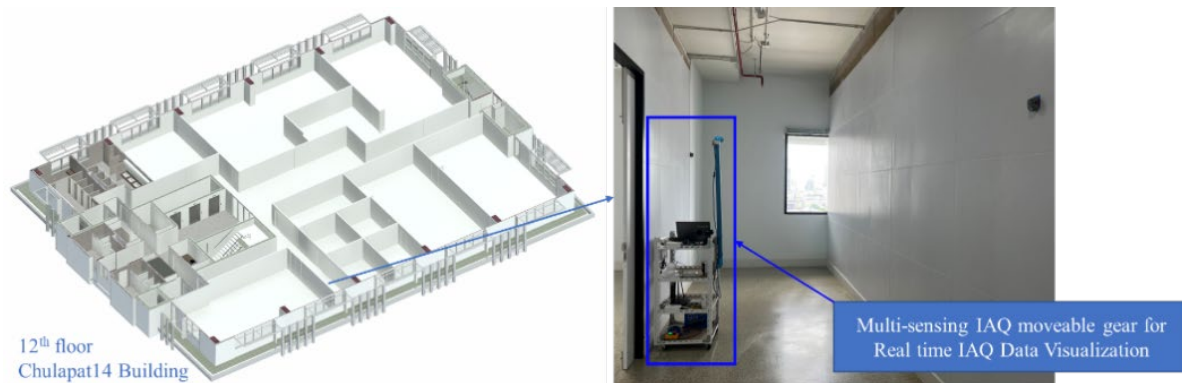


Figure 5. Real world experimental of Case3

(4) Case4: Digital Twin experimental implement 02: As same as Case3, this could be counted as the pioneer group of implement Digital Twin Building experiment in Thailand. Pine and Grass Building was selected as case representative Digital Twin Building, based on its experimental objective focusing on integration of the whole Digital Twin building space with Physical to Virtual (P2V) and Virtual to Physical (V2P) performance thru smart home devices as shown in Figure 6, to reconfirm its 3 basic functional interaction status in each of 6 framework layers.

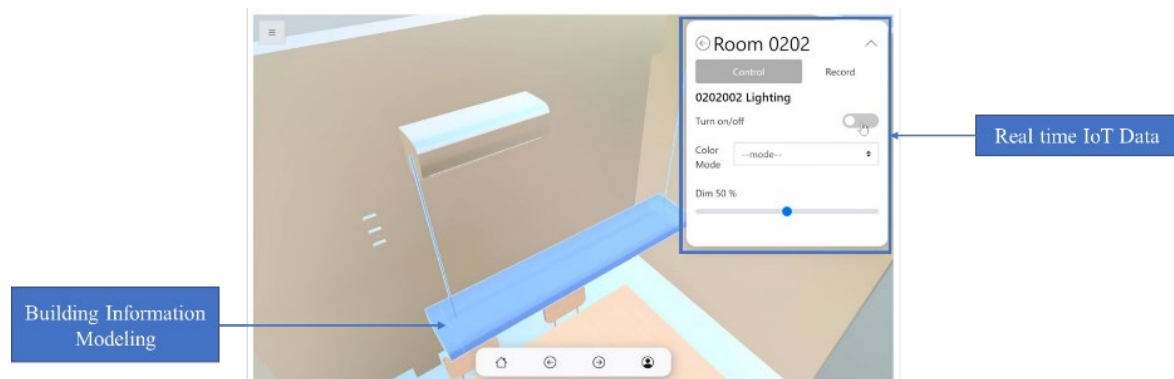


Figure 6. User interface of Case4

(5) Case5: Digital Twin experimental implement 02: In Europe, more Digital Twin Building implement could be identified. Cambridge university was selected as case representative Digital Twin Building, based on its experimental objective focusing on integration of the Digital Twin Building concept into existing faculty management BMS (Lu et al.,2020) as shown in Figure 7, to reconfirm its 3 basic functional interaction status in each of 6 framework layers.

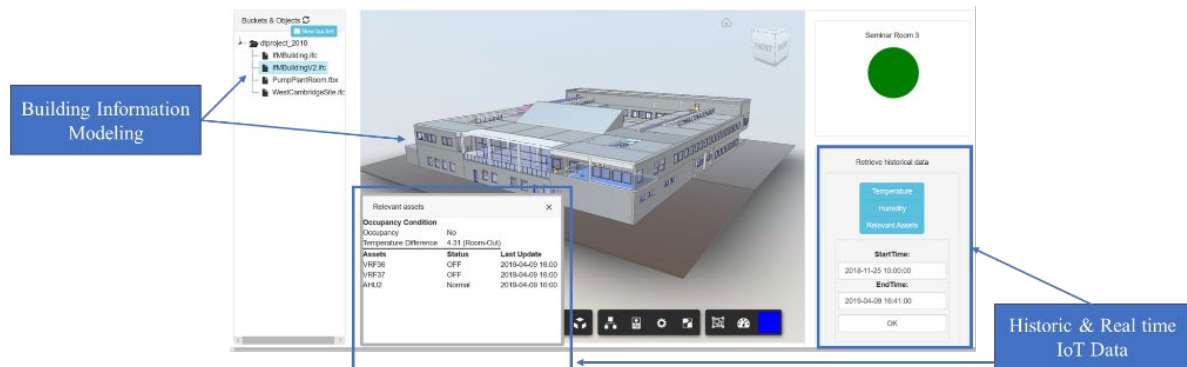


Figure 7. User interface of Case5

2.2 Analytical Procedure

DT Building framework was introduced for input of 5 selective cases into, by considering 3 basic functional interaction: according to PNG building experiment and patrol experiment, there are 3 basic functional interaction from Digital Twin performance identify including (1) Data managing: automatic data digitalizing and accumulating from all operating devices, (2) Monitoring: Visual interaction by user with operating devices through any level of application or interface, (3) Controlling: Physical interaction by user with operating devices through any level of application or interface, in each layer of DT Building Framework including (Layer1) Physical Layer (Layer2) Data Layer, (Layer3) Transmission Layer, (Layer4) Data Modeling Layer, (Layer5) Data Integration Layer, (Layer6) Application and Service layer, specified in Table 1, which originally based on OSI reference model, covering all IT ecosystem.

3. CONCLUSION

Even though this initial concept of hypothetical demonstration, without formal standard procedure and systematic criteria, could not be the ultimate guideline or standard for the Level of Digital Twin establishment. With this, we could logically identify a significant status of “the Level of Digital Twin” by means of comparison of these 5 selective cases specified in Table 2.

Following are description of table 1, to show how DT Building Framework could differentiate each case, both their Digital twin status and further characters;

(1) Group1: Digital Twin Status = Non-Digital Twin and incomplete Digital Twin

(1.1) No Layer1, Layer2 and Layer3 from DT Building Framework: Without P2V and V2P interaction, due to no physical component existing, simulation case could not even be fulfilled a minimum requirement of Digital Twin.

(1.2) No Layer4 from DT Building Framework: P2V and V2P interaction taken place without real connection between a virtual platform and a real physical component (coordination in real architectural space), due to non-BIM application as middleware and integration platform, Home IoT Solution case could be counted as incomplete Digital Twin. However, with their original data management system and platform, they could be upgraded to Digital Twin after proper middleware employment.

Table 2. Comparison of case study

	Group 1		Group 2			Full Employment
	Case 1	Case 2	Case 3	Case 4	Case 5	Case 4 (Future)
(Layer 1) Physical Layer						
Coverage of building service		●	○	●	○	●
Coverage of building area		●	○	○	●	●
(Layer 2) Data Layer						
Environment Data		●	●	●	●	●
Device Data		●		●	●	●
Building Data			○	●	●	●
User Data		●		●		●
(Layer 3) Transmission layer						
Number of Communication Protocol		2	2	3	2	3
(Layer 4) Data Modeling Layer						
BIM	●		●	●	●	●
Additional BIM			●	●		●
Multiple BIM integration			○		●	
(Layer 5) Data Integration Layer						
BIM on platform	●		●	●	●	●
Number of IoT platform		3	2	2	3	2
(Layer 6) Application and Service Layer						
Data Visualization	●	●	●	●	●	●
Building Equipment Control		●		●		●
Data Analysis	●				●	●

Note: BIM = Building Information Modeling, ● = Complete functional interaction,
○ = Partial functional interaction

(2) Group2: Digital Twin Status = complete DT Building in various level

(2.1) Complete Digital Twin status based on DT Building Framework, with focusing on data managing and monitoring with no controlling: Smart patrol case shows its complete Digital Twin status with P2V and V2P interaction taken place with real connection between a BIM platform of IAQ measurement and a real physical component of movable unit correlating to coordination in real architectural space.

(2.2) Complete Digital Twin status based on DT Building Framework, with focusing on data managing and monitoring with partial controlling: Cambridge University shows its complete Digital Twin with P2V and V2P interaction taken place with real connection between a BIM platform of facility management system, based on existing BMS, and a real physical component of IoT devices correlating to coordination in real architectural space.

(2.3) Complete Digital Twin status based on DT Building Framework, with focusing on data managing and monitoring with partial controlling: PNG building shows its complete Digital Twin status with P2V and V2P interaction taken place with real connection between a BIM platform of BMS and a real physical component of IoT devices correlating to coordination in real architectural space.

(3) Relevant Factors

Considering case of PNG building as complete Digital Twin status; with partial P2V and V2P interaction, due to incomplete IoT devices employment, it could be upgraded by means of more investment on budget to fulfill capacity by IoT devices employment into all building floors. This could complete each of 6 layers in DT building framework to the optimum level. As well as more investment in operation team is required, for continuity of handling the whole ecosystem of DT building framework. However, any investment has to be under well-planning referred to objectives and business model. These relevant factors, in correlation with DT building framework, could be analyzed together in order to evaluate the Level of Digital Twin in architectural sector properly.

ACKNOWLEDGMENTS

This study was supported by Panasonic Solutions (Thailand) Co., Ltd. for the information of ZEN smart-living unit project.

REFERENCES

- Autodesk. (2016). *Forge Fader - RCDB*. Retrieved from Autodesk website: <https://forge-rcdb.autodesk.io/>
- Dave, B., Buda, A., Nurminen, A. and Främling, K. (2018). A Framework for Integrating BIM and IoT Through Open Standards, *Automation in Construction*, 95, 35-45.
- IoTAnalytics. (2021). *IoT Platforms Competitive Landscape 2021*. Retrieved from Autodesk website: <https://iot-analytics.com/product/iot-platforms-competitive-landscape-2021/>
- Lu, Q., Parlikad, A.K., Woodall, P., Don Ranasinghe, G., Xie, X., Liang, Z., Konstantinou E., Heaton, J. and Schooling, J. (2020). Developing a digital twin at building and city levels: Case study of West Cambridge campus, *Journal of Management in Engineering*, 8 (3).

FROM BIM TO DIGITAL TWIN: A CASE STUDY EXPERIENCE

Prapaporn Rattanatamrong¹, Jarunchai Srisawat², Peemapat Podsoonthorn³,
Thapana Boonchoo⁴, Wanida Putthividhya⁵ and Veerasak Likhitrungsilp⁶

- 1) Ph.D., Asst. Prof., Department of Computer Science, Faculty of Science and Technology, Thammasat University, Pathum Thani, Thailand. Email: rattanat@tu.ac.th
- 2) B. Sc., Graduate Student, Department of Computer Science, Faculty of Science and Technology, Thammasat University, Pathum Thani, Thailand. Email: jarunchai.sri@dome.tu.ac.th
- 3) Undergraduate Student, Department of Computer Science, Faculty of Science and Technology, Thammasat University, Pathum Thani, Thailand. Email: peemapat.pod@dome.tu.ac.th
- 4) Ph.D., Asst. Prof., Department of Computer Science, Faculty of Science and Technology, Thammasat University, Pathum Thani, Thailand. Email: thapana@cs.tu.ac.th
- 5) Ph.D., Asst. Prof., Department of Computer Science, Faculty of Science and Technology, Thammasat University, Pathum Thani, Thailand. Email: pwanida@tu.ac.th
- 6) Ph.D., Assoc. Prof., Department of Civil Engineering, Faculty of Engineering, Chulalongkorn University, Bangkok, Thailand. Email: Veerasak.L@chula.ac.th

Abstract: In the construction business, Building Information Modeling (BIM) provides a digital representation of the geometrical and non-geometrical information of a building. A BIM model can be used for a range of tasks, including design collaboration, construction planning, and building management. The term “Digital Twin” (DT) refers to a recently developed technology that is used to represent a virtual replica of a building that includes not only physical properties but also dynamic data from various sources, such as sensors and BIM models. This paper explains our real case experience in creating a digital twin based on BIM for the administration and maintenance of an academic building in Thailand. A Unity application based on the building's BIM model is created and enhanced with the appropriate graphics for exhibiting real-time building states that were collected by Internet of Things (IoT) sensors as well as additional interactive controls for navigation and drill down focus. From data ingestion to dashboard presentation, the complete data pipeline takes place in the cloud. The digital twin development technique for building management is suggested for future applicants after we successfully overcame a number of challenges with the use of already accessible tools and technologies.

Keywords: Digital twin, Building information modeling, Smart building, Internet of things, Cloud computing

1. INTRODUCTION

The concept of "smart buildings" has evolved as a result of the development of IoT technology, and it is currently applied to newly constructed facilities. The Building Information Modeling (BIM) model of the building can give detailed information starting with the design phase and continuing through planning, construction, and completion. Although the BIM model's information on building components, including their positions, is essential for building maintenance, some dynamic data of the building is still lacking. According to (Jia et al., 2018), the data from a variety of interconnected components (such as equipment, appliances, sensing, and control infrastructure) can enhance the intelligence and effectiveness of smart buildings in optimizing various desirable outcomes, e.g., occupant health, comfort, diagnosis, operational costs, and energy efficiency. The vast amount of disparate data, however, also makes it difficult to plan smart buildings and guarantee their effectiveness.

Digital Twin (DT) gives you the ability to view, manage, and optimize your operational assets, processes, and resources by employing real-time data. This provides essential, real-time information regarding activity and performance of the physical building. A number of past works explored BIM-based DT for buildings. For examples, (Kaewunruen & Xu, 2018; Kaewunruen et al., 2018) studied the use of digital twins for building energy management, however the twins do not involve widespread sensor networks or real-time building status data. An integration of BIM model and IoT was proposed by (Khajavi et al., 2019) as a framework for the deployment of wireless sensor network (WSN) on a building façade for implementing digital twins of buildings. However, the review by (Liu et al. 2021) shows that out of all the published works investigating the use of DT for building maintenance, only a third are use cases. The remaining focuses on the development of concepts or new implementation methodologies.

This paper describes how we converted an existing BIM model of an academic building in Thailand into a digital twin. Our main contributions are the following:

- Presenting actual use cases for digital twins in smart buildings
- Providing the lessons discovered from methods that can be used in real-world applications.

2. DIGITAL TWIN DEVELOPMENT

2.1 Design Requirements

Our case study is to create a digital twin of Chulalongkorn University's building ENG30 that will enable real-time analysis and visualization of the building's current condition. The building maintenance team can utilize the digital twin to track the dynamic states of the facility and use that information to inform future maintenance decisions rather than analyzing data from many sources on several fragmented reports.

The following are, in brief, the main requirements for the digital twin of this building:

- Easily accessible through web browsers
- Preloaded with initial static data from the building's BIM model
- Providing real-time indoor environmental monitoring (e.g., temperature, humidity, and light) of a single control room and restrooms that do not have any network connectivity or power outlets.

2.2 Overall Architecture of the Digital Twin and Its Workflow

The system architecture of the digital twin is depicted in Figure 1. The Amazon Web Service (AWS) cloud is used for all of the processes in the data pipeline, including ingestion, data transformation, storage, and visualization. First, using the cloud-based message broker AWS IoT Core (AWS IoT Core, 2023), distributed real-time data from IoT sensors located in various locations across the building is ingested and buffered (labelled as 1). The data was then prepared using an AWS Lambda serverless function (labeled as 2) and sent to InfluxDB (InfluxDB, 2023), a time-series database. The BIM model was transformed into a Unity (Unity, 2023) Web-based application, and building metadata and data schema was kept in a cloud-based object storage called an Amazon S3 bucket (labeled as 3). The virtual cloud server hosting the digital twin's components is referred to as an EC2 instance. The Web application of the digital twin connects to an API gateway to receive the most recent data from InfluxDB's REST API (labeled as 4), which is then presented as information cards in the related rooms of the building's 3D model. Grafana (Grafana Labs, 2023), an open-source visualization and analytics web tool, is used to create the graphs for the collected time-series data (labeled as 5). Grafana allows us to link digital twin data through customized panels and dashboard layouts. The challenges that were encountered when designing and putting each element of the digital twin into use are covered in more detail in the following subsections.

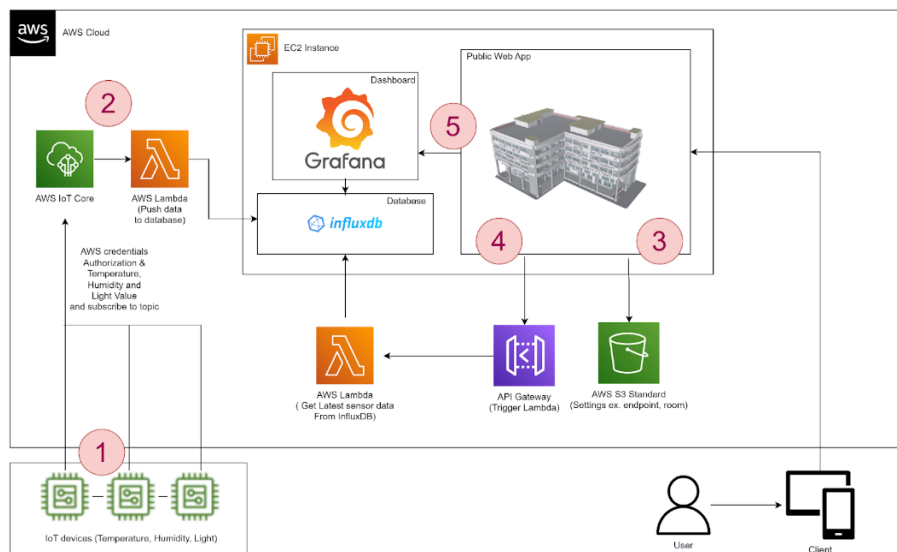


Figure 1. The overall system architecture of the ENG30 digital twin.

2.3 Indoor Environmental Monitoring using IoT Sensors

The room temperature, relative humidity, and lighting conditions serve as models for the indoor atmosphere of the building. We installed a photosensitive sensor (LDR) and a temperature and humidity sensor (DHT11) on a compact-sized ESP32 Arduino-compatible board with a built-in Wi-Fi antenna (as shown in Figure 2(a)). Our C++ data collecting script collects sensor data at every 15 minutes along with the timestamp provided by the DS3231 AT24C32 Real Time Clock Module. Sensors were calibrated and recorded values were validated. The IoT board is powered by two rechargeable 18650 batteries (3.7V 2600mAh Lithium Ion) because there are no power outlets available in the rooms to place IoT sensors. IoT boards can connect to the Internet via 4G LTE routers without the need for conventional wiring. Figure 2(b) shows the locations where the 4G routers and IoT boards were deployed. According to our experimental study, the gathered data needs to be saved locally and delivered in batches of JSON encoded data to the cloud server every hour to use as low power as feasible.

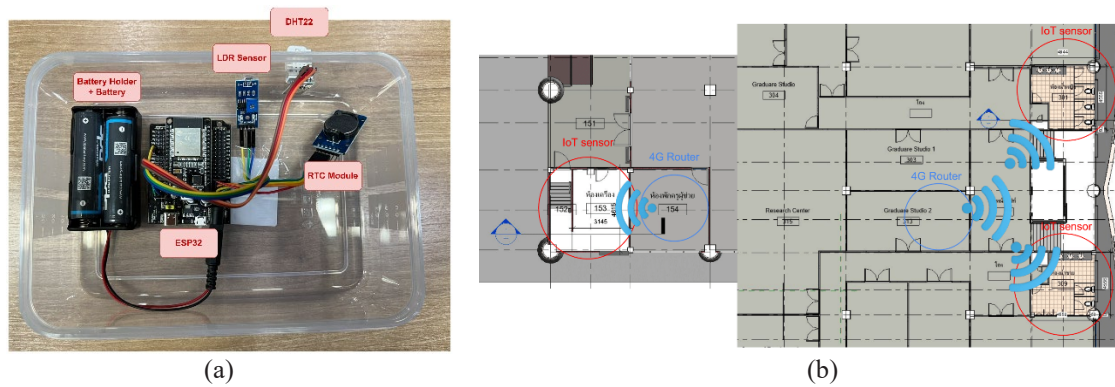


Figure 2. (a) Components of the IoT board (b) Installed locations of 4G routers and IoT boards

2.4 BIM-based Digital Twin Web Application

The building's BIM was previously produced using the well-known BIM authoring program Autodesk Revit (Revit, 2023). We exported the Revit BIM model file into an Industry Foundation Class (IFC) file, an open format for building data models used in construction and design projects in various technologies. BIM in the IFC format were imported into Unity as Game Object hierarchies using the IFC importer plugin (IFC importer, 2020), available from the Unity Asset Store. The plugin maintains the hierarchy and semantic information of the IFC file, allowing us to search objects using their IFC id, presentation layer, and element type.

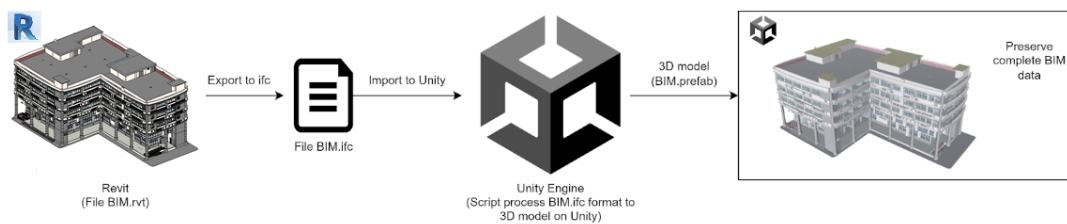


Figure 3. General structure of reports, papers, and essays

Further modifications were implemented in order to overlay 3D cubical objects that represent rooms of interest with installed IoT boards and pertinent micro interactions according to the digital twin's schema. As a result, we managed to create a prefab or a blueprint of a Unity-compatible BIM object, which we can then utilize when creating the Web interface for the digital twin. The whole process is illustrated in Figure 3.

3. RESULTS

The resulting Web-based digital twin of the ENG30 building is shown in Figure 4. The focus view for the entire building or a specific floor can be changed by users. Additionally, they can rotate the angle and separate floors from one another to view each floor on the inside in greater detail.

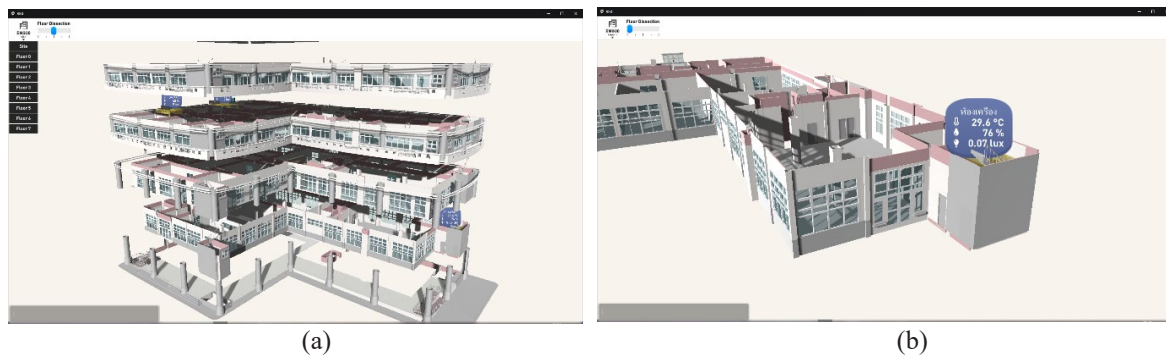


Figure 4. Web-based digital twin features (a) floor dissection (b) real-time in-context information display

The interactive Grafana dashboards in the cloud receive data from InfluxDB. A realistic solution to the necessity for human involvement with the data at two different levels of detail and context was to incorporate data visualization into the digital twin. The current data values for each room are first displayed in an information card that is displayed above the room. Second, if further information is needed, users can choose a specific room to display a dashboard with time-series graphs showing both the current and past value. Figure 5 illustrates the dashboard showing data from the first 10 days after deployment. Different hues and colors represent various degrees of temperature, humidity, and light intensity. Users can examine different room dashboards and a range of data levels for context and comparison in each unique analytical scenario.

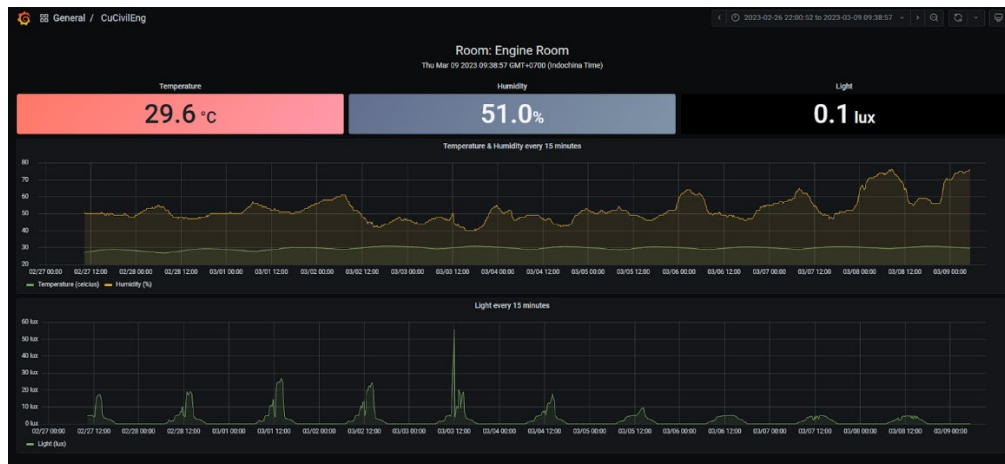


Figure 5. A room-specific dashboard showing time-series of indoor environmental data

4. DISCUSSION

According to our experience, the greatest challenge to the creation of a digital twin for the building in our case study is the absence of an adequate power supply for IoT boards. Only 5 to 6 days can be expected from each pack of 2 cells, necessitating manual and frequent replacement with fresh ones. In addition to changing the operation mode in software like we did, we intend to optimize power usage further via a hardware solution.

After the sensors in a target region have acquired the necessary data (temperature, humidity, and light), we can consider how artificial intelligence and machine learning (AI & ML) can support the DT system. Depending on the issues with a task, different AI & ML applications might be used. For instance, using the data gathered, a machine learning model may be created that can conduct an inference for room occupancy, which is essential for the power-saving planning policy. Additionally, the machine learning model can facilitate the room/building simulation in the digital counterpart in the DT. Similarly, AI can be thought of as creating an autonomous system for the entire room or even the entire building based on such machine learning models, starting with simple tasks like automatically turning off the air conditioning to save energy to more complex tasks like sounding an evacuation alarm when serious anomaly events are detected.

Better control and building operations are made possible by integrated data. In this work, we use IFC and our own schema for implementing DT, but we are aware of the value of a standard data model that can facilitate data interoperability between the building subsystems and external data sources and applications. We are currently looking into using Brick Schema (Brick Schema, 2023) and Real Estate Core (Real Estate Core, 2023) to improve the DT development and utilization. When integrating semantic graph or network model databases with built-in relationship schema, Digital Twin functions as a greatly powerful spatially aware data model. This enables the execution of "what if?" scenarios from financial, business strategy, or even organizational structure perspectives, as well as the simulation of future plans.

Future research will look into ways to simplify the back-end maintenance needed for digital twin applications and evaluate the requirements for human interaction that cannot be satisfied by off-the-shelf technologies and call for more specialized methods.

5. CONCLUSIONS

A Digital Twin (DT) creates a complete digital representation of a building by combining data from all sources, including the physical BIM and dynamic data elements (such as people and activity aspects). The implementation of a DT from a BIM model is still hindered by a number of technological barriers, despite the potential benefits they may have for how we manage and maintain smart buildings. Contextual limitations, stakeholder demands, and technological capabilities all have a substantial impact on the architecture used for the development and deployment of digital twins. In this study, we demonstrate how to develop a successful DT use

case on top of already-available technology, such as cloud and IoT. Given that we can address network connectivity and power issues, IoT can offer real-time dynamic information for the DT. In addition to storage and processing capabilities, cloud computing technology can offer a wide range of other services and frameworks that can support the creation and implementation of digital twins. Lastly, when combined with semantic graph or network model databases with built-in relationship schema, rapid ideation, prototyping, and policy validation may be carried out using DT in an almost risk-free setting.

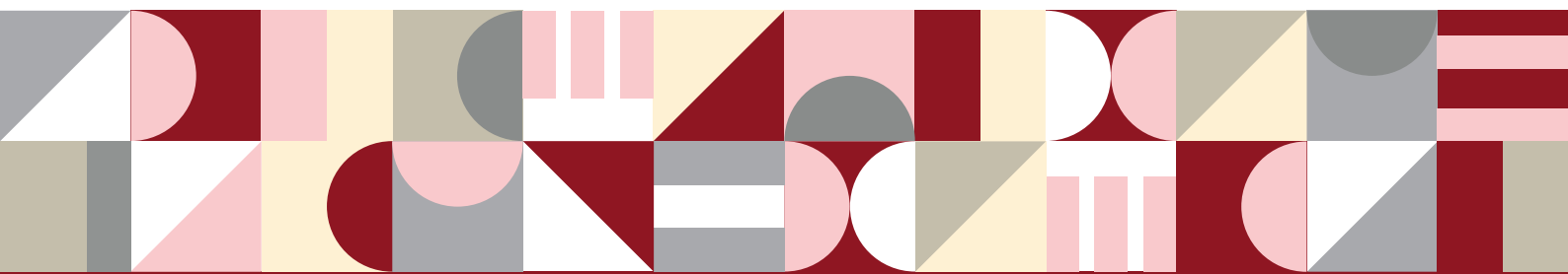
ACKNOWLEDGMENTS

This work was supported in part by research grant from Department of Civil Engineering, Faculty of Engineering, Chulalongkorn University.

REFERENCES

- AWS IoT Core. (2023). Retrieved from AWS IoT Core website: <https://docs.aws.amazon.com/iot/latest/developerguide/what-is-aws-iot.html>
- BrickSchema. (2023). Retrieved from BrickSchema website: <https://brickschema.org/>
- Grafana Labs. (2023). Retrieved from Grafana Labs website: <https://grafana.com/grafana/dashboards/>
- IFC importer. (2020). Retrieved from Unity Asset Store website: <https://assetstore.unity.com/packages/tools/utilities/ifc-importer-162502>
- InfluxDB. (2023). Retrieved from InfluxDB website: <https://www.influxdata.com/>
- Jia, R., Jin, B., Jin, M., Zhou, Y., Konstantakopoulos, I. C., Zou, H., Kim, J., Li, D., Gu, W., Arghandeh, R., Nuzzo, P., Schiavon, S., Sangiovanni-Vincentelli, A. L., and Spanos, C. J. (2018). Design Automation for Smart Building Systems, *Proceedings of the IEEE*, 106(9), 1680-1699.
- Kaewunruen, S., and Xu, N. (2018). Digital Twin for Sustainability Evaluation of Railway Station Building, *Frontiers in Built Environment*, 4(77).
- Kaewunruen, S., Rungskunroch, P. and Welsh, J. (2018). A Digital-Twin Evaluation of Net Zero Energy Building for Existing Buildings, *Sustainability*, 11(1), 159.
- Khajavi, S., Motlagh, N. H., Jaribion, A., Werner, L., Holmström, J. (2019). Digital Twin: Vision, Benefits, Boundaries, and Creation for Buildings. *IEEE Access*. 7. 147406-147419. 10.1109/ACCESS.2019.2946515.
- Liu, M., Fang, S., Dong, H., and Xu, C. (2021) Review of digital twin about concepts, technologies, and industrial applications, *Journal of Manufacturing Systems*, 58, 346-361.
- RealEstateCore. (2023). Retrieved from RealEstateCore website: <https://www.realestatecore.io/>
- Revit. (2023). Retrieved from Revit website: <https://asean.autodesk.com/products/revit/overview>
- Unity. (2023). Retrieved from Unity website: <https://docs.unity.com/>

Green Construction and Sustainability



CIRCULAR ECONOMY CRITICAL SUCCESS FACTORS FOR SUSTAINABLE CONSTRUCTION: AN EXPLORATORY APPROACH

Abdulrahman Haruna¹, and Veerasak Likhitrungsilp²

1) Ph.D., Department of Building Technology, Faculty of Environmental Technology, Abubakar Tafawa Balewa University Bauchi Nigeria. Email: abkabo360@gmail.com

2) Ph.D., Assoc. Prof., Department of Civil Engineering, Faculty of Engineering, Chulalongkorn University, Bangkok, Thailand. Email: veerasakl@gmail.com

Abstract: The circular economy agenda emphasizes the need of reducing carbon footprint and achieve sustainability in the construction industry. To maximize benefits while maintaining the functionality of Building projects, sustainability concepts should be applied throughout all decision-making stages in the construction of buildings particular with regard to CE. In this study, the critical successful factors (CSFs) needed to achieve the circular economy (CE) in residential construction projects were identified and studied. Regarding the long-term viability of such undertakings. The CSFs for CE were found in previous research and contextually modified utilizing semi-structured interviews and a pilot study using the Exploratory Factor Analysis (EFA) method. The EFA findings revealed three constructs into which the CE CSFs may be divided: Political Factors, Technological Factors and Organizational Factors. The Nigerian construction industry's stakeholders were then given a questionnaire to complete. The CSFs model was created and the results obtained indicated that political and technological factors were significant CSFs for implementing CE, despite the fact that Nigerian experts with limited practice experience were fairly informed about CE. The findings of this study will help increase sustainability in the Nigerian construction industry while also serving as a guide for decision-makers regarding the impact of global warming and carbon footprint.

Keywords: Circular, Economy, Exploratory, Success, Sustainability, Factors

1. INTRODUCTION

Sustainability idea has encouraged the change mantra for the built environment in energy usage and natural resource exhaustion that have been required in traditional building life cycle. Several sustainability obstacles which include environmental change and related monetary and ecological disturbances, with suggestions for human and ecosystem, and social request will progressively challenge the society (Mora, Frazier et al. 2013, Steffen and Hughes 2013, Wright, Nyberg et al. 2013, Semenza 2014). Sustainable building procedures can be characterized as those in which the general nature of the procedure empowers the conveyance of reasonable structures in a way that addresses the issues of all individuals included (Häkkinen, Kuittinen et al. 2015). With growing demand for construction materials, shortage of supply and growing environmental concerns resulting to increase in carbon emission and embodied energy. Embodied energy reduction for Reinforced concrete structures through the usage of more efficient materials from the optimization of structural design, rather than the use of normal building materials, such as low carbon cement and clinker (Yeo and Gabbai 2011). An important segment of the building life cycle impacts are determined by early decision at the design stage (Basbagill, Flager et al. 2013). Structures are built with an assortment of building materials and every material consumes energy all through its phases of fabrication, use and deconstruction (Wallbaum, Ostermeyer et al. 2012). The stages include raw material extraction, transportation, fabrication, assembly, establishment and additionally its dismantling, deconstruction and decay.

Resource efficient construction is significant topic around the world, especially since the concept of circular economy (CE) has emerged at various levels in recent years (Reike, Vermeulen et al. 2018) (Kirchherr, Reike et al. 2017). The circular economy's (CE) importance is becoming more universally acknowledged among scholars and professional in industry, society, and academia (Merli, Preziosi et al. 2018). Since the linear economic model is connected with mass production and resource usage without regard for the physical limit of resources, a fundamental change to a CE model is necessary (Geissdoerfer, Savaget et al. 2017). There is a deeper understanding of the value of resources and the significance of using them wisely, which places the CE notion at the vanguard of resource conservation and efficient use. The linear economy of "take-make-use-dispose" that is currently in place is to be replaced by the circular economy (CE) idea. Resource usage, waste, and emissions are reduced in CE, a restorative and regenerative system, by shortening (efficient resource use), lengthening (temporarily extended use), and closing (cycling) material loops (Reike, Vermeulen et al. 2018). Utilizing CE solutions like reuse, repair, refurbishment, recycling, and recovery helps to operationalize CE. Although strategies for CE building design and construction are being created and implemented more frequently, the process has been inconsistent and lacks a widely accepted or set direction within the building sector (Eberhardt, Birkved et al. 2022). A circular economy (CE) model is particularly gaining ground as a means of addressing environmental challenges such as the depletion of natural resources, greenhouse gas (GHG) emissions, and disposal of waste from

construction and demolition (C&D)(Charef and Lu 2021). A lot of studies have been conducted to explain the benefits of circular economy in the construction industry, but an exploratory approach towards circular economy in the construction industry was not found, hence necessitate the study to be performed.

2. METHOD

This study adopts a mixed method approach to gather in depth data on Circular economy critical success factors. From the literature reviewed, 31 CSFs of effective implementation of CE were discovered. The factors chosen from the previous research were then reviewed and modified using the qualitative approach, which included 13 semi-structured interviews. Sending a list of CSFs of CE to residential building experts with pertinent industrial expertise was conducted in a pilot study (Questionnaire I). The Exploratory Factor Analysis (EFA) analysis was used to examine the comprehensiveness and clarity of the CSFs of CE in conjunction with the research of these variables and their categories. Due to the expert interviews, two additional factors were added, resulting in a total of 33 CSFs of CE as shown in Table 1.

Table 1. CSFs of CE in the construction industry.

CE CSFs	Item code	Item Name
Political Factors	CESF.PL1	Standard for recovered materials
	CESF.PL2	Lack of codes and guidelines for reclaimed components
	CESF.PL3	Policies weaknesses
	CESF.PL4	Inappropriate regulations
	CESF.PL5	Inappropriate contracts
	CESF.PL6	Lack of incentives for using reclaimed component
Technological Factors	CESF.PL7	Low landfill taxes
	CESF.PL8	Lack of environment regulation
	CESF.TL1	Management of data
	CESF.TL2	Data availability & accessibility
	CESF.TL3	Data reliability
	CESF.TL4	Difficulty to separate material composite
	CESF.TL5	Material composition and data knowledge
	CESF.TL6	Material recoverability
	CESF.TL7	Material reliability
	CESF.TL8	Barriers associated to the use of BIM
	CESF.TL9	Lack of technologies for EOL Management
	CESF.TL10	Lack of technologies for recovered materials
	CESF.TL11	Building life span, duration & composition update
	CESF.TL12	Building type and size
	CESF.TL13	Barriers related to project phases
Organizational Factors	CESF.OG1	Complexity to implement new approach
	CESF.OG2	Flexibility and Planning
	CESF.OG3	Lack of support for the implementation of new approach
	CESF.OG4	Fragmented sector
	CESF.OG5	Lack of holistic view
	CESF.OG6	Inappropriate organization
	CESF.OG7	Multidisciplinary team
	CESF.OG8	Communication issues
	CESF.OG9	Lack of research in sustainable approach
	CESF.OG10	Lack of education and information within all part of the industry
	CESF.OG11	Lack of appropriate training for deconstruction
	CESF.OG12	Lack of skills

3. DATA COLLECTION

3.1 Semi Structure Interview

Through a "purposive sampling" method, twelve experts certified as fellows by Nigerian Institute of civil engineer (NICE) were chosen based on three factors: years of experience, educational attainment, position and Sustainable construction performed. Following the management of the degree of variation amongst interview subjects, this tactic assisted researchers in achieving their research objectives. The method was developed and enriched by further interviews. In order to reexamine and investigate the facts as well as the preexisting CSFs constructions in a local context, this study adopted the abduction approach.

As a result, the experts who were consulted concurred that a more formal plan for CE adoption in mass housing projects should be offered. The CSFs of CE are categories into three sections and two additional variables were added to the list. The CSFs that had been altered and added to were utilized to create a pilot study questionnaire.

3.2 Pilot Survey

By sending 210 questionnaires to mass housing developers in Nigeria, an exploratory factor analysis (EFA) was used to perform a pilot study to investigate the construction industry. The sample size was within a reasonable range and may be considered representative (Tabachnick, Fidell et al. 2007). The classification of all CSFs, as presented in Table 1, was supported by the EFA results.

3.3 Main Survey

The CSF classes were appropriately modified and categorize to produce the main survey (Questionnaire II) in accordance with the preliminary interviews and the EFA assessment (Questionnaire I). A larger pool of potential mass housing building participants was contacted for Questionnaire II in the Nigerian cities of Kano, Kaduna, and Abuja in order to evaluate the CSFs of CE. The survey was divided into three main sections: the respondent's demographic profile, the CSFs of CE (Table 1), and the open-ended questions (to add any more CSFs that the participants felt were crucial to be discovered). Contact was made with three important groups: clients, consultants, and contractors. The following professions/occupations could be further classified into: architects, electrical engineers, quantity surveyors, structural engineers, builders and mechanical engineers. Respondents evaluated CSFs of CE using a Likert 5-point scale, where 5 was extremely high, 4 was high, 3 was average, 2 was small, and 1 was no or very small based on information and experience (Phyo and Cho 2014). In Nigeria, CE is relatively new, hence stratified sampling of that population was taken into consideration. Only 205 entities contributed to the study despite the screening study assessing over 250 entities. Additionally, this study's sample size was determined through methodological purpose analysis (Badewi 2016).

4. DATA ANALYSIS

4.1 Exploratory Factor Analysis

Factor analysis is a technique used to reduce a large number of variables into fewer numbers of factors. This technique extracts maximum common variance from all variables and puts them into a common score. The KMO test and spherical test were performed before conducting EFA to assist the date factorability. Kaiser–Meyer–Olkin (KMO) and Barlett's test of Sphericity results was 0.948 and significant (sign = 0.001) (Tavakol and Dennick 2011). The data of this research were excellent factorability. The factorability structure of 33 items related to CSFs of CE has been determined through an exploratory factor analysis (EFA) technique. The diagonals of the anti-image correlation matrix are all greater than 0.5, indicating that each variable's inclusion in the factor analysis is genuine. Initial communities are projections of variation for each variable that all components have taken into consideration. Small values (0.3) point to variables that don't fit the factor solution well. All of the initial communities are above the threshold for this examination. Every factor loading has a significance value greater than 0.5. The results obtained as showed in Table 2 indicates that the factor loadings are above 0.5 and the cronbach alpha reliability is also excellent for all construct ranging from 0.928 to 0.953.

Table 2. Factor Loading of CSFs of CE in the construction industry.

Code	Components Loading				Cronbach alpha (α)	Naming
	1	2	3	Ranking		
CESF.PL6	0.834			1	0.928	Political Factors
CESF.PL4	0.790			2		
CESF.PL7	0.767			3		
CESF.PL2	0.765			4		
CESF.PL1	0.717			5		
CESF.PL3	0.696			6		
CESF.PL5	0.558			7		
CESF.TL5		0.858		1	0.936	Technological Factors
CESF.TL7		0.796		2		
CESF.TL6		0.780		3		
CESF.TL8		0.776		4		
CESF.TL1		0.658		5		
CESF.TL11		0.625		6		
CESF.TL4		0.618		7		
CESF.TL13		0.607		8		
CESF.TL2		0.598		9		
CESF.TL10		0.554		10		
CESF.TL9		0.526		11		
CESF.TL12		0.514		12		
CESF.TL3		0.505		13		
CESF.OG1			0.745	1	0.953	Organizational Factors
CESF.OG5			0.727	2		
CESF.OG3			0.727	3		
CESF.OG6			0.725	4		
CESF.OG2			0.717	5		
CESF.OG10			0.703	6		
CESF.OG4			0.685	7		
CESF.OG12			0.670	8		
CESF.OG7			0.668	9		
CESF.OG8			0.623	10		
CESF.OG9			0.590	11		
CESF.OG11			0.585	12		
Eigenvalues	5.768	5.114	4.618			
% of Variance	15.162	9.476	5.034			

4.2 CE Implementation Status

Respondents are categorized based on their years of experience, area of specialization, and organizational role. Respondent with over 20 years' experience is represented by 1.2 percent, which is the less in this survey while those that have 16 to 20 years experienced accounted for 23.1 percent and 11 to 15 years experienced represent 29.9 percent. Respondents with working experience up to 5 years were represented by 11.8 percent as shown in Figure 1. Since the respondent's experience is quite respectable, views and opinions acquired through the study can be considered significant and reliable. Most participants had reasonable experience in construction, further demonstrating that respondents are adequately experienced to provide reliable information. Analysis of the returned questionnaire showed that Civil engineers are majority of the respondent with about 27.4 percent which were then followed by Architect with 20.2 percent and Builders with 19.1%. Quantity surveyors represent 16.3 percent of the total respondent in the survey with M & E accounting for about 10.8 percent. Others respondent which include Interior decorators, Planners and estate valuers represent 6.2 percent as shown in Figure 2.

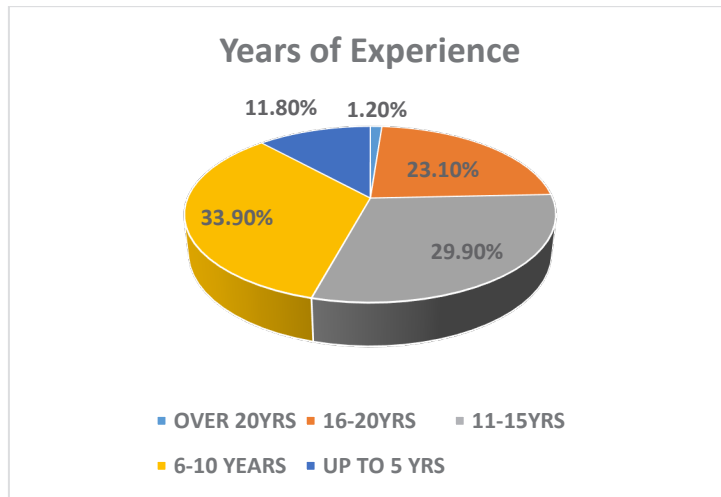


Figure 1. Respondent years of experience

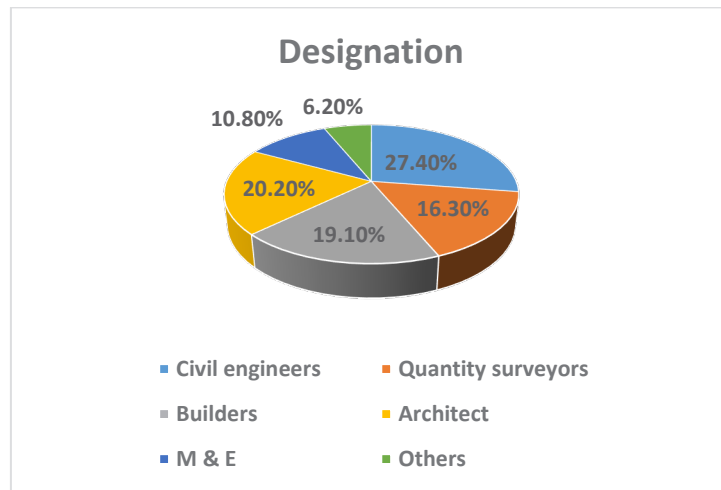


Figure 2. Respondent Designation

The respondents' opinions on CE differ, as seen in Figure 3. According to the findings, 18% of respondents think of CE as a concept of repair, 14% as production, 26% as recycling, 23% as consumption, and 19% as leasing. This result demonstrates that almost 95% of respondents see CE as either an idea or a strategy.

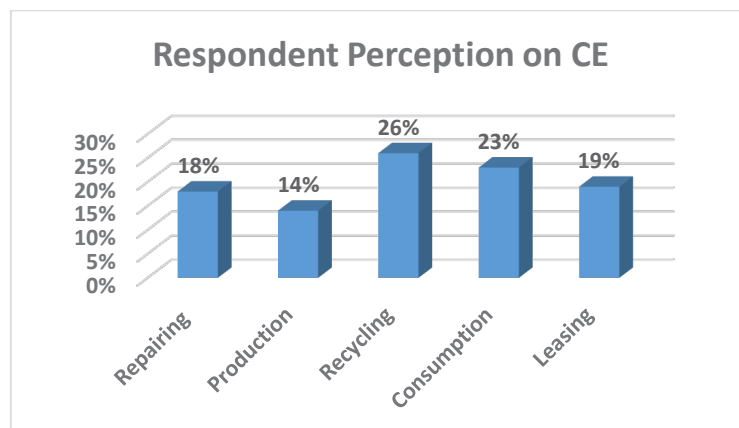


Figure 3. Respondent Perception on CE

5. DISCUSSION

The principal component analysis method was employed in this research, and the factors were extracted based on eigenvalue, which is greater than one. Oblique Simple Structure Promax was chosen because each factor should have a few high loadings, with the rest of the loadings being zero or close to zero. Results obtained indicated that organisational factors having when improved have high tendency towards improving circular economy adoption and will aid in achieving sustainable construction.

6. CONCLUSIONS

For many countries, CE is primarily employed and approved as a highly helpful instrument for maximizing the use of resources, boosting a project's objectives, and ensuring its sustainability. In contrast, there is very little use of CE in emerging economies. Like many other developing nations, Nigeria has had irregularities and disparities with regard to high-quality housing, particularly large-scale projects. CE is advised to treat this problem. As a result, this study uses a semi-structured interview and an EFA to identified CSFs of CE based on the literature review. The findings indicates that organizational factors are the main criteria that when improved can lead to effective CE implementation.

ACKNOWLEDGMENTS

The authors want to express their profound appreciation to Department of Civil Engineering, Faculty of Engineering, Chulalongkorn University.

REFERENCES

- Ajayi, S. O., L. O. Oyedele, M. Bilal, O. O. Akinade, H. A. Alaka, H. A. Owolabi and K. O. Kadiri (2015). "Waste effectiveness of the construction industry: Understanding the impediments and requisites for improvements." *Resources, Conservation and Recycling*, 102: 101-112.
- Akbarnezhad, A., K. C. G. Ong and L. R. Chandra (2014). "Economic and environmental assessment of deconstruction strategies using building information modeling." *Automation in construction*, 37: 131-144.
- Akinade, O. O., L. O. Oyedele, S. O. Ajayi, M. Bilal, H. A. Alaka, H. A. Owolabi, S. A. Bello, B. E. Jaiyeoba and K. O. Kadiri (2017). "Design for Deconstruction (DfD): Critical success factors for diverting end-of-life waste from landfills." *Waste management* 60: 3-13.
- Badewi, A. (2016). "Investigating benefits realisation process for enterprise resource planning systems."
- Basbagill, J., F. Flager, M. Lepech and M. Fischer (2013). "Application of life-cycle assessment to early stage building design for reduced embodied environmental impacts." *Building and Environment*, 60: 81-92.
- Benachio, G. L. F., M. d. C. D. Freitas and S. F. Tavares (2020). "Circular economy in the construction industry: A systematic literature reviews." *Journal of Cleaner Production*, 260: 121046.
- Bouwens, G., F. Mooij, M. Lafta, R. Lafta and J. Van Uiter (2016). "Towards circular economy in architecture." *Res. Archit. Urban. II*.
- Cabeza, L. F., C. Barreneche, L. Miró, M. Martínez, A. I. Fernández and D. Urge-Vorsatz (2013). "Affordable construction towards sustainable buildings: review on embodied energy in building materials." *Current Opinion in Environmental Sustainability*, 5(2): 229-236.
- Chang, R.-d., V. Soebarto, Z.-y. Zhao and G. Zillante (2016). "Facilitating the transition to sustainable construction: China's policies." *Journal of Cleaner Production*, 131: 534-544.
- Charef, R. and W. Lu (2021). "Factor dynamics to facilitate circular economy adoption in construction." *Journal of Cleaner Production*, 319: 128639.
- Chileshe, N., R. Rameezdeen and M. R. Hosseini (2016). "Drivers for adopting reverse logistics in the construction industry: a qualitative study." *Engineering, Construction and Architectural Management*.
- Council, U. G. B. (2019). "Circular economy guidance for construction clients: How to practically apply circular economy principles at the project brief stage." *UK GBC*.
- Couto, A. and J. P. Couto (2010). "Guidelines to improve construction and demolition waste management in Portugal." *Process Management*, 285-308.
- Dantas, T. E., E. De-Souza, I. Destro, G. Hammes, C. Rodriguez and S. Soares (2021). "How the combination of Circular Economy and Industry 4.0 can contribute towards achieving the Sustainable Development Goals." *Sustainable Production and Consumption*, 26: 213-227.
- De Jesus, A. and S. Mendonça (2018). "Lost in transition? Drivers and barriers in the eco-innovation road to the circular economy." *Ecological economics*, 145: 75-89.
- Eberhardt, L. C. M., M. Birkved and H. Birgisdottir (2022). "Building design and construction strategies for a circular economy." *Architectural Engineering and Design Management*, 18(2): 93-113.
- Fellows, R. F. and A. M. Liu (2021). *Research methods for construction*, John Wiley & Sons.
- Fivet, C. and J. Brütting (2020). "Nothing is lost, nothing is created, everything is reused: structural design for a

- circular economy." *The Structural Engineer*, 98(1): 74-81.
- Geissdoerfer, M., P. Savaget, N. M. Bocken and E. J. Hultink (2017). "The Circular Economy—A new sustainability paradigm?" *Journal of cleaner production*, 143: 757-768.
- Gorgolewski, M. (2008). "Designing with reused building components: some challenges." *Building Research & Information*, 36(2): 175-188.
- Häkkinen, T., M. Kuittinen, A. Ruuska and N. Jung (2015). "Reducing embodied carbon during the design process of buildings." *Journal of Building Engineering*, 4: 1-13.
- Harvey, N. (2001). *Life Expectancy of Building Components. Surveyors' Experience of Building in Use: A Practical Guide*, London, UK: Building Cost Information Service.
- Hossain, M. U. and S. T. Ng (2018). "Critical consideration of buildings' environmental impact assessment towards adoption of circular economy: An analytical review." *Journal of Cleaner Production*, 205: 763-780.
- Hueso-González, P., J. Martínez-Murillo and J. Ruiz-Sinoga (2018). "Benefits of adding forestry clearance residues for the soil and vegetation of a Mediterranean mountain forest." *Science of the Total Environment*, 615: 796-804.
- Jaillon, L., C.-S. Poon and Y. H. Chiang (2009). "Quantifying the waste reduction potential of using prefabrication in building construction in Hong Kong." *Waste management*, 29(1): 309-320.
- Julianelli, V., R. G. G. Caiado, L. F. Scavarda and S. P. d. M. F. Cruz (2020). "Interplay between reverse logistics and circular economy: critical success factors-based taxonomy and framework." *Resources, Conservation and Recycling*, 158: 104784.
- Kassem, M., N. Iqbal, G. Kelly, S. Lockley and N. Dawood (2014). "Building information modelling: protocols for collaborative design processes." *Journal of Information Technology in Construction*, 19: 126-149.
- Kibert, C. J. (2003). "Deconstruction: the start of a sustainable materials strategy for the built environment." *Industry and environment*, 26(2): 84-88.
- Kifokeris, D. and Y. Xenidis (2017). "Constructability: outline of past, present, and future research." *Journal of Construction Engineering and Management*, 143(8): 04017035.
- Kirchherr, J., D. Reike and M. Hekkert (2017). "Conceptualizing the circular economy: An analysis of 114 definitions." *Resources, conservation and recycling*, 127: 221-232.
- Leising, E., J. Quist and N. Bocken (2018). "Circular Economy in the building sector: Three cases and a collaboration tool." *Journal of Cleaner production*, 176: 976-989.
- Merli, R., M. Preziosi and A. Acampora (2018). "How do scholars approach the circular economy? A systematic literature review." *Journal of cleaner production*, 178: 703-722.
- Mora, C., A. G. Frazier, R. J. Longman, R. S. Dacks, M. M. Walton, E. J. Tong, J. J. Sanchez, L. R. Kaiser, Y. O. Stender and J. M. Anderson (2013). "The projected timing of climate departure from recent variability." *Nature*, 502(7470): 183-187.
- Munaro, M. R., S. F. Tavares and L. Bragança (2020). "Towards circular and more sustainable buildings: A systematic literature review on the circular economy in the built environment." *Journal of Cleaner Production*, 260: 121134.
- Osobajo, O., T. Omotayo, A. Oke and L. Obi (2020). "Transition towards circular economy implementation in the construction industry: a systematic review."
- Phyo, W. W. M. and A. M. Cho (2014). "Awareness and practice of value engineering in Myanmar construction industry." *International Journal of Scientific Engineering and Technology Research*, 3(10): 2022-2027.
- Pomponi, F. and A. Moncaster (2017). "Circular economy for the built environment: A research framework." *Journal of cleaner production*, 143: 710-718.
- Pulaski, M., C. Hewitt, M. Horman and B. Guy (2004). "Design for deconstruction: The complete sustainable-design cycle includes provisions for the re-use of building components at the end of a structure's design life." *Modern steel construction*.
- Pun, S. K., C. Liu, C. Langston, G. Treloar and Y. Itoh (2006). "Promoting the reuse and recycling of building demolition materials." *World Transactions on Engineering and Technology Education*, 5(1): 195.
- Reike, D., W. J. Vermeulen and S. Witjes (2018). "The circular economy: new or refurbished as CE 3.0? — exploring controversies in the conceptualization of the circular economy through a focus on history and resource value retention options." *Resources, Conservation and Recycling*, 135: 246-264.
- Rios, F. C., W. K. Chong and D. Grau (2015). "Design for disassembly and deconstruction-challenges and opportunities." *Procedia engineering*, 118: 1296-1304.
- Semenza, J. C. (2014). *Climate change and human health*, Multidisciplinary Digital Publishing Institute.
- Steffen, W. and L. Hughes (2013). *The Critical Decade 2013: Climate change science, risks and response*.
- Tabachnick, B. G., L. S. Fidell and J. B. Ullman (2007). *Using multivariate statistics*, Pearson Boston, MA.
- Tan, A. Z. T., A. Zaman and M. Sutrisna (2018). "Enabling an effective knowledge and information flow between the phases of building construction and facilities management." *Facilities*.

- Tavakol, M. and R. Dennick (2011). "Making sense of Cronbach's alpha." *International journal of medical education*, 2: 53.
- Volk, R., T. H. Luu, J. S. Mueller-Roemer, N. Sevilmis and F. Schultmann (2018). "Deconstruction project planning of existing buildings based on automated acquisition and reconstruction of building information." *Automation in construction*, 91: 226-245.
- Wallbaum, H., Y. Ostermeyer, C. Salzer and E. Z. Escamilla (2012). "Indicator based sustainability assessment tool for affordable housing construction technologies." *Ecological Indicators* **18**: 353-364.
- Wright, C., D. Nyberg, C. De Cock and G. Whiteman (2013). "Future imaginings: organizing in response to climate change." *Organization*, 20(5): 647-658.

A BLOCKCHAIN-BASED CARBON AUDITING FRAMEWORK FOR CONSTRUCTION MATERIAL AND PRODUCT CERTIFICATION

Yuqing Xu¹, Xingyu Tao², Moumita Das³, Helen H.L. Kwok⁴, Hao Liu⁵, and Jack C.P. Cheng⁶

- 1) Ph.D. Student, Department of Civil and Environmental Engineering, The Hong Kong University of Science and Technology, Hong Kong. Email: yxudv@connect.ust.hk
- 2) Ph.D. Candidate, Department of Civil and Environmental Engineering, The Hong Kong University of Science and Technology, Hong Kong. Email: xtaoab@connect.ust.hk
- 3) Ph.D., Postdoc, Department of Civil and Environmental Engineering, The Hong Kong University of Science and Technology, Hong Kong. Email: moumitadas@ust.hk
- 4) Ph.D., Postdoc, Department of Civil and Environmental Engineering, The Hong Kong University of Science and Technology, Hong Kong. Email: hlkwokab@connect.ust.hk
- 5) Ph.D. Candidate, Department of Civil and Environmental Engineering, The Hong Kong University of Science and Technology, Hong Kong. Email: h.liu@connect.ust.hk
- 6) Ph.D., Prof., Department of Civil and Environmental Engineering, The Hong Kong University of Science and Technology, Hong Kong. Email: cejcheng@ust.hk

Abstract: The construction industry has an indispensable role in global carbon reduction as it is one of the largest generators of carbon footprint emissions. Of various emission sources at different stages of the construction life cycle, construction materials and products contribute a considerable proportion, and thus their importance should not be neglected. Although multiple carbon certification or labelling schemes for Construction Materials and Products (CMPs) have been launched to assess their carbon emissions, such efforts and practices still rely heavily on traditional centralized data storage and publishment, which suffer data non-transparency and manipulation problems, making it difficult to identify and track carbon footprints of CMPs. Therefore, this paper proposes a transparent and reliable carbon auditing framework for CMP certification based on blockchain technology, which aims to facilitate the management of carbon footprints ranging from raw material extraction, transportation to plants, and manufacturing. In the proposed framework, a two-level privacy blockchain data model summarizing carbon footprints is first developed under data transparency and privacy concerns. An asymmetric encryption scheme integrating with an online document-sharing system, the InterPlanetary File System (IPFS), is then proposed to secure data storage and access during the carbon auditing process. Besides, smart contracts are developed to interact with the blockchain network, which supports generating immutable distributed ledgers of construction material and product carbon footprints. A prototype using Ethereum, a public blockchain development tool, was deployed and evaluated. The feasibility of the framework is validated through an illustrative example, showing that the blockchain-based framework is a promising solution in auditing and tracking the carbon footprints of CMPs.

Keywords: Carbon Auditing, Blockchain, Carbon Footprint, Carbon Tracking, Carbon Privacy

1. INTRODUCTION

The construction industry is among the leading industries contributing the largest carbon emissions (Sizirici et al., 2021), facing increasing pressure to reduce its life cycle carbon emissions (Huang et al., 2018). As it is reported that the extraction and manufacturing of construction materials contribute 70% of carbon footprint emissions of various emission sources at the construction stage (Fieldson & Rai, 2009), multiple carbon certification or labelling schemes have been developed in different regions as practical and meaningful yardsticks to effectively measure and manage the carbon footprints of Construction Materials and Products (CMPs). However, the existing carbon certification or labelling schemes for CMPs have been challenged for not providing enough transparent carbon footprint data since the limited data disclosure of CMP carbon footprints (Wu et al., 2014a). The use of traditional centralized data management methods in these schemes also makes it difficult to verify the reliability and authenticity of carbon footprints, which tend to be tampered with by central administrators.

As an emerging and promising technology, blockchain offers a powerful solution to prevent data untransparent, unreliable, and hard-to-track problems (Tao et al., 2022). Blockchain refers to a distributed database sharing and storing all committed transaction records through a chain of blocks among a number of participants (Xu et al., 2023). Unlike centralized systems, blockchain operates under a distributed peer-to-peer network without intermediaries, minimizing reliance on centralized organizations (Braeken et al., 2020). Thus, data transparency, reliability, and traceability are guaranteed with blockchain. Based on such advantages, blockchain could be a powerful tool to manage carbon footprint data in CMP certification. Without an intermediary or central authority, the carbon footprint data of CMPs can be maintained collectively under a transparent environment in a reliable manner. However, applying blockchain in the field of CMP certification has yet to be addressed since such integration still faces the leakage of sensitive carbon footprint data, such as information about partner material suppliers and the consumption quantity of raw materials in CMP manufacturing.

Therefore, this study develops a novel blockchain-based framework for CMP certification, especially towards the process of carbon auditing in CMP certification, which aims to facilitate the transparency, reliability and trackability of CMP carbon footprints. The proposed framework also secures the sensitive carbon footprint data-sharing under the transparent blockchain environment by developing a two-level privacy blockchain data model for CMP certification and implementing asymmetric encryption to realize the data access control. This paper is organized as follows. Section 2 briefly introduces CMP certification schemes, including the general process map and information flows. Section 3 provides details of our proposed blockchain-based framework. An illustrative example to validate the proposed framework is given in Section 4. The discussion is elaborated in Section 5. Finally, conclusions are drawn in Section 6.

2. CMP CERTIFICATION

Since CMPs contribute a large proportion of the life cycle carbon emissions of buildings, there is an increasing trend within the construction industry for well-regarded certification schemes for CMPs to assess and manage their carbon footprints. Several internationally recognized CMP certification schemes include the Carbon Trust Product Carbon Footprint Label in the UK, the Singapore Green Labelling Scheme (SGLS), the Green Product Certification Scheme in Hong Kong, and the CarbonCounted in Canada (Wu et al., 2014b). Normally, the CMP certification process in these schemes can be divided into three main stages in Figure 1: (1) carbon auditing stage for collecting relevant data and measuring the Carbon Footprint of the Product (CFP), (2) application stage for preparing certification documents, and (3) certification stage for verifying and issuing CMP certificates.

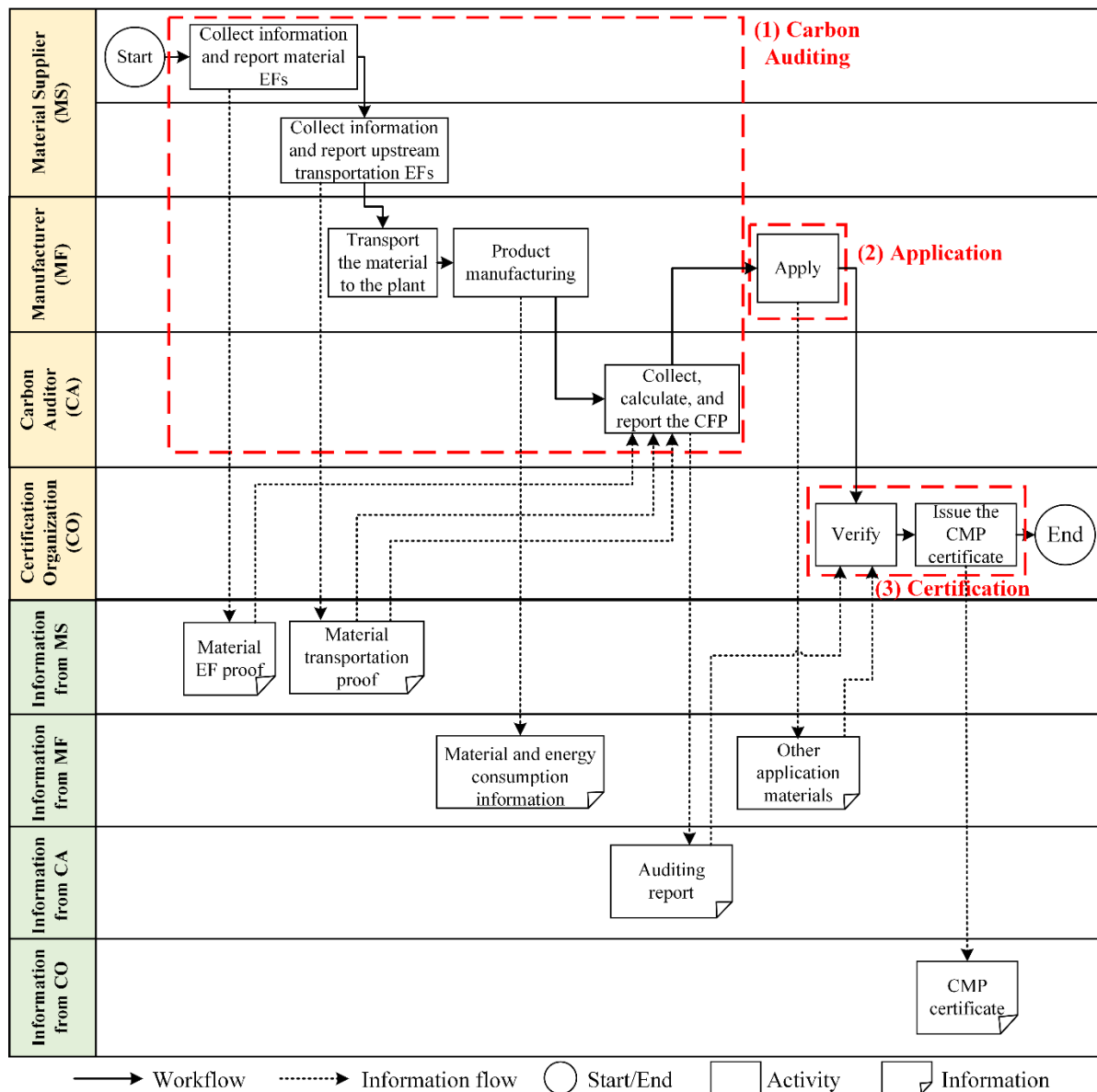


Figure 1. Process map and information flows of CMP certification

Figure 1 also shows a process map with information flows during the CMP certification process. The CMP certification starts with raw material suppliers providing carbon footprint data, especially for material Emission Factor (EF) and transportation EF when transferring raw materials to the manufacturer's plant. After that, the manufacturer starts to record carbon footprints generated from CMP manufacturing, which contains the material and energy consumption details. Based on the data collected in the previous two steps, the professional carbon auditor hired by the manufacturer measures the total CFP, generates the audit report for CMP certification, and finishes the carbon auditing stage. At the next application stage, the manufacturer sends the application files with the audit report and all relevant proof documents to the certification organization for verification. The certification organization issues the CMP certificate after successful verification at the final certification stage. This paper mainly focuses on the carbon auditing stage in CMP certification. Multiple carbon footprint-related data and files are collected during the carbon auditing process in hard-copies stored in the non-transparent environment, making it difficult and time-costly to verify this data and track carbon footprints of CMPs. Thus, this paper aims to implement blockchain to provide an efficient data management platform for carbon auditors to collect CMP carbon footprints and to facilitate transparency, reliability, and traceability when verifying and tracking carbon footprints during CMP certification.

3. METHOD

This section illustrates the proposed blockchain-based carbon auditing framework for CMP certification (shown in Figure 2). Material suppliers, manufacturers, and carbon auditors are the three main stakeholders in the proposed framework. In the beginning, encryption transactions are generated and distributed in the blockchain network for each stakeholder, which will be used to control the access of sensitive carbon footprint data (see details in Section 3.2). Material suppliers record CMP carbon footprints from raw material extraction and transportation to plants via blockchain transactions, while manufacturers record CMP carbon footprints from material and energy consumption during the manufacturing process. When generating these recording transactions, sensitive carbon footprint data is first processed based on asymmetric encryption and then stored in the distributed ledgers, which allows the data recipients to access sensitive carbon footprint data after decryption. Thus, the carbon footprint data-sharing is secured under the transparent blockchain network. In this proposed framework, CMP carbon footprints are recorded and synchronized in every peer's ledger, which allows carbon auditors to efficiently collect carbon footprint data and generate the carbon audit report. It also facilitates the transparency, reliability, and traceability of CMP certification, as certification organizations can search and verify CMP carbon footprints with immutable blockchain transactions.

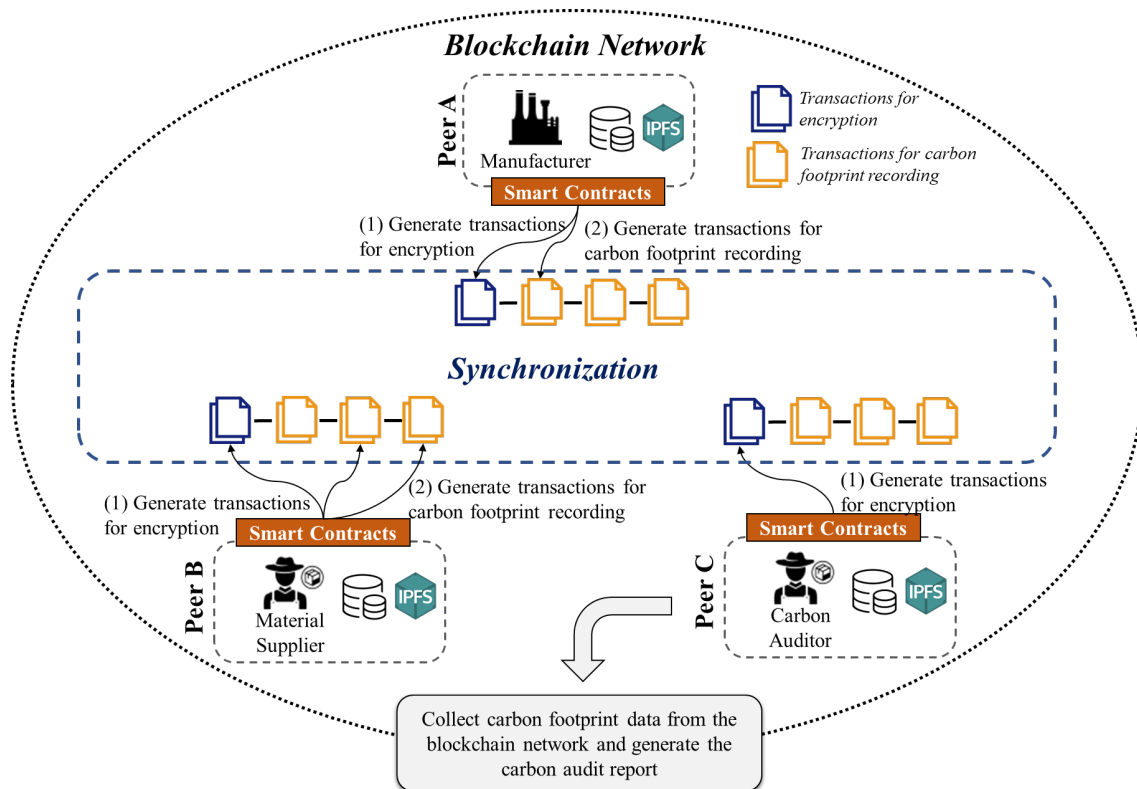


Figure 2. Blockchain-based carbon auditing framework for CMP certification

As shown in Figure 3, the architecture of the proposed framework involves four technical layers: (1) data access layer to receive user inputs of carbon footprint data required for CMP certification, in which a two-level privacy blockchain data model is developed, (2) data privacy layer to pre-process sensitive carbon footprint data identified in the developed data model based on asymmetric encryption, (3) smart contract layer to interact with blockchain network and automatically generate blockchain transactions, and (4) data storage layer to store different types of carbon footprint data. The details of these layers are described in the following subsections.

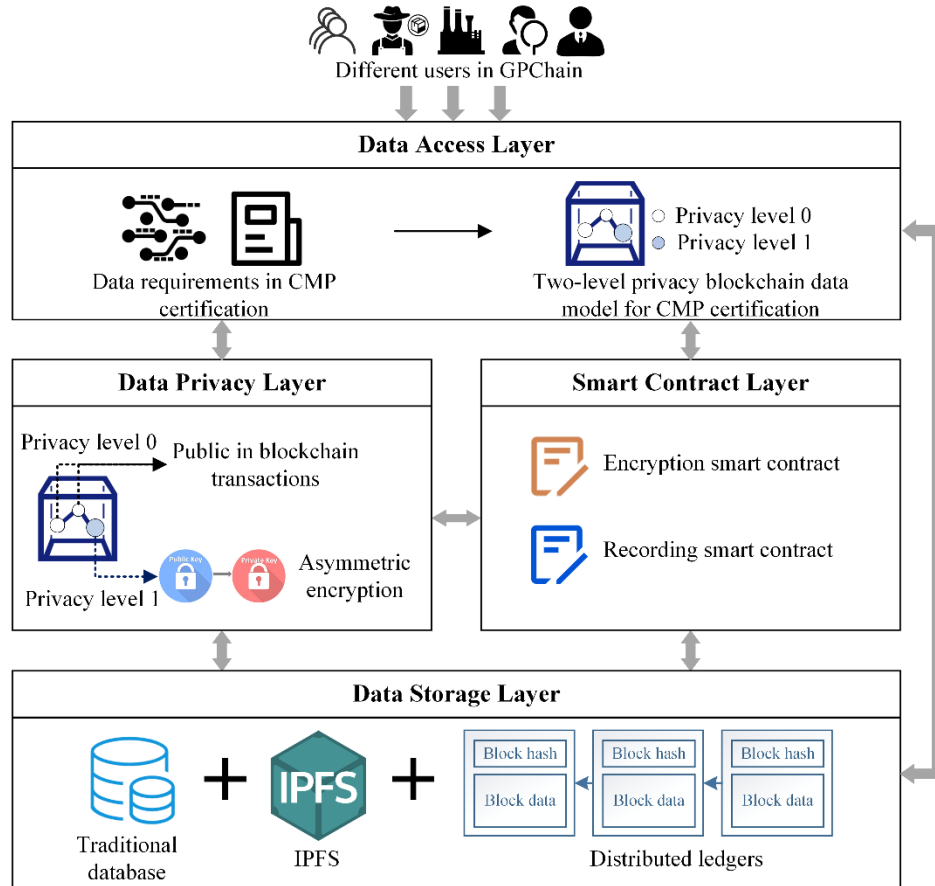


Figure 3. Architecture of the proposed framework

3.1 Data Access Layer

The data access layer is the front end of the proposed framework. This layer is mainly designed to receive the carbon footprint data required for CMP certification and to provide the basis for CMP carbon auditing. According to the information flows identified in Figure 1, data requirements for carbon auditing in CMP certification are thus specified as information exchanges at the carbon auditing stage, which includes the material EF proof documents, material transportation proof documents, and material and energy consumption information. Based on the identified data requirements, a two-level privacy blockchain data model for CMP certification is developed in Figure 4.

In this developed data model, the inputs of material suppliers are modelled based on the material EF proof documents and material transportation proof documents, which will generate a blockchain transaction summarizing material origin information. This type of transaction contains basic supply chain information (“Material supplier” and “Material type”), and the most vital information to track, which are material emission factors (EFs) from material extraction (“Material EF” and “Unit of material EF”) and upstream transportation (“Transportation EF” and “Unit of transportation EF”). Meanwhile, the original proof documents of material EF and transportation are also input and stored in the blockchain network via the unique document hash value provided by the InterPlanetary File System (IPFS) (see details in Section 3.4). For manufacturers, there are two types of user inputs: material consumption transaction and energy consumption transaction. Material consumption and energy consumption information are modelled to cover (1) the specific product information such as “Manufacturer”, “Product category”, and “Product batch ID”, and (2) detailed quantity information affecting the CFP calculation like “Material consumption” and “Processing EF”.

However, since the information in blockchain transactions is totally transparent to network peers, it tends

to raise concerns about the leakage of sensitive carbon footprint data required in CMP certification, such as partner raw material suppliers of manufacturers and material consumption during CMP manufacturing. Therefore, the proposed data model considers stakeholders' concerns about the privacy of carbon footprint data and identifies two privacy levels of carbon footprint data, which are presented below.

- Privacy level 0 is for non-sensitive information that all users can access. To provide efficient and reliable tracking of CMP carbon footprints in CMP certification, carbon emissions from the CMP's components and transportation, especially their EFs, are made transparent when recording. Meanwhile, the manufacturer's information and CMP's general information are also covered at this level, since these kinds of information are available when certifying a specific CMP following traditional certification schemes.
- Privacy level 1 is for private information that should only be accessed by intended recipients, specific to carbon footprint data that is transparent to the carbon auditor and not accessed by irrelevant stakeholders. Although the proposed framework aims to improve the transparency of CMP certification, manufacturers are not willing to share information about their cooperative suppliers and manufacturing details with others. However, such partner material supplier information and material consumption information are needed for carbon auditors to generate the auditing report. Therefore, "Material supplier", "Material type", proof documents provided by suppliers, "Material consumption", and proof documents of energy consumption during product processing are identified as privacy level 1 information that should be available to carbon auditors, while cannot be accessed by other peers.

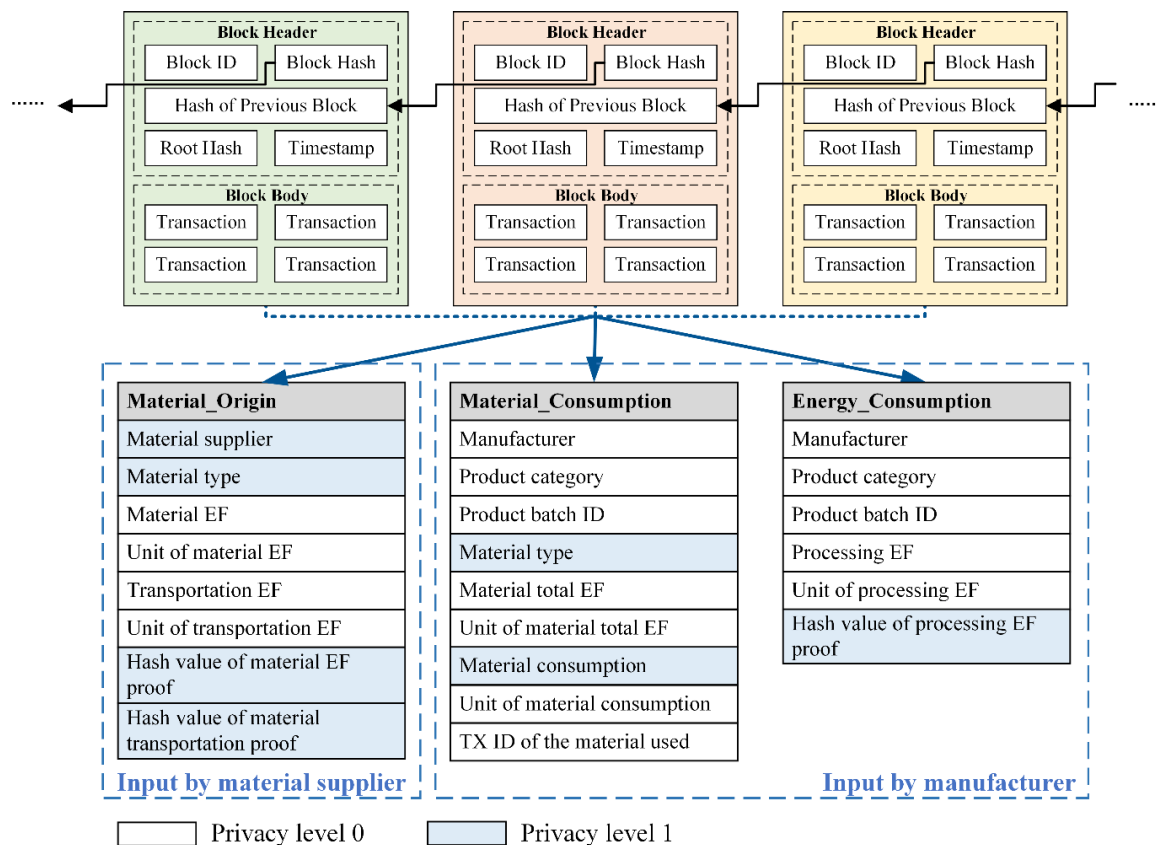


Figure 4. Two-level privacy blockchain data model for CMP certification

3.2 Data Privacy Layer

As transaction information is accessible to all blockchain network peers, concerns regarding data security of private carbon footprint data for CMP certification tend to be raised. Thus, the proposed framework adopts the data privacy layer by integrating asymmetric encryption to facilitate data security and confidentiality of CMP carbon footprints. Asymmetric encryption is a type of encryption scheme that uses a pair of keys, including a public key to encrypt the plaintext message and a private key to decrypt the ciphertext message (Simmons, 1979). The public keys will be available in public so that anyone who wants to send a message to a recipient can use the recipient's public key for encryption. Private keys under the asymmetric encryption scheme are kept secret to ensure only the recipient can know the plaintext message after decryption.

Figure 5 shows a transaction of raw material origins generated by Material Supplier A that wants to be shared with the carbon auditor. Initially, material suppliers, manufacturers, and carbon auditors distribute their asymmetric public keys via transactions in the blockchain network. Carbon footprint data at privacy level 0, such as “Material EF” and “Transportation EF”, is input directly in blockchain transactions, and everyone can access it. When sharing privacy level 1 information identified in Figure 4, including “Material supplier”, “Material type”, and original hash values of proof documents (generated by IPFS), Material Supplier A first encrypts them with the carbon auditor’s public key, and the transaction with encrypted ciphertexts is generated and broadcast in the blockchain network. After decryption with the private key, the carbon auditor successfully accesses the information shared by Material Supplier A, while others can only access the meaningless encrypted version of privacy level 1 information.

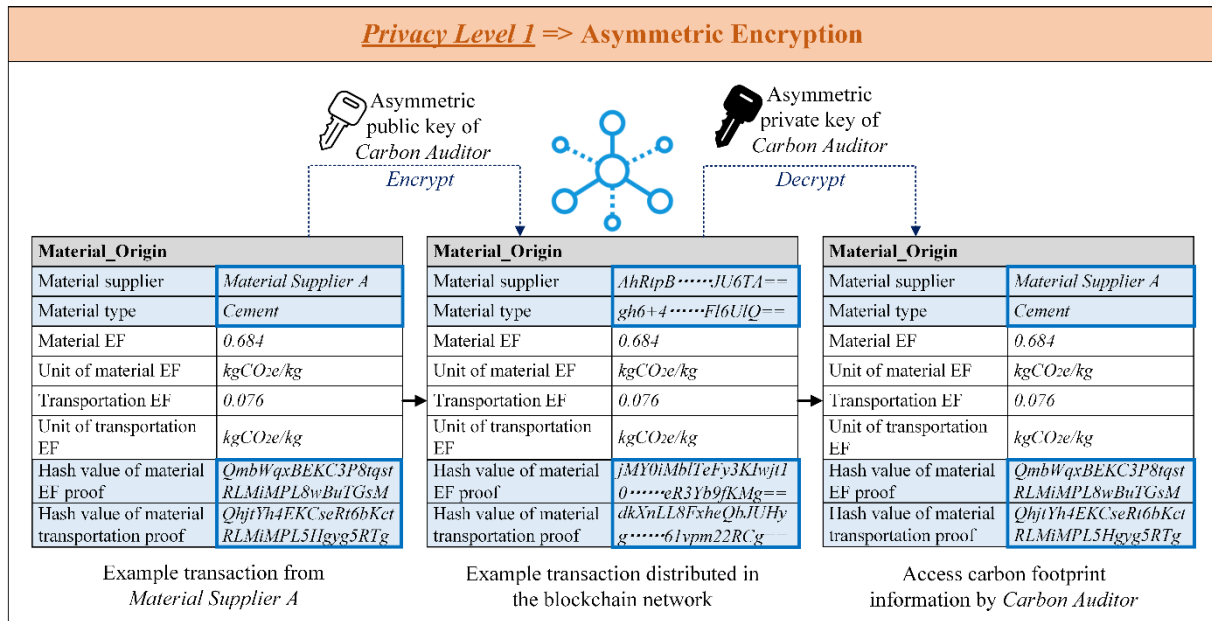


Figure 5. An example of securing carbon footprint data using asymmetric encryption

3.3 Smart Contract Layer

The smart contract layer is mainly designed to connect user inputs after pre-processing in the data privacy layer with the blockchain network via smart contracts. Smart contracts are automatically executed codes stored in the blockchain that can interact with the distributed ledgers, which can realize functions such as sharing information and executing payments (Macrinici, 2018). In the proposed framework, there are two types of smart contracts, which are encryption smart contract and recording smart contract.

- Encryption smart contract is designed to secure carbon footprint data-sharing. This smart contract has two main functions: key distribution and key retrieval. Key distribution allows network peers to input and distribute their asymmetric public keys for privacy protection, while the key retrieval function enables peers to get the public keys of intended information receivers (such as the carbon auditor) for carbon footprint data encryption.
- Recording smart contract helps to transfer user inputs of processed carbon footprint data to immutable records distributed in the blockchain network. There are three types of recording functions corresponding to three types of transactions identified in Figure 4, which facilitate the generation of material origin transactions for material suppliers, and material consumption transactions and energy consumption transactions for manufacturers.

3.4 Data Storage Layer

This section presents the data storage layer in the proposed framework for storing carbon footprint data with three methods, integrating a conventional database and two distributed databases (blockchain and IPFS). The conventional database is designed to store original carbon footprint data and corresponding blockchain transaction indexes for stakeholders’ own management, while blockchain stores public carbon footprint data in original text and private carbon footprint data in encrypted versions. IPFS is a decentralized file-sharing and storage platform that identifies files based on contents (IPFS community, 2015). When a file is uploaded to IPFS, a unique hash value summarizing file contents will be generated, which is a unique record of the uploaded file. Files stored on IPFS can be requested and accessed by anyone with the matching hash values. In this paper, IPFS is designed to

store and share hard-copy proof documents required for CMP certification, such as source letters of raw materials provided by raw material suppliers and annual electricity bills provided by manufacturers. Considering the data requirements during CMP certification and blockchain's unachievable ability to store hard copy files, IPFS serves as a decentralized file-sharing and storage platform to facilitate efficient and reliable communication and information exchange among participants. Material suppliers and manufacturers first upload proof documents in IPFS and then get unique hash values of files returned by IPFS. These hash values are then encrypted with the carbon auditor's public key. After decryption, the carbon auditor can get the original hash value in IPFS and access the shared files for auditing.

4. RESULTS

4.1 Prerequisites

To validate the proposed framework, a public blockchain platform, Ethereum (Wood, 2014), is used to develop the prototype. Blockchain functions supported by smart contracts are developed with Solidity language. Three blockchain nodes (material supplier, manufacturer, and carbon auditor) are generated and deployed in the Ethereum testnet, Goerli. Besides, the Rivest–Shamir–Adleman (RSA) (Badertscher et al., 2017), an asymmetric encryption protocol widely used for data transmission, is selected in this experiment. An IPFS desktop is also set up for storing hard copies of proof documents required for CMP certification. An Ethereum transaction search engine called Etherscan (Etherscan, 2015) is used in this test for illustrating and tracking blockchain transactions.

4.2 Conduction of Proposed Framework

First, a pair of asymmetric encryption keys are generated for the carbon auditor in this test. By invoking the encryption smart contract, the carbon auditor distributes its public key based on the newly generated encryption transaction in the blockchain network. Second, the material supplier collects the carbon footprint information of material origins, including the hash value obtained from the IPFS after uploading the proof documents. Then the material supplier retrieves the carbon auditor's public key from the encryption transaction and uses this key to encrypt private carbon footprint data identified in Figure 4. After this step, pre-processed carbon footprint data is used as the input of the recording smart contract, and a blockchain transaction of material origin is then generated in the distributed ledgers which can be searched and tracked through Etherscan. Similarly, the manufacturer sends the public carbon footprint data and encrypted carbon footprint data to the recording smart contract as the input, and different transactions for material consumption and energy consumption are generated and broadcast. Figure 6 (a) shows the recording smart contract developed in this test as well as three carbon footprint transactions generated, which can be tracked in Etherscan in Figure 6 (b). Figure 6 (c) is the detailed information contained in the transaction of recording material origin, and the original information can be accessed by anyone after decoding (Figure 6(d)).

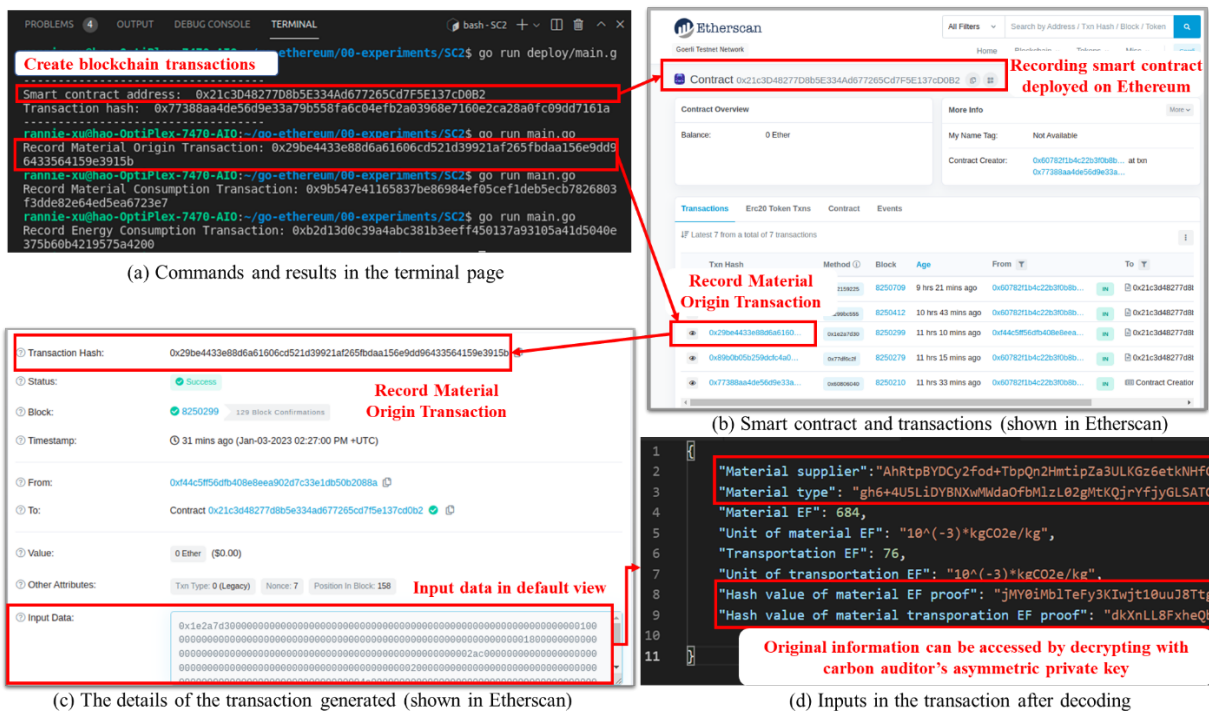


Figure 6. Results of the test

Finally, the carbon auditor gets a series of transactions of CMP carbon footprint data for auditing. For the encrypted carbon footprint information in transactions, the original information is accessed after decrypting it with the carbon auditor's private key. Therefore, based on the immutable blockchain transactions containing CMP carbon footprints, the carbon auditor measures CMP's total CFP and generates an auditing report for certification. Moreover, these blockchain transactions also provide reliable data sources for further carbon footprint verification, helping to facilitate the transparency, reliability, and traceability of CMP certification.

5. DISCUSSION

Compared with previous studies, the blockchain-based carbon auditing framework serves as a more appropriate data management tool for CMP certification. First, recording CMP carbon footprints in the proposed framework is more transparent than traditional certification schemes, allowing carbon auditors, certification organizations, and even public users to track CMP carbon footprints. Second, as the transparency-privacy trade-off commonly exists in blockchain networks, this proposed framework provides balances between maintaining a transparent carbon footprint data-sharing environment and protecting sensitive carbon footprint data during CMP certification by developing the two-level privacy data model and using asymmetric encryption. Last, this paper not only contributes to the academy by exploring blockchain's potential for carbon auditing in CMP certification but also has industry contributions. Based on the transparent carbon footprints recorded in the framework, industry consumers are encouraged to cultivate purchasing habits in selecting low-carbon products before construction.

6. CONCLUSIONS

This research proposes a blockchain-based carbon auditing framework for CMP certification. First, a general framework with workflows for carbon auditing in CMP certification under the blockchain context is proposed, which identifies the main types of stakeholders and their activities. Second, a two-level privacy blockchain data model for CMP certification is developed in this paper, identifying the carbon footprint data inputs of the proposed framework and their sensitivity. Based on the data model, asymmetric encryption is implemented to secure private carbon footprint data-sharing in the blockchain network. An experimental test is conducted in this paper to validate the proposed framework, which demonstrates its feasibility. However, this framework is an initial exploration of applying blockchain in CMP certification. In the future, a user-friendly application page and more performance tests need to be implemented.

REFERENCES

- Badertscher, C., Matt, C., and Maurer, U. (2017). Strengthening access control encryption. *In Advances in Cryptology—ASIACRYPT 2017: 23rd International Conference on the Theory and Applications of Cryptology and Information Security*, Hong Kong, China, pp. 502-532.
- Braeken, A., Liyanage, M., Kanhere, S. S., and Dixit, S. (2020). Blockchain and cyberphysical systems. *Computer*, 53(09), 31-35.
- Etherscan. (2015). *The Ethereum blockchain explorer*. Retrieved from Etherscan website: <https://etherscan.io/>.
- Fieldson, R., & Rai, D. (2009). An assessment of carbon emissions from retail fit-out in the United Kingdom. *Journal of Retail & Leisure Property*, 8, 243-258.
- Huang, L., Krigsvoll, G., Johansen, F., Liu, Y., & Zhang, X. (2018). Carbon emission of global construction sector. *Renewable and Sustainable Energy Reviews*, 81, 1906-1916.
- IPFS community. (2015). *How IPFS works*, Retrieved from IPFS website: <https://ipfs.tech/>.
- Macrinici, D., Cartoceanu, C., and Gao, S. (2018). Smart contract applications within blockchain technology: A systematic mapping study. *Telematics and Informatics*, 35(8), 2337-2354.
- Simmons, G. J. (1979). Symmetric and asymmetric encryption. *ACM Computing Surveys*, 11(4), 305-330.
- Sizirici, B., Fseha, Y., Cho, C. S., Yildiz, I., and Byon, Y. J. (2021). A review of carbon footprint reduction in construction industry, from design to operation. *Materials*, 14(20), 6094.
- Tao, X., Liu, Y., Wong, P. K. Y., Chen, K., Das, M., and Cheng, J. C. (2022). Confidentiality-minded framework for blockchain-based BIM design collaboration. *Automation in Construction*, 136, 104172.
- Wood, G. (2014). Ethereum: A secure decentralised generalised transaction ledger. *Ethereum project yellow paper*, 151(2014), 1-32.
- Wu, P., Low, S. P., Xia, B., and Zuo, J. (2014a). Achieving transparency in carbon labelling for construction materials—Lessons from current assessment standards and carbon labels. *Environmental science & policy*, 44, 11-25.
- Wu, P., Xia, B., Pienaar, J., and Zhao, X. (2014b). The past, present and future of carbon labelling for construction materials—a review. *Building and Environment*, 77, 160-168.
- Xu, Y., Tao, X., Das, M., Kwok, H. H., Liu, H., Wang, G., and Cheng, J. C. (2023). Suitability analysis of consensus protocols for blockchain-based applications in the construction industry. *Automation in Construction*, 145, 104638.

RESEARCH ON VISUALIZATION BASED ON CLIMATE ANALYSIS OF THE INFLUENCE OF GREEN SPACE ON THE THERMAL ENVIRONMENT USING MSSG MODEL

Takumi Makio¹, Kaoru Matsuo², Shigeaki Takeda³, Hiroyuki Kaga⁴, and Makoto Yokoyama⁵

1) Graduate Student, Graduate School of Agriculture, Osaka Metropolitan University, Osaka, Japan. Email: makio.omu@gmail.com

2) Ph.D., Assist. Prof., Graduate School of Agriculture, Osaka Metropolitan University, Osaka, Japan. Email: kmatsuo@omu.ac.jp

3) Ph.D., Assoc. Prof., Graduate School of Agriculture, Osaka Metropolitan University, Osaka, Japan. Email: takeda@omu.ac.jp

4) Ph.D., Prof., Graduate School of Agriculture, Osaka Metropolitan University, Osaka, Japan. Email: kaga@omu.ac.jp

5) Ph.D., Lecturer, Faculty of Urban Management, Fukuyama City University, Hiroshima, Japan. Email: m-yokoyama@fcu.ac.jp

Abstract: In addition to climate change, a lack of green space has caused urban warming. In Osaka city, severe urban warming reportedly leads to high temperatures. Under these circumstances, the "Grand Green Osaka" project is currently underway in a central business district in front of the Osaka central station. This urban development project will include a hotel, commercial facilities, and a large 8-hectare green space on a 17-hectare site. This study aims to visualize the impact of green space making in a development on the surrounding thermal environment based on the climate analysis result by numerical simulation. As a result, a relatively cooler temperature zone was further extended within the development area. On the west side of the developed area, the newly developed green space was contiguous with the existing green space, which enhanced the high temperature mitigation effect and lowered the temperature. On the east side of the developed area, the wind turbulence caused by the appearance of buildings and the lower temperature in the developed area brought cooler and stronger wind speeds than the current conditions, which contributed to the lower temperature.

Keywords: Green spaces, Climate analysis, Multi-scale simulator for the geoenvironment, 3D city model.

1. BACKGROUND AND OBJECT

In addition to climate change, a lack of green space networks has caused urban warming. Osaka is the second largest metropolitan area in Japan. The population is concentrated and there are many tall buildings and a large skyline. Osaka has been reported to experience high temperature due to the intense urbanization (Takebayashi & Moriyama, 2005). In order to mitigate or adapt urban warming, various studies have dealt with understanding of climate condition (Kitao et al., 2010; Liqing et al., 2023; Yamasaki et al., 2022), analyzing the relationship between temperature and factors (Noguchi et al., 2014; Sasaki et al., 2018) and reflecting these results to urban planning or landscape planning (Chao et al., 2012; Inoue et al., 2020; Matsuo et al., 2019). Under these circumstances, the "Grand Green Osaka" project has been currently underway in a central business district in front of the Osaka central station, within the year 2024. This urban development project will include a hotel, commercial facilities, and a large 8-hectare green space on a 17-hectare site. In addition, this aims to realize a new urban model for Osaka that incorporates the concepts of SDGs, based on the integrating nature and the city, which will be created around the green space making.

This study aims to visualize the impact of green space making in a development on the surrounding thermal environment based on the climate analysis result. It is a city block-level climate analysis based on current conditions and post-development numerical calculations using the "MSSG: Multi-scale Simulator for the Geoenvironment."

2. METHOD

2.1 Outline of MSSG Model

The MSSG model is a coupled atmosphere-ocean model being developed by the Japan Agency for Marine-Earth Science and Technology, and is a multi-simulation model capable of numerically computing physical phenomena at scales ranging from the entire Earth to a single street space. The simulation consists of two steps. First, mesoscale meteorological calculations were performed. The calculation was performed using the nesting method, with Domain 1 and Domain 2 centered on a central business district in front of the Osaka central station, and with initial and boundary values of the atmosphere and land surface data as calculation conditions. Second, building-resolving meteorological calculations were performed with Domain 3 using the results of mesoscale meteorological calculations as initial and boundary values.

Table 1. Numerical calculation conditions

Domain1,2 Numerical calculation conditions

Calculation Period		August 9, 2022 00:00:00 - August 10, 2022 00:00:00 (JST)
Domain1	Resolution	1km
	Calculation area	240×240
Domain2	Resolution	100m
	Calculation area	480×480
Weather Data		Meso Scale Model Data with 3 hours interval, resolution of approx.10km (Japan Meteorological Agency)
Surface Data	Elevaion	10m-mesh Digital Topographic Data (Fundamental Geospatial Data 2016)
	Land use	Land use mesh data with resolution of approx. 100 m (National Land Information 2016)

Doamin3 Numerical calculation conditions

Calculation Period		August 9, 2022 1:00 p.m. - August 9, 2022 1:20 p.m. (JST)
Clculation Area	Grid size	5m×5m×5m
	Grid number	992×992×151
Time Step		0.25 seconds, every 10 seconds
Weather Data		Meso-Meteorological Calculations, per 100 m and per hour
Surface Data	Land Use	Osaka City Building Use Data (2019, Pasco Corporation). Project PLATEAU (2020, Ministry of Land, Infrastructure, Transport and Tourism).
	Green Cover	Satellite Imagery spatial resolution of approx. 10m). (Sentinel-2 MSI sensor, October 2, 2021)
	Elevation	Numerical Elevation 5m-mesh (Fundamental Geospatial Data 2016)
	Building Height	Project PLATEAU (2020, Ministry of Land, Infrastructure, Transport and Tourism)

2.2 Calculation Condition

Table 1 shows the numerical calculation conditions, Figure 1 shows the land use data of Domain 1 and Domain 2 and Figure 2 shows the land use data of Domain 3. The calculation period for the mesoscale meteorological calculations was set from 00:00 on August 9, 2022 to 00:00 on August 10, 2022. A nesting method was used for the calculation domain, with Domain 1 consisting of 240×240 grids with a grid size of 1 km and Domain 2 consisting of 480×480 grids with a grid size of 100 m, centered on the Osaka central station area. As the initial value and boundary values, weather data is used Meso Scale Model data with 3-hour intervals, the resolution of 10 km. For surface data, the numerical elevation data from the Geospatial Information Authority of Japan in 2016 and land use data from the National Land Information in 2016 are used for the calculations. The calculation period for the building-resolving meteorological calculations was 13:00-13:20 on August 9, 2022, when the daytime temperature was the highest, with the first 10 minutes omitted from the analysis as the run-up period. Domain 3 was set to 992×992 grids in the xy direction and 151 grids in the z direction with a grid size of 5 m, and centered on the Osaka central station area. The meso-meteorological calculation results were used for the initial and boundary values. The land use data is composed of five categories, “Building,” “Building Site,” “Road,” “Greenspace,” “Waters.” “Building” is made from the data of Project PLATEAU, a 3D city model published in Japan. The others were made by corresponding the land use data from that’s published in Osaka City Government to land use categories of MSSG. Green cover was made using satellite imagery taken on October 2, 2021 by the Multispectral Imager (MSI) sensor on Sentinel-2. Building height was determined using the Project PLATEAU.

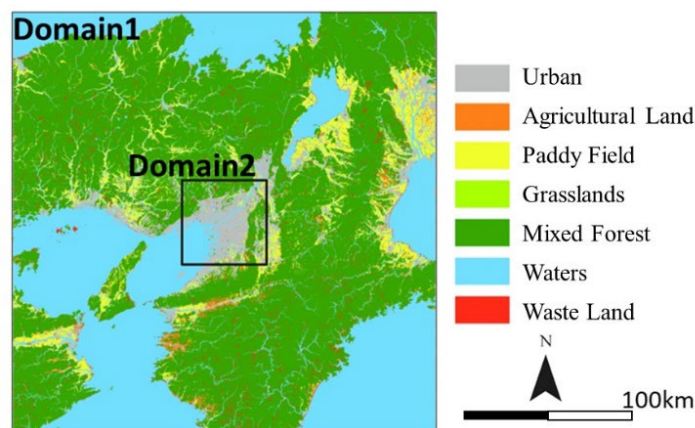


Figure 1. Land use data of Domain1,2

From the above, climate current situation was performed. In this study, the analysis of the simulation results are in Domain 3 area. We call Domain 3 area “Osaka area” and the central business district in Osaka area is defined as “Osaka central station area”.

After the analyzing the simulation results of current situation, climate future situation after the development in the Osaka central station area was simulated. When this simulation is performed, the land use data category is changed to refer to the site plan in the Osaka central station area. Figure 3 shows the land use data of before and after development. Specifically, the current land use classified as "Building Site" was changed to "Greenspace," "Building," and "Road," respectively. In addition, the green cover data is modified and added the new green spaces to be created by the development, and the building height is modified height information for new buildings by the development. We call these areas as “developed area.”

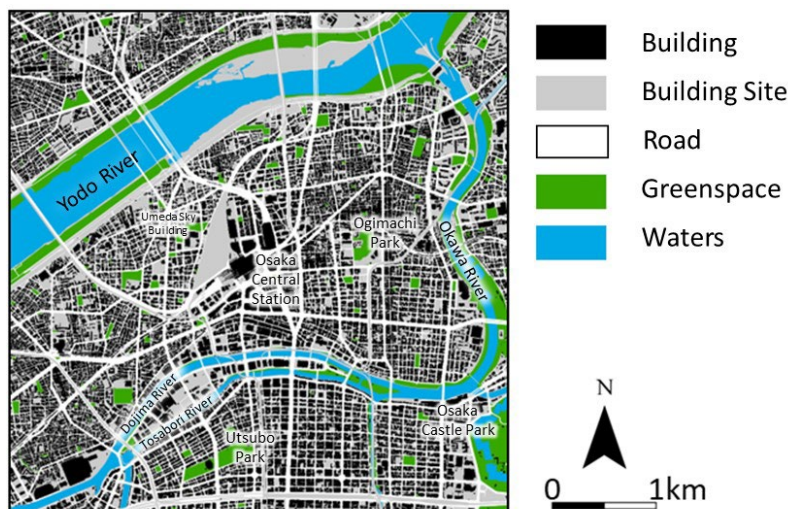


Figure 2. Land use data of Osaka area

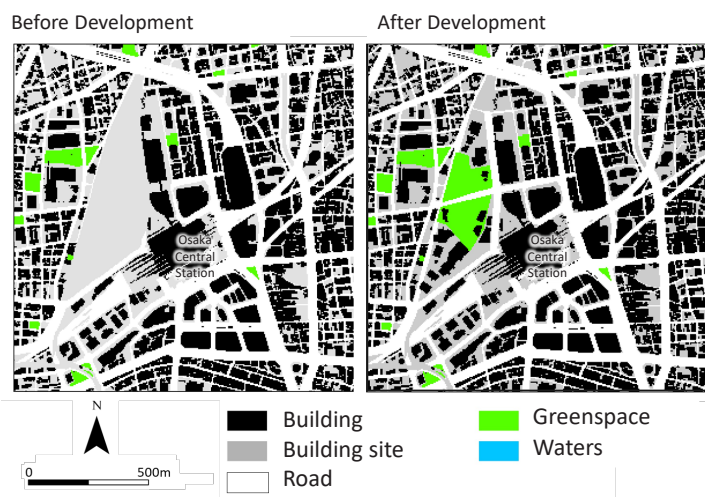


Figure 3. Land use data of before and after development

3. RESULTS AND DISCUSSION

3.1 Current Situation Simulation Results in The Osaka Central Station Area

Figure 4 shows the simulation results of the daytime temperature and wind distribution in Osaka area. The results are averaged from 13:10 to 13:20 and are at 1 m above the ground. Sea breeze blowing from west to east is observed in Osaka area. In Yodo River, 3.0 - 6.0 m/s and slightly stronger northwest wind blows. It can be seen flowing into the open space north of Osaka central station, and the wind speed is very high at 6 m/s or more. Wind speeds 2.0 - 3.0 m/s are also observed along the Dojima River, Tosabori River, and Okawa River upstream. The effect is cooler temperatures in the river and surroundings. For example, the Yodo River is the lowest at 30.5 - 32.0°C, and the Okawa, Tosabori, and Dojima Rivers are also low at 31.5 - 33.0°C. In addition, parks and green spaces such as Ogimachi Park, Utsubo Park, and Osaka Castle Park are relatively slightly lower at 31.0 - 33.0°C

due to low convective heat is low. On the other hand, wide roads have relatively high temperatures of 35.0 - 36.0°C. This is due to the warming of the ground surface caused by the large amount of solar radiation, which raises the temperature near the ground surface. In addition, high temperatures are observed away from the river such as Tosabori River and the Okawa River within the wide roads. This is because the temperatures are also significantly higher, where the distance from the Tosabori River and the Okawa River is greater and the river breezes do not reach the area.

Figure 5 shows the daytime temperature and wind distribution in the Osaka central station area. In this area, the temperature is 32.5 - 36.5°C. This shows that the temperature varies greatly depending on the location. First, the temperature within the district that will change in the future due to development, the temperature is 32.5 - 33.5°C, with the high temperatures being mitigated. This is thought to be due to cool sea breezes blowing from the southwest and river breezes flowing in from the Yodo River, as wind speeds are as high as 4.0 - 6.0 m/s. The temperature on the north side of the Umeda Sky Building was also lower than 32.5°C. This can be attributed to the green space at the foot of the Umeda Sky Building. The wind also becomes a valley wind between the north and south buildings of Grand Front Osaka, blowing at 4.0 - 6.0 m/s up to the Hankyu Osaka Umeda Station. On the other hand, the temperature is relatively high between 35.0 and 36.5°C on the west side of the track of the Osaka central station, northwest of Nishi-Umeda Station, east of the Diamond District, and between the buildings southeast of Hankyu Osaka-Umeda Station.

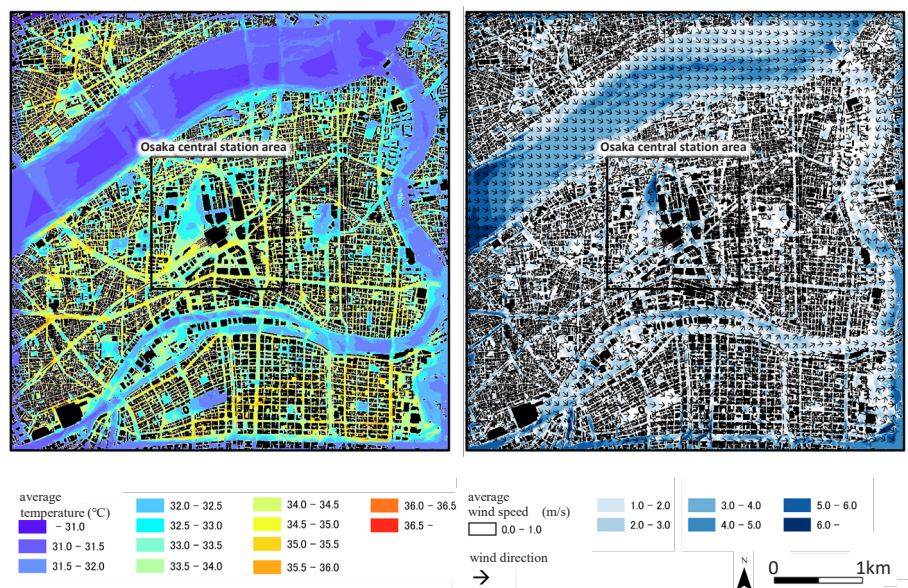


Figure 4. Temperature and wind distribution of Osaka area

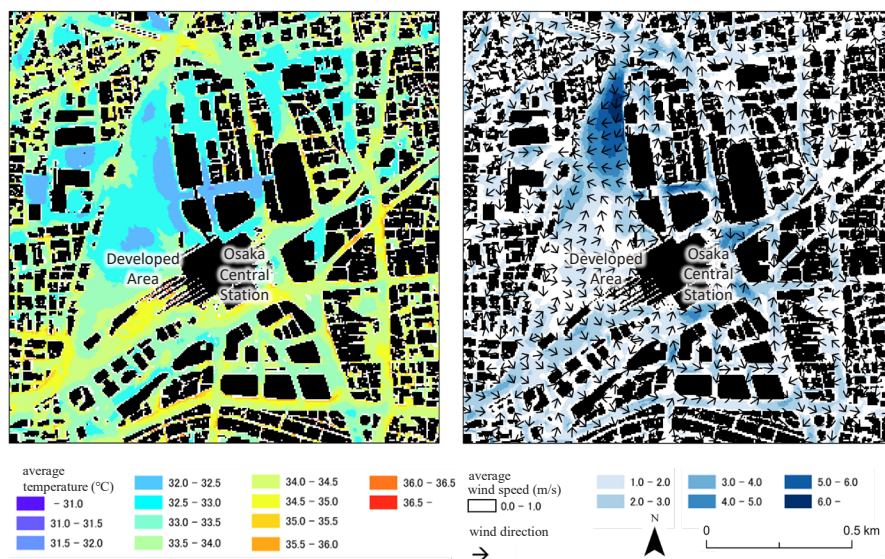


Figure 5. Temperature and wind distribution in the Osaka central station area

3.2 Changes Climate Condition by Comparing Current and After Development Simulation Results

Figure 6 shows the simulation results of the temperature and wind distribution in the Osaka central station area. Compared with the current condition, a lower range of 2.0 °C to 1.0 °C was confirmed in the developed area, and the temperatures are lower than 32.0 °C. In particular, the temperatures of the center of the developed area, where the new green spaces are to be created, and its surroundings are 31.0 - 32.0 °C. The wind speeds decreased by more than 2.0 m/s in the northern part developed area and increased in the southern part. Small wind turbulence caused by the newly constructed buildings was observed at several locations, and wind speeds were seen lower compared current situation. Looking at the area around developed area, temperatures in the eastern area were lower than 32.0°C in some places, which is thought to be due to the cool valley winds that were 1.0 - 2.0 m/s higher than the current conditions from the developed area and carried to the east side of the area. In addition, a lower range of 0.5°C to 1.0 °C compared to the current condition was spread to the north side. In the western area, the cool breeze from the developed area can be seen to have lowered the temperature. This is presumably due to the sequence between the green space at the foot of the Umeda Sky Building and the newly developed green space. In the south side area, a lower range of 1.0°C to 2.0 °C compared to the current condition was also spread. On the other hand, some temperature increases or were observed. In the green areas on the west side of the Umeda Sky Building, a higher range of 0.5 °C to 1.0 °C was observed compared to the current condition. In addition, temperatures between 33.5 and 36.0°C were relatively high on the track of Osaka central station on the west side and on the north side Hankyu Osaka Umeda station, and the intersection of the east side of Hankyu Osaka Umeda station.

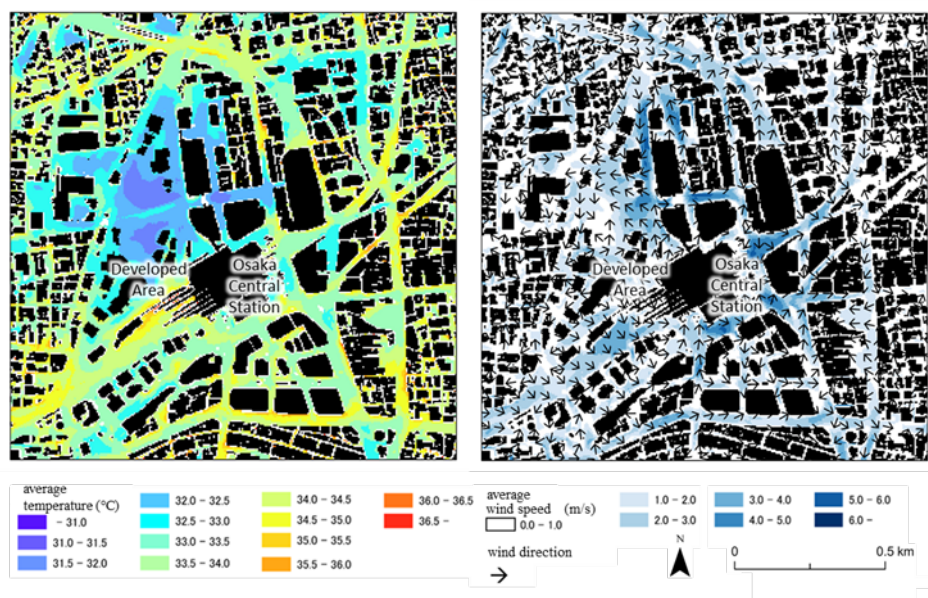


Figure 6. Temperature and wind distribution in the Osaka central station area after development

4. CONCLUSION

It was found that the implementation of the Grand Green Project further expanded the relatively cool temperature area within the developed area. On the west side of the developed area, the effect of mitigating the high temperature and lowering the temperature was enhanced because the newly developed green space was sequenced with the current green space. On the east side of the developed area, the temperatures were also lower than the current condition because the wind turbulence caused by the emergence of buildings and the lower temperatures in the developed area brought cooler and stronger wind speeds than the current conditions. In addition, the lower temperature as compared to the current condition was also spread to the area on the south side. In this project area, many utilizations and activities are expected to expand in the future. Therefore, mitigation and adaptation to urban warming is essential. This study revealed that the project will improve the thermal environment, with the development district having a temperature range equivalent to that of a parks or green spaces in Osaka City, and further visualized the results of the project. In the future, these results help in understanding the current situation and issue from the perspective of climate in urban planning or landscape planning.

ACKNOWLEDGMENTS

This study was supported by Grant-in-Aid for Young Scientists (21K14873). And, we appreciate financial supports from the Nippon Life Insurance Foundation. Numerical calculations were performed using the Earth Simulator with support from the Japan Agency for Marine-Earth Science and Technology (JAMSTEC).

REFERENCES

- Chao, R., Tejo, S., Sanda, L., Hung, L., Bert, H., Bert, H., Sebastian, K., Rene, B., and Lutz, K. (2012). Urban Climate Map System for Dutch spatial planning, *International journal of Applied Earth Observation and Geoinformation*, 18, 207-221
- Inoue, K., Tanaka, K., Tanaka, T., Matsuo, K. and Yokoyama, M. (2020). A study on the summer outdoor temperature distribution in the urban central area of Hiroshima Delta -Analysis of factors for forming temperature distribution and extraction of areas for promoting heat mitigation measures, *Journal of the City Planning Institute of Japan*, 55(3), 931-938.
- Kitao, N., Moriyama, M., Tanaka, T., and Takebayashi, H. (2010). Analysis of urban heat island phenomenon in Osaka region using WRF model -To estimate the effects of the urbanization using the concept of potential natural vegetation, *AIJ Journal of Environmental Engineering*, 75(651), 465-471.
- Liqing, Z., Chao, Y., (2023). Multi-scale climate-sensitive planning framework to mitigate urban heat island effect: A case study in Singapore, *Urban Climate*, 49, 101451.
- Matsuo, K. and Tanaka, T. (2019). 16. Analysis of spatial and temporal distribution patterns of temperatures in urban and rural areas: Making urban environmental climate maps for supporting urban environmental planning and management in Hiroshima, *Sustainable Cities and Society*, 47.
- Noguchi, S., Tanaka, T. and Sadohara, S. (2014). Analysis on the factors of summer temperature in the basin city -Measurement results and analysis by GIS-, *AIJ Journal of Technology and Design*, 20(46), 1029-1034.
- Sasaki, Y., Matsuo, K., Yokoyama, M., Sasaki, M., Tanaka, T., and Sadohara, S. (2018). Sea breeze effect mapping for mitigating summer urban warming: For making urban environmental climate map of Yokohama and its surrounding area, *Urban Climate*, 24, 529-550.
- Takebayashi, H. and Moriyama, M. (2005). Urban heat island phenomena influenced by sea breeze, *AIJ Journal of Technology and Design*, 11(21), 199-292.
- Yamasaki, J., Masubuchi, M., Iizuka, S., Yoshida, T., Nitani, R., Manabe, R., and Murayama, A. (2022). Thermal Environment Simulation for Urban Center Neighborhood by Using 3D City Model of Project PLATEAU: Toward Heat Adaptation in Community Planning, *Papers on Environmental Information Science* 36.

EMISSIONS TRACKING CONTROL OPTIMIZATION TO SUPPORT SUSTAINABLE CONSTRUCTION IN ROAD CONSTRUCTION PROJECTS

Phattadon Khathawatcharakun¹, Charinee Limsawasd², and Nathee Athigakunagorn³

1) Ph.D. Student, Department of Civil Engineering, Faculty of Engineering, Chulalongkorn University, Bangkok 10330, Thailand. Email: phattadon.kha@gmail.com

2) Ph.D., Assoc. Prof., Department of Civil Engineering, Faculty of Engineering, Chulalongkorn University, Bangkok 10330, Thailand. Email: charinee.l@chula.ac.th

3) Ph.D., Assoc. Prof., Department of Civil Engineering, Faculty of Engineering at Kamphaeng Saen, Kasetsart University, Nakhon Pathom 73140, Thailand. Email: nathee.a@ku.th

Abstract: Utilizing green contracting is a prominent technique to advocate sustainable construction in reducing CO₂ emissions from nonroad heavy construction equipment. Although sustainable equipment regulations have established the standard for controlling emissions from equipment, it still mostly executes in the preconstruction phase. However, a method to control emissions during the construction phase to adhere to the green contracting requirements has not been fully developed. Therefore, there is a pressing need for new research to develop a tracking support and control system for monitoring emissions during the construction phase. This paper presented a tracking control optimization model with the capability to identify the potential key date(s) for monitoring the contractor's green performance to secure the onsite emissions within the terms of the contract agreement. The tracking control model is implemented based on the concept of earned value management for estimating emissions variation and predicting emissions toward project completion. The model is applied to a hypothetical example of a road construction project with an expected result presenting optimal solutions of the emission-tracking date that enables a suggestion for improving sustainable options on the construction equipment fleet. The proposed optimization model should prove useful as a sustainable tracking and control mechanism facilitating project owners in identifying sustainable key date(s) for monitoring the emissions to assure the effectiveness of green contract implementation.

Keywords: CO₂ emission, Optimization, Earned value management, Road construction projects.

1. INTRODUCTION

According to the Federal Office for the Environment (FOEN), the construction sector is the highest diesel consumer, with approximately 40% of the total diesel consumed in the nonroad sector, especially nonroad heavy construction equipment. Importantly, the use of diesel also affects the environment, and it is an essential cause of greenhouse gas emissions. The equipment are the main sources of air pollutants including carbon oxides (CO and CO₂), hydrocarbons (HC), nitrogen oxides (NO_x) and particulate matter (PM). FOEN (2015) reported that construction equipment is the most polluting source of greenhouse gas emissions into the atmosphere compared to all nonroad sectors (34% of nonroad emissions). These emissions can cause a variety of health effects, such as, asthma, lung cancer, and respiratory disease (Kenny & Priyadarshini, 2020).

The stakeholders, including the government, private sector, trade organizations, and others involved in the construction industry have been conscious of the need to reduce greenhouse gas emissions and promote clean diesel technology, such as Diesel Particulate Filter (DPF), Catalyzed Converter/Muffler (CCM) and CMX Catalyst Muffler (EPA, 2005; NEDC, 2011). For example, the Northeast Diesel Collaborative (NEDC) work group adopted the model construction contract and specifications to promote the use of emission controls in the construction industry. Some projects incorporate sustainable equipment regulations certified by the United States Environmental Protection Agency (US EPA) in the contract specification to reduce and control emissions from nonroad heavy construction equipment. However, it is still challenging to manage and control the emissions of the construction operation throughout the preconstruction and construction phases. Although the current emission reduction regulation has a great benefit on environment as the equipment control standard (Shao, 2016). However, it still unattractive to contractors in adopting the equipment standard in their projects in terms of the financial perspective.

To achieve the goal of air quality improvement in the construction sector, Huang and Fan (2022b) proposed a responsibility-sharing subsidy policy that helps the government determine subsidy value and emission limits, as well as developed the decision-support tool for construction equipment replacement and retrofitting strategies. Patcharachavalit et al. (2023) developed a decision-support optimization model for selecting a sustainable equipment fleet by considering an availability of equipment investment budget and construction time.

The subsidy and incentive policies have been used for motivating the contractor in many studies (Huang & Fan, 2022a; Huang & Fan, 2022b; Metham & Benjaoran, 2018). Nevertheless, the implementation lacks a method for monitoring and controlling emissions from contractor operations during the construction phase. Thus, to address this problem, this study aims to introduce a tracking control optimization model to identify the potential key date(s) for monitoring the contractor's green performance to secure the emissions during the construction

phase. Moreover, the proposed tracking control optimization model can find the key date(s) for improving the sustainable option on the construction equipment fleet for emissions reduction before exceeding the predetermined emission limit.

2. METHOD

The tracking control optimization model to identify the potential key date(s) for securing the emissions within the terms of the contract agreement consists of five modules: (1) determining project performance baseline; (2) monitoring contractor's green performance; (3) predicting contractor's green performance at completion; (4) improving sustainable option; and (5) developing optimization model. The details of each module are provided in the following subsections:

2.1 Determining Project Performance Baseline

The project performance baseline during construction is essential for owners or controllers in monitoring the CO₂ emissions due to the impact of the different uses of equipment. It is calculated as the planned CO₂ emissions from construction equipment usage according to the construction method and project scheduling incorporating with the CO₂ emission reduction goal. The project performance baseline will be used to control the predicted of CO₂ emissions at completion and ensure if it is within the limit. In this study, the budgeted CO₂ of work scheduled (BCO₂WS) based on earned value management theory was applied as the project performance baseline. The CO₂ emissions factor is defined in kgCO₂/liter based on the fuel consumption usage (EPA, 2018), as shown in Equation (1).

$$BCO_2WS = PWH \times PFR \times EF \quad (1)$$

where BCO₂WS = budgeted CO₂ of work scheduled (kgCO₂); PWH = planned work hour (hr); PFR = planned fuel consumption rate (liter/hr); and EF = CO₂ emission factor (kgCO₂/liter).

2.2 Monitoring Contractor's Green Performance

This step determines the contractor's performance using the concept of earned value analysis. The CO₂ emission performance index (CO₂PI) is applied to represent the actual green performance from contractor's operations, calculated as the ratio of the budgeted CO₂ of work performed (BCO₂WP) and the actual CO₂ of work performed (ACO₂WP) by using Equations (2) - (4), respectively. There are three cases for calculating the CO₂ emission performance index (CO₂PI): (1) CO₂PI is less than 1, indicating that actual CO₂ emissions are greater than the CO₂ emission budget; (2) CO₂PI greater than 1, indicating actual CO₂ emission less than the CO₂ emission budget; and (3) CO₂PI equal to 1, indicating actual CO₂ emission equal to the CO₂ emission budget.

$$BCO_2WP = AWH \times PFR \times EF \quad (2)$$

$$ACO_2WP = AWH \times AFR \times EF \quad (3)$$

$$CO_2PI = BCO_2WP / ACO_2WP \quad (4)$$

where BCO₂WP = budgeted CO₂ of work performed (kgCO₂); AWH = actual work hour (hr); ACO₂WP = actual CO₂ of work performed (kgCO₂); AFR = actual fuel consumption rate (liter/hr); and CO₂PI = CO₂ emission performance index.

2.3 Predicting Contractor's Green Performance at Completion

To predict the CO₂ emission at project completion, the owners or controllers need to measure the current states of CO₂ emission at a point of time based on the contractor's green performance, and then forecast the at-completion emission based on the current CO₂PI (see Equations (5) – (6)).

$$CO_2BAC = \sum BCO_2WS \quad (5)$$

$$ECO_2AC = CO_2BAC / CO_2PI \quad (6)$$

where CO₂BAC = budgeted CO₂ emission at completion (kgCO₂); and ECO₂AC = estimated CO₂ at completion (kgCO₂).

2.4 Improving Sustainable Options

The purpose of this module is to help the owners or controllers to estimate CO₂ emissions under a suggestion for improving sustainable options on the construction equipment fleet for the contractor towards

emission mitigation. The sustainable option will be applied to the fleet right after a tracking date in case that ECO_2AC is higher than the sum of BCO_2WS . Notably, the percentage of CO_2 emission reduction was assigned depending on the implementation of sustainable options. Equation (7) presents this calculation step:

$$CO_2SO = ECO_2AC \times RE \quad (7)$$

where CO_2SO = CO_2 emissions after sustainable option implementation; and RE = percentage of CO_2 emissions reduction from sustainable improvement.

2.5 Developing Optimization Model

As aforementioned, the main objective in this study is to optimize potential key date(s) for monitoring the contractor's green performance in order to secure the emission during the construction phase, subject to the restriction of the estimated CO_2 emission at completion. The optimization model is proposed to help the owners or controllers find the optimal key date(s) for monitoring CO_2 emissions, in which the amount of CO_2 emission of the entire equipment fleet can be reduced by the sustainable option strategies application, as shown in Figure 1.

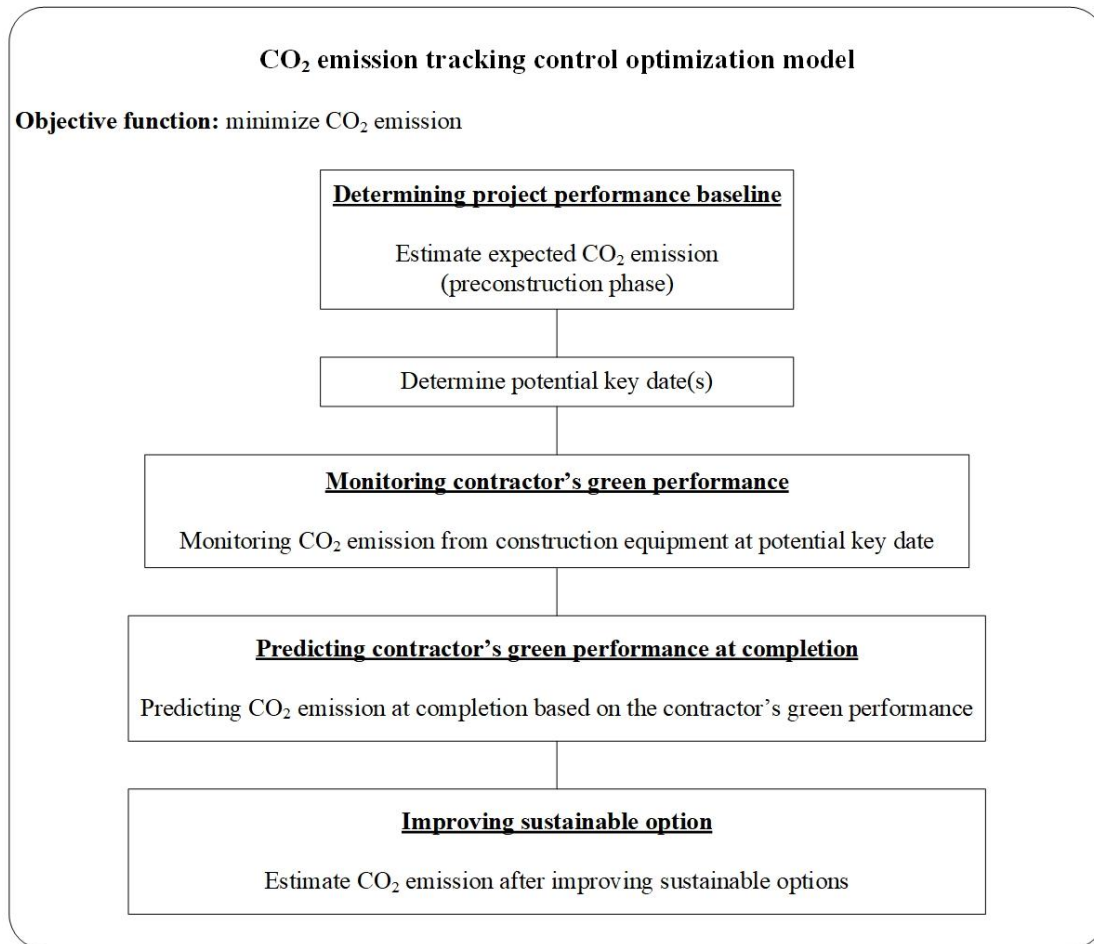


Figure 1. CO_2 emission tracking control optimization model

3. APPLICATION EXAMPLE AND PRELIMINARY RESULTS

This paper exemplified an application example with six equipment types working during a 10-day period, as shown in Table 1, to demonstrate the capabilities of the CO_2 emission tracking control optimization model in identifying the potential key date(s). The key date(s) was defined as decision variables by which date the owners or controllers should monitor the CO_2 emissions from the equipment fleet and applying the sustainable options to reduce CO_2 emissions. This can prevent the onsite emissions from exceeding the CO_2 emission baseline. In this study, the actual CO_2 emission was assumed with an additional 10% from the planned CO_2 emission and a 20% emission reduction due to the improvement in the construction equipment fleet after using sustainable options. It was also assumed that if the CO_2 emissions exceeded the baseline, such types of equipment working on tracking date must be improved. Notably, for the construction equipment, the sustainable option was installed only once on the next working day.

Table 1. Equipment usage during 10-days period

Equipment type	Number of pieces of equipment									
	Day									
	1	2	3	4	5	6	7	8	9	10
Excavator	2	2	2	2	2	2	2	2	2	2
Truck	-	3	1	3	1	1	1	1	1	1
Grader	1	-	1	1	-	1	1	1	1	1
Rubber-tired roller	-	2	1	2	1	1	1	1	1	1
Steel-wheeled roller	-	-	-	1	-	1	1	1	1	1
Vibrating roller	-	-	-	-	2	-	-	-	-	-

Figure 2 demonstrates the potential key date(s) under the objective of minimizing CO₂ emissions. After investigation, it reveals that the model will identify the potential key date(s) when new equipment types(s) were used. Comparing between Day 2 and Day 3, more potential key date was set on Day 2 due to different use of equipment from the previous key date (truck and rubber-tired roller). This is because the same equipment types were still used on Day 3 with no effect on CO₂ emission reduction. Furthermore, Day 5 could not be identified as a potential date. It is noticeable that no other equipment type was applied afterwards (see Days 6 - 10) that can cause a reduction in CO₂ emissions.

Equipment type	Number of pieces of equipment									
	Day									
	1	2	3	4	5	6	7	8	9	10
Excavator	2	2	2	2	2	2	2	2	2	2
Truck	-	3	1	3	1	1	1	1	1	1
Grader	1	-	1	1	-	1	1	1	1	1
Rubber-tired roller	-	2	1	2	1	1	1	1	1	1
Steel-wheeled roller	-	-	-	1	-	1	1	1	1	1
Vibrating roller	-	-	-	-	2	-	-	-	-	-

Figure 2. Potential key date(s)

Table 2 illustrates the preliminary conclusion for the different potential key date(s). Alternative A shows more promising key date(s) in reducing CO₂ emissions when compared to Alternative B. The excavator and grader working from the first day can substantially reduce emissions if applying the sustainable options early. For the small-scale project as the application example, CO₂SO can basically reduce at least 8% from BCO₂WS and can be different around 400 kg of CO₂ between both key date alternatives. The magnitude of impact would definitely be gigantic on a larger scale project with a longer construction duration. To sum up at this stage, it tends to be more beneficial to monitor emissions early at the first day of such equipment type employed.

Table 2. CO₂ emission of different potential key date(s)

Alternative	Tracking status										BCO ₂ WS (kg)	CO ₂ SO (kg)
	Day											
	1	2	3	4	5	6	7	8	9	10		
A	✓	✓	x	✓	x	x	x	x	x	x	30,199	27,750
B	x	✓	x	✓	x	x	x	x	x	x		

Remark: ✓ = tracking; × = not tracking

5. CONCLUSIONS

In this study, the conceptual framework of an emission tracking control optimization model is introduced to help the project owners in controlling emissions from equipment during the construction phase. The model was aimed to identify the potential key date(s) and simultaneously optimize for monitoring the contractor's green performance from the construction equipment fleet with the objective of minimizing CO₂ emissions.

The application example shows that the emission tracking control model can reach emission mitigation

and secure CO₂ emissions within the terms of the contract agreement. The model can suggest the date for monitoring emissions from the viewpoint of owners or controllers to prevent emissions from exceeding the baseline. From the contractor's perspective, the date for improving sustainable options can be obtained when monitoring the contractor's green performance is implemented.

However, at this beginning stage, other comprehensive and detailed CO₂ emission calculations should be further analyzed to investigate the impact of different potential key date(s). For example, the actual CO₂ emissions of each equipment type should be different and more realistic. Nevertheless, the improvement of the construction equipment fleet in the current model is still limited, as it is allowed to change all pieces of equipment when CO₂ emissions exceed the baseline on the tracking date. In addition, the further study and information are still required to improve the model performance and efficiency.

ACKNOWLEDGMENTS

The authors would like to express our special thank to the Expressway Authority of Thailand for their valuable contribution to this study during interviews conduct and data collection stage.

REFERENCES

- EPA. (2005). *National Clean Diesel Campaign: Innovative Strategies for Cleaner Air*. Retrieved from EPA website: <https://nepis.epa.gov/Exe/ZyPURL.cgi?Dockey=P10009B4.TXT>
- EPA. (2018). *Emission factors for greenhouse gas inventories*. Retrieved from EPA website: https://www.epa.gov/sites/default/files/2018-03/documents/emission-factors_mar_2018_0.pdf
- FOEN. (2015). *Non-road energy consumption and pollutant emissions*. Retrieved from FOEN website: https://www.bafu.admin.ch/dam/bafu/en/dokumente/luft/umwelt-wissen/energieverbrauchundschadstoffemissionendesnon-road-sektors.pdf.download.pdf/non-road_energy_consumptionandpollutantemissions.pdf
- Huang, Z. and Fan, H. (2022a). A novel quantitative model for determining subsidy levels to accelerate the replacement of in-use construction equipment for emissions reduction, *Journal of Management in Engineering*, 38 (2), 04021100.
- Huang, Z. and Fan, H. (2022b). Responsibility-sharing subsidy policy for reducing diesel emissions from in-use off-road construction equipment, *Applied Energy*, 320, 119301.
- Kenny, C. and Priyadarshini, A. (2020). Do greenhouse gases impact our respiratory system? A study of the effect of greenhouse gas emissions on respiratory disease related mortality in Ireland,
- Metham, M. and Benjaoran, V. (2018). Incentive contracts for road construction to reduce greenhouse gas emissions, *Engineering Journal*, 22 (5), 105-122.
- NEDC. (2011). *NEDC: Diesel Emission Controls in Construction Projects-Model Construction Contract Specifications, December 2010*. Retrieved from NEDC website: <https://www.epa.gov/sites/default/files/2015-09/documents/nedc-model-contract-sepcification.pdf>
- Patcharachavalit, N., Limsawasd, C. and Athigakunagorn, N. (2023). Multiobjective Optimization for Improving Sustainable Equipment Options in Road Construction Projects, *Journal of Construction Engineering and Management*, 149 (1), 04022160.
- Shao, Z. (2016). An emissions inventory for agricultural tractors and construction equipment in India, *The International Council on Clean Transportation (ICCT)*.

GREEN INFRASTRUCTURE PLANNING WITH POPULATION DECREASING FOR ADAPTING TO CLIMATE CHANGE BY USING GIS AND NUMERICAL MODELS: CASE OF KURE CITY IN HIROSHIMA PREFECTURE

Takahiro Tanaka¹, Shinji Hirai², Ryota Araki², Riki Yamaga², Shota Tamura³, Makoto Yokoyama⁴, Kaoru Matsuo⁵, and Toru Sugiyama⁶

1) Professor, Department of Architecture, Graduate School of Advanced Science and Engineering, Hiroshima University, Higashi-Hiroshima, Japan. Email: ttanaka@hiroshima-u.ac.jp

2) Graduate Student, Department of Architecture, Graduate School of Advanced Science and Engineering, Hiroshima University, Higashi-Hiroshima, Japan.

3) Assistant Professor, Department of Architecture, Graduate School of Advanced Science and Engineering, Hiroshima University, Higashi-Hiroshima, Japan.

4) Lecturer, Faculty of Urban Management, Fukuyama City University, Fukuyama, Japan.

5) Assistant Professor, Department of Environmental Sciences and Technology, Graduate School of Agriculture, Osaka Metropolitan University, Sakai, Japan.

6) Japan Agency for Marine-Earth Science and Technology

Abstract: Due to climate change, many Japanese cities are experiencing severe flooding and severe summer thermal environments in the outdoor spaces. Under such circumstances, the use of green infrastructure is considered to be one of the effective options to adapt to climate change (mitigation of flood damage and severe thermal environment). On the other hand, many provincial cities in Japan are facing a declining population and an increasing amount of low-used lands and un-used lands, which will require land use re-arranging in the near future. This increase in low-used and un-used lands can be considered an opportunity to introduce green infrastructure. Therefore, in this study, authors utilized GIS and numerical simulation models to identify suitable sites for effective green infrastructure building by evaluating multiple scenarios. This study shows that the introduction of G.I. into underutilized land has some positive effects on both urban flood control and the improvement of the thermal environment.

Keywords: Green Infrastructure, Climate Change, Flood Control, Urban Warming, Population Decreasing

1. INTRODUCTION

With climate change on the rise, green infrastructure must be introduced into urban spaces because of its various benefits, such as flood control and severe thermal environment mitigation (Matthews et al., 2015; Matsuo & Tanaka, 2019). Therefore, it is necessary to consider how to introduce green infrastructure (G.I.) in actual urban spaces, but the major challenge is to supply sufficient places for its introduction. On the other hand, in recent years, many local cities have seen a marked increase in vacant houses, vacant lots, and other underutilized land as a result of population decline and aging, pointing to the need for urban contraction in terms of safety and convenience of living (Sakamoto et al., 2017; Tamura et al., 2023). In such cities with declining populations, we considered it effective to utilize underutilized land as a place to introduce G.I. Therefore, the purpose of this report is to understand the effects of G.I. introduction on flood control and improvement of thermal environment in low-underutilized lands by using numerical analysis, and to identify areas where G.I. introduction is highly effective.

The study area covered the Central District of Kure City, Hiroshima Prefecture. In the district, the following phenomena have been observed in recent years: (1) a rapid increase in the number of vacant houses and land, mainly in the sloping urban areas, due to population decline; (2) an increase in flood damage; and (3) a rise in average temperatures.

2. SCENARIO DESIGN FOR G.I. INTRODUCTION







Vacant houses, vacant lots, and parking lots (monthly parking lots and coin-operated parking lots) were defined as "low-underutilized land. Using residential map data, residential address number control maps, etc., sites with an average area for each type of low-underutilized land in the subject area were extracted, and a G.I. introduction model was created for these sites with reference to previous cases. In addition, three G.I. introduction scenarios were developed for use in the scenario evaluation. The specifics are as follows:

(Scenario 1) Scenario that does not assume the demolition of vacant houses (no demolition): Vacant buildings, vacant sites, vacant land, and parking lots are subject to G.I. introduction, without assuming the demolition of vacant houses.

(Scenario 2) Scenario assuming demolition of vacant houses (with demolition): Vacant houses are assumed to be demolished, and the current building area is also assumed to be target to G.I. introduction.

(Scenario 3) Scenario assuming double the current ratio of vacant houses (double the current ratio of vacant houses): G.I. introduction is conducted assuming a case in which the ratio of vacant houses in the target land becomes double the current ratio in the future. The vacant houses are assumed to be demolished.

Table 1. Image of green infrastructure installed

	Vacant House	Vacant Land	Parking Lot
Current			
Green Infrastructure Installed			

3. SCENARIO EVALUATION FOR THE FLOOD CONTROL EFFECTS

3.1 Numerical Model for Flood

A numerical analysis model was developed to predict the flood control effects of the G.I. implementation scenario. The model was constructed using InfoWorks ICM, combining surface data (land use and river information) and subsurface data (boreholes and culverts) to reproduce water flows such as rainwater infiltration and surface runoff at the target site. Numerical analysis was performed on this model using the rainfall data of Heavy Rain in July 2018 as the target rainfall. The results of this numerical analysis (inundation area) were confirmed to generally overlap with the actual damage area, and this model was used in the subsequent analysis.

3.2 Scenario Evaluation

The values of inundated area and total inundation volume for each scenario are shown in Figure 1. No significant effect on inundated area can be expected for scenarios (1) no demolition and (2) with demolition. However, a certain effect can be seen for the total inundation volume, and the effect is relatively large especially for the case of “(2) with demolition”. Comparing the results of “(1) no demolition” (i.e., installing rainwater harvesting facilities) and “(2) with demolition” (i.e., installing G.I. with infiltration functions) for vacant buildings, a difference in effectiveness can be seen, indicating that the storage function alone is not expected to have a significant effect. On the other hand, a significant effect is seen in “(3) double the current ratio of vacant houses”. Proactive introduction of G.I.s, especially in areas where population is expected to decline in the future, is considered effective.

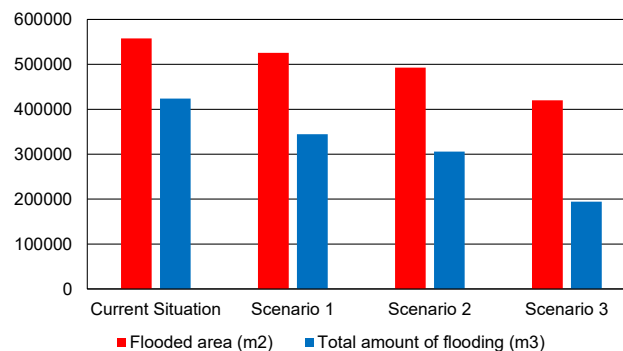


Figure 1. Flood control effect for each scenario

3.3 Identification of G.I.-Introduced Areas with High Flood Control Effectiveness

In order to identify areas where G.I. introduction is highly effective, the target area was divided into 10 catchment areas, and scenarios were created for each catchment area with G.I. introduction. Numerical analysis was then conducted for each scenario to identify catchment areas with high G.I. introduction effects. The catchment areas were compared by defining the “G.I. introduction effect (flood control)” as the reduction in inundated area divided by the area of G.I. introduction in each catchment area. Figure 2 shows the results. The areas with the highest introduction effect can be seen on the north and west slopes of the target district.

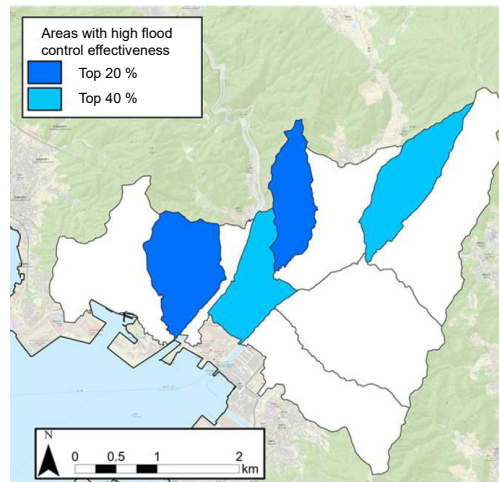


Figure 2. Area with high flood control effectiveness

4. SCENARIO EVALUATION FOR THE SEVERE THERMAL ENVIRONMENT MITIGATION EFFECTS

4.1 Numerical Model for Urban Climate

To predict the effect of G.I. introduction on the thermal environment improvement, an MSSG model was set up in a supercomputer (Earth Simulator) owned by JAMSTEC (Japan Agency for Marine-Earth Science and Technology). The numerical model was set up using GIS data on land use, building height, elevation, and tree location to reproduce the distribution of the thermal and wind environment at the target site (spatial resolution of 5 m). Comparison of the results of the numerical calculation with the results of the temperature measurement survey conducted on August 1, 2021 showed a high correlation between the two (correlation coefficient of 0.86), and we considered that the temperature distribution trend at the subject site was generally reproduced. Therefore, we decided to use this model in the following analysis.

4.2 Scenario Evaluation

Table 2 shows the average temperatures of the residential areas across the target sites for each scenario. Even for “(3) double the current ratio of vacant houses,” not much effect is observed for the entire target area. On the other hand, seeing the distribution of temperature change for “(2) with demolition” (Figure 3), areas where the temperature decreases by more than -0.5°C can be seen in various locations. Therefore, there are some areas where the effect is locally significant. In particular, the temperature decrease is large on the northern and eastern slopes of the subject site, and this is thought to be due not only to G.I.-Introduction, but also to the ventilation environment improvement effect of the entire target area due to the removal of vacant houses.

Table 2. Scenarios evaluations

Scenarios	Average Temperature (degree C.)	Temperature Change (degree C.)
Current Situation	31.92	-
Scenario 1 (no demolition)	31.85	-0.07
Scenario 2 (with demolition)	31.79	-0.13
Scenario 3 (double the current ratio of vacant houses)	31.70	-0.22

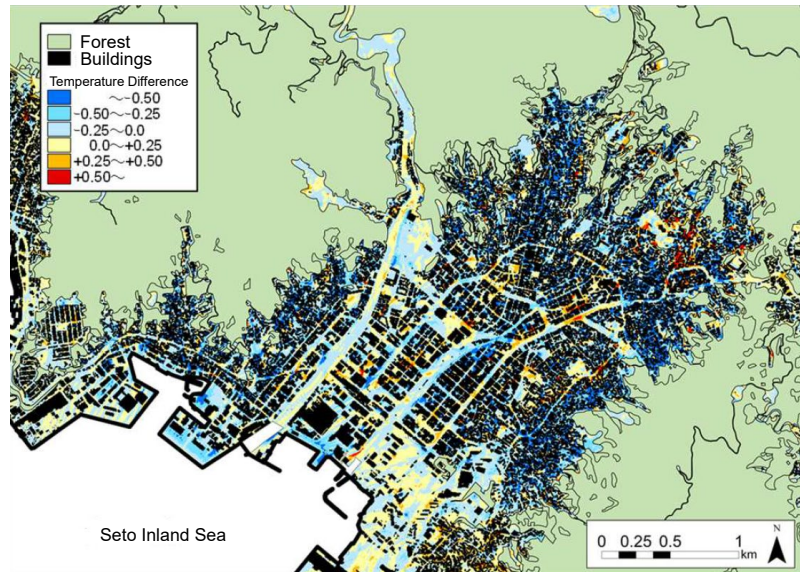


Figure 3. Temperature differences between “Scenario 2” and “Current Situation” (Unit: degree C.)
([Scenario 2] – [Current Situation])

4.3 Identification of G.I.-Introduced Areas with High Thermal Environment Mitigation Effectiveness

In order to identify areas where the G.I. introduction effect is significant, we defined “G.I. introduction effect (thermal environment)” as the temperature change (average value) in each administrative district (100 districts in total) in the “(2) with demolition” scenario divided by the G.I. introduction area, and compared the administrative districts. Figure 4 shows the results. High introduction effect is obtained in the northern and western slopes, especially in the middle of the slope (elevation 30-60 m) where the current building density is higher.

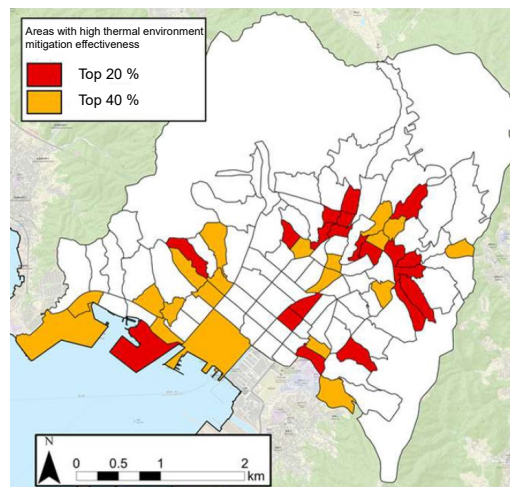


Figure 4. Area with high thermal environment mitigation effectiveness

5. EXTRACTION OF AREAS WHERE BOTH OF THE TWO EFFECTS ARE SIGNIFICANT

Overlaying the areas with large G.I. introduction effects extracted in Chapters 3 and 4, areas with large effects in terms of both flood control and severe thermal environment mitigation (G.I. introduction priority areas) were extracted. This is the G.I. introduction priority area map (Figure 5). Priority areas for GI introduction are often found in sloping urban areas with a high rate of population decline. This may be due to the fact that sloping urban areas are densely built, poorly ventilated, and have weak infrastructure such as sewage pipes.

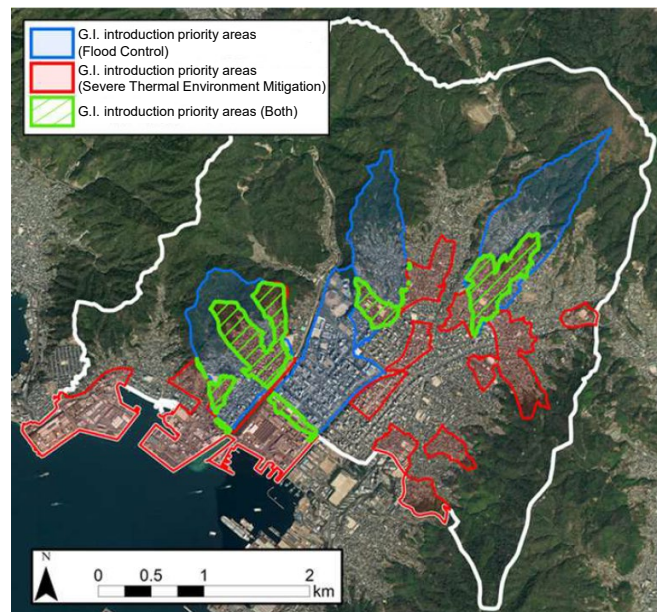


Figure 5. Area with high thermal environment mitigation effectiveness

6. SUMMARY

This study shows that the introduction of G.I. into underutilized land has some positive effects on both urban flood control and the improvement of the thermal environment. The study also indicated areas where the effect is significant. In sloping urban areas where population is expected to decline in the future, it is desirable to actively introduce G.I. to underutilized land.

ACKNOWLEDGMENTS

This work was supported by JSPS KAKENHI Grant Numbers 20H02331, 22K18847. Numerical calculations with the MSSG model were performed using the Earth Simulator at JAMSTEC (Japan Agency for Marine-Earth Science and Technology). And we would like to thank Kure Satellite Office of Hiroshima University, for their cooperation in conducting this study.

REFERENCES

- Matthews, T., Lo, A. Y., Byrne, J. A. (2015). Reconceptualizing green infrastructure for climate change adaptation: Barriers to adoption and drivers for uptake by spatial planners, *Landscape and Urban Planning*, 138, 155-163.
- Matsuo, K., Tanaka, T. (2019). Analysis of spatial and temporal distribution patterns of temperatures in urban and rural areas: Making urban environmental climate maps for supporting urban environmental planning and management in Hiroshima, *Sustainable Cities and Society*, 47, 101419.
- Sakamoto, K., Iida, A., Yokohari, M. (2017). Spatial emerging patterns of vacant land in a Japanese city experiencing urban shrinkage: a case study of Tottori City, *Urban and Regional Planning Review*, 4, 111-128.
- Tamura, S., Kajie, K., Tanaka, T. (2023). Factors influencing the occurrence of vacant houses in a small provincial town in Japan, *Applied Spatial Analysis and Policy*, (<https://doi.org/10.1007/s12061-023-09517-y>)

COMPARATIVE ANALYSES OF SIMULATION AND MEASUREMENT DATA OF BUILDINGS ENERGY CONSUMPTION USING TYPICAL WEATHER DATA AND REAL WEATHER DATA IN HOT-HUMID CLIMATE

Sarin Pinich¹, Terdsak Tachakitkachorn², Atch Sreshthaputra³

1) Dr.techn., Department of Architecture, Faculty of Architecture, Chulalongkorn University, Bangkok, Thailand. Email: sarin.pi@chula.ac.th

2) Ph.D., Asst. Prof., Architecture for Creative Community Research Unit, Department of Architecture, Faculty of Architecture, Chulalongkorn University, Bangkok, Thailand. Email: terdsak.t@chula.ac.th

3) Ph.D., Assoc. Prof., Department of Architecture, Faculty of Architecture, Chulalongkorn University, Bangkok, Thailand. Email: atch.s@chula.ac.th

Abstract: For decades, improving energy efficiency and performance of buildings has been a challenge. Nowadays, in order to predict the building's energy performance to support decision-making in the selection of design retrofit options, energy simulation tools have become very useful and well-known among designers and researchers. Great accuracy in the related input parameters is required to generate a dependable simulation model. Outdoor climate is one of the most affected parameters in the simulation results. This study aims to investigate the reliability of simulation in a hot and humid climate. A Thai construction located in Bangkok is selected as a case study. The method is to compare measured values of energy consumption with the same parameters calculated in the software using outdoor climate data from in situ measurement and typical outdoor climate data. The evaluation of the predictive performance of the simulation model using local climate data and data from the ASHRAE weather database will be presented.

Keywords: Energy simulation, Typical weather file, Buildings energy consumption, Hot-humid climate

1. INTRODUCTION

Building performance and energy efficiency improvements have been a challenge for decades. Simulation tools, such as dynamic building performance modeling software, are known to deploy the prediction of the whole energy consumption, the indoor thermal environment, and the amount of indoor heat gain to support decision-making in the selection of design options. Furthermore, building simulation issues today go beyond only building design to include building operation, diagnostics, and commissioning (Monetti et al., 2015). Concerns regarding a discrepancy between buildings' predicted and actual measured energy performance, known as 'performance gap' (Zero Carbon Hub, 2010; Menezes et al., 2011), are growing in the construction sector (Wilde, 2014). For many years, various studies have been conducted to find solutions to reduce this gap and increase the accuracy of the simulation models. According to previous research regarding the predicted and actual energy performance of non-domestic buildings (Menezes et al., 2011), the measured energy use can be up to 2.5 times greater than the expected energy use, which highlights the magnitude of this gap. There are various factors affecting the error between predicted and actual energy performance, such as occupancy behaviors, building material properties, local surroundings, and indoor and outdoor climate conditions (Sarna, Ferdyn-Grygierek, & Grygierek, 2022; Lam et al., 2014). The temperature difference between the two sides of the building envelope components directly affects the heat gain, making the outdoor weather data and indoor climate condition ones of the most important factors influencing the accuracy of the energy modeling performance (Kiesel, Vuckovic, & Mahdavi, 2013; Erbaa, Causonea, & Armani, 2017). In addition, although research regarding weather data inputs has been done in several places (for example, Crawley, Lawrie 2019; Erbaa, Causonea, & Armani, 2017; Kiesel, Vuckovic, & Mahdavi, 2013), hot and humid regions have received less attention from the related studies despite having a significant number of performance simulations conducted in the related research and design processes. In hot and humid regions, there has been some research conducted in the field of building performance simulation validation which concentrates on comparing fieldwork data to simulated data (Al-Tamimi, Fadzilb, 2010; Indana, Dinapradipta, & Samodra, 2020). However, the optimization-based calibration approach focusing on the weather data is a rarity. Hence, in this study, various simulations will be conducted with varied weather data inputs, both outdoor and indoor, under the hot-humid climate conditions (Bangkok, Thailand). The simulations' outcomes will be discussed. Moreover, a comparison of the simulation results with actual data on energy use will be discussed.

2. METHOD

2.1 Methodology

To achieve the purpose of this study, a simplified process for calibrating dynamic building energy models that can be used by both professionals and researchers is presented (Chong et al., 2021; Fabrizio & Monetti, 2015). The calibration in this paper will focus only on adjusting the inputs of climate condition data in order to reduce the performance gap by applying an optimization-based calibration approach (Monetti et al., 2015). Optimization

refers to the adjustment of parameters for a better match with the actual measured data when used in calibration. This study conducts the four steps of optimization-based calibration using climate factors. Firstly, a dynamic energy simulation tool is used to conduct the building energy evaluation. The model that is currently being defined is uncalibrated and is based on design data and typical boundary conditions. Secondly, preparing data for tuning, which is known as "pre-processing of the calibration," is performed in this stage. In this process, collected data and building model input data were analyzed. In this particular case, we focus only on the boundary condition factors, including indoor and outdoor weather data. For one of the simulation scenarios, a real weather file was created using in-situ monitoring meteorological data (such as outdoor dry bulb air, values of solar radiation, etc.). In addition, indoor environment monitoring data (i.e., indoor ambient temperature) is also analyzed to form another scenario. However, please note that in the common calibration process, sensitivity and uncertainty assessments should be conducted to account for the presence of various sources of uncertainty (Heo, 2011) while calibrating a building model. Due to the time limitation, sensitivity and uncertainty analyses are not within the scope of this study. Alternative configurations of input data (i.e., initial condition as well as indoor and outdoor climate) were considered in order to improve the predictive performance. These configurations are labeled Initial Model, Scenario 1, and Scenario 2 (see Table 1). To improve the predictive performance of the simulation, on-site measurement data, including indoor and outdoor, is proposed as an input for the optimized options. Lastly, post-processing of the optimization outcome is conducted to validate the calibrated building model's accuracy. Comparing the simulated scenarios to the initial model and to the actual measurement, the total consumption of the energy use (in kWh) of the generated data and the on-site monitoring data were calculated for comparison.

Table 1. Building performance simulation scenarios

Simulation scenarios	Indoor condition	Outdoor climate
Initial model	25°C	ASHRAE as typical data
1	25°C	On-site measurement data
2	On-site measurement data (actual room temperature)	On-site measurement data

2.2 Building Case Study Characteristics

The case study building is selected as an experimental room constructed in the parking lot area at the department of industrial design, Chulalongkorn University, Bangkok. The case study is a one-story building with dimensions of 2.30 meters in width, 5.40 meters in length, and 3.20 meters in height. The building envelope comprises three layers, including (1) fiber cement board with a thickness of 12 mm as an exterior layer, (2) glass wool (density 24 kg.m⁻³ with a k-value of 0.035 W.m⁻¹.oC⁻¹ with a thickness of 100 mm as a middle layer, and (3) gypsum board with a thickness of 9 mm (doubled layer) as an interior layer.

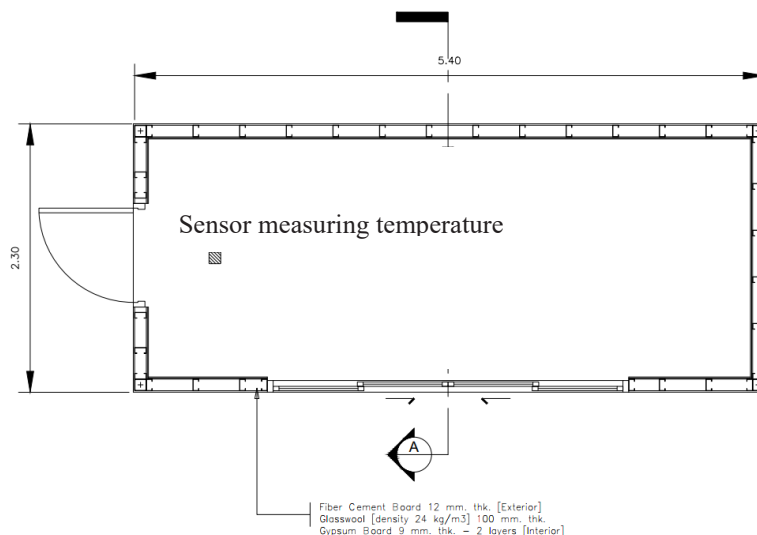


Figure 1. Case study building floor plan with the location of the sensor measuring indoor temperature

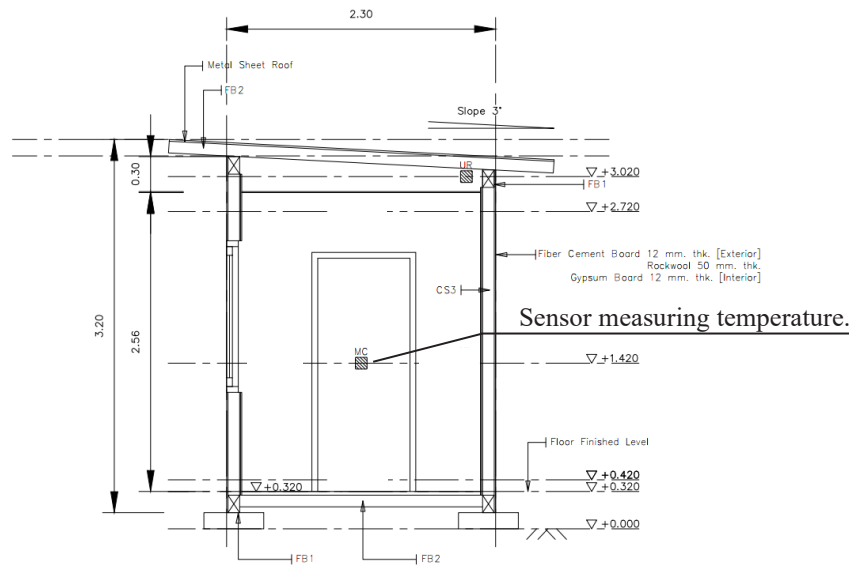


Figure 2. Case study building section with the location of the sensor measuring indoor temperature

2.3 Building Operation and Simulations Settings

The case study operation and the on-site measurements (i.e., outdoor and indoor temperature, AC electrical power consumption, and outdoor solar radiation) were conducted between March 14th, 2023, and March 26th, 2023. The air conditioning operates from 8:00 a.m. to 16:00 p.m. every day, with the temperature set at 25 °C. The properties of the building component materials correspond to the values of the actual material properties. The value of the air conditioning COP is 3.50. The conditions for all simulations are shown in Figure 3. The simulation software used in this study is TRNSYS with the TESS library, which is used to model the performance of transient systems commonly known for energy simulation (TESS, 2019). To determine how much electricity was used, the cooling sensible heat load of the AC (kWh) must be simulated. Using a COP of 3.5, the cooling sensible heat load is converted to AC electrical power consumption. The three simulation models are performed with different boundary conditions. Regarding the initial model, the outdoor boundary condition of the simulation is set using ASHRAE as typical climate data. Created in collaboration with White Box Technologies (WBT), IWEC2 weather files from ASHRAE are available instantly via the website (ASHRAE, n.d.) for individual purchase or in sets by nation or region. Simulation scenario 1 uses onsite measurement data as an outdoor climate condition. While the first two models use an indoor thermostat set point of 25 degrees Celsius as an indoor condition setting, the third model, labeled Simulation Scenario 2, uses on-site indoor monitoring data (i.e., indoor temperature) as an input for indoor condition. The location of the sensor is illustrated in Figure 1 and Figure 2.

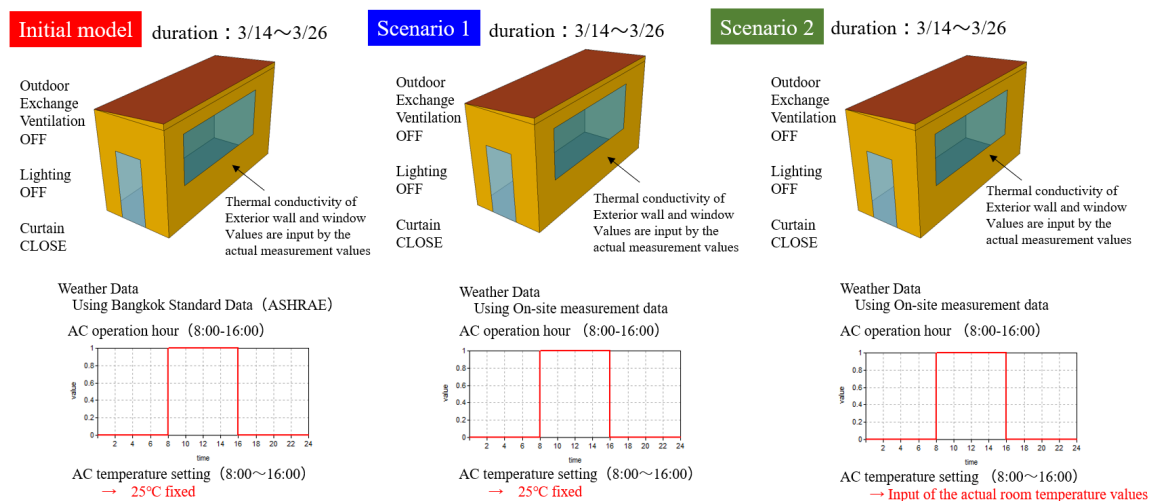


Figure 3. Conditions for the three simulation cases: initial model, scenario 1, and scenario 2.

3. RESULTS

The three simulation models (the initial model, scenario 1, and scenario 2) are conducted with different boundary conditions for indoor and outdoor. The simulation results presented as the AC electrical power consumption (kWh) accumulating the power used every day from March 14th to March 26th, 2022, are shown in Table 2 with the actual measurement of AC electrical power consumption (kWh). Overall, it can be clearly seen that using either the typical weather data or the in-situ outdoor climate data as boundary conditions leads to the occurrence of a performance gap approximately 10–20% different from the actual cooling power consumption. However, the actual indoor climate data, including dry bulb temperature as an input, can provide a more accurate result as cooling energy consumption (kWh) with an error of 5% compared to the actual energy consumption collection.

Table 2. AC electrical power consumption (kWh) of Initial model, scenario 1 model, and scenario 2 model

Simulation model	AC electrical power consumption (kWh)	The percentage of the consumption different from the actual data (%)
Initial model (ASHRAE)	25.3	8.3
Scenario 1 (Local outdoor climate)	21.7	21.4
Scenario 2 (Local indoor climate)	26.3	4.7
Actual measurement	27.6	-

4. DISCUSSION

The difference in AC electrical power consumption (kWh) between the initial model (using ASHRAE weather data) and Scenario 1 (local outdoor climate) can be assumed to be caused by the different degree of solar radiation. Figure 4 shows the hourly solar radiation rate of ASHRAE climate data and on-site outdoor measurements and temperatures (T) from different sources and locations on March 14th, 2022. The on-site outdoor temperature values are higher than the temperature values generated from the typical weather file (Figure 4b), even though the on-site solar radiation rate is lower (Figure 4a). It can be inferred that solar radiation has a stronger effect on envelope heat gain compared to outdoor temperatures. And the simulated indoor temperature presents higher values than the onsite indoor measurement (Figure 4b). This finding might be caused by the greater amount of heat gained through the exterior walls. Moreover, scenario 2's outcome, energy consumption, gives the highest accuracy with the lowest percent error of approximately 5%. It can be argued that this case performs the simulation without dependency on inputs related to internal heat gain, for example, building materials, surface temperature, and surrounding conditions. According to this argument, the simulation of scenario 2 is conducted with fewer effects due to the many uncertain inputs related to heat transfer via the building facade.

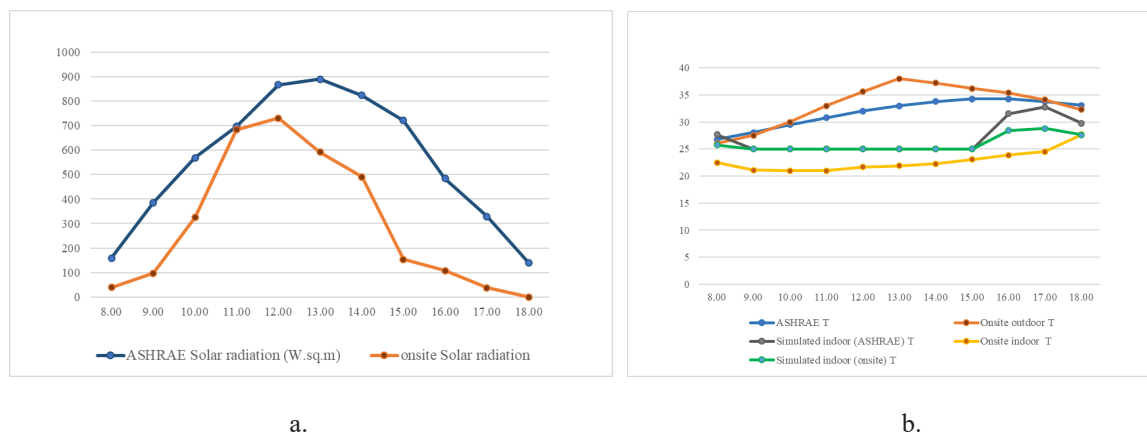


Figure 4. (a) hourly solar radiation rate of ASHRAE climate data and on-site outdoor measurement monitoring, and (b) temperatures (T) from different sources on March 14th, 2022.

5. CONCLUSIONS

This contribution provides findings from a case study on the comparative analyses of measurement simulation and measurement data of building energy consumption in a daytime-operated building in a hot and humid climate (Bangkok, Thailand). Compared to typical and local weather data deployed as simulation inputs, the indoor measured data provide a more accurate simulation model with building energy consumption as an outcome. Other related factors affecting the simulation results should be observed and studied in the future.

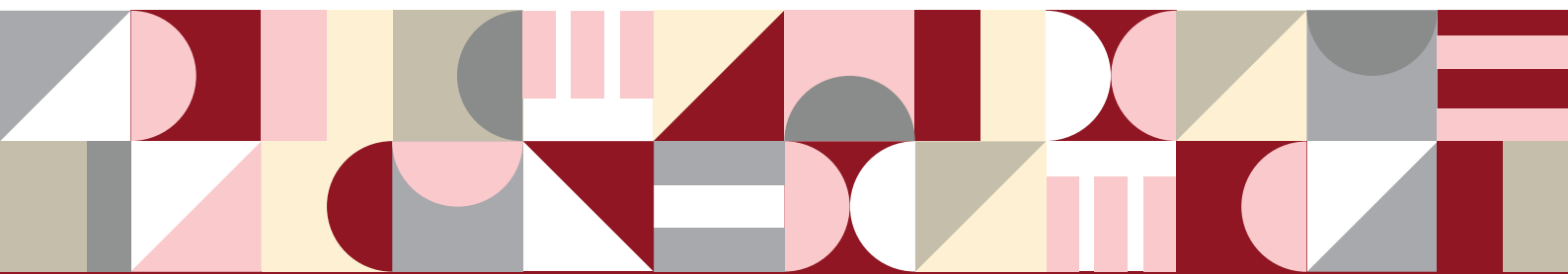
ACKNOWLEDGMENTS

This study was supported by Panasonic Solution (Thailand) Co., Ltd. for the building case study information and the results of all simulation scenarios.

REFERENCES

- Al-Tamimi, N.A.M., Fadzilb, S.F.S. (2010). Experimental and Simulation Study for Thermal Performance Analysis in Residential Buildings in Hot-Humid Climate (Comparative Study). *Journal of Science & Technology*, Vol. (15) No.(1).
- ASHRAE. (n.d.). Weather data. Retrieved from ASHRAE website: <https://www.ashrae.org/technical-resources/bookstore/ashrae-international-weather-files-for-energy-calculations-2-0-iwec2>
- Chong, A., Gu, Y., and Jia, H. (2021) calibrating building energy simulation models: A review of the basics to guide future work. *Energy & Buildings*, 253, 111533.
- Crawley, D.B., Lawrie, L.K. (2019). Should We Be Using Just ‘Typical’ Weather Data in Building Performance Simulation?, *Proceeding of 16th International Building Performance Simulation Association Conference, IBPSA 2019*, 2nd - 4th September 2019, Rome. DOI: 10.26868/25222708.2019.210594
- Erbaa, S., Causonea, F., and Armani, R. (2017). The effect of weather datasets on building energy simulation outputs, *Proceeding of 9th International Conference on Sustainability in Energy and Buildings*, SEB-17, 5th -7th July 2017, Chania, Crete, Greece.
- Fabrizio E., Monetti E. (2015). Methodologies and advancements in the calibration of building energy models, *Energies*, 8 (4), 2548-2574.
- Heo, Y. (2011). *Bayesian calibration of building energy models for energy retrofit decision-making under uncertainty*. PhD Thesis. Georgia Institute of Technology. USA.
- Indana, H.D., Dinapradipta, A., and Samodra, F.X.T.B. (2020). Simulation Validation for Thermal Performance of Building Envelope Material in Humid Tropical Highland Climate. *Proceeding of 6th International Seminar on Science and Technology (ISST) 2020, IPTEK Journal of Proceedings Series No. (6) (2020), ISSN (2354-6026)*, July 25th, 2020, Institut Teknologi Sepuluh November, Surabaya, Indonesia.
- Kiesel, K., Vuckovic, M., and Mahdavi, A. (2013). Representation of Weather Conditions in Building Performance Simulation: A Case Study of Microclimatic Variance in Central Europe. *Proceedings of 13th Conference of International Building Performance Simulation Association*, 26th -28th August 2013, Chambéry, France.
- Lam, K.P., Zhao, J., Ydstie, E.B., Wirick, J., Qi, M., & Park, J.H. (2014). An EnergyPlus Whole Building Energy Model calibration method for office buildings using occupant behaviour data mining and empirical data. *In Proceeding of the Building Simulation Conference*, 10th –12th September 2014, Atlanta, GA, USA.
- Menezes, C., Cripps, A., Bouchlaghem, D., and Buswell, R. (2012). Predicted vs. actual energy performance of non-domestic buildings: using post-occupancy evaluation data to reduce the performance gap, *Appl. Energy*, 97, 355–364.
- Monetti, V., Davin, E., Fabrizio, E., André, P., and Filippi, M. (2015). Calibration of building energy simulation models based on optimization: a case study. *Proceeding of 6th International Building Physics Conference, IBPC 2015, Energy Procedia*, 78 (2015) 2971 – 2976.
- Sarna, I., Ferdyn-Grygierek, J., and Grygierek, K. (2022). Thermal Model Validation Process for Building Environment Simulation: A Case Study for Single-Family House. *Atmosphere* 2022, 13, 1295. <https://doi.org/10.3390/atmos13081295>
- TESS. (2019). TRNSYS Overview. Retrieved from TESS website: <http://www.tess-inc.com/trnsys/trnsys.html>.
- Wilde, P. (2014). The gap between predicted and measured energy performance of buildings: A framework for investigation, *Automation in Construction*, 41, 40-49.
- Zero Carbon Hub. (2010). A Review of the Modelling Tools and Assumptions: Topic 4, Closing the Gap between Designed and Built Performance, *Zero Carbon Hub*, London, UK.

Information Process and Management



THE INTEGRATION OF DESIGN AND FABRICATION FOR PREFABRICATED UHPC PANELS OF BUILDING FACADES

Kevin Harsono¹, ShenGuan Shih², and YenJui Chen³

1) Doctoral student, Department of Architecture, College of Design, National Taiwan University of Science and Technology, Taipei, Taiwan. Email: D11113803@mail.ntust.edu.tw

2) Ph.D., Prof., Department of Architecture, College of Design, National Taiwan University of Science and Technology, Taipei, Taiwan. Email: sgshih@mail.ntust.edu.tw

3) Ph.D., General Manager, Taiwan Sobute New Materials Co. Ltd., Taipei, Taiwan. Email: rodney.chen24@gmail.com

Abstract: Prefabricated ultra-high-performance concrete (UHPC) panels have gained more and more attention for building facades due to their superiority of aesthetic appeal, strength, customization, sustainability, and ease of installation. Despite its many advantages, many barriers exist to using UHPC panels for construction. Most noticed is the cost of materials, limited availability, the complexity of fabrication, lack of standards, and limited experience in the industry. The key to resolving the difficult situations would be the ability to integrate the knowledge regarding the best use of the material, as well as the ways to optimize the fabrication and installation of UHPC panels in the design phases. This paper discusses the use of digital technologies to support the integrated project delivery process for building facades built with prefabricated UHPC panels. The scope of the study covers the communication pattern between the client, the architect and the UHPC experts across the schematic design phase, the design development phase, and the construction documentation phase. Parametric design tools, performance simulation tools, and a common data environment are used to facilitate communication across multiple disciplines so that domain knowledge regarding UHPC can be effectively integrated into the design decision process in all design phases. A construction project in which it was decided to use metal panels for the façade in the schematic design phase, but in the design development phase the architect and the client changed their decisions to use UHPC panels was used as a case study to uncover the difficulties for a conventional design communication process to integrate knowledge about new materials and technology. Scenarios that show how digital technology may facilitate communication among stakeholders that are not familiar with the domain expertise of others are displayed and explained in this paper.

Keywords: Ultra-High-Performance Concrete, Design Knowledge Integration, Fabrication, Digital Technology.

1. INTRODUCTION

The building façade is a crucial element in building construction, acting as a protective boundary between outdoor and indoor spaces and accounting for a substantial proportion of total construction expenses, which can reach up to 30% (Montali et al., 2019). To achieve the aims of constructing cost-effective high-performance buildings, it is necessary to explore innovative solutions that balance aesthetic, functional, and economic aspects of building façades. The construction industry is now striving to satisfy the demand for high-performance buildings at acceptable costs. However, by utilizing advances in building material technology, architects and consultants can create designs that are both aesthetically pleasing and function remarkably well. To achieve this, careful design and planning from the earliest stages are necessary. On the other hand, prefabricated UHPC panels are becoming increasingly popular among architects and engineers as a building envelope material due to their exceptional structural performance and capacity to produce distinctive organic forms (Amran et al., 2022). However, there are some barriers to implementing the UHPC prefabricated methods such as poor design considerations, resistance among architects and engineers to embracing new technology, and a lack of knowledge of the possibilities and limits of the materials (Wang et al., 2020). To fully embrace the potential of new materials such as UHPC, integration between all project stakeholders is necessary from the earliest stage of the project (Chang & Shih, 2018). This requires a robust communication model such as the Business Process Model and Notation (BPMN), which can be used to model project workflows and processes, enabling effective communication and collaboration among the customer, architect, and consultant at every stage of the project.

The challenges of incorporating information about new materials and technology into practical design communication procedures are highlighted in this paper through a case study method. In this study, communication patterns between consultants and architects are examined, along with the use of performance and structural analysis as design tools. The research also explores the role that digital technologies may play in effective project delivery, both throughout the design and manufacturing phases. The primary objective of this research is to provide a novel approach for developing UHPC façade panels that takes structural and efficiency assessments into account from the very beginning of the construction project. In-depth discussion of how digital technologies were used to enhance communication and incorporate UHPC expertise from other disciplines

during the design process is also included in the paper.

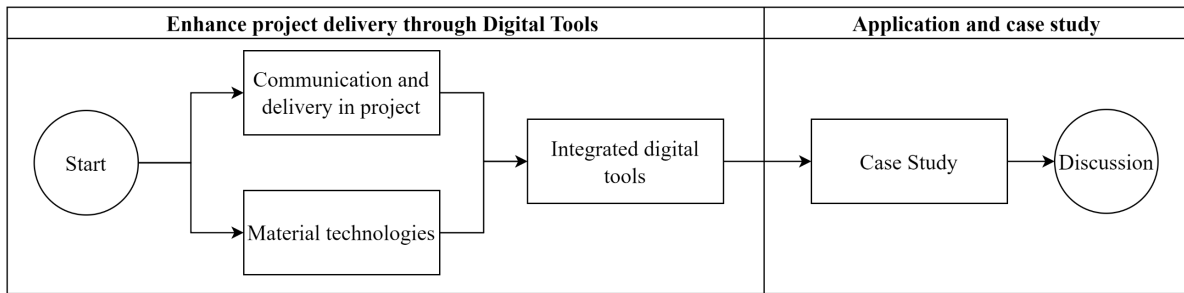


Figure 1. Research Method

Figure 1 illustrates the research method, which is divided into two main sections. The first section outlines the proposed method of communication between stakeholders and introduces the design tools that can help the architect integrate the process of design and performance analysis. The second section focuses on the use of digital tools in façade design during the early stages of a case study in Taiwan. The case study is described to illustrate the importance of improved communication between architects and consultants during the early stages of a project. This allows architects to create effective designs without needing to rely on direct contact with consultants during the early phase of the project.

2. ENHANCING PROJECT DELIVERY THROUGH DIGITAL TOOLS

2.1 Communication and Delivery in Project

To ensure the successful delivery of a project, effective communication between stakeholders is essential. Additionally, it is also crucial to integrate information at an early stage. This can help minimize conflicts and avoid unnecessary waste. Unfortunately, the industry has not yet found a practical and effective solution for this issue (Yin et al., 2008). Digital technologies have the potential to make communication between architects and consultants more efficient and cost-effective. Common delivery methods such as Design-Bid-Build, Design-Build, or Construction Manager at Risk have drawbacks, including frequent disputes and claims. To overcome these challenges, integration between stakeholders is required, and Integrated Project Delivery (IPD) was proposed. To ensure smooth IPD, the involvement of digital tools technology and a culture of open information sharing is necessary. Digital tools technologies offer essential capabilities, including multi-disciplinary performance analysis and modeling, which help to achieve integrated and efficient project delivery (Ma et al., 2018).

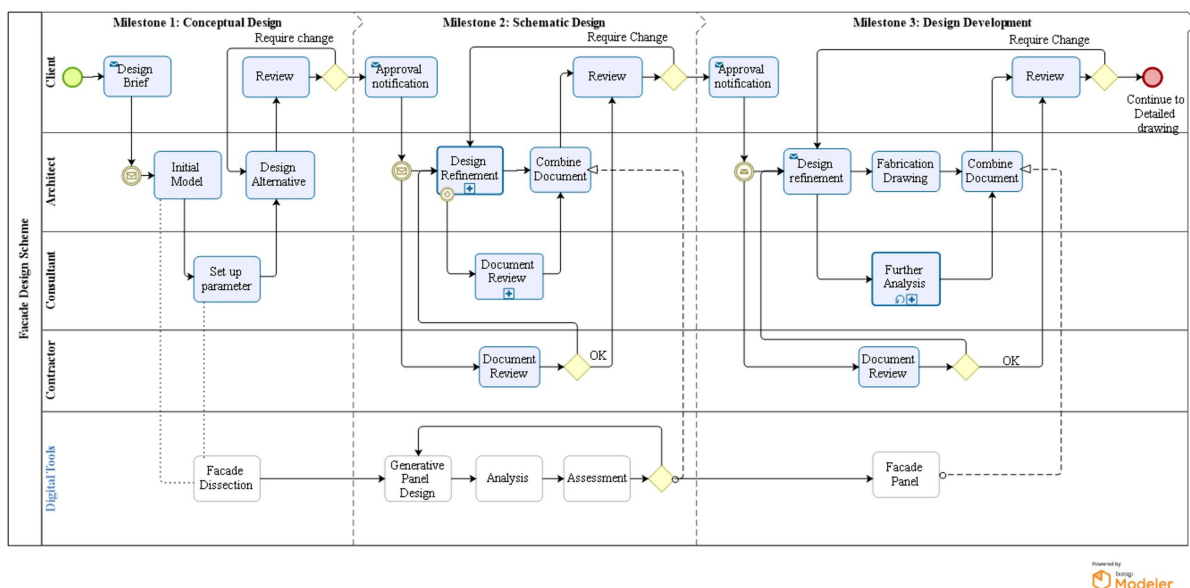


Figure 2. BPMN between stakeholders in facade construction.

The study utilizes the Bizagi modeler software to generate a BPMN model. The purpose of this model is to visualize the communication flow between stakeholders involved in the project. The proposed BPMN model used in this study is based on previous research that emphasizes the collaborative process throughout all project

phases within stakeholders. BPMN is a workflow-based notation which has two sets of elements. BPMN elements can be divided into two types, namely node and edge. The nodes represent the event, activities, and processes in the project workflow. The edge represents the connection between the nodes (Houhou et al., 2022). The proposed BPMN model in this study is based on previous research (Ma et al., 2018) that emphasizes the collaborative process throughout all project phases within stakeholders, which iterates the "design - evaluation/compare - modify" process. The BPMN model's progress in the integrated project delivery is illustrated in Figure 2.

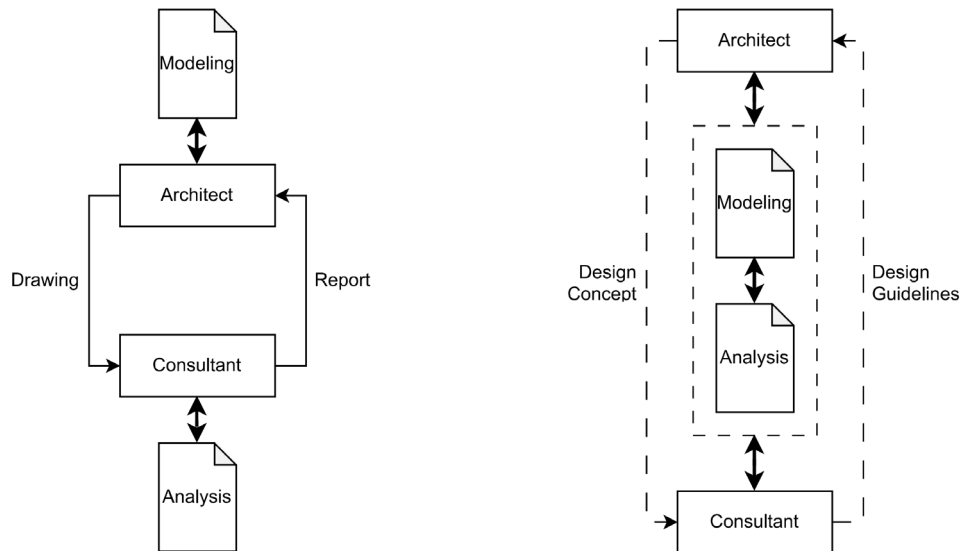


Figure 3. Left: Conventional (Left) and Shifted Paradigm (Right) of communication between stakeholders.

This study proposes an integration between architects and consultants in the early stages of the design process to improve project delivery efficiency and effectiveness, as shown in Figure 3. Conventionally, communication between architects and consultants relies heavily on iterated interactions between them. The architect creates models intensively and sends drawings to the consultant, who then analyzes the building based on the drawings and provides a report for the architect to finalize for the client. However, if there are any changes to the design, the process must be repeated from the beginning, resulting in increased time and money spent on communication between the architect and the consultant.

In contrast, early communication between architects and consultants can result in better use of the selected materials and more effective design, taking into consideration the performance and fabrication of selected materials from the beginning. As seen in Figure 3 (right), by integrating the knowledge of the materials from the beginning and making use of the right tools, architects can generate numerous design alternatives with performance analysis automatically. By using digital technologies to communicate, the flow of communication will change from being intensely communicative between architect and consultant during the entire process to being less intense. Direct communication between the architect and the consultants is required only in the early stage of the project, where they discuss the design concept, and the consultant provides the architect with design guidelines, based on the selected material. The remaining communication process is carried out through software that can model and analyze automatically. Performance analysis is considered throughout the initial design process that is provided to clients as a result of the knowledge integration between the consultant and architect in the early stages of the project. The consultant provides the analytical parameter during the initial stakeholder meeting before the design process begins. However, the expected outcome of the conceptual design stage is more likely to be very simplified massing. During this phase, contractors may have less involvement, since the output is only representing the basic shape of the façade panels. After the design is approved, the project moves from conceptual design to schematic design, marked by approval from the client. At this point, the consultant can begin further analysis.

This approach can significantly reduce revision time, resulting in a more streamlined design process that meets all desired criteria. Moreover, this method emphasizes the importance of considering material waste, structure performance, and aesthetic value in the early stages of the project. This ensures satisfactory outcomes and better use of UHPC as a building envelope material, given its mechanical properties and structural behaviors. In addition, by using this method architects may create the design while also performing the analysis, allowing for rapid adjustments and reducing overall design mistakes. As a result, using digital technologies to facilitate communication between the consultant and architects has the potential to greatly improve the efficacy and efficiency of the design process.

2.2 Mechanical Properties of Ultra-High-Performance Concrete

First created in France in the 1990s, Reactive Powder Concrete (RPC) or Ultra-High-Performance Concrete (UHPC) is a kind of cementitious material. The extraordinary mechanical qualities of this special concrete, such as its great flowability, early and ultimate strengths, and outstanding durability, are very well known. The high durability of UHPC is attributed to significant reduction in the number and size of the pores within the material (Abbas et al., 2016). The Federal Highway Administration (FHWA) describes UHPC as a form of concrete that includes considerable amounts of internal fiber reinforcement, granular components with an optimum gradation, and a water-to-cement ratio of less than 0.25. Apart from its discontinuous pore structure, UHPC provides an extensive list of additional desired qualities that make it an outstanding material for a variety of building applications. High compressive strength, which is normally up to 250 MPa, is one of its most noticeable characteristics. Its strength enables the construction of structures that are lighter and thinner, hence minimizing a building's overall weight and carbon footprint. UHPC is perfect for usage in tough settings or regions with heavy traffic since it is also incredibly strong and resistant to weathering, abrasion, and impact (Akhnoukh & Buckhalter, 2021). In this study, the UHPC parameter was sourced from the consultant of the project. Table 1 provides an overview of the mechanical properties of UHPC used in this research, which will be used to examine the effectiveness of UHPC facade panels in building design.

Table 1. UHPC Mechanical Properties.

Parameter	Value
Young Modulus	40000 MPa
Poisson Ratio	0.20
Density	24000 Kg.m ⁻³
Compressive Strength	130 MPa

3. FACADE TECTONIC AND INTEGRATION OF DIGITAL TOOLS

The use of novel materials like UHPC in the construction of façade systems presents a significant challenge to both façade fabricators and architects, emphasizing the significance of façade tectonics. Prefabricated UHPC panels provide a solution to the fabrication issue in UHPC facade construction. The common practice for the facade construction process includes manufacturing in a factory and transporting the panels to the construction site for assembly based on the design drawing. This prefabrication process can speed up the construction process, improve the quality of the building, and reduce the waste of resources, as stated by Wang et al. However, despite the numerous advantages of prefabricated building technology, its full potential is still not being exploited in many projects. Therefore, the development of integrated digital tools for building façade design is necessary to optimize the use of UHPC material in façades.

To achieve this optimization, integrated digital tools should be designed to facilitate the design and analysis of building facades, especially in the early stages of the project. The digital tools can help the architect as well as the consultant and fabricator to achieve an optimized panel design that is not only aesthetically pleasing but also has good performance. By integrating UHPC material properties and the required structural design parameters, the digital tools can optimize the panel's design while ensuring that the construction and production costs are reasonable. The result is a façade system that maximizes the potential of UHPC material, improves building quality, and reduces resource waste. This study proposes a comprehensive set of tools for designing building facades that include modeling tools, performance evaluation, and structural analysis during the initial stages of the design process. Figure 4 illustrates the proposed program workflow.

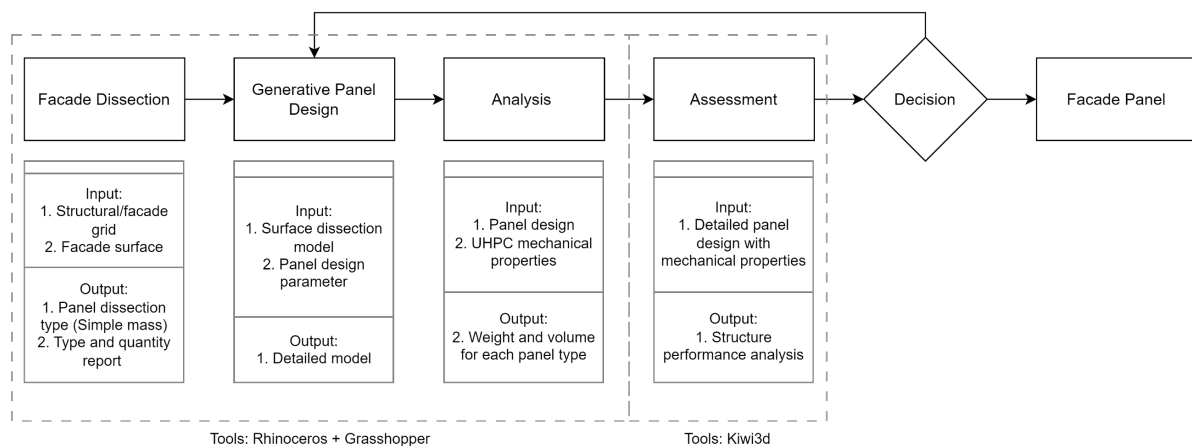


Figure 4. Generative tools flowchart.

This research proposes the utilization of digital tools for the creation of building facades that integrate modeling tools and structural analysis at the initial phase of the design process. Rhinoceros and Grasshopper plugins are utilized for this purpose. The software's workflow begins with inputting the building facade mass, which is then divided by the program. The user can also input the grid for the facade dissection, which can be determined by the material or transportation module. For the subsequent step, the software generates the panel design based on predetermined parameters. The next step involves calculating the weight and volume of each panel type so that the contractor can estimate the cost at the project's earliest stage. At these stages, the model already includes material information. The output from this phase will contain early information regarding the material. The model will be automatically analyzed using performance assessment software, Kiwi3d, which can generate finite element analysis model with simple structural performance analysis. This approach allows architects to design an efficient and cost-effective facade while integrating knowledge at the project's early stage. This integration reduces communication costs between architects and consultants and minimizes the time wasted on revisions between the two parties. By utilizing these digital tools, architects can simplify the design process and create high-quality and cost-efficient building facades.

4. CASE STUDY

The study presented in this paper examines a specific construction site in Taiwan of the building façade as a case study. Initially, the building was designed with a secondary skin material made of metal. However, during the design phase of the project, a significant design change occurred. The architect and client decided to switch to a different material, which is UHPC, due to the humid weather conditions at the site. This decision might have a significant impact on the overall design of the building, as well as its construction cost. The switch to UHPC material posed new challenges and opportunities for the project team. On one hand, the material's unique properties allow for more creative and innovative design solutions. On the other hand, the new material required the project team to adjust their approach and consider new factors, such as the material's structural integrity and fabrication feasibility. This change had a significant impact on the overall design and construction cost of the building, necessitating effective cost and time management. To address this issue, digital tools were utilized to redesign the façade panel using UHPC material.

The first step of designing the UHPC panel façade is to import the model into the rhinoceros's software and assign the surface to the grasshopper plug-in cluster. To determine the façade panel type and dimension the surface is input together with the façade grid. Figure 5 (left) shows the dissection of the surface, resulting in simple façade panel dissections. Accurate knowledge of the kind and quantity of materials that are needed is crucial since the manufacturing phase of a building project may be difficult and expensive. During this stage, the software assesses the type and quantity of each panel, which is crucial information for the fabrication phase of the project.

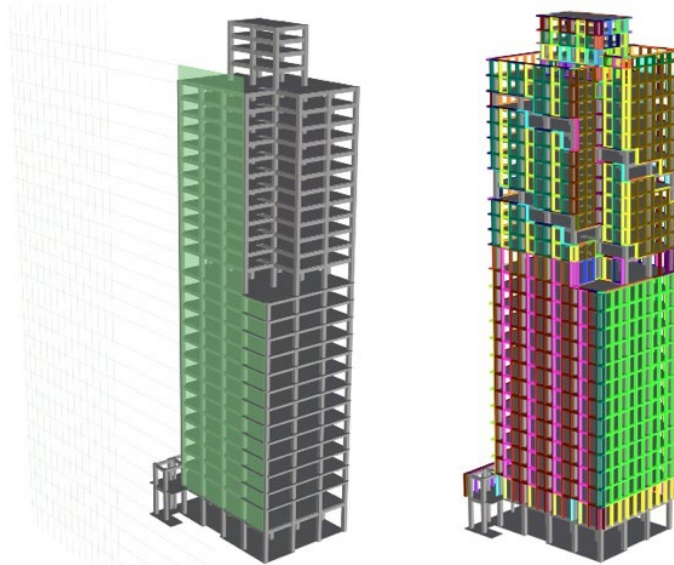


Figure 5. Left: Surface dissection based on façade grid. Right: Façade panel type.

As depicted in the right panel of Figure 5, despite the absence of essential details in this early façade model, the software's output can automatically determine the type and quantity of the façade. This helps the contractor in providing a rough estimate of the construction cost. Figure 6 displays the output of the dissection, which comprises the approximate dimensions and quantities of each panel. The dissection of the façade into uncomplicated UHPC panels can facilitate the optimization of the fabrication process, leading to greater efficiency and cost-effectiveness in subsequent stages.

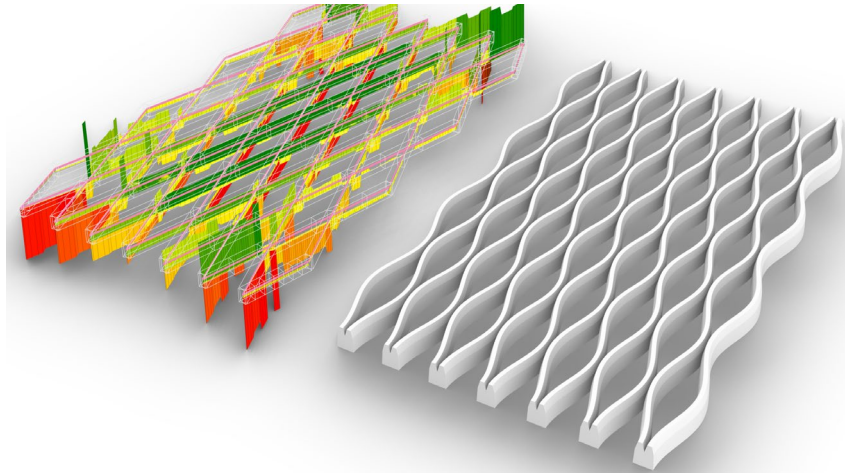


Figure 8. Right: Architectural Model; Left: Structure model.

As this paper is written, the project is undergoing the construction phase. Some of the construction images are shown in Figure 9, which highlight how well the design and construction processes were carried out. Early knowledge integration together with digital technologies has produced a project that exceeds customer expectations as well as industry benchmarks.



Figure 9. Construction Process.

5. DISCUSSION

The integration of design and fabrication has become increasingly important in the construction industry, especially with the rise of prefabrication and the use of advanced materials such as UHPC. By aligning material knowledge and digital technology, it is possible to streamline project delivery and achieve significant cost efficiencies. This paper highlights the potential benefits of early communication and integration of material knowledge and digital technology to achieve cost efficiency and streamlined project delivery. To achieve this, a new paradigm of communication needs to be proposed. The traditional method of modeling and analysis can be slow and cumbersome, requiring intensive communication between the architect and consultant throughout the entire process. However, with the integration of material knowledge and digital technology, direct communication is only necessary in the early stages of the project. The remaining communication is carried out through software, reducing the need for repetitive communication and improving the design process's efficiency. The study also introduces a set of digital tools that are designed to make the process of design and production more seamless by integrating the knowledge of the material in the early stage of the design process. These tools include automated panel dissection, generative panel design, and performance analysis. With the use of these technologies, architects can create complex panels more efficiently while automatically generating the performance analysis simultaneously. Additionally, the performance analysis results in this set of tools can also serve as a basis for the engineer to further analyze the panel. To demonstrate the effectiveness of these tools, a case study is chosen as an example of a successful attempt to integrate design and fabrication in ongoing projects. This research is a pilot study that focuses on the integration of design and fabrication of prefabricated UHPC

façade panels. However, the study has some limitations, such as performance analysis only based on wind pressure and the tools limited to façade panel design. These limitations provide opportunities for future research, such as incorporating more sophisticated technology like robots and 3D printers, improving the precision of analysis, and including additional performance evaluations such as life cycle, thermal transmittance, and lighting.

6. CONCLUSION

This paper focuses on using UHPC panels as a building envelope material for their exceptional structural performance and ability to create unique organic forms. It proposes a new method for designing UHPC façade panels by integrating knowledge from stakeholders early in the project and utilizing digital tools for multidisciplinary performance analysis and modeling. The study emphasizes collaborative processes throughout all project phases using the BPMN model, which iterates the "design - evaluation/compare - modify" process. Early collaboration between architects and consultants can improve project delivery, efficiency, and effectiveness, leading to better material utilization and performance. The case study emphasizes the value of digital technologies in redesigning the UHPC façade panel, resulting in cost and time savings while ensuring safety criteria are met. The knowledge integration and utilization of digital tools have played a crucial role in streamlining the project. In conclusion, this study highlights the importance of early-stage collaboration between stakeholders, and the value of digital technologies in improving project delivery, efficiency, and effectiveness. The proposed method for designing UHPC façade panels shows promise in achieving optimal designs that meet client needs while utilizing materials efficiently.

ACKNOWLEDGEMENTS

The author wishes to express their gratitude to all the stakeholders involved in the project that was used as a case study in this paper and for allowing its publication. The construction pictures in this paper were generously provided by Guo Yuan Construction Co., Ltd., who also acted as the UHPC fabricator in the project.

REFERENCES

- Abbas, S., Nehdi, M. L., & Saleem, M. A. (2016). Ultra-High Performance Concrete: Mechanical Performance, Durability, Sustainability and Implementation Challenges. *International Journal of Concrete Structures and Materials*, 10(3), 271–295. <https://doi.org/10.1007/s40069-016-0157-4>
- Akhnoukh, A. K., & Buckhalter, C. (2021). Ultra-high-performance concrete: Constituents, mechanical properties, applications and current challenges. *Case Studies in Construction Materials*, 15, e00559. <https://doi.org/10.1016/j.cscm.2021.e00559>
- Amran, M., Huang, S.-S., Onaizi, A. M., Makul, N., Abdelgader, H. S., & Ozbakkaloglu, T. (2022). Recent trends in ultra-high performance concrete (UHPC): Current status, challenges, and future prospects. *Construction and Building Materials*, 352, 129029. <https://doi.org/10.1016/j.conbuildmat.2022.129029>
- Chang, Y. F., & Shih, S. G. (2018). *Exploring Multi-Disciplinary Communication Based on Generative Modeling at the Early Architectural Design Stage* [Preprint]. SOCIAL SCIENCES. <https://doi.org/10.20944/preprints201806.0230.v1>
- Houhou, S., Baarir, S., Poizat, P., Quéinnec, P., & Kahloul, L. (2022). A First-Order Logic verification framework for communication-parametric and time-aware BPMN collaborations. *Information Systems*, 104, 101765. <https://doi.org/10.1016/j.is.2021.101765>
- Ma, Z., Zhang, D., & Li, J. (2018). A dedicated collaboration platform for Integrated Project Delivery. *Automation in Construction*, 86, 199–209. <https://doi.org/10.1016/j.autcon.2017.10.024>
- Montali, J., Sauchelli, M., Jin, Q., & Overend, M. (2019). Knowledge-rich optimisation of prefabricated façades to support conceptual design. *Automation in Construction*, 97, 192–204. <https://doi.org/10.1016/j.autcon.2018.11.002>
- Wang, C., Li, F., Zhang, J., Guo, J., & Li, S. (2020). Tectonic Methodology on the Façade Composition Pattern of Prefabricated Building Enclosure Wallboards. *IOP Conference Series: Earth and Environmental Science*, 510(5), 052086. <https://doi.org/10.1088/1755-1315/510/5/052086>
- Yin, S. Y. L., Tserng, H. P., & Tsai, M. D. (2008). A model of integrating the cycle of construction knowledge flows: Lessons learned in Taiwan. *Automation in Construction*, 17(5), 536–549. <https://doi.org/10.1016/j.autcon.2007.10.002>

CONSIDERING OF BIM DATA SCALE INTERFACES FOR VARIOUS APPLICATION: CASE STUDIES OF SMART PATROL PROJECT IN CHULAPAT 14 BUILDING CHULALONGKORN UNIVERSITY

Kaweekrai Srihiran¹, Terdsak Tachakitkachorn², and Chalumpon Thawanapong³

1) Assoc. Prof., Regional, Urban, and Built Environmental Analytics: RUBEA, Department of Architecture, Faculty of Architecture, Chulalongkorn University, Bangkok, Thailand. Email: Kaweekrai.s@chula.ac.th

2) Ph.D., Asst. Prof., Architecture for Creative Community Research Unit, Department of Architecture, Faculty of Architecture, Chulalongkorn University, Bangkok, Thailand. Email: Terdsak.t@chula.ac.th

3) Ph.D. Student, Department of Architecture, Faculty of Architecture, Chulalongkorn University, Bangkok, Thailand. Email: Jchalumpon@gmail.com

Abstract: BIM in the design and construction industry consists of graphical and non-graphical data, from the scale at the production level of parts and assembly to the scale at the design and construction level of elements and buildings to the scale at city levels of buildings and infrastructure, is big data for use in city management. However, when the data becomes larger, it causes problems in the efficiency of data management and processing. Case studies from digital twin experiment and BIM modeling procedure in Chulalongkorn university based on consideration of BIM data scale interfaces by organizing of a graphical data transformation to a non-graphical data from the scale at the production level of parts and assembly to the scale at the design and construction level of elements and buildings to the scale at city levels of buildings and infrastructure clarified significant procedures of data management efficiency.

Keywords: BIM data, Management, Processing, Scale interface

1. INTRODUCTION

Building Information Modeling (BIM) in the design and construction industry consists of graphical and non-graphical data (Aish, 1986), from the scale at the production level of parts (Autodesk, 2023) and assembly to the scale at the design and construction level of elements and buildings (Autodesk, 2018) to the scale at city levels of buildings and infrastructure, is big data for use in city management (Lu et al., 2020). Chulalongkorn university transformed 2D drafting of all existing campus buildings into BIM and requires BIM for the newly constructed building, to be utilized in smart city development in campus site, shown in Figure 1. According to BIM guideline in Thailand, BIM can be classified by the building element e.g., floor, wall, door, with the different Level of Development (LoD) for each process of construction, consist of Conceptual, Design development, Construction document, Shop drawing, and As built drawing (ASA, 2015), which is the precise building information for delivering to building owner when the construction is complete. (ISO, 2020)

However, the delivered BIM with large amount of data, has caused problems in the efficiency of data management and processing of BIM utilization in Operation and Maintenance (O&M) phase of the building. This study is a case studies from digital twin experiment in Chulalongkorn university with clarification of BIM utilization in term of background of the project in section 2.1, BIM processing in section 2.2, BIM application in section 2.3, based on consideration of BIM data scale interfaces by organizing of a graphical data transformation to a non-graphical data from the scale at the production level of parts and assembly, to the scale at the design and construction level of elements and buildings to the scale at city levels of buildings and infrastructure clarified significant procedures of data management efficiency.

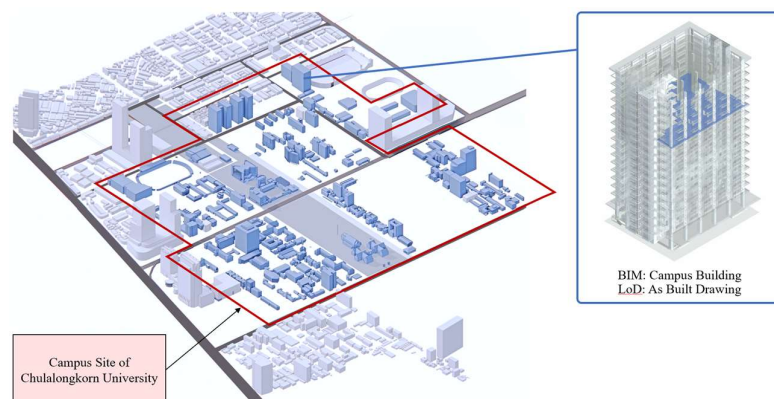


Figure 1. BIM of campus building in Chulalongkorn university

2. CASE STUDIES

2.1 Background of the Project

Smart patrol project is a digital twin experimental project in 2022, in the experimental area of 800 sq.m., in 12th floor of Chulapat 14 building, to create a real time spatial application for Indoor Air Quality (IAQ) data visualization from IAQ patrol, multi-sensing IAQ moveable gear, with a built in network device and rechargeable battery, and Ultra-wideband (UWB) tag to connect with 40 UWB anchors in the experimental area to detect the location of the patrol as shown in Figure 2.

The measurement data is real time IoT data consisting of IAQ data e.g., Temperature, Humidity, CO, CO₂, etc., and Indoor Positioning System (IPS) data in term of cartesian coordinate system, consists of X-coordinate and Y-coordinate.

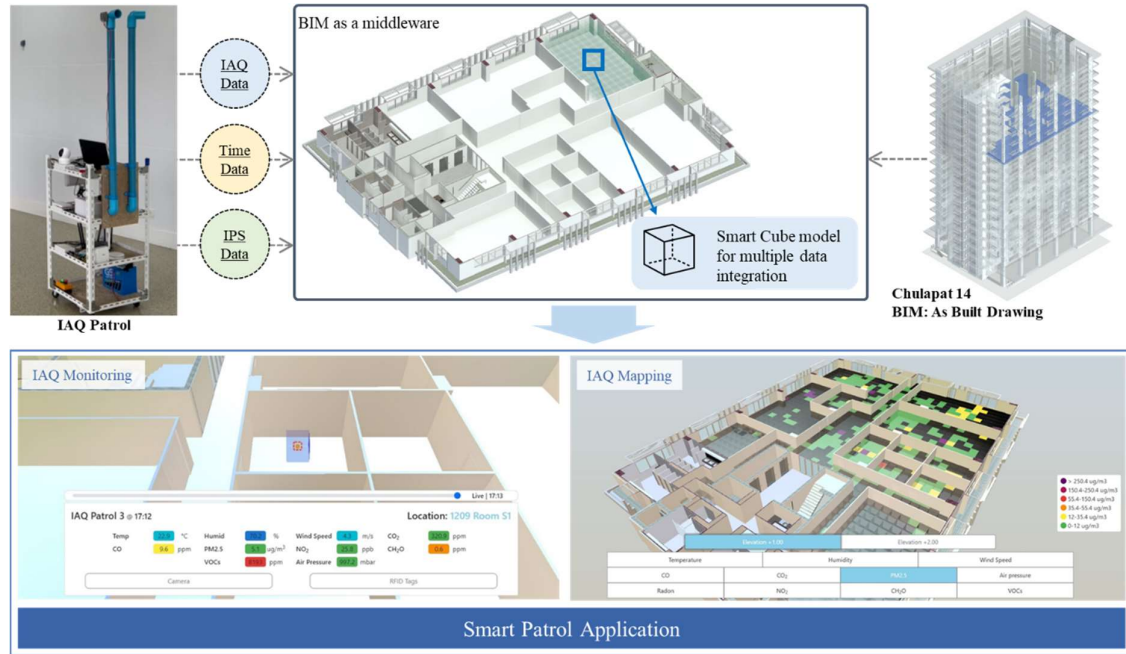


Figure 2. Development framework of Smart patrol project

2.2 BIM Processing

According to the number of measurement data types, non-graphical data of each subdivision of space in As built drawing BIM of Chulapat14, in term of Rooms (Autodesk, 2020), has been used to generate Smart cube model, an additional BIM for IoT data management by classifying IAQ data with its location with IPS data, and IoT data visualization thru Viewer API in Autodesk web service (Autodesk, 2022). The model is a geometry model, representation of 1 m³ of the experimental area with parameter in BIM software specified in Table 1.

Table 1. Parameter and description of Smart cube model in BIM software

Parameter	Value	Description
Element id	1154480	string data, to identify the model in BIM software and called from BIM server for data visualization
Associated floor	12	string data, to identify location of the model in term of floor name in Chulapat 14 building
Associated room	1209 Room S1	string data, to identify location of the model in term of room name in Chulapat 14 building
X-coordinate	8.17	numeric data of x value of the model in project coordinate system in BIM software
Y-coordinate	4.76	numeric data of y value of the model in project coordinate system in BIM software

In addition, Using of As built drawing BIM of Chulapat 14 graphical data as a spatial 3D Graphical User Interface (GUI) in Smart patrol application, the excessive detail has to be organized in BIM software specified in Table 2, for the clear and effective communication as shown in Figure 3.

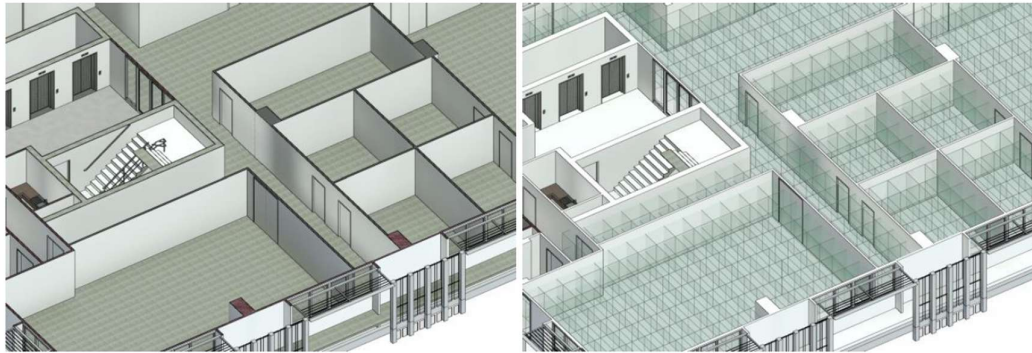


Figure 3. BIM Graphical data transformation in Smart patrol project

Table 2. BIM utilization in Smart patrol project

	LoD of Existing BIM	Usage of BIM in application	
		LoD	Purpose
Electrical	As Built Drawing	Not use	-
Mechanical	As Built Drawing	Not use	-
Plumbing	As Built Drawing	Not use	-
Structure	As Built Drawing	Not use	-
Architecture			
- Wall	As Built Drawing	Design Development	3D GUI
- Curtain Wall	As Built Drawing	Construction Document	3D GUI
- Floor	As Built Drawing	Design Development	3D GUI
- Column	As Built Drawing	Construction Document	3D GUI
- Ceiling	As Built Drawing	Design Development	3D GUI
- Door	As Built Drawing	Construction Document	3D GUI
- Window	As Built Drawing	Construction Document	3D GUI
- Roof	As Built Drawing	Construction Document	3D GUI
- Stair	As Built Drawing	Design Development	3D GUI
- Railing	As Built Drawing	Construction Document	3D GUI
- Furniture	As Built Drawing	Construction Document	3D GUI
- Room	As Built Drawing	As Built Drawing	Generate Smart cube model
Additional Model			
- Smart cube model		Design Development	2D and 3D GUI

2.3 BIM Application

Smart patrol application is a real time IAQ data visualization on BIM and IoT integration platform with 3D GUI from graphical data of building model and Smart cube model, and 2D GUI to display 10 types of IAQ data included Temperature, Humidity, Wind speed, CO, CO₂, PM 2.5, NO₂, CH₂O, VOCs, Air pressure, and IPS data in term of room name.

- IAQ Monitoring, real time data visualization from showing Smart cube model via element id (Kunkel, 2018), with the matching of X-coordinate and Y-coordinate parameter with IPS data to show the location of IAQ data. 2D GUI shows the details of IAQ data and room name, which is the associated room parameter of the shown model.
- IAQ Mapping, cumulative IAQ data heat map with all Smart cube models in different color according to the latest IAQ data in each type, with 2D GUI for the data description.

3. CONCLUSION

3.1 BIM Utilization in Smart Patrol Project

Although the case study of digital twin experimental project in Chulalongkorn university is the proof that BIM utilization is not deploying the full details of BIM but depends on the development goal, the case study has

revealed that BIM data scale might be classified in term of spatial development scale from single coordinate point to subdivision of space in room level and floor level, and magnify to the building and city level as shown in Figure 4.

3.2 BIM Utilization Project Standard

According to the challenge of the various project development goals classification in BIM utilization project, a proper standard for BIM utilization is needed, with pragmatic tools e.g., template, procedure, guideline.

3.3 Future Development Plan

To invent the comprehensive BIM utilization project standard, prototype of the project should be embraced in terms of spatial development scale and development goal for comparative analysis as shown in Figure 5. Chulalongkorn university has a plan to develop BIM utilization project in the whole building scale and city infrastructure in campus site by the cooperation between faculty of architecture and faculty of engineering.

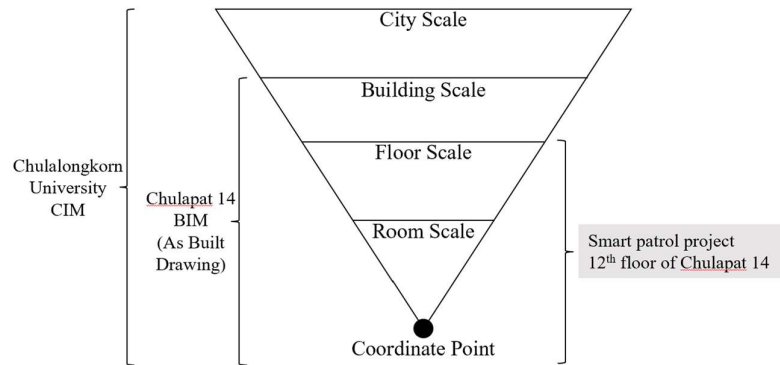


Figure 4. BIM data scale interfaces from coordinate point to the city

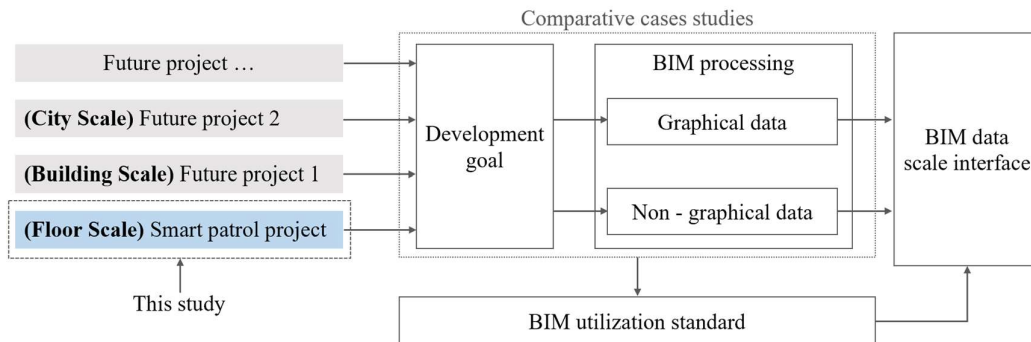


Figure 5. The Current research and future plan for BIM data scale interfaces

REFERENCES

- Aish, R. (1986). *Building modeling the key to integrated construction CAD*. CIBSE.
- ASA. (2015). *Thailand BIM Guideline*. ASA.
- Autodesk. (2018). *BIM Collaborate Coordinate teams and models from one place*. Retrieved from Autodesk website: <https://construction.autodesk.com/products/autodesk-bim-collaborate/>
- Autodesk. (2020). *About Rooms*. Retrieved from Autodesk website: <https://help.autodesk.com/view/RVT/2020/>
- Autodesk. (2022). *Autodesk.Viewing. GuiViewer3D*. Retrieved from Autodesk website: <https://aps.autodesk.com/en/docs/viewer/v2/reference/javascript/guiviewer3d/>
- Autodesk. (2023). *Autodesk Inventor: Mechanical design software for ambitious ideas*. Retrieved from Autodesk website: <https://asean.autodesk.com/products/inventor/overview?term=1-YEAR&tab=subscription>
- ISO. (2020). *ISO 19650-3:2020 Organization and digitization of information about buildings and civil engineering works, including building information modelling (BIM) — Information management using building information modelling — Part 3: Operational phase of the assets*. ISO.

- Kunkel, J. (2018). *Revit Element ID - How to Get It and What to Do with It*. Retrieved from CADD microsystem website: <https://www.caddmicrosystems.com/blog/revit-element-id-how-to-get-it-and-what-to-do-with-it/>
- Lu, Q., Parlikad, A.K., Woodall, P., Don Ranasinghe, G., Xie, X., Liang, Z., Konstantinou E., Heaton, J. and Schooling, J. (2020). Developing a digital twin at building and city levels: Case study of West Cambridge campus, *Journal of Management in Engineering*, 8 (3).

DEVELOPMENT OF ROADWAY GEOMETRIC DESIGN PROCESS MODEL FOR KNOWLEDGE MANAGEMENT

Koji Makanae¹

1) Ph.D., Prof., School of Project Design, Miyagi University, Miyagi, Japan. Email: makanae@myu.ac.jp

Abstract: This paper discusses a design process model for knowledge management in roadway geometric design. In this model, the design process is classified into four stages: Conceptual Design, Outline Design, Basic Design, and Recursive Design, and it shows that the roadway design process can be viewed as a function of the designer's thought process. Moreover, a method for analyzing the fluctuation in roadway distance was proposed. A distance-conversion table for each measurement that lengthens the roadway can be linked to the dispositional information. Using this method, we can start compiling knowledge from the beginning about changes in distance and will be able to reproduce the route-selection process in a system.

Keywords: Information management, Knowledge management, Roadway geometric design, BIM

1. INTRODUCTION

Building information modeling (BIM) is a technique continuously gaining popularity in the construction sector, and is increasingly being applied to public infrastructure. For example, U.S. CAD vendors in particular, are developing "BIM for Infrastructure" systems and working on their application in construction projects. Also, building SMART, the BIM standards body, has established an infrastructure sub-committee, and is exploring applications of industry foundation classes (IFCs), which are the standards in building construction for railways and roadways. Mean-while, Japan is also following this trend: in 2012, a construction information modeling (BIM/CIM) concept was promoted by the Ministry of Land, Infrastructure, Transport and Tourism (MLIT), while construction-production systems using 3D models and ICT were developing fast. The BIM/CIM concept has also expanded into management and can be expected to extend into information management that covers the construction lifecycle, including the maintenance management and handover to the next cycle. Till date, for BIMs in the construction sector, work has been done on knowledge-based BIM systems during project management (Motawa and Almarshad, 2013).

Knowledge management (KM) was based on keyword searches in the early stages, but later ontologies were used in KM systems (Anumba et al., 2008). Regarding KM in design, after the concept of BIM for KM was proposed by Lee et al. (2006), the importance of it KM for BIM was pointed out in existing studies (e.g., Fruchter et al., 2009). However KM for BIM is still in the emerging stage as Wang and Meng (2021) pointed out, and there are few studies on KM related to roadway geometric design.

By contrast, we proposed a conceptual model as a foundation for information management in the previous studies (Makanae, 2016, 2017, 2022). This paper summarizes the pyramid information model as a foundation for information management and the connector model for information, which can include knowledge and wisdom. Moreover, this paper shows a design process model for KM in roadway geometric design.

2. MODELING INFRASTRUCTURE INFORMATION STRUCTURE

Compared to other industries, public infrastructure is distinct, such that its work products are larger, and the lifecycles are longer, including production processes. These processes progress through stages of conceptual planning, detailed planning, surveying, designing, and fabrication. Among them, the design information is driven towards finer granularity and higher precision, ultimately forming the actual production on site. The authors demonstrated that information structures in production processes followed a "pyramid" model moving from abstract to specific and an information-structure model along the time axis throughout the lifecycle (Makanae, 2010, 2012). The pyramid-scheme design information structure used in the previous studies is shown in Figure 1 (a).

Information is produced by obtaining various types of external information, including actual space information, and abstract information is related to concrete information in the pyramid scheme, which expands downward from the top regardless of the shape of its base.

The relationship between the pyramid scheme and time is considered here. Figure 1 (b) shows the relationship between the pyramid scheme and time by reproducing Figure 1 (a) as seen from the side. Pieces of information are related to each other in the design and construction phases. In these processes, information is produced, while information in the actual space is being obtained. The time efficiency of the construction process is represented by the slope of the entire pyramid.

Abstract information becomes concrete over a period that can span a few years or decades, although this period varies according to the type and scale of the infrastructure. The natural and social environments around the

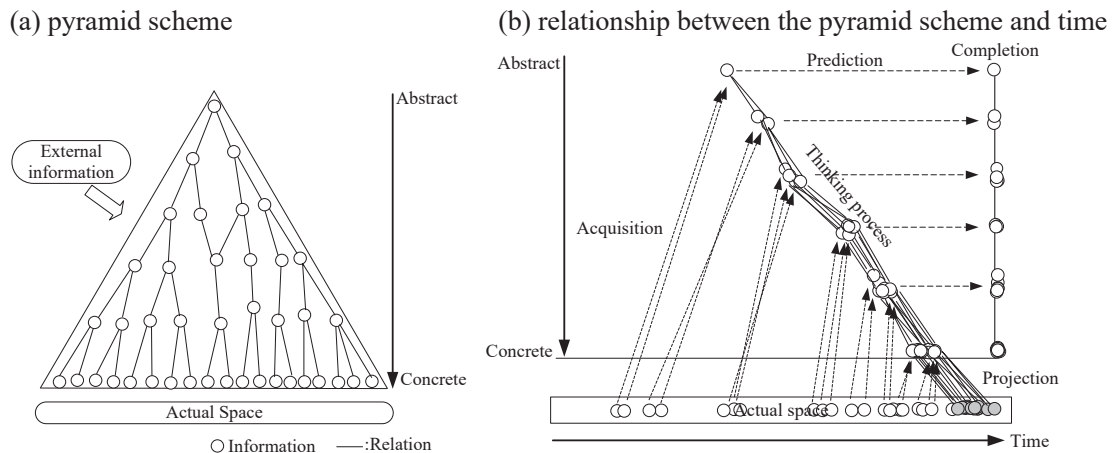


Figure 1. The pyramid model of public-infrastructure information

scheme vary during the period, and the information varies accordingly. Information variations may cause the information pyramid scheme to collapse. Continuity from the abstract to concrete information should be ensured in the construction process of the scheme.

3. AN INFORMATION-CONNECTOR MODEL FOR COMPILING KNOWLEDGE AND WISDOM

In the pyramid model shown in Figure 1, all generated information is connected to the thing itself in real space via links. However, when viewing a production process at the micro-scale, there also exists discarded information without any linkage to the thing itself. Taking a roadway-design project as an example, when selecting an alignment, there are multiple possible routes connecting the starting and endpoints, each of whose draft designs will be produced. Each candidate route is evaluated for its pros and cons according to numerous factors, followed by a decision-making, with only the selected candidate proceeding to the execution stage.

Although the course of this decision-making process will be documented in reports, it will not leave behind an information structure. However, such a process uses all the knowledge and wisdom of the people involved, and the basis for the decision (why a certain route was selected) may remain useful over the course of multiple lifecycles. The field of KM uses a "data-information-knowledge-wisdom" (DIKW) pyramid (Rowley, 2007), but when applied to infrastructure information management, there still exists a need for a way to collect and create knowledge and wisdom, not just data and information—the upper layers of DIKW.

A conceptual diagram of information connectors, including decision-making, is shown in Figure 2. The individual connectors can be expressed as a "swelling of knowledge" when there are multiple options. Those bulges contain the decision-making process for one of the options. Compiling these decision-making processes leads to developing the rules of thumb, which can be used as a way of creating wisdom.

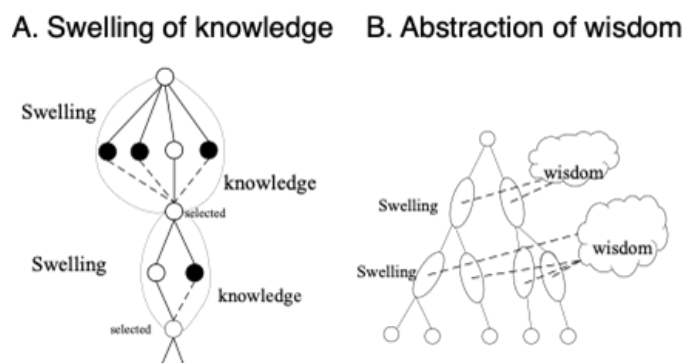


Figure 2. The connector model of information, including knowledge and wisdom

4. A METHOD OF COMPILING INFORMATION FOR CONTINUITY OF KNOWLEDGE

4.1 Development of Design Process Model for Roadway Geometric Design

In order to develop a knowledge structure model required for roadway geometric design, we analyzed an actual roadway design process and flow analysis from the viewpoint of information distribution. The roadway design process used as a reference is a large-scale mountain roadway reconstruction project in Japan (Gassan highway, 30.9 km long, 5 tunnels, 36 bridges, completed in 1981, Figure 3).

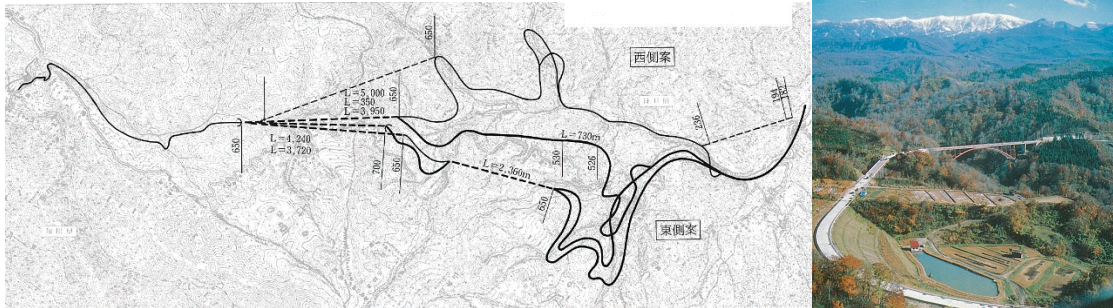


Figure 3. Roadway reconstruction planning of Gassan roadway (MLIT, Japan)

The road construction process was elucidated by analyzing the road construction record issued by the construction office of MLIT. Terms related to the design were extracted as design information. To build the schema for knowledge management, Wnag and Meng (2019) proposed a framework based on UML diagrams. In this study, the relationships among the extracted information were represented on a mind-map diagram to show the chain relationship of the data because a mind-map diagram makes it easy to show hierarchical relationships.

Figure 4 shows a part of the results of the analysis. The historical records included the reconstruction and the previous generation of roadway in the 19th century.

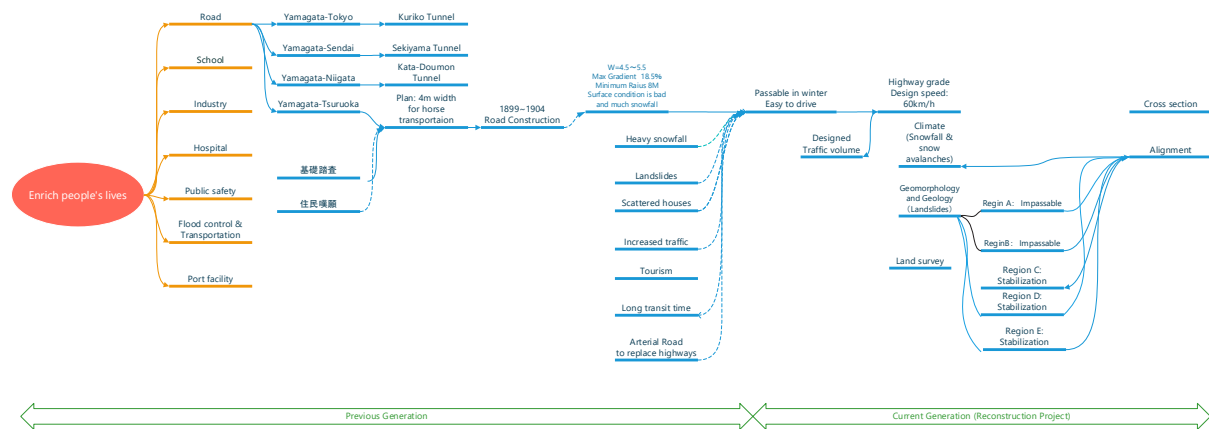


Figure 4. Construction process analysis using mind-map diagram

Although the geometric design at that time was paper-based and did not involve digital information, the flow analysis was conducted considering the application of BIM. The resulting design process schema is shown in Figure 5. The design process is classified into four stages: Conceptual Design, Outline Design, Basic Design, and Recursive Design. Each stage encompasses the function *f* of human intellectual activity.

In the Conceptual Design stage, the basic information for roadway route design (origin, destination, and waypoints) and the level of service of the roadway are determined based on the design standard. Function *f1* outputs the origin, destination, and waypoints that should be set to realize the concept and the level of service of the roadway to be built, based on a statistical analysis of regional and traffic conditions and geographical information.

The Outline Design stage defines the actual roadway locations and the information underlying the cross-section configuration. The function *f2A* defines the outline road alignment based on the terrain model, and the function *f2C* defines the cross-section configuration based on the level of service.

The Basic Design is the process of defining the basic geometry of the roadway using function f_3 based on more detailed terrain, geological, and environmental information. As in the previous process, the specific shape is defined by parameters. In most cases, the site for the roadway is determined at this stage, and the land acquisition proceeds sequentially.

In the Recursive Refinement stage, sectioning is performed on the established roadway alignment based on differences in structure type, and design is performed for each individual structure. The geometry is constructed using parameters according to the structural type, such as earthwork for function f_4E , bridge for f_4B , tunnel for f_4T .

As described above, the roadway design process can be viewed as a function of the designer's thought process. Therefore, design object Obj can be shown as Eq (1).

$$Obj = f_n (\text{terrain, geology/environment, parameters (design conditions)}) \quad (1)$$

The knowledge information modeling process is the definition of these functions. We plan to define these functions for the knowledge information model.

4.2 A Method of Compiling Information for Knowledge Continuity

When selecting a roadway route, natural conditions such as topography, soil quality, climate, flora and fauna, and scenery, as well as societal conditions, such as the locations of existing roadways, land use, schools and other facilities, will act as control points, while the goal is to lay out an optimized roadway that satisfies these various conditions or minimizes their impact. In order to compile design dispositions (know-how) at the route design stage, connecting the map information consisting of curves that show the centerlines of roadways is the main challenge. The geometric structure of a roadway is defined as a single dimension representing the linear distance of the roadway centerline. Similarly, distance is the central piece of information for specifying the position. Hence, connecting dispositional information and distance becomes desirable. However, at the route-selection stage, the centerline has yet to be decided to obtain the central piece of information, the distance.

An example of the route design process is shown in Figure 6. Once the starting and end points have been set, the roadway could be defined as a single straight line, but in reality, it may need to be a curve due to topographic and other constraints, thus, lengthening the roadway compared to a straight line. Also, as shown in the example, if the roadway involves tunnels or bridges, it may actually be shorter than following the topographic contours. In this study, as a method for analyzing the fluctuation in roadway distance, we prepared a distance-conversion table for each measurement that has the effect of lengthening the roadway and proposed that this can be linked to dispositional information. Using this method, we can start compiling knowledge from the beginning about changes in distance and will be able to reproduce the route design process in a system. In the future, a system that implements this method, as well as its continuous testing, will become necessary.

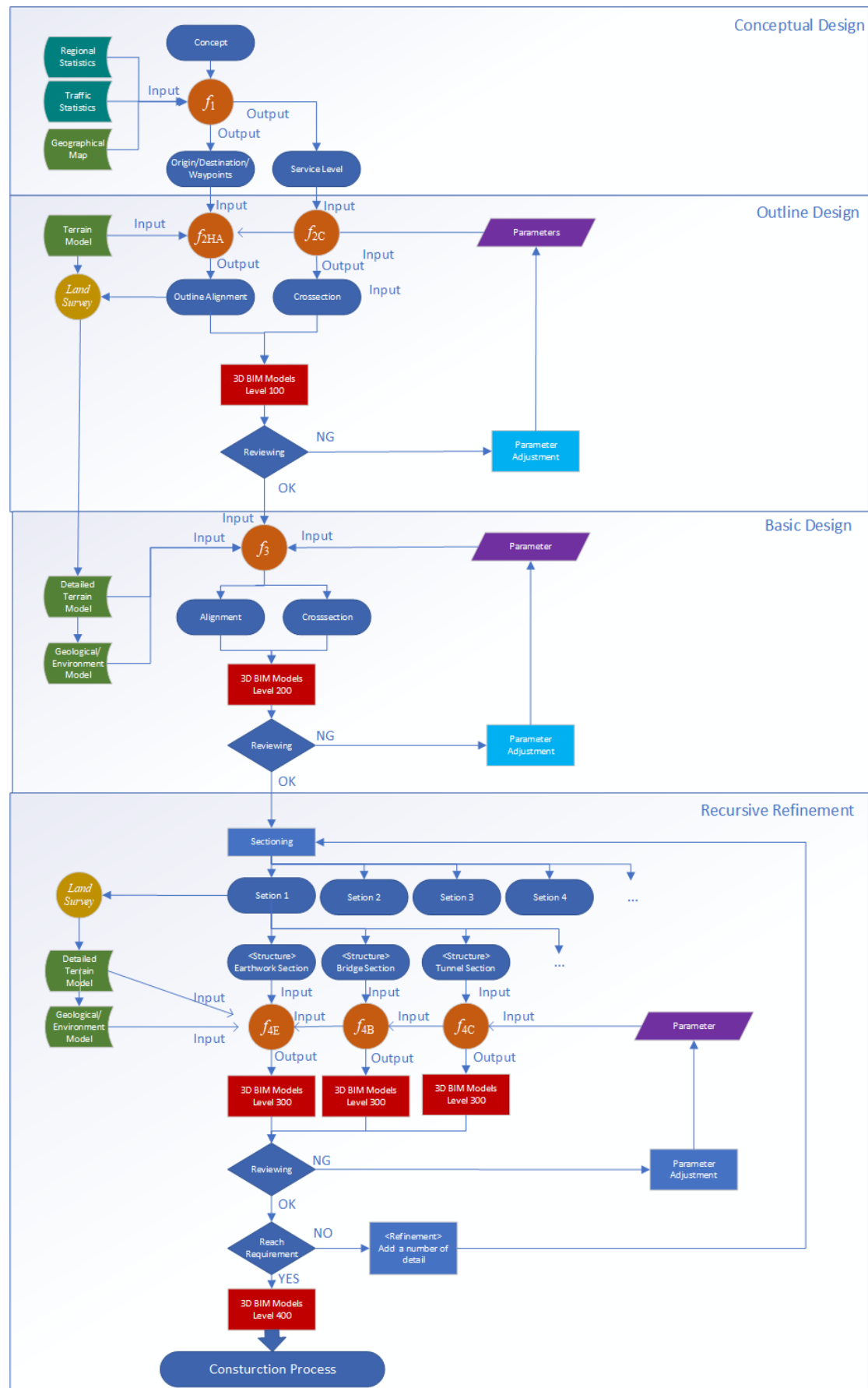


Figure 5. Design process model in roadway geometric design

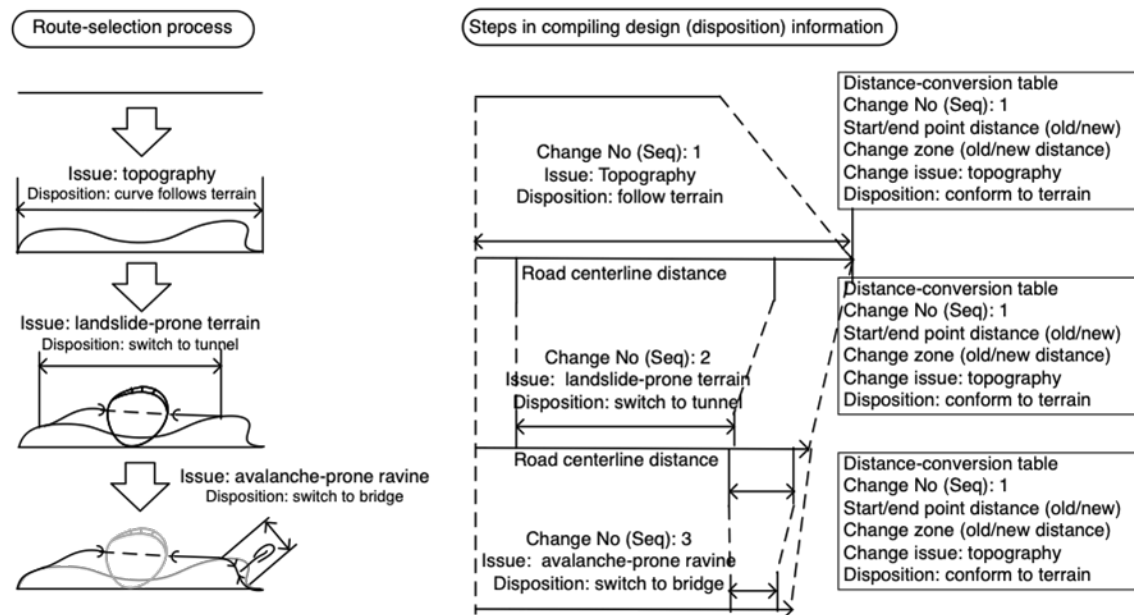


Figure 6. Information-compilation process in route design (disposition)

5. CONCLUSIONS

In this paper, we presented a design process model required for roadway route design and studied how to compile information, including knowledge and wisdom. The road reconstruction process was elucidated by analyzing the road construction records using a mind-map diagram to show the chain relationship of the information. In this schema, the design process is classified into four stages: Conceptual Design, Outline Design, Basic Design, and Recursive Design, and it shows that the roadway design process can be viewed as a function of the designer's thought process. Moreover, a method for analyzing the fluctuation in roadway distance was proposed.

In the future, continuous work is necessary to build a system for compiling the design dispositions based on our proposed method. As the process analysis was performed in a mountainous area in this study, there are few stakeholders related to the targeted project. However, the highway construction process is more complex in urban areas with various stakeholders. We should continue the analysis for more complex conditions to reveal highway design mechanisms.

Also, more experiments and analyses of knowledge acquisition need to be done. Along with clarifying the knowledge-acquisition process, research needs to be carried out on ways to create knowledge and wisdom from the information compiled based on the expertise formed in this manner.

ACKNOWLEDGMENTS

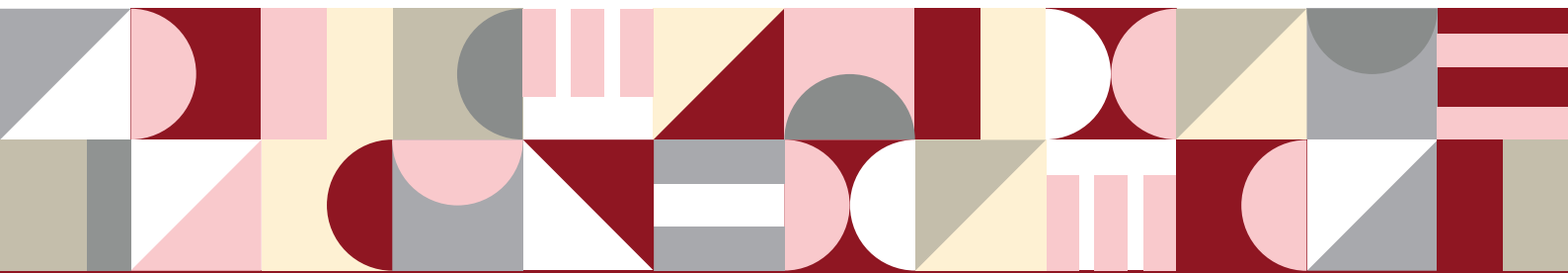
JSPS KAKENHI Grant Number 19K04641 supported this work.

REFERENCES

- Anumba, C.J., Issa, R.R.A., Pan, J., Mutis, I. (2008), "Ontology-based information and knowledge management in construction", *Construction Innovation*, 8(3), 218-239.
- Fruchter, R., T. Schrotenboer, and G. P. Luth. 2009. "From building information model to building 644 knowledge model." *In Proceedings of International Workshop on Computing in Civil Engineering*, Austin, Texas: ASCE, 380–389.
- Makanae, K. (2010). Analysis of Information Structure in Infrastructure Lifecycle, *Proc. 1st International Conference on Sustainable Urbanization*, Hong Kong, 202-207.
- Makanae, K. (2012). "Development and Analysis of Time-Spatial Information Model for Infrastructure Lifecycle Management", *Proc. 14th International Conference on Computing in Civil and Building Engineering*, Moscow.
- Makanae, K. (2016). The Conceptual Model of Information Management in Infrastructure Lifecycles, *Proc. 7th Civil Engineering Conference in the Asian Region (CECAR 7)*, 7p.
- Makanae, K. (2017). The concept of information and knowledge management in civil infrastructure lifecycles, *Proc. in International Conference on Civil and Building Engineering Informatics (ICCBEI)*, Taipei, Taiwan, 343-346.

- Makanae, K. (2022). Development of Knowledge Information Model for Highway Route Design, Book of Abstract, 19th International Conference on Computing in Civil & Building Engineering, Cape Town, 17.
- Motawa, I., Almarshad, A. (2013). A knowledge-based BIM system for building maintenance. *Automation in Construction*, 29, 173–182.
- Rowley, J. (2007). The wisdom hierarchy: representations of the DIKW hierarchy, *Journal of Information and Communication Science*, 33(2): 163–180.
- Wang, H., Meng, X. (2019). Transformation from IT-based knowledge management into BIM-supported knowledge management: A literature review, *Expert Systems with Applications*, 121, 170-187.
- Wang, H., Meng, X. (2021). BIM-supported knowledge management: Potentials and expectations. *Journal of Management in Engineering*, 37(4), 04021032-1 - 04021032-13.

Laser and Image Scanning



FOOTPRINT DETECTION OF CEILING EQUIPMENT FROM TLS POINT CLOUDS

Riho Akiyama¹, Hiroaki Date², Satoshi Kanai³, and Kazushige Yasutake⁴

1) Master Course Student, Graduate School of Information Science and Technology, Hokkaido University, Sapporo, Japan. Email: r_akiyama@sdm.ssi.ist.hokudai.ac.jp

2) D. Eng., Assoc. Prof., Faculty of Information Science and Technology, Hokkaido University, Sapporo, Japan. Email: hdate@ssi.ist.hokudai.ac.jp

3) D. Eng., Prof., Faculty of Information Science and Technology, Hokkaido University, Sapporo, Japan. Email: kanai@ssi.ist.hokudai.ac.jp

4) Kyudenko Corporation, Fukuoka, Japan. Email: kazu-yas@kyudenko.co.jp

Abstract: In recent years, 3D scanning technology using a terrestrial laser scanner (TLS) has become widespread and is used in a wide range of fields such as plants, civil engineering, and architecture. The point clouds acquired by scanning are used for measurement, creating drawings, and 3D model generation and recognition. The reflected ceiling plan (RCP) is one of the 2D drawings of facilities that represents ceiling equipment such as lighting, fire alarm, inspection hole, and so on, and is often created for existing facilities for renovations, inspections, and safety standard checks. For large-scale facilities, the creation of RCPs becomes a labor-intensive and quite time-consuming process. This paper presents a method of footprint detection of ceiling equipment for supporting the creation of RCPs using laser scanning technology. The proposed method detects circle and square shape footprints of the equipment from TLS point clouds of the facility, and by labeling the equipment information, RCP can be created. In the experiment for two datasets, the performance of the method is evaluated, and footprints of about 90% are detected.

Keywords: Laser scanning, Point cloud, Ceiling equipment, Object detection, Reflected ceiling plan.

1. INTRODUCTION

The reflected ceiling plan (RCP) as shown in Figure 1 is one of the 2D drawings of facilities that represents ceiling equipment such as lighting, fire alarm, access door, sprinkler, speaker, and so on, and is often created for existing facilities for renovations, inspection, and safety standard checks. For large-scale facilities, the creation of RCPs becomes a labor-intensive and quite time-consuming process. The technology for efficiently recognizing the equipment and its positions on the ceiling is required for solving the problems.



Figure 1. An example of the reflected ceiling plan

Automatic recognition of scenes from 3D scan data is an important research topic and many algorithms, theories, and methods have been developed in relation to this. 3D scan data has the 3D coordinates, and the result of the recognition includes the object's position and orientation. Therefore, it is suitable for generating 2D drawings and 3D models of existing environments and scenes. This research aims to develop a system for efficient RCP creation using point clouds of facilities acquired by terrestrial laser scanners. This paper proposes a method to detect the footprint of ceiling equipment. The footprint is a boundary shape of the ceiling equipment on the ceiling, as shown in Figure 2(a). The shape of the footprint of almost all ceiling equipment is classified into square or circle as shown in Figure 2(b). If it is possible to detect the footprints accurately, a label of the equipment can be assigned to each footprint, and efficient RCP creation will be realized.

Research on recognition of the scene and objects from point clouds has been conducted for a long time and can be roughly classified into rule-based methods (Macher et al., 2017), model-based methods (Drost et al., 2010), and methods based on machine learning (Golovinskiy et al., 2009; Poux et al., 2020; Qi et al., 2017). Model-based methods prepare a 3D model of the recognition target and determine its existence, position, and posture from a point cloud. In the problem setting of this research, it is difficult to prepare all the 3D models of the target

equipment, so the model-based method cannot be applied. In the machine-learning based method, Support Vector Machines or Random Forest have been used to recognize objects in the scene (Golovinskiy et al., 2009; Poux et al., 2020). Recently, many point cloud segmentation and object recognition methods based on deep learning have been proposed (Qi et al., 2017). However, the equipment targeted in this study contain a lot of noise and lack of points due to their surface specular reflection (Figure 2(a), some of the equipment is very small and there are many variations, making it difficult to apply recognition methods based on point clouds on equipment only.

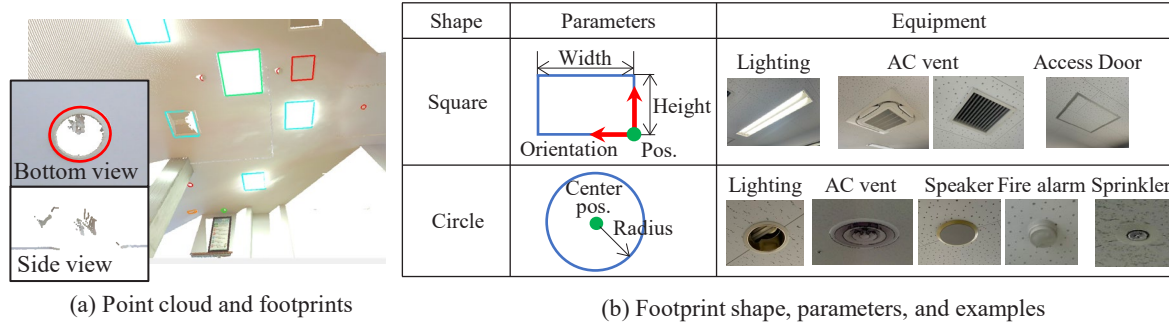


Figure 2. Footprints of ceiling equipment

Some research for detecting ceiling equipment has been conducted. Recently, a recognition method that uses both images and point clouds and includes equipment attached to the ceiling surface has emerged (Hossain et al., 2022). Pan et al. (Pan et al., 2022) also used a combination of AI-based image recognition, image-based 3D reconstruction, and laser scanning to extract indoor objects, including ceiling equipment. However, there are issues in creating training data and improving the recognition accuracy of small equipment such as smoke detectors, and some equipment for RCP creation was out of scope. Takahashi et al. (Takahashi et al., 2020) proposed a method for detecting the footprint of ceiling equipment from TLS point clouds and achieving a much higher extraction rate compared with the above machine learning-based methods without preparing additional data. The method provides a high detection rate of circular footprints, but the method requires prior knowledge of the footprint. This research extends the method of Takahashi et al to be able to also detect square footprints without prior knowledge and to improve the detection accuracy by developing an accurate ceiling plane and its boundary extraction method.

2. METHOD

2.1 Overview of the Proposed Method

Figure 2 shows footprint information and examples of ceiling equipment to be extracted by our method. In this study, it is assumed that the ceiling surfaces consist of flat horizontal planes, and the regions surrounded by the ceiling regions are regarded as the equipment regions, and the boundary of each equipment region is extracted as a footprint. The proposed method estimates the parameters of the footprint (Figure 2(b)) for each equipment.

Figure 3 shows an overview of the proposed method. Because point clouds are generally obtained by multiple scanning at different scanner positions depending on the size of the facility, in our method, first the footprints are extracted from each scan and then the resulting footprints are integrated for all scans. In footprint extraction for each scan, first, structuring and normal estimation are done for the point cloud as a pre-process. Then, the ceiling regions are extracted using the region-growing algorithm. Next, the equipment boundary points are extracted from the ceiling regions, and footprints are extracted by fitting circles and rectangles to the boundary points. Finally, the facility footprints obtained from each scan are integrated.

2.2 Preprocess

To improve the processing efficiency of the neighbor search in region extraction and normal estimation, the point cloud is structured. Because TLS performs laser range measurement while changing the azimuth and elevation angles at regular intervals (Figure 4(a)), a structured point cloud like an image (Figure 4(b)) can be generated by taking the azimuth and elevation angles of the laser measurement as axes and assigning each point in each cell (Masuda&Tanaka, 2010). Next, the normal vector \mathbf{n}_i of each point i in the point cloud is estimated by normalizing the sum of the outer products of the difference vectors between the point and its neighbor points of four directions on the structured point cloud.

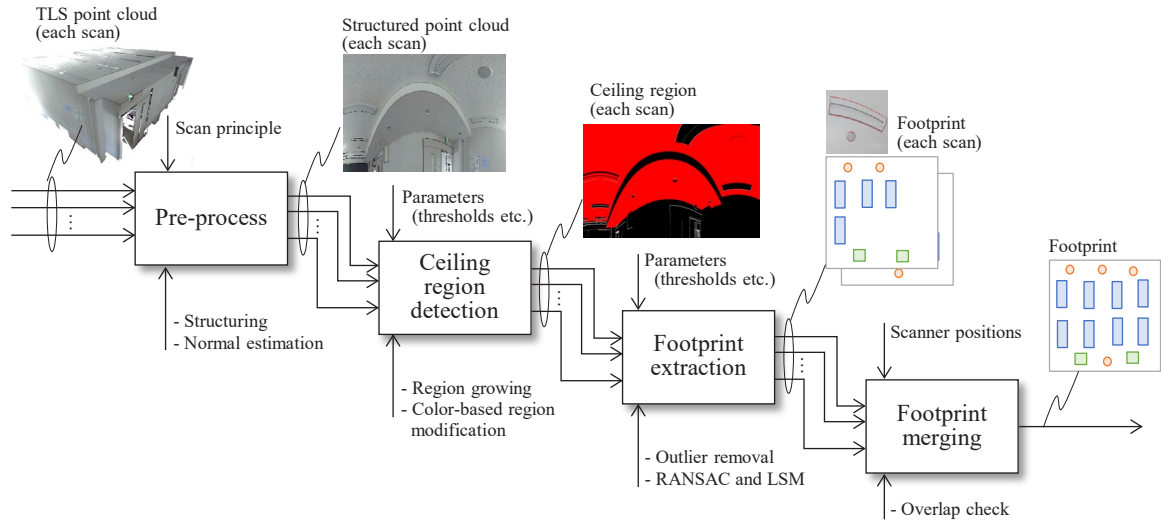


Figure 3. Algorithm of the proposed method

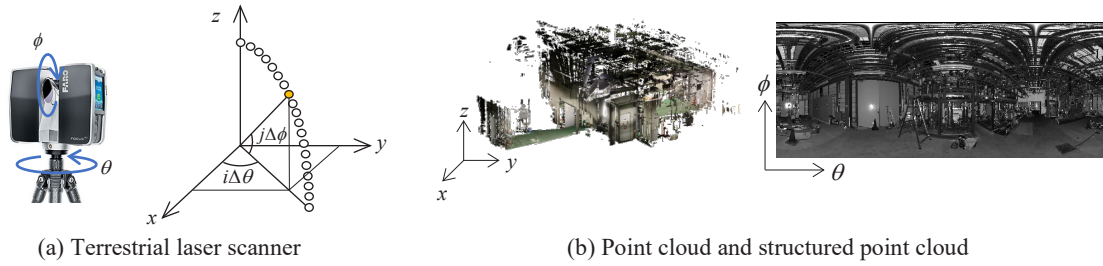


Figure 4. TLS and structured point cloud

2.3 Ceiling Region Detection

Each region of ceiling equipment is regarded as a region bounded by the bumps on the planar ceiling region. The ceiling regions are detected using a region-growing algorithm (Poux et al., 2022), and a new method for accurately detecting the ceiling region is proposed in this paper. In our research, two growing conditions for height difference C_1 and point normal C_2 shown in Equations (1) and (2) are evaluated for accurate ceiling region detection.

$$C_1 : d_{ij} \leq \tau_d \quad (1)$$

$$C_2 : \theta_i \leq \tau_\theta \quad (2)$$

Here, θ_i is the angle between a normal of point i and vertically downward direction $\mathbf{n}^v = (0, 0, -1)$, d_{ij} is the height difference between point i and j , the point i is a candidate for adding the current region, and j is a front point of the current region (Figure 5(a)), and τ_d, τ_θ are given thresholds.

Figure 5(b) shows ceiling region detection results on the structured point cloud with different growing conditions. Condition C_1 can detect most ceiling regions well, but under-detection (false negative) at areas distant from the scanner was observed (Figure 5(b) left). Although C_2 often results in over-detection (false positive) at equipment with small boundary steps and under-detection just above the scanner, problems of C_1 could be solved (Figure 5(b) center). In addition, it is observed that the conditions have directionality, that is, height difference works well for the growth to the front side (from down to top direction in the structured point cloud), and normal works for the backside. From these observations, in our method, a hybrid condition is used, that is, C_2 is used for growth from the front side to the back side, C_1 is used for growth from the backside to the front side, and $C_1 \vee C_2$ is for other directions. The results using the hybrid condition are shown in Figure 5(b) right.

In the experiments, over-detection of the ceiling at the access door which has quite small steps at its boundary is often observed as shown in Figure 6(a). To solve this problem, modification of the ceiling region by color information is done as shown in Figure 6(b). First, a grayscale image is created from structured point clouds, and adaptive thresholding is applied to it. Then, connected black cells are connected and the size of the connected component is estimated by an axis-aligned bounding box. Smaller components are deleted, and finally, points corresponding to the remaining components and their inside region are classified into non-ceiling regions.

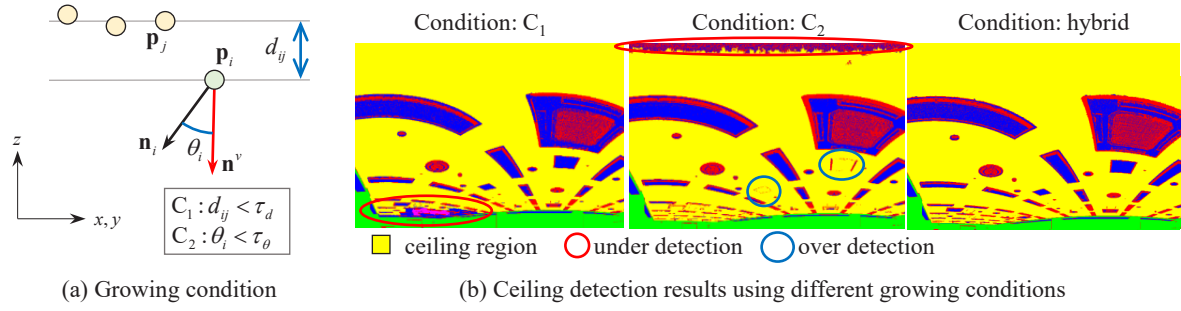


Figure 5. Ceiling region detection by region growing

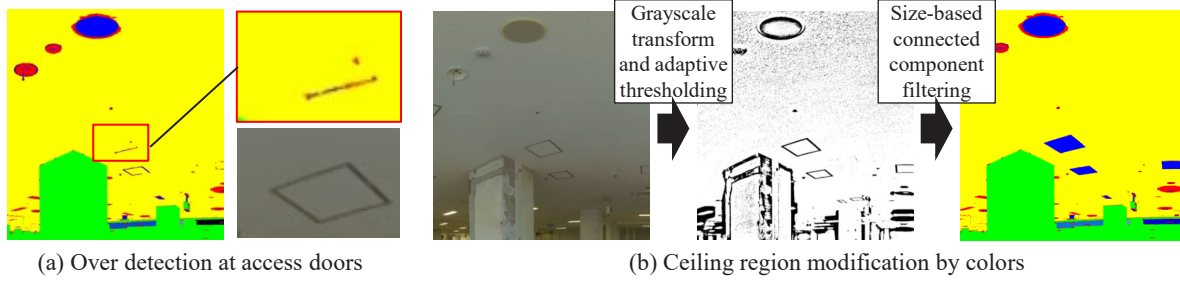


Figure 6. Color-based ceiling region modification

2.4 Equipment Boundary Point Extraction

First, boundary points of the extracted ceiling regions are extracted. The boundary points involve the boundary of equipment, occlusions caused by equipment, walls, and beams. First, boundary points from occlusions are removed by deleting the boundary points on the far side from the scanner when the protrusion height of the equipment exceeds a certain value (Takahashi et al., 2020). Then, vertical planar regions are detected by region growing as walls, and boundary points near the walls are also removed. Finally, boundary points from beams are removed by thresholding the height difference between the boundary point i and a point j just below i on the structured point cloud, that is, the boundary point i satisfying Equation (3) is removed.

$$z_j - z_i > \tau_b \quad (3)$$

Here, z_i is the height of the point i , z_j is the height of the point j , and τ_b is a given threshold. The remaining boundary points are clustered, and each cluster can be a candidate for the footprint of the equipment.

Recognition of the type of footprint and parameter estimation can be done using circle and square fitting to each candidate. The fitting process is done on the horizontal plane. First, circle fitting by RANSAC (Fischler&Balls, 1981) is applied to each candidate. If the inlier ratio is larger than a threshold, the candidate is classified into equipment with a circular footprint. Then, a least-square circle fit is applied to the inliers to compute the center point and radius of the circular footprint. Next, an orthogonal two-line fit using RANSAC is applied to the candidates that are not classified into circular footprints. The candidates are classified into square footprints if they have a large inlier ratio in RANSAC and the distance between the endpoints of the fit line segments is shorter than the threshold. Then, orthogonal two-line fitting using the least-squares method (Takahashi et al., 2019) is applied to the inliers, and the final footprint is defined using the inscribed orthogonal lines parallel to the fitted line obtained by the least-squares method. The reference position, width, and length of the square footprint are computed using the final footprint. In RANSAC, since the point interval varies depending on the distance from the scanner, the threshold for inlier determination is set according to the point spacing (Takahashi et al., 2020). In addition, footprints that include a sufficient number of ceiling region points in its inside are also removed as false detection.

2.5 Merging

Using the results of point cloud registration, all extracted footprints in each scan are integrated into a single-coordinate system. Then, overlaps of footprints on 2D horizontal planes are checked. If the overlap is detected for multiple footprints, a footprint that is closest to the scanner position is retained and the others are removed.

3. RESULTS

The proposed method is applied to two data sets shown in Figure 7(a). Laser scanning was done using a TLS FARO FOCUS 3D S120. Data_A is one scan and the point cloud includes about 43M points. Data_B consists of 12 scans and 520M points. In our implementation, first, the point clouds are uniformly down-sampled on the structured point clouds, and the number of points in one scan becomes approximately 11 million. In the experiments, the down-sampling had little effect on the detection rate, but computational time is drastically reduced (By using the down-sampling for Data_A, the calculation time was reduced from 603s to 100s, and the number of total detected footprints was unchanged, although the numbers of detected circle and rectangle footprints were slightly changed, respectively).

Figure 7(b)(c) shows the results of footprint extraction by our method for Data A and B. To evaluate the performance of our method, the ground truth of footprints was manually created and compared with the extraction results. The footprints were judged as correct if the error of the reference position was less than 10 cm and the difference in dimensions was less than half of the ground truth. In the figure, red squares and circles show correctly extracted footprints, green squares and circles with blue boundary lines are undetected footprints (showing ground truth), and other squares and circles show false detection. From Figure 7(b), some undetected footprints and false detections can be observed at the distant area from the scanner caused by a large point interval, but almost all footprints were extracted near the scanner, including small equipment. Similar trends can be observed in Data_B, as shown in Figure 7(c).

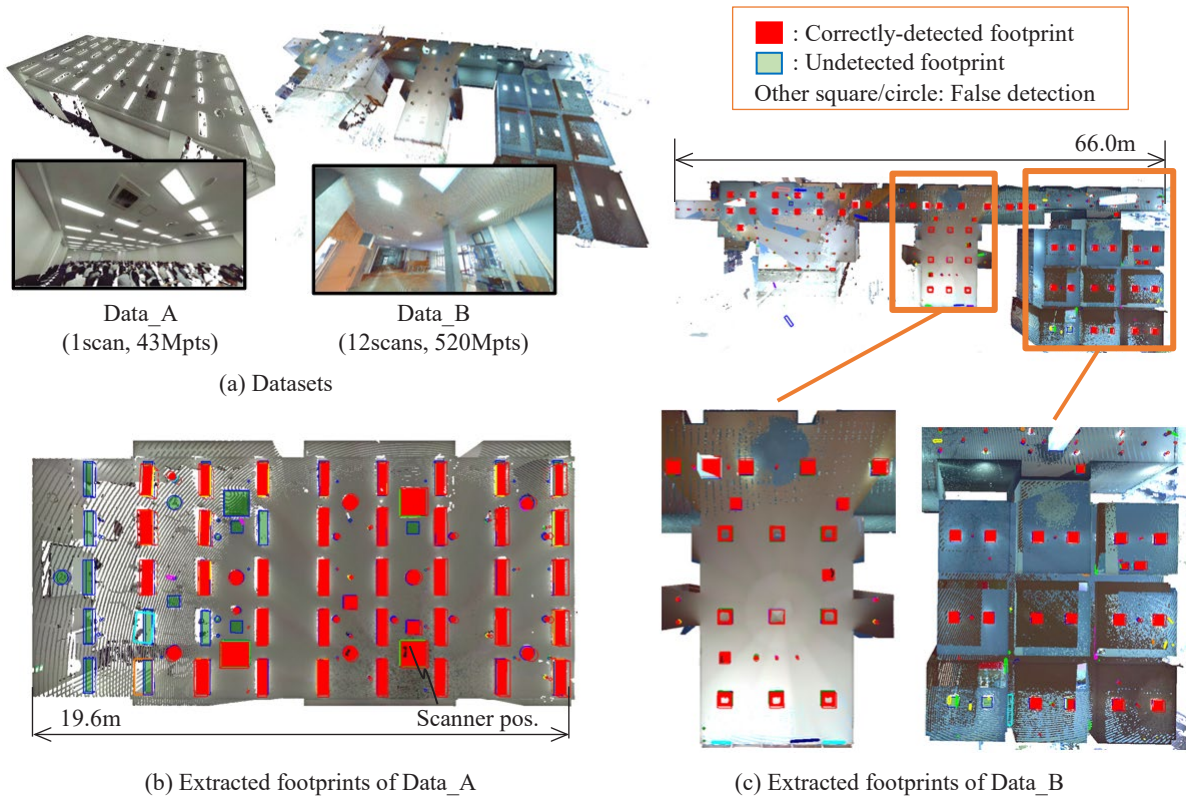


Figure 7. Point clouds for experiments and results of footprint extraction

Quantitative evaluation of the detection rate showed that footprints of equipment within 6 meters on the ceiling plane from just above the scanner can be extracted well, and the rate becomes smaller according to the distance from the scanner. In the scanning, the distance between scanner positions is often set to less than 10m, therefore evaluation within 6m is appropriate. Table 1 summarizes the footprint extraction rates of each equipment for Data_A. The evaluation was done for equipment within 6m of the scanner on the ceiling. The values in the brackets show the extraction rates of the footprint in the whole room shown in Figure 7(b). Almost all footprints, including small equipment, could be extracted, and the extraction rate for circle and square footprints was about 94%. In Data_B, detection rates for circle and square footprints were 92% (80/87) and 88% (57/65), respectively. Undetected footprints were observed in the distant area from the scanner. It is expected that scan planning considering the detection performance will improve the detection rate.

Table 1. Footprint extraction rates of Data_A*

Square FP				Circle FP					
Lighting	AC vent	Access door	Total (%)	AC vent	Speaker	Sprinkler	Camera	Fire alarm	Total (%)
14/14 (36/45)	1/1 (3/4)	2/3 (2/6)	94.4 (74.5)	2/2 (7/9)	5/5 (8/10)	4/5 (9/20)	2/2 (3/9)	2/2 (5/5)	93.8 (60.1)

* Detection rates within 6 meters on the ceiling plane. The values in the brackets show detection rates in the whole room.

4. CONCLUSIONS

In this paper, a detection method of footprints of ceiling equipment from TLS point clouds was proposed for supporting the creation of a reflected ceiling plan. The method consists of normal estimation, region growing for ceiling region extraction, circle and square fitting for detecting footprints, and footprint merging from several scans. Footprint detection rates were about 90% for two datasets of facilities with different scales. The quantitative evaluation showed that our method can detect almost all footprints of equipment within 6m from the scanner on the horizontal plane.

In future work, we will extend our method for semi-automatic RCP generation. The current method only extracts the footprints of the ceiling equipment. To realize RCPs creation, equipment labels should be assigned to each footprint. It may be difficult to automatically assign the label for footprints using only the parameters. To cluster the extracted footprints, and manually assign the label to each cluster may be one of the effective methods for efficient RCP creation.

REFERENCES

- Drost, B., Ulrich, M., Navab, N. and Ilic, S. (2010). Model Globally, Match Locally: Efficient and Robust 3D Object Recognition, *Proceedings of IEEE Computer Society Conference on Computer Vision and Pattern Recognition*, 998-1005.
- Fischler, M. A. and Bolles, R. C. (1981). Random Sample Consensus: A paradigm for model fitting with applications to image analysis and automated cartography, *Communications of the ACM*, 24 (6), 381-395.
- Golovinskiy, A., Kim, A. G., and Funkhouser, T. (2009). Shape-based Recognition of 3D Point Clouds in Urban Environments, *International Conference on Computer Vision*.
- Hossain, M., Ma, T., Watson, T., Simmers, B., Khan, J.A., Jacobs, E., and Wang, L. (2022). Building Indoor Point Cloud Datasets with Object Annotation for Public Safety, *Smart Cities, Green Technologies, and Intelligent Transport Systems*, 173-196.
- Macher, H., Landes, T. and Grussenmeyer, P. (2017). From Point Clouds to Building Information Models: 3D Semi-Automatic Reconstruction of Indoors of Existing Buildings, *Applied Sciences*, 7, 1030 (2017)
- Masuda, H. and Tanaka, I. (2010). As-Built 3D Modeling of Large Facilities Based on Interactive Feature Editing, *Computer-Aided Design and Applications*, 7(3), 349-360.
- Pan, Y., Braun, A., Brilakis, I., and Borrmann, A. (2022). Enriching geometric digital twins of buildings with small objects by fusing laser scanning and AI-based image recognition, *Automation in Construction*, 140, 104375.
- Poux, F., Mattes, C., and Kobbelt, L. (2020). Unsupervised Segmentation of Indoor 3D Point Cloud: Application to Object-based Classification, *The International Archives of the Photogrammetry, Remote Sensing and Spatial Information Sciences*, Volume XLIV-4/W1-2020, 111-118.
- Poux, F., Mattes, C., Selman, Z., and Kobbelt, L. (2022). Automatic region-growing system for the segmentation of large point clouds, *Automation in Construction*, 138, 104250.
- Qi, C. R., Yi, L., Su, H., and Guibas, L. J. (2017). PointNet++: Deep Hierarchical Feature Learning on Point Sets in a Metric Space, *Proceedings of the 31st International Conference on Neural Information Processing Systems*, 5105-5114.
- Takahashi, H., Date, H., and Kanai, S. (2019). Automatic Indoor Environment Modeling from Laser-scanned Point Clouds Using Graph-Based Regular Arrangement Recognition, *Proceedings of the 4th International Conference on Civil and Building Engineering Informatics*, 368-375.
- Takahashi, H., Date, H., Kanai, S., and Yasutake, K. (2020). Detection of Indoor Attached Equipment from TLS Point Clouds using Planar Region Boundary, *The International Archives of the Photogrammetry, Remote Sensing and Spatial Information Sciences*, XLIII-B2-2020, 495-500.

AN ALTERNATIVE METHOD FOR CABLE TENSION EVALUATION BASED ON THE TERRESTRIAL LASER SCANNING DATA

Thaniyaphat Srimontriphakdi¹, Peerasit Mahasuwanchai², Phutawan Yawananont³, Chainarong Athisakul⁴, Ekkachai Yooprasertchai⁵, Sutat Leelataviwat⁶, and Somchai Chucheeepsakul⁷

- 1) Ph.D. Candidate, Department of Civil Engineering, Faculty of Engineering, King Mongkut's University of Technology Thonburi, Bangkok, Thailand. Email: thaniyaphat.srim@kmutt.ac.th, s.thaniyaphat@gmail.com
- 2) Ph.D., Department of Civil Engineering, Faculty of Engineering, King Mongkut's University of Technology Thonburi, Bangkok, Thailand. Email: peerasit.maha@mail.kmutt.ac.th
- 3) Department of Civil Engineering, Faculty of Engineering, King Mongkut's University of Technology Thonburi, Bangkok, Thailand. Email: phutawanservice@gmail.com
- 4) Ph.D., Assoc. Prof., Department of Civil Engineering, Faculty of Engineering, King Mongkut's University of Technology Thonburi, Bangkok, Thailand. Email: chainarong.ath@kmutt.ac.th, athisakul@gmail.com
- 5) Ph.D., Department of Civil Engineering, Faculty of Engineering, King Mongkut's University of Technology Thonburi, Bangkok, Thailand. Email: ekkachai.yoo@kmutt.ac.th
- 6) Ph.D., Assoc. Prof., Department of Civil Engineering, Faculty of Engineering, King Mongkut's University of Technology Thonburi, Bangkok, Thailand. Email: sutat.lee@kmutt.ac.th
- 7) Ph.D., Prof., Department of Civil Engineering, Faculty of Engineering, King Mongkut's University of Technology Thonburi, Bangkok, Thailand. Email: somchai.chu@kmutt.ac.th

Abstract: This paper presents the results of applying terrestrial laser scanning (TLS) data to evaluate cable tension. TLS is a current technology for collecting building data with high precision. Consequently, TLS technology can be used to measure existing cable structure profiles. Generally, the actual slack cable shape profile indicates the cable tension. Therefore, the precise cable tension can be evaluated by matching the cable profile to the corresponding tension based on cable mechanics theory. In addition, the study used the nonlinear finite element method to assess the correct cable tension for the case in which bending rigidity has a significant effect. Finally, the paper presents experimental verification to demonstrate the accuracy of the proposed method.

Keywords: Cable tension evaluation, Cable structures, Nonlinear finite element, Terrestrial laser scanning, 3D point cloud data.

1. INTRODUCTION

Cable structures are applied in many infrastructure projects. Their advantages include high-tension resistance, light weight, and flexibility. However, due to the environmental loads, creep, and fatigue, the cables may become damaged, which is not easy to detect by visual inspection alone. Consequently, cable structures should be periodically monitored to evaluate cable tension and observe any damage, thus ensuring safety. Many instruments, such as accelerometers, vision cameras, laser vibrometers, are available for cable structure inspection. In addition, terrestrial laser scanning (TLS) is a current technology that can produce high-accuracy data for infrastructure monitoring. Therefore, using TLS to obtain data represents an alternative non-contact procedure for cable tension evaluation.

Many studies have previously examined methods of cable tension measurement. One of the most frequently used methods is the natural frequency-based or vibration method, which can estimate tension from the measured natural frequencies using beam theory or string theory. For example, Kim and Kim (2013) and Kim et al. (2013) proposed a method for estimating the dynamic characteristics of cables using a vision-based system combined with a digital image processing technique. This method calculates the cable tensions using vibration to evaluate the natural frequency and mode shape. However, camera vibration can occur when using this method, which generates camera-induced motion. This can be compensated for by installing an additional stationary target or using an inertial measurement system to estimate camera motion (Lee et al., 2020; Ma et al., 2022). The results of this method have been verified by comparing them to accelerometer data. Mehrabi and Farhangdoust (2018) used a laser vibrometer to record cable vibration and then calculated the dynamic properties of the cable. Their mathematical formulation for estimating tension force considers the effect of sag-extensibility and bending stiffness.

Recently, several studies have researched the cable tension evaluation method based on the static profile shape of the cables. For example, Jo et al. (2021) proposed a cable tension force evaluation method based on parabolic cable theory and the measurement of cable sag, which can be obtained from multiple digital images. The researchers performed an experiment on a cable-stayed bridge during construction. They verified the proposed method by comparing the evaluated tensions with those from the lift-off test. Zhou et al. (2021) used TLS to collect the static shape of suspension bridge cables. They identified the suspender centerline using point cloud density and then evaluated the suspender forces using a reverse calculation method based on a catenary equation. They verified the proposed method by analyzing a suspension bridge under controlled load conditions. Zhang et al.

(2022) presented an analytical approach to evaluate hanger forces based on the main cable profile. They used the high-precision total station to measure the data. Then, they applied the method to a suspension bridge to demonstrate its feasibility and effectiveness. The results of this method were verified by comparing them to those of the frequency-based method.

The current study adopts the TLS method to collect the static profile of the cable, achieving high performance and accuracy. A massive data set was collected digitally, and the geometry and dimensions of the cable profile were measured using computer software. The cable tensions were then evaluated from the static shape using a nonlinear finite element procedure and a matching process. In addition, an experiment was performed to demonstrate the presented method's effectiveness and accuracy. The study also investigated the significant effect of bending rigidity, including in the finite element model formulation.

2. METHOD

Theoretically, the different static profiles of a cable represent its corresponding internal forces. Moreover, the cable's internal force can be calculated if the cable sizes and material properties are known. However, the cable profile is essential for evaluating the tension in the cable. Therefore, this study presents the methodology for cable tension evaluation using TLS data, as shown in Figure 1. In the first step, TLS was applied to acquire data for the cable's static profile. Then, the data were processed to obtain a 3D point cloud dataset for the cable profile, as explained in Section 2.1. After that, the cable profile measurement procedure was performed to determine the sampling points and measure their coordinates. Finally, the cable tension was evaluated using the finite element procedure and optimization technique described in Section 2.2. In addition, experimental verification was performed to show the accuracy of the proposed method, as explained in Section 2.3.

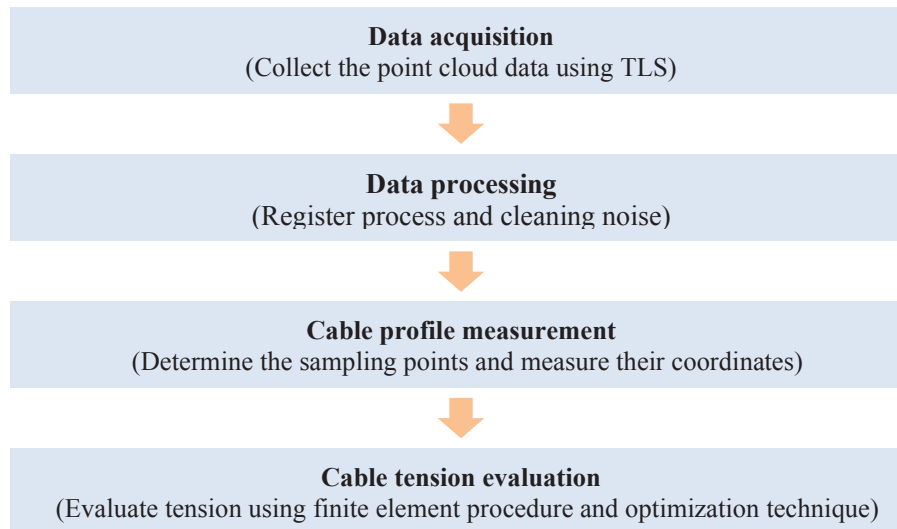


Figure 1. Cable tension evaluation workflow using terrestrial laser scanning data

2.1 Terrestrial Laser Scanning and Point Cloud Registration

The study collected data using a FARO Focus X-330 terrestrial laser scanner, which has a high performance and records massive point cloud data. TLS occurs in the horizontal and vertical directions over 360-degree and 300-degree ranges, respectively. According to the phase-shift technology principle, the scanner registers the object's surface point distance and the corresponding vertical and horizontal angles. In this study, the resolution was set at 28.2 million points for each scan, and the measurement speed was 122,000 points per scan. In the experimental verification, TLS was used to collect the data from three positions, at the middle of the span and both ends.

The registration method is a combination methodology used to analyze the point cloud dataset. This study used SCENE software to carry out the registration method on the cable. This software uses the iterative closest point (ICP) algorithm for targetless registration (cloud-to-cloud registration). Figure 2a exhibits point cloud datasets 1, 2, and 3 before the registration process, defined as blue, red, and green, respectively. At this point, the three sets of scan data had yet to be merged. After the registration procedure was carried out successfully, the cable's point cloud datasets were combined, as shown in Figure 2b. After that, each point cloud dataset was exported as an RCP file for cable evaluation.

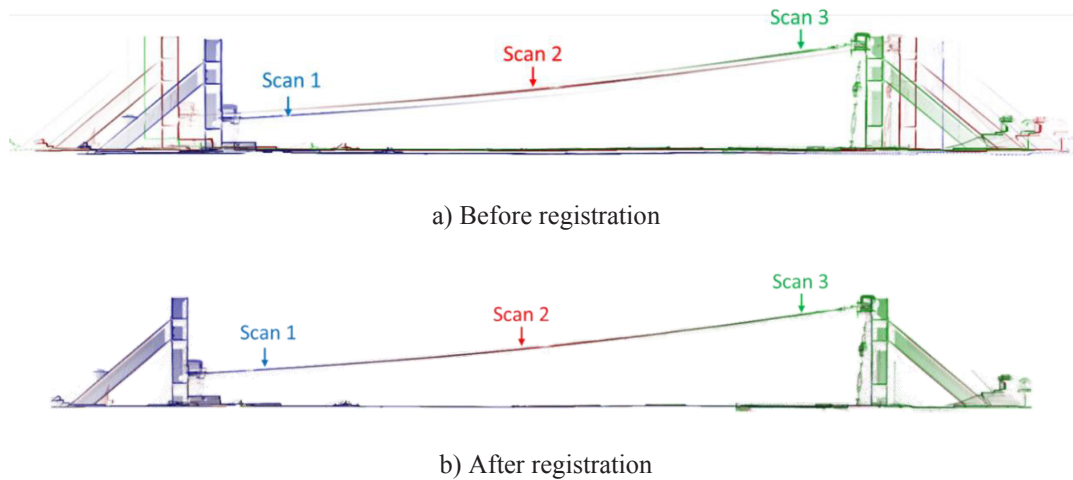


Figure 2. Point cloud registration procedure for cable profile measurement

2.2 Cable Tension Evaluation

The process of evaluating the appropriate tension is based on the idea that the corresponding profile is the shape that best fits the 3D point cloud data. Therefore, the cable coordinates obtained from the 3D point cloud data are necessary for determining the shape. This study divided the cable into six intervals with equal horizontal lengths, as shown in Figure 3. Tangent lines of the rod were created in the neighboring regions of the sampling points. The intersections of the tangent lines and interval-dividing lines were considered the coordinates of the sampling points. The bottom-end support is defined as the origin (0, 0). The coordinates of the five sampling points along the cable length and the top-end support were obtained by measuring their dimensions. This procedure was carried out using the computer software Autodesk Revit 2023.

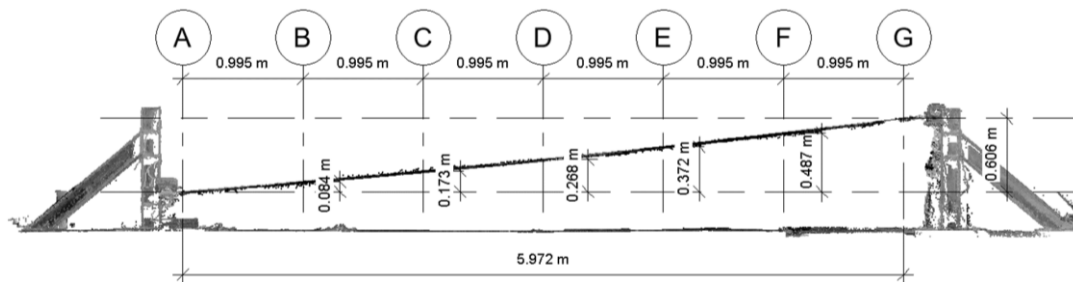


Figure 3. Measurement coordinates from the point cloud dataset

The cable profiles at any applied loads were calculated using a nonlinear finite element procedure considering the effect of bending rigidity. The vertical coordinates at the sampling points were compared with those measured from the 3D point cloud data. The best-fit shape was determined using the curve-fitting optimization technique. The criterion was to minimize the summation of the squared residuals of vertical coordinates between the finite element method and the 3D point cloud data. The cable was divided into 48 elements for the finite element procedure, and then curve-fitting optimization techniques were carried out. The overall computational time for the cable tension evaluation process was less than 1 minute for each case. During this step, the study adopted the nonlinear finite element model presented by Athisakul et al. (2011, 2012, 2014) and Chucheepsakul et al. (2003) to match the appropriate cable tension with the current cable profiles.

2.3 Experiment

In this study, cable tension was evaluated using the finite element procedure, which requires the investigation of the static shape. Therefore, experimental testing was conducted in the laboratory to verify the accuracy of the 3D point cloud registration process and the finite element procedure. The cable tension from the finite element procedure was compared to the tension from the load cell reading. The experiment used steel rods of various sizes as samples to show the effect of bending rigidity. Table 1 presents the dimensions and material properties of the rods. Samples 1 and 2 were steel rods with 17.1 mm and 21.4 mm outer diameters, respectively, with a length of 6 m. Samples 3 and 4 had 27.2 mm outer diameters with lengths of 6 m and 12 m, respectively. Samples 1 and 2 were tested for seven load cases, while samples 3 and 4 were tested for three load cases.

The experimental testing involved the following steps: The steel rods were hung on two supports at different levels to represent an inclined shape scenario. Both supports were hinges, that could rotate freely. The support on the right-hand side had a mechanism for applying force in the rods, which included a cable wire, a single pulley, a load cell, a turnbuckle, and pad eye support. The terrestrial laser scanner was used to collect data for each load case, as shown in Figure 4. The cable wire connected the rod and load cell through the single pulley. The turnbuckle was connected to the load cell and the pad eye support and could be tightened and loosened to adjust the applied load. The load cell had a maximum capacity of 300 kg with an accuracy of 0.1 kg. The details of the experimental schematic and the actual test are shown in Figures 5a and 5b, respectively.

Table 1. Dimensions and material properties of samples

Sample	Length (m)	Outer Diameter (mm)	Inner Diameter (mm)	Density (kg/m ³)	Elastic Modulus (N/m ²)
1	6	17.1	12.7	7,850	2.07x10 ¹¹
2	6	21.4	16.2		
3	6	27.2	22.2		
4	12	27.2	22.2		

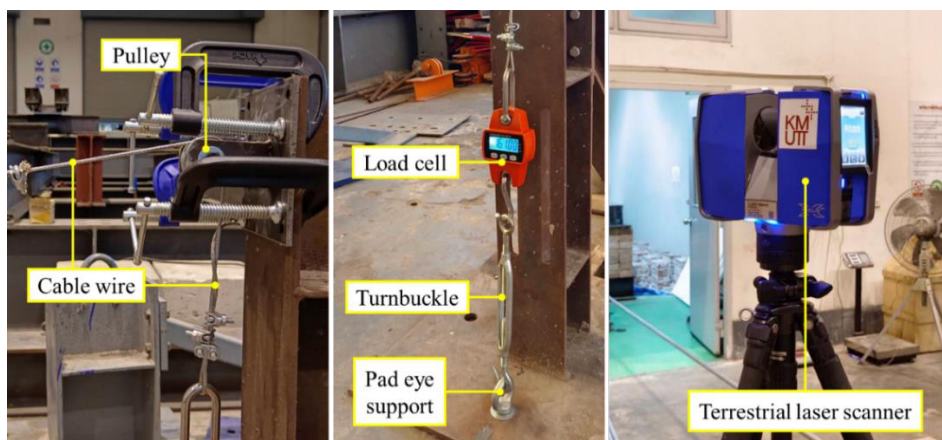
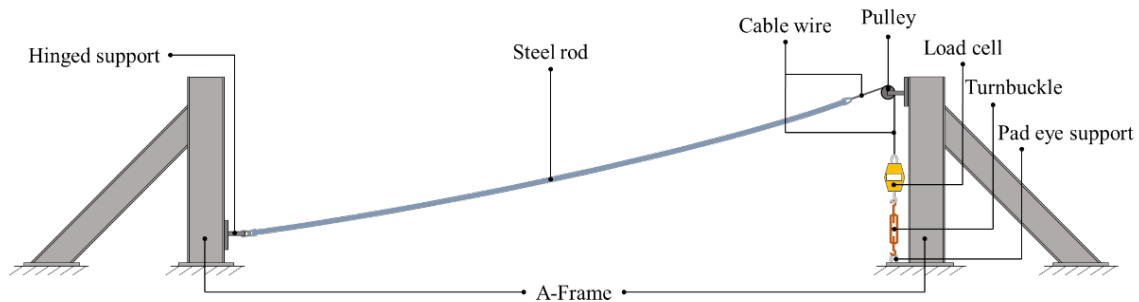


Figure 4. Equipment employed in the laboratory testing



a) Experimental schematic



b) Actual test setup

Figure 5. Experiment test setup details

For the point cloud data acquisition in the laboratory test, the steel rod's static profile was collected using a terrestrial laser scanner. The scanner was installed at a higher level than the rod. Scans were performed at three scan locations for each load case at mid-span and both end supports. Afterward, the 3D point cloud data from each scan were combined following the procedure described in Section 2.1. Finally, the tension results determined by following the procedure in Section 2.2 were compared to those collected from the load cell reading.

3. RESULTS

This study tested four steel rods samples with various applied loads experimentally. Table 2 presents the tension results evaluated from the static profile of the cable using the finite element procedure and the optimization technique. It also shows the effect of bending rigidity in the model formulation.

Table 2. Comparison between the evaluated tensions and load cell readings

Sample	Outer diameter (mm)	Length (m)	Load cell (N)	Evaluated tension (N)			
				Include bending rigidity	(%Diff.)	Exclude bending rigidity	(%Diff.)
1	17.1	6	389.6	382.7	(-1.8)	549.8	(41.1)
			574.2	565.6	(-1.5)	732.9	(27.6)
			771.4	741.3	(-3.9)	908.4	(17.8)
			967.7	968.0	(0.1)	1,135.9	(17.4)
			1,163.0	1,186.5	(2.0)	1,354.5	(16.5)
			1,356.3	1,350.5	(-0.4)	1,517.9	(11.9)
			1,551.3	1,576.6	(1.6)	1,745.6	(12.5)
2	21.4	6	587.1	595.7	(1.5)	989.0	(68.5)
			879.5	881.4	(0.2)	1,274.0	(44.9)
			1,169.0	1,177.3	(0.7)	1,570.7	(34.4)
			1,461.2	1,466.0	(0.3)	1,859.8	(27.3)
			1,752.0	1,791.0	(2.2)	2,185.3	(24.7)
			2,054.4	2,081.2	(1.3)	2,475.5	(20.5)
			2,305.3	2,310.5	(0.2)	2,702.7	(17.2)
3	27.2	6	787.0	793.8	(0.9)	1,652.8	(110.0)
			1,215.4	1,204.3	(-0.9)	2,030.0	(67.0)
			1,522.7	1,521.1	(-0.1)	2,365.2	(55.3)
4	27.2	12	1,514.7	1,460.0	(-3.6)	1,665.9	(10.0)
			2,190.4	2,161.2	(-1.3)	2,368.9	(8.2)
			2,536.7	2,525.4	(-0.4)	2,738.3	(7.9)

4. DISCUSSION

In the experimental testing, only partial 3D point cloud data was collected along the cable. More specifically, data was only collected along the top edge of the cable. A similar approach is necessary in the real world, where most cable structures are hung at a high level while the TLS processes occur at a lower level. Therefore, while the entire cable length is scanned, this only includes its bottom edge. Ideally, the profile should be measured from the centerline of the cable. However, measuring cable's top or bottom edge only is sufficient to determine the profile if the cable diameter size is known or can be measured directly through fieldwork. Consequently, the profile can be determined by perpendicularly shifting the top or bottom edge to the centerline by a distance equal to half the cable diameter.

As the results in Table 2 indicate, the tensions evaluated using the proposed method were less than 5% different from those taken from the load cell reading. All of the tensions estimated from the model formulation, excluding the effect of bending rigidity, were significantly different from those of the load cell reading. The most considerable difference, at 110.0%, occurred in the largest-size rod with the smallest applied load. When considering the same applied load of approximately 1,500 N with the same sample length, the differences were 12.5%, 27.3%, and 55.3% for rod sizes of 17.1 mm, 21.4 mm, and 27.2 mm, respectively. Moreover, the same rod size of 27.2 mm with different sample lengths of 6 and 12 m generated differences in evaluated tension up to 55.3% and 10.0%, respectively. Thus, it can be concluded that bending rigidity significantly affects cable tension. Consequently, the nonlinear finite element model formulation that considers bending rigidity is strongly recommended in the cable tension evaluation process. However, the effect of bending rigidity is reduced when either the slenderness ratio of the cable or the applied tension is increased.

5. CONCLUSIONS

This study presented an alternative method for cable tension evaluation based on TLS data. It showed that the accuracy of 3D point cloud data from a terrestrial laser scanner is sufficient for evaluating cable tension. The nonlinear finite element method was applied to assess cable tension. The experimental results show the accuracy and reliability of the finite element procedure and curve-fitting optimization technique. Considering bending rigidity in the model formulation gives better, more accurate results. However, the effect of bending rigidity is diminished as the tension or the slenderness ratio of the cable is increased.

ACKNOWLEDGEMENTS

The authors gratefully acknowledge the financial support from the Petchra Pra Jom Klao Ph.D. Research Scholarship with Grant No. 37/2564 from King Mongkut's University of Technology Thonburi to the first author and Thailand Science Research and Innovation (TRSI) Basic Research Fund: Fiscal year 2023 under project number FRB660073/0164 (Advanced and Sustainable Construction Towards Thailand 4.0).

REFERENCES

- Athisakul, C., Klaycham, K., and Chucheeepsakul, S. (2014). Critical top tension for static equilibrium configuration of steel catenary riser, *China Ocean Engineering*, 28 (6), 829-842.
- Athisakul, C., Monprapussorn, T., and Chucheeepsakul, S. (2011). A variational formulation for three-dimensional analysis of extensible marine riser transporting fluid, *Ocean Engineering*, 38 (4), 609-620.
- Athisakul, C., Phanyasachart, T., Klaycham, K., and Chucheeepsakul, S. (2012). Static equilibrium configurations and appropriate applied top tension of extensible marine riser with specified total arc-length using finite element method, *Engineering Structures*, 34, 271-277.
- Chucheeepsakul, S., Monprapussorn, T., and Huang, T. (2003). Large strain formulations of extensible marine pipes transporting fluid, *Journal of Fluids and Structures*, 17 (2), 185-224.
- Jo, H.C., Kim, S.H., Lee, J., Sohn, H.G., and Lim, Y.M. (2021). Sag-based cable tension force evaluation of cable-stayed bridges using multiple digital images, *Measurement*, 186, 110053.
- Kim, S.W., and Kim N.S. (2013). Dynamic characteristics of suspension bridge hanger cables using digital image processing, *NDT&E International*, 59, 25-33.
- Kim, S.W., Jeon, B.G., Kim, N.S., and Park, J.C. (2013). Vision-based monitoring system for evaluating cable tensile forces on a cable-stayed bridge, *Structural Health Monitoring*, 12 (5-6), 440-456.
- Lee, J., Lee, K.C., Jeong, S., Lee, Y.J., and Sim, S.H. (2020). Long-term displacement measurement of full-scale bridges using camera ego-motion compensation, *Mechanical Systems and Signal Processing*, 140, 106651.
- Ma, Z., Choi, J., and Sohn, H. (2022). Noncontact cable tension force estimation using an integrated vision and inertial measurement system, *Measurement*, 199, 111532.
- Mehrabi, A.B., and Farhangdoust, S. (2018). A laser-based noncontact vibration technique for health monitoring of structural cables: background, success, and new developments, *Advances in Acoustic and Vibration*, 2018, 1-3.
- Zhang W.M., Tian, G.M., Zhao, H.X., Wang, Z.W., and Liu, Z. (2019). Analytical methods for the assessment of hanger forces of a suspension bridge based on measured main cable configuration, *Advances in Structural Engineering*, 23 (7), 1-15.
- Zhou, Y., Xiang, Z., Zhang, X., Wang, Y., Han, D., and Ying, C. (2021). Mechanical state inversion method for structural performance evaluation of existing suspension bridges using 3D laser scanning, *Computer-Aided Civil and Infrastructure Engineering*, 37 (5), 650-665.

INTEGRATING BIM INTO WEB GIS TO ENHANCE THE VISUALIZATION OF PORT INFRASTRUCTURE

Le Vin Tran^{1,3,4*}, Minh Chung Bui^{1,3,4}, Van Tan Nguyen^{1,3,4},
Tuan Anh Le^{1,3}, Danh Thao Nguyen^{1,3}, Bao Binh Luong^{2,3}, Hiep Hoang⁴

1) Department of Port and Coastal Engineering, Faculty of Civil Engineering, Ho Chi Minh City University of Technology (HCMUT), 268 Ly Thuong Kiet, District 10, Ho Chi Minh, Vietnam

2) Department of Geomatic Engineering, Faculty of Civil Engineering, Ho Chi Minh City University of Technology (HCMUT), 268 Ly Thuong Kiet, District 10, Ho Chi Minh, Vietnam

3) Vietnam National University Ho Chi Minh City, Linh Trung Ward, Thu Duc District, Ho Chi Minh, Vietnam

4) Portcoast Consultant Corporation, Ho Chi Minh City, Vietnam

*Corresponding author's email: tlvin.sdh221@hcmut.edu.vn

Abstract: This paper provides a detailed procedure to transform a seaport into a digital format, with the objective of creating a precise, effective BIM model of the port infrastructure. We execute on-site surveys to acquire point cloud data of the port infrastructure, encompassing a variety of data types from terrestrial to underwater regions. Additionally, we suggest a solution for data collection in inaccessible areas, by utilizing a range of equipment and combining advanced survey technologies to overcome the limitation of each separate survey type. The collected data undergoes processing to generate a comprehensive BIM model of the port, which encompasses data from the land to the underwater area. This BIM model is subsequently converted to a GIS-compatible format, and then integrated into the ArcGIS online platform. This fusion allows the merging of engineering design data with geospatial attributes into a comprehensive model. The final output, as demonstrated in a real case study of seaport in Vietnam, will be presented along with insights into optimizing data processing for integration.

Keywords: BIM, GIS, Laser scanning, USVs, UAS, Point cloud

1. INTRODUCTION

Building Information Modeling (BIM) is a digital process used in the construction and management of a virtual designed model for building or infrastructure projects. This innovative method employs various software tools to foster collaboration among diverse stakeholders such as designers, architects, engineers, and contractors, who all contribute to a singular, cohesive model of the construction project. This model contains 3D visuals along with the specifications of individual building components, including their materials, size, performance metrics, and maintenance requirements. Prior to integrating the BIM process into any building project, it's crucial to perform a 3D survey to collect essential geometric data for producing the 'as-built' model of the structure (Murphy et al., 2017), in addition to gathering other types of relevant data. This step calls for the use of cutting-edge 3D survey techniques like 3D laser scanning or photogrammetry, which generate point clouds as the foundation for the subsequent parametric modeling phase (Wang et al., 2019). There are several proven methods to transform point clouds into a BIM model, as documented in a wide array of literature (Moyano et al., 2020; Pepe & Costantino, 2020).

The use of 3D digital models and the object parameterization within the Building Information Modeling (BIM) environment allows for a comprehensive association of physical and mechanical characteristics with each structural or architectural component, along with any additional relevant information. However, most contemporary research primarily concentrates on the generation of BIM models for terrestrial structures. The question remains on how to handle data not based on land, such as underwater data, which is relatively important for projects like seaports.

Moreover, the capacity of the BIM environment to store and detail elements is somewhat restricted. This limitation can be addressed by associating semantics, images, or other forms of information with model components using a specialized field. Applications of these models can be seen in Cultural Heritage contexts (Pepe & Costantino, 2020), and in complex structures like historical bridges and cathedrals.

To counteract the constraints of BIM, initiatives are underway to connect BIM with external databases for streamlined data management. These solutions are expected to enhance flexibility in data access and administration in the future (Adami et al., 2018).

Addressing these limitations requires the identification of an efficient environment capable of managing various databases and bridging them with 3D spatial objects. In this context, a 3D Geographical Information System (GIS) environment provides the ability to establish numerous fields and link multiple databases from a variety of sources. These sources can encompass satellite images, aerial photos, terrestrial and underwater surveys, and more. The 3D GIS environment is further useful for generating maps and performing spatial data analyses. In addition, Web GIS, a variant of GIS, leverages the internet to provide access to geospatial data and analysis tools. This system allows users to retrieve GIS data and tools from any location via a web browser, thus facilitating data sharing and collaboration. Since users can access the same data from anywhere with internet connectivity, Web

GIS broadens accessibility to a more diverse range of users, including those without prior GIS expertise. (Narindri et al., 2022)

Building Information Modeling (BIM) and Geographic Information Systems (GIS) can work together to enhance building and infrastructure planning, design, and operation. However, integrating data from various survey technologies into GIS can be challenging due to disparities in data formats, resolution, accuracy, and georeferencing methods.

This paper will detail the process of high-accuracy field data collection for BIM models and integrating BIM data into web GIS. This approach has been applied to a port infrastructure project in Vietnam, where the BIM model includes data from aerial, terrestrial, and underwater sources.

2. METHODOLOGY AND PROCEDURES

2.1. Data Acquisition

Data collection for a BIM-GIS project requires details on a building or infrastructure's physical and functional attributes, along with its spatial context. This data aids in crafting a precise digital model for design, construction, and operation. Various surveying techniques are often combined to solve the problem of location challenges, especially when surveying objects such as the seaport, situated at land-sea interfaces. Terrestrial Laser Scanning (TLS) was utilized for on-land surveys, while a UAV photogrammetric survey targeted upper building parts inaccessible from the ground. Additionally, a USV multibeam sonar system collected data for the underwater and front-side port regions.

The Trimble GNSS R12i, known for its high-precision capabilities, was used during the survey to collect GPS data and create accurate control points, thereby enhancing the point cloud and grid model data's accuracy. The data's reliability was crucial for accurate analyses.

- **Terrestrial 3D laser scanning**

3D laser scanning, an advanced technique using directed laser beams, records characteristics of various objects around a structure (Guo et.al., 2020). This highly accurate process can create a detailed 3D model of the surveyed area, covering large expanses across diverse terrains without line of sight (Zhou et al., 2019).

In this study, laser scanning was employed on land to gather precise point cloud data of equipment and buildings. Preceding the scan, a traverse network was established and adjusted, with each point's coordinates and elevation measured via a Leica TS60 total station and LS10 digital level, respectively, to ensure high accuracy. Leica RTC360, P50, and Trimble SX12 scanners were then used to capture all physical features of the existing facilities. Main scanners were stationed at each traverse point, with additional scanners closer to the traverse network to record shape, size, and surface color details of existing objects. Figure 1.a displays the onsite 3D laser scanning process. The TLS collected data then was processed using professional software like Cyclone to serve as the source for BIM model creation and the base map in GIS.

- **Aerial surveying with drones**

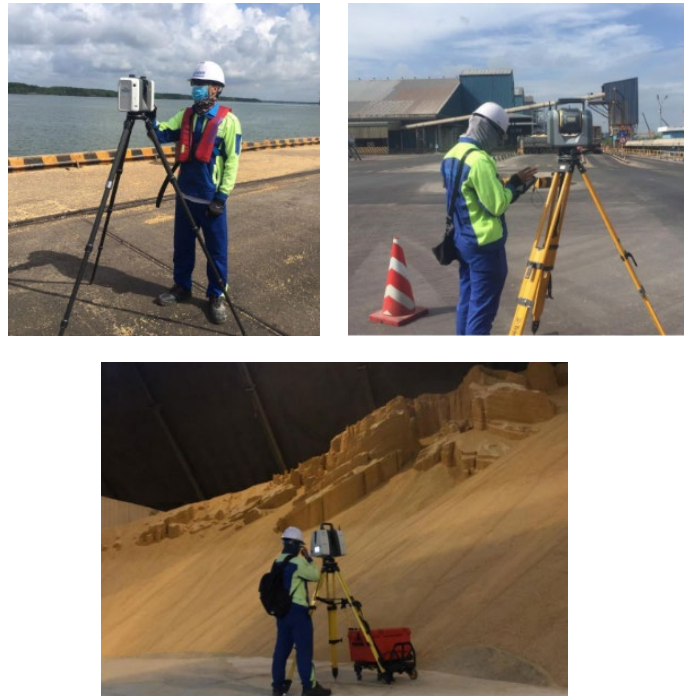
Aerial surveys are utilized to address on-land surveying limitations, particularly when terrestrial laser scanning is less effective due to large site size or inaccessible areas like high roofs. Modern unmanned aerial systems (UAS) with high-quality cameras, onboard GPS, and other sensors have streamlined aerial surveys (Abdulla Al-Kaff et al., 2018). The captured images undergo processing using photogrammetry techniques for delivering accurate and detailed 3D information from measured image correspondences at any scale.

In this project, a 3D map of the port area was field-collected using a DJI Matrice RTK300- Zenmuse P1 with a 45MP Full-frame Sensor (Figure 1.b). The drone followed designed flight paths to capture overlapping aerial photos every 0.7 seconds over the worksite (Figure 1b- right hand side). The Zenmuse P1 can capture centimeter-accurate data with real-time position and orientation compensation technology. In essence, the drone's GPS and onboard sensors embed latitude, longitude, and altitude data in the image metadata as it's captured. These images are then processed and analyzed using DJI Terra software, which employs photogrammetry techniques to generate photorealistic 3D representations of land surfaces and various objects within the port area.

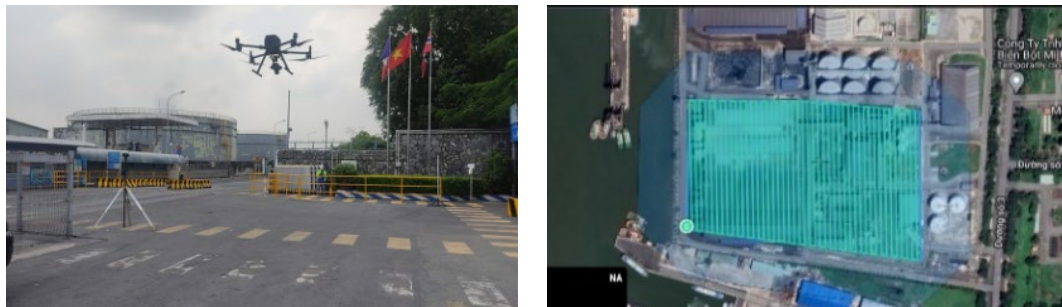
- **Underwater surveying with USVs**

Neither aerial nor terrestrial surveys can collect data from the wharf's edge to the underwater area. Thus, Unmanned Surface Vehicles (USVs) equipped with integrated iLiDAR and multibeam echo sounders are used to gather bathymetric and point cloud data of the wharf's front side. For this project, the Otter USV system, which includes two GNSS devices to receive coordinate, elevation, and orientation data, is utilized (Figure 1c).

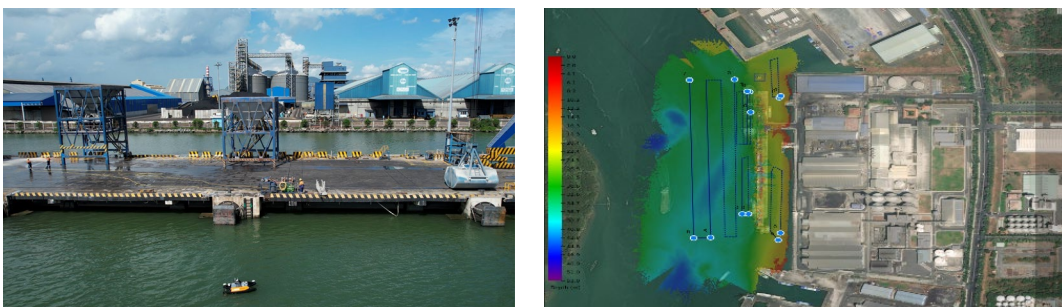
Before surveying, a high-precision control grid based on a coordinate system is established, setting the elevation for the entire project. Concurrently, an automatic water level monitoring station is set up on the shore as an RTK measurement method base station. Once the iLiDAR and Norbit iWBMS devices are attached to the Otter system, the USVs are launched to collect bathymetric data and 3D point cloud data of the wharf's front side.



a) Terrestrial 3D laser scanning



b) Aerial survey



c) Underwater survey

Figure 1. Conducting the field surveys

2.2. BIM

The process of reconstructing 3D models from profiles, as discussed by D. Costantino in 2021, can be used to construct a 3D model. This technique leverages a 3D point cloud to reconstruct the object or structure's 3D form using either a curve or a parametric surface. The collected point cloud data is then exported and imported into suitable software such as Revit, which aids in the model's creation (as shown in Figure 2). By considering the distance between the object surface's points within the point cloud and the similarity in direction of the neighboring standard faces, an engineer can create an as-built model. After this data is integrated into the software, building

components are designed in the BIM model, utilizing the point cloud data and the collected images. The final stage involves correlating the BIM model's components with the point cloud to ensure each component aligns with its respective points in the point cloud.

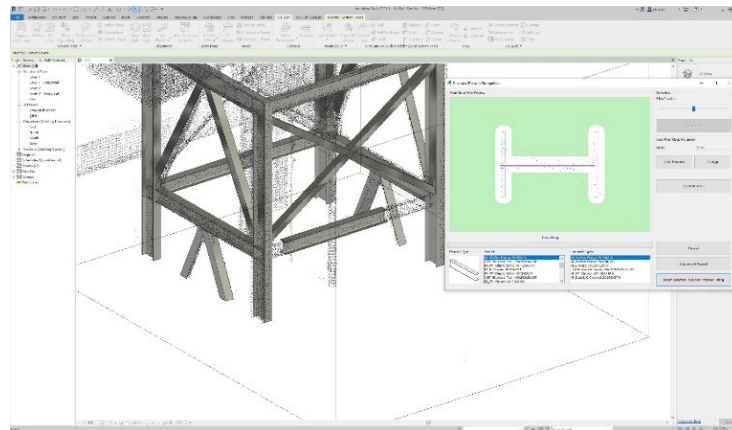


Figure 2. Building Revit model from point cloud data

2.3. Web GIS

ArcGIS Online is a cloud-based platform that integrates numerous powerful geospatial analysis tools and capabilities from Esri. Currently, this WebGIS platform is widely used for visualizing both 2D and 3D data, particularly 3D models such as building information models (BIM), 3D meshes, and 3D point clouds. Choosing a common platform like ArcGIS Online for storing and sharing data can facilitate access to and retrieval of data from any location, thus providing convenience for data management and analysis.

2.4. BIM – GIS Integration

Due to the benefits that the integration of Building Information Modeling (BIM) and Geographical Information Systems (GIS) offers, it has been the subject of extensive research and implementation across a diverse range of application field, particularly in planning and operation (Matrone et.al., 2019). The overall process of integration is illustrated in Figure 3. The accepted data format and procedure for uploading each type of data are described in the following sections.

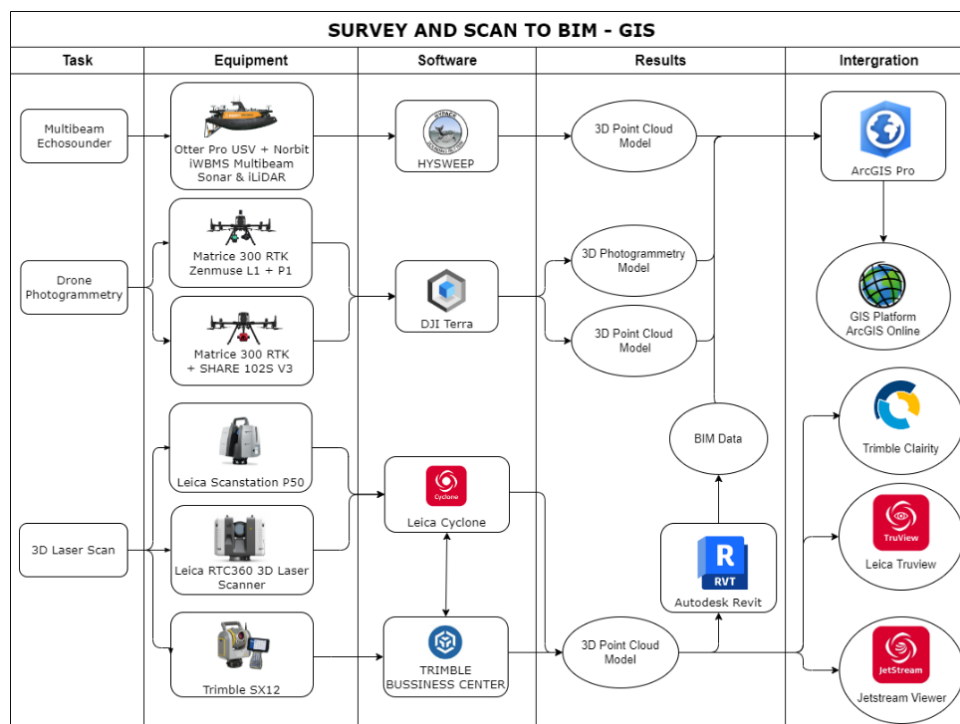


Figure 3. Workflow for collecting, processing and integrating data.

3. RESULTS

The South Vietnam port case study involved conducting several surveys to gather detailed information, which included bathymetric details, 3D laser scanning point cloud data, and aerial images. These data were merged to create a comprehensive digital model of the port. For the 3D laser scanning the cluster approach was applied to organize 3D laser scanning into logical sections. The precision achieved in internal areas was 1-3mm, and in external areas, it was 3-5mm. The survey results obtained through terrestrially conducted surveys are illustrated in Figure 4.

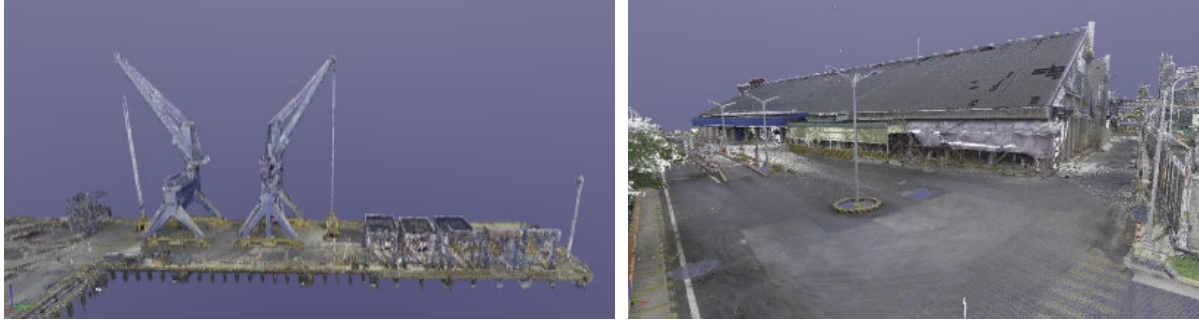


Figure 4. 3D point cloud of the wharf and the warehouse

The drone survey involves processing aerial images using DJI Terra software (Figure 5a). The images are captured with an approximate overlap of 70-80%. The initial steps involve stitching the images and generating a preliminary point cloud model. In order to adjust the images to the desired coordinate system, Ground Control Points (GCPs) are added. The deviations between the GCPs and the 3D Mesh model are shown on Table 1. Once the images are adjusted, they are exported to digital models, like 3D Mesh, which are evaluated based on mapping regulations. The 3D mesh data for the entire port area is exported in *.slpk format and uploaded onto ArcGIS Online, where it is displayed alongside other survey data which includes underwater topography and 3D laser scans.

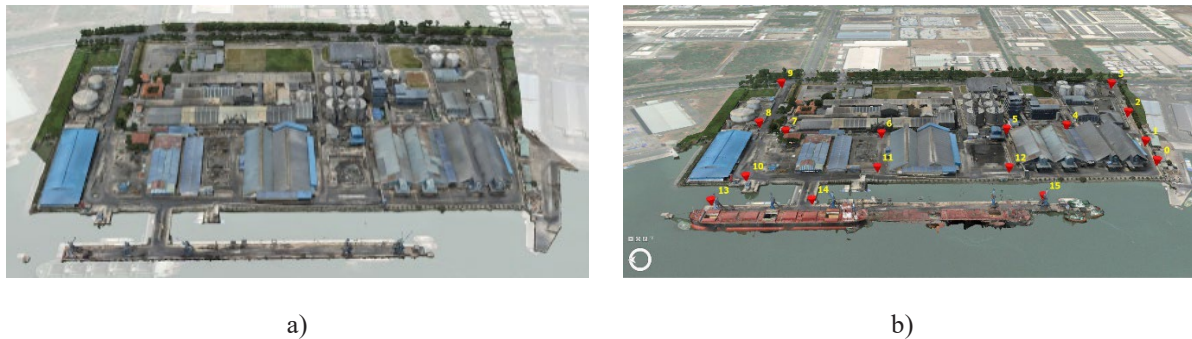


Figure 5. (a) 3D photogrammetry model of the port area, (b) Targets (Ground control points) layout.

Table 1. Detailed Comparison Table of Point Position Errors between GCPs and 3D Mesh model

Point ID	3D Photogrammetry model			Targets			Deviation
	x	y	z	x	y	z	
1	421038.131	1170449.281	2.774	421038.130	1170449.280	2.770	0.004
2	421167.175	1170435.472	2.724	421167.170	1170435.470	2.720	0.007
3	421325.556	1170417.005	3.144	421325.550	1170417.000	3.140	0.009
4	421110.122	1170563.385	2.653	421110.120	1170563.380	2.650	0.006
5	421097.127	1170670.862	2.944	421097.120	1170670.860	2.940	0.008
6	421085.373	1170886.116	3.215	421085.370	1170886.110	3.210	0.008
7	421101.143	1171049.992	3.092	421101.140	1171049.990	3.090	0.004
8	421141.386	1171102.745	2.704	421141.380	1171102.740	2.700	0.009

Point ID	3D Photogrammetry model			Targets			Deviation
	x	y	z	x	y	z	
9	421355.751	1171099.625	2.931	421355.750	1171099.620	2.930	0.005
10	420933.363	1171081.334	2.906	420933.360	1171081.330	2.900	0.008
11	420956.994	1170889.284	2.852	420956.990	1170889.280	2.850	0.006
12	420949.666	1170689.862	2.554	420949.660	1170689.860	2.550	0.007
13	420861.055	1171112.697	3.643	420861.050	1171112.690	3.640	0.009
14	420860.183	1170975.995	3.053	420860.180	1170975.990	3.050	0.007
15	420858.766	1170657.021	3.476	420858.760	1170657.020	3.470	0.009

(*) Note:

- Unit (m)
- Coordinates and elevations of Targets are measured using electronic total station devices.

The bathymetric and iLiDAR data from the USV survey were processed and checked for errors using Hysweep software. A raw point cloud model in *.e57 or *.las format was then generated, mapping the underwater terrain and the wharf's front side. For the accuracy checking, the comparison between the 3D Point Cloud model and Ground Control Points (Figure 6) are conducted (Table 2). This point cloud data was then imported to Autodesk Recap Pro or Leica Cyclone software for noise removal and data integration. Ultimately, the highly precise point cloud data for the area in front of the port was exported (Figure 7). To enhance storage efficiency, processing time, and rendering speed on the ArcGIS Online platform, the file formats *.las and *.e57 will be transformed into the Point Cloud Scene Layer format (*.slpk). Point cloud scene layers are capable of swiftly rendering significant amounts of symbolized and filtered point cloud data, ensuring rapid display of such datasets.

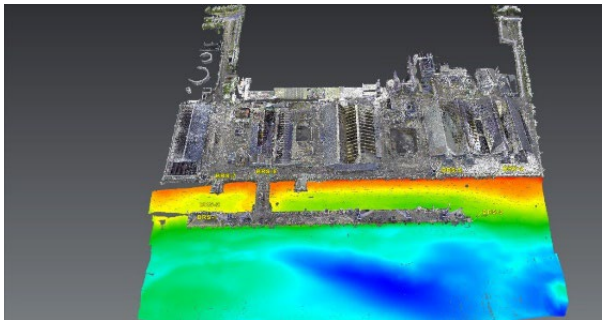


Figure 6. Targets (Ground control points) layout.

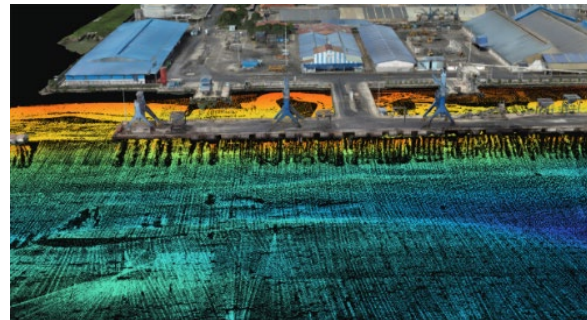


Figure 7. The point cloud model of the water area in front of the wharf and the slope of the shoreline and 3D mesh model of port.

Table 2. Detailed comparison of Point Position Errors

Point ID	Point Cloud			Targets			Deviation
	x	y	z	x	y	z	
BRS-1	420836.927	1171114.459	3.32	420836.917	1171114.459	3.315	0.011
BRS-2	420861.34	1171114.479	3.277	420861.34	1171114.478	3.279	0.002
BRS-3	420833.758	1170611.984	3.304	420833.757	1170611.985	3.303	0.001
BRS-4	420921.616	1170553.975	1.771	420921.617	1170553.976	1.773	0.002
BRS-5	420921.833	1170669.987	0.423	420921.832	1170669.988	0.423	0.001
BRS-6	420928.025	1171019.57	1.28	420928.026	1171019.576	1.289	0.010
BRS-7	420921.174	1171094.753	0.099	420921.173	1171094.752	0.097	0.002

(*) Note:

- Unit (m)
- Coordinates and elevations of Targets are measured using electronic total station devices.

Formula for evaluating Point Position Error:

$$\text{Deviation} = \sqrt{(X2 - X1)^2 + (Y2 - Y1)^2 + (Z2 - Z1)^2} \quad (1)$$

The final product from the BIM-GIS integration can be observed in Figure 8. With this WebGIS based model, the data can be shared, together with the huge amount of data to other stakeholders. Noted that the integrated model provides all information of all types of available measurable data related to the port. Furthermore, the 3D visualization makes the representation of the port more intuitive.

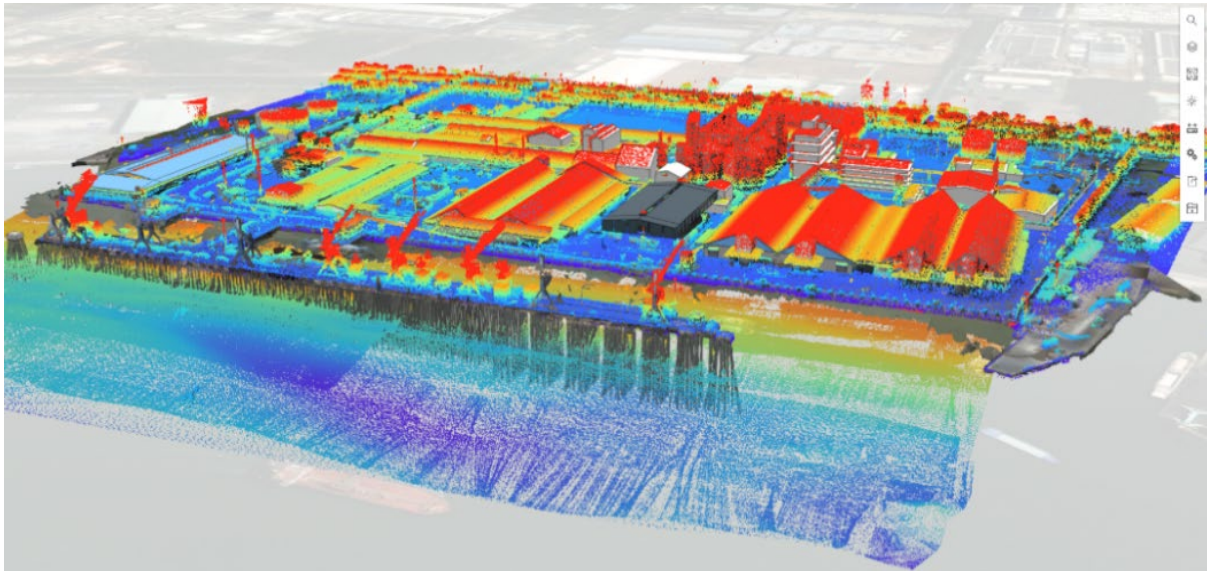


Figure 8. Integrated model visualization on ArcGIS online

4. CONCLUSIONS

This research provides a valuable case study for the application of innovative technology in infrastructure management. Through the integration of Building Information Modeling (BIM) with a WebGIS platform, we have constructed a comprehensive 3D representation of a port infrastructure system. This integration not only enriches the visual understanding of the data but also improves its practical applicability for engineering design and geographical information. The fusion of BIM and WebGIS technologies demonstrates the potency of combined systems in streamlining complex procedures and enhancing the user experience. This combination serves as a significant step in the digital transformation era, highlighting the progressiveness of innovation. As the result of data integrating, the format of output data as *. slpk is recommended to enhance the process speed in WebGIS environment. Future research should focus on improving the user interface, including additional data types, assessing performance, and addressing potential security and privacy concerns.

ACKNOWLEDGEMENTS

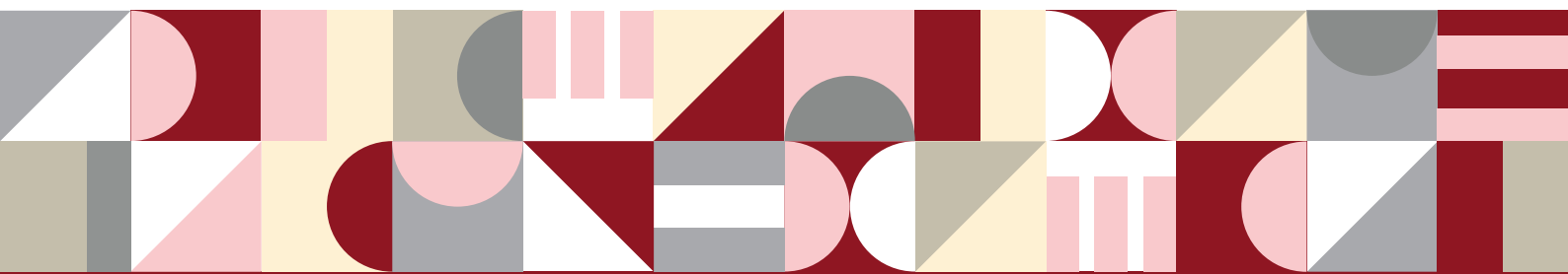
We express our gratitude to Ho Chi Minh City University of Technology (HCMUT), VNU-HCM for their support in facilitating this study. Our sincere thanks also go to Portcoast Consultant Corporation for their valuable time and resources contributed to this research.

REFERENCES

- Abdulla Al-Kaff, David Martín, Fernando García, Arturo de la Escalera, José María Armingol (2018). Survey of computer vision algorithms and applications for unmanned aerial vehicles, *Expert Systems with Applications*, Volume 92, Pages 447-463.
- Adami, A., Bruno, N., Rosignoli, O., Scala, B. (2018). HBIM for planned conservation: a new approach to information management, *Proceedings of the Visual Heritage*.
- Costantino, D., Pepe, M., Restuccia A.G. (2021). Scan-to-HBIM for conservation and preservation of cultural heritage building: the case study of San Nicola in Montedoro church (Italy), *Appl. Geomat.*

- Moyano, J., Odriozola, C.P., Nieto-Julián, J.E., Vargas, J.M., Barrera, J.A., León, J. (2020). Bringing BIM to archaeological heritage: interdisciplinary method/strategy and accuracy applied to a megalithic monument of the Copper Age, *J. Cult. Herit.* 303–314.
- Guo, J., Wang, Q. and Park, J.-H. (2020). Geometric quality inspection of prefabricated MEP modules with 3D laser scanning, *Automation in Construction*, vol. 111, p. 103053.
- Pepe, M., Costantino D., (2020). UAV Photogrammetry and 3D Modelling of Complex Architecture for Maintenance Purposes: The Case Study of the Masonry Bridge on the Sele River, Italy, *Periodica Polytechnica Civil Engineering*.
- Pepe, M., Costantino, D., Restuccia Garofalo, A. (2020). An efficient pipeline to obtain 3D model for HBIM and structural analysis purposes from 3D point clouds, *Appl. Sci.* 10 (4) 1235.
- Matrone, F., Colucci, E., De Ruvo, V., Lingua, A., and Spanò, A. (2019). HBIM in a Semantic 3D GIS Database, *ISPRS Ann. Photogramm. Remote Sens. Spat. Inf. Sci.*, 42(2/W11), 2019, pp. 857– 865, doi: 10.5194/isprs-Archives-XLII-2-W11- 857-2019.
- Murphy, M., Corns, A., Cahill, J., Eliashvili, K., Chenau, A., Pybus, C., Shaw, R., Devlin, G., Deevy, A., and Truong-Hong, L., (2017). Developing historic building information modelling guidelines and procedures for architectural heritage in Ireland. *Int. Arch. Photogramm. Remote Sens. Spatial Inf. Sci.*, XLII-2/W5, 539–546, <https://doi.org/10.5194/isprs-archives-XLII-2-W5-539-2017>.
- Narindri, B. P. K., et al. (2022). Developing Building Management System Framework using Web-based-GIS and BIM Integration, *Civil Engineering Dimension* 24(2): 71-84.
- Wang, Q., Guo, J., Kim, M.-K., (2019). An Application Oriented Scan-to-BIM Framework. *Remote Sensing*, 11(3), 365, 2-27. <https://doi.org/10.3390/rs11030365>.
- Zhou, Y.-W., Hu, Z.-Z., Lin, J.-R. and Zhang, J.-P. (2019). A review on 3D spatial data analytics for building information models, *Archives of Computational Methods in Engineering*, vol. 27, no. 2, pp. 1–15.

Smart Cities and Infrastructure Management



ON THE VISUAL ASPECT OF THE INFORMATION SCAPE IN THE BUILT ENVIRONMENT: SHILIN NIGHT MARKET AS AN EXAMPLE

Ye Yint Aung¹ and ShenGuan Shih²

1) Doctoral Student, Department of Architecture, College of Design, National Taiwan University of Science and Technology, Taipei, Taiwan. Email: D11013803@mail.ntust.edu.tw

2) Ph.D., Prof., Department of Architecture, College of Design, National Taiwan University of Science and Technology, Taipei, Taiwan. Email: sgshih@mail.ntust.edu.tw

Abstract: How would a restaurant guest choose her favorite seat to dine in? How would prey animals place and orient themselves when feeding on grassland where predators might be around? Is it possible that the answers to the two questions might have similar traces of reasoning? Our perception of space is inherited from our ancestors, who were capable of sensing danger and opportunities for food and mates in the environment. An information scape is a representation of the flow of information that is accessible to a specific location in the environment. The hypothesis is that the tendency to locate oneself at an advantageous information scape is a part of human nature. The spatial experience of a person in a specific space can be diverse in terms of the availability of information within the environment. The information can be acquired through various senses such as odor, vision, taste, audition, and contact. Vision is the distinct sensory source of a human's perception of acquiring information in the built environment. Isovist analysis is a useful measurement of the visible field from a specified location in architectural and urban contexts. Isovist is adopted and extended in this study with Monte Carlo simulation to analyze information scape in an urban space. Shilin night market in Taipei, one of the well-known business and tourist attraction areas, exemplifies as the research area for information scape analysis. A measurement based on information scape analysis is used to quantify the accessibility and availability of information regarding the visible boundary from different spatial metrics of the Shilin environs. Overall, this paper displays that information scape analysis has the potential for studying the complex interaction between spatial configuration and human behavior in the aspect of information availability.

Keywords: Information scape, Information availability, Isovist analysis, Visibility, Spatial experience.

1. INTRODUCTION

Our perception of space is genetically inherited from our ancestors, who were capable of sensing danger and opportunities for food and other benefits from the environment. It can be imagined that preferring a corner table against a wall or a post where a panoramic view of the surrounding can be enjoyed in a restaurant, or crowds of visitors sitting in certain spots and appreciating the landmark of the specific location are some of the scenarios of people sensing information and making beneficial or directional decisions from the given environment. In other words, human nature involves a desire to position oneself in a favorable informative periphery to take advantage of own sake. Information scape in a built environment can be conceptualized as the network of spatial information perceived and processed that influences the human being to navigate, wayfinding, percept, and adapt it to take benefit of their own in terms of their various natural senses. It is vital to learn about information landscapes to design appropriate spaces and neighborhoods that promote human activity and well-being. Yet, since the intricate connection between spatial information and arrangement, conceptualizing the framework for assessing information scape is generally a challenging matter.

The medium of spatial information can be acquired depending on the type of information being conveyed and the situation in which it is presented. Billboards, directional signages, advertisements, digital displays, and sometimes, even human being themselves are some of the forms of information sources in public areas. Shreds of evidence and information can be attained by different kinds of natural sensors belonging to human beings: odor, vision, taste, audition, and contact. Among other sensory abilities, vision is the distinct sensory source of a human's perception for collecting information and activating consequent behaviors.

To address this challenge, isovist has emerged as a viable approach for studying visible and spatial experience in both architectural and urban environments. Isovist and isovist fields have been prevalent in assessing various social, visual, cognitive, and behavioral patterns of architectural and urban neighborhoods. Benedikt (Benedikt, 1979) argued the idea of isovist which involves either isovist or a series of isovists, isovist field, and a number of their measurables can be derived to statistically quantify the visual quality of a space. The isovist field is more beneficial for understanding the building as a whole than the individual isovist, which is valuable for understanding specific places in a structure or the experience of a particular type of user (Dawes & Ostwald, 2021). Despite a collection of research on social and spatio-visual properties of the environment using isovist, it is found that the relationship between information availability and isovist has not been fully explored.

In this paper, isovist is proposed and extended with Monte Carlo simulation to analyze information scape in the environment. It aims to investigate how the physical setting can influence the availability and accessibility

of information and, in turn, how individuals traverse and engage with the environment regarding the limited available source. The approached framework is demonstrated through a case study of Shilin night market, a well-known business district in Taipei. Overall, this research contributes that information scape analysis has the potential for architects and urban designers to comprehend the complex interaction between spatial configuration and human behavior in the aspect of information availability.

2. ISOVIST AND INFORMATION SCAPE IN THE BUILT ENVIRONMENT

The term “built environment” simply refers to all buildings and amenities created by man to support their activities (Portella, 2014, p. 454). The concept of the built environment becomes intricate when it comes to analyzing its quality regarding a web of social, behavioral, visual, ecological, cultural, and economic relationships leading to the built environment as a complex system. The framework measuring the quality of a particular space or area in a built environment has been made using different research methodologies in the past decades. Geoff Boeing (Boeing, 2018) identified the framework of indicators measuring the complexity of spaces in urban environments regarding the temporal, visual, spatial, scaling, and connectivity of the spaces, enabling the designer to analyze and access diverse aspects of the built environment. This matrix can assist designers to study the current complex design problem in both top-down and longitudinal directions and help to assist predicted anticipated or unanticipated deviations in the built environment. Among them, visual complexity is the issue that closely impacts visual perception and information availability in the architectural and urban fabric.

Visual complexity refers to the degree of arrangement among physical components of the environment such as the characteristics of buildings, walkways, directional and business signs, etc. It is closely tied to information scape and isovist among mentioned indicators since information availability in the environment can have an impact on visual complexity. In other words, a space with less information tends to be visually simple, whereas a space with dense information is likely to be visually complex. Urban activist Jane Jacobs argued that visual diversity impacts the behavioral pattern of people walking in urban neighborhoods (Jacobs, 1961). She extended that people tend to walk along streets which flourished of information, for instead, restaurants, cafes, stores, and shops that have a high level of visual complexity facades leading the street safe and preventing crime attempts. One of the innovative ideas to assess the quality of visual complexity by quantifying the information available in the environment since it is linked with the level of information richness in the information.

In the built environment, the phrase “information scape” can be conceptualized as the networks of spatial information perceived and processed through physical components within the physical space. Information scapes are intended to assist individuals in navigating and comprehending complex surroundings such as buildings, urban areas, and transit hubs. As our physical environments become more intricate and people rely on technology to navigate their surroundings, information scapes are becoming increasingly crucial in the modern world. A well-designed information scape may significantly alter how people view and interact with a space, thereby increasing their overall contentment and well-being. In this case, considering how we can assess the quality of information scape, and its accessibility and availability in our built environment become a prominent matter in the perspective of architecture and urban design. Visual analysis methodology i.e., isovist, is closely associated with weighing the distance of information availability from a particular point in each location.

Isovist has been utilized as a research methodology to assess visual perception and behavior patterns in different disciplines from Landscape, architecture, and built environment to Psychology for many years. Several academics from a range of different academic subjects have long been interested in the roots of the isovist to describe what is observable from a single, specific position in space. Tandy, for instance, appears to have been the first person in landscape studies and geography to utilize and develop the word, isovist (Tandy, 1967). Nonetheless, this may be considered a continuation of a long-standing practice among geographers to consider a location's viewshed and/or the idea of a vista. The idea of isovists is also arguably most directly related to Gibson's research on the ambient optic array in psychology. The ambient optic array was thought to represent the “scene” that appears when light rays enter the eye and so provide information about the visible environment to a situated observer (Gibson, 1979). Benedikt developed the well-defined idea of isovist which is now widely accepted and theorized its statistically measurable methods. Benedikt presents that an isovist is the set of all points visible from a given vantage point in space and concerning an environment (Benedikt, 1979).

In architecture, isovist is portrayed as a polygon that provides a simple graphic interpretation of spatial geometry for a certain point. Moreover, it has many geometric measurable qualities such as isovist area, perimeter, radial lengths, edges, and other statistical measurements such as variance, skewness, compactness, occlusivity, and circularity, etc. Such metrics are not just attributes of the polygon, but they also capture many elements of the environment from which is created. This isovist measurement can be used to model or anticipate a person's comprehension of, and potential reaction to, the environment (Dawes & Ostwald, 2021). To interpret the behavior of research issues, Academics usually apply different theoretical models such as “prospect and refuge theory” to interpret the mathematical measures of isovist in their research (Dosen & Ostwald, 2013; Ostwald & Dawes, 2018, p. 249; Xiang et al., 2021). Isovists are also frequently associated with the “space syntax” set of theories and approaches for studying architectural and urban settings, which are frequently linked to the evaluation of various

social and cognitive qualities of architectural plans (Dawes & Ostwald, 2021).

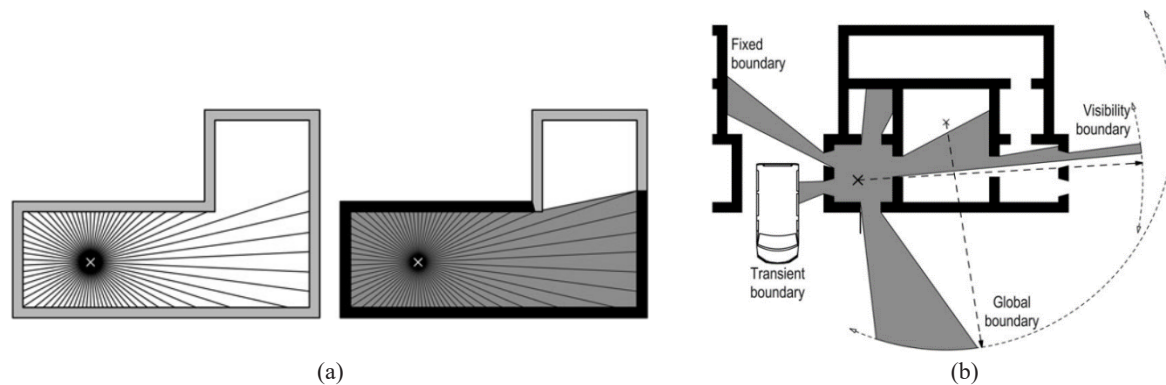


Figure 1. (a) Isovist construction with vertex lines & (b) Different types of isovist boundary conditions (Ostwald & Dawes, 2018, pp. 104, 106)

A limit or spread of isovist can be determined by a variety of edge constraints. Several academics defined the different ideas of visible boundaries to limit the isovist dispersion, which impacts on length of a radial line. The most basic edge condition is a fixed surface, but other useful limits include a fixed distance from the observation point (visible boundary) global perimeters enclosing the environment (global boundary), and dynamic or transient edges, which can be seen in Figure 1(b). For instance, Gibson claimed there are two kinds of space: 'local,' where the horizon is obscured by other surfaces, and 'aerial,' which is constrained by the earth's surface, horizon, and sky. According to Thiel, local space extends to about 60 meters, while aerial space or boundary is beyond around 140 meters. The transition area refers to the area between these boundaries according to Camillo Sitte (1945), Kevin Lynch, and Gary Hack (1984). According to Benedikt (1979), an isovist's range is limited to the edge of the environment, which is determined by an artificial and seemingly arbitrary global border. An alternate option is to set a standard maximum viewable distance, or visibility boundary, for each observation point (Ostwald & Dawes, 2018, p. 103).

In modern days of the advanced computational era, isovist can be constructed by a series of lines in 360 degrees extending from the given position to the environment. These lines which are known as radial lines or radials, spread out from the observation point with equal angular dissemination forming the isovist polygon by connecting the opposite edges of the lines. These lines are crucial for accessing the quality of information availability since they are associated with the surface border of the wall in which available information may be conceived to be placed (Ostwald & Dawes, 2018, p. 106). In this paper, isovist radial length, a measurable indicator, is adopted to determine the information accessibility matrix in the Shilin area.

3. FRAMEWORK OF INFORMATION SCOPE IN THE BUILT ENVIRONMENT

This section presents scenarios of information scope in the built environment, framework, and process of information scope analysis to assess information accessibility and availability in the Shilin night market.

3.1 Information Scope in the Built Environment

Information scope can be defined as the networks of spatial information perceived and processed through physical components within the physical space. Information source and receiver play the important roles in this situation. Information sources can be found in any types of mediums which can generate, establish, and portray any form of information in the environments. In the context of information scope, the situation of information accessibility and availability can have remarkably vital in acquiring information to perform essential daily routine. The situation of information scope in the environment can vary in accordance with its spatial context, surroundings, and information density distribution, and human's necessity and mode of existence. The information density distribution of information scope is likely to be varied and complex in the built environment. For instance, available information quantity may be relatively lower in suburban area than in downtown area. Furthermore, the density of information may be higher in nearby landmark area compared to the edges of the landmark boundary. Another example of information density is that the information availability in the office may be richer and more diverse than in office parking area in the architectural scale.

Subsequently, different people necessitate different information preferences or priorities regarding their mode of activities in different scenarios to fulfill their needs and desires. Based on state of actions and information acquisition behaviors, a person can be an information receiver who attain the information from his or her surrounding information scope. Conversely, he or she can be an information source who disseminate information to the neighborhoods. Choosing a favorable table in a restaurant, giving a speech in lecture hall, preferring working

next to the panoramic view window, staying at home during COVID outbreaks are some of the examples how people behave for his or her own sake of taking information advantage in the environment.

The information proximity between information source and given location also has impact the amount of prevalent information we received and the level of urgency to be counter-reacted for us depending on the acquired information. In other words, information which appear near us is more concerned on our existence than information that is distant from us, especially if it potentially affects the need of our instant interactions. For example, if a traffic accident occurs on a nearby road, this information may be more instantly relevant and significant than news about a political event taking place on the other side of the continent.

The information landscape has a profound influence on our everyday lives, impacting our capacity to collect and act on information. Despite its importance, the information scape remains a largely unexplored field of research. The complexity and diversity of the built environment, along with individual variances in information preferences, make it a difficult area. Furthermore, the closeness of information has a tremendous influence on our perception and response to it. Further study is needed to better understand the ramifications of the information scape and to build environments that encourage optimal information accessibility and availability.

3.2 Isovist Measures on the Perspective of Information Scape

Assessing the quality of information scape based on its information accessibility and availability become a significant matter for designers to comprehend the spatial quality of the built environment. Information scape can be appraised by a variety of approaches. Owing to the ability of acquiring the relationship of perceptual experience and characteristic of a space with its measures, and human behavior and cognition, isovist can be used as an information scape analysis tool to access the quality of the given environment. There are different measurables of isovist can conceptually interpret the quality of information scape regarding its area, perimeter, radial length, relationship between skewness and mode of human activities in the environment, etc.

It can be hypothetically assumed that the information density is randomly distributed in the space as the information weight of each part of the whole area can significantly vary even in the similar built environment. One of the perspectives of countability on information scape is the amount of information density in each location accessed by using isovist area per information source ratio. Then, we can extend it with the distance measure between observation point and information source because the distance of information we obtained within each isovist area reflects the degree of urgency or reaction of human perception on that information.

The more information near to us, the more concern on the decision we have to make regarding to those information behaviors, raising the issue of significance and proximity of information. In order to weight the information significance and proximity, specifically, in each location, the degree of information priorities in the isovist can be ranked by the distance indicator between information source and observation points, extended with the coefficient of information intensity, for labeling the significance of information.

In the context of information scape, the amount of information density can be significantly impacted on the direction of viewer where he or she is facing. A wealth of information may have accessed in the direction of the sight line whereas certain degree of information must be compromised in the out of sight. As a result, there is an information tradeoff phenomenon eventualize as a result of the condition between information acquisition by looking a specific direction and information lost on the blind side. This tradeoff points out the importance of considering information dispersion in the physical environment. Because of the directional benefits of isovist measure, the information tradeoff may evaluate by using Half isovist (180 degree) or third isovist (120 degree) instead of full isovist.

Skewness, one of the statistics measures of isovist, may also be analyzed the spatial reasoning of information dispersion relationship between chosen location and the information he or she may receive from it. Skewness, variance of the radial length distance of isovist, is the third moment of about the mean of the radial, M_3 (Ostwald & Dawes, 2018, p. 115). Stamps (Stamps, 2005) shows that high skewness implies that the observation point is close to an isovist's edge or corner, and low skewness suggests that the observation site is more central to the isovist. Since the tendency to select the different locations in each area, for instance, sitting next to the wall or corner, hiding in a narrow space, and performing arts at the center of the plaza, can be associated with the likeliness of prevalent information availability in the physical environment, it has the potential to access the human behavioral pattern of location selection in the perspective of information scape.

Overall, isovist measurables has the potential to analysis the information scape and this aspect of research have not well explored in the built environment discipline. Designers and planners should recognize the importance of information scape and how people interact with information dissemination in different contexts by analyzing the spatial distribution and accessibility of information in the built environment using isovist indicators. Ultimately, comprehending and analyzing information scape can lead to better design decisions that increase the spatial quality of the built environment.

3.3 Measuring Information accessibility by Isovist Radial Length

Shilin night market area, one of Taipei's business and cultural districts popular with both tourists and locals, is designated as a study area. The research is emphasized on the area where the old night market emerged and thrived near Cixian Temple along the Danan road and the intersection of Danan and Dadong road. It can be

highlighted in Figure 2.

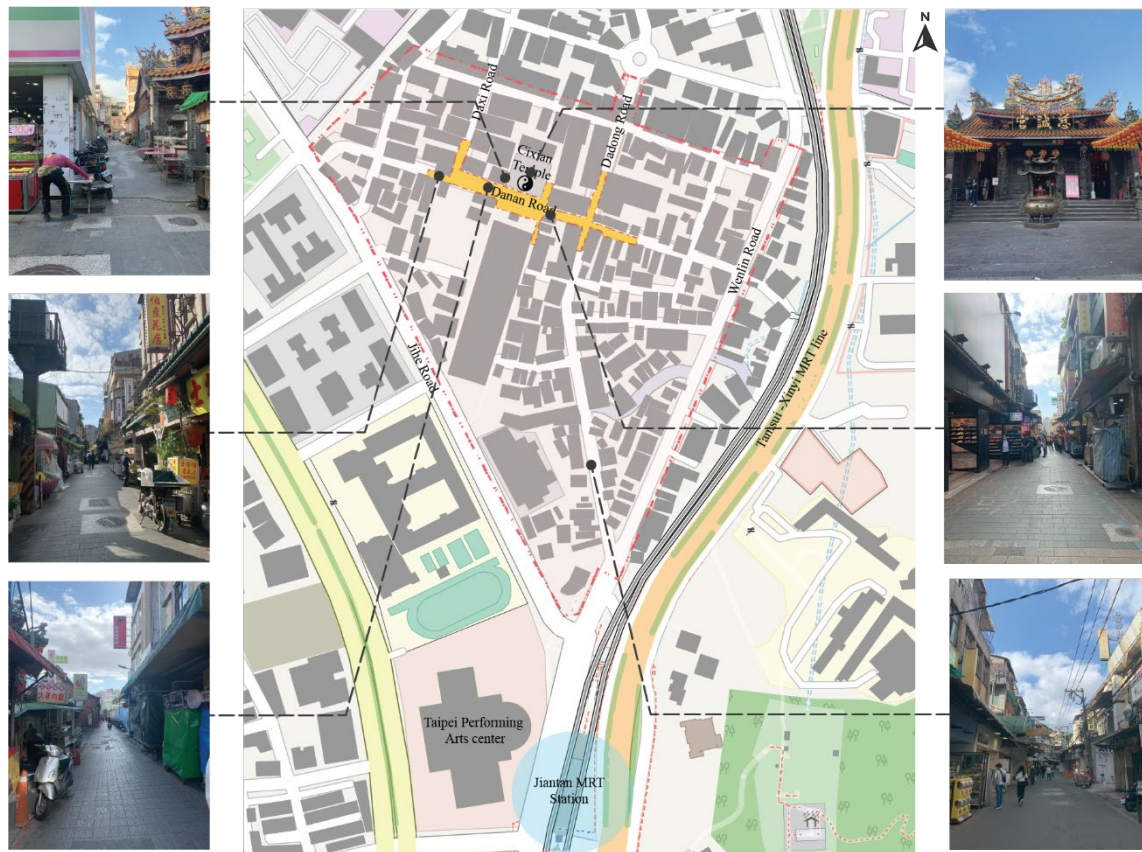


Figure 2. Shilin night market area and its neighborhood (*OpenStreetMap*, n.d.)

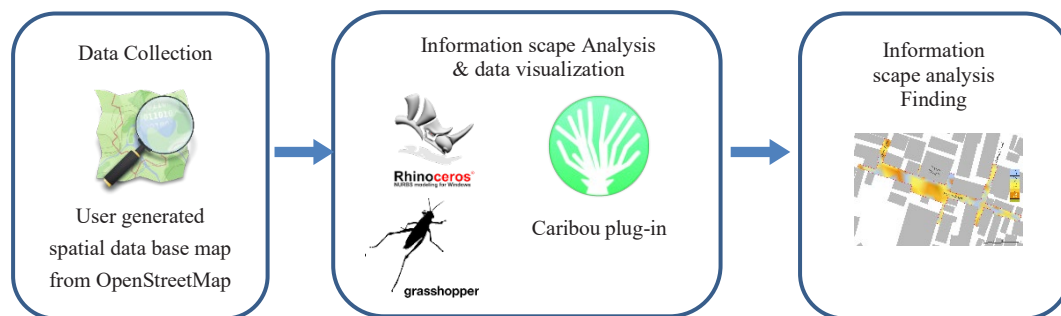


Figure 3. Flowchart of research framework

Rhino 3D computer-aid design software and grasshopper which is visual programming tool embedded in it, are primarily utilized in this research for establishing the base map, initiating isovists and calculating the isovist fields and radial lengths of isovist indicators. There are three main parts regarding research methodological concern such as data collection, information scape analysis and research outcome evaluation. First, a based map meta data is extracted from the OpenStreetMap and its generated geometrical parameters in grasshopper environment using Caribou plug-in. Information scape sources are, conceptually, arbitrarily dispersed around the area, with a significantly larger density found along both sides of the street, which are filled with shophouses that serve as primary information sources for visitors. Second, the map of arbitrary isovist locations is generated using Monte Carlo simulation with the help of grasshopper script. Then, it continues to establish isovist fields on the randomly generated locations. Finally, information scape analysis regarding its accessibility and availability is portrayed with the gradient map or heatmap.

While conducting research or dealing with geographical data, it is critical to have a reliable and up-to-date base map. While maps can be obtained from a variety of sources, such as government organizations or other websites, they are not always conveniently accessible or give the required amount of detail. In these cases,

employing an OpenStreetMap (OSM) file is a possible option. OpenStreetMap is a free and open-source globe map, created by a global community of mappers who contribute and maintain data about roads, building footprints and other geospatial data. OSM data can be obtained in a variety of forms, including shapefiles and GeoJSON, and used to generate a base map for research purposes. Researchers can get a detailed and up-to-date map that can be altered to meet their specific needs by utilizing OSM. In this situation, the OSM file of research area is extracted from OpenStreetMap for attaining the base map meta data. OSM files are usually large datasets that contains detail information about numerous geospatial elements. In a result, specific tools are required to efficiently visualize the meta data. In this appeal, the OSM file is parsed into grasshopper geometry and parameters through the Caribou, grasshopper plug-in in Rhino 3D software.

Due to the fact that the concept of information scape is ambiguous, isovists are established in the research boundary by generating random observation spots using Monte Carlo simulation. Randomizing observation points can help to avoid potential bias in their sample, as each location has equal chance of being chosen. This can help to guarantee that the data gathered is a true depiction of the information landscape in the study area. Furthermore, random sampling can help to improve the reliability and validity of the results by reducing the possibility of selecting points that are outliers or unrepresentative of the entire population. In this case, randomly generated 200 sample isovist locations are set up by applying Monte Carlo method of sample randomization in the research area (3007.54 sq-m), which can be seen in Figure 4.



Figure 4. Isovist random sampling in research boundary

Once the isovist location is established, radial nodes are polar arrayed in 360 degrees with 5-degree interval creating 72 radial lines from the central location point in each isovist. In isovist, radial length can be hypothesized to the distance of information availability from the given point to the information source. The maximum radial distance or visible boundary is limited to 60 meters. Then, each radial length of isovist and mean radial length of each isovist are evaluated.

The proximity between an observer and a source point can have a considerable impact on the amount of information gathered. Portraying this scenario, the relationship between distance of two points and information accessibility can be modeled using exponential decay weighted function. Then, we assume that the coefficient of exponential value can be either less than one or negative number as information accessibility is inversely proportional to the radial length distance between observer and source nodes. It should be noted that the coefficient of exponential value can vary in an accordance with different location contexts, information behavior, cultural aspects and enclosed or exposed environment. In this circumstance, in order to enhance the weightage of the information scape, the coefficient of exponential value (0.5) is assumed to be applied to the value of mean radial length. Finally, the accessibility of information scape is investigated according to the distance-weighted information scape factor of isovist and illustrated with gradient map or heat map.

4. DISCUSSION

This section presents the result of an information scape analysis of the Shilin market area. The establishment of the research environment, isovist construction and simulation are carried out with the help of grasshopper, visual programming tool in the Rhino 3D software environment. The Figure 5 shows the gradient matrix of intensity distribution of information scape of the Shilin night market area.

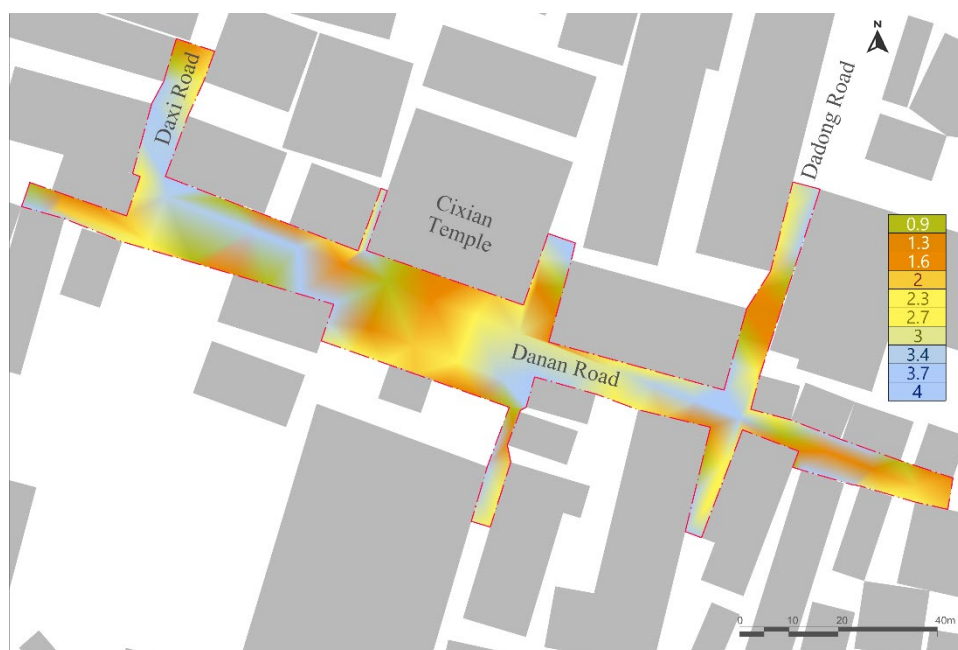


Figure 5. Information scape scale of Shilin night market area

There are two aspects of information scape availability can be discussed: information significance and proximity, in this study. First, the more information we have in proximity, the more concerned we are with the decision we must make on those information behaviors regarding the aspect of significance of information. Subsequently, observation locations, information proximity concern, that are closer to the source points will more likely provide a more accurate and richer of the information landscape than those farther away. Since the quality of the information accessibility is inversely proportional to the distance of radial length and information scape indicator, the chances of information scape quality are likely to be higher and significant when the radial distances and indicator factors decrease.

According to the quantitative indicator of information available from the simulation result and gradient information scape intensity map of the Shilin research area (Figure 5), the average information availability is 2.67, contributing to the 26 percentage of the area. The area where the poor quality of information accessibility has a maximum value of 4.04 which represent 17 percent of the area. This result can be experienced firstly, in the area where the width of the road is relatively wider and, secondly, the area near the street junction surrounding and, thirdly, built density is comparably lower than its neighborhood area. A person standing these spaces may unlikely get the chance of enriched and significant information as he or she is distant from the information sources and has less access to relevant information in proximity. It may lead them making poor informed decision.

On the one hand, one may likely to find a rich amount of information where the area of which the intensity of information scape has relatively lower, ranging from 1 to 2, representing 20 percent of the whole area. This condition can be observed in the area with narrower roads as well as the edges of building footprints along the road. The closer and significant information may help the individuals access and process the necessary information, resulting in improving decision making process.

The idea of an information scape is used in this study to examine the availability of information in the physical environment. The result showed that the availability of information can affect people's capacity to make decisions. The study also demonstrated how the quality of information accessibility may be influenced by factors such as road width, building density, and observer position. The study suggests that in order to improve information accessibility, which can improve decision-making, the built environment should take into account the distribution of information availability and proximity.

5. CONCLUSION

In this paper, we conceptualize the framework of information scape analysis and present the potential of isovist measures to quantify the quality of isovist by information proximity, density, location, and direction of the observer aspects in the physical surrounding. It extends with randomly populated 200 isovists to assess the average tendency of information accessibility and availability in the built environment. Then, the information available is evaluated with mean isovist radial length, one of the isovist measurables, extended with the coefficient of information exponential decay to identify the level of information importance or urgency for the human behavioral

patterns being reshaped. The study aims to understand the information scape between human behavior and the spatial situation in the built environment and provide a framework of measurable aspects for information accessibility for the architects and urban designers to optimize the arrangement of information sources in the environment for ease of navigation and accessibility leading to the human-centric environment. This study has some limitations. As this paper explore the information scape in the light of information accessibility and significance, it should be noted that the human behavioral pattern and state of mode is neglected. The physical conditions of the environment may have other aspects to be considered such as the type, height, entropy of information sources, weather situations, and crowd density. Moreover, the calibration of coefficient of information decay based on the contextual environment can be another interesting topic to be explored. Overall, this research displays that information scape analysis has the potential for studying the complex interaction between spatial configuration and human behavioral patterns for user experience, enhancing accessibility, and encouraging communication and engagement in the aspect of information availability.

REFERENCES

- Benedikt, M. L. (1979). To Take Hold of Space: Isovists and Isovist Fields. *Environment and Planning B: Planning and Design*, 6(1), 47–65. <https://doi.org/10.1068/b060047>
- Boeing, G. (2018). Measuring the complexity of urban form and design. *URBAN DESIGN International*, 23(4), 281–292. <https://doi.org/10.1057/s41289-018-0072-1>
- Dawes, M. J., & Ostwald, M. J. (2021). Isovists: Spatio-visual Mathematics in Architecture. In B. Sriraman (Ed.), *Handbook of the Mathematics of the Arts and Sciences* (pp. 1419–1431). Springer International Publishing. https://doi.org/10.1007/978-3-319-57072-3_5
- Dosen, A., & Ostwald, M. (2013). Prospect and refuge theory: Constructing a critical definition for architecture and design. *International Journal of Design in Society*, 6, 9–23. <https://doi.org/10.18848/2325-1328/CGP/v06i01/38559>
- Gibson, J. J. (1979). *The ecological approach to visual perception*. Boston: Houghton Mifflin Company.
- Jacobs, J. (1961). *The death and life of great American cities* (Vintage Books ed). Vintage Books.
- OpenStreetMap. (n.d.). OpenStreetMap website: <https://www.openstreetmap.org/>
- Ostwald, M. J., & Dawes, M. J. (2018). *The Mathematics of the Modernist Villa* (Vol. 3). Springer International Publishing. <https://doi.org/10.1007/978-3-319-71647-3>
- Portella, A. A. (2014). Built Environment. In A. C. Michalos (Ed.), *Encyclopedia of Quality of Life and Well-Being Research* (pp. 454–461). Springer Netherlands. https://doi.org/10.1007/978-94-007-0753-5_240
- Stamps, A. E. (2005). Isovists, Enclosure, and Permeability Theory. *Environment and Planning B: Planning and Design*, 32(5), 735–762. <https://doi.org/10.1068/b31138>
- Tandy, C. R. V. (1967). The isovist method of landscape survey. *Methods of Landscape Analysis*, 10, 9–10.
- Xiang, L., Papastefanou, G., & Ng, E. (2021). Isovist indicators as a means to relieve pedestrian psycho-physiological stress in Hong Kong. *Environment and Planning B: Urban Analytics and City Science*, 48(4), 964–978. <https://doi.org/10.1177/2399808320916768>

ACCUMULATION AND CLASSIFICATION OF SMART LIVING FRAMEWORK FROM ACADEMIC STUDIES AND REAL SECTOR

Suchanad Phuprasoet¹, Terdsak Tachakitkachorn², and Kaweekrai Srihiran³

1) M. Arch, Department of Architecture, Faculty of Architecture, Chulalongkorn University, Bangkok, Thailand. Email: ping_phuprasert@hotmail.com

2) Ph.D., Asst. Prof., Architecture for Creative Community Research Unit, Department of Architecture, Faculty of Architecture, Chulalongkorn University, Bangkok, Thailand. Email: Terdsak.t@chula.ac.th

3) Assoc. Prof., Regional, Urban, and Built Environmental Analytics: RUBEA, Department of Architecture, Faculty of Architecture, Chulalongkorn University, Bangkok, Thailand. Email: Kaweekrai.s@chula.ac.th

Abstract: Information & Communication Technologies (ICTs) and Internet of Things (IoTs) are fundamental technologies of Industry 4.0. The technologies can be globally used to manage several fields. Due to 56% of the world's population living in cities nowadays, the management of Smart city projects over the World is increasingly getting attention. Integrating ICTs and IoTs with the electricity grid in a smart city creates alternative solutions for energy management and helps to increase the amount of energy saving in cities. This way of integration not only helps to handle urbanization and climate changes but also improves the citizens' all aspects of quality of life, which is called 'Smart living'. Smart living in an aspect of housing quality, also began to integrate IoTs into Smart buildings or Smart homes to enhance the quality of life. A Smart living idea is widely known but still lacks comprehensive and up-to-date data accumulation and classification to create a Smart living framework in an aspect of housing quality, used as the tool for considering several dimensions of Smart living projects from the real sector. This research aims to accumulate and classify the Smart living framework, which is comprehensive and applicable nowadays. A research methodology based on guidelines for performing systematic literature reviews. The researcher screened up to 30 academic studies about Smart buildings or Smart homes in a literature review. Academic studies that have proposed the kind of guidelines, main criteria, indicators, or conceptual models of Smart homes, Smart buildings, or Smart living, and have been published within five years were selected. Subsequently, data exploration, accumulation, and classification of similar keywords relating to Smart living have been done respectively. Later, the researcher refines the details and synthesizes the Smart living framework used to consider Smart living projects from the real sector. The result showed that the Smart living framework could be classified into 2 classes; Management and Enhancement. This Smart living framework includes 9 criteria and 32 indicators, and findings of gaps in Smart living studies were found. In this paper, academic studies have conceptual Smart living frameworks as guidelines, which are more comprehensive than the real sector. In other words, the real sector will not be able to completely follow academic studies until the levels of technological advancement can support them.

Keywords: Framework, Smart living, Academic sector, Real sector

1. INTRODUCTION

It is now the fourth industrial revolution (4IR), also called 'Industry 4.0' (Ajayi et al., 2022). 4IR is not only about industries but also overall transformation using both Digital integration and Intelligent engineering (Muhuri et al., 2019). Moreover, the ICTs, IoTs, and sensor networks are fundamental technologies of 4IR (Ajayi et al., 2022). Along with the fact that over 56 percent of the world's population (4.4 billion) currently lives in cities (Ivers & Fleury, 2022), hence countries around the world face the challenges of urbanization and climate change. As a result, ICTs, technology that supports activities involving information, and IoTs, the connection of all devices to the internet and each other, have been introduced to better manage and control the activities in cities (ARC Advisory Group, 2022; Gokhe, 2018; Plummer, 2021).

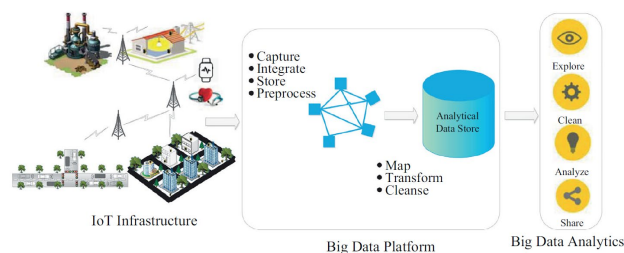


Figure 1. Big data line diagram connected to the Internet of Things within a Smart city.

In addition, the Smart city Ranking among European Mid-Sized Cities, a report that compiles data on Smart cities from the early stages of the Smart city movement, presents a prototype of Smart city structure as follows. Smart cities consist of six characteristics: Smart economy, Smart people, Smart governance, Smart mobility, Smart environment, and Smart living. Smart living in this case refers to the concept of enhancing people's quality of life in various aspects of quality of life. The housing quality also included as one aspect of Smart living (Giffinger et al., 2007). Simultaneously, Integrating ICTs and IoT technologies from the planning and design stages of architecture is the beginning process to create the Smart building and Smart home. The concept of a Smart building is a set of communication technologies enabling different objects, sensors, and functions within a building to communicate and interact with each other and also to be managed, controlled, and automated in a remote way (Bonneau et al., 2017). In the same way, the concept of a Smart home is a house that has the ability to associate and communicate amongst itself whereas the user can remote from near or far through the internet and Smartphone (ch.aunchalee, 2021). Obviously, both are concepts that enhance the housing quality in all aspects such as energy management for energy saving, security systems management, or the convenience of living in Smart homes, etc., which also brings Smart living to become reality.

However, by doing the literature reviews in the area of Smart building and Smart home researches existing nowadays, researchers found that the research on Smart living has not been much studied. Besides that, most studies are conducted in the form of IT-based research such as proposing a network system, creating software, or creating applications more than non-IT-based research such as social, environmental, physical space, and other aspects. Additionally, the information on Smart living study is also kind of a wide dataset, distributed, and interpolated under the field of Smart building and Smart home. The data have not yet been collected and classified in a systematic way, easy to understand, and truly up-to-date. Therefore, the researcher carried out this research to bridge the gap in order to answer the research questions as follows: 1) What is a tool that is used to give design guidelines for various Smart projects (e.g. Smart home or Smart building) to support the Smart living readiness in an aspect of housing quality? 2) What is the overall scope of the Smart living concept until the present? under conditions that integrate both IT and other non-IT aspects, which collect data from both academic studies and Smart living projects from the real sector. 3) Does the current Smart living projects from the real sector consistent with academic study's Smart living concept? If not, what are the differences? Lastly, 4) Are there basic elements, important to future Smart living studies? If so, what does it consist of?

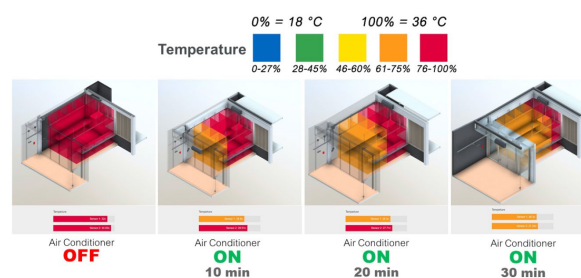


Figure 2. shows dynamic 'Smart cube', the automatic color-transabled 3D representation of room temperature, generated by using BIM-Based Indoor Environmental Monitoring System

2. METHOD

2.1 Overview

This research's methodology based on guidelines for performing systematic literature reviews (Kitchenham & Charters, 2007). Due to a systematic literature review, researchers identify, evaluate and interpret all available research relevant to the research questions mentioned above. The guidelines for performing systematic literature reviews summarized that there are three main phases including planning the review, conducting the review, and reporting the review (Kitchenham & Charters, 2007). Thus, the researcher will explain and detail the stages associated with planning and conducting the review below, where the conducting stage consists of the implementation of the planning stage. It has been articulated in terms of three activities: (a) Definition of the need for a review, (b) Definition of the research question, and (c) Definition of the review protocol.

(a) The need for a review

The need for the study is motivated by the lack of Smart living studies in terms of non-IT-based research, the information on Smart living studies is too broad data set under the field of Smart buildings and Smart homes studies, and the mentioned data have not yet been studied and summarized in a systematic way, easy to understand, and truly up-to-date.

(b) The research questions

- What is a tool that is used to give design guidelines for any Smart projects to support Smart living readiness in an aspect of housing quality?

- What is the overall scope of the Smart living concept until the present? under conditions that integrate both IT and other non-IT aspects, which collect data from both academic studies and Smart living projects from the real sector.
 - Does the current Smart living projects from the real sector consistent with academic criteria? If not, what are the differences?
 - Are there basic elements, important to future Smart living studies? If so, what does it consist of?
- (c) The review protocol

For the searching process, the researcher implemented a manual search of articles in the Scopus repository. Scopus was created by Elsevier in 2004. It is the largest curated scientific database where major publishers are indexed in Scopus. That is the reason for querying on Scopus.

In terms of the inclusion criteria, the search string which the Scopus engine is case-insensitive, included “Smart homes evaluation” OR “Smart building evaluation” OR “Smart homes criteria” OR “Smart building criteria”

For data collection, the researcher downloaded a PDF file to archive the title, authors’ name, keywords, abstract, and DOI for each article.

For data analysis, at this stage the title, keywords, and abstract of about 20 reviews were read only by the first author of the present paper. Despite the fact that, in systematic mapping studies, the investigation is usually limited to taking into account the title and abstract of each selected item, the first author downloaded the PDF of the 20 reviews to give a correct answer to the research questions. Then read the introduction and conclusion sections of those articles. This approach was applied iteratively until all the reviews had been explored and mapped.

After the researchers have reviewed more than 20 pieces of literature related to Smart living both IT-based and non-IT-based research. Reviewing the structure of the Smart city initiated in 2007, indicates that the concept of Smart living has started (Giffinger et al., 2007). Smart living has been continuously studied more than a decade. Thus, researchers have set the scope, where every case study must be published under 5 years from 2018-2021 for up-to-date information. The selected researches include the topic of Smart building, Smart home, developing evaluation of Smartness, Smart Readiness Indicator (SRI) in Smart building, and empirical study of BIM-IoT integration in the Smart building, as shown in Table 1.

Table 1. List of academic case studies selected for this research

Case Study	Title	Published year
A	Intelligent Building, Definitions, Factors and Evaluation Criteria of Selection	2018
B	Final Report on the Technical Support to the Development of a Smart Readiness Indicator for Buildings	2018
C	Development of a Smart Building Evaluation System for Office Buildings	2019
D	Developing a Scoring System to Evaluate the Level of Smartness in Commercial Buildings: A Case of Sri Lanka	2021
E	An Intelligent, Secure, and Smart Home Automation System	2020
F	The social issues of Smart home: a review of four European cities’ experiences	2021
G	BIM-Base Indoor Environmental Monitoring System	2020

As there is a cluster of the database from 20 reviews, a comprehensive overview of a research area is needed to better understand the scope of this study. Researcher started the classification method according to the systematic mapping studies (Kitchenham & Charters, 2007), the topics covered in the 20 reviews were classified into two main classes. The topics extracted from the 20 reviews were classified into 9 criteria, which consist of 5 criteria for the management class; 4 criteria for the enhancement class, as shown in the figure 3.

The classified data were synthesized and presented as the Smart living framework proposed in this research. Lastly, the Smart living framework was comparatively analyzed with Smart living projects from the real sector, in order to determine whether both case studies are consistent or different or not. If so, what are they?

For the selection of Smart living projects from the real sector, all selected projects have been conducted and experimented with the Smart features consistent with Smart living products; 3 Smart living projects were selected. The scale of each project is slightly different, but each has its own significant point as being a part of early Smart protocols in Thailand. The selected projects include: (a) Zen Model - Panasonic's smart home unit; (b) Saladaeng Digital Twin building; and (c) Smart patrol - Smart environmental monitoring system, experimented in Chulapat 14 Building. All of these three projects take placed or located in Bangkok, Thailand. Figure 3 shows an overview of the proposed method.

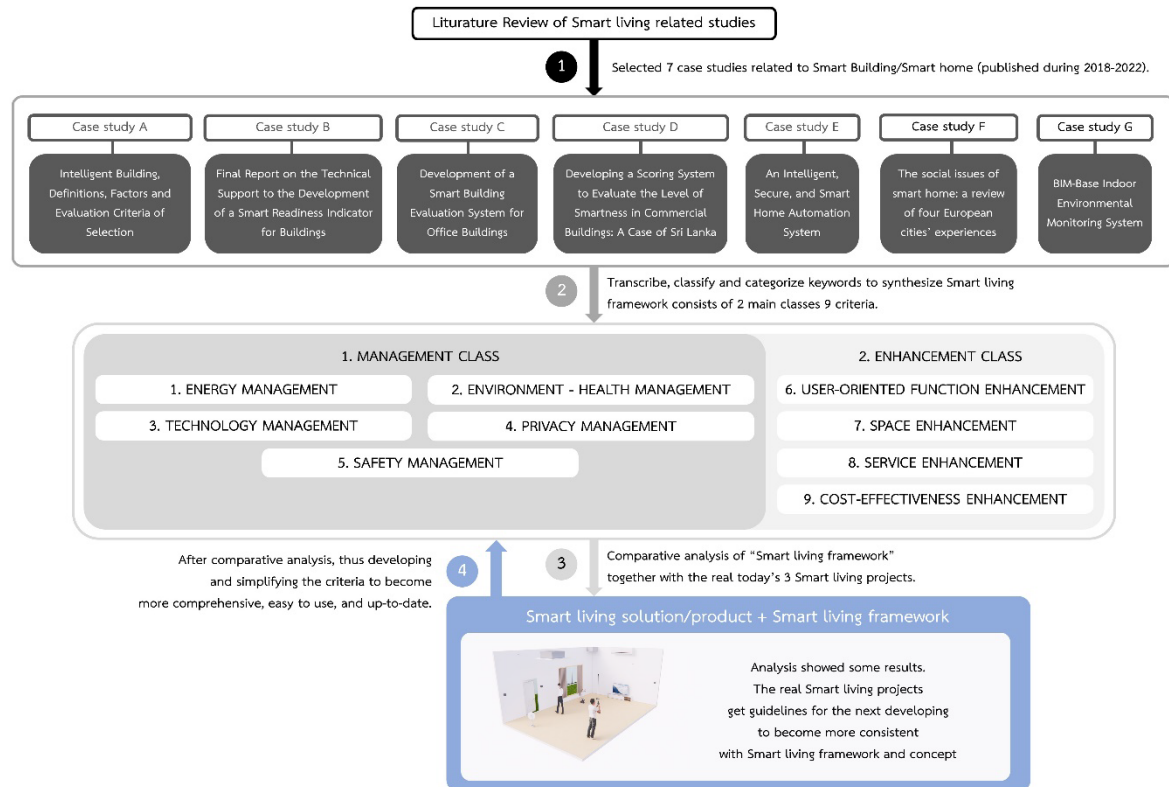


Figure 3. Research methodology model

2.2 Literature Review

A review of relevant literature on both Smart living in aspect of housing quality, which refers to Smart buildings and Smart homes. In order to understand the meaning and scope of Smart living in terms of housing quality, and the relationship between smart buildings and smart homes that affect today's Smart living. In addition, meanings and the relation between ICTs, IoTs and Smart living will be described.

(1) Definition and Scope of Smart Living

Smart living refers to the concept of enhancing people's quality of life, which comprises of various aspects of the quality of life as 1) Cultural facilities 2) Health conditions 3) Individual safety 4) Housing quality 5) Education facilities 6) Touristic attractivity and 7) Social cohesion. Its main objective is to improve the quality of life of people in all aspects mentioned above (Giffinger et al., 2007).

(2) The Relationship Between Smart Living, Smart Building and Smart Home

Building sector is the most energy consumption sector in many developing countries (Asadian et al., 2018). The main purpose of smart building design is to reduce energy consumption and CO₂ emissions from the building sector. In order to meet the main purpose, both architectural and technological solutions should be used to contribute enhancing the quality of life, which will directly affect the productivity and satisfaction of the building user (Gunatilaka et al., 2021; Omar, 2018). For this reason, Smart building is another significant element that contributes to the promotion of Smart living.

Smart home is one of the options to achieve the purpose of Smart living in terms of housing quality. The main purpose of a smart home is integration of service and management system together to provide users with an efficient, comfortable, safe, and environmentally friendly living environment (Pira, 2021). Smart home allows users to monitor and change the status of home appliances, and also to check the status of sensors (Majeed et al., 2020), therefore a smart home is also important for Smart living.

(3) Concepts of ICTs and Communication Networks Related to Smart Living

ICT is technology that supports activities involving information. Such activities include gathering, processing, storing and presenting data. Increasingly these activities also involve collaboration and communication. Hence IT has become ICT, for instance, personal computers, email, and etc.(Gokhe, 2018). Obviously, The 4IR is characterized by rapid digitization. Digitalization means the process of converting something to digital form (Merriam-Webster, n.d.). For instance, over the years communication networks have evolved through five

generations. Consequently, some key application areas will be significantly enhanced by the 5G mobile network such as residential use, Internet-of-things, etc. (Ajayi et al., 2022). For this reason, ICT has become an important foundation for driving Smart living.

(4) Concept of IoTs and Sensor Network Related to Smart Living

IoT is the connection of all devices to the internet and each other (ARC Advisory Group, 2022). It is one of the key components of the Industry 4.0 era, causing the data explosion, which is called when the large scale of data is rapidly generated and stored in computer systems (Zhu et al., 2009). IoTs has grown exponentially over the past year (Ajayi et al., 2022). For instance, IoT acts as a network of devices and buildings that have technology embedded in them. This could be in the form of sensors, tags and network connectivity that allow us to view its activities and performance. Information provided by IoT devices allows users to access and control the technologies through the internet network, which helps to enhance housing quality (NEW PC PLANET, 2019).

3. RESULTS AND DISCUSSION

ICTs and IoTs are fundamental technologies in the age of Industry 4.0. ICTs and IoTs integrated with smart technologies are used to manage Smart cities and develop various fields. Developing a Smart city directly enhance Smart living concept, the concept of improving the citizens' quality of life in all aspects. Smart living in an aspect of housing quality can be implemented by integrating ICTs in the Smart building or Smart home. At present, Smart living still lacks of a framework that can be used as a tool for considering technologies for Smart living and used as a basis for decision-making in selecting suitable technology for the general public. Moreover, Information in the area of Smart living lack of systematically organized and up-to-date information. Hence, this research aims to bridge the gap.

The study related to today's Smart living concepts, beginning with a literature review methodology of academic case studies and the Smart living projects from the real sector including Smart home and Smart building. Then the process of data accumulation, transcription, and classification, were done in order to synthesize the framework respectively. The results of the study revealed that the framework can be classified into 2 main classes: management class and enhancement class, including 9 criteria: 1) Energy management 2) Environmental and health management 3) Technology management 4) Privacy management 5) Safety management 6) User-oriented function enhancement 7) Space enhancement 8) Service enhancement 9) Cost-effectiveness enhancement, which totally consists of 32 indicators, as show in Table 2.

Table 2. The proposed Smart living framework
comparing between Academic studies and Smart living projects form the real sector

No.	Main criteria	Sub criteria	Detail	A	B	C	D	E	F	G	ZEN MODEL	SLD DT BLDG	CU PAT 14
				Profile of building definitions, factors and evaluation criteria of selection	Final report on the Technical Support to the Development of a Smart Readiness Indicator for Buildings	Development of a Smart Building Evaluation System for office buildings	Developing a Smart System to Evaluate the level of Smartness in Commercial Buildings: A Case of Seville	As intelligent, secure, and smart home Automation System	The focus point of a smart home: a review of four European cities' experiences	With New Indoor Environmental Monitoring System	Smart home smart home unit	Building digital twin building	Smart control experiment in Shanghai 55 Building
01 ENERGY MANAGEMENT													
1	1	a	Energy saving & conservation	✓	✓	✓	✓	✓	✓	✓	✓	✓	✓
2	1	b	Energy recovery	✓	✓	✓	✓	✓	✓	✓	✓	✓	✓
3	1	c	Energy regeneration	✓	✓	✓	✓	✓	✓	✓	✓	✓	✓
4	1	d	Energy grid integration (Smart grid)	✓	✓	✓	✓	✓	✓	✓	✓	✓	✓
02 ENVIRONMENT-HEALTH MANAGEMENT													
5	2	a	IAQ Monitoring	✓	✓	✓	✓	✓	✓	✓	✓	✓	✓
6	2	b	Thermal comfort control	✓	✓	✓	✓	✓	✓	✓	✓	✓	✓
7	2	c	Visual comfort control	✓	✓	✓	✓	✓	✓	✓	✓	✓	✓
8	2	d	Acoustical comfort control	✓	✓	✓	✓	✓	✓	✓	✓	✓	✓
03 TECHNOLOGY MANAGEMENT													
9	3	a	System Integration capability	✓	✓	✓	✓	✓	✓	✓	✓	✓	✓
10	3	b	Control and monitoring capability	✓	✓	✓	✓	✓	✓	✓	✓	✓	✓
11	3	c	Application of high-tech design	✓	✓	✓	✓	✓	✓	✓	✓	✓	✓
04 PRIVACY MANAGEMENT													
12	4	a	Surveillance monitoring and control	✓	✓	✓	✓	✓	✓	✓	✓	✓	✓
13	4	b	Surveillance recording	✓	✓	✓	✓	✓	✓	✓	✓	✓	✓
14	4	c	Data protection	✓	✓	✓	✓	✓	✓	✓	✓	✓	✓
05 SAFETY MANAGEMENT													
15	5	a	Emergency escape capability	✓	✓	✓	✓	✓	✓	✓	✓	✓	✓
16	5	b	Fire/Smoke detection	✓	✓	✓	✓	✓	✓	✓	✓	✓	✓
17	5	c	Disaster monitoring	✓	✓	✓	✓	✓	✓	✓	✓	✓	✓
18	5	d	Movement detection	✓	✓	✓	✓	✓	✓	✓	✓	✓	✓
06 USER-ORIENTED FUNCTION ENHANCEMENT													
19	6	a	Demand side management	✓	✓	✓	✓	✓	✓	✓	✓	✓	✓
20	6	b	Ease of installation	✓	✓	✓	✓	✓	✓	✓	✓	✓	✓
21	6	c	EV charging - connectivity	✓	✓	✓	✓	✓	✓	✓	✓	✓	✓
22	6	d	Controls for optimizing user comfort	✓	✓	✓	✓	✓	✓	✓	✓	✓	✓
07 SPACE ENHANCEMENT													
23	7	a	Space flexibility	✓	✓	✓	✓	✓	✓	✓	✓	✓	✓
24	7	b	Spatial utilization	✓	✓	✓	✓	✓	✓	✓	✓	✓	✓
08 SERVICE ENHANCEMENT													
25	8	a	Maintenance management	✓	✓	✓	✓	✓	✓	✓	✓	✓	✓
26	8	b	Land conservation - Waste management strategies	✓	✓	✓	✓	✓	✓	✓	✓	✓	✓
27	8	c	System performance checking	✓	✓	✓	✓	✓	✓	✓	✓	✓	✓
28	8	d	Building automation control system	✓	✓	✓	✓	✓	✓	✓	✓	✓	✓
09 COST-EFFECTIVENESS ENHANCEMENT													
29	9	a	Initial set up cost	✓	✓	✓	✓	✓	✓	✓	✓	✓	✓
30	9	b	Operating cost	✓	✓	✓	✓	✓	✓	✓	✓	✓	✓
31	9	c	Maintenance cost	✓	✓	✓	✓	✓	✓	✓	✓	✓	✓
32	9	d	Electricity cost	✓	✓	✓	✓	✓	✓	✓	✓	✓	✓

Analyzing data through all 32 indicators of 9 criteria found that, current Smart living projects from the real sector are unable to cover all of Smart living framework on the academic study side. The Smart living framework proposed in this research can be generally used as a decision-making tool for considering and choosing which Smart living projects for implementation. Elements within the Smart living framework can be used as a guideline for designing buildings that respond to the Smart living concept. In addition, it is also for those who are interested in studying in details of the elements within the Smart living framework.

In summary, the academic case studies on Smart living have set the conceptual framework provided as a guideline that is quite comprehensive and complete in many aspects. At the same time, the real sector can help answer some of questions in Smart living studies which are not covered by the academic cases studies. In other words, Unpractical Smart living concepts in real sector, which have already been proposed comprehensively through academic case studies, will not be brought into reality until the level of technological advancement can support the real sector in the future. Thus, the integration between academic case studies and the real sector is a rational principle that yields a more complete framework. Therefore, the framework can be developed to be more complete as time changes.

4. RECOMMENDATION

The proposed Smart living in this research can also be further developed to evaluation criteria for technologies related to Smart living, which will help standardize the Smart living field. For instance, applying the multi-criteria decision-making (MCDM) techniques by Analytical Hierarchy Process (AHP) helps decision makers find one that best suits their goal and their understanding of the problem. This can be use to determine the criteria and understand the relative importance of each criterion in determining the level of smartness of Smart living projects in the real sector. This can lead to the development of a scoring system (Gunatilaka et al., 2021; Majumder, 2015).

REFERENCES

- Ajayi, O., Bagula, A., and Maluleke, H. (2022). The Fourth Industrial Revolution: A Technological Wave of Change. In M. Gordan, K. Ghaedi, & V. Saleh (Eds.), *Industry 4.0* (pp. Ch. 1). IntechOpen. <https://doi.org/10.5772/intechopen.106209>
- ARC Advisory Group. (2022). *Five Key Industry 4.0 Technologies*. Retrieved from OTTO Motors website: <https://ottomotors.com/blog/5-industry-4-0-technologies>
- Asadian, E., Azari, K.T., and Vakili Ardebili, A. (2018). Chapter 1.5 - Multicriteria Selection Factors for Evaluation of Intelligent Buildings—A Novel Approach for Energy Management. In I. Dincer, C. O. Colpan, & O. Kizilkan (Eds.), *Exergetic, Energetic and Environmental Dimensions* (pp. 87-102). Academic Press. <https://doi.org/10.1016/B978-0-12-813734-5.00005-6>
- Bonneau, V., Ramahandry, T., IDATE, Probst, L., Pedersen, B., and Dakkak-Arnoux PwC, L. (2017). *Smart Building- Energy efficiency application*.
- Ch.aunchalee. (2021). *I o t 302* 47. <https://pubhtml5.com/ktnj/oyuw/basic/>
- Giffinger, R., Fertner, C., Kramar, H., Kalasek, R., Milanović, N., and Meijers, E. (2007). *Smart cities - Ranking of European medium-sized cities*.
- Gokhe, M. (2018). *IV.1 Information and Communication Technolo*. TSCER. https://www.hzu.edu.in/csit/IV.1_information_and_communication_technology.pdf
- Gunatilaka, R.N., Abdeen, F.N., and Sepasgozar, S.M.E. (2021). Developing a Scoring System to Evaluate the Level of Smartness in Commercial Buildings: A Case of Sri Lanka, *Buildings*, 11(12), 644. <https://doi.org/10.3390/buildings11120644>
- Ivers, L., and Fleury, M. (2022, 2022, October 6). *Urban Development*. Retrieved from World Bank website: <https://www.worldbank.org/en/topic/urbandevelopment/overview>
- Kitchenham, B., and Charters, S. (2007). Guidelines for performing Systematic Literature Reviews in Software Engineering, 2.
- Majeed, R., Abdullah, N.A., Ashraf, I., Zikria, Y.B., Mushtaq, M.F., and Umer, M. (2020). An Intelligent, Secure, and Smart Home Automation System, *Scientific Programming*, 2020, 1-14. <https://doi.org/10.1155/2020/4579291>
- Majumder, M. (2015). Multi Criteria Decision Making. In *Impact of Urbanization on Water Shortage in Face of Climatic Aberrations* (1 ed., pp. IX, 98). Springer Singapore. <https://doi.org/https://doi.org/10.1007/978-981-4560-73-3>
- Merriam-Webster. (n.d.). Digitalization. In *Merriam-Webster.com dictionary*. Retrieved April 11, 2023, from <https://www.merriam-webster.com/dictionary/digitalization>
- Muhuri, P.K., Shukla, A.K., and Abraham, A. (2019). Industry 4.0: A bibliometric analysis and detailed overview, *Engineering Applications of Artificial Intelligence*, 78, 218-235. <https://doi.org/10.1016/j.engappai.2018.11.007>

- NEW PC PLANET. (2019). *Smart Living with the Internet of Things*. <https://pcplanet-eg.com/smart-living-internet-things/>
- Omar, O. (2018). Intelligent building, definitions, factors and evaluation criteria of selection, *Alexandria Engineering Journal*, 57(4), 2903-2910. <https://doi.org/10.1016/j.aej.2018.07.004>
- Pira, S. (2021). The social issues of smart home: a review of four European cities' experiences, *European Journal of Futures Research*, 9(1). <https://doi.org/10.1186/s40309-021-00173-4>
- Plummer, L. (2021). *Insight Report: Industry 4.0 and the Digital Transformation of Cities*. <https://www.smartcitiesworld.net/whitepapers/whitepapers/insight-report-industry-40-and-the-digital-transformation-of-cities>
- Zhu, Y., Zhong, N., and Xiong, Y. (2009). Data Explosion, Data Nature and Dataology. In N. Zhong, K. Li, S. Lu, & L. Chen, *Brain Informatics* Berlin, Heidelberg.

CRACK DETECTION OF BRIDGES FROM SELF-WEIGHT DEFORMATION PROFILES

Suphanat Wang¹

1) Graduate student, Department of Civil Engineering, Faculty of Engineering, Chulalongkorn University, Bangkok, Thailand. Email: 6470287921@student.chula.ac.th

Abstract: Bridges have been a main part of transportation systems for a long time and their structures may be eroded and damaged by many kinds of effects. The Bridge Health Monitoring system has been applied to automatically observe the abnormal condition of the structures before the structures will lead to collapse. One practical monitoring technique is to install tiltmeters or inclinometers on the bridges to detect their damages. Previous researchers have proposed many methodologies to detect crack locations and damage severity in bending structures such as reinforced concrete beams and bridges using periodic measured load tests. Although their effectiveness is verified using finite element model, laboratory model and a real bridge. The researchers reported that the methodology can only predict the very severe locations of the damage but cannot detect other smaller damages or cracks. In addition, the method requires a repeated bridge load test which is rather time-consuming and expensive. Unlike the previous studies, the present research, therefore, proposes the new methodology for crack detection from bridge deformation profile due to self-weight. Using a simple comparison of bridge inclinations under its self-weight before and after damages, the Crack Index is then computed and used to indicate the damage along the bridge without any load test requirement. The algorithm of computing the Crack Index taking into account the measurement accuracy is presented. Based on the computer simulations of bridge cracks, the Crack Index is determined and compared to the existing methods under various crack patterns and crack depths. It is found from the obtained results that the newly proposed method can significantly improve the precision of crack detection of the bridges and can be approved by reliable numerical model.

Keywords: Bridge crack, Crack detection, Bridge deformation, Bridge inclination, Bridge self-weight, Bridge health monitoring system

1. INTRODUCTION

One of the significant superstructures that facilitates transportation technologies, such as expressways and overpasses, is bridge. Reinforced concrete bridge is the most popular type at which we observe around the world. Many bridge structures in the world were constructed and it still have been utilized. How we know that the structures are still safe and ready for use has been the question that a lot of engineers have attempted to seek the solutions.

The concept of detecting abnormal occurrences in the bridge structures, such as crack developments and significant overgrowth of deflection, is the preliminary remark which inform the authorities to apply law enforcement for rehabilitation or permanent closing. Unfortunately, many severe and sudden deteriorate situations that affected to many lives and their assets still happened in the past. To better follow the conditions of existing bridges, there were some previous researchers seeking the approaches to early detect failure in each bridge structure, such as Ultrasonic approach (Kong et al., 2020) and Infrared thermography (Ichi & Dorafshan, 2022).

However, there were some restrictions of those methods that can only find cracks occurring with certain depth or some specific conditions. To comprehensively and regularly inspect the existing structures, Bridge Health Monitoring system, which is the application of sensors to follow the responses of bridge structures, came with more advantages. The general type of testing, which appeared in the past researches, consisted of the static, dynamic and crawl-speed test and used the heavy trucks to perform the analyses.

When the bridge structures tend to collapse, their dynamic and static responses will be changed due to the failure condition. The dynamic responses of each structure, such as mode shapes and natural frequencies, have been taken into consideration for a period of time since they present some changes when some cracks develop. However, these responses can only present the notable values when major cracks in the structures occurs and cannot specify the location of the failure. On the contrary, the static responses come up with more advantages, especially bending structures governed by the moment-curvature relation. The curvature of the damaged parts is noticeably increased due to the reduction of bending stiffness around those areas.

2. LITERATURE REVIEW

2.1 Bridge Health Monitoring system

The Bridge Health Monitoring system is adopted by installation of developed sensors in bridge structures to perform periodic load test and notice unusual values. The sensors often used for measuring the responses of the bridges in many researches and field works are composed of accelerometer, inclinometer, displacement sensor and strain sensor.

Some previous researchers assessed the Indian River Inlet Bridge located at Delaware in the United States and provided Bridge Health Monitoring sensors. They designed the methodology to generate the baseline responses received from the first time that the bridge was opened, and 6 months and a year after that. The static, crawl-speed, and dynamic test were contributed by using calibrated trucks. The results did not show any unusual conditions (Al-Khateeb et al., 2019).

Other utilizations of the Bridge Health Monitoring system appeared and varied by the implementation and indices computed by the selected responses. There were lots of researchers provided the example interesting approaches in this scope (Ferguson et al., 2022; Sun et al., 2016; Zhang et al., 2021).

2.2 The Influence Line of the Change of Inclination Angle and The Deformation Area Difference Method

When cracks occur in each bridge structure, stiffness of cracked sections will be decrease due to crack enlargement and they impact on the curvature at that area described by the moment-curvature relation as shown in the equation below.

$$-\frac{M(u)}{EI(u)} = \kappa(u) \approx \frac{d}{du} \varphi(u) = \frac{d^2}{du^2} w(u) \quad (1)$$

$M(u)$ presents the value of bending moment at the section. $EI(u)$ presents the stiffness of the section. $\kappa(u)$, $\varphi(u)$ and $w(u)$ represents the value of curvature, rotation and deflection at the section.

In 2020, there was the group of researchers who studied about how to use the influence line of the change of rotation to detect possible crack locations in bridge structures. They concluded that the area of support location is the most appropriate position for setting up inclinometer sensors. Although this method found the correct points of crack, to apply this method in practice needed moving calibrated trucks to generate influence lines. It was necessary to control speed and use the advance techniques to analyze and divide an influence line of each axle using axle configuration (Huseynov et al., 2020).

The Deformation Area Difference method presents the simpler way to define crack areas on bridges. The static test using trucks was involved in the method to increase the sensitivity of results. However, there were some false predictions due to the restriction of measurement accuracy. (Erdenebat & Waldmann, 2020; Erdenebat et al., 2018).

2.3 The Principle of Gradual Strain Distribution

Reinforced concrete is the type of structure that can simply design for beam or bridge structures. In this part, the previous researches will be described. The details are about the strain distribution and other related parameters of cracking happened on reinforced concrete bending structures. The distribution of the cracked structure can be illustrated as shown in the figure.

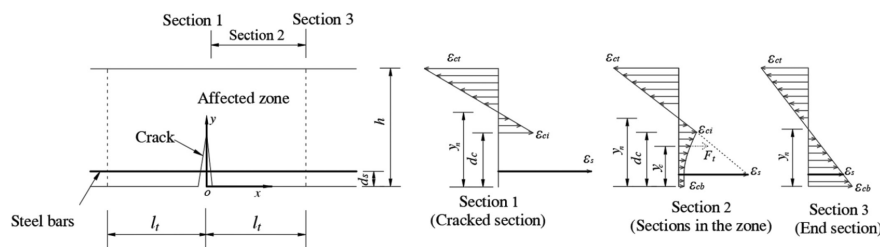


Figure 1. Strain distribution of cracked reinforced concrete beam structure (Fu et al., 2022)

By equation (2), The strain distribution of concrete in each section is proposed by the researchers to describe behavior of the crack model. The crack is developed at the section 1 and the section 2 represents the section of the area affected by the nearest crack location. The strain distribution of rebar is simply calculated by using the plane section remains plane assumption and represented by the equation (3). Lastly, the length of affected area is computed by the equation (4).

Concrete strain distribution:

$$\begin{aligned} \text{Section1: } \varepsilon_c(y) &= \begin{cases} 0 & ; y < d_c \\ (\varepsilon_{ct} \times \frac{y - y_n}{h - y_n}) & ; y \geq d_c \end{cases} \\ \text{Section2: } \varepsilon_c(y) &= \begin{cases} \left(\varepsilon_{ct} \frac{d_c - y_n}{h - y_n} - \varepsilon_{cb} \right) \left(\frac{y}{d_c} \right)^3 + \varepsilon_{cb} & ; y < d_c \\ (\varepsilon_{ct} \times \frac{y - y_n}{h - y_n}) & ; y \geq d_c \end{cases} \\ \text{Section3: } \varepsilon_c(y) &= \left(\varepsilon_{ct} \times \frac{y - y_n}{h - y_n} \right) \end{aligned} \quad (2)$$

$$\text{The strain distribution of steel bar: } \varepsilon_s = \left(\frac{d_s - y_n}{h - y_n} \right) \varepsilon_{ct} \quad (3)$$

$$\begin{aligned} \text{Affected length} &= \min \left(l_t, \frac{l_c}{2} \right) \\ l_t &= c + \frac{f_{ctm} D_s}{4 \tau_{bms} \rho_{ef}} \end{aligned} \quad (4)$$

c represents the concrete covering of the tension rebar in unit of meters. f_{ctm} represents the average tensile strength of the concrete in unit of MPa. D_s is the diameter of the tension rebar in unit of meters. ρ_{ef} represents the reinforcement ratio. l_c represents the distance between the considered crack and the adjacent crack in unit of meters. τ_{bms} represents the bonding stress between rebar and concrete in unit of MPa. For the stabilized cracking stage, τ_{bms} can be computed by the formula $\tau_{bms} = 1.8 f_{ctm}$

By applying the equilibrium equation of each section, the location of neutral-axis and the moment of inertia at each section can be proved. The second moments of area varied slightly in the affected area depends on the distance from the crack location.

$$I_{eq} = A_{ef}(y_n - y_c)^2 + \frac{E_s}{E_c} A_s (y_n - d_s)^2 + \frac{b(h - y_n)^3}{3} \quad (5)$$

A_{ef} represents the effective tensile section of concrete in unit of meter². A_s represents the whole area of the tension steel bars in unit of meter². y_n represents the neutral axis of the section in unit of meters. y_c represents the acting point of the resultant tensile force of concrete in unit of meters. d_s represents the location of tension steel bar measured from the bottom of the section in unit of meters. E_c and E_s are the modulus of elasticity of the concrete and steel respectively in unit of MPa.

More details about the principle of gradual strain distribution proved by the laboratory test and finite element model are already described by the previous researches (Fu et al., 2022; Fu et al., 2020).

3. METHODOLOGY

The new proposed index to investigate damage on bridge structures comes directly from the moment-curvature relation. Based on the assumption that interested cracks affect to bending stiffness of the damaged sections, there are the evident growths of the curvature values at the cracked sections. The below formula describes the change of curvature near to deformed sections and the definition of each variable.

$$(\kappa_d - \kappa_o)_i \approx \frac{(\varphi_d(x_i) - \varphi_d(x_{i-1})) - (\varphi_o(x_i) - \varphi_o(x_{i-1}))}{(x_i - x_{i-1})} \quad (6)$$

$(\kappa_d - \kappa_o)_i$ represents the changes of the curvature at the i^{th} section. $\varphi_d(x_i)$ presents the inclination angle of the deformed structure at the i^{th} section. $\varphi_o(x_i)$ presents the inclination angle of the initial structure at the i^{th} section. x_i represents the location of the measurement point at the i^{th} section.

From the above equation, only using the numerator can define the possible crack zone. The denominator of the formula is varied by the distance between the position of each inclinometer installation. Crack Index is defined by the concept.

3.1 Inclinometer

Rotation or inclination angle of bridge structures are focused on because of the existing of high-accuracy and conveniently installed instruments. Inclinometer is the measuring instrument set up to compute rotation output based on the direction of the gravitational acceleration. The efficiency of the sensor depends on the sensitivity of each one. The mainly used inclinometer involved in the calculation of theoretical model is referred by the SOLAR-05. The resolution of this instrument written in the specification is 0.001 degree which is equivalent to about 0.000017 radian. Nevertheless, it is difficult to combine the effect of that resolution into the adjustment of rotation from the theoretical computation. By decreasing the resolution to be equal to 0.00002 radian, the output values can be easily adjusted in the theoretical computation by rounding to even number.

The resolution only uses to describe the maximum accuracy that the instrument can measure. In practice, there are many influences that affects to the instruments. The accuracy at 20 °C that is another detail in the specification come instead and represent the on-site efficiency of each inclinometer more reliably. The accuracy of the SOLAR-05 detailed in the specification equal to 0.01 degree. At present, many high-resolution inclinometers are developed expeditiously. The instruments with the accuracy in the range of 0.01 to 0.001 degree or the resolution in the range of 0.001 to 0.0001 degree are applied extensively since they are sufficient to detect small changes of inclination angle.

3.2 Crack Index

Crack Index is formed by combination of the change of inclination angle collected from the deformed structure and the resolution or accuracy of the instrument. The equation which describes the Crack Index is simply created. It can be concluded from the figure 2 and 3. that the value of rotation changes will be gained in only the boundary of affected area due to the principle of gradual strain distribution no matter where the crack occurs. Due to the adoption of these ideas, the algorithm to generate the Crack Index can be computed by the equation (7).

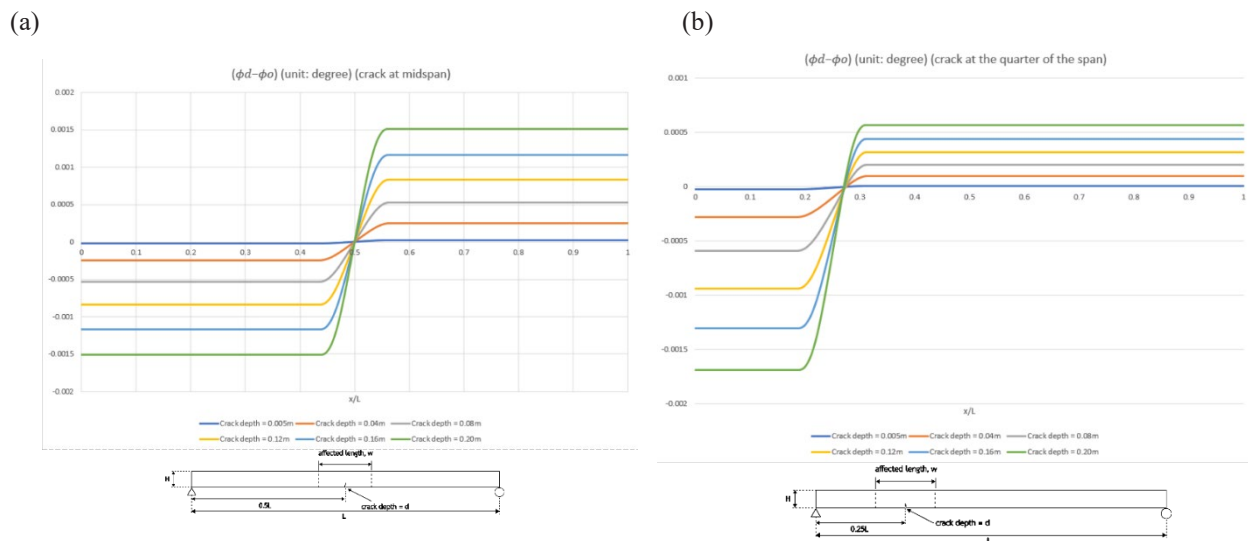


Figure 2. Rotation change at each crack depth due to the single crack (a) at the midspan and (b) at the quarter of the span respectively.

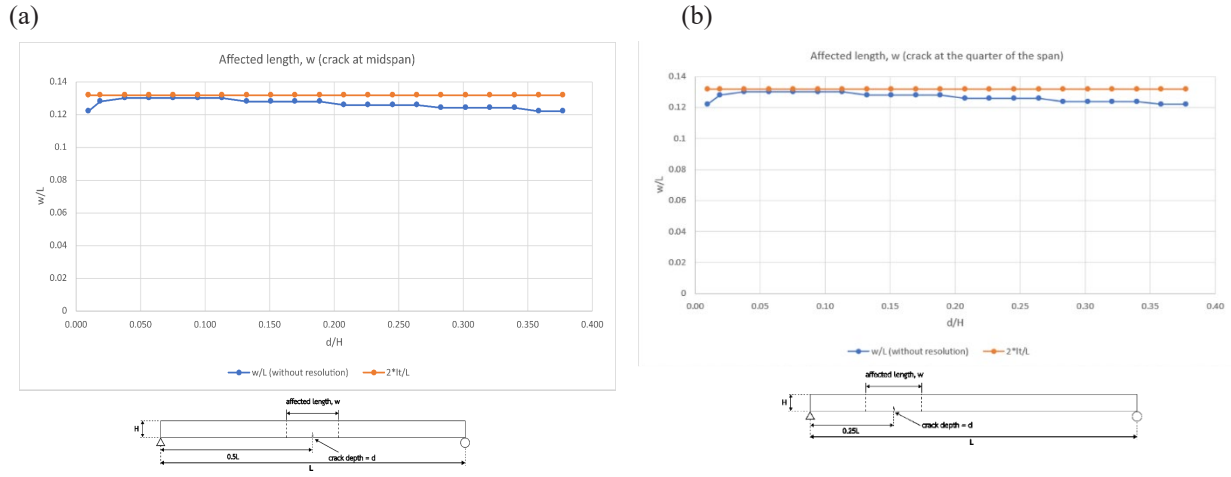


Figure 3. Affected length (w) at each crack depth due to the single crack (a) at the midspan and (b) at the quarter of the span respectively.

$$\begin{aligned}
 & (\text{Crack Index})_{x=x_i} \\
 & = \begin{cases} 0, & (\varphi_d(x_{i+m}) - \varphi_o(x_{i+m})) - \min((\varphi_d - \varphi_o)_{i-1}) < 2\varepsilon \text{ and } (x_{i+m} - x_{i-1}) \leq 2l_t \\ 0.1, & 0 \leq (\varphi_d(x_i) - \varphi_o(x_i)) - (\varphi_d(x_{i-1}) - \varphi_o(x_{i-1})) \leq \varepsilon, (\varphi_d(x_{i+m}) - \varphi_o(x_{i+m})) - \min((\varphi_d - \varphi_o)_{i-1}) \geq 2\varepsilon \text{ and } (x_{i+m} - x_{i-1}) \leq 2l_t \\ 0.2n, & n\varepsilon \leq (\varphi_d(x_i) - \varphi_o(x_i)) - (\varphi_d(x_{i-1}) - \varphi_o(x_{i-1})) < (n+1)\varepsilon \text{ for } n \in \{2,3,4\} \\ 1, & (\varphi_d(x_i) - \varphi_o(x_i)) - (\varphi_d(x_{i-1}) - \varphi_o(x_{i-1})) > 5\varepsilon \end{cases} \quad (7) \\
 & \min((\varphi_d - \varphi_o)_{i-1}) = \min[(\varphi_d(x_{i-1}) - \varphi_o(x_{i-1})), (\varphi_d(x_N) - \varphi_o(x_N))]
 \end{aligned}$$

$\min[a(x_i), a(x_j)]$ represents the algorithm that compute for the minimum value of the function a within the range of $x \in [x_i, x_j]$. ε represents resolution or accuracy of the inclinometers. N is the total number of inclinometers installed on each model.

The equation above used for algorithm design of the proposed Crack Index describe that Crack Index will signal about some abnormal conditions which is possibly occurring between the location of i^{th} and $(i-1)^{th}$ sensor if there is the growth of the rotation changes more than two times within affected length. By determination the spacing of instrument installation to be greater than 2 times of the affected length or the length $2l_t$, the formula above can be simply modified to be equation (8), which is considered only the adjacent sensors.

$$\begin{aligned}
 & (\text{Crack Index})_{x=\frac{x_i+x_{i-1}}{2}} \\
 & = \begin{cases} 0, & (\varphi_d(x_i) - \varphi_o(x_i)) - (\varphi_d(x_{i-1}) - \varphi_o(x_{i-1})) < \varepsilon \\ 0, & \varepsilon \leq (\varphi_d(x_i) - \varphi_o(x_i)) - (\varphi_d(x_{i-1}) - \varphi_o(x_{i-1})) < 2\varepsilon \text{ and } (\varphi_d(x_{i+1}) - \varphi_o(x_{i+1})) - (\varphi_d(x_i) - \varphi_o(x_i)) < \varepsilon \\ 0.1, & \varepsilon \leq (\varphi_d(x_i) - \varphi_o(x_i)) - (\varphi_d(x_{i-1}) - \varphi_o(x_{i-1})) < 2\varepsilon \text{ and } \varepsilon \leq (\varphi_d(x_i) - \varphi_o(x_i)) - (\varphi_d(x_{i-1}) - \varphi_o(x_{i-1})) < 2\varepsilon \\ 0.2n, & n\varepsilon \leq (\varphi_d(x_i) - \varphi_o(x_i)) - (\varphi_d(x_{i-1}) - \varphi_o(x_{i-1})) < (n+1)\varepsilon \text{ for } n \in \{2,3,4\} \\ 1, & (\varphi_d(x_i) - \varphi_o(x_i)) - (\varphi_d(x_{i-1}) - \varphi_o(x_{i-1})) \geq 5\varepsilon \end{cases} \quad (8)
 \end{aligned}$$

In conclusion, Crack Index represents the possibility that the cracks develop at each interval due to significant growths of rotation changes. If Crack Index equals to 1 or the increase in the value of rotation change is more than 5 times than the accuracy of the instrument within the interval of two adjacent instruments, it can be surely concluded that some cracks occur around that area.

3.3 Numerical Model and Details

By applying the principle of Gradual Strain Distribution, the moment-curvature relation and the geometric relations, the static responses of the structures, such as curvature, rotation and displacements, are computed. Herein, the bridge section from the specification with the assumption that the cracked bridge has the same behavior as the cracked reinforced concrete beam structure is simply adjusted to verify the methodology and the efficiency of proposed Crack Index.

Modified reinforced concrete bridge model applied for verification of the approach is one of the types in the standard drawing written by Ministry of Transport, Thailand. The model is simplified to be the rectangular section, consists of 15 meters width and have the span length 10 meters long. The figure 4a and 4b represent the simplified model that is updated from the original model in the specification. To easily analyze, the type of simply supported structure is overcome to use. Compressive strength of concrete is specified to be the same as the

specification and equal to 35 MPa. Steel rebar is referred by the standard of TIS24 Grade SD40. Clear concrete covering is determined to be 40 centimeters. In this paper, only self-weight load condition is focused on since it is convenient to control the condition without vary effects due to external loads and other factors.

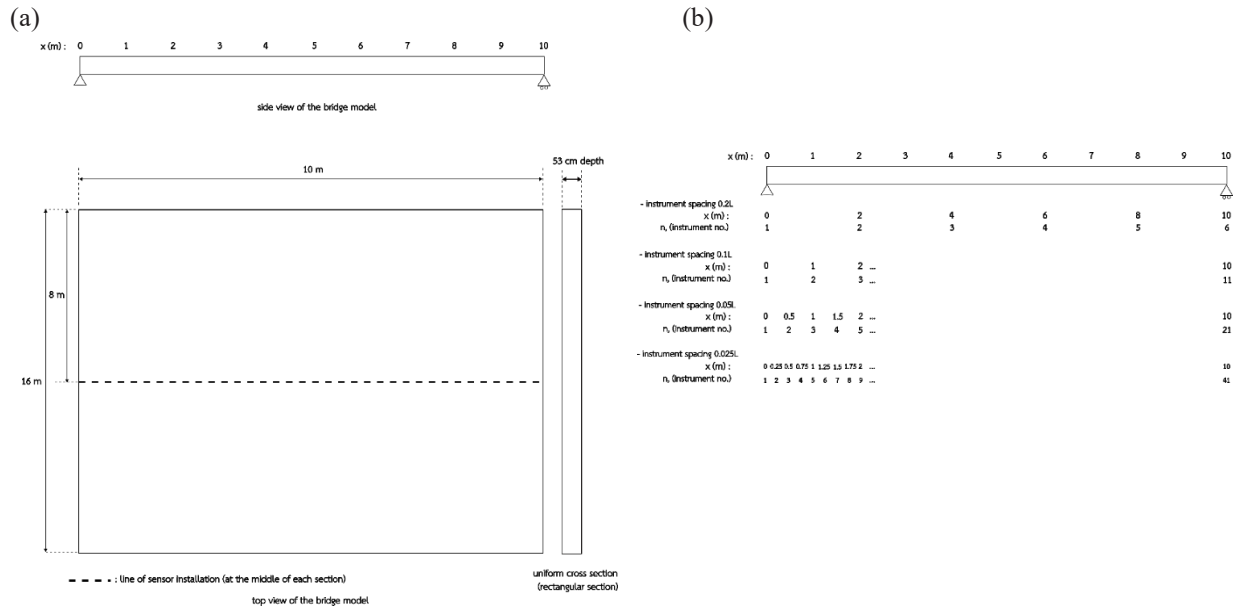


Figure 4. (a) Side and top view of the bridge model adopted for theoretical analysis and referred by the standard drawing together with the crack pattern throughout the section at the midspan.

(b) Location of instrument installation using the constant spacing of measurement point 0.2L, 0.1L, 0.05L and 0.025L or using 6, 11, 21 and 41 inclinometers respectively

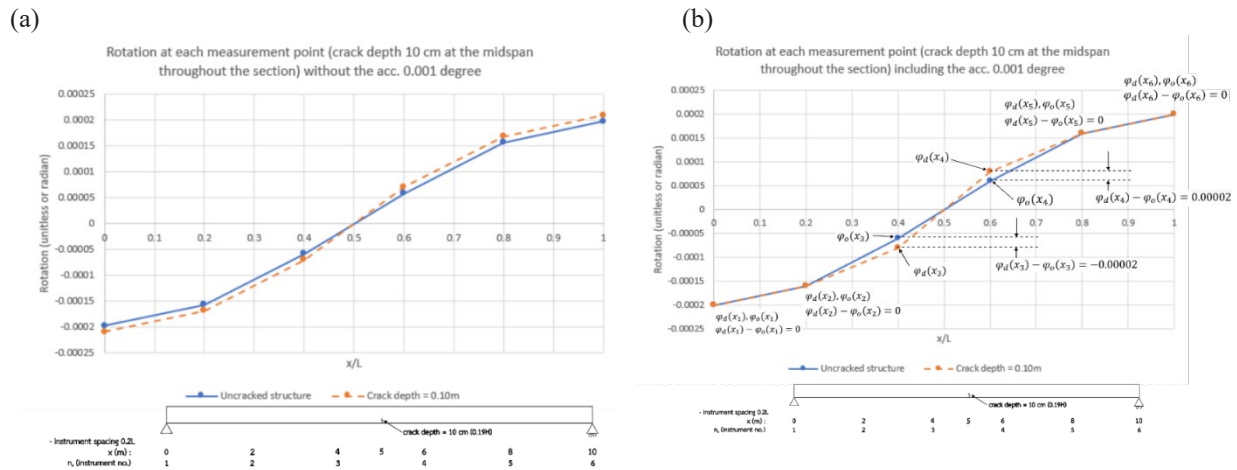
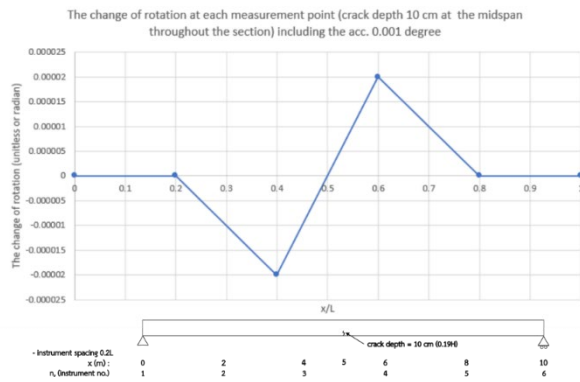


Figure 5. Rotation (a) without the accuracy 0.001 degree and (b) with the accuracy 0.001 degree respectively at each measurement point using the spacing 0.2L. The crack occurs at the midspan with the crack depth 10 centimeters (0.19H).

(a)



(b)

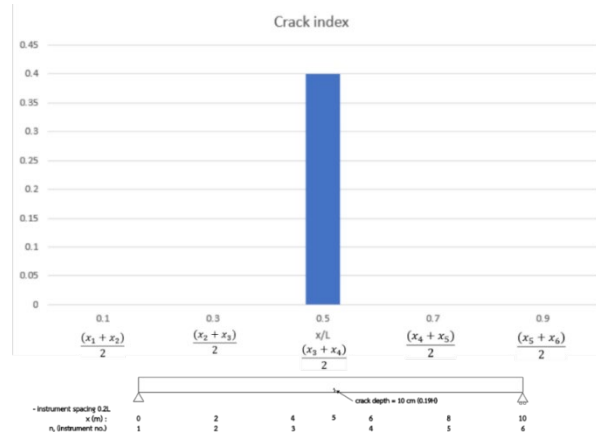


Figure 6. (a) Rotation change at each measurement point computed from the figure 5b
(b) Crack Index using the rotation changes in the figure 6a

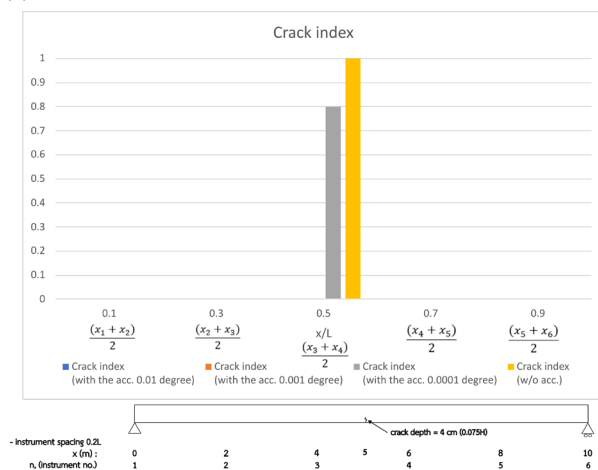
Figure 5a and 5b represent the rotation at each measurement point of the model with and without the effect of accuracy 0.001 degree respectively. The value of rotation change at each point shown in the figure 6a compute from subtraction the uncracked rotation (blue, solid) from the cracked (orange, dash) as presented in figure 5b. Due to the fact that the location of measuring instruments will be set up using the spacing $0.2L$, which is more than 2 times of the affective length or l_t , the rotation changes of the adjacent sensors are only taken into account.

4. RESULTS FROM NUMERICAL MODEL AND DISCUSSION

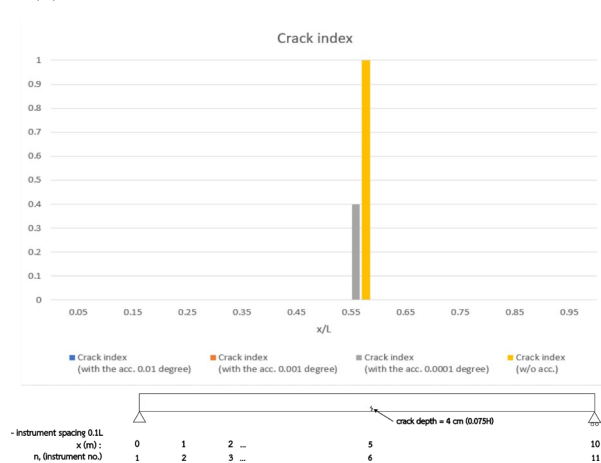
4.1 Results from Numerical Model

From the first crack scenario or the single crack 4 centimeters (crack depth = $0.075H$) at midspan throughout the section, by using the instrument spacing $0.2L$, Crack Index can be presented in the figure 7a. The figure 7b, 7c and 7d represent the illustration of Crack Index in case of measurement points increased to 11, 21 and 41 points respectively (the spacing of instrument installation $0.1L$, $0.05L$ and $0.025L$). The different instrument accuracies, consisting of 0.01 (blue), 0.001 (red) and 0.0001degree (grey) are collected in order to consider how the sensor quality improve this methodology. Meanwhile, the theoretical results without accuracy effect are also presented in the graph (orange).

(a)



(b)



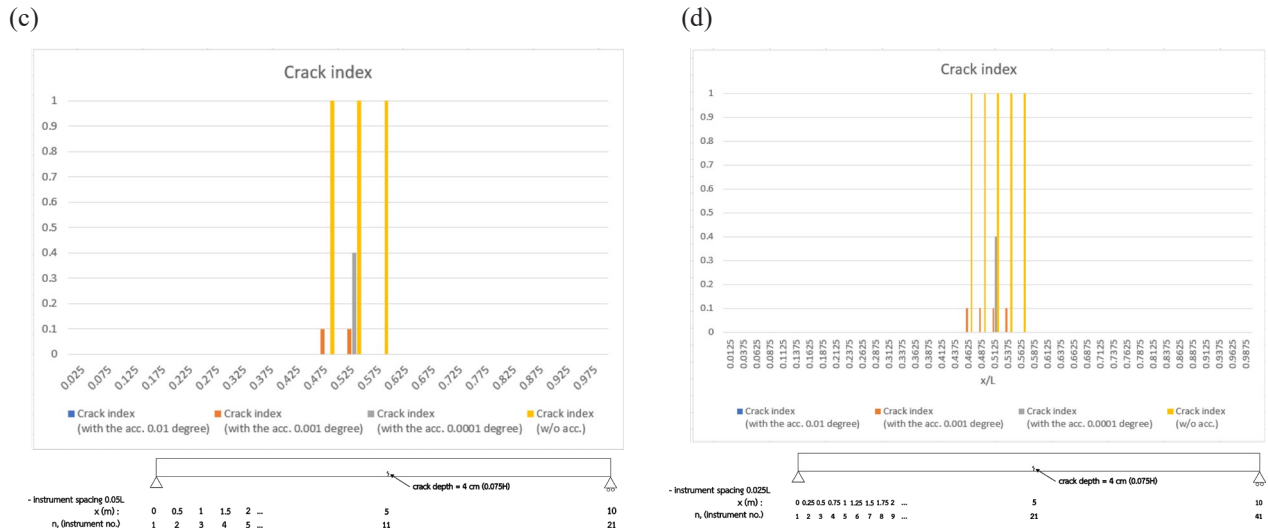


Figure 7. Crack Index of the bridge model that consists of single crack (crack depth = 4 centimeters (0.075H)) at the midspan throughout the section with the various accuracies of the instrument using the number of instruments (a) 6, (b) 11, (c) 21 and (d) 41 as illustrated in the figure 4

According to the figure 7a to 7d, the values of Crack Index appear within the area that are affected from the stiffness reduction due to the cracks. It can be concluded from these graphs that the more accurate instrument we use, the more effective the proposed approach to detect small cracks and specify accurate crack positions we receive.

After that, the condition of crack depth 10 centimeters (crack depth = 0.19H) from the bottom throughout the cross section at the midspan is determined to notice that how the values of Crack Index are affected and it can be concluded that Crack Index computed together with 6 sensors that have the accuracy 0.001 degree can represent the accurate crack location in this scenario.

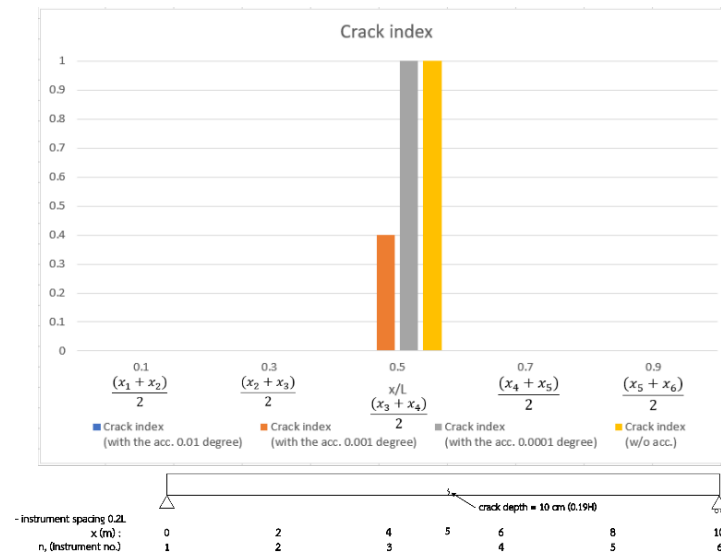


Figure 8. Crack Index of the bridge model that consists of single crack (crack depth = 10 centimeters (0.19H)) at the midspan throughout the section with the various accuracies of 6 sensors as illustrated in the figure 4

4.2 The Effect of Crack Location to the Proposed Crack Index

At the location composing of small amount of curvature, Crack Index will slowly detect the small failure due to the relationship between level of stiffness change and an initial curvature at each position. The case of single crack at the quarter of the span is set up to compare how different location of crack affects to Crack Index. In this

scenario, the condition of crack depth 10 centimeters or 0.19H throughout the section is adopted to compare with the one at the midspan.

Crack Index computed from the single crack at the quarter of the span are less than the ones computed from the midspan and it only appears when spacing of measurement points is less than 0.025L. It means that the proposed Crack Index is less sensitive to cracks that occur near to the supports. However, Crack Index is proposed for crack conditions due to the bending mode failure that more possibly occurs near to midspan; therefore, this effect is not a lot taken into consideration.

4.3 The Spacing Between Each Inclinometer

Due to the comparison of Crack Index as shown in the figure 7, it can be concluded that the less spacing between measurement points, the more possibility to find correct locations of crack by this algorithm. However, the installation of many sensors is not practical and difficult and the effect is not concerning since it will not impact on the proposed Crack Index when cracks are grown up large enough. As shown by the examples above, only six high-resolution sensors are sufficient to predict the area at which cracks occur.

4.4 The Comparison Between the Proposed Crack Index and the DAD-Value

The Deformation Area Difference method is one of the approaches that is applied for bridge assessment based on abrupt changes of curvature at each crack location due to bending stiffness reduction. The DAD-value can theoretically identify possible locations of crack that may occur at bridge structures. Nevertheless, the accuracy due to the instruments comes to be the influence of the approach since it affects to the rounding of inclination angle measured from instrument due to both the initial and the cracking state.

The graphs in the figure 9 illustrate the comparison between the curvature-based DAD-value (blue) and the proposed Crack Index (red) that are computed from the single crack condition occurring throughout the section at the midspan. Crack depth is constantly determined to be equal to 4 centimeters (0.075H) and the adjustment of the results by the effect of accuracy 0.001 degree is also represented. By consideration of the same number of instruments for assessment, the values of Crack Index tend to effectively point out the accurate location of crack. Due to the fact that the notion to generate the algorithm of Crack Index is developed from the equation of curvature-based DAD-value, Crack Index mitigates noises that are occurred by the effect of instrument accuracy and is more sensitive to small cracks.

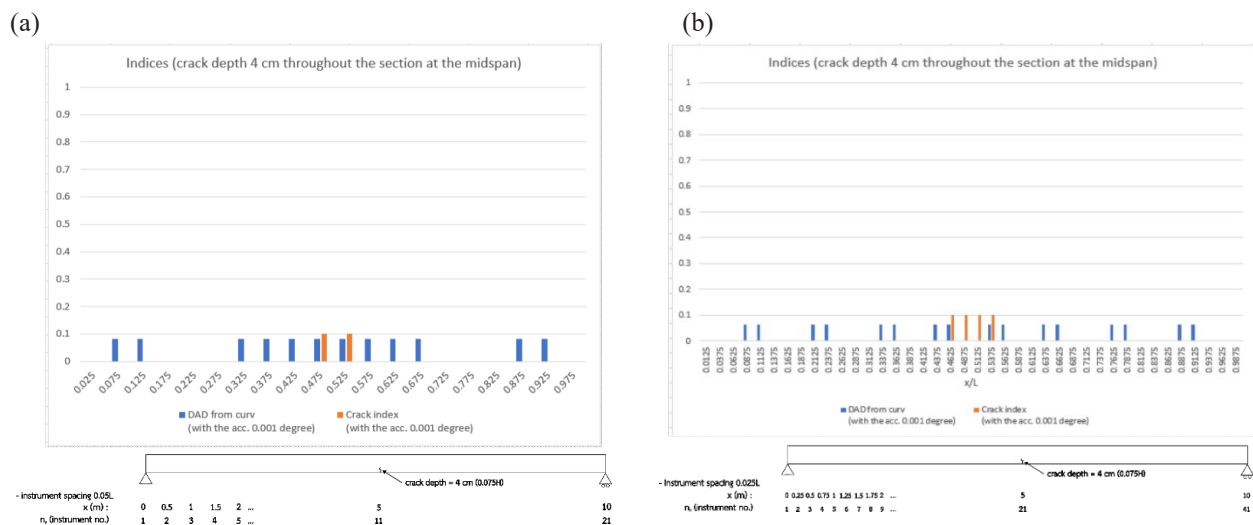


Figure 9. Curvature-based DAD-value and Crack Index of the crack depth 0.075H at the midspan throughout the section with the instrument accuracy 0.001 degree using the number of instruments (a) 21 and (b) 41 as illustrated in the figure 5.

5. CONCLUSION

The solutions to detect cracks that develop in bridge structures are still in the spotlight and the approaches that can specify the accurate possible locations of cracks are proposed by many researchers. However, those methods have many restrictions to assess. In this research, Crack Index due to the only self-weight load condition is developed from the previous idea of curvature changes around each crack location. To resolve the effect of noises of the Deformation Area Difference method, the algorithm of Crack Index as shown in the equation (7) and (8) are presented. Crack Index is theoretically effective to predict crack locations as other indices can do. The crack location, spacing between each sensor and the accuracy of sensors affect to the sensitive of Crack Index.

From the results in the previous chapter, it can be concluded that the Crack Index specifies the accurate location of each crack and is sensitive to crack locations that have larger value of curvature. In this paper, the type of structure model is simply supported with uniform section and it can clearly indicate cracks near to midspan. A number of instruments using for assessment encourage to quickly predict the small crack condition. On the contrary, when cracks develop to be large enough, all arrangements of measuring instruments will represent the accurate position of cracks. Moreover, the field of development of the inclinometer sensor in the future that improve the accuracy of instrument are very important since it will increase the efficiency of Crack Index. The change of temperature gradient is the variable that are often noticeably mentioned and it can be resolved by collection inclination angle from each sensor at the same temperature condition. The main restriction of the methodology that is to certainly recognize the accuracy of inclinometer in the field test are ensured by laboratory test.

However, the scope of the future studies about Crack Index is extensive. The other conditions that can occur in the real structure, such as the support settlement, and the study on the real bridge structure are still excluded but those areas need to be considered in the future since it may affect to the sensitive of this methodology.

REFERENCES

- Al-Khateeb, H. T., Shenton, H. W., Chajes, M. J., & Aloupis, C. (2019). Structural Health Monitoring of a Cable-Stayed Bridge Using Regularly Conducted Diagnostic Load Tests [Original Research]. *Frontiers in Built Environment*, 5. <https://doi.org/10.3389/fbuil.2019.00041>
- Erdenebat, D., & Waldmann, D. (2020). Application of the DAD method for damage localisation on an existing bridge structure using close-range UAV photogrammetry [Article]. *Engineering Structures*, 218, Article 110727. <https://doi.org/10.1016/j.engstruct.2020.110727>
- Erdenebat, D., Waldmann, D., Scherbaum, F., & Teferle, N. (2018). The Deformation Area Difference (DAD) method for condition assessment of reinforced structures. *Engineering Structures*, 155, 315-329. <https://doi.org/10.1016/j.engstruct.2017.11.034>
- Ferguson, A. J., Hester, D., & Woods, R. (2022). A direct method to detect and localise damage using longitudinal data of ends-of-span rotations under live traffic loading [Article]. *Journal of Civil Structural Health Monitoring*, 12(1), 141-162. <https://doi.org/10.1007/s13349-021-00533-5>
- Fu, C., Gao, Z., & Yan, P. (2022). Calculation of Effective Section of Cracked Concrete Beams Based on Gradual Strain Distributions [Article]. *ACI Structural Journal*, 119(5), 217-226. <https://doi.org/10.14359/51734832>
- Fu, C., Tong, D., & Wang, Y. (2020). Assessing the Instantaneous Stiffness of Cracked Reinforced Concrete Beams Based on a Gradual Change in Strain Distributions [Article]. *Advances in Materials Science and Engineering*, 2020, Article 7453619. <https://doi.org/10.1155/2020/7453619>
- Huseynov, F., Kim, C., Obrien, E. J., Brownjohn, J. M. W., Hester, D., & Chang, K. C. (2020). Bridge damage detection using rotation measurements – Experimental validation [Article]. *Mechanical Systems and Signal Processing*, 135, Article 106380. <https://doi.org/10.1016/j.ymssp.2019.106380>
- Ichi, E., & Dorafshan, S. (2022). Effectiveness of infrared thermography for delamination detection in reinforced concrete bridge decks. *Automation in Construction*, 142, 104523. <https://doi.org/10.1016/j.autcon.2022.104523>
- Kong, X., Zhang, Z., Meng, L., & Tomiyama, H. (2020). Machine Learning Based Features Matching for Fatigue Crack Detection. *Procedia Computer Science*, 174, 101-105. <https://doi.org/10.1016/j.procs.2020.06.063>
- Sun, Z., Nagayama, T., & Fujino, Y. (2016). Minimizing noise effect in curvature-based damage detection [Article]. *Journal of Civil Structural Health Monitoring*, 6(2), 255-264. <https://doi.org/10.1007/s13349-016-0163-x>
- Zhang, Y., Xie, Q., Li, G., & Liu, Y. (2021). Multi-damage identification of multi-span bridges based on influence lines [Article]. *Coatings*, 11(8), Article 905. <https://doi.org/10.3390/coatings11080905>

DYNAMIC RESPONSE EVALUATION OF RAILWAY TRACK TRANSITIONS WITH RESILIENT MATERIALS

Surapan Noppharat¹, Anand Raj², and Chayut Ngamkhanong³

1) Master's degree Student, Department of Civil Engineering, Faculty of Engineering, Chulalongkorn University, Bangkok, Thailand. Email: 6470299421@chula.ac.th

2) Ph.D., Post Doctoral Research Fellow, Department of Civil Engineering, Faculty of Engineering, Chulalongkorn University, Bangkok, Thailand. Email: anandrajce@gmail.com

3) Ph.D., Lecturer, Department of Civil Engineering, Faculty of Engineering, Chulalongkorn University, Bangkok, Thailand. Email: Chayut.ng@chula.ac.th

Abstract: Railway infrastructure development is a growing trend around the globe, offering numerous benefits. However, one of the significant challenges is the track transition problem that arises from changing track sections. This leads to abrupt changes in track stiffness, resulting in substantial damage to the track structure due to the differential settlement, thereby increasing maintenance costs. In Thailand, the first phase of Thailand's high speed rail project has introduced a slab track system from China combined with traditional ballasted tracks at several sections. It is important to note that transition area can be critical and. There have been several methods to reduce differential stiffness. However, the combined method of using both Under Sleeper Pads (USPs) and Under Slab Mats (USMs) has not been widely adopted, even though it has the potential to reduce track vibration, impact load, and differential settlement. This paper presents the 3D train-track-soil finite element model at railway track transition zone with USPs and USMs. Several types of pads are proposed at different locations on the tracks subjected to various train speeds. Numerical results from a train-track-soil model computed using LS-DYNA are validated with field measurements and previous numerical results. One of the main advantages of using USPs is that they help to reduce ballast degradation. Similarly, USMs can be used to control track stiffness. While there are various ways to address these problems, the mixed method of using USPs and USMs is found to be an alternative to mitigate the problem at railway track transition. It is important to use resilient pads with caution, as improper selection or application of these pads can lead to further problems. Therefore, additional research is required to assess the potential benefits of this approach in reducing track vibration, impact load, and differential settlement on other tracks and soil types.

Keywords: Track Transition, Dynamic Train-Track-Soil Interactions, Under Sleeper Pads (USPs), Under Slab Mats (USMs)

1. INTRODUCTION

Engineering advancements in construction technologies have led to the development of efficient transportation systems, and railway infrastructure is at the forefront of this trend. Rail transportation has several advantages over other modes of transportation, such as high load capacity, punctuality, and convenience. The developments of railway infrastructure are crucial for driving economic growth and social development.

Recently, Thailand has adopted a new construction technology from China, the Chinese Railway Track System (CRTS) Type III, for the first phase of high-speed rail line project. However, there are concerns regarding the design and construction of the railway track system, particularly the issue of track transition. The route for the project includes a region where the track section changes from ballasted track to slab track. Changing the track section abruptly can cause a sudden change in the vertical track stiffness of the structures, leading to an increase in dynamic forces and vertical acceleration. This can result in differential settlement of the track, leading to increased maintenance costs over time. In the past, several solutions, such as pile, subgrade modification, Hot-Mixed Asphalt, and approach slab, have been proposed to solve track transition problems. However, these methods are cost effective and difficult to install after the tracks have been constructed.

Note that literature on solving transition problems with mixed methods is limited (Grossoni et al. 2019). Therefore, in this study, we propose a mixed method using two types of resilient materials that are made of rubber such as Under Sleeper Pads (USPs) and Under Slab Mats (USMs) to address this problem. USPs can be installed conveniently under sleepers in ballasted tracks, which are the primary type of track structures used for other lines in Thailand, whereas USMs can be used as an isolation layer in slab track CRTS type III panels. It is very important to note that these materials are usually made of synthetic materials which have a high carbon footprint. Therefore, using natural rubber as a sustainable alternative is important for Thailand as a leading producer.

2. METHOD

In this research, we develop 3D Finite Element Method (FEM) models of railway track transition with the consideration of train, track and ground using LS-DYNA, as shown in Figure 1. Dynamic analysis is performed under various train speeds. The focus of the analysis is on the track transition zone, where USPs and USMs are installed. This section includes train modelling, track modelling, ground modelling and USPs and USMs.

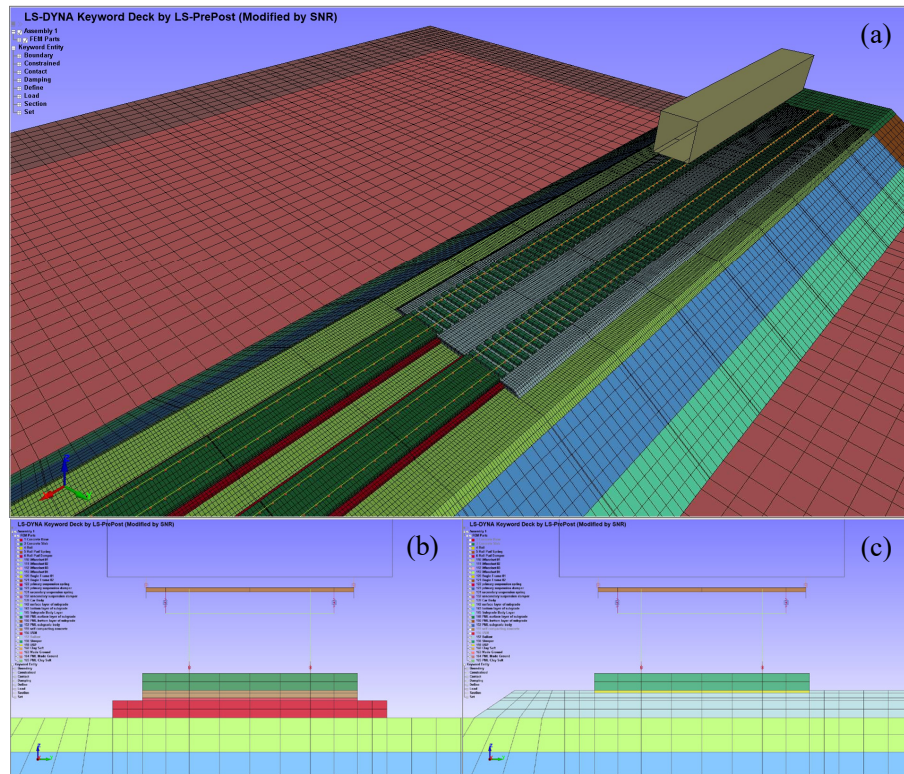


Figure 1. (a) 3D FEM Track Transition Model in LS-DYNA, (b) Section of Slab Track CRTS type III with USMs, (c) Section of Ballasted Track with USPs

2.1 Train Modeling

The train model is developed based on multi-body simulations as presented in (Huang et al., 2014) and consists of three main components: car body, bogies, and wheelsets. The first component is the car body modelled as a rigid body using shell element. This simplifies the analysis of the effects on other parts of the train. The second component models the bogies using shell elements. This is because bending effects need to be considered for this part of the train. The third component models the wheelsets are modelled using beam elements. These components are connected through a suspension system composed of a spring and damper or discrete element.

This study considers the CR 400 BF, Fuxing Hao EMU Train. The vehicle properties are presented in Table 1. To analyze the vertical response, the train model is separated into 10 parts based on their Degree of Freedoms (DOFs). These parts include the vertical translation and rotation of one rigid car body, the vertical displacement and rotation of two bogies, and the vertical translation of four wheelsets (Ting et al. 2020). Note that we mainly aim to examine the vertical displacement and rotation of these specific parts to better understand the train's vertical response so that the transverse translation and rotation are neglected.

Table 1. Properties CR 400BF, Fuxing Hao EMU Train (Qi & Zhou, 2020).

Properties	Value	Unit
Mass of car body	45,200	[kg]
Mass of bogie frame	2,276	[kg]
Mass of wheelset	1,627	[kg]
Inertia of Pitch Motion of the Car Body	5.47×10^5	[kg.m ²]
Inertia of Pitch Motion of the Bogies	6,800	[kg.m ²]
Primary Suspension Stiffness	1.04×10^6	[N/m]
Primary Suspension Damping	5×10^3	[N.s/m]
Secondary Suspension Stiffness	4×10^5	[N/m]
Secondary Suspension Damping	6×10^3	[N.s/m]

2.2 Track Modeling

At transition zone, track section is divided into two: slab track and ballasted track. Steel rails are modelled using beam element and are connected to rail pads and fasteners, which are modelled using spring and damper elements. In order to accurately capture the behavior of the rail system, the effect of track irregularities is included in the model. The track irregularity is computed using the Power Spectrum Density (PSD) Function, as shown in Figure 2. This approach has been validated using data from Germany's high-speed rail network, ensuring that the model accurately represents the behavior of the rail system.

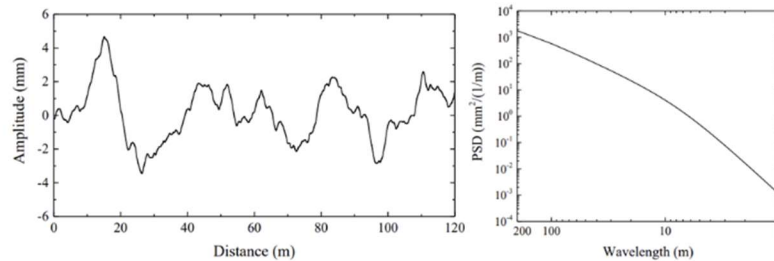


Figure 2. Roughness with Distance and PSD Wavelength (Li. Ting, 2020).

Ballasted tracks consist of various components, including sleepers, USPs, and ballast. Additionally, slab tracks of CRTS type III feature reinforced concrete slabs, a filling layer of self-compacting concrete, and a supporting layer of plain concrete. Note that the 3D solid element is considered for these components.

Tables 2 and 3 contain all the material and section properties for the ballasted track and slab track, respectively, that are utilized in the analysis. The dynamic properties with strain-rate dependent are considered using the keyword STRAIN_RATE_DEPENDENT_PLASTICITY.

Table 2. Material Properties of Ballasted Track (Gavin et al., 2010).

Properties	Value	Unit
Mass Density of the Ballast	1800	[kg/m ³]
Poisson's Ratio of the Ballast	0.30	[mm/mm]
Modulus of Elasticity of the Ballast	1.50×10^8	[N/m ²]
Mass Density of the Sleeper	2400	[kg/m ³]
Poisson's Ratio of the Sleeper	0.25	[mm/mm]
Modulus of Elasticity of the Sleeper	3.00×10^{10}	[N/m ²]
Stiffness of the Rails Pads	5.0×10^7	[N/m]
Damping of the Rail Pads	7.5×10^4	[N.s/m]
Mass Density of the Rail Pads	1500	[kg/m ³]

Table 3. Material Properties of Slab Track, CRTS Type III (Wang et al., 2017).

Properties	Value	Unit
Mass Density of the Rail	7830	[kg/m ³]
Modulus of Elasticity of the Rail	2.059×10^{11}	[N/m ²]
Poisson's Ratio of the Rail	0.30	[mm/mm]
Stiffness of the Rails Pads*	5.0×10^7	[N/m]
Damping of the Rail Pads	7.5×10^4	[N.s/m]
Thickness of Concrete Slab	0.20	[m]
Mass Density of the Concrete Slab	2500	[kg/m ³]
Modulus of Elasticity of the Concrete Slab**	3.6×10^{10}	[N/m ²]
Poisson's Ratio of the Concrete Slab	0.20	[mm/mm]
Thickness of Self Compacting Concrete	0.09	[m]
Mass Density of the SC Concrete	2500	[kg/m ³]
Modulus of Elasticity of SC Concrete**	3.4×10^9	[N/m ²]
Poisson's Ratio of Self Compacting Concrete	0.2	[mm/mm]
Thickness of Concrete Base	0.2	[m]
Mass Density of the Concrete Base	2500	[kg/m ³]
Modulus of Elasticity of the Concrete Base**	3.2×10^{10}	[N/m ²]
Poisson's Ratio of the Concrete Base	0.2	[mm/mm]

* Dynamics Stiffness.

** Reference Static Value, Strain Rate Dependent.

2.3 Ground Modeling

The analysis of soil needs to be tailored to the different layers of soil and material properties specific to construction in Bangkok, Thailand. In particular, this research focuses on Bangkok Clay Soil, which is a common soil type in the area. Bangkok Clay Soil is complex and composed of four layers, namely Soft Clay (SC), Medium Stiff Clay (MC), Hard Stiff Clay (HC), and Sand. To accurately model this soil, 3D Finite Element Method (FEM) solid elements are used for all parts of the soil. Additionally, the soil layers are modelled as Visco-Elastic materials. To prevent wave reflection at the edges of the ground, Perfectly Matched Layers (PML) elements are used. The Bangkok's soil profile and properties used are from previous literature (Likitlersuang et al., 2018)

The soil used for validation purposes is the original soil design from the Beijing-Shanghai High-Speed Line in China, which consists of five layers, namely the top clay layer, bottom clay layer, completely weathered amphibolite layer, highly weathered amphibolite layer, and weakly weathered amphibolite layer (Li et al. 2020). In field measurements, it is difficult to obtain experimental values for the different layers of the soil, making it challenging to define an accurate damping coefficient. To address this issue, Rayleigh damping of the soil was used in the simulation to approximate the damping ratio, C , as shown in equation (1) and to overcome the complexity of obtaining direct experimental values for ground layers (Connolly et al. 2015).

$$C = \alpha M + \beta K \quad (1)$$

where C = Rayleigh damping of soil, M = Mass matrix of the structures, K = Stiffness matrix of whole model, assumed $\alpha = 0$ and $\beta = 0.0002$ to be more convenient to calculate Rayleigh Damping, or damping effect depends on the value of the stiffness of all layers of soil. (Li et al. 2019)

Table 4. Material Properties of Soil (M. Wang, 2016).

Properties	Value	Unit
Depth of Surface Layer of the Subgrade	0.40	[m]
Density of Surface Layer of the Subgrade	2300	[kg/m ³]
Elastic Modulus of Subgrade Surface Layer	5.47 x 10 ⁵	[N/m ²]
Poisson's Ratio of Subgrade Surface Layer	0.25	[mm/mm]
Depth of Bottom Layer of the Subgrade	2.30	[m]
Density of Bottom Layer of the Subgrade	1950	[kg/m ³]
Elastic Modulus of Subgrade Bottom Layer	1.50 x 10 ⁸	[N/m ²]
Poisson's Ratio of subgrade Bottom Layer	0.35	[mm/mm]
Depth of the Subgrade	2.00	[m]
Density of Subgrade	2100	[kg/m ³]
Elastic Modulus of the Subgrade	1.10 x 10 ⁸	[N/m ²]
Poisson's Ratio of Subgrade	0.30	[mm/mm]
Depth of 1st Layer of Ground	2.0	[m]
Density of 1st Layer of Ground	1835.49	[kg/m ³]
Elastic Modulus of the 1st Layer of Ground	4.56 x 10 ⁷	[N/m ²]
Poisson's Ratio of 1st Layer of Ground	0.20	[mm/mm]
Depth of 2nd Layer of Ground	3.0	[m]
Density of 2nd Layer of Ground	1835.49	[kg/m ³]
Elastic Modulus of the 2nd Layer of Ground	8.50 x 10 ⁵	[N/m ²]
Poisson's Ratio of 2nd Layer of Ground	0.20	[mm/mm]

2.4 Under Sleeper Pads and Under Slab Mats

The design case of this study aims to investigate the effects of installed under sleeper pads (USPs) and under slab mats (USMs) on track transition, from the moving direction of the train at the ballasted track zone to the slab track side. Specifically, the study seeks to examine the impact of using different types of pads with varying stiffness in terms of bedding modulus on reducing track vibration and differential settlement on both the track and ground. USPs are installed underneath sleepers on ballasted track while USMs are installed on the isolation layer of slab track.

To achieve these objectives, the program utilizes USP and USM models with solid elements, incorporating materials properties as shown in Tables 5 and 6. Different pad types are considered based on the recommended bedding modulus from previous literature (International Union of Railway, 2011; International Union of Railway, 2015; Kaewunruen et al., 2018; Ngamkhanong et al., 2020). The study seeks to explore how the different pad types impact the tracks and ground stability and vibration reduction.

Table 5. Properties of Under Sleeper Pads, USPs (Ngamkhanong et al. 2020).

Properties	Value	Unit
Thickness of USPs	0.10	[m]
Density of USPs	1100	[kg/m ³]
Poisson's Ratio of USPs	0.45	[mm/mm]
Bedding Modulus of the Soft USPs	0.15	[N/mm ³]
Bedding Modulus of Medium Stiff USPs	0.25	[N/mm ³]
Bedding Modulus of Stiff USPs	0.35	[N/mm ³]
Bedding Modulus of Very Stiff USPs	1.00	[N/mm ³]

Table 6. Properties of Under Slab Mats, USMs (Kaewunruen et al. 2018).

Properties	Value	Unit
Thickness of USMs	0.10	[m]
Density of USMs	700	[kg/m ³]
Poisson's Ratio of USMs	0.35	[mm/mm]
Bedding Modulus of Soft USMs	0.07	[N/mm ³]
Bedding Modulus of Typical USMs	0.11	[N/mm ³]
Bedding Modulus of Medium Stiff USMs	0.15	[N/mm ³]
Bedding Modulus of Stiff USMs	0.23	[N/mm ³]

Based on the design of this study, it will be divided into five cases. The first case is a control group, where no pads are installed on transition zone. This case enables the comparison of the differential displacement and other dynamic response between the no pad case and the installed pad cases. The second case involves the use of Stiff USPs on ballasted track and Medium Stiff USMs on slab track. The third case uses Medium Stiff USPs with Medium Stiff USMs. The fourth case uses Stiff USPs with Typical USMs, and the fifth case uses Medium USPs with Typical USMs.

The analysis also varies the train speed in increments of 50 km/hr, up to a maximum of 250 km/hr, to determine the critical speed and most effective mixed types of pads that can improve track stiffness while reducing track and ground vibrations.

3. RESULTS AND DISCUSSIONS

3.1 Model Validation

Before interpreting the results obtained in this study, the modified models are executed and validated with results from other articles. The comparison of dynamic response is made in terms of the interaction between Wheel-Rail contact force, Rail displacement, and the settlement of the track, as well as the ground acceleration along the track transition. Tables 7-8 present a comparison of simulation results from this study with field measurements conducted by Cai et al. (2017), demonstrating the validation of the Train-Track-Soil interaction on both ballasted track and slab track, respectively.

Table 7. Validation Results of Train-Track-Soil Interaction on Ballasted Track.

Dynamic Response	Simulation Results from Cai et al. (2017)	Simulation Results from this study	Unit
Wheel-Rail Contact Force	100	115	[kN]
Displacement of Rail (Rail Seat)	2.606	2.292	[mm]
Displacement of Rail (Mid-Span)	2.604	2.396	[mm]

Table 8. Validation Results of Train-Track-Soil Interaction on Slab Track.

Dynamic Response	Simulation results from Cai et al. (2017)	Simulation results from this study	Unit
WR Contact Force	98.7	93.36	[kN]
Rail Pad Force	37.648	35.53	[kN]
Displacement of Rail	0.827	1.198	[mm]

3.2 Rail Displacement

Figure 3 presents the rail displacement and track stiffness along the location of the transition zone under the train speed of 50 km/hr. The track stiffness can be computed from the dynamic train load divided by the displacement of the rail. The dash lines present the rail displacement while the solid lines present the track stiffness along the section. The abrupt change in rail displacement and track stiffness can be seen clearly when there are no pads installed. While the smoothness can be found when the USPs and USMs are installed. Despite the fact that

the use of Under Sleeper Pads (USPs) can cause a slight increase in rail displacement, they still fall within an acceptable range. Moreover, USPs can provide other benefits such as reducing vibrations in the underlying layers. By analyzing the track stiffness along the transition zone, we can determine how the track responds to the dynamic load of the train. Therefore, it is essential to ensure that the track stiffness is appropriately designed in order to maintain safety and efficient operation of the railway system.

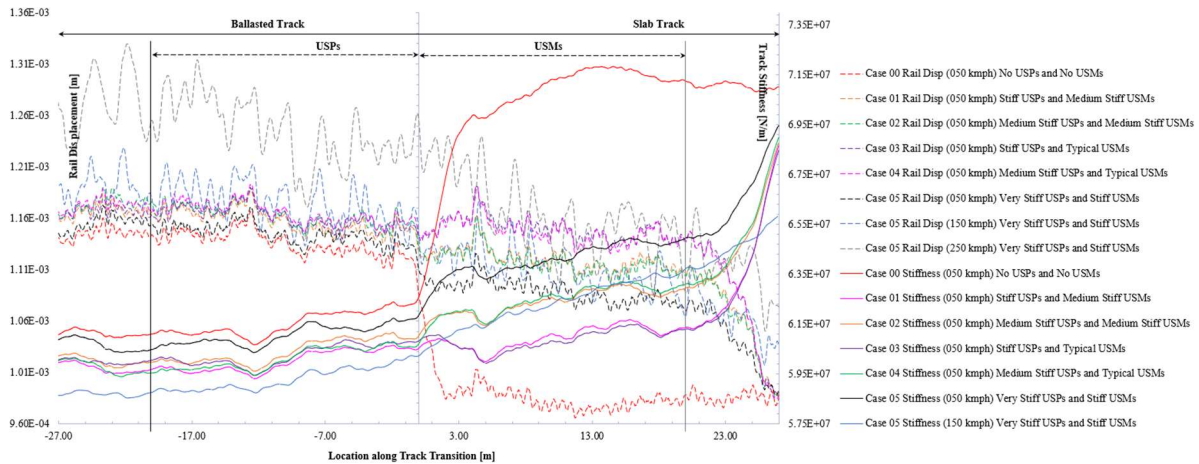


Figure 3. Rail Displacement and Track Stiffness along the Transition Zone

3.2 Track Acceleration

This section discusses the effectiveness of different types of pads in reducing vibrations in tracks, particularly in terms of acceleration on ballasted and slab tracks. The comparison is made between acceleration responses subjected to 250 km/hr when using pads versus when not using pads. Figure 4a displays the USPs in the ballasted track zone, while Figure 4b shows USMs in the slab track zone. The results show that using a very stiff USP is the most effective in reducing track vibrations. Furthermore, all types of USMs can reduce the acceleration response by up to 40% when compared to not using any pads.

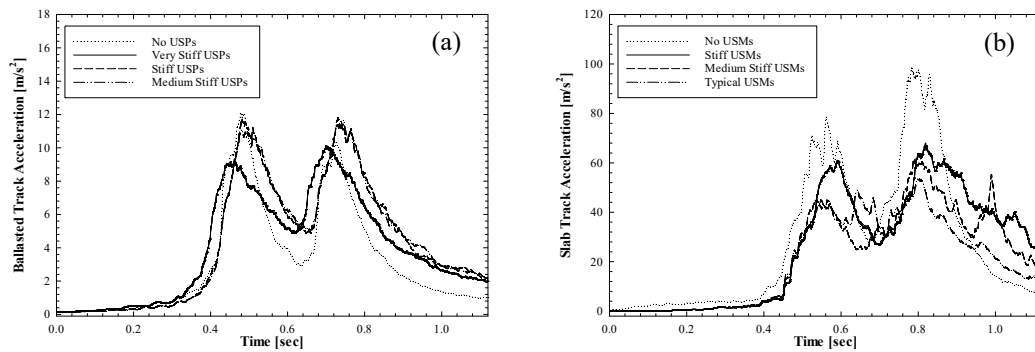


Figure 4. Track Acceleration on Transition zone, in case of 250 [km/hr].
(a) USPs in Ballasted Track (b) USMs on Slab Track.

3.3 Ground Acceleration

As previously mentioned, while the use of resilient pads on the transition zone can reduce track acceleration and improve track stability, they may not significantly reduce ground vibrations. Figure 5 shows the dynamic responses of ground under the train speed of 250 km/hr. It is found that ground vibration can be observed even it is far away from the track center. Figure 6 describes ground acceleration responses at critical section in a controlled case without the use of USPs and USMs. It indicates that as train speed increases in the transition zone, ground acceleration increases. Interestingly, it is observed that ground vibration on adjacent side of the track is lower than another side when especially when the lower speed train approaches.

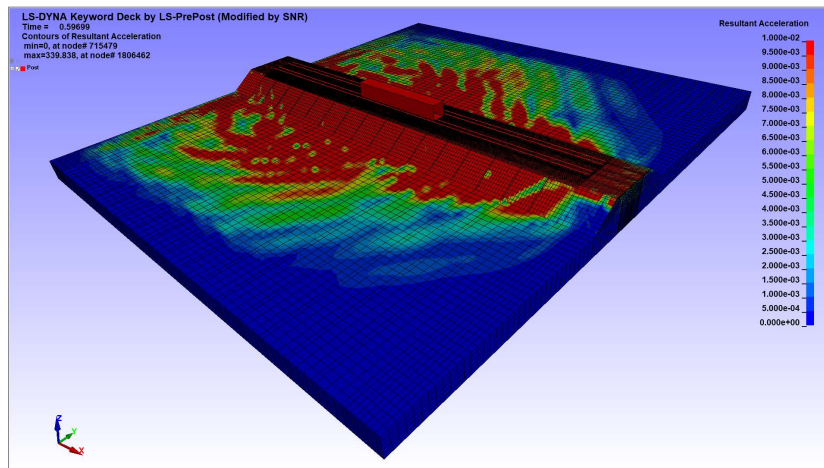


Figure 5. Ground Dynamic Response of Transition Zone with USPs and USMs in 3D FEM Modeling under 250 km/hr.

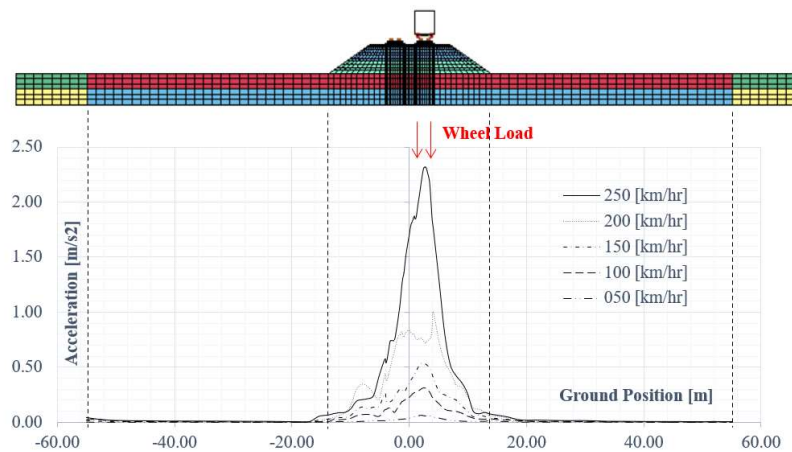


Figure 6. Ground Acceleration at Critical Section.

4. CONCLUSIONS

The study highlights some key findings related to the use of resilient materials on railway track transition zone. Firstly, it recommends the use of Under Sleeper Pads (USPs) and Under Sleeper Mats (USMs) to reduce train vibrations and minimize track degradation in the long term, which can ultimately result in cost savings in maintenance. Additionally, USPs have been found to be effective in reducing stress on the ballast and substructure. Stiff USMs are also recommended on slab track for smoothing the transition between ballasted track and slab track.

Secondly, the study suggests that mixed methods are more effective than simple solutions for smoothing track stiffness during track transition. However, it is important to note that the choice of pads must be carefully considered to ensure they have the proper bedding modulus on the railway tracks as using inappropriate type may lead to higher dynamic responses. Thirdly, the study emphasizes the importance of taking into account track and ground characteristics. Matching track properties with the passing of trains at critical speeds can cause more dynamic responses and potentially lead to resonance effects on track structures so that using different pads may create different natural frequencies of track system.

In conclusion, the study highlights that track transition can lead to long-term differential settlement. Therefore, it is crucial to use appropriate components to improve track stiffness and minimize track vibrations. The use of USPs and USMs, along with carefully considered mixed methods can be effective in achieving this goal. The outcome will provide useful information for designers and engineers to improve decisions on construction and maintenance processes.

ACKNOWLEDGMENTS

This Research is funded by Thailand Science research and Innovation Fund Chulalongkorn University (BCG66210020). This project is also funded by National Research Council of Thailand (NRCT).

REFERENCES

- Connolly, D. P., Kouroussis, G., Laghrouche, O., Ho, C. L., and Forde, M. C. (2015). Benchmarking railway vibrations—Track, vehicle, ground and building effects. *Construction and Building Materials*, 92, 64-81
- Huang, H., Gao, Y., and Shelley Stoffels, S. (2014). Fully Coupled Three-Dimensional Train-Track-Soil Model for High-Speed Rail. *Transportation Research Board of the National Academies*, 2448, 87–93.
- International Union of Railway. (2011). UIC Recommendation R917-1 Under ballast mat, Paris, France.
- International Union of Railway. (2015). UIC Leaflet 917 Guidelines for under sleeper pad, Paris, France.
- Keping, Z., Xiaohui, Z. and Shunhua, Z. (2023). Analysis on dynamic behavior of 400 km/h high-speed train system under differential settlement of subgrade. *Engineering Structures*, 278, 0141-0296.
- Li, T., Su, Q., and Kaewunruen, S. (2020). Influences of piles on the ground vibration considering the train-track-soil dynamic interactions. *Computers and Geotechnics*, 120, 103455.
- Li, T., Su, Q., Shao, K., and Liu, J. (2019). Numerical analysis of vibration responses in highspeed railways considering mud pumping defect. *Shock and Vibration*, 2019
- Likitlersuang, S., Pholkainuwatra, P., Chompoorat, T. and Keawsawasvong, S. (2018). Numerical Modelling of Railway Embankments for High-Speed Train Constructed on Soft Soil. *Journal of GeoEngineering*, 13(3), 149-159
- Ngamkhanong, C., Ming, Q. Y., Li, T., and Kaewunruen, S. (2020). Dynamic train-track interactions over railway track stiffness transition zones using baseplate fastening systems. *Engineering Failure Analysis*, 118.
- Galvin, P., Romero, A., and J. Dominguez, J. (2010). Fully three-dimensional analysis of high-speed train–track–soil-structure dynamic interaction. *Journal of Sound and Vibration*, 329, 5147–5163.
- Kaewunruen, S., Ngamkhanong, C., Papaelis, M., Roberts, C.. (2018). Wet/dry influence on behaviors of closed-cell polymeric cross-linked foams under static, dynamic and impact loads. *Construction and Building Materials*, 187, 1092–1102.
- Kaewunruen, S., Ngamkhanong, C. and Ng, J.. (2019). Influence of time-dependent material degradation on life cycle serviceability of interspersed railway tracks due to moving train loads. *Engineering Structures*, 119, 0141-0296.
- Takeshi, I., Dongqin, Z. and Yosuke, N. (2016). Numerical study of dynamic response of railway vehicles under tunnel exit winds using multibody dynamic simulations. *Engineering Structures*, 127, 673-678.
- Qi, Y. and Zhou, L. (2020). The Fuxing: The China Standard EMU. *Engineering, Engineering Achievements*, 6.
- Wang, M., Cai, C., Zhu, S., and Zhai, W. (2017). Experimental study on dynamic performance of typical non ballasted track systems using a full-scale test rig. *Proceedings of the Institution of Mechanical Engineers, Part F: Journal of Rail and Rapid Transit*, 231(4), 470-481
- Zheng, W.Q. and Zhu, Z. (2019) Properties of rubber under-ballast mat used as ballast less track isolation layer in high-speed railway. *Construction and Building Materials*, 0950-0618.

ONE-DIMENSIONAL COMPRESSION MODEL FOR UNSATURATED CRUSHABLE GRANULAR MATERIALS

Pongsapak Kanjanatanalert¹, and Veerayut Komolvilas²

1) M.Eng. Candidate, Department of Civil Engineering, Faculty of Engineering, Chulalongkorn University, Bangkok, Thailand. Email: 6470227221@student.chula.ac.th

2) Ph.D., Asst. Prof., Centre of Excellence in Geotechnical and Geoenvironmental Engineering, Chulalongkorn University, Bangkok, Thailand. Email: veerayut.k@chula.ac.th

Abstract: Particle crushing is a phenomenon that occurs in crushable materials, such as granular soils, when subjected to high stress conditions that exceed the crushing strength of the particles, resulting in the breakdown of particles into smaller fragments. This can cause soil stiffness reduction and significant soil deformation. Furthermore, an increase in degree of saturation can also contribute to hydraulic collapse due to the higher stiffness of unsaturated soil compared to saturated soil. Experimental evidence suggests that the presence of water can further reduce the crushing strength of the soil. Consequently, the combined effects of particle crushing and changes in the saturation degree can cause excessive deformation and a reduction in soil strength. While existing constitutive models can predict the effects of unsaturated soils and particle crushing separately, a model that can simulate the combined effect of both phenomena is required to study the behavior of unsaturated crushable soils. Therefore, this study aims to propose a one-dimensional compression model for unsaturated crushable soils that can simulate the combined effect of particle crushing and unsaturated soils.

Keywords: One-dimensional compression model, Crushing strength, Particle crushing, Unsaturated soils.

1. INTRODUCTION

Particle crushing is a phenomenon that occurs in crushable materials such as granular soils when they are subjected to high stress levels exceeding the crushing strength (Hardin, 1985; Lade et al., 1996; Nakata et al., 2001). This leads to the crushing of soil particles into smaller ones. For instance, when a pile is driven into the soil, the soil at the pile tip experiences extremely high driving stress, leading to particle crushing (Wu et al., 2013). The occurrence of particle crushing is influenced by several factors, including stress, particle size, initial density, particle shape, mineral composition, and the presence of water (Hardin, 1985; Lade et al., 1996; Nakata et al., 2001). Particle crushing significantly affects the mechanical behavior of soils. For example, it alters the grading observed in the experimental results of ring shear tests (Coop et al., 2004), decreases the void ratio due to the smaller particles filling up the void spaces (Hardin, 1985; Kikumoto & Wood et al., 2010; Lade et al., 1996; Wu et al., 2013; Yu, 2018), and reduces soil strength (Miura & Ohara, 1979; Nakata et al., 2001; Wu et al., 2013).

Another phenomenon that affects soil behavior is the collapse of soil due to changes in the degree of saturation. Unsaturated soil typically has a higher stiffness and can exist in a looser state than saturated soil, which affects the soil behavior (Kikumoto & Kyokawa et al., 2010; Komolvilas et al., 2022). Previous research has suggested that suction depends on the degree of saturation following the Soil-Water Characteristic Curve (SWCC) (Van Genuchten, 1980). However, Tarantino and Tombolato (2005) demonstrated that the SWCC is influenced by changes in the void ratio. Hence, volumetric compression can lead to an increase in the degree of saturation, even under constant suction, eventually resulting in the soil becoming saturated. Compression and soaking tests on air-dried silt (Jennings & Burland, 1962) showed that samples soaked at a constant applied pressure exhibit significant volumetric deformation, known as hydraulic collapse. Therefore, an increase in the degree of saturation results in a decrease in the void ratio and soil stiffness.

When considering the combined effect of particle crushing and unsaturated soils, void ratio and soil strength can be reduced due to particle crushing. Moreover, the decrease in void ratio caused by particle crushing can lead to an increase in the degree of saturation, resulting in hydraulic collapse. These combined effects can cause significant soil deformation and failure. Therefore, the interplay between these behaviors must be considered when dealing with unsaturated crushable soils. To address this problem, two important factors need to be considered. First, previous studies have suggested that the presence of water has a dominant effect on crushing strength (Manso et al., 2021; Oldecop & Alonso, 2001; Ovalle et al., 2015; Ventini et al., 2020). Second, numerous experimental results have been carried out to investigate the evolution of Soil-Water Characteristic Curve (SWCC) of granular materials subjected to particle crushing. The findings indicate that particle breakage causes a significant alteration of the SWCC, with a notable increase in the degree of saturation during particle crushing under constant suction (Gao et al., 2016; Jamei et al., 2011; Zhang et al., 2017). As particle crushing leads to a change in grading, these results are consistent with various grain-size-dependent SWCC models that can estimate the SWCC under different gradings (Arya & Paris, 1981; Fredlund et al., 2002). Therefore, a one-dimensional compression model for unsaturated crushable soil is needed to capture these coupling effects between suction and crushing behavior. Previous studies have proposed several constitutive models that utilize the critical state concept (Schofield &

Wroth, 1968) to predict the behavior of unsaturated soils (Kikumoto & Kyokawa et al., 2010; Komolvilas et al., 2022) and particle crushing (Nguyen & Kikumoto, 2018) separately. In this study, the objective is to develop a one-dimensional compression model for unsaturated crushable granular materials that could simulate the combined effect of particle crushing and unsaturated soils.

2. MODEL FORMULATION

2.1 Basic Concept of Particle Crushing in Unsaturated Soils.

To quantify the amount of particle crushing, the definition of grading index is needed. Muir Wood and Maeda (2008) proposed the grading state index (I_G), the definition of I_G is shown in Figure 1. The formulation of I_G assumes that grain size distribution (GSD) gradually changes from the single size grading (line AB) to a limit grading (curve AD), the value of I_G ranges from 0 to 1 respectively.

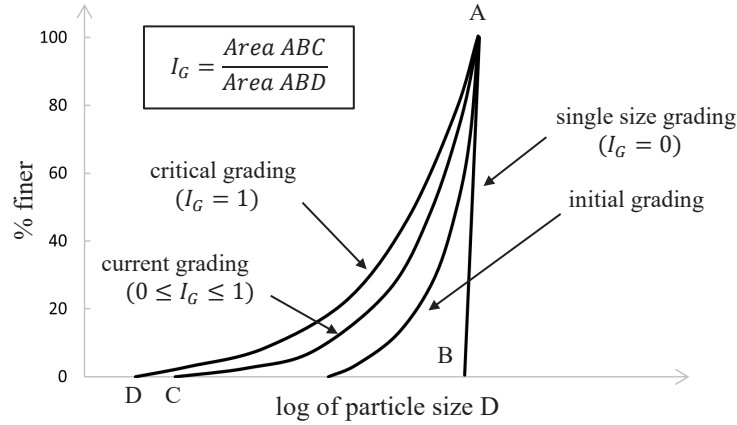


Figure 1. Definition of grading state index I_G (Muir Wood & Maeda, 2008)

As the previous studies indicated that crushing strength reduced due to an increase in degree of saturation (Manso et al., 2021; Oldecop & Alonso, 2001; Ovalle et al., 2015; Ventini et al., 2020). Therefore, the crushing strength of unsaturated soils can be determined by adding state parameter ψ_c to the crushing strength of saturated soils as Equation (1).

$$p_c = p_{c_{sat}} + \psi_c(S_r) \quad (1)$$

Where p_c and $p_{c_{sat}}$ is the crushing strength of unsaturated and saturated soils respectively. When degree of saturation increases, the value of ψ_c decreases. For simplicity, the simple linear relationship can be assumed as Equation (2). The material constant parameter ξ_c represents the difference in crushing strength under dried and saturated conditions.

$$\psi_c(S_r) = \xi_c(1 - S_r) \quad (2)$$

An evolution law for the grading state index is necessary to explain the impact of changes in grading. Kikumoto & Wood et al. (2010) proposed a method to describe the evolution of grading state index by linking it to crushing strength (p_c), as shown in Equation (3). Where p_{ci} is the initial crushing strength when $I_G = 0$, and material parameter p_r controls the rate of particle crushing.

$$I_G = 1 - \exp\left(-\frac{p_c - p_{ci}}{p_r}\right) \quad (3)$$

When the unsaturated soil is subjected to isotropic compression, particle crushing occurs once the stress reaches the crushing strength (p_c). However, in case of shearing, the combined effects of both mean effective stress (p'') and deviator stress (q) determine when particle crushing occurs. To account for this, a crushing surface for unsaturated soils has been proposed to describe the onset of particle crushing as shown in Equation (4).

$$f_c = \log\left(\frac{p''}{p_c}\right) + \log\left(1 + \left(\frac{\eta''}{M_c}\right)^2\right) \quad (4)$$

As p_c monotonically increases when particle crushing occurs ($f_c = 0$), the increment of p_c can be

determined by the consistency condition of crushing strength ($df_c = 0$) as shown in Equation (5)

$$dp_c = \langle p_c \frac{\partial f_c}{\partial \sigma''} d\sigma'' \rangle \quad (5)$$

where $\langle \rangle$ is the macauley bracket define as $\langle x \rangle = \begin{cases} 0, & x < 0 \\ x, & x \geq 0 \end{cases}$.

The critical state concept has been extended to incorporate the behavior of crushable soils. Muir Wood and Maeda (2008) indicated that particle crushing causes a downward parallel shift of the critical state line (CSL) in the specific volume (v) and logarithm of mean effective stress (p'') plane. To represent downward shift of the state boundary surface due to particle crushing, a state parameter ψ_{IG} has been introduced (Nguyen & Kikumoto, 2018). The value of ψ_{IG} increases monotonically from 0 ($I_G = 0$) to ξ_{IG} ($I_G = 1$). For simplicity, a linear relationship is assumed as shown in Equation (6).

$$\psi_{IG} = \xi_{IG} I_G \quad (6)$$

2.2 Basic Concept of Unsaturated Soils Exhibiting Particle Crushing.

Bishop's effective stress (σ'') is selected to determine the effective stress of unsaturated soils (Bishop, 1959). The experimental results (Bishop & Donald, 1961) suggested that Bishop's effective stress parameter (χ) could be considered equivalent to the degree of saturation (S_r). Thus, Bishop's effective stress (σ'') can be expressed by Equation (7).

$$\sigma'' = (\sigma - u_a) + S_r(u_a - u_w) \quad (7)$$

The SWCC model is needed to describe the hydraulic behavior of unsaturated soils under various loading conditions. In this study, the classical SWCC model (Van Genuchten, 1980), which establishes a relationship between suction (s) and the degree of saturation (S_r), is selected as Equation (8).

$$S_r^A = S_{min} + (S_{max} - S_{min})[1 + (\alpha^A s)^n]^{-m}; A = d \vee w \quad (8)$$

Where α , n , and m are material parameters, S_{max} and S_{min} are the maximum and minimum degree of saturation, superscripts d and w denote the main drying and wetting curves.

The classical SWCC has been extended to account the effect of void ratio and hysteresis (Kikumoto & Kyokawa et al., 2010; Komolvilas et al., 2022) utilizing the modified suction (s^*) and ratio (I_h) as expressed in Equation (9) and Equation (10), respectively.

$$s^* = s \left(\frac{e}{e_{ref}} \right)^{\xi_e} \quad (9)$$

$$I_h = \frac{S_r - S_r^w}{S_r^d - S_r^w} \quad (10)$$

However, experimental findings have indicated that particle breakage significantly alters the SWCC, leading to a notable increase in the degree of saturation during particle crushing under constant suction (Gao et al., 2016; Jamei et al., 2011; Zhang et al., 2017). Fortunately, the decrease in void ratio due to particle crushing has a direct impact on the modified suction (s^*). As a result, the evolution of the SWCC due to grain crushing is automatically incorporated through the change of the modified suction (s^*).

As unsaturated soils have relatively high stiffness and are able to exist in a looser state compared to saturated soils, the behavior of unsaturated soils can be captured by assuming the state parameter ψ_{S_r} represent the upward parallel shift of the normally consolidated line (NCL) as the degree of saturation (S_r) decreases (Kikumoto & Kyokawa et al., 2010; Komolvilas et al., 2022). The value of ψ_{S_r} increases monotonically from 0 (fully saturated) to ξ_{S_r} (fully dried). The simple linear relationship is assumed to be Equation (11).

$$\psi_{S_r} = \xi_{S_r}(1 - S_r) \quad (11)$$

2.3 One-Dimensional Compression Model for Unsaturated Crushable Granular Materials.

Since soil exhibits elastoplastic behavior even under the yield surface, the model takes into account the effect of density to predict the behavior of over-consolidated soils by using sub-loading surface concept

(Hashiguchi, 1989) and a state variable Ω , which represents the difference in specific volume between the current state and the NCL. As plastic deformation occurs, Ω decreases and eventually reaches 0 (on the NCL). The evolution law of Ω is defined by Equation (12).

$$d\Omega = -\omega v_0 \Omega |\Omega| \|d\varepsilon^p\| \quad (12)$$

The associated flow rule is assumed to calculate the increment of plastic strain. Finally, the yield function of unsaturated crushable soils based on modified Cam clay can be expressed as Equation (13). The overview of the yield function and the movement of normally consolidated line (NCL) are summarized in Figure 2.

$$f = (\lambda - \kappa) \left[\ln \frac{p'' \left\{ 1 + \left(\frac{\eta''}{M} \right)^2 \right\}}{p_0'' \left\{ 1 + \left(\frac{\eta_0''}{M} \right)^2 \right\}} \right] - v_0 \varepsilon_v^p - d\psi_{S_r} + d\psi_{I_G} + d\Omega \quad (13)$$

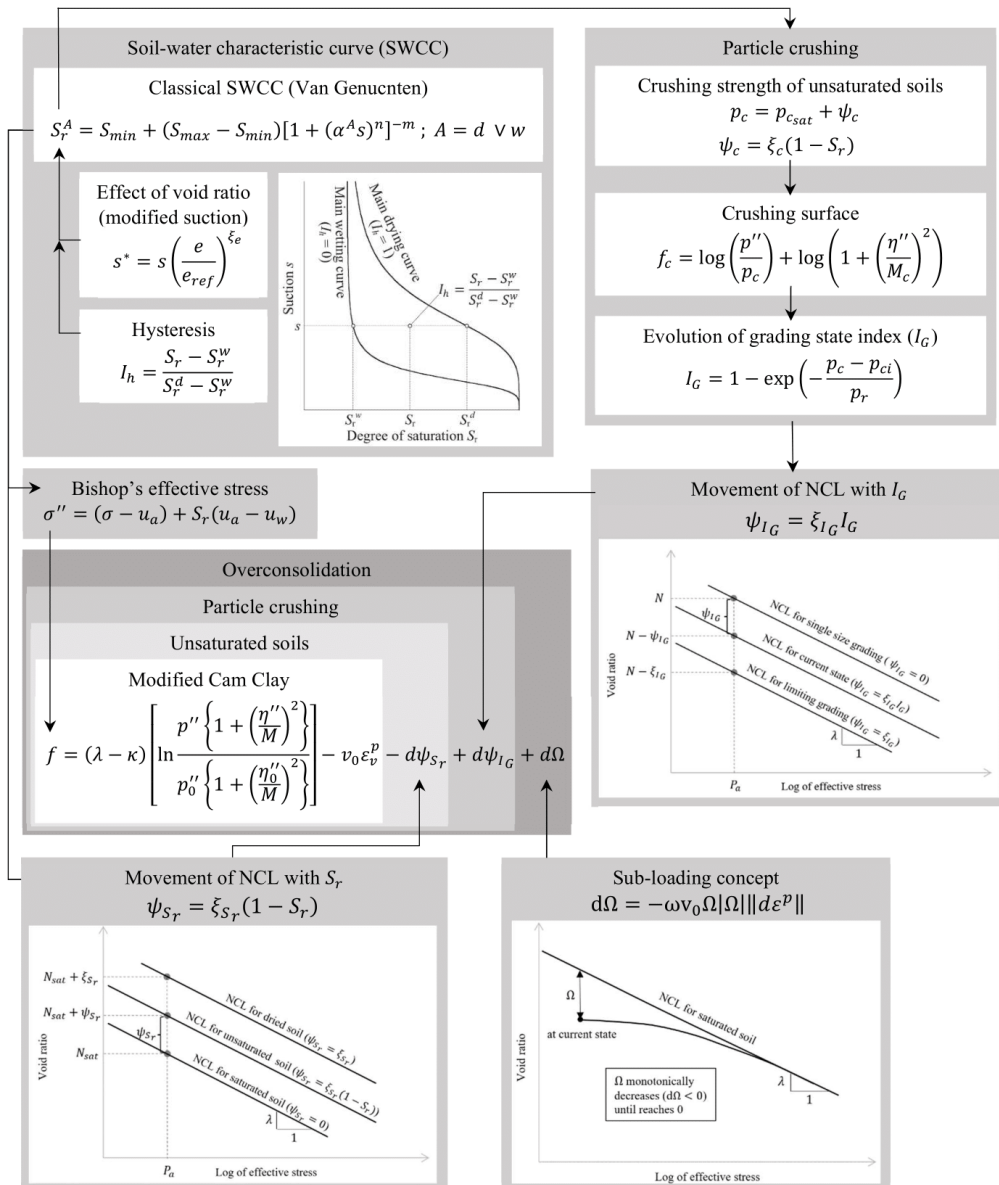


Figure 2. The yield function of unsaturated crushable granular materials

3. SIMULATION

In this study, the impact of unsaturated crushable soils was investigated through the simulation of one-dimensional compression tests. The simulation consisted of three parts. Firstly, the material parameters were calibrated using the experimental results of saturated Ottawa sand exhibiting particle crushing by Valdes (2003). The comparison between the simulation and experimental data is shown in Figure 3. Secondly, the simulation of one-dimensional compression tests focused on the behavior of unsaturated and saturated soils, with or without particle crushing, utilizing an initial void ratio (e_0) of 0.698. Thirdly, a one-dimensional compression tests of unsaturated crushable materials under 4 different suctions were simulated with the initial void ratio ($e_0 = 1.6$) to discuss the effect of changes in the degree of saturation on the crushing behavior. The reason for using different initial void ratios in the second and third parts is due to the tendency of loose soils to exhibit hydraulic collapse more readily than denser soils. Therefore, the loose samples are more effective to clearly illustrate the effect of suction on the compression behavior of soils. The material parameters for the simulation are listed in Table 1. To simulate the case without crushing, materials parameter p_{ci} was assigned to be a very high value ($p_{ci} = 1,000,000$ kPa).

Table 1. Parameters for unsaturated crushable granular materials

Parameters for particle crushing		
Symbol	Material parameters	Description
p_{ci}	5000	Crushing strength for single size grading ($I_G = 0$)
p_r	5000	Crushing resistance
M_c	0.58	Slope of crushing surface
ξ_{p_c}	500.0	Effects of S_r to crushing strength
Parameters for water retention curves (SWCC)		
S_{max}	1.00	Parameters for Van Genuchten SWCC model
S_{min}	0.15	
α_d	0.01	
α_w	0.04	
n	1.80	
m	0.30	
ξ_h	100.0	Effect of hysteresis
ξ_e	4.0	Effect of void ratio
Parameters for stress-strain characteristics		
λ	0.246	Compression index
κ	0.01	Swelling index
M	1.65	Critical state stress ratio
ν_e	0.20	Poisson's ratio
N	3.10	Reference specific volume on NCL under $p' = p_a$, $q = 0$, $I_G = 0$, and $S_r = 1$
ω	2000.0	Sub-loading parameter
ξ_{I_G}	0.20	Effect of I_G on NCL
ξ_{S_r}	0.50	Effect of S_r on NCL

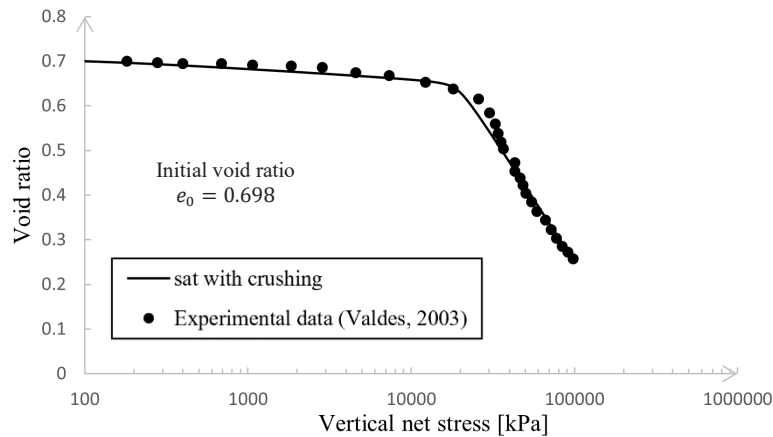


Figure 3. Simulation result of one-dimensional compression test on Ottawa sand

4. RESULTS

One-dimensional compression tests were simulated to study the behavior of particle crushing on unsaturated soils under 4 conditions, including unsaturated ($s = 2048$ kPa) and saturated soils ($s = 0$ kPa), with or without particle crushing. The results are shown in Figure 4. When considering the case with crushing, the compression line (Figure 4a) indicates a rapid decrease in void ratio compared to the case without crushing. Additionally, particle crushing ultimately affected the change in degree of saturation (Figure 4b), which is consistent with experimental findings demonstrating a notable increase in degree of saturation during particle crushing under constant suction (Gao et al., 2016; Jamei et al., 2011; Zhang et al., 2017), and the effect of grain size distribution on SWCC models (Arya & Paris, 1981; Fredlund et al., 2002). In terms of strength, a reduction in deviator stress was observed when crushing occurs as shown in Figure 4c.

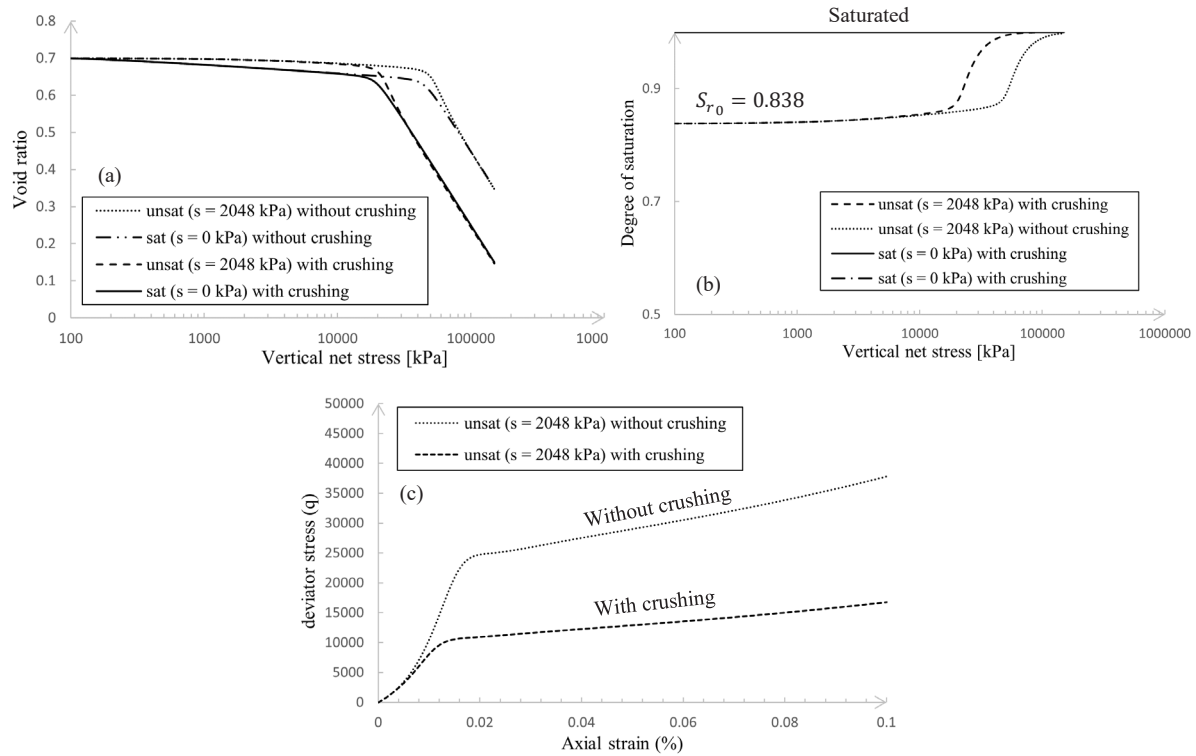


Figure 4 The simulation results of one-dimensional compression tests of unsaturated crushable soils

The effect of degree of saturation on particle crushing was studied by simulating a one-dimensional compression test for unsaturated crushable materials under 4 different suctions (Figure 5a). When comparing the unsaturated ($s = 98, 248, 598$ kPa) and saturated ($s = 0$ kPa) cases, the unsaturated soils initially exhibited higher stiffness compared to the saturated soils.

As particles crushing displays (I_G increases), S_r also increases due to the reduction in void ratio caused by grain crushing (Figure 5d). This is because volumetric compression affects the change in degree of saturation even under constant suction (Figure 5c). Therefore, the compression line of unsaturated soils finally converged to the compression line of saturated soils (Figure 5a).

The onset of crushing under different suctions are plotted in terms of deviator stress (q) and mean effective stress (p'), as shown in Figure 5b, which illustrates that the crushing stress depends on the degree of saturation (S_r). As the suction increases (S_r decreases), particles break at a higher value of effective stress. This is because cracks can grow even under the crushing strength of materials, a phenomenon known as subcritical crack growth. The onset of cracking stress depends on the amount of water in the pores of particles (Nara et al., 2010), which can be explained by stress corrosion theory (Atkinson, 1982; Michalske & Freiman, 1983). This theory suggests that when the inter-atomic bond at the crack tip is strained, it can be easily attacked by a corrosive agent such as water, ultimately leading to material weakness that can break at a lower stress.

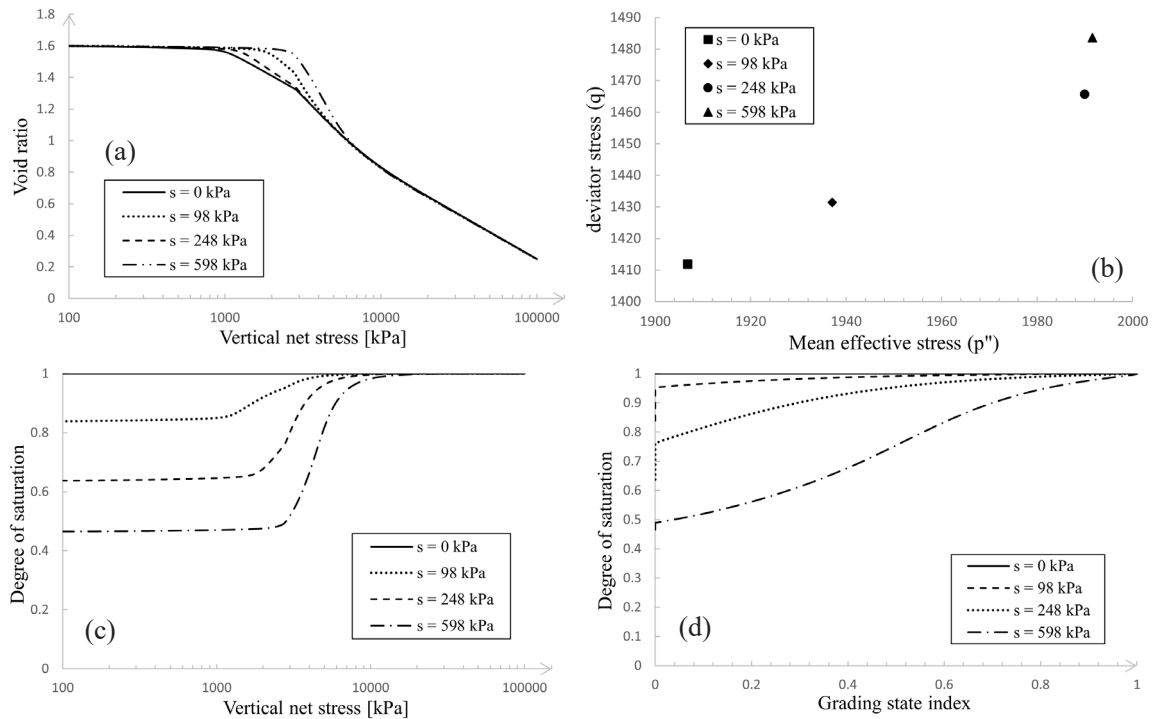


Figure 5 The simulation result of one-dimensional compression tests for unsaturated crushable soils under 4 different suctions

5. CONCLUSIONS

This paper proposed a one-dimensional compression model for unsaturated crushable granular materials. The simulation outcomes demonstrate that this model can effectively represent significant aspects of unsaturated crushable soils, such as the reduction in crushing strength caused by an increase in degree of saturation (S_r), and the evolution of S_r resulting from grain crushing. Furthermore, this model can be extended to a three-dimensional compression model to simulate Triaxial tests under various loading conditions in future research.

ACKNOWLEDGMENTS

This research is supported by the Civil Engineering Centennial Scholarship of Chulalongkorn University to the first author. This work was financially supported by Office of the Permanent Secretary, Ministry of Higher Education, Science, Research and Innovation: Grant No. RGNS 63- 019 to the second author.

REFERENCES

- Arya, L. M., & Paris, J. F. (1981). A physicoempirical model to predict the soil moisture characteristic from particle - size distribution and bulk density data. *Soil science society of America journal*, 45(6), 1023-1030.
- Atkinson, B. K. (1982). Subcritical crack propagation in rocks: theory, experimental results and applications. *Journal of Structural Geology*, 4(1), 41-56.
- Bishop, A., & Donald, I. (1961). Proceedings of the Fifth International Conference on Soil Mechanics and Foundation Engineering, Paris. 17-22 July 1961.
- Bishop, A. W. (1959). The principle of effective stress. *Teknisk ukeblad*, 39, 859-863.
- Coop, M., Sorensen, K., Bodas Freitas, T., & Georgoutsos, G. (2004). Particle breakage during shearing of a carbonate sand. *Géotechnique*, 54(3), 157-163.
- Fredlund, M. D., Wilson, G. W., & Fredlund, D. G. (2002). Use of the grain-size distribution for estimation of the soil-water characteristic curve. *Canadian Geotechnical Journal*, 39(5), 1103-1117.
- Gao, S., Zhang, Y. D., Sonta, A., & Buscarnera, G. (2016). Evolution of the water retention characteristics of granular materials subjected to grain crushing. *Journal of Geotechnical and Geoenvironmental Engineering*, 142(9), 06016006.
- Hardin, B. O. (1985). Crushing of soil particles. *Journal of geotechnical engineering*, 111(10), 1177-1192.
- Hashiguchi, K. (1989). Subloading surface model in unconventional plasticity. *International journal of solids and structures*, 25(8), 917-945.

- Jamei, M., Guiras, H., Chtourou, Y., Kallel, A., Romero, E., & Georgopoulos, I. (2011). Water retention properties of perlite as a material with crushable soft particles. *Engineering Geology*, 122(3-4), 261-271.
- Jennings, J., & Burland, J. (1962). Limitations to the use of effective stresses in partly saturated soils. *Géotechnique*, 12(2), 125-144.
- Lade, P. V., Yamamuro, J. A., & Bopp, P. A. (1996). Significance of particle crushing in granular materials. *Journal of geotechnical engineering*, 122(4), 309-316.
- Manso, J., Marcelino, J., & Caldeira, L. (2021). Single-particle crushing strength under different relative humidity conditions. *Acta Geotechnica*, 16(3), 749-761.
- Michalske, T. A., & Freiman, S. W. (1983). A molecular mechanism for stress corrosion in vitreous silica. *Journal of the American Ceramic Society*, 66(4), 284-288.
- Miura, N., & Ohara, S. (1979). Particle Crushing of a decomposed Grained Soil Under Shear. *Soils and Foundation*, 19(3), 61-76.
- Muir Wood, D., & Maeda, K. (2008). Changing grading of soil: effect on critical states. *Acta Geotechnica*, 3, 3-14.
- Nakata, Y., Kato, Y., Hyodo, M., Hyde, A. F., & Murata, H. (2001). One-dimensional compression behaviour of uniformly graded sand related to single particle crushing strength. *Soils and foundations*, 41(2), 39-51.
- Nara, Y., Hiroyoshi, N., Yoneda, T., & Kaneko, K. (2010). Effects of relative humidity and temperature on subcritical crack growth in igneous rock. *International Journal of Rock Mechanics and Mining Sciences*, 47(4), 640-646.
- Nguyen, V. P., & Kikumoto, M. (2018). An elastoplastic model for soils exhibiting particle breakage. Proceedings of the 4th Congrès International de Géotechnique-Ouvrages-Structures: CIGOS 2017, 26-27 October, Ho Chi Minh City, Vietnam 4,
- Oldecop, L. A., & Alonso, E. (2001). A model for rockfill compressibility. *Géotechnique*, 51(2), 127-139.
- Ovalle, C., Dano, C., Hicher, P.-Y., & Cisternas, M. (2015). Experimental framework for evaluating the mechanical behavior of dry and wet crushable granular materials based on the particle breakage ratio. *Canadian Geotechnical Journal*, 52(5), 587-598.
- Schofield, A. N., & Wroth, P. (1968). *Critical state soil mechanics* (Vol. 310). McGraw-hill London.
- Tarantino, A., & Tombolato, S. (2005). Coupling of hydraulic and mechanical behaviour in unsaturated compacted clay. *Géotechnique*, 55(4), 307-317.
- Van Genuchten, M. T. (1980). A closed - form equation for predicting the hydraulic conductivity of unsaturated soils. *Soil science society of America journal*, 44(5), 892-898.
- Ventini, R., Flora, A., Lirer, S., Mancuso, C., & Cammarota, A. (2020). An experimental study of the behaviour of two rockfills accounting for the effects of degree of saturation. E3S Web of Conferences,
- Wu, Y., Yamamoto, H., & Yao, Y. (2013). Numerical study on bearing behavior of pile considering sand particle crushing. *Geomech. Eng*, 5(3), 241-261.
- Zhang, Y., Park, J., Gao, S., Sonta, A., Horin, B., & Buscarnera, G. (2017). Effect of grain crushing and grain size on the evolution of water retention curves. In *PanAm unsaturated soils 2017* (pp. 268-278).

A COMBINED DROUGHT INDEX (CDI) SYSTEM FOR DROUGHT EARLY WARNING, MONITORING, AND RISK ASSESSMENT IN EEC THAILAND

Sasin Jirasirirak¹, Aksara Putthividhya^{2*}, Somkiat Prajamwong³, and Wimonpat Bumbudsanpharoke Kamkanya⁴

1) Ph.D. Candidate, Department of Water Resources Engineering, Faculty of Engineering, Chulalongkorn University, Bangkok, Thailand. Email: sasin_sk@hotmail.com

2) Ph.D., Assoc. Prof., Department of Water Resources Engineering, Faculty of Engineering, Chulalongkorn University, Bangkok, Thailand. Email: dr.aksara.putthividhya@gmail.com

3) Ph.D., Special Advisor of Strategic Water Resources Management, Eastern Economic Corridor Office, Bangkok, Thailand

4) Ph.D., Senior Expert in Economic Analysis of Water Resources Development Project, Office of the National Water Resources, Bangkok, Thailand

*Corresponding Author

Abstract: Thailand is facing increasing water risks as a growing population, economic growth and the looming threats posed by climate change are expected to make sustainable water management and water security significantly more difficult. The government thus needs to move from a crisis response to a risk-management approach by maintaining acceptable levels of risk in 4 main areas including (1) drought risk; (2) flood risk; (3) the risk of inadequate water quality (water pollution); and (4) the risks of undermining the resilience of freshwater systems (water use and water allocation). This paper aims to enhance and facilitate the move to a risk-based approach to water security by making better use of drought analysis instruments using appropriate indices/indicators to reduce water shortages in drought-stricken areas especially under prolonged weather events hopefully to formulate water policies for justified spatio-temporal water allocation and access in the Eastern Economic Corridor (EEC) region. Long-term analysis of meteorological and hydrological drought indices is conducted to characterize and monitor drought trends in EEC using the Standardized Precipitation Index (SPI), the Standardized Precipitation Evapotranspiration Index (SPEI), and the Streamflow Drought Index (SDI). Computed time series of the 3 selected indices are compared with observed drought events by assimilating the weekly rainfall and monthly streamflow and evapotranspiration (PET) data from ground observations and remotely-sensed Earth observing satellites (i.e., MODIS, Aqua MODIS, TRMM, and GPM) data and climate drought indices are calculated. The performances of 3 climatic indices seem to be able to capture the main characteristics of drought conditions in EEC region and the indices also designate extreme drought frequency and severity since early 2000s. The 2 indices obviously can also detect notable drought episodes during year 1997-98, 2003-04, and 2015-16 consistent with El Niño years. The overstating the frequency of droughts at the 1-month timescale by SPEI and SDI still exists just like the case of SPI. SPEI indicated substantial higher severity and longer duration of drought events compared to those of SPI especially for the year 1991-92 drought episode, while SPI under-quantified the magnitude and missed to represent extreme droughts during that period. SPI climatic indices shows diverse effects on drought conditions under the prolonged records with certain restrictions, while multivariate index (i.e., SPEI) illustrates the obvious advantage of temporal variation of drought frequency, magnitude, and severity characteristics detection. The better performance of SPEI indices compared to SPI emphasizes that PET plays an important role in hydrologic cycle in Thailand with tropical monsoon weather system and its variation is primarily affected by precipitation as well as land use and land coverage change. Development of multiple drought indices demonstrated in this study can be beneficial for drought assessment, early warning, and future projections for planning and support the implementation of preventive measures or mitigation of drought impacts.

Keywords: Drought index, Drought early warning, EEC Thailand, Drought risk, ENSO.

1. INTRODUCTION

Droughts occur in virtually all climatic zones and are mostly related to the reduction in the amount of precipitation received over an extended period of time. Droughts are recognized as an environmental disaster and have attracted the attentions owing to the rise in water demand from population growth and expansion of agricultural-energy-industrial sectors as well as looming climate change, recent years have witnessed much focus on global drought scenarios including Thailand. The period between extreme events seems to have become shorter in certain regions and floods and droughts have made references to this change in the occurrence of extreme hydrologic events including higher peaks and severity levels (Lettenmaier et al., 1996; Aswathanarayana, 2001).

Difference in hydrometeorological variables and socio-economic factors as well as the stochastic nature of water demands in different regions around the world become an obstacle to having a precise definition of drought. But, drought can be generally categorized into 4 categories (Dracup et al., 1980; Heim Jr, 2002; Zargar et al., 2011): meteorological, hydrological, agricultural, and socioeconomic. Meteorological drought is defined usually on the basis of the degrees of dryness (in comparison to some “normal” or average amount) and the duration of the dry period. Definitions of meteorological drought must be considered as regional specific since the atmospheric conditions that result in deficiencies of precipitation are highly variable from region to region. Hydrological

drought is associated with the effects of periods of precipitation shortfalls on surface or subsurface water supply (i.e., streamflow, reservoir and lake levels, groundwater) and how this deficiency plays out through the hydrologic system. Agricultural drought links various characteristics of meteorological (or hydrological) drought to agricultural impacts, focusing on precipitation shortages, differences between actual and potential evapotranspiration, soil water deficits, reduced groundwater or reservoir levels, and so forth. Socio-economic drought is associated with failure of water resources systems to meet water demands and thus associating droughts with supply of and demand for an economic good (water) (AMS, 2004). Socio-economic drought occurs when the demand for an economic good exceeds the supply as a result of a weather-related shortfall in water supply.

Assessment of droughts is of primary importance for water resources planning and management under well-recognized climate change impacts and threats. According to the Intergovernmental Panel on Climate Change (IPCC) report (IPCC, 2007), instrumental observations over the past 157 years show that temperatures at the surface have risen globally, with significant regional variations. This warming definitely intensifies the global hydrologic cycle (Milly et al., 2002) not in changing the averages but the overall increase of extreme events, resulting in increasing the globally averaged precipitation, evaporation, and runoff. Among the extreme meteorological events, droughts are possibly the most slowly developing ones, that often have the longest duration, and at the moment the least predictability among all atmospheric hazards. (Mishra and Singh, 2010). For the global average, warming in the last 20th century has occurred in 2 phases, from the 1910s to 1940s (0.35°C), and more strongly from 1970s to the present (0.55°C). An increasing rate of warming has taken place over the last 25 years, and 11 of the 12 warmest years on record have occurred in the past 12 years.

For Thailand, it is considered one of the most drought-affected countries in the Asia-Pacific region and is marred by frequent drought. Recently, observed extreme weather events (drought in year 2011/2012 2015/2016 and 2018/2019) reflect the more frequent occurrence of severe drought in Thailand. Assessment of the recent drought in Thailand reveals that it is mainly due to a shorter-than-normal monsoon season and below-average annual rainfall in 2018 and 2019 as the monsoon rain cycle arrived almost 2 weeks later than averaged cycle and departed 3 weeks earlier in Thailand. Average annual precipitation in 2019 of 1,343 mm was reported and considered 15% below the 30-yr average and 19% lower than the previous year's levels (1,661 mm). Royal Irrigation Department (RID) Thailand reported that water supplies in major reservoirs totaled 3.8 billion m³, down 60% from the same period last year as of January 2020. River ran low and stages were substantially below the mean sea level, resulting in saltwater intrusion creeping way upstream and threatening drinking water supplies. Insufficient water availability at the end of 2019 rainy season impact food, agriculture, and industrial security and manifested disputes among all water sectors with economic competition.

Owing to the rising water demand, looming climate change, aging water resources infrastructure, and the economy with rapidly rising incremental costs of new supplies and increasing conflict among water sectors, a wider view is needed to handle water scarcity problems specifically focusing on developing measures for mitigating the impacts of drought, especially among Thai responsible agencies that are highly centralized but fragmented. The Thai government thus needs to move from a crisis response to a risk management approach by maintaining acceptable levels of risk in 4 main areas including (1) drought risk; (2) flood risk; (3) the risk of degrading water quality; and (4) the risk associating with water use and water allocation. These force stress the urgent need to develop drought assessment for water resources planning and management using indices/indicators to characterize spatio-temporal drought magnitudes especially under prolonged weather events.

A number of different drought indices have been developed utilizing the climatic and hydrological variables to describe drought characteristics such as duration, severity, and frequency (Hao and Singh, 2015), each with its own strengths and weaknesses, including Palmer Drought Severity Index (PDSI) (Palmer, 1965); the Drought Area Index (Bhalme and Mooley, 1980); the Standardized Precipitation Index (SPI) (McKee et al., 1993); the Reconnaissance Drought Index (RDI) (Tsakiris and Vagelis, 2005); and Standardized Precipitation Evapotranspiration Index (SPEI) (Vicente-Serrano, et al. 2010), Rainfall Anomaly Index (RAI) (van Rooy, 1965), Surface Water Supply Index (SWSI) (Shafer and Dezman, 1982), etc. SPI and SPEI are extensively used because they both offer ease in calculating and interpreting, are multi-scalar in nature, and are spatially and temporally comparable. The major difference between the two indices is that SPI uses only precipitation as the climatic variable for drought computation with the underlying assumption that the temporal variability of precipitation is much higher than other climatic variables (e.g., temperature); while SPEI considers the variabilities in other climatic variables (e.g., temperature, humidity, winds, etc.) by incorporating the evaporative demands in the drought index (Vicente-Serrano et al., 2010). This is more relevant in the context of climate change, where the assumption of stationarity of climate variables such as temperature is no longer valid (Dubrovsky et al., 2009). Several recent researchers have used SPEI for historical and future drought assessments (Zhang et al., 2018). Vicente-Serrano et al. (2012) conducted a global assessment of the performance of SPI, SPEI, and 4 variants of PDSI and found that SPEI is superior in identifying the drought impacts. Zhang et al. (2018) found that SPEI is highly correlated with the total water storage in the Chinese river basin, underlining its usefulness in assessing the water resources. Moreover, several previous studies have demonstrated that projected increased drought severities under climate change and the magnitude of increments using SPEI is higher than using SPI (Ahmadalipour et al.,

2017; Marcos-Gracia et al., 2017). Currently, there is no particular index that is capable of adequately characterizing drought conditions for every place and every time period (Svoboda et al., 2015).

This study aims to enhance and facilitate the move to a risk-based approach to water security by making better use of appropriate drought indices analysis instruments to reduce water shortages in drought-stricken areas especially under prolonged weather events hopefully to formulate water policies for justified spatio-temporal water allocation and access in the Eastern Economic Corridor (EEC) region of Thailand. Long-term analysis of meteorological and hydrological drought indices is conducted to characterize and monitor drought trends in the EEC using the Standardized Precipitation Index (SPI; precipitation-based less complicated drought index as it requires only simple inputs), the Standardized Precipitation Evapotranspiration Index (SPEI; an index taking into account the difference between precipitation and potential evapotranspiration), and the Streamflow Drought Index (SDI) input with various types of data sources, including ground observations and remotely-sensed data. Computed time series of the 3 selected indices are compared with observed drought events by assimilating weekly rainfall and monthly streamflow and evapotranspiration data from ground observations and remotely-sensed Earth observing satellites (i.e., MODIS, Aqua MODIS, TRMM, and GPM) data and climate drought indices are calculated.

2. METHOD

2.1 Study Area

Thailand is located close to the equatorial Indo-Pacific basins; this monsoon precipitation has strong correlation with the Southern Oscillation Index (SOI), a sea level pressure-based El Niño-Southern Oscillation (ENSO) index (Singhtrattna et al., 2005). The region is characterized by a monsoon tropical climate with distinctive dry and rainy seasons causing repetitive droughts and floods. The country average range of annual rainfall of 1,300-2,000 mm per year with peak rainfall in August and September.

The target study area is known as Eastern Economic Corridor (EEC) located in the East of Thailand, spanning from East to West and covering 3 provinces namely Chonburi, Rayong, and Chachoengsao shown in Figure 1. Monthly average rainfall of the region falls between 5.4-284.2 mm with the minimum rainfall in December and maximum rainfall in September and October. Annual average rainfall is approximately 1,308.5 mm which is considered lower than the nation-wide average. Current water demand of 739 million m³/year versus the allocated 941 million m³/year with substantial rise to 1.21 billion m³/year in the future (year 2037) from rapid investment in EEC to support industrial expansion and population growth, surpassing the amount possibly allocated, is anticipated. Changing climate pattern with less rain projected in the future based on the long-term climate projection imposes major challenges for water management as competition for water will become worse, particularly for policy makers and regulators in EEC.

2.2 Climatic Data

The daily precipitation datasets employed in this study were referenced from Asian Precipitation-Highly-Resolved Observational Data Integration Towards Evaluation of Water Resources (APHRODITE) available free-of-charge at <http://www.chikyu.ac.jp/precip/>. Observed daily climatic data, including maximum and minimum temperatures, relative humidity, wind speed, evaporation, and solar radiation for the period from 1987-2017 were kindly provided from Royal Irrigation Department (RID) and Thai Meteorological Department (TMD) shown in Figure 2 (for Rayong, Chonburi, and Chachoengsao provinces).

2.3 Drought Indices

(1) Standardized Precipitation Index

The Standardized Precipitation Index (SPI) (McKee et al., 1993) is an index based on probability of the long term precipitation representing either abnormal wetness or dryness conditions. The SPI was designed to quantify precipitation deficits for different time scales such as 3, 6, 9, 12, and 24 months of cumulative precipitation. This allows SPI index to reflect impacts resulting from the availability of different hydrological parameters. We fit long term series of monthly station-based precipitation observations to determine the cumulative probability of density function (PDF) and then transformed into a normal distribution with a mean set to zero and standard deviation of one as shown in Figure 3. The original concept of the SPI applied the two-parameter gamma distribution according to McKee et al (1993) as shown in Equation 1.

$$g(x) = \frac{1}{\beta^a \Gamma(a)} X^{a-1} e^{-\frac{x}{\beta}} \quad (1)$$

where β is a scale parameter, a is a shape parameter, $g(x)$ is the gamma probability density function, e is Euler's number for exponentiation, and $\Gamma(a)$ is the ordinary gamma function of a . The estimation of β and a can be found in more detail from McKee et al. (1993).

(2) Standardized Precipitation Evapotranspiration Index

The Standardized Precipitation Evapotranspiration Index (SPEI) (Vincente-Serrano et al., 2010) has been developed based on a monthly climatic water balance driven by precipitation and Potential Evapotranspiration

(*PET*). The procedure of SPEI compilation relies mainly on the original concept of SPI calculation but employs the monthly difference between *P* and *PET*, representing the water surpluses or deficits at different time scales as shown in Equation 2.

$$D = P - PET \quad (2)$$

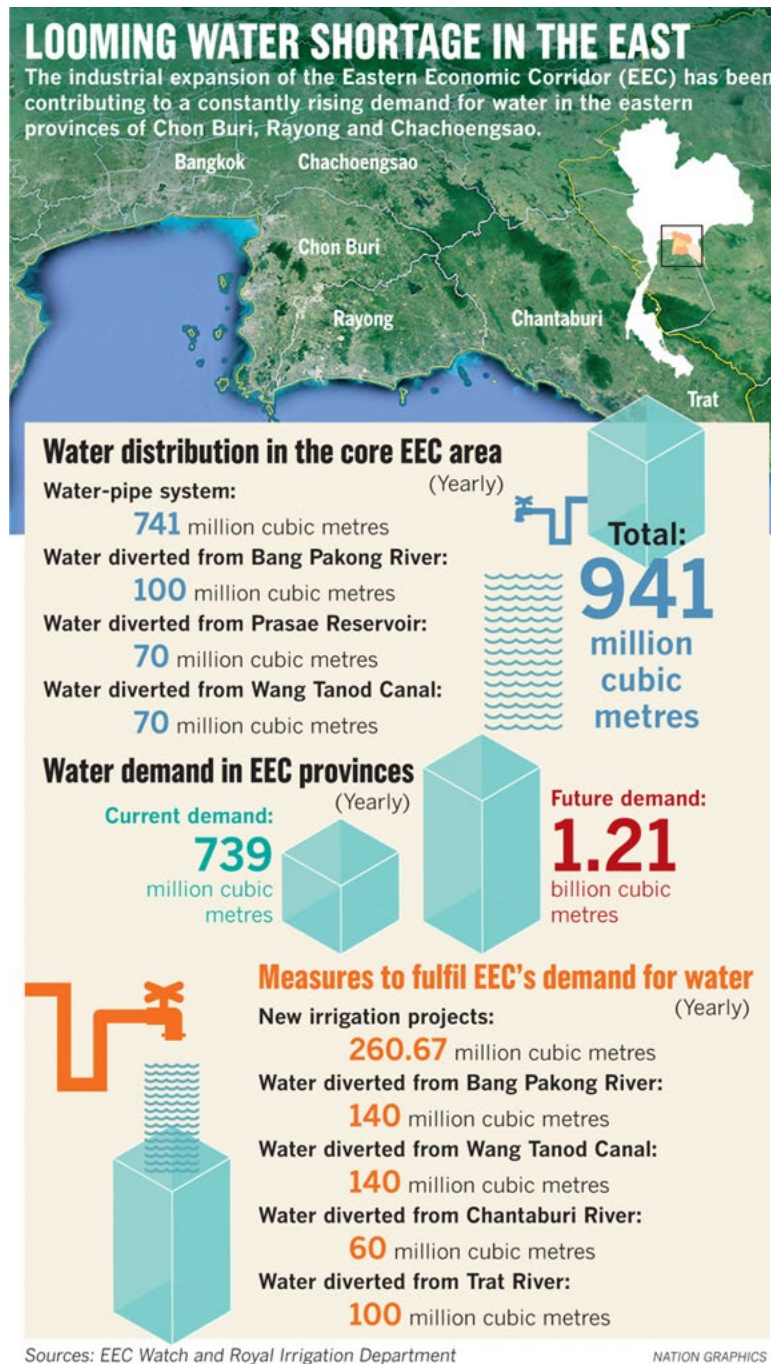


Figure 1. Study area EEC region in Thailand with current and future (year 2037) water demand

The difference in *P* and *PET* are then fitted to several parametric statistical probability distribution functions to standardize the original data sets. *PET* is calculated using Penman-Monteith (PM) equation (Allen et al., 1998) per recommendation by World Meteorological Organization (WMO) (WMO, 2009).

3. RESULTS AND DISCUSSION

The variation of observed droughts in EEC region Thailand is temporally evaluated as shown in Figure 4 based on SPI calculation for 1, 3, 6, 9, 12, and 24 months, respectively. Drought events are generally indicated when the results of SPI, for whichever timescale is being investigated, become continuously negative and reach a

value of -1. The degree of drought can be computed as a factor of the highlighted area size. The different timescales of the SPI demonstrated differences in magnitude and duration of droughts. Longer timescales showed a higher severity and longer duration of droughts than the short timescales. For longer timescales (> 6 months), water scarcity was less frequent, but lasted longer.

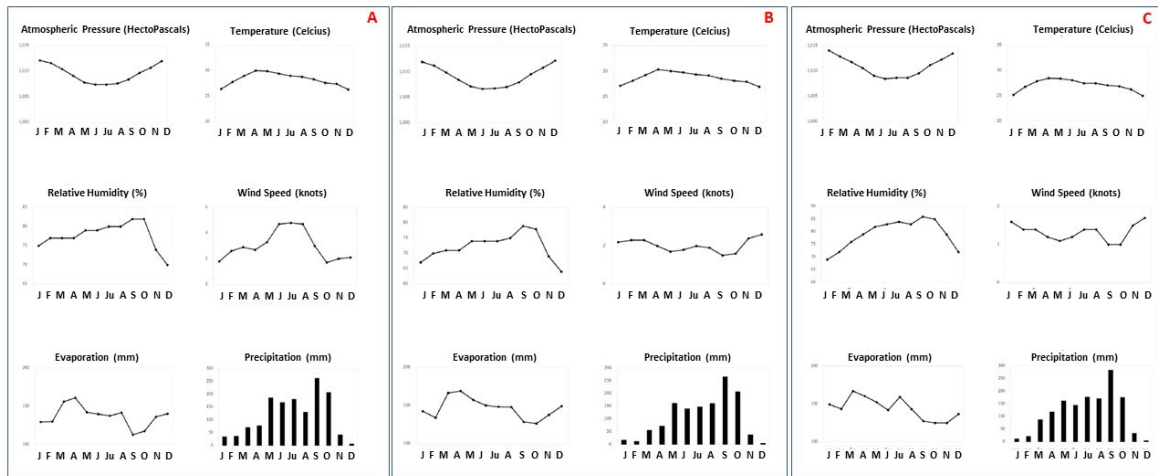


Figure 2. Observed daily climatic data for EEC region for the period from 1987-2017 (A) Rayong province; (B) Chonburi province; and (C) Chachonegsao province

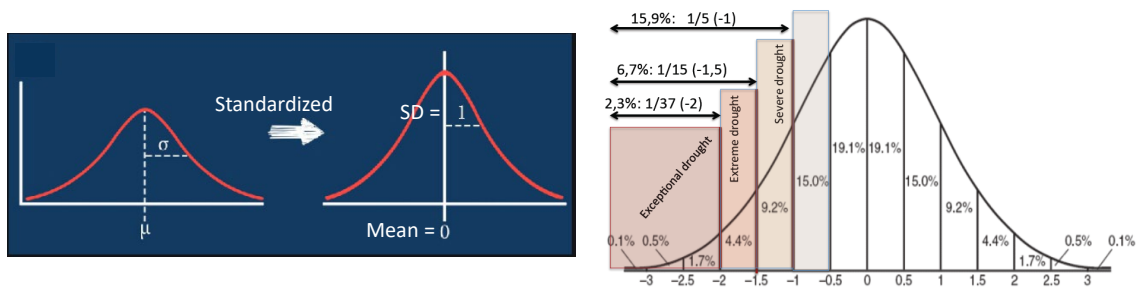


Figure 3. Standardized precipitation index concept

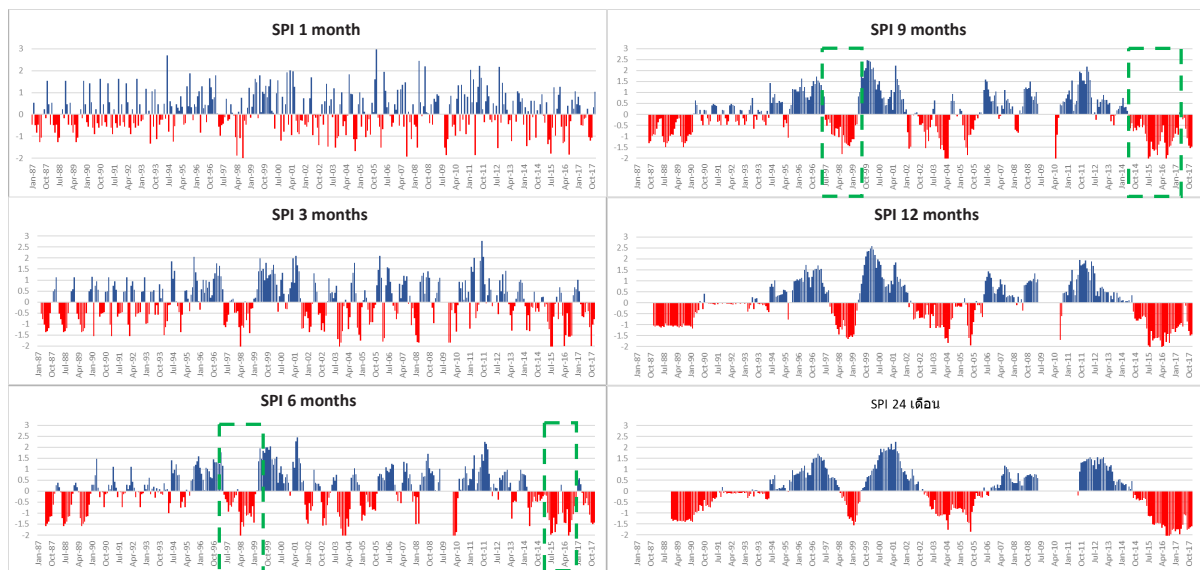


Figure 4. Long-term Standardized Precipitation Index (SPI) analysis in EEC region Thailand. Drought events identified any time an SPI value reaches an intensity of -1 or less

It is clear from times series SPI plots in Figure 5 that drought events in Thailand were likely happening every year on the 1-month analysis timescale, perhaps due to the limitation from using monthly precipitation data causing standardization of the SPI fail to differentiate between the real drought events and monthly variation at such timescales. The interpretation and utilization of the SPI over the tropical monsoon region with distinct precipitation should be carefully carried out to avoid any misleading interpretation when being applied to the short timescale. A direct relationship between drought events defined by SPI and the ENSO conditions based on climate parameter variability is illustrated in Figure 5 as SPI 3-month conformed to El Niño years. Anomalies of the 3-month moving average sea surface temperature (SST) in Niño 3.4 region (5N-5S, 120-170W) for period from 1950-2020 reveal El Niño and La Niña period, frequency, and intensities during the 30+ yrs history in Thailand. Analysis of Figure 5 indicates that droughts significantly struck Thailand from both frequency- and intensity-wise in late 1980s to early 2000s perhaps due to the warmer climatic trend in Thailand since 1980s (Singhrattna et al., 2005) based on declining precipitation intensity and rising temperature trend over this region which causes increasing in PET (National Oceanic and Atmospheric Administration, 2015; Dai, 2011; Sheffield et al., 2012). Results from attempts to validate the performance of drought indices (SPI, SPEI, and SDI) through drought events reported also shown in Figure 4 indicate that moderate timescale SPI (i.e., SPI 6-months, SPI 9-months) can consistently define drought events in the study area.

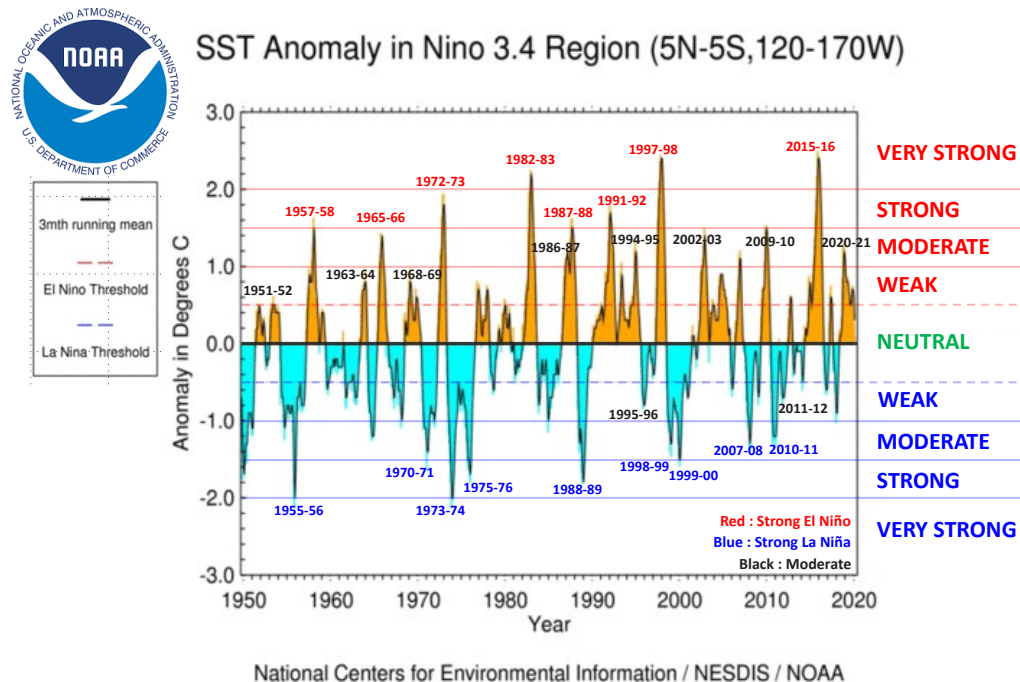


Figure 5. SST anomalies (3 month moving average) in Niño 3.4 region (5N-5S, 120-170W) for 1950-2020 indicating El Niño and La Niña period and intensities (modified from NOAA)

Figures 6 and 7 illustrate the performance SPEI and SDI at multiple timescales (1-24 months). The performances of both climatic indices seem to be able to capture the main characteristics of drought conditions in EEC region and both indices also designate extreme drought frequency and severity since early 2000s. The overstating the frequency of droughts at the 1-month timescale still exists just like the case of SPI. The 2 indices obviously can also detect notable drought episodes during year 1997-98, 2003-04, and 2015-16 consistent with El Niño years. SPEI indicated substantial higher severity and longer duration of drought events compared to those of SPI especially for the year 1991-92 drought episode, while SPI under-quantified the magnitude and missed to represent extreme droughts during that period. The better performance of SPEI indices compared to SPI emphasizes that PET plays an important role in hydrologic cycle in Thailand with tropical monsoon weather system and its variation is primarily affected by precipitation as well as land use and land coverage change.

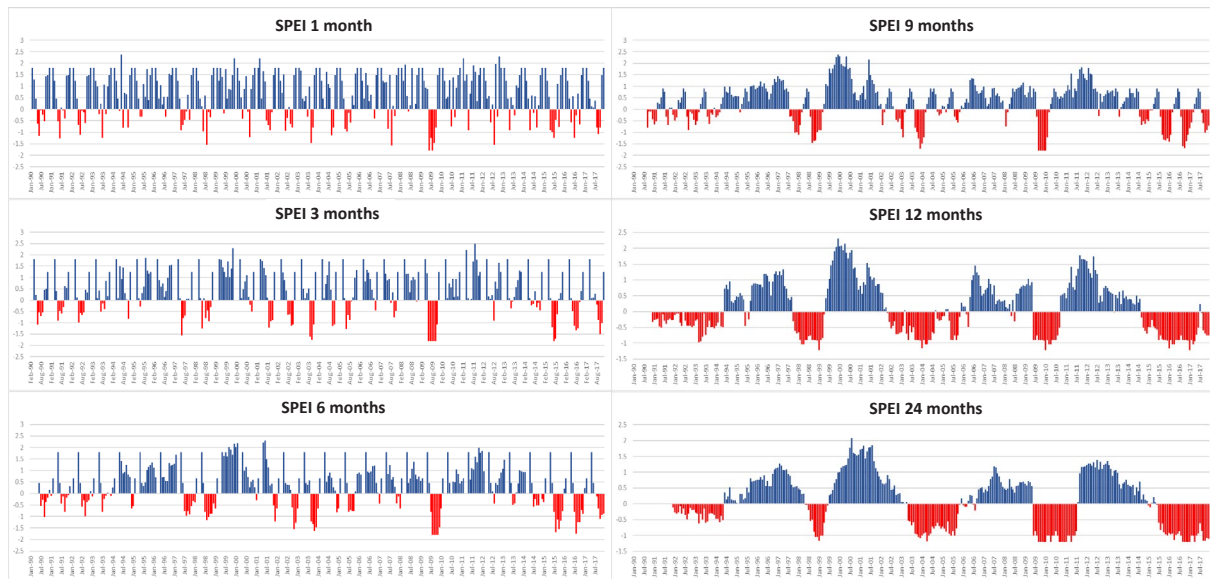


Figure 6. Long-term Standardized Precipitation Evapotranspiration Index (SPEI) analysis in EEC region Thailand. Drought events identified any time an SPEI value reaches an intensity of -1 or less.

4. CONCLUSIONS

This study aims to enhance and facilitate the move to a risk-based approach to water security by making better use of appropriate drought indices analysis instruments to reduce water shortages in drought-stricken areas especially under prolonged weather events hopefully to formulate water policies for justified spatio-temporal water allocation and access in the Eastern Economic Corridor (EEC) region of Thailand. Long-term analysis of meteorological and hydrological drought indices is conducted to characterize and monitor drought trends in the EEC using the Standardized Precipitation Index (SPI; precipitation-based less complicated drought index as it requires only simple inputs), the Standardized Precipitation Evapotranspiration Index (SPEI; an index taking into account the difference between precipitation and potential evapotranspiration), and the Streamflow Drought Index (SDI) input with various types of data sources, including ground observations and remotely-sensed data. Computed time series of the 3 selected indices are compared with observed drought events by assimilating weekly rainfall and monthly streamflow and evapotranspiration data from ground observations and remotely-sensed Earth observing satellites (i.e., MODIS, Aqua MODIS, TRMM, and GPM) data and climate drought indices are calculated.

The performances of 3 climatic indices seem to be able to capture the main characteristics of drought conditions in EEC region and the indices also designate extreme drought frequency and severity since early 2000s. SPI analysis indicates that drought events in Thailand are likely happening every year on the 1-month analysis timescale, perhaps due to the limitation from using monthly precipitation data causing standardization of the SPI fail to differentiate between the real drought events and monthly variation at such timescales. The interpretation and utilization of the SPI over the tropical monsoon region with distinct precipitation should be carefully conducted to avoid any misleading interpretation when being applied to the short timescale. A direct relationship between drought events defined by SPI and the ENSO conditions based on climate parameter variability exists as SPI 3-month conforms to El Niño years. Anomalies of the 3-month moving average sea surface temperature (SST) in Niño 3.4 region (5N-5S, 120-170W) for period from 1950-2020 reveal El Niño and La Niña period, frequency, and intensities during the 30+ yrs history in Thailand. Analysis carried out in this study indicates that droughts significantly struck Thailand from both frequency- and intensity-wise in late 1980s to early 2000s perhaps due to the warmer climatic trend in Thailand since 1980s (Singhrattana et al., 2005) based on declining precipitation intensity and rising temperature trend over this region which causes increasing in PET (National Oceanic and Atmospheric Administration, 2015; Dai, 2011; Sheffield et al., 2012). Results from attempts to validate the performance of drought indices (SPI, SPEI, and SDI) through drought events reported indicate that moderate timescale SPI (i.e., SPI 6-months, SPI 9-months) can consistently define drought events in the study area.

The selected indices obviously can also detect notable drought episodes during year 1997-98, 2003-04, and 2015-16 consistent with El Niño years. The overstating the frequency of droughts at the 1-month timescale by SPEI and SDI exists just like the case of SPI. SPEI indicated substantial higher severity and longer duration of drought events compared to those of SPI especially for the year 1991-92 drought episode, while SPI under-quantified the magnitude and missed to represent extreme droughts during that period. SPI climatic indices shows diverse effects on drought conditions under the prolonged records with certain restrictions, while multivariate index (i.e., SPEI) illustrates the obvious advantage of temporal variation of drought frequency, magnitude, and

severity characteristics detection. The better performance of SPEI indices compared to SPI emphasizes that *PET* plays an important role in hydrologic cycle in Thailand with tropical monsoon weather system and its variation is primarily affected by precipitation as well as land use and land coverage change. Development of multiple drought indices demonstrated in this study can be beneficial for drought assessment, early warning, and future projections for planning and support the implementation of preventive measures or mitigation of drought impacts.

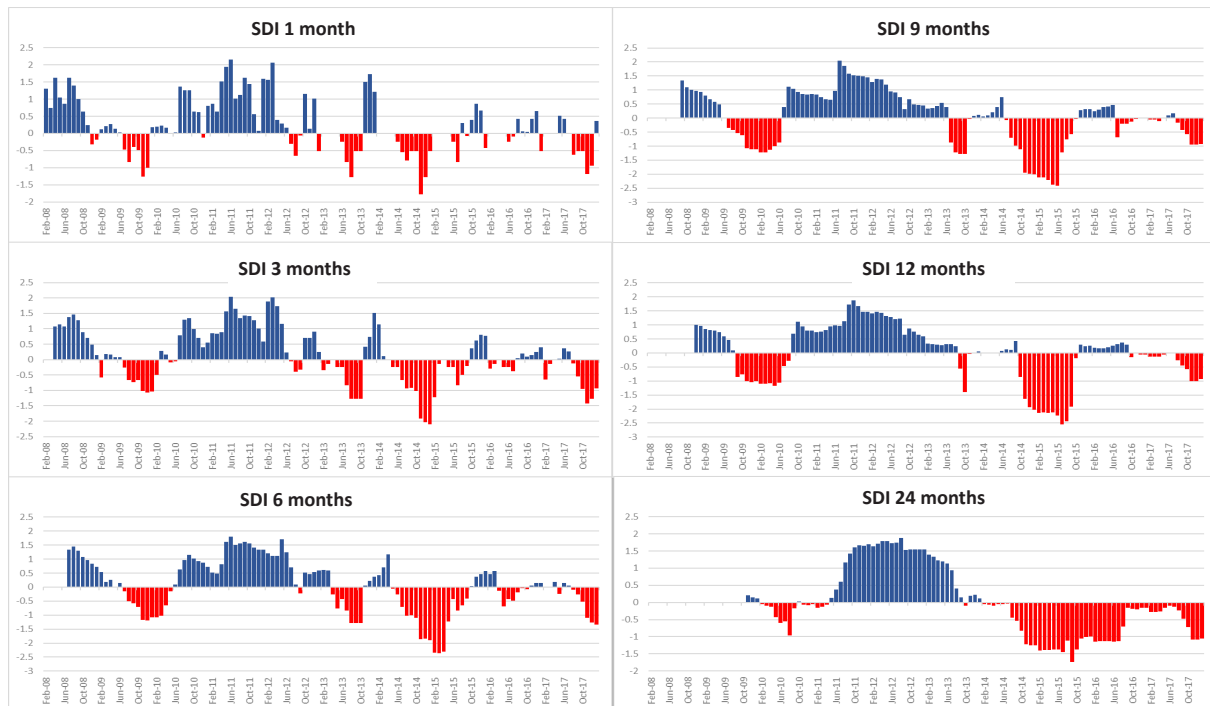


Figure 7. Long-term Streamflow Drought Index (SDI) analysis in EEC region Thailand. Drought events identified any time an SDI value reaches an intensity of -1 or less.

ACKNOWLEDGMENTS

We are very grateful with the Royal Irrigation Department (RID) and Thai Meteorological Department (TMD) for collecting and providing climatic datasets. The financial support to SJ is partially funded by Chulalongkorn University C2F Fund and the Science and Technology Research Partnership for Sustainable Development, JST_JICA, Japan.

REFERENCES

- Ahmadalipour, A., Moradkhani, H. and Demirel, M.C. (2017) A comparative assessment of projected meteorological and hydrological droughts: elucidating the role of temperature. *J. Hydrol.*, 553, 785-797.
- Allen, R., Pereira, L., Raes, D. and Smith, M. (1998). Crop evapotranspiration: guidelines for computing cropwater requirements. FAO Irrigation and Drainage Paper 56. FAO, Rome, pp. 377e384.
- American Meteorological Society (AMS) (2004). Statement on meteorological drought. *Bull. Am. Meteorol. Soc.*, 85, 771-773.
- Aswathanarayana, U. (2001). Water Resources Management and the Environment. Balkema, Rotterdam, The Netherlands.
- Bhalme, H.N. and Mooley, D.A. (1980). Large-scale droughts/floods and monsoon circulation. *Mon. Weather Rev.*, 108, 1197-1211.
- Dai, A. (2011). Drought under global warming: a review. *Wiley Interdiscip. Rev. Clim. Change*, 2, 45e65.
- Dracup, J.A., Lee, K.S. and Paulson, E.G. (1980). On the statistical characteristics of drought events. *Water Resour. Res.*, 16 (2), 289-296.
- Dubrovsky, M., Svoboda, M.D., Trnka, M., Hayes, M.J., Wilhite, D.A., Zalud, Z. and Hlavinka, P. (2009) Application of relative drought indices in assessing climate-change impacts on drought conditions in Czechia. *Theoretical and Applied Climatology*, 96, 155-171.
- Hao, Z. and Singh, V.P. (2015). Drought characterization from a multivariate perspective: a review. *J. Hydrol.* 527, 668e678.

- Heim Jr., R.R. (2002). A review of twentieth-century drought indices used in the United States. *Bull. Am. Meteorol. Soc.*, 83, 1149e1165.
- Intergovernmental Panel on Climate Change (IPCC) (2007). The physical science basis. In: Solomon, S., Qin, D., Manning, M., Chen, Z., Marquis, M., Averyt, K.B., Tignor, M., Miller, H.L. (Eds.), Contribution of working group I to the fourth assessment report of the Intergovernmental Panel on Climate Change. Cambridge University Press, Cambridge, United Kingdom and New York, NY, USA, p. 996.
- Lettenmaier, D.P., McCabe, G. and Stakhiv, E.Z. (1996). Global climate change: effects on hydrologic cycle. In: Mays, L.W. (Ed.), *Water Resources Handbook*, Part V. McGraw-Hill, New York.
- McKee, T.B., Doesken, N.J. and Kleist, J. (1993). The relationship of drought frequency and duration to time scales. In: *Proceedings of the 8th Conference on Applied Climatology* Boston, MA, USA, pp. 179e183.
- Milly, P.C.D., Wetherald, R.T., Dunne, K.A. and Delworth, T.L. (2002). Increasing risk of great floods in a changing climate. *Nature*, 415, 514–517.
- Mishra, A.K. and V.P. Singh (2010): A review of drought concepts. *Journal of Hydrology*, 391, 202–216.
- National Oceanic and Atmospheric Administration, 2015. Historical El Nino/La Nino Episodes (1950epresent), Climate Prediction Center. Retrieved from website:
http://www.cpc.ncep.noaa.gov/products/analysis_monitoring/ensostuff/ensoyears.shtml, 19 October 2015.
- Palmer, W.C. (1965). *Meteorological Drought*. US Department of Commerce, Weather Bureau Washington, DC, USA.
- Shafer, B.A. and Dezman, L.E. (1982). Development of a surface water supply index (SWSI) to assess the severity of drought conditions in snowpack runoff areas. In: *Preprints, Western SnowConf.*, Reno, NV, Colorado State University, pp. 164–175.
- Sheffield, J., Wood, E.F. and Roderick, M.L. (2012). Little change in global drought over the past 60 years. *Nature*, 491, 435e438.
- Singhrattana, N., Rajagopalan, B., Kumar, K.K. and Clark, M. (2005). Interannual and interdecadal variability of Thailand summer monsoon season. *J. Clim.*, 18, 1697e1708.
- Svoboda, M.D., Fuchs, B.A., Poulsen, C.C., and Nothwehr, J.R. (2015). The drought risk atlas: enhancing decision support for drought risk management in the United States. *J. Hydrol.*, 526, 274e286.
- Tsakiris, G. and Vangelis, H. (2005). Establishing a drought index incorporating evapotranspiration. *Eur. Water*, 9, 3e11.
- Van Rooy, M.P. (1965). A rainfall anomaly index independent of time and space. *Notos*, 14, 43.
- Vicente-Serrano, S.M., Begueria, S. and Lopez-Moreno, J.I. (2010). A multiscalar drought index sensitive to global warming: the standardized precipitation evapotranspiration index. *J. Clim.*, 23, 1696e1718.
- Vicente-Serrano, S.M., Van der Schrier, G., Begueria, S., AzorineMolina, C., LopezeMoreno, J.I. (2015). Contribution of precipitation and reference evapotranspiration to drought indices under different climates. *J. Hydrol.*, 526, 42e54.
- World Meteorological Organization (WMO) (2009). Lincoln declaration on Drought Indices. World Meteorological Organization. Retrieved from website:
http://www.wmo.int/pages/prog/wcp/agm/meetings/wies09/documents/Lincoln_Declaration_Drought_Indices.pdf, Retrieved 22 April 2023.
- Zargar, A., Sadiq, R., Naser, B. and Khan, F.I. (2011). A review of drought indices. *Environmental Reviews*, 19, 333–349.
- Zhang, Y., Yu, Z. and Niu, H. (2018). Standardized precipitation evapotranspiration index is highly correlated with total water storage over China under future climate scenarios. *Atmospheric Environment*, 194, 123–133.

DISASTER EDUCATION ON FLOOD PREVENTION USING CARD GAME THROUGH DIGITAL PLATFORM

Mari Tanaka¹ and Kenji Nakamura²

1) D. Eng., Prof., Cooperative Faculty of Education, Gunma University, Maebashi, Japan. Email: mari@gunma-u.ac.jp

2) D. Health and Welfare Science., Lecturer., Gunma University Center for Mathematics and Data Science, Maebashi, Japan. Email: nac-k@gunma-u.ac.jp

Abstract: In General, disaster management has been mentioned in term of engineering both soft and hard implement hardly understand by local people. On the other hand, disaster education would be an efficient tool for getting community to recognize this. In disaster education, it is important not only to focus on the dangers of disasters, but also to develop a sense of attachment to and pride in the community in which one lives, while enjoying the benefits of nature, so that one can proactively evacuate in the event of a disaster.

In this study, a workshop was planned and conducted to deepen understanding of the wisdom and ingenuity of predecessors and their lifestyles in dealing with floods, and to create cards to introduce the local knowledge of the community and their predecessors' flood response. Then we created a digital card game using these cards, which enables participants to learn about the local wisdom of the community and its response to flood disasters while playing the game by themselves. The digital karuta system was constructed so that it could be run on low-spec equipment, and was designed to be simple enough to be implemented by elementary school students. In addition, brain activity was investigated using NIRS to see if the digitalization of the system had any effect on the learning effect.

Keywords: Disaster education, Living environment, Local wisdom, Digital disaster prevention card game

1. INTRODUCTION

In recent years, natural disaster such as torrential rains and typhoons have become more frequent and severe due to the effects of climate change. We should realize priority on protecting precious lives from any disaster. In order for all residents to be able to protect their own lives from disasters, it is important that each people be able to take appropriate actions in the event of a disaster. From this perspective, the government has revised the Basic Act on Disaster Control Measures, which has strengthened the system to ensure smooth and prompt evacuation of residents in the event of a disaster, such as by improving the clarity of evacuation information and enhancing measures for those who require assistance for evacuation actions.

In addition, since the Great East Japan Earthquake, the importance of disaster education has increased, and the contents and education methods of disaster education have been greatly enhanced of the new government curriculum guidelines. In the curriculum guidelines of elementary school social studies implemented from 2020, the part about natural disasters occurring in the prefecture was added: Among earthquake disasters, tsunami disasters, wind and flood disasters, volcanic disasters, and snow disasters, those that have occurred in the prefecture in the past should be selected and discussed. In the commentary to the curriculum guideline of Home Economics in junior high schools implemented since 2021, in the section on housing, “Regarding natural disasters, examples of past disasters may be taken up in accordance with the actual conditions of the region. The word “according to the actual conditions of the region” was added. As described above, it is expected that students will learn about past disasters, but there is a lack of teaching materials that are suited to the past disaster of the region.

In disaster education, it is important not only to focus on the dangers of disasters, but also to develop a attachment to the community and pride in the community in which one lives, while enjoying the benefits of nature, so that one can proactively evacuate in the event of a disaster. In this study, a workshop was planned and conducted to deepen understanding of the wisdom and ingenuity of predecessors and their lifestyles in coping with flood, and to create cards to introduce the good points of the community and their predecessor's response to the flood, targeting communities that have coped with frequent floods. This is intended to be used in the production of disaster prevention materials tailored to the actual conditions of the community. Furthermore, we organized an exchange meeting between local elderly and elementary school student using these cards, many of the children (29/35 person: 83%) expressed a desire to play with the cards more. Therefore, we attempted to digitize the cards so that the children could learn about the features and local wisdoms while playing alone and by themselves. The card system was constructed so that it could be operated even with low-spec equipment, and was designed to be simple enough to be implemented by elementary school students. In addition, brain activity was investigated using NIRS to see if the digitalization had any effect on the learning effect.

2. METHOD

This study to make learning about community disaster management was conducted in three phases (Table

1). First, a workshop was held (June 26, 2022) to deepen understanding of local flood experiences and responses and to make cards. At a community center in the town of Itakura, Gunma Prefecture, participants were introduced to the town of Itakura and its lifestyles in the event of flooding. They visited a flood prevention building in the event of flooding while listening to a talk about the town's lifestyles, and created playing cards to introduce local lifestyles in anticipation of flooding. Twenty participants, including elementary school students and university students (Fig.1, Fig.2), took part in the project. Secondly, on February 14, 2023, we held a meeting between local elderly and elementary school student using the completed playing cards at an elementary school, creating an opportunity for disaster education in which participants could share their experiences of disasters in the community while playing (Fig.3). Finally, we constructed an online card game and tested whether it could be implemented even in a remote and impersonal setting (March 2023). We called this online card "Digital Karuta". The effectiveness of the paper karuta and the online digital karuta was measured (Fig.4).

Table 1. Disaster education process and digitized cards

	1	2	3
Date	2022.06.26	2023.02.14	2023.03
	Workshop	Meeting	Experiment
Contents	Quiz, Visiting flood evacuation building, Discussions, Making playing card to show local wisdom to cope with flood	Game, Playing card game, Discussion, Card battle children VS local senior residents	Paper Karuta, Digital Karuta, NIRS experiment
Participants	7 Elementary students 1 High school student 11 University students & graduate 4 Local senior volunteers	35 Elementary students 8 University students 9 Local senior volunteers school teachers	6 University students (3 men, 3 women)



Figure1. Workshop of visiting and making playing card "Karuta"



Figure 2. Playing cards (Paper Karuta) to show local wisdom made by workshop



Figure 3. Exchange meeting (local seniors, elementary school student and university students)



Figure 4. Experiment

3. RESULTS

3.1 Novelty of the System (novelty of performance/function, novelty of configuration, novelty of development method)

Karuta is an interactive task that uses a tool called cards. The cards are displayed on the system, and the karuta is acquired using the skeletal estimation function of the web camera. It is classified as an XR technology because it reproduces information from the real world in real time on the system. By implementing a text-to-speech function, the task can be performed by one person, but it is also possible for two people to perform the task online at the same time. The system is built on Amazon's Web Services and published using a dedicated domain. AR-type karuta cards have existed in the past. There are also memorization-type karuta cards that display cards in succession, but there is no XR-type karuta card game that uses a skeletal estimation function. There are application that use skeletal estimation technology for training, but they have not yet been implemented because skeletal estimation technology often makes recognition errors due to the non-uniformity of background regions. Our digital karuta, which is still in the demonstration stage, avoids recognition errors by cropping the background region of the recognized human body. Figure 5 show the processing flow of the system and the test environment.

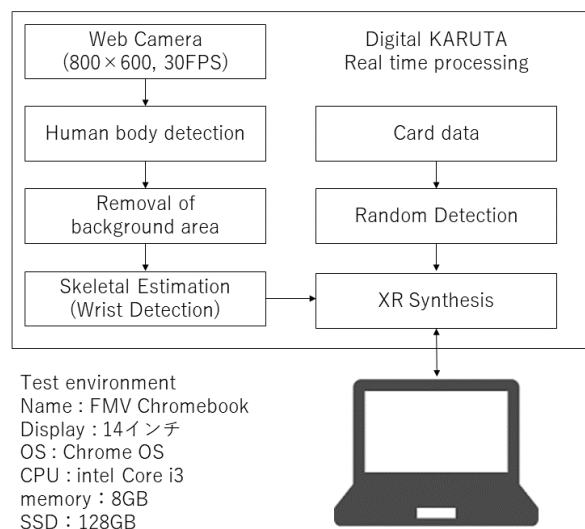


Figure 5. Processing flow of the system and the test environment

3.2 System Effectiveness

The frame rate for this system is 30 FPS, which is the standard frame rate for TV and video. Since real-time processing is done at the terminal side, it is not affected by line delays. Therefore, we focused on cerebral blood flow changes in real-world karuta and digital karuta, targeting the prefrontal regions that are activated during language activity and concentration.

3.3 System Reliability

NIRS (Near Infrared Spectroscopy) is a system that uses near-infrared light to estimate the amount of hemoglobin in cerebral blood flow. In the medical field, it is used to measure depression, and in the basic field, it is used to study learning effects such as short-term memory (Michael et al., 2021). A Neu HOT-2000 was used as the equipment, and six volunteer students were participated. The task consisted of a 30-second rest (Rest1), a 30-second task (Task), and a 30-second rest (Rset2). The average waveforms of the six subjects are shown below (Fig.6, Fig.7).

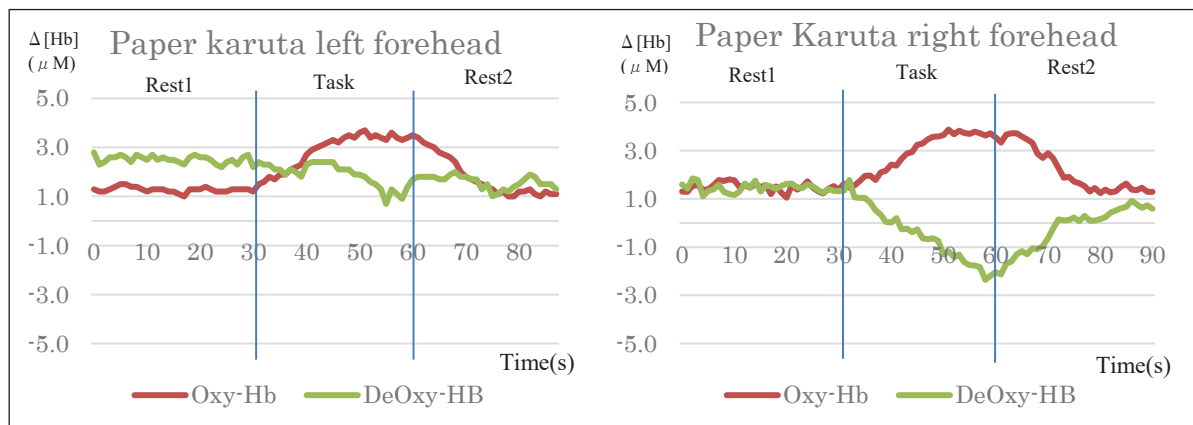


Figure 6. NIRS waveform of paper Karuta

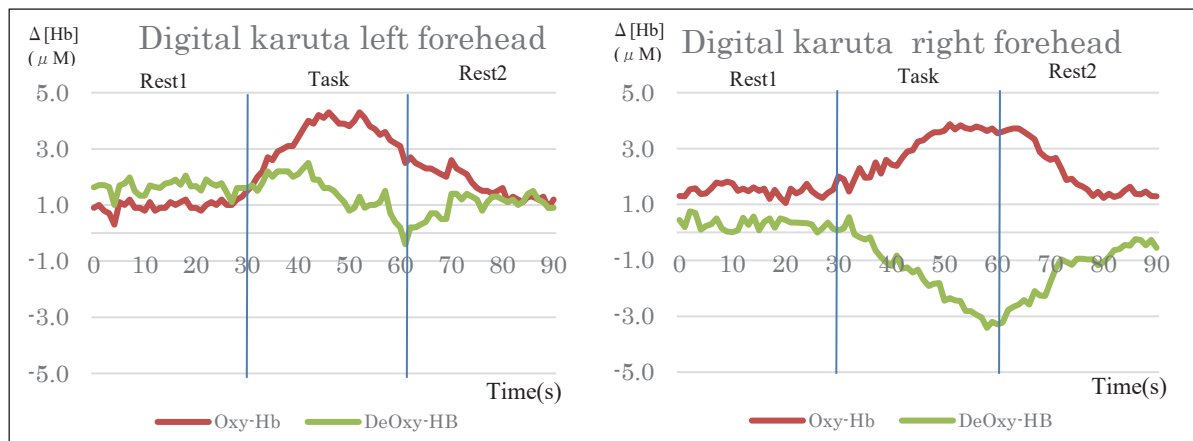


Figure 7. NIRS waveform of digital Karuta

4. DISCUSSION

We hypothesized that there would be no change in oxyhemoglobin between rest and task time. Since the number of N was too small to assume a normal distribution, a Wilcoxon signed-rank sum test was used. As a result, Oxyhemoglobin has p-value = 0.0004883 in paper Karuta, Oxyhemoglobin has p-value = 0.0004883 in digital Karuta. Deoxyhemoglobin has p-value = 0.03418 in paper Karuta, Oxyhemoglobin has p-value = 0.01611 in digital Karuta. Comparing the paper and digital karuta, both of them showed an increase in oxyhemoglobin. The table shows the average values for each state (Table 2).

Table 2. Average values for each state

		Rest1 (μ M)	Task (μ M)	Rest2 (μ M)
Paper Karuta	Oxy-Hb	1.239927	2.360296	1.677265
	DeOxy-Hb	1.271493	-0.40051	-0.06321
Digital Karuta	Oxy-Hb	0.942886	2.35513	1.408666
	DeOxy-Hb	0.697754	-1.11253	-0.80124

There was no difference between the rest and task times. Nguyen evaluated the concentration phase by activation of the NIRS waveform during operation, suggesting a possible link between elevated Oxyhemoglobin and concentration (Nguyen et al., 2017). The higher value during the task condition indicates that users are in a state of concentration and their memory is activated during digital Karuta.

However, estimating memory effects with NIRS has its challenges, NIRS measures changes in the amount of hemoglobin in cerebral blood flow, and there are many examples by assessing brain activity and concentration states, such as the N-back test (Michael et al., 2021). All of these tasks assess short-term memory and do not guarantee long-term memory. Takeuchi have just measured the effects of learning by video games using NIRS and showed students with higher increases in oxyhemoglobin tended to perform better in video games (Takeuchi et al., 2016). Dennis found that NIRS responses were high during highly effective learning (Dennis, 2017). These results indicate that there is a proportional relationship between the amount of oxyhemoglobin increase and learning effectiveness. However, there are many unknowns about brain activity, and there is no guarantee that activation of short-term memory will facilitate transfer to long-term memory (Nakamura et al., 2020). Further validation and innovation are needed in the future. We plan to conduct long-term memory tests and follow-up surveys to verify the effectiveness of digital Karuta.

5. CONCLUSIONS

When brain activity was measured by NIRS for paper Karuta and digital Karuta, it was found that brain activity was activated in both cases. Since Karuta involves hand and body movements, it is possible that effects other than brain activity have a synergistic effect on the NIRS waveform, but further verification is needed. However, the mean oxyhemoglobin value of the paper Karuta increased by 1.12μ M, whereas the mean oxyhemoglobin value of the digital Karuta increased by 1.41μ M. The results suggest that digital Karuta may be more brain active. In addition, digital Karuta can be implemented non-face-to-face and is not limited to Covid19 or face-to-face activities. This suggests that digital Karuta also has a distance learning component.

In the future, we would like to make effective use of the cards to learn about local wisdom for disaster prevention while playing, for example by holding a digital Karuta tournament at elementary school. In the first of three phases of the disaster study was workshop. We emphasized hands-on experiences, such as visiting evacuation building, listening to a story about the use of it during floods. Then we tasted river fish at the lunch time. Afterwards, the children were asked to draw painting to express what impressed them and what they wanted to introduce. All of the children responded that this was the first time they had seen flood evacuation building after participating in this workshop. In their impressions, many of them mentioned the various innovations they had seen in the building, indication a certain level of effectiveness. At the 3rd step of meeting, while looking at the cards, the participants were able to hear stories from local senior residents about their responding to disasters in the past. Many flood evacuation buildings and boats still remain in the town, and by providing more opportunities to learn about local resources through digitalization and other means, we can learn about how people lived in the past in response to flooding and think about how we should do when the flood.

The authors have been involved in activities to pass on the flood experience and response not only in Japan but also in Thailand, producing story books and playing cards. We would like to develop these activities while digitizing them in Thailand.

ACKNOWLEDGMENTS

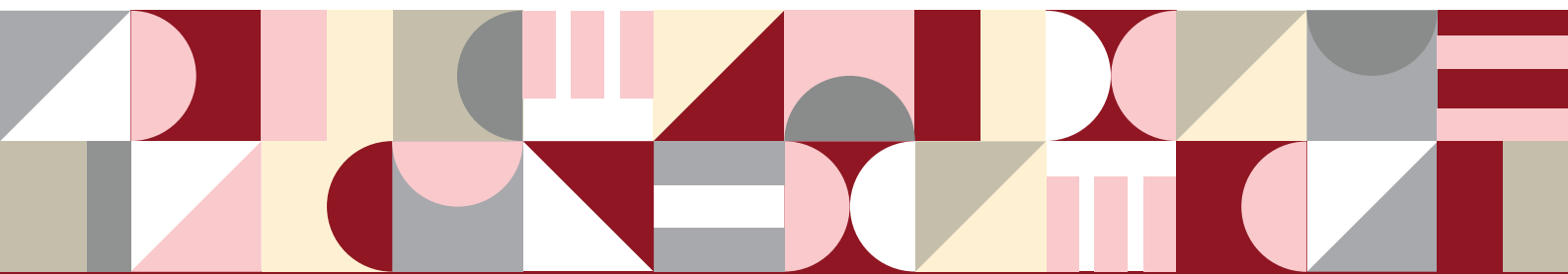
The authors appreciate principal, teachers and students at Itakura east elementary school and senior volunteers for their cooperation in conducting this research. Our thanks extended to students at Gunma university. Part of this research was supported by JSPS 19k04748 and JPMJPF2112.

REFERENCES

Cabinet office Japan. (2021). *Proposal by the disaster education team*. Retrieved from cabinet office website: https://www.bousai.go.jp/kaigirep/teigen/pdf/teigen_06.pdf

- Ministry of education culture, sports, science and technology Japan. (2017). *Education guideline* Retrieved from Mext website: https://www.mext.go.jp/content/20230308-mxt_kyoiku02-100002607_003.pdf
https://www.mext.go.jp/component/a_menu/education/micro_detail/_icsFiles/afieldfile/2019/03/18/1387018_009.pdf
- Tanaka, M. and Tachakitkachorn, T. (2023). Adaptive revitalizing of water-coexisting dwelling under climate change -Comparative significant characteristics on flood recognition and adaptation measures in riverine village in central Thailand and Japan-, *Proceedings 13th International Symposium on Architectural Interchanges in Asia, China*, 358-364
- Tachakitkachorn, T. and Tanaka, M. (2023). Adaptive revitalizing of deltaic dwelling for a typical inundation under climate change: Gunma-based applied art production for enhancing of waterfront knowledge inheritance in Ayudhaya, *Proceedings 13th International Symposium on Architectural Interchanges in Asia, China*, 191-196
- Tanaka, M. (2023). The potential of regional indigenous playing card to understand local living culture including natural disaster, *Annual bulletin of Cooperative Faculty of Education Gunma University*, 58, 55-64
- Wongphyat, W. and Tanaka, M. (2020). A Prospect of disaster education and community development in Thailand: Learning from Japan, *Nakhara: Journal of Environmental Design and Planning*, 19,1-24
- Tanaka, M., Hasumi, Y., Iwashita, T. and Tachakitkachorn, T. (2020). Story-telling towards Japanese and Thai school children by using story book based on the past flood experience, *Proceedings of Architectural Institute of Japan Hokkaido Architectural Research Conference*, 93, 333-336
- Tanaka, M., Kubo, H. and Anbo, E. (2019). Learning Living Environment by Making and Using Indigenous Playing Cards Base on Year-round Event Including Awareness of Natural Disaster, *Annual bulletin of Education Practice Center Gunma University*, 36, 125-134
- Tanaka, M. and Chaimuk, P. (2018). Disaster Education by Sharing Flood Experience in Thailand, *Proceedings 12th International Symposium on Architectural Interchanges in Asia*, 904-943
- Tanaka, M. (2016). Education about Disaster Reduction by Sharing Flood Experiences, *Proceedings 11th International Symposium on Architectural Interchanges in Asia*, 2133-2136
- Tanaka, M. (2012). Learning regional living environments by making and playing indigenous playing cards, *Annual bulletin of Education Practice Center Gunma University*, 29, 103-110
- Michael, K. and Jingxia, L. (2021). Probing depression, schizophrenia, and other psychiatric disorders using fNIRS and the verbal fluency test: A systematic review and meta-analysis, *Journal of Psychiatric Research*, 140, 416-435.
- Michael, K., Tsz, L., Yvonne, M., Han, Y., Agnes, S. (2021). Prefrontal activation and pupil dilation during n-back task performance: A combined fNIRS and pupillometry study, *Neuropsychologia*, 159 (20), 107954
- Nakamura, K., Shiroto, Y., Tamura, Y., Koyama, K., Takeuchi, K., Amanuma, M., Nagasawa, Toru., Ozawa, Seiji. (2020). An increase in the deoxygenated hemoglobin concentration induced by a working memory task during the refractory period in the hemodynamic response in the human cerebral cortex, *Neuroscience Letters*, 714, 134531
- Dennis, Norris. (2017). Short-term memory and long-term memory are still different, *Psychological Bulletin*, 143(9). 992–1009.
- Takeuchi, N., Mori, T., Suzukamo, Y., Izumi, S. (2016). Integration of Teaching Processes and Learning Assessment in the Prefrontal Cortex during a Video Game Teaching-learning Task, *Frontiers in Psychology*, 7, 2052
- Nguyen, T., Ahn, S., Jang, H., Jun, S.C., Kim, J.G. (2017). Utilization of a combined EEG/NIRS system to predict driver drowsiness. *Scientific Reports*. 7, 43933.

Visualization and XR



CONSTRUCTION OF A LOCATION-BASED MIXED-REALITY VISUALIZATION SYSTEM USING GLOBAL NAVIGATION SATELLITE SYSTEM DATA

Ryoudai Nakaso¹, Masahiro Suzuki², Hiroshi Okawa³, Tsuyoshi Kotoura⁴ and Kazuo Kashiya⁵

1) Department of Civil and Environmental Engineering, Chuo University, Tokyo, Japan. Email: a19.pj7j@g.chuo-u.ac.jp

2) Graduate School of Civil, Human, and Environmental Engineering, Chuo University, Tokyo, Japan. Email: a17.6rjs@g.chuo-u.ac.jp

3) Graduate School of Civil, Human, and Environmental Engineering, Chuo University, Tokyo, Japan. Email: ookawa-hi@ej-hds.co.jp

4) Penta-Ocean Construction CO., Tokyo, Japan. Email: tsuyoshi.kotoura@mail.penta-ocean.co.jp

5) Professor, Department of Civil and Environment Engineering, Chuo University, Tokyo, Japan. Email: kaz.90d@g.chuo-u.ac.jp

Abstract: Visualization techniques are increasingly being used in civil engineering. Mixed reality (MR), which allows hands-free visualization with eye contact, is suitable for civil engineering because safety can be ensured during visualization. Location-based methods (as examples of superimposition techniques) in which the accuracy is affected only by location information does not require marker placement so it is suitable for use on construction sites. This paper presents the development of a location-based MR visualization system based on global navigation satellite system (GNSS) data, aiming to support work at construction sites. This system uses GNSS receivers capable of centimeter-level positioning using network real-time kinematic surveying to superimpose accurately and automatically a three-dimensional model onto real space. The visualization position was recalculated every second so that it could be moved. The effectiveness of this system was evaluated by comparing the accuracy of the superimposition of the marker-based method with that of a real, buried underground structure.

Keywords: Mixed reality, Hololens2, Location-based visualization, Global navigation satellite system

1. INTRODUCTION

In recent years, visualization technology has been utilized in various fields, such as entertainment and beauty (Jeong et al., 2021; Valentina et al., 2018). As another example, visualization techniques can be used to confirm the completed form of a building during its construction. A disadvantage of mixed reality (MR) visualization technology (Milgram and Kishino, 1994) is that it requires a dedicated head-mounted device. However, one advantage is that both hands are free during visualization, which ensures safety. Therefore, MR is considered more useful than augmented reality (Caudell & Mizell, 1992), a technology similar to that used at construction sites.

Kawagoe et al. (2022) developed a marker-based MR visualization system. However, this system has limitations, such as the need to place markers onsite accurately and the significant decrease in superimposition accuracy when the moving distance is large. Therefore, we have focused on location-based methods in this study. This method determines the visualization position based on location information; because it eliminates the need to place markers onsite, it is possible to visualize difficult locations, such as the sea, where markers cannot be placed, or at night, during which markers cannot be recognized. Additionally, because the superimposition accuracy depends on the accuracy of the acquired location information, high-precision superimposition is possible using a high-precision global navigation satellite system (GNSS) receiver. The purpose of this study is to develop a location-based MR visualization system using GNSS data; accordingly, this paper presents the system development, angle-correction accuracy verification, and application to virtually buried pipe visualization. The paper is organized as follows. Section 2 describes the development environment, preprocess, and main process, including the accuracy verification of the GNSS receiver used for the MR visualization system. Section 3 presents an evaluation of the relationship between the distance between two receivers and the angle correction accuracy, thus showing how the distance that achieves the highest accuracy in this system is obtained. Section 4 shows the application of the proposed system to virtually buried pipe visualization on campus. Section 5 presents the conclusions of this paper and future tasks.

2. MR VISUALIZATION SYSTEM

A flowchart of this system is shown in Figure 1.

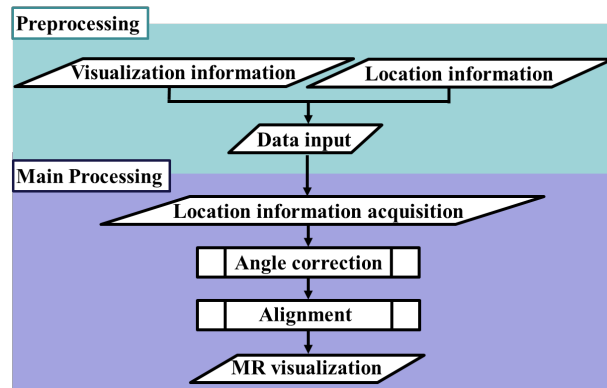


Figure 1. Mixed reality (MR) visualization system flowchart

2.1 Development Environment

We used Unity as the integrated development environment and MRTK as the development kit. We used Hololens2, a head-mounted computer device manufactured by Microsoft (Figure 2). A QZNEO made by the CORE GROUP was the GNSS receiver that was used to obtain location information. The communication protocol used to transmit position information from the GNSS receiver to Hololens2 was UDP, which can communicate with multiple terminals simultaneously and has a higher communication speed than TCP.



Figure 2. Hololens2 and two global navigation satellite system (GNSS) receivers for visualization

2.2 Receiver Position Information Accuracy of GNSS

Table 1 shows the definitions of the reception state of this machine (QZNEO file server 2023). To confirm the position accuracy of the machine, we measured the change in the received position at two points: open- and nonopen-sky environments (Figure 3). In Table 1, the reception state was fixed and floated in open- and nonopen-sky environments, respectively. Hereafter, we use the numerical notations in the table for the reception condition. Figure 4 shows the variation in the position information obtained in each environment. It is shown that the variation range of the position information received every second is several centimeters in the open-sky environment. Specifically, an accurate superposition is possible in an open-sky environment.

Table 1. Definition of each positional accuracy of the GNSS receiver

Number	Positioning state	Estimation accuracy
0	No positioning	—
1	Single positioning	3.0 m
2	Relative positioning	40 cm
5	Float (Preliminary stage of real-time kinematic (RTK) positioning)	20 cm
4	Fixed (RTK positioning completed)	2 cm

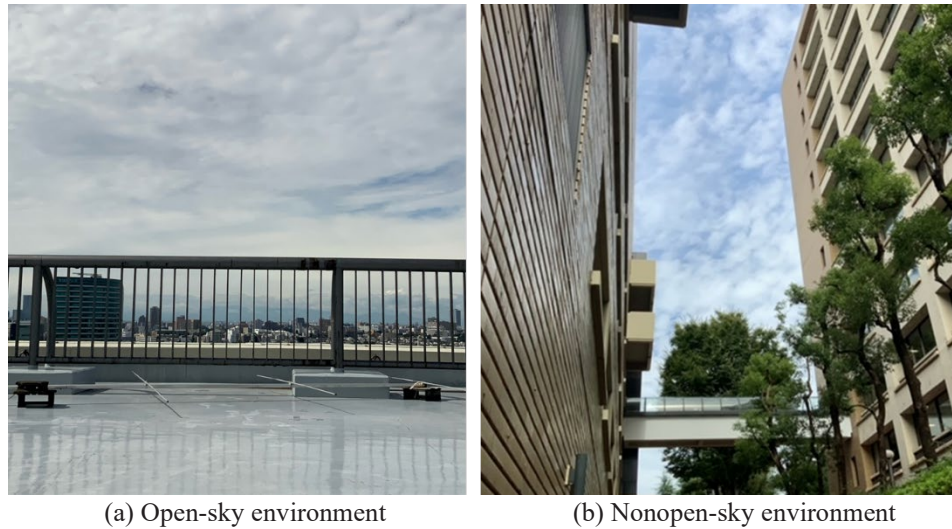


Figure 3. Measurement environment

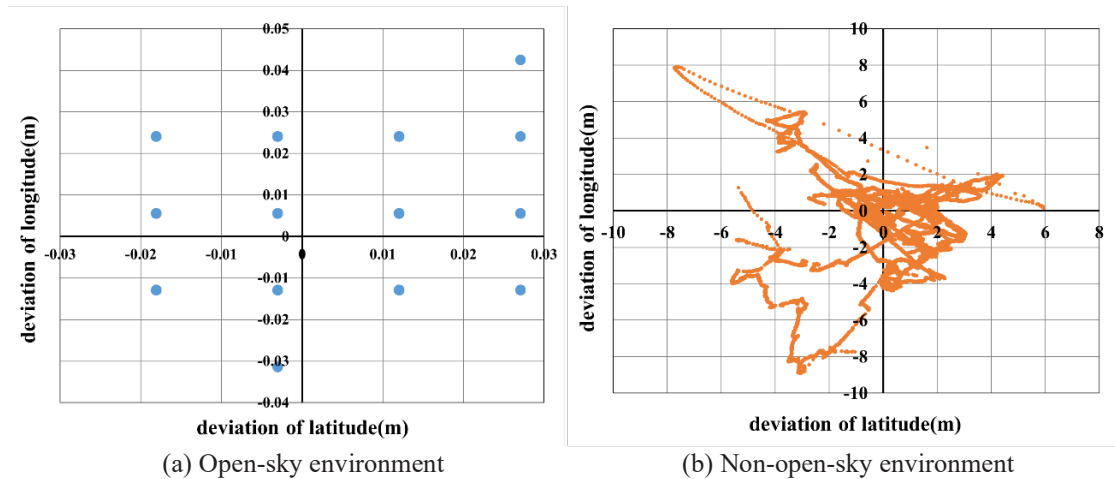


Figure 4. Range of deviation (m) of the positional information of GNSS receiver

2.3 Preprocessing

We input the three-dimensional (3D) data of the model to be visualized as visualization information. As location information, we input the latitude, longitude, and ellipsoidal height of the superimposed position of the model.

2.4 Main Processing

In the initial setup, when the application was launched, a left-handed coordinate system was constructed with the device's position as the origin, vertically upward direction as the positive y-axis, and the device's front direction as the positive z-axis. During positional alignment, this system's north direction is along the positive z-axis, east as the positive x-axis, and vertical as the positive y-axis, using latitude, longitude, and ellipsoidal height for calculations. Therefore, as shown in Figure 4, angle correction was performed to match the north and east directions with the z- and x-axes, respectively. The size of the azimuthal angle in the front direction of the device was calculated from the latitude difference $\Delta z(m)$ and longitude difference $\Delta x(m)$ of the position information acquired by the two GNSS receivers at the application startup. Angle correction was completed by rotating the coordinate system by θ around the y-axis. In the corrected coordinate system, the distance from the device to the superimposed position was calculated by subtracting the superimposed from the device position information and by determining the superimposed position; because the position information was updated every second, it also corresponds to device movement. The average value of the positional information acquired by the two GNSS receivers was used as the device position. For latitude and longitude, degrees were used as units and converted to meters using the circumference formula.

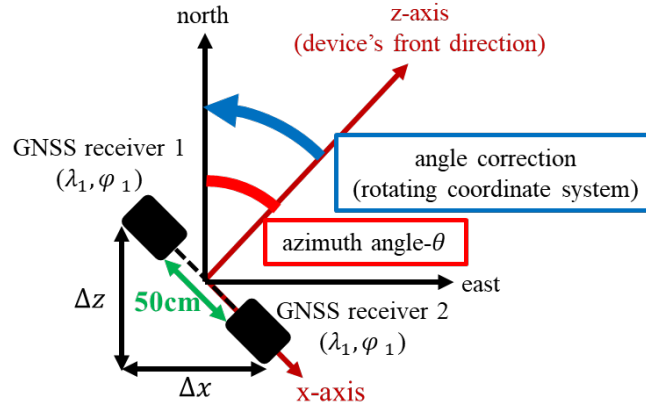


Figure 5. Angle correction method

3. ANGLE CORRECTION ACCURACY VERIFICATION

Because the angle correction is based on position information, its accuracy is affected by the accuracy of the acquired position information. Additionally, the magnitude of the effect of the position information error on the angle correction accuracy varies depending on the distance between the two receivers. Therefore, we evaluated the relationship between the distance between the two receivers and the angle correction accuracy based on verification and adopted the distance that achieved the highest accuracy in this system. For visualization, two GNSS receivers were installed on top of the Hololens2. Therefore, the maximum distance between two GNSS receivers was set to 50 cm.

3.1 Comparison by Measuring the Azimuthal Angle

First, we measured the azimuthal angle for five distances (that ranged from 10 to 50 cm) for approximately 20 min each, and compared and evaluated the accuracy based on the range of deviation. As shown in Figure 6, when the distance between the two receivers was 30 cm or more, the deviation was low and the accuracy was high; conversely, for distances equal to 10 or 20 cm, the range of deviation was large, and the accuracy was low; thus, these distances were not considered in the system.

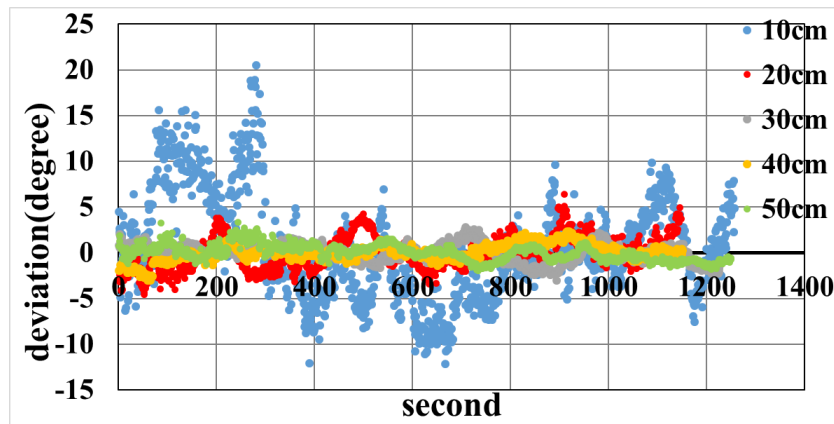


Figure 6. Deviation (°) for distances in the range of 10–50 cm between the two GNSS receivers

3.2 Comparison by Measuring the Azimuthal Angle

We also superimposed the model five times for each distance (for distances that ranged from 30 and 50 cm) and compared and evaluated the accuracy based on the superimposed accuracy of the 3D model after angle correction. The results were assessed visually by taking and synthesizing photographs from the same location. As shown in Figure 7, the superimposed position is on a white line in the depth direction of the image; the angle-correction accuracy improved as the distance between the two receivers increased. Therefore, we adopted a distance of 50 cm between the two receivers.

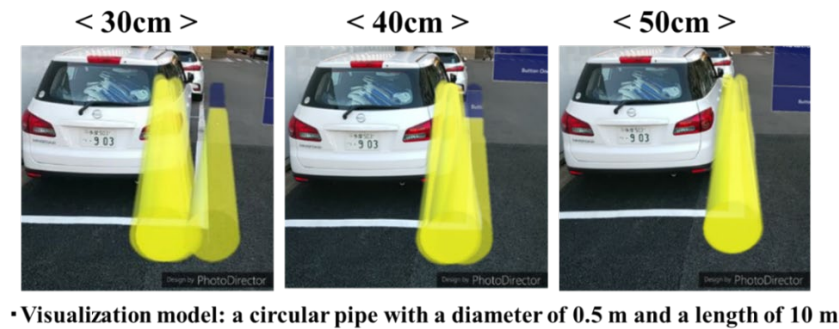


Figure 7. Visualization results

4. APPLICATION TO VIRTUAL BURIED PIPE VISUALIZATION

4.1 Implementation Environment

The implementation environment was around Building No. 1 of the Korakuen campus of Chuo University. For actual visualization in a city, multipath interference may occur because of the arrival delay caused by the reflection of radio waves by surrounding high-rise buildings, thus making accurate positioning difficult; therefore, part of the area with high-rise buildings was adopted, as shown in Figure 8 (Geospatial Information Authority of Japan, 2023). The blue area in the figure represents the highest accuracy defined by the GNSS receiver at 4, whereas the green area represents 5, and the yellow-green area represents intermediate values.

The visualization target was a 3D model of a cylinder with a diameter of 0.5 m and a total length of approximately 250 m modeled after a water pipe. As an evaluation method for the superimposed accuracy, the relationship between the moving distance, position information accuracy, and superimposed accuracy was verified and evaluated by measuring the size of the horizontal superimposed position error at seven points, including points a to f and point a (after one lap). In this application example, the vertical superimposed position was fixed on the ground and only the magnitude of the horizontal error was investigated. Additionally, the usefulness of this system was evaluated by performing a similar visualization using the marker-based method used in previous studies and by comparing it with the superimposed accuracy.

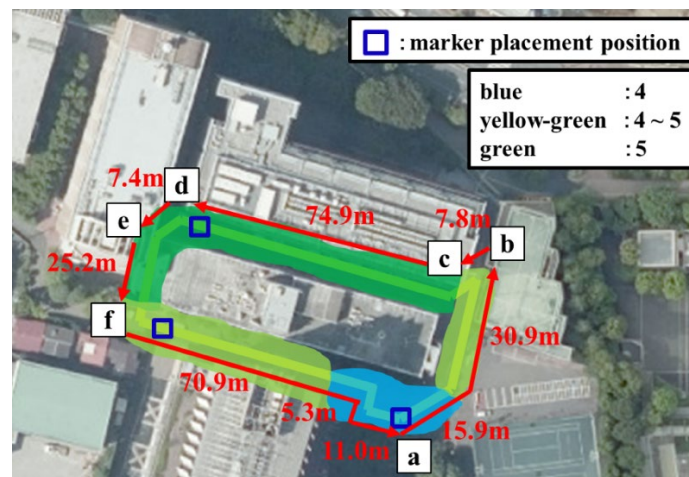


Figure 8. Implementation environment

4.2 Application Outcome

Figure 9 shows the visualization results obtained using our location-based method and the magnitude of the superimposed position error measured with a measuring tape at each point. Figure 10 shows the relationship between the moving distance, position information accuracy, and magnitude of error in the superimposed position at each point and the comparison outcome with the marker-based method. Consequently, the location-based method of our system can maintain high accuracy even if the moving distance is large compared with the marker-based method because the size of the superimposed position error is small even at point a (after one lap). This is because the marker-based method senses device movement by acquiring the surrounding feature points with the camera of the device and adjusting the superimposed position of the model, whereas the location-based method recalculates the superimposed position of the model every second by acquiring the position information of the

device. However, because the size of the superimposed position error is large at points d and e, the superimposed accuracy decreases if the position information accuracy decreases, compared with the marker-based method.

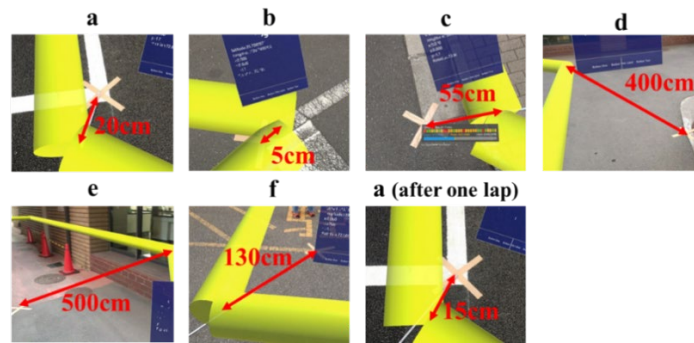


Figure 9. Visualization results and the size of the horizontal superimposed position error

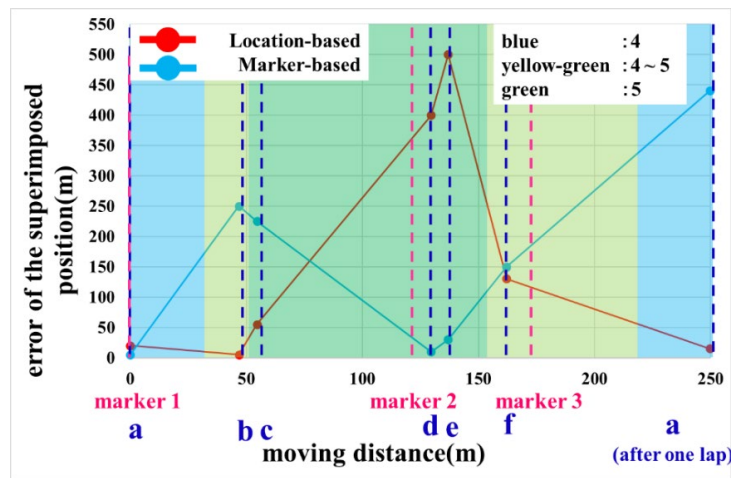


Figure 10. Magnitude of the error of the superimposed position at each tested point

5. CONCLUSIONS

In this study, we aimed to develop a location-based MR visualization system based on GNSS data through system construction, angle correction accuracy verification, and application to virtually buried pipe visualization paradigms; the following conclusions were drawn:

- Longer distance between the two GNSS receivers resulted in a higher accuracy of the angle correction
- The effectiveness of our method was confirmed in an open-sky environment with good GNSS data-reception conditions. However, in a nonopen-sky environment, where the reception condition is poor, the marker-based method was found to be more suitable.

In the future, we plan to apply this system to various visualization targets, including the sea.

REFERENCES

- Caudell, T. P. and Mizell, D. W. (1992). Augmented reality: An application of heads-up display technology to manual manufacturing processes, *IEEE Hawaii International Conference on System Sciences*, 659–669
- Geospatial Information Authority of Japan (2023). Retrieved from Geospatial Information Authority of Japan website: <https://www.gsi.go.jp/>
- Jeong, B. W. and Ji, H. S. and Boreum, C. and Jong, H. L. (2021). The effect of Augmented Reality on purchase intention of beauty products: The roles of consumers' control, *Journal of Business Research*, 133(2), 275-284.
- Kawagoe, T. and Teng, F. and Kashiya, K. and Yoshinaga, T. and Kotoura, T. and Ishida, H. (2022). Development of a visualization system for underground structures using MR Technology, *Japanese Journal of JSCE*, 78 (2), 73–81.
- Milgram, P. and Kishino, F. (1994). A Taxonomy of Mixed Reality Visual Displays, *IEICE Transactions on Information Systems*, 77(12), 1321-1329.

- QZNEO file server (2023). Retrieved from CORE GROUP website: https://www.core.co.jp/service/gnss/qzneo/dl/qzneo_fileserver
- Valentina, N. and Mara, D. and Mary, B. and Nuno, N. (2018). A Mixed Reality neighborhood tour: Understanding visitor experience and perceptions, *Entertainment Computing*, 27, 89-100.

ADVANCED AUGMENTED REALITY OBJECT PLACEMENT IN CONSTRUCTION SITES USING GEOSPATIAL API AND VISUAL POSITIONING SYSTEMS

Haein Jeon¹, Youngsu Yu², Sihyun Kim³, and Bonsang Koo⁴

1) Ph.D. Student, Department of Civil Engineering, Seoul National University of Science and Technology, Seoul, Korea. Email: haeinjeon@seoultech.ac.kr

2) Ph.D. Candidate, Department of Civil Engineering, Seoul National University of Science and Technology, Seoul, Korea. Email: youngsu@seoultech.ac.kr

3) Ph.D. Student, Department of Civil Engineering, Seoul National University of Science and Technology, Seoul, Korea. Email: sihyun@seoultech.ac.kr

4) Ph.D., Prof., Department of Civil Engineering, Seoul National University of Science and Technology, Seoul, Korea. Email: bonsang@seoultech.ac.kr

Abstract: Augmented Reality (AR), used in conjunction with Building Information Modeling (BIM) models, has enabled 3D models and associated information to be used directly on-site. Alignment of AR content is generally achieved using fiducial markers, namely QR codes. However, these markers are not suited for construction sites, as placement needs constant changes and updates with the progress of the project. Recent studies for BIM and AR have also focused on content creation rather than investigating technical advances to improve the practical application of AR use in the field, especially towards placement accuracy and stability. This study explored the use of Geospatial API which places AR content within a 3D map created by integrating the local GPS coordinates of AR devices and the global coordinates attained from Google Street View via a Visual Positioning System (VPS). Experiments on a bridge expansion project identified that additional images must be uploaded onto Google Street View for remote locations. This study determined the optimal conditions for image number, location, and spacing to enhance and secure the performance of Geospatial API in such cases. The results demonstrated that the approach obviated the need to first map a space of interest, previously a prerequisite and time-consuming task for marker-based approaches.

Keywords: Augmented Reality, Building Information Modeling, Geospatial API, Visual Positioning System, Projection Stability, Placement Accuracy

1. INTRODUCTION

Building Information Modeling (BIM), which includes life-cycle information from project design to construction and maintenance, provides an excellent medium for enhancing site management. However, since BIM models are typically viewed on desktop PCs or laptops, direct access to their data has been somewhat limited. As a consequence, their use in the construction stage has been mostly confined to pre-construction services such as 4D simulations and constructability evaluations. Augmented Reality (AR) enables virtual objects and associated data to be overlaid onto real world scenes, allowing for a more intuitive avenue to access the BIM data. Recent studies have confirmed that the application of AR technology on construction sites considerably diminishes the time and effort required to access and manage project data in the field (Chu et al., 2018). Investigations also showed that AR is more effective in recognizing and addressing potential jobsite risks (Huang, 2020; Chai et al., 2019).

However, the rapid and precise overlap between the actual structure of interest and the AR content has remained a challenge. Fiducial markers (e.g., QR code), which are typically used to anchor AR objects onto real world scenes, are not suited for construction sites: constantly changing field conditions and time-consuming marker placement processes make their use cumbersome and impractical.

In this study, Geospatial API, Google's state-of-the-art AR placement method, was proposed to address these issues. The Geospatial API enables the placement of AR content within a single coordinate system by integrating AR and global coordinates via a Visual Positioning System (VPS). Through multiple experiments on a bridge expansion project, this study explored the feasibility and challenges of this technology for enhancing the placement stability and accuracy of projections on construction sites. Because bridge projects are often located in remote areas, additional images had to be uploaded onto Google Street View for Geospatial API to work correctly. This study identified the optimal image number, location, and spacing conditions for enhancing and securing the performance of Geospatial API in such cases.

2. RESEARCH BACKGROUND

2.1 AR Applications in the Construction Industry

AR has been evaluated as a means to enhance the productivity of the construction industry by allowing the virtual overlay of 3D models on actual structures and by readily providing relevant project management data on-site. Research and technological development related to AR, used in conjunction with BIM data, have been

carried out in the areas of safety, quality, and process management.

Park & Kim (2013) proposed a new Safety Management and Visualization System (SMVS), which integrates BIM, location tracking, and AR to identify safety risks in construction sites and improve workers' hazard perception ability. Kim et al. (2017) developed a system that utilizes wearable devices to provide workers with AR-based risk information within the site to prevent safety accidents in advance.

Mirshokraei et al. (2019) proposed a web-based quality management system that combines BIM and AR, allowing real-time quality assessment and data management from a single mobile device on construction sites. Hyundai E&C (2020) also developed a quality management platform that visualizes BIM data on-site through AR devices to allow better intuition of the work environment.

AR has also been leveraged to monitor and manage on-site progress. Kim et al. (2018) proposed a way to integrate 4D CAD models with AR to visualize construction sequences directly in the field. KICT (2020) developed an AR-based process management system that employs BIM drawings with linked process information for remote construction site monitoring.

Despite these studies, AR has seen limited adoption in practice. One of its restrictions stems from the difficulty in aligning and maintaining the stability of the AR objects to specific locations in the field. Current methods for the alignment of the objects make it cumbersome and also suffer from misplacements. This study focused on exploring a novel technique for model projections, i.e., Google's Geospatial API, and investigating specific measures required to ensure projection accuracy and stability.

2.2 AR Projection Method Overview

AR projection methods are mainly divided into three types: 1) marker-based, 2) markerless-based, and 3) projector-based approaches (Marner et al., 2014; Cheng & Chen, 2017). Marker-based approaches are one of the most common, utilizing physical markers such as QR codes as the anchor point for model projections. While this method provides stable and accurate projections, it has the disadvantage of requiring multiple physical markers to be installed at predefined locations. Secondly, markerless methods generate projections by tracking the features of local objects in real world scenes and/or by utilizing GPS coordinates, negating the need for separate markers. However, it frequently suffers from misalignments and misplacements of its projections. Finally, projector-based approaches use proprietary projectors that track, calibrate, and adjust the content to synchronize with physical surfaces such as walls, tables, or even people. The method is mainly used on large installations such as museum exhibitions and advertising campaigns. While this method ensures accuracy, it is presumed unsuitable for use at construction sites as it requires a separate projector and exhibits poor visibility in areas of high illumination.

The Geospatial API employed in this study is a type of markerless approach. It obviates the need for physical markers by incorporating a novel coordinate placement technique called the 'Visual Positioning System' (VPS). VPS utilizes computer vision algorithms to analyze images from a device's camera to create a 3D map, and then identifies the user's location and orientation. This is achieved by one or more of the following methods employed in VPS (Jeong&Jeong, 2021):

- Structure-based localization: this method estimates location by generating a 3D structure of the physical environment. The approach entails comparing and matching the device's 2D camera images with a 3D model derived from point cloud data, enabling the precise determination of the user's location.
- Image-based localization: this method estimates location using visual features of images. The approach entails matching images from the device's camera with those archived in large-scale databases, which could be derived from big data-enabled social networks or street view, enabling the precise determination of the user's location.
- Learning-based localization: location is estimated from images using deep learning algorithms. This approach entails training the algorithms on a substantial amount of image data, which then form the basis for analyzing images captured by the device's camera, enabling precise user location determination.

It is worth noting that VPS are distinguished from Visual Place Recognition (VPR) systems, which are principally concerned with identifying a specific place and distinguishing it from others, and thereby facilitating self-localization. VPR is predominantly utilized in robotic systems, and autonomous driving systems, etc. In contrast, VPS places significant emphasis on tracking the user's location and orientation in real-time based on images and is mainly used in AR applications and indoor navigation systems.

In the implementation of VPS, the three methods above can either be employed concurrently or selectively, depending on the specific situation at hand. Although the precise selection among the three methods utilized by VPS in the Geospatial API has not been publicly disclosed, it has been ascertained that the system leans on image-based localization methods. The subsequent section elaborates on how Geospatial API operates in conjunction with VPS.

2.3 Geospatial API With VPS

Geospatial API is a part of Google's ARCore, an SDK for developing AR applications. Geospatial API combines the local GPS coordinates of AR devices and the global coordinates attained from Google Maps to determine an accurate single coordinate for content placement. The technique, referred to as 'Global localization,' in effect allows 'cloud anchors' to be generated at a global scale, which previously could only work in local, indoor environments (Figure 1). More specifically, the technique is executed using the following steps:

- First, Geospatial API utilizes VPS to identify the location and orientation of the AR device via images from its camera. VPS uses computer vision algorithms to analyze real-world images from the camera of the AR device to create a 3D map of the surroundings. This map consists of a single coordinate system created by extracting and mapping point cloud data from the device's camera view with those stored in Google Street View images. The device's camera view includes the user's location information, which is determined based on the local GPS coordinates of the device, while the Google Street View image data contains Google Earth's geographic coordinates, i.e., the information of real-world locations. Using the map created in this manner, the surrounding environment is analyzed, and the precise placement of AR objects in physical space is achieved by determining the device's position and orientation in real-time.
- Secondly, the specific latitude, longitude, and altitude of the generated single coordinate system are designated as anchors for the AR object. Anchors refer to a point or coordinates used to fix an AR object at a specific location in the real world to ensure its consistent placement. Through this process, the AR object is projected at the designated coordinate. Geospatial API tracks real-time changes in the user's location and direction while the AR device moves so that the AR object can be fixed to the pre-designated location.

The VPS relies on images in the Google Street View database to locate its coordinates, and therefore having multiple images of the real world subject, and its nearby surroundings is a prerequisite for Geospatial API to operate correctly. Consequently, VPS works well in urban areas where Google Street View contains abundant images of the location of interest. However, this is often not the case in remotely located construction sites.

In such cases, new images need to be taken of the location of interest and loaded onto Google Street View. A goal of this study was then to specifically determine the number, spacing, and location of the images required to get the required placement accuracy.

The performance indicators of the Geospatial API include 'Horizontal Accuracy (HA)', 'Vertical Accuracy (VA)', and 'Heading Accuracy (HDA)'. These represent the range of error in the 'latitude and longitude, altitude, and bearing angle', respectively, as perceived by the device relative to the current location, with smaller values indicating a more precise coordinate (ARCore, 2023). Through several validations, it was observed that a small value of HDA correlates with small values of VA and HA simultaneously. Considering that the VA and HA fall within a one-meter range when HDA is less than 10 degrees, this HDA value was deemed appropriate and was used as the target value in our study.

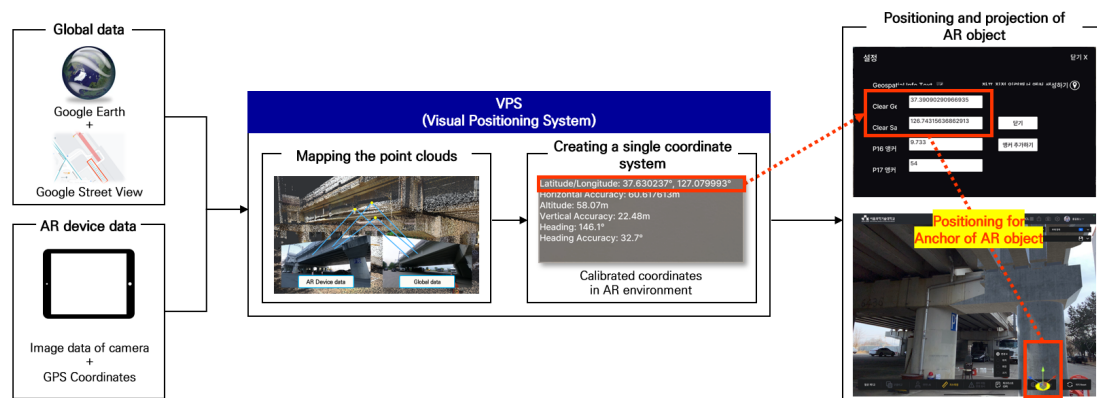


Figure 1. Geospatial API -based AR object projection process

3. AR SYSTEM USING GEOSPATIAL API FOR SITE MANAGEMENT

3.1 System Development and Overview

To apply Geospatial API on the construction site, a BIM-based AR system, termed AROS¹, was developed and optimized for use with Apple's iPad Pro². The system was developed using Unity3D, which converts BIM models to 3D meshes that can be visualized in AR devices. Apple's AR Kit was used as the SDK to develop the

¹ Augmented Reality On-Site (AROS)

² Specs of iPad Pro: Wi-Fi version, A12Z Bionic chip, 12.9-inch

user interface. Geospatial API was subsequently mounted as the model anchoring and projection method, which was also implemented in Unity 3D.

AROS was developed with the goal of providing the information needed for safety and quality inspections for infrastructure projects. AROS provides AR objects and inspection checklists on the screen and also allows measurements and on-site images to be taken and stored. These functions enable site personnel to perform inspection tasks as well as save the inspection results.



Figure 2. UI for AROS, the BIM-based AR system

3.2 Initial Testing of Geospatial-based AR System

For Geospatial API to be effective, the projected models need to be correctly placed even when users move through a site and also exhibit minimal projection errors between the actual structure and the model.

A railway bridge project, (Wolgot-Pangyo line, Korea) which involved expanding its lanes, was selected as an initial test subject. The section of the railway bridge used had a span of 71.64 meters and consisted of 12 piles, two piers, two copings, nine girders, and five slabs. AROS, mounted with Geospatial API, was used to place a virtual model of the expansion portion of the bridge adjacent to the existing structure.

Figure 3(a) shows the correct placement of the AR object in relation to the existing structure. However, as shown in Figure 3(b), the projection was way off the mark. Multiple tests recorded HDA measurements above 40 degrees, much higher than the 10 degrees limit. The tests also showed that the placements were unstable when the AR device was moved to different locations.

The problem lay primarily in the insufficient number of images stored in Google Street View, which was attributed to the site's remote location. Unfortunately, Geospatial API does not document the number of images required nor the appropriate locations and spacing needed. Thus, these values needed to be attained through a trial and error process.

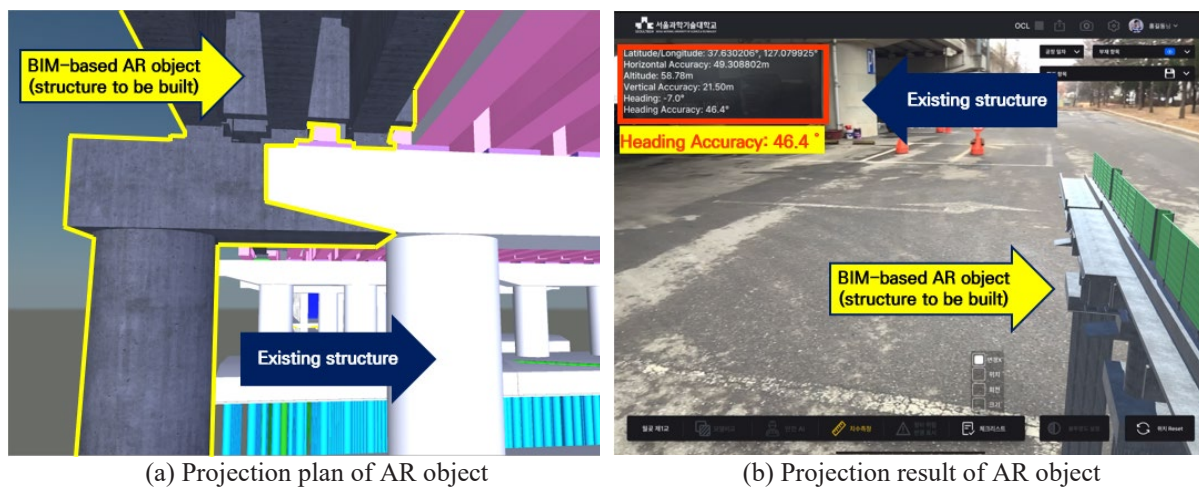


Figure 3. Plan and result of Geospatial API-based AR object projection





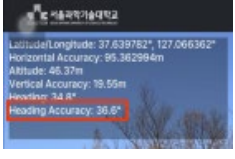
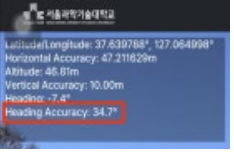






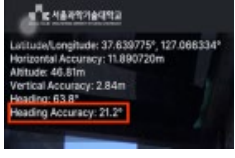
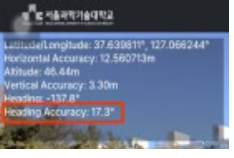
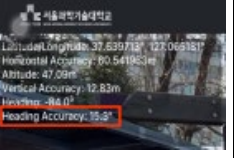
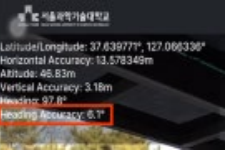
4. IMPROVEMENT OF PROJECTION STABILITY AND PLACEMENT ACCURACY

4.1. Experiments for Attaining the Optimal Image Number, Location, and Spacing

To deduce the optimal number, location, and spacing of images, an experiment was conducted in which the number of registered images was increased consecutively with equal spacing and measuring the HDA at each increment. A series of locations were preselected from which the images would be taken. The selected locations did not have images registered on Google Street View.

An open area measuring $629.2m^2$ was selected as a test site. The size of the area was used as it would approximate the size of a single bridge span. Two images at specific points at regular intervals of five meters spacing in a grid formation were taken, loaded onto Google Street View, and subsequently measured for their HDA Table 1 shows the rounds of tests performed and the average HDA for each round, with a red dot indicating the data registration point. Results showed that at least 15 street view images were needed for the HDA to measure less than the minimum requirement of 10 degrees. As shown in the table, the actual had for this round measured at 6.1 degrees.

Table 1. Test results for deriving an appropriate number of registered image data

Validation round	1	2	3	4
Number of image data registrations				
	No. of image: 1	No. of image: 3	No. of image: 5	No. of image: 7
Average of heading accuracy				
	36.6°	34.7°	33.2°	25.1°
Conformity to the accuracy range	X	X	X	X
Validation round	5	6	7	8
Number of image data registrations				
	No. of image: 9	No. of image: 11	No. of image: 13	No. of image: 15
Average of heading accuracy				
	21.2°	17.3°	10°~15.3°	6.1°
Conformity to the accuracy range	X	X	X	X

4.2. Validation of Projection Performance Improvement

For the railway bridge, a total of 28 images at five meters intervals were taken in a similar grid pattern and subsequently registered on Google Street View. HDA measurements ranged between one and four degrees. Tests on site also confirmed that the projections maintained its correct position even when the user moved to different locations underneath and around the bridge structure. However, as shown in Figure 4(a), projection errors ranging from a minimum of one to a maximum of two meters still persisted.

The misplacement was found to be due to the errors in GPS coordinates provided by the iPad Pro used as the AR device. Because the version of the iPad Pro deployed did not have its own GPS tracking chip, it used Wi-Fi signals to provide approximated GPS coordinates. These approximations caused errors in the coordinates ranging between ± 10 meters. This issue was resolve simply by upgrading the hardware. Specifically, a cellular

model of iPad Pro³, which was equipped with its own GPS tracker, was used to test the placement accuracy once more. The results showed that this time around, the HDA was within three degrees, with an error range of less than one meter (Figure 4(b)).

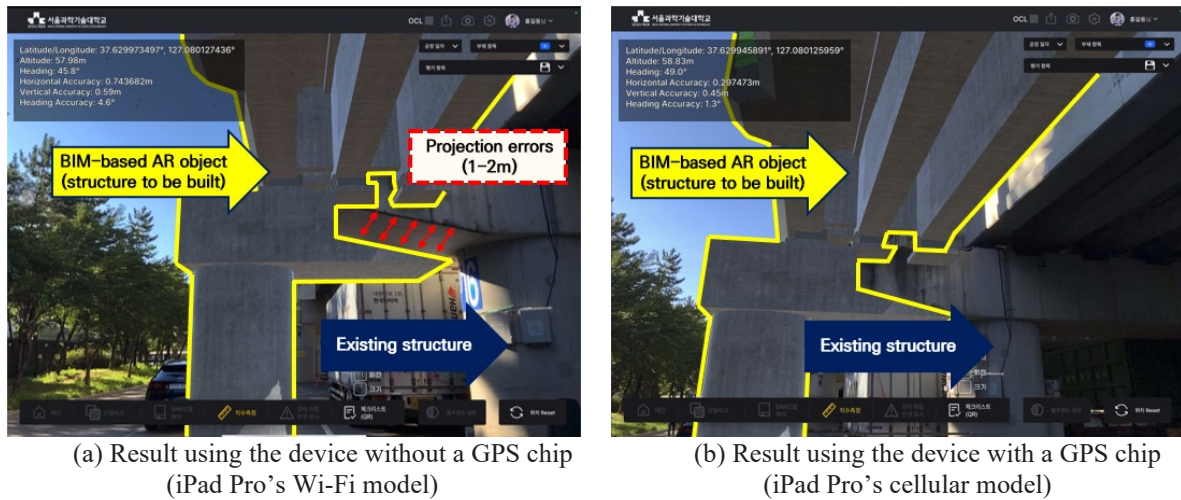


Figure 4. Result of placement accuracy improvement on site

5. CONCLUSIONS

This study explored the applicability of Geospatial API, a state-of-the-art AR markerless projection method for use on construction sites. The markerless approach had the advantage of obviating the need for fiducial markers, which originally made it cumbersome and impractical to use AR devices in the field.

The initial validation of Geospatial API in a bridge construction site revealed that the lack of images of the target location resulted in severe deterioration of projection accuracy and stability. This issue arose from the Geospatial API's reliance on using VPS via Google Street View. Experiments were conducted to determine the minimal number, optimal location, and spacing of images needed to reduce HDA to within 10 degrees. Repetitive tests on an open area showed that at least 15 images taken at five meters intervals in a grid pattern were needed to satisfy the requirement.

For the bridge, 28 images using the same grid formation were taken and uploaded to Google Street View. Subsequent projections demonstrated that placement stability was obtained at multiple perspectives around the bridge structure. However, the projections still revealed offset errors to the actual structure ranging between one and two meters. The issue was identified as miscalculations encountered in the GPS coordinates within the AR device. This was identified as a hardware problem, which was easily solved by upgrading the AR device with its own GPS and processor. Follow up tests revealed projection errors reduced to less than one meter, with HDA values also a complaint three degrees.

The experiments provide an initial validation and applicability of incorporating a Geospatial API-based AR projection approach for construction sites. The study contributes specifically by identifying the number and structural disposition of the images needed for obtaining placement stability using the novel technology. The study also revealed the need for higher performing GPS hardware to minimize placement errors.

Although Geospatial API requires these additional steps, its advantage in obviating the need for marker-based approaches has the potential to make it convenient and easy to use AR technologies in the construction domain. In this regard, our study contributes to the advancement of AR in the construction industry by formalizing the adoption of a novel markerless method for on-site project management.

Future work includes using video images and loading it to Google Street View in lieu of individual images. This method was recently opened by Google and should allow much larger amounts of image data points to be utilized by Geospatial API. Application of the technique also needs to be implemented for other infrastructure such as roads or tunnels, where distinct structural features may be less defined compared to bridges.

ACKNOWLEDGMENTS

This research was supported by the Korea Agency for Infrastructure Technology Advancement (KAIA) (grant no. RS-2020-KA158185, Fourth year of the third phase).

³ Spec of iPad Pro's cellular model: Cellular version, A12Z Bionic chip, 12.9-inch, Built-in GPS/GNSS

REFERENCES

- ARCore. (2023). *Google.XR.ARCoreExtensions.GeospatialPose*. Retrieved from ARCore website: <https://developers.google.com/ar/reference/unity-arf/struct/Google.XR.ARCoreExtensions.GeospatialPose>
- Chai, C., Mustafa, K., Kuppusamy, S., Yusof, A., Lim, C. S., and Wai, S. H. (2019). BIM integration in augmented reality model, *International Journal of Technology*, 10 (7), 1266-1275.
- Cheng, J. C., Chen, K., and Chen, W. (2017). Comparison of marker-based AR and markerless AR: A case study on indoor decoration system, In *Lean and Computing in Construction Congress (LC3)*, *Proceedings of the Joint Conference on Computing in Construction (JC3)*, 2, 483-490.
- Chu, M., Matthews, J., and Love, P. E. (2018). Integrating mobile building information modelling and augmented reality systems: an experimental study, *Automation in Construction*, 85, 305-316.
- Huang, Z. (2020). Application research on BIM+AR technology in construction safety management, *Journal of physics, conference series*, 1648 (4), 1-5.
- Hyundai E&C. (2020). *Hyundai E&C seeks quality innovation with Augmented Reality (AR) technology*, Retrieved from Hyundai Engineering & Construction website: https://www.hdec.kr/en/company/press_view.aspx?CompanyPressSeq=52#YopLJXZByUk.
- Jeong, T., & Jeong, G. (2021). Deep learning-based Visual Positioning System (VPS) for AR navigation, *Broadcasting and Media Magazine*, 26(2), 67-72.
- KICT. (2020). Development of Virtualization and Simulation Technology for smart Construction Based on VR/AR, 19.
- Kim, H. (2018). Status and Prospects about VR/AR Industry, National IT Industry Promotion Agency (nipa), 44, 2-12.
- Kim, H., Kim, K., Bormann, A., and Kang, L. (2018). Improvement of realism of 4D objects using augmented reality objects and actual images of a construction site, *KSCE Journal of Civil Engineering*, 22 (8), 2735-2746.
- Kim, K. N., Kim, H. J. and Kim, H. K. (2017). Image-based construction hazard avoidance system using augmented reality in wearable device, *Automation in Construction*, 83, 390-403.
- Marnier, M. R., Smith, R. T., Walsh, J. A., and Thomas, B. H. (2014). Spatial user interfaces for large-scale projector-based augmented reality, *IEEE computer graphics and applications*, 34 (6), 74-82.
- Mirshokraei, M., De Gaetani, C. I., and Migliaccio, F. (2019). A web-based BIM-AR quality management system for structural elements, *Applied Sciences*, 9 (19), 3984.
- Park, C., and Kim, H. (2013). A framework for construction safety management and visualization system, *Automation in Construction*, 33, 95-103.

AUTOMATED DIMENSIONAL CHECKING IN MIXED REALITY FOR STAIRCASE FLIGHT

Michelle Siu Zhi Lee¹, Nobuyoshi Yabuki², and Tomohiro Fukuda³

1) Ph.D. Candidate, Division of Sustainable Energy and Environmental Engineering, Graduate School of Engineering, Osaka University, Osaka, Japan. Email: u521745c@ecs.osaka-u.ac.jp

2) Ph.D., Prof., Division of Sustainable Energy and Environmental Engineering, Graduate School of Engineering, Osaka University, Osaka, Japan. Email: yabuki@see.eng.osaka-u.ac.jp

3) Ph.D., Assoc. Prof., Division of Sustainable Energy and Environmental Engineering, Graduate School of Engineering, Osaka University, Osaka, Japan. Email: fukuda.tomohiro.see.eng@osaka-u.ac.jp

Abstract: Building inspections have always been required to serve as a quality check to ensure that constructed building elements comply with national and local standards. Some of these checks involve dimensional checks such as checking for minimum headroom or clear widths. These checks are often done as spot checks using a tape measure. The efficiency of such checks could potentially be improved with new technology such as the use of Mixed Reality (MR) solutions that have in-built native sensors. Current and previous research for MR in the construction industry involves using MR for visualizing designs, facilitating information transfer in construction management, training construction workers, or operations and maintenance purposes. The objective of this research is to identify the accuracy of automatically computed dimensional checks in MR against dimensions measured from generated meshes, against ground truth. The results computed by the MR application are compared with dimensions measured from the exported mesh object in Computer-aided Design (CAD) to determine the accuracy of the MR-generated dimensions. Preliminary results show that MR-generated dimensions are generally accurate in conditions where meshes have sufficient coverage, but are not accurate when identified surfaces are too small to generate proper meshes. Future research includes ways to improve the accuracy of dimensional checks for smaller surfaces.

Keywords: Wearable technology, Mixed reality, Smart inspection, Digital inspection, Construction inspection

1. INTRODUCTION

Building inspections are always done after a building is constructed to ensure contractors have constructed buildings according to national or local standards. These inspections involve checks such as dimensional clearances, verticality checks, flatness checks, etc., to ensure buildings are safe and serviceable for the general public (Fakunle et al, 2020). Inspection checks are usually done by multiple experts visually, with the help of measuring tools, which can lead to inconsistencies due to the heavy reliance on the human factor (Prieto et al, 2021). With investments in construction technology increasing over the years (Bartlett et al, 2020), technology could potentially be used to improve the accuracy and efficiency of inspections. A state-of-the-art review on Mixed-Reality (MR) applications in the Architecture, Engineering, Construction, and Operations (AECO) industry found that 49% of such research focused on applications in the construction phase including using MR for site monitoring and inspections; for construction simulations; as a training tool for assembly; or for improving construction safety (Cheng et al, 2020). The studies cited in the review relating to inspections generally require a Building Information Model (BIM) for comparison of design BIM with real-world data (Kwon et al, 2014; Nguyen et al, 2021; Zhou et al, 2017). However, BIM might not always be available for every construction project, and checking against design BIM assumes that the design BIM already complies with building code standards.

Koshelham et al (2021) reported that headsets with mapping capabilities had significantly higher efficiency and flexibility to map indoor environments compared to laser scanning technologies, and that centimeter accuracy can be achieved while experimenting using the Microsoft HoloLens. However, since then, newer eyewear with improved sensors and processors have been released in the market that could potentially achieve better accuracy. In this study, the use of an MR head-mounted device (HMD) with edge computing is proposed to automatically compute dimensions for building staircase components that can be checked against building codes. Staircase components were selected due to the complexity of the required dimensional checks such as riser height, tread depth, staircase width and headroom, as opposed to general clear corridor widths, or ceiling height clearances. The computed dimensions are compared against raw data exported from the MR HMD and actual site-measured data to evaluate the accuracy of the results, then to determine the potential for on-site implementation of MR building dimensional checks against building code compliances.

2. METHODOLOGY

The overall flow of the analysis is shown in Figure 1. Manual measurements using common construction measurement tools will first be done to obtain control dimensions. For edge computing to be possible, an untethered MR HMD compatible application will be developed where its function will be to analyze sensor data collected by the MR HMD, and display data according to user's requirements. The application will perform an

algorithm to identify staircase features and calculate feature dimensions, referred to as MR-computed dimensions, from the captured data for compliance checks. Subsequently, the data collected is then exported for manual processing to validate the dimensions computed by the MR application. Both MR and post-processed dimensions will be compared against the control dimensions to determine the accuracy of the computed results against measured results.

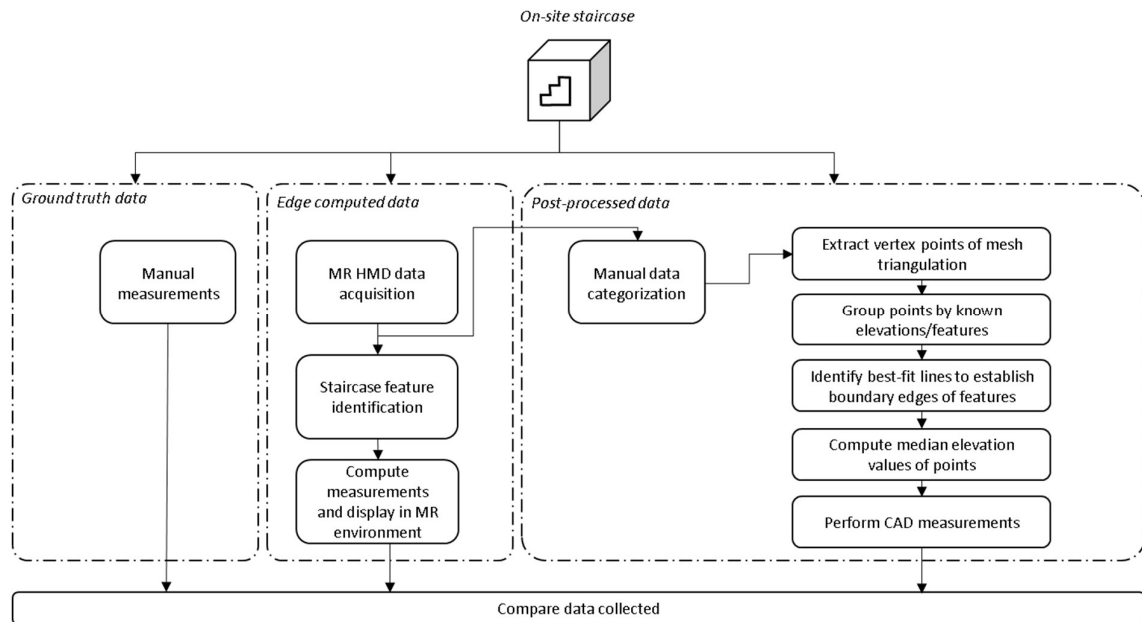


Figure 1. Overall research methodology

2.1 Defining Staircase Components

Each staircase component to be measured is shown in Figure 2.

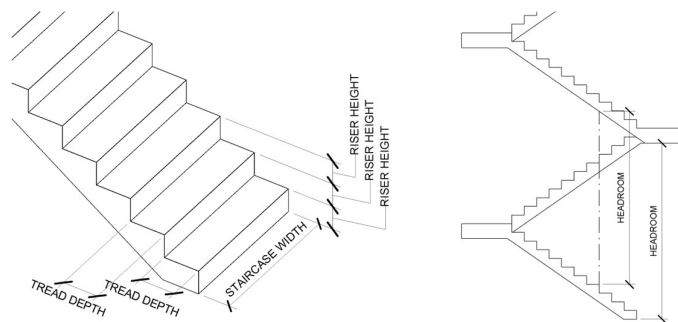


Figure 2. Staircase components to be measured

2.2 Manual Measurements

The measuring tools used to obtain the control measurements consist of a metal 5-meter tape measure and a laser measure. The tape measure is used when measuring shorter lengths such as the riser height, tread depth and tread width, while the laser measure is used for measuring longer lengths, such as headroom.

Measurements will be taken at the left, center and right edges of each tread for riser height, tread depth and headroom, to account for minor variations in workmanship. The average value is then used as the baseline value. However, due to the small surface of each tread depth-wise, only a single value will be taken for staircase width.

2.3 MR Application Computed Measurements

An MR device that has native sensors and edge computing capabilities is required for this research

application. A software application will then be developed to read the data gathered from the native sensors, understand the scene, and compute the data to give dimensions of the various staircase components. The results obtained from the MR application will be used for compliance checks.

2.4 Post-processed Data for CAD Measurements

The gathered data from the MR device's sensors is exported for further processing by extracting vertex points of the mesh. Points are visually grouped into categories such as wall, ceiling, landing, and treads, with the latter further subcategorized by elevation values for riser height computation. Subsequently, best-fit lines or median values are used to demarcate virtual boundaries of the tread surfaces and staircase soffit surfaces. The computed dimensions are then measured in CAD.

2.4 Evaluating Measurements

International Organization for Standardization (ISO) standards define accuracy as the closeness of agreement between a test result and the accepted reference value; and trueness as the closeness of agreement between the average value obtained from a large series of test results and an accepted reference value (ISO, 1994). The results from the manual method of measurement, which is the current commonly used method in the industry, will be taken as the reference value for evaluating the accuracy and trueness of the results obtained from the MR method and CAD method.

3. APPLICATION AND RESULTS

3.1 MR HMD and MR Application

An application was developed in Unity for the Microsoft Hololens 2 using the Microsoft Mixed Reality Toolkit (MRTK) and the Scene Understanding Software Development Kit (SDK). A summary of the technical specification of the Hololens 2 is presented in Table 1 for reference, and a high-level overview of the software architecture is presented in Figure 3. The Scene Understanding SDK acts as a communication layer between the application and the Scene Understanding runtime, generating meshes that classifies real world surfaces into components (Scene Understanding SDK overview, 2022).

Table 1. Hololens 2 Technical Specification¹

Component	Specification
Processor	Second-generation Microsoft custom-built holographic processing unit
System on chip	Qualcomm Snapdragon 850 Compute Platform
Operating System	Windows Holographic OS
Memory	4GB LPDDR4x system DRAM
Storage	64GB UFS 2.1
Display	See-through holographic waveguide lenses at 2k resolution
Sensors	4 visible light cameras for head tracking 2 infrared cameras for eye tracking 1MP Time-of-Flight depth sensor 8MP RGB Camera, 1080p 30fps video capability
Connectivity	Wi-Fi, Bluetooth 5.0, USB-C
Weight	566 grams
Battery Life	2-3 hours of active use

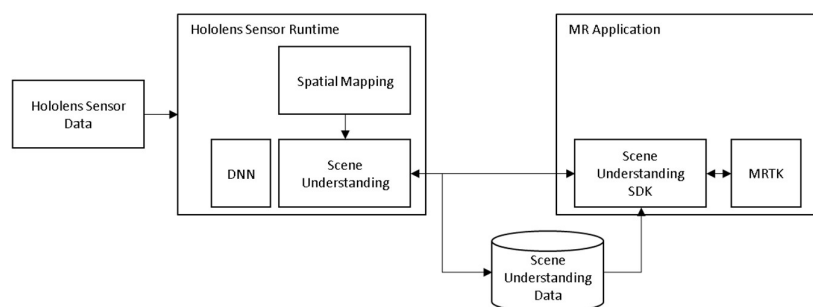


Figure 3. MR Application Architecture Overview²

¹ *About Hololens 2*. March 13, 2023. Retrieved from <https://learn.microsoft.com/en-us/hololens/hololens2-hardware> on May 06, 2023.

² Adapted from S. Stachniak, Microsoft. (2020, June 9). *Digitizing the physical world: An intro to Mixed Reality*

3.1.1 Automated Calculation using Sensor Data

The Scene Understanding SDK generates SceneObjects, made up of Quads that represent real world surfaces (Scene Understanding SDK overview, 2022). The software queries the position of each Quad, sorts them into lists, then calculates the distance between the positions of each Quad to obtain riser heights. The extents of each Quad are also queried to report the length and width distances. Since staircase soffits are typically sloping surfaces, Raycast (Physics.Raycast, 2023) is used so that it can report the distance between the origin and the point it intersects with a ceiling surface to give the headroom value. Objects are then spawned for visualization of these dimensions as shown in Figure 4. The staircase used in the experiment, as well as the mesh generated from Hololens 2 is shown in Figure 5.

A manual point-to-point measurement was also built into the application for cases where dimensions could not be automatically computed.

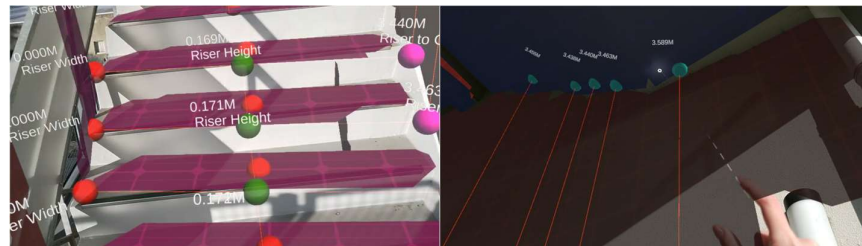


Figure 4. Riser Height and Staircase Width Dimensions (left) and Headroom Dimensions (right) generated in MR

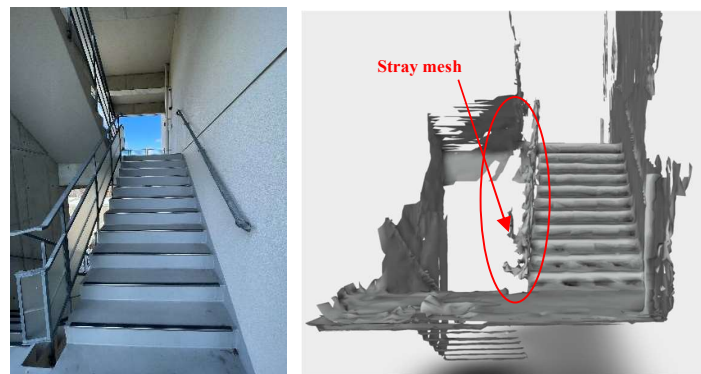


Figure 5. Staircase flight at Osaka University (left) and generated mesh from Hololens 2 (right)

3.2 CAD Measurement

The mesh generated by the Hololens 2 was exported as a .obj file and Rhino software was used to extract the vertices of the mesh triangulation into a points file in .csv format. The points were then imported into Civil 3D, rotated to match the axes as shown in Figure 6. Stray points occurred mostly on the left edge of the tread, where there is a void between the railing and the floor. The scene understanding runtime attempted to close up the mesh, resulting in these stray points beyond the railing as seen in Figure 5.

In Figure 6, points belonging to the wall are presented in pink and the representative reference is obtained by computing the best-fit line along the wall points. The handrail on the right side of the flight, and railing on the left side of the flight is represented in purple. It is known that the staircase width is 1.385m from manual measurement, and a line is offset to represent the leftmost edge of the staircase. Due to the stray points, utilizing a best-fit line on the left edge of the staircase flight will not produce relevant results. Hence, in this experiment, staircase width was unable to be determined.

In Figure 6, treads were presented in alternating green and blue colors, landings in orange, and other points in red. Points were initially categorized using a search criterion of +/- 20mm from the reference elevation. Subsequently, tread edge best-fit lines were computed using the outermost points that satisfy this search criterion. Left, middle and right dimensions are measured in CAD, and averaged to obtain the tread depth for comparison. Subsequently, points within the boundaries of these best-fit lines, regardless of the initial +/-20mm criterion were

Scene Understanding [Video]. Microsoft. <https://learn.microsoft.com/en-us/shows/mixed-reality/digitizing-the-physical-world-an-intro-to-mixed-reality-scene-understanding>

added to their respective riser group of points. Each group is further subdivided into 3 regions – left, center and right equally along the staircase width for further analysis to determine if the stray mesh affects the results. Riser heights were computed taking the median of each sub-group's point elevation. Using the coordinates of each tread edge point at left, center, right, into the equation of the best fit line, the headroom elevation is computed, and subtracting the riser elevation would give the headroom value at each staircase region.

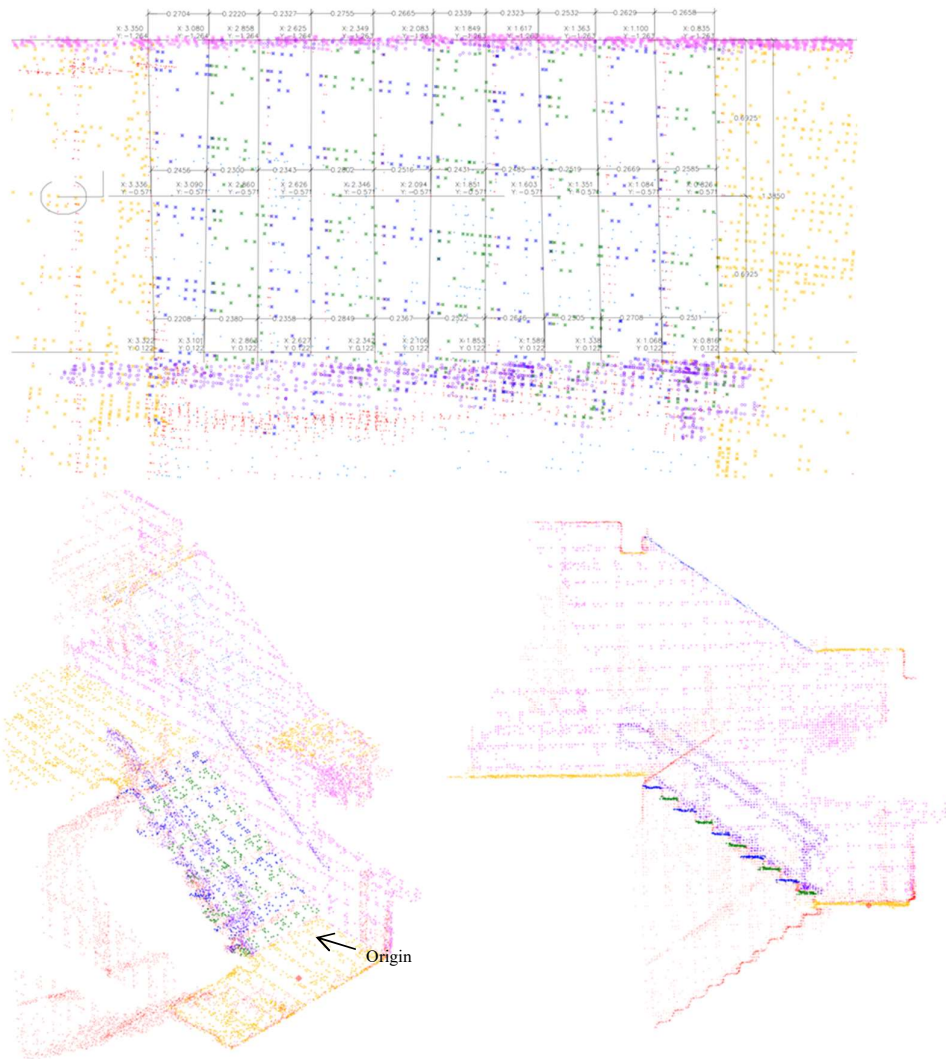


Figure 6. Categorized points extracted from Hololens 2 mesh – plan view, isometric view (bottom left), elevation view (bottom right)

3.2 Measurement Results

The percentage error comparison for tread depth, riser height and headroom measurements between the MR application computed dimensions and the CAD measurements against the reference measured dimensions are presented in Figure 8, Figure 9 and Figure 10 respectively. As shown in Figure 4, the MR application was unable to compute the staircase width or tread depth automatically, reporting a 0.000m width. Manual measurement in the application relies on the user placing 2 points, which are represented as spheres on the meshes that were generated. Obtaining tread depth measurements by pointing right at the edge of each mesh to obtain MR manual measurement was not feasible, and hence was not computed.

4. DISCUSSION

4.1 Accuracy of Vertical Measurements - Riser Height & Headroom

The results presented in Figure 9 show that the MR measurements generated for riser heights vary between -2.9% to a maximum of 3.4% when comparing riser height values. This corresponds to a value of 5-6mm difference with the reference value of 177mm. While regulatory code allows for riser heights up to a maximum of 180mm

(Hasegawa, n.d), the results suggest that due to the error generated by the MR application, should the MR app be used for compliance checks, there might be instances where the MR application will report a non-compliance case. Table 2 presents the instances of non-compliance readings as compared with the readings taken using traditional methods. Figure 9 also shows that the trueness of the computed measurements is better than the results obtained from CAD measurements. Such inaccuracies may be attributed to the subjective nature of inspections where Phares et al (2004) established that there is significant variability in reporting the condition state of a bridge inspection. Similarly, when using a tape measure to take “actual” readings, there is a possibility of human error as humans are unable to perceive differences in millimeters without the aid of more precise tools. Previous research has also shown that inaccuracies when using conventional measuring tools may have contributed to reported defects that may actually fall within allowable construction tolerances (Talebi et al, 2021).

From Figure 9, the largest errors result from the left region of the stairs. This large error is largely attributed to the stray mesh as shown in Figure 5.

The measurements of headroom reflect similar results as riser height measurements where MR application readings were found to be more accurate than CAD-measured readings. However, since the staircase was constructed more than the required standard of 2.1m (Hasegawa, n.d), useful results could not be obtained to compare occurrences of non-compliance. Figure 10 also shows that the left region of the stairs has the largest errors compared with the center and right region, but does not differ as much as riser height values.

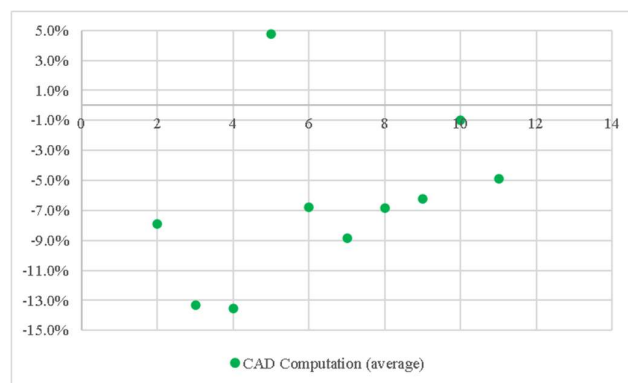


Figure 8. Percentage error against measured values between CAD-computed tread depth

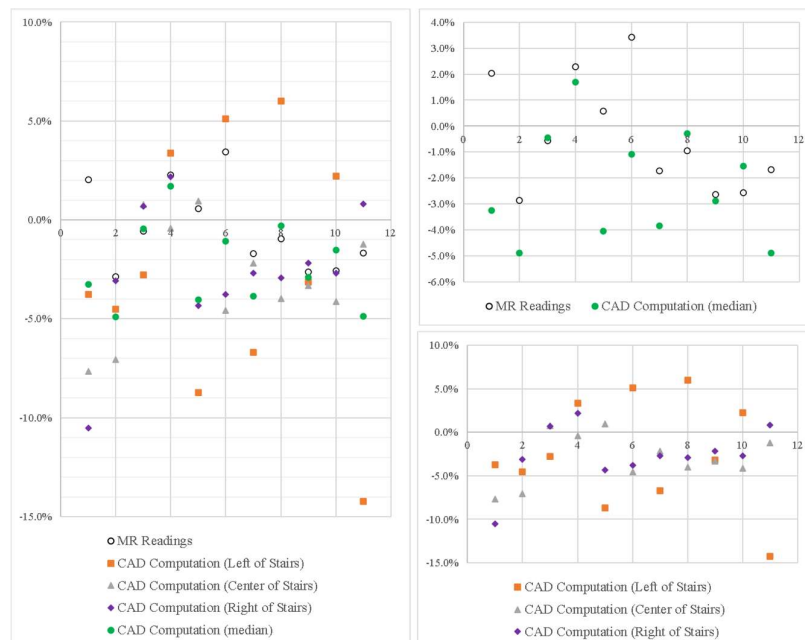


Figure 9. Percentage error against measured values between MR readings and all CAD-computed riser heights (Left), MR readings and CAD-computed average riser heights (Right-Top), CAD-computed left, right and center riser heights of staircase flight (Right-bottom).

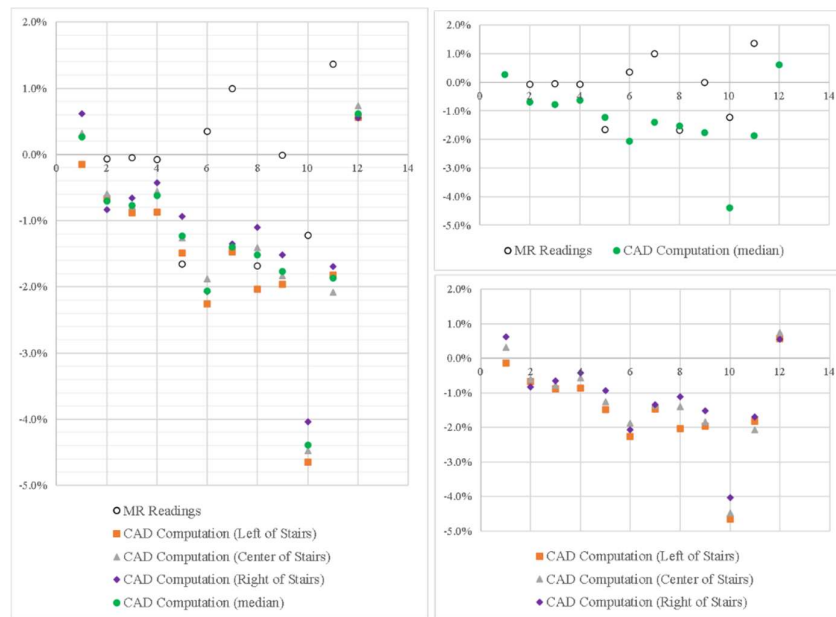


Figure 10. Percentage error against measured values between MR readings and all CAD-computed headroom (Left), MR readings and CAD-computed average headroom (Right-Top), CAD-computed left, right and center headroom of staircase flight (Right-bottom).

4.2 Accuracy of Horizontal Measurements - Tread Depth and Staircase Width

Due to the large number of stray points on the left edge of the staircase, plotting a best-fit line to determine the staircase width would not give a reasonable staircase width. Hence, data points beyond +50mm from the known staircase width of 1.385m were excluded from the analysis. The difficulty in clearly identifying the left edge of the staircase using data could be the reason why the MR application could not compute staircase width results as well.

Best-fit lines were drawn on the perceived edge points of each tread as shown in Figure 4. The average value of the dimensions is taken as the tread depth measurement for comparison. The largely manual process of identifying which points shall form the best-fit line, and the large variability of computed tread depth could be the reason why the MR application could not compute the tread depth automatically using the spatial map. Nonetheless, Table 2 shows that the proposed method of measuring tread depth in CAD gave largely inaccurate results, and the measured tread depths were largely less than the conventionally measured reference values.

Table 2. Occurrences of non-compliance from measured results

Staircase Component Measurement	Riser Height		Headroom		Tread Depth	
	MR Measurement	CAD Measurement	MR Measurement	CAD Measurement	MR Measurement	CAD Measurement
No. of Non-compliances	3	1	0	0	NIL	8
% of Non-compliances	27.3%	9.1%	0.0%	0.0%	NIL	72.7%
No. of Non-compliances by Ref. measurement	1		0		0	
% of Non-compliances by Ref. measurement	9.1%		0.0%		0.0%	

Khoshelham et al. (2019) reported that HoloLens 1, the predecessor of HoloLens 2, had a plane-fitting precision of 22.5mm and a mean distance of approximately 50mm compared to a registered laser scanner point cloud. In this study, automated riser height dimensions computed using the MR application showed an error within +/-6mm, while headroom measurement errors were closer to the reported accuracy of about 50mm. The percentage

error observed fell within a range of $\pm 5\%$ in both measurements suggesting that there might be compounded error due to the surface of interest being farther from the headset user. The larger value of error that was observed on the sloping surface could be attributed to errors either in mesh generation, or human error when taking measurements over longer distances using conventional measuring tools since CAD measured dimensions utilizing the exported mesh on landings, i.e., flat surfaces, gave almost zero error. The MR application could not compute headroom dimensions on landings, likely due to a programming error that needs further study.

5. CONCLUSIONS

The study showed that a spatial map generated by an MR device could be used to compute dimensions in an MR environment and yielded an accuracy of up to $\pm 5\%$ when computing vertical measurements. This suggests that measurements in MR could result in larger errors when measuring longer distances. However, the larger distance measured in this study was of a sloping surface, which could also be a reason for the larger errors encountered.

Although vertical measurements were computed successfully using the MR application, it was unable to compute horizontal distances. This limitation may be attributed to a large number of stray points observed in the exported mesh generated by the MR device, likely due to the void between the staircase railing and flight. Additionally, difficulty in identifying a clear boundary for each tread likely hindered the computation of tread depth. This was further evident during manual attempts to obtain best-fit lines for tread boundaries using the exported mesh, which yielded rather inaccurate tread depth measurements as well. Future research will focus on identifying more accurate methods for determining tread boundaries and incorporating this logic into the MR application to compute horizontal measurements.

REFERENCES

- Bartlett, K., Blanco, J.L., Fitzgerald, B., Johnson, J., Mullin, A.L., and Ribeirinho, M.J. (2020). *Rise of the platform era: The next chapter in construction technology*, McKinsey & Company.
- Fakunle, F.F., Opiti, C., Sheikh, A.A., and Fashina, A.A. (2020). Major barriers to the enforcement and violation of building codes and regulations: a global perspective, *SPC Journal of Environmental Sciences*, 2(1), 12-18
- Hasegawa, T. (nd). *Building Control in Japan Part D (ver. 1910)*. Institute of International Harmonization for Building and Housing (iibh). pp.78-79. Retrieved from iibh website: http://www.iibh.org/kijun/pdf/BCinJ_Part_D_1910.pdf
- International Organization for Standardization. (1994). *Accuracy (trueness and precision) of measurement methods and results – Part 1: General principles and definitions (ISO Standard No. 5725-1)*. Retrieved from website: <https://www.iso.org/obp/ui/#iso:std:iso:5725:-1:ed-1:v1:en>
- Khoshelham, K., Tran, H., and Acharya, D. (2019). Indoor mapping eyewear: geometric evaluation of spatial mapping capability of hololens, *The International Archives of the Photogrammetry, Remote Sensing and Spatial Information Sciences, Volume XLII-2/W13*,
- Kwon, O., Park, C., and Lim, C. (2014). A defect management system for reinforced concrete work utilizing BIM, image-matching and augmented reality, *Automation in Construction*, 46, 74-81.
- Microsoft. (2022). *Scene understanding SDK overview*. February, 08 2022. Retrieved from <https://learn.microsoft.com/en-us/windows/mixed-reality/develop/unity/scene-understanding-sdk>
- Microsoft. (2023). *About Hololens 2*. Retrieved from Microsoft website: <https://learn.microsoft.com/en-us/hololens/hololens2-hardware>
- Nguyen, D., Nguyen, T., Jin, R., Jeon, C., and Shim, C. (2021). BIM-based mixed-reality application for bridge inspection and maintenance, *Construction Innovation*, 22(3), 487-503.
- Phares, B.M., Washer, G.A., Rolander, D.D., Graybeal, B.A., and Moore, M. (2004). Routine Highway Bridge Inspection Condition Documentation Accuracy and Reliability, *Journal of Bridge Engineering*, 9(4), 403-413.
- Physics.Raycast. Retrieved from website: <https://docs.unity3d.com/ScriptReference/Physics.Raycast.html>
- Prieto, S.A., Giakoumidis, N., and Garcia de Soto, B. (2021). AutoCIS: An Automated Construction Inspection System for Quality Inspection of Buildings, *38th International Symposium on Automation and Robotics in Construction*.
- Talebi, S., Koskela, L., Tzortzopoulos, P., Kagioglou, M., Rausch, C., Elghaish, F., and Poshdar, M. (2021). Causes of Defects Associated with Tolerances in Construction: A Case Study, *Journal of Management Engineering*, 37(4).
- Zhou, Y., Luo, H., and Yang, Y. (2017). Implementation of augmented reality for segment displacement inspection during tunneling construction, *Automation in Construction*, 82, 112-121.

BIM-BASED AND AUGMENTED REALITY COMBINED WITH A REAL-TIME FIRE EVACUATION SYSTEM FOR THE CONSTRUCTION INDUSTRY

Somjintana Kanangkaew¹, Noppadon Jekkaw², and Tanit Tongthong³

1) Ph.D. Candidate, Department of Civil Engineering, Faculty of Engineering, Chulalongkorn University, Bangkok, Thailand.
Email: 6171424921@student.chula.ac.th

2) Ph.D., Assoc. Prof., Department of Civil Engineering, Faculty of Engineering, Chulalongkorn University, Bangkok, Thailand.
Email: Noppadon.j@chula.ac.th

3) Ph.D., Assoc. Prof., Department of Civil Engineering, Faculty of Engineering, Chulalongkorn University, Bangkok, Thailand.
Email: Tanit.t@chula.ac.th

Abstract: In the past decade, the drawings of construction projects' standard fire evacuation routes are usually presented in two-dimensional (2-D) views to explain the construction area and evacuation routes. Common users find it difficult to interpret the 2-D drawings quickly, accurately determine their position within the building, and choose the appropriate evacuation routes. Thus, in the event of a fire, the construction project can lead to damage and result in numerous fatalities and injuries among the workers. Nowadays, Visualization technology such as Building Information Modeling (BIM) and Augmented Reality (AR) are used in construction projects to create construction in a three-dimensional (3-D) visualization. This study aims to develop a prototype application that combines Building Information Modeling (BIM) and Augmented Reality (AR) to improve the fire evacuation system and provide real-time access to information for evacuating from hazardous locations. A marker-based location system was implemented, using a marker as a spatial index to link the physical location and virtual information. The results showed that the proposed system could provide real-time access to information such as the current location, exit, distance of the shortest route from the current location to the destination, and virtual green line, voice, and arrow direction for evacuation guidance. Regarding obstacle avoidance, the proposed system recommended the appropriate evacuation route to the user in real-time. Therefore, this proposed system is effective and convenient for decision-making, helping users find destinations quickly and efficiently.

Keywords: Fire Evacuation System, Building Information Modeling, Augmented Reality

1. INTRODUCTION

Construction projects, in particular, are prone to high numbers of fire accidents compared to other phases in the construction project lifecycle. Fire is one of the six fatal accidents in the construction sector. In addition, fire accident is growing in economic loss, loss of life, and social impacts such as the incapacity to work due to an injury (Lee et al., 2014). According to statistics from 2012 to 2018, the Bangkok Fire and Rescue Department responded to an estimated average of 889 reported structure fires yearly (D.o.E, 2021). These fires caused an average of 20 civilian deaths and 152 civilian injuries (Kanangkaew et al., 2023). In addition, many construction project fires occurred during this period and caused severe damage to users. Therefore, evacuating people to a safety zone in most emergency management becomes a crucial step. Furthermore, because of the characteristics of construction phases, continuously changed workplaces, the number of occupants, spaces, and evacuation routes change from one day to another (Marzouk & Daour, 2018). Furthermore, the construction site has less protection, such as fire alarms, sprinklers, smoke detectors, and other fire suppression systems that have not been implemented. Therefore, evacuation conditions in the construction phases differ from the other phases, and the disasters are becoming diverse (Cheng et al., 2016) and challenging to predict the appropriate evacuation routes.

Generally, Construction site environments have many temporary works and continuously changed workplaces, which means the number of occupants, spaces, and evacuation routes change from one day to another (Marzouk & Daour, 2018). Furthermore, evacuation routes cannot identify locations due to continuously evolving workplaces obstructed hallways from materials and equipment. The lack of identification of evacuation routes on-site frequently results in additional cost growth schedule delays during construction phases (Choi et al., 2014). However, in the common evacuation routes in construction projects, the drawings were usually guided in two-dimensional (2-D) views to explain hazardous areas and evacuation routes. Therefore, common users cannot interpret the drawings quickly, understand their position within the building, and select appropriate evacuation routes (Wang et al., 2014). Recent relevant research has identified the cause of a high proportion of emergency casualties as a direct link with the delayed evacuation service of the facility (Fahy & Proulx, 2001), which the lack of real-time information updates can cause such as building users in an emergency cannot get the real-time location evacuation route (Wang et al., 2014). To reduce the number of injuries and fatalities from fire accidents in construction projects, it is essential to prepare safety evacuation tools and guidelines to direct workers and staff to evacuate as fast and safely as possible from the hazard location.

This study aims to create a prototype application that combines Building Information Modeling (BIM) and Augmented Reality (AR) to improve the fire evacuation system and provide real-time access to information for evacuating from hazardous locations.

2. LITERATURE REVIEW

2.1 Fire Emergency Procedures

Efficient fire evacuation is one of the most critical primitive responses to a possible emergency situation (Chen et al., 2017). However, the building's environment constantly changes, disasters are becoming more diverse and challenging to predict, and evacuation routes cannot be identified due to obstructed hallways caused by materials and equipment in the workplace. Therefore, predicting potential hazards when a fire occurs in construction projects is difficult. Despite the constraints in work conditions, the researcher still developed tools in this process to protect construction workers and staff from fire accidents.

2.2 Visualization Technology in The Construction

According to Hosseini & Maghrebi (2021), visualization technology is an effective communication tool for fire evacuation systems in construction projects. Its advantages include the ability to display complex data in an easily understandable way, visually identify hazard areas, facilitate decision-making, and promote interaction between staff and engineers to solve problems.

2.3 Building Information Modeling (BIM)

Building Information Modeling (BIM), as defined by international standards, is a shared digital representation of any constructed object's physical and functional characteristics, which serves as a dependable foundation for decision-making. It is considered one of the most significant recent developments in the architecture, engineering, and construction industry and is particularly valuable for high-rise and complex buildings. BIM facilitates visualization and coordination of work, error avoidance, clash detection, safety management improvement, and communication and productivity enhancement (Han et al., 2009) in construction projects. It encourages integration and collaboration, linking applications effectively across various building life cycle stages through shared information (Wang et al., 2014). Building Information Modeling (BIM) also enables virtual 3-D coordination of construction activities related to emergency evacuation, presenting the unique site layout in 3-D visualization and rapidly identifying fire conditions in construction projects (Cheng et al., 2016).

2.4 Augmented Reality (AR)

Augmented Reality (AR) is a technology or environment where virtual information created by a computer is superimposed onto the user's view of a real-world scene (Limsupreeyarat, 2012) through a display device. This technology allows for visualizing the real environment, with computer-generated digital content such as text, images, 3-D models, and sound overlaid after stimulation (Chen et., 2019). However, workers and staff, except engineers and architects, typically do not use BIM technology, which can be difficult to understand. Therefore, Augmented Reality (AR) offers digital information, such as 3-D models, images, and animations, to be overlaid on the real world and achieve a natural interaction between the user and their environment (Cheng et al., 2017), making it easier for workers and staff to understand information.

3. METHODOLOGY

3.1 Project Framework

The system architecture developed in this study consists of four elements: 1) BIM authoring, 2) a marker-based location, 3) application authoring, and 4) the experiment. Overall, the study demonstrated that the integration of BIM and AR could be applied to facilitate the automatic update of the digital model, storage of data in a standard file format (Rahimiana et al., 2019), display of the user's location in the virtual environment, obstacle avoidance system in real-time. Additionally, this study posits that this can be used as an effective tool for supporting decision-making and enabling users to perceive and understand the information clearly and easily.

Figure 1 demonstrates the framework of the proposed system. Seamless information exchange was a significant focus of this study; the Industry Foundation Classes (IFC) file format and the Autodesk Revit and Autodesk Navisworks (NWD) file formats were utilized as standard files. Firstly, the IFC model is exported into an Autodesk Filmbox (FBX) file format and integrated into the Unity game engine to create a virtual model in the virtual environment. This virtual model generates a dataset of fire exits and markers, which display the user's location in the virtual environment. Then, scripts are used to calculate the shortest evacuation route and obstacle avoidance system in real-time. Finally, the proposed system can visualize and detect markers that trigger the display of the user's location and the shortest and obstacle avoidance system in real-time on a real-world scene.

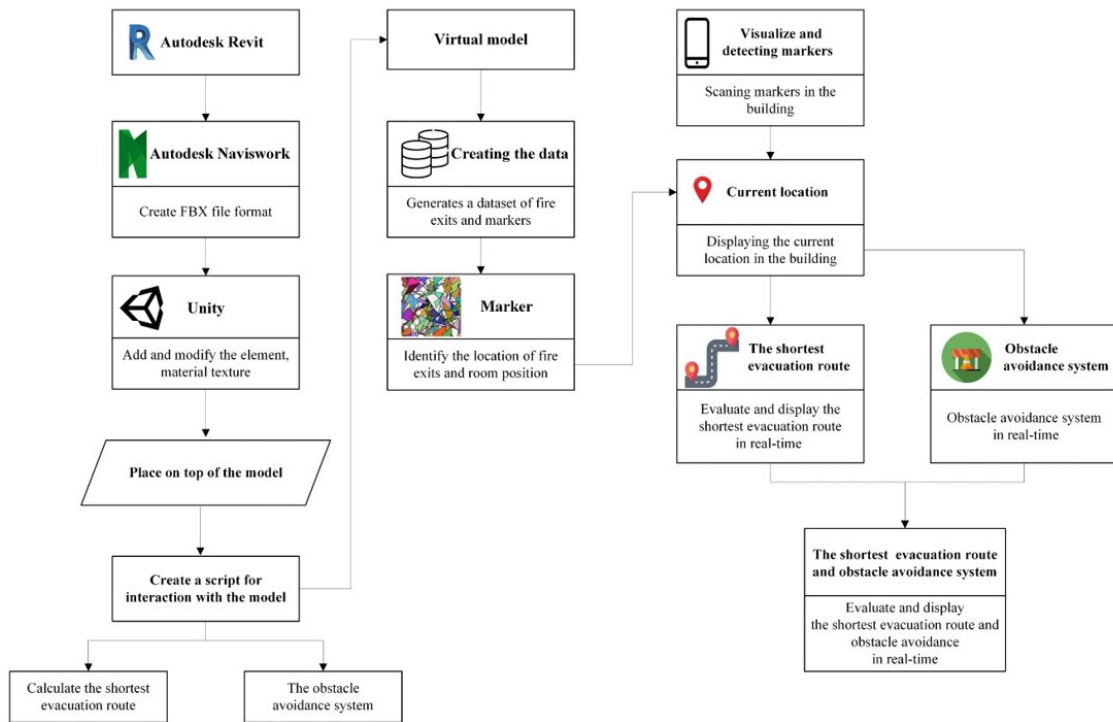


Figure 1. The framework of the proposed system

3.2 BIM Authoring

A prototype application combining Building Information Modeling (BIM) and Augmented Reality (AR) was implemented to demonstrate the proposed framework. For this study, the proposed system was used for people to evacuate from an existing building. Therefore, the Department of Civil Engineering Building at Chulalongkorn University was selected as a case study. This five-story building is used for classrooms, offices, and meeting rooms, with a total area of 5,832 square meters and a height of 26 meters. First, a 3-D model of the building's architecture was created with a Level of Detail (LOD) of 300 using Autodesk Revit 2019 based on as-built drawings. As a result, the room and exit locations in the 3-D model are the same as those in the real world. Next, the IFC file format was utilized to save the 3D model, which was then converted to the Autodesk Naviswork (NWD) file format and saved in the Autodesk Filmbox (FBX) file format, as shown in Figure 2.

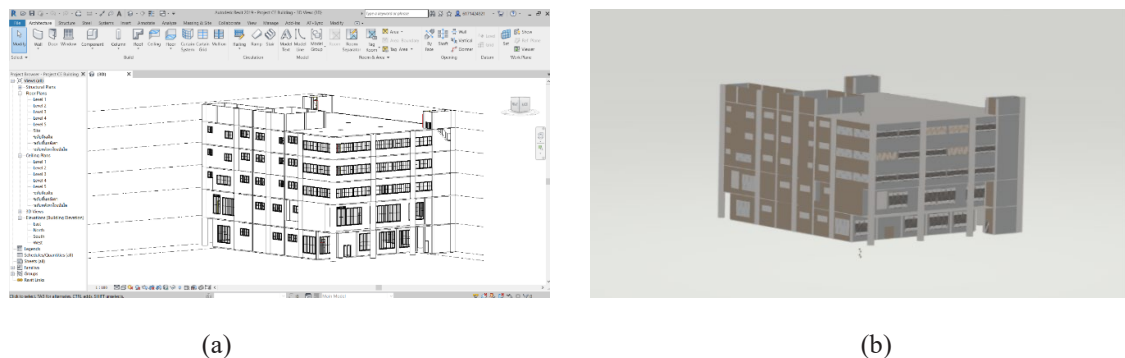


Figure 2. The 3-D model of the Department of Civil Engineering Building at Chulalongkorn University.

3.3 Linking the FBX Model and the Unity Game Engine

The primary platform used for creating the application and integrating visualization technologies such as Building Information Modeling (BIM) and Augmented Reality (AR) was the Unity game engine, a cross-platform toolkit developed by Unity Technologies for creating video games and simulations for computers, consoles, and mobile devices. Additionally, this study utilized a previously developed method of linking a digital model to support the integration of the information in the 3-D model, including 3-D rendering, physics, and collision detection, which was established using the FBX file format and incorporated programming with C# scripting in combination with other related classes and APIs.

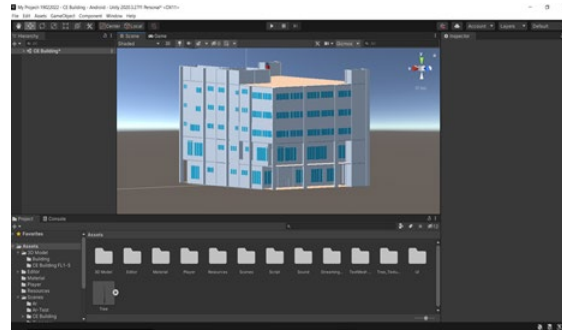


Figure 3. A virtual environment of the building was created using the Unity game engine.

3.4 A Marker-Based Location

The developed marker-based location system utilizes a marker as a spatial index to connect physical locations with virtual information. The system functions as follows: Firstly, the camera captures an image with a marker on the mobile device. The image is then forwarded to the classifier algorithm, which is designed to classify data into different categories or classes and assumes a relatively balanced distribution of classes to create the marker ID by generating the code. Then, the marker code is sent to the database as a key value to look for associated information. Next, the system sets the location and direction in the virtual environment. However, the system does not display any data if the code is not recognized in the database. As the mobile device moves, the system transmits updated data concerning the location and direction to the real world in real-time. The system does not update any data if the mobile device has not moved.

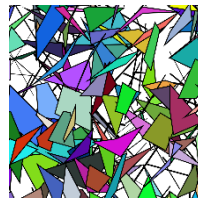


Figure 4. Example of the markers.

3.5 Application Authoring

The proposed system provides real-time information, such as the user's current location, which is used to calculate the distance to the exit via a virtual green line. The system also provides voice and arrow directions for evacuation guidance, virtual green line, exit, and distance from the current location to the exit and recommends the appropriate evacuation route in case of obstacle avoidance. In the proposed system, the starting point is an image containing a marker, which is used to measure the distance to the exit, determine whether the evacuation route adheres to safety rules, and plan the corresponding exits for each room in the building. If the user moves away from the exit or does not follow the evacuation guidance, the system will recalculate the distance from the current location and display real-time information to the user on their next interaction. Additionally, in the case of obstacle avoidance, the proposed system will recommend the appropriate evacuation route to the user in real-time.

3.6 The Shortest Fire Evacuation Route

The proposed architecture for a fire evacuation system is an integrated framework that stores location data in a 3-D model, calculates the shortest fire evacuation route for each user, and generates a green line to display the virtual evacuation route with voice and arrow directions in the building. Building Information Modeling (BIM) is an effective visualization tool that helps allocate evacuation areas in the building to each exit based on the latest locations of fires and evacuees. C# is the primary programming language used for scripting in this study. The shortest evacuation route is calculated using the A* algorithm.

A* algorithm is a heuristic search algorithm that finds the shortest paths between a starting node and an end node and uses a heuristic function to estimate the cost of reaching the goal, which helps it to search for the optimal path efficiently. The advantage of the A* algorithm is that it is simple and relatively fast (Erke et al., 2020). Moreover, the A* algorithm can be computed By Equation (1).

$$f(n) = g(n) + h(n) \quad (1)$$

Where: $f(n)$ is the cost function from an initial point to the destination; $g(n)$ is the actual cost from an

initial point to the node n in state space; $h(n)$ is the estimated cost of the optimal path from the node n to the destination.

7	6	5	6	7	8	9	10	11	18	19	20	21	22
6	5	4	5	6	7	8	9	10	17	18	19	20	21
5	4	3	4	5	6	7	8	9	16	17	18	19	20
4	3	2	3	4	5	6	7	8	15	16	17	18	19
3	2	1	2	3	4	5	6	7	14	15	16	17	18
2	1	0	1	2	3	4	5	6	13	14	15	16	17
3	2	1	2	3	4	5	6	7	12	13	14	15	16
4	3	2	3	4	5	6	7	8	11	12	13	14	15
5	4	3	4	5	6	7	8	9	10	11	12	13	14
6	5	4	5	6	7	8	9	10	11	12	13	14	15

Figure 5. The example of finding the shortest paths using the A* algorithm (Mahadevi et al., 2012)

3.7 The Real-Time Obstacle Avoidance System

Construction site environments involve many temporary works and constantly changing workplaces. As a result, the number of occupants, spaces, and evacuation routes can vary daily (Marzouk & Daour, 2018). Additionally, obstructed hallways from materials and equipment can make it challenging to identify evacuation routes. Therefore, it is essential to design an evacuation route application that can avoid obstacles in real-time.

The proposed architecture for the real-time obstacle avoidance system is an integrated framework that stores location data in the 3-D model and avoids obstacles in the building. Building Information Modeling (BIM) is an effective visualization tool that helps allocate evacuation areas in the building, and Google Sheets is a web-based spreadsheet program developed by Google. It allows users to create, edit, and collaborate on spreadsheets in real-time, which use internet access to identify and update the position of materials and temporary works in the 3-D model. C# is the primary programming language used for scripting in this study.

The real-time obstacle avoidance system using A* algorithm is an effective approach for planning collision-free paths in complex environments. It is widely used in robotics and autonomous systems for navigation and the range of information provided by Google Sheets. The system must sense the environment and detect obstacles to plan a collision-free path. The detected obstacles are then marked in the graph as nodes or edges that cannot be traversed. The A* algorithm is then applied to find the shortest path from the starting node to the goal while avoiding obstacles.

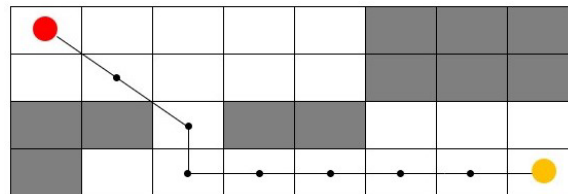


Figure 6. The concept obstacles avoidance system using A* algorithm

3.8 The Experiment

In this study, the proposed system was tested through an experiment to visualize and display the user's location, the shortest evacuation route, and an obstacle avoidance system in real-time on a real-world scene. Based on the application's built-in calibration system, 36 markers with patterns were installed on the 4th floor as nodes, such as rooms, corners, and fire exits, as shown in Figure 8, and were defined in the 3-D model in both virtual and real environments.

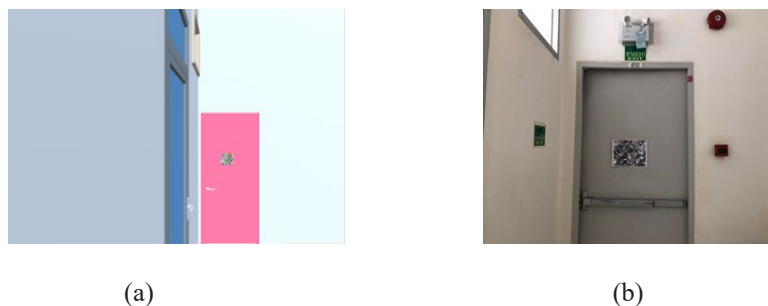


Figure 7. Example of the marker's location in the virtual and real environment.

The authors of this study designed three case studies for data collection in the case of obstacles avoidance systems as follows:

1. Case 1: the real environment in normal condition
2. Case 2: Adding one obstacle location
3. Case 3: Adding two obstacle locations

The proposed system integrated the evacuation route and exit in the experiment by capturing images containing the marker. The proposed system then detected markers that triggered the display of the user's location and the shortest obstacle avoidance system in real-time on a real-world scene. Finally, the system calculated the shortest evacuation route based on distance and recommended the appropriate evacuation route to the user in real-time.

4. RESULTS

4.1 The Shortest Fire Evacuation Route

From the experiment, the proposed system could detect markers and provide real-time access to information such as the current location, exit, distance of the shortest route from the current location to the destination, and virtual green line, voice, and arrow direction for evacuation guidance to the user in real-time.

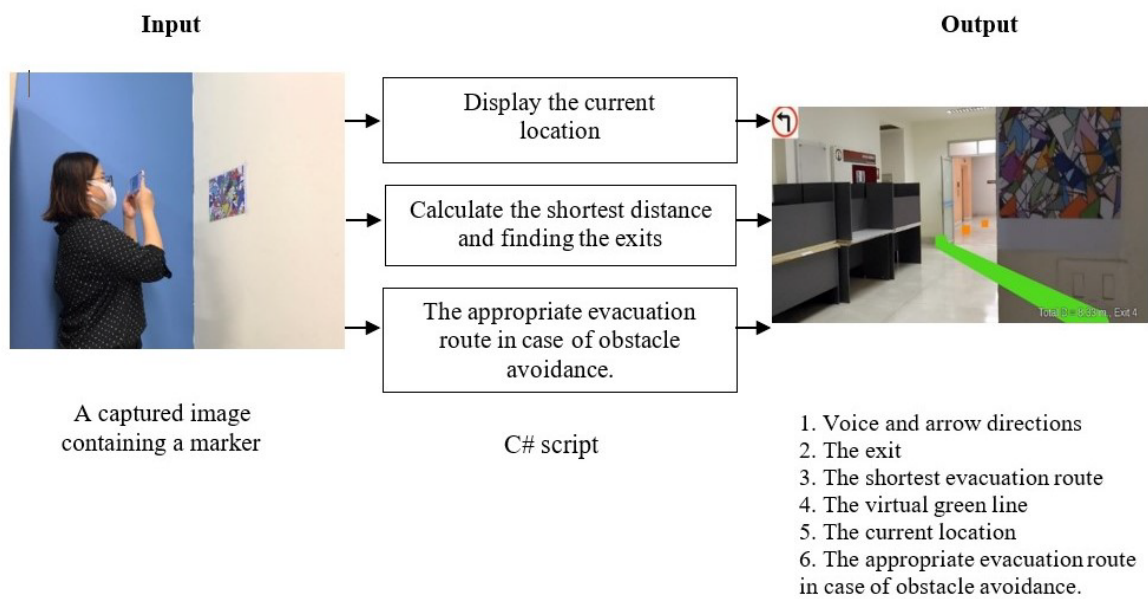


Figure 8. Details the method for integrating the evacuation route and exit using the proposed system.

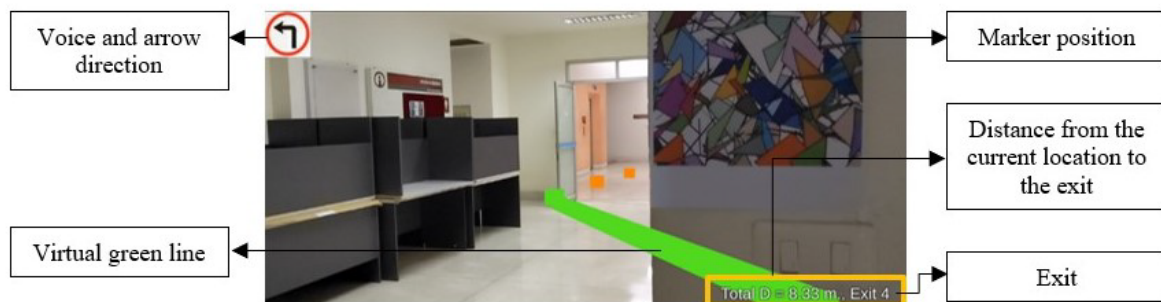


Figure 9. The output of the proposed system.

4.2 The Real-Time Obstacle Avoidance System

The result showed that the proposed system could identify the position of obstacles and detect obstacles from a Google Sheet in real-time, which uses internet access to identify and update the position of obstacles. When an obstacle appears in a building, the proposed system could avoid obstacles and immediately recommend an appropriate evacuation route to the user.

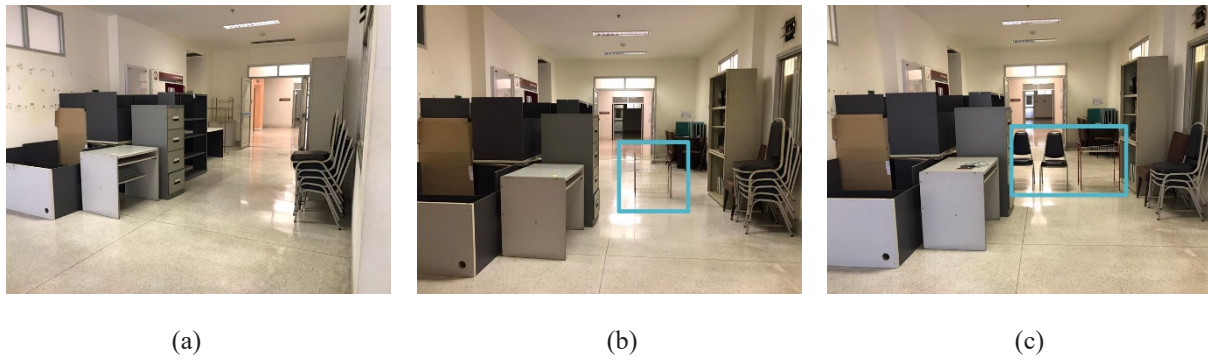


Figure 10. Three case studies of obstacles positions for the experiment.



Figure 11. The output of the obstacle avoidance system in cases 1 and 2.

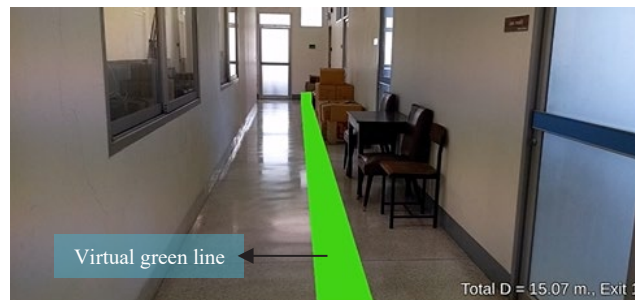


Figure 12. The output of the obstacle avoidance system in case 3.

Figures 11 and 12 present the results of the proposed system in case of an obstacle avoidance system. The results show that the proposed system could be recommended the appropriate evacuation route to the user in real-time regarding obstacle avoidance, which is exit 3 and 4 in cases 1 and 2, respectively. In addition, in case 3, it was impossible to walk through due to obstructions. Therefore, instead, the proposed system could be recommended to the user to the next exit, which is exit 1.

5. CONCLUSIONS

In conclusion, the proposed system is a BIM-based and Augmented Reality (AR) application that improves fire evacuation systems and provides real-time access to information for evacuating from hazardous locations. In the case study, the proposed system was tested through an experiment to visualize and display the user's location, the shortest evacuation route, and an obstacle avoidance system in real-time on a real-world scene. The experiment was conducted using the proposed system on the 4th floor of the Department of Civil Engineering Building at Chulalongkorn University, based on the application's built-in calibration system. The results showed that the proposed system could provide real-time access to information such as the current location, exit, distance of the shortest route from the current location to the destination, and virtual green line, voice, and arrow direction for evacuation guidance. Furthermore, the proposed system could recommend the appropriate evacuation route to the user in real-time regarding obstacle avoidance. If it was impossible to walk through due to obstructions, the proposed system could recommend the user to the next exit. Therefore, this proposed system is effective and convenient for decision-making, helping users find destinations quickly and efficiently.

However, this study has some limitations that need to be addressed in the future. One limitation is that the

proposed system can only provide real-time information if the user captures an image containing a marker on their mobile device. This means that if the user is not near a marker location, they will not receive real-time information from the system. In addition, more types of sensors will be embedded into the proposed system in future work, including temperature, smoke, and flammable sensors, to calculate and prevent the system from selecting the next exit, which is safe from the location of the fire, and provide information to the users.

ACKNOWLEDGMENTS

The author would like to thank the Department of Civil Engineering, Faculty of Engineering, Chulalongkorn University, for providing the data analysis and facilitating the data collection process for this research project.

REFERENCES

- Cheng, J., Chen, K., and Chen, W. (2017). Comparison of Marker-Based and Markerless AR: A Case Study of An Indoor Decoration System. *Lean and Computing in Construction Congress (LC3): Volume 1B Proceedings of the Joint Conference on Computing in Construction (JC3)*, Heraklion, Greece.
- Cheng, M., Chiu, K.-C., Hsieh, Y., Yang, I. and Chou, J. (2016). Development of BIM-based Real-time Evacuation and Rescue System for Complex Building, *Proceeding of the 33rd International Symposium on Automation and Robotics in Construction (ISARA 2016)*, Auburn, Alabama, USA.
- Chen, Y., Wang, Q., Chen, H., Song, X., Tang, H., and Tian, M. (2017). An overview of augmented reality technology. *IOP Conf. Series: Journal of Physics: Conf.* 1237.
- Chen, Y., Wang, Q., Chen, H., Song, X., and Tang, H. (2019). An overview of augmented reality technology, *Journal of Physics Conference Series*, 1237(2):022082
- Choi, J., Choi, J., and Kim, I. (2014). Development of BIM-based evacuation regulation checking system for high-rise and complex buildings. *Automation in Construction*. 46, 38-49.
- Department of Alternative Energy Development and Efficiency, D. o. E. (2021). Building Energy Codes.
- Fahy, R. and Proulx, G. (2001). Toward creating a database on delay times to start evacuation and walking speeds for use in evacuation modeling, *Proceeding of the 2nd International Symposium on Human Behaviour in Fire*, Boston, MA., USA.
- Hosseini O. and Maghrebi. M. (2021). Risk of fire emergency evacuation in complex construction sites: Integration of 4D-BIM, social force modeling, and fire quantitative risk assessment. *Advanced Engineering Informatics*, 50, 101378.
- Han, S., Peña-Mora, F., Golparvar-Fard M., and Roh, S. (2009). Application of a Visualization Technique for Safety Management. *International Workshop on Computing in Civil Engineering 2009*, Austin, Texas, United States.
- Kanangkaew, S., Jekkaw, N., and Tongthong, T. (2023). A real-time fire evacuation system based on the integration of Building Information Modeling and Augmented Reality, *Journal of Building Engineering*, 67:105883
- Lee, K., Lee, H.-S., Park M., Kim, H., and Han, S. (2014). A Real-Time Location-Based Construction Labor Safety Management System. *Journal of Civil Engineering and Management*, 20(5), 724-736.
- Khatib, O. and Quinlan, S. (1993). Elastic Bands: Connecting, Path Planning and Control. *Proceeding of IEEE International Conference on Robotics and Automation*, Atlanta, GA, United States.
- Limsupreeyarat, P. (2012). Supporting Construction Personnel in the Safety and Planning of Construction Activities Performed at High Elevations via Augmented Reality Technology. [Doctoral dissertation, Chulalongkorn University]. Bangkok, Thailand.
- Mahadevi S., Shylaja, K.R., and Ravinandan, M. E. (2012). Memory Based A-Star Algorithm for Path Planning of a Mobile Robot, *International Journal of Science and Research (IJSR)*, 3(6), 1351-1355.
- Marzouk, M. and Daour, I. (2018). Planning labor evacuation for construction sites using BIM and agent-based simulation. *Safety Science*, 109, 174-185.
- Rahimiana, F., Chavdarova, V., Oliver, S., and Chamo, F. (2019). OpenBIM-tango integrated virtual showroom for offsite manufactured production of self-build housing. *Automation in Construction*, 102, 1-16.
- Wang, B., H. Li., Rezgui, Y., Bradley, A., and Ong, H. N. (2014). BIM-Based Virtual Environment for Fire Emergency Evacuation. *The Scientific World Journal*, 14, 1-22.



5th ICBEI
BANGKOK, THAILAND



The 5th International Conference on Civil and Building
Engineering Informatics (ICCBEI 2023)
Bangkok, Thailand

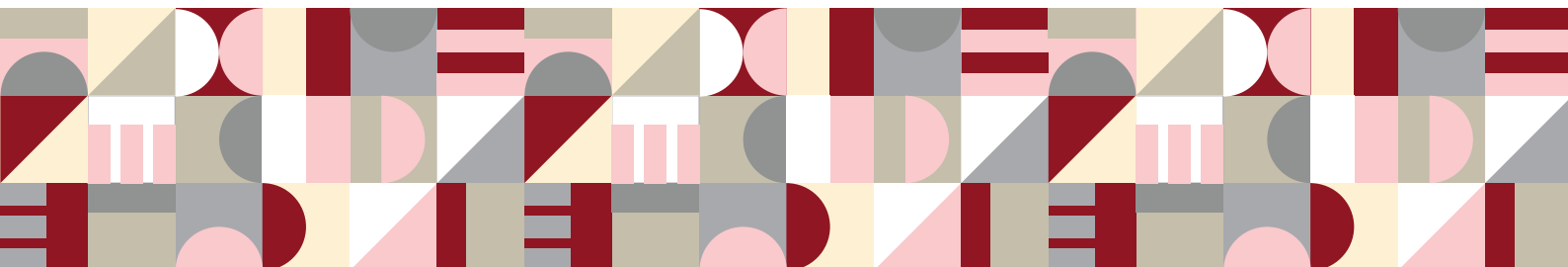
Graphic Design and Book layout by

Weerana Talodsuk

puii6704@gmail.com / cweerana@gmail.com

ICCBEI 2023

BANGKOK THAILAND



The 5th International Conference
on Civil and Building Engineering Informatics
July 19-21, 2023